UNIVERSITAT ROVIRA I VIRGILI

IMMOBILIZATION OF 2,4-CIS-DIARYLPROLINOL SILYL ETHERS, ISOTHIOUREAS, SPINOL-DERIVED PHOSPHORIC ACIDS AND THEIR APPLICATION IN THE CATALYTIC ENANTIOSELECTIVE SYNTHESIS IN BATCH AND FLOW

Junshan Lai

UNIVERSITAT
ROVIRA i VIRGILI

Immobilization of 2,4-cis-Diarylprolinol Silyl Ethers, Isothioureas, SPINOL-Derived Phosphoric Acids and Their Application in the Catalytic Enantioselective Synthesis in Batch and Flow

Junshan Lai

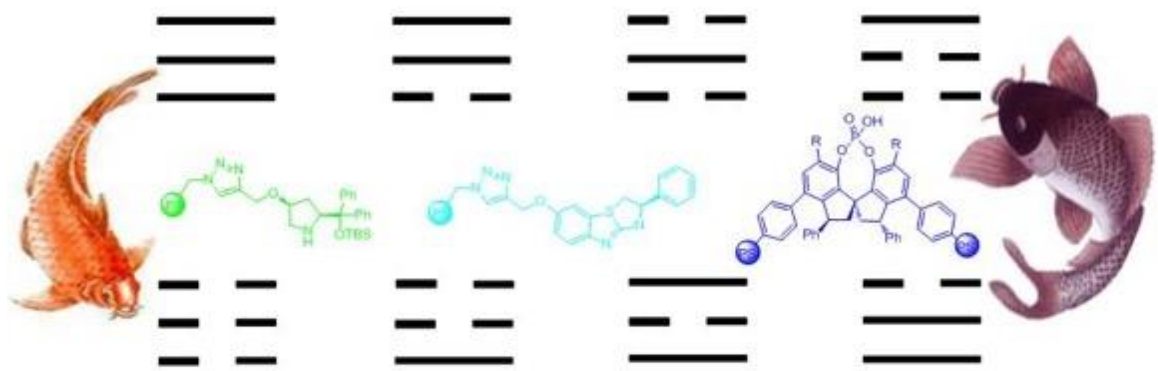

TESI DOCTORAL – TESIS DOCTORAL- DOCTORAL THESIS
2020

Immobilization of 2,4-cis-Diarylprolinol Silyl Ethers, Isothioureas, SPINOL-Derived Phosphoric Acids and Their Application in the Catalytic Enantioselective Synthesis in Batch and Flow

PhD Thesis by

Junshan Lai

Supervised by

Prof. Miquel A. Pericàs Brondo, Dr. M. Sonia Sayalero Sanz

Departament de Química Analítica i Química Orgànica, Universitat Rovira i Virgili (URV)

Institute of Chemical Research of Catalonia (ICIQ)

Tarragona 2020

Universitat Rovira i Virgili

Institut Català d'Investigació Química

UNIVERSITAT ROVIRA I VIRGILI

ICIQ
Institut Català d'Investigació Química

Prof. Miquel A. Pericàs Brondo, Group Leader and Director of the Institute of Chemical Research of Catalonia (ICIQ) and,

Dr. M. Sonia Sayalero Sanz, Researcher and former Group Coordinator of the Pericàs Research Group (ICIQ),

STATE, that the present Doctoral Thesis entitled: **"Immobilization of 2,4-cis-Diarylprolinol Silyl Ethers, Isothioureas, SPINOL-Derived Phosphoric Acids and Their Application in the Catalytic Enantioselective Synthesis in Batch and Flow "**, presented by Junshan Lai to receive the degree of Doctor, has been carried out under our supervision at the Institute of Chemical Research of Catalonia (ICIQ).

Tarragona, 15th of September, 2020

PhD Thesis Supervisor	PhD Thesis Co-supervisor
Prof. Miquel A. Pericàs Brondo	Dr. M. Sonia Sayalero Sanz

Acknowledgements

Let's imagine an enantiomerically pure compound existing as a pair of diastereomers that we plan to use as a catalyst. For diastereomeric excesses between 80% and 90%, we can consider that it already has a practical value in view of its application in catalysis. If we observe the HPLC trace and the NMR spectrum of our catalyst candidate, although the peaks due to the minor isomer are lower than those corresponding to the major isomer, its presence has a particularly important effect on the catalytic activity and selectivity of the considered compound (in some cases positive and in some cases negative). For my life, the four-year PhD study is like this minor isomer---short but very important for my life and future career choices. I am grateful for the positive impact that these four years in ICIQ has exerted on me.

During my four years PhD study in ICIQ, a lot of people have made my life here unforgettable and meaningful.

First of all, I would like to thank my supervisor Prof. Miquel A. Pericàs (Miquel) for his guidance, caring, encouragement, professional advice and constant support during the time of my career in ICIQ. And giving me the opportunity to do my research in an international team which has given me a lot of adventure and experience.

At the same time, I wish to thank Dr. Carles Rodríguez Escrich and Dr. Sonia Sayalero Sanz for their invaluable advice and help in the development of the projects. In addition, I would like to thank all the technical support and administrative staff of ICIQ, especially thanks to Ms. Sara Gacia for all her help.

I am also grateful to all the past and present members of the Pericàs group. Special thanks to Dr. Patricia Llanes for her help for renting a house in Tarragona, and advice and help in the experiments set up. Special thanks to Dr. Parijat Borah for his professional advice during discussion.

In addition, I would like to thank the friends I made in Tarragona for their support and friendship. Special thanks to Nicola Zanda for his funny jokes in the lab.

Special thanks to my family---my parents, grandparents, my sister and my girlfriend---for their endless love and unconditional supports during all my life.

Thank you very much to all of you!

The present doctoral thesis has been possible thanks to the funding received from AEI/MINECO/FEDER (FPI Fellowship BES-2016-078937) and ICIQ Foundation (ICIQ grant 2016/13) as well as from the following projects: CERCA Programme/Generalitat de Catalunya, AEI/MINECO/FEDER (Grants: CTQ2015-69136-R and PID2019-109236RB-I00) and AGAUR (Grants: 2014SGR827 and 2017SGR1139)

Abbreviations

In this document the abbreviations and acronyms most commonly used in organic chemistry have been used, according to the recommendations of the ACS "Guidelines for authors":

http://pubs.acs.org/paragonplus/submission/joceah/joceah_authguide.

Table of Contents

Thesis Overview

Chapter I. General Introduction

The first chapter is a general introduction of immobilized organocatalysis dealing with the general concept, general principles for immobilization, supports and strategies, continuous flow process and device. Some representative immobilized organocatalysts are presented in this chapter as well.

Chapter II. Immobilization of *cis*-4-Hydroxydiphenylprolinol Silyl Ethers and application in the Synthesis of 5-Hydroxyisoxazolidines

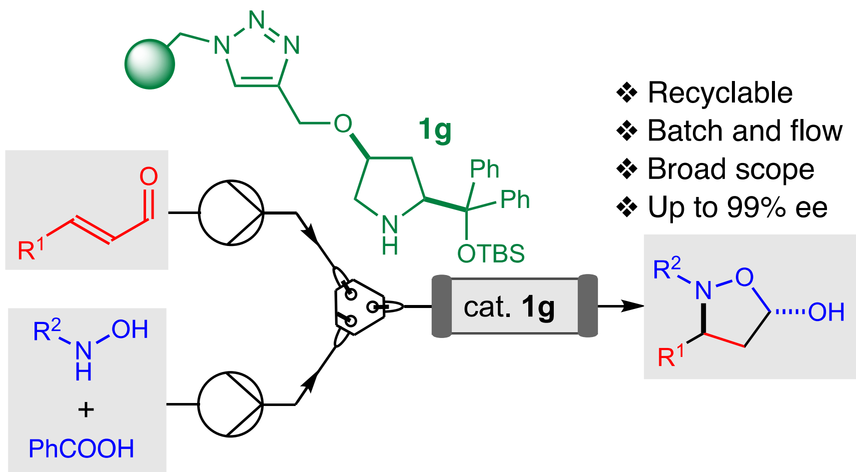

In chapter II, a new family of polystyrene-supported *cis*-4-hydroxydiphenylprolinol has been prepared, and the resulting polymers have been evaluated as organocatalysts to promote the tandem reaction between *N*-protected hydroxylamines and α,β-unsaturated aldehydes in batch and flow. The new PS-supported catalysts compare favorably with well-established immobilized Jørgensen-Hayashi catalysts, affording 5-hydroxyisoxazolidines as single diastereoisomers with high enantioselectivities and good yields (up to 83% yield, up to 99% ee).

Chapter III. Continuous Flow Preparation of Enantiomerically Pure BINOL(s) by Acylative Kinetic Resolution

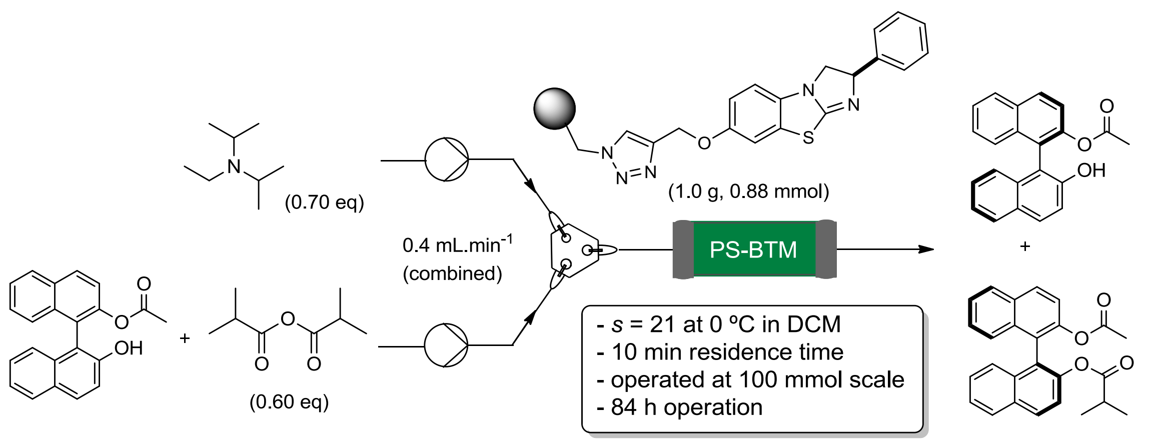

A polystyrene-immobilized isothiourea has been applied to the enantioselective acylative kinetic resolution (KR) of monoacylated BINOL(s) with inexpensive isobutyric anhydride in batch and flow. High selectivity values (*s* = 35 at 0 ºC) and a remarkable stability of the catalytic system in the operation conditions have been recorded for unsubstituted BINOL. No significant loss of activity/selectivity is recorded after 10 consecutive KR cycles in batch. A continuous flow process has been implemented and operated with a 100 mmol (32.8 g) sample of racemic monoacetylated BINOL in an 84 hours experiment with a packed bed reactor containing 1 g (f = 0.37 mmol.g^{-1}) of the functional resin. Residence time can be decreased to 10 min with the same reactor to achieve a conversion of 58% with a selectivity factor *s* = 17 in dichloromethane solution when a more highly functionalized catalyst (f = 0.88 mmol.g^{-1}) is used. This translates into a remarkable combined productivity of 5.5 $mmol_{prod}\cdot mmol_{cat}^{-1}\cdot h^{-1}$.

Chapter IV. Development of Immobilized SPINOL-Derived Chiral Phosphoric Acids for Catalytic Continuous Flow Processes. Use in the Catalytic Desymmetrization of 3,3-Disubstituted Oxetanes

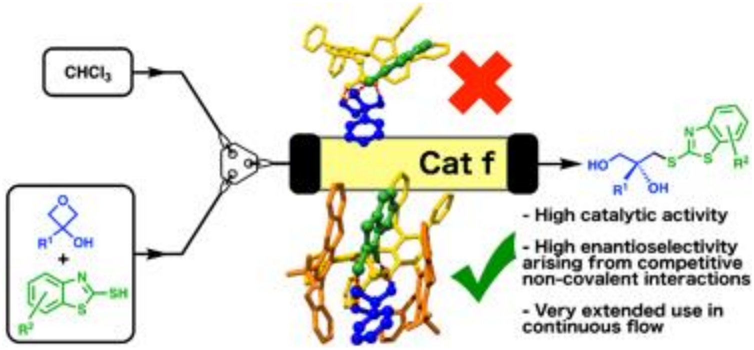

A family of C2-symmetrical 1,1′-spirobiindane-7,7′-diol (SPINOL) derivatives containing polymerizable styryl units has been prepared through a highly convergent approach. Radical co-polymerization of these monomers with styrene has allowed the synthesis of a new family of immobilized SPINOL-derived chiral phosphoric acids (SPAs) where the combination of the restricted axial flexibility of the SPINOL units and the existence of extended and adaptable chiral walls adjacent to them leads to enhanced stereocontrol in catalytic processes. The optimal immobilized species (**Cat f**) brings about the catalytic desymmetrization of 3,3-disubstituted oxetanes in up to 90% yield with up to >99% enantioselectivity, exhibiting a very high recyclability (no decrease in conversion or enantioselectivity after sixteen, 16-hour runs). To exploit these characteris-tics, a continuous flow process has been implemented and operated for the sequential preparation of 17 diverse enantioen-riched products. The suitability of the flow setup for gram scale preparations (20 mmol scale) and its deactiva-tion/reactivation by treatment with pyridine/hydrochloric acid in dioxane have been demonstrated. Density Functional Theo-ry has been employed to provide a rational justification of the deep effect on enantioselectivity arising from the presence of sterically bulky substituents at the 6,6´-positions of the SPINOL unit. The main structural features of **Cat f** have subse-quently been incorporated to the design of a simplified homogeneous analog available in a straightforward manner (**Cat g**) that performs the benchmark desymmetrization reaction with similar yields and enantioselectivities as **Cat f**, providing a convenient alternative for cases when single use in solution is sought.

Chapter V. Manganese/Copper Co-Catalyzed Electrochemical Wacker-Tsuji-Type Oxidation of Aryl-Substituted Alkenes

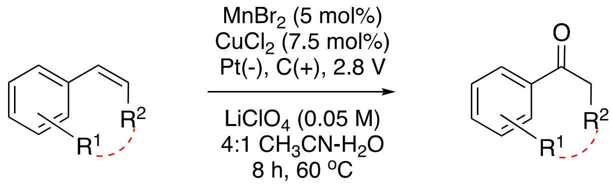

A manganese/copper co-catalyzed electrochemical Wacker-Tsuji oxidation of aryl-substituted olefins has been developed. The process involves the use of 5 mol% $MnBr_2$ and 7.5 mol% $CuCl_2$, in 4:1 acetonitrile/water in an undivided cell at 60 ºC, with 2.8 V constant applied potential. α-Aryl ketones are formed in moderate to excellent yields, with the advantages of avoidance of palladium as a catalyst and any external chemical oxidant, in an easily operated, cost effective procedure.

Chapter I

General Introduction

1.1. General introduction of immobilization of chiral organocatalysts

Optically active compounds are very important molecules in the fields of medical, pharmaceutical, and agricultural science.[1] The synthesis of optically active compounds requires in most cases the use of asymmetric transformation methodology. Within this approach, asymmetric organocatalysis represents one of the most useful methods to synthesize optically active compounds. Since 2000, when MacMillan introduced chiral imidazolidinones as catalysts for asymmetric Diels-Alder reactions using the term *organocatalysis* for the first time,[2] and List *et al*. reported on the direct asymmetric aldol reaction catalyzed by proline,[3] this topic has raised paramount interest worldwide. In the past twenty years, organocatalysis has become a hot field and has been used to achieve a variety of diverse organic transformations.[4]

---

[1] a) Kobayashi, S.; Ishitani, H. *Chem. Rev.* **1999**, *99*, 1069–1094; b) Brunel, J. M. *Recent Res. Dev. Org. Chem.* **2003**, *7*, 155-190; c) Cobley, C. J.; Henschke, J. P. *Adv. Synth. Catal.* **2003**, *345*, 195-201.

[2] Ahrendt, K. A.; Borths, C. J.; MacMillan, D. W. C. *J. Am. Chem. Soc.* **2000**, *122*, 4243-4244.

[3] List, B.; Lerner, R. A.; Barbas III, C. F. *J. Am. Chem. Soc.* **2000**, *122*, 2395-2396.

[4] a) *Asymmetric Organocatalysis: From Biomimetic Concepts to Applications in Asymmetric Synthesis*, (Eds. Berkessel, A.; Gröger, H.), Wiley-VCH, Weinheim, Germany, **2005**; b) Benaglia, M.; Puglisi, A.; Cozzi, F. *Chem. Rev.* **2003**, *103*, 3401–3430; c) Dalko, P. I.; Moisan, L. *Angew.Chem. Int. Ed.* **2004**, *43*, 5138–5175; d) Houk K.N.; List B. *Acc. Chem. Res.* **2004**, *37*, 631-847; e) Guillena, G.; Ramón, D. J. *Tetrahedron: Asymmetry* **2006**, *17*, 1465-1492; f) List B. *Chem. Rev.* **2007**, *107*, 5413–5883; g) Guillena, G.; Nájera, C.; Ramón, D. J. *Tetrahedron: Asymmetry* **2007**, *18*, 2249–2293; h) Pellissier, H. *Tetrahedron* **2007**, *63*, 9267-9331.

Homogeneous asymmetric organocatalysis is one of the most useful methodologies for preparing chiral compounds. However, in most cases a relatively large amount (at least 10 mol%) of organocatalyst is required to complete the desired reaction within a reasonable time. Isolation of these catalysts from the reaction mixture, required for purification purposes and advisable from an economic perspective, is relatively hard due to the similar organic nature of catalyst and reaction product and thus results poorly economic. In this context, Immobilized organocatalysts were designed to overcome these limitations of their homogeneous counterparts by simultaneously allowing easy product purification and catalyst recovery. [5]

Immobilization of chiral catalysts onto polymers for catalytic asymmetric reactions represents an important, useful and green approach to increased sustainability in organic synthesis. The approach has received considerable attention for the preparation of optically active compounds and has become one of the basic technology in organic synthesis. [6] As already pointed out, there are several

[5] a) *Chiral Catalyst Immobilization and Recycling*, (Ed.: De Vos, D. E.; Van-kelecom, I. F. J.; Jacobs, P. A.), Wiley-VCH, Weinheim, **2000**; b) *Fine Chemicals Through Heterogeneous Catalysis*, (Ed.: Sheldon, R. A.; Bekkum, H.), Wiley-VCH, Weinheim, **2001**; c) McMorn, P.; Hutchings G. J. *Chem. Soc. Rev.* **2004**, *33*, 108-122; d) *Handbook of Asymmetric Heterogeneous Catalysis* (Eds.: Ding, K.; Uozumi, Y.), Wiley-VCH, Weinheim, **2008**; e) *Recoverable and Recyclable Catalysts*, (Eds.: Benaglia, M.), John Wiley & Sons, Chichester, **2009**; f) *Heterogenized Homogeneous Catalysts for Fine Chemicals Production Catalysis by Metal Complexes*, (Eds.: Barbaro, P.; Liguari, F.), Springer, Heidelberg, *Vol. 33*, **2010**; g) *Enantioselective Homogeneous Supported Catalysts*, (Eds.: Šebesta, R.), RCS Publishing, Cambridge, **2011**.

[6] a) El-Shahawy, A. A.; Itsuno, S. *Current Topics in Polymer Research* (Ed.: Bregg, R. K.), Nova Science, New York, *chapter 1*, **2005**, pp. 1-69; b) Itsuno, S.; Haraguchi, N. *Heterogeneous Enantioselective Catalysis Using Organic Polymeric Suopports* in *Handbook of Asymmetric Heterogeneous Catalysis*, (Eds.: Ding, K.; Uozumi, Y.), Wiley-VCH, Weinheim, Germany, *chapter 3*, **2008**, pp. 73-129; c) Clapham, B.; Reger, T. S.; Janda, K.D. *Tetrahedron* **2001**, *57*, 4637-4662; d) Miguel, Y. R.; Brule, E.; Margue, R. G. *J. Chem. Soc. Perkin. Trans.* **2001**, *1*, 3085-3094; e) Fan, Q. H.; Li, Y. M.; Chan, A. S. C. *Chem. Rev.* **2002**, *102*, 3385-3466; f) Dickerson, T. J.; Reed, N. N.; Janda, K. D. *Chem. Rev.* **2002**, *102*, 3325-3344; g) McNamara, C. A.; Dixon, M. J.; Bradley, M. *Chem. Rev.* **2002**, *102*, 3275-3300; h) Itsuno, S.; Haraguchi, N.; Arakawa, Y. *Recent Res. Dev.*

advantages associated to the use of polymer-supported chiral organocatalysts for organic transformations. The catalysts can be recovered by simple filtration if the immobilized chiral organocatalysts is not soluble in the reaction mixture, and, if soluble polymeric chiral organocatalysts are used, the catalysts can be recovered by adding appropriate solvents to precipitate them from the reaction mixture. After several runs of recovery and reusing, very high cumulative turnover numbers (TONs) can be achieved. Moreover, it´s possible to apply the immobilized chiral organocatalysts in the development of catalytic enantioselective continuous flow processes.

1.2. General principles for immobilization of chiral organocatalysts

The goal of immobilization of chiral catalysts onto polymers aims at combining the positive properties of the corresponding homogeneous catalysts with the additional stability, recyclability and separation properties of support materials. However, some general principles that need to be considered during the immobilization process to maintain both reactivity and efficiency of the immobilized catalysts.

The nature of the catalyst support and the immobilization process affect the performance of the immobilized catalysts. Up to now, a big variety of catalytic supports, both organic and inorganic, combined with different methodologies for the immobilization of homogeneous catalysts have been designed and applied in catalysis.[7] The physico-chemical properties, porosity and dimensions of supports; the properties and length of the spacer and linker connecting catalyst and support;

Org. Chem. **2005**, *9*, 27-47; i) Itsuno, S.; Arakawa, Y.; Haraguchi, N. *J. Soc. Rubber Ind. Jpn.* **2006**, *79*, 448-454; j) Chen, J.; Yang, G.; Zhang, H.; Chen, Z. *React. Funct. Polym.* **2006**, *66*, 1434-1451; k) Trindade A. F.; Gois P. M. Afonso C. A. *Chem. Rev.* **2009**,*109*, 418-514; l) Altava B.; Burguete M. I.; García-Verdugo E.; Luis S.V. *Chem. Soc. Rev.* **2018**, *47*, 2722-2771.

[7] *Supported Catalysts and Their Applications*, (Eds.: Sherrington, D.C.; Kybett, A.P.), Cambridge: The Royal Society of Chemistry, **2001**.

the catalytic active sites density on the surface of supports are parameters that will mainly affect the activity and efficiency of catalysts.[8] The deleterious interactions between catalytic active sites and support must be restricted to avoid deactivation, undesired cooperative effects, and loss of efficiency in catalysts. In addition, the catalyst supports should be chemically inert and not harmful to the environment. Moreover, the linker or spacer connecting catalyst and support should be chemically inert in the reaction conditions, and should present a conformational behavior that contributes to projecting the catalytic units away from the polymer backbone, thus facilitating mass transfer.

1.3. Supports and strategies for immobilization of chiral organocatalysts

The immobilization of organocatalysts can be divided into three different types: covalent immobilization, non-covalent interactions, and encapsulation.

In covalent immobilization, the catalyst is covalently bound to the support. This is the preferred approach, due to the very strong binding established between the homogeneous organocatalysts and the support that renders leaching essentially impossible. In the non-covalent immobilization, the catalysts are adsorbed on the surface of the support *via* weak intermolecular interactions such as hydrogen bonding and electrostatic or van der Waals forces. Finally, in encapsulation, the catalyst is physically trapped in the pores or cavities of the support. It is worth mentioning that immobilization based on non-covalent interactions and encapsulation is less convenient, because of the weak interactions involved, the problem of catalyst leaching, the instability of the catalyst/support assembly, and the occurrence of pore size problems in the entrapment immobilization.[8]

[8] a) Heitbaum, M.; Glorius, F.; Escher, I. *Angew. Chem. Int. Ed.* **2006**, *45*, 4732-4762; b) Cozzi, F. *Adv. Synth. Catal.* **2006**, *348*, 1367-1390.

Consequently, we will mainly focus on covalent immobilization of chiral organocatalysts in this thesis.

Generally, organic polymers,[9] organic–inorganic materials,[10] inorganic bulk supports,[11] inorganic oxides,[12] nanomaterials and magnetic nanoparticles (MNPs)[13] are conveniently used as supports in the literature.

In the following introduction, we will briefly introduce Immobilization of chiral organocatalysts on polymeric resins, silica and magnetic nanoparticles, and will discuss the copper-catalyzed azide-alkyne cycloaddition reaction (CuAAC reaction; a copper-catalyzed Huisgen 1,3-dipolar cycloaddition) as the preferred tool to build 1,4-disubstituted-1,2,3-triazole moieties as broadly used linkers for covalent immobilization.

1.3.1 Immobilization of chiral organocatalysts on polymeric resins

Polymeric resins were introduced by Merrifield in the 1960s. The first example was based on polystyrene (PS), and used divinylbenzene (DVB) as the cross-linker. Several organic insoluble and soluble polymers have been investigated as catalyst

---

[9] a) Altava, B.; Burguete, M.I.; García-Verdugo, E.; Luis, S.V. *Chem.Soc. Rev.* **2018**, *47*, 2722-2771; b) *Polymeric Materials in Organic Synthesis and Catalysis*, (Ed.: Buchmeiser, M.R.), Wiley-VCH Weinheim., **2005**; c) Lu, J.; Toy, P.H. *Chem. Rev.* **2009**, *109*, 815-838.

[10] Bridging Heterogeneous and Homogeneous Catalysis: Concepts, Strategies, and Applications, (Eds.: Li, C.; Liu, Y.), Weinheim: Wiley-VCH, **2014**.

[11] a) Catalyst Preparation: Science and Engineering, (Ed.: Regalbuto, J.), Boca Raton, FL: CRC Press, Taylor & Francis Group, **2007**; b) Freire, C.; Pereira, C.; Rebelo, S. *Catalysis* **2012**, *24*, 116-203.

[12] a) Ying, J. Y.; Mehnert, C. P.; Wong, M. S. *Angew. Chem. Int. Ed.* **1999**, *38*, 56-77; b) Alcón, M. J.; Corma, A.; Iglesias, M.; Sánchez, F. *J. Organomet. Chem.* 2002, *655*, 134-145; c) Tao, Y.; Kanoh, H.; Abrams, L.; Kaneko, K. *Chem. Rev.* **2006**, *106*, 896-910.

[13] Rossi, L.M.; Costa, N.J.S.; Silva, F.P.; Wojcieszak, R. *Green Chem.* **2014**, *16*, 2906-2933.

supports during the next years with the advantages of easy separation, catalyst recovery and robustness.[9, 14]

Polymeric resins-supported chiral organocatalysts are mainly prepared by coupling reaction of functional polymeric resins with modified chiral organocatalyst containing an additional functional group for immobilization purposes. Less commonly, the whole immobilized system is prepared by co-polymerization of a vinyl- or styryl-substituted organocatalyst with appropriate co-monomers. An important condition, to be fulfilled in all cases, is that the anchoring point in the catalytic unit should be away from the active site in order to avoid perturbations in the enantiodetermining transition state.

There are several functionalized polymeric resins are commercially available in reagents supply companies. The structures of some functionalized polymers based on polystyrene (PS) such as Merrifield Resin, Wang resin, TentaGel™ and ArgoGel™ are presented in Figure 1. In addition, polyethyleneglycol (PEG) and poly(ethylene oxide) (PEO) and cellulose are also commonly used as supports.

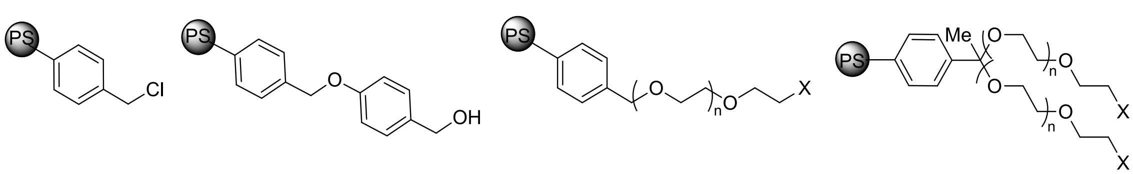

Merrifield resin **I-1** Wang resin **I-2** TentaGel™ **I-3** ArgoGel™ **I-4**

Figure 1. Commercially available functionalized polymers based on PS

With the advantages of inexpensive, easy to prepare, easy to functionalize, mechanistically robust, chemically inert, and commercially available, PS is still one of the most common polymeric resins.

[14] Altava, B.; Burguete, M.I.; García-Verdugo, E.; Luis, S.V. Chem.Soc. Rev. 2018, 47, 2722-2771;

1.3.2 Immobilization of chiral organocatalysts on silica

With the advantages of bio-friendly nature, inertness, and impressive thermal stability, porous property, and with the possibility of being designed to fit different shapes and pore sizes, silica is becoming an ideal support for catalysts immobilization.[15]

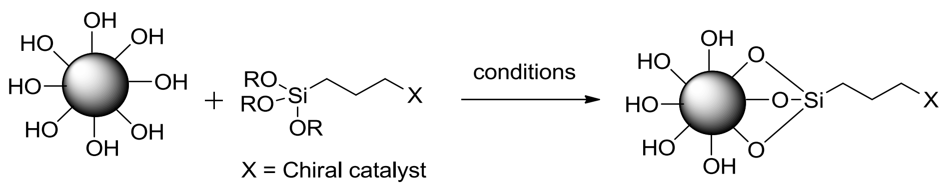

I-5 **I-6** **I-7**

Scheme 1. Post-synthetic methods for the immobilization of catalysts onto silica supports

The supporting of catalysts onto functionalized silica can be performed using post-synthetic methods by attaching the desired compound onto the surface of pristine silica supports (Scheme 1).[16]

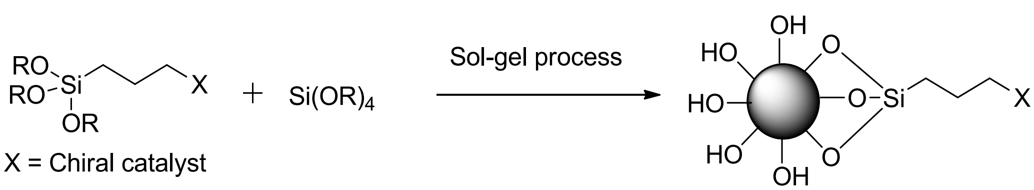

I-6 **I-8** **I-7**

Scheme 2. The immobilization of catalysts onto silica supports by sol-gel process

[15] a) Giraldo, L. F.; López, B. L.; Pérez, L.; Urrego, S.; Sierra, L.; Mesa, M. *Macromol. Symp.* **2007**, *258*, 129-141; b) Liang, J.; Liang, Z.; Zou, R.; Zhao, Y. *Adv. Mater.* **2017**, *29*, 1701139.

[16] a) Walcarius, A.; Etienne, M.; Bessière, J. *Chem. Mater.* **2002**, *14*, 2757-2766; b) González-Arellano, C.; Corma, A.; Iglesias, M.; Sánchez, F. *Adv.Synth. Catal.* **2004**, *346*, 1316-1328; c) Kume, Y.; Qiao, K.; Tomida, D.; Yokoyama, C. *Catal. Commun.* **2008**, *9*, 369-375; d) Bruhwiler, D. *Nanoscale* **2010**, *2*, 887-892; e) Karimi, B.; Khorasani, M. *ACS Catal.* **2013**, *3*, 1657.

Alternatively, a functional trialkoxysilane co-condensates with other silane monomers (usually tetraethoxysilane, TES) in the sol-gel process to produce silica supported catalysts. This second approach is conceptually equivalent to the copolymerization of vinyl monomers discussed above, and has been used in different contexts (Scheme 2).[17]

1.3.3 Immobilization of chiral organocatalysts on magnetic nanoparticles

Magnetic nanoparticles (MNPs) have attracted significant interest as alternative support for catalyst immobilization. MNPs have properties such as high surface area, high dispersion, outstanding stability, low toxicity and superparamagnetic behavior.[18]

Among their unique properties, high surface area allows high catalyst loading and the superparamagnetic nature allows nanoparticle an efficient separation and recovery from the reaction medium by magnetic decantation. In addition, MNPs presents a large number of hydroxyl groups on the surface of their particles. This characteristic allows the immobilization of catalysts by covalent bonds. Fe_3O_4 is the most exploited iron oxide nanomaterial for magnetic nanoparticles supports (Scheme 3).[19]

[17] a) Parish, R.V.; Habibi, D.; Mohammadi, V. *J. Organomet. Chem.* **1989**, *369*, 17-28; b) Burkett, S.L.; Sims, S.D.; Mann, S. *Chem. Commun.* **1996**, 1367-1368; c) Che, S.; Liu, Z.; Ohsuna, T.; Sakamoto, K.; Terasaki, O.; Tatsumi, T. *Nature* **2004**, *429*, 281-284.

[18] a) Wendy, T.; Ageeth, A. B.; John, W. G. *Catal. Today* **1999**, *48*, 329-336; b) Ko, S.; Jang, J. *Angew. Chem. Int. Ed.* **2006**, *45*, 7564-7567; c) Yi, D. K.; Lee, S. S.; Ying, J. Y. *Chem. Mater.* **2006**, *18*, 2459-2461.

[19] McCafferty, E.W.; Wightman J. P. *Surf. Interface Anal.* **1998**, *26*, 549.

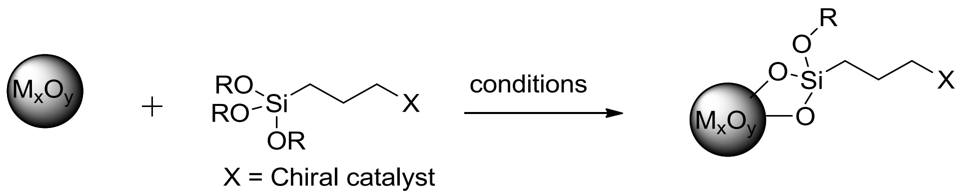

I-9 **I-6** **I-10**

Scheme 3. Immobilization of chiral organocatalysts on magnetic nanoparticles

1.3.4 The copper-catalyzed azide-alkyne cycloaddition reaction as a tool for the formation of 1,4-disubstituted-1,2,3-triazole linkers for covalent organocatalyst immobilization

The copper-catalyzed Azide-Alkyne cycloaddition (CuAAC, namely Cu-catalyzed Huisgen 1,3-dipolar cycloaddition) is probably the most known example of click reaction.[20] It is a very convenient strategy for immobilization of catalysts due to its broad scope, easy realization and mild reaction conditions. On the other hand, the progress of the reaction can be easily monitored by IR spectroscopy, through the disappearance of the characteristic triple bond bands of the reactants. Depending on the different immobilization strategies, both alkyne-functionalized and azido-functionalized resins are available. In every case, the partner organocatalyst must be functionalized in a complementary manner (Scheme 4).

I-11 **I-12** **I-13**

[20] a) Huisgen, R. *Centenary Lecture-1,3-Dipolar Cycloadditions* **1961**, 357-396; b) Vsevolod, V. R.; Luke, G. G.; Valery, V. F.; Sharpless, K. B. *Angew. Chem. Int. Ed.* **2002**, *41*, 2596-2599; c) Tornøe, C. W.; Christensen, C.; Meldal, M. *J. Org. Chem.* **2002**, *67*, 3057-3064; d) Bock, V. D.; Hiemstra, H.; Van Maarseveen, J. H. *Eur. J. Org. Chem.* **2006**, 51-68; e) Meldal, M.; Tornøe, C. W. *Chem. Rev.* **2008**, *108*, 2952-3015; f) Hein, J. E.; Fokin, V. V. *Chem. Soc. Rev.* **2010**, *39*, 1302-1315.

Scheme 4. The CuAAC reaction as a tool for the formation of triazole linkers for covalent organocatalyst immobilization

The possible interaction of the triazole linker with the catalytic active sites should be taken into consideration, since it can interfere with the catalytic activity both in a positive and in a negative manner.[21] The experience of our group has shown that CuAAC reaction is an efficient technique to immobilize organocatalysts. The role of triazole linker was related to an increase in the swelling ability of PS-support, probably through forming a hydrogen bond-based aqueous microphase around the hydrophobic resin.[22]

1.3.5 Immobilization of chiral organocatalysts by copolymerization of a monomer with a chiral organocatalyst

Chiral organocatalysts can also be supported by the polymerization of the chiral monomers with an achiral comonomer and cross-linker.

A variety of monomers can be used according to the type of polymerization. Styrene derivatives have been most frequently used as the chiral monomer because of their easy ability to co-polymerize with other vinyl monomers. In any case, many other types of derivatives, such as acrylates, acrylamides, ethylene oxide, ethylene imine, and methacrylates have also been sometimes used as the chiral monomers. Divinylbenzene (DVB) is the most commonly used difunctional monomer as a cross-linker. In addition, ethyleneglycol dimethacrylate, N,N´-bis(acrylamide), and a difunctional styrene derivative with oligo(ethylene glycol) spacer have been used as cross-linkers in vinyl polymerization.

---

[21] For a case of negative influence in metal-catalyzed processes, see: Bastero, A.; Font, D.; Pericàs, M. A. *J. Org. Chem.* **2007**, *72*, 2460-2468.

[22] For a case of cooperativity between the triazole linker and the organocatalytic unit, see: Font, D.; Sayalero, S.; Bastero, A.; Jimeno, C.; Pericàs, M. A., *Org. Lett.* **2008**, *10*, 337-340.

A variety of copolymerization techniques can be used for the preparation of a polymer-supported catalyst. One of the most efficient copolymerization methods employed in our laboratory can be summarized as shown in Scheme 5. Representatively, the polymer supported organocatalysts could be prepared by radical copolymerization of chiral vinyl monomers, styrene, and DVB with 2,2´-azabis(2-methylpropionitrile) (AIBN) or benzoyl peroxide (BPO) as an initiator.

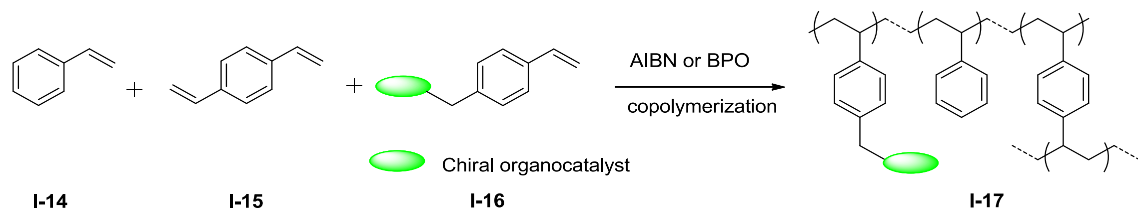

Scheme 5. Immobilization of chiral organocatalysts by copolymerization

1.4. Continuous flow process based on immobilized chiral organocatalysts

In addition to the recovery and reuse ability of solid-supported catalysts mentioned above, one of the main advantages of immobilized catalysts is the possibility of implementing continuous flow (CF) processes, in which the initial reactants are pumped through a reactor and the product flows out in a continuous manner. [23]

CF systems can be divided into two different types according to the use of soluble or insoluble catalysts. [24]

In many cases, soluble catalysts are more active and selective than the analogous insoluble ones; accordingly, much effort has been devoted to explore separation and

[23] a) Jas, G.; Kirschning, A. *Chem. -Eur. J.* **2003**, *9*, 5708-5723; b) Puglisi, A.; Benaglia, M.; Chiroli, V. *Green Chem.* **201**3, *15*, 1790-1813; c) Tsubogo, T.; Ishiwata, T.; Kobayashi, S. *Angew. Chem. Int. Ed.* **2013**, *52*, 6590-6604.

[24] For a field guide to flow chemistry, see: Plutschack, M. B.; Pieber, B.; Gilmore, K.; Seeberger, P. H. *Chem. Rev.* **2017**, *117*, 11796-11893.

recovery strategies of the former in view of their use in continuous flow processes. Although such processes avoid the catalyst immobilization step, the use of soluble catalytic system is still facing the question of how to perform the separation and recycling of the catalyst in an effective and truly continuous manner.

In many cases, soluble catalysts have higher activity and selectivity than the analogous insoluble ones. Although using soluble catalysts in CF avoids the immobilization of the catalysts, the use of soluble catalyst system still faces the problem of how to separate and recover the catalyst effectively and continuously. Accordingly, much effort has been devoted to explore separation and recovery strategies of the former in view of their use in continuous flow processes.

The use of insoluble catalysts in the CF devices is one of the most obvious and common methods to achieve its continuous recylcling. Therefore, it is not surprising that efforts to use polymer-supported catalysts in laboratory-scale fine chemical transformations were reported the early 1980s.[25] In such processes, the insoluble catalysts can be confined inside a CF device by mechanical means or using magnetic fields (when MNPs are used as a support). The absence of need to fine-tune the system properties for solubility and phase distribution of products and active species represent an important advantage of this approach. Thus, the packed-bed immobilized catalysts can be separated and recovered easily in a single operation. On the other hand, no mechanical stirring is needed in flow systems, which contributes to increase the lifetime of the material supporting the immobilized catalyst. Compared with conventional batch systems, CF systems have advantages of significant time, space and energy savings by simplifying operation. In addition,

[25] a) Ragaini, V.; Saed, G. *Z. Phys. Chem.* **1980**, *119*, 117-128; b) Ragaini, V.; Verzella, G.; Ghignone, A.; Colombo, G. *Ind. Eng. Chem. Process Des. Dev.* **1986**, *25*, 878-885; c) Itsuno, S.; Ito, K.; Maruyama, T.; Kanda, N.; Hirao, A.; Nakahama, S. *Bull. Chem. Soc. Jpn.* **1986**, *59*, 3329-3331; d) Hodge, P.; Sung, D.W.L.; Stratford, P.W. *J. Chem. Soc., Perkin Trans.* **1999**, *1*, 2335-2342.

continuous flow processes are easy to scale up, more cost-effective, and sometimes give higher and stereoselectivities than the corresponding batch processes.[24] The use of continuous flow processes is expected to grow significantly in the next few years, especially in industrial applications.

A possible reaction set-up for CF with the symbols of all the components and the description of the critical parts is provided below (Figure 2).

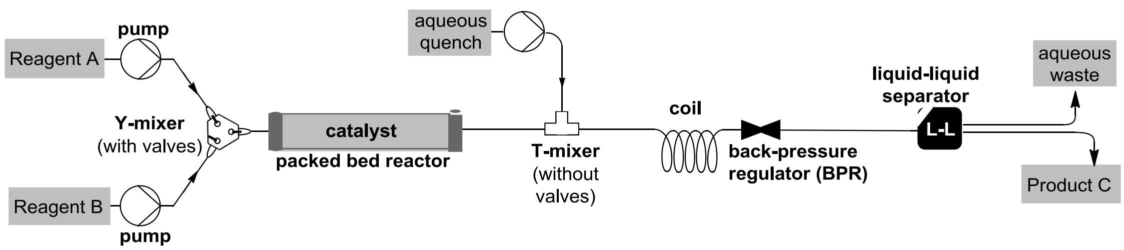

Figure 2. Schematic representation of a flow set-up with some of the devices.

Pumbs. Most flow processes require the use of pumps to ensure stable flow. There are several options, but we tend to use regular syringe pumps or HPLC-like piston pumps.

Tubing. Most commonly PTFE tubing of 1/16” is used.

Packed bed reactor. It refers to the cylindrical laboratory utensils filled with solvent-swelled resin. It can be made of any material, such as PTFE, glass or steel. Since we usually do not need high pressure, our most common choice is a glass column with a diameter of 1 cm.

Check valve. The small tool can ensure that the flow direction is one-way, avoiding the backflow situation that may damage the internal catalyst of the packed bed reactor.

Back-pressure regulator. Commonly abbreviated as BPR. It is a device that can put a certain pressure on each part of the upstream system. It can work with gas and avoid the use of low boiling point solvents to form bubbles.

Liquid-liquid separator. It is a device that can separate a two-phase mixture in a flowing state through their different polarities.

Residence time. For a given device operating at a given total flow rate, it is the time for the reactants to enter the column and contact the catalyst.

Accumulated TON. For batch operation, yield is the best parameter for product generated in a given catalytic experiment. In flow operation, the best parameter is the accumulated TON instead of yield.

1.5. Examples of immobilized chiral organocatalysts in batch and continuous flow system

Some examples of immobilization of organocatalysts such as proline-derived catalysts, prolinamides, pyrrolidine derivatives, amino acid derivatives, chiral imidazolidinone (MacMillan) catalysts, Cinchona alkaloids, cinchona alkaloid quaternary ammonium salts, chiral DMAP Analogue, chiral thioureas ureas and squaramide organocatalysts will be briefly introduced in this Chapter. The immobilization of diarylprolinol and their silyl ethers derivatives, chiral benzotetramisole analogues, and chiral phosphoric acid will be described in Chapters II, III, IV, respectively.

1.5.1 Immobilized proline-derived catalysts.

L-Proline and its derivatives are quite effective organocatalysts for a plenty of asymmetric transformations, where they have been extensively used. Catalytic processes involving proline take place via the formation of activated enamines

(HOMO activation) or iminium ions (LUMO activation)[26] intermediates between the carbonyl substrates and L-Proline or its derivatives.[27] It's not unusual that these processes require high catalyst loadings, in the 20–30 mol% range or even higher. Since L-proline is inexpensive, its immobilization could be considered worthless; however, proline derivatives are usually expensive materials whose preparation from the natural amino acid involves multistep sequences. One should add to this economic argument the often costly separation of these organocatalysts in monomeric form from reaction crudes. In this regard, in the last few years, immobilized proline derivatives have been developed and used as efficient catalysts for a plethora of asymmetric reactions.[4,28] The immobilization strategies used for L-proline and its derivatives involve both covalent linking to the support and immobilization by noncovalent interactions.

The first examples of supported proline involved covalent linking to a cross-linked polystyrene and were reported in 1985 by the Takemoto group. These polymeric prolines were used in a Robinson cyclization reaction and produced the corresponding diketones in modest yield and enantioselectivity.[29] (Scheme 6).

---

[26] HOMO: Highest Occupied Molecular Orbital; LUMO: Lowest Unoccupied Molecular Orbital.

[27] a) Mukherjee, S.; Woon Yang, Y.; Hoffmann, S.; List, B. *Chem. Rev***.** **2007**, *107*, 5471-5569; b) Erkkilä, A., Majander, I.; Pihko, P. M. *Chem. Rev.* **2007**, *107*, 5416-5470.

[28] a) *Catalyst Separation, Recovery and Recycling. Chemistry and Process Design*, (Eds.: Cole-Hamilton, D. J.; Tooze, R. P.), Springer, Dordrecht, Netherlands, **2006**; b) *The Power of Functional Resins in Organic Synthesis*, (Eds.: Albericio, F.; Tulla-Puche, J.), Wiley-VCH, Weinheim, Germany, **2008**; c) Cozzi, F. *Adv. Synth. Catal.* **2006**, *348*, 1367-1390; e) Benaglia, M. *New J. Chem.* **2006**, *30*, 1525-1533; f) Gruttadauria, M.; Giacalone, F.; Noto, R. *Chem. Soc. Rev.* **2008**, *37*, 1666-1688; g) Gruttadauria, M.; Giacalone, F.; Noto, R. *Chem. Soc. Rev.* **2008**, *37*, 1666-1688; h) Trindade, A. F.; Gois, P. M. P.; Afonso, C. A. M. *Chem. Rev.* **2009**, *109*, 418-514; i) Bergbreiter, D. E.; Tian, J.; Hongfa, C. *Chem. Rev***.** **2009**, *109*, 530–582; j) Lu, J.; Toy, P. H. *Chem. Rev.* **2009**, *109*, 815-838; k) Kristensen, T. E.; Hansen, T. *Eur. J. Org. Chem.* **2010**, *17*, 3179-3204.

[29] Kondo, K.; Yamano, T.; Takemoto, K. *Makromol. Chem.* **1985**, *186*, 1781–1785.

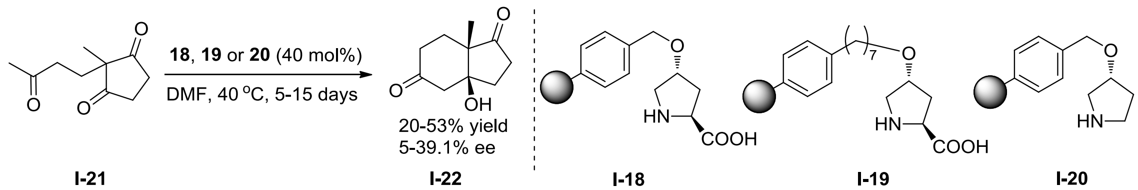

Scheme 6. The first examples of supported proline and application for Robinson cyclization

Asymmetric aldol reactions between cyclic ketones and aldehydes are the most common used to test newly developed immobilized proline derivatives. Some recent examples are summarized in Scheme 7. In 2012, our laboratory reported the asymmetric aldol reactions catalyzed by a novel polystyrene-immobilized proline derivative **I-26**. The reactions were completed in short reaction times and took place with excellent diastereo- and enantioselectivity. The catalyst could be recovered by simple filtration and exhibited very high reusability in batch, which prompted its application in packed-bed reactors for continuous flow processing. The high catalytic activity of **I-26** allowed a short residence time of 26 minutes in the flow process,[30] in sharp contrast with the initially developed supported prolines, involving shorter linkers and lacking the synergistic triazole linker, where reaction time in batch was in the range of days.

[30] C. Ayats, A. H. Henseler, M. A. Pericàs, *ChemSusChem* **2012**, *5*, 320-325.

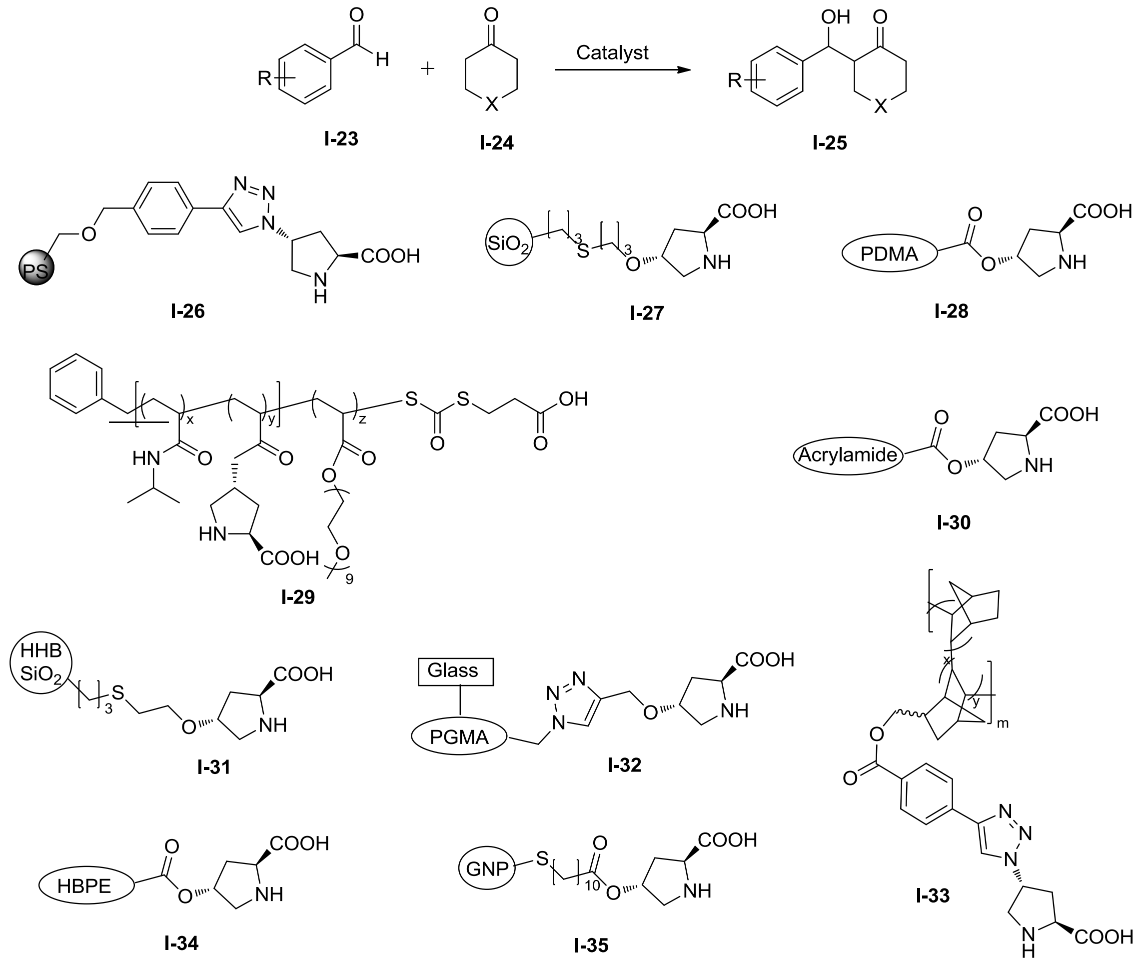

Scheme 7. Immobilized prolines for organocatalytic applications in aldol reactions

In 2013, Massi and co-workers reported silica-supported proline derivative **I-27**. It was packed in a microreactor to be used in continuous flow. The gathered information by reaction-progress kinetic analysis allowed them to assess optimal operating parameters and reaction conditions.[31]

[31] Bortolini, O.; Cavazzini, A.; Giovannini, P. P.; Greco, R.; Marchetti, N.; Massi, A.; Pasti, L. *Chem. Eur. J.* **2013**, *19*, 7802-7808.

In the same year, O'Reilly and Monteiro group reported the bounding of L-proline moieties to a thermoresponsive polymer nanoreactor (**I-28**) that consisted of a permanently hydrophilic block (poly(dimethylacrylamide), PDMA) and a thermoresponsive block, which above its lower critical solution temperature (LCST) becomes hydrophobic block. When temperatures were higher than the LCST (ranging from 25 to 40°C), the polymer-bound proline formed micelles promoted the aldol reaction; decreasing the temperature to below the LCST of the polymer, it became fully water-soluble, and allowed to separate the catalyst from the water with insoluble aldol product. It provided recyclability over five runs with yield decreased slightly and selectivity remained high.[32] Still in the same year, Suzuki group reported the bounding of (S)-proline moieties on block copolymers (**I-29**) that consisted of thermoresponsive poly(N-isopropylacrylamide) (PNIPAAm) and PEG-grafted polyacrylate blocks. The copolymer dissolved in water at temperatures below LCST (25 °C), and they formed micelles at temperatures above the LCST (50 °C). The conducted Aldol reactions between 4-Nitrobenzaldehyde and cyclohexanone in aqueous solution obtained products in a high yield with high diastereo- and enantioselectivity (96% ee). The catalyst could be reused up to 3 times.[33] In 2014, Fan and Hua group showed the preparation of **I-30** by copolymerization between N-isopropylacrylamide (NIPAM) and a hydroxyproline derivative. This polymeric material was applied to the catalysis of aldol reactions in aqueous media, with excellent activity and stereoselectivity. For its recycling, the polymer could be recovered by adding diethyl ether or brine as precipitating agents. This allowed its use in ten consecutive runs without loss of conversion and stereoselectivity. [34] The

---

[32] Zayas, H. A.; Lu, A.; Valade, D.; Amir, F.; Jia, Z.; O'Reilly, R. K.; Monteiro, M. J. *ACS Macro Lett.* **2013**, *2*, 327-331.

[33] Suzuki, N.; Inoue,T.; Asada, T.; Akebi, R.; Kobayashi, G.; Rikukawa, M.; Masuyama, Y.; Ogasawara, M.; Takahashi, T.; Thang, S. H. *Chem. Lett.* **2013**, *42*, 1493–1495.

[34] Liu, Y.; Tong, Q.; Ge, L.; Zhang, Y.; Hua, L.; Fan, Y. *RSC Adv.* **2014**, *4*, 50412-50416.

same year, the He group reported the preparation of L-proline-grafted mesoporous silica with alternating hydrophobic and hydrophilic blocks (**I-31**). The aldol product afforded in good results in neat or aqueous media and **I-31** could be reused three times.[35] In 2015, the Verboom group reported the covalent attachment of L-proline derivatives onto the inner walls of a microreactor via glycidyl methacrylate polymer brushes. Catalyst **I-32** in a microreactor afforded good diastereo- and enantioselectivity but low conversions (23%) in the tested aldol reaction.[36] In the same year, the Albéniz group in collaboration with our laboratory reported the immobilization of L-proline derivatives onto rationally designed vinyl addition polynorbornene (VA-PNB) resins through click reactions. The resulting recoverable and highly reusable resins **I-33** are very active in the aldol reaction in aqueous media. The results provided a promising strategy for the immobilization of organocatalyst with the combination of modular VA-PNB resins. [37] In the same year, the Wang group reported the bounding of L-proline onto hyperbranched polyethylene (HBPE), which was prepared by copolymerization of ethylene with an acryloyl-derivatized hydroxyproline (**I-34**). Good yields and stereoselectivities were reported with very good recyclability up to seven runs. [38] In 2016, the Mase group reported the self-assembling gold nanoparticle (GNP)-supported L-proline derivative **I-35**. Moderate to good selectivities were afforded in the asymmetric aldol reaction, and the catalyst could be reused for five cycles without significant loss of weight and efficiency. [39]

---

[35] An, Z.; Guo, Y.; Zhao, L.; Li, Z.; He, J. *ACS Catal.* **2014**, *4*, 2566-2576.

[36] Munirathinam, R.; Leoncini, A.; Huskens, J.; Wormeester, H.; Verboom, W. *J. Flow Chem.* **2015**, *5*, 37-42.

[37] Sagamanova, I. K.; Sayalero, S.; Martínez-Arranz, S.; Albéniz, A. C. Pericàs, MA.*Catal. Sci. Technol.* **2015**, *5*, 754-764.

[38] Wang, S.; Liu, P.; Wang, W. J.; Zhang, Z.; Li, B. G. *Catal. Sci. Technol.* **2015**, *5*, 3798-3805.

[39] Soti, P. L., Yamashita, H., Sato, K., Narumi, T., Toda, M., Watanabe, N.; Marosi, G.; Mase, N. (2016). Tetrahedron 72: 1984–1990.

Immobilized prolines also have been applied in other reactions besides the aldol reactions between cyclic ketones and aldehydes.

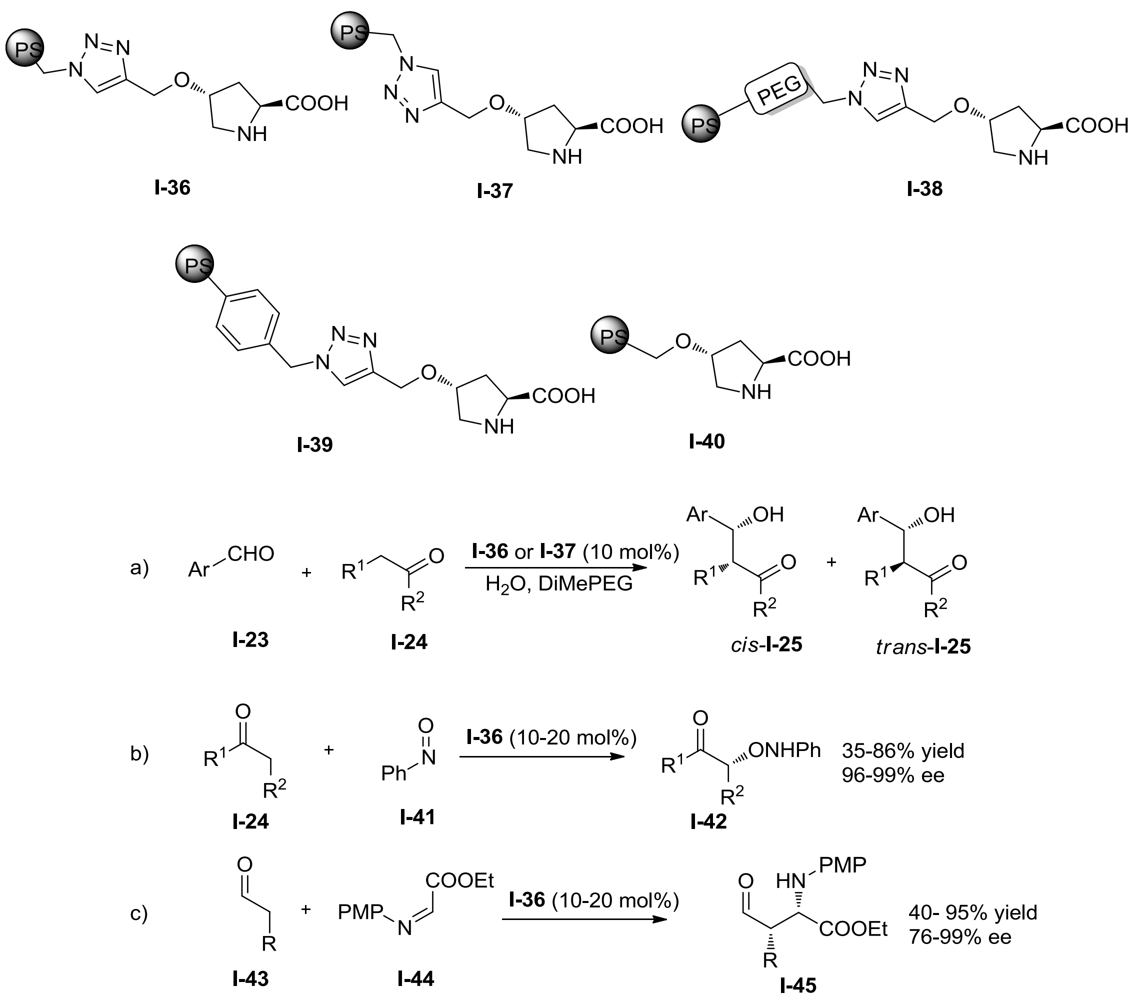

Scheme 8. Immobilized prolines for organocatalytic applications

In 2006, our laboratory prepared and tested several resins obtained mainly by means of azide-alkyne Huisgen cycloaddition in the key steps (scheme 8). [37, 40, 41, 42, 43] Catalysts (**I-36)** - (**I-40)** proved to be very active and selective polymers. Catalyst **36** has been applied in the aldol reaction between several ketones and benzaldehydes in water.[40] The high hydrophobicity of the resin and the presence of water are key to obtaining high stereoselectivity, whereas yield can be increased by using catalytic amounts of DiMePEG. Resin **I-36** was the first immobilized insoluble organocatalyst active in the -aminoxylation of aldehydes and ketones giving a good yield and a high enantioselectivity and higher reaction rates than those reported with L-proline.[43] In all the mentioned cases, recycle and reuse of the catalyst was accomplished with no losses in either activity or stereoselectivity.

Finally, **I-36** was also applied to Mannich reactions both in batch and in continuous flow.[45] In this pioneer example of an organocatalytic, highly enantioselective flow process using an immobilized species, a simple ¼" PTFE tube filled with **I-36** was used as the flow reactor, and a mixture of both reagents was pumped through it at 0.2 mL min^{-1}. Two different examples provided the corresponding *syn*-Mannich products with very good results, replicating the batch process but with higher productivities. Notably, residence time for complete conversion in these experiments was only 6 minutes (Figure 3).

[40] Font, D.; Jimeno, C.; Pericàs, M. A. *Org. Lett.* **2006**, *8*, 4653-4656.

[41] Font, D.; Bastero, A.; Sayalero, S.; Jimeno, C.; Pericàs, M. A. *Org. Lett.* **2007**, *9*, 1943-1946.

[42] Font, D.; Sayalero, S.; Bastero, A.; Jimeno, C.; Pericàs, M. A. *Org. Lett.* **2008**, *10*, 337-340.

[43] Alza, E.; Rodríguez - Escrich, C.; Sayalero, S.; Bastero, A.; Pericàs, M. A. *Chem. Eur. J.* **2009**, *15*, 10167-10172.

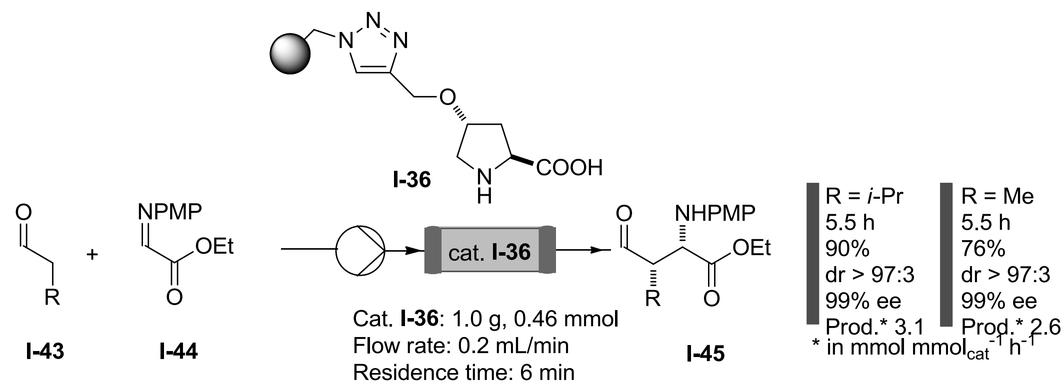

Figure 3. Polystyrene-supported proline for the *syn*-selective Mannich reaction in flow

For supported catalysts, the longer the continuous flow system runs, the lower the overall catalyst loading and the higher the total TON. The robustness of the supported catalyst is thus fundamental to prolong operation time and increase the total TON. Encouraged by the behavior of **I-36** in the alfa-aminoxylation of aldehydes with nitrosobenzene, we decided to inplement **I-36** to a packed-bed reactor. It turned out to be very active and in 5 min residence time the desired products were obtained in good conversions (Figure 4).[44] However, the practicality of this process was hampered by a side reaction of the catalyst that led to deactivation of the resin.

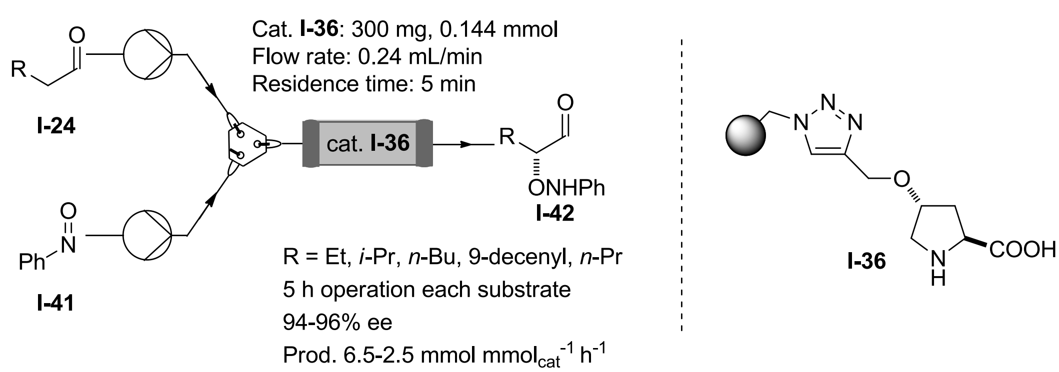

Figure 4. Immobilized proline for the flow aminoxylation of aldehydes

[44] Cambeiro, X. C.; Martín-Rapún, R.; Miranda, P. O.; Sayalero, S.; Alza, E.; Llanes, P.; Pericàs, M. A. *Beilstein J. Org. Chem.* **2011**, *7*, 1486-1493.

In 2007, the Gruttadauria group reported the immobilization of 4-hydroxy-L-proline on a mercaptomethyl-functionalized resin.[45] These authors showed that the proline resin could be applied in direct asymmetric aldol reactions in water as the sole solvent without any additive with good-to-excellent conversions and parallel stereoselectivities (Scheme 9). The proline resin **I-46** can be reused for five cycles without loses in reactivity or selectivity. As mentioned in this paper, the formation of a hydrophobic core in the inner surface of the resin accompany with the hydrophilic proline moiety lies at the resin/water interface, this microenvironment both promoted the aldol reaction and increased the stereoselectivity.

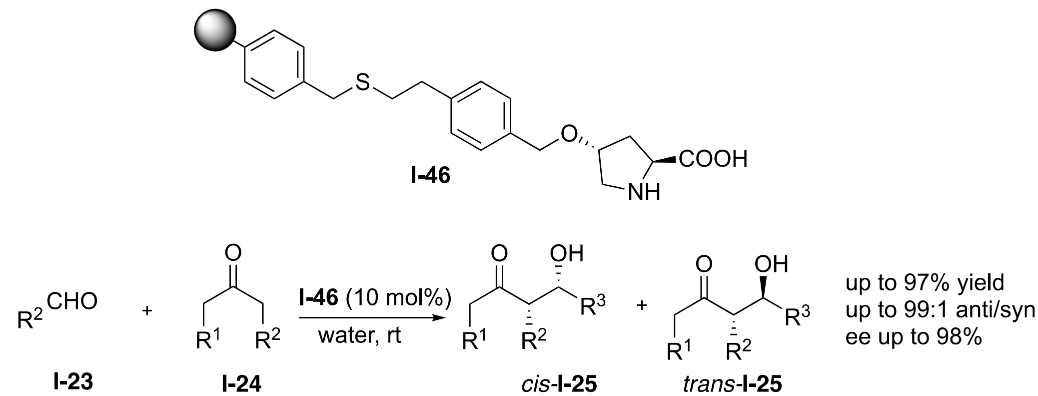

Scheme 9. Immobilization of 4-hydroxy-L-proline on a mercaptomethyl-functionalized PS resin

In 2016, our group reported the preparation of a PS-immobilized triazolylproline by a bottom-up approach involving co-polymerization with full regiocontrol. The resulting supported resin swelled in water and was applied to the enantioselective cross-aldol reaction and self-aldol reaction of aldehydes under neat conditions with excellent yields and stereoselectivities. (Scheme 10) [46]

---

[45] a) Giacalone, F.; Gruttadauria, M.; Mossuto Marculescu, A.; Noto R. *Tetrahedron Lett.* **2007**, *48*, 255–259; b) Gruttadauria, M.; Giacalone, F.; Mossuto Marculescu, A.; Lo Meo, P.; Riela, S.; Noto, R. *Eur. J. Org. Chem.* **2007**, 4688–4698.

[46] Llanes, P.; Sayalero, S.; Rodríguez-Escrich, C.; Pericàs, M. A. *Green Chem.* **2016**, *18*, 3507-3512.

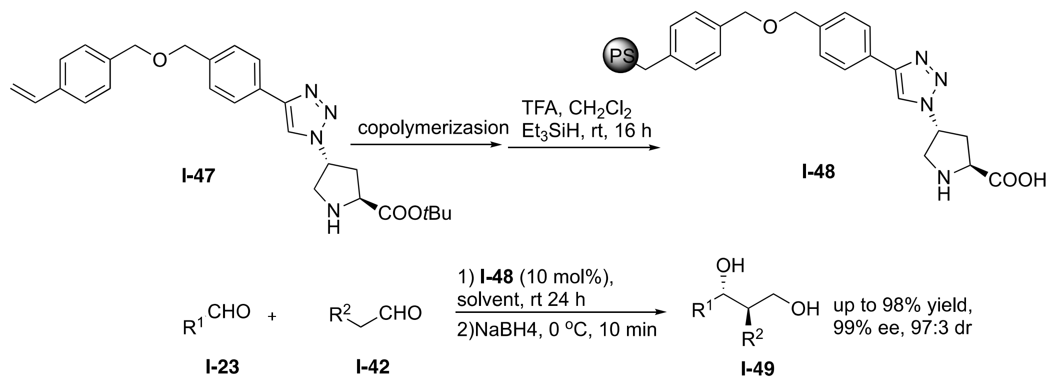

Scheme 10. PS immobilized triazolylproline by a bottom-up approach

In summary, several strategies have been developed to immobilize proline derivatives. A significant feature of immobilized proline catalysts is that some of them tend to swell in water. Obviously, the presence of proline units can compensate for the low affinity of polystyrene resins for polar proton transfer solvents.

1.5.2 Polymer-supported prolinamides

Recently, several chiral prolinamides have been found to be active and highly stereoselective catalysts for the direct aldol reaction both in organic solvents [47] and in aqueous conditions. [48] In 2009, the Gruttadauria group developed a highly recoverable and regenerable supported organocatalyst **I-50** for the aldol reaction between ketones and substituted benzaldehydes afforded high stereoselectivities at

---

[47] a) Raj, M.; Maya, V.; Ginotra, S. K.; Singh, V. K. *Org. Lett.* **2006**, *8*, 4097-4099; b) Tang, Z.; Jiang, F.; Yu, L. T.; Cui, X.; Gong, L. Z.; Mi, A. Q.; Jiang, Y. Z.;Wu, Y. D. *J. Am. Chem. Soc.* **2003**, *125*, 5262-5263; c) Tang, Z.; Yang, Z. H.; Chen, X. H.; Cun, L. F.; Mi, A. Q.; Jiang, Y. Z.; Gong, L. Z. *J. Am. Chem. Soc.* **2005**, *127*, 9285-9289.

[48] a) Raj, M.; Maya, V.; Ginotra, S. K.; Singh, V. K. *Org. Lett.* **2006**, *8*, 4097-4099; b) Tang, Z.; Jiang, F.; Yu, L. T.; Cui, X.; Gong, L. Z.; Mi, A. Q.; Jiang, Y. Z.;Wu, Y. D. *J. Am. Chem. Soc.* **2003**, *125*, 5262-5263; c) Tang, Z.; Yang, Z. H.; Chen, X. H.; Cun, L. F.; Mi, A. Q.; Jiang, Y. Z.; Gong, L. Z. *J. Am. Chem. Soc.* **2005**, *127*, 9285-9289.

room temperature, while prolinamide **I-51** was used at -5 or -10 °C. [49] (Scheme 11). When the resins were recovered by filtration and reused in the next cycle, the catalysts were deactivated. This happened might because the excess of ketone reacted with the catalyst and formed the corresponding imidazolidinone. Therefore, when the recovered polymers were treated with formic acid, the catalysts' activity could be regenerated.

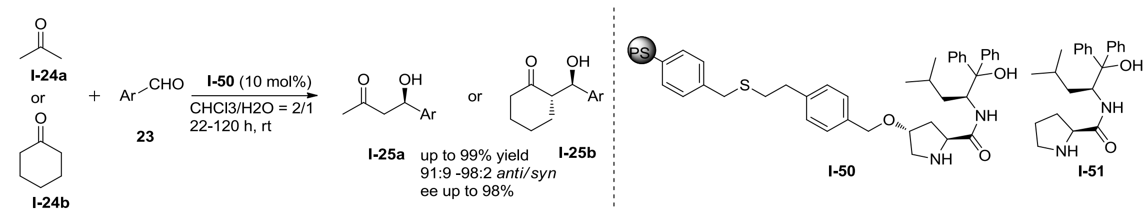

Scheme 11. Polymer-supported prolinamides for the direct aldol reaction

In 2013, the Pedrosa group reported a prolylsulfonamide derived from ethylene diamine and its supported counterpart **I-53**. They showed to excellent yields and enantioselectivities in the Robinson annulation of cyclic and acyclic triketones under solvent free conditions. (Scheme 12).[50]

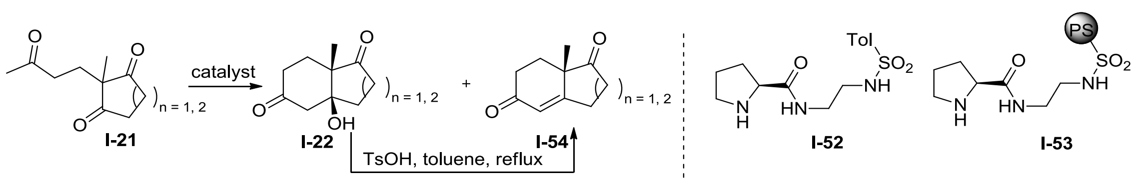

Scheme 12. Prolylsulfonamide derived from ethylene diamine and its supported counterpart

In 2013, Gröger and co-workers developed the combination of an asymmetric organocatalytic reaction with a biotransformation toward a "one-pot like" process for

[49] Gruttadauria, M.; Giacalone, F.; Mossuto Marculescu, A.; Salvo, A. M. P.; Noto, R. *ARKIVOC* **2009**, 8, 5-15.

[50] Pedrosa, R.; Andrés, J. M.; Manzano, R.; Pérez-López, C. *Tetrahedron Lett.* **2013**, *54*, 3101-3104.

the preparation of 1,3-diols based on immobilized organo- and biocatalysts. A (*S*)-proline functionalized chiral amide alcohol was bounded to a polymer gave catalyst **I-55**. It was used for the asymmetric aldol reaction, and a subsequent reduction of the aldol adduct catalyzed by an alcohol dehydrogenase (ADH) afforded the *anti*-1,3-diol via the combined organocatalytic/biocatalytic approach with high yield and excellent diastereo- and enantioselectivity (d.r. >35:1, >99% ee). Moreover, **I-55** showed excellent reusability.[51] (Scheme 13).

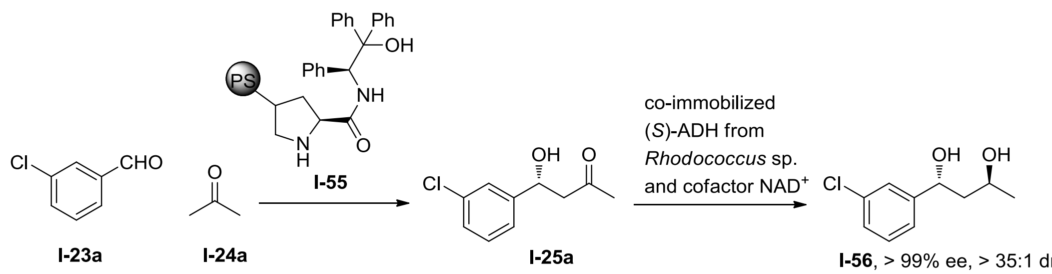

Scheme 13. “One-pot like” process for 1,3-diols based on immobilized organo- and biocatalysts

In the same year, the same group conducted a detailed study on the impact of the non-immobilized and immobilized prolinamide catalyst loading on reactivity and selectivity for a direct aldol reaction in aqueous medium. The use of 5.0 mol% non-immobilized proline amide catalysts **I-57** for 24 hours led to a significant impact of the retro-aldol reaction and a thermodynamic control of the reaction. In contrast, excellent enantioselectivities with high conversions were achieved within this reaction time at an amount of 0.5 mol% catalyst **I-57**. On the other hand, the immobilized proline amide **I-58** led to a kinetically controlled reaction within a broad range (0.5 to 10 mol%) of catalyst amount because of a lower reactivity of the

[51] Heidlindemann, M.; Rulli, G.; Berkessel, A.; Hummel, W.; Gröger, H. *ACS Catal.* **2014**, *4*, 1099-1103.

heterogeneous catalyst. Catalyst **I-58** also showed a good recyclability in five reaction cycles.[52] (Scheme 14).

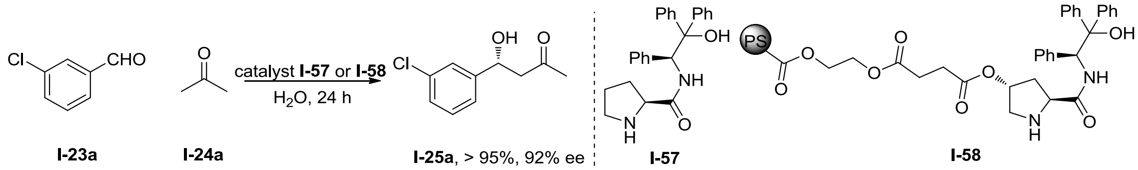

Scheme 14. Polymer-supported prolinamides for the direct aldol reaction

In 2014, the Cui group designed a strategy for the immobilization of (S)-prolinamide. The *N*-(p-hydroxyhenyl) (*S*)-prolinamide **I-60** was enzymatically polymerized using horseradish peroxidase (HRP) to give the polymer immobilized prolinamide **I-61**. **I-61** was tested as an organocatalyst for direct asymmetric aldol reaction between aromatic aldehydes and cyclohexanone to give the aldol addition products in good yields (up to 91%) and with high diastereoselectivity (up to 6:94 dr), and medium enantioselectivity (up to 87% ee). In addition, **I-61** can be recovered and reused for at least 5 cycles without significant loss in reactivity and selectivity.[53] (Scheme 15).

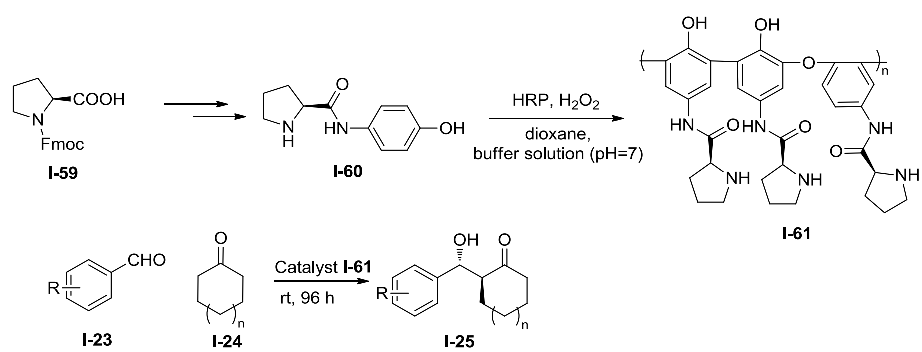

Scheme 15. Polymer immobilized prolinamide prepared by enzymatically HRP

[52] Rulli, G.; Fredriksen, K. A.; Duangdee, N.; Bonge-Hansen, T.; Berkessel, A.; Gröger, H. *Synthesis* **2013**, *45*, 2512-2519.

[53] Qu, C.; Zhao, W.; Zhang, L.; Cui, Y. *Chirality* **2014**, *26*, 209-213.

In 2015, the Yilmaz group reported the supporting of a L-proline-derived Calix[4]arene chiral organocatalyst onto well-defined (15±3 nm) magnetic Fe_3O_4 nanoparticles (**I-62**). This catalyst showed high catalytic activity (up to 95%), enantioselectivity (up to 94%) and diastereoselectivity (up to 97:3) for the asymmetric aldol reaction of aromatic aldehydes and cyclohexanone in water. Magnetically recoverable **I-62** could be easily be separated from the reaction crude by application of an external magnetic field and reused for several times without any significant loss of activity. (Scheme 16)[54]

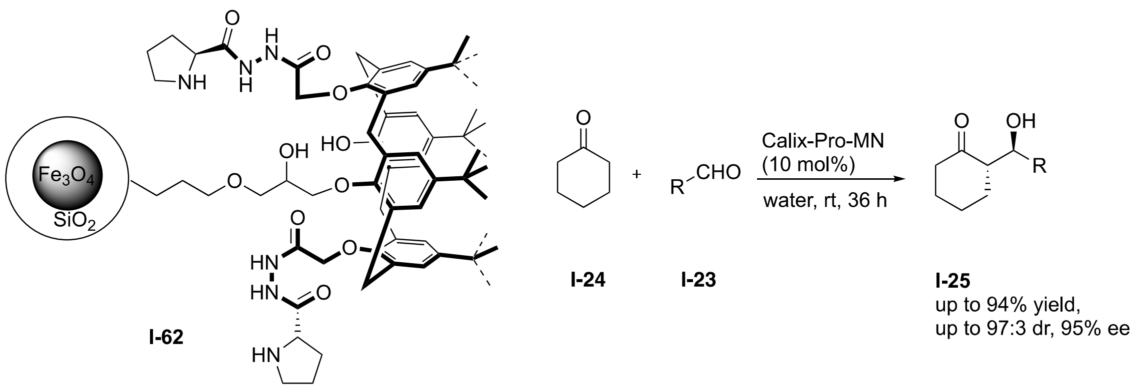

Scheme 16. Calix-Pro-MN and application in asymmetric aldol reaction

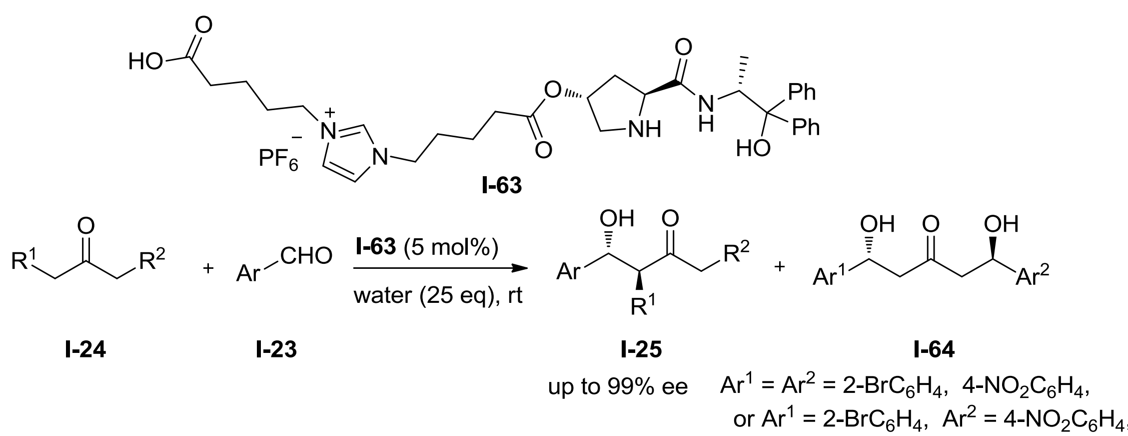

[54] Akceylan, E.; Uyanik, A.; Eymur, S.; Sahin, O.; Yilmaz, M. *Appl. Catal. A-Gen.* **2015**, *499*, 205-212.

Scheme 17. Prolinamide derived ionic liquid supported organocatalyst

In 2015, the Zlotin group reported a recyclable prolinamide-derived organocatalyst supported onto an ionic liquid bearing and bearing an auxiliary Brønsted acidic group (**I-63**). This species catalyzed asymmetric mono- and bis-aldol reactions of aromatic aldehydes with cyclic or linear ketones in aqueous medium with excellent catalytic performance (up to 96:4 dr and 81–99 % ee) over ten cycles. (Scheme 17)[55]

1.5.3 Polymer-immobilized pyrrolidine derivatives

Chiral pyrrolidines are one of the most efficient motifs as a chiral organocatalyst. Oriyama and coworkers reported on the utility of chiral pyrrolidine-based ligands as catalysts for kinetic resolution.[56] In 2001, the Janda group reported the preparation of polymer-supported proline-based diamine catalyst **I-65** for the kinetic resolution of racemic mixtures of secondary alcohols. It can be recovered and reused several times without loss of reactivity and selectivity.[57] A series of racemic secondary alcohols were resolved using **I-65**. 2-Phenylcyclohexanol and 2-Phenylcyclopentanol were resolved with excellent selectivity (S = 134 and 27, respectively), whereas some fused ring cycloalkanols and open-chain alcohols such as 1-naphthylethanol and 1-phenylethanol resulted in little or no selective resolution. (Scheme 18)

[55] Kucherenko, A. S.; Gerasimchuk, V. V.; Lisnyak, V. G.; Nelyubina, Y. V.; Zlotin, S. G. *Eur. J. Org. Chem.* **2015**, 5649-5654.

[56] Oriyama, T.; Hori, Y.; Imai, K.; Sasaki, R. Tetrahedron Lett. 1996, 37, 8543–8546. Sano, T.; Imai, K.; Ohashi, K.; Oriyama, T. *Chem. Lett.* **1999**, 265-266.

[57] Clapham, B.; Cho, C. W.; Janda, K. D. *J. Org. Chem.* **2001**, *66*, 868-873.

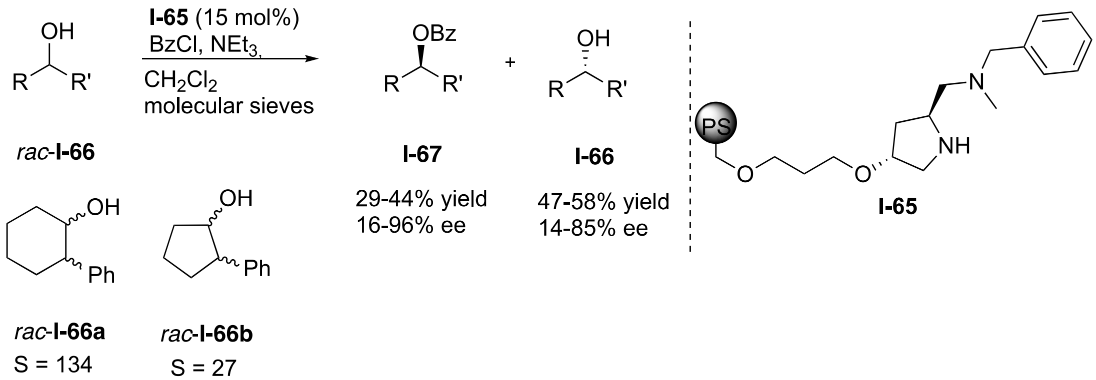

Scheme 18. Immobilized pyrrolidine for kinetic resolution of secondary alcohols

In 2007, our laboratory reported the preparation of PS-immobilized chiral pyrrolidines bearing 2-triazolylmethyl substituents by the copper-mediated Azide-alkyne Huisgen cycloaddition between the pyrrolidine derivative with azide and alkyne bounded PS resins. [58] It represented the first insoluble mediator of the reaction and achieved the performance of the soluble counterpart in the same process. Catalyst **I-68** was applied to the Michael addition of ketones to -nitrostyrenes in good yields with excellent selectivity. It was also tested in the Michael addition of aldehydes to -nitrostyrenes. Quantitative conversions and high diastereoselectivities were achieved for linear aldehydes with moderate enantioselectivities (Scheme 19). In 2008, Wang and coworkers reported a similar polymer-immobilized chiral pyrrolidine bearing a triazole block. [59] It was also used in the Michael reaction of cyclohexanone to nitroolefins with high yields (up to >99%), excellent diastereoselectivities (up to >99:1 dr) and enantioselectivities (up to >99% ee) in the presence of TFA. The supported catalyst could be recovered and recycled by a simple filtration and reused for more than 10 cycles without significant loss of efficiency.

[58] Alza, E.; Cambeiro, X. C.; Jimeno, C.; Pericàs, M. A. *Org. Lett.* **2007**, *9*, 3717–3720.

[59] Miao, T.; Wang, L. *Tetrahedron Lett.* **2008**, *49*, 2173–2176.

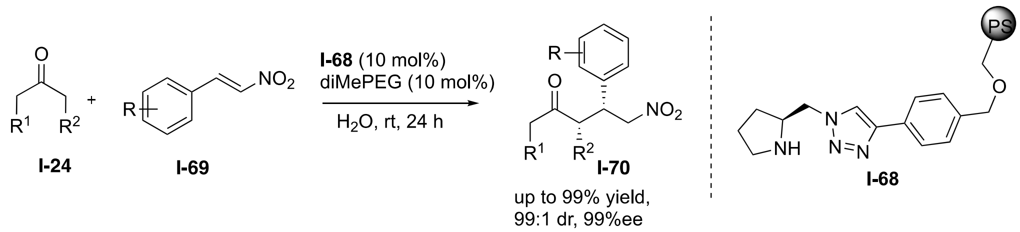

Scheme 19. Immobilized pyrrolidine for Michael addition of aldehydes to nitrostyrene

In 2008, the Zhang group reported a new type of polymer - immobilized pyrrolidine - based chiral ionic liquid, synthesized from Merrifield resin with N-Boc–protected chiral pyrrolidine substituted by the imidazole moiety. [60] Upon deprotection, the immobilized catalyst efficiently mediated the Michael addition reaction of ketones and aldehydes with -nitrostyrenes in high yields, excellent enantioselectivies, and diastereoselectivities in neat conditions. The catalyst **I-71** could be reused up to 8 times without significant loss of catalytic activity and stereoselectivity (Scheme 20).

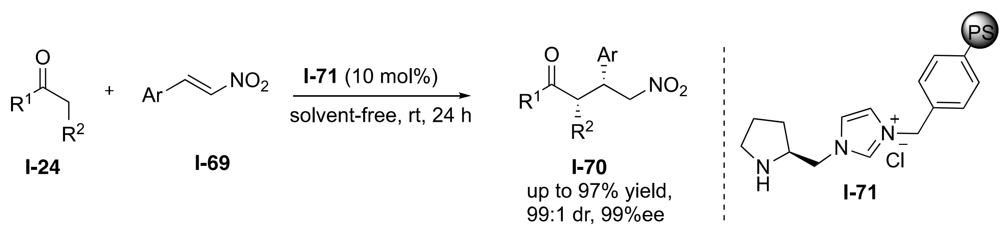

Scheme 20. Immobilized pyrrolidine-based chiral ionic liquid in Michael addition reaction

In 2015, our group in collaboration with the Gilmour laboratory reported a polymer-supported fluorinated pyrrolidine derivative **I-72** and applied it to the enantioselective Michael addition of aldehydes to nitroalkenes. Catalyst **I-72** exhibited high activity and displayed excellent selectivities with a wide variety of substrates. The implementation of a continuous flow process based on **I-72** allowed either the multigram synthesis of a single Michael adduct over a 13 h period or the sequential

[60] Li, P.; Wang, L.; Wang, M.; Zhang, Y. *Eur. J. Org. Chem.* **2008**, 1157–1160.

generation of a library of enantiopure Michael adducts from different combinations of substrates (13 examples, 16 runs, 18.5 h total operation). A customized in-line aqueous workup, followed by liquid–liquid separation in flow, allowed for product isolation without the need of chromatography or other separation techniques (figure 5). [61]

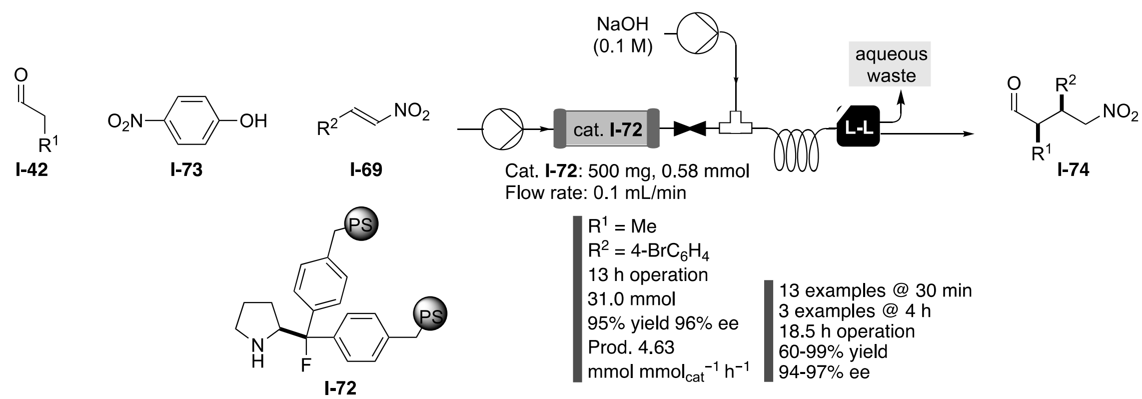

Figure 5. A co-polymerized version of the Gilmour catalyst for the continuous Michael addition of aldehydes to nitroalkenes.

In 2011, our laboratory developed pyrrolidine derivative **I-75** and its solid-supported version **I-76** and applied them to the *anti*-selective Mannich addition of aldehydes and ketones to imines. [62] **I-76** exhibited very high activity and excellent stereoselectivity whith low catalyst loadings and short reaction times. The polymeric atalyst **I-76** was later used for the successful implementation of a continuous flow process allowing both the sequential preparation of small libraries of enantiopure

[61] Sagamanova, I.; Rodríguez-Escrich, C.; Molnár, I. G.; Sayalero, S.; Gilmour, R.; Pericàs, M. A. *ACS Catal.* **2015**, *5*, 6241-6248.

[62] Martín‐Rapún, R.; Fan, X.; Sayalero, S.; Bahramnejad, M.; Cuevas, F.; Pericàs, M. A. *Chem. Eur. J.* **2011**, *17*, 8780-8783.

anti-Mannich adducts and for the preparation of single adducts at the 0.05–0.1 mol scale with close to 300 of TONs (Figure 6).[63]

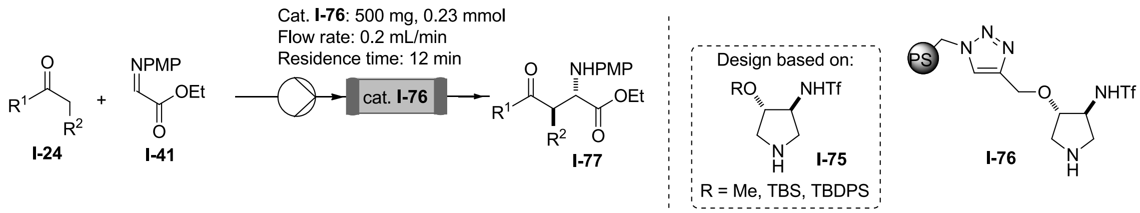

Figure 6**.** *anti*-Selective Mannich reaction in flow promoted by a PS-supported pyrrolidine derivative

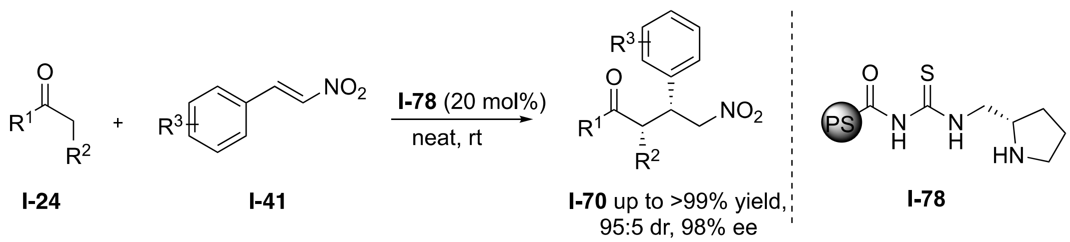

Scheme 21. Immobilized pyrrolidine-based swellable pearl-like copolymer in Michael addition

In 2016, the Drabina group reported the preparation by copolymerization of a swellable, pearl-like (20–600 μm diameter), PS-supported benzoylthiourea-pyrrolidine organocatalyst **I-78**, and its use as a recyclable mediator for the Michael addition of ketones to functionalized β-nitrostyrenes with quantitatively yields and up to 98% ee (scheme 21).[64] Interestingly, **I-78** retained most of its activity and enantioselectivity after five consecutive uses.

1.5.4 Immobilized primary amino acids

[63] Martín-Rapún, R.; Sayalero, S.; Pericàs, M. A. *Green Chem.* **2013**, *15*, 3295-3301.

[64] Androvič, L.; Drabina, P.; Svobodová, M.; Sedlák, M. *Tetrahedron: Asymmetry* **2016**, *27*, 782-787.

In addition to proline and its derivatives, primary amino acids chiral organocatalysts have been immobilized onto polymers also.

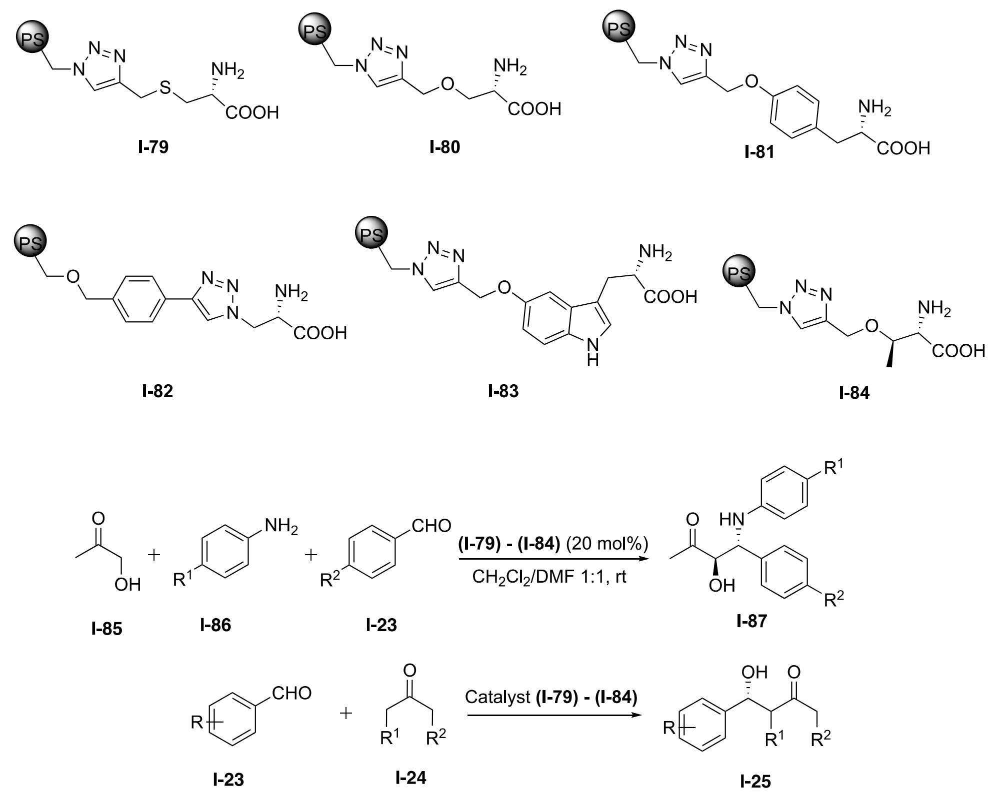

Scheme 22. Immobilized primary amino acids and application

In 2014, our laboratory reported the immobilization of a series of primary amino acid-derived PS-supported organocatalysts through alkyne-azide cycloaddition reactions. The resulting polymers (**I-79)** - (**I-84)** were tested as organocatalysts in *anti*-selective Mannich reactions. The immobilized threonine derivative **I-84** performed best reactivity and selectivity in three-component Mannich reactions to provide *anti*-β-amino-α-hydroxycarbonyl compounds (up to 95% ee). A family of five different enantioenriched *anti*-Mannich adducts has been prepared under the sequential continuous flow process by passing different combinations of anilines and aromatic aldehydes through the same catalyst sample.[65] Those immobilized catalysts also were tested in asymmetric aldol reactions. The easily recyclable polymeric catalyst **I-84** performed highly reactive and stereoselective (up to 99% ee) in the aldol reaction of both cyclic and acyclic ketone donors with aromatic aldehydes in aqueous media.[66] (Scheme 22)

1.5.5 Immobilized peptide catalysts.

Peptides are also promising candidates for chiral organocatalysts.[67] Some of the peptides developed with this purpose showed efficient catalytic activity in asymmetric reactions, although sometimes they have problems to separate and recover. To overcome these problems, the immobilization of peptides have recently been developed and used as catalysts for asymmetric synthesis.

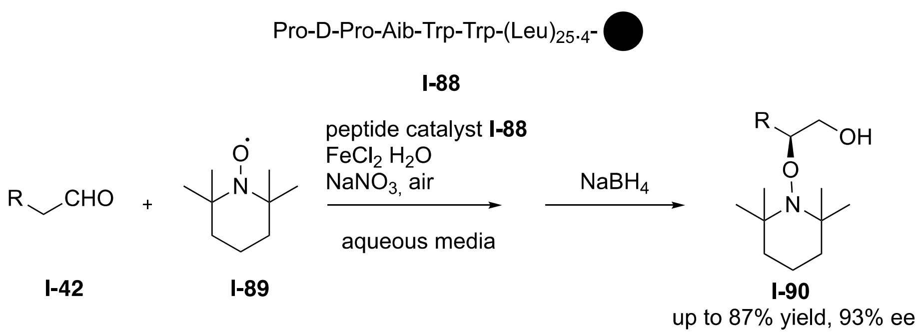

Scheme 23. Immobilized peptide catalysts Pro-D-Pro-Aib-Trp-Trp combined with polyleucine

In 2010, Kudo and Akagawa designed the peptide catalyst **I-88**, which contained a terminal five-residue Pro-D-Pro-Aib-Trp-Trp and polyleucine, and was bounded to a polymer support. **I-88** performed as an effective catalyst in the asymmetric

[65] Ayats, C.; Henseler, A. H.; Dibello, E.; Pericàs, M. A. *ACS Catal.* **2014**, *4*, 3027-3033.

[66] Henseler, A. H.; Ayats, C.; Pericas, M. A. *Adv. Synth. Catal.* **2014**, *356*, 1795-1802.

[67] Kudo, K.; Akagawa, K. in *Polymeric Chiral Catalyst Design and Chiral Polymer Synthesis*, (Ed.: Itsuno, S.), Wiley, New Jersey, **2011**, pp. 91-123.

asymmetric *R*-oxyamination of aldehydes in aqueous media (Scheme 23). The structure and chirality of the hydrophobic segment play a decisive role in its reactivity and enantioselectivity.[68]

In 2013, the same group developed a similar immobilized peptide catalyst **I-91** and applied it to the asymmetric reduction of unsaturated aldehydes. The peptide polymer **I-91** performed a highly regio- and enantioselectivity in the reduction of α,β,γ,δ-unsaturated aldehyde (Scheme 24).[69]

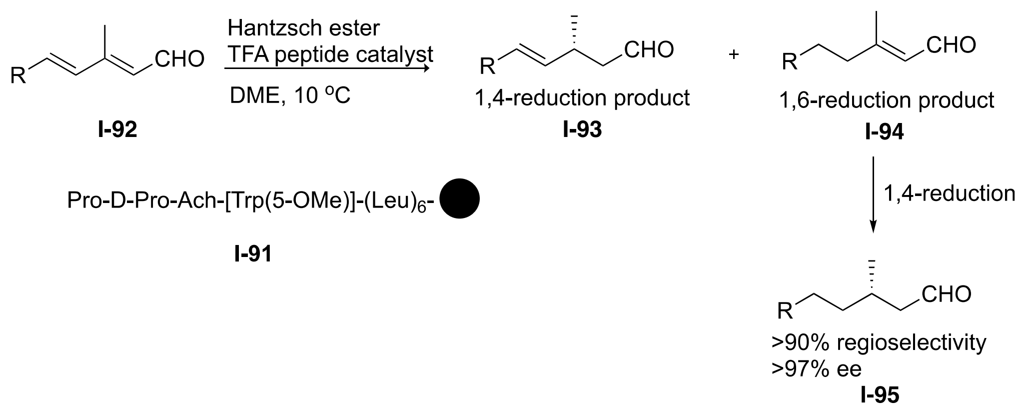

Scheme 24. Immobilized peptide catalysts for asymmetric reduction of unsaturated aldehydes

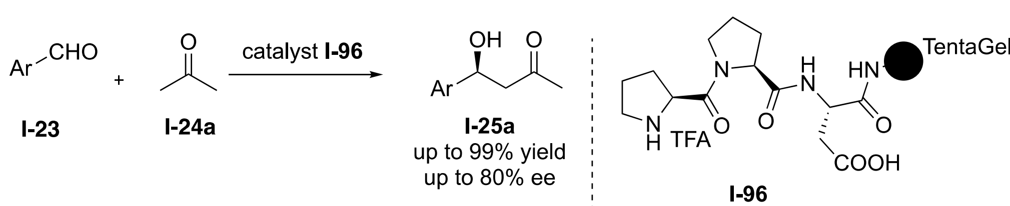

Scheme 25. Immobilized peptide catalysts for aldol reaction

[68] Akagawa, K.; Fujiwara, T.; Sakamoto, S.; Kudo, K. *Org. Lett.* **2010**, *12*, 1804-1807.

[69] Akagawa, K.; Sen, J.; Kudo, K. *Angew. Chem. Int. Ed*, **2013**, *52*, 11585-11588.

The most reactive peptidic organocatalysts developed to date for the asymmetric aldol[70] reaction and Michael addition[71] were reported by the Wennemers group in 2008. Based on these works, in 2012, the Fülöp group developed a heterogeneous catalytic continuous-flow process using an immobilized Wennemers' tripeptide as heterogeneous organocatalyst (**I-96**) for asymmetric aldol reactions. The peptide was synthetized by solid-phase peptide synthesis and immobilized in the same step. The yields and stereoselectivities of β-hydroxyketone products were obtained both high and comparable to the best homogeneous catalytic batch results. (Scheme 25).[72]

In 2015, the Chen group reported the synthesis of supported organocatalysts **I-97** by immobilizing valine-derived formamide onto the surface of Fe_3O_4 magnetic nanoparticles. The immobilizied catalyst **I-97** performed high reactivity and enantioselectivity in the asymmetric reduction of imines with trichlorosilane at room temperature with toluene as solvent (Scheme 26). **I-97** can be recovered with the help of an external magnet, and can be reused five cycles without a significant loss of reactivity and selectivity.[73]

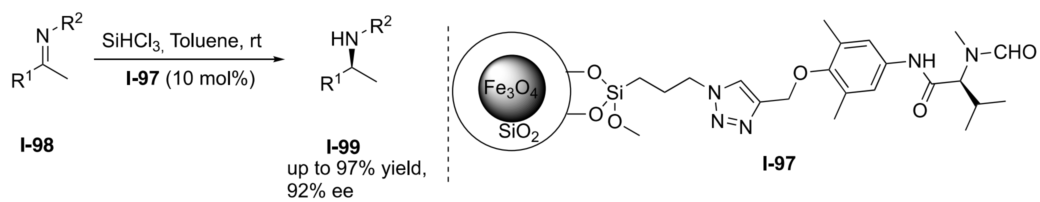

Scheme 26. Immobilized peptide catalysts for asymmetric reduction of imines

[70] Krattiger, P.; Kovasy, R.; Revell, J. D.; Ivan, S.; Wennemers, H. *Org. Lett.* **2005**, *7*, 1101-1103.

[71] a) Wiesner, M.; Revell, J. D.; Wennemers, H. *Angew. Chem., Int. Ed.* **2008**, *47*, 1871-1874; b) Wiesner, M.; Revel,l J. D.; Tonazzi, S.; Wennemers, H. *J. Am. Chem. Soc.* **2008**, *130*, 5610-5611.

[72] Ötvös, S. B.; Mándity, I. M.; Fülöp, F. *J. Catal.* **2012**, *295*, 179-185.

[73] Ge, X.; Qian, C.; Ye, X.; Chen, X. *RSC Adv.* **2015**, *5*, 65402-65407.

1.5.6 Immobilized chiral imidazolidinone (MacMillan) catalysts.

The series of chiral imidazolidinones, known as MacMillan catalysts, is one of the most powerful and applicable designed organocatalysts. The iminium salt generated as an intermediate from these species can be widely applied to mediate asymmetric reactions.[74] Like for the different conventional effective chiral catalysts that have been reported, several research groups have been working on the immobilization of chiral imidazolidinone catalysts both for immobilization strategy and materials.

The first example was reported by Benaglia and Cozzi and coworkers in 2002. A tyrosine-derived imidazolidinone was immobilized onto a modified poly(ethylene glycol) and converted *in situ* into a soluble polymer-supported catalyst (**I-100**). The polymeric catalyst **I-100** was applied for the enantioselective Diels-Alder cycloaddition of acrolein with 1,3-cyclohexadiene, moderate yield (67%) and high enantioselectivity (92% ee) of products were obtained. Some loss of chemical efficiency and slight erosion of enantioselectivity was observed during the recycling of catalysts.[75] The polymeric catalyst **I-100** was also used in some 1,3−dipolar cycloadditions involving α,β - unsaturated aldehydes and nitrones. The immobilized catalyst showed similar enantioselectivity with the unsupported MacMillan catalysts, but a lower yield of products are obtained.[76] However, the polymeric catalyst can't be effective reuse in these two studied reactions, due to the chemical instablility under these reaction conditions. (Scheme 27)

---

[74] a) Lelais, G.; MacMillan, D. W. D. In New Frontiers in Asymmetric Catalysis (Mikami, K.; Lautens, M., Eds.), Wiley, New York, **2007**, pp. 319–331; b) Lelais, G.; MacMillan, D. W. C. *Aldrichim. Acta* **2006**, *39*, 79-87; b) MacMillan, D. W. C. *Nature* **2008**, *455*, 304-308; c) Erkkila, A.; Majander, I.; Pihko, P. M. *Chem. Rev.* **2007**, *107*, 5416-–5470; d) Mukherjee, S.; Yang, J. W.; Hoffmann, S.; List, B. *Chem. Rev.* **2007**, *107*, 5471-5569.

[75] Benaglia, M.; Celentano, G.; Cinquini, M.; Puglisi, A.; Cozzi, F. *Adv. Synth. Catal.* **2002**, *344*, 149-152.

[76] Puglisi, A.; Benaglia, M.; Cinquini, M.; Cozzi, F.; Celentano, G. *Eur. J. Org. Chem.* **2004**, 567-573.

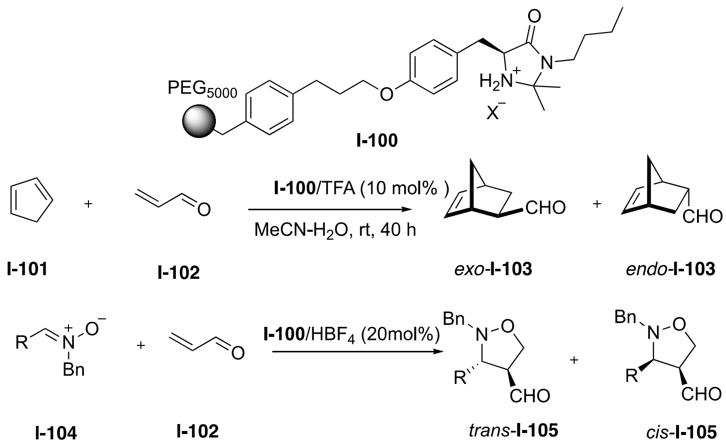

Scheme 27. Immobilized chiral MacMillan's imidazolidinone for Diels-Alder and 1,3 - dipolar cycloadditions

In the same year, the Pihko group used *J*anda*J*el™ and silica as supports, and immobilized the catalyst using the *N*-position of the amide moiety, which is not directly involved in the catalytic event. The *J*anda*J*el™ supported polymer **I-106** performed significantly higher enantioselectivity than the silica-supported one in the Diels–Alder reaction of cyclopentadiene and cinnamaldehyde, and the adducts were obtained in 70% yield with 99% ee (endo) and 99% ee (exo). Furthermore, the catalytic activity can be easily adjusted by changing the support medium; it can be easily recovered by filtration and directly reused in the next cycle (Scheme 28). [77]

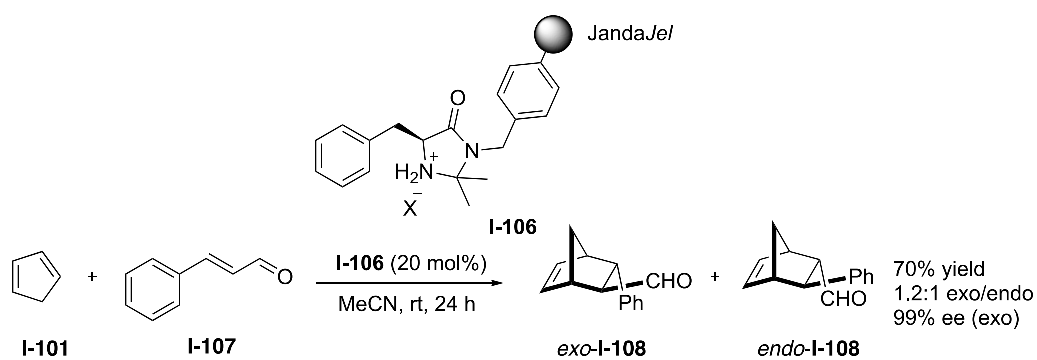

[77] Selkälä, S. A.; Tois, J.; Pihko, P. M.; Koskinen, A. M. P. *Adv. Synth. Catal.* **2002**, *344*, 941-945.

Scheme 28. Immobilized chiral imidazolidinone for Diels-Alder cycloaddition

In 2006, the Ying group reported the immobilization of a chiral imidazolidinone onto siliceous meso-cellular foams (MCF) and polymer-coated MCF, and the resulting materials (**I-109**) were used for asymmetric Friedel-Crafts alkylation and Diels-Alder reaction. High activity and excellent recyclability were achieved with the polymer-coated MCF immobilized catalyst (scheme 29).[78]

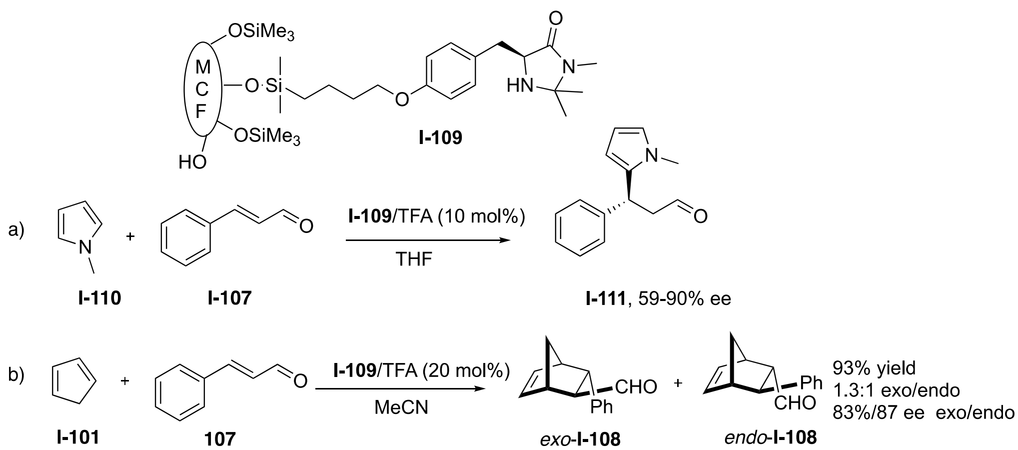

Scheme 29. Immobilized chiral imidazolidinone for Friedel-Crafts alkylation and Diels-Alder reaction

The chiral imidazolidinone sulfonate salt was an effective catalyst for the Diels–Alder reaction of cyclopentadiene and cinnamaldehyde. In 2009, the Itsuno group reported the preparative of the polymer-supported organocatalyst imidazolidinone sulfonate salt **I-114** by ion exchange reaction of MacMillan iminium catalyst with PS-supported sulfonic acids (Scheme 30). The immobilized recyclable catalyst **I-114** performed good enantioselectivity and effectively in the asymmetric Diels–Alder reaction of 1,3-cyclopentadiene and *trans*-cinnamaldehyde in CH_3OH/H_2O.[79] Later in 2012, the same group reported the synthesis a polymer **I-117** with chiral imidazolidinone

[78] Zhang, Y.; Zhao, L.; Lee, S. S.; Ying, J. Y. *Adv. Synth. Catal.* **2006**, *348*, 2027-2032.

[79] Haraguchi, N.; Takemura, Y.; Itsuno, S. *Tetrahedron Lett.* **2010**, *51*, 1205-1208.

incorporated into the main-chain by reacting chiral imidazolidinone dimers with naphthalene 2,6-disulfonic acid via ionic bonding. Polymer **I-117** were tested in the Diels–Alder reactions and afforded the chiral adducts with good enantioselectivity. [80]

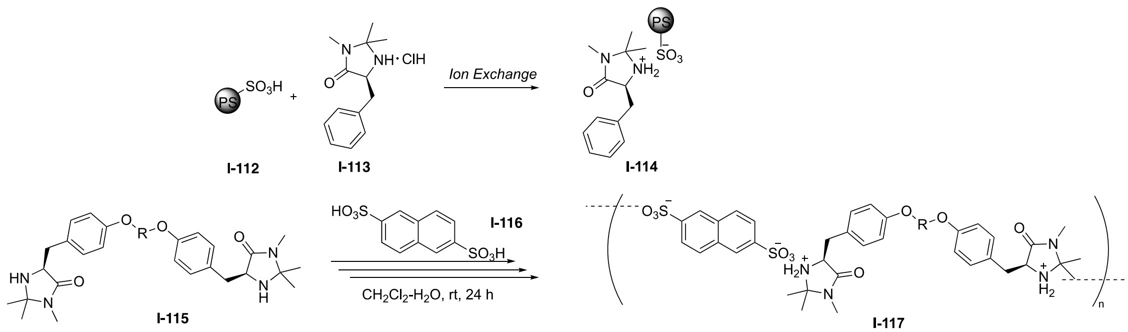

Scheme 30. Supporting chiral imidazolidinone by ion exchange reaction

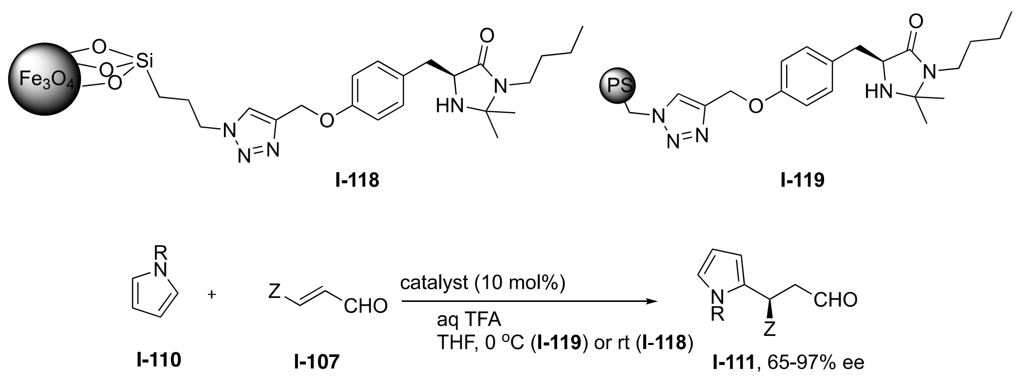

Scheme 31. Supporting chiral imidazolidinone onto magnetic nanoparticles

In 2012, Our laboratory reported the bounding of a chemically modified, first generation MacMillan imidazolidinone onto Fe_3O_4 (5.3 ± 1.4 nm) magnetic nanoparticles (**I-118**) and 1% DVB Merrifield resin (**I-119**) via click reactions. Both of the catalysts were used in the asymmetric Friedel-Crafts alkylation of N-substituted pyrroles with α,β-unsaturated aldehydes. The PS-supported catalyst (**I-119**) showed

[80] Haraguchi, N.; Kiyono, H.; Takemura ,Y.; Itsuno, S. *Chem. Commun.* **2012**, *48*, 4011-4013.

higher catalytic activity and enantioselectivity, while the MNP-supported one (**I-118**) showed higher recyclability. (Scheme 31). [81]

Radical co-polymerization of DVB with a properly modified chiral imidazolidinone inside a stainless-steel column with dodecanol and toluene as porogens afforded a MacMillan-type chiral organocatalyst immobilized monolith (**I-122**) (Scheme 32). It was implemented into continuous flow process for the cycloadditions of cyclopentadiene and α,β-unsaturated aldehydes, the chiral adducts were obtained with good enantioselectivities (90% ee at 25 °C) and high productivities (higher than 330). The same catalytic reactor was also used for three different stereoselective transformations (Diels-Alder, 1,3-dipolar nitrone-olefin cycloaddition, and Friedel-Crafts alkylation) in a sequential manner; up to 99% yield with 93% *ee* and 71% yield with 90% *ee* at 25 °C were obtained in the case of the former two reactions, respectively. In addition to simplifying product recovery, the monolithic reactor can continuously work for more than 8 days.[82]

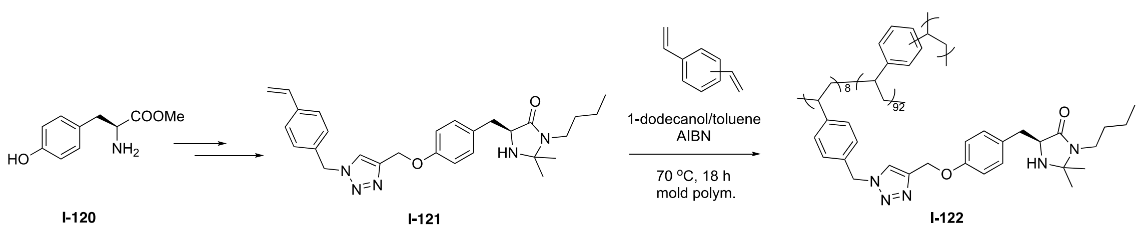

Scheme 32. Supporting chiral imidazolidinone through radical co-polymerization

In 2016, our laboratory reported two supported versions of the second-generation MacMillan imidazolidinone. This organocatalyst was immobilized on 1% DVB Merrifield resin (**I-123**) and Fe_3O_4 magnetic nanoparticles by the copper-catalyzed

---

[81] Riente, P.; Yadav, J.; Pericàs, M. A. *Org. Lett.* **2012**, *14*, 3668-3671.

[82] Chiroli, V.; Benaglia, M.; Puglisi, A.; Porta, Rv Jumde, R. P.; Mandoli, A. *Green Chem.* **2014**, *16*, 2798-2806.

"click reaction". Both of the polymeric catalysts were applied to the asymmetric Friedel-Crafts alkylation of indoles with α,β-unsaturated aldehydes. While both polymeric catalysts could be easily recovered and exhibited good recyclability, the PS-based catalyst **I-123** showed higher stability and provided better stereoselectivities. (Scheme 32).[83]

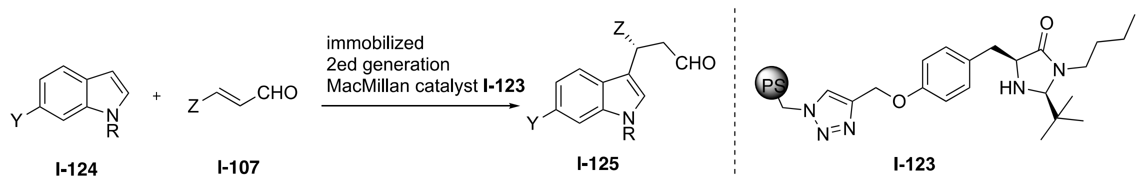

Scheme 32. Supported chiral imidazolidinone for asymmetric Friedel-Crafts alkylation of indoles

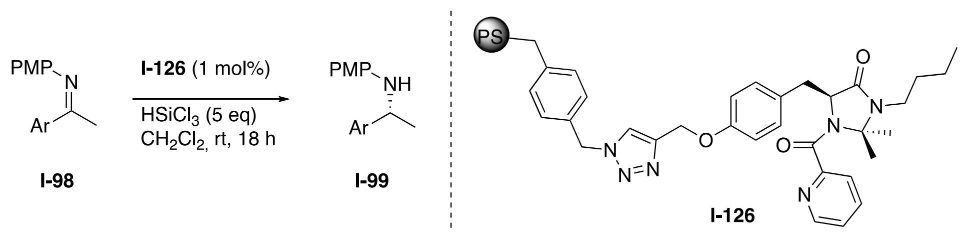

Scheme 33. PS-Supported imidazolidinone **I-126** for the catalytic reduction of imines with trichlorosilane

In 2017, the Puglisi group reported the solid supported chiral imidazolidinone organocatalysts **I-126** for the catalytic asymmetric reduction of imines with trichlorosilane. PS showed better effect as a support than silica in this case in terms of both chemical and stereochemical efficiency. Even at 1 mol% loading **I-126** showed a remarkable activity and stereocontrol ability, promoting the reduction with excellent enantioselectivities (up to 98% *ee* and in most cases ranging between 90–95% *ee*). Functional polymer **I-126** was implemented into continuous flow process;

[83] Ranjbar, S.; Riente, P.; Rodríguez-Escrich, C.; Yadav, J.; Ramineni, K.; Pericàs, M. A. *Org. Lett.* **2016**, *18*, 1602-1605.

chiral amines were obtained in excellent yields and enantioselectivities (Scheme 33).[84]

1.5.7 Immobilized Cinchona alkaloids

Cinchona alkaloids are isolated from the bark of several species of cinchona trees. Readily available and inexpensive cinchona alkaloids, such as quinine, quinidine, cinchonine and cinchonidine, have been widely applied in some catalytic asymmetric transformations.[85] Some active sites in cinchona alkaloids are suitable for the immobilization onto a polymer: the vinyl group at C-3, hydroxyl group at C'-6 of the quinoline moiety after demethylation, and hydroxyl group at C-9 are readily available for further transformation and for immobilization. Supporting through the nitrogen of the amino functionalities is also possible. The resulting quaternary ammonium salt has been used as a phase-transfer catalyst (PTC).

In 2001, the Lectka group reported the use of PS-immobilized quinine that constitute the packing of a series of "reaction columns" for catalytic asymmetric reaction process. This process was applied to the [2+2] Staudinger reactions of ketenes and imines to yield β-lactams with excellent enantio- and diastereoselectivity. The polymeric catalyst can be reused up to 60 cycles without significant loss of catalytic efficiency (scheme 34).[86]

---

[84] Porta, R.; Benaglia, M.; Annunziata, R.; Puglisi, A.; Celentano, G. *Adv. Synth. Catal.* **2017**, *359*, 2375-2382.

[85] a) *Cinchona alkaloids in synthesis and catalysis: ligands, immobilization and organocatalysis*, (Ed.: Song, C. E.) John Wiley & Sons. **2009**; b) Tian, S. K.; Chen, Y.; Hang, J.; Tang, L.; McDaid, P.; Deng, L. *Acc. Chem. Res.* **2004**, *37*, 621-631; c) Marcelli, T.; Hiemstra, H. *Synthesis* **2010**, 1229-1279; d) Kacprzak, K.; Gawroński, J. *Synthesis* **2001**, 961-998.

[86] Hafez, A. M.; Taggi, A. E.; Dudding, T.; Letcka, T. *J. Am. Chem. Soc.* **2001**, *123*, 10853-10859.

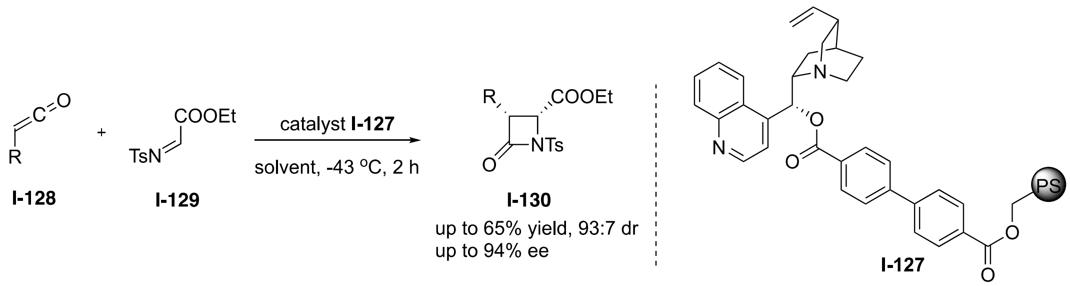

Scheme 34. PS-immobilized quinine for [2+2] Staudinger reaction

In 2004, the Cahard group reported the synthesis of linear PS-immobilized cinchona alkaloids **I-131** and applied them to enantioselective α-fluorination of carbonyl compounds. The the PS-bound cinchona alkaloid soluble polymers **I-131** can be easily recovered by solid/liquid separation and exhibite an efficient recycling without any loss of enantioselectivity (Scheme 35). [87]

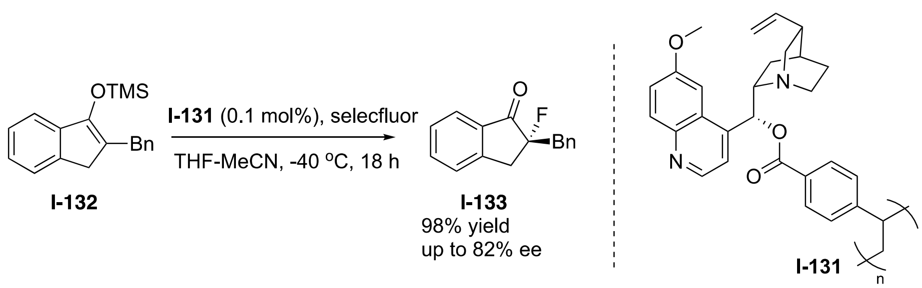

Scheme 35. PS-immobilized quinine for enantioselective α-fluorination

In 2005, Lectka and coworkers reported a flow system based on Wang resin-immobilized quinine packed in a column (**I-134**), that promoted the asymmetric α-chlorination of acid chlorides to afford chiral α-chloroesters with excellent enantioselectivities up to 94% ee and in good yields (Scheme 36).[88]

---

[87] Thierry, T.; Audouard, C.; Plaquevent, J. C.; Cahard, D. *Synlett* **2004**, *2004*, 856-860.

[88] Bernstein, D.; France, S.; Wolfer, J.; Lectka, T. *Tetrahedron: Asymmetry* **2005**, *16*, 3481-3483.

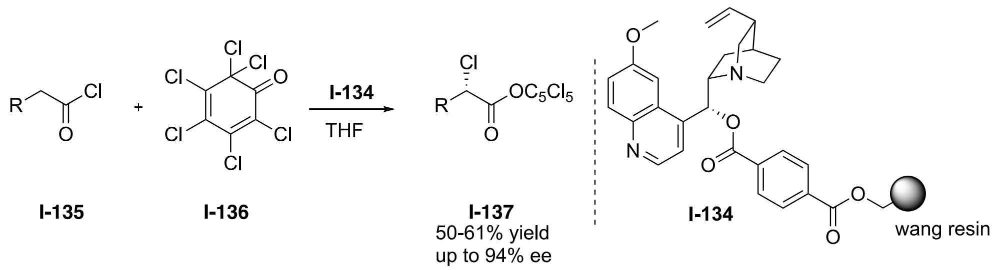

Scheme 36. PS-immobilized quinine for asymmetric α-chlorination of acid chlorides

Cinchona-based bifunctional thiourea [89] and sulfonamide [90] organocatalysts are also highly effective in a variety of asymmetric reactions. In 2009, Song and coworkers reported a polymer-supported bifunctional Cinchona-based sulfonamide organocatalyst **I-140**. It showed excellent activity and enantioselectivity (up to 97% ee) in the methanolytic desymmetrization of meso-cyclic anhydrides. Moreover, the polymeric catalyst showed long-term stability under catalytic conditions, which made it reusable without decrease in TOF or in enantioselectivity (Scheme 37).[91]

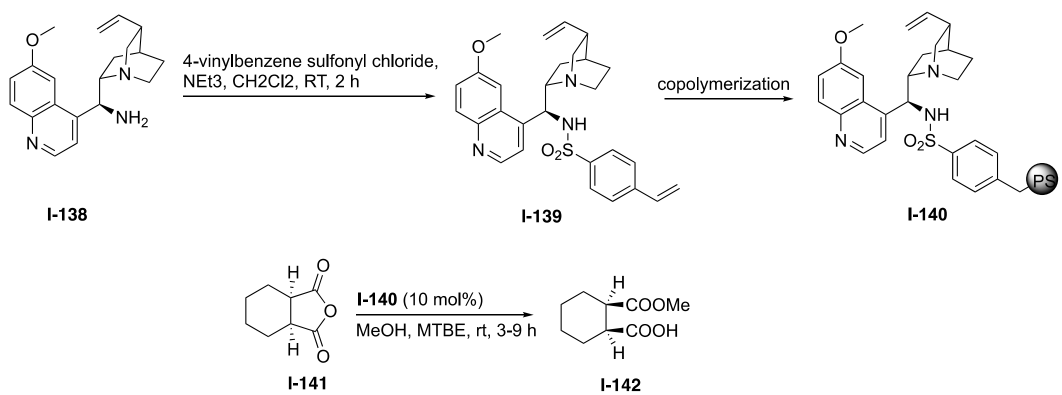

[89] Connon, S. J. *Chem. Comm.* **2008**, 2499-2510.

[90] Oh, S. H.; Rho, H. S.; Lee, J. W.; Lee, J. E.; Youk, S. H.; Chin, J.; Song, C. E. *Angew. Chem. Int. Ed.* **2008**, *47*, 7872-7875.

[91] Youk, S. H.; Oh, S. H.; Rho, H. S.; Lee, J. E.; Lee, J. W.; Song, C. E. *Chem. Comm.* **2009**, 2220-2222.

Scheme 37. PS-immobilized Cinchona alkaloid **I-140** for the desymmetrization of *meso*-cyclic anhydrides

In 2012, the Hansen group developed the immobilization of Cinchona alkaloids by copolymerization of polyfunctional thiols and alkenes together with unmodified Cinchona precursors. In this way, bead polymerization and catalyst immobilization were combined in a single step. The supported Cinchona derivatives **(I-143)** – **(I-145)** have been successfully applied in several asymmetric transformations, but catalyst recycling ability is relatively poor so far (Figure 7).[92]

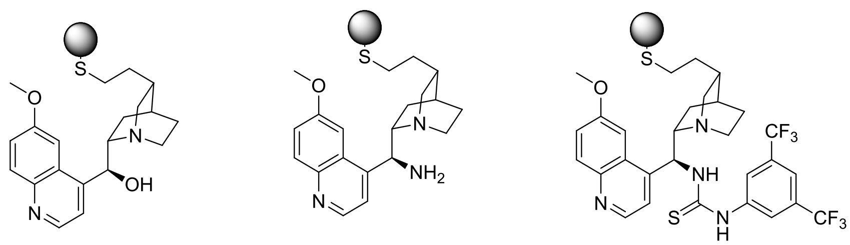

I-143 **I-144** **I-145**

Figure 7. PS-immobilized Cinchona alkaloids **(I-143) – (I-145)** prepared by copolymerization of polyfunctional thiols and alkenes together with unmodified Cinchona precursors

In addition to synthetic polymer supports, biopolymers such as chitosan have also been applied for the immobilization of cinchona alkaloids. In 2012, the Cui group reported the use of chitosan-supported cinchona alkaloids **(I-149) - (I-150)** as catalysts for the asymmetric Michael addition of 1,3-dicarbonyl compounds to maleimides, achieving high yields and high stereoselectivities. The catalyst was recovered by simple filtration and reused several times without a significant loss in activity (Scheme 38).[93]

---

[92] Fredriksen, K. A.; Kristensen, T. E.; Hansen, T. *Beilstein J. Org. Chem.* **2012**, *8*, 1126-1133.

[93] Qin, Y.; Zhao, W.; Yang, L.; Zhang, X.; Cui, Y. *Chirality* **2012**, *24*, 640-645.

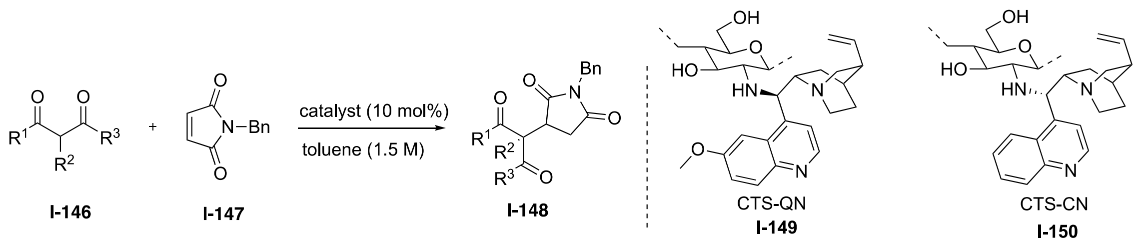

Scheme 38. Chitosan-immobilized cinchona alkaloids derivatives **(I-149) - (I-150)** for the asymmetric Michael addition

In 2015, our group reported the synthesis of a PS-supported 9-amino(9-deoxy)*epi* quinine derivative **I-151** and used it to catalyse Michael additions of a variety of nucleophiles and enones, affording excellent conversion and enantioselectivity. Catalyst **I-151** was used for the implementation of a single-pass continuous flow process, which could be used for the sequential synthesis of a small library of enantiopure compounds, being operated for 21 hours without significant decrease in conversion and with improved enantioselectivity with respect to batch operation (Figure 8).[94]

Figure 8. PS-Supported Cinchona-derived primary amine for continuous flow Michael additions.

In 2016, the Mandoli group reported the preparation of Merrifield resin-immobilized dimeric quinidine **I-154** by a click reaction of an alkyne-functionalized dimeric quinidine bounding onto azido-functionalized Merrifield resin. Excellent yields and enantioselectivities (89–95% ee) were attained in 100 performed reaction cycles in

[94] Izquierdo, J.; Ayats, C.; Henseler, A. H.; Pericàs, M. A. *Org. Biomol. Chem.* **2015**, *13*, 4204-4209.

the enantioselective *α*-amination of 2-oxindoles with diethyl azodicarboxylate catalysed with polymeric catalyst **I-154**. Operation time for more than 5300 hours over 8 months, showing excellent stability (Scheme 39).[95]

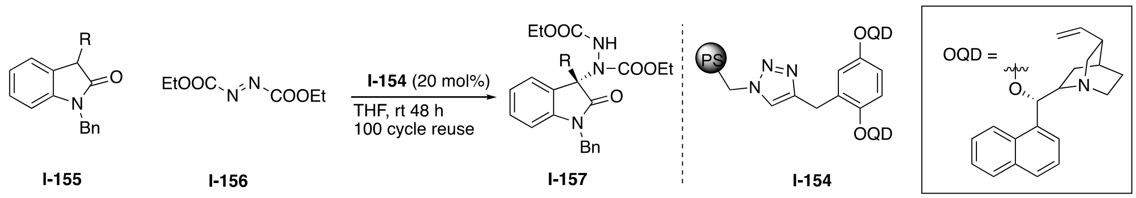

Scheme 39. Merrifield resin-immobilized dimeric quinidine for the enantioselective *α*-amination of 2-oxindoles with diethyl azodicarboxylate

1.5.8 Polymer-immobilized cinchona alkaloid-derived quaternary ammonium salts

One of the most promising applications of cinchona alkaloids in asymmetric reactions are probably the application of the derived quaternary ammonium salts to phase-transfer catalysis (PTC). As already discussed, the cinchona alkaloid can be immobilized onto a polymer mainly through the nitrogen (R^1), the hydroxyl group of C-9 position (R^2), the vinyl group of C-3, and 6'-position (4-position of quinolone moiety). The resulting polymer-supported cinchona alkaloid quaternary ammonium salts can be applied to a variety of organic reactions, including alkylation of amino acids imine,[96] hydrocyanation of imines,[97] the aldol reaction,[98] and epoxidation,[99] as representative examples.

[95] Jumde, R.P.; Mandoli, A. *ACS Catal.* **2016**, *6*, 4281-4285.

[96] O'Donnell, M. J.; Bennett, W. D.; Wu, S. *J. Am. Chem. Soc.* **1989**, *111*, 2353-2355.

[97] Sigman, M. S.; Vachal, P.; Jacobsen, E. N. *Angew. Chem. Int. Ed.* **2000**, *39*, 1279-1281.

[98] Sakthivel, K.; Notz, W.; Bui, T.; Barbas III, G. F. *J. Am. Chem. Soc.* **2001**, *123*, 5260-5267.

[99] Berkessel, A.; Gasch, N.; Glaubitz, K.; Koch, C. *Org. Lett.* **2001**, *3*, 3839-3842.

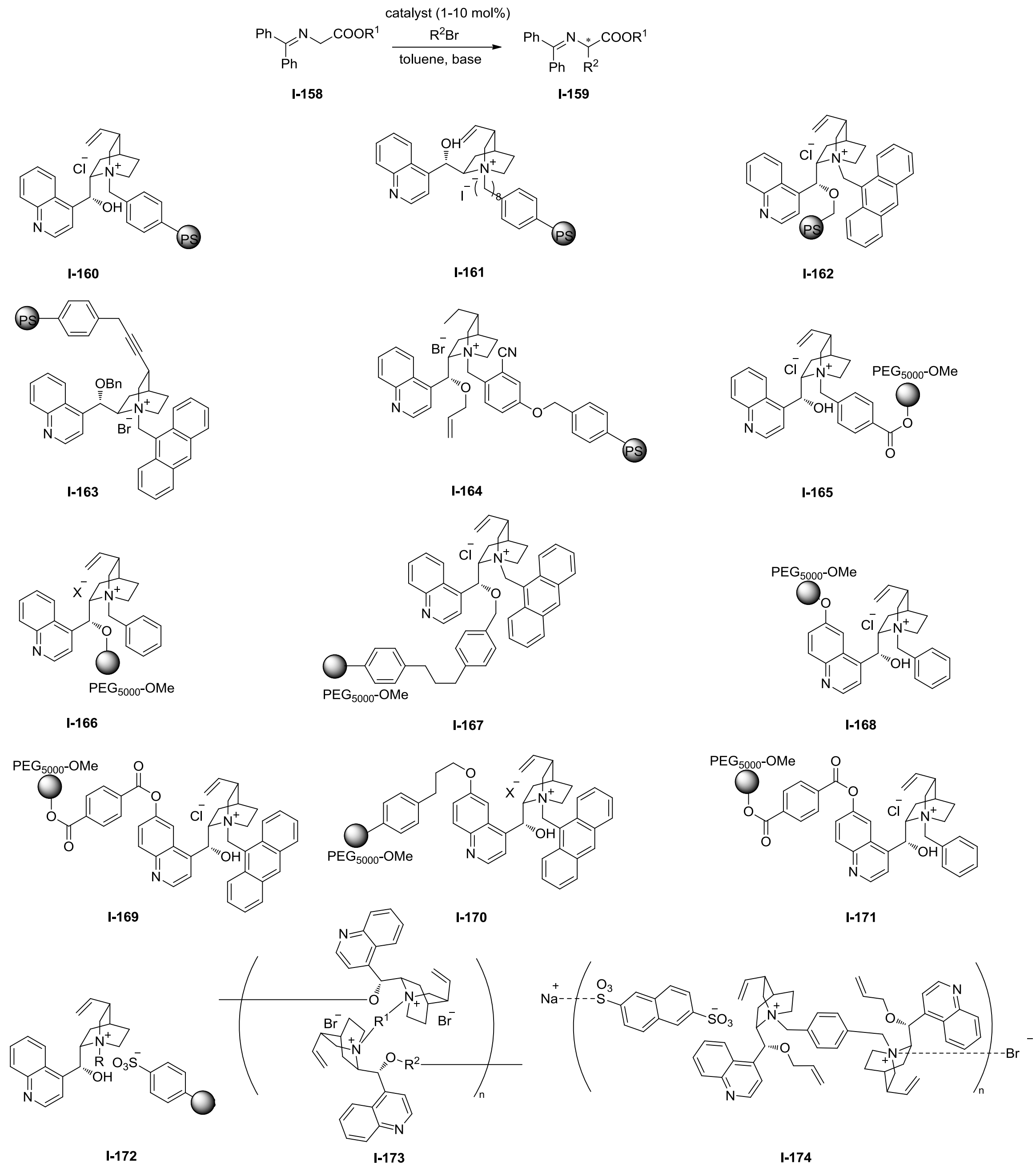

Scheme 40. Polymer-immobilized cinchona alkaloid quaternary ammonium salts

The asymmetric alkylation of glycine derivatives to produce optically active *α*-amino acids have been commonly used as model reaction to test the catalytic activity of cinchona alkaloid quaternary ammonium salts. In 1989, O'Donnell and co-workers reported the alkylation of a glycine Schiff base[100] under PTC conditions catalysed by cinchona alkaloid quaternary ammonium salt, highly enantioselective afforded desired products.[96] A variety of modified cinchona alkaloid quaternary ammonium salts, as well as the polymeric version of those catalysts ((**I-160)** - (**I-174)**) have been reported since the initial report in this field (Scheme 40).[101]

1.5.9 Polymer-immobilized chiral DMAP Analogues

Chiral DMAP analogues have been well explored since the late 1990s, and have been used for enantioselective acyl transfer reactions (kinetic resolution (KR), dynamic kinetic resolution (DKR), desymmetrization, rearrangements, and opening *meso* anhydride) and regioselective acylations of carbohydrates.[102]

---

[100] O'Donnell, M. J.; Polt, R. L. *J. Org. Chem.* **1982**, *47*, 2663–2666.

[101] a) Zhengpu, Z.; Yongmer, Y.; Zhen, W.; Hodge, P. *React. Funct. Polym.* **1999**, *41*, 37-43; b) Chinchilla, R.; Mazo´n, P.; Najera, C. *Tetrahedron: Asymmetry* **2000**, *11*, 3277-3281; c) Chinchilla, R.; Mazo´n, P.; Najera, C. *Adv. Synth. Catal.* **2004**, *346*, 1186-1194; d) Thierry, B.; Plaquevent, J. C.; Cahard, D. *Tetrahedron: Asymmetry* **2001**, *12*, 983-986; e) Thierry, B.; Perrard, T.; Audouard, C.; Plaquevent, J. C.; Cahard, D. *Synthesis* **2001**, *11*, 1742-1746; f) Thierry, B.; Plaquevent, J. C.; Cahard, D. *Mol. Divers.* **2005**, *9*, 277-290; g) Shi, Q.; Lee, Y. J.; Song, H.; Cheng, M.; Jew, S. S.; Park, H. G.; Jeong, B. S. *Chem. Lett.* **2008**, *37*, 436-437; h) Thierry, B.; Plaquevent, J. C.; Cahard, D. *Tetrahedron: Asymmetry* **2003**, *14*, 1671-1677; i) Lv, J.; Wang, X.; Liu, J.; Zhang, L.; Wang, Y. *Tetrahedron: Asymmetry* **2006**, *17*, 330-335; j) Wang, X.; Yin, L.; Yang, T.; Wang, Y. *Tetrahedron: Asymmetry* **2007**, *18*, 108-114; k) Arakawa, Y.; Haraguchi, N.; Itsuno, S. *Angew. Chem. Int. Ed.* **2008**, *47*, 8232-8235; l) Itsuno, S.; Paul, D. K.; Ishimoto, M.; Haraguchi, N. *Chem. Lett.* **2010**, *39*, 86-87; m) Itsuno, S.; Paul, D. K.; Salam, M. A.; Haraguchi, N. *J. Am. Chem. Soc.* **2010**, *132*, 2864-2865.

[102] a) Wurz, R. P. *Chem. Rev.* **2007**, *107*, 5570-5595; b) Atodiresei, I.; Schiffers, I.; Bolm, C. *Chem Rev.* **2007**, *107*, 5683-5712; c) Alba, A. -N. R.; Rios, R. *Chem Asian J.* **2011**, *6*, 720-734; d) Müller, C.E.; Schreiner, P. R. *Angew. Chem. Int. Ed.* **2011**, *50*, 6012-6042; e) Pellissier, H. *Adv Synth Catal.* **2011**, *353*, 1613-1666; f) Taylor, J. E.; Bull, S. D.; Williams, J. M. *Chem. Soc. Rev.* **2012**, *41*, 2109-2121; g) Krasnov, V.P.; Gruzdev, D. A.; Levit, G. L. *Eur J Org Chem.* **2012**, 1471-1493; h) Diaz-de-Villegas, M. D.; Galvez, J. A.; Badorrey, R.; Lopez-Ram-de-Viu, M. P. *Chem Eur J.* **2012**, *18*, 13920-13935; i) Enriquez-Garcia, A.; Kündig, E. P. *Chem Soc Rev.* **2012**, *41*, 7803-7831; j) Lee, D.; Taylor, M. S. *Synthesis-Stuttgart.* **2012**, *44*, 3421-3431; k) Candish, L.; Nakano,

In 2003, the Anson group reported the synthesis of a family of immobilized chiral DMAP analogues as enantioselective acylation catalysts in two steps and identified the best candidates in the acylative KR of racemic sec - alcohols. Wang resin-immobilized DMAP analogue **I-175**, turned out to be optimal for the enantioselective acylation reactions of secondary alcohols, including a variety of cis-2-substituted cycloalkanols (Scheme 41).[103]

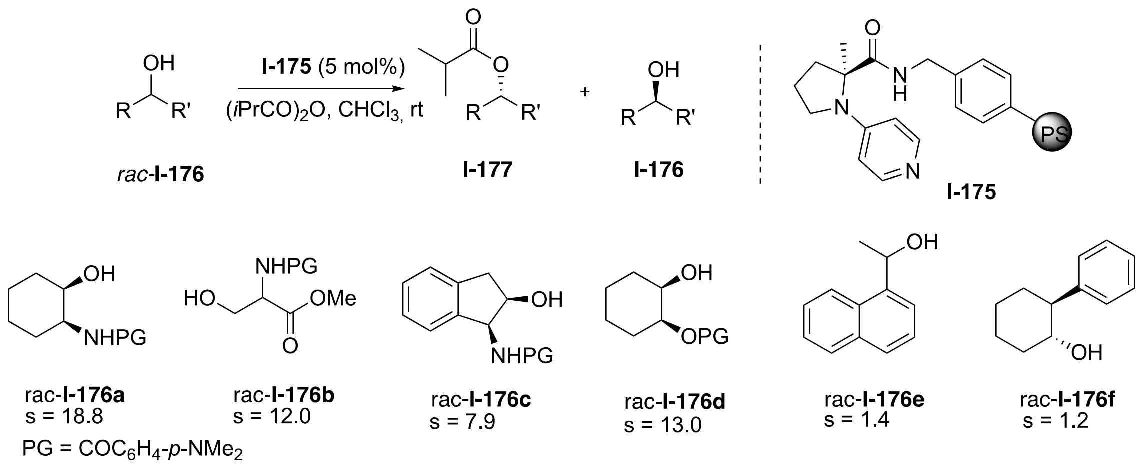

Scheme 41. Polymer-immobilized chiral DMAP Analogue for KR of second alcohol

In 2009, Connon and Gun'ko reported the immobilization of a chiral DMAP analogue **I-178** onto magnetic nanoparticles. This system was used to the acylative KR of racemic sec - alcohols, affording moderate selectivity. The magnetic catalyst is simple to prepare, insensitive to air/moisture and easily recoverable by magnetic

Y.; Lupton, D. W. *Synthesis-Stuttgart.* **2014**, *46*, 1823-1835; l) Seidel, D. *Synlett.* **2014**, *25*, 783-794; m) Lawandi, J.; Rocheleau, S.; Moitessier, N.; *Tetrahedron.* **2016**, *72*, 6283-6319; n) Zeng, X.-P.; Cao, Z. -Y.; Wang, Y.-H.; Zhou, F.; Zhou, J. *Chem Rev.* **2016**, *116*, 7330-7396; o) Suzuki, T. *Tetrahedron Lett.* **2017**, *58*, 4731-4739; p) Pellissier, H. *Tetrahedron* **2018**, *74*, 3459-3468; q) Mandai, H.; Fujii, K.; Suga, S. *Tetrahedron Lett.* **2018**, *59*, 1787-1803; r) Yang, H.; Zheng, W. H. *Tetrahedron Lett.* **2018**, *59*, 583-591

[103] Pelotier, B.; Priem, G.; Campbell, I. B.; Macdonald, S. J. F.; Anson, M. S. *Synlett* **2003**, 679-683.

decantation. It retained excellent activity and selectivity after 32 iterative cycles (Scheme 42).[104]

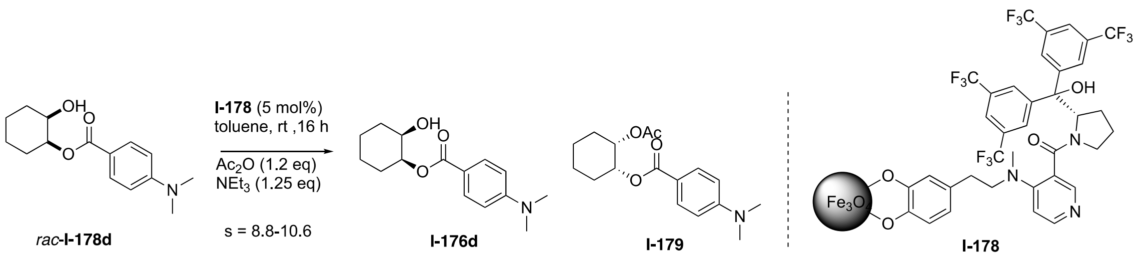

Scheme 42. Magnetic nanoparticles immobilized Chiral DMAP analogue **I-178** for the KR of secondary alcohols

1.5.10 Polymer-immobilized chiral thioureas and squaramides organocatalysts

Recently, chiral thioureas and squaramides have emerged as a promising class of organocatalysts based on non−covalent interactions. The immobilization of them onto polymers have attracted a plenty of attention in the past years.

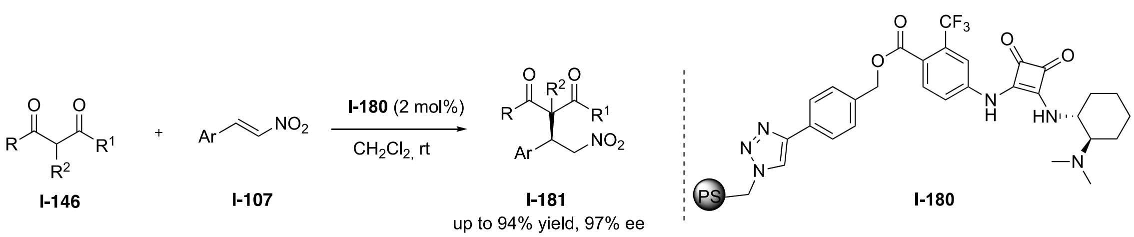

Scheme 43. Polymer-immobilized chiral squaramide organocatalyst for Michael addition

In 2012, our laboratory reported the first example of bounding a chiral squaramide organocatalyst covalently onto a Merrifield type resin with a copper-catalyzed azide-alkyne cycloaddition strategy. The functional resin **I-180** was explored in the asymmetric Michael addition of 1,3−dicarbonyl compounds to β−nitrostyrenes,

[104] Gleeson, O.; Tekoriute, R.; Gun'ko, Y, K.; Connon ,S. J. *Chem. Eur. J.* **2009**, *15*, 5669-5673.

affording good to excellent yields and enantioselectivities. The 1,2,3–triazole linker provided the functional resin **I-180** with excellent catalytic stability, allowing its reuse in 10 consecutive reaction cycles (Scheme 43).[105]

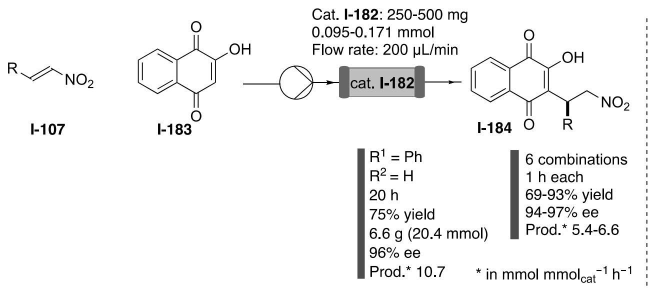

Figure 9. Supported squaramide catalyst **I-182** for the continuous flow conjugate addition of hydroxynaphthoquinones to nitroalkenes.

In 2013, our laboratory applied the immobilized, minimalistic catalyst **I-182** to promote the fast Michael addition of 2-hydroxy-1,4-naphthoquinone to β–nitroalkenes, obtaining excellent enantioselectivities at low catalyst loadings. The PS-supported catalyst **I-182** can be recycled up to 10 times without any decrease in enantioselectivity and adapted to long (24 h) continuous flow operation (Figure 9).[106]

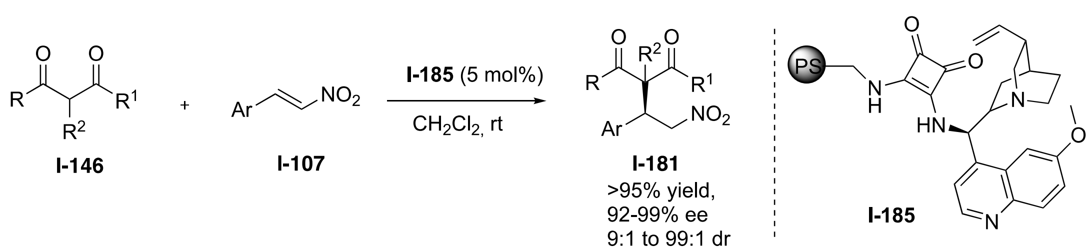

Scheme 44. Polymer-immobilized quinidine-squaramide for the asymmetric Michael addition

[105] Kasaplar, P.; Riente, P.; Hartmann, C.; Pericàs, M. A. *Adv. Synth. Catal.* **2012**, *354*, 2905-2910.

[106] Kasaplar, P.; Rodriguez-Escrich, C.; Pericas, M. A. *Org. Lett.* **2013**, *15*, 3498-3501.

In 2013, the Soós group reported the immobilization of quinine- and quinidine-squaramide organocatalysts (**I-185**) for batch and continuous‐flow applications. These organocatalysts were used in the asymmetric addition of 1,3-dicarbonyl compounds to β-nitrostyrenes, affording Michael adducts in excellent yields with enantioselectivities, even on the gram scale. Moreover, these immobilized catalysts exhibited stability to survive several cycles without significant loss of activity (Scheme 44).[107]

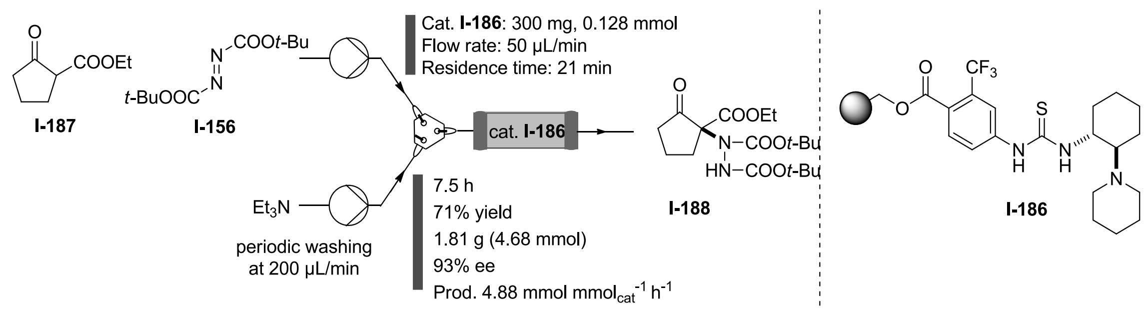

Figure 10**.** Immobilized thiourea for the enantioselective amination of ketoesters.

In 2015, Our laboratory prepared an immobilized bifunctional thiourea organocatalyst (PS-TU) and used it in the enantioselective α-amination of 1,3-dicarbonyl compounds with azodicarboxylates. Homogeneous thioureas can be irreversibly deactivated by the azodicarboxylate reagents, in contrast, PS-TU could be recovered by simple washing with triethylamine between runs, which allowed the reuse up to 9 cycles. Finally, the PS-TU had also been implemented to continuous flow process (7.5 h operation, 21 min residence time, TON = 37) (Figure 10).[108]

[107] Kardos, G.; Soós, T. *Eur. J. Org. Chem.* **2013**, 4490-4494.

[108] Kasaplar, P.; Ozkal, E.; Rodríguez-Escrich, C.; Pericàs, M. A. *Green Chem.* **2015**, *17*, 3122-3129.

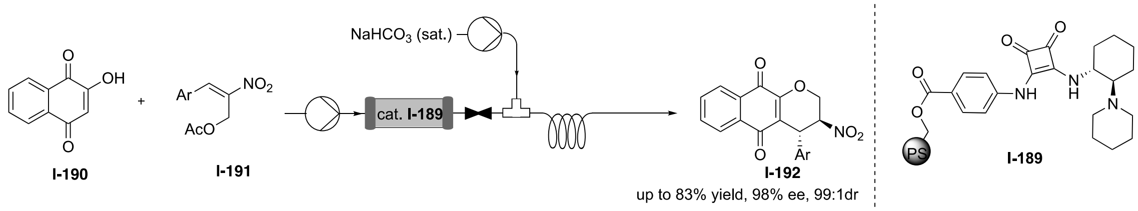

Figure 11. Immobilized chiral squaramide **I-189** for the enantioselective production of a library of pyranonaphthoquinones **I-192** in continuous flow

In 2016, our group reported the development of the new, cost-effective PS-supported squaramide **I-189** and the implement of it to a continuous flow setup for the enantioselective production of a library of pyranonaphthoquinones. This was accomplished by a two-step process took place in aequence, which involved a squaramide-catalyzed Michael reaction and *oxa*-Michael cyclization reaction (Figure 11).[109]

In 2017, Itsuno and coworkers reported the synthesis of a chiral polymer containing cinchona-based chiral squaramides in their main chain structure (**I-193**). Resin **I-193** was applied to the asymmetric addition of β-ketoesters to β−nitroolefins, achieving the Michael adducts in good yields and enantioselectivities of up to 99% ee.[110] In the next year, the same group reported the synthesis of another chiral polymers containing cinchona-based squaramide dimers that contain two cinchona squaramide units connected by diamines in the main chain structure (**I-195**). The chiral polymers were applied in asymmetric Michael addition reactions, where they induced the formation of the corresponding Michael adducts **I-194** in good yields with excellent enantio- and diastereoselectivities. The polymeric catalysts **I-193** and **I-195**

[109] Osorio-Planes, L.; Rodríguez-Escrich, C.; Pericàs, M. A. *Catal. Sci. Technol.* **2016**, *6*, 4686-4689.

[110] Ullah, M. S.; Itsuno, S. *Molecular Catal.* **2017**, *438*, 239-244.

could be easily recovered and reused several times without loss of catalytic activity (Scheme 45). [111]

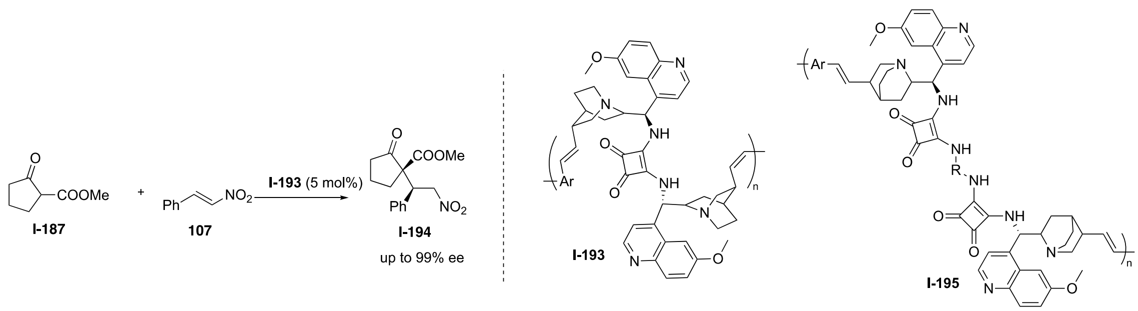

Scheme 45. Immobilized cinchona-based squaramides for the Michael addition of β-ketoesters to nitroolefins

1.5.11 Immobilizaiton of other types of organocatalyst

Motivated by works of the application of diamine **I-196** to Robinson annulations reported by the Luo group,[112] in 2017, our laboratory reported its supported version (**I-198**) and tested it in the enantioselective Robinson annulation with a good recyclability. In this case, the immobilized catalyst **I-198** presented clear advantages over the homogeneous analogue **I-197**.[113] A continuous flow process based on **I-198** was implemented by placing the polymeric catalyst in a jacketed packed bed reactor. With it, 11.7 g of the Wieland-Miescher ketone (**I-203**) in 91% ee was prepared with a 24-h flow experiment. A library of eight diverse structure cylohexenones were prepared with a similar set-up. (Figure 12).

[111] Ullah, M. S.; Itsuno, S. *ACS Omega* **2018**, *3*, 4573-4582.

[112] a) Zhou, P.; Zhang, L.; Luo, S.; Cheng, J. P. *J. Org. Chem.* **2012**, *77*, 2526-2530; b) Xu, C.; Zhang, L.; Zhou, P.; Luo, S.; Cheng, J. P. *Synthesis* **2013**, *45*, 1939-1945.

[113] Cañellas, S.; Ayats, C.; Henseler, A. H.; Pericàs, M. A. *ACS Catal.* **2017**, *7*, 1383-1391.

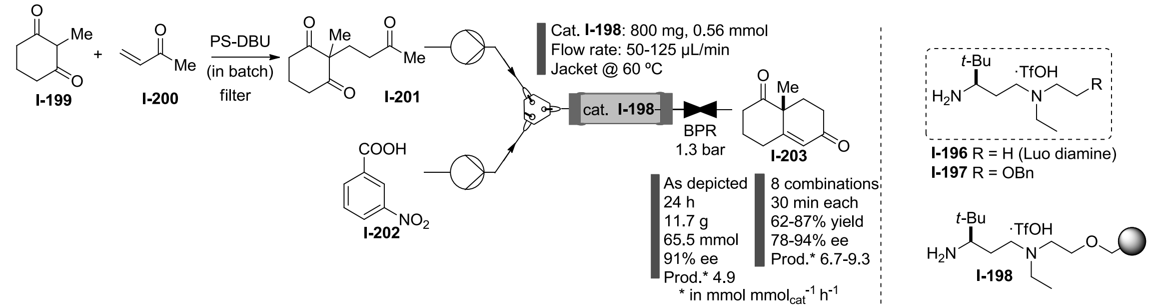

Figure 12. Immobilized chiral diamine catalyst for the flow Robinson annulation.

Apart from a non-recyclable MNP-supported chiral NHC catalyst,[114] the Massi group reported in 2017 the only recyclable example of supported chiral NHC catalyst. The chiral NHC was immobilized onto silica and PS. Both functionalized resins were applied to the asymmetric intramolecular Stetter reaction to produce chromanones **I-206** (Scheme 46).[115] The PS-supported catalyst **I-204** exhibited better results in this reaction and good recyclability of up to 10 times. Then, a monolithic version of **I-204** was prepared and used for 120 hours in a single flow experiment at 10 µl/min with a TON of 132.

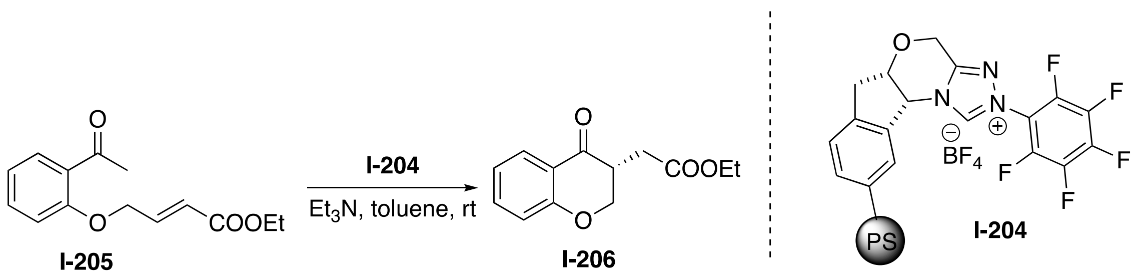

Scheme 46. Immobilized chiral NHC catalyst

[114] Ranganath, K.V.S.; Schäfer, A.H.; Glorius, F. *ChemCatChem* **2011**, *3*, 1889-1891.

[115] Ragno, D., Di Carmine, G., Brandolese, A., Bortolini, O., Giovannini, P. P., & Massi, A. *ACS Catal.* **2017**, *7*, 6365–6375.

1.6 Aim of this thesis

The immobilization of chiral catalysts onto polymers for catalytic asymmetric reactions represents an important and useful approach to increase sustainability in organic synthesis through a significant number of clear advantages (minimization of solvent usage through simplified work-up, easy catalyst separation by filtration or magnetic decantation, opportunities for recycling and continuous flow processing.). According to this, the immobilization of organocatalysts and the implementation of continuous flow processes based on them is attractive for its potential in practical applications in the future in industry.

Thus, the aims of this thesis cover three main areas: (a) studies towards the immobilization of organocatalysts with known ability for high enantiocontrol in asymmetric reactions, and application of the resulting immobilized species in batch and continuous flow processes; (b) development of new methodology for the preparation of highly sterically congested, polymerizable chiral phosphoric acids and demonstration of their potential in asymmetric catalysis; (c) within the broad area of developing green and economically viable alternatives for relevant, synthetic processes, the development a non-palladium dependent, electrochemical Wacker-Tsuji-type oxidation.

Chapter II

Immobilization of *cis*-4-Hydroxydiphenylprolinol Silyl Ethers onto Polystyrene. Application in the Catalytic Enantioselective Synthesis of 5-Hydroxyisoxazolidines in Batch and Flow

2.1. Polymer-supported prolinol and diarylprolinol derivatives

The pursuit of preparing optically enriched compounds has greatly promoted the development of asymmetric catalysis, which has been greatly expanding the toolkit of synthetic chemists.[116] Organocatalysis has been providing varieties of synthetic approach to optically active compounds under generally mild conditions. In the past years, prolinol is becoming a promising candidate for asymmetric organocatalysis.[117] Some of its derivatives such as diarylprolinols and their silyl ethers (generally known as Jørgensen–Hayashi catalysts, one of the most versatile chiral organo-aminocatalysts) have been widely used in varieties of asymmetric processes.[118]

---

[116] a) *Asymmetric Organocatalysis: from Biomimetic Concepts to Applications in Asymmetric Synthesis* (Eds.: Berkessel, A.; Groeger, H.) Wiley-VCH, **2005**; b) *Enantioselective Organocatalysis: Reactions and Experimental Procedures* (Eds.: Dalko, P. I.) Wiley-VCH: Weinheim, **2007**; c) Mukherjee, S.; Yang, J. W.; Hoffmann, S.; List, B. *Chem. Rev.* **2007**, *107*, 5471–5569; d) Doyle, A. G.; Jacobsen, E. N. *Chem. Rev.* **2007**, *107*, 5713–5743; e) MacMillan, D. W. C. *Nature* **2008**, *455*, 304-308; f) Dondoni, A.; Massi, A. *Angew. Chem., Int. Ed.* **2008**, *47*, 4638-4660.

[117] a) Juhl, K.; Jørgensen, K. A. *Angew. Chem. Int. Ed.* **2003**, *42*, 1498-1501; b) Zhong, G.; Fan, J.; Barbas, III, C. F. *Tetrahedron Lett.* **2004**, *45*, 5681-5684.

[118] a) Palomo, C.; Mielgo, A. *Angew. Chem. Int. Ed.* **2006**, *45*, 7876-7880; b) Verkade, J. M.; van Hemert, L. J.; Quaedflieg, P. J.; Rutjes, F. P. *Chem. Soc. Rev.* **2008**, *37*, 29-41; c) Mielgo, A.; Palomo, C. *Chem. Asian. J.* **2008**, *3*, 922-948; d) Bertelsen, S.; Jørgensen, K. A. *Chem. Soc. Rev.* **2009**, *38*, 2178-2189; e) Wong, C. T. *Tetrahedron* **2009**, *65*, 7491-7497; f) Jensen, K. L.; Dickmeiss, G.; Jiang, H.; Albrecht, Ł.; Jørgensen, K. A. *Acc. Chem. Res.* **2012**, *45*, 248-264; g) Volla, C. M.; Atodiresei, I.; Rueping, M. *Chem. Rev.* **2013**, *114*, 2390-2431; h) Donslund, B. S.; Johansen, T. K.; Poulsen, P. H.; Halskov, K. S.; Jørgensen, K. A. *Angew. Chem. Int.*

For prolinol and its derivatives in the asymmetric organocatalysis, it´s quite common a relatively large amount (in the 10–30 mol% range or even higher) of organocatalyst is required to complete the desired reaction within a reasonable time. Isolation of these catalysts from the reaction mixture, required for purification purposes and advisable from an economic perspective, is relatively hard due to the similar organic nature of catalyst and reaction product and thus results poorly economic.[119] To solve those problems, immobilized organocatalysts have been designed with the aim of overcoming these limitations by simultaneously allowing easy product purification and recovery.[120] In the last few years, immobilized prolinol derivatives have been developed and used as efficient catalysts for a plenty of asymmetric reactions.

In 2008, Wendorff and Studer reported the synthesis and immobilization of α,α-diphenylprolinol-oligostyrene conjugates into a polystyrene (PS) matrix by electrospinning affording fibers with a large surface area (fiber diameter of 1.2 µm).[121] The fibers (**II-1**) were tested in the asymmetric Michael addition of dimethyl

Ed. **2015**, *54*, 13860-13874; i) Halskov, K. S.; Donslund, B. S.; Paz, B. M.; Jørgensen, K. A. *Acc. Chem. Res.* **2016**, *49*, 974-986; j) Klier, L.; Tur, F.; Poulsen, P. H.; Jørgensen, K. A. *Chem. Soc. Rev.* **2017**, *46*, 1080-1102.

[119] a) Patora-Komisarska, K.; Benohoud, M.; Ishikawa, H.; Seebach, D.; Hayashi, Y. *Helv. Chim. Acta* **2011**, *94*, 719-745; b) Burés, J.; Armstrong, A.; Blackmond, D. G. *Acc. Chem. Res.* **2016**, *49*, 214-222.

[120] a) *Chiral catalyst immobilization and recycling*, (Eds.: De Vos, D. E.; Vankelecom, I. F. J.; Jacobs, P. A.) Wiley-VCH, Weinheim; New York, **2000**; b) Benaglia, M.; Puglisi, A.; Cozzi, F. *Chem. Rev.* **2003**, *103*, 3401-3430; c) Benaglia, M. *New J. Chem.* **2006**, *30*, 1525-1533; d) Cozzi, F. *Adv. Synth. Catal.* **2006**, *348*, 1367-1390; e) Gruttadauria, M.; Giacalone, F.; Noto, R. *Chem. Soc. Rev.* **2008**, *37*, 1666-1688; f) Margelefsky, E. L.; Zeidan, R. K.; Davis, M. E. *Chem. Soc. Rev.* **2008**, *37*, 1118-1126; g) *Recoverable and recyclable catalysts*, *1st ed.* (Eds.: Benaglia, M.) Wiley, Hoboken, N.J., **2009**; h) Trindade, A. F.; Gois, P. M. P.; Afonso, C. A. M. *Chem. Rev.* **2009**, *109*, 418-514; i) Kristensen, T. E.; Hansen, T. *Eur. J. Org. Chem.* **2010**, 3179-3204; j) *Polymeric chiral catalyst design and chiral polymer synthesis* (Eds.: Itsuno, S.) John Wiley & Sons, **2011**.

[121] Röben, C.; Stasiak, M.; Janza, B.; Greiner, A.; Wendorff, J. H.; Studer, A. *Synthesis* **2008**, 2163-2168.

malonate to cinnamaldehyde. However, the selected immobilization strategy turned out to be non-optimal, since a decrease of the catalyst activity was observed in the study of its recyclability (Scheme 1).

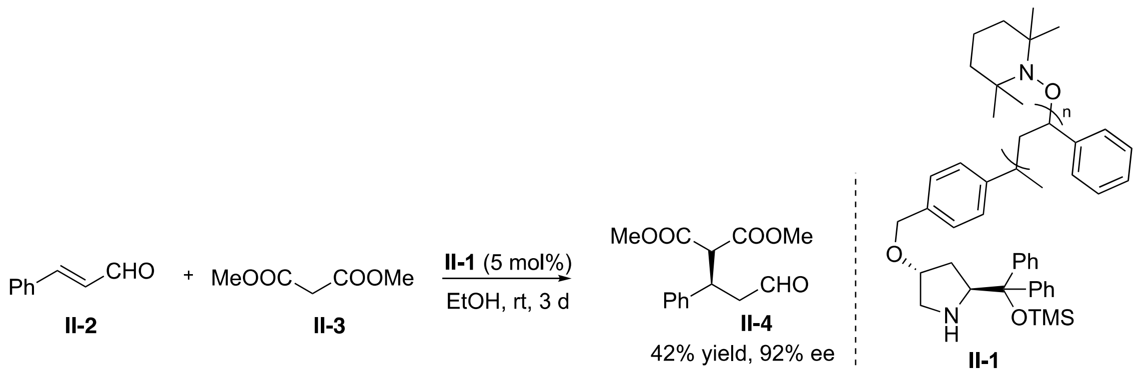

Scheme 1. diarylprolinol derivatives functionalized fibers and application in the Michael reaction

In 2010, the Zeitler group reported a MeOPEG-immobilized recyclable Jørgensen−Hayashi catalyst (**II-5**). **II-5** provided the same reactivity and selectivity with its homogeneous version in the Michael addition of nitromethane to α,β-unsaturated aldehydes.[122] In 2011, our laboratory reported the bounding of two α,α - diphenylprolinol ethers onto a PS-resin through copper-catalyzed azide-alkyne cycloaddition (**II-6**). These catalysts were tested in the asymmetric addition of aldehydes to nitroolefins (Scheme 2, a) and the addition of malonates (Scheme 2, b) or nitromethane (Scheme 2, c) to α,β - unsaturated aldehydes.[123] As a general trend, the triazole-linked diarylprolinol ethers immobilized onto insoluble PS resins showed high catalytic activity, and it can be easily recovered by filtration and can be reused in new reaction cycles.[123] In the same year, our laboratory used **II-6** as catalysts in the enantioselective domino Michael-Knoevenagel reaction of dimethyl 3-oxoglutarate and 3-substituted acrolein derivatives (Scheme 2, d). With the

[122] I. Mager, I.; Zeitler, K. *Org. Lett.* **2010**, *12*, 1480-1483.

[123] Alza, E.; Sayalero, S.; Kasaplar, P.; Almaşi, D.; Pericas, M. A. *Chem.-Eur. J.* **2011**, *17*, 11585-11595.

developed polymeric catalyst **II-6**, highly functionalized cyclohexane derivatives were prepared in a simple and effective manner both under batch and continuous flow conditions.[124]

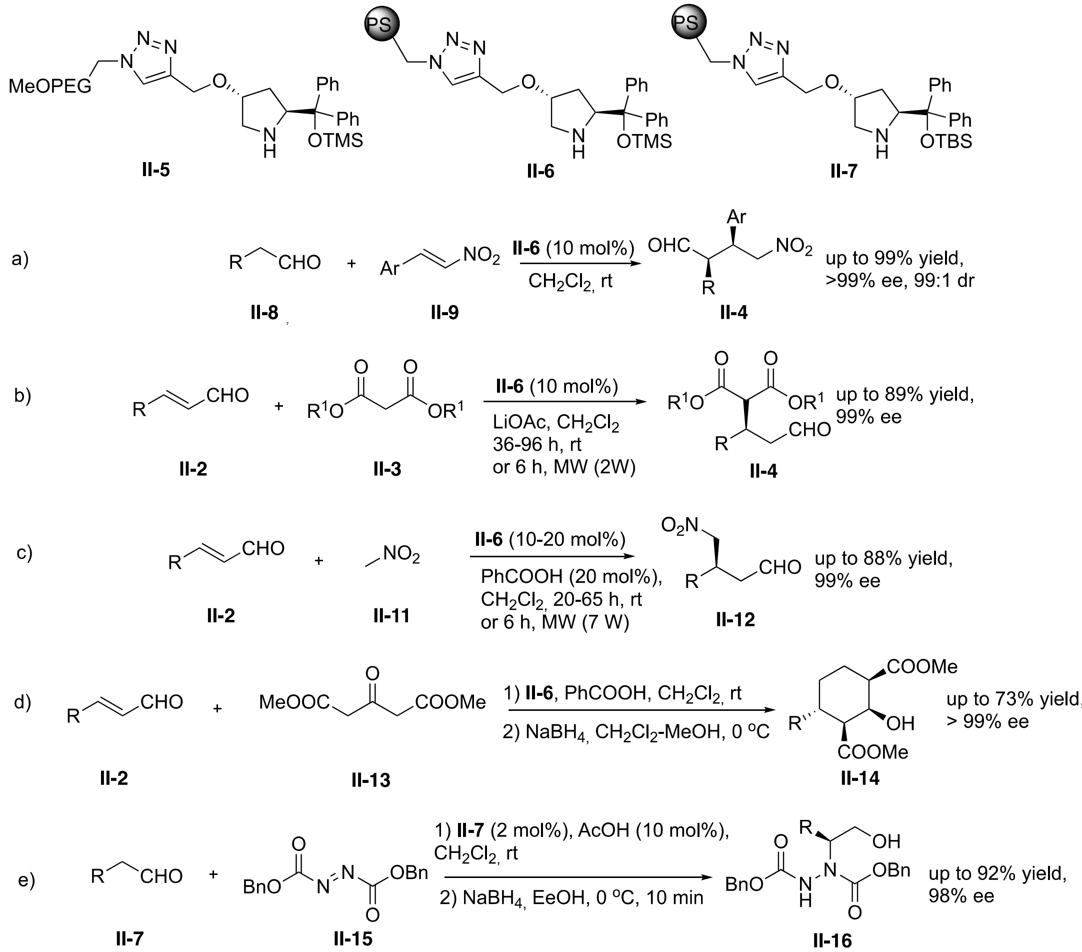

Scheme 2. PS-supported Jørgensen−Hayashi catalyst and application.

In 2012, our laboratory developed the immobilized species **II-7** as an highly active catalyst for the enantioselective α - amination of aldehydes (Scheme 2, e).[125] The

[124] Alza, E.; Sayalero, S.; Cambeiro, X. C.; Martín-Rapún, R.; Miranda, P. O.; Pericas, M. A. *Synlett* **2011**, 464-468.

[125] Fan, X.; Sayalero, S.; Pericas, M. A. *Adv. Synth. Catal.* **2012**, *354*, 2971-2976.

desired products obtained with high yields and enantioselectivities in short times at low (1–2 mol%) catalyst loading. Catalyst **II-7** could be reused 10 times, achieving with an accumulated TON of 480. A long‐standing continuous flow operation with very short residence time (6 min) could also be implemented.

In 2012, the Wang group reported the bounding of Jørgensen–Hayashi catalysts into a robust chiral porous polymer (**II-17**) through a ¨bottom‐up¨ strategy. The high BET surface area (881 m^2/g), wide openings, and interconnected nanopores increased the accessibility of catalytic sites of the immobilized catalysts and promoted the mass transport process, these behaviors are the key to its high catalytic activity. Polymer **II-17** showed excellent activity in the asymmetric Michael addition of aldehydes to nitroalkenes as a recoverable polymeric catalyst. It can be reused 4 times without significant loss of enantio- and diastereoselectivity.[126] In 2013, the Ouali group reported the immobilization of the Jørgensen–Hayashi catalyst by grafting the catalyst *via* triazole linkers onto the surface of two different supports, PS‒functionalized Co/C MNPs (**II-18**) and phosphorus dendrimers (**II-19**). These supported catalysts were tested in Michael additions of various aldehydes to different nitroolefins, displaying high activities and selectivities. Moreover, **II-19** could be recovered by precipitation/filtration and reused in 7 consecutive cycles without loss of efficiency (Figure 1).[127]

[126] Wang, C. A.; Zhang, Z. K.; Yue, T.; Sun, Y. L.; Wang, L.; Wang, W. D.; Zhang, Y.; Liu, C.; Wang, W. *Chem. -Eur. J.* **2012**, *18*, 6718-6723.

[127] Keller, M.; Perrier, A.; Linhardt, R.; Travers, L.; Wittmann, S.; Caminade, A. M.; Majoral, J. P.; Reiser, O.; Ouali, A. *Adv. Synth. Catal.* **2013**, *355*, 1748-1754.

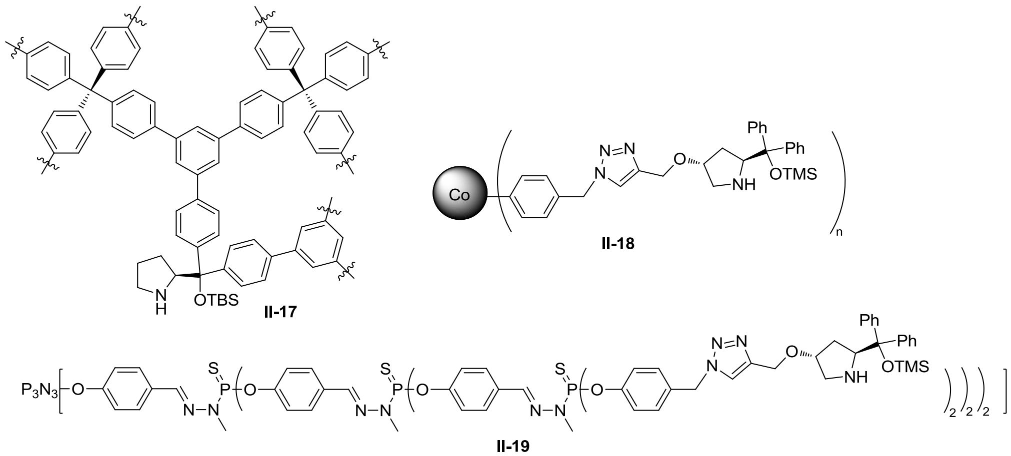

Figure 1. Jørgensen–Hayashi catalysts embedded into a nanoporous polymer

In 2010, the Wang group reported the immobilization of a (S)-diarylprolinol trimethylsilyl ether onto superparamagnetic nanoparticle $Fe_3O_4@SiO_2$ (**II-20**) and applied for the asymmetric Michael addition of aldehydes to nitroalkenes in water, obtaining the desired adducts with moderate to good yields and selectivities (up to 90% ee and 99:1 dr). The NMP-immobilized catalyst **II-20** could be easily separated from the reaction by an external magnet and reused for four cycles.[128] In 2011, our group reported the supporting of (*S*)-α,α-Diphenylprolinol trimethylsilyl ether onto well-defined (5.7 ± 1.1 nm) Fe_3O_4 NMPs (**II-21**). NMPs catalyst **II-21** exhibited high activity, high enantioselectivity and showed to be magnetically recoverable and reusable in the same reactions. The assembly process of nanoparticles and their catalytic use in CH_2Cl_2 solution didn´t cause particle growth or agglomeration. This behavior ensured its high catalytic activity and recyclability (Scheme 3).[129]

[128] Wang, B. G.; Ma, B. C.; Wang, Q.; Wang, W. *Adv. Synth. Catal.* **2010**, *352*, 2923.

[129] Riente, P.; Mendozaa, C.; Pericás, M. A. *J. Mater. Chem.* **2011**, *21*, 7350-7355.

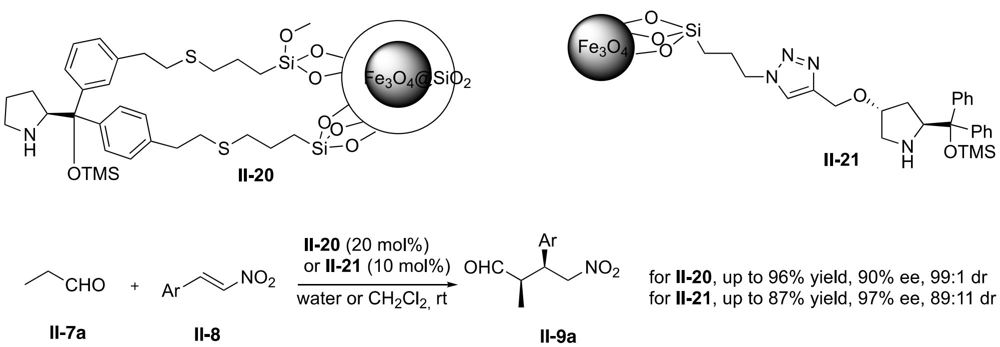

Scheme 3. Jørgensen–Hayashi catalysts supported onto superparamagnetic nanoparticle $Fe_3O_4@SiO_2$ and applied for the asymmetric Michael addition

Since acetaldehyde is highly volatile and susceptible to oligomerization, it is best used by *in situ* generation from its cyclic trimer, 2,4,6-trimethyl-1,3,5-trioxane (**II-23**), with an acidic catalyst. However, acid catalysts cannot coexist with amine-type organocatalysts because of mutual deactivation. By taking advantage of the properties inherent to immobilized species, our laboratory proposed a new approach for combining two otherwise incompatible catalysts, using a tea bag to hold the polymer-immobilized sulfonic acid catalyst, physically separating in this manner the acidic species (**II-22**) from the chiral amine organocatalyst (**II-6**). With the polymeric sulfonic acid in the tea bag, trioxane was easily decomposed to form acetaldehyde, whose enamine gave Michael adducts **II-24** in good yields with excellent enantioselectivities (Scheme 4).[130]

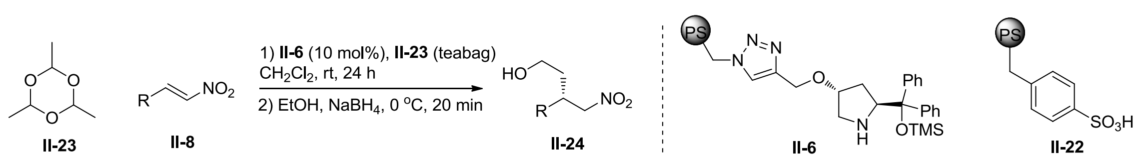

Scheme 4. Immobilized Jørgensen–Hayashi catalysts working with polymeric sulfonic acid in the tea bag for the Michael addition

[130] Fan, X.; Rodriguez-Escrich, C.; Sayalero, S.; Pericas, M. A. *Chem. -Eur. J.* **2013**, *19*, 10814-10817.

In 2014, our laboratory reported two hybrid magnetic materials which were prepared from κ-carrageenan and Fe_3O_4 nanoparticles and exhibited good reactivities and selectivities in the Michael addition of aldehydes to nitroalkenes. After the reaction process was completed, the catalysts could be conveniently retrieved from the reaction mixture by simple magnetic decantation. (Scheme 5)[131]

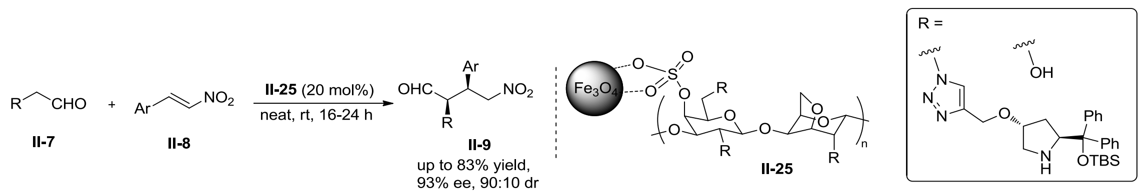

Scheme 5. Immobilized Jørgensen–Hayashi catalysts onto κ-carrageenan and Fe3O4 nanoparticles **25** and use in the Michael addition of aldehydes to nitroalkenes

In 2016, our laboratory reported the synthesis of six solid-supported diarylprolinol catalysts and applied them to the enantioselective cyclopropanation reactions. Among those prepared catalysts, **II-26** afforded excellent results and exhibited remarkable robustness under the conditions of the cyclopropanation reaction. The use of **II-26** allowed the implementation of a long flow experiment (48 h) and could be adapted to the generation of a library of 12 different cyclopropanes by sequential flow experiments. (Figure 2)[132]

[131] Mak, C. A.; Ranjbar, S.; Riente, P.; Rodríguez-Escrich, C.; Pericàs, M. A. *Tetrahedron* **2014**, *70*, 6169-6173.

[132] Llanes, P.; Rodríguez-Escrich, C.; Sayalero, S.; Pericàs, M. A. *Org. Lett.* **2016**, *18*, 6292-6295.

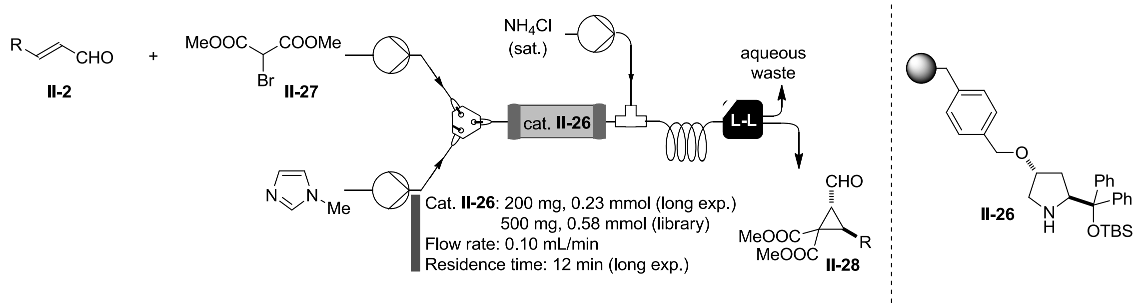

Figure 2. Continuous flow asymmetric cyclopropanation.

2.2 Isoxazolidines

Isoxazolidines are valuable chiral building blocks that can be easily converted to γ-amino alcohols, β-lactams and β-amino acids, important scaffolds for chemical and biological applications.[133] This has prompted several authors to develop novel asymmetric methods for their preparation. For instance, in 2000, the MacMillan group reported an imidazolidinone-catalyzed enantioselective synthesis of isoxazolidines that relied on 1,3-dipolar cycloaddition reactions of an iminium ion intermediate.[134] This represented the first example of a chiral organocatalyst catalyzed 1,3-dipolar cycloaddition.

---

[133] a) Chiacchio, U.; Rescifina, A.; Corsaro, A.; Pistarà, V.; Romeo, G.; Romeo, R. *Tetrahedron: Asymmetry* **2000**, *11*, 2045-2048; b) Sibi, M. P.; Liu, M. *Org. Lett.* **2001**, *3*, 4181-4184; c) Lee, H. S.; Park, J. S.; Kim, B. M.; Gellman, S. H. *J. Org. Chem.* **2003**, *68*, 1575-1578; d) Sibi, M. P.; Prabagaran, N.; Ghorpade, S. G.; Jasperse, C. P. *J. Am. Chem. Soc.* **2003**, *125*, 11796-11797; e) Chiacchio, U.; Balestrieri, E.; Macchi, B.; Iannazzo, D.; Piperno, A.; Rescifina, A.; Mastino, A. *J. Med. Chem.* **2005**, *48*, 1389-1394; f) Chiacchio, U.; Rescifina, A.; Iannazzo, D.; Piperno, A.; Romeo, R.; Borrello, L.; Romeo, G. *J. Med. Chem.* **2007**, *50*, 3747-3750; g) Pagar, V. V.; Liu, R. S. *Angew. Chem. Int. Ed.* **2015**, *54*, 4923-4926; h) Diethelm, S.; Carreira, E. M. *J. Am. Chem. Soc.* **2015**, *137*, 6084-6096; i) Berthet, M.; Cheviet, T.; Dujardin, G.; Parrot, I.; Martinez, J. *Chem. Rev.* **2016**, *116*, 15235-15283.

[134] Jen, W. S.; Wiener, J. J.; MacMillan, D. W. *J. Am. Chem. Soc.* **2000**, *122*, 9874-9875.

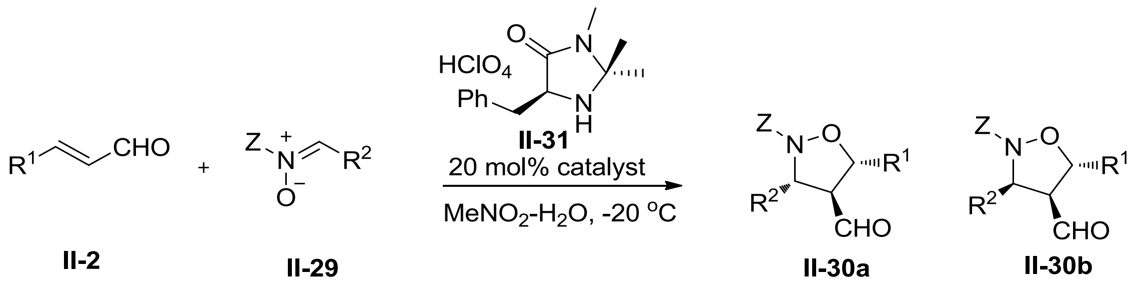

Scheme 6. Imidazolidinone-catalyzed enantioselective synthesis of isoxazolidines

In 2007, Córdova reported α,α-diarylprolinol TMS ether catalyzed asymmetric domino Michael reaction between *N*-protected hydroxylamines and enals,[135] the reaction provided the preparation of 5-hydroxyisoxazolidines and β-amino acids in high yields and highly chemo- and enantioselectivity (Scheme 7, cat. **II-34**). Later in 2016, the Wang group developed a spiro - pyrrolidine catalyst for this asymmetric domino Michael reaction with excellent enantioselectivity (Scheme 7, cat. **II-35**).[136]

In 2010, the Zlotin group reported the using of recoverable α,α-diarylprolinol-derived chiral ionic liquids catalyst for this asymmetric domino Michael reaction. Corresponding adducts were obtained in excellent yields and with moderate to high enantioselectivities. The supported chiral ionic liquids catalyst can be easily recycled and reused for more than four times in this domino reaction (Scheme 7, cat. **II-36**).[137]

---

[135] a) Ibrahem, I.; Rios, R.; Vesely, J.; Zhao, G. L.; Córdova, A. *Chem. Commun.* **2007**, 849-851; b) Ibrahem, I.; Rios, R.; Vesely, J.; Zhao, G. L.; Córdova, A. *Synthesis* **2008**, 1153-1157.

[136] Dou, Q. Y.; Tu, Y. Q.; Zhang, Y.; Tian, J. M.; Zhang, F. M.; Wang, S. H. *Adv. Synth. Catal.* **2016**, *358*, 874-879.

[137] Maltsev, O. V.; Kucherenko, A. S.; Chimishkyan, A. L.; Zlotin, S. G. *Tetrahedron: Asymmetry* **2010**, *21*, 2659-2670.

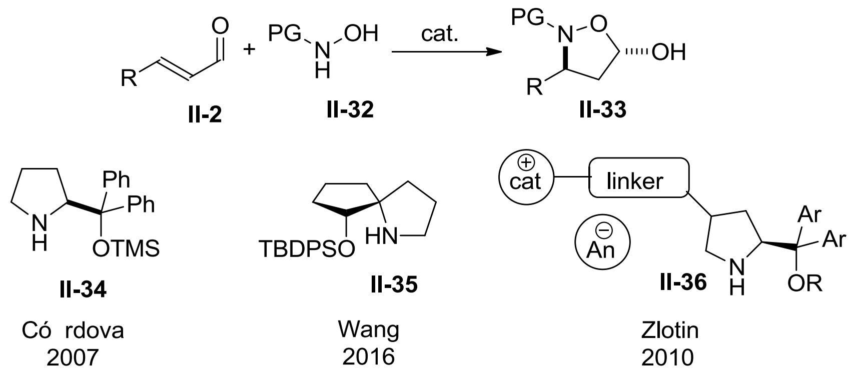

Scheme 7. Asymmetric domino Michael reaction between N-protected hydroxylamines and enals

2.3 Aim of this project

In 2017, our group reported the preparation of a diverse family (37 compounds) of *cis*‐4‐alkoxydiorganylprolinol derivatives starting from trans-4-hydroxyproline. Through the combined use of high-throughput-experimentation (HTE) techniques and Design of Experiments (DoE), the most promising catalysts were identified in the asmmetric *aza*-Michael addition of succinimide to α,β‐unsaturated aldehydes, affording corresponding adducts **II-39** in good yields and excellent enantioselectivities (Scheme 8).[138]

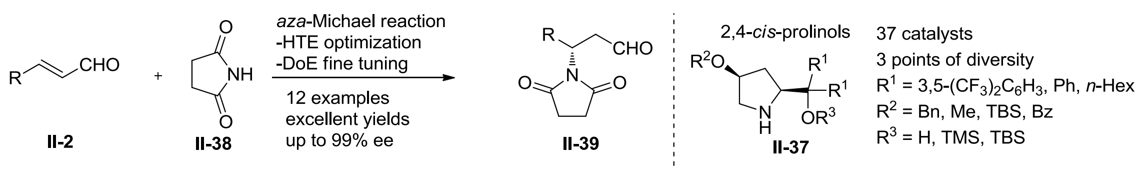

Scheme 8. *Cis*‐4‐alkoxydiorganylprolinol derivatives **II-37** for the enantioselective *aza*-Michael addition of succinimide to α,β‐unsaturated aldehydes

[138] Arenas, I.; Ferrali, A.; Rodríguez-Escrich, C.; Bravo, F.; Pericàs, M. A. *Adv. Synth. Catal.* **2017**, *359*, 2414-2424.

Encouraged by the behavior of the *cis* derivatives, which performed better than their *trans* analogues, we planned to develop immobilized versions of **II-37** and to apply these heterogeneous catalysts in the development of new organocatalytic processes. Thus, in this project, we aim at study the immobilization of *cis*-4-hydroxyprolinol derivatives and establish a direct comparison with the *trans* series we have previously reported in the formation of isoxazolidines.

With this aim in mind, we prepared two members of this family, bearing TMS and TBDMS protecting groups (**II-45a** and **II-45b**), according to the sequence outlined in Scheme 9. With comparison purposes, we decided to evaluate as well the activity in the same process of supported diarylprolinol catalysts previously reported in our group, either having a 2,4-trans array[139] or prepared by co-polymerization of a distyrylprolinol derivative.[140] And the addition of Cbz protected hydroxylamine to cinnamaldehyde as model reaction.

[139] Fan, X.; Sayalero, S.; Pericàs, M. A. *Adv. Synth. Catal.* **2012**, *354*, 2971-2976.

[140] a) Llanes, P.; Rodríguez-Escrich, C.; Sayalero, S.; Pericàs, M. A. *Org. Lett.* **2016**, *18*, 6292-6295; b) Sagamanova, I.; Rodríguez-Escrich, C.; Gábor Molnár, I.; Sayalero, S.; Gilmour, R.; Pericàs, M. A. *ACS Catal.* **2015**, *5*, 6241-6248.

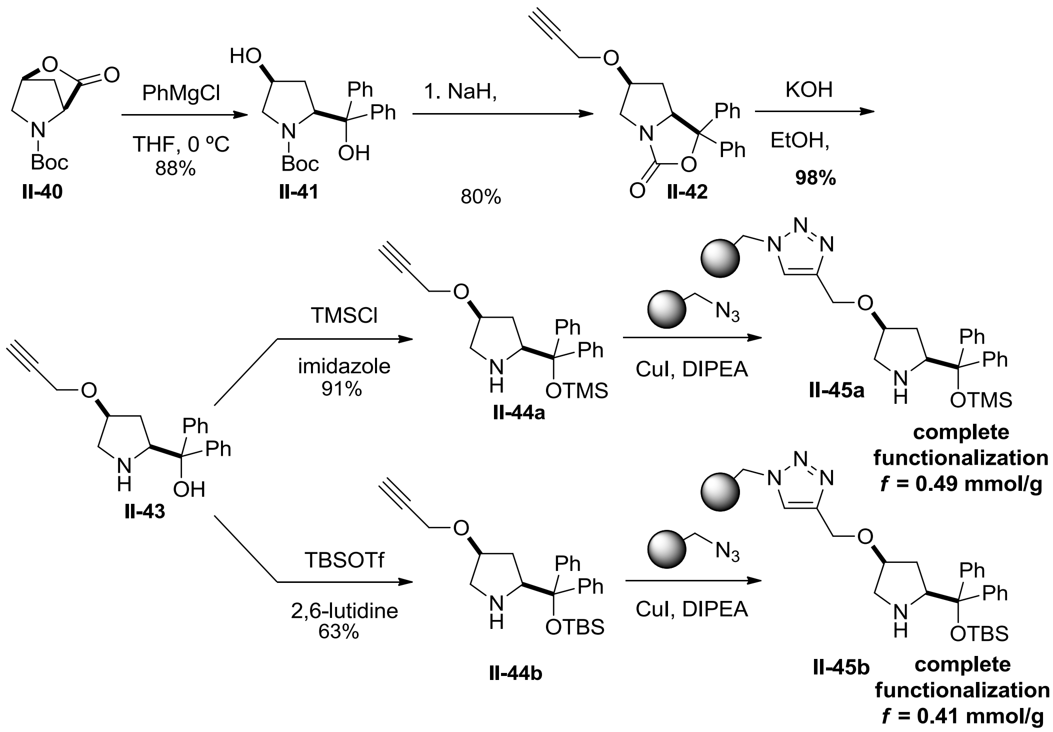

Scheme 9. Synthetic sequence for the preparation of resins **II-45a** and **II-45b**.

This manuscript was later published in Advanced Synthesis & Catalysis. (*Adv. Synth. Catal.* **2018,** *360*, 2914-2924)

Immobilization of *cis*-4-Hydroxydiphenylprolinol Silyl Ethers onto Polystyrene. Application in the Catalytic Enantioselective Synthesis of 5-Hydroxyisoxazolidines in Batch and Flow

Junshan Lai,[a,c] Sonia Sayalero,[a] Alessandro Ferrali,[a] Laura Osorio-Planes,[a] Fernando Bravo,[a] Carles Rodríguez-Escrich,*,[a] and Miquel A. Pericàs*[a,b]

[a] Institute of Chemical Research of Catalonia (ICIQ), The Barcelona Institute of Science and Technology, Av. Països Catalans, 16, 43007 Tarragona (Spain). crodriguez@iciq.es; mapericas@iciq.es; (+34) 977-920-200.

[b] Departament de Química Inorgànica i Orgànica, Universitat de Barcelona (UB), 08028 Barcelona (Spain).

[c] Universitat Rovira i Virgili, Departament de Química Analítica i Química Orgànica, c/Marcel·lí Domingo, 1, 43007 Tarragona, Spain

Abstract. A new family of polystyrene-supported *cis*-4-hydroxydiphenylprolinol has been prepared, and the resulting polymers have been evaluated as organocatalysts to promote the tandem reaction between *N*-protected hydroxylamines and α,β-unsaturated aldehydes in batch and flow. The new PS-supported catalysts compare favorably with well-established immobilized Jørgensen-Hayashi catalysts, affording 5-hydroxyisoxazolidines as single diastereoisomers with high enantioselectivities and good yields (up to 83% yield, up to 99% ee).

Keywords: supported catalysts; organic catalysis; flow chemistry; asymmetric catalysis; isoxazolidines

Introduction

The development of asymmetric catalysis has significantly expanded the toolkit of synthetic chemists when tackling the preparation of optically enriched compounds.[1] The advent of organocatalysis, that arrived to complement biocatalysis and transition metal-based approaches, has provided new opportunities to activate very reactive intermediates in generally mild conditions. a,a-Diarylprolinols, generally known as Jørgensen-Hayashi catalysts, are amongst the most successful aminocatalysts.[2] Their main drawback is the high catalyst loadings usually required as a consequence of unfavourable equilibria and the formation of off-cycle species.[3] To address this issue, our research group, as well as others, have studied their immobilization in an attempt to increase their lifespan.[4] In the cases where the anchoring strategy has proven successful, the resulting solid-supported Jørgensen-Hayashi catalysts display high catalytic activity and selectivity, while being recyclable and even amenable to application in continuous flow.[5]

Recently, we reported the preparation of a family of 37 modular *cis*-4-hydroxyprolinol derivatives starting from *trans*-4-hydroxyproline. The synthesis relied on the intermediacy of the bicyclic lactone depicted in Figure 1 (previously described by Joullié[6]) to invert the stereochemistry at C4. With the help of high-throughput-experimentation (HTE) techniques and Design of Experiments (DoE) we were able identify the most promising catalysts for the *aza*-Michael addition and fine-tune the reaction conditions to optimize yield and enantioselectivity.[6c] Encouraged by the behavior of the *cis*-derivatives, which performed better than their *trans* analogues, we decided to study the immobilization of *cis*-4-hydroxyprolinol derivatives and establish a direct comparison with the *trans* series we have previously reported (Figure 1).

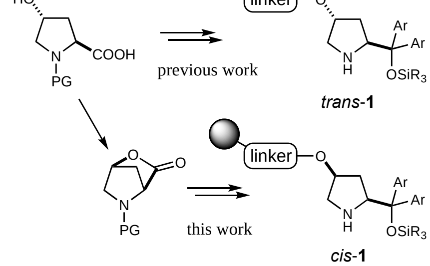

Figure 1. Immobilized *cis*- and *trans*-diarylprolinols.

Isoxazolidines[7] are valuable chiral building blocks that can be easily converted to γ-amino alcohols,[8] β-lactams[9] and β-amino acids,[10,7e,f] important scaffolds for chemical and biological applications. This has prompted several authors to develop novel asymmetric methods for their preparation. For instance, in 2000, MacMillan and co-workers were the first to report an imidazolidinone-catalyzed enantioselective synthesis of isoxazolidines that relied on 1,3-dipolar cycloaddition reactions of an iminium ion intermediate.[11] In 2007, Córdova reported the preparation of 5-hydroxyisoxazolidines mediated by a,a-diarylprolinol TMS ether via an asymmetric domino Michael reaction pathway between *N*-protected hydroxylamines and enals,[12] for which

Wang later employed a spiranic catalyst[13] (Scheme 1). In 2010, Zlotin and co-workers used recoverable α,α-diarylprolinol-derived chiral ionic liquids which could be easily recycled and reused more than four times in this domino reaction.[14] However, to the best of our knowledge, the asymmetric organocatalytic synthesis of 5-hydroxyisoxazolidines in flow remains unexplored.

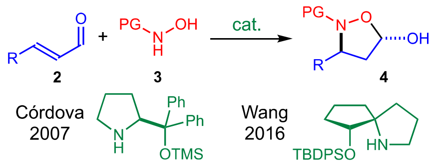

Scheme 1. Organocatalytic isoxazolidine formation.

When dealing with supported catalysts, besides the type of monomer and the immobilization strategy, the choice of solid phase is crucial because poor mechanical stability of non-properly selected supports can counterbalance the putative advantages of easy recycling and reuse.[15] In our experience, polystyrene resins have proven reliable in terms of thermal and mechanical stability. In this context, the implementation of flow processes entails a further advantage because, once the resin is packed, the beads are not shaken nor stirred. In light of the above-mentioned, we thought the addition of hydroxylamine derivatives to enals catalyzed by immobilized diarylprolinol derivatives would be a good benchmark to assess the relative merits of the *cis* and *trans* series both in batch and flow.

Results and Discussion

In order to establish the catalytic behavior of the supported *cis*-diarylprolinols, we prepared two members of this family, bearing TMS and TBDMS protecting groups, according to the sequence outlined in Scheme 2. First, lactone **5**[6] was treated with phenylmagnesium chloride to generate the 2,4-*cis* diphenylprolinol derivative **6**. Propargylation of the secondary alcohol took place with concomitant oxazolidinone formation and the product **7** was then hydrolyzed to the amino alcohol **8**. This intermediate was protected as a TMS (**9**) or TBS (**10**) ether which, after immobilization via azide-alkyne cycloaddition with azidomethyl-polystyrene, gave rise to resins **1b** and **1c**, respectively with full functionalization.

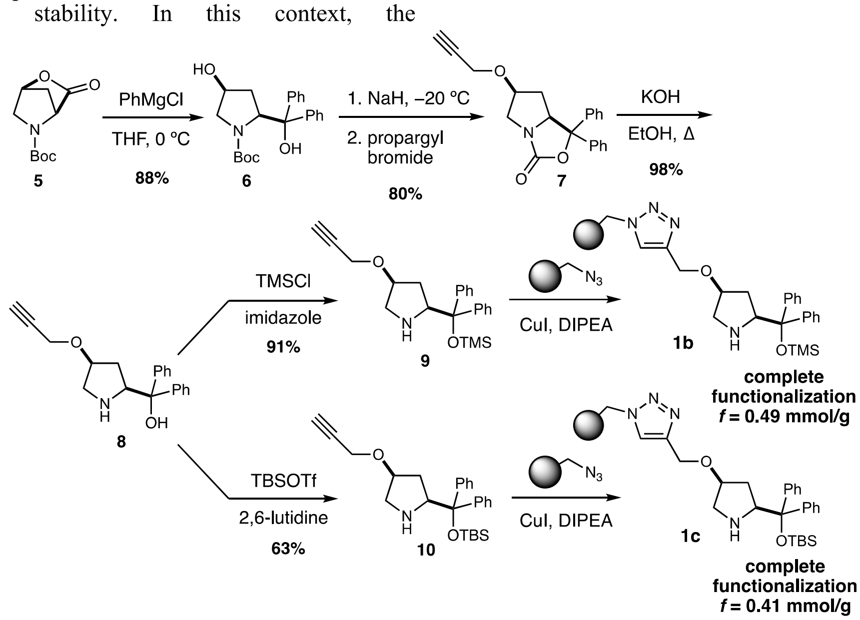

Scheme 2. Synthetic sequence for the preparation of resins **1b** and **1c**.

For the sake of comparison, we decided to evaluate as well the activity of supported diarylprolinol catalysts previously reported in our group, either having a 2,4-*trans* array[5c] (**1d**) or prepared by co-polymerization of a distyrylprolinol derivative[5e,16] (**1e,f**). Finally, homogeneous *cis*-**1g** would also tested in an attempt to assess the impact of the triazole linker.

Thus, the stage was set to run a comparative study of catalysts **1a-1g** (Table 1), placing special emphasis on the stereochemistry at C4. The model reaction selected was the addition of protected hydroxylamine **3a** to cinnamaldehyde **2a**, which afforded chiral 5-hydroxyisoxazolidine **4aa** via a tandem sequence consisting of aza-Michael addition followed by hemiacetalization. Preliminary tests run with **1b** established $CHCl_3$ and rt as a good starting point to optimize reaction conditions (see SI for details).

Table 1. Solid-supported catalyst screening for the enantioselective formation of isoxazolidines.

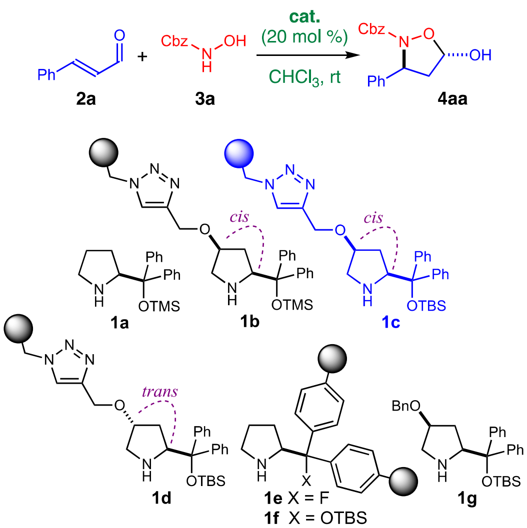

Entry[a)]	Cat.	time (h)	Conv. (%)	Yield (%)	ee (%)
1	**1a**	6	99	65	89
2	**1b**	6	99	80	90
3	**1c**	**7**	**100**	**76**	**95**
4	**1d**	7	98	71	92
5	**1e**	18	100	74	76
6	**1f**	18	97	68	95
7	**1g**	6	98	70	93

[a)] Conversion and yield determined by ^{1}H NMR using mesitylene as an internal standard; for the functionalization level of catalysts, see SI.

According to literature precedents,[12] diarylprolinol TMS ether **1a** proved competent in this reaction (entry 1). In comparison, the supported catalysts from the novel 2,4-*cis* series **1b** and **1c** (bearing a TMS and a TBS group, respectively; entries 2 and 3) displayed improved activity and enantioselectivity. Interestingly, the results were also better than those recorded for the *trans* analog **1d** (entry 4). A direct comparison between **1c** and **1d**, which differ only on the relative stereochemistry of the pyrrolidine 2,4 substituents allows to establish the superiority of the *cis*-derivatives over the *trans* ones, at least for this reaction. Then, the two catalysts prepared by co-polymerization of a distyrylprolinol were submitted to the reaction conditions: **1e** (with a fluorine; entry 5) gave moderate enantioselectivity, whereas **1f**, bearing a silyl ether (entry 6), matched the ee's of **1c**, albeit with a slightly lower activity. Finally, an homogeneous analogue of **1c**, without the triazole (**1g**[6c] entry 7) was shown to behave similarly in terms of yield and selectivity, which points out to a steric rather than electronic effect of the linker. In summary, the catalyst of choice for this reaction is **1c**, with a *cis*-2,4 arrangement and a TBS group.

During the investigation of this tandem reaction, we found that the addition of acid had a significant impact on the reaction rate and selectivity, leading in most cases to full conversions in shorter times (Scheme 3).[17] While strong acids like TFA or TsOH completely shut down the catalytic activity, with less acidic co-catalysts the ee value increased (acids **11c-e**) and full conversion was reached in 6 h. Among all carboxylic acids tested, cinnamic acid turned out to give the best enantioselectivity in $CHCl_3$. Because of the toxicity of $CHCl_3$ which may limit the utilization of the immobilized diarylprolinol in flow, we carried out a similar screening in CH_2Cl_2 (see SI). In this solvent, benzoic and cinnamic acid behave similarly; given that the former is inexpensive, we established a second set of conditions involving CH_2Cl_2 and benzoic acid as an additive.

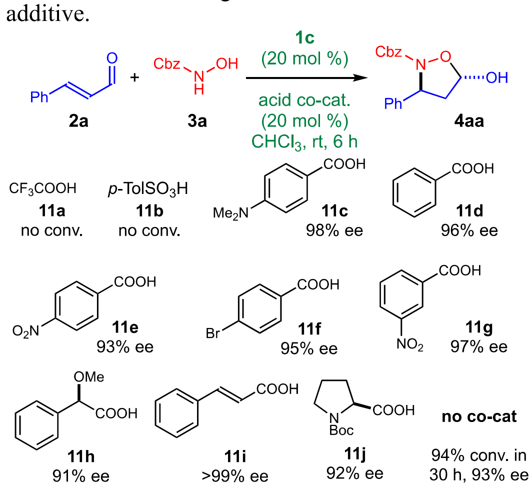

Scheme 3. Screening of the acidic co-catalyst. [a)] Conv. determined by ^{1}H NMR using mesitylene as internal standard; full conversion recorded with acids **11c-11j** in 6 h.

Thus, we decided to investigate the scope of the catalytic asymmetric tandem reaction in batch using immobilized diarylprolinol **1c** with cinnamic acid as additive in $CHCl_3$ (Scheme 4, conditions A) or benzoic acid as additive in CH_2Cl_2 (Scheme 4, conditions B), in both cases at room temperature. Indeed, β-substituted enals provided the corresponding 5-hydroxyisoxazolidines **4** as single diastereoisomers with high enantioselectivities and moderate to good yields (34-83% yield, 71–99% ee). Moreover, the reactions with *N*-Boc-NHOH **3b** gave the corresponding products in 51–74% yield and in 71–99% ee. Cinnamaldehyde and its derivatives containing halogen atoms (F or Cl) or a nitro group at the *para*-position of the aromatic ring afforded the desired isoxazolidines in a short time. Introduction of a group in the *ortho*-position or the presence of a methoxy group at the *para*-position slowed down the reaction.

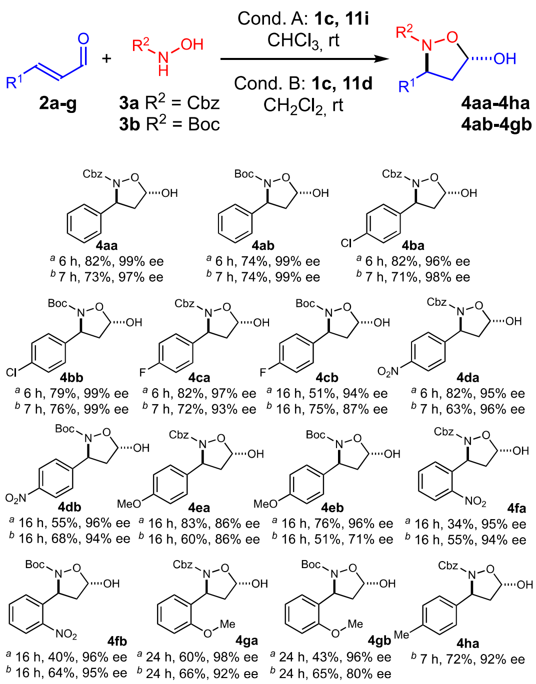

Scheme 4. Scope of the catalytic reaction in batch. [a)] Reaction conditions: **2** (0.05 mmol, 1 eq.), **3** (10 mg, 0.06 mmol, 1.2 eq.), **1c** (23 mg, 20 mol %), **11i** (1.5 mg, 20 mol %), $CHCl_3$ (0.25 mL), rt. [b] Reactions run in CH_2Cl_2 (0.5 mmol of **2**) with **11d** (12 mg, 20 mol %) as co-catalyst.

The good results recorded prompted us to study the recyclability of the catalyst in batch. To our delight, the reaction between **2a** and **3a** catalyzed by **1c** could be run for 10 consecutive cycles after simply filtering and recovering the resin. As shown in Table 2, the results obtained in the tenth cycle match those recorded in the initial one, which bears witness of the catalyst robustness. Indeed, the accumulated TON in these ten runs was 36.5.

Encouraged by the robustness of the supported catalyst, a family of α,β-unsaturated aldehydes was submitted to the flow process with **3a** or **3b** as reaction partners (Scheme 5). To this end, a packed bed reactor was filled with catalyst **1c** (1.00 g, 0.41 mmol) and two channels were used to feed the reagents through the system. Due to compatibility issues, the first contained a solution of **2** while the second had a mixture of hydroxylamine **3** and benzoic acid (**11d**); the use of a single syringe pump equipped with two syringe slots ensured that both flow rates were equal. For each experiment, 9.84 mmol of **2** were passed through the packed bed reactor, at a combined flow rate of 100 µL min^{-1}. When the solutions of starting materials were consumed, the column was rinsed with CH_2Cl_2 to remove all organic products.

Table 2. Study of the catalyst recyclability.

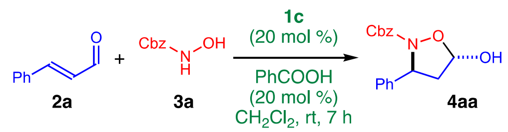

Run	Conv. (%)	Yield (%)	ee (%)
1	98	73	94
2	97	79	95
3	97	89	95
4	97	80	96
5	96	71	95
6	97	68	96
7	97	65	96
8	96	72	96
9	92	64	96
10	91	69	96

With this sequential approach, up to ten different 5-hydroxyisoxazolidines were prepared with excellent enantioselectivities and moderate to good yields. As shown in Scheme 5, cinnamaldehyde and its electron poor derivatives afforded the corresponding products in good yields and excellent ee's working at 100 µL min^{-1}. On the other hand, the slower kinetics observed for **2e** forced us to lower the flow rate to 50 µL min^{-1}; under these conditions, even if the yields were not fully satisfactory, the enantioselectivities remained excellent. Overall, the accumulated TON in these flow processes was of 134. Remarkably, the same packed bed reactor was used for all the flow experiments (preliminary runs and scope), carried out within a period of 2 months without apparent decrease in performance.

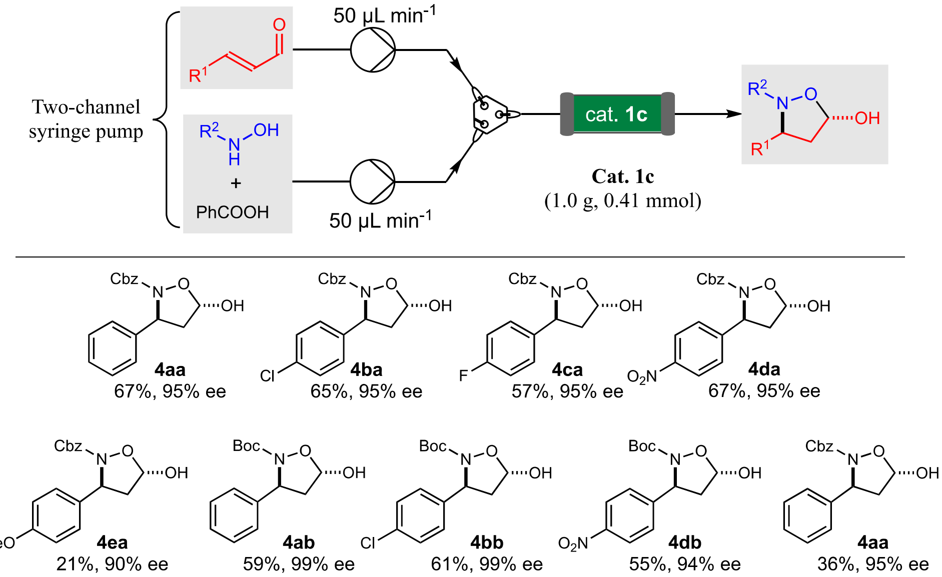

Scheme 5. Set-up and results of the continuous flow reaction promoted by **1c**.

The synthetic versatility of the products was demonstrated by taking the crude mixture from one of the reactions and submitting it to oxidation to furnish isoxazolidinone **12** (Scheme 6). Even more interestingly, this could be reduced to a β-amino acid in a continuous flow experiment carried out with a H-cube reactor (90 atm of H_2, 0.5 mL min^{-1}, 50 °C) that involved N-O bond reduction and hydrogenolysis of the Cbz protecting group. Remarkably, this allows the generation of enantioenriched β-amino acids in only three steps, two of which are carried out in a continuous flow manner. Moreover, the use of the H-cube enables to carry out the reduction without a bottle of gaseous hydrogen (it is generated in situ from water), which greatly improves the safety profile of the procedure.

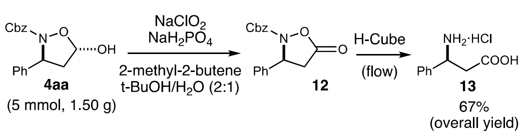

Scheme 6. Derivatization of Product **4aa**.

Conclusion

In summary, a solid-supported organocatalyst has been applied to the enantioselective domino reaction between α,β-unsaturated aldehydes and *N*-protected hydroxylamines in batch and flow. Immobilized diarylprolinol **1c**, has afforded the best results while proving remarkably stable under the reaction conditions. This has allowed to run ten consecutive cycles of the same reaction, providing the same enantioselectivity and without significant loss of yield. In addition, eleven flow experiments involving nine different substrates have been carried out over a period of 2 months with the same packed column. Finally, a sequence consisting of oxidation and continuous flow hydrogenation allowed the preparation of β-amino acids, thus proving the synthetic potential of this methodology.

Experimental Section

Preparation of immobilized 2,4-*cis*-diarylprolinols 1b,1c

A solution of the lactone **5**[6] (1.377 g, 6.46 mmol) in dry THF (38 ml) under Ar was cooled to 0 °C and PhMgCl (2.0 M in THF, 6.5 ml, 12.92 mmol) was added dropwise. The mixture was stirred for 2 h (conversion was checked by TLC). Then, the reaction mixture was quenched with aq. sat. NH_4Cl (50 mL), the layers were separated, the aqueous phase was extracted with TBME (3 x 40 mL) and dried over Na_2SO_4. Purification by flash column chromatography (Cy/EtOAc 80:20 - 70:30 - 65:35 - 60:40) gave 2.11 g of product **6** (88% yield).

tert*-Butyl (2*S*,4*S*)-4-hydroxy-2-(hydroxydiphenylmethyl)pyrrolidine-1-carboxylate (6)**. White solid. **Melting point**: 197.3-199.5. ***Rf: 0.30 (Cy/EtOAc 60:40). **[α]$_D^{25}$** = +122.3 (*c* 1.00, DCM). **^{1}H NMR** (400, $CDCl_3$): δ = 7.52-7.48 (m, 2H), 7.41-7.35 (m, 4H), 7.33-7.28 (m, 1H), 7.26-7.17 (m, 3H), 4.92 (d, *J* = 9.1 Hz, 1H), 4.54 (br s, 1H), 4.35 (br s, 1H), 4.20-3.70 (br s, 2H), 3.33 (br s, 1H), 2.30 (ddd, *J* = 14.6, 9.3, 7.6 Hz, 1H), 1.82 (d, *J* = 14.6 Hz, 1H), 1.14 (br s, 9H). **^{13}C NMR** (100.4, $CDCl_3$): δ = 154.8, 145.0, 144.7, 128.2 (2C), 127.8 (2C), 127.2, 127.1 (3C), 126.9 (2C), 81.4, 79.7, 70.1, 64.7, 57.1, 38.2, 27.9 (3C). **HRMS** (ESI+): calcd for $C_{22}H_{27}NNaO_4$ [M+Na]$^+$: 392.1832, found: 392.1840.

A suspension of NaH (60% in mineral oil, 0.200 g, 5.0 mmol) in 9 mL of anhydrous DMF under N_2 was cooled to –25 °C (internal temperature) and a solution of alcohol **6** (0.924 g, 2.5 mmol) in 7 mL of DMF was added dropwise. The mixture was stirred at this temperature for 20 min and then propargyl bromide (80% in toluene, 0.28 mL, 2.5 mmol) was added dropwise. The resulting mixture was stirred at 0 °C for 1 h and then brought to RT. When TLC analysis showed complete conversion of the starting material, 35 mL of NH_4Cl were added and it was extracted with EtOAc (3 × 60 mL). the combined organic phases were dried over Na_2SO_4 and concentrated in vacuo. Purification by flash column chromatography (Cy/EtOAc 90:10 to 60:40) gave the propargylated derivative **7** in 80% yield (0.668 g, 2.00 mmol) as a white solid.

(6*S*,7a*S*)-1,1-Diphenyl-6-(prop-2-yn-1-yloxy)tetrahydro-1H,3H-pyrrolo[1,2-c]oxazol-3-one (7). White solid. **Melting point**: 140.0-141.8. ***Rf***: 0.27 (Cy/EtOAc 70:30). **[α]$_D$^{25}** = −209.8 (*c* 1.00, DCM). **^{1}H NMR** (400, $CDCl_3$): δ = 7.53-7.48 (m, 2H), 7.38-7.25 (m, 8H), 4.64 (dd, *J* = 9.0, 7.1 Hz, 1H), 4.41 (qd, *J* = 5.9, 3.2 Hz, 1H), 4.04 (dd, *J* = 16.1, 2.4 Hz, 1H), 3.96 (dd, *J* = 16.1, 2.4 Hz, 1H), 3.89 (dd, *J* = 12.6, 3.2 Hz, 1H), 3.30 (dd, *J* = 12.6, 5.9 Hz, 1H), 2.39 (t, *J* = 2.4 Hz, 1H), 2.09 (ddd, *J* = 13.4, 7.1, 6.2 Hz, 1H), 1.42 (dddd, *J* = 13.5, 9.1, 5.4, 0.8 Hz, 1H). **^{13}C NMR** (125.0, $CDCl_3$): δ = 160.3, 143.2, 139.9, 128.6 (2C), 128.4 (2C), 128.3, 127.8, 126.0 (2C), 125.7 (2C), 86.2, 79.0, 78.0, 74.9, 67.4, 56.3, 52.0, 35.5. **HRMS** (ESI+): calcd. for $C_{21}H_{19}NNaO_3$ [M+Na]$^+$: 356.1257, found: 356.1251.

A solution of the oxazolidinone **7** (503 mg, 1.51 mmol) in EtOH (11 mL) was treated with a solution of KOH (423 mg, 7.54 mmol) in water (0.8 M). The mixture was heated at reflux overnight turning from a slurry to a clear yellowish solution. The next morning, TLC analysis (Cy/EA 50:50) shows that the starting material has disappeared, so the reaction mixture is concentrated in vacuo. The resulting slurry is diluted with water, extracted with EtOAc (3 × 25 mL), dried over Na_2SO_4 and evaporated. Purification by flash column chromatography gave 456 mg (1.51 mmol) of the amino alcohol **8** (98%).

Diphenyl((2*S*,4*S*)-4-(prop-2-yn-1-yloxy)pyrrolidin-2-yl)methanol (8). Colourless oil. **[α]$_D$^{25}** = −44.5 (*c* 1.00, DCM). **^{1}H NMR** (400 MHz, $CDCl_3$): δ = 7.62-7.56 (m, 2H), 7.53-7.47 (m, 2H), 7.32-7.25 (m, 4H), 7.20-7.14 (m, 2H), 4.32 (dd, *J* = 8.2, 7.1 Hz, 1H), 4.23 (dddd, *J* = 6.1, 5.1, 3.7, 2.3 Hz, 1H), 4.15 (dd, *J* = 15.9, 2.4 Hz, 1H), 4.08 (dd, *J* = 15.9, 2.4 Hz, 1H), 3.16 (ddd, *J* = 10.9, 2.3, 1.4 Hz, 1H), 3.04 (dd, *J* = 10.9, 5.1 Hz, 1H), 2.38 (t, *J* = 2.4 Hz, 1H), 1.90 (ddd, *J* = 14.4, 8.2, 6.3 Hz, 1H), 1.80 (dddd, *J* = 14.1, 7.1, 3.7, 1.4 Hz, 1H). **^{13}C NMR** (100.4 MHz, $CDCl_3$): δ = 147.2, 145.4, 128.2 (2C), 128.0 (2C), 126.5, 126.4, 125.9 (2C), 125.5 (2C), 79.7, 77.6, 76.9, 74.2, 63.8, 55.8, 51.9, 32.6. **HRMS** (ESI+): calcd for $C_{20}H_{22}NO_2$ [M+H]$^+$: 308.1645, found: 308.1641.

A solution of the amino alcohol **8** (250 mg, 0.813 mmol) in CH_2Cl_2 (8133 µl) was cooled to 0 °C. Then, imidazole (166 mg, 2.440 mmol) and chlorotrimethylsilane (258 µl, 2.033 mmol) were sequentially added. The solution was then allowed to reach 0 °C and stirred at this temperature for 3 h. Then, it was quenched with water and the aqueous layer was extracted with EtOAc (3 x 20 mL). The combined organic extracts were dried over Na^2SO^4 and concentrated under reduced pressure. Flash chromatography on silica gel with 2.5% Et_3N (Cy/EtOAc 50:50) afforded 282 mg of the silylated product **9** (91% yield, 0.813 mmol).

(2*S*,4*S*)-2-(Diphenyl((trimethylsilyl)oxy)methyl)-4-(prop-2-yn-1-yloxy)pyrrolidine (9). Colourless oil. ***R$_f$***: 0.42 (Cy/EtOAc 80:20). **[α]$_D$^{25}** = −50.0 (*c* 1.00, DCM). **^{1}H NMR** (400 MHz, $CDCl_3$): δ = 7.51-7.47 (m, 2H), 7.35-7.31 (m, 2H), 7.29-7.18 (m, 6H), 4.14 (dtd, *J* = 6.7, 5.2, 3.0 Hz, 1H), 3.98 (dd, *J* = 15.8, 2.4 Hz, 1H), 3.92 (dd, *J* = 15.8, 2.4 Hz, 1H), 3.89 (dd, *J* = 9.3, 6.9 Hz, 1H), 3.01 (ddd, *J* = 12.0, 3.1, 1.0 Hz, 1H), 2.94 (dd, *J* = 12.0, 5.6 Hz, 1H), 2.34 (t, *J* = 2.4 Hz, 1H), 1.82 (br s, 1H), 1.74 (dt, *J* = 13.5, 6.9 Hz, 1H), 1.58 (dddd, *J* = 13.5, 9.4, 4.9, 1.0 Hz, 1H), −0.08 (s, 9H). **^{13}C NMR** (100.4 MHz, $CDCl_3$): δ = 146.8, 145.2, 128.7 (2C), 127.7 (2C), 127.6 (2C), 127.2 (2C), 127.1, 126.8, 82.4, 80.0, 78.6, 73.8, 65.8, 55.8, 53.2, 34.6, 2.1 (3C). **HRMS** (ESI+): calcd. for $C_{23}H_{30}NO_2Si$ [M+H]$^+$: 380.2040, found: 380.2050.

Azidomethylpolystyrene (*f* = 0.60, 5.90 g, 3.52 mmol) was suspended in DMF (53 ml) and THF (53 ml). Then, DIPEA (6.1 ml, 35.2 mmol) and copper(I) iodide (34 mg, 0.176 mmol) were added, followed by a solution of the alkyne **9** (1.61 g, 4.23 mmol) in the same solvent mixture (via cannula). The resulting mixture was shaken overnight at 40 ºC. The next morning, after checking a small aliquot by IR to confirm full conversion, the resin **1b** was filtered and washed with water, water/MeOH, MeOH, MeOH/CH_2Cl_2 and CH_2Cl_2. Then, it was dried overnight in the vacuum oven at 40 °C.

f_{max} = 0.49; *f* = 0.49 (based on N Elemental Analysis). Complete functionalization.

A solution of the diphenylprolinol derivative **8** (350 mg, 1.139 mmol) in DCE (5.5 mL) under Ar was cooled to 0 °C and treated with 2,6-lutidine (1.05 mL, 9.11 mmol) and TBSOTf (1.05 mL, 4.55 mmol). Then, it was heated at reflux overnight under vigorous stirring. The next morning, the reaction mixture was quenched with sat. aq. NH_4Cl (25 mL) and the aqueous layer was extracted with CH_2Cl_2 (3 × 25 mL). The combined organic extracts were dried over Na_2SO_4 and concentrated under reduced pressure. Purification by flash chromatography on silica gel with 2.5% Et_3N (Cy/EtOAc 90:10) gave silyl ether **10** in 63% yield (302 mg, 1.14 mmol).

(2*S*,4*S*)-2-(((*tert*-Butyldimethylsilyl)oxy)diphenylmethyl)-4-(prop-2-yn-1-yloxy)pyrrolidine (10). yellow oil. ***R$_f$***: 0.28 (Cy/EtOAc 80:20). **[α]$_D$^{25}** = −33.3 (*c* 1.00, DCM). **^{1}H NMR** (400 MHz, $CDCl_3$): δ = 7.61-7.55 (m, 2H), 7.38-7.32 (m, 2H), 7.32-7.22 (m, 6H), 4.13 (dtd, *J* = 6.8, 5.0, 3.2 Hz, 1H), 3.95 (dd, *J* = 15.8, 2.4 Hz, 1H), 3.89 (dd, *J* = 15.8, 2.4 Hz, 1H), 3.88 (dd, *J* = 9.5, 7.0 Hz, 1H), 2.99-2.89 (m, 2H), 2.34 (t, *J* = 2.4 Hz, 1H), 1.92 (br s, 1H), 1.77 (dt, *J* = 13.6, 6.9 Hz, 1H), 1.56 (ddd, *J* = 13.6, 9.7, 4.7 Hz, 1H), 0.99 (s, 9H), −0.12 (s, 3H), −0.51 (s, 3H). **^{13}C NMR** (100.4 MHz, $CDCl_3$): δ = 146.5, 144.8, 129.5, 127.7 (2C), 127.6 (2C), 127.4 (2C), 127.3 (2C), 126.9, 82.2, 80.0, 78.5, 73.7, 66.1, 55.7, 53.2, 35.0, 26.3 (3C), 19.1, −2.5, −3.6. **HRMS** (ESI+): calcd for $C_{26}H_{36}O_2$ [M+H]$^+$: 422.2510, found: 422.2513.

Azidomethylpolystyrene (*f* = 0.509, 6 g, 3.05 mmol) was suspended in DMF (46 ml) and THF (46 ml). Then, DIPEA (5.3 ml, 30.5 mmol) and copper(I) iodide (29 mg, 0.153 mmol) were added, followed by a solution of the alkyne (1.545 g, 3.66 mmol) in the same solvent mixture (via cannula). The resulting mixture was shaken overnight at 40 ºC. The next morning, after checking a small aliquot by IR to confirm full conversion, the resin **1c** was filtered and washed with water, water/MeOH, MeOH, MeOH/CH_2Cl_2 and CH_2Cl_2. Then, it was dried overnight in the vacuum oven at 40 °C.

f_{max} = 0.42; *f* = 0.41 (based on N Elemental Analysis). Complete functionalization.

General Procedures for the Batch Experiments

Conditions A

To a 2 mL glass vial were sequentially added PS-catalyst **1c** (*f* = 0.41 mmol/g, 0.01mmol, 23 mg, 20 mol % loading), 0.25 mL $CHCl_3$ and **11i** (1.5 mg, 20 mol %), followed by **2** (1 eq., 0.05 mmol) and **3** (1.2 eq., 0.06 mmol) at room temperature. The reaction mixture was shaken until TLC analysis showed consumption of the enal (for reaction times, see Scheme 4). Then, it was filtered and the resin beads were washed with DCM (5 x 0.25 mL). The solvent was concentrated under reduced pressure and the product was isolated after purification by column chromatography on silica gel with cyclohexane/ethyl acetate (EtOAc/*c*-Hex = 1:5) to yield **4**.

Conditions B

To a 5 mL glass vial were sequentially added PS-catalyst **1c** (*f* = 0.41 mmol/g, 0.1 mmol, 232 mg, 20 mol % loading), 2.5 mL CH_2Cl_2 and **11d** (12 mg, 0.1mmol, 20 mol %), followed by **2** (1 eq., 0.5 mmol) and **3** (1.2 eq., 0.6 mmol) at room temperature. The reaction mixture was shaken until TLC analysis showed consumption of the enal (for reaction times, see Scheme 4). Then, it was filtered and the resin beads were washed with DCM (8 x 1.5 mL). The solvent was concentrated under reduced pressure and the product was isolated after purification by column chromatography on silica gel with cyclohexane/ethyl acetate (EtOAc/*c*-Hex = 1:5) to yield **4**.

General Procedure for the Flow Experiments

Using the set-up depicted in Scheme 5, the packed bed reactor (Omnifit glass column, 10 mm Ø) was filled with 1.0 g of catalyst **1c**, which was swollen by pumping CH_2Cl_2 at 0.1 mL min^{-1} for one hour. The reagents were then introduced in the system in two separate streams (50 μL min^{-1} each unless otherwise stated) using a dual syringe pump: (a) containing **2** (0.4 M, 1.0 eq) in 21.5 mL of CH_2Cl_2 and (b) containing a mixture of **3** (0.48 M, 1.2 eq.) and PhCOOH in 21.5 mL of CH_2Cl_2. When the solutions of reagents were consumed, the packed bed reactor was rinsed with CH_2Cl_2 at 0.1 mL min^{-1} for 2 h. The collected outstream was concentrated under reduced pressure and purified by column chromatography on silica gel with cyclohexane/ethyl acetate (EtOAc/*c*-Hex 1:5) to yield the corresponding product **4**.

Preparation of b-Amino Acid Hydrochloride 13

To a 25 mL round-bottom flask were sequentially added **4aa** (1.50 g, 5 mmol), *tert*-butanol (8 mL), H_2O (4 mL), 2-methylbut-2-ene (2 mL), KH_2PO_4 (1088 mg, 8 mmol), $NaClO_2$ (720 mg, 8 mmol). The reaction mixture was stirred at room temperature for 16 h and then it was washed with saturated Na_2SO_3 and concentrated under reduced pressure. The residue obtained was dissolved in MeOH (200 mL), filtered to remove insoluble material and circulated through the H-Cube at 0.5 mL min^{-1} flow rate (90 atm, 50 ºC). The outstream collected was concentrated in vacuo and the residue was washed with 2 M HCl in diethyl ether (10 mL), then with diethyl ether (5 x 10 mL), to give hydrochloride **13** in 67% yield (673 mg, 3.35 mmol).

Compound Characterization Data

Benzyl (3*S*,5*S*)-5-hydroxy-3-phenylisoxazolidine-2-carboxylate (4aa).[12] ^{1}H NMR (400 MHz, $CDCl_3$) δ 7.37-7.17 (m, 10H), 5.91 (d, *J* = 4.4 Hz, 1H), 5.38 (t, *J* = 8.2 Hz, 1H), 5.17 (s, 2H), 2.79 (dd, *J* = 12.6, 8.4 Hz, 1H), 2.30 (ddd, *J* = 12.6, 8.2, 4.5 Hz, 1H). ^{13}C NMR (101 MHz, $CDCl_3$) δ 159.3, 141.4, 135.6, 128.6 (x2), 128.4 (x2), 128.1, 127.7 (x2), 127.4, 126.0 (x2), 98.8, 68.1, 61.3, 45.3. IR (neat): 3362, 3063, 3032, 2860,1707, 1496, 1453, 1390, 1301, 1238, 1027, 902, 754, 696 cm^{-1}. $[\alpha]_D^{25}$ = –29.5 (*c* = 1.0, $CHCl_3$). HPLC (Daicel Chiralpak AD-H, hexane/*i*-PrOH = 90:10, flow rate 1.0 mL/min, λ = 210 nm): major isomer: t_R = 13.2 min; minor isomer: t_R = 15.3 min.

***tert*-Butyl (3*S*,5*S*)-5-hydroxy-3-phenylisoxazolidine-2-carboxylate (4ab).**[12] ^{1}H NMR (400 MHz, $CDCl_3$) δ 7.34 (d, *J* = 4.4 Hz, 4H), 7.26 (dd, *J* = 8.2, 4.5 Hz, 1H), 5.92 (d, *J* = 4.0 Hz, 1H), 5.29 (dd, *J* = 8.9, 7.7 Hz, 1H), 2.76 (dd, *J* = 12.5, 8.3 Hz, 1H), 2.33-2.21 (m, 1H), 1.42 (s, 9H). ^{13}C NMR (101 MHz, $CDCl_3$) δ 158.8, 142.1, 128.5 (x2), 127.2, 126.1 (x2), 98.6, 82.5, 61.4, 45.3, 28.1 (x3). IR (neat): 3347, 2977, 2933, 1703, 1456, 1367, 1346, 1316, 1247, 1162, 1070, 911, 848, 758, 697 cm^{-1}. $[\alpha]_D^{25}$ = –15.2 (*c* = 1.0, $CHCl_3$). HPLC (Daicel Chiralpak AD-H, hexane/*i*-PrOH = 90:10, flow rate 1.0 mL/min, λ = 210 nm): major isomer: t_R = 6.3 min; minor isomer: t_R = 7.5 min.

Benzyl (3*S*,5*S*)-3-(4-chlorophenyl)-5-hydroxyisoxazolidine-2-carboxylate (4ba). ^{1}H NMR (400 MHz, $CDCl_3$) δ 7.40-7.21 (m, 9H), 5.94-5.83 (m, 1H), 5.38 (t, *J* = 8.2 Hz, 1H), 5.21 (s, 2H), 2.80 (dd, *J* = 12.6, 8.4 Hz, 1H), 2.33-2.21 (m, 1H). ^{13}C NMR (101 MHz, $CDCl_3$) δ 159.1, 139.9, 135.5, 133.2, 128.8 (x3), 128.4 (x2), 128.2, 127.8, 127.4 (x2), 98.7, 68.2, 60.8, 45.2. IR (neat): 3356, 3033, 2961, 1707, 1492, 1391, 1296, 1237, 1087, 1014, 903, 825, 736, 696 cm^{-1}. HRMS (ESI): m/z: $[M+Na]^+$ ($C_{17}H_{16}ClNNaO_4$), calcd.: 356.0660; found: 356.0660. $[\alpha]_D^{25}$ = –33.2 (c = 1.0, $CHCl_3$). HPLC (Daicel Chiralpak AD-H, hexane/*i*-PrOH = 90:10, flow rate 1.0 mL/min, λ = 210 nm): major isomer: t_R = 14.911 min; minor isomer: t_R = 17.611 min.

***tert*-Butyl (3*S*,5*S*)-3-(4-chlorophenyl)-5-hydroxyisoxazolidine-2-carboxylate (4bb).**[12] ^{1}H NMR (400 MHz, $CDCl_3$) δ 7.36-7.22 (m, 4H), 5.91 (d, *J* = 4.4 Hz, 1H), 5.27 (t, *J* = 8.3 Hz, 1H), 2.76 (dd, *J* = 12.4, 8.3 Hz, 1H), 2.22 (ddd, *J* = 12.6, 8.5, 4.4 Hz, 1H), 1.43 (s, 9H). ^{13}C NMR (126 MHz, $CDCl_3$) δ 158.7, 140.6, 133.1, 128.7 (x2), 127.5 (x2), 98.6, 82.8, 60.9, 45.3, 28.1 (x3). IR (neat): 3378, 2979, 2931, 2854, 1702, 1491, 1351, 1325, 1249, 1163, 1089, 1014, 956, 907, 847, 821, 769 cm^{-1}. $[\alpha]_D^{25}$ = –14.6 (*c* = 1.0, $CHCl_3$). HPLC (Daicel Chiralpak AD-H, hexane/*i*-PrOH = 98:2, flow rate 1.0 mL/min, λ = 210 nm): minor isomer: t_R = 22.3 min; major isomer: t_R = 24.7 min.

Benzyl (3*S*,5*S*)-3-(4-fluorophenyl)-5-hydroxyisoxazolidine-2-carboxylate (4ca). ^{1}H NMR (400 MHz, $CDCl_3$) δ 7.35-7.15 (m, 7H), 7.00 (t, *J* = 8.7 Hz, 2H), 5.84 (d, *J* = 4.2 Hz, 1H), 5.34 (t, *J* = 8.2 Hz, 1H), 5.17 (s, 2H), 2.76 (dd, *J* = 12.6, 8.4 Hz, 1H), 2.24 (ddd, *J* = 12.6, 8.1, 4.5 Hz, 1H). ^{13}C NMR (101 MHz, $CDCl_3$) δ 162.1 (d, *J* = 245.8 Hz), 159.2, 137.1 (d, *J* = 3.1 Hz), 135.5, 128.4 (x2), 128.2, 127.8 (x2), 127.7 (x2, d, *J* = 8.0 Hz), 115.5 (x2, d, *J* = 21.6 Hz), 98.7, 68.2, 60.8, 45.3. ^{19}F NMR (376 MHz, $CDCl_3$) δ –115.1. IR (neat): 3367 (s), 3035, 2962, 1709, 1605, 1509, 1454, 1390, 1297, 1224, 1070, 905, 835, 736, 697 cm^{-1}. HRMS (ESI): m/z: $[M+Na]^+$ ($C_{17}H_{16}FNNaO_4$), calcd.: 340.0956; found: 340.0961. $[\alpha]_D^{25}$ = –33.2 (c = 1.0, $CHCl_3$). HPLC (Daicel Chiralpak AD-H, hexane/*i*-PrOH = 90:10, flow rate 1.0 mL/min, λ = 210 nm): major isomer: t_R = 13.3 min; minor isomer: t_R = 15.8 min.

***tert*-Butyl (3*S*,5*S*)-3-(4-fluorophenyl)-5-hydroxyisoxazolidine-2-carboxylate (4cb).** ^{1}H NMR (400 MHz, $CDCl_3$) δ 7.37-7.26 (m, 2H), 7.10-6.99 (m, 2H), 5.93-5.82 (m, 1H), 5.29 (t, *J* = 8.3 Hz, 1H), 2.77 (dd, *J* = 12.5, 8.3 Hz, 1H), 2.26 (dddd, *J* = 12.6, 8.3, 4.4, 1.7 Hz, 1H), 1.45 (s, 9H). ^{13}C NMR (101 MHz, $CDCl_3$) δ 162.1 (d, *J* = 245.41), 158.6, 137.8 (d, *J* = 3.2), 127.7 (x2, d, *J* = 8.1), 115.4 (x2, d, *J* = 21.5), 98.5, 82.6, 60.8, 45.4, 28.1 (x3). ^{19}F NMR (376 MHz, $CDCl_3$) δ –115.52. IR (neat): 3395, 2979, 2935, 1714, 1604, 1367, 1321, 1248, 1221, 1155, 1069, 910, 833, 766, 551 cm^{-1}. HRMS (ESI): m/z: $[M+Na]^+$ ($C_{14}H_{18}FNO_4Na$), calcd.: 306.1112; found: 306.1112. $[\alpha]_D^{25}$ = –10.7 (c = 1.0, $CHCl_3$). HPLC (Daicel Chiralpak AD-H, hexane/i-PrOH = 90:10, flow rate 1.0 mL/min, λ = 210 nm): major isomer: t_R = 9.3 min; minor isomer: t_R = 11.3 min.

Benzyl (3*S*,5*S*)-5-hydroxy-3-(4-nitrophenyl)isoxazolidine-2-carboxylate (4da).[12] ^{1}H NMR (400 MHz, $CDCl_3$) δ 8.17 (d, *J* = 8.7 Hz, 2H), 7.49 (d, *J* = 8.7 Hz, 2H), 7.37-7.16 (m, 5H), 5.94 (d, *J* = 4.2 Hz, 1H), 5.48 (t, *J* = 8.3 Hz, 1H), 5.18 (s, 2H), 2.87 (dd, *J* = 12.5, 8.5 Hz, 1H), 2.25 (ddd, *J* = 12.5, 8.2, 4.4 Hz, 1H). ^{13}C NMR (101 MHz, $CDCl_3$) δ 159.1, 148.6, 147.2, 135.1, 128.4 (x2), 128.3, 127.8 (x2), 126.8 (x2), 123.9 (x2), 98.7, 68.5, 60.8, 45.0. IR (neat): 3363, 2958, 2837, 1706, 1612, 1513, 1455, 1392, 1319, 1290, 1243, 1113, 1029, 903, 849, 747, 695 cm^{-1}. HRMS (ESI):

m/z: $[M+Na]^+$ ($C_{17}H_{16}N_2NaO_6$), calcd.: 367.0901; found: 367.0903. $[\alpha]_D^{25}$ = –40.5 (*c* = 1.0, $CHCl_3$). HPLC (Daicel Chiralpak AD-H, hexane/*i*-PrOH = 80:20, flow rate 1.0 mL/min, λ = 210 nm): minor isomer: t_R = 19.7 min; major isomer: t_R = 22.1 min.

***tert*-Butyl (3*S*,5*S*)-5-hydroxy-3-(4-nitrophenyl)isoxazolidine-2-carboxylate (4db).**[12] ^{1}H NMR (400 MHz, $CDCl_3$) δ 8.22 (d, *J* = 8.8 Hz, 2H), 7.53 (d, *J* = 8.6 Hz, 2H), 5.94 (d, *J* = 4.3 Hz, 1H), 5.40 (t, *J* = 8.4 Hz, 1H), 2.85 (dd, *J* = 12.4, 8.4 Hz, 1H), 2.23 (ddd, *J* = 12.6, 8.5, 4.4 Hz, 1H), 1.44 (s, 9H). ^{13}C NMR (101 MHz, $CDCl_3$) δ 158.6, 149.4, 147.25, 126.9 (x2), 123.9 (x2), 98.5, 83.3, 61.0, 45.1, 28.0 (x3). IR (neat): 3329, 2960, 2931, 2840, 1702, 1614, 1514, 1455, 1368, 1336, 1299, 1246, 1159, 1088, 1064, 1032, 965, 913, 868, 835, 807 cm^{-1}. $[\alpha]_D^{25}$ = –26.9 (*c* = 1.0, $CHCl_3$). HPLC (Daicel Chiralpak AD-H, hexane/*i*-PrOH = 90:10, flow rate 1.0 mL/min, λ = 210 nm): minor isomer: t_R = 12.1 min; major isomer: t_R = 14.1 min.

Benzyl (3*S*,5*S*)-5-hydroxy-3-(4-methoxyphenyl)isoxazolidine-2-carboxylate (4ea).[1]H NMR (400 MHz, $CDCl_3$) δ 7.35-7.17 (m, 7H), 6.86 (d, *J* = 8.7 Hz, 2H), 5.90 (d, *J* = 4.2 Hz, 1H), 5.33 (t, *J* = 8.2 Hz, 1H), 5.17 (s, 2H), 3.79 (s, 3H), 2.75 (dd, *J* = 12.6, 8.3 Hz, 1H), 2.29 (ddd, *J* = 12.6, 8.3, 4.5 Hz, 1H). ^{13}C NMR (101 MHz, $CDCl_3$) δ 159.2, 159.0, 135.7, 133.4, 128.4 (x2), 128.1, 127.7 (x2), 127.3 (x2), 114.0 (x2), 98.7, 68.0, 60.9, 55.3, 45.2. IR (neat): 3475, 3120, 2960, 2850, 1707, 1610, 1513, 1396, 1346, 1324, 1261, 1124, 1012, 962, 833, 758, 694, 518 cm^{-1}. HRMS (ESI): m/z: $[M+Na]^+$ ($C_{18}H_{19}NNaO_5$), calcd.: 352.1155; found: 352.1152. $[\alpha]_D^{25}$ = –51.7 (*c* = 1.0, $CHCl_3$). HPLC (Daicel Chiralpak AD-H, hexane/*i*-PrOH = 85:15, flow rate 1.0 mL/min, λ = 210 nm): major isomer: t_R = 16.1 min; minor isomer: t_R = 19.8 min.

***tert*-Butyl (3*S*,5*S*)-5-hydroxy-3-(4-methoxyphenyl)-isoxazolidine-2-carboxylate (4eb).** ^{1}H NMR (400 MHz, $CDCl_3$) δ 7.25 (d, *J* = 8.6 Hz, 2H), 6.86 (d, *J* = 8.8 Hz, 2H), 5.93-5.82 (m, 1H), 5.23 (t, *J* = 8.2 Hz, 1H), 3.79 (s, 3H), 2.71 (dd, *J* = 12.5, 8.3 Hz, 1H), 2.26 (dddd, *J* = 12.6, 8.3, 4.5, 2.0 Hz, 1H), 1.42 (s, 9H). ^{13}C NMR (101 MHz, $CDCl_3$) δ 158.8, 158.7, 134.1, 127.4 (x2), 113.9 (x2), 98.6, 82.3, 60.9, 55.3, 45.3, 28.1 (x3). IR (neat): 3329, 2960, 2931, 1702, 1613, 1514, 1455, 1336, 1299, 1246, 1159, 1088, 1064, 1032, 965, 91, 807 cm^{-1}. HRMS (ESI): m/z: $[M+Na]^+$ ($C_{15}H_{21}NNaO_5$), calcd.: 318.1312; found: 318.1311. $[\alpha]_D^{25}$ = –33.8 (*c* = 1.0, $CHCl_3$). HPLC (Daicel Chiralpak AD-H, hexane/*i*-PrOH = 90:10, flow rate 1.0 mL/min, λ = 210 nm): major isomer: t_R = 9.1 min; minor isomer: t_R = 10.0 min.

Benzyl (3*S*,5*S*)-5-hydroxy-3-(2-nitrophenyl)isoxazolidine-2-carboxylate (4fa). ^{1}H NMR (400 MHz, $CDCl_3$) δ 8.04 (dd, *J* = 8.2, 1.2 Hz, 1H), 7.79 (dd, *J* = 8.0, 1.3 Hz, 1H), 7.65 (td, *J* = 7.8, 1.2 Hz, 1H), 7.49 – 7.41 (m, 1H), 7.35-7.20 (m, 5H), 6.09 (t, *J* = 7.8 Hz, 1H), 5.91 (d, *J* = 4.3 Hz, 1H), 5.24-5.15 (m, 2H), 3.17 (dd, *J* = 12.9, 8.6 Hz, 1H), 2.28-2.16 (m, 1H). ^{13}C NMR (101 MHz, $CDCl_3$) δ 158.8, 147.3, 137.7, 135.3, 134.1 (x2), 128.5 (x2), 128.3 (x2), 127.9, 127.8, 124.8, 98.9, 68.4, 58.7, 45.2. IR (neat): 3366, 3067, 3035, 2961, 1710, 1609, 1578, 1523, 1446, 1391, 1339, 1292, 1067, 907, 738, 676 cm^{-1}. HRMS (ESI): m/z: $[M+Na]^+$ ($C_{17}H_{16}N_2NaO_6$), Calcd.: 367.0901. Found: 367.0910. $[\alpha]_D^{25}$ = +67.7 (*c* = 1.0, $CHCl_3$). HPLC (Daicel Chiralpak AD-H, hexane/*i*-PrOH = 90:10, flow rate 1.0 mL/min, λ = 210 nm): major isomer: t_R = 11.3 min; minor isomer: t_R = 14.7 min.

***tert*-Butyl (3*S*,5*S*)-5-hydroxy-3-(2-nitrophenyl)isoxazolidine-2-carboxylate (4fb).** ^{1}H NMR (400 MHz, $CDCl_3$) δ 7.89 (d, *J* = 8.2 Hz, 1H), 7.70 (d, *J* = 7.8 Hz, 1H), 7.60-7.50 (m, 1H), 7.42-7.28 (m, 1H), 5.92-5.76 (m, 2H), 3.01 (dd, *J* = 12.7, 8.4 Hz, 1H), 2.10 (ddd, *J* = 7.9, 4.6, 2.1 Hz, 1H), 1.32 (s, 9H). ^{13}C NMR (101 MHz, $CDCl_3$) δ 158.1, 147.6, 138.2, 133.9, 128.1(x2), 124.4, 98.8, 83.1, 58.4, 45.3, 28.0 (x3). IR (neat): 3348, 2977, 2927, 2854, 1707, 1345, 1244, 1138, 1066, 958, 913, 848, 788, 744 cm^{-1}. HRMS (ESI): m/z: $[M+Na]^+$ ($C_{14}H_{18}N_2NaO_6$), calcd.: 333.1057; found: 333.1059. $[\alpha]_D^{25}$ = +83.4 (*c* = 1.0, $CHCl_3$). HPLC (Daicel Chiralpak AD-H, hexane/*i*-PrOH = 95:5, flow rate 1.0 mL/min, λ = 210 nm): minor isomer: t_R = 19.0 min; major isomer: t_R = 20.2 min.

Benzyl (3*S*,5*S*)-5-hydroxy-3-(2-methoxyphenyl)isoxazolidine-2-carboxylate (4ga). ^{1}H NMR (400 MHz, $CDCl_3$) δ 7.42 (d, *J* = 7.6 Hz, 1H), 7.32-7.18 (m, 6H), 6.94 (t, *J* = 7.5 Hz, 1H), 6.86 (d, *J* = 8.2 Hz, 1H), 5.81 (s, 1H), 5.72 (t, *J* = 7.8 Hz, 1H), 5.19 (s, 2H), 3.80 (s, 3H), 2.89 (dd, *J* = 12.7, 8.4 Hz, 1H), 2.13 (ddd, *J* = 12.4, 7.2, 4.8 Hz, 1H). ^{13}C NMR (101 MHz, $CDCl_3$) δ 159.3, 156.1, 135.9, 129.9, 128.3 (x2), 128.2, 128.1, 127.7 (x2), 125.8, 120.6, 110.3, 98.8, 67.9, 56.8, 55.3, 44.2. IR (neat): 3360, 2960, 2838, 1707, 1601, 1491, 1460, 1389, 1339, 1285, 1239, 1068, 1025, 908, 751, 696 cm^{-1}. HRMS (ESI): m/z: $[M+Na]^+$ ($C_{18}H_{19}NNaO_5$), calcd.: 352.1155; found: 352.1154. $[\alpha]_D^{25}$ = –42.0 (*c* = 1.0, $CHCl_3$). HPLC (Daicel Chiralpak AD-H, hexane/*i*-PrOH = 90:10, flow rate 1.0 mL/min, λ = 210 nm): major isomer: t_R = 7.8 min; minor isomer: t_R = 13.2 min.

***tert*-Butyl (3*S*,5*S*)-5-hydroxy-3-(2-methoxyphenyl)isoxazolidine-2-carboxylate (4gb).** ^{1}H NMR (400 MHz, $CDCl_3$) δ 7.43 (dd, *J* = 7.6, 1.5 Hz, 1H), 7.29-7.16 (m, 1H), 6.94 (td, *J* = 7.5, 0.9 Hz, 1H), 6.86 (dd, *J* = 8.2, 0.7 Hz, 1H), 5.84 (dd, *J* = 4.2, 2.8 Hz, 1H), 5.64 (t, *J* = 7.9 Hz, 1H), 3.84 (s, 3H), 2.85 (dd, *J* = 12.7, 8.4 Hz, 1H), 2.14-2.03 (m, 1H), 1.43 (s, 9H). ^{13}C NMR (101 MHz, $CDCl_3$) δ 158.8, 156.1, 130.6, 128.0, 126.0, 120.6, 110.2, 98.7, 82.1, 56.7, 55.3, 44.2, 28.1 (x3). IR (neat): 3356, 2976, 2930, 2850, 1703, 1602, 1491, 1461, 1348, 1315, 1239, 1160, 1066, 1027, 916, 848, 806, 751 cm^{-1}. HRMS (ESI): m/z: $[M+Na]^+$ ($C_{15}H_{21}NNaO_5$), calcd.: 318.1312; found: 318.1312. $[\alpha]_D^{25}$ = –22.0 (*c* = 1.0, $CHCl_3$). HPLC (Daicel Chiralpak AD-H, hexane/*i*-PrOH = 90:10, flow rate 1.0 mL/min, λ = 210 nm): major isomer: t_R = 7.9 min; minor isomer: t_R = 11.1 min.

(*S*)-3-Amino-3-phenylpropanoic acid hydrochloride (13).[18] ^{1}H NMR (400 MHz, Deuterium Oxide) δ 7.38 (s, 5H), 4.69 (m, 5 H), 3.10 (dd, *J* = 17.2, 7.7 Hz, 1H), 2.98 (dd, *J* = 17.2, 6.6 Hz, 1H). ^{13}C NMR (101 MHz, D_2O) δ 173.4, 135.1, 129.7, 129.4 (x2), 127.1 (x2), 51.5, 37.7. $[\alpha]_D^{25}$ = +2.8 (*c* = 0.28, H_2O).

Acknowledgements

Financial support from CERCA Programme/Generalitat de Catalunya, MINECO (CTQ2015-69136-R, AEI/MINECO/ FEDER, UE and Severo Ochoa Excellence Accreditation 2014–2018, SEV-2013-0319) and the CELLEX Foundation [CELLEX-ICIQ High Throughput Experimentation (HTE) platform] is gratefully acknowledged.

References

[1] a) *Asymmetric Organocatalysis: from Biomimetic Concepts to Applications in Asymmetric Synthesis* (Eds.: A. Berkessel, H. Groeger) Wiley-VCH, **2005**; b) *Enantioselective Organocatalysis: Reactions and Experimental Procedures* (Eds.: P. I. Dalko) Wiley-VCH: Weinheim, **2007**; c) S. Mukherjee, J. W. Yang, S. Hoffmann, B. List, *Chem. Rev.* **2007**, *107*, 5471–5569; d) A. G. Doyle, E. N. Jacobsen, *Chem. Rev.* **2007**, *107*, 5713–5743; e) D. W. C. MacMillan, *Nature* **2008**, *455*, 304-308; f) A. Dondoni, A. Massi, *Angew. Chem., Int. Ed.* **2008**, *47*, 4638-4660.

[2] a) C. Palomo, A. Mielgo, *Angew. Chem., Int. Ed.* **2006**, *45*, 7876-7880; b) J. M. Verkade, L. J. van Hemert, P. J. Quaedflieg, F. P. Rutjes, *Chem. Soc. Rev.* **2008**, *37*, 29-

41; c) A. Mielgo, C. Palomo, *Chem. - Asian J.* **2008**, *3*, 922-948; d) S. Bertelsen, K. A. Jørgensen, *Chem. Soc. Rev.* **2009**, *38*, 2178-2189; e) C. T. Wong, *Tetrahedron* **2009**, *65*, 7491-7497; f) K. L. Jensen, G. Dickmeiss, H. Jiang, Ł. Albrecht, K. A. Jørgensen, *Acc. Chem. Res*. **2011**, *45*, 248-264; g) C. M. Volla, I. Atodiresei, M. Rueping, *Chem. Rev.* **2013**, *114*, 2390-2431; h) B. S. Donslund, T. K. Johansen, P. H. Poulsen, K. S. Halskov, K. A. Jørgensen, *Angew. Chem. Int. Ed.* **2015**, *54*, 13860-13874; i) K. S. Halskov, B. S. Donslund, B. M. Paz, K. A. Jørgensen, *Acc. Chem. Res.* **2016**, *49*, 974-986; j) L. Klier, F. Tur, P. H. Poulsen, K. A. Jørgensen, *Chem. Soc. Rev.* **2017**, *46*, 1080-1102.

[3] a) K. Patora-Komisarska, M. Benohoud, H. Ishikawa, D. Seebach, Y. Hayashi, *Helv. Chim. Acta* **2011**, *94*, 719-745; b) J. Burés, A. Armstrong, D. G. Blackmond, *Acc. Chem. Res.* **2016**, *49*, 214-222.

[4] a) *Chiral catalyst immobilization and recycling*, (Eds.: D. E. De Vos, I. F. J. Vankelecom, P. A. Jacobs) Wiley-VCH, Weinheim; New York, **2000**; b) M. Benaglia, A. Puglisi, F. Cozzi, *Chem. Rev.* **2003**, *103*, 3401-3430; c) M. Benaglia, *New J. Chem.* **2006**, *30*, 1525-1533; d) F. Cozzi, *Adv. Synth. Catal.* **2006**, *348*, 1367-1390; e) M. Gruttadauria, F. Giacalone, R. Noto, *Chem. Soc. Rev.* **2008**, *37*, 1666-1688; f) E. L. Margelefsky, R. K. Zeidan, M. E. Davis, *Chem. Soc. Rev.* **2008**, *37*, 1118-1126; g) *Recoverable and recyclable catalysts*, *1st ed.* (Eds.: M. Benaglia) Wiley, Hoboken, N.J., **2009**; h) A. F. Trindade, P. M. P. Gois, C. A. M. Afonso, *Chem. Rev.* **2009**, *109*, 418-514; i) T. E. Kristensen, T. Hansen, *Eur. J. Org. Chem.* **2010**, 3179-3204; j) *Polymeric chiral catalyst design and chiral polymer synthesis* (Eds.: S. Itsuno) John Wiley & Sons, **2011**.

[5] a) P. Riente, C. Mendoza, M. A. Pericàs, *J. Mater. Chem.* **2011**, *21*, 7350-7355; b) E. Alza, S. Sayalero, X. C. Cambeiro, R. Martín-Rapún, P. O. Miranda, M. A. Pericàs, *Synlett* **2011**, 464-468; c) X. Fan, S. Sayalero, M. A. Pericàs, *Adv. Synth. Catal.* **2012**, *354*, 2971-2976; d) X. Fan, C. Rodríguez-Escrich, S. Sayalero, M. A. Pericàs, *Chem. - Eur. J.* **2013**, *19*, 10814-10817; e) P. Llanes, C. Rodríguez-Escrich, S. Sayalero, M. A. Pericàs, *Org. Lett.* **2016**, *18*, 6292-6295.

[6] a) M. M. Bowers-Nemia, M. M. Joullié, *Heterocycles* **1983**, *20*, 817–828; b) J. Seo, P. Martásek, L. J. Roman, R. B. Silverman, *Bioorg. Med. Chem.* **2007**, *15*, 1928–1938; c) I. Arenas, A. Ferrali, C. Rodríguez-Escrich, F. Bravo, M. A. Pericàs, *Adv. Synth. Catal.* **2017**, *359*, 2414-2424.

[7] a) U. Chiacchio, A. Rescifina, A. Corsaro, V. Pistarà, G. Romeo, R. Romeo, *Tetrahedron: Asymmetry* **2000**, *11*, 2045-2048; b) M. P. Sibi, M. Liu, *Org. Lett.* **2001**, *3*, 4181-4184; c) H. S. Lee, J. S. Park, B. M. Kim, S. H. Gellman, *J. Org. Chem.* **2003**, *68*, 1575-1578; d) M. P. Sibi, N. Prabagaran, S. G. Ghorpade, C. P. Jasperse, *J. Am. Chem. Soc.* **2003**, *125*, 11796-11797; e) U. Chiacchio, E. Balestrieri, B. Macchi, D. Iannazzo, A. Piperno, A. Rescifina, A. Mastino, *J. Med. Chem.* **2005**, *48*, 1389-1394; f) U. Chiacchio, A. Rescifina, D. Iannazzo, A. Piperno, R. Romeo, L. Borrello, G. Romeo, *J. Med. Chem.* **2007**, *50*, 3747-3750; g) V. V. Pagar, R. S. Liu, *Angew. Chem. Int. Ed.* **2015**, *54*, 4923-4926; h) S. Diethelm, E. M. Carreira, *J. Am. Chem. Soc.* **2015**, *137*, 6084-6096; i) M. Berthet, T. Cheviet, G. Dujardin, I. Parrot, J. Martinez, *Chem. Rev.* **2016**, *116*, 15235-15283.

[8] a) S. Tang, J. He, Y. Sun, L. He, X. She, *J. Org. Chem.* **2010**, *75*, 1961-1966; b) A. P. Kozikowski, C. Yon-Yih, B. C. Wang, Z. B. Xu, *Tetrahedron* **1984**, *40*, 2345-2358.

[9] a) B. Alcaide, P. Almendros, C. Aragoncillo, *Chem. Rev.* **2007**, *107*, 4437-4492; b) F. M. Cordero, F. Pisaneschi, A. Goti, J. Ollivier, J. Salaün, A. Brandi, *J. Am. Chem. Soc.* **2000**, *122*, 8075-8076; c) F. M. Cordero, M. Salvati, F. Pisaneschi, A. Brandi, *Eur. J. Org. Chem.* **2004**, 2205-2213.

[10] a) M. Liu, M. P. Sibi, *Tetrahedron* **2002**, *58*, 7991-8035; b) N. Sewald, *Angew. Chem. Int. Ed.* **2003**, *42*, 5794-5795; c) A. R. Minter, A. A. Fuller, A. K. Mapp, *J. Am. Chem. Soc.* **2003**, *125*, 6846-6847.

[11] W. S. Jen, J. J. Wiener, D. W. MacMillan, *J. Am. Chem. Soc.* **2000**, *122*, 9874-9875.

[12] a) I. Ibrahem, R. Rios, J. Vesely, G. L. Zhao, A. Córdova, *Chem. Commun.* **2007**, 849-851; b) I. Ibrahem, R. Rios, J. Vesely, G. L. Zhao, A. Cordova, *Synthesis* **2008**, 1153-1157.

[13] Q. Y. Dou, Y. Q. Tu, Y. Zhang, J. M. Tian, F. M. Zhang, S. H. Wang, *Adv. Synth. Catal.* **2016**, *358*, 874-879.

[14] O. V. Maltsev, A. S. Kucherenko, A. L. Chimishkyan, S. G. Zlotin, *Tetrahedron: Asymmetry* **2010**, *21*, 2659-2670.

[15] a) A. Kirschning, W. Solodenko, K. Mennecke, *Chem. - Eur. J.* **2006**, *12*, 5972-5990; b) X. Y. Mak, P. Laurino, P. H. Seeberger, *Beilstein J. Org. Chem.* **2009**, *5*, 19; c) T. Tsubogo, T. Ishiwata, S. Kobayashi, *Angew. Chem. Int. Ed.* **2013**, *52*, 6590-6604; d) D. Zhao, K. Ding, *ACS Catal.* **2013**, *3*, 928-944; e) I. Atodiresei, C. Vila, M. Rueping, *ACS Catal.* **2015**, *5*, 1972-1985; f) C. Rodríguez-Escrich, M. A. Pericàs, *Eur. J. Org. Chem.* **2015**, *2015*, 1173-1188; g) R. Porta, M. Benaglia, A. Puglisi, *Org. Process Res. Dev*. **2016**, *20*, 2-25.

[16] I. Sagamanova, C. Rodríguez-Escrich, I. Gábor Molnár, S. Sayalero, R. Gilmour, M. A. Pericàs, *ACS Catal.* **2015**, *5*, 6241-6248.

[17] L. Hong, W. Sun, D. Yang, G. Li, R. Wang, *Chem. Rev.* **2016**, *116*, 4006-4123.

[18] a) E. Forró, T. Paál, G. Tasnádi, F. Fülöp, *Adv. Synth. Catal*. **2006**, *348*, 917-923; b) O. Marianacci, G. Micheletti, L. Bernardi, F. Fini, M. Fochi, D. Pettersen, V. Sgarzani, A. Ricci, *Chem. Eur. J*. **2007**, *13*, 8338-8351; c) G. Tasnádi, E. Forró, F. Fülöp, *Tetrahedron: Asymmetry* **2008**, *19*, 2072-2077.

Supporting Information

Immobilization of *cis*-4-Hydroxydiphenylprolinol Silyl Ethers onto Polystyrene. Application in the Catalytic Enantioselective Synthesis of 5-Hydroxyisoxazolidines in Batch and Flow

Junshan Lai, Sonia Sayalero, Alessandro Ferrali, Laura Osorio-Planes,

Fernando Bravo, Carles Rodríguez-Escrich* and Miquel A. Pericàs*

crodriguez@iciq.es, mapericas@iciq.es

–Institute of Chemical Research of Catalonia (ICIQ), The Barcelona Institute of Science and Technology, Av. Països Catalans, 16, 43007 Tarragona (Spain),

–Departament de Química Inorgànica i Orgànica, Universitat de Barcelona (UB), 08028 Barcelona (Spain)

Table of Contents

1. General information

Unless otherwise noted, all reactions were conducted under air. All commercial reagents were used as received except cinnamaldehyde derivatives, that were purified by flash chromatography. Flash chromatography was carried out using 60 mesh silica gel and dry-packed columns. Thin layer chromatography was carried out using Merck TLC Silicagel 60 F254 aluminum sheets. Components were visualized by UV light (λ = 254 nm) and stained with phosphomolybdic dip. NMR spectra were recorded at 298 K on a Bruker Avance 400 Ultrashield apparatus. ^{1}H NMR spectroscopy chemical shifts are quoted in ppm relative to tetramethylsilane (TMS). $CDCl_3$ was used as internal standard for ^{13}C NMR spectra. Chemical shifts are given in ppm and coupling constants in Hz. IR spectra were recorded on a Bruker Tensor 27 FT-IR spectrometer and are reported in wavenumbers (cm^{-1}). High performance liquid chromatography (HPLC) was performed on Agilent Technologies chromatographs (1100 and 1200 Series), using Chiralpak AD-H columns and guard columns. FAB mass spectra were obtained on a Fisons V6-Quattro instrument, ESI mass spectra were obtained on a Waters LCT Premier Instrument and CI and EI spectra were obtained on a Waters GCT spectrometer. Specific optical rotation measurements were carried out on a Jasco P-1030 polarimeter.

Catalysts **1b** and **1c** were prepared as described below (see Section 2) based on the protocol described in a previous paper.[1] Catalysts **1d**,[2] **1e**,[3] **1f**[2] and **1g**[1] were prepared according to procedures previously reported by our laboratories. Catalyst loading was determined by elemental analysis: **1b** (f = 0.49 mmol g^{-1}); **1c** (f = 0.41 mmol g^{-1}); **1d** (f = 0.49 mmol g^{-1}); **1e** (f = 0.45 mmol g^{-1}); **1f** (f = 0.72 mmol g^{-1}).

2. Preparation of the 2,4-*cis* catalysts 1b and 1c

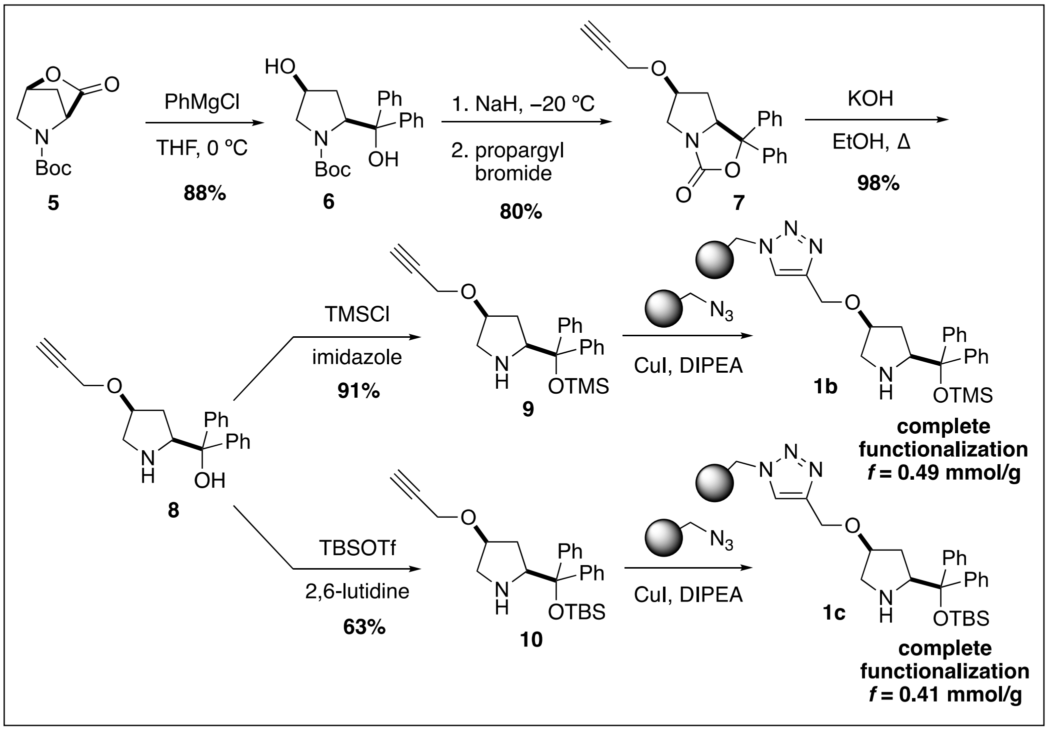

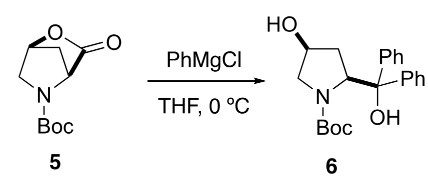

A solution of the lactone **5**[1] (1.377 g, 6.46 mmol) in dry THF (38 ml) under Ar was cooled to 0 °C and PhMgCl (2.0 M in THF, 6.5 ml, 12.92 mmol) was added dropwise. The mixture was stirred for 2 h (conversion was checked by TLC). Then, the reaction mixture was quenched with aq. sat. NH_4Cl (50 mL), the layers were separated, the aqueous phase was extracted with TBME (3 x 40 mL) and dried over Na_2SO_4. Purification by flash column chromatography (Cy/EtOAc 80:20 - 70:30 - 65:35 - 60:40) gave 2.11 g of product **6** (88% yield).

tert*-Butyl (2*S*,4*S*)-4-hydroxy-2-(hydroxydiphenylmethyl)pyrrolidine-1-carboxylate (6)**. White solid. **Melting point**: 197.3-199.5. ***R_f: 0.30 (Cy/EtOAc 60:40). **$[\alpha]_D^{25}$** = +122.3 (*c* 1.00, DCM). **^{1}H NMR** (400, $CDCl_3$): δ = 7.52-7.48 (m, 2H), 7.41-7.35 (m, 4H), 7.33-7.28 (m, 1H), 7.26-7.17 (m, 3H), 4.92 (d, *J* = 9.1 Hz, 1H), 4.54 (br s, 1H), 4.35 (br s, 1H), 4.20-3.70 (br s, 2H), 3.33 (br s, 1H), 2.30 (ddd, *J* = 14.6, 9.3, 7.6 Hz, 1H), 1.82 (d, *J* = 14.6 Hz, 1H), 1.14 (br s, 9H). **^{13}C NMR** (100.4, $CDCl_3$): δ = 154.8, 145.0, 144.7, 128.2 (2C), 127.8 (2C), 127.2, 127.1 (3C), 126.9 (2C), 81.4, 79.7, 70.1, 64.7, 57.1, 38.2, 27.9 (3C). **HRMS** (ESI+): calcd for $C_{22}H_{27}NNaO_4$ $[M+Na]^+$: 392.1832, found: 392.1840.

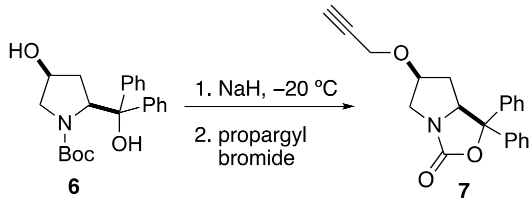

A suspension of NaH (60% in mineral oil, 0.200 g, 5.0 mmol) in 9 mL of anhydrous DMF under N_2 was cooled to –25 °C (internal temperature) and a solution of alcohol **6** (0.924 g, 2.5 mmol) in 7 mL of DMF was added dropwise. The mixture was stirred at this temperature for 20 min and then propargyl bromide (80% in toluene, 0.28 mL, 2.5 mmol) was added dropwise. The resulting mixture was stirred at 0 °C for 1 h and then brought to RT. When TLC analysis showed complete conversion of the starting material, 35 mL of NH_4Cl were added and it was extracted with EtOAc (3 × 60 mL). the combined organic phases were dried over Na_2SO_4 and concentrated in vacuo. Purification by flash column chromatography (Cy/EtOAc 90:10 to 60:40) gave the propargylated derivative **7** in 80% yield (0.668 g, 2.00 mmol) as a white solid.

(6*S*,7a*S*)-1,1-Diphenyl-6-(prop-2-yn-1-yloxy)tetrahydro-1H,3H-pyrrolo[1,2-c]oxazol-3-one (7). White solid. **Melting point**: 140.0-141.8. ***R**f*: 0.27 (Cy/EtOAc 70:30). **$[\alpha]_D^{25}$** = −209.8 (*c* 1.00, DCM). **^{1}H NMR** (400, $CDCl_3$): δ = 7.53-7.48 (m, 2H), 7.38-7.25 (m, 8H), 4.64 (dd, *J* = 9.0, 7.1 Hz, 1H), 4.41 (qd, *J* = 5.9, 3.2 Hz, 1H), 4.04 (dd, *J* = 16.1, 2.4 Hz, 1H), 3.96 (dd, *J* = 16.1, 2.4 Hz, 1H), 3.89 (dd, *J* = 12.6, 3.2 Hz, 1H), 3.30 (dd, *J* = 12.6, 5.9 Hz, 1H), 2.39 (t, *J* = 2.4 Hz, 1H), 2.09 (ddd, *J* = 13.4, 7.1, 6.2 Hz, 1H), 1.42 (dddd, *J* = 13.5, 9.1, 5.4, 0.8 Hz, 1H). **^{13}C NMR** (125.0, $CDCl_3$): δ = 160.3, 143.2, 139.9, 128.6 (2C), 128.4 (2C), 128.3, 127.8, 126.0 (2C), 125.7 (2C), 86.2, 79.0, 78.0, 74.9, 67.4, 56.3, 52.0, 35.5. **HRMS** (ESI+): calcd. for $C_{21}H_{19}NNaO_3$ $[M+Na]^+$: 356.1257, found: 356.1251.

NOTE: if more equivalents of NaH are used or higher temperatures are reached the corresponding allene **7'** can be generated in significant amounts. Characterization for this allene is as follows:

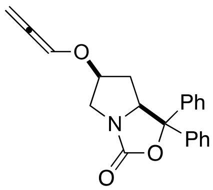

(6*S*,7a*S*)-6-((2λ⁵-Propa-1,2-dien-1-yl)oxy)-1,1-diphenyltetrahydro-1H,3H-pyrrolo[1,2-c]oxazol-3-one (7'). White solid. **Melting point**: 127.8-129.2. ***R**$_f$*: 0.40 (Cy/EtOAc 70:30). **[α]$_D^{25}$** = −207.6 (*c* 1.00, DCM). **^{1}H NMR** (400, $CDCl_3$): δ = 7.55-7.48 (m, 2H), 7.40-7.26 (m, 8H), 6.53 (t, *J* = 6.0 Hz, 1H), 5.44 (dd, *J* = 8.2, 6.0 Hz, 1H), 5.35 (dd, *J* = 8.2, 6.0 Hz, 1H), 4.64 (dd, *J* = 9.2, 7.2 Hz, 1H), 4.39 (qd, *J* = 5.9, 2.6 Hz, 1H), 3.95 (dd, *J* = 13.0, 2.6 Hz, 1H), 3.26 (dd, *J* = 13.0, 5.9 Hz, 1H), 2.13 (dt, *J* = 13.9, 6.9 Hz, 1H), 1.52 (dddd, *J* = 14.1, 9.2, 5.0, 0.8 Hz, 1H). **^{13}C NMR** (125.0, $CDCl_3$): δ = 201.0, 160.1, 143.1, 139.9, 128.6 (2C), 128.4 (2C), 128.3, 127.8, 125.9 (2C), 125.6 (2C), 120.1, 91.0, 86.1, 77.7, 67.5, 52.7, 35.7. **HRMS** (ESI+): calcd for $C_{21}H_{19}NNaO_3$ [M+Na]$^+$: 356.1257, found: 356.1258.

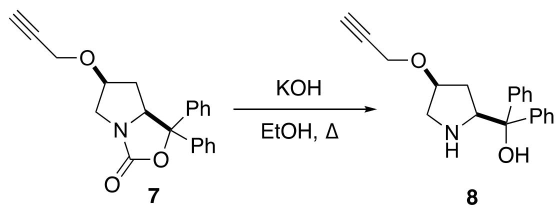

A solution of the oxazolidinone **7** (503 mg, 1.51 mmol) in EtOH (11 mL) was treated with a solution of KOH (423 mg, 7.54 mmol) in water (0.8 M). The mixture was heated at reflux overnight turning from a slurry to a clear yellowish solution. The next morning, TLC analysis (Cy/EA 50:50) shows that the starting material has disappeared, so the reaction mixture is concentrated in vacuo. The resulting slurry is diluted with water, extracted with EtOAc (3 × 25 mL), dried over Na_2SO_4 and evaporated. Purification by flash column chromatography gave 456 mg (1.51 mmol) of the amino alcohol **8** (98%).

Diphenyl((2*S*,4*S*)-4-(prop-2-yn-1-yloxy)pyrrolidin-2-yl)methanol (8). Colourless oil. **[α]$_D^{25}$** = −44.5 (*c* 1.00, DCM). **^{1}H NMR** (400 MHz, $CDCl_3$): δ = 7.62-7.56 (m, 2H), 7.53-7.47 (m, 2H), 7.32-7.25 (m, 4H), 7.20-7.14 (m, 2H), 4.32 (dd, *J* = 8.2, 7.1 Hz, 1H), 4.23 (dddd, *J* = 6.1, 5.1, 3.7, 2.3 Hz, 1H), 4.15 (dd, *J* = 15.9, 2.4 Hz, 1H), 4.08 (dd, *J* = 15.9, 2.4 Hz, 1H), 3.16 (ddd, *J* = 10.9, 2.3, 1.4 Hz, 1H), 3.04 (dd, *J* = 10.9, 5.1 Hz, 1H), 2.38 (t, *J* = 2.4 Hz, 1H), 1.90 (ddd, *J* = 14.4, 8.2, 6.3 Hz, 1H), 1.80 (dddd, *J* = 14.1, 7.1, 3.7, 1.4 Hz, 1H). **^{13}C NMR** (100.4 MHz, $CDCl_3$): δ = 147.2, 145.4, 128.2 (2C), 128.0 (2C), 126.5, 126.4, 125.9 (2C), 125.5 (2C), 79.7, 77.6, 76.9, 74.2, 63.8, 55.8, 51.9, 32.6. **HRMS** (ESI+): calcd for $C_{20}H_{22}NO_2$ $[M+H]^+$: 308.1645, found: 308.1641.

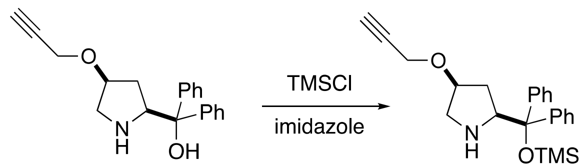

A solution of the amino alcohol **8** (250 mg, 0.813 mmol) in CH_2Cl_2 (8133 µl) was cooled to 0 °C. Then, imidazole (166 mg, 2.440 mmol) and chlorotrimethylsilane (258 µl, 2.033 mmol) were sequentially added. The solution was then allowed to reach 0 °C and stirred at this temperature for 3 h. Then, it was quenched with water and the aqueous layer was extracted with EtOAc (3 x 20 mL). The combined organic extracts were dried over Na^2SO^4 and concentrated under reduced pressure. Flash chromatography on silica gel with 2.5% Et_3N (Cy/EtOAc 50:50) afforded 282 mg of the silylated product **9** (91% yield, 0.813 mmol).

(2*S*,4*S*)-2-(Diphenyl((trimethylsilyl)oxy)methyl)-4-(prop-2-yn-1-yloxy)pyrrolidine (9). Colourless oil. ***R_f***: 0.42 (Cy/EtOAc 80:20). **$[\alpha]_D^{25}$** = −50.0 (*c* 1.00, DCM). **^{1}H NMR** (400 MHz, $CDCl_3$): δ = 7.51-7.47 (m, 2H), 7.35-7.31 (m, 2H), 7.29-7.18 (m, 6H), 4.14 (dtd, *J* = 6.7, 5.2, 3.0 Hz, 1H), 3.98 (dd, *J* = 15.8, 2.4 Hz, 1H), 3.92 (dd, *J* = 15.8, 2.4 Hz, 1H), 3.89 (dd, *J* = 9.3, 6.9 Hz, 1H), 3.01 (ddd, *J* = 12.0, 3.1, 1.0 Hz, 1H), 2.94 (dd, *J* = 12.0, 5.6 Hz, 1H), 2.34 (t, *J* = 2.4 Hz, 1H), 1.82 (br s, 1H), 1.74 (dt, *J* = 13.5, 6.9 Hz, 1H), 1.58 (dddd, *J* = 13.5, 9.4, 4.9, 1.0 Hz, 1H), −0.08 (s, 9H). **^{13}C NMR** (100.4 MHz, $CDCl_3$): δ = 146.8, 145.2, 128.7 (2C), 127.7 (2C), 127.6 (2C), 127.2 (2C), 127.1, 126.8, 82.4, 80.0, 78.6, 73.8, 65.8, 55.8, 53.2, 34.6, 2.1 (3C). **HRMS** (ESI+): calcd. for $C_{23}H_{30}NO_2Si$ $[M+H]^+$: 380.2040, found: 380.2050.

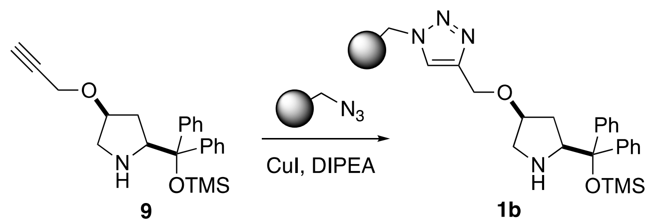

Azidomethylpolystyrene (*f* = 0.60, 5.90 g, 3.52 mmol) was suspended in DMF (53 ml) and THF (53 ml). Then, DIPEA (6.1 ml, 35.2 mmol) and copper(I) iodide (34 mg, 0.176 mmol) were added, followed by a solution of the alkyne **9** (1.61 g, 4.23 mmol) in the same solvent mixture (via cannula). The resulting mixture was shaken overnight at 40 °C. The next morning, after checking a small aliquot by IR to confirm full conversion, the resin **1b** was filtered and washed with water, water/MeOH, MeOH, MeOH/CH_2Cl_2 and CH_2Cl_2. Then, it was dried overnight in the vacuum oven at 40 °C.

f_{max} = 0.49; *f* = 0.49 (based on N Elemental Analysis). Complete functionalization.

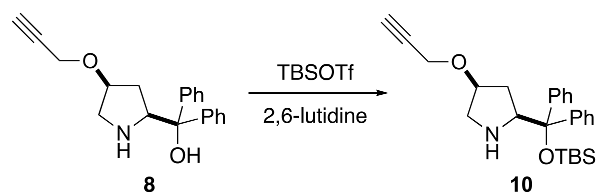

A solution of the diphenylprolinol derivative **8** (350 mg, 1.139 mmol) in DCE (5.5 mL) under Ar was cooled to 0 °C and treated with 2,6-lutidine (1.05 mL, 9.11 mmol) and TBSOTf (1.05 mL, 4.55 mmol). Then, it was heated at reflux overnight under vigorous stirring. The next morning, the reaction mixture was quenched with sat. aq. NH_4Cl (25 mL) and the aqueous layer was extracted with CH_2Cl_2 (3 × 25 mL). The combined organic extracts were dried over Na_2SO_4 and concentrated under reduced pressure. Purification by flash chromatography on silica gel with 2.5% Et_3N (Cy/EtOAc 90:10) gave silyl ether **10** in 63% yield (302 mg, 1.14 mmol).

(2*S*,4*S*)-2-(((*tert*-Butyldimethylsilyl)oxy)diphenylmethyl)-4-(prop-2-yn-1-yloxy)pyrrolidine (10). yellow oil. ***R**f*: 0.28 (Cy/EtOAc 80:20). $[\alpha]_D^{25}$ = −33.3 (*c* 1.00, DCM). **^{1}H NMR** (400 MHz, $CDCl_3$): δ = 7.61-7.55 (m, 2H), 7.38-7.32 (m, 2H), 7.32-7.22 (m, 6H), 4.13 (dtd, *J* = 6.8, 5.0, 3.2 Hz, 1H), 3.95 (dd, *J* = 15.8, 2.4 Hz, 1H), 3.89 (dd, *J* = 15.8, 2.4 Hz, 1H), 3.88 (dd, *J* = 9.5, 7.0 Hz, 1H), 2.99-2.89 (m, 2H), 2.34 (t, *J* = 2.4 Hz, 1H), 1.92 (br s, 1H), 1.77 (dt, *J* = 13.6, 6.9 Hz, 1H), 1.56 (ddd, *J* = 13.6, 9.7, 4.7 Hz, 1H), 0.99 (s, 9H), −0.12 (s, 3H), −0.51 (s, 3H). **^{13}C NMR** (100.4 MHz, $CDCl_3$): δ = 146.5, 144.8, 129.5, 127.7 (2C), 127.6 (2C), 127.4 (2C), 127.3 (2C), 126.9, 82.2, 80.0, 78.5, 73.7, 66.1, 55.7, 53.2, 35.0, 26.3 (3C), 19.1, −2.5, −3.6. **HRMS** (ESI+): calcd for $C_{26}H_{36}O_2$ $[M+H]^+$: 422.2510, found: 422.2513.

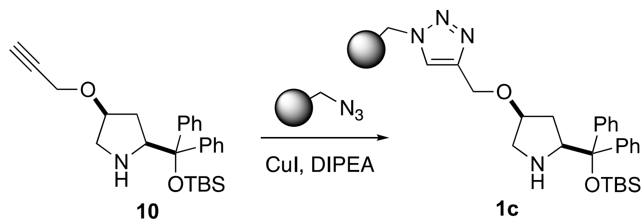

Azidomethylpolystyrene (*f* = 0.509, 6 g, 3.05 mmol) was suspended in DMF (46 ml) and THF (46 ml). Then, DIPEA (5.3 ml, 30.5 mmol) and copper(I) iodide (29 mg, 0.153 mmol) were added, followed by a solution of alkyne **10** (1.545 g, 3.66 mmol) in the same solvent mixture (via cannula). The resulting mixture was shaken overnight at 40 °C. The next morning, after checking a small aliquot by IR to confirm full conversion, the resin **1c** was filtered and washed with water, water/MeOH, MeOH, MeOH/CH_2Cl_2 and CH_2Cl_2. Then, it was dried overnight in the vacuum oven at 40 °C.

f_{max} = 0.42; *f* = 0.41 (based on N Elemental Analysis). Complete functionalization.

3. Experimental procedures

3.1. Optimization of reaction temperature

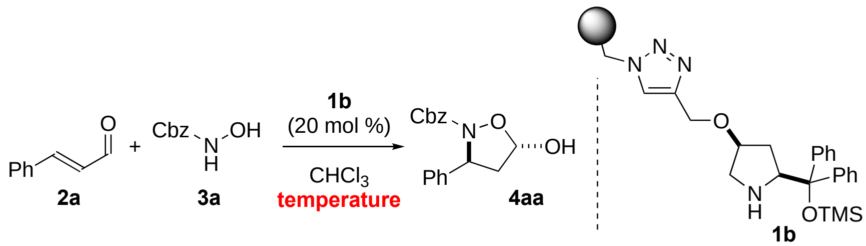

To a 2 mL glass vial were sequentially added PS-catalyst **1b** (*f* = 0.49 mmol/g, 21 mg, 20 mol % loading) and 0.25 mL $CHCl_3$, followed by cinnamaldehyde **2a** (6.7 mg, 0.05 mmol) and **3a** (10 mg, 0.06 mmol) at the indicated reaction temperature. The reaction mixture was shaken until TLC analysis showed consumption of the enal. Then, it was filtered and the resin beads were washed with DCM (5 x 0.25 mL). The solvent was concentrated under reduced pressure. Conversion and yield were determined by ^{1}H NMR using mesitylene as an internal standard.

Table S1. Optimization of reaction temperature

Temperature	Conversion (%)	Yield	Time (h)	ee (%)
60	99	70	6	74
rt	**99**	**73**	**6**	**92**
0	100	68	23	92

[a] Reaction conditions: **2a** (6.7 mg, 0.05 mmol, 1 eq.), **3a** (10 mg, 0.6 mmol, 1.2 eq.) PS-cat. **1b** (21 mg, 20 mol %), $CHCl_3$ (0.25 mL). Conversion and yield determined by ^{1}H NMR using mesitylene as an internal standard.

3.2. Solvent screening

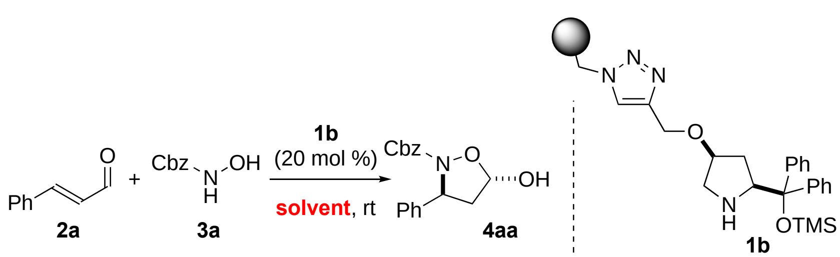

To a 2 mL glass vial were sequentially added PS-catalyst **1b** (f = 0.49 mmol/g, 0.01mmol, 21 mg, 20 mol % loading) and 0.25 mL of the solvent indicated, followed by cinnamaldehyde **2a**

(6.7 mg, 0.05 mmol) and **3a** (10 mg, 0.06 mmol) at room temperature. The reaction mixture was shaken until TLC analysis showed consumption of the enal. Then, it was filtered and the resin beads were washed with DCM (5 x 0.25 mL). The solvent was concentrated under reduced pressure. Conversion and yield were determined by ^{1}H NMR using mesitylene as an internal standard.

Table S2. Solvent screening

Entry	Solvent	Conversion (%)	Yield (%)	Time	ee (%)
1	$CHCl_3$	99	76	6	90
2	DCM	96	72	6	88
3	CH_3CN	75	71	30	86
4	DMF	0	0	30	–
5	EtOH	47	28	30	90
6	toluene	94	74	16	92

[a] Reaction conditions: **2a** (6.7 mg, 0.05 mmol, 1 eq.), **3a** (10 mg, 0.06 mmol, 1.2 eq.) PS-cat. **1b** (21 mg, 20 mol %), solvent (0.25 mL), rt. Conversion and yield determined by ^{1}H NMR using mesitylene as an internal standard.

3.3. PS-catalyst screening with $CHCl_3$ as solvent

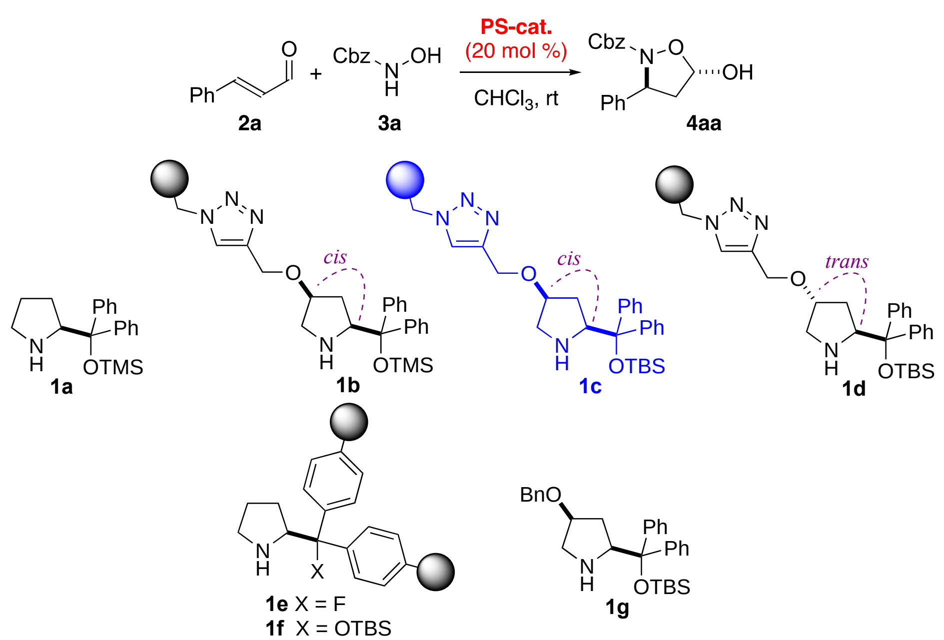

To a 2 mL glass vial were sequentially added indicated PS-catalyst (20 mol % loading) and 0.25 mL $CHCl_3$, followed by cinnamaldehyde **2a** (6.7 mg, 0.05 mmol) and **3a** (10 mg, 0.06 mmol) at room temperature. The reaction mixture was shaken until TLC analysis showed consumption of the enal. Then, it was filtered and the resin beads were washed with DCM (5 x 0.25 mL). The solvent was concentrated under reduced pressure. Conversion and yield were determined by ^{1}H NMR using mesitylene as an internal standard.

Table S3. PS-catalyst screening with $CHCl_3$ as solvent

Entry	Cat.[b]	Conversion (%)	Yield (%)	Time (h)	ee (%)
1	**1a**	99	65	6	89
2	**1b**	99	80	6	90
3	1c	**100**	**76**	**7**	**95**
4	**1d**	98	71	7	92
5	**1e**	100	74	18	76
6	**1f**	97	68	18	95
8	**1g**	98	70	6	93

[a] Reaction conditions: **2a** (6.7 mg, 0.05 mmol, 1 eq.), **3a** (10 mg, 0.06 mmol, 1.2 eq.) PS-cat. (20 mol % loading), $CHCl_3$ (0.25 mL), rt. Conversion and yield determined by ^{1}H NMR using mesitylene as an internal standard. [b] **1b** (f = 0.49 mmol/g); **1c** (f = 0.41 mmol/g); **1d** (f = 0.49 mmol/g); **1e** (f = 0.45 mmol/g); **1f** (f = 0.72 mmol/g).

3.4. Acid co-catalyst screening with $CHCl_3$ as solvent

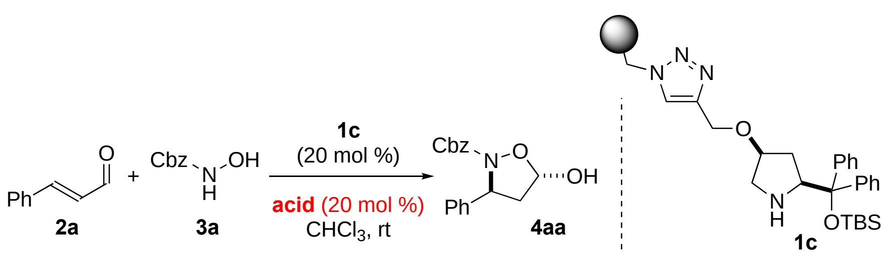

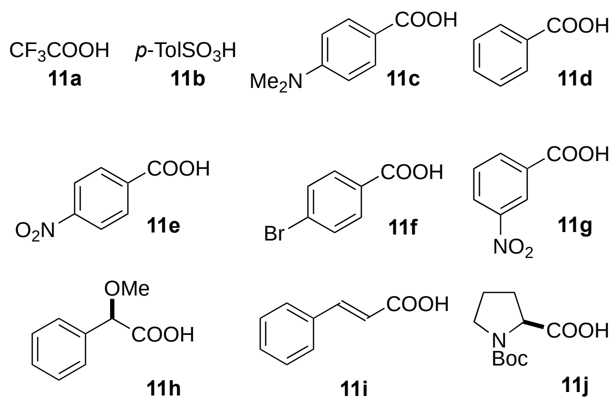

To a 2 mL glass vial were sequentially added PS-catalyst **1c** (f = 0.41 mmol/g, 0.01mmol, 23 mg, 20 mol % loading), 0.25 mL $CHCl_3$ and the indicated acid co-catalyst **11** (20 mol %), followed by cinnamaldehyde **2a** (6.7 mg, 0.05 mmol) and **3a** (10 mg, 0.06 mmol) at room temperature. The reaction mixture was shaken until TLC analysis showed consumption of the enal. Then, it was filtered and the resin beads were washed with DCM (5 x 0.25 mL). The solvent was concentrated under reduced pressure. Conversion and yield were determined by ^{1}H NMR using mesitylene as an internal standard.

Table S4. Acid co-catalyst screening with $CHCl_3$ as solvent

Entry	Acid	Time (h)	ee (%)
1	**11a**	48	–
2	**11b**	48	–
3	**11c**	6	98
4	**11d**	6	96
5	**11e**	6	93
6	**11f**	6	95
7	**11g**	6	97
8	**11h**	6	91
9	**11i**	**6**	**>99**
10	**11j**	6	92

11	–	30	93

[a] Reaction conditions: **2a** (6.7 mg, 0.05 mmol, 1 eq.), **3a** (10 mg, 0.06 mmol, 1.2 eq.) PS-cat. **1c** (23 mg, 20 mol %), acid (20 mol %), $CHCl_3$ (0.25 mL), rt. Conversion and yield determined by ^{1}H NMR using mesitylene as an internal standard.

3.5. Re-evaluation of reaction conditions with different PS-catalysts in $CHCl_3$

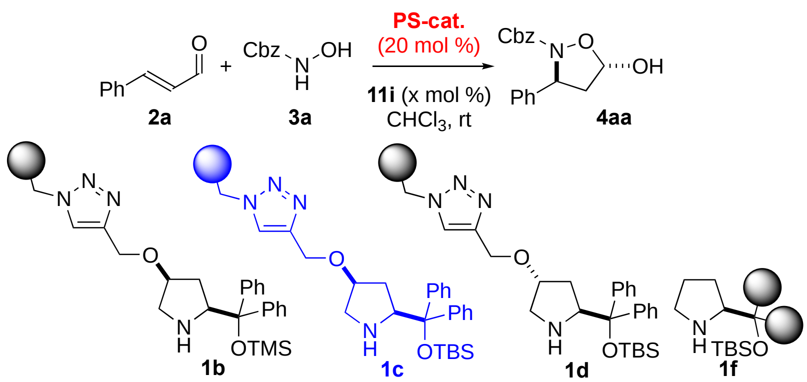

To a 2 mL glass vial were sequentially added indicated PS-catalyst, 0.25 mL $CHCl_3$ and **11i**, followed by cinnamaldehyde **2a** (6.7 mg, 0.05 mmol) and **3a** (10 mg, 0.06 mmol) at room temperature. The reaction mixture was shaken until TLC analysis showed consumption of the enal. Then, it was filtered and the resin beads were washed with DCM (5 x 0.25 mL). The solvent was concentrated under reduced pressure. Conversion and yield were determined by ^{1}H NMR using mesitylene as an internal standard.

Table S5. Re-evaluation of reaction conditions with different PS-catalysts in $CHCl_3$

Entry	PS-cat.	**5i** (x mol%)	Time (h)	ee (%)
1	**1c**	–	>30	92
2	**1c**	5	15	93
3	**1c**	10	15	96
4	**1c**	**20**	**6**	**>99**
5	**1b**	20	6	95
6	**1d**	20	6	95
7	**1f**	20	18	99

[a] Reaction conditions: **2a** (6.7 mg, 0.05 mmol, 1 eq.), **3a** (10 mg, 0.06 mmol, 1.2 eq.) PS-cat. (20 mol %), **11i** (x mol %), $CHCl_3$ (0.25 mL), rt. Conversion and yield determined by ^1H NMR using mesitylene as an internal standard.

3.6. Acid co-catalyst screening with CH_2Cl_2 as solvent

To a 2 mL glass vial were sequentially added PS-catalyst **1c** (f = 0.41 mmol/g, 0.01mmol, 23 mg, 20 mol % loading), 0.25 mL CH_2Cl_2 and the indicated co-catalyst acid (20 mol %), followed by cinnamaldehyde **2a** (6.7 mg, 0.05 mmol) and **3a** (10 mg, 0.06 mmol) at the indicated temperature. The reaction mixture was shaken until TLC analysis showed consumption of the enal. Then, it was filtered and the resin beads were washed with DCM (5 x 0.25 mL). The solvent was concentrated under reduced pressure. Conversion and yield were determined by ^1H NMR using mesitylene as an internal standard.

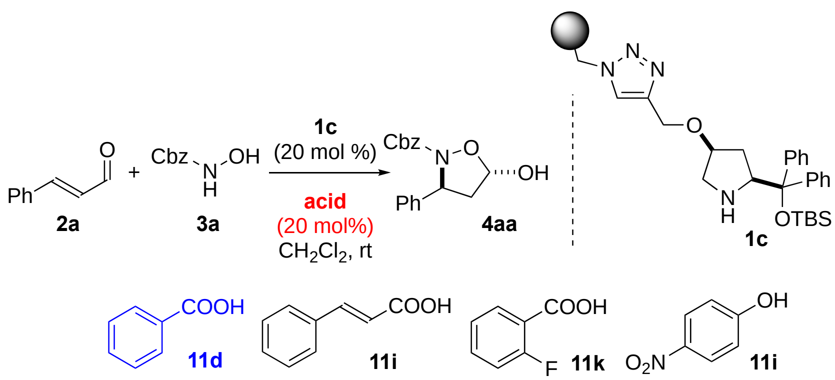

Table S6. Acid co-catalyst screening with CH_2Cl_2 as solvent

Entry	Temp (°C)	Acid	Time (h)	Conv (%)	ee (%)
1	**rt**	**11d**	**7**	**98**	**97**
2	rt	**11i**	7	97	97
3	rt	**11k**	7	99	93
4	rt	**11l**	7	95	94
5	rt	–	24	82	95
6	0	**11d**	24	98	98
7	40	**11d**	7	95	0

[a] Reaction conditions: **2a** (6.7 mg, 0.05 mmol, 1 eq.), **3a** (10 mg, 0.6 mmol, 1.2 eq.) PS-cat. **1c** (21 mg, 20 mol %), acid (20 mol %), CH_2Cl_2 (0.25 mL). Conversion and yield determined by [1]H NMR using mesitylene as an internal standard.

3.7. Re-evaluation of reaction conditions with different PS-catalysts in CH_2Cl_2

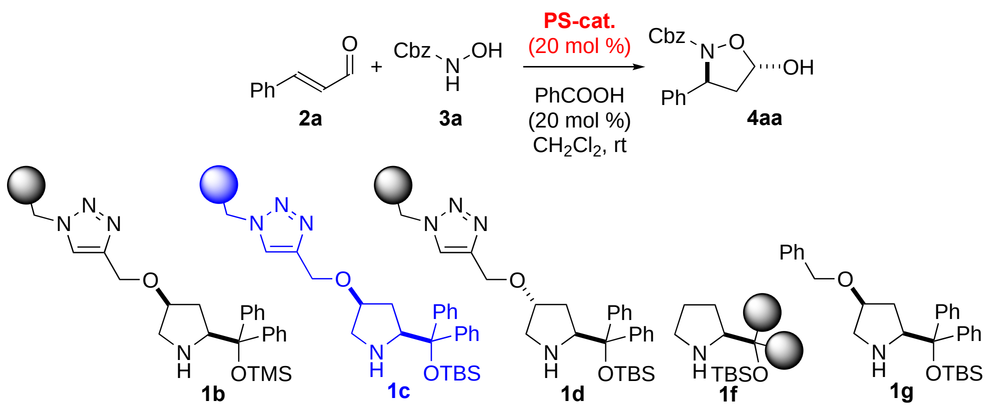

To a 2 mL glass vial were sequentially added the indicated catalyst, 0.25 mL CH_2Cl_2 and PhCOOH (1.2 mg, 20 mol %), followed by cinnamaldehyde **2a** (6.7 mg, 0.05 mmol) and **3a** (10 mg, 0.06 mmol) at room temperature. The reaction mixture was shaken until TLC analysis showed consumption of the enal. Then, it was filtered and the resin beads were washed with DCM (5 x 0.25 mL). The solvent was concentrated under reduced pressure. Conversion and yield were determined by [1]H NMR using mesitylene as an internal standard.

Table S7. Re-evaluation of reaction conditions with different PS-catalysts in CH_2Cl_2

Entry	Cat.	Conversion (%)	NMR yield (%)	ee (%)
1	**1b**	96	81	89
2	**1c**	**97**	**79**	**97**
3	**1d**	98	74	90
4	**1f**	96	72	97
5	**1g**	97	76	99

[a] Reaction conditions: **2a** (6.7 mg, 0.05 mmol, 1 eq.), **3a** (10 mg, 0.06 mmol, 1.2 eq.) PS-cat. (20 mol %), PhCOOH (5-20 mol%), CH_2Cl_2 (0.25 mL), 7 h, rt.

3.8. General procedure for the gram scale experiment in batch

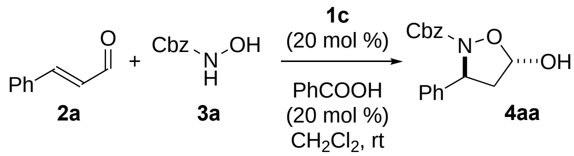

To a 50 mL round-bottom flask were sequentially added PS-catalyst **1c** (*f* = 0.41 mmol/g, 1 mmol, 2.32 g, 20 mol% loading), 25 mL CH_2Cl_2 and PhCOOH (122 mg, 1 mmol, 20 mol%), followed by cinnamaldehyde **2a** (670 mg, 5 mmol) and **3a** (1.0 g, 6 mmol) at room temperature. The reaction mixture was shaken overnight. Then, it was filtered and the resin beads were washed with DCM (8 x 10 mL). The solvent was concentrated under reduced pressure and the product was isolated after purification by column chromatography on silica gel with cyclohexane/ethyl acetate (EtOAc/*c*-Hex = 1:5) to yield **4aa** (65%, 972 mg).

3.9. General procedure for the scope of the reaction in batch

Conditions A: To a 2 mL glass vial were sequentially added PS-catalyst **1c** (*f* = 0.41 mmol/g, 0.01 mmol, 23 mg, 20 mol % loading), 0.25 mL $CHCl_3$ and **11i** (1.5 mg, 20 mol %), followed by cinnamaldehyde **2** (1 eq., 0.05 mmol) and **3** (1.2 eq., 0.06 mmol) at room temperature. The reaction mixture was shaken until TLC analysis showed consumption of the enal. Then, it was filtered and the resin beads were washed with DCM (5 x 0.25 mL). The solvent was concentrated in vacuo and the product was isolated after purification by column chromatography on silica gel with cyclohexane/ethyl acetate (EtOAc/*c*-Hex = 1:5) to yield **4**.

Conditions B: To a 5 mL glass vial were sequentially added PS-catalyst **1c** (*f* = 0.41 mmol/g, 0.1 mmol, 232 mg, 20 mol % loading), 2.5 mL CH_2Cl_2 and **11d** (12 mg, 0.1mmol, 20 mol %), followed by cinnamaldehyde **2** (1 eq., 0.5 mmol) and **3** (1.2 eq., 0.6 mmol) at room temperature. The reaction mixture was shaken until TLC analysis showed consumption of the enal. Then, it was filtered and the resin beads were washed with DCM (8 x 1.5 mL). The solvent was concentrated in vacuo and the product was isolated after purification by column chromatography on silica gel with cyclohexane/ethyl acetate (EtOAc/*c*-Hex = 1:5) to yield **4**.

3.10. Recycling experiments of the PS-Supported catalyst 1c in batch

To a 5 mL glass vial were sequentially added cinnamaldehyde **2a** (67 mg, 0.5 mmol), **3a** (100 mg, 0.6 mmol), PS-catalyst **1c** (*f* = 0.41 mmol/g, 0.1 mmol, 232 mg, 20 mol % loading), PhCOOH (12 mg, 20 mol%) and 2.5 mL CH_2Cl_2 at room temperature. The reaction mixture was shaken at room temperature for 7 hours. Then, it was filtered and the resin beads were washed with DCM (8 x 1.5 mL). The solvent was concentrated under reduced pressure and the product was isolated after purification by column chromatography on silica gel with cyclohexane/ethyl acetate (EtOAc/*c*-Hex = 1:5) to yield **4aa**.

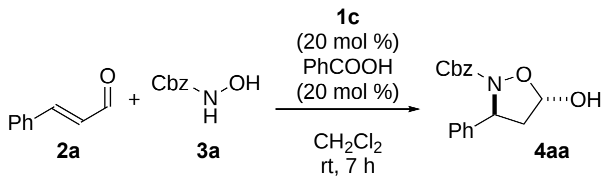

Table S8. Recycling experiments in batch

Run	Conversion (%)	Yield (%)	ee (%)
1	98	73	94
2	97	79	94
3	97	89	95
4	97	80	96
5	96	71	95
6	97	68	96
7	97	65	96
8	96	72	96
9	92	64	96
10	91	69	96

Reaction condition: **2a** (67 mg, 0.5mmol, 1 eq.), **3a** (100 mg, 0.6 mmol, 1.2 eq.) PS-cat. **1c** (232 mg, 20 mol %), PhCOOH (12 mg, 20 mol%), CH_2Cl_2 (2.5 mL), rt, 7 h. Isolated yield.

3.11. Parameter optimization for the flow experiment

The amount of catalyst **1c** indicated was placed in a glass Omnifit column (10 mm Ø). A stream of CH_2Cl_2 was passed for one hour at 0.1 mL min^{-1}. The reagents were then introduced in the system in two separate streams using a dual syringe pump: (a) containing **2a** (0.4 M in CH_2Cl_2, 1.0 eq) and (b) containing a mixture of **3a** (1.2 eq.) and the amount of PhCOOH indicated in CH_2Cl_2 (0.48 M of **3a**). When the flow finished the packed bed reactor was rinsed with CH_2Cl_2 at 0.1 mL min^{-1} for 2 h. The collected outstream was concentrated under reduced pressure and purified by column chromatography on silica gel with cyclohexane/ethyl acetate (EtOAc/*c*-Hex = 1:5) to yield **4aa**.

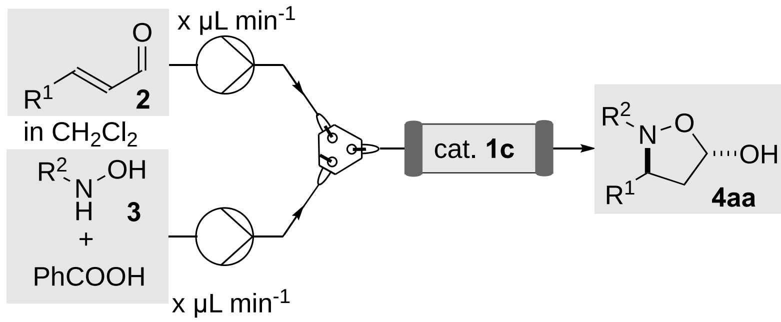

Table S9. Parameter optimization for the flow experiment

Amount of **2a**	Flow rate (µL min^{-1})	**11d** (eq.)	Cat. **1c** (g, mmol)	Conversion (%)	Yield (%)	ee (%)
0.2 M (4.8 mmol)	100	0.5	0.5, 0.21	68	47	95
0.2 M (2.4 mmol)	100	0.5	0.8, 0.33	84	58	96
0.2 M (2.4 mmol)	50	0.5	0.8, 0.33	95	77	96
0.1 M (2.4 mmol)	100	0.5	0.8, 0.33	76	50	95
0.2 M (2.4 mmol)	100	1	0.8, 0.33	87	72	96
0.2 M (2.4 mmol)	100	1	1.0, 0.41	95	75	95
0.2 M (8.2 mmol)	100	1	1.0, 0.41	81	67	95

Reaction conditions: **2a** (1 eq.), **3a** (1.2 eq.) PS-cat. **1c** (*f* = 0.41 mmol/g), PhCOOH, CH_2Cl_2, rt. Isolated yield.

3.12. Continuous flow process

Using the same set-up depicted above, the packed bed reactor (Omnifit glass column, 10 mm Ø) was filled with 1.0 g of catalyst **1c**, which was swollen by pumping CH_2Cl_2 at 0.1 mL min^{-1} for one hour. The reagents were then introduced in the system in two separate streams (50 µL min^{-1} each unless otherwise stated) using a dual syringe pump: (a) containing **2** (0.4 M, 1.0 eq) in 21.5 mL of CH_2Cl_2 and (b) containing a mixture of **3** (0.48 M, 1.2 eq.) and PhCOOH in 21.5 mL of CH_2Cl_2. When the solutions of reagents were consumed, the packed bed reactor was rinsed with CH_2Cl_2 at 0.1 mL min^{-1} for 2 h. The collected outstream was concentrated under reduced pressure and purified by column chromatography on silica gel with cyclohexane/ethyl acetate (EtOAc/*c*-Hex = 1:5) to yield the corresponding product **4**.

3.13. Preparation of β-amino acid hydrochloride 13

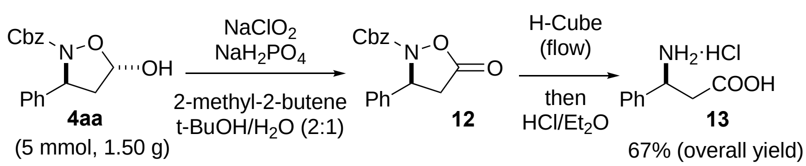

To a 25 mL round-bottomed flask were sequentially added **4aa** (1.50 g, 5 mmol), *tert*-butanol (8 mL), H_2O (4 mL), 2-methylbut-2-ene (2 mL), KH_2PO_4 (1088 mg, 8 mmol), $NaClO_2$ (720 mg, 8 mmol). The reaction mixture was stirred at room temperature for 16 h and then it was washed with saturated Na_2SO_3 and concentrated under reduced pressure. The residue obtained was dissolved in MeOH (200 mL), filtered to remove insoluble material and circulated through the H-Cube at 0.5 mL min^{-1} flow rate (90 atm, 50 °C). The outstream collected was concentrated in vacuo and the residue was washed with 2 M HCl in diethyl ether (10 mL), then with diethyl ether (5 x 10 mL), to give hydrochloride **13** in 67% yield (673 mg, 3.35 mmol).

3.14. Comparative kinetic studies of catalysts 1c and 1d

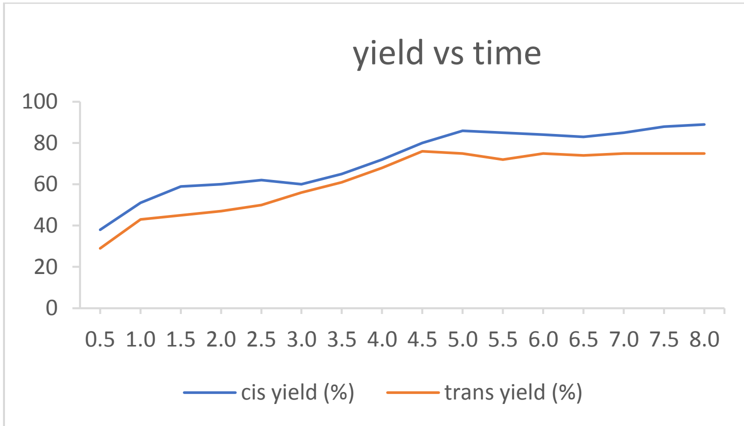

Reactions were run in $CDCl_3$ in an NMR tube according to the procedure described in Section 3.9 of this Supporting Information (using mesitylene as internal standard).

4. Compound characterization data

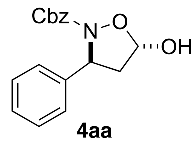

4aa

Benzyl (3*S*,5*S*)-5-hydroxy-3-phenylisoxazolidine-2-carboxylate[5]

^{1}H NMR (400 MHz, $CDCl_3$) δ 7.37-7.17 (m, 10H), 5.91 (d, *J* = 4.4 Hz, 1H), 5.38 (t, *J* = 8.2 Hz, 1H), 5.17 (s, 2H), 2.79 (dd, *J* = 12.6, 8.4 Hz, 1H), 2.30 (ddd, *J* = 12.6, 8.2, 4.5 Hz, 1H).

^{13}C NMR (101 MHz, $CDCl_3$) δ 159.3, 141.4, 135.6, 128.6 (x2), 128.4 (x2), 128.1, 127.7 (x2), 127.4, 126.0 (x2), 98.8, 68.1, 61.3, 45.3.

IR (neat): 3362, 3063, 3032, 2860,1707, 1496, 1453, 1390, 1301, 1238, 1027, 902, 754, 696 cm^{-1}.

$[\alpha]_D^{25}$ = –29.5 (*c* = 1.0, $CHCl_3$).

HPLC (Daicel Chiralpak AD-H, hexane/*i*-PrOH = 90:10, flow rate 1.0 mL/min, λ = 210 nm): major isomer: t_R = 13.2 min; minor isomer: t_R = 15.3 min.

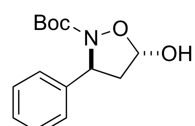

4ab

tert-Butyl (3*S*,5*S*)-5-hydroxy-3-phenylisoxazolidine-2-carboxylate[5]

^{1}H NMR (400 MHz, $CDCl_3$) δ 7.34 (d, *J* = 4.4 Hz, 4H), 7.26 (dd, *J* = 8.2, 4.5 Hz, 1H), 5.92 (d, *J* = 4.0 Hz, 1H), 5.29 (dd, *J* = 8.9, 7.7 Hz, 1H), 2.76 (dd, *J* = 12.5, 8.3 Hz, 1H), 2.33-2.21 (m, 1H), 1.42 (s, 9H).

^{13}C NMR (101 MHz, $CDCl_3$) δ 158.8, 142.1, 128.5 (x2), 127.2, 126.1 (x2), 98.6, 82.5, 61.4, 45.3, 28.1 (x3).

IR (neat): 3347, 2977, 2933, 1703, 1456, 1367, 1346, 1316, 1247, 1162, 1070, 911, 848, 758, 697 cm^{-1}.

$[\alpha]_D^{25}$ = –15.2 (*c* = 1.0, $CHCl_3$).

HPLC (Daicel Chiralpak AD-H, hexane/*i*-PrOH = 90:10, flow rate 1.0 mL/min, λ = 210 nm): major isomer: t_R = 6.3 min; minor isomer: t_R = 7.5 min.

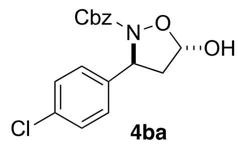

4ba

Benzyl (3*S*,5*S*)-3-(4-chlorophenyl)-5-hydroxyisoxazolidine-2-carboxylate

^{1}H NMR (400 MHz, $CDCl_3$) δ 7.40-7.21 (m, 9H), 5.94-5.83 (m, 1H), 5.38 (t, *J* = 8.2 Hz, 1H), 5.21 (s, 2H), 2.80 (dd, *J* = 12.6, 8.4 Hz, 1H), 2.33-2.21 (m, 1H).

^{13}C NMR (101 MHz, $CDCl_3$) δ 159.1, 139.9, 135.5, 133.2, 128.8 (x3), 128.4 (x2), 128.2, 127.8, 127.4 (x2), 98.7, 68.2, 60.8, 45.2.

IR (neat): 3356, 3033, 2961, 1707, 1492, 1391, 1296, 1237, 1087, 1014, 903, 825, 736, 696 cm^{-1}.

HRMS (ESI): m/z: $[M+Na]^+$ ($C_{17}H_{16}ClNNaO_4$), calcd.: 356.0660; found: 356.0660.

$[\alpha]_D^{25}$ = –33.2 (c = 1.0, $CHCl_3$).

HPLC (Daicel Chiralpak AD-H, hexane/*i*-PrOH = 90:10, flow rate 1.0 mL/min, λ = 210 nm): major isomer: t_R = 14.911 min; minor isomer: t_R = 17.611 min.

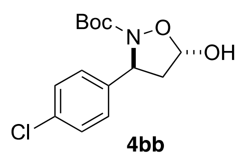

4bb

tert-Butyl (3*S*,5*S*)-3-(4-chlorophenyl)-5-hydroxyisoxazolidine-2-carboxylate[5]

^{1}H NMR (400 MHz, $CDCl_3$) δ 7.36-7.22 (m, 4H), 5.91 (d, *J* = 4.4 Hz, 1H), 5.27 (t, *J* = 8.3 Hz, 1H), 2.76 (dd, *J* = 12.4, 8.3 Hz, 1H), 2.22 (ddd, *J* = 12.6, 8.5, 4.4 Hz, 1H), 1.43 (s, 9H).

^{13}C NMR (126 MHz, $CDCl_3$) δ 158.7, 140.6, 133.1, 128.7 (x2), 127.5 (x2), 98.6, 82.8, 60.9, 45.3, 28.1 (x3).

IR (neat): 3378, 2979, 2931, 2854, 1702, 1491, 1351, 1325, 1249, 1163, 1089, 1014, 956, 907, 847, 821, 769 cm^{-1}.

$[\alpha]_D^{25}$ = –14.6 (*c* = 1.0, $CHCl_3$).

HPLC (Daicel Chiralpak AD-H, hexane/*i*-PrOH = 98:2, flow rate 1.0 mL/min, λ = 210 nm): minor isomer: t_R = 22.3 min; major isomer: t_R = 24.7 min.

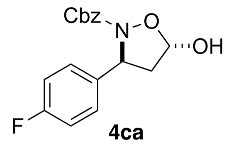

4ca

Benzyl (3*S*,5*S*)-3-(4-fluorophenyl)-5-hydroxyisoxazolidine-2-carboxylate

^{1}H NMR (400 MHz, $CDCl_3$) δ 7.35-7.15 (m, 7H), 7.00 (t, *J* = 8.7 Hz, 2H), 5.84 (d, *J* = 4.2 Hz, 1H), 5.34 (t, *J* = 8.2 Hz, 1H), 5.17 (s, 2H), 2.76 (dd, *J* = 12.6, 8.4 Hz, 1H), 2.24 (ddd, *J* = 12.6, 8.1, 4.5 Hz, 1H).

^{13}C NMR (101 MHz, $CDCl_3$) δ 162.1 (d, *J* = 245.8 Hz), 159.2, 137.1 (d, *J* = 3.1 Hz), 135.5, 128.4 (x2), 128.2, 127.8 (x2), 127.7 (x2, d, *J* = 8.0 Hz), 115.5 (x2, d, *J* = 21.6 Hz), 98.7, 68.2, 60.8, 45.3.

^{19}F NMR (376 MHz, $CDCl_3$) δ –115.1.

IR (neat): 3367 (s), 3035, 2962, 1709, 1605, 1509, 1454, 1390, 1297, 1224, 1070, 905, 835, 736, 697 cm^{-1}.

HRMS (ESI): m/z: $[M+Na]^+$ ($C_{17}H_{16}FNNaO_4$), calcd.: 340.0956; found: 340.0961.

$[\alpha]_D^{25}$ = –33.2 (c = 1.0, $CHCl_3$).

HPLC (Daicel Chiralpak AD-H, hexane/*i*-PrOH = 90:10, flow rate 1.0 mL/min, λ = 210 nm): major isomer: t_R = 13.3 min; minor isomer: t_R = 15.8 min.

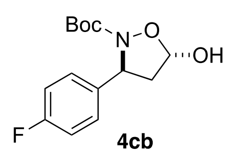

4cb

tert-Butyl (3*S*,5*S*)-3-(4-fluorophenyl)-5-hydroxyisoxazolidine-2-carboxylate

^{1}H NMR (400 MHz, $CDCl_3$) δ 7.37-7.26 (m, 2H), 7.10-6.99 (m, 2H), 5.93-5.82 (m, 1H), 5.29 (t, *J* = 8.3 Hz, 1H), 2.77 (dd, *J* = 12.5, 8.3 Hz, 1H), 2.26 (dddd, *J* = 12.6, 8.3, 4.4, 1.7 Hz, 1H), 1.45 (s, 9H).

^{13}C NMR (101 MHz, $CDCl_3$) δ 162.1 (d, *J* = 245.41), 158.6, 137.8 (d, *J* = 3.2), 127.7 (x2, d, *J* = 8.1), 115.4 (x2, d, *J* = 21.5), 98.5, 82.6, 60.8, 45.4, 28.1 (x3).

^{19}F NMR (376 MHz, $CDCl_3$) δ –115.52.

IR (neat): 3395, 2979, 2935, 1714, 1604, 1367, 1321, 1248, 1221, 1155, 1069, 910, 833, 766, 551 cm^{-1}.

HRMS (ESI): m/z: [M+Na]$^+$ ($C_{14}H_{18}FNO_4Na$), calcd.: 306.1112; found: 306.1112.

$[\alpha]_D^{25}$ = –10.7 (c = 1.0, $CHCl_3$).

HPLC (Daicel Chiralpak AD-H, hexane/i-PrOH = 90:10, flow rate 1.0 mL/min, λ = 210 nm): major isomer: t_R = 9.3 min; minor isomer: t_R = 11.3 min.

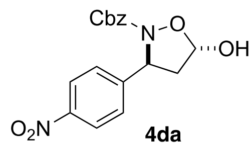

4da

Benzyl (3*S*,5*S*)-5-hydroxy-3-(4-nitrophenyl)isoxazolidine-2-carboxylate[5]

^{1}H NMR (400 MHz, $CDCl_3$) δ 8.17 (d, *J* = 8.7 Hz, 2H), 7.49 (d, *J* = 8.7 Hz, 2H), 7.37-7.16 (m, 5H), 5.94 (d, *J* = 4.2 Hz, 1H), 5.48 (t, *J* = 8.3 Hz, 1H), 5.18 (s, 2H), 2.87 (dd, *J* = 12.5, 8.5 Hz, 1H), 2.25 (ddd, *J* = 12.5, 8.2, 4.4 Hz, 1H).

^{13}C NMR (101 MHz, $CDCl_3$) δ 159.1, 148.6, 147.2, 135.1, 128.4 (x2), 128.3, 127.8 (x2), 126.8 (x2), 123.9 (x2), 98.7, 68.5, 60.8, 45.0.

IR (neat): 3363, 2958, 2837, 1706, 1612, 1513, 1455, 1392, 1319, 1290, 1243, 1113, 1029, 903, 849, 747, 695 cm^{-1}.

HRMS (ESI): m/z: [M+Na]$^+$ ($C_{17}H_{16}N_2NaO_6$), calcd.: 367.0901; found: 367.0903.

$[\alpha]_D^{25}$ = –40.5 (*c* = 1.0, $CHCl_3$).

HPLC (Daicel Chiralpak AD-H, hexane/*i*-PrOH = 80:20, flow rate 1.0 mL/min, λ = 210 nm): minor isomer: t_R = 19.7 min; major isomer: t_R = 22.1 min.

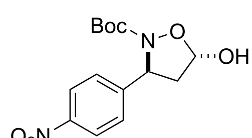

4db

tert-Butyl (3*S*,5*S*)-5-hydroxy-3-(4-nitrophenyl)isoxazolidine-2-carboxylate[5]

^{1}H NMR (400 MHz, $CDCl_3$) δ 8.22 (d, *J* = 8.8 Hz, 2H), 7.53 (d, *J* = 8.6 Hz, 2H), 5.94 (d, *J* = 4.3 Hz, 1H), 5.40 (t, *J* = 8.4 Hz, 1H), 2.85 (dd, *J* = 12.4, 8.4 Hz, 1H), 2.23 (ddd, *J* = 12.6, 8.5, 4.4 Hz, 1H), 1.44 (s, 9H).

^{13}C NMR (101 MHz, $CDCl_3$) δ 158.6, 149.4, 147.25, 126.9 (x2), 123.9 (x2), 98.5, 83.3, 61.0, 45.1, 28.0 (x3).

IR (neat): 3329, 2960, 2931, 2840, 1702, 1614, 1514, 1455, 1368, 1336, 1299, 1246, 1159, 1088, 1064, 1032, 965, 913, 868, 835, 807 cm^{-1}.

$[\alpha]_D^{25}$ = –26.9 (*c* = 1.0, $CHCl_3$).

HPLC (Daicel Chiralpak AD-H, hexane/*i*-PrOH = 90:10, flow rate 1.0 mL/min, λ = 210 nm): minor isomer: t_R = 12.1 min; major isomer: t_R = 14.1 min.

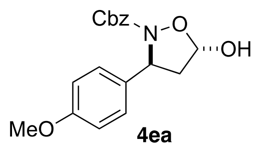

4ea

Benzyl (3*S*,5*S*)-5-hydroxy-3-(4-methoxyphenyl)isoxazolidine-2-carboxylate

^{1}H NMR (400 MHz, $CDCl_3$) δ 7.35-7.17 (m, 7H), 6.86 (d, *J* = 8.7 Hz, 2H), 5.90 (d, *J* = 4.2 Hz, 1H), 5.33 (t, *J* = 8.2 Hz, 1H), 5.17 (s, 2H), 3.79 (s, 3H), 2.75 (dd, *J* = 12.6, 8.3 Hz, 1H), 2.29 (ddd, *J* = 12.6, 8.3, 4.5 Hz, 1H).

^{13}C NMR (101 MHz, $CDCl_3$) δ 159.2, 159.0, 135.7, 133.4, 128.4 (x2), 128.1, 127.7 (x2), 127.3 (x2), 114.0 (x2), 98.7, 68.0, 60.9, 55.3, 45.2.

IR (neat): 3475, 3120, 2960, 2850, 1707, 1610, 1513, 1396, 1346, 1324, 1261, 1124, 1012, 962, 833, 758, 694, 518 cm^{-1}.

HRMS (ESI): m/z: $[M+Na]^+$ ($C_{18}H_{19}NNaO_5$), calcd.: 352.1155; found: 352.1152.

$[\alpha]_D^{25}$ = –51.7 (*c* = 1.0, $CHCl_3$).

HPLC (Daicel Chiralpak AD-H, hexane/*i*-PrOH = 85:15, flow rate 1.0 mL/min, λ = 210 nm): major isomer: t_R = 16.1 min; minor isomer: t_R = 19.8 min.

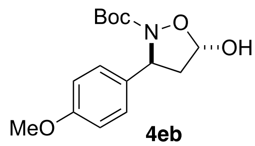

4eb

tert-Butyl (3*S*,5*S*)-5-hydroxy-3-(4-methoxyphenyl)isoxazolidine-2-carboxylate

^{1}H NMR (400 MHz, $CDCl_3$) δ 7.25 (d, *J* = 8.6 Hz, 2H), 6.86 (d, *J* = 8.8 Hz, 2H), 5.93-5.82 (m, 1H), 5.23 (t, *J* = 8.2 Hz, 1H), 3.79 (s, 3H), 2.71 (dd, *J* = 12.5, 8.3 Hz, 1H), 2.26 (dddd, *J* = 12.6, 8.3, 4.5, 2.0 Hz, 1H), 1.42 (s, 9H).

^{13}C NMR (101 MHz, $CDCl_3$) δ 158.8, 158.7, 134.1, 127.4 (x2), 113.9 (x2), 98.6, 82.3, 60.9, 55.3, 45.3, 28.1 (x3).

IR (neat): 3329, 2960, 2931, 1702, 1613, 1514, 1455, 1336, 1299, 1246, 1159, 1088, 1064, 1032, 965, 91, 807 cm^{-1}.

HRMS (ESI): m/z: [M+Na]$^+$ ($C_{15}H_{21}NNaO_5$), calcd.: 318.1312; found: 318.1311.

$[\alpha]_D^{25}$ = –33.8 (*c* = 1.0, $CHCl_3$).

HPLC (Daicel Chiralpak AD-H, hexane/*i*-PrOH = 90:10, flow rate 1.0 mL/min, λ = 210 nm): major isomer: t_R = 9.1 min; minor isomer: t_R = 10.0 min.

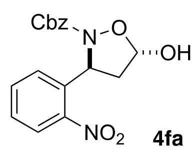

4fa

Benzyl (3*S*,5*S*)-5-hydroxy-3-(2-nitrophenyl)isoxazolidine-2-carboxylate

^{1}H NMR (400 MHz, $CDCl_3$) δ 8.04 (dd, *J* = 8.2, 1.2 Hz, 1H), 7.79 (dd, *J* = 8.0, 1.3 Hz, 1H), 7.65 (td, *J* = 7.8, 1.2 Hz, 1H), 7.49 – 7.41 (m, 1H), 7.35-7.20 (m, 5H), 6.09 (t, *J* = 7.8 Hz, 1H), 5.91 (d, *J* = 4.3 Hz, 1H), 5.24-5.15 (m, 2H), 3.17 (dd, *J* = 12.9, 8.6 Hz, 1H), 2.28-2.16 (m, 1H).

^{13}C NMR (101 MHz, $CDCl_3$) δ 158.8, 147.3, 137.7, 135.3, 134.1 (x2), 128.5 (x2), 128.3 (x2), 127.9, 127.8, 124.8, 98.9, 68.4, 58.7, 45.2.

IR (neat): 3366, 3067, 3035, 2961, 1710, 1609, 1578, 1523, 1446, 1391, 1339, 1292, 1067, 907, 738, 676 cm^{-1}.

HRMS (ESI): m/z: [M+Na]$^+$ ($C_{17}H_{16}N_2NaO_6$), Calcd.: 367.0901. Found: 367.0910.

$[\alpha]_D^{25}$ = +67.7 (*c* = 1.0, $CHCl_3$).

HPLC (Daicel Chiralpak AD-H, hexane/*i*-PrOH = 90:10, flow rate 1.0 mL/min, λ = 210 nm): major isomer: t_R = 11.3 min; minor isomer: t_R = 14.7 min.

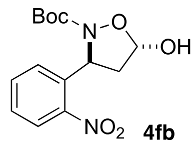

4fb

tert-Butyl (3*S*,5*S*)-5-hydroxy-3-(2-nitrophenyl)isoxazolidine-2-carboxylate

^{1}H NMR (400 MHz, $CDCl_3$) δ 7.89 (d, *J* = 8.2 Hz, 1H), 7.70 (d, *J* = 7.8 Hz, 1H), 7.60-7.50 (m, 1H), 7.42-7.28 (m, 1H), 5.92-5.76 (m, 2H), 3.01 (dd, *J* = 12.7, 8.4 Hz, 1H), 2.10 (ddd, *J* = 7.9, 4.6, 2.1 Hz, 1H), 1.32 (s, 9H).

^{13}C NMR (101 MHz, $CDCl_3$) δ 158.1, 147.6, 138.2, 133.9, 128.1(x2), 124.4, 98.8, 83.1, 58.4, 45.3, 28.0 (x3).

IR (neat): 3348, 2977, 2927, 2854, 1707, 1345, 1244, 1138, 1066, 958, 913, 848, 788, 744 cm^{-1}.

HRMS (ESI): m/z: $[M+Na]^+$ ($C_{14}H_{18}N_2NaO_6$), calcd.: 333.1057; found: 333.1059.

$[\alpha]_D^{25}$ = +83.4 (*c* = 1.0, $CHCl_3$).

HPLC (Daicel Chiralpak AD-H, hexane/*i*-PrOH = 95:5, flow rate 1.0 mL/min, λ = 210 nm): minor isomer: t_R = 19.0 min; major isomer: t_R = 20.2 min.

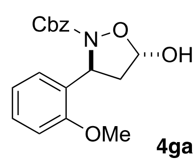

4ga

Benzyl (3*S*,5*S*)-5-hydroxy-3-(2-methoxyphenyl)isoxazolidine-2-carboxylate

^{1}H NMR (400 MHz, $CDCl_3$) δ 7.42 (d, *J* = 7.6 Hz, 1H), 7.32-7.18 (m, 6H), 6.94 (t, *J* = 7.5 Hz, 1H), 6.86 (d, *J* = 8.2 Hz, 1H), 5.81 (s, 1H), 5.72 (t, *J* = 7.8 Hz, 1H), 5.19 (s, 2H), 3.80 (s, 3H), 2.89 (dd, *J* = 12.7, 8.4 Hz, 1H), 2.13 (ddd, *J* = 12.4, 7.2, 4.8 Hz, 1H).

^{13}C NMR (101 MHz, $CDCl_3$) δ 159.3, 156.1, 135.9, 129.9, 128.3 (x2), 128.2, 128.1, 127.7 (x2), 125.8, 120.6, 110.3, 98.8, 67.9, 56.8, 55.3, 44.2.

IR (neat): 3360, 2960, 2838, 1707, 1601, 1491, 1460, 1389, 1339, 1285, 1239, 1068, 1025, 908, 751, 696 cm^{-1}.

HRMS (ESI): m/z: $[M+Na]^+$ ($C_{18}H_{19}NNaO_5$), calcd.: 352.1155; found: 352.1154.

$[\alpha]_D^{25}$ = –42.0 (*c* = 1.0, $CHCl_3$).

HPLC (Daicel Chiralpak AD-H, hexane/*i*-PrOH = 90:10, flow rate 1.0 mL/min, λ = 210 nm): major isomer: t_R = 7.8 min; minor isomer: t_R = 13.2 min.

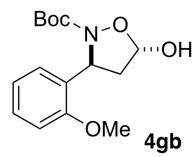

4gb

tert-Butyl (3*S*,5*S*)-5-hydroxy-3-(2-methoxyphenyl)isoxazolidine-2-carboxylate

^{1}H NMR (400 MHz, $CDCl_3$) δ 7.43 (dd, *J* = 7.6, 1.5 Hz, 1H), 7.29-7.16 (m, 1H), 6.94 (td, *J* = 7.5, 0.9 Hz, 1H), 6.86 (dd, *J* = 8.2, 0.7 Hz, 1H), 5.84 (dd, *J* = 4.2, 2.8 Hz, 1H), 5.64 (t, *J* = 7.9 Hz, 1H), 3.84 (s, 3H), 2.85 (dd, *J* = 12.7, 8.4 Hz, 1H), 2.14-2.03 (m, 1H), 1.43 (s, 9H).

^{13}C NMR (101 MHz, $CDCl_3$) δ 158.8, 156.1, 130.6, 128.0, 126.0, 120.6, 110.2, 98.7, 82.1, 56.7, 55.3, 44.2, 28.1 (x3).

IR (neat): 3356, 2976, 2930, 2850, 1703, 1602, 1491, 1461, 1348, 1315, 1239, 1160, 1066, 1027, 916, 848, 806, 751 cm^{-1}.

HRMS (ESI): m/z: $[M+Na]^+$ ($C_{15}H_{21}NNaO_5$), calcd.: 318.1312; found: 318.1312.

$[\alpha]_D^{25}$ = –22.0 (*c* = 1.0, $CHCl_3$).

HPLC (Daicel Chiralpak AD-H, hexane/*i*-PrOH = 90:10, flow rate 1.0 mL/min, λ = 210 nm): major isomer: t_R = 7.9 min; minor isomer: t_R = 11.1 min.

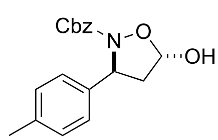

4ha

Benzyl (3*S*,5*S*)-5-hydroxy-3-(*p*-tolyl)isoxazolidine-2-carboxylate

^{1}H NMR (400 MHz, $CDCl_3$) δ 7.30–7.16 (m, 7H), 7.11 (d, *J* = 7.8 Hz, 2H), 5.89 (d, *J* = 4.3 Hz, 1H), 5.38 – 5.29 (m, 1H), 5.20 – 5.08 (m, 2H), 2.80 – 2.68 (m, 1H), 2.33 – 2.21 (m, 4H).

^{13}C NMR (101 MHz, $CDCl_3$) δ 159.3, 138.4, 137.0, 135.6, 129.2 (x2), 128.3 (x2), 128.0, 127.6 (x2), 125.9 (x2), 98.7, 68.0, 61.1, 45.1, 20.9.

IR (neat): 3363, 3062, 3032, 2860, 1708, 1515, 1454, 1390, 1337, 1302, 1237, 1068, 906, 806, 731, 696 cm^{-1}.

HRMS (ESI): m/z: $[M+Na]^+$ ($C_{18}H_{19}NNaO_4$), Calcd.: 336.1206. Found: 336.1198.

$[\alpha]_D^{25}$ = –34.5 (*c* = 1.0, $CHCl_3$).

HPLC (Daicel Chiralpak AD-H, hexane/*i*-PrOH = 90:10, flow rate 1.0 mL/min, λ = 210 nm): major isomer: t_R = 11.5 min; minor isomer: t_R = 15.6 min.

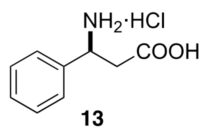

13

(*S*)-3-Amino-3-phenylpropanoic acid hydrochloride[6]

^{1}H NMR (400 MHz, Deuterium Oxide) δ 7.38 (s, 5H), 4.69 (m, 5 H), 3.10 (dd, J = 17.2, 7.7 Hz, 1H), 2.98 (dd, J = 17.2, 6.6 Hz, 1H).

^{13}C NMR (101 MHz, D2O) δ 173.4, 135.1, 129.7, 129.4 (x2), 127.1 (x2), 51.5, 37.7.

$[\alpha]_D^{25}$ = +2.8 (*c* = 0.28, H_2O). Lit.: +3.0[6a] (*c* = 0.28, H_2O), +3.0[6b] (*c* = 0.47, H_2O) and +4.0[6c] (*c* = 0.3, H_2O).

5. References

[1] I. Arenas, A. Ferrali, C. Rodríguez-Escrich, F. Bravo, M. A. Pericàs, *Adv. Synth. Catal.* **2017**, *359*, 2414.

[2] X. Fan, S. Sayalero, M. A. Pericàs, *Adv. Synth. Catal.* **2012**, *354*, 2971-2976.

[3] I. Sagamanova, C. Rodríguez-Escrich, I. Gábor Molnár, S. Sayalero, R. Gilmour, M. A. Pericàs, *ACS Catal.* **2015**, *5*, 6241-6248.

[4] P. Llanes, C. Rodríguez-Escrich, S. Sayalero, M. A. Pericàs, *Org. Lett.* **2016**, *18*, 6292-6295.

[5] a) I. Ibrahem, R. Rios, J. Vesely, G. L. Zhao, A. Córdova, *Chem. Commun.* **2007**, 849-851; b) I. Ibrahem, R. Rios, J. Vesely, G. L. Zhao, A. Cordova, *Synthesis* **2008**, 1153-1157.

[6] a) E. Forró, T. Paál, G. Tasnádi, F. Fülöp, *Adv. Synth. Catal*. **2006**, *348*, 917-923; b) O. Marianacci, G. Micheletti, L. Bernardi, F. Fini, M. Fochi, D. Pettersen, V. Sgarzani, A. Ricci, *Chem. Eur. J*. **2007**, *13*, 8338-8351; c) G. Tasnádi, E. Forró, F. Fülöp, *Tetrahedron: Asymmetry* **2008**, *19*, 2072-2077.

6. NMR spectra

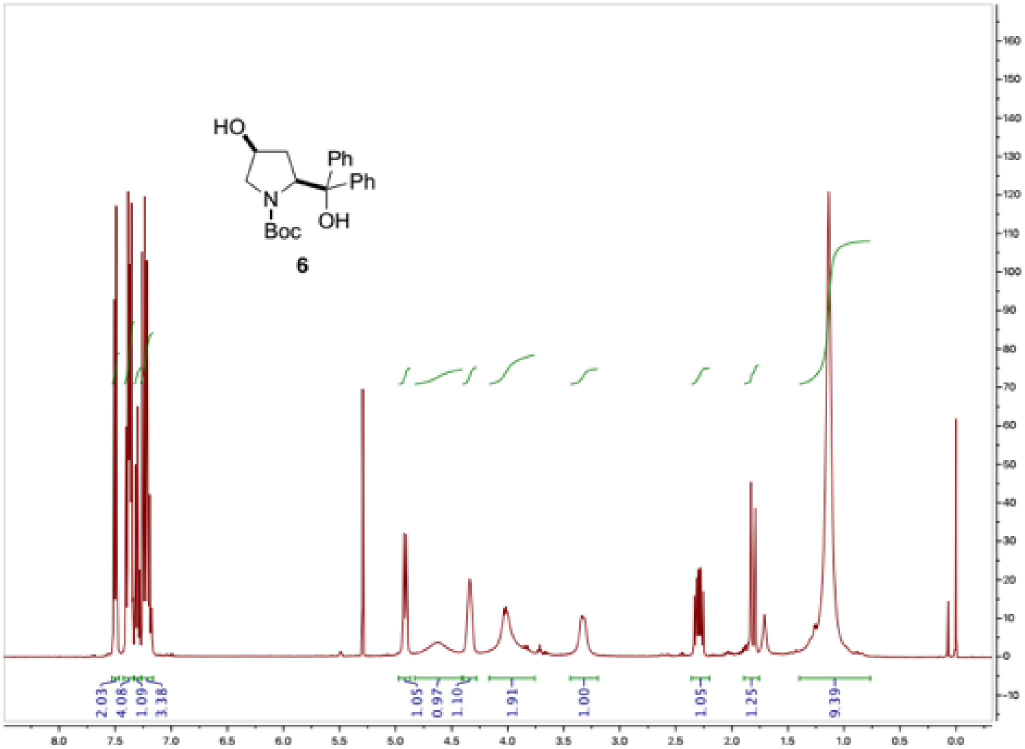

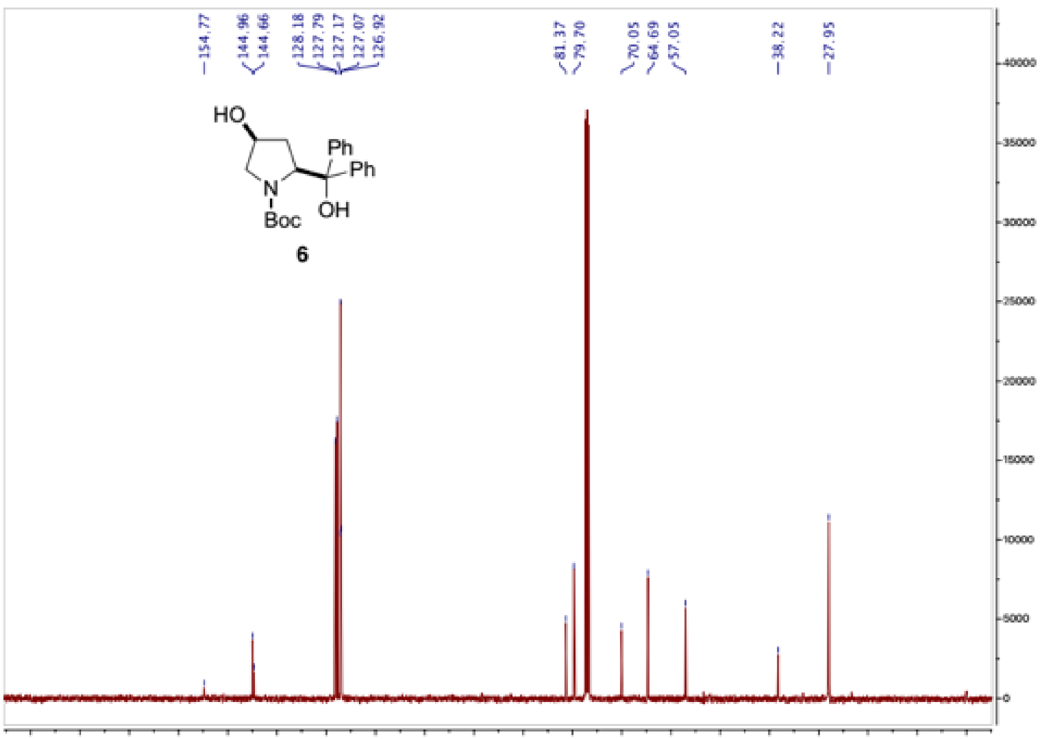

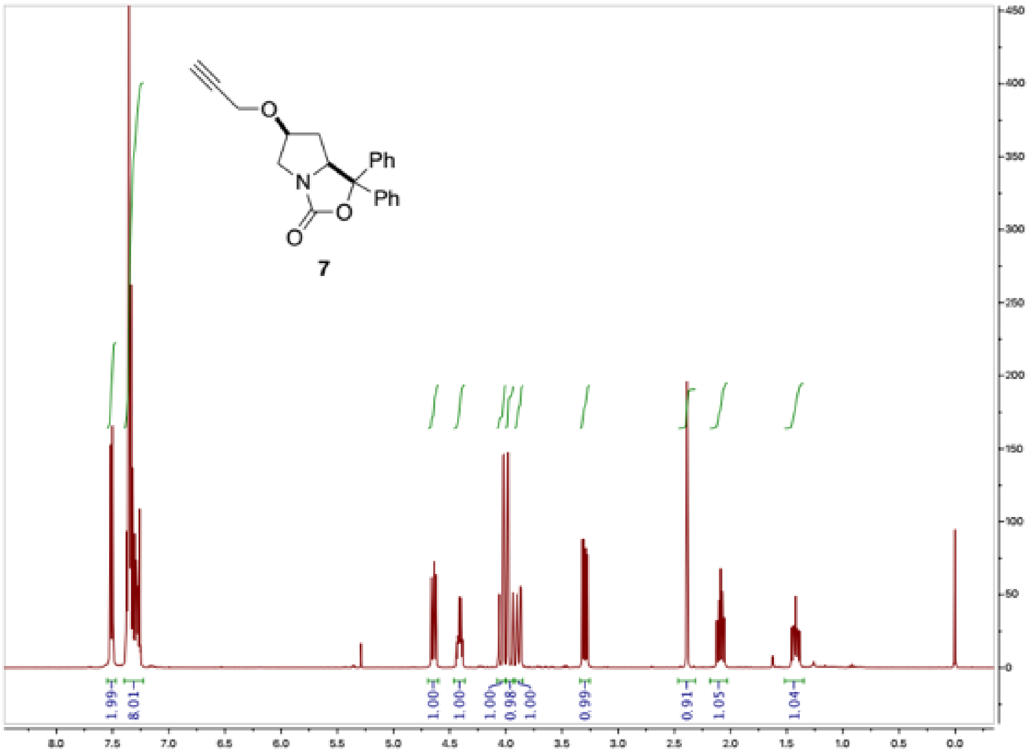
Ph
Ph
N
O
O
O
7
1.99
8.01
1.00
1.00
1.00
0.98
1.00
0.99
0.91
1.05
1.04

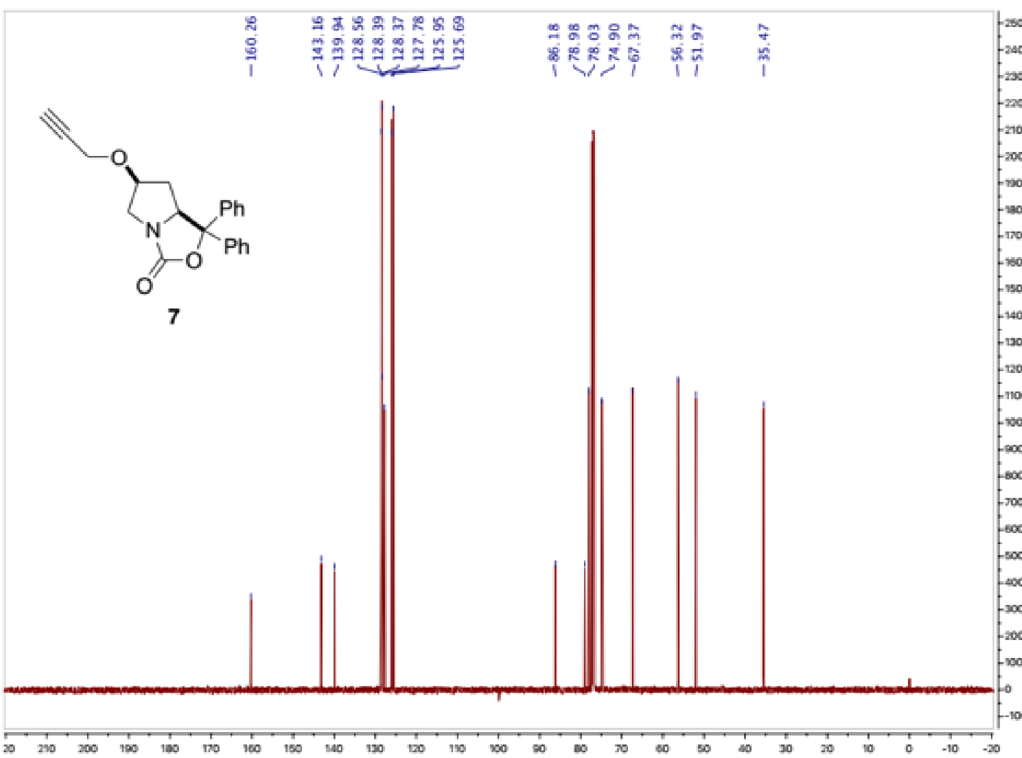
160.26
143.16
139.94
128.56
128.39
128.37
127.78
125.95
125.69
86.18
78.98
78.03
74.90
67.37
56.32
51.97
35.47
Ph
Ph
N
O
O
O
7

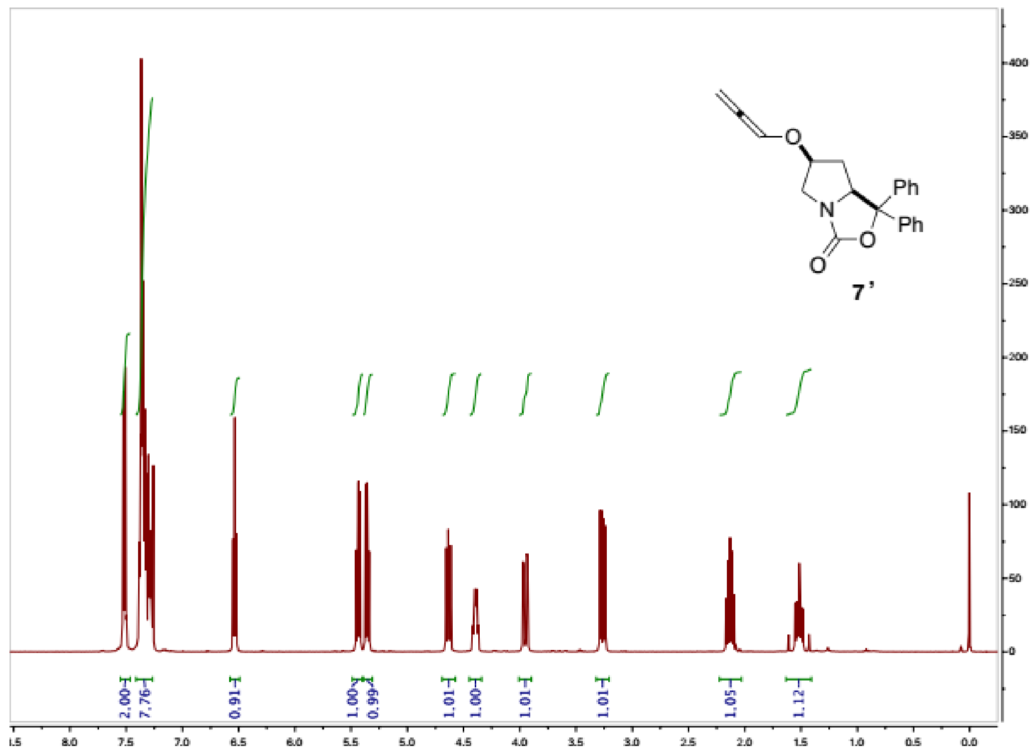
7'
2.00
7.76
0.91
1.00
0.99
1.01
1.00
1.01
1.01
1.05
1.12

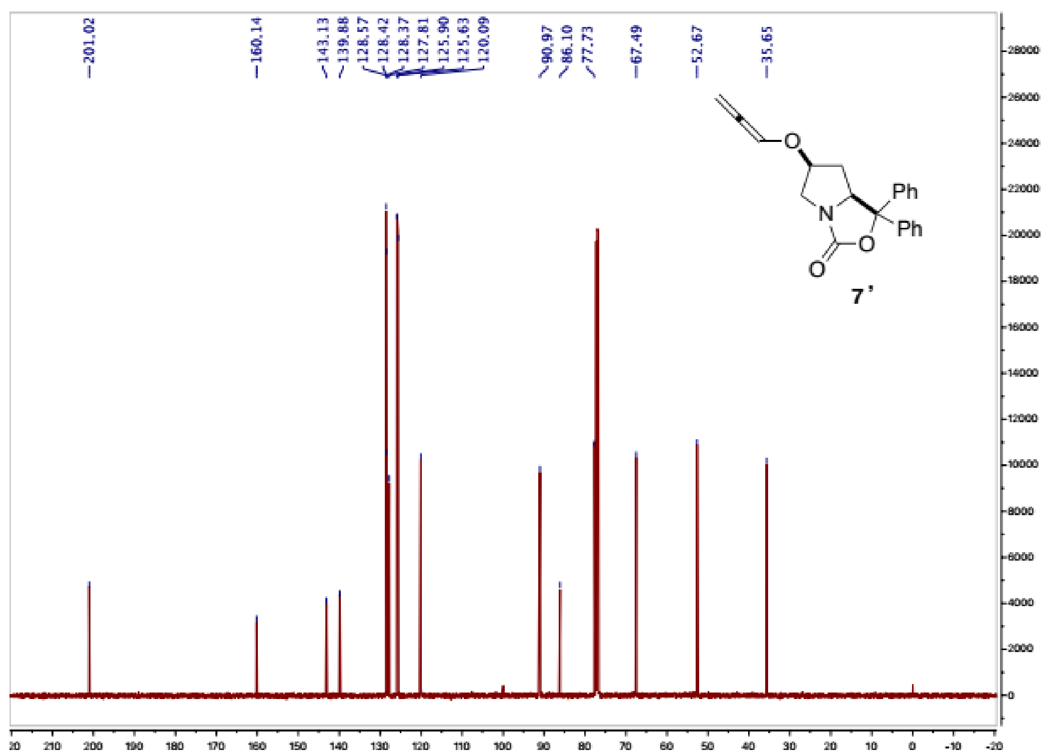
201.02
160.14
143.13
139.88
128.57
128.42
128.37
127.81
125.90
125.63
120.09
90.97
86.10
77.73
67.49
52.67
35.65
7'

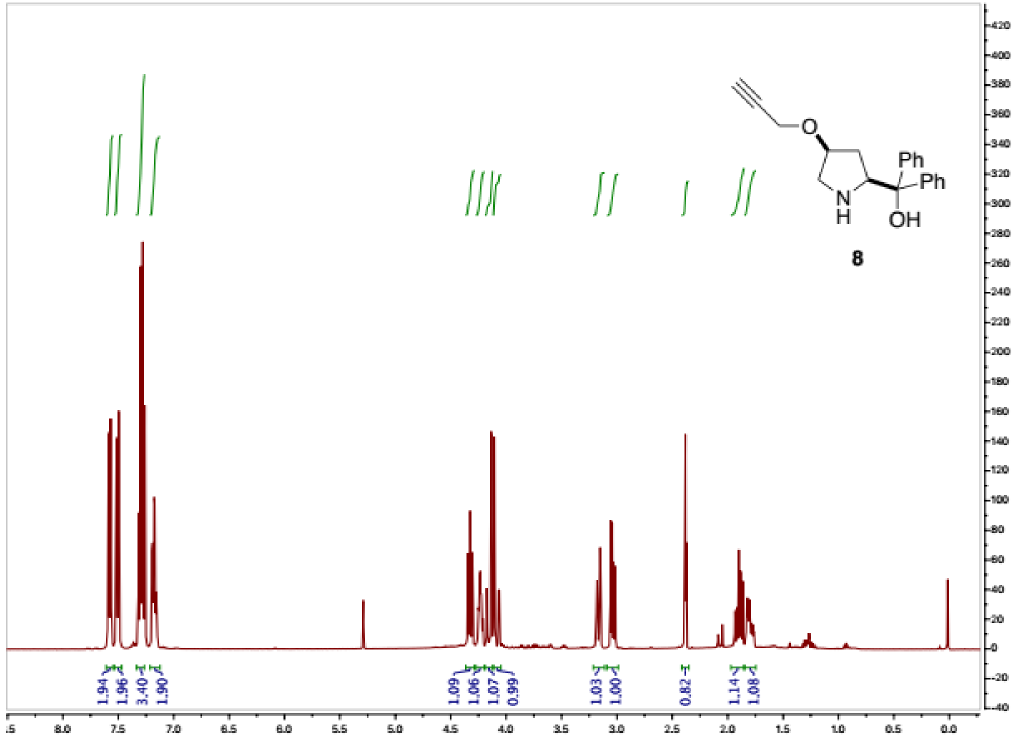
Ph
Ph
N
H
OH
O
8
1.94
1.96
3.40
1.90
1.09
1.06
1.07
0.99
1.03
1.00
0.82
1.14
1.08

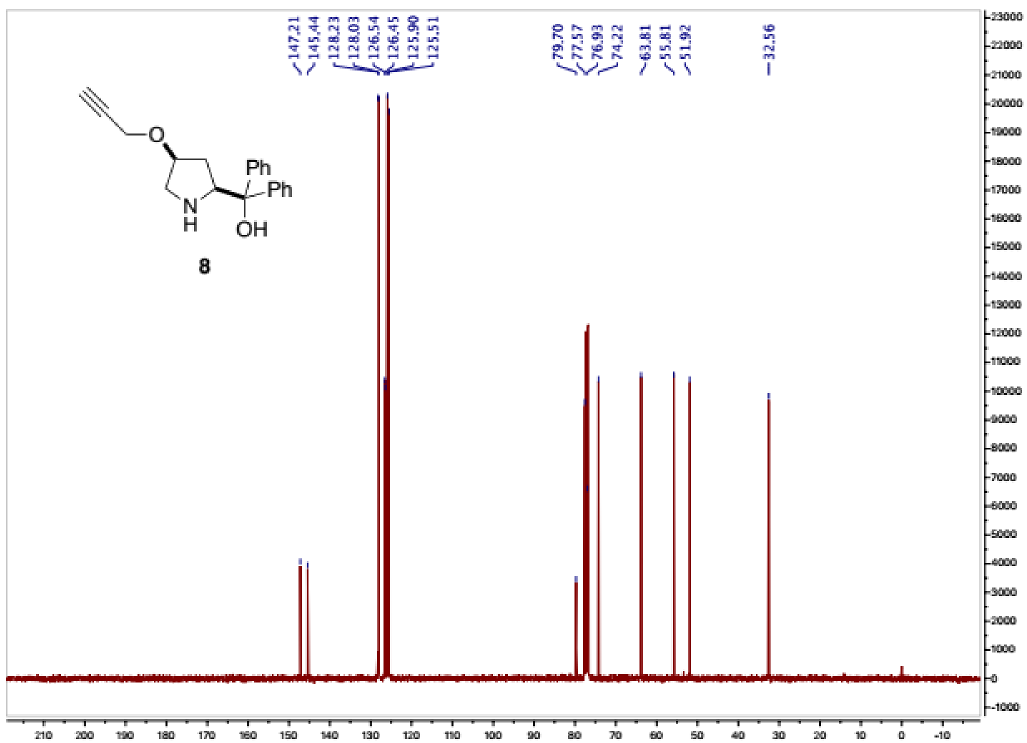
147.21
145.44
128.23
128.03
126.54
126.45
125.90
125.51
79.70
77.57
76.93
74.22
63.81
55.81
51.92
32.56
Ph
Ph
N
H
OH
O
8

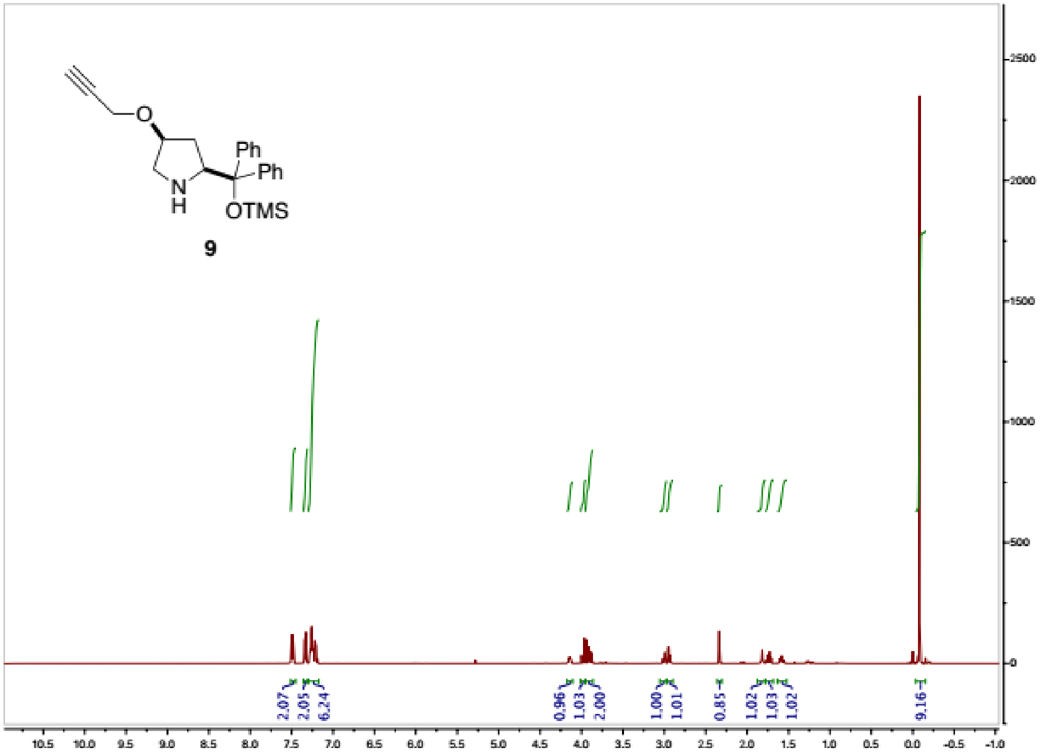
Ph
Ph
O
N
H
OTMS
9
2.07
2.05
6.24
0.96
1.03
2.00
1.00
1.01
0.85
1.02
1.03
1.02
9.16

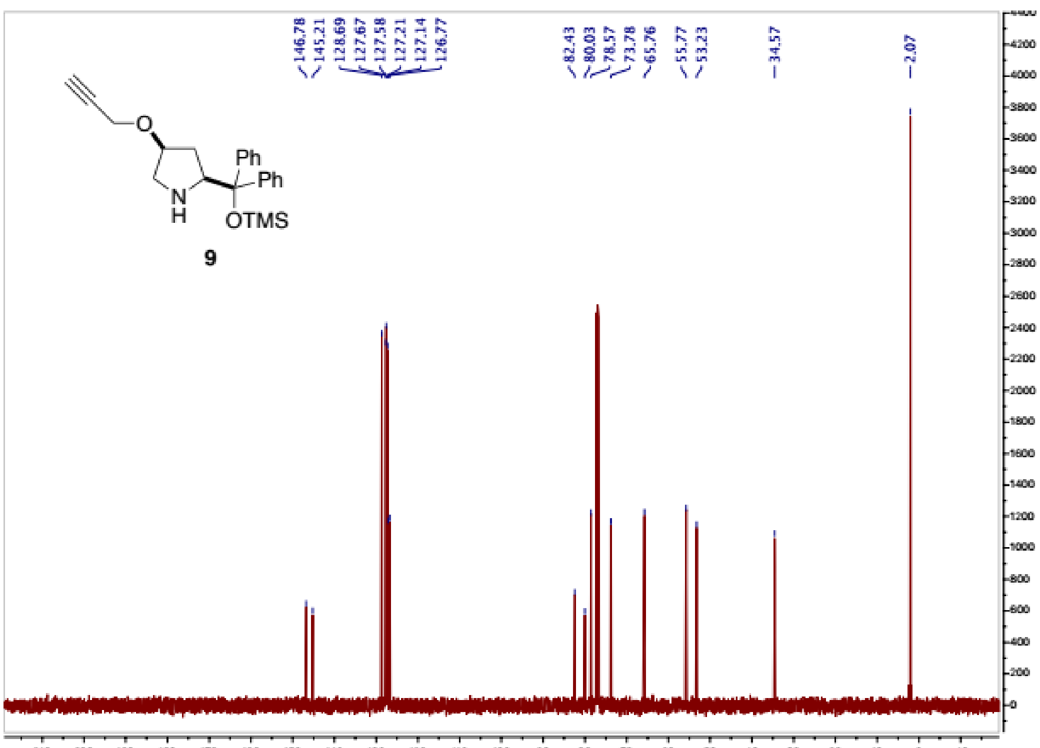
146.78
145.21
128.69
127.67
127.58
127.21
127.14
126.77
82.43
80.03
78.57
73.78
65.76
55.77
53.23
34.57
2.07
Ph
Ph
O
N
H
OTMS
9

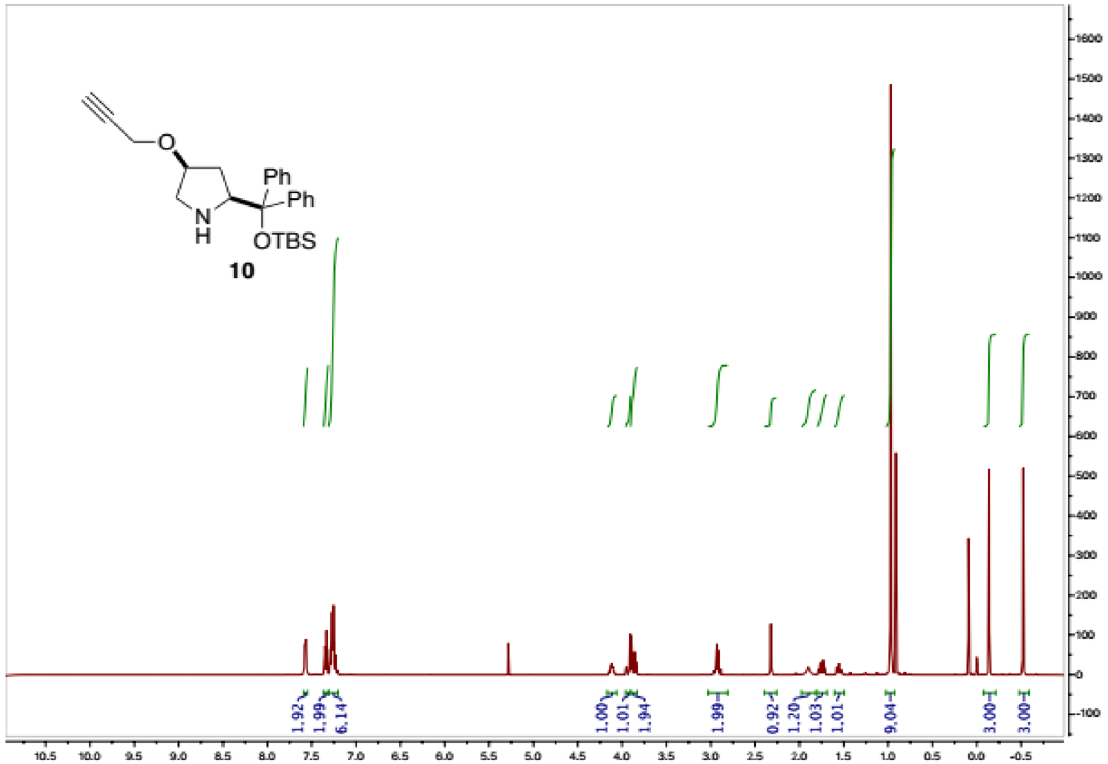
Ph
Ph
N
H
OTBS
10
1.92
1.99
6.14
1.00
1.01
1.94
1.99
0.92
1.20
1.03
1.01
9.04
3.00
3.00

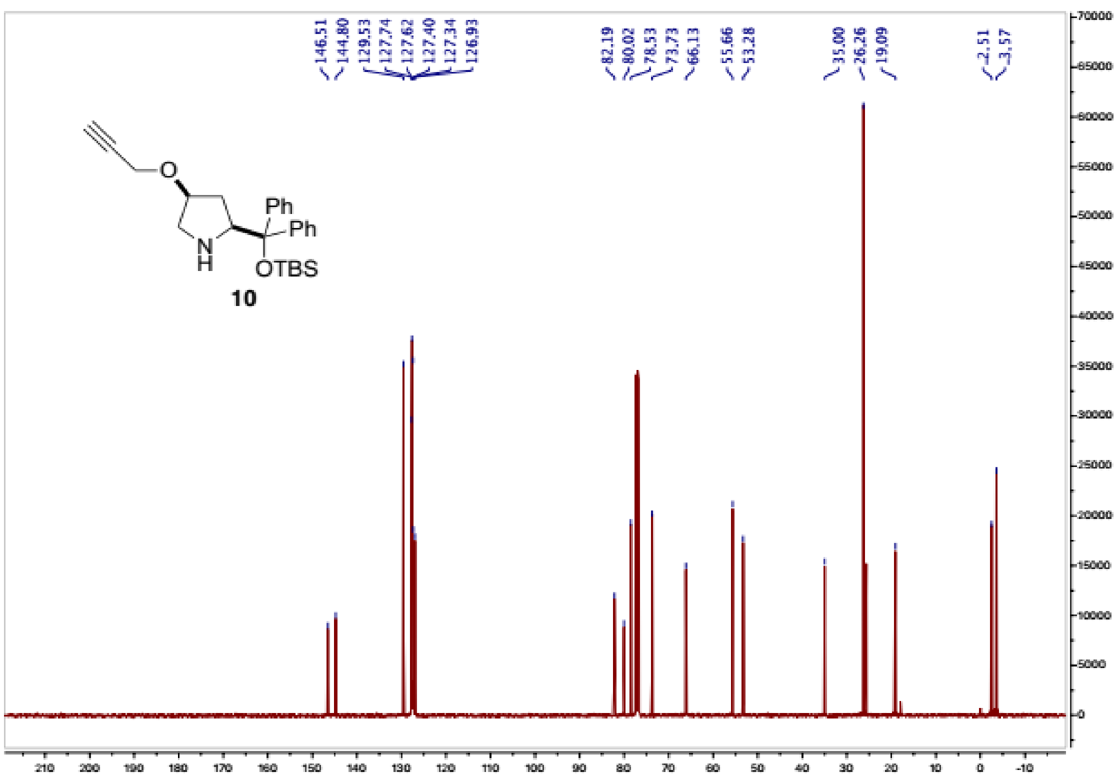
146.51
144.80
129.53
127.74
127.62
127.40
127.34
126.93
82.19
80.02
78.53
73.73
66.13
55.66
53.28
35.00
26.26
19.09
-2.51
-3.57
Ph
Ph
N
H
OTBS
10

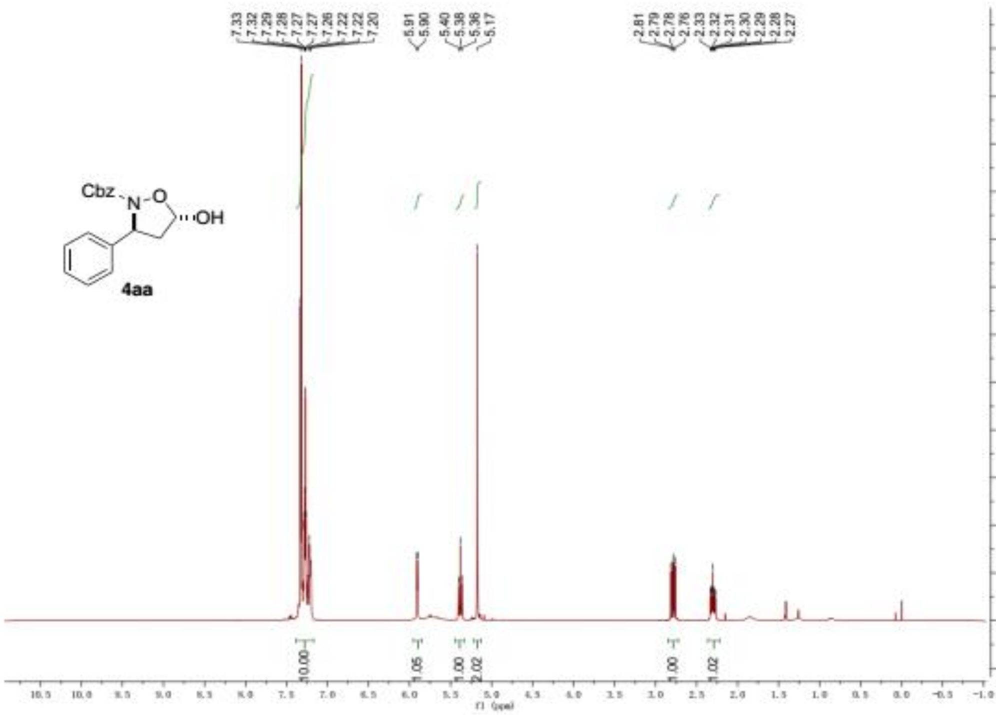
7.33
7.32
7.29
7.28
7.27
7.27
7.26
7.22
7.22
7.20
5.91
5.90
5.40
5.38
5.36
5.17
2.81
2.79
2.78
2.76
2.33
2.32
2.31
2.30
2.29
2.28
2.27
Cbz
N
O
OH
4aa
10.00
1.05
1.00
2.02
1.00
1.02
f1 (ppm)

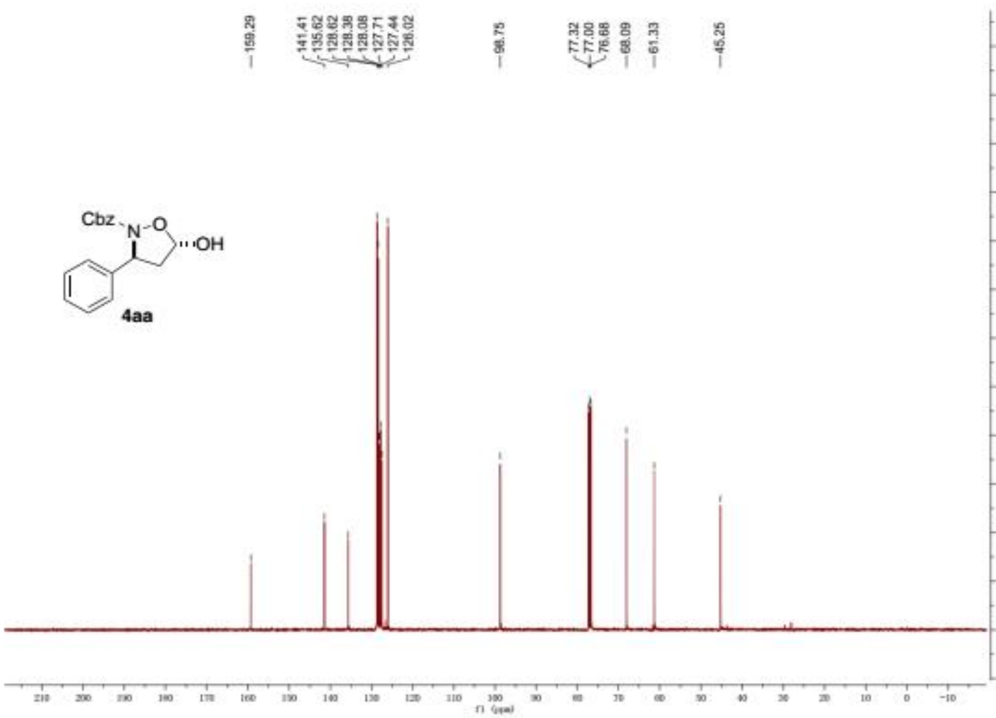
159.29
141.41
135.62
128.62
128.38
128.08
127.71
127.44
126.02
98.75
77.32
77.00
76.68
68.09
61.33
45.25
Cbz
N
O
OH
4aa
f1 (ppm)

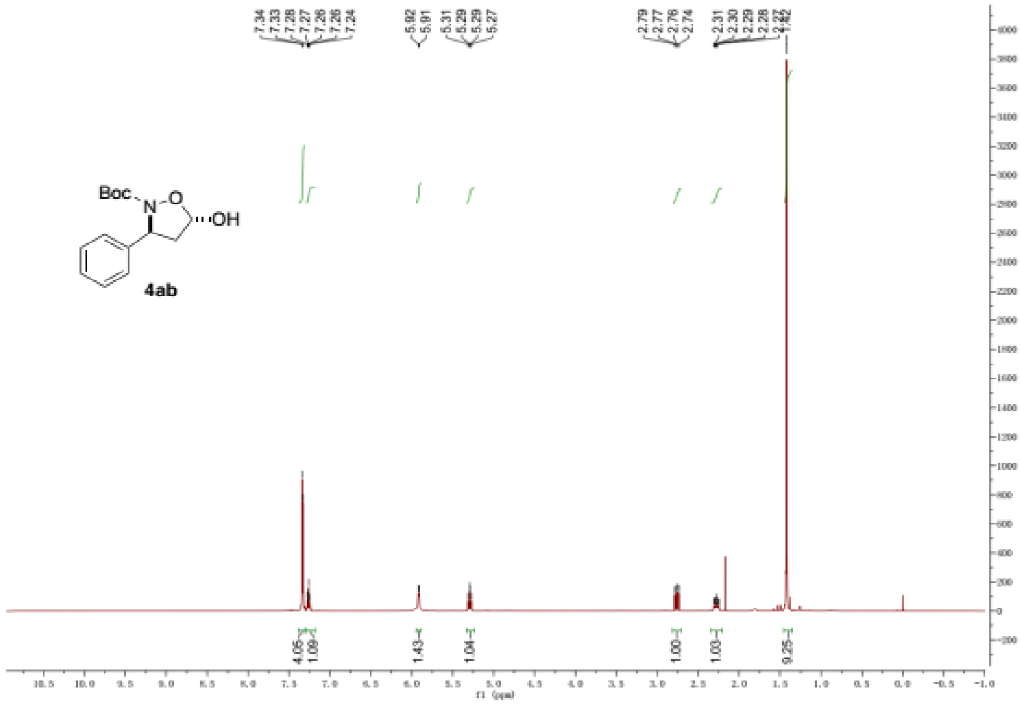
7.34
7.33
7.28
7.27
7.26
7.26
7.24
5.92
5.91
5.31
5.29
5.29
5.27
2.79
2.77
2.76
2.74
2.31
2.30
2.29
2.28
2.27
1.42
Boc
N
O
OH
4ab
4.05
1.09
1.43
1.04
1.00
1.03
9.25
f1 (ppm)

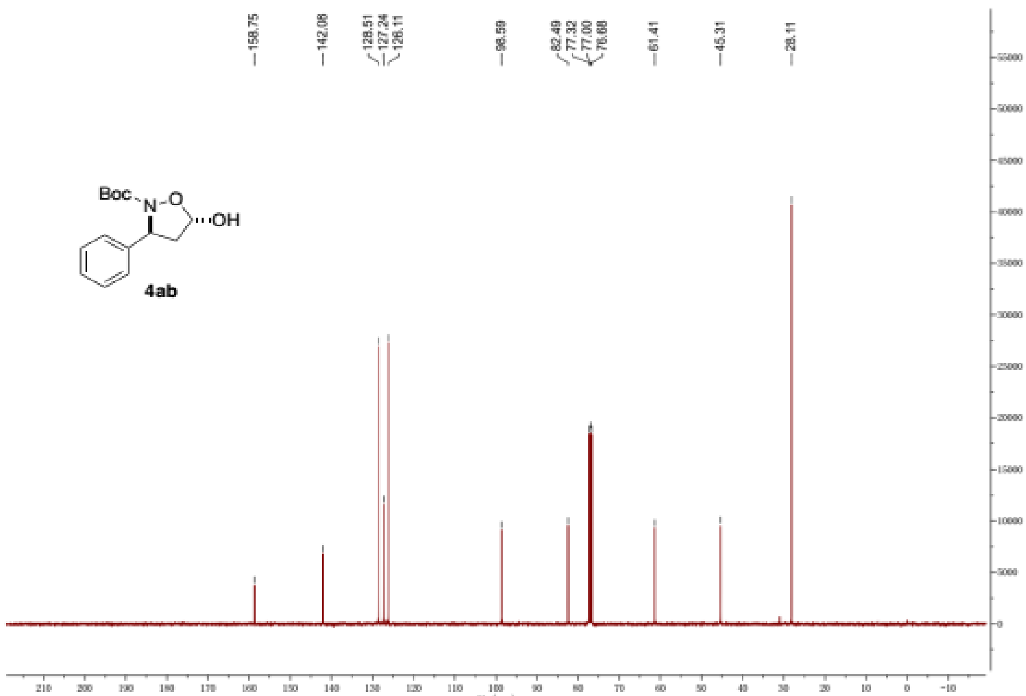
158.75
142.08
128.51
127.24
126.11
98.59
82.49
77.32
77.00
76.68
61.41
45.31
28.11
Boc
N
O
OH
4ab
f1 (ppm)

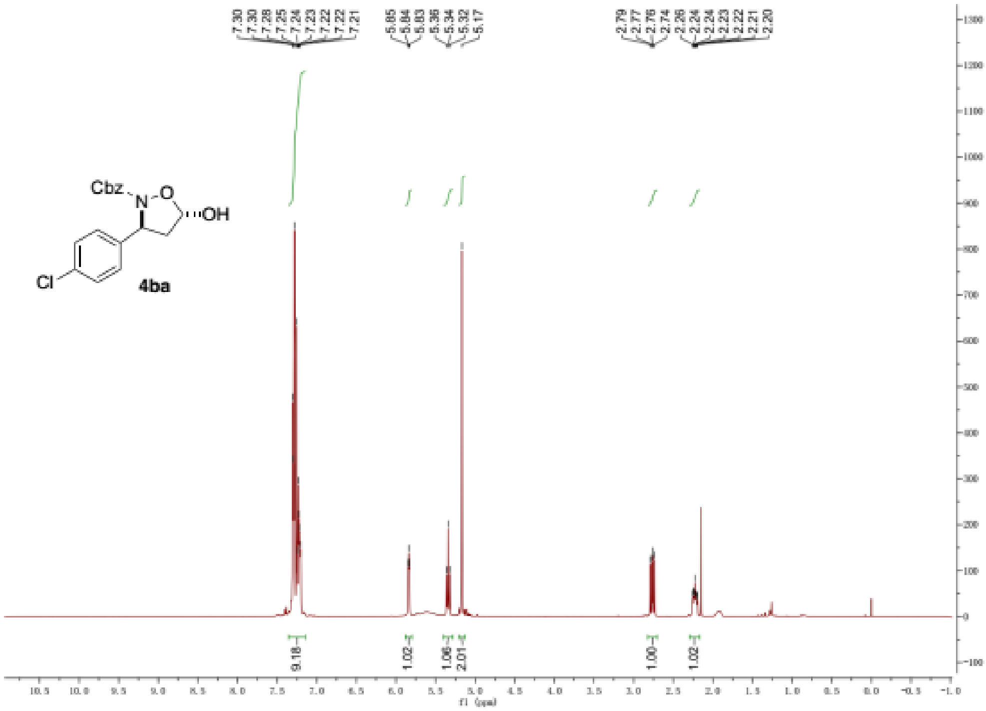
7.30 7.30 7.28 7.25 7.24 7.23 7.22 7.22 7.21
5.85 5.84 5.83 5.36 5.34 5.32 5.17
2.79 2.77 2.76 2.74 2.26 2.24 2.24 2.23 2.22 2.21 2.20
Cbz
N
O
OH
Cl
4ba
9.18
1.02
1.06
2.01
1.00
1.02
f1 (ppm)

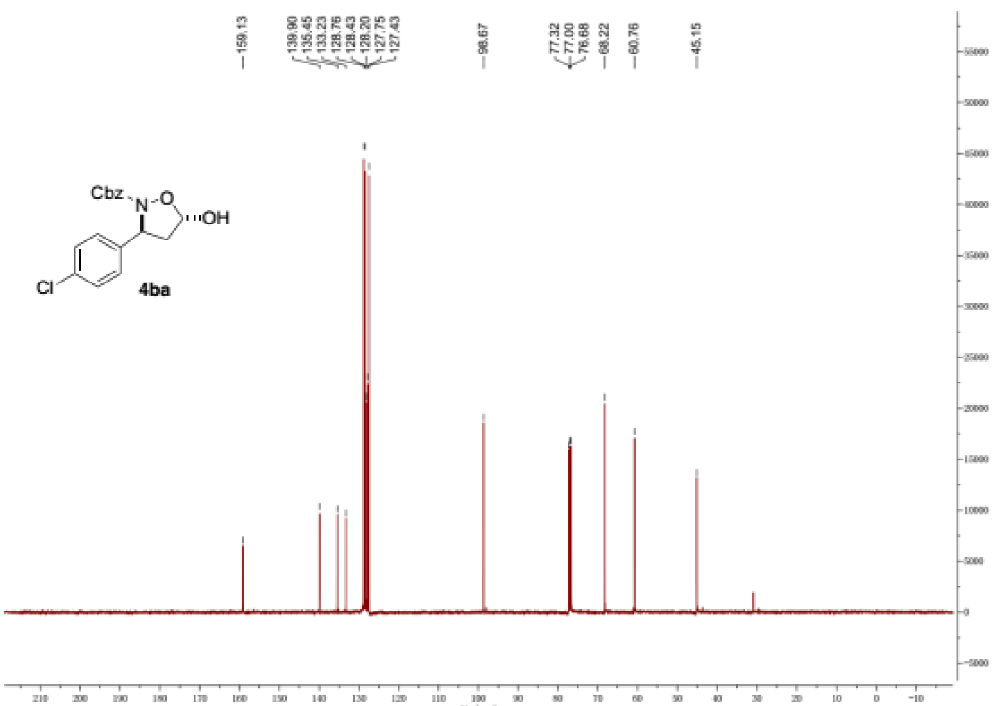
159.13
139.90 135.45 133.23 128.76 128.43 128.20 127.75 127.43
98.67
77.32 77.00 76.68
68.22
60.76
45.15
Cbz
N
O
OH
Cl
4ba
f1 (ppm)

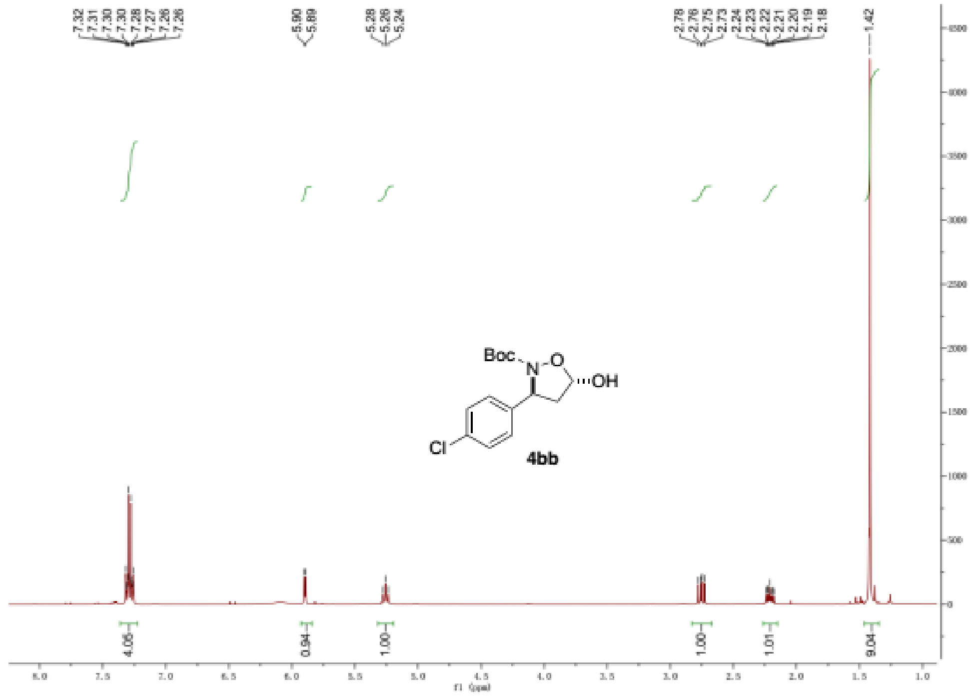

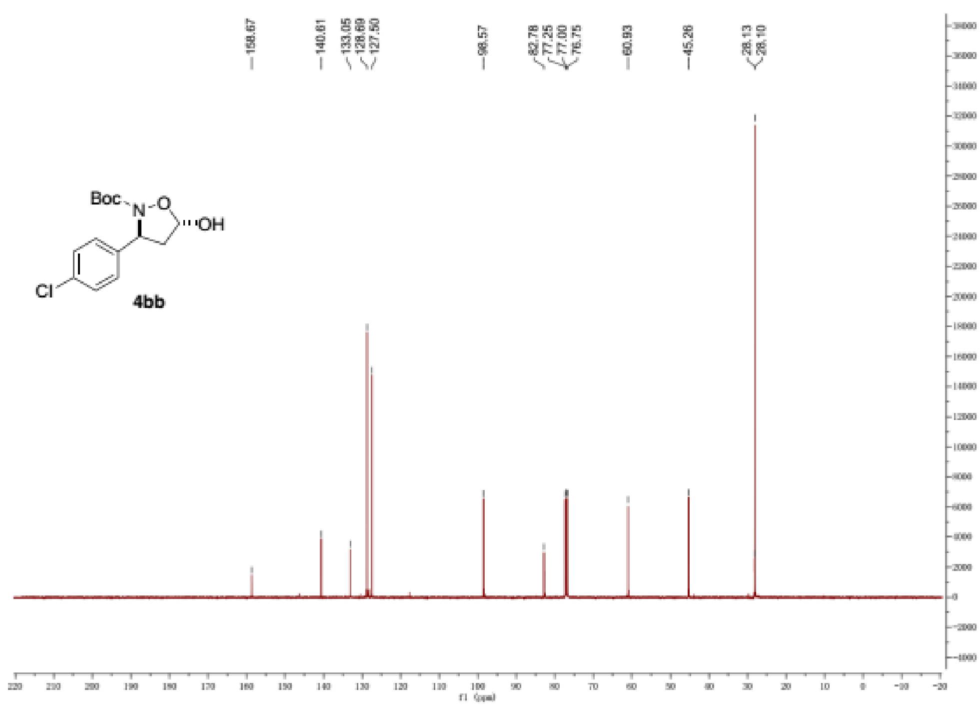

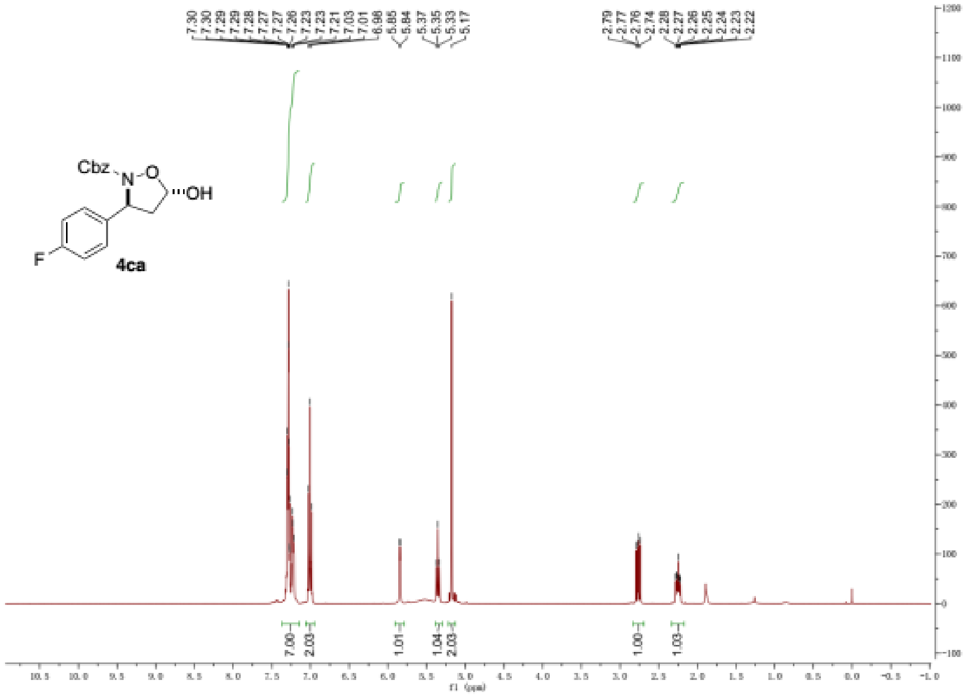

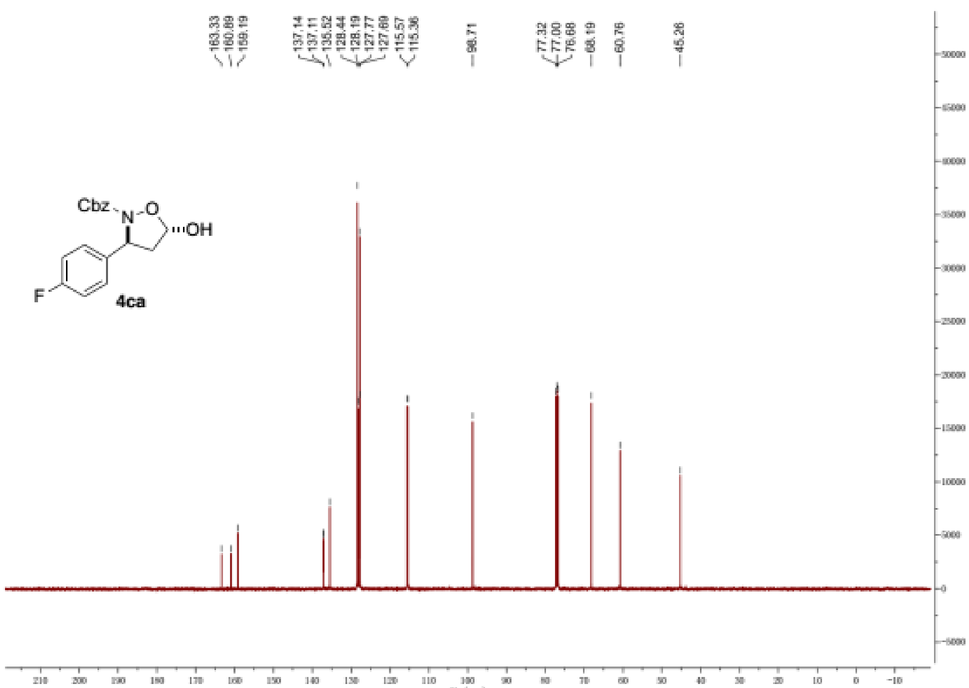

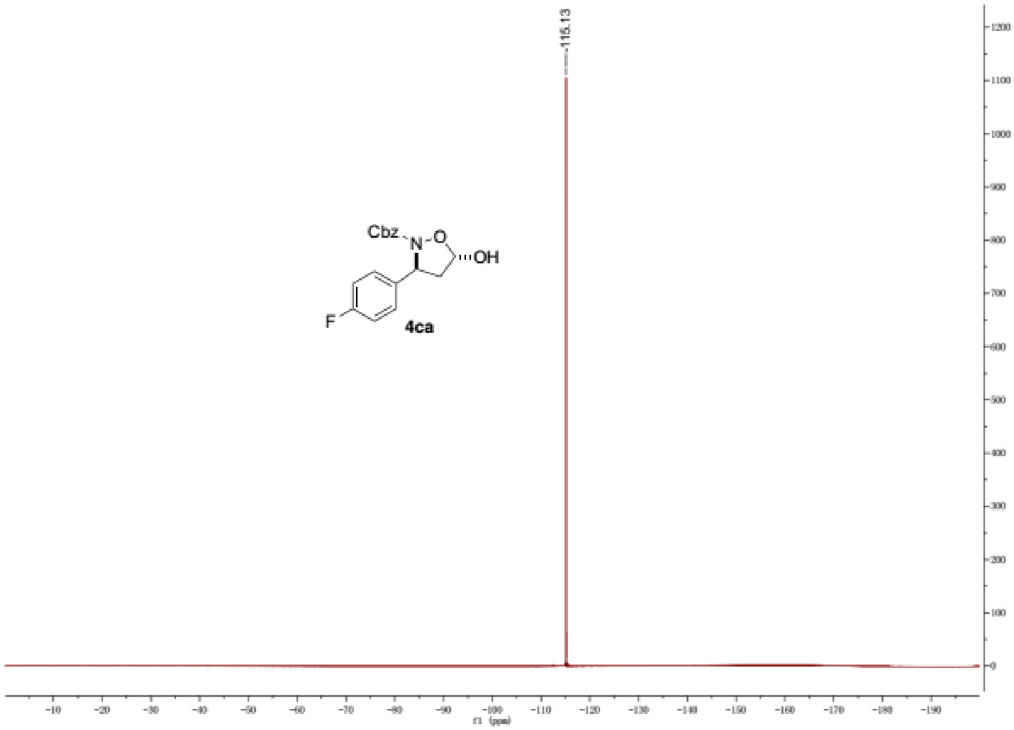
-115.13
Cbz
N
O
OH
F
4ca
f1 (ppm)

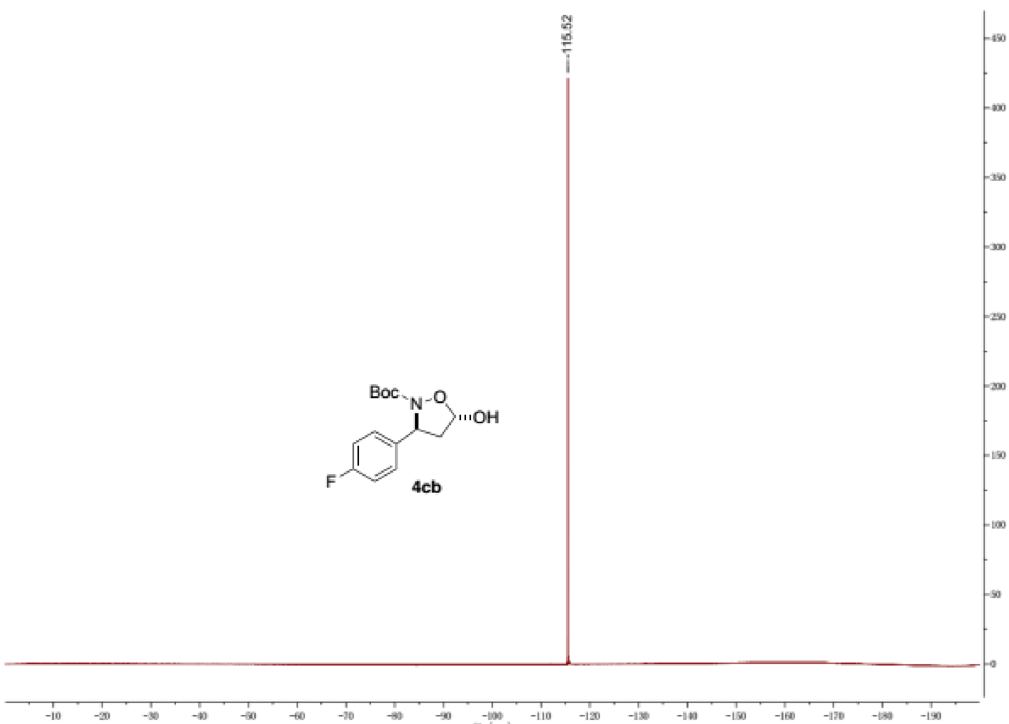
-115.52
Boc
N
O
OH
F
4cb
f1 (ppm)

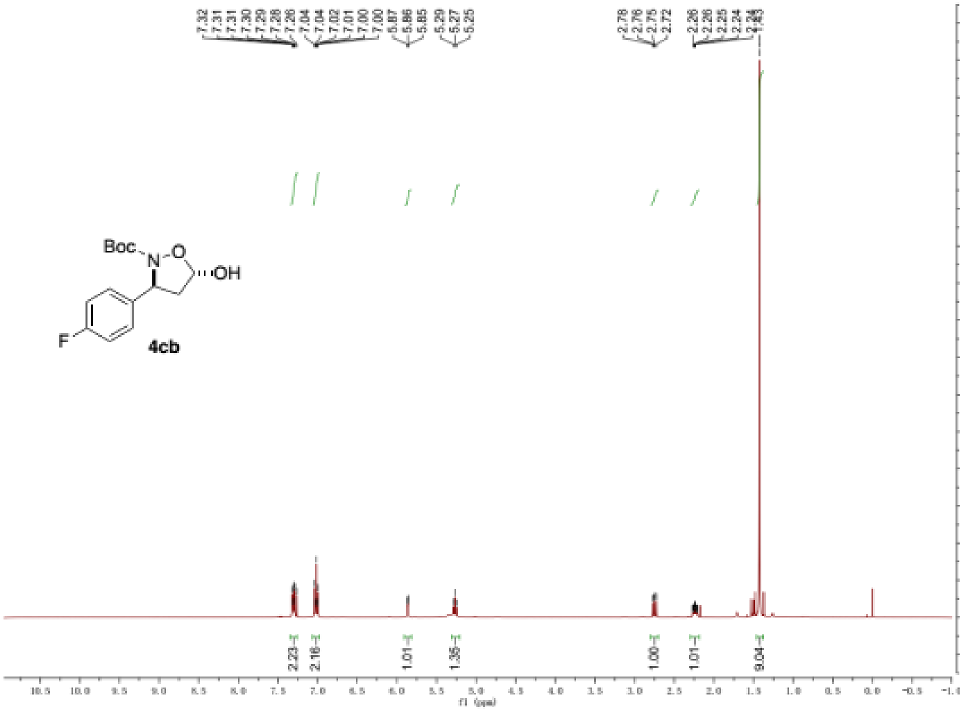
Boc
N
O
OH
F
4cb
f1 (ppm)

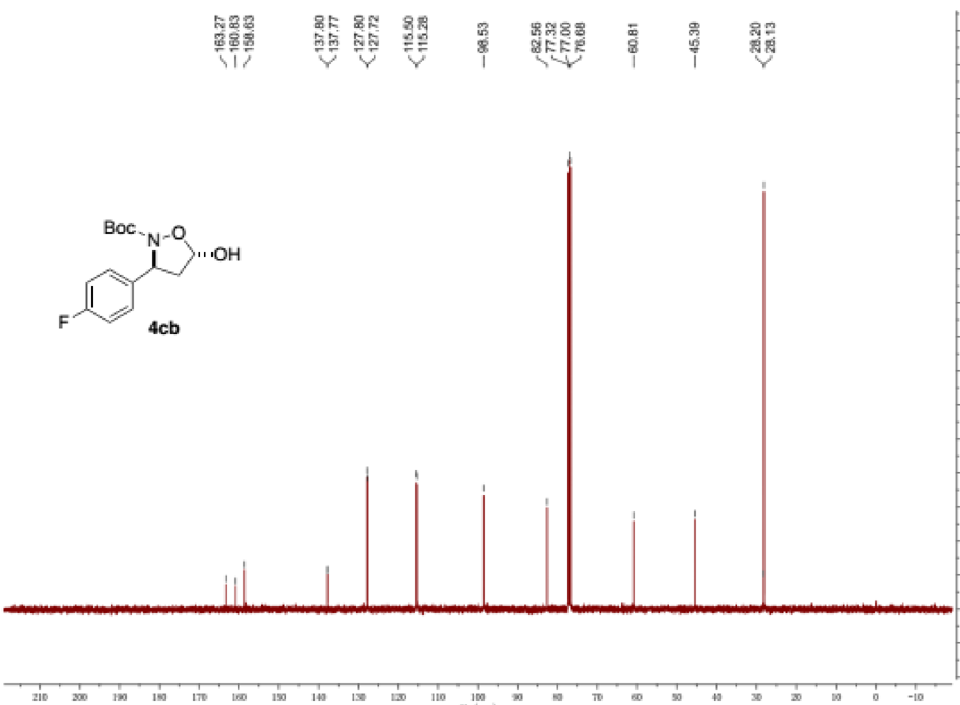
Boc
N
O
OH
F
4cb
f1 (ppm)

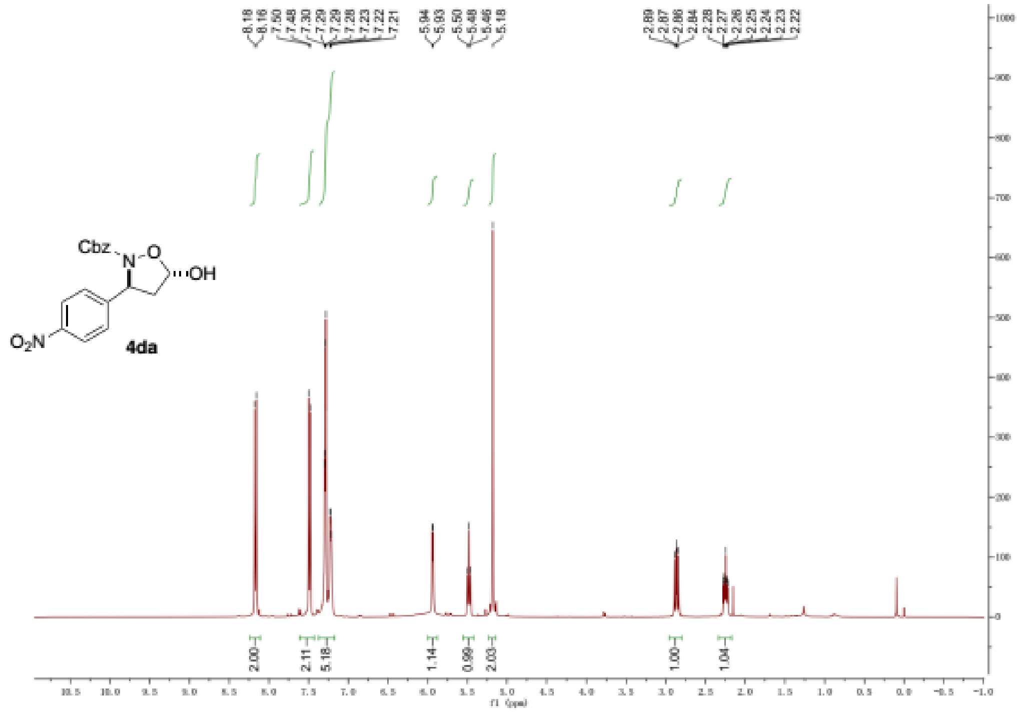
Cbz
N
O
OH
O_2N
4da

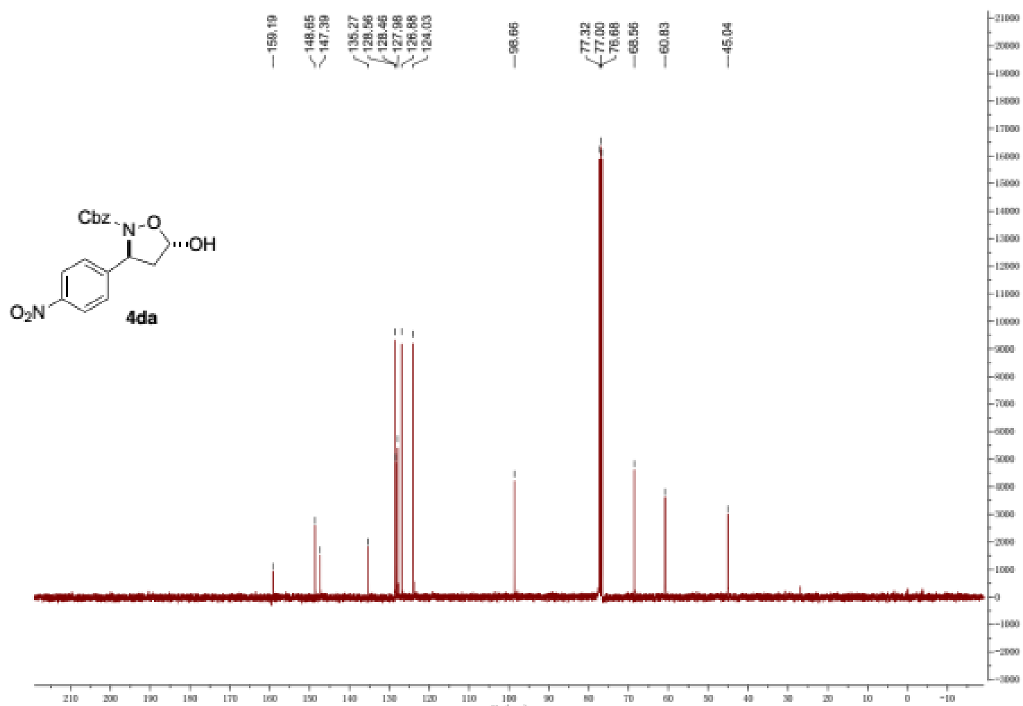
Cbz
N
O
OH
O_2N
4da

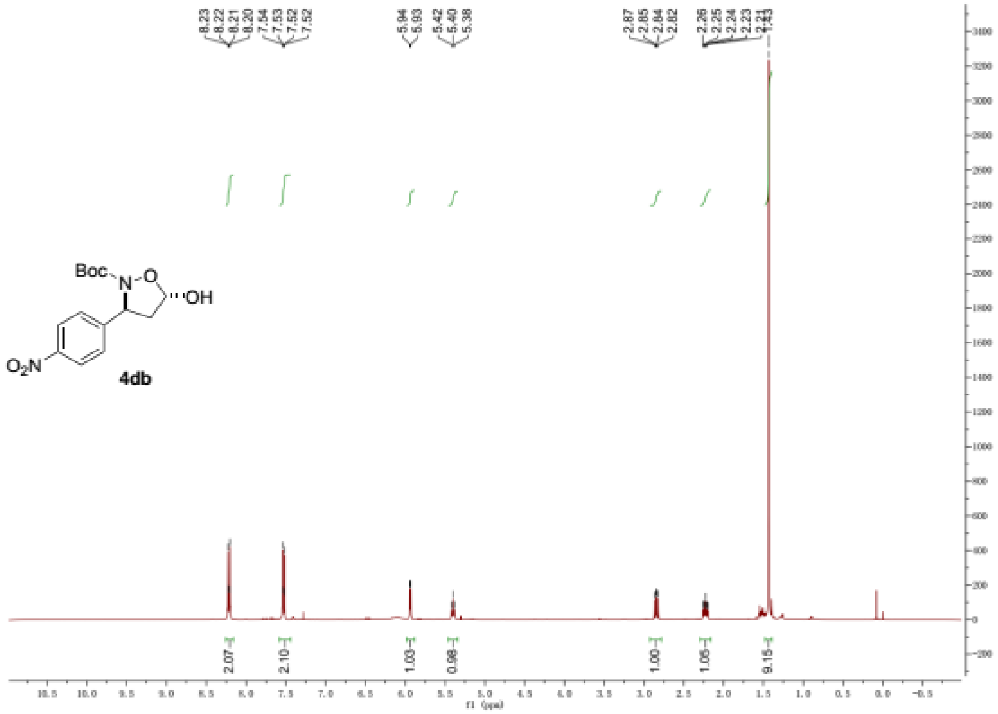
8.23
8.22
8.21
8.20
7.54
7.53
7.52
7.52
5.94
5.93
5.42
5.40
5.38
2.87
2.85
2.84
2.82
2.26
2.25
2.24
2.23
2.21
1.43
Boc
N
O
OH
O2N
4db
2.07
2.10
1.03
0.98
1.00
1.06
9.15
f1 (ppm)

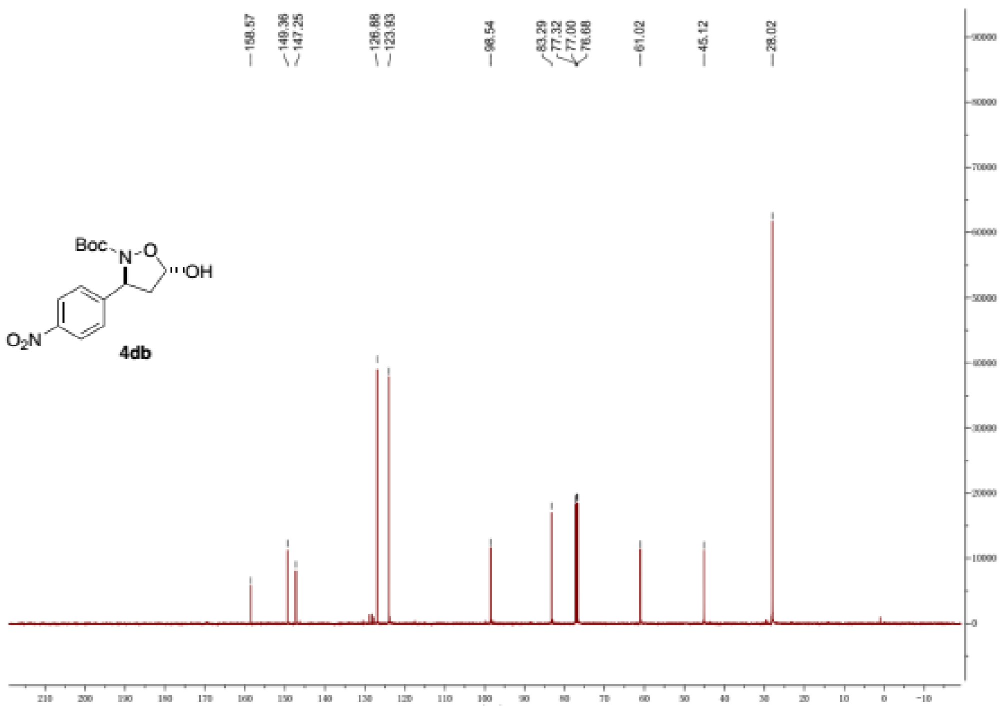
158.57
149.36
147.25
126.88
123.83
98.54
83.29
77.32
77.00
76.68
61.02
45.12
28.02
Boc
N
O
OH
O2N
4db
f1 (ppm)

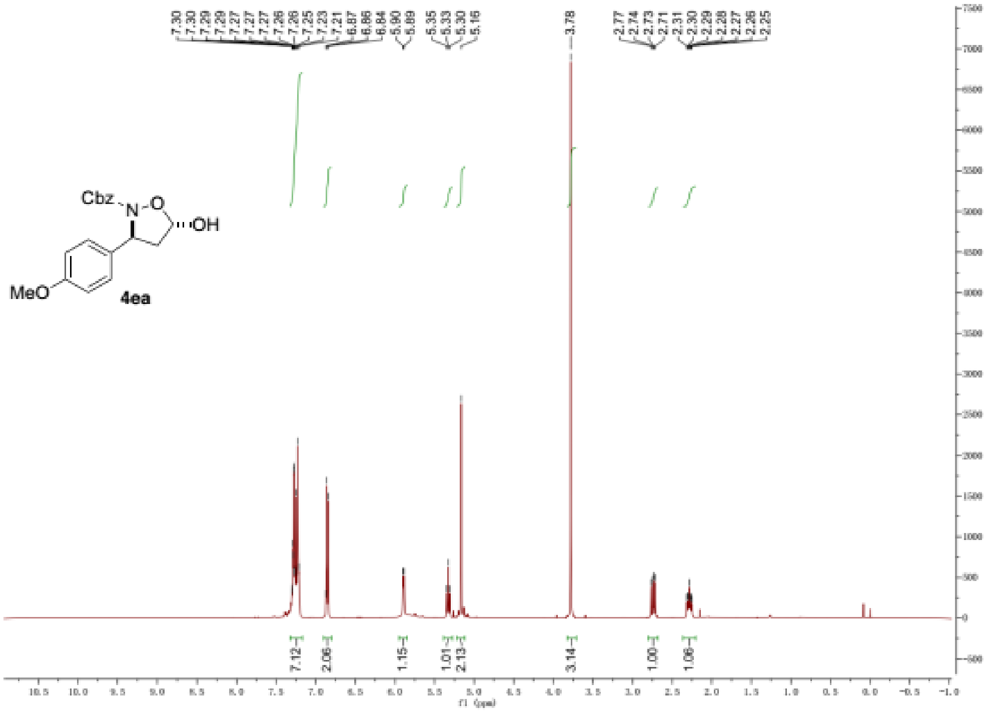

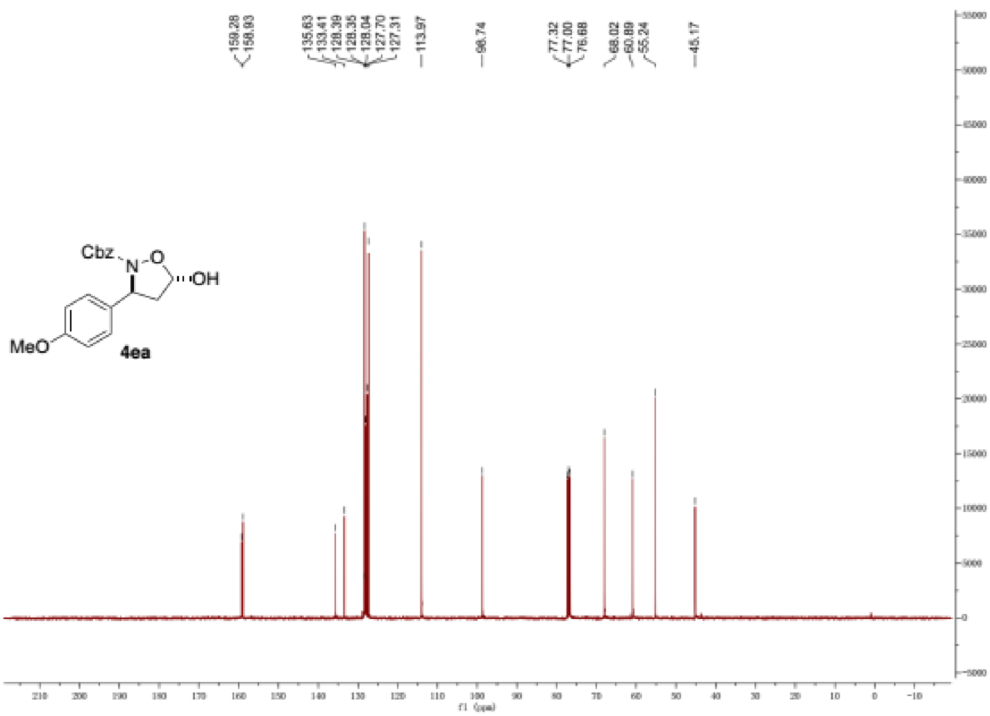

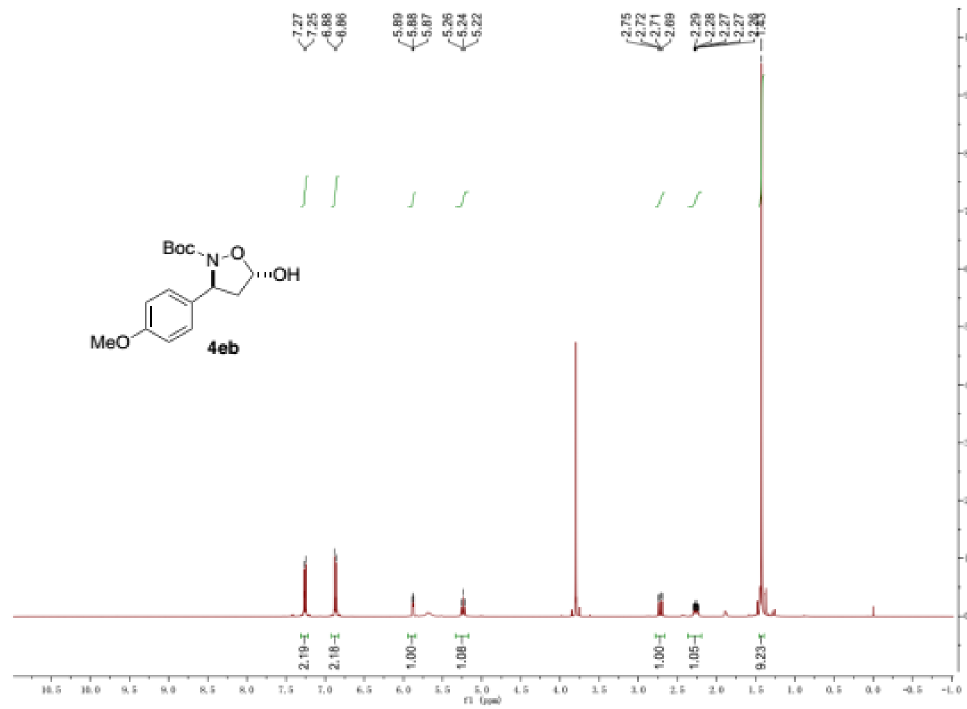
7.27
7.25
6.88
6.86
5.89
5.88
5.87
5.26
5.24
5.22
2.75
2.72
2.71
2.69
2.29
2.28
2.27
2.27
2.26
1.43
Boc
N
O
OH
MeO
4eb
2.19
2.18
1.00
1.08
1.00
1.05
9.23
f1 (ppm)

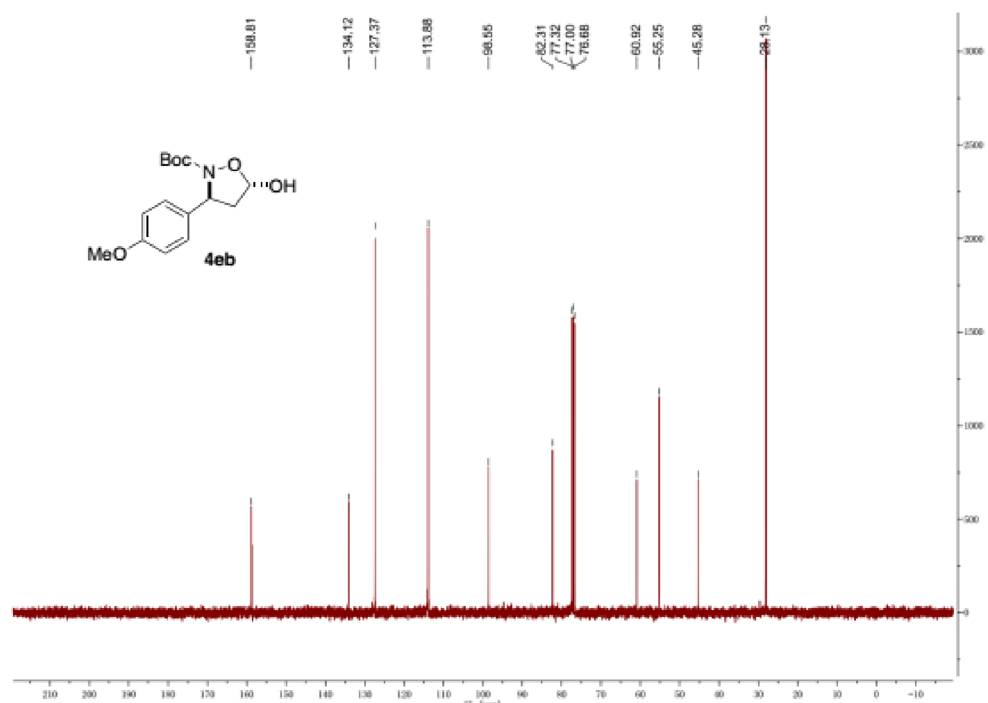
158.81
134.12
127.37
113.88
98.55
82.31
77.32
77.00
76.68
60.92
55.25
45.28
28.13
Boc
N
O
OH
MeO
4eb
f1 (ppm)

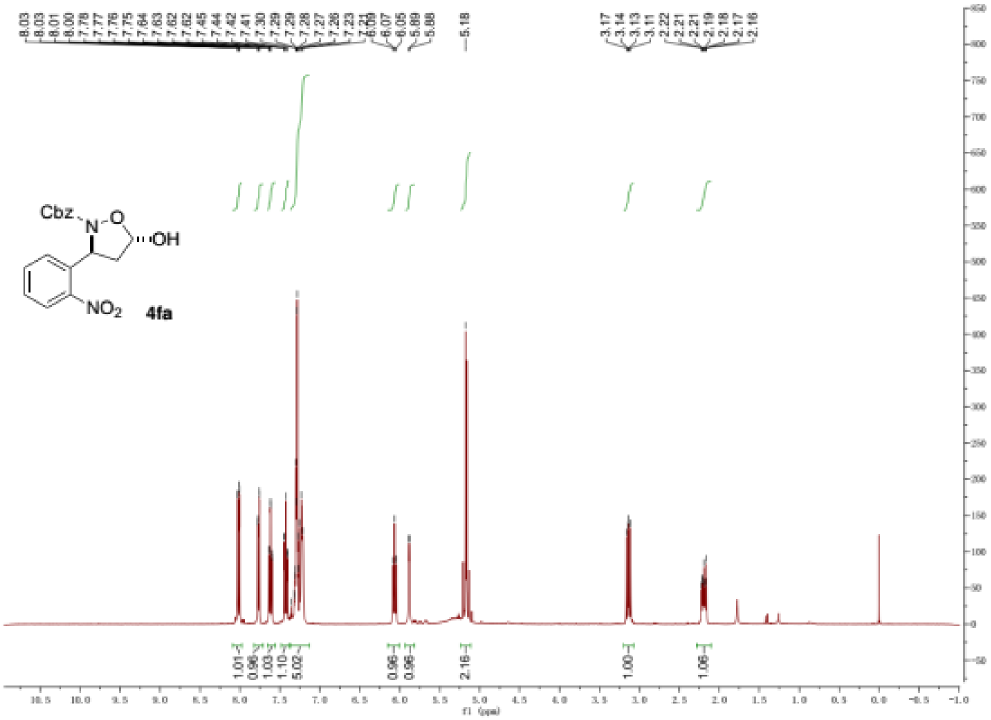
Cbz
N
O
OH
NO2
4fa
1.01
0.98
1.03
1.10
5.02
0.98
0.98
2.16
1.00
1.06
f1 (ppm)

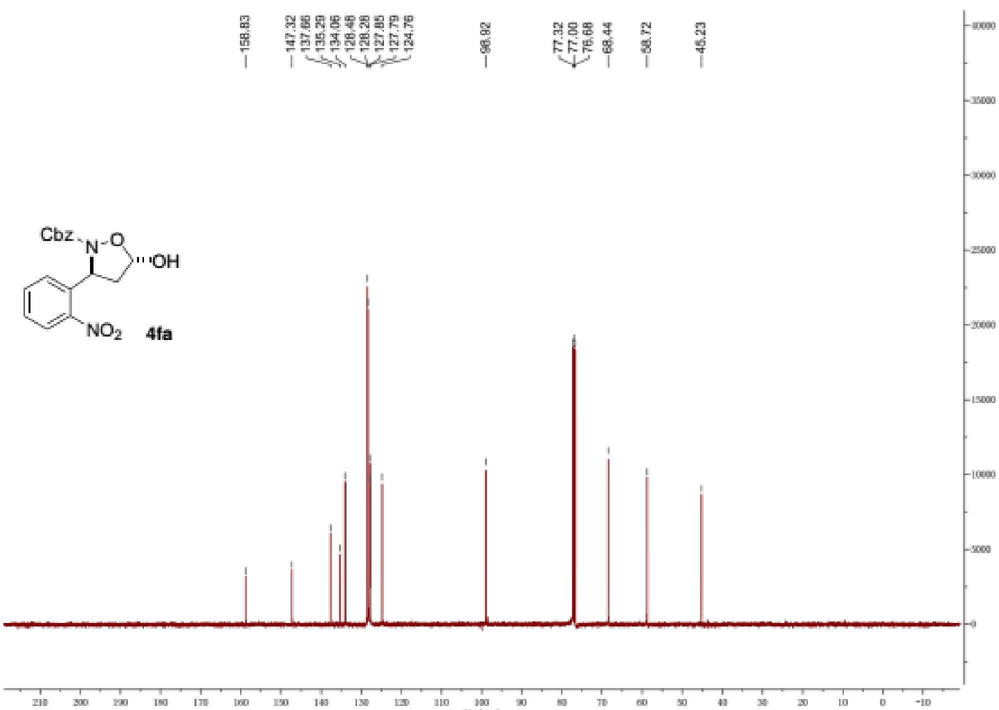
Cbz
N
O
OH
NO2
4fa
158.83
147.32
137.66
135.29
134.06
128.48
128.28
127.85
127.79
124.76
98.82
77.32
77.00
76.68
68.44
58.72
45.23
f1 (ppm)

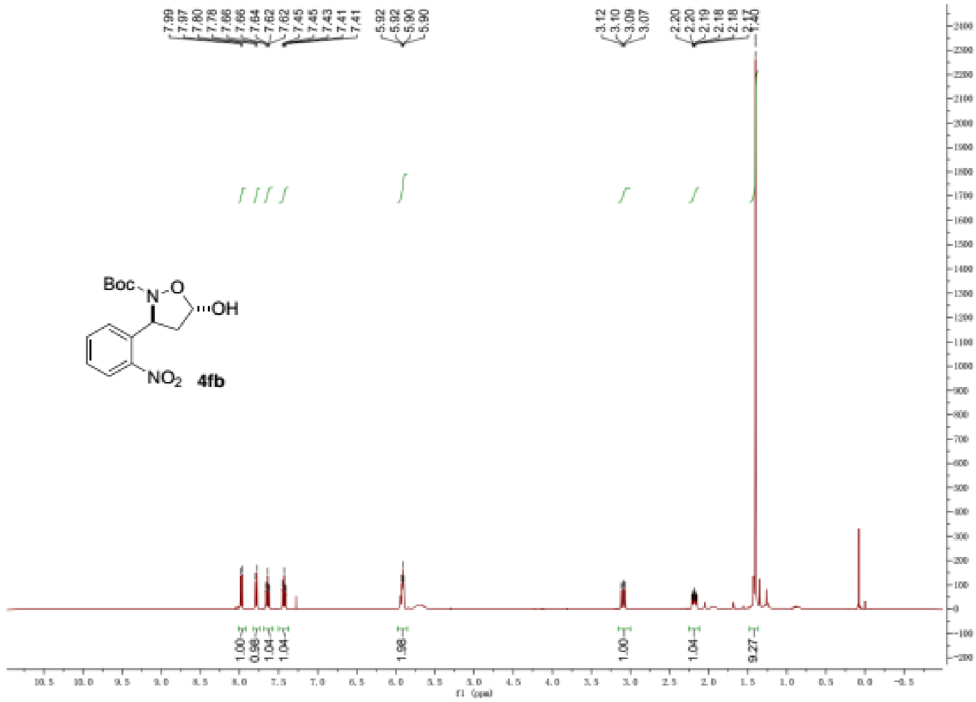
Boc
N
O
OH
NO2
4fb
7.99
7.97
7.80
7.78
7.66
7.64
7.62
7.45
7.43
7.41
5.92
5.90
3.12
3.10
3.09
3.07
2.20
2.19
2.18
2.17
1.40
1.00
0.98
1.04
1.04
1.98
1.00
1.04
9.27
f1 (ppm)

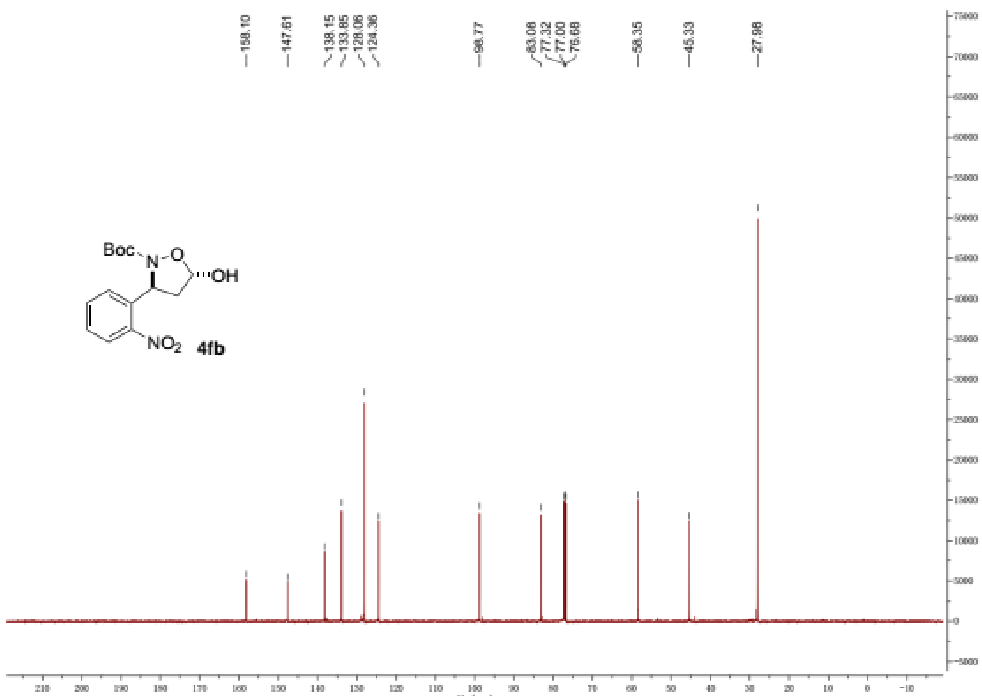
158.10
147.61
138.15
133.85
128.06
124.36
98.77
83.08
77.32
77.00
76.68
58.35
45.33
27.98
Boc
N
O
OH
NO2
4fb
f1 (ppm)

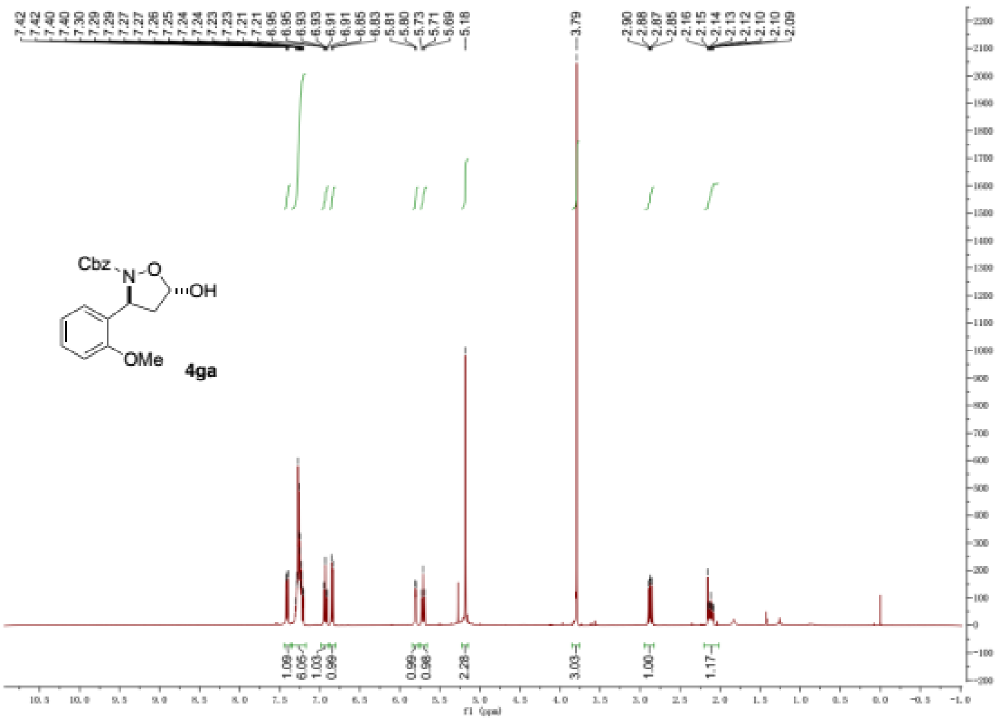
4ga

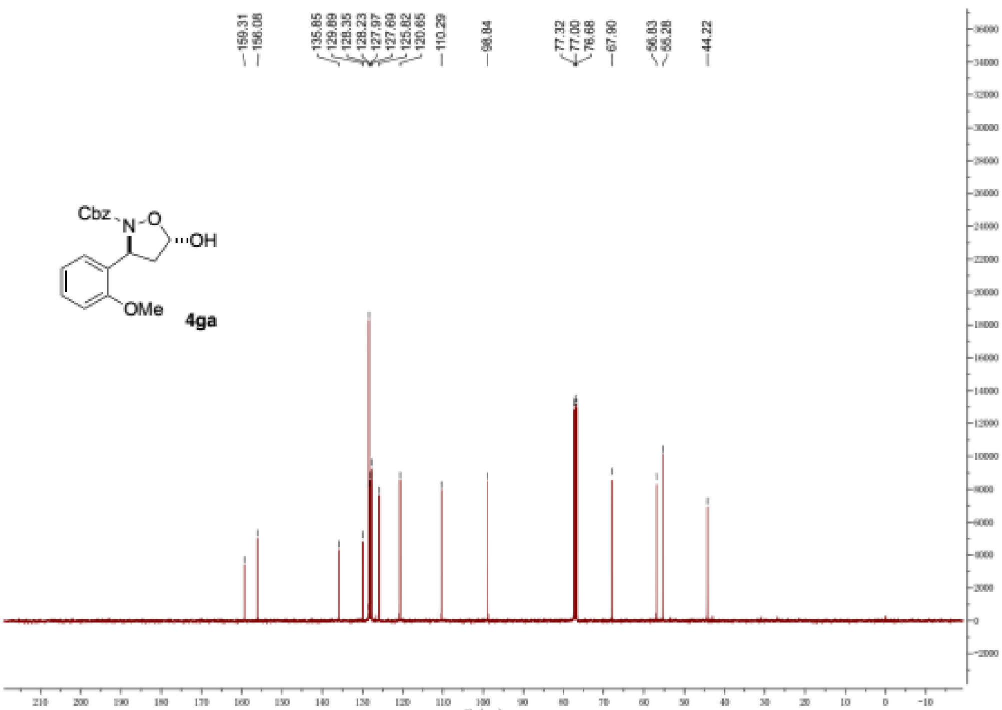
4ga

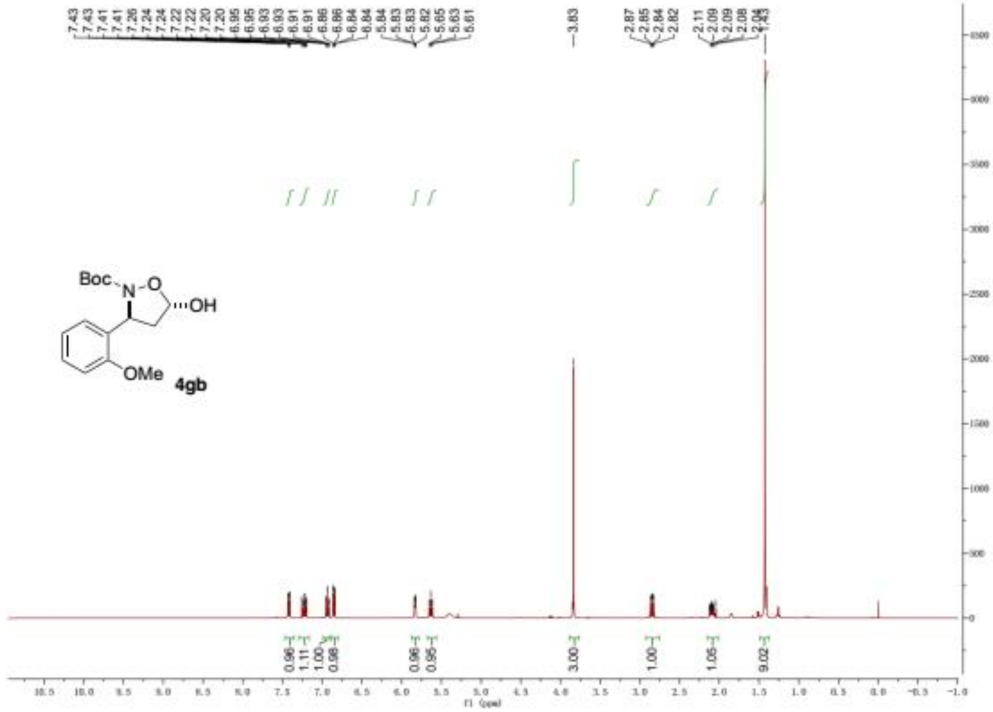

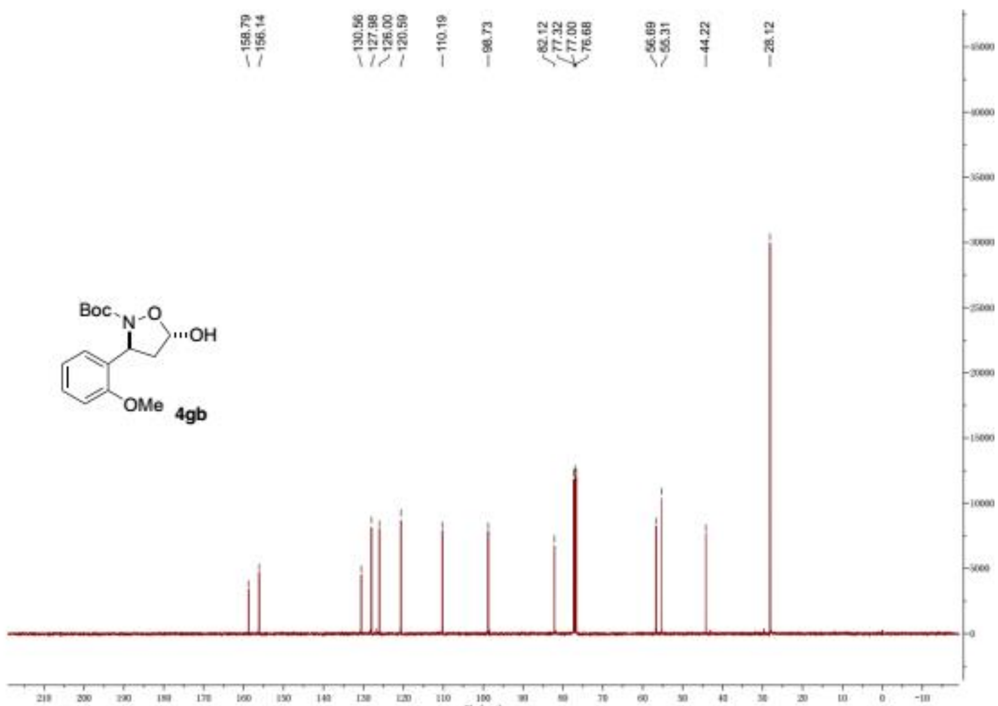

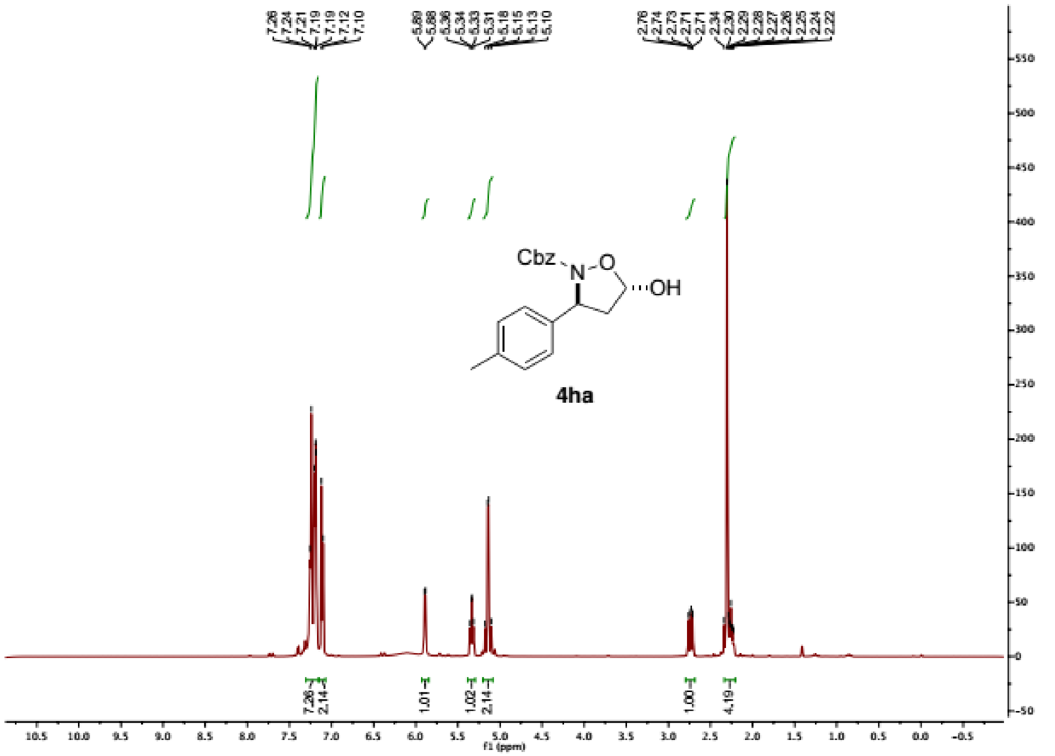
Cbz
N
O
OH
4ha
f1 (ppm)

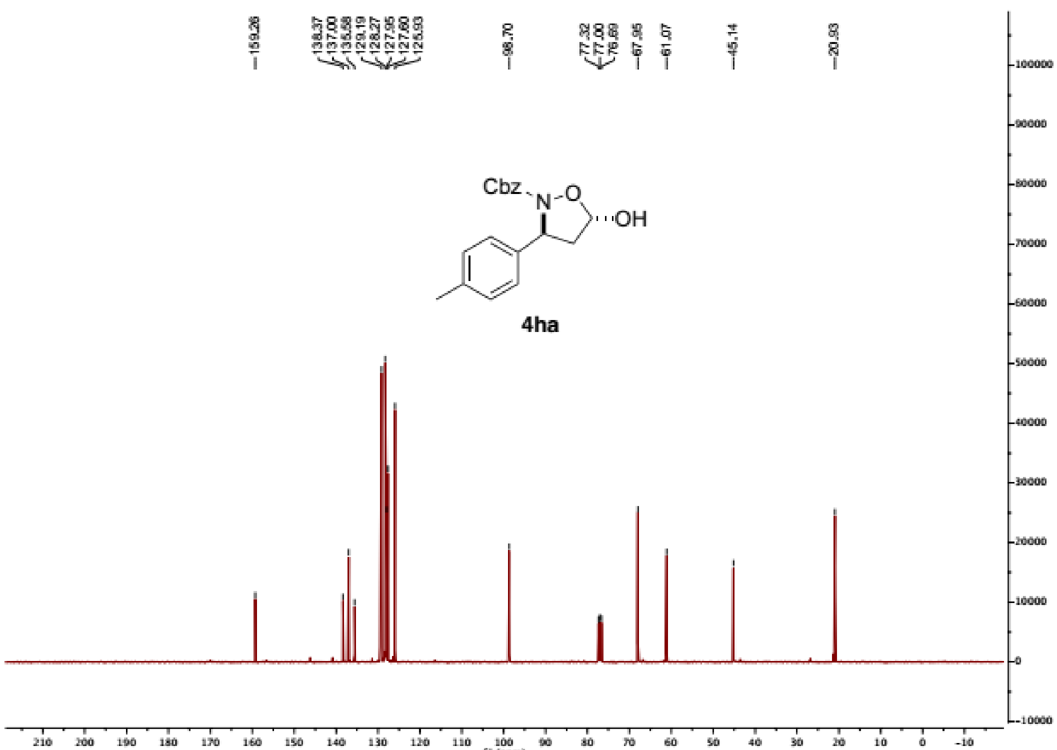
Cbz
N
O
OH
4ha
f1 (ppm)

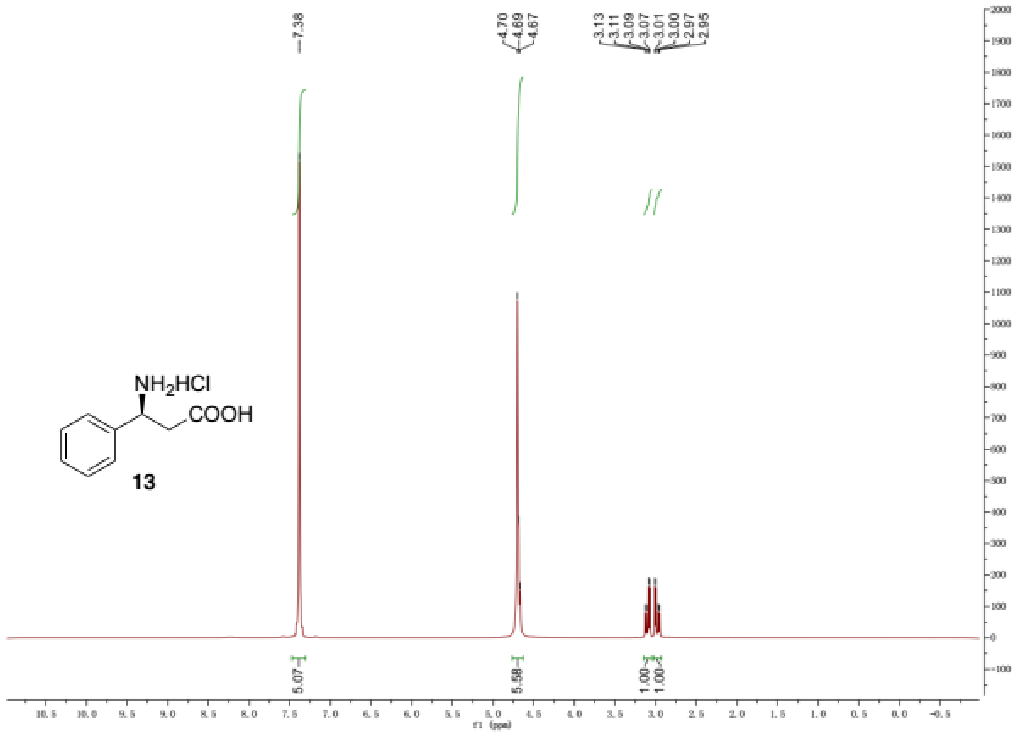
7.38
4.70
4.69
4.67
3.13
3.11
3.09
3.07
3.01
3.00
2.97
2.95
NH2HCl
COOH
13
5.07
5.58
1.00
1.00
f1 (ppm)

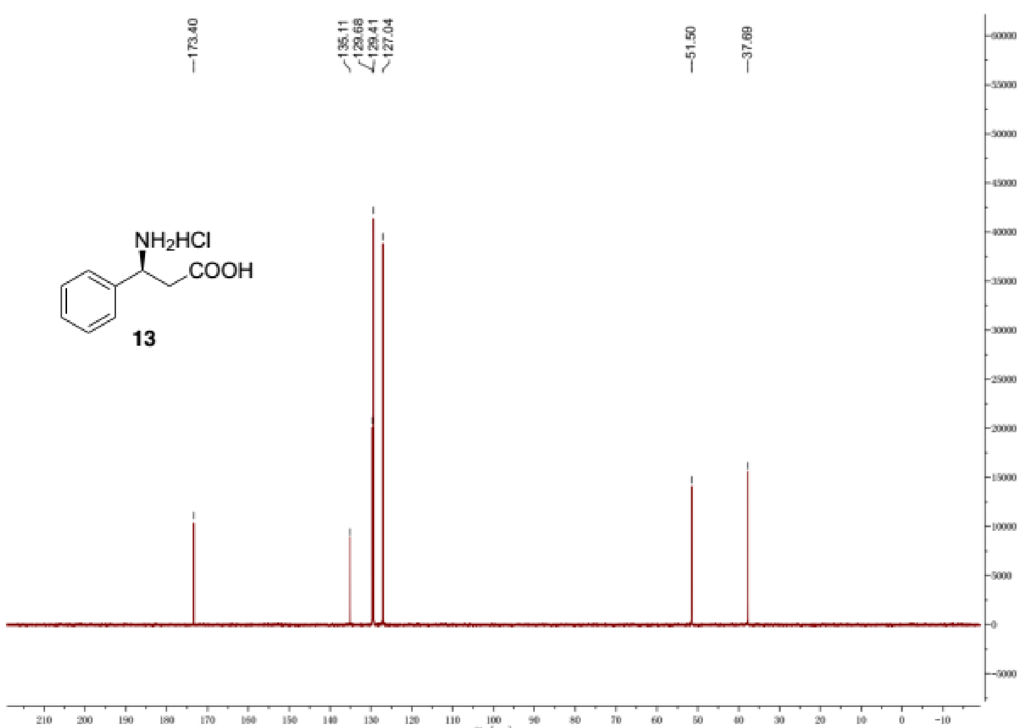
173.40
135.11
129.68
129.41
127.04
51.50
37.69
NH2HCl
COOH
13
f1 (ppm)

7. HPLC chromatograms

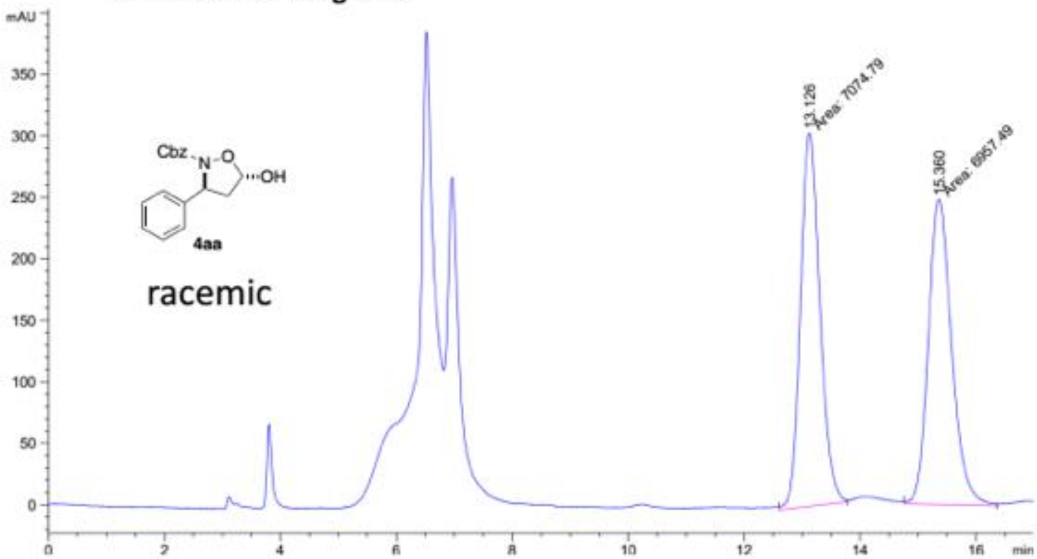

Peak #	RetTime [min]	Type	Width [min]	Area [mAU*s]	Height [mAU]	Area %
1	13.126	MM	0.3883	7074.78613	303.65152	50.4179
2	15.360	MM	0.4668	6957.49121	248.41331	49.5821

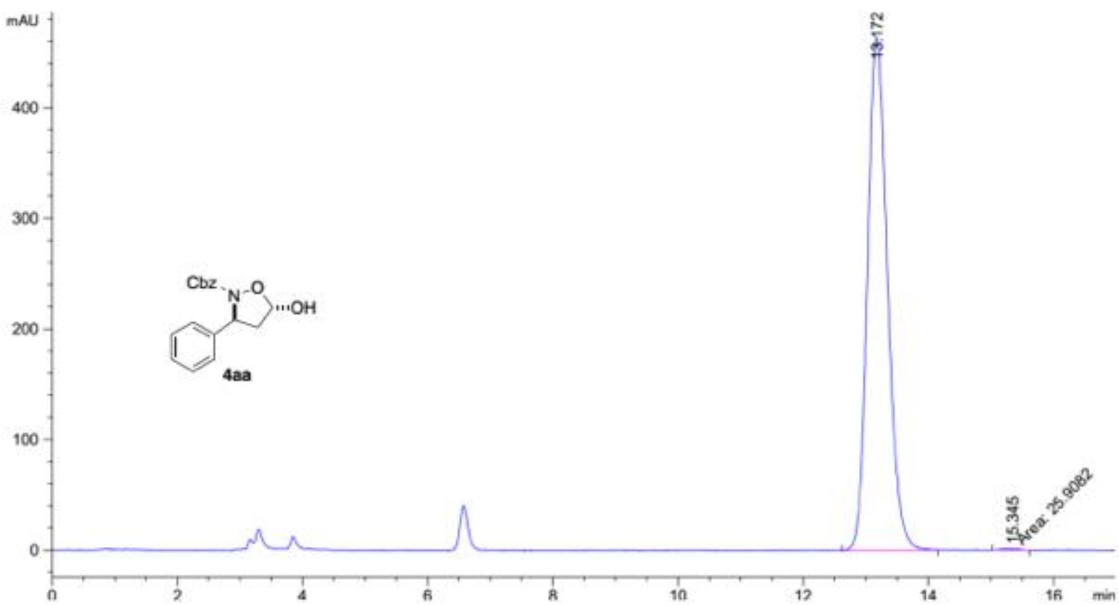

Peak #	RetTime [min]	Type	Width [min]	Area [mAU*s]	Height [mAU]	Area %
1	13.172	BB	0.3442	1.02645e4	463.79126	99.7482
2	15.345	MM	0.3253	25.90824	1.32721	0.2518

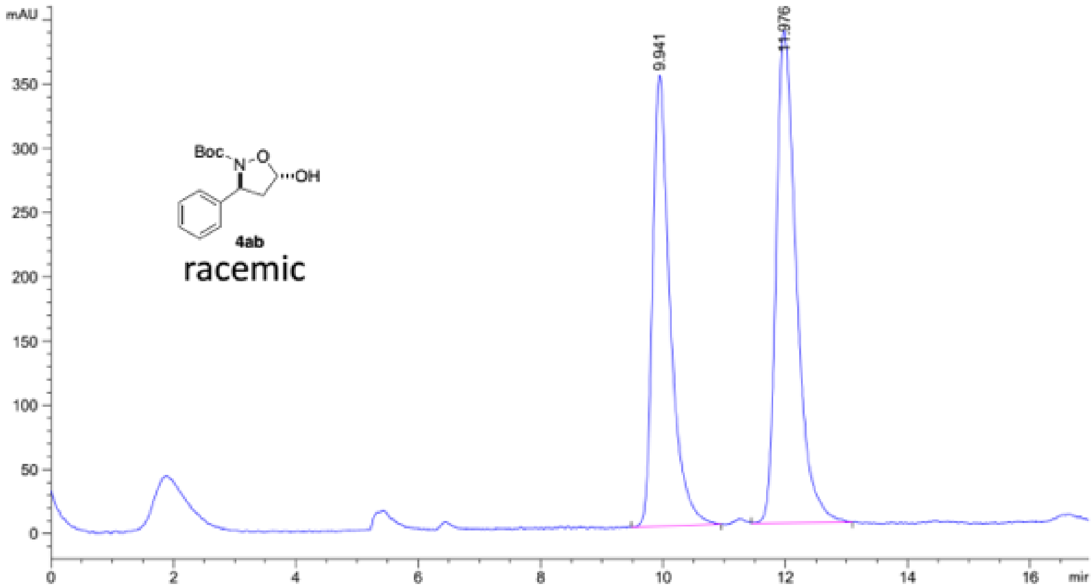

Peak #	RetTime [min]	Type	Width [min]	Area [mAU*s]	Height [mAU]	Area %
1	6.296	BB	0.1940	8209.96094	647.35596	49.5907
2	7.518	BB	0.1747	8345.47754	682.11053	50.4093

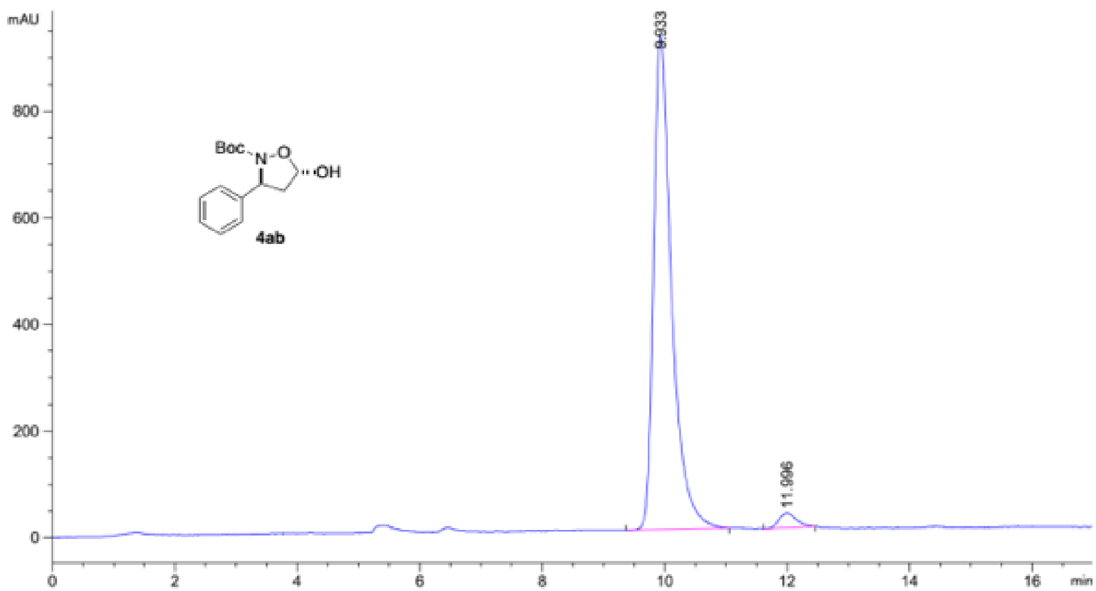

Peak #	RetTime [min]	Type	Width [min]	Area [mAU*s]	Height [mAU]	Area %
1	6.260	BB	0.2377	2.18061e4	1464.46118	99.7553
2	7.483	BB	0.1141	53.49866	6.63165	0.2447

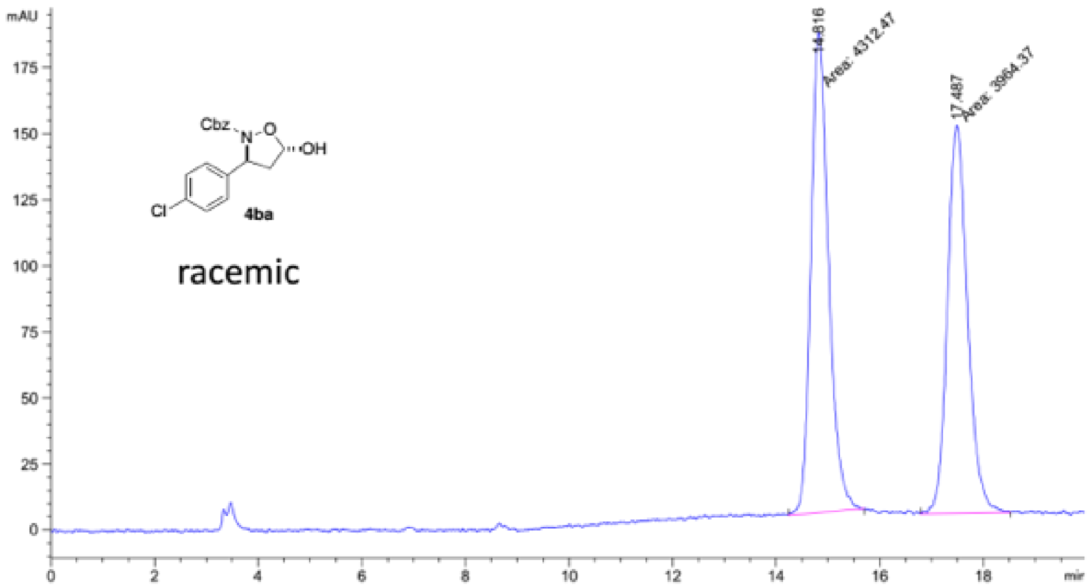

Peak #	RetTime [min]	Type	Width [min]	Area [mAU*s]	Height [mAU]	Area %
1	14.816	BB	0.3613	4318.26221	181.67305	52.9487
2	17.487	BB	0.3935	3837.30347	145.58012	47.0513

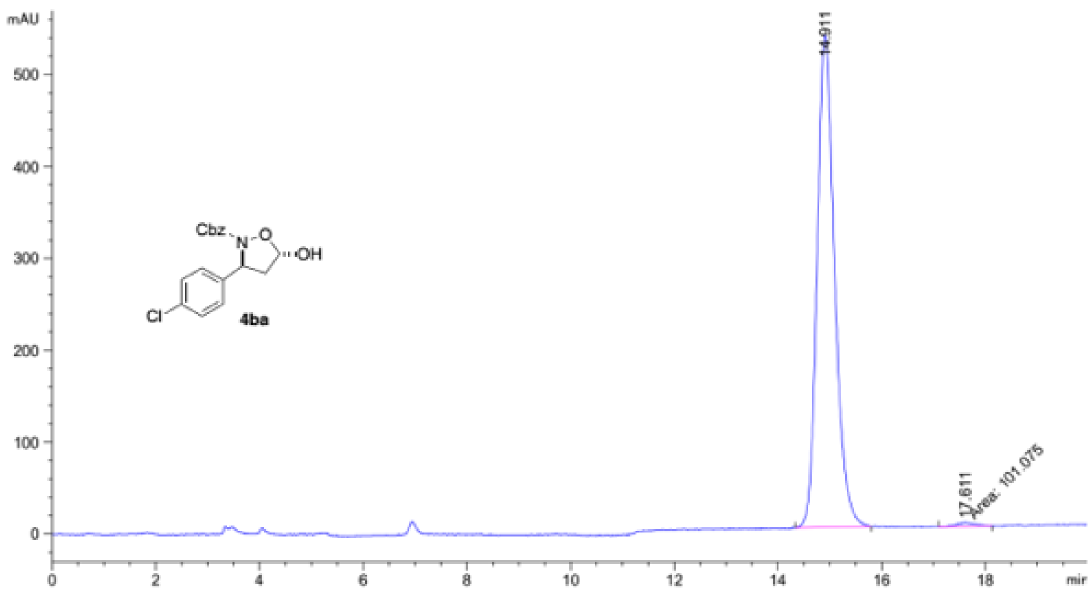

Peak #	RetTime [min]	Type	Width [min]	Area [mAU*s]	Height [mAU]	Area %
1	14.911	BB	0.3557	1.25634e4	535.50610	99.2019
2	17.611	MM	0.4360	101.07498	3.86343	0.7981

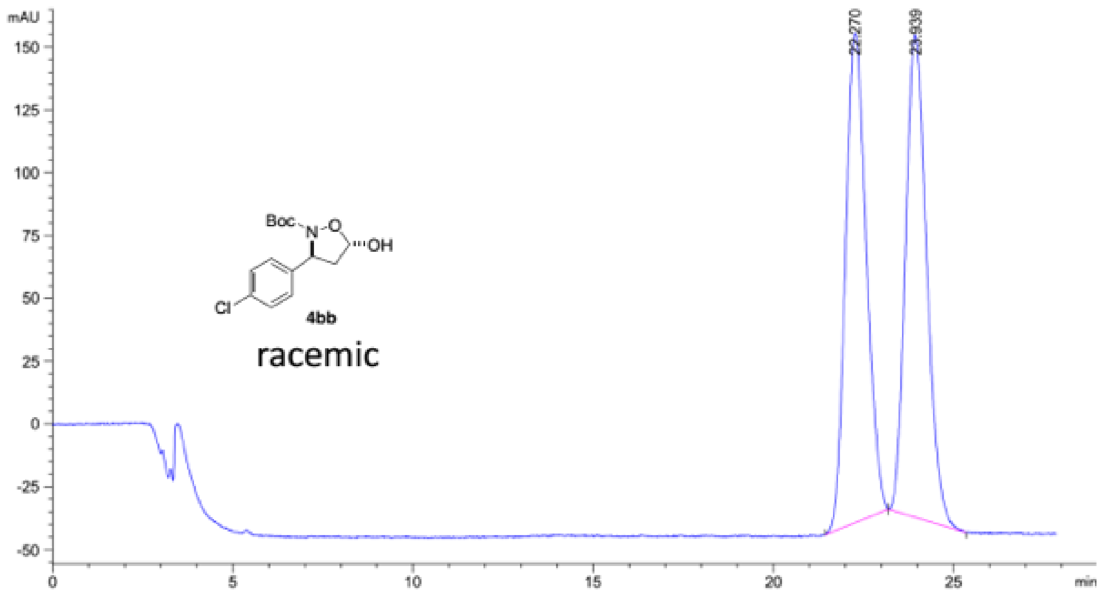

Peak #	RetTime [min]	Type	Width [min]	Area [mAU*s]	Height [mAU]	Area %
1	22.270	BB	0.5886	7816.17041	194.60812	49.9525
2	23.939	BB	0.6000	7831.04443	191.92555	50.0475

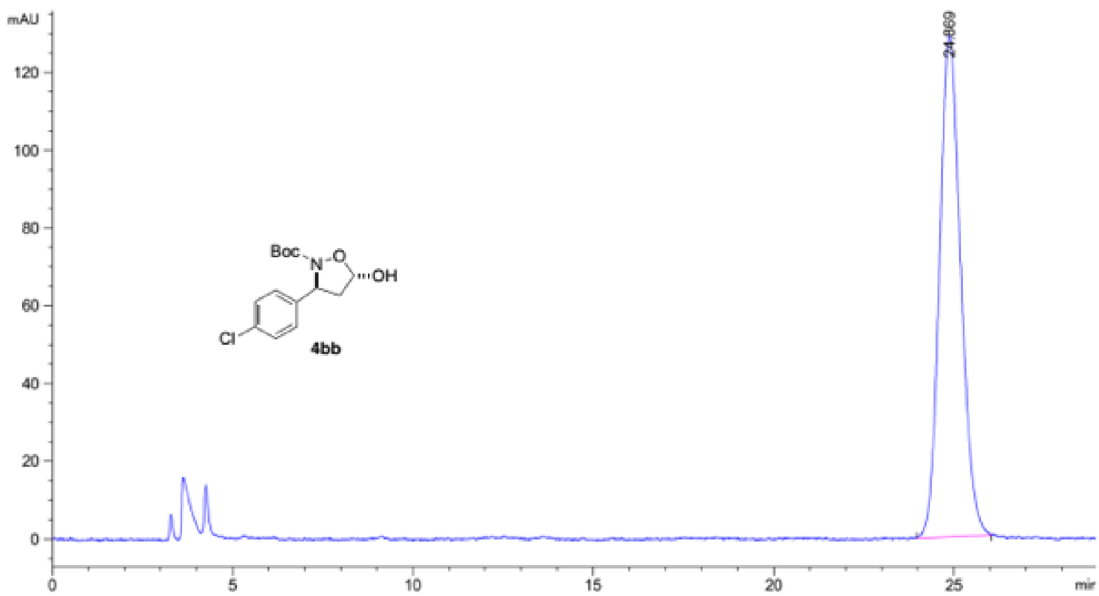

Peak #	RetTime [min]	Type	Width [min]	Area [mAU*s]	Height [mAU]	Area %
1	24.869	BB	0.5331	5268.50928	128.83727	100.0000

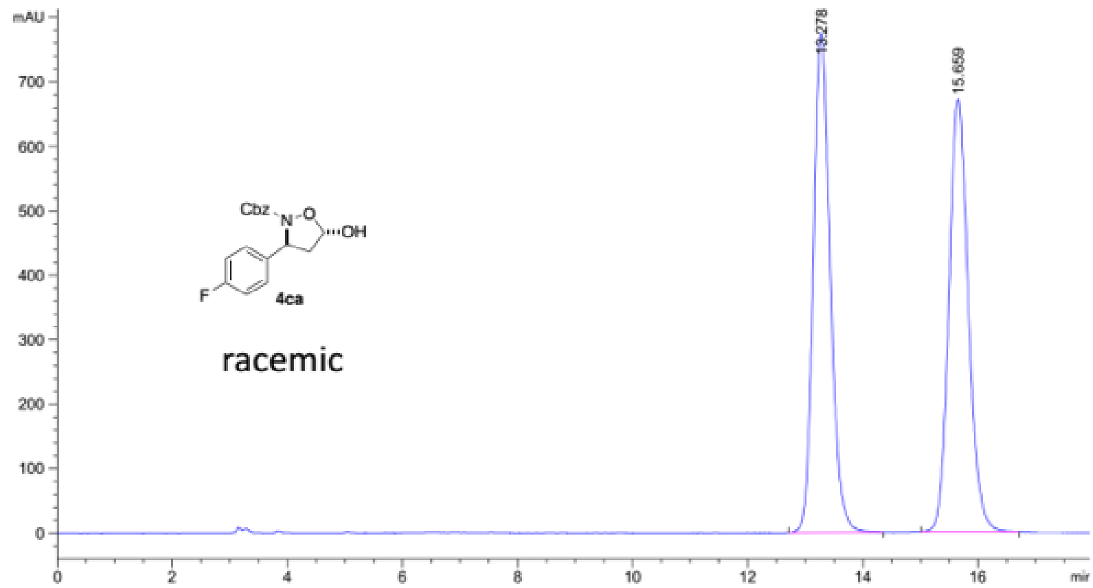

Peak #	RetTime [min]	Type	Width [min]	Area [mAU*s]	Height [mAU]	Area %
1	13.278	BB	0.3122	1.58151e4	774.50507	49.9609
2	15.659	BB	0.3633	1.58399e4	671.20117	50.0391

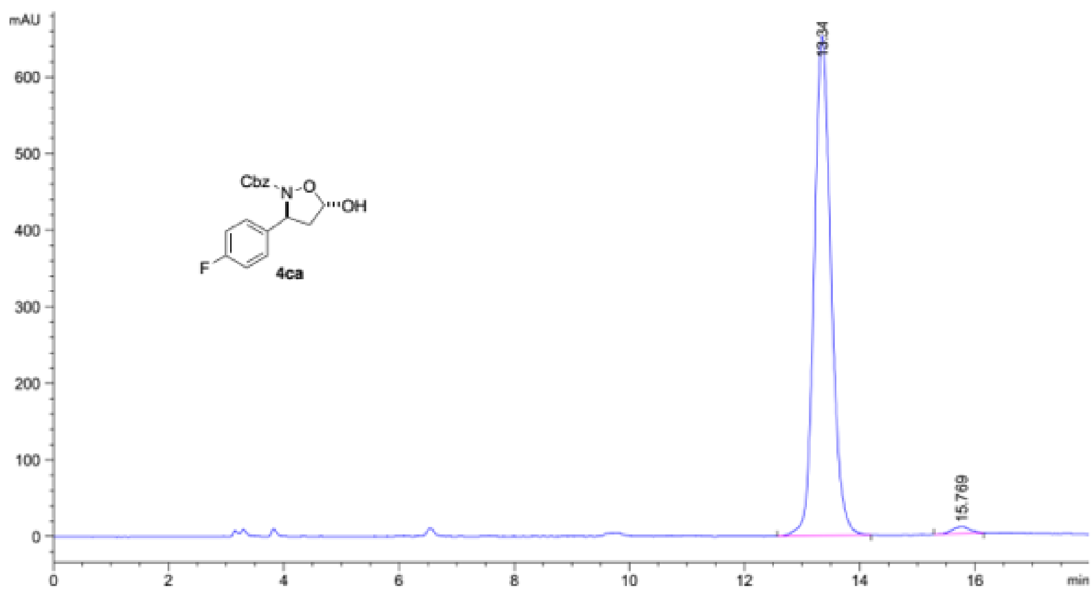

Peak #	RetTime [min]	Type	Width [min]	Area [mAU*s]	Height [mAU]	Area %
1	13.349	BB	0.3175	1.33866e4	652.08160	98.4949
2	15.769	BB	0.2692	204.55771	9.13807	1.5051

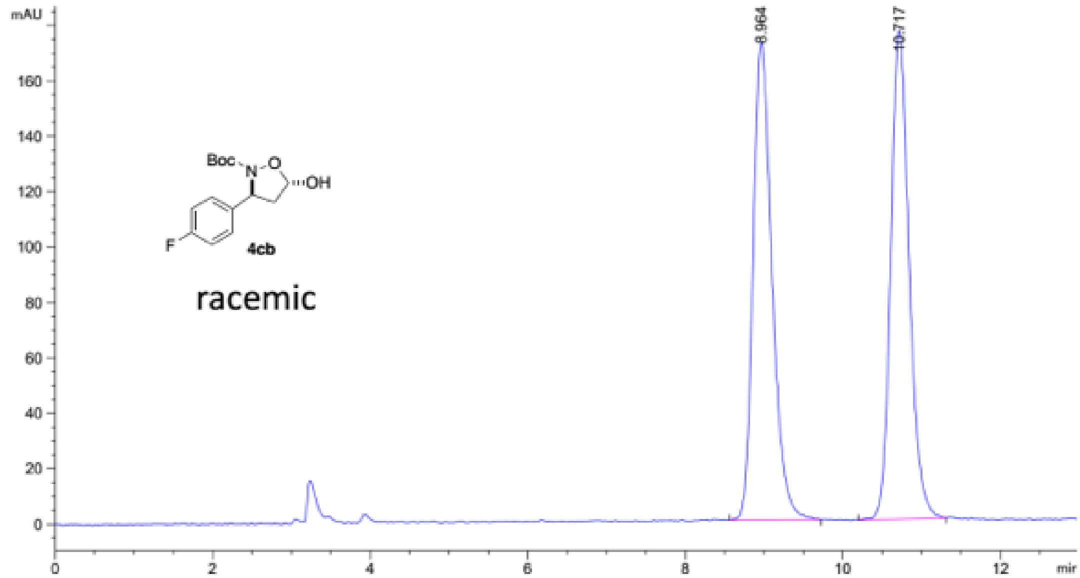

Peak #	RetTime [min]	Type	Width [min]	Area [mAU*s]	Height [mAU]	Area %
1	8.964	BB	0.2590	2882.64551	172.47208	50.2143
2	10.717	BB	0.2471	2858.03735	176.36497	49.7857

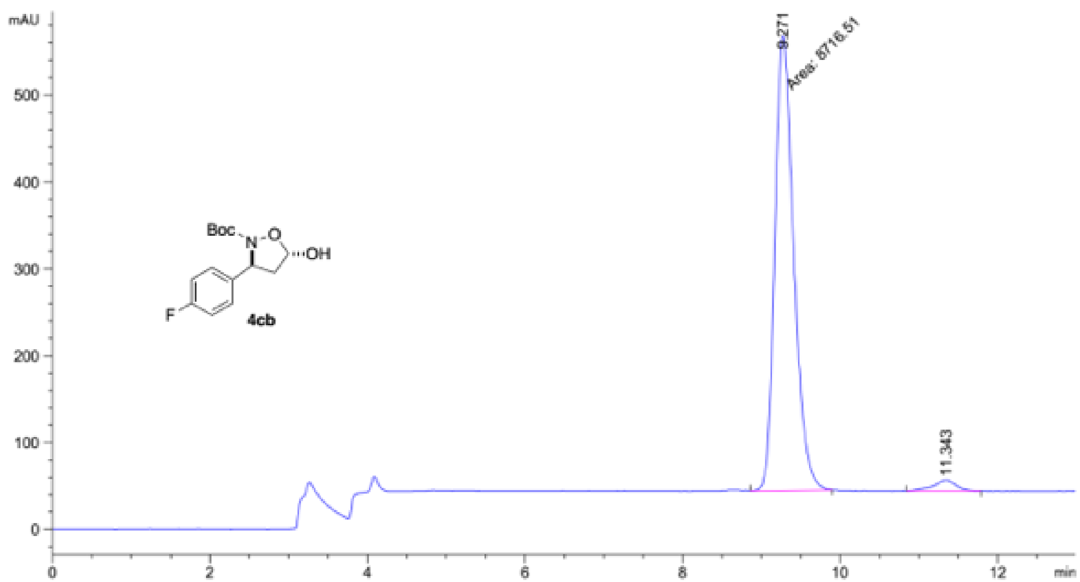

Peak #	RetTime [min]	Type	Width [min]	Area [mAU*s]	Height [mAU]	Area %
1	9.271	MM	0.2777	8716.51270	523.14294	97.1924
2	11.343	BB	0.2724	251.79427	12.42615	2.8076

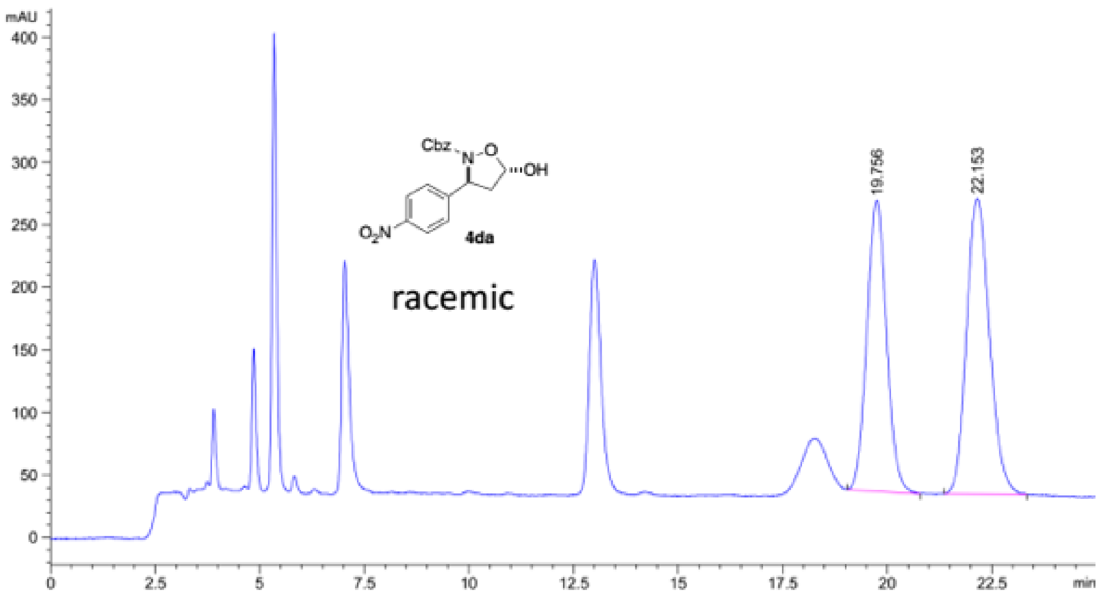

Peak #	RetTime [min]	Type	Width [min]	Area [mAU*s]	Height [mAU]	Area %
1	19.756	BB	0.4945	7574.17188	232.21043	45.6341
2	22.153	BB	0.5755	9023.43164	236.32964	54.3659

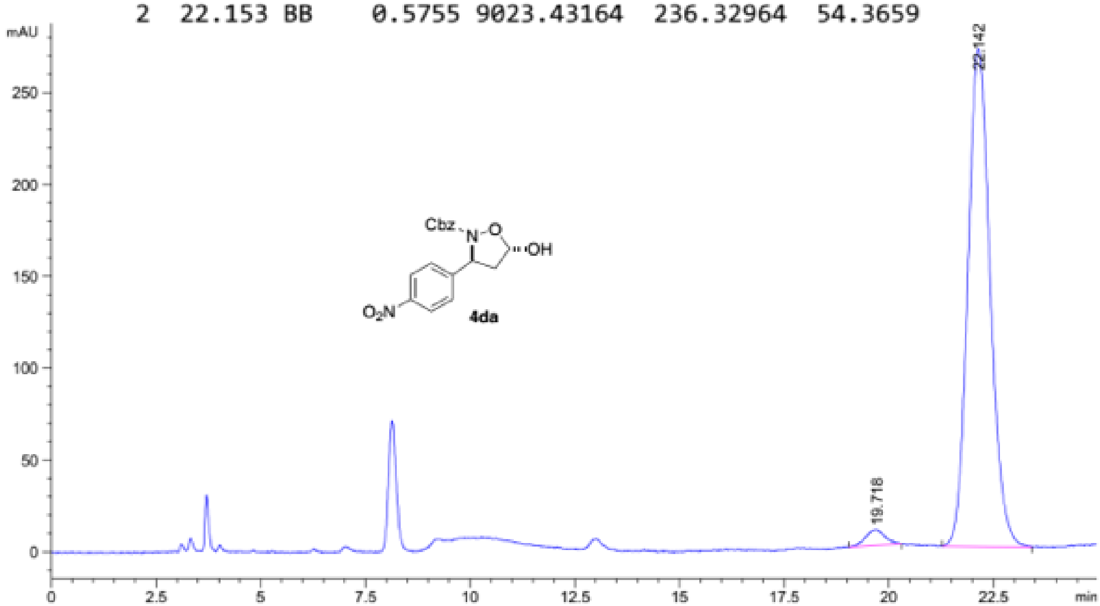

Peak #	RetTime [min]	Type	Width [min]	Area [mAU*s]	Height [mAU]	Area %
1	19.718	BB	0.3940	282.78375	8.63579	2.7388
2	22.142	BB	0.5559	1.00422e4	271.23340	97.2612

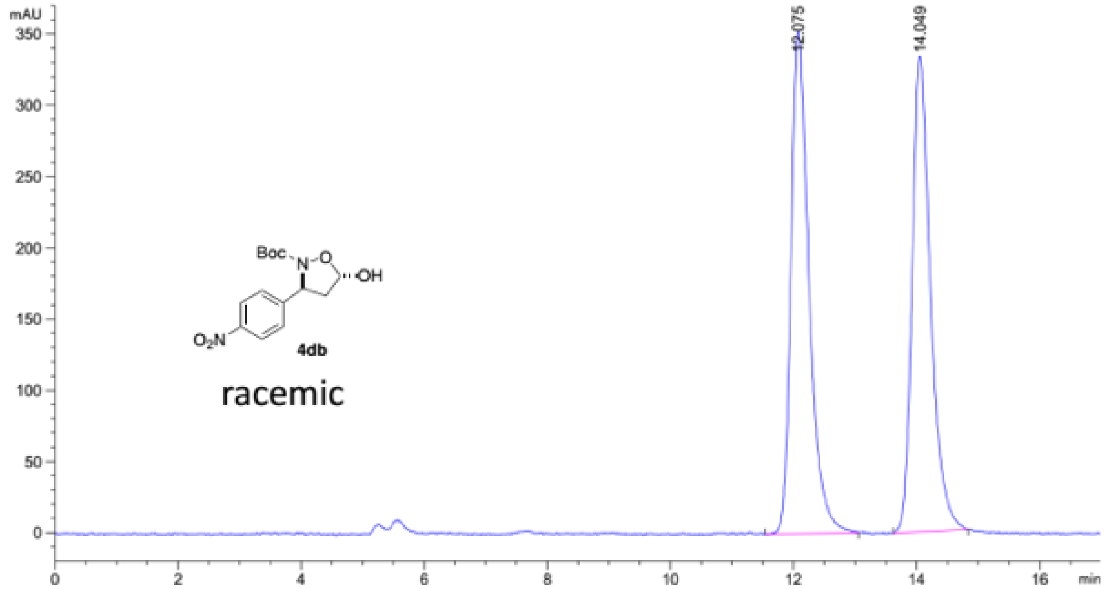

Peak #	RetTime [min]	Type	Width [min]	Area [mAU*s]	Height [mAU]	Area %
1	12.075	BB	0.2947	7166.46826	353.27213	50.6443
2	14.049	BB	0.3118	6984.11670	334.18558	49.3557

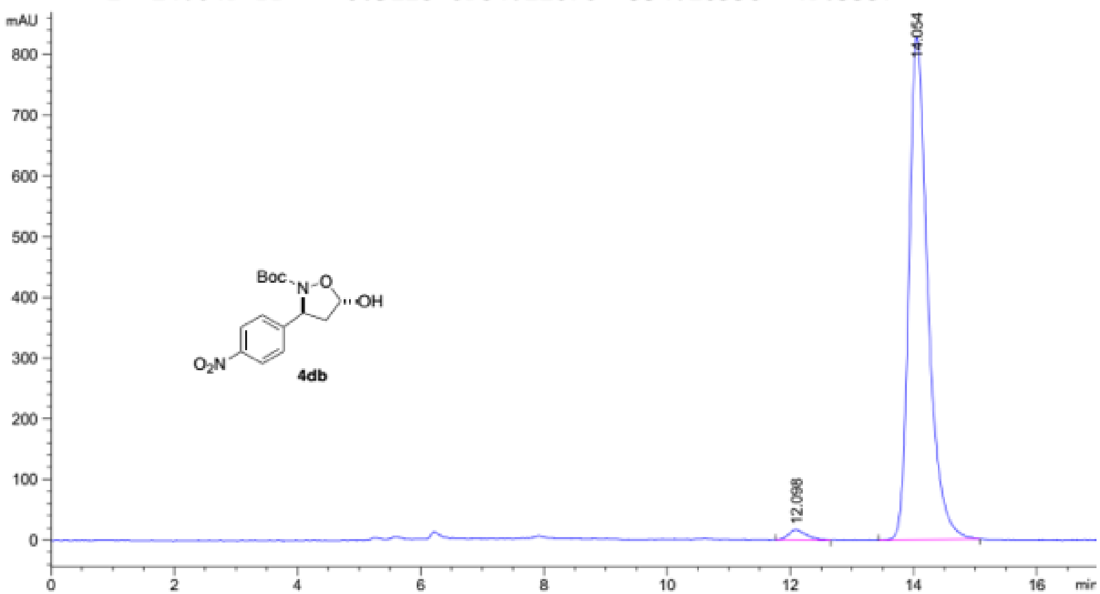

Peak #	RetTime [min]	Type	Width [min]	Area [mAU*s]	Height [mAU]	Area %
1	12.098	BB	0.2402	348.09653	17.48797	1.9282
2	14.054	BB	0.3212	1.77051e4	828.94922	98.0718

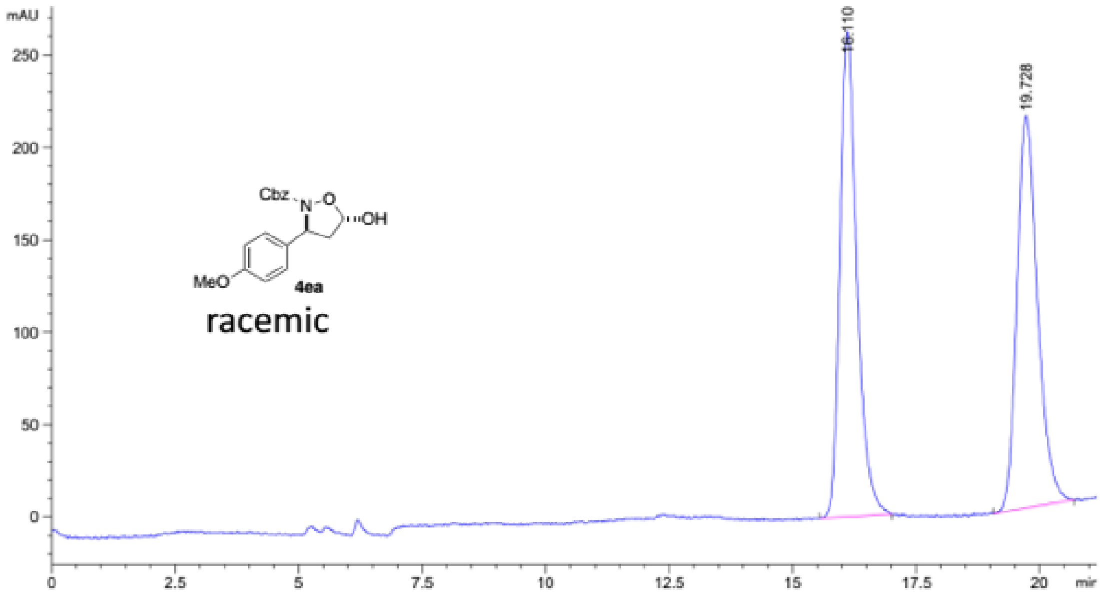

Peak #	RetTime [min]	Type	Width [min]	Area [mAU*s]	Height [mAU]	Area %
1	16.110	BB	0.3538	6292.95654	262.43561	50.4373
2	19.728	BB	0.4239	6183.84277	212.22551	49.5627

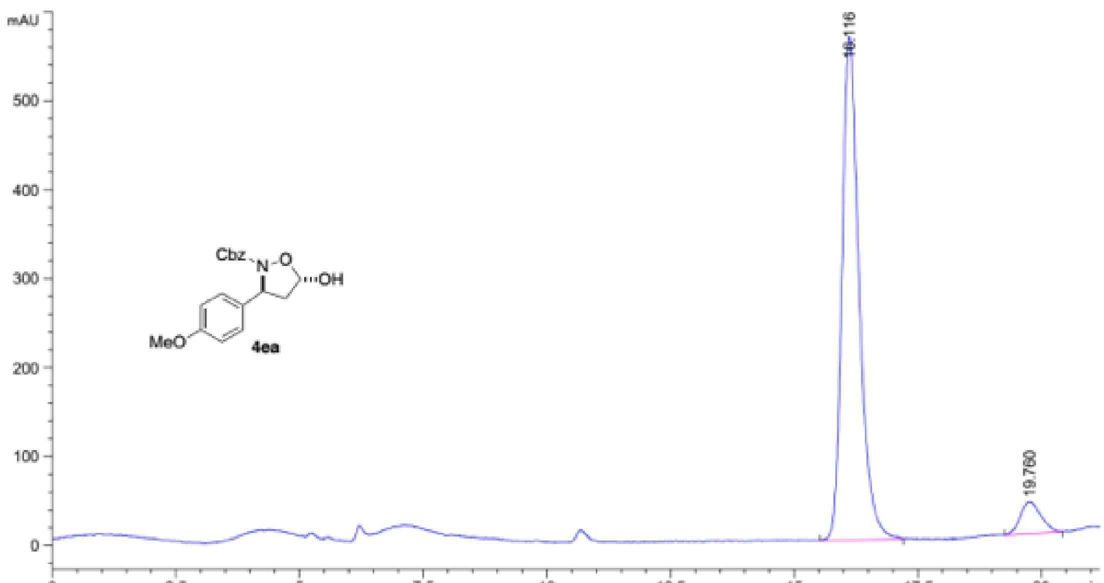

Peak #	RetTime [min]	Type	Width [min]	Area [mAU*s]	Height [mAU]	Area %
1	16.116	BB	0.3574	1.36430e4	565.71735	92.9998
2	19.760	BB	0.3549	1026.92090	35.56075	7.0002

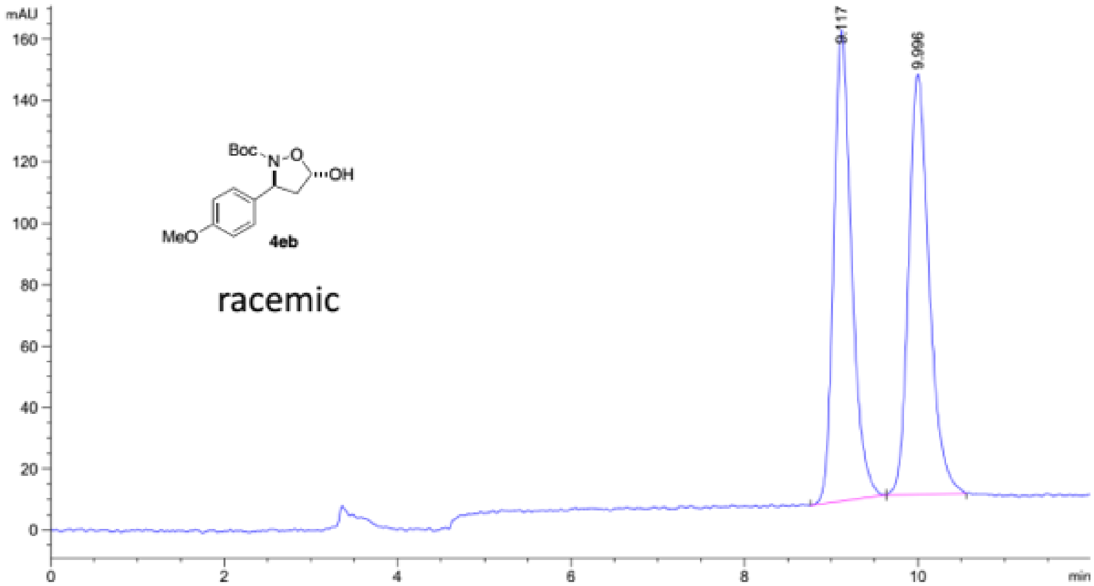

Peak #	RetTime [min]	Type	Width [min]	Area [mAU*s]	Height [mAU]	Area %
1	9.117	BB	0.2170	2195.71558	153.36635	49.2974
2	9.996	BB	0.2504	2258.30176	136.90877	50.7026

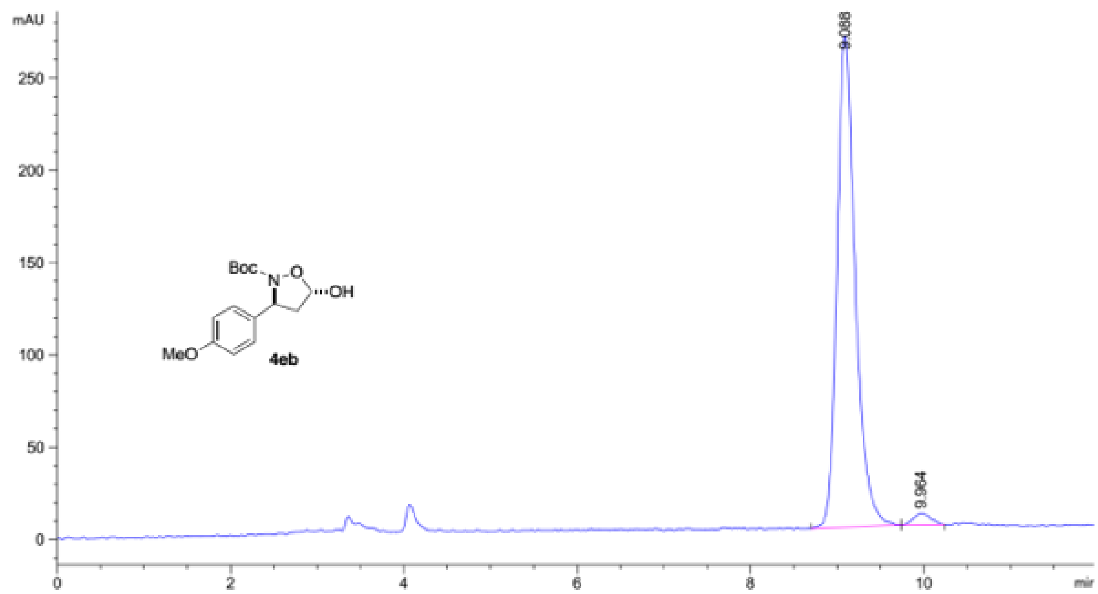

Peak #	RetTime [min]	Type	Width [min]	Area [mAU*s]	Height [mAU]	Area %
1	9.088	BB	0.2224	3883.91626	265.95953	97.8883
2	9.964	BB	0.1737	83.78580	6.19845	2.1117

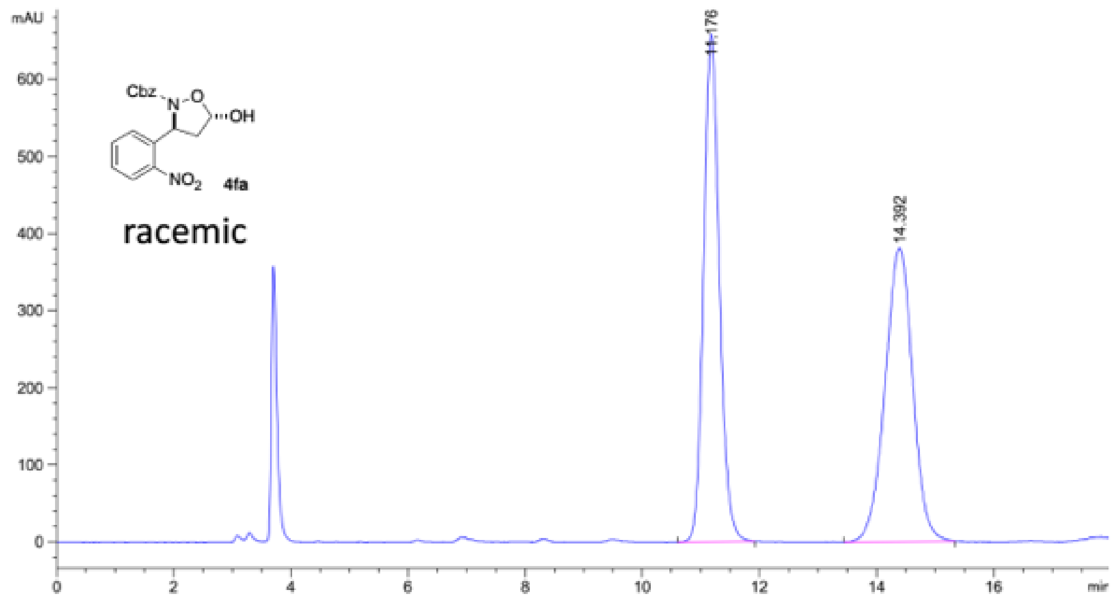

Peak #	RetTime [min]	Type	Width [min]	Area [mAU*s]	Height [mAU]	Area %
1	11.176	BB	0.2883	1.23152e4	658.22516	49.5975
2	14.392	BB	0.5116	1.25151e4	380.65091	50.4025

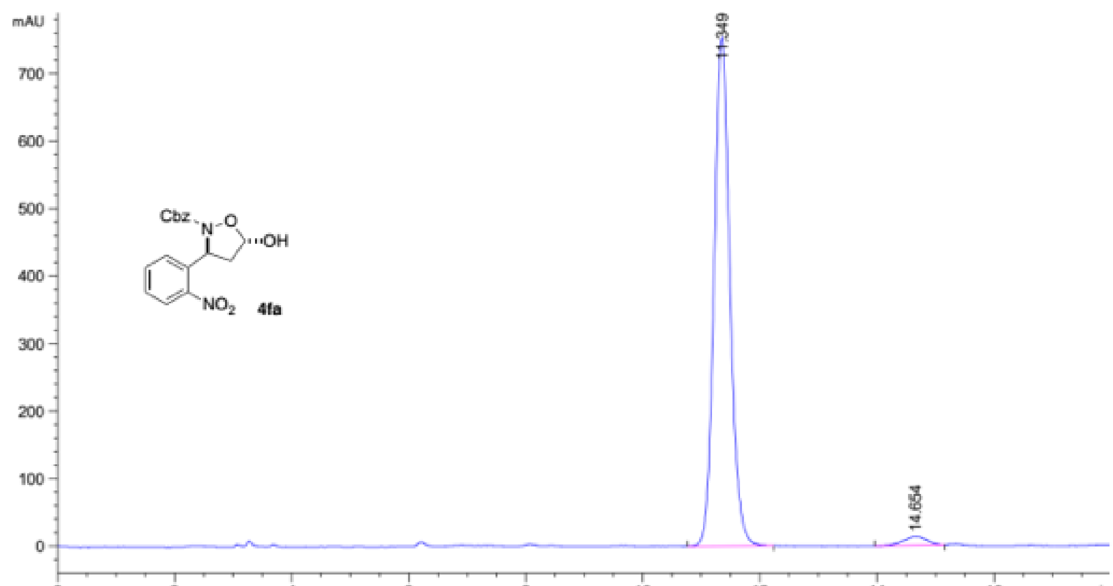

Peak #	RetTime [min]	Type	Width [min]	Area [mAU*s]	Height [mAU]	Area %
1	11.349	BB	0.2922	1.42190e4	753.25641	97.3934
2	14.654	BB	0.3501	380.55173	13.20872	2.6066

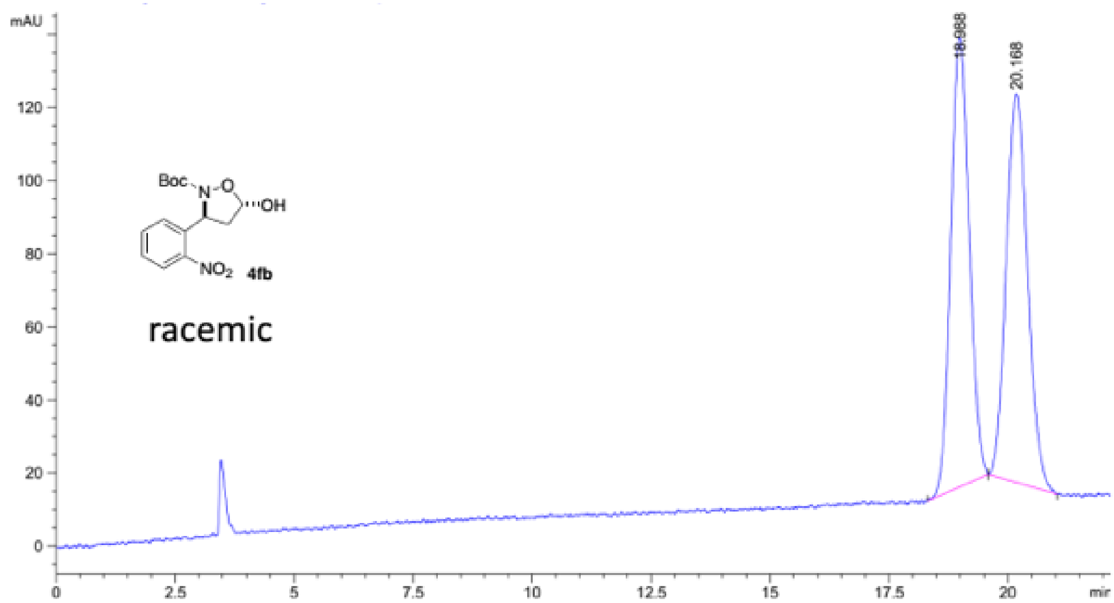

Peak #	RetTime [min]	Type	Width [min]	Area [mAU*s]	Height [mAU]	Area %
1	18.988	BB	0.3734	3325.79980	123.01029	49.9775
2	20.168	BB	0.4273	3328.79053	106.30922	50.0225

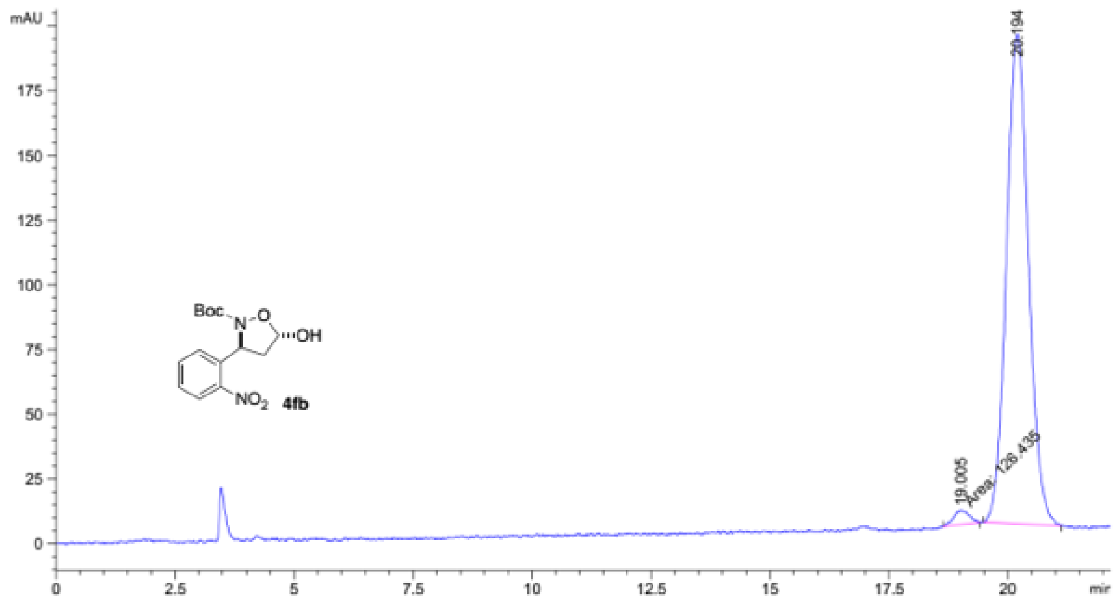

Peak #	RetTime [min]	Type	Width [min]	Area [mAU*s]	Height [mAU]	Area %
1	19.005	MM	0.3784	126.43514	5.56816	2.0348
2	20.194	BB	0.4420	6087.18848	188.88759	97.9652

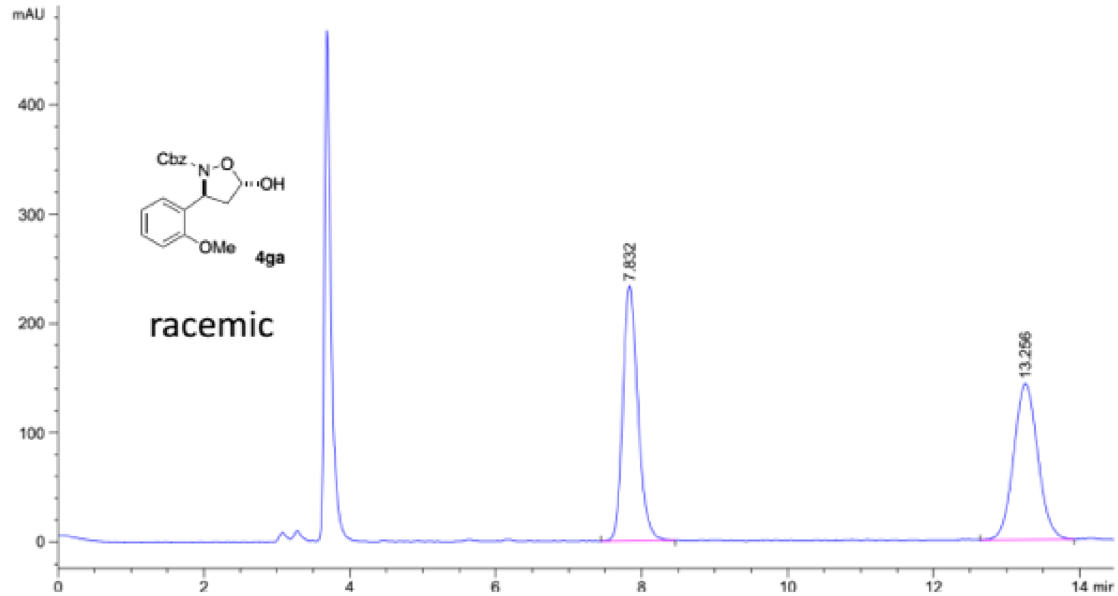

Peak #	RetTime [min]	Type	Width [min]	Area [mAU*s]	Height [mAU]	Area %
1	7.832	BB	0.2233	3384.69019	233.19429	50.5226
2	13.256	BB	0.3667	3314.67407	142.88220	49.4774

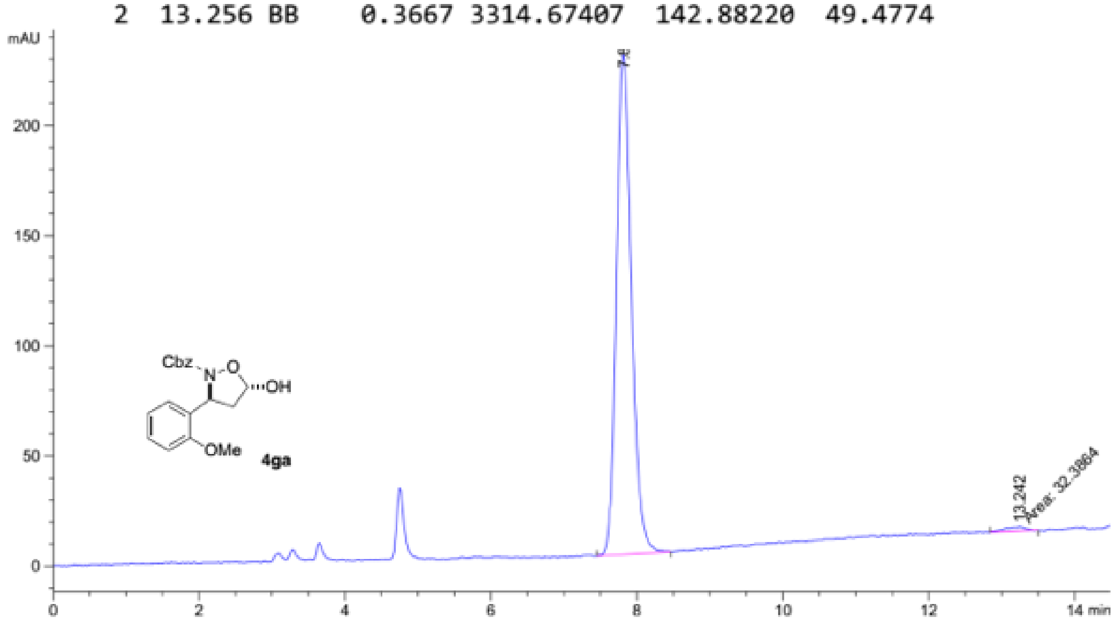

Peak #	RetTime [min]	Type	Width [min]	Area [mAU*s]	Height [mAU]	Area %
1	7.812	BB	0.2202	3268.44946	226.70520	99.0188
2	13.242	MM	0.3078	32.38636	1.75339	0.9812

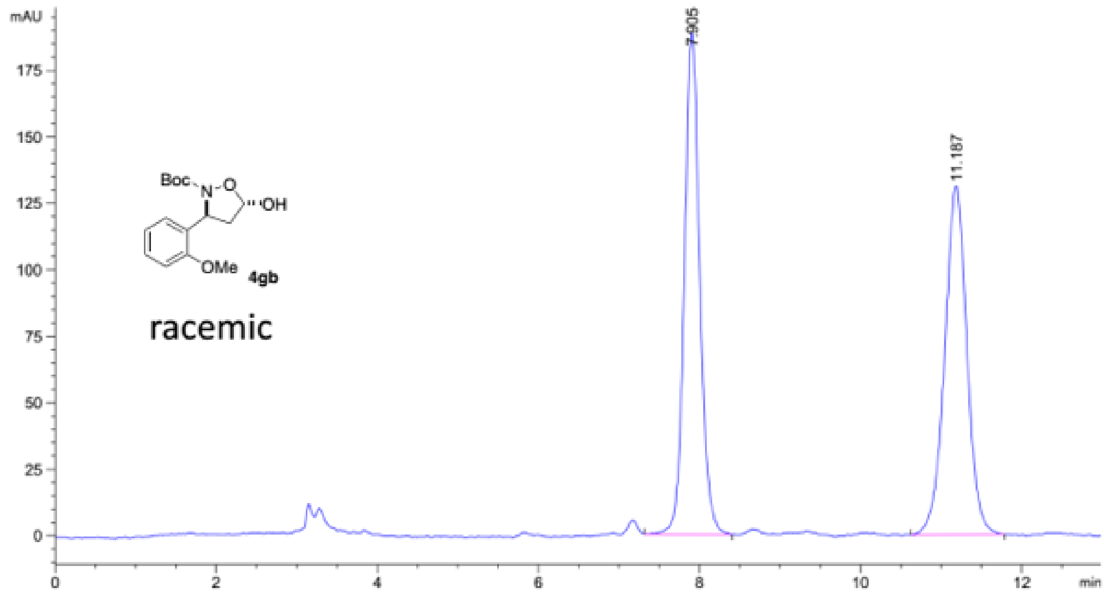

Peak #	RetTime [min]	Type	Width [min]	Area [mAU*s]	Height [mAU]	Area %
1	7.905	BB	0.2010	2506.98486	188.63969	49.8926
2	11.187	BB	0.2900	2517.77466	131.15120	50.1074

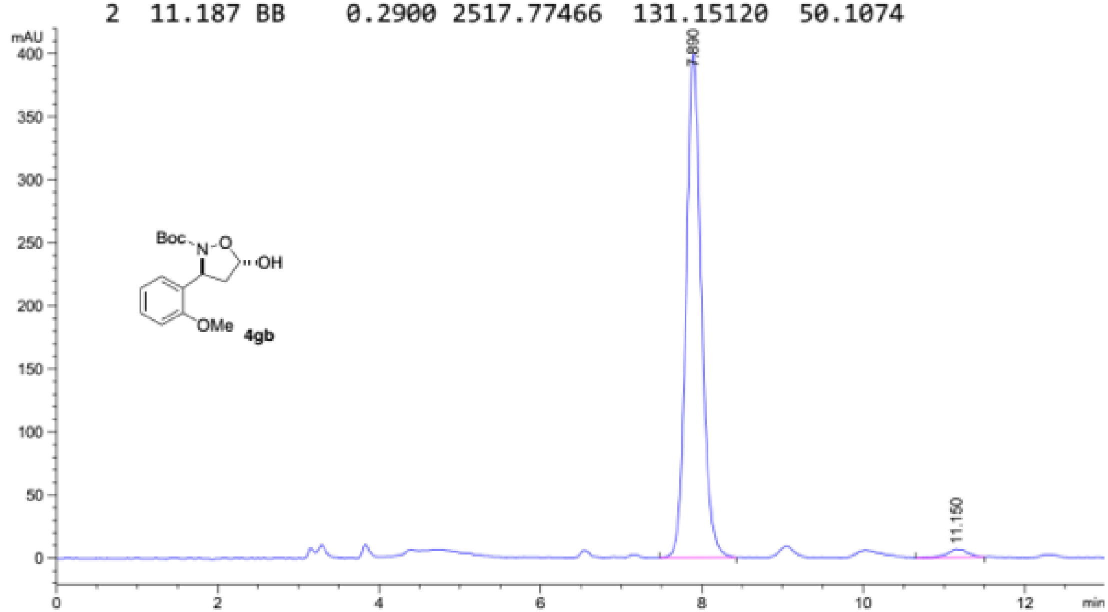

Peak #	RetTime [min]	Type	Width [min]	Area [mAU*s]	Height [mAU]	Area %
1	7.890	BB	0.2000	5275.11865	399.61581	97.8295
2	11.150	BB	0.2354	117.03419	6.39896	2.1705

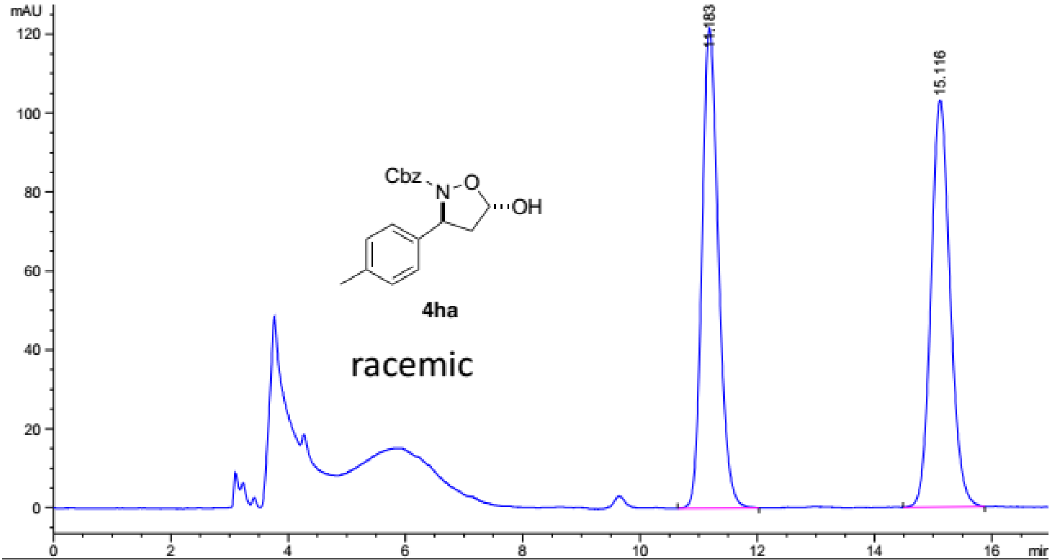

Peak #	Ret Time [min]	Type	Width [min]	Area [mAU*s]	Height [mAU]	Area %
1	11.183	BB	0.2997	2375.24243	121.69804	50.3420
2	15.116	BB	0.3491	2342.96533	103.11539	49.6580

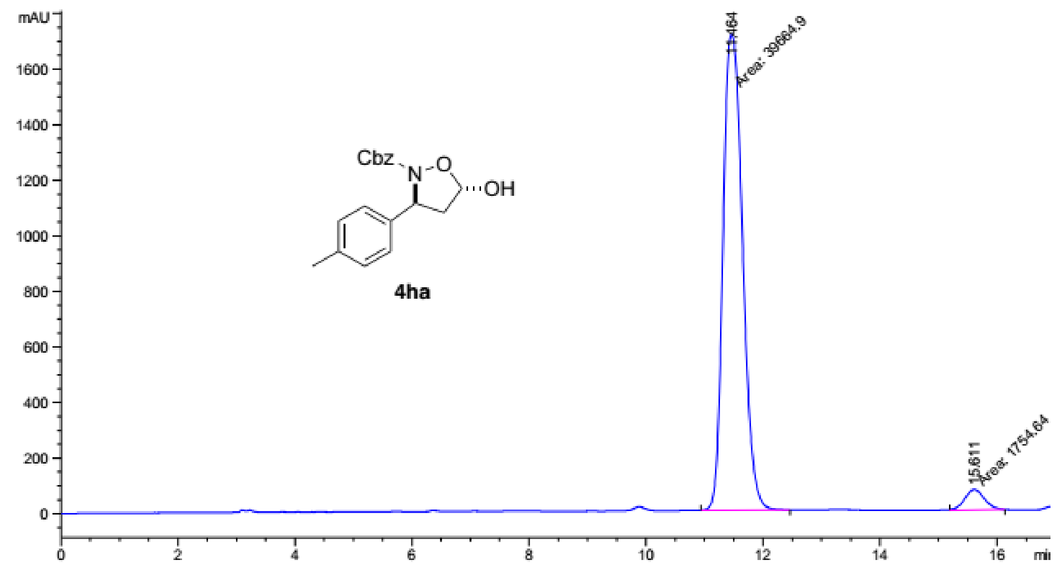

Peak #	Ret Time [min]	Type	Width [min]	Area [mAU*s]	Height [mAU]	Area %
1	11.464	MF	0.3859	3.96649e4	1713.17957	95.7637
2	15.611	MM	0.3937	1754.63977	74.27271	4.2363

Chapter III

Continuous Flow Preparation of Enantiomerically Pure BINOL(s) by Acylative Kinetic Resolution

3.1. Introduction

Enantiopure 1,1'-binaphthol (BINOL) and its derivative are probably the most versatile building blocks for the preparation of chiral catalysts, including Brønsted/Lewis acid/base catalysts.[141]

Although the development of the asymmetric oxidative dimerization of naphthyl derivatives has experienced a significant progress in recent years,[142] the kinetic resolution (KR) of racemic biaryl derivatives (and, in particular, of unsubstituted BINOL) continues to be the main entrance to the ever growing family of 1,1'-binaphthols and derivatives.[141,143] Within this approach, the acylative KR of 1,1'-

[141] For some reviews on the use of BINOL-based, chiral biaryl ligands in asymmetric catalysis, see: a) Noyori, R.; Takaya, H. *Acc. Chem. Res.* **1990**, *23*, 345-350; b) Tang, W.; Zhang, X. *Chem. Rev.* **2003**, *103*, 3029-3070; c) Chen, Y.; Yekta, S.; Yudin, A. K. *Chem. Rev.* **2003**, *103*, 3155-3212; d) Xia, Q. H.; Ge, H. Q.; Ye, C. P.; Liu, Z. M.; Su, K. X. *Chem. Rev.* **2005**, *105*, 1603-1662; e) Shibasaki, M.; Matsunaga, S. *Chem. Soc. Rev.* **2006**, *35*, 269-279; f) Akiyama, T.; Itoh, J.; Fuchibe, K. *Adv. Synth. Catal.* **2006**, *348*, 999-1010; g) Connon, S. J. *Angew. Chem. Int. Ed.* **2006**, *45*, 3909-3912; h) Xie, J.-H.; Zhou, Q.-L. *Acc. Chem. Res.* **2008**, *41*, 581-593; i) Rueping, M.; Kuenkel, A.; Atodiresei, I. *Chem. Soc. Rev.* **2011**, *40*, 4539-4549; j) D. Parmar; E. Sugiono; S. Raja; M. Rueping, *Chem. Rev.* **2014**, *114*, 9047-9153; k) Sunoj, R. B. *Acc. Chem. Res.* **2016**, *49*, 1019-1028.

[142] For some recent examples, see: a) Narute, S.; Parnes, R.; Toste, F. D.; Pappo, D. *J. Am. Chem. Soc.* **2016**, *138*, 16553-16560; b) Kim, H. Y.; Takizawa, S.; Sasai, H.; Oh, K. *Org. Lett.* **2017**, *19*, 3867-3870; c) Tian, J. M.; Wang, A. F.; Yang, J. S.; Zhao, X. J.; Tu, Y. Q.; Zhang, S. Y.; Chen, Z. M. *Angew. Chem. Int. Ed.* **2019**, *58*, 11023-11027.

[143] For the catalytic non-enzymatic KR of biaryl compounds, see: a) Aoyama, H.; Tokunaga, M.; Kiyosu, J.; Iwasawa, T.; Obora, Y.; Tsuji, Y. *J. Am. Chem. Soc.* **2005**, *127*, 10474-10475. For KR with biaryl-derived

binaphthyl derivatives has received comparatively little attention in spite of its potential.

In 2014, the Sibi group reported the KR of racemic 1,1'-binaphthols derivatives with chiral 4-dimethylaminopyridine (DMAP) catalysts achieving selectivity factors of up to 51 (Scheme 1).[144] The developed chiral DMAP was also evaluated in the KR of racemic secondary alcohols achieving selectivity factors of up to 37. In this report, a low operation temperature at -50 ºC was used, which render them impractical for large scale operation.

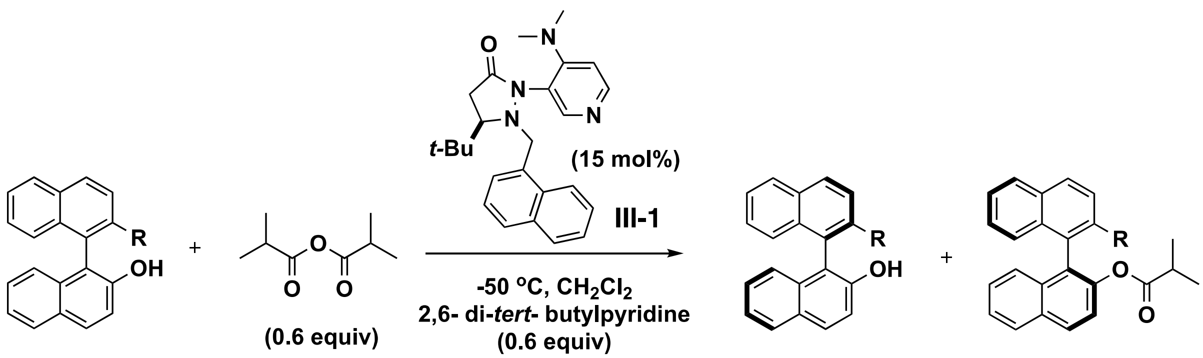

rac-**III-2** **III-3** **III-2** **III-4**

Scheme 1. Chiral DMAP in the KR of racemic methylated 1,1'-binaphthols and derivatives

In the same year, the Zhao group reported the acylative KR of a wide range of 1,1'-biaryl-2,2'-diols and NOBIN derivatives with a chiral NHC **III-5**, leading to acylated products with excellent enantiomeric purity (99% ee) with selectivity factors of up to

catalysts, see: b) Mori, K.; Ichikawa, Y.; Kobayashi, M.; Shibata, Y.; Yamanaka, M.; Akiyama, T. *J. Am. Chem. Soc.* **2013**, *135*, 3964-3970; c) Shirakawa, S.; Wu, X.; Maruoka, K. *Angew. Chem. Int. Ed.* **2013**, *52*, 14200-14203; d) Cheng, D. J.; Yan, L.; Tian, S. K.; Wu, M. Y.; Wang, L. X.; Fan, Z. L.; Zheng, S. C.; Liu, X. Y.; Tan, B. *Angew. Chem. Int. Ed.* **2014**, *53*, 3684-3687; e) Arseniyadis, S.; Mahesh, M.; McDAID, P.; Hampel, T.; Davey, S. G.; Spivey, A. C. *Collect. Czech. Chem. Commun.* **2011**, *76*, 1239-1253.

[144] Ma, G.; Deng, J.; Sibi, M. P. *Angew. Chem. Int. Ed.* **2014**, *53*, 11818-11821.

52 (Scheme 2).[145] In the case of KR of 1,1'-binaphthyl-2,2'-diol, the unsubstituted BINOL, the KR process worked with selectivity factors of up to 52. However, when the reaction scaled up to 1 g, the s factor decreased to 25, which may limit the application of this process in bigger scales.

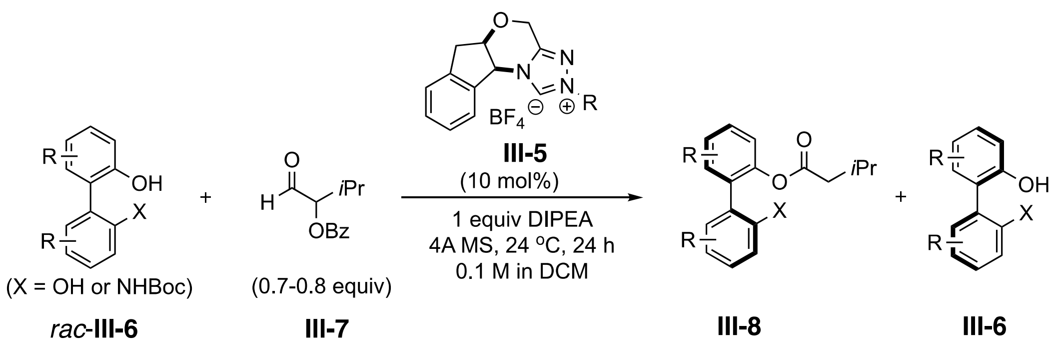

Scheme 2. Chiral NHC-catalyzed acylative KR of a wide range of 1,1'-biaryl-2,2'-diols and NOBIN derivatives

In 2019, during our study of the acylative KR of 1,1'-binaphthyl derivatives with immobilized isothiourea catalysts, the Smith group reported an chiral isothiourea - catalysed acylative KR of unprotected 1,1′ - biaryl - 2,2′ - diol derivatives in highly enantioenriched form (s values up to 190). In this study, 2,2 - diphenylacetic pivalic anhydride was used to minimize diacylation and to achieve high selectivity.[146]

[145] Lu, S.; Poh, S. B.; Zhao, Y. *Angew. Chem. Int. Ed.* **2014**, *53*, 11041-11045.

[146] Qu, S.; Greenhalgh, M. D.; Smith, A. D. *Chem. Eur. J.* **2019**, *25*, 2816-2823.

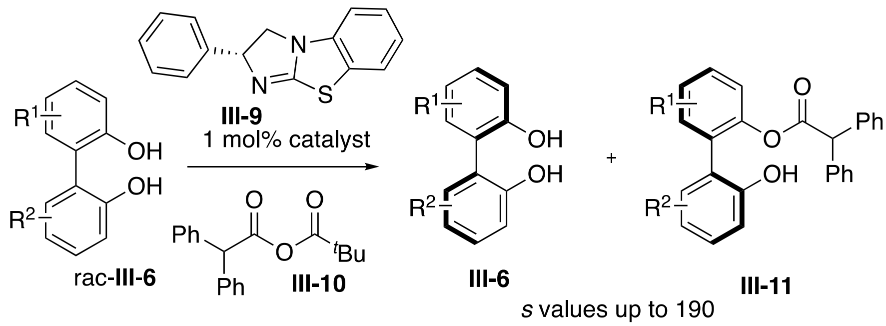

Scheme 3. Chiral isothiourea - catalysed acylative KR of 1,1′ - biaryl - 2,2′ - diol derivatives

3.2. Polymer-immobilized chiral benzotetramisole analogues

Chiral isothioureas, an amidine-based catalyst first reported by Birman group in 2006,[147] have become very useful catalysts for nonenzymatic enantioselective acyl transfer for the KR of alcohols[148] and carboxylic acids,[149] and desymmetrization of axially chiral diols.[150] Benzotetramisole (BTM), the archetypical example of chiral isothioureas, is among the most readily available and effective nonenzymatic enantioselective acylation catalysts[151] reported to date.[147,152] Over the last years, the Smith group has expanded its use to a variety of processes.[153]

[147] Birman, V. B.; Li, X. *Org. Lett.* **2006**, *8*, 1351–1354.

[148] Merad, J.; Borkar, P.; Bouyon Yenda, T.; Roux, C.; Pons, J.-M.; Parrain, J.-L.; Chuzel, O.; Bressy, C. *Org. Lett.* **2015**, *17*, 2118-2121.

[149] Yang, X.; Birman, V. B. *Adv. Synth. Catal.* **2009**, *351*, 2301-2304.

[150] Qu, S.; Greenhalgh, M. D.; Smith, A. D. *Chem. Eur. J.* **2019**, *25*, 2816-2823.

[151] Vedejs, E.; Jure, M. *Angew. Chem. Int. Ed.* **2005**, *44*, 3974-4001.

[152] a) Birman, V. B.; Guo, L. *Org. Lett.* **2006**, *8*, 4859-4861; b) Birman, V. B.; Jiang, H.; Li, X.; Guo, L.; Uffman, E. W. *J. Am. Chem. Soc.* **2006**, *128*, 6536-6537; c) Birman, V. B.; Jiang, H.; Li, X. *Org. Lett.* **2007**, *9*, 3237-3240.

[153] a) Belmessieri, D.; Morrill, L. C.; Simal, C.; Slawin, A. M. Z.; Smith, A. S. *J. Am. Chem. Soc.* **2011**, *133*, 2714-2720; b) Simal, C.; Lebl, T.; Slawin, A. M. Z.; Smith, A. D. *Angew. Chem. Int. Ed.* **2012**, *51*, 3653-3657;

In 2016, our group reported the preparation of a PS-supported BTM analogue (**III-12**). The functional resin **III-12** was used in the domino Michael addition/cyclization reaction of *in situ* activated arylacetic acids with chalcone-type tosylimines (Scheme 4, a), affording the cyclization products dihydropyridinones **15** with high yields and excellent enantioselectivities (*ee* up to 99%). Recycling studies suggested that pivaloyl chloride was the main reason of deactivation of **III-12**, an otherwise very stable catalyst.[154] In 2017, our group reported the use of this supported BTM (**III-12**) as a highly efficient organocatalyst in a variety of formal [4+2] cycloaddition reactions, leading to six-membered heterocycles and spiro-heterocycles (**III-17**) in high yields and excellent enantioselectivities (Scheme 4, b) and exhibiting notable chemical stability under operation conditions with high recyclability (11 cycles, accumulated TON of 76.8). Finally, this supported BTM (**III-12**) was implemented into an extended-operation continuous flow process (no decrease in yield or ee after 18 h).[155] In the same year, our labratory reported the use of this immobilized BTM **III-12** in the periselective [8+2] cycloaddition between *in situ* generated chiral ammonium enolates and azaheptafulvenes, producing enantioenriched cycloheptatrienes fused

c) Morrill, L. C.; Douglas, J.; Lebl, T.; Slawin, A.M. Z.; Fox, D. J.; Smith, A. D. *Chem. Sci.* **2013**, *4*, 4146-4155; d) Morrill, L. C.; Stark, D. G.; Taylor, J. E.; Smith, S. R.; Squires, J. A.; D'Hollander, A. C. A.; Simal, C.; Shapland, P.; O'Riordanc, T. J. C.; Smith, A. D. *Org. Biomol. Chem.* **2014**, *12*, 9016-9027; e) Smith, R. S.; Douglas, J.; Prevet, H.; Shapland, P.; Slawin, A. M. Z.; Smith, A. D. *J. Org. Chem.* **2014**, *79*, 1626-1639; f) Morrill, L. C.; Smith, S. M.; Slawin, A. M. Z.; Smith, A. D. *J. Org. Chem.* **2014**, *79*, 1640-1655; g) Smith, S. R.; Leckie, S. M.; Holmes, R.; Douglas, J.; Fallan, C.; Shapland, P.; Pryde, D.; Slawin, A. M. Z.; Smith, A. D. *Org. Lett.* **2014**, *16*, 2506-2509; h) Morrill, L. C.; Ledingham, L. A.; Couturier, J. P.; Bickel, J.; Harper, A. D.; Fallan, C.; Smith, A. D. *Org. Biomol. Chem.* **2014,** *12*, 624-636; i) Yeh, P. P.; Daniels, D. S. B.; Fallan, C.; Gould, E.; Simal, C.; Taylor, J. E.; Slawin, A. M. Z.; Smith, A. *Org. Biomol. Chem.* **2015**, *13*, 2177-2191.

[154] Izquierdo, J.; Pericàs, M. A. *ACS Catal.* **2016**, *6*, 348-356.

[155] Wang, S.; Izquierdo, J.; Rodríguez-Escrich, C.; Pericàs, M. A. *ACS Catal.* **2017**, *7*, 2780-2785.

to a pyrrolidone ring in good yields and excellent enantioselectivities (Scheme 4, c).[156]

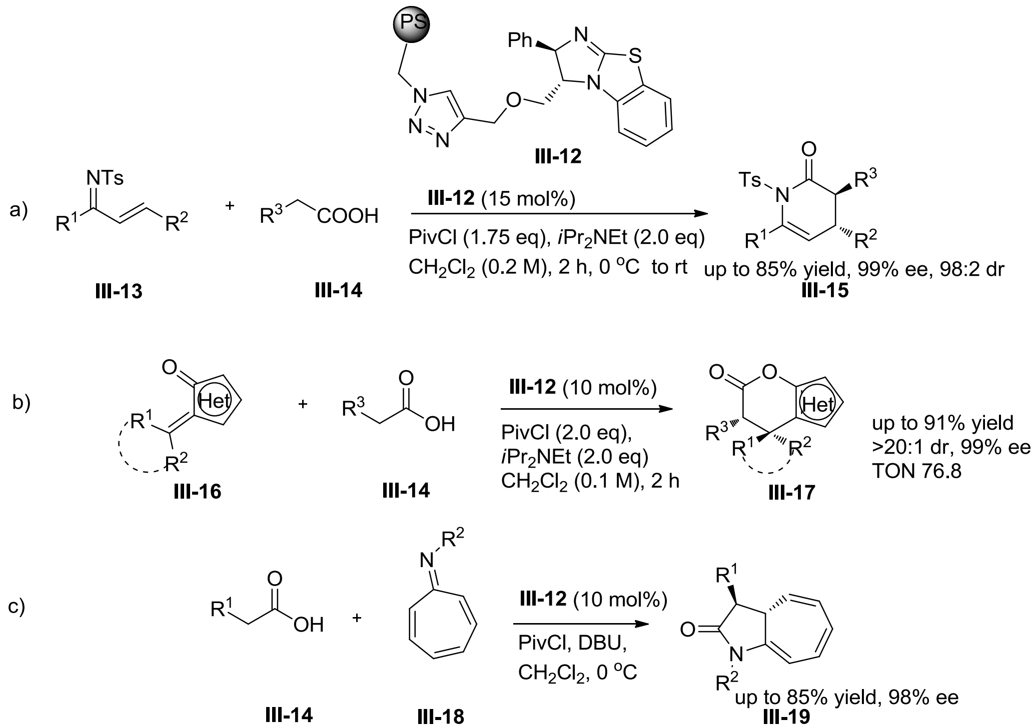

Scheme 4. PS-supported BTM analogue and application in asymmetric transformation

In 2018, in a joint effort of our laboratories, the Smith group reported the PS-immobilized of a Hyper-BTM based chiral isothiourea catalyst (**III-20**). The polymeric catalyst was evaluated in the acylative KR of a wide range of secondary alcohols *rac* **III-21**, including benzylic, allylic, and propargylic alcohols, cycloalkanol derivatives, and one 1,2-diol, obtaining good to excellent selectivity factors of up to 600. The good recyclability allowed the implementation of it into a continuous flow process.[157] A few months later, it was reported the application in the acylative KR of secondary

[156] Wang, S.; Rodríguez-Escrich, C.; Pericàs, M. A. *Angew. Chem. Int. Ed.* **2017**, *56*, 15068-15072.

[157] Neyyappadath, R. M.; Chisholm, R.; Greenhalgh, M. D.; Rodríguez-Escrich, C.; Pericàs, M. A.; Hähner, G.; Smith, A. D. *ACS Catal.* **2018**, *8*, 1067-1075.

and tertiary heterocyclic alcohols, including secondary benzylic, propargylic, allylic and cycloalkanols, and a range of 22 privileged 3-hydroxyoxindoles and 3-hydroxypyrrolidinones, obtaining up to excellent selectivity (s = 7–190). Finally, it was applied in a packed bed reactor to a continuous flow process with high selectivities (Scheme 5).[158]

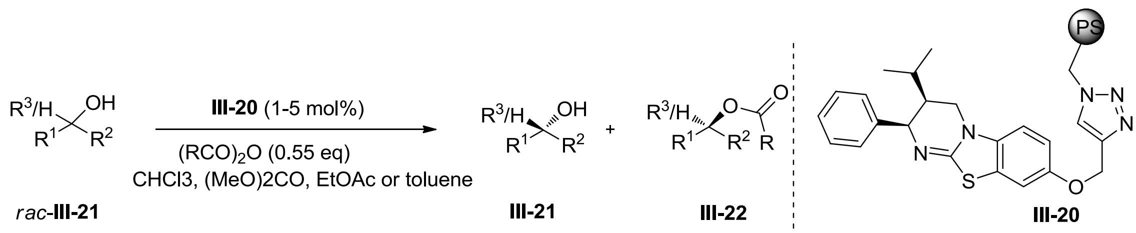

Scheme 5. PS-supported BTM analogue and application in the KR of alcohols

3.3. Aim of this project

In spite of the performance of the acylative KR of 1,1'-binaphthyl derivatives, these methods involve reaction conditions, such as low operation temperature or long reaction time, that render them impractical for large scale operation.

With these limitations in mind, and taking into account the industrial importance of enantiopure BINOLs and their derivatives, we considered alternative processes that could be operated under mild reaction conditions with high turnover frequencies, with the ultimate goal of developing a continuous flow process for the preparation of enantiomerically pure BINOL.

There are currently no examples where immobilized BTM catalysts have been applied for the acylative KR of 1,1'-bi-2-naphthol (BINOL). We wish to report the application of second generation immobilized BTM in the acylative KR of BINOLs in

[158] Guha, N. R.; Neyyappadath, R. M.; Greenhalgh, M. D.; Chisholm, R.; Smith, S. M.; McEvoy, M. L.; Young, C. M.; Rodríguez-Escrich, C.; Pericàs, M. A.; Hähner, G.; Smith, A. D. *Green Chem.* **2018**, *20*, 4537-4546.

batch and long-term continuous flow, allowing the preparation of highly enantioenriched BINOL in large scale.

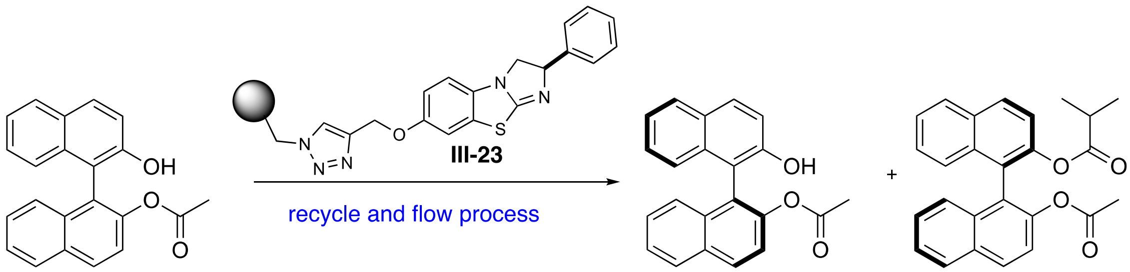

Scheme 6. Aim of this project

This manuscript was later published in Advanced Synthesis & Catalysis. (*Adv. Synth. Catal*. **2020**, **362**, 1370-1377)

Continuous Flow Preparation of Enantiomerically Pure BINOL(s) by Acylative Kinetic Resolution

Junshan Lai,[a,b] Rifahath M. Neyyappadath,[c] Andrew D. Smith[c] and Miquel A. Pericàs[a,d,*]

[a] Institute of Chemical Research of Catalonia (ICIQ), The Barcelona Institute of Science and Technology, Av. Països Catalans, 16, 43007 Tarragona (Spain). mapericas@iciq.es; (+34) 977-920-200.
[b] Departament de Química Analítica i Química Orgànica, Universitat Rovira i Virgili, 43007 Tarragona, Spain
[c] EaStCHEM, School of Chemistry, University of St Andrews, North Haugh, St Andrews, KY16 9ST, U.K.
[d] Departament de Química Inorgànica i Orgànica, Universitat de Barcelona (UB), 08028 Barcelona (Spain)

Abstract. A polystyrene-immobilized isothiourea has been applied to the enantioselective acylative kinetic resolution (KR) of monoacylated BINOL(s) with inexpensive isobutyric anhydride in batch and flow. High selectivity values (s = 35 at 0 ºC) and a remarkable stability of the catalytic system in the operation conditions have been recorded for unsubstituted BINOL. No significant loss of activity/selectivity is recorded after 10 consecutive KR cycles in batch. A continuous flow process has been implemented and operated with a 100 mmol (32.8 g) sample of racemic monoacetylated BINOL in an 84 hours experiment with a packed bed reactor containing 1g (f = 0.37 mmol.g^{-1}) of the functional resin. Resident time can be decreased to 10 min with the same reactor to achieve a conversion of 58% with a selectivity factor s = 17 in dichloromethane solution when a more highly functionalized catalyst (f = 0.88 mmol.g^{-1}) is used. This translates into a remarkable combined productivity of 5.5 mmol$_{prod}$·mmol$_{cat}$$^{-1}$·h^{-1}.

Keywords: BINOL; Kinetic resolution; Isothiourea organocatalysts; Immobilization; Continuous flow

Introduction

Enantiopure 1,1'-binaphthols (BINOLs) are probably the most versatile building blocks for the preparation of chiral catalysts. Their almost unlimited applicability cover the broad areas of metal catalysis and organocatalysis, and simple structural variations lead to applications in the comprehensive area of Brønsted/Lewis acid/base catalysis.[1] Although the development of methods for the asymmetric oxidative dimerization of naphthyl derivatives has experienced a significant progress in recent years,[2] the kinetic resolution (KR) of racemic biaryl derivatives (and, in particular, of unsubstituted BINOL) continues to be the main entrance to the ever growing family of 1,1'-binaphthols and derivatives.[1, 3] Within this approach, the acylative KR of 1,1'-binaphthyl derivatives has received comparatively low attention in spite of its potential.[4] In 2014, Sibi reported chiral 4-dimethylaminopyridine catalysts achieving selectivity factors of up 51 in the considered acylative process (Scheme 1a).[5] In the same year, Zhao (Scheme 1b)reported the highly efficient NHC-catalyzed acylative KR of a wide range of 1,1'-biaryl-2,2'-diols and amino alcohols leading to products with consistently very high enantiomeric purity (99% ee).[6] In spite of its performance, these methods involve reaction conditions, such as low operation temperature[5] or long reaction time,[6] that render them impractical for large scale operation.

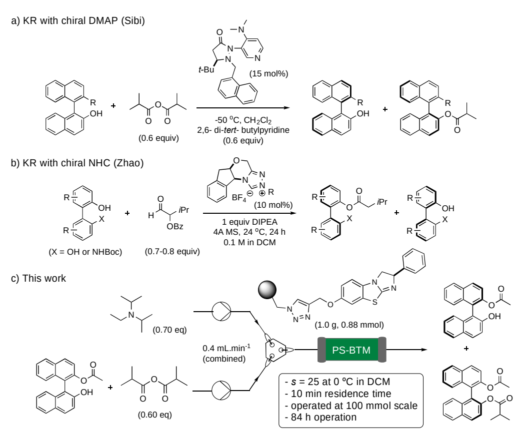

Scheme 1. Approaches to the acylative KR of BINOL and related compounds.

With these limitations in mind, and taking into account the industrial importance of enantiopure BINOLs and their derivatives, we considered alternative processes that could be operated under mild reaction conditions with high turnover frequencies, with the ultimate goal of developing a continuous flow process for the preparation of enantiomerically pure BINOL (Scheme 1c).[7]

Chiral isothioureas, first reported by Birman in 2006,[8] have become useful catalysts for the acylative KR of alcohols[9] and carboxylic acids[10] and, quite recently, for the desymmetrization of axially chiral diols.[11] Benzotetramisole (BTM), the archetypical example of chiral isothioureas, is among the most readily available and effective nonenzymatic enantioselective acylation catalysts[12] reported to date.[8, 13] In 2016, we reported the preparation of a polystyrene-supported BTM analogue which was successfully used in the domino Michael addition/cyclization reaction with excellent yields and very high enantioselectivities, [14] and later applied to asymmetric [4+2] and [8+2] annulation reactions.[15] More recently, in a joint effort of our laboratories, new polystyrene-supported isothiourea catalysts, based on the homogeneous catalysts BTM and HyperBTM, have been prepared and used for the acylative KR of secondary[16a] and secondary and tertiary heterocyclic alcohols[16b] in batch and in continuous flow. However, there are currently no examples where BTM catalysts have been applied for the acylative KR of 1,1'-bi-2-naphthol (BINOL). We report herein the application of second generation immobilized BTM in the acylative KR of BINOLs with high selectivity in batch and continuous flow, and we show that the flow procedure can be operated at the 100 mmol scale (32.8 g) without any decrease in the performance of the catalyst.

Results and Discussion

We decided to evaluate isothioureas **5a-d** as catalysts for this study. The selection includes monomers **5b-c** as well as the first and second generation PS-immobilized BTM-type catalysts **5a**[14] and **5d**,[16b] and is guided by previous results in the KR of axially chiral diols with homogeneous isothioureas (Figure 1).[11]

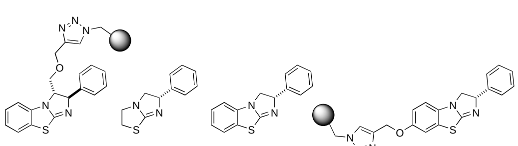

Figure 1. Catalysts used in this study.

For the preparation of **5d** (Scheme 2) we used a slight modification of the reported procedure that simplifies the installment of the propargyl anchor by performing the replacement of the methoxy by a propargyloxy group at the beginning of the sequence. Thus, 2-chloro-6-methoxybenzothiazole (**1**) was demethylated with BBr_3 and alkylated without isolation with propargyl bromide (**2**) to afford 2-chloro-6-propynyloxybenzo[d]thiazole (**3**) in 93% yield. Then, following a modification of a literature procedure, [17] neat **3** was heated in a pressure tube (135 ºC, 24 h) with a stoichiometric amount of (*S*)-2-amino-2-phenylethanol and Hunig's base (2 eq.) followed by in situ cyclization to afford 8-propynyloxy-BTM (**4**) in 58% yield (3 steps). Immobilization of **4** onto azidomethyl polystyrene, prepared from commercial Merrifield resin, was achieved by a Cu-catalyzed azide−alkyne cycloaddition reaction. The nitrogen content of the resulting polymer, determined by elemental analysis, was used to calculate the functionalization[18] of **5d** (0.37 mmol g^{-1}), and this value was used to determine the catalyst loading in all subsequent KRs.

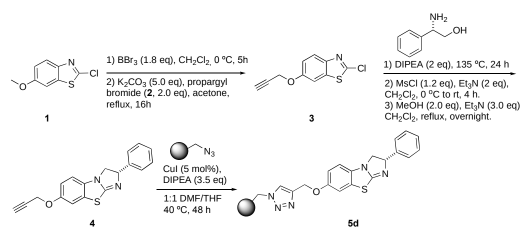

Scheme 2. Synthesis of the second-generation polystyrene-supported BTM catalyst (**5d**).

Our initial studies focused on the KR of parent BINOL **6a** with anhydrides, using 5 mol % of BTM **5**c as the catalyst (Scheme 3). Unfortunately, the reactions were poorly selective, mixtures of binol with its monoacylated and bisacylated products being always obtained. Moreover, the reproducibility of these experiments was rather poor.

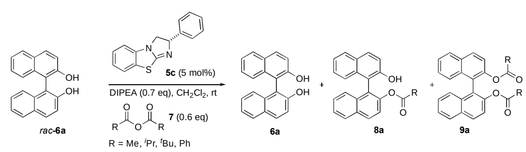

Scheme 3. Acylative KR of *rac*-BINOL (**6a**).

In light of these results, we modified our strategy to the acylative KR of monoacylated BINOLs (Table 1). We first used isobutyric anhydride as an acyl donor (0.6 equiv) for the KR of a series of monoacylated BINOLs in CH_2Cl_2 at room temperature. As shown in entry 1, the KR of monoacetyl BINOL with isobutyric anhydride took place with a selectivity factor $s = 14$ at 58% conversion. The use of larger acyl groups on the monoacylated BINOL substrate, such as isobutyryl, pivaloyl or benzoyl, gave much lower selectivities (entries 2-4). According to this, monoacetyl BINOL **8a** was used as the model substrate to optimise the nature of the acylating agent **7**. As shown in entry 6, pivalic anhydride did not work in this reaction, while both acetic anhydride and benzoic anhydride (entries 5 and 7) gave low selectivities. Accordingly, the combination of **8a** and isobutyric anhydride was established as optimal for the planned KR process.

Table 1. Acylative KR of monoacylated BINOLs.[a)]

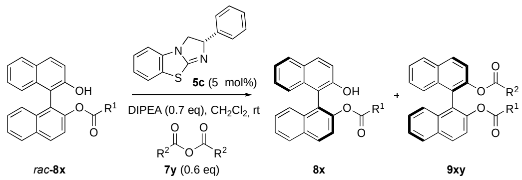

	8	R^1	**9**	R^2	**8** ee$^{b)}$ [%]	**9** ee$^{b)}$ [%]	c$^{c)}$ [%]	*s*$^{d)}$
1	**8a**	Me	**9ab**	^{i}Pr	91	65	58	14
2	**8b**	^{i}Pr	**9bb**	^{i}Pr	52	42	55	4
3	**8c**	^{t}Bu	**9cb**	^{i}Pr	43	33	56	3
4	**8d**	Ph	**9db**	^{i}Pr	78	51	60	7
5	**8a**	Me	**9aa**	Me	24	18	57	2
6	**8a**	Me	**9ac**	^{t}Bu	-	-	-	-
7	**8a**	Me	**9ad**	Ph	34	31	52	3

a) Reaction conditions: (+/-) **8** (0.5 mmol, 1 eq.), **7y** (0.3 mmol, 0.6 eq.) and *i*Pr$_2$NEt (45.2 mg, 61 µL, 0.35 mmol, 0.7 eq.), catalyst (0.025 mmol), CH_2Cl_2 (2.5 mL), rt. b) ee determined by HPLC. c) Conversion determined by Kagan's equations. d) Selectivity factors calculated from ee data.

Since the main goal of this project was applying immobilized isothiourea catalysts to the KR process, **5d** featuring an almost unperturbed BTM structure was directly used to optimise the reaction solvent (Table 2). Gratifyingly, the reaction rate was not affected by the heterogeneous nature of the catalyst (in both cases the process was complete in 10 h) and the *s* value even increased (*s* = 18) when chloroform was used at room temperature (entry 1). Slightly lower selectivity (*s* = 14) was recorded in dichloromethane under the same conditions (entry 4), while non-chlorinated solvents like DMF, CH_3CN, Dioxane, Et_2O, toluene and THF provided only moderate selectivities (entries 7-11). With halogenated solvents, the effect of temperature was also studied. Working in chloroform, a temperature decreased to 0 ºC led to an increased s value of 29 (Table 2, entry 2) without any significant decrease in catalytic activity. However, when the reaction temperature was increased to 60 °C (4 h reaction time), the s value decreased to 6. According to these results, we decided to use $CHCl_3$ and CH_2Cl_2 as solvents in the acylative KR performed in batch, and CH_2Cl_2 for the processes in continuous flow.

Table 2. Solvent optimization for the acylative KR. [a)]

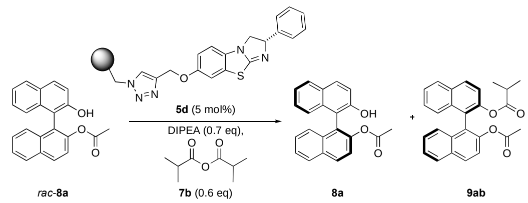

	solvent	**8a** ee$^{b)}$ [%]	**9ab** ee$^{b)}$ [%]	c$^{c)}$ [%]	*s*$^{d)}$
1	$CHCl_3$	95	67	58	18
2	**$CHCl_3$ (0 ºC)**	**95**	**78**	**55**	**29**
3	$CHCl_3$ (60 ºC)	70	47	60	6
4	CH_2Cl_2	90	65	58	14
5	**CH_2Cl_2 (0 ºC)**	**92**	**74**	**55**	**21**
6	CH_3CN	26	21	55	2
7	DMF	28	23	55	2
8	toluene	83	61	58	10
9	THF	89	61	59	12
10	dioxane	83	58	59	9
11	Et_2O	77	55	58	8

a) Reaction conditions: *rac*-**8a** (164 mg, 0.5 mmol, 1 eq.), **7b** (47.4 mg, 50 µL, 0.3 mmol, 0.6 eq.) and iPr$_2$NEt (45.2 mg, 61 µL, 0.35 mmol, 0.7 eq.), **5d** (135 mg, 5 mol %, f = 0.37 mmol%), solvent (2.5 mL), rt or indicated temperature. b) ee determined by HPLC. c) Conversion determined by Kagan's equations. d) Selectivity factors calculated from ee data.

As a final step in the optimization process, we wanted to compare the first- and second-generation polystyrene-supported BTM analogues (**5a** and **5d**) in the acylative KR (Table 3) in the optimal solvent. Results with the homogeneous catalysts **5b** and **5c** have been included for comparison purposes. The comparison gave a clear result in favour of **5d**. Thus, as shown in entry 1, **5a** proved unsuitable for this transformation, affording enantioenriched **8a** and **9ab** with very poor selectivity (*s* = 3). It is thus strongly suggested that the presence of the linker in position 3 of the heterocyclic nucleus leads to a much less efficient *chemzyme* for this particular process. To gain some further indication on the structural factors of **5** affecting selectivity, the reaction was also tested with **5b** and **5c**. With tetramisole **5b** (entry 2) the reaction was poorly selective, but benzotetramisole **5c** afforded the best selectivity results over a temperature range ranging from room temperature to -20 °C, where a selectivity of 36 was reached (entries 3-5). A similar decrease in temperature working with **5d** (entry 8) proved deleterious for catalytic activity and selectivity, and this can be attributed to the arrest of mobility of the polymer at this temperature, preventing swelling and the achievement of an optimal conformation. From a structural perspective it can be concluded that the presence of a condensed benzo ring in positions 2,3 of tetramisole is necessary for high selectivity in the acylative KR. Furthermore, a bulky substituent (the polymer chain) in one of the distal positions on the benzo group is well tolerated in terms of both catalytic activity and enantioselectivity.

Table 3. Comparison of catalysts **5a** and **5d** in the acylative KR of **8a** with **7b**.a)

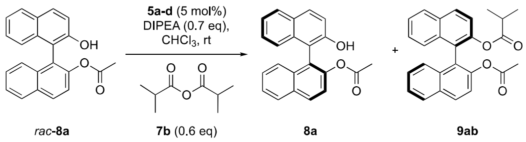

	Cat.	t [h]	**8a** ee$^{b)}$ [%]	**9ab** ee$^{b)}$ [%]	c$^{c)}$ [%]	s$^{d)}$
1	**5a**	8	-41	-33	57	3
2	**5b**	8	42	30	58	3
3	**5c**	8	98	73	57	28
4	**5c** (0 ºC)	8	99	71	58	30
5	**5c** (-20ºC)	16	98	78	56	36
6	**5d**	10	95	67	59	18
7	**5d** (0 ºC)	12	95	78	55	29
8	**5d** (-20 ºC)	24	33	61	35	6

a) Reaction conditions: *rac*-**8a** (164 mg, 0.5 mmol, 1 eq.), **7b** (47.4 mg, 50 µL, 0.3 mmol, 0.6 eq.), *i*Pr_2NEt (45.2 mg, 61 µL, 0.35 mmol, 0.7 eq.), **5a-d** (0.025 mmol), $CHCl_3$ (2.5 mL), rt or indicated temperature. b) ee determined by HPLC. c) Conversion determined by Kagan's equations. d) Selectivity factors calculated from ee data.

Although our main goal in this project was the development of a practical procedure for the preparation of enantiopure BINOL, we decided to investigate the scope of the catalytic acylative KR reaction in batch using the immobilized BTM catalyst **5d** in $CHCl_3$ (Table 4) at 0 ºC. Catalyst **5d** does not behave as a promiscuous chemzyme being rather specific with respect to the nature and substitution of the substrate. Substituents on the distal ring are generally well tolerated (**8e**, **8h**, **8i**), but excessive steric congestion (**8f**) leads to a significant decrease in enantioselectivity. Acylation of one of the oxygen atoms in the BINOL system (**8g**) and the presence of the two connected naphthyl units (**8g**, **8l**, **8m**) seem to be strict structural requirements, as the absence of substitution in *o*-, *o'*- in the BINOL system (**8j**, **8k**, **8m**) also seems to be. Fortunately, the parent substrate of interest **8a**, stands as the optimal substrate for the acylative KR, achieving a selectivity of up to 29 with the immobilized catalyst **5d** and up to 36 with the homogeneous BTM **5c**. It is worth noting that either scalemic **8a** or the diester **9ab** can be easily converted into the enantiomeric forms of BINOL through saponification and recrystallization from either toluene or chloroform (ESI).

Table 4. Scope of the acylative KR of BINOLs catalyzed by **5d**.a)

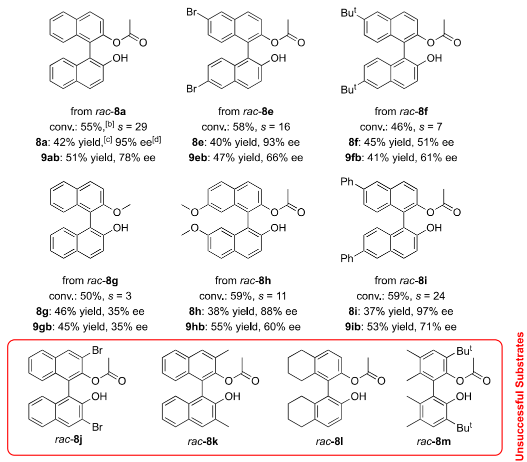

a) Reaction conditions: *rac*-**8** (0.5 mmol, 1 eq.), **7b** (47.4 mg, 50 µL, 0.3 mmol, 0.6 eq.), *i*Pr_2NEt (45.2 mg, 61 µL, 0.35 mmol, 0.7 eq.), **5d** (135 mg, 5 mol %), $CHCl_3$ (2.5 mL), 0 ºC, 10 h. b) Conversion determined by Kagan's equations. c) Isolated yield. d) ee determined by HPLC.

In view of the excellent results achieved with catalyst **5d** in the acylative KR of **8a**, the study of the recyclability of the catalyst in this particular process was undertaken. The process was initially studied in chloroform, however, slow deactivation of the catalyst was observed although selectivity remained constant over ten consecutive cycles (see Table S1). The deactivation process can be tentatively attributed to hydrolysis of the intermediate acylisothiouronium species as suggested by Birman,[17a] and we reasoned that using the less labile and less toxic anhydrous CH_2Cl_2 could minimize the deactivation problem without requiring solvent pre-treatments. As shown in Table 5, no decrease in catalytic activity or enantioselectivity was observed in a ten-cycle experiment in this solvent.

Table 5. Recycling of **5d** in the acylative KR of *rac*-**8a** with **7b** in CH_2Cl_2.a)

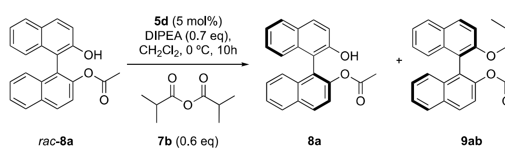

run	**8a** ee$^{b)}$ [%]	**9ab** ee$^{b)}$ [%]	conv$^{c)}$ [%]	*s*$^{d)}$
1	92	74	55	21
2	91	75	55	22
3	92	74	55	21
4	93	73	56	21
5	92	74	55	21
6	92	73	55	20
7	91	73	55	20
8	91	73	55	20

9	91	73	55	20
10	90	73	55	19

a) Reaction conditions: *rac*-**8a** (164 mg, 0.5 mmol, 1 eq.), **7a** (50 uL, 0.3 mmol, 0.6 eq.) *i*Pr$_2$NEt (61 uL, 0.35 mmol, 0.7 eq), PS-cat. **5d** (135 mg, 5 mol %), CH_2Cl_2 (2.5 mL), 0 ºC, 10 h. b) ee determined by HPLC. c) Conversion determined by Kagan's equations. d) Selectivity factors calculated from ee data.

Once the robustness of **5d** in dichloromethane had been established, a large scale (100 mmol) experiment in continuous flow was planned. The employed setup is shown in Figure 3. Catalyst **5d** (1.0 g, 0.37 mmol) was swollen in CH_2Cl_2 in a size-adjustable medium pressure glass column to create a packed bed reactor, and a cooling jacket was attached to maintain an internal temperature of 0 ºC. Two syringes mounted on a single syringe pump were used to feed the reagents to the flow reactor. One of the syringes contained a solution of **8a** and isobutyric anhydride (**7b**) in dichloromethane, and the second one a solution of *i*Pr$_2$NEt in dichloromethane, with concentrations adapted to secure the desired ratio (0.2 M in **8a** in the combined flow). The optimal combined flow rate was initially determined as 0.1 mL.min^{-1} at a reaction temperature of 0 ºC. Then, the preparative experiment was performed under the optimal condition from 250 mL of a 0.4 M solution of *rac*-**8a** (32.8 g, 100 mmol) in CH_2Cl_2. The experiment took 84 h to completion, and the measured residence time of the employed setup (visual inspection with a solution of methyl red) was *ca*. 40 min. Data at different operation times have been summarized in Table 6.

Table 6. Continuous flow acylative KR of **8a** with isobutyric anhydride (**7b**) catalyzed by **5d** (f = 0.37 mmol.g^{-1}).a)

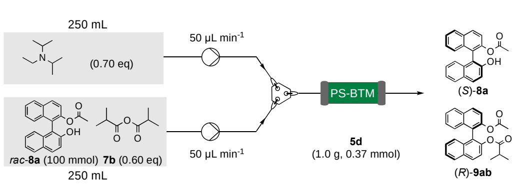

Operation time [h]	8a ee[b] [%]	8a yield[c] [%]	9ab ee[b] [%]	9ab yield[c] [%]	Conv[d] [%]	s[e]
0	94	40	62	57	60	14
2	91	43	69	50	57	17
12	96	40	64	58	60	17
21	96	40	64	55	60	17
32	96	41	66	56	59	18
42	96	43	67	52	59	19
56	97	39	66	55	60	20
66	96	43	69	55	58	21
76	96	42	69	50	58	21
84	90	45	74	49	55	20

a) Reaction conditions: *rac*-**8a** (1 eq., 0.2 M in CH_2Cl_2), **7b** (0.6 eq., 0.2 M in CH_2Cl_2), *i*Pr$_2$NEt (0.7 eq., 0.2 M in CH_2Cl_2), **5d** (1.0 g), 0 ºC, 0.1 mL.min^{-1} combined flow, residence time 40 min. b) ee determined by HPLC. c) Isolated yield d) Conversion determined by Kagan's equations. e) Selectivity factors calculated from ee data.

It was highly rewarding to see that **5d** does not show any sign of deterioration after 84 hours operation. This was clearly an indication of potential practical applicability in the continuous preparation of both enantiomers of BINOL. Taking into account that the original preparation of *ent*-**5d**[16a] provided a more highly functionalized resin (f = 0.88 mmol.g^{-1}), we reasoned that the use of this particular resin could lead to an important increase in the productivity of the acylative KR. To test this possibility a new packed bed reactor was prepared with 1.0 g of *ent*-**5d** with f = 0.88 mmol.g^{-1}. Working with this resin under the same experimental conditions of the previous flow process, we could easily determine that a combined flow rate of 0.4 mL.min^{-1} provided a conversion of *ca*. 58% (Table 7). At this rate, the acylative KR of a sample of 12.6 g (38.4 mmol) of *rac*-**8a** could be completed in a 8 hours experiment. This represents an impressive four-fold increase in productivity relative to the use of **5d** with f = 0.37 mmol.g^{-1}, resulting in residence times of *ca.* 10 min. Interestingly, no variation in selectivity or catalytic activity could be detected during the whole experiment.

Table 7. Continuous flow acylative KR of **8a** with isobutyric anhydride (**7b**) catalyzed by *ent*-**5d** (f = 0.88 mmol.g^{-1}).a)

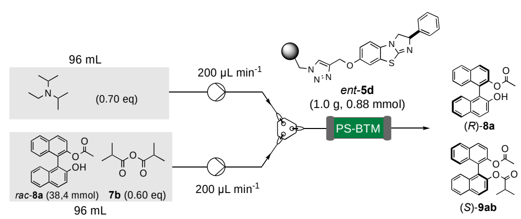

Operation time [h]	8a [%]	ee[b]	9ab [%]	ee[b]	conv c) [%]	s d)
0.5	-90		-66		58	14
1	-92		-67		58	16
2	-93		-68		58	17
3	-93		-68		58	17
4	-93		-68		58	17
5	-93		-67		58	17
6	-92		-68		57	17
7	-93		-67		58	17
8	-93		-68		58	17

a) Reaction conditions: *rac*-**8a** (12.6 g, 1 eq., 0.2 M in CH_2Cl_2), **7b** (0.6 eq., 0.2 M in CH_2Cl_2), *i*Pr$_2$NEt (0.7 eq., 0.2 M in CH_2Cl_2), *ent*-**5d** (1.0 g, 0.88 mmol), 0 ºC, 0.4 mL.min^{-1} combined flow, residence time 10 min. b) ee determined by

HPLC. c) Conversion determined by Kagan's equations. d) Selectivity factors calculated from ee data.

Although the hydrolysis of BINOL mono- and diesters and the enantioenrichment of scalemic BINOL (**6**) by recrystallization are well documented,[19] we wanted to show that both enantiomers of **6** can be easily obtained in highly enantiopure form from either **8a** or **9ab** resulting from the flow process. To this end, representative samples (500 mg) of both compounds, isolated from the effluent of the flow process mediated by **5d** were treated with finely powdered K_2CO_3 (4 eq.) in MeOH for 2 h at room temperature, and the resulting **6** submitted to enantioenrichment by slow crystallization from toluene (Scheme 4). Through this non-optimized process (*S*)-**8a** with 96% ee afforded (*S*)-**6** with 99.2% ee in 75-85% yield. Starting from the diester (*R*)-**9ab** with 67% ee, (*R*)-**6** with 99.6% ee was obtained in 35-41% yield.

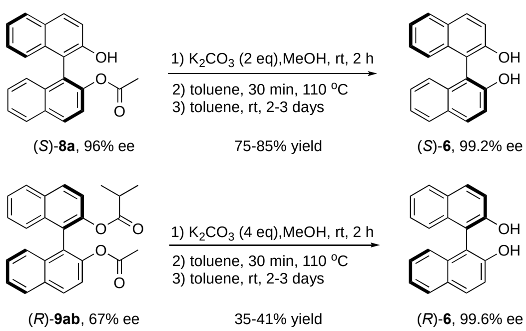

Scheme 4. Recovery of enantiopure BINOL (**6**) from its mono- and diesters.

In summary, the polystyrene-immobilized isothiourea **5d** is a suitable catalyst for the acylative KR of O-acetyl BINOL **8a** and some of its derivatives with isobutyric anhydride **7b**. Working in dichloromethane, the catalyst can used in batch for ten consecutive cycles or in continuous flow for 84 h without showing any decrease in catalytic activity or in selectivity. With the use of a highly functionalized resin (f = 0.88 mmol.g^{-1}), a 58% conversion is achieved with a residence time of 10 min. in a packed bed reactor containing 1 g. of the functional resin. In this manner, a productivity of 5.5 $\text{mmol}_{(R)\text{-}\mathbf{8a}+(S)\text{-}\mathbf{9ab}}\cdot\text{mmol}_{ent\text{-}\mathbf{5d}}^{-1}\cdot\text{h}^{-1}$ can be achieved in a very simple manner. Although some optimization work for the conversion of enantioenriched **8a** and **9ab** into the enantiomers of BINOL (**6**) is still required, the present procedure appears as a most promising alternative for the large-scale preparation of these industrially important materials.

Experimental Section

General procedure for the AKR in batch. To a 5 mL glass vial at 0 °C (ice bath), cat. **5d** (f = 0.37 mmol/g, 135 mg, 5 mol % loading) and 2.5 mL $CHCl_3$, followed by *rac*-**8** (0.5 mmol, 1 eq.), **7b** (47.4 mg, 50 µL, 0.3 mmol, 0.6 eq.) and ^{i}Pr$_2$NEt (45.2 mg, 61 µL, 0.35 mmol, 0.7 eq.), were sequentially added. The reaction mixture was shaken 10 hours. Then, it was filtered and the resin beads were washed with $CHCl_3$ (3 x 1 mL). The solvent was concentrated in vacuo and the product was isolated after purification by column chromatography on silica gel with cyclohexane/ethyl acetate (EtOAc/*c*-Hex = 1:10). In the recycling experiments, the functional resin **5d** was used directly in the next reaction cycle. After each cycle, the organic phase was concentrated under vacuum, and the product was isolated after purification by column chromatography as indicated above.

Continuous flow AKR of rac-8a with isobutyric anhydride 7b using catalyst 5d. Catalyst **5d** (1.0 g, 0.37 mmol), contained in a size-adjustable medium pressure glass column (Omnifit glass column, 10 mm Ø) to create a packed bed reactor, was swollen by pumping CH_2Cl_2 at 0.1 mL. min^{-1} for one hour and a cooling jacket was attached to the reactor to maintain an internal temperature of 0 ºC. Two syringes mounted on a single syringe pump were used to feed the reagents to the flow reactor,one containing a solution of **8a** and isobutyric anhydride (**7b**) in dichloromethane, and the second one a solution of DIPEA in dichloromethane, with concentrations adapted to secure the desired ratio (0.2 M in **8a** in the combined flow). The optimal combined flow rate was initially determined as 0.1 mL.min^{-1} at a reaction temperature of 0 ºC. Then, the preparative experiment was performed under the optimal condition from 250 mL of a 0.4 M solution of *rac*-**8a** (32.8 g, 100 mmol) and **7b** (10.0 mL, 60 mmol) in dichloromethane, and 250 mL of a solution of DIPEA (11.9 mL, 70 mmol) in dichloromethane. The experiment took 84 h to completion, and the measured residence time of the employed setup (visual inspection with a solution of methyl red) was *ca*. 40 min. Data at different operation times have been summarized in Table S3.5 (see Supporting Information). When the solutions of reagents were consumed, CH_2Cl_2 was circulated at 0.1 mL min^{-1} until TLC analysis showed no product in the effluent (ca. 1.5 h). The collected outstream was concentrated under reduced pressure and purified by column chromatography on silica gel with cyclohexane/ethyl acetate (20:1) to yield the corresponding products (*S*)-**8a** and (*R*)-**9ab**.

Acknowledgements

Financial support from CERCA Programme/Generalitat de Catalunya, MINECO (CTQ2015-69136-R) and AGAUR/ Generalitat de Catalunya (2017 SGR 1139) is gratefully acknowledged.

References

[1] For some reviews on the use of BINOL-based, chiral biaryl ligands in asymmetric catalysis, see: a) R. Noyori, H. Takaya, *Acc. Chem. Res.* **1990**, *23*, 345; b) W. Tang, X. Zhang, *Chem. Rev.* **2003**, *103*, 3029; c) Y. Chen, S. Yekta, A. K. Yudin, *Chem. Rev.* **2003**, *103*, 3155; d) Q.-H. Xia, H.-Q. Ge, C.-P. Ye, Z.-M. Liu, K.-X. Su, *Chem. Rev.* **2005**, *105*, 1603; e) M. Shibasaki, S. Matsunaga, *Chem. Soc. Rev.* **2006**, *35*, 269; f) T. Akiyama, J. Itoh, K. Fuchibe, *Adv. Synth. Catal.* **2006**, *348*, 999; g) S. J. Connon, *Angew. Chem. Int. Ed.* **2006**, *45*, 3909; h) J.-H. Xie, Q.-L. Zhou, *Acc. Chem. Res.* **2008**, *41*, 58; i) M. Rueping, A. Kuenkel, I. Atodiresei, *Chem. Soc. Rev.*

2011, *40*, 4539; j) D. Parmar; E. Sugiono; S. Raja; M. Rueping, *Chem. Rev.* **2014**, *114*, 9047; k) R. B. Sunoj, *Acc. Chem. Res.* **2016**, *49*, 1019.

[2] For some recent examples, see: a) S. Narute, R. Pames, F. D. Toste, D. Pappo, *J. Am. Chem. Soc.* **2016**, *138*, 16553; b) H. Y. Kim, S. Takizawa, H. Sasai, K. Oh, *Org. Lett.* **2017**, *19*, 3867; c) J.-M. Tian, A.-F. Wang, J.-S. Yang, X.-J. Zhao, Y.-Q. Tu, S.-Y. Zhang, Z.-M. Chen, *Angew. Chem. Int. Ed.* **2019**, *58*, 11023.

[3] For the catalytic non-enzymatic KR of biaryl compounds, see: a) H. Aoyama, M. Tokunaga, J. Kiyosu, T. Iwasawa, Y. Obora, Y. Tsuji, *J. Am. Chem. Soc.* **2005**, *127*, 10474. For KR with biaryl-derived catalysts, see: b) K. Mori, Y. Ichikawa, M. Kobayashi, Y. Shibata, M. Yamanaka, T. Akiyama, *J. Am. Chem. Soc.* **2013**, *135*, 3964; c) S. Shirakawa, X. Wu, K. Maruoka, *Angew. Chem. Int. Ed.* **2013**, *52*, 14200; d) D.-J. Cheng, L. Yan, S.-K. Tian, M.-Y. Wu, L.-X. Wang, Z.-L. Fan, S.-C. Zheng, X.-Y. Liu, B. Tan, *Angew. Chem. Int. Ed.* **2014**, *53*, 3684; e) S. Arseniyadis, M. Mahesh, P. McDaid, T. Hampel, S. G. Davey, A. C. Spivey, Collect. Czech. *Chem. Commun.* **2011**, *76*, 1239.

[4] H. B. Kagan, J. C. Fiaud, *Top. Stereochem.* **1988**, *18*, 249

[5] G. Ma, J. Deng, M. P. Sibi, *Angew. Chem. Int. Ed.* **2014**, *53*, 11818.

[6] S. Lu, S. B. Poh, Y. Zhao, *Angew. Chem. Int. Ed.* **2014**, *53*, 11041.

[7] For recent work on organocatalysed flow processes, see: a) S. Watanabe, N. Nakaya, J. AkaiKenji, Kanaori, T. Harada, *Org. Lett.* **2018**, *20*, 2737; b) J. Lai, S. Sayalero, A. Ferrali, L. Osorio‐Planes, F. Bravo, C. Rodríguez‐Escrich, M.A. Pericàs, *Adv Synth Catal.* **2018**, *360*, 2914; c) L. Clot-Almenara, C. Rodriguez-Escrich, M.A. Pericàs, *RSC Adv.* **2018**, *8*, 6910; d) C. Rodríguez-Escrich, M.A. Pericàs, *Chem Rec.* **2019**, *19*, 1872; e) A. Ciogli, D. Capitani, N. Di Iorio, S. Crotti, G. Bencivenni, M. Pia Donzello, C. Villani, *Eur. J. Org. Chem.* **2019**, 2020; f) M. G. Russell, C. Veryser, J. F. Hunter, R. L. Beingessner, T. F. Jamison, *Adv. Synth. Catal.* **2019**, https://doi.org/10.1002/adsc.201901185; g) S. B. Ötvös, M. A. Pericàs, C. O. Kappe, *Chem. Sci.* **2019**, 10.1039/C9SC04752.

[8] V. B. Birman, X. Li, *Org. Lett.* **2006**, *8*, 1351–1354.

[9] J. Merad, P. Borkar, T. Bouyon Yenda, C. Roux, J.-M. Pons, J.-L. Parrain, O. Chuzel, C. Bressy, *Org. Lett.* **2015**, *17*, 2118.

[10] X. Yang, V. B. Birman, *Adv. Synth. Catal.* **2009**, *351*, 2301.

[11] S. Qu, M. D. Greenhalgh, A. D. Smith, *Chem. Eur. J.* **2019**, *25*, 2816.

[12] E. Vedejs, M. Jure, *Angew. Chem. Int. Ed.* **2005**, *44*, 3974.

[13] a) V. B. Birman, L. Guo, *Org. Lett.* **2006**, *8*, 4859; b) V. B. Birman, H. Jiang, X. Li, L. Guo, E. W. Uffman, *J. Am. Chem. Soc.* **2006**, *128*, 6536; c) V. B. Birman, H. Jiang, X. Li, *Org. Lett.* **2007**, *9*, 3237.

[14] J. Izquierdo, M. A. Pericàs. *ACS Catal.* **2016**, *6*, 348.

[15] a) S. Wang, J. Izquierdo, C. Rodríguez-Escrich, M. A. Pericàs, *ACS Catal.* **2017**, *7*, 2780; b) S. Wang, C. Rodríguez-Escrich, M. A. Pericàs, *Angew. Chem. Int. Ed.* **2017**, *56*, 15068.

[16] a) R. M. Neyyappadath, R. Chisholm, M. D. Greenhalgh, C. Rodríguez-Escrich, M. A. Pericàs, G. Hähner, A.D. Smith, *ACS Catal.* **2018**, *8*, 1067; b) N. Ranjan Guha, R. M. Neyyappadath, M. D. Greenhalgh, R. Chisholm, S. M. Smith, M. L. McEvoy, C. M. Young, C. Rodríguez-Escrich, M. A. Pericàs, G. Hähner, A. D. Smith, *Green Chem.* **2018**, *20,* 4537.

[17] a) X. Li, H. Jiang, E. X. Uffman, L. Guo, Y. Zhang, X. Yang, V. B. Birman, *J. Org. Chem.* **2012**, *77*, 1722; b) J. Merad, J.-M. Pons, O. Chuzel, C. Bressy, *Eur. J. Org. Chem.* **2016**, 5589.

[18] A. Vidal-Ferran, N. Bampos, A. Moyano, M. A. Pericàs, A. Riera, J. K. M. Sanders, *J. Org. Chem.* **1998**, *63*, 6309.

[19] a) N. Aoyagi, N. Ogawa, T. Izumi, *Tetrahedron Lett.* **2006**, *47*, 4797; b) M. Juárez-Hernandez, D. V. Johnson, H. L. Holland, J. McNulty, A. Capretta, *Tetrahedron: Asymmetry* **2003**, *14*, 289.

Supporting Information

Continuous Flow Preparation of Enantiomerically Pure BINOL(s) by Acylative Kinetic Resolution

Junshan Lai,[a,b] Rifahath M. Neyyappadath,[c] Andrew D. Smith[c] and Miquel A. Pericàs[a,d,*]

mapericas@iciq.es

[a]Institute of Chemical Research of Catalonia (ICIQ), The Barcelona Institute of Science and Technology, Av. Països Catalans, 16, 43007 Tarragona (Spain)
[b]Departament de Química Analítica i Química Orgànica, Universitat Rovira i Virgili, 43007 Tarragona, Spain
[c]EaStCHEM, School of Chemistry, University of St Andrews, North Haugh, St Andrews, KY16 9ST, U.K.
[d]Departament de Química Inorgànica i Orgànica, Universitat de Barcelona (UB), 08028 Barcelona (Spain)

Table of Contents

1. General information

Unless otherwise noted, all reactions were conducted under air. All commercial reagents were used as received; Substituted binaphthols was synthesized according to the reported procedures.[1] $CHCl_3$ were sequentially washed with concentrated sulfuric acid, water, 1N NaOH solution and water, dried with Na_2SO_4, refluxed with $CaCl_2$ and distilled. Flash chromatography was carried out using 60 mesh silica gel and dry-packed columns. Thin layer chromatography was carried out using Merck TLC Silica gel 60 F254 aluminum sheets. Components were visualized by UV light (λ = 254 nm) and stained with phosphomolybdic dip. NMR spectra were recorded at 298 K on a Bruker Avance 400 Ultrashield apparatus. ^{1}H NMR spectroscopy chemical shifts are quoted in ppm relative to tetramethylsilane (TMS). $CDCl_3$ was used as internal standard for ^{13}C NMR spectra. Chemical shifts are given in ppm and coupling constants in Hz. IR spectra were recorded on a Bruker Tensor 27 FT-IR spectrometer and are reported in wavenumbers (cm^{-1}). High performance liquid chromatography (HPLC) was performed on Agilent Technologies chromatographs (1100 and 1200 Series), using Chiralpak AD-H columns and guard columns. FAB mass spectra were obtained on a Fisons V6-Quattro instrument, ESI mass spectra were obtained on a Waters LCT Premier Instrument and CI and EI spectra were obtained on a Waters GCT spectrometer. Specific optical rotation measurements were carried out on a Jasco P-1030 polarimeter.

2. Preparation of the immobilized isothiourea 5d.

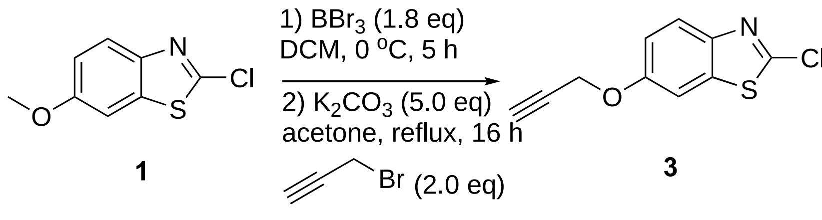

a) Propargyl ether **3**: A solution of the 2-chloro-6-methoxybenzothiazole **1** (2.0 g, 10 mmol) in dry DCM (100 ml) under Argon was cooled to 0 °C with ice bath and BBr_3 (1.0 M in DCM, 18 ml, 18 mmol, 1.8 eq.) was added dropwise. The mixture was stirred for 5 h in the same temperature. Then, the reaction mixture was washed with aq. sat. $NaHCO_3$ (3x20 mL) and dried over Na_2SO_4. Removed the solvent and used in the next step without purification. Acetone (50 mL) was added to the mixture, followed by K_2CO_3 (6.4 g, 50 mmol, 5 eq) and 3-bromopropyne (3.0 g, 20 mmol, 2 eq, 80% w.t. in toluene). The mixture was heated under reflux overnight, then cooled to room temperature and filtered. The solid residue was washed with a small amount of acetone, the filtrates were collected and the solvent was evaporated under reduced pressure. Purification by flash column chromatography (Cyclohexane/EtOAc 98:2) afforded the desired propargyl ether **3** in 93% yield (2.07 g, 9.3 mmol) as a white solid.

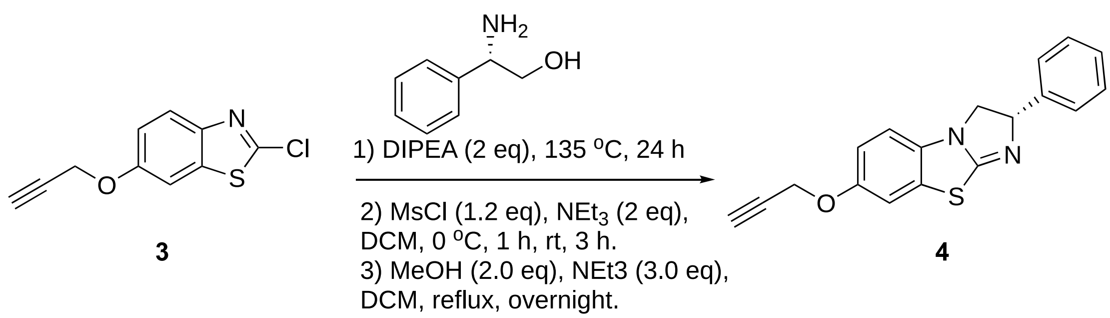

b) Propargyloxy-BTM **4**: Following a modification of a literature procedure[1], a suspension of 2-chloro-6- methoxybenzo[d]thiazole **3** (2.0 g, 9.0 mmol, 1.0 eq.), $^{i}Pr_2NEt$ (3.13 mL, 18 mmol, 2.0 eq.), and (*S*)-phenylglycinol (2.0 g, 10.0 mmol, 1.11 eq.) was heated at 135 °C for 24 h. The orange mixture was allowed to cool to 40 °C, 100 mL of CH_2Cl_2 were then added to the viscous reaction crude, and the mixture was left at room temperature till a solution was formed (around 2-3 hours). The mixture was then cooled to 0 °C in an ice bath under Ar and treated with freshly distilled Et_3N (2.5 mL, 18 mmol, 2 eq.), and methanesulfonyl chloride (0.83 mL, 10.8 mmol, 1.2 eq.) was added dropwise. The mixture was stirred at 0 °C for 1 h and then at to room temp for 3 hours. MeOH (0.7 mL, 2 eq) was then added, and the reaction was heated under reflux overnight. When cold (room temperature), the reaction was quenched with 50 mL of water. Phases were separated, and the aqueous one was extracted with CH_2Cl_2 (2 x 50 mL). The combined organic extracts were dried over Na_2SO_4, filtered, and concentrated to dryness in the rotatory evaporator. The obtained dark-red oil was purified by column chromatography eluting with cyclohexane: EtOAc (10-100 %) to afford **4** as a yellow oil (1.60 g, 58% yield).

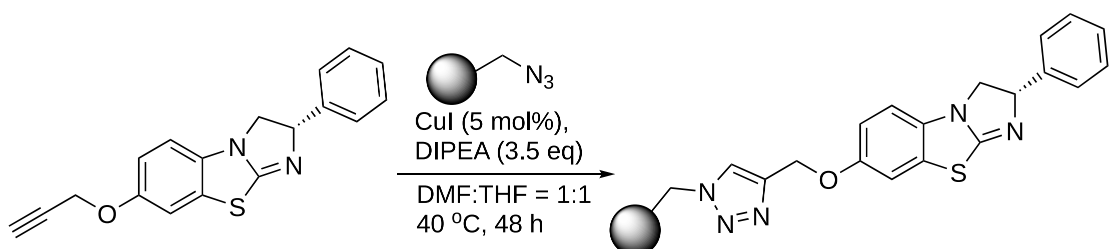

4 **5d**

c) Immobilized catalyst **5d**: To a round bottom flask, azidomethylpolystyrene (7.0 g, 4.13 mmol, f = 0.59 mmol/g, 1 equiv.) suspended in a 1:1 mixture of THF and DMF (60 mL), (S)-2-phenyl-7-(prop-2- yn-1-yloxy)-2,3-dihydrobenzo[d]imidazo[2,1-b]thiazole **4** (1.39 g, 4.54 mmol, 1.1 equiv.), iPr_2NEt (2.4 mL, 14 mmol, 3.5 equiv.) and CuI (38 mg, 0.2 mmol, 5 mol%), were added. The mixture was shaken (orbital stirrer) at 40 °C and the reaction progress was monitored by IR. The reaction mixture was stirred until disappearance of the azide band (~2094 cm^{-1}) was confirmed by IR (*ca*. 48 h). The resin was filtered and washed with water, water/MeOH, MeOH, MeOH/CH_2Cl_2 and CH_2Cl_2. Then, it was dried overnight in a vacuum oven at 40 °C. In this way, 8.0 g of light brown resin **5d** were obtained. Elemental analysis indicated a functionalization of 0.37 mmol/g.

3. Experimental procedures

3.1. Solvent screening for the acylative kinetic resolution of BINOLs

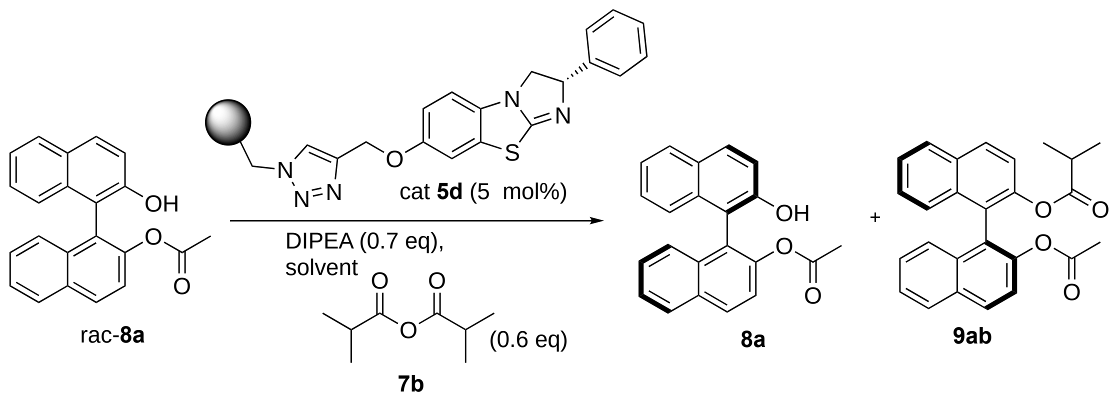

To a 5 mL glass vial, cat. **5d** (*f* = 0.37 mmol/g, 135 mg, 5 mol % loading) and 2.5 mL solvent, followed by **(+/-)8a** (164 mg, 0.5 mmol, 1 eq.), **7b** (47.4 mg, 50 µL, 0.3 mmol, 0.6 eq.) and iPr_2NEt (45.2 mg, 61 µL, 0.35 mmol, 0.7 eq.), were sequentially added at room temperature or the indicated reaction temperature. The reaction mixture was shaken for 10 hours at rt, or 12 hours at 0 °C or 4 h at 60 °C. Then, it was filtered and the resin beads were washed with CH_2Cl_2 (3 x 0.5 mL). The combined organic phases were concentrated under reduced pressure, and the residue was used to measure conversion and ee's for the determination of the selectivity (*s*) of the transformation.

Table S3.1. Solvent screening[a]

entry	solvent	**8a** ee[b] [%]	**9ab** ee[b] [%]	c[c][%]	*s*[d]
1	$CHCl_3$	95	67	58	18
2	**$CHCl_3$ (0 °C)**	**95**	**78**	**55**	**29**
3	$CHCl_3$ (60 °C)	70	47	60	6
4	CH_2Cl_2	90	65	58	14
5	**CH_2Cl_2 (0 °C)**	**92**	**74**	**55**	**21**
6	CH_3CN	26	21	55	2
7	DMF	28	23	55	2
8	toluene	83	61	58	10
9	THF	89	61	59	12
10	dioxane	83	58	59	9
11	Et_2O	77	55	58	8

[a] Reaction conditions: *rac*-**8a** (164 mg, 0.5 mmol, 1 eq.), **7b** (47.4 mg, 50 µL, 0.3 mmol, 0.6 eq.) and $^iPr_2NEt$ (45.2 mg, 61 µL, 0.35 mmol, 0.7 eq.), cat. **5d** (135 mg, 5 mol %, f = 0.37 mmol%), solvent (2.5 mL), rt or indicated temperature. Conversions were determined by Kagan's equations and ee's by HPLC. [b] Reaction time was 4 h.

3.2. Optimization of reaction temperature

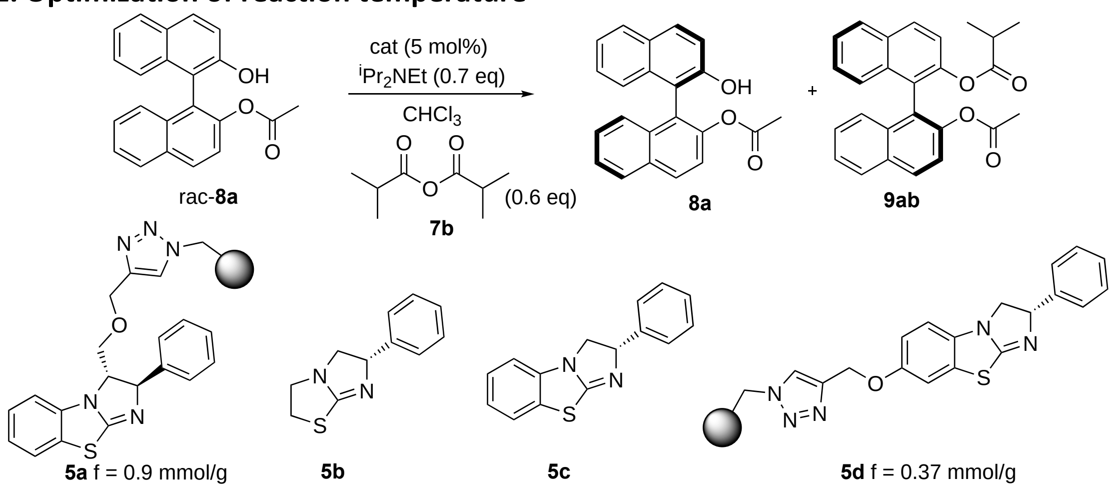

To a 5 mL glass vial were sequentially added the indicated amount of catalyst and 2.5 mL $CHCl_3$, followed by *rac*-**8a** (164 mg, 0.5 mmol, 1 eq.), **7b** (47.4 mg, 50 µL, 0.3 mmol, 0.6 eq.), $^iPr_2NEt$ (45.2 mg, 61 µL, 0.35 mmol, 0.7 eq.) at room temperature or at the indicated reaction temperature. The reaction mixture was shaken (orbital stirrer) for the indicated time. Then, it was filtered and the resin beads were washed with CH_2Cl_2 (3 x 0.5 mL). The combined organic phases were concentrated under reduced pressure, and the residue was used to measure conversion and ee's for the determination of the selectivity (*s*) of the transformation.

Table S3.2. Optimization of reaction temperature[a]

Entry	cat	time (h)	Ee of **8a** (%)	Ee of **9ab**	Conv. (%)	*s*
1	5a	8	-41	-33	57	3
2	5b	8	42	30	58	3
3	5c	8	98	73	57	28
4	5c (0 °C)	8	99	71	58	30
5	5c (-20 °C)	16	98	78	56	36

6	5d	10	95	67	59	18
7	5d (0 °C)	12	95	78	55	29
8	5d (-20 °C)	24	33	61	35	6

[a] Reaction conditions: **(+/-)8a** (164 mg, 0.5 mmol, 1 eq.), **7b** (47.4 mg, 50 μL, 0.3 mmol, 0.6 eq.) and iPr_2NEt (45.2 mg, 61 μL, 0.35 mmol, 0.7 eq.), catalyst, $CHCl_3$ (2.5 mL), rt or indicated temperature. Conversions determined by Kagan's equations. *ee*s were determined by HPLC.

3.3. General procedure for the AKR in batch

To a 5 mL glass vial at 0 °C (ice bath), cat. **5d** (*f* = 0.37 mmol/g, 135 mg, 5 mol % loading) and 2.5 mL $CHCl_3$, followed by *rac*-**8** (0.5 mmol, 1 eq.), **7b** (47.4 mg, 50 μL, 0.3 mmol, 0.6 eq.) and $^iPr_2NEt$ (45.2 mg, 61 μL, 0.35 mmol, 0.7 eq.), were sequentially added. The reaction mixture was shaken 10 hours. Then, it was filtered and the resin beads were washed with $CHCl_3$ (3 x 1 mL). The solvent was concentrated in vacuo and the product was isolated after purification by column chromatography on silica gel with cyclohexane/ethyl acetate (EtOAc/*c*-Hex = 1:10).

3.4. Recycling of 5d in batch ($CHCl_3$)

To a 5 mL glass vial at 0 °C (ice bath), filled with Ar, cat. **5d** (*f* = 0.37 mmol/g, 135 mg, 5 mol % loading) and 2.5 mL $CHCl_3$, followed by rac-**8a** (0.5 mmol, 1 eq.), **7b** (47.4 mg, 50 μL, 0.3 mmol, 0.6 eq.) and $^iPr_2NEt$ (45.2 mg, 61 μL, 0.35 mmol, 0.7 eq.), were sequentially added. The reaction mixture was shaken for the indicated time, the liquid phase was separated and the resin beads were washed with $CHCl_3$ (3 x 0.5 mL) under Ar. After that, the functional resin **5d** was used directly in the next recycle. After each cycle, the organic phase was concentrated under vacuum, and the product was isolated after purification by column chromatography on silicagel eluting with cyclohexane/ethyl acetate (10:1).

Table S3.3. Recycling of 5d in batch (reactions in $CHCl_3$)[a]

run	time (h)	Ee of **8a** (%)	Ee of **9a** (%)	Conv. (%)	*s*
1	10	95	78	55	29
2	10	95	77	55	28

3	10	95	77	55	28
4	10	94	78	55	28
5	10	94	78	55	28
6	14	94	78	55	28
7	14	94	77	55	27
8	14	93	77	55	26
9	14	93	77	55	26
10	14	94	76	55	25

[a] Reaction conditions: *rac*-**8a** (164 mg, 0.5 mmol, 1 eq.), **7b** (50 uL, 0.3 mmol, 0.6 eq.) DIPEA (61 uL, 0.35 mmol, 0.7 eq), PS-cat. **5d** (135 mg, 5 mol %), $CHCl_3$ (2.5 mL), 0 ºC. Conversions were determined by Kagan's equations and ee's by HPLC.

3.5. Recycling of 5d in batch (CH_2Cl_2)

The same procedure described under 3.4 was repeated in CH_2Cl_2. The reaction time was 10 hours in all cases. The results are summarized in Table S3.4.

Table S3.4. Recycling experiments in batch with CH_2Cl_2

run	ee of **8a** (%)	ee of **9a** (%)	conv. (%)	*s*
1	92	74	55	21
2	91	75	55	22
3	92	74	55	21
4	93	73	56	21
5	92	74	55	21
6	92	73	55	20
7	91	73	55	20
8	91	73	55	20
9	91	73	55	20
10	90	73	55	19

[a] Reaction conditions: (+/-)**8a** (164 mg, 0.5 mmol, 1 eq.), **7b** (50 uL, 0.3 mmol, 0.6 eq.) DIPEA (61 uL, 0.35 mmol, 0.7 eq), PS-cat. **5d** (135 mg, 5 mol %), DCM (2.5 mL), 0 ºC, 10 h. Conversions determined by Kagan's equations. ees were determined by HPLC.

3.6. Continuous flow process with catalyst 5d

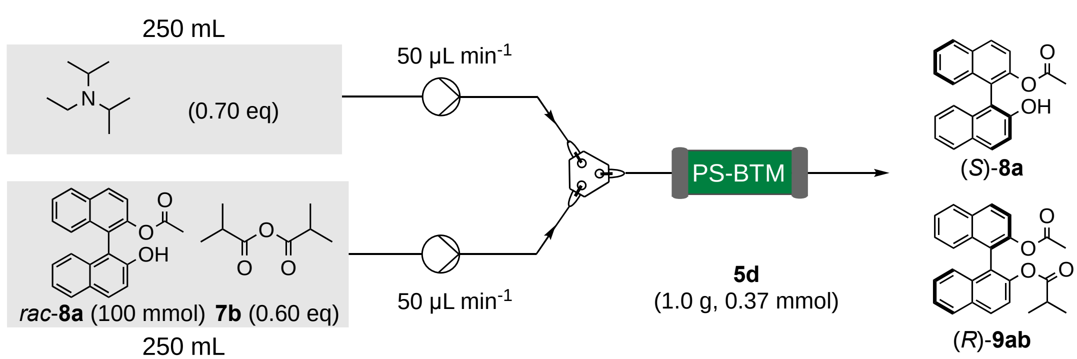

Catalyst **5d** (1.0 g, 0.37 mmol), contained in a size-adjustable medium pressure glass column (Omnifit glass column, 10 mm Ø) to create a packed bed reactor, was swollen by pumping CH_2Cl_2 at 0.1 mL. min^{-1} for one hour and a cooling jacket was attached to maintain an internal temperature of 0 ºC. Two syringes mounted on a single syringe pump were used to feed the reagents to the flow reactor,one containing a solution of **8a** and isobutyric anhydride (**7b**) in dichloromethane, and the second one a solution of DIPEA in dichloromethane, with concentrations adapted to secure the desired ratio (0.2 M in **8a** in the combined flow). The optimal combined flow rate was initially determined as 0.1 mL.min^{-1} at a reaction temperature of 0 ºC. Then, the preparative experiment was performed under the optimal condition from 250 mL of a 0.4 M solution of *rac*-**8a** (32.8 g, 100 mmol) and **7b** (10.0 mL, 60 mmol) in dichloromethane, and 250 mL of a solution of DIPEA (11.9 mL, 70 mmol) in dichloromethane. The experiment took 84 h to completion, and the measured residence time of the employed setup (visual inspection with a solution of methyl red) was *ca*. 40 min. Data at different operation times have been summarized in Table S3.5. When the solutions of reagents were consumed, CH_2Cl_2 was circulated at 0.1 mL min^{-1} until TLC analysis showed no product in the effluent (ca. 1.5 h). The collected outstream was concentrated under reduced pressure and purified by column chromatography on silica gel with cyclohexane/ethyl acetate (20:1) to yield the corresponding product (*S*)-**8a** and (*R*)-**9ab**.

Table S3.5. Preparative scale continuous flow process with catalyst 5d[a]

Operation time [h]	**8a** ee[b] [%]	**8a** yield[c] [%]	**9ab** ee[b] [%]	**9ab** yield[c] [%]	conversion[d] [%]	*s*[e]
0	94	40	62	57	60	14
2	91	43	69	50	57	17
12	96	40	64	58	60	17
21	96	40	64	55	60	17
32	96	41	66	56	59	18
42	96	43	67	52	59	19
56	97	39	66	55	60	20

66	96	43	69	55	58	21
76	96	42	69	50	58	21
84	90	45	74	49	55	20

[a] Reaction conditions: *rac*-**8a** (1 eq., 0.2 M in DCM), **7b** (0.6 eq., 0.2 M in DCM) DIPEA (0.7 eq., 0.2 M in DCM), **5d** (1.0 g), 0 ºC, 0.1 mL.min^{-1} combined flow, residence time 40 min. [b] ee determined by HPLC. [c] Isolated yield [d] Conversion determined by Kagan's equations. [e] Selectivity factors calculated from ee data.

3.7. Continuous flow process with catalyst *ent*-5d

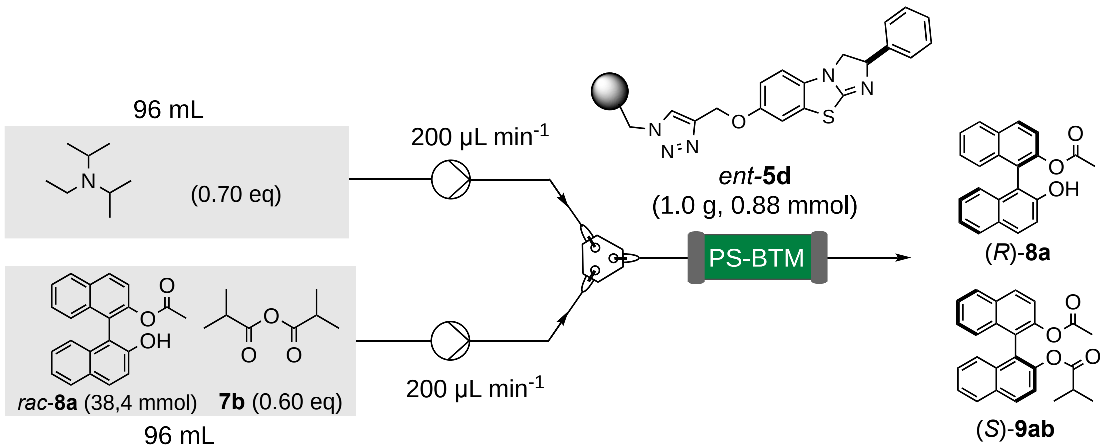

For this experiment, the packed bed reactor (Omnifit glass column, 10 mm Ø) was filled with 1 g (0.88 mmol) of catalyst *ent*-**5d**, which was swollen by pumping CH_2Cl_2 at 0.1 mL min^{-1} for one hour. The column was connected with cooling system and the temperature was set at 0 ºC, and the reagents were then introduced in the system in two separate streams (0.2 mL min^{-1} each) using a dual syringe pump, as in the previous case. The preparative experiment was performed from 96 mL of a 0.4 M solution of *rac*-**8a** (12.6 g, 38.4 mmol) and **7b** (3.85 mL, 23.0 mmol) in dichloromethane, and 96 mL of a solution of DIPEA (4.57 mL, 26.9 mmol) in dichloromethane. The experiment took 8 h to completion, and the measured residence time of the employed setup was *ca*. 10 min. Data at different operation times have been summarized in Table S3.6. When the solutions of reagents were consumed, CH_2Cl_2 was circulated at 0.1 mL min^{-1} until TLC analysis showed no product in the effluent (ca. 1.5 h). The collected outstream was concentrated under reduced pressure and purified by column chromatography on silica gel with cyclohexane/ethyl acetate (20:1) to yield the corresponding product (*R*)-**8a** and (*S*)-**9ab**.

Table S3.6. Preparative scale continuous flow process with catalyst ent-5d[a]

Operation time [h]	**8a** ee[b] [%]	**9ab** ee[b] [%]	conv.[c] [%]	*s*[d]
0.5	-90	-66	58	14
1	-92	-67	58	16
2	-93	-68	58	17
3	-93	-68	58	17
4	-93	-68	58	17
5	-93	-67	58	17
6	-92	-68	57	17
7	-93	-67	58	17
8	-93	-68	58	17

[a] Reaction conditions: *rac*-**8a** (12.6 g, 1 eq., 0.2 M in DCM), **7b** (0.6 eq., 0.2 M in DCM) DIPEA (0.7 eq., 0.2 M in DCM), *ent*-**5d** (1.0 g, 0.88 mmol), 0 °C, 0.4 mL.min^{-1} combined flow, residence time 10 min. [b] ee determined by HPLC. [c] Conversion determined by Kagan's equations. [d] Selectivity factors calculated from ee data.

3.8. Recovery of enantiopure BINOL (6) from its mono- and diesters

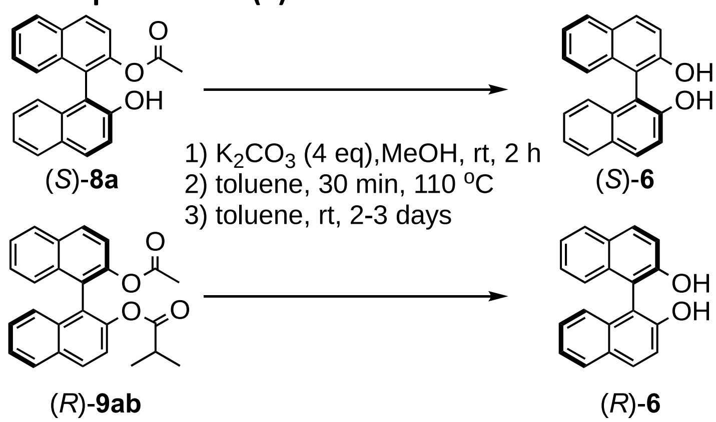

To a 10 mL round-bottom flask, 5 mL MeOH, enantioentiched (*R*)-**9ab** (500 mg, 1.19 mmol, 1 eq; 68% ee), finely powdered K_2CO_3 powder (657 mg, 4.76 mmol, 4 eq). [**Important**: for this procedure, it is necessary to grind K_2CO_3 into a fine powder; otherwise, saponification will not work or will take a much longer time] were sequentially added. The reaction mixture was stirred at rt until TLC analysis showed complete consumption of the starting diester (ca.

2 hours). The mixture was then diluted with ethyl acetate (20 mL) and sequentially washed with 1 N HCl (2 x 20 mL) and water (20 mL). The ethyl acetate phase was then dried with $MgSO_4$ and the solvent removed under vacuum. The crude product was dissolved in the minimal amount of toluene at 110 °C, to make sure that the solution was oversaturated. The heating bath was then removed, and the solution was kept at room temperature overnight. At this point a quasi-racemic (11-23% ee) BINOL precipitate was separated by filtration, and the resulting solution showed a 89-91% ee. This solution was left in an uncapped flask at room temperature for 2 to 3 days, when abundant crystallization of (*R*)-**6** took place. This crystalline material was separated by filtration and washed with a small amount of cold toluene to give 120-140 mg (35% to 41% yield) of (*R*)-**6** with >99.6% ee.

By following an analogous procedure from the same amount of (*S*)-**8a** with 96% ee, the enantiomeric diol (*S*)-**6** with 99.2% enantiomeric excess was obtained in 75-85% yield.

4. Compound characterization data

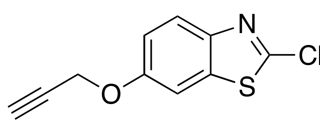

2-chloro-6-(prop-2-yn-1-yloxy)benzo[*d*]thiazole (3)

2.07 g, 93% yield. Colourless solid. m. p. 60–61 °C.

^{1}H NMR (400 MHz, Chloroform-*d*) δ 7.81 (d, *J* = 9.0 Hz, 1H), 7.30 (d, *J* = 2.6 Hz, 1H), 7.11 (dd, *J* = 9.0, 2.6 Hz, 1H), 4.73 (d, *J* = 2.5 Hz, 2H), 2.57 (t, *J* = 2.4 Hz, 1H) ppm.

^{13}C NMR (101 MHz, $CDCl_3$) δ 155.7, 150.5, 145.8, 137.0, 123.3, 116.12, 105.4, 77.9, 76.1, 56.3 ppm.

IR (neat): 3300, 3279, 3228, 2928, 2114, 1601, 1557, 1486, 1453, 1383, 1257, 1226, 1200, 1014, 826, 808, 676 cm^{-1}.

HRMS (ESI): m/z: $[M+H]^+$ ($C_{10}H_7ClNOS$), calcd.: 223.9931; found: 223.9923.

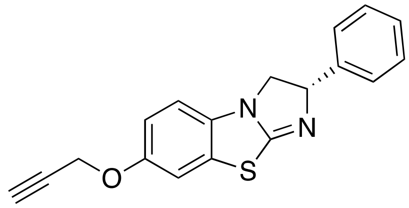

(*S*)-2-phenyl-7-(prop-2-yn-1-yloxy)-2,3-dihydrobenzo[*d*]imidazo[2,1-b]thiazole (4)

1.60 g, 58% yield. Light yellow oil.

^{1}H NMR (400 MHz, Chloroform-*d*) δ 7.37 – 7.33 (m, 4H), 7.29 – 7.24 (m, 1H), 6.99 (d, *J* = 2.5 Hz, 1H), 6.81 (dd, *J* = 8.6, 2.5 Hz, 1H), 6.56 (d, *J* = 8.5 Hz, 1H), 5.62 (dd, *J* = 10.2, 8.3 Hz, 1H), 4.62 (d, *J* = 2.4 Hz, 2H), 4.26 – 4.15 (m, 1H), 3.63 (t, *J* = 8.5 Hz, 1H), 2.52 (t, *J* = 2.4 Hz, 1H) ppm.

^{13}C NMR (101 MHz, $CDCl_3$) δ 166.8, 152.6, 142.8, 132.0 (x2), 128.5, 128.2, 127.4, 126.4 (x2), 113.5, 111.1, 108.5, 78.3, 75.7, 75.2, 56.8, 52.8 ppm.

IR (neat): 3285, 3060, 3030, 2929, 2871, 2117, 1760, 1697, 1596, 1569, 1485, 1364, 1191, 1024, 697 cm^{-1}.

HRMS (ESI): m/z: $[M-H]^+$ ($C_{18}H_{13}N_2OS$), calcd.: 305.0749; found: 305.0739.

$[\alpha]_D^{25}$ = -81.4 (*c* = 0.1, CH_2Cl_2).

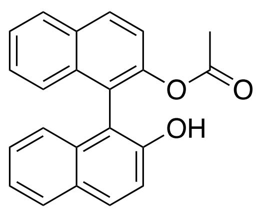

(*S*)-2'-hydroxy-[1,1'-binaphthalen]-2-yl acetate (8a)

69 mg, 42% yield. Colourless oil.

^{1}H NMR (400 MHz, Chloroform-*d*) δ 8.02 (d, *J* = 8.9 Hz, 1H), 7.96 – 7.79 (m, 3H), 7.46 (ddd, *J* = 8.1, 6.6, 1.4 Hz, 1H), 7.37 (d, *J* = 8.9 Hz, 1H), 7.34 – 7.18 (m, 5H), 7.03 (dt, *J* = 8.4, 1.1 Hz, 1H), 1.82 (s, 3H) ppm.[2]

$[\alpha]_D^{25}$ = -10.3 (*c* = 0.1, CH_2Cl_2).

HPLC (Daicel Chiralpak AD-H, hexane/^{i}PrOH = 90:10, flow rate 1.0 mL/min, λ = 210 nm): major isomer: t_R = 12.9 min; minor isomer: t_R = 15.1 min.

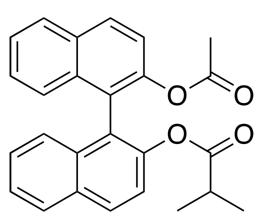

(*R*)-2'-acetoxy-[1,1'-binaphthalen]-2-yl isobutyrate (9ab)

101 mg, 51% yield. Colourless oil.

^{1}H NMR (400 MHz, Chloroform-*d*) δ 7.97 (t, *J* = 7.9 Hz, 2H), 7.90 (t, *J* = 7.7 Hz, 2H), 7.48 – 7.36 (m, 4H), 7.32 – 7.18 (m, 4H), 2.45 – 2.25 (m, 1H), 1.78 (s, 3H), 0.75 (d, *J* = 6.7 Hz, 3H), 0.67 (d, *J* = 6.9 Hz, 3H) ppm.

^{13}C NMR (101 MHz, $CDCl_3$) δ 175.1, 169.1, 146.7 (x2), 133.3 (x2), 131.5, 131.4, 129.4, 129.3, 127.9 (x2), 126.7, 126.6, 126.1 (x2), 125.6 (x2), 123.5 (x2), 121.9, 121.8, 33.74, 20.5, 18.1 (x2) ppm.

IR (neat): 3059, 2974, 2935, 2875, 1752, 1508, 1469, 1365, 1185, 1091, 807, 756 cm^{-1}.

HRMS (ESI): m/z: $[M+Na]^+$ ($C_{26}H_{22}NaO_4$), calcd.: 421.1416; found: 421.1410.

$[\alpha]_D^{25}$ = –8.2 (*c* = 0.1, CH_2Cl_2).

HPLC (Daicel Chiralpak AD-H, hexane/^{i}PrOH = 90:10, flow rate 1.0 mL/min, λ = 210 nm): major isomer: t_R = 6.9 min; minor isomer: t_R = 11.4 min.

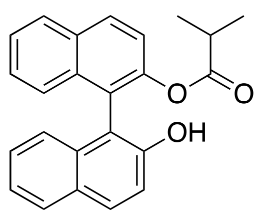

(*S*)-2'-hydroxy-[1,1'-binaphthalen]-2-yl isobutyrate (8b)

75 mg, 42% yield. Colourless solid. m. p. 147–148 °C.

^{1}H NMR (300 MHz, Chloroform-*d*) δ 8.07 (d, *J* = 8.9 Hz, 1H), 7.97 (d, *J* = 8.1 Hz, 1H), 7.86 (dd, *J* = 17.0, 8.4 Hz, 2H), 7.50 (ddd, *J* = 8.2, 6.2, 1.9 Hz, 1H), 7.43 – 7.19 (m, 6H), 7.05 (d, *J* = 8.2 Hz, 1H), 5.15 (s, 1H), 2.38 (p, *J* = 7.0 Hz, 1H), 0.77 (d, *J* = 7.0 Hz, 3H), 0.60 (d, *J* = 7.0 Hz, 3H) ppm.[3]

$[\alpha]_D^{25}$ = –15.3 (*c* = 0.1, CH_2Cl_2).

HPLC (Daicel Chiralpak AD-H, hexane/^{i}PrOH = 90:10, flow rate 1.0 mL/min, λ = 210 nm): major isomer: t_R = 9.8 min; minor isomer: t_R = 11.8 min.

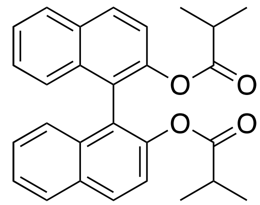

(*R*)- [1,1'-binaphthalene]-2,2'-diyl bis(2-methylpropanoate) (9bb)

109 mg, 51% yield. Colourless solid. m. p. 66–68 °C.

^{1}H NMR (400 MHz, Chloroform-*d*) δ 8.02 – 7.94 (m, 2H), 7.91 (dt, *J* = 8.3, 1.1 Hz, 2H), 7.51 – 7.37 (m, 4H), 7.34 – 7.24 (m, 4H), 2.32 (p, *J* = 7.0 Hz, 2H), 0.71 (d, *J* = 7.0 Hz, 6H), 0.62 (d, *J* = 7.0 Hz, 6H) ppm.[4]

$[\alpha]_D^{25}$ = +41.6 (*c* = 0.1, CH_2Cl_2).

HPLC (Daicel Chiralpak AD-H, hexane/^{i}PrOH = 90:10, flow rate 1.0 mL/min, λ = 210 nm): major isomer: t_R = 5.1 min; minor isomer: t_R = 9.2 min.

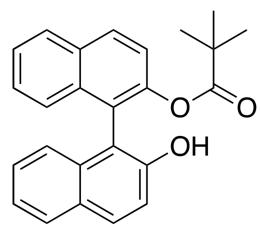

(*S*)-2'-hydroxy-[1,1'-binaphthalen]-2-yl pivalate (8c)

74 mg, 40% yield. Colourless solid. m. p. 108–110 °C.

^{1}H NMR (400 MHz, Chloroform-*d*) δ 8.07 (d, *J* = 8.8 Hz, 1H), 7.97 (d, *J* = 8.3 Hz, 1H), 7.92 – 7.77 (m, 2H), 7.50 (ddd, *J* = 8.1, 5.9, 2.1 Hz, 1H), 7.42 – 7.20 (m, 6H), 7.06 (d, *J* = 8.4 Hz, 1H), 5.14 (s, 1H), 0.78 (s, 9H) ppm.[5]

$[\alpha]_D^{25}$ = +60.3 (*c* = 0.1, CH_2Cl_2).

HPLC (Daicel Chiralpak AD-H, hexane/^{i}PrOH = 90:10, flow rate 1.0 mL/min, λ = 210 nm): major isomer: t_R = 7.1 min; minor isomer: t_R = 10.6 min.

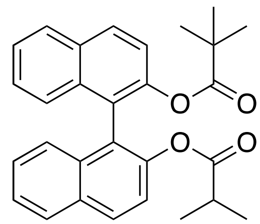

(*R*)-2'-(isobutyryloxy)-[1,1'-binaphthalen]-2-yl pivalate (9cb)

119 mg, 54% yield. Colourless oil.

^{1}H NMR (400 MHz, Chloroform-*d*) δ 7.97 (dd, *J* = 8.9, 2.1 Hz, 2H), 7.91 (ddt, *J* = 8.3, 2.1, 1.0 Hz, 2H), 7.48 – 7.37 (m, 4H), 7.30 (ddd, *J* = 5.7, 2.5, 1.1 Hz, 4H), 2.31 (p, *J* = 7.0 Hz, 1H), 0.74 (s, 9H), 0.69 (d, *J* = 7.0 Hz, 3H), 0.61 (d, *J* = 7.0 Hz, 3H) ppm.

^{13}C NMR (101 MHz, $CDCl_3$) δ 176.4, 174.9, 146.9, 146.8, 133.4 (x2), 131.5, 131.4, 129.2 (x2), 127.9, 127.8, 126.6, 126.1, 126.0, 125.6 (x2), 123.7, 123.6, 121.9 (x2), 38.6, 33.8, 26.3 (x3), 18.1, 18.0 ppm.

IR (neat): 3063, 2975, 2930, 1757, 1737, 1509, 1450, 1368, 1262, 1185, 1059, 876, 807, 704 cm^{-1}.

HRMS (ESI): m/z: $[M+Na]^+$ ($C_{29}H_{28}NaO_4$), calcd.: 463.1880; found: 463.1884.

$[\alpha]_D^{25}$ = –1.5 (*c* = 0.1, CH_2Cl_2).

HPLC (Daicel Chiralpak AD-H, hexane/^{i}PrOH = 90:10, flow rate 1.0 mL/min, λ = 210 nm): major isomer: t_R = 4.5 min; minor isomer: t_R = 8.8 min.

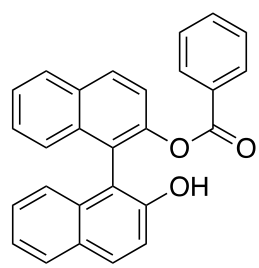

(*S*)-2'-hydroxy-[1,1'-binaphthalen]-2-yl benzoate (8d)

74 mg, 38% yield. Colourless solid. m. p. 180–181 °C.

^{1}H NMR (400 MHz, Chloroform-*d*) δ 8.11 (d, *J* = 8.9 Hz, 1H), 7.99 (dt, *J* = 8.3, 1.0 Hz, 1H), 7.82 – 7.74 (m, 2H), 7.70 – 7.61 (m, 2H), 7.57 – 7.48 (m, 2H), 7.42 (d, *J* = 7.4 Hz, 1H), 7.39 – 7.20 (m, 7H), 7.15 (dd, *J* = 8.3, 1.5 Hz, 1H), 5.33 (s, 1H) ppm.[6]

$[\alpha]_D^{25}$ = -114.4 (*c* = 0.1, CH_2Cl_2).

HPLC (Daicel Chiralpak AD-H, hexane/^{i}PrOH = 90:10, flow rate 1.0 mL/min, λ = 210 nm): major isomer: t_R = 9.6 min; minor isomer: t_R = 15.1 min.

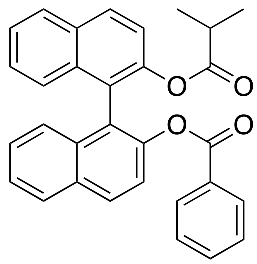

(*R*)-2'-(isobutyryloxy)-[1,1'-binaphthalen]-2-yl benzoate (9db)

131 mg, 57% yield. Colourless oil.

^{1}H NMR (400 MHz, Chloroform-*d*) δ 8.02 (d, *J* = 8.9 Hz, 1H), 7.97 – 7.77 (m, 3H), 7.68 – 7.53 (m, 3H), 7.50 – 7.25 (m, 8H), 7.20 (t, *J* = 7.8 Hz, 2H), 2.35 (dt, *J* = 14.0, 6.9 Hz, 1H), 0.68 (dd, *J* = 26.9, 7.0 Hz, 6H) ppm.

^{13}C NMR (101 MHz, $CDCl_3$) δ 175.0, 164.6, 146.9, 146.8, 133.3 (x2), 133.1, 131.5 (x2), 129.7 (x2), 129.4, 129.3, 129.2, 128.1 (x2), 127.9 (x2), 126.7 (x2), 126.1, 126.0, 125.7, 125.5, 123.6, 123.5, 121.8 (x2), 33.7, 18.1 (x2) ppm.

IR (neat): 3079, 2976, 2934, 1760, 1587, 1490, 1466, 1366, 1317, 1191, 1082, 1011, 986, 937, 883, 826 cm^{-1}.

HRMS (ESI): m/z: $[M+Na]^+$ ($C_{31}H_{24}NaO_4$), calcd.: 483.1572; found: 483.1567.

$[\alpha]_D^{25}$ = +38.5 (*c* = 0.1, CH_2Cl_2).

HPLC (Daicel Chiralpak AD-H, hexane/^{i}PrOH = 80:20, flow rate 1.0 mL/min, λ = 210 nm): major isomer: t_R = 6.7 min; minor isomer: t_R = 13.0 min.

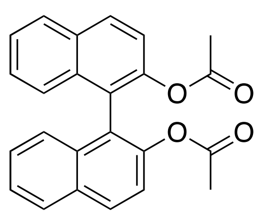

(*R*)- [1,1'-binaphthalene]-2,2'-diyl diacetate (9aa)

102 mg, 55% yield. Colourless solid. m. p. 112–114 °C.

^{1}H NMR (400 MHz, Chloroform-*d*) δ 8.03 – 7.97 (m, 2H), 7.96 – 7.89 (m, 2H), 7.51 – 7.39 (m, 4H), 7.31 – 7.24 (m, 2H), 7.23 – 7.13 (m, 2H), 1.85 (s, 6H) ppm.[7]

$[\alpha]_D^{25}$ = +4.2 (c = 0.1, CH_2Cl_2).

HPLC (Daicel Chiralpak AD-H, hexane/^{i}PrOH = 90:10, flow rate 1.0 mL/min, λ = 210 nm): major isomer: t_R = 9.7 min; minor isomer: t_R = 11.0 min.

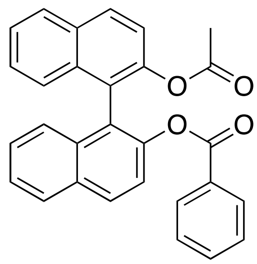

(*R*)-2'-acetoxy-[1,1'-binaphthalen]-2-yl benzoate (9ad)

106 mg, 49% yield. Colourless oil.

^{1}H NMR (400 MHz, Chloroform-*d*) δ 8.04 (d, *J* = 8.9 Hz, 1H), 7.98 – 7.83 (m, 3H), 7.68 – 7.57 (m, 3H), 7.50 – 7.18 (m, 10H), 1.81 (s, 3H) ppm.

^{13}C NMR (101 MHz, $CDCl_3$) δ 169.1, 164.8, 146.8 (x2), 133.3, 133.1, 131.5, 129.8 (x2), 129.5 (x2), 129.2 (x2), 128.2 (x2), 128.0 (x2), 127.9 (x2), 126.7(x2), 126.2, 126.1, 125.7, 125.6, 123.6, 121.8, 121.7, 20.5 ppm.

IR (neat): 3063, 2975, 2930, 1757, 1737, 1509, 1450, 1368, 1262, 1185, 1059, 876, 807, 704 cm^{-1}.

HRMS (ESI): m/z: $[M+Na]^+$ ($C_{29}H_{20}NaO_4$), calcd.: 455.1259; found: 455.1254.

$[\alpha]_D^{25}$ = –4.6 (c = 0.1, CH_2Cl_2).

HPLC (Daicel Chiralpak AD-H, hexane/^{i}PrOH = 80:20, flow rate 1.0 mL/min, λ = 210 nm): major isomer: t_R = 10.7 min; minor isomer: t_R = 19.0 min.

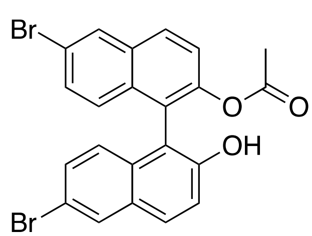

(*S*)-6,6'-dibromo-2'-hydroxy-[1,1'-binaphthalen]-2-yl acetate (8e)

97 mg, 40% yield. Colourless solid. m. p. 161–163 °C.

^{1}H NMR (400 MHz, Chloroform-*d*) δ 8.08 (d, *J* = 2.0 Hz, 1H), 7.97 (d, *J* = 2.1 Hz, 1H), 7.91 (d, *J* = 8.9 Hz, 1H), 7.76 (d, *J* = 9.0 Hz, 1H), 7.36 (dd, *J* = 8.9, 2.0 Hz, 2H), 7.27 (dd, *J* = 9.0, 1.6 Hz, 2H), 7.06 (d, *J* = 9.0 Hz, 1H), 6.85 (d, *J* = 9.0 Hz, 1H), 5.39 (s, 1H), 1.83 (s, 3H) ppm.[9]

$[\alpha]_D^{25}$ = +75.3 (*c* = 0.1, CH_2Cl_2).

HPLC (Daicel Chiralpak AD-H, hexane/^{i}PrOH = 80:20, flow rate 1.0 mL/min, λ = 210 nm): major isomer: t_R = 8.6 min; minor isomer: t_R = 10.5 min.

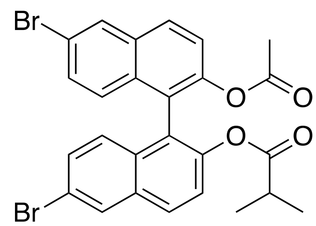

(*R*)-2'-acetoxy-6,6'-dibromo-[1,1'-binaphthalen]-2-yl isobutyrate (9eb)

130 mg, 47% yield. Colourless solid. m. p. 155–155 °C.

^{1}H NMR (400 MHz, Chloroform-*d*) δ 8.08 (dd, *J* = 5.1, 2.2 Hz, 2H), 7.89 (dd, *J* = 8.9, 5.6 Hz, 2H), 7.53 – 7.29 (m, 4H), 7.05 (t, *J* = 9.6 Hz, 2H), 2.37 (qd, *J* = 7.1, 4.7 Hz, 1H), 1.83 (s, 3H), 0.75 (dd, *J* = 24.4, 6.9 Hz, 6H) ppm.

^{13}C NMR (101 MHz, $CDCl_3$) δ 174.9, 168.8, 147.0 (x2), 132.5, 131.7, 131.6, 130.2 (x2), 130.0 (x2), 129.9 (x2), 128.7 (x2), 127.7, 127.6, 123.3, 123.2, 123.1, 123.0, 120.0, 33.7, 20.5, 18.2 (x2). ppm

IR (neat): 3079, 2976, 2934, 1760, 1587, 1490, 1466, 1366, 1317, 1191, 1082, 1011, 986, 937, 883, 826 cm^{-1}.

HRMS (ESI): m/z: $[M+Na]^+$ ($C_{26}H_{20}BrNaO_4$), calcd.: 576.9621; found: 576.9619.

$[\alpha]_D^{25}$ = +6.2 (*c* = 0.1, CH_2Cl_2).

HPLC (Daicel Chiralpak AD-H, hexane/^{i}PrOH = 80:20, flow rate 1.0 mL/min, λ = 210 nm): major isomer: t_R = 6.3 min; minor isomer: t_R = 11.6 min.

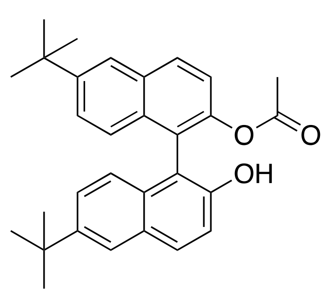

(*S*)-6,6'-di-tert-butyl-2'-hydroxy-[1,1'-binaphthalen]-2-yl acetate (8f)

99 mg, 45% yield. Colourless solid. m. p. 206-208 °C.

^{1}H NMR (400 MHz, Chloroform-*d*) δ 8.02 (d, *J* = 8.9 Hz, 1H), 7.91 – 7.73 (m, 3H), 7.45 – 7.16 (m, 5H), 6.99 (d, *J* = 8.9 Hz, 1H), 5.17 (s, 1H), 1.87 (s, 3H), 1.38 (s, 18H) ppm.

^{13}C NMR (101 MHz, $CDCl_3$) δ 170.6, 151.3, 149.0, 147.5, 146.0, 132.2, 131.7, 131.6 (x2), 130.2, 128.8, 126.4, 125.5 (x2), 124.3, 123.3, 123.0, 122.9, 121.5, 118.0, 113.9, 34.8, 34.5, 31.2 (x3), 31.1 (x3), 20.5 ppm.

IR (neat): 3494, 3068, 2958, 2904, 2868, 1749, 1597, 1502, 1463, 1364, 1263, 1199, 1067, 1014, 945, 885, 825 cm^{-1}.

HRMS (ESI): m/z: $[M-H]^+$ ($C_{30}H_{31}O_3$), calcd.: 438.2279; found: 439.2270.

$[\alpha]_D^{25}$ = 56.5 (*c* = 0.1, CH_2Cl_2).

HPLC (Daicel Chiralpak AD-H, hexane/^{i}PrOH = 90:10, flow rate 1.0 mL/min, λ = 210 nm): major isomer: t_R = 4.7 min; minor isomer: t_R = 9.4 min.

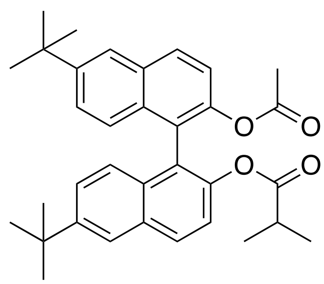

(*R*)-2'-acetoxy-6,6'-di-tert-butyl-[1,1'-binaphthalen]-2-yl isobutyrate (8fb)

105 mg, 41% yield. Colourless solid. m. p. 82–84 °C.

^{1}H NMR (400 MHz, Chloroform-*d*) δ 7.93 (t, *J* = 8.4 Hz, 2H), 7.83 (dd, *J* = 9.9, 1.9 Hz, 2H), 7.37 (t, *J* = 7.9 Hz, 4H), 7.18 (ddd, *J* = 15.1, 8.8, 1.2 Hz, 2H), 2.34 (td, *J* = 7.0, 1.1 Hz, 1H), 1.80 (s, 3H), 1.38 (d, *J* = 4.3 Hz, 18H), 0.76 (d, *J* = 7.0 Hz, 3H), 0.67 (d, *J* = 7.0 Hz, 3H) ppm.

^{13}C NMR (101 MHz, $CDCl_3$) δ 175.2, 169.2, 148.3, 148.2, 146.2 (x2), 131.5 (x2), 131.5, 131.4, 129.2, 129.1, 125.9, 125.8, 125.5 (x2), 123.2 (x2), 122.9, 122.8, 121.8, 121.6, 34.7 (x2), 33.7, 31.2 (x6), 20.6, 18.2, 18.1 ppm.

IR (neat): 2962, 2906, 2871, 1754, 1596, 1500, 1364, 1263, 1191, 1123, 1093, 1014, 887, 826, 731 cm^{-1}.

HRMS (ESI): m/z: $[M+Na]^+$ ($C_{34}H_{38}NaO_4$), calcd.: 533.2668; found: 533.2657.

$[\alpha]_D^{25}$ = -76.0 (*c* = 0.1, CH_2Cl_2).

HPLC (Daicel Chiralpak AD-H, hexane/^{i}PrOH = 90:10, flow rate 1.0 mL/min, λ = 210 nm): major isomer: t_R = 7.6 min; minor isomer: t_R = 10.7 min.

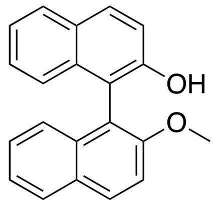

(*S*)-2'-methoxy-[1,1'-binaphthalen]-2-ol (8g)

83 mg, 46% yield. Colourless solid. m. p. 152–154 °C.

^{1}H NMR (400 MHz, Chloroform-*d*) δ 7.99 (d, *J* = 9.1 Hz, 1H), 7.85 (q, *J* = 8.8 Hz, 3H), 7.42 (d, *J* = 9.1 Hz, 1H), 7.37 – 7.12 (m, 6H), 7.10 – 6.97 (m, 1H), 4.94 (s, 1H), 3.74 (s, 3H) ppm.[7]

$[\alpha]_D^{25}$ = +43.2 (*c* = 0.1, CH_2Cl_2).

HPLC (Daicel Chiralpak AD-H, hexane/^{i}PrOH = 90:10, flow rate 1.0 mL/min, λ = 210 nm): major isomer: t_R = 13.5 min; minor isomer: t_R = 19.2 min.

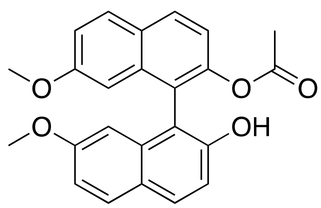

(*S*)-2'-hydroxy-7,7'-dimethoxy-[1,1'-binaphthalen]-2-yl acetate (8h)

74 mg, 38% yield. Light yellow oil.

^{1}H NMR (400 MHz, Chloroform-*d*) δ 7.90 (d, *J* = 8.8 Hz, 1H), 7.84 – 7.65 (m, 3H), 7.27 – 7.06 (m, 3H), 6.96 (dd, *J* = 8.9, 2.5 Hz, 1H), 6.58 (t, *J* = 2.7 Hz, 1H), 6.39 (t, *J* = 3.1 Hz, 1H), 5.28 (s, 1H), 3.50 (d, *J* = 5.5 Hz, 6H), 1.79 (s, 3H) ppm.

^{13}C NMR (101 MHz, $CDCl_3$) δ 170.2, 158.8, 158.3, 152.1, 148.6, 134.8, 134.7, 130.2, 130.0, 129.8, 129.4, 127.6, 124.3, 121.8, 119.2, 118.6, 115.5, 115.4, 113.2, 104.0, 103.5, 55.0, 54.9, 20.3 ppm.

IR (neat): 3438, 3060, 3002, 2937, 2833, 1755, 1619, 1509, 1459, 1423, 1367, 1271, 1193, 1136, 1017, 902, 831, 729 cm^{-1}.

HRMS (ESI): m/z: $[M-H]^+$ ($C_{24}H_{19}O_5$), calcd.: 387,1232; found: 387.1238.

$[\alpha]_D^{25}$ = +97.8 (*c* = 0.1, CH_2Cl_2).

HPLC (Daicel Chiralpak AD-H, hexane/^{i}PrOH = 60:40, flow rate 1.0 mL/min, λ = 210 nm): major isomer: t_R = 8.0 min; minor isomer: t_R = 8.7 min.

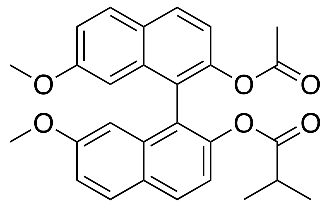

(*R*)-2'-acetoxy-7,7'-dimethoxy-[1,1'-binaphthalen]-2-yl isobutyrate (9hb)

126 mg, 55% yield. Yellow oil.

^{1}H NMR (400 MHz, Chloroform-*d*) δ 7.88 (dd, *J* = 8.8, 6.9 Hz, 2H), 7.80 (dd, *J* = 8.9, 7.6 Hz, 2H), 7.25 (dd, *J* = 8.8, 6.0 Hz, 2H), 7.11 (ddd, *J* = 8.9, 5.0, 2.5 Hz, 2H), 6.61 (dd, *J* = 9.5, 2.5 Hz, 2H), 3.55 (d, *J* = 1.2 Hz, 6H), 2.31 (hept, *J* = 7.0 Hz, 1H), 1.74 (s, 3H), 0.74 (d, *J* = 6.9 Hz, 3H), 0.58 (d, *J* = 7.0 Hz, 3H) ppm.

^{13}C NMR (101 MHz, $CDCl_3$) δ 175.1, 169.2, 158.2, 158.2, 147.3, 147.2, 134.7, 134.6, 129.5, 129.4, 129.0 (x2), 127.0, 126.9, 122.5 (x2), 119.5, 119.4, 118.5, 118.4, 104.4, 104.3, 55.1 (x2), 33.8, 20.6, 18.1, 18.0 ppm.

IR (neat): 2972, 2938, 2834, 1752, 1622, 1508, 1459, 1420, 1383, 1366, 1177, 1135, 1017, 959, 899, 833, 731 cm^{-1}.

HRMS (ESI): m/z: $[M+H]^+$ ($C_{28}H_{27}O_6$), calcd.: 459.1808; found: 459.1809.

$[\alpha]_D^{25}$ = -12.2 (*c* = 0.1, CH_2Cl_2).

HPLC (Daicel Chiralpak AD-H, hexane/^{i}PrOH = 60:40, flow rate 1.0 mL/min, λ = 210 nm): major isomer: t_R = 4.3 min; minor isomer: t_R = 15.2 min.

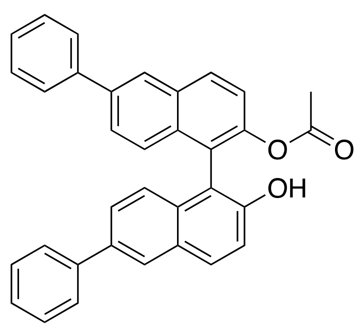

(*S*)-2'-hydroxy-6,6'-diphenyl-[1,1'-binaphthalen]-2-yl acetate (8i)

89 mg, 37% yield. Colourless solid. m. p. 96–98 °C.

^{1}H NMR (400 MHz, Chloroform-*d*) δ 8.11 (d, *J* = 1.8 Hz, 1H), 8.04 (dd, *J* = 5.4, 3.5 Hz, 2H), 7.91 (d, *J* = 8.9 Hz, 1H), 7.62 (d, *J* = 8.3 Hz, 4H), 7.57 – 7.52 (m, 1H), 7.49 (dd, *J* = 8.8, 1.9 Hz, 1H), 7.41 – 7.27 (m, 9H), 7.14 (d, *J* = 8.8 Hz, 1H), 5.39 (s, 1H), 1.83 (s, 3H) ppm.

^{13}C NMR (101 MHz, $CDCl_3$) δ 170.4, 151.9, 147.9, 140.8, 140.4, 139.0, 136.2, 132.6 (x2), 132.5, 130.9, 130.7, 129.2, 128.8 (x2), 128.7 (x2), 127.5, 127.3 (x2), 127.1 (x4), 126.3 (x2), 126.0, 125.9, 125.1, 123.0, 122.2, 118.7, 113.9, 20.3 ppm.

IR (neat): 3511, 3027, 1754, 1594, 1491, 1360, 1194, 1076, 1013, 889, 809, 754, 695 cm^{-1}.

HRMS (ESI): m/z: $[M-H]^+$ ($C_{34}H_{23}O_3$), calcd.: 479,1653; found: 479.1632.

$[\alpha]_D^{25}$ = +259.0 (*c* = 0.1, CH_2Cl_2).

HPLC (Daicel Chiralpak AD-H, hexane/^{i}PrOH = 60:40, flow rate 1.0 mL/min, λ = 210 nm): major isomer: t_R = 9.8 min; minor isomer: t_R = 27.3 min.

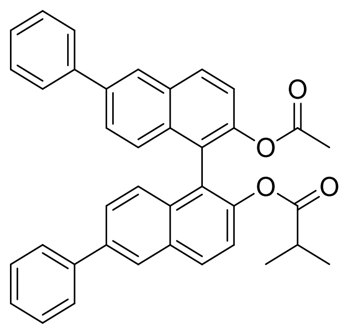

(*R*)-2'-acetoxy-6,6'-diphenyl-[1,1'-binaphthalen]-2-yl isobutyrate (9ib)

146 mg, 53% yield. Colourless solid. m. p. 107–109 °C.

^{1}H NMR (400 MHz, $CDCl_3$) δ 8.13 (d, *J* = 5.0 Hz, 2H), 8.04 (dd, *J* = 8.8, 6.8 Hz, 2H), 7.68 (d, *J* = 7.7 Hz, 4H), 7.57 (dd, *J* = 8.8, 0.9 Hz, 2H), 7.50 – 7.40 (m, 6H), 7.39 – 7.30 (m, 4H), 2.40 (dt, *J* = 14.0, 7.0 Hz, 1H), 1.85 (s, 3H), 0.80 (d, *J* = 7.0 Hz, 3H), 0.74 (d, *J* = 7.0 Hz, 3H) ppm.

^{13}C NMR (101 MHz, $CDCl_3$) δ 175.2, 169.1, 146.8 (x2), 140.6 (x2), 138.3 (x2), 132.5 (x2), 131.8 (x2), 129.7, 129.6, 128.8 (x4), 127.4 (x2), 127.3 (x2), 126.7, 126.6, 126.4 (x2), 125.8, 125.7, 123.4, 123.3, 122.4 (x2), 122.3 (x2), 33.8, 20.6, 18.2 (x2) ppm.

IR (neat): 3027, 2973, 2935, 2875, 1753, 1594, 1491, 1367, 1191, 1092, 1012, 905, 890, 754, 729, 695 cm^{-1}.

HRMS (ESI): m/z: $[M+Na]^+$ ($C_{38}H_{30}NaO_4$), calcd.: 573,2042; found: 573,2036.

$[\alpha]_D^{25}$ = -60.6 (*c* = 0.1, CH_2Cl_2).

HPLC (Daicel Chiralpak AD-H, hexane/^{i}PrOH = 60:40, flow rate 1.0 mL/min, λ = 210 nm): major isomer: t_R = 8.2 min; minor isomer: t_R = 14.5 min.

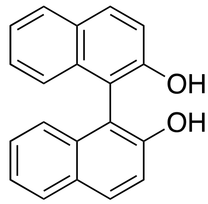

[1,1'-binaphthalene]-2,2'-diol (6)

^{1}H NMR (400 MHz, $CDCl_3$) δ 7.95 (d, *J* = 9.0 Hz, 2H), 7.87 (d, *J* = 8.0 Hz, 2H), 7.41 – 7.33 (m, 4H), 7.29 (ddd, *J* = 8.2, 6.8, 1.4 Hz, 2H), 7.14 (d, *J* = 8.9 Hz, 2H), 5.02 (s, 2H) ppm.

^{13}C NMR (101 MHz, $CDCl_3$) δ 152.7 (x2), 133.4 (x2), 131.4 (x2), 129.4 (x2), 128.4 (x2), 127.5 (x2), 124.2 (x2), 124.0 (x2), 117.7 (x2), 110.8 (x2) ppm.

HPLC (Daicel Chiralpak AD-H, hexane/*i*-PrOH = 80:20, flow rate 1.0 mL/min, λ = 210 nm): major isomer: t_R = 16.4 min; minor isomer: t_R = 19.8 min.

5. References

[1] V. B. Birman, X. Li, *Org. Lett.* **2006**, *8*, 1351-1354.
[2] O. Karam, A. Martin-Mingot, M. P. Jouannetaud, J. C. Jacquesy, A. Cousson, *Tetrahedron*, **2004**, *60*, 6629-6638.
[3] S. Lu, S. B. Poh, Y. Zhao, Y. *Angew. Chem. Int. Ed.* **2014**, *53*, 11041-11045.
[4] L. Gialih, L. Shih-Huang, C. Show-Jane, W. Fang-Chen, S. Hwey-Lin, *Tetrahedron Lett.* **1993**, *34*, 6057-6058.
[5] H. Aoyama, M. Tokunaga, J. Kiyosu, T. Iwasawa, Y. Obora, Y. Tsuji, *J. Am. Chem. Soc.* **2005**,*127*, 10474-10475.
[6] J. Green, J. S. Woodward, *Synlett* **1995**, *1995*, 155-156.
[7] S. T. Kadam, H. B. Lee, S. S. Kim, *B. Kor. Chem. Soc.* **2009**, *30*, 1071-1076.
[8] G. Ma, J. Deng, M. P. Sibi, *Angew. Chem. Int. Ed.* **2014**, *53*, 11818-11821.
[9] M. Juárez-Hernandez, D. V. Johnson, H. L. Holland, J. McNulty, A. Capretta, *Tetrahedron: Asymmetry* **2003**, *14*, 289-291.

6. NMR spectra

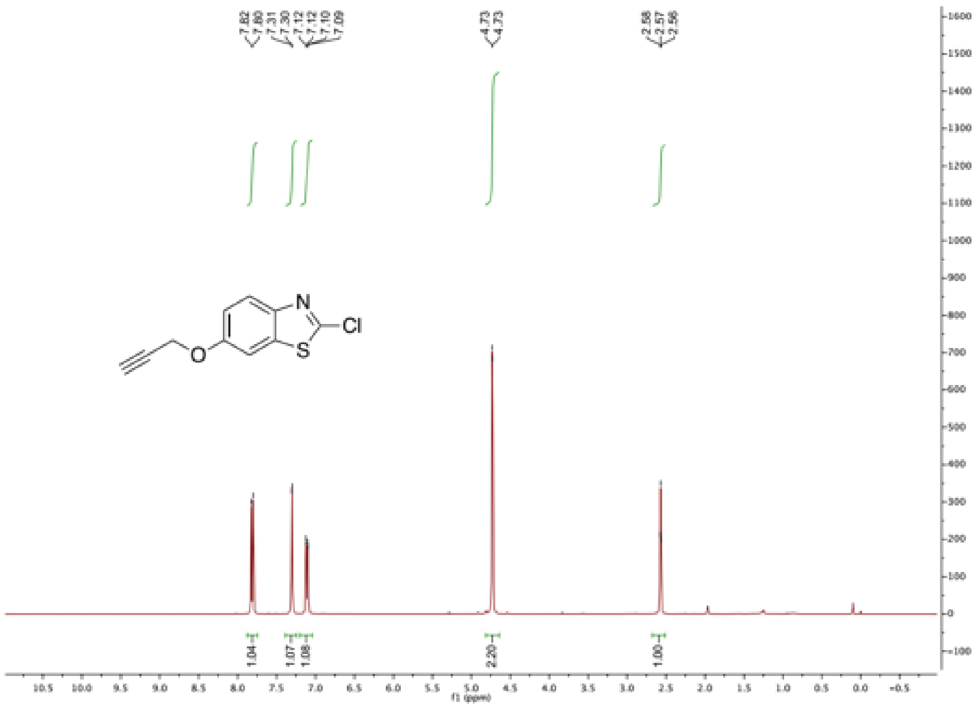

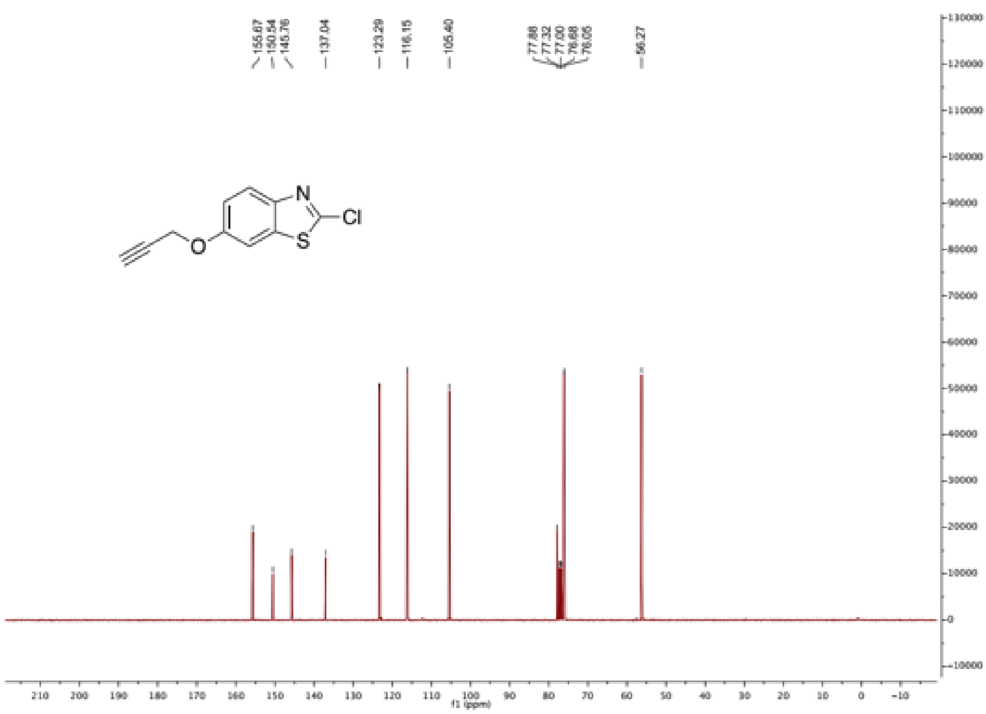

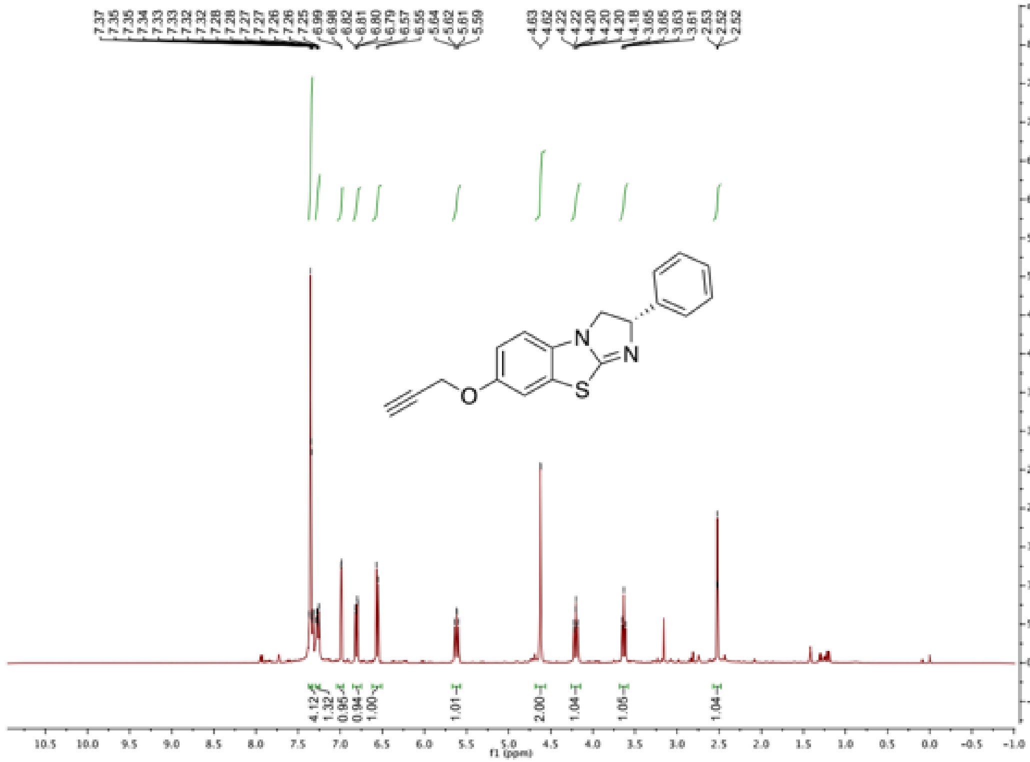
7.37
7.35
7.35
7.34
7.33
7.33
7.32
7.32
7.28
7.28
7.27
7.27
7.26
7.26
7.25
6.99
6.98
6.82
6.81
6.80
6.79
6.57
6.55
5.64
5.62
5.61
5.59
4.63
4.62
4.22
4.22
4.20
4.20
4.20
4.18
3.65
3.65
3.63
3.61
2.53
2.52
2.52
N
N
O
S
4.12
1.32
0.95
0.94
1.00
1.01
2.00
1.04
1.05
1.04
f1 (ppm)

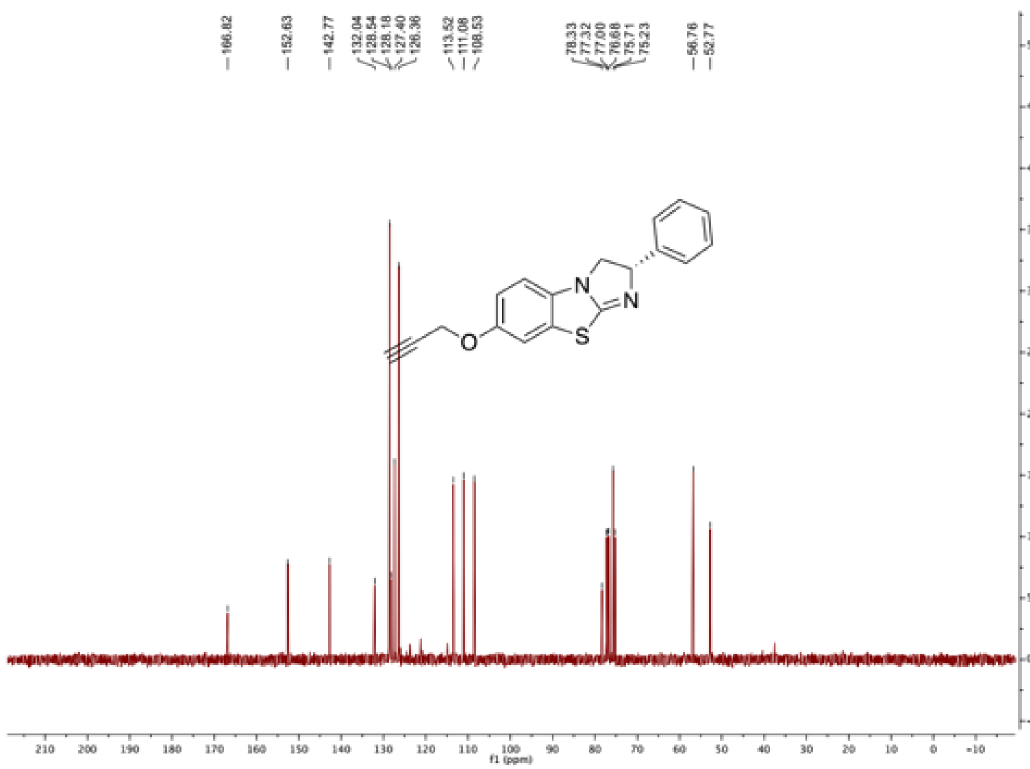
166.82
152.63
142.77
132.04
128.54
128.18
127.40
126.36
113.52
111.08
108.53
78.33
77.32
77.00
76.68
75.71
75.23
56.76
52.77
N
N
O
S
f1 (ppm)

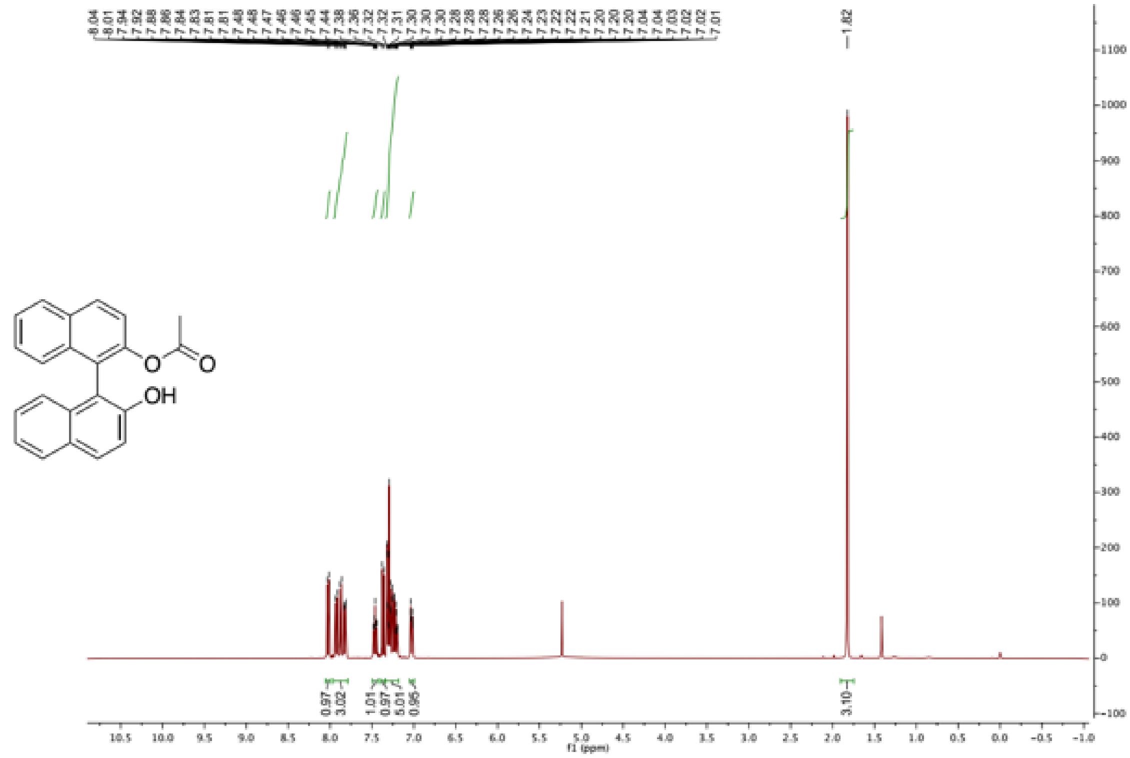
OH
f1 (ppm)

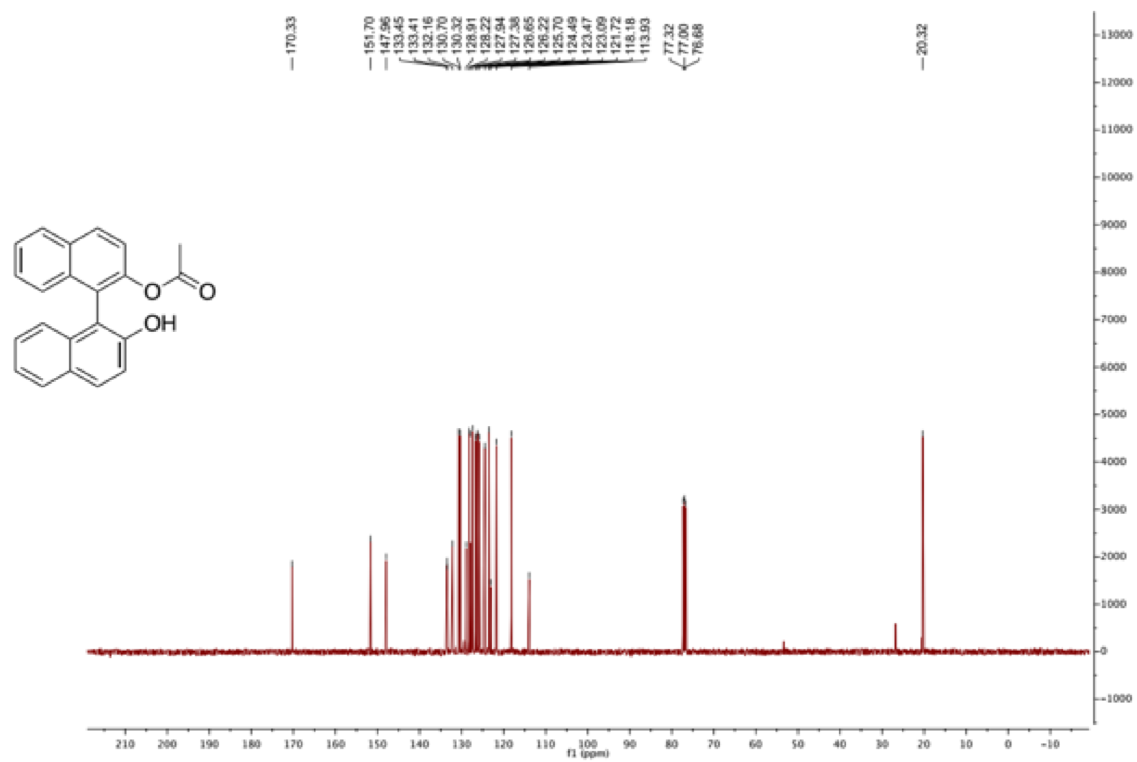
OH
f1 (ppm)

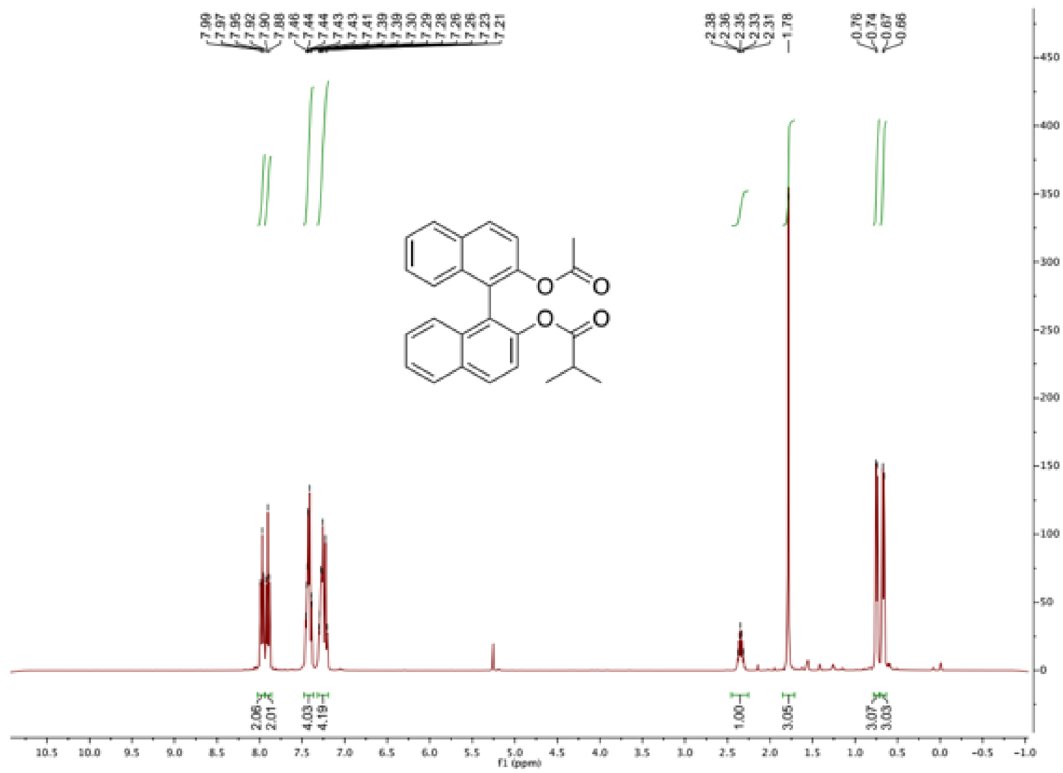

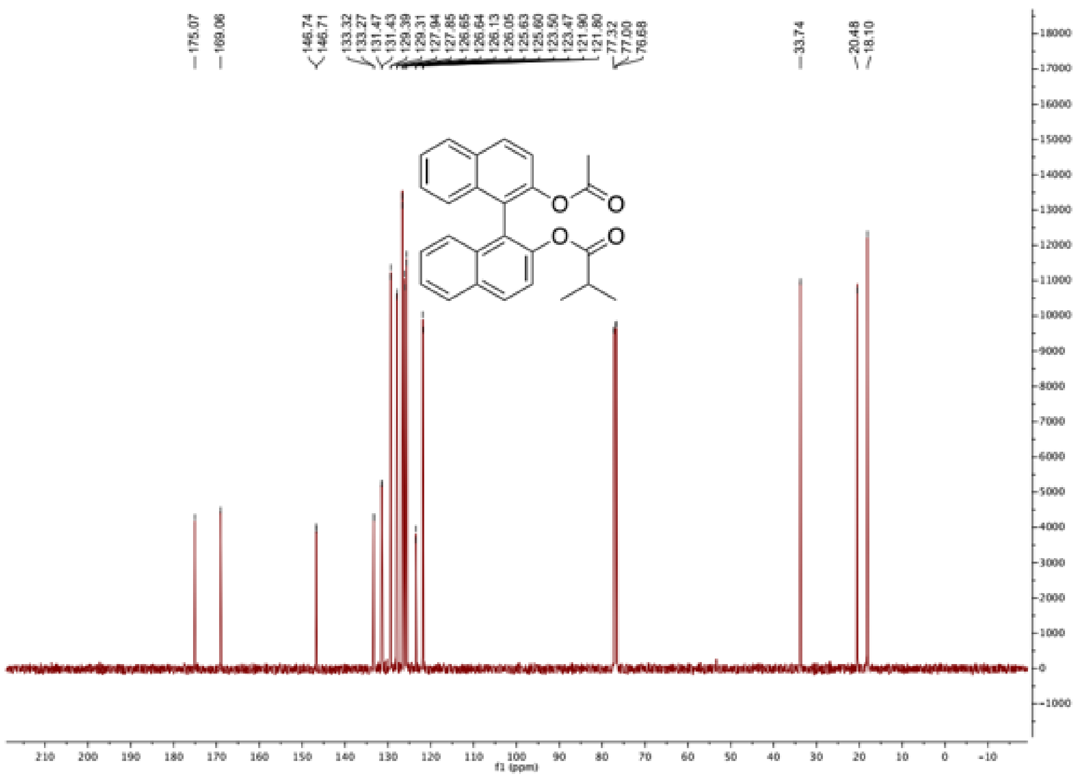

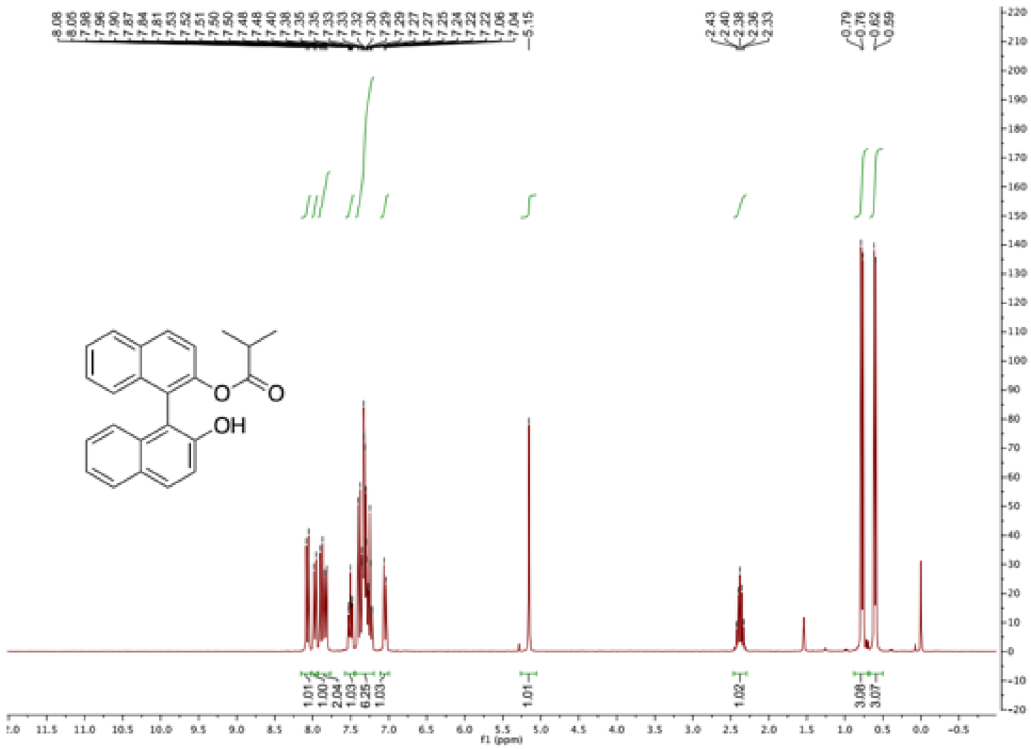

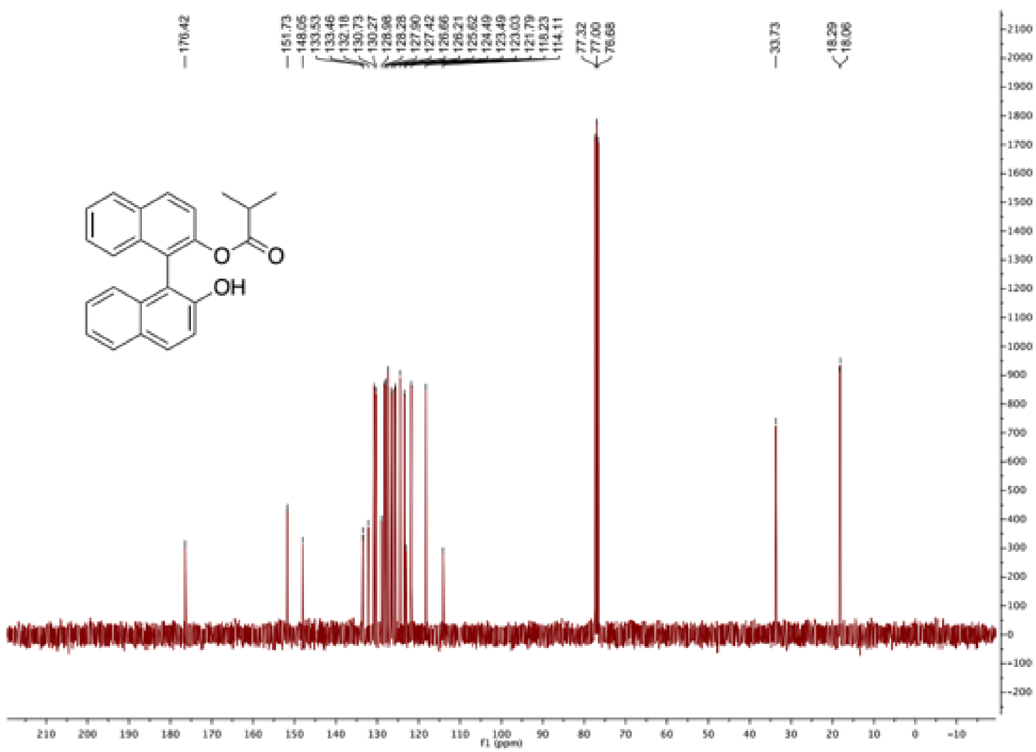

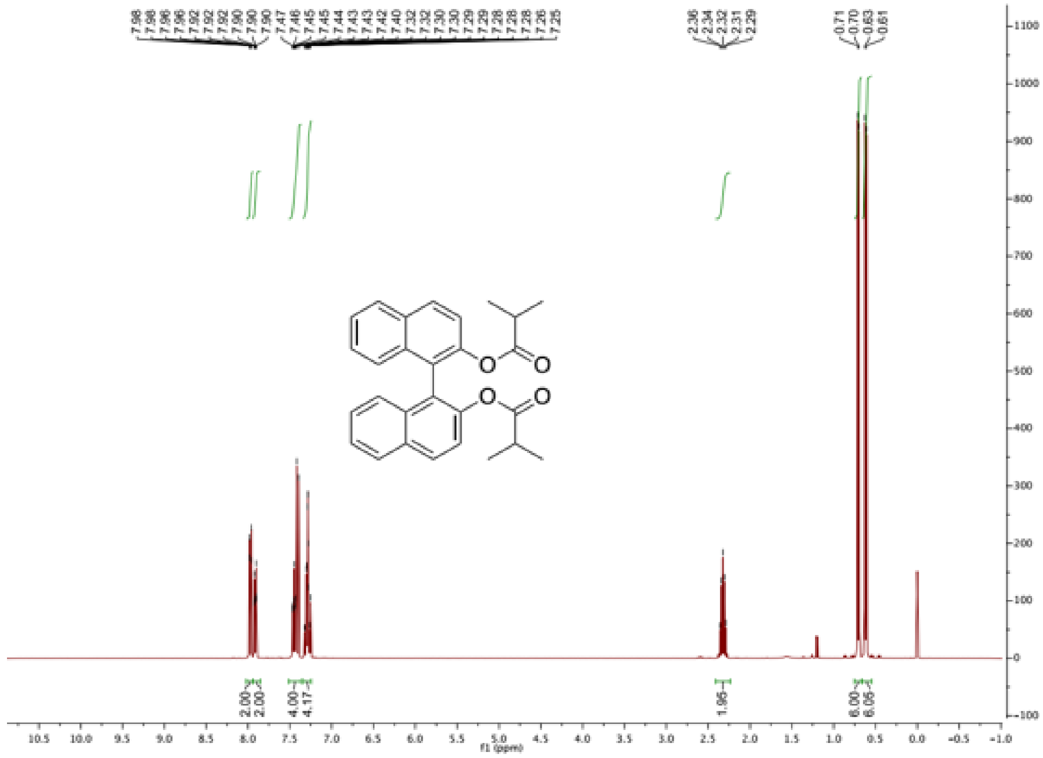
7.98 7.98 7.96 7.96 7.92 7.92 7.90 7.90 7.90 7.47 7.46 7.45 7.45 7.44 7.43 7.43 7.42 7.40 7.32 7.32 7.30 7.30 7.29 7.29 7.28 7.28 7.28 7.26 7.25
2.36 2.34 2.32 2.31 2.29
0.71 0.70 0.63 0.61
2.00 2.00 4.00 4.17
1.96
6.00 6.05
f1 (ppm)

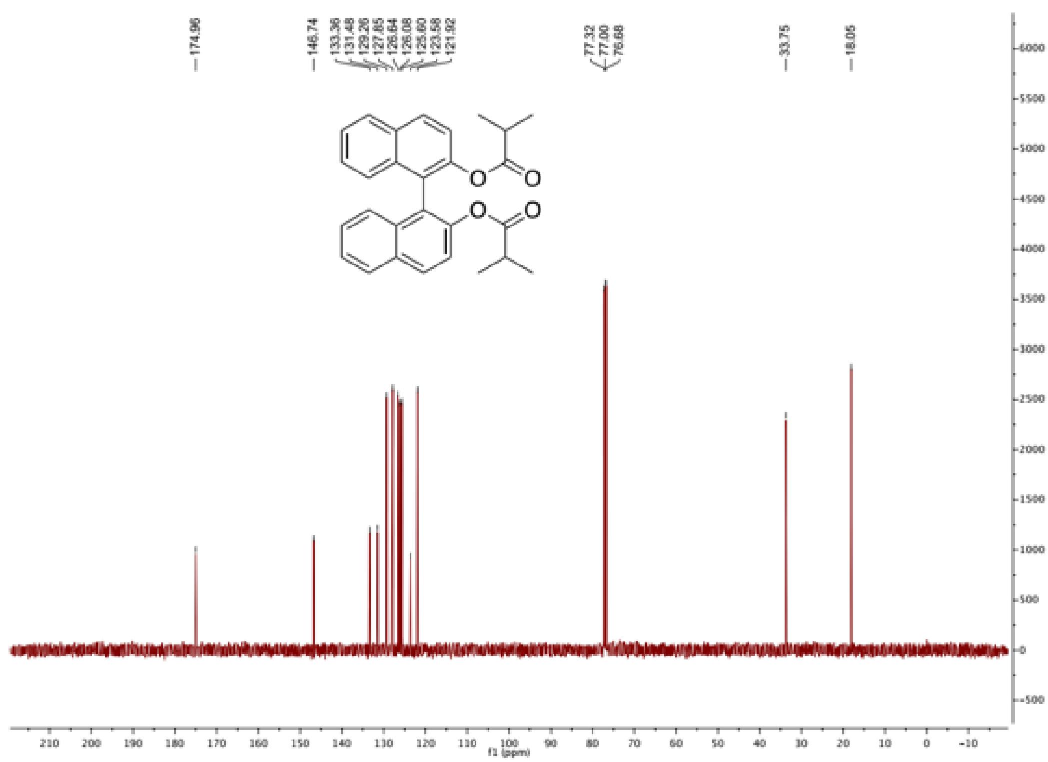
174.96
146.74
133.36 131.48 129.26 127.85 126.64 126.08 125.60 123.58 121.92
77.32 77.00 76.68
33.75
18.05
f1 (ppm)

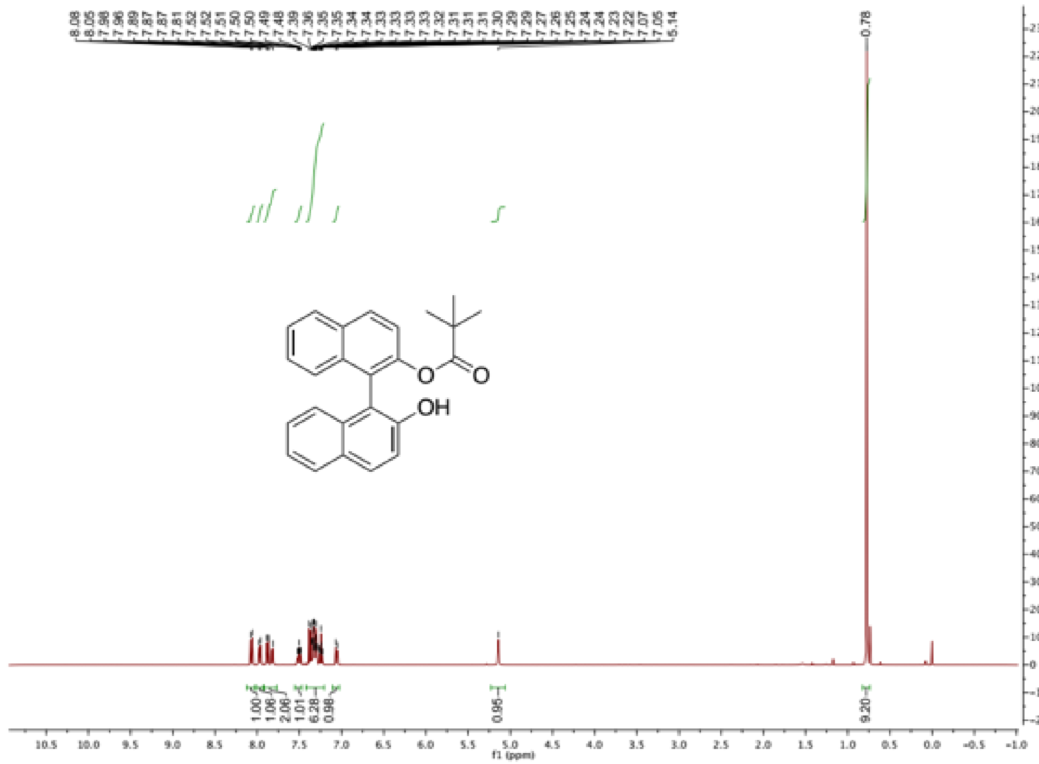

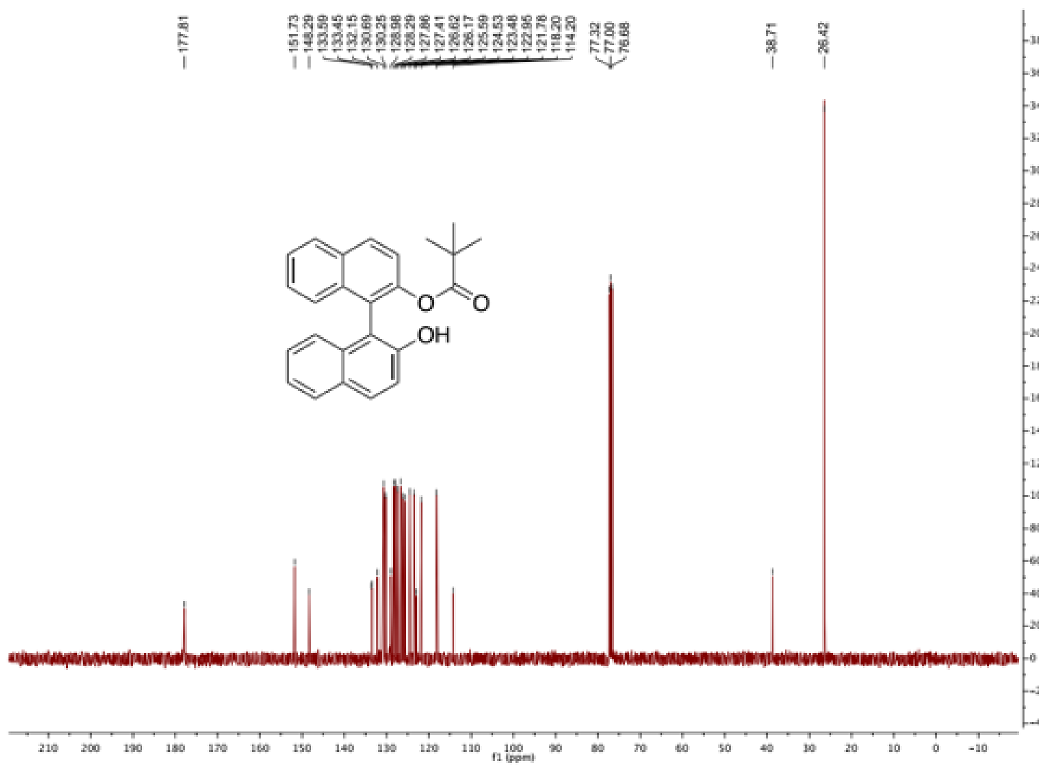

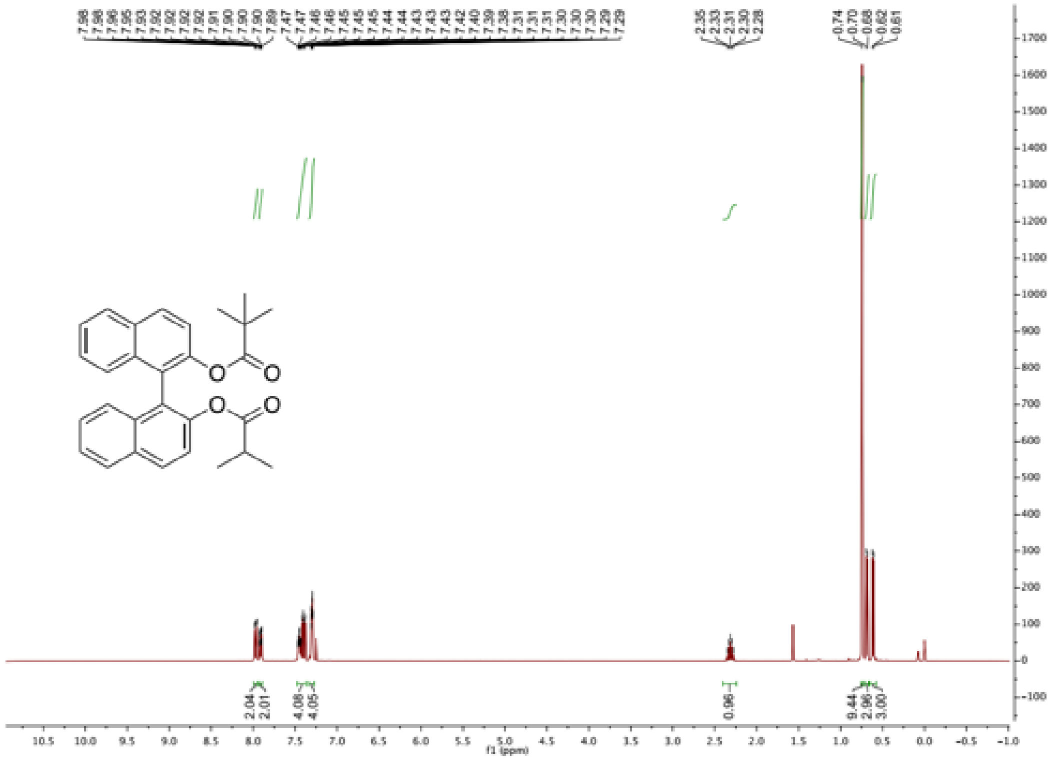

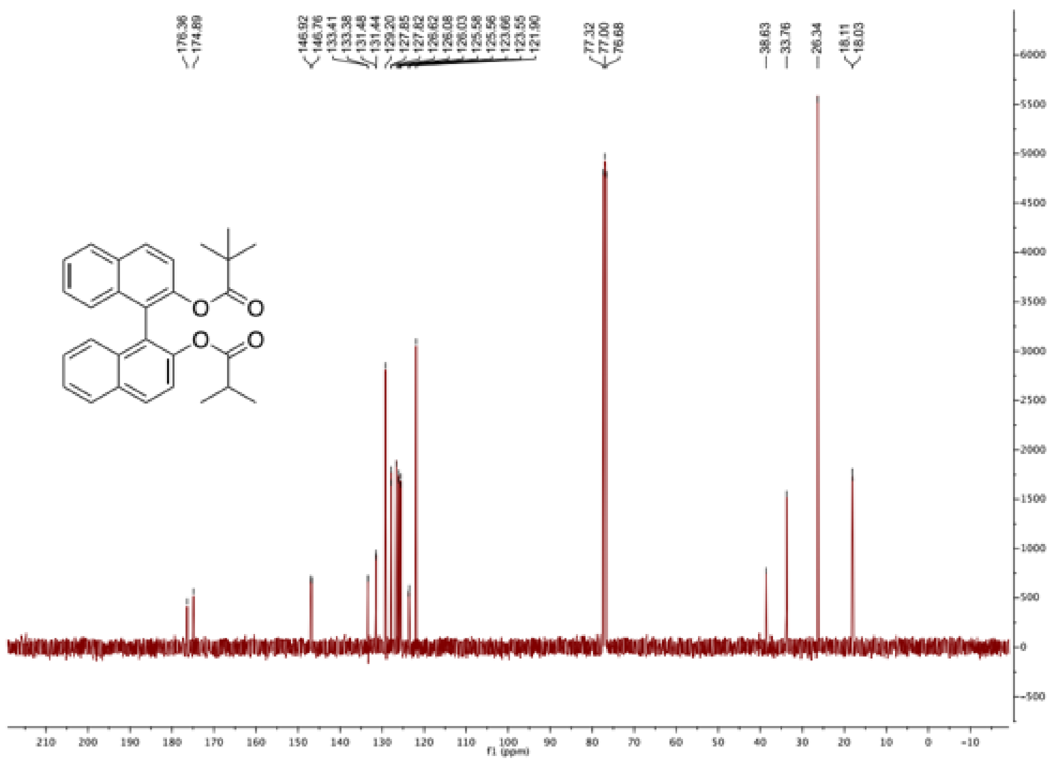

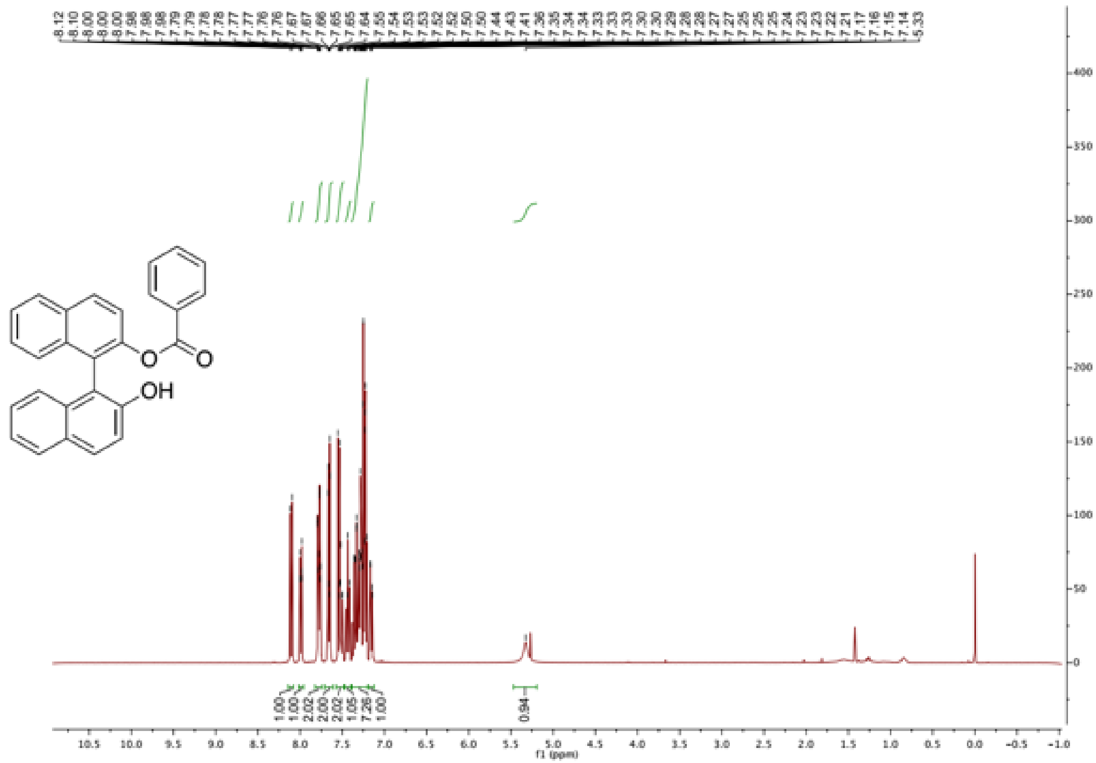

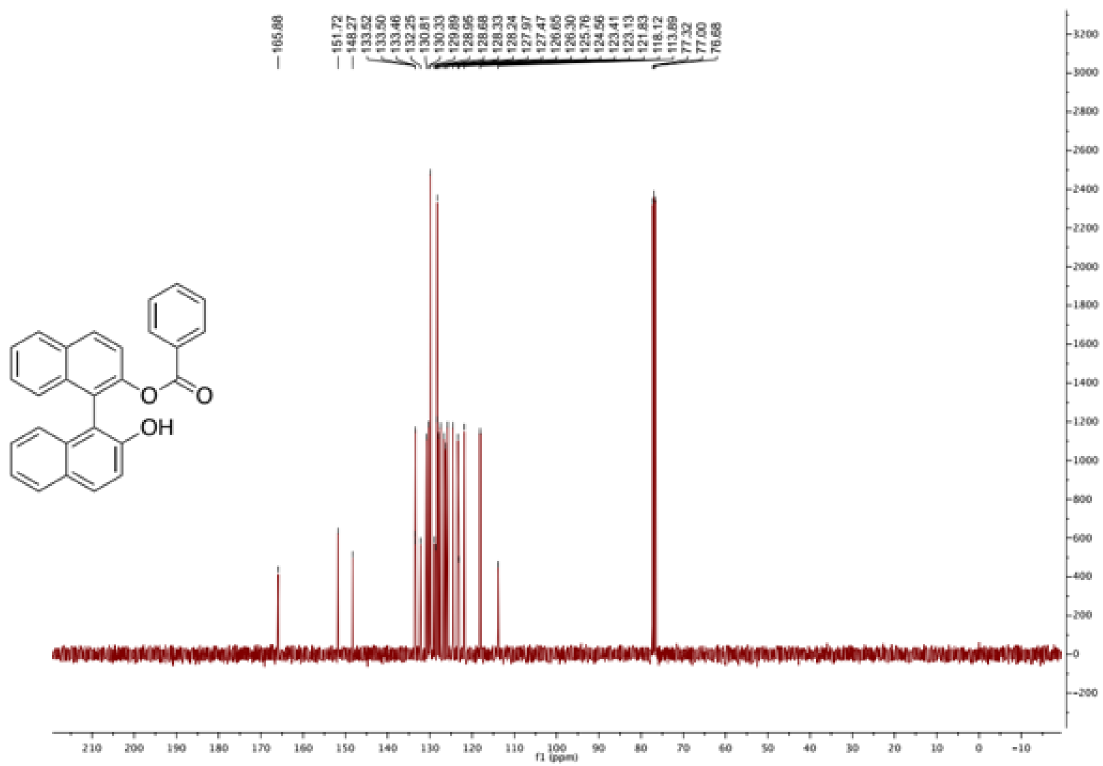

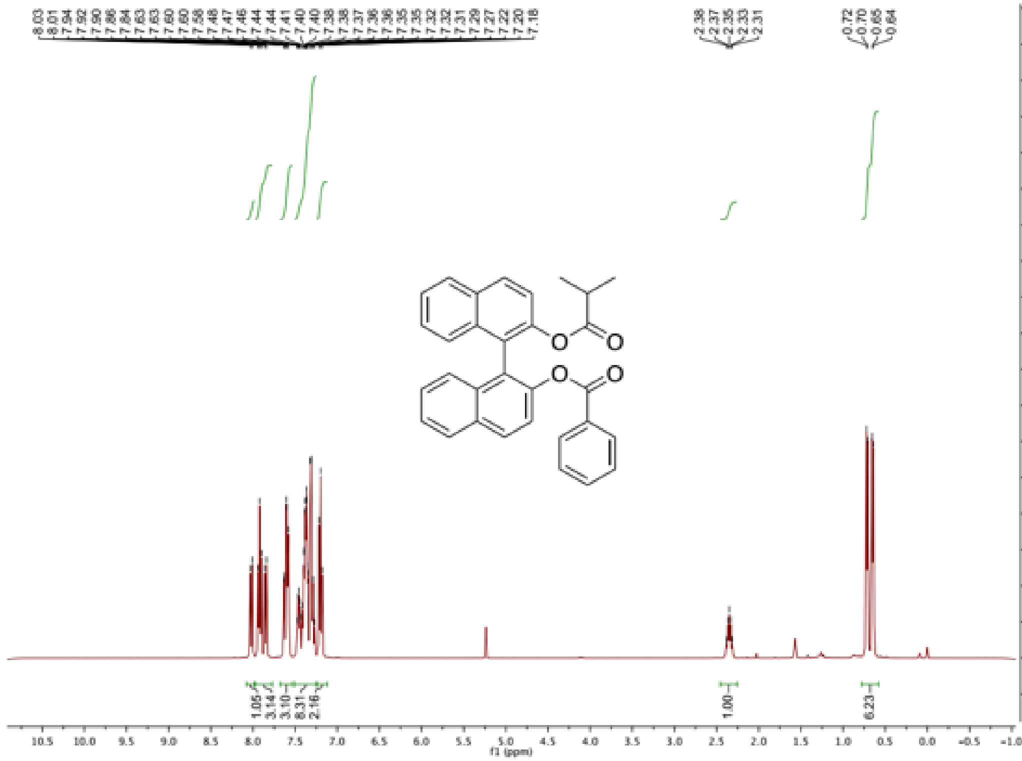

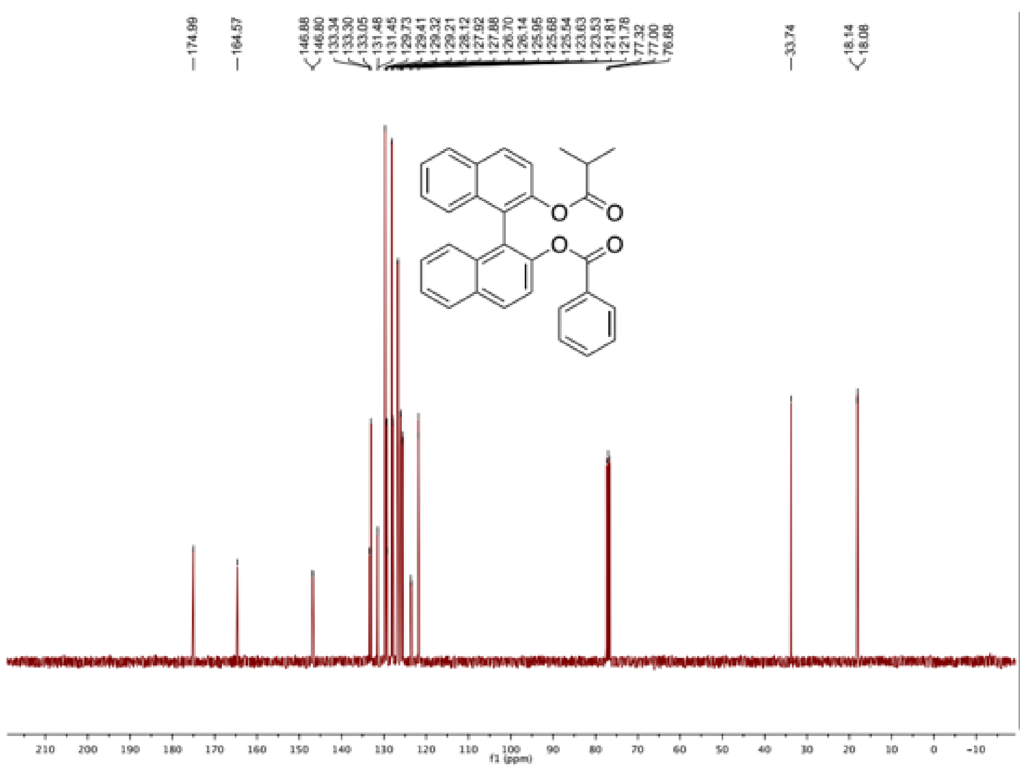

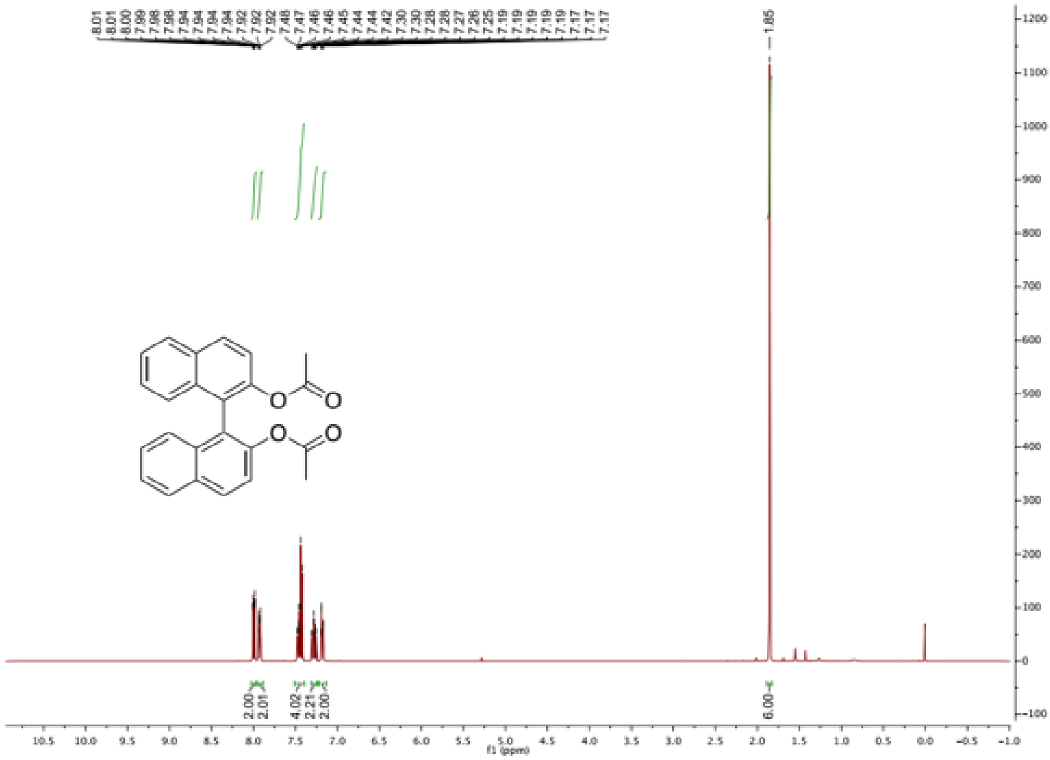
1.85
2.00
2.01
4.02
2.21
2.00
6.00
f1 (ppm)

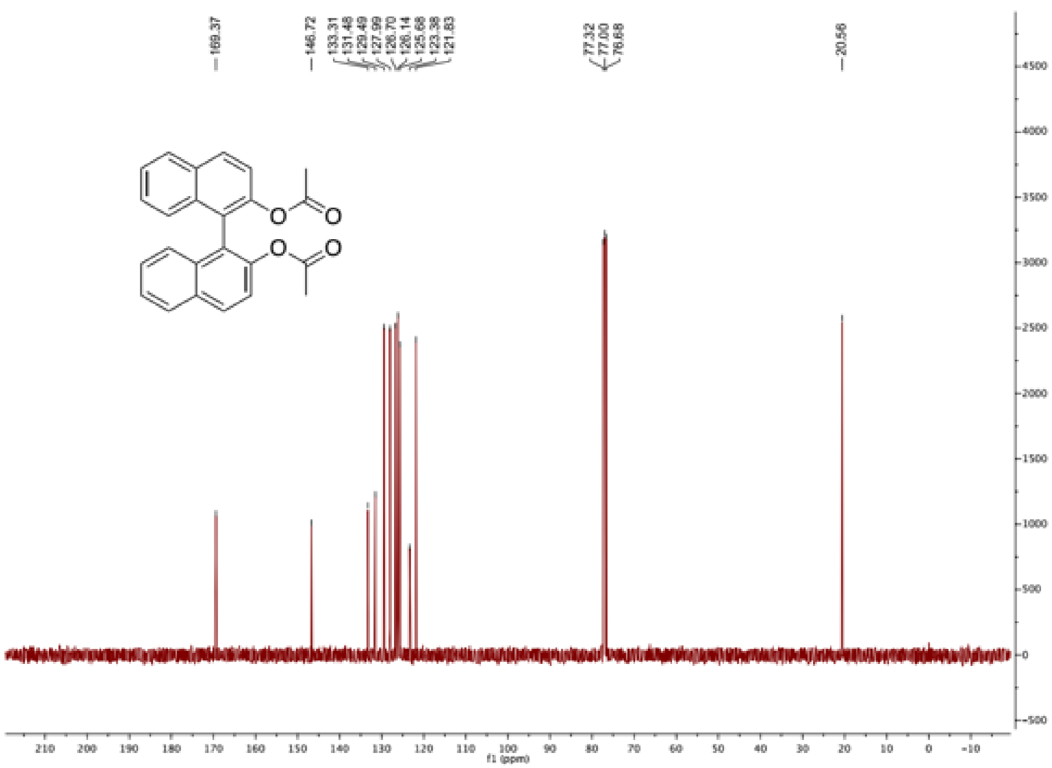
169.37
146.72
133.31
131.48
129.49
127.99
126.70
126.14
125.68
123.38
121.83
77.32
77.00
76.68
20.56
f1 (ppm)

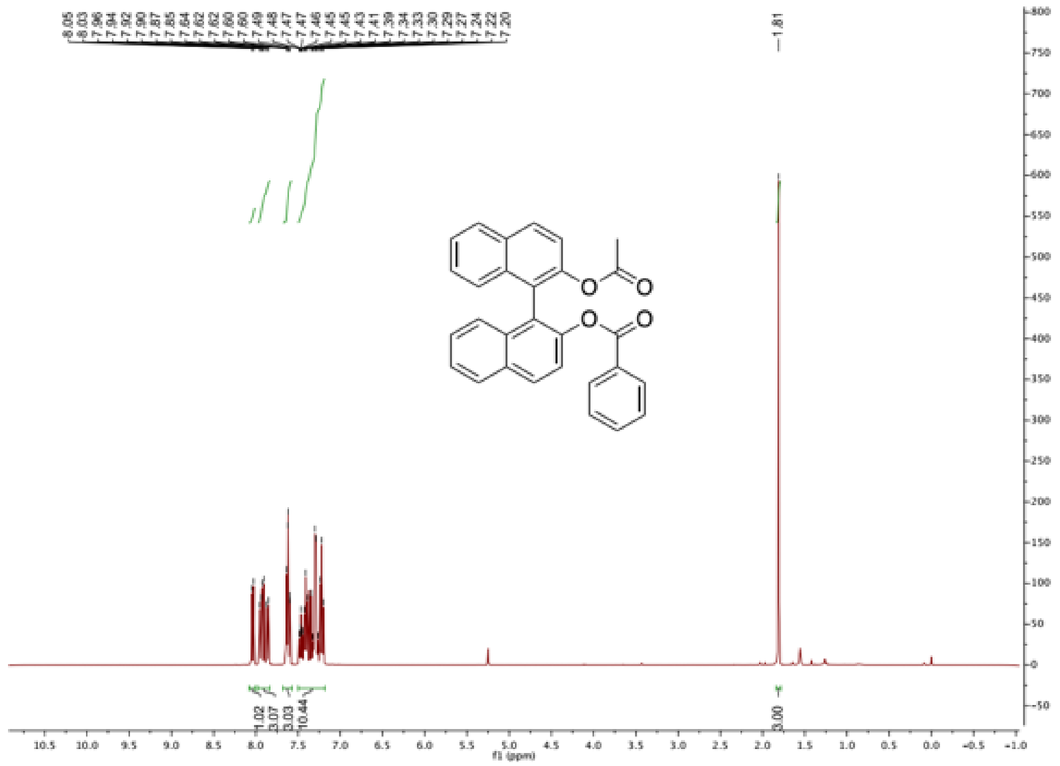

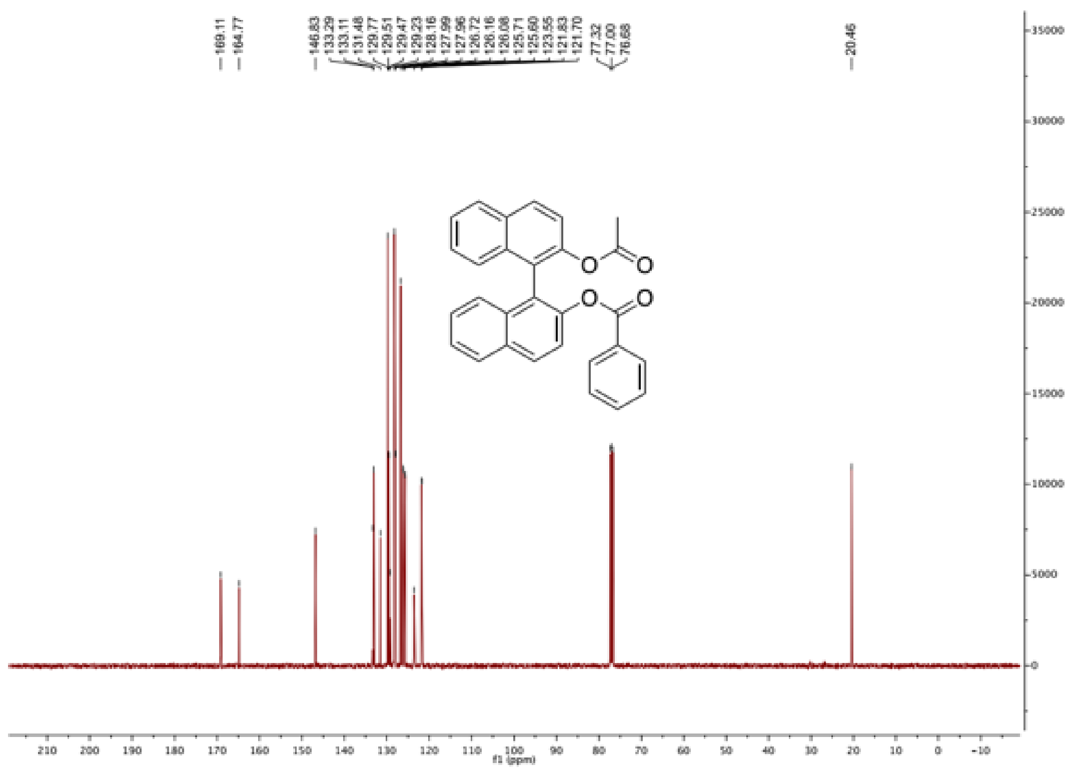

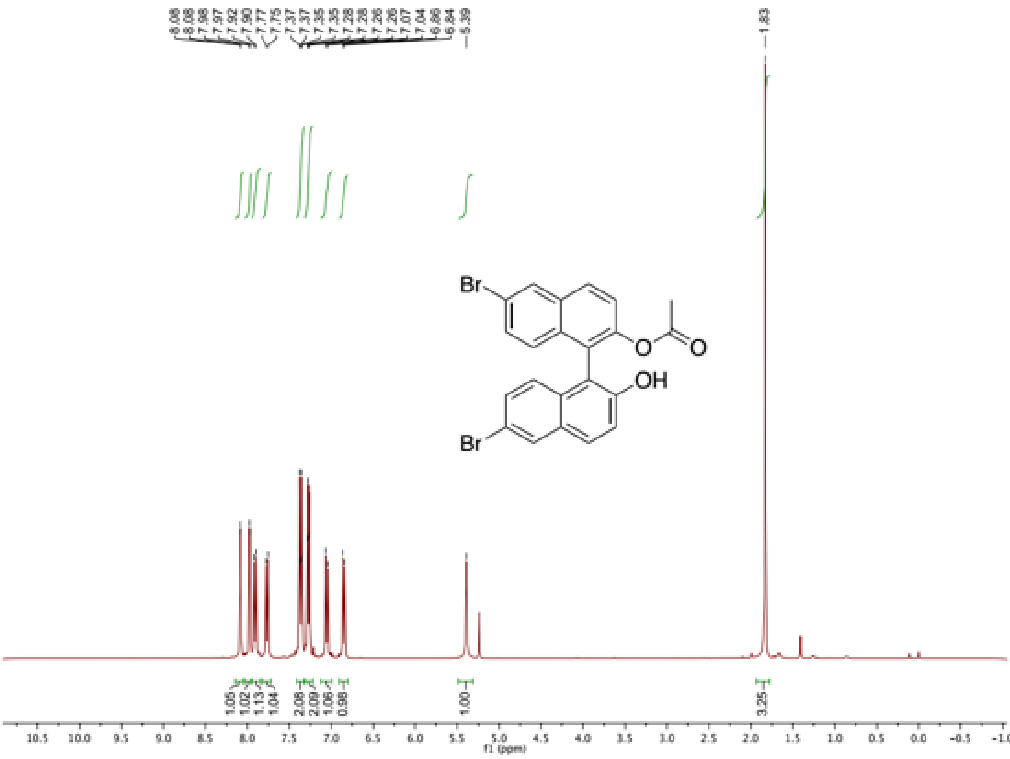

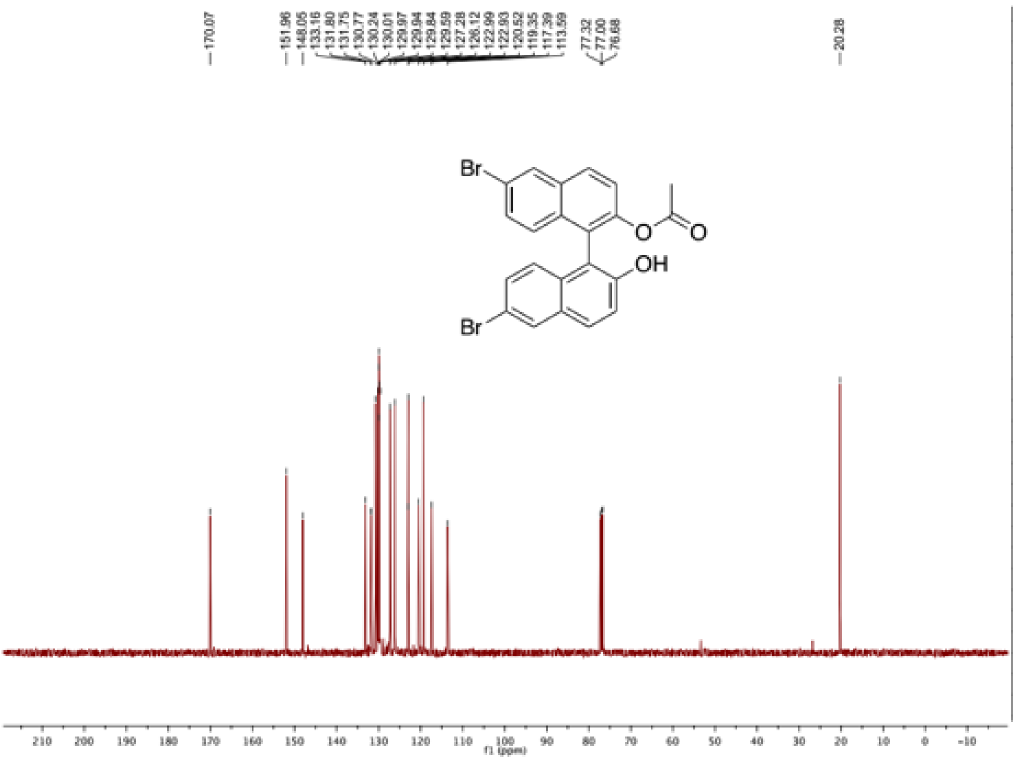

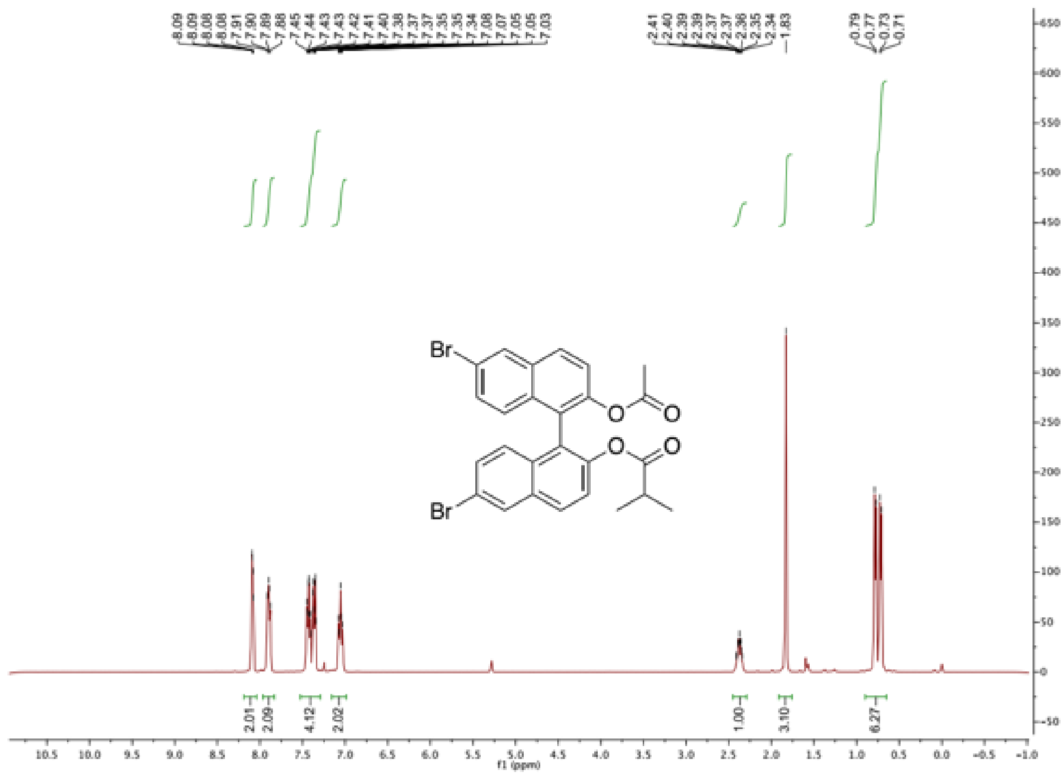
Br
O
O
Br
2.01
2.09
4.12
2.02
1.00
3.10
6.27
f1 (ppm)

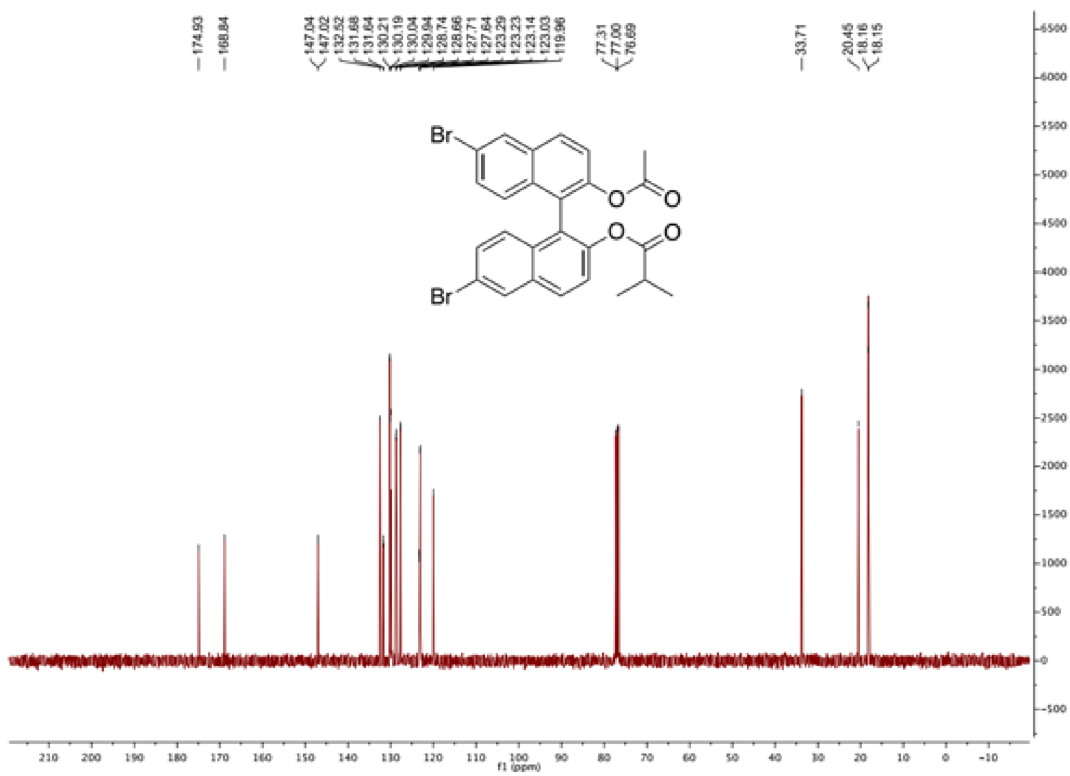
Br
O
O
Br
f1 (ppm)

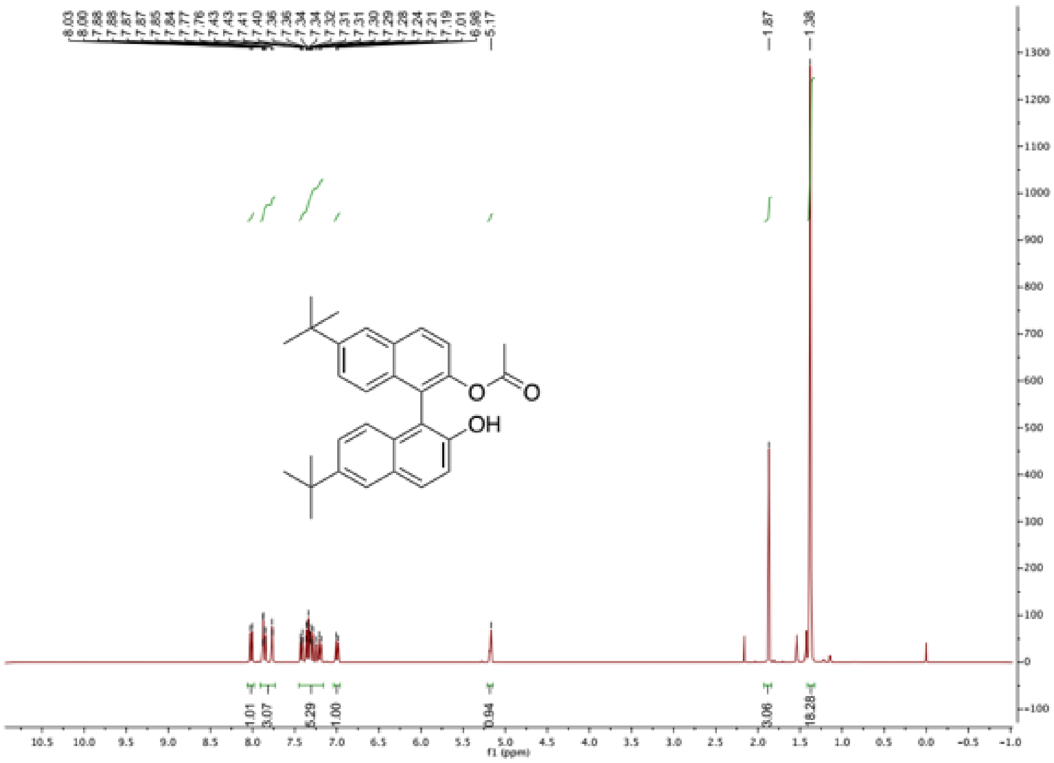

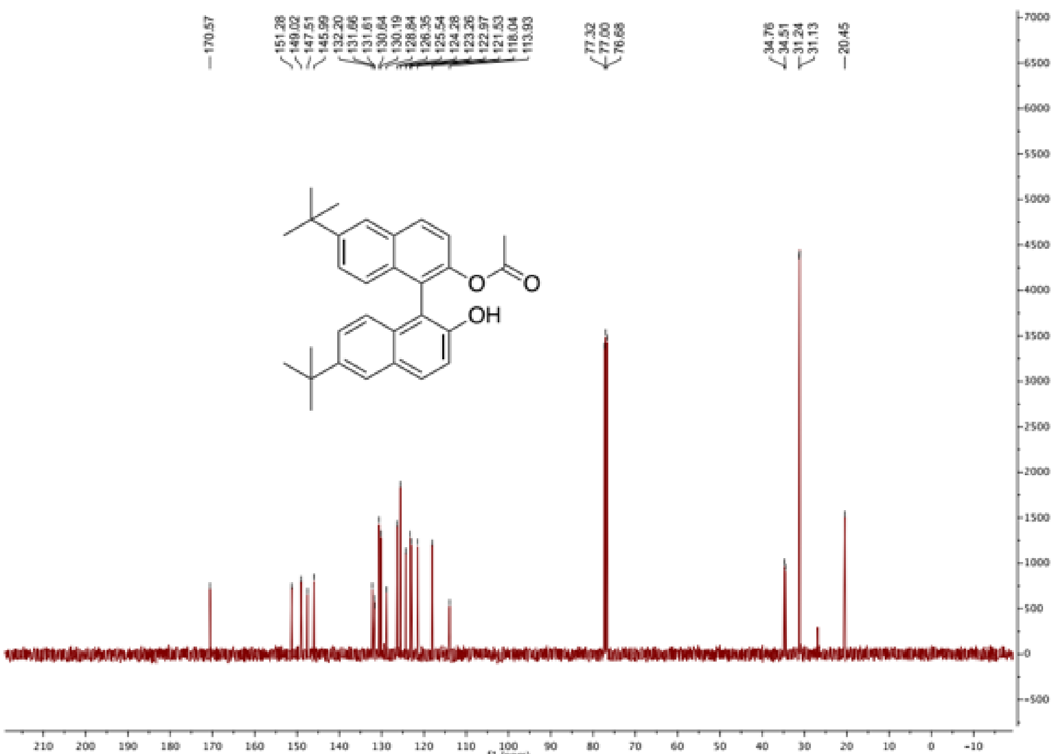

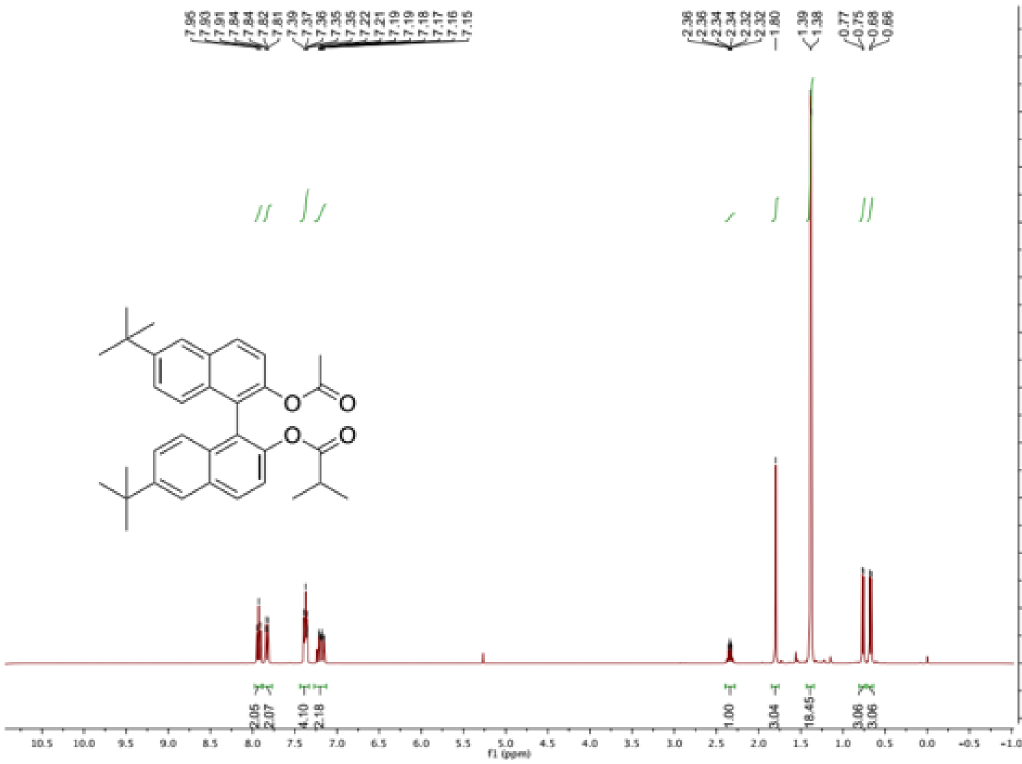

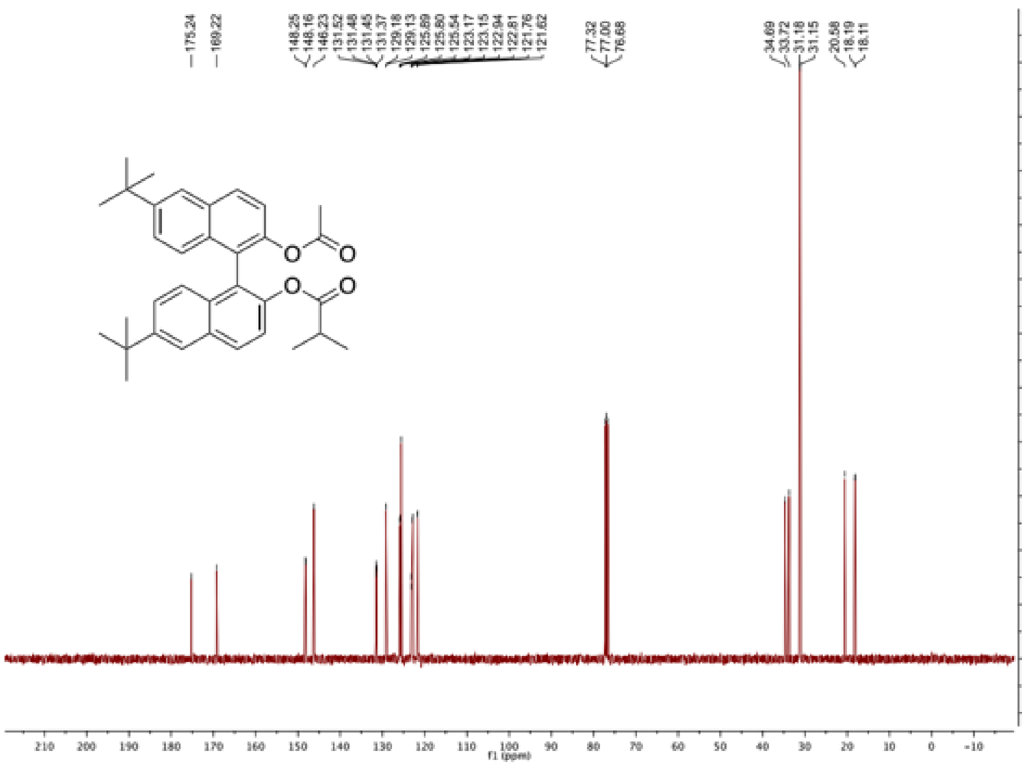

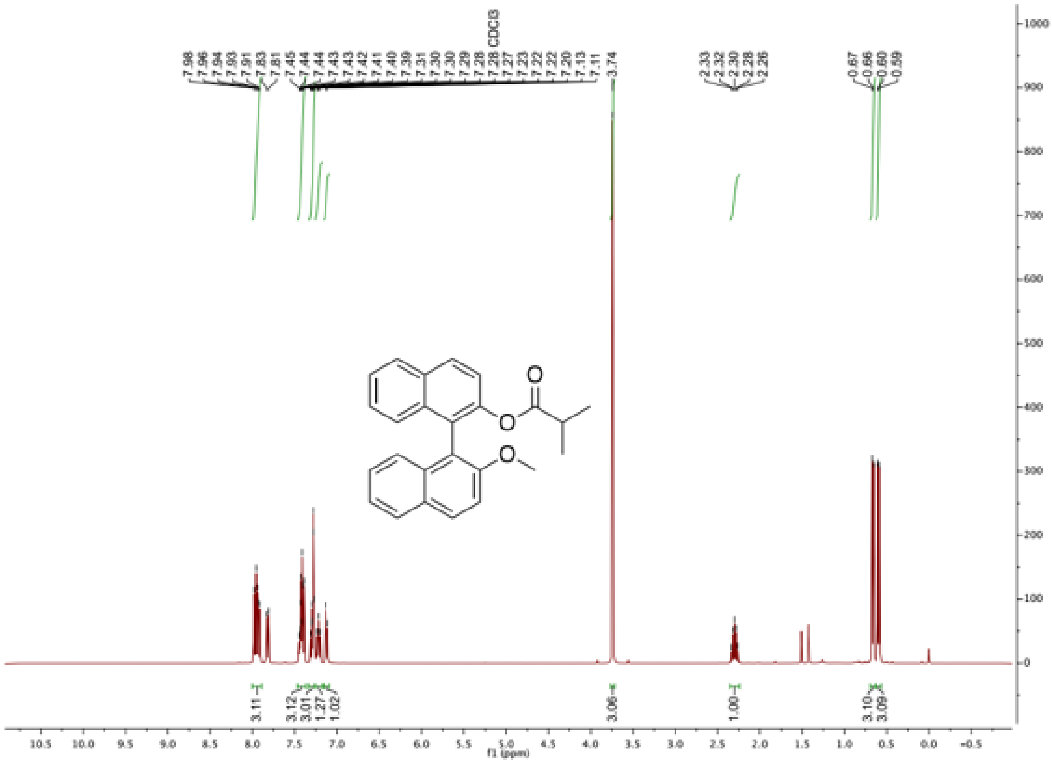

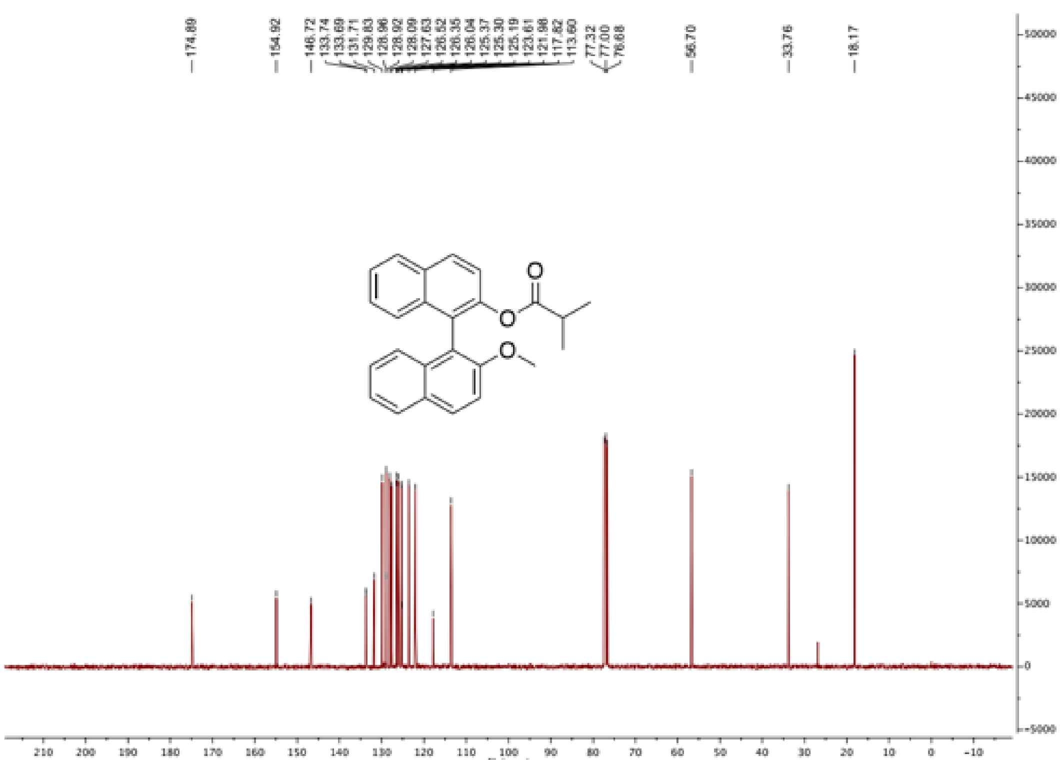

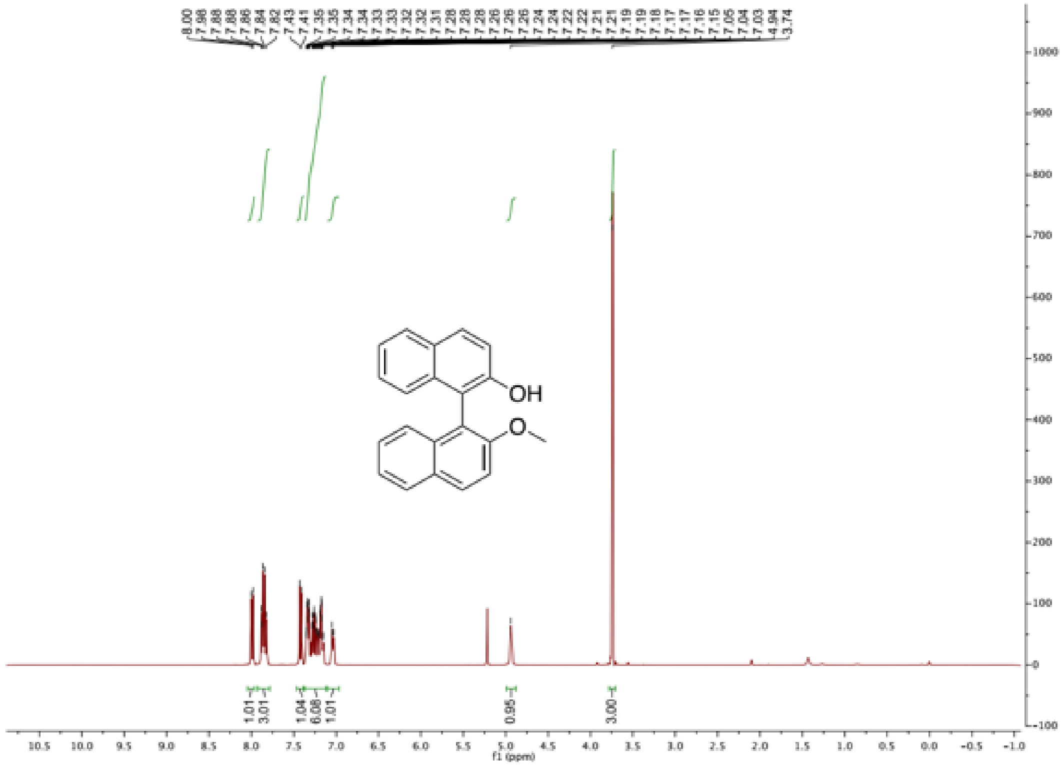

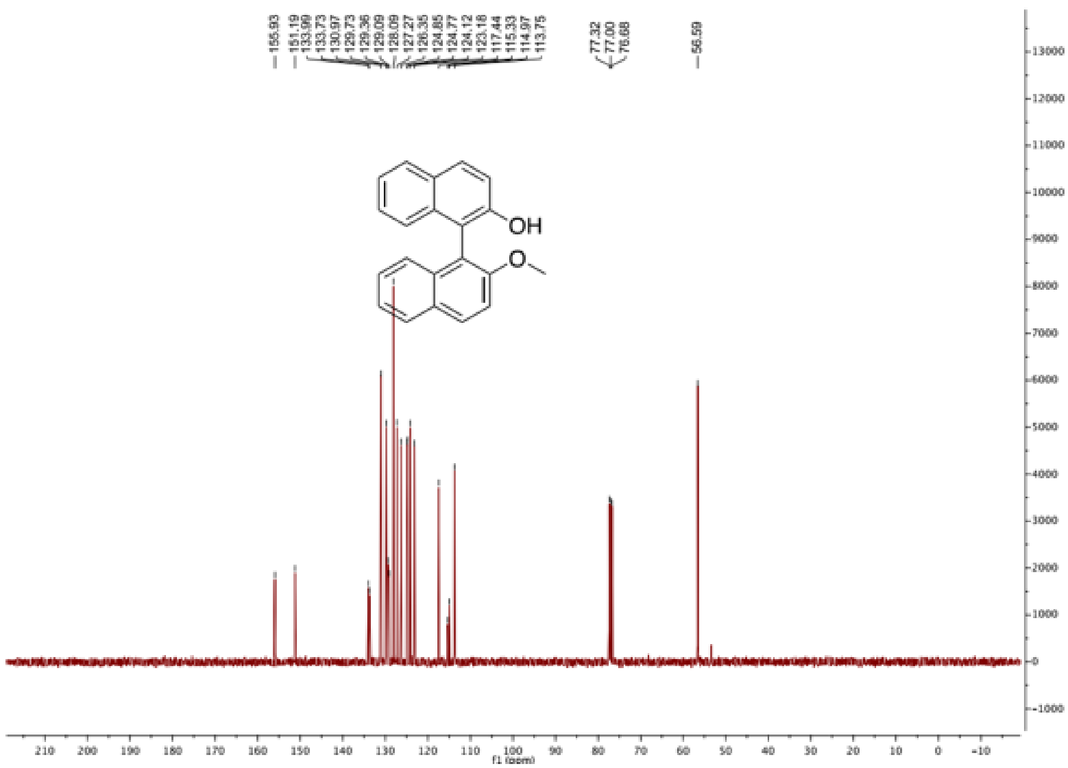

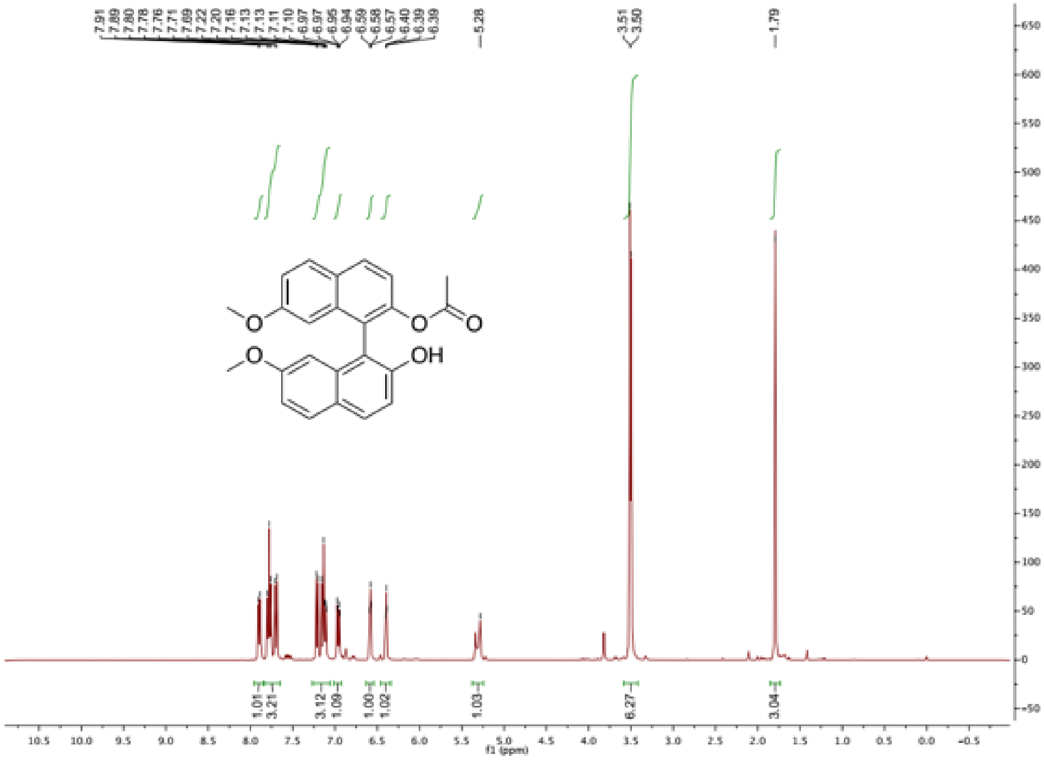

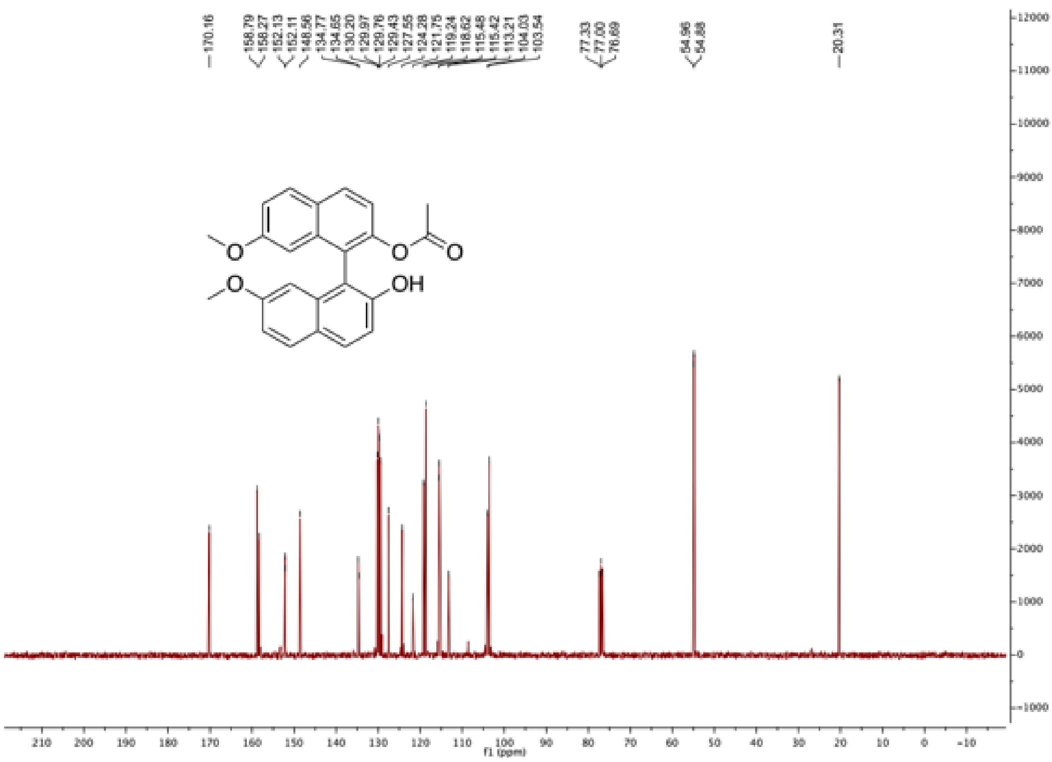

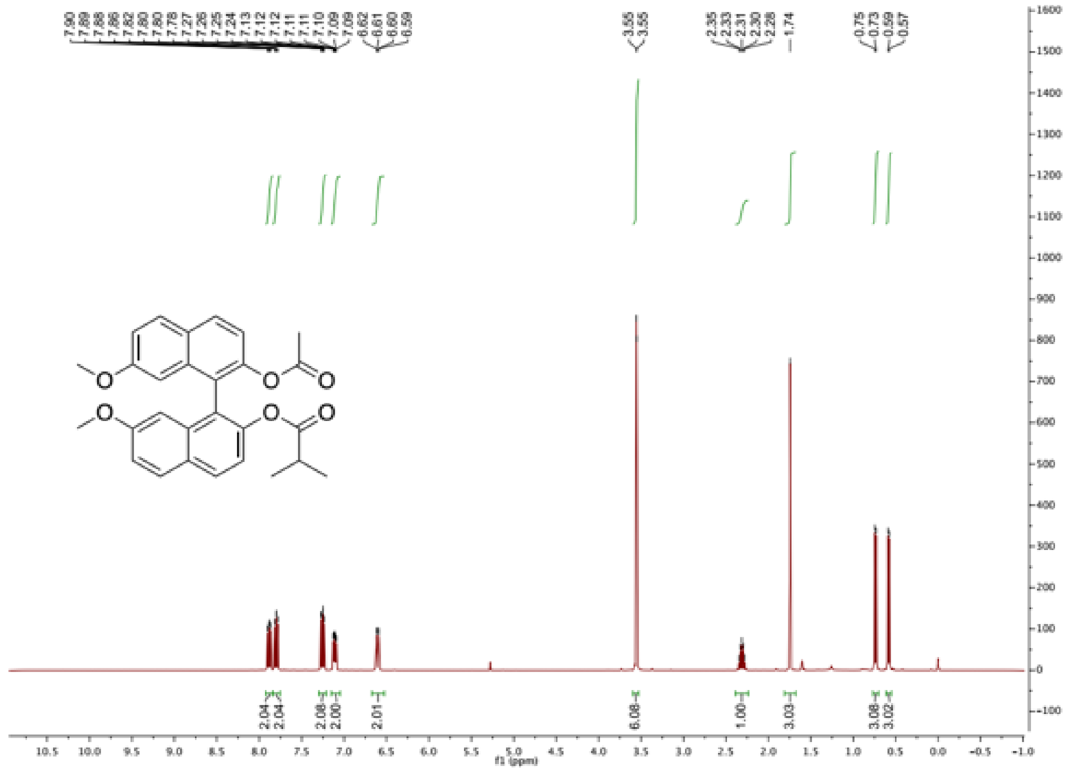

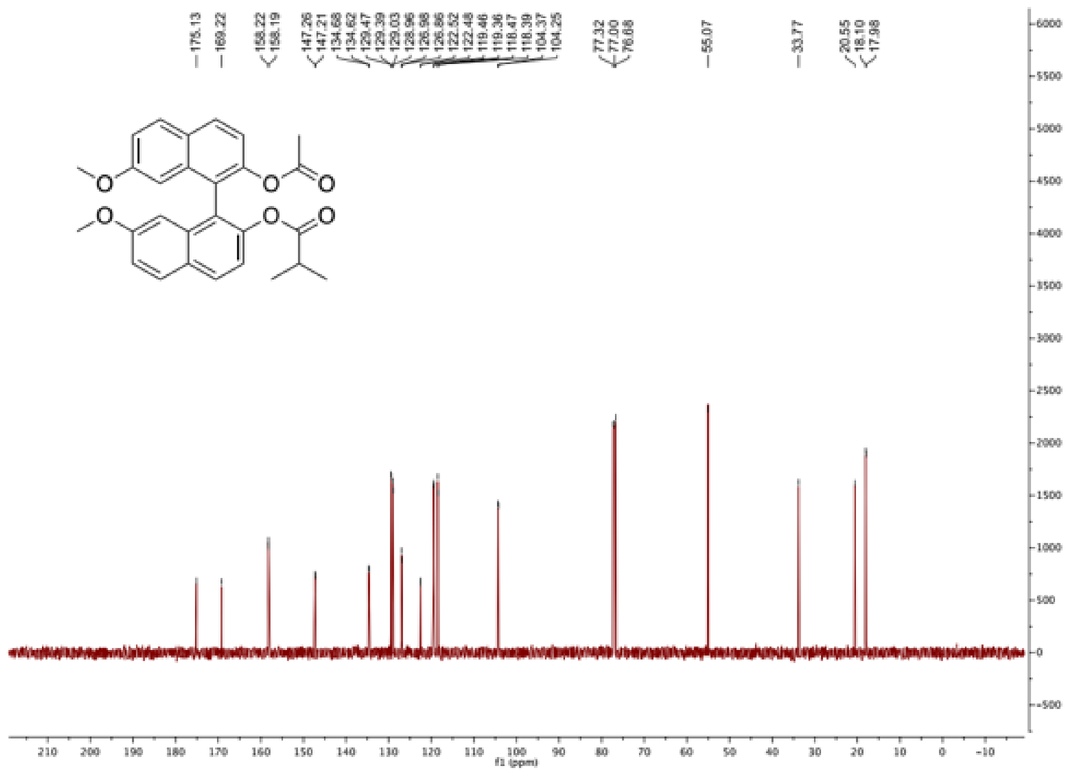

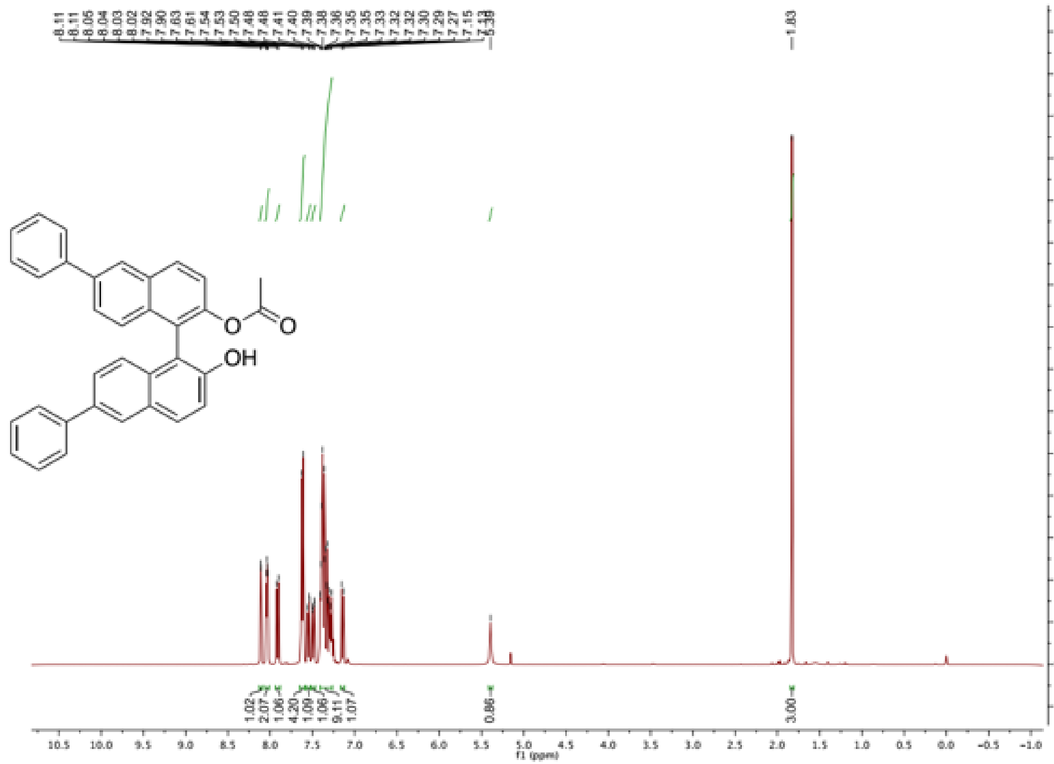

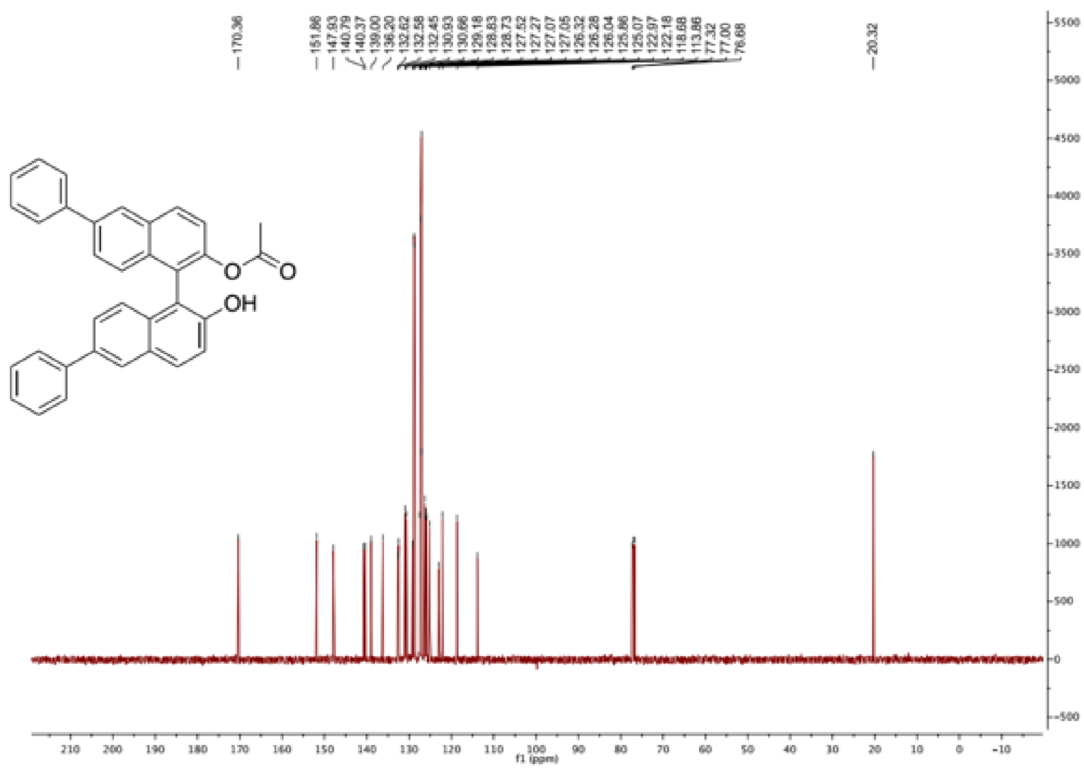

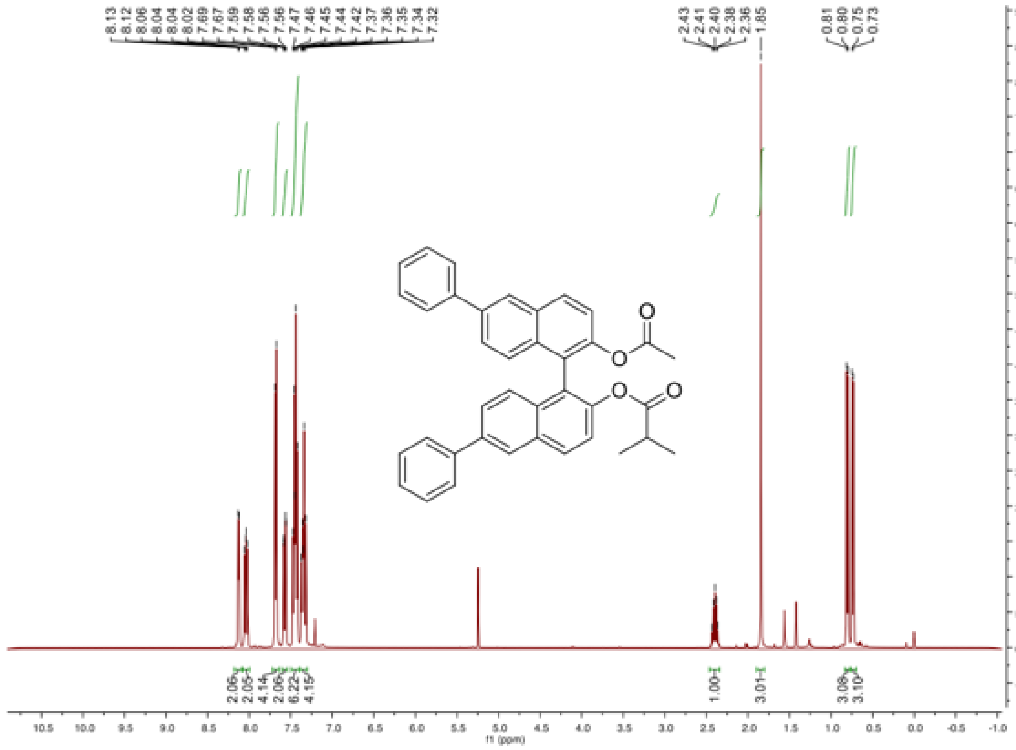

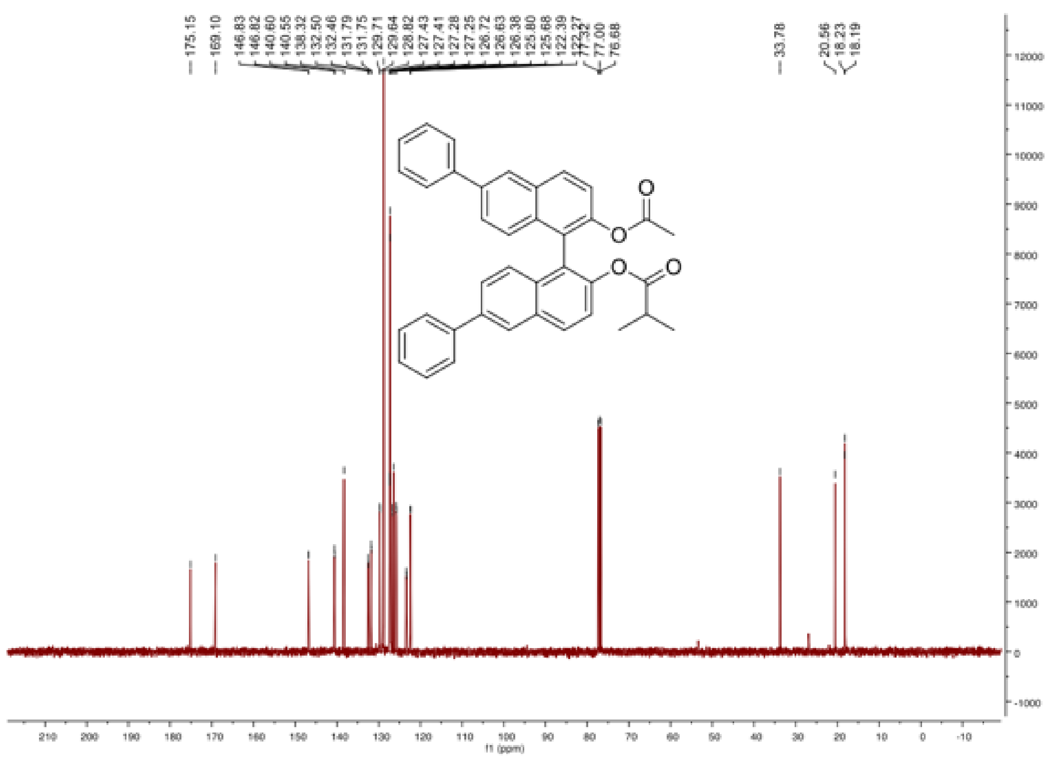

7. HPLC chromatograms

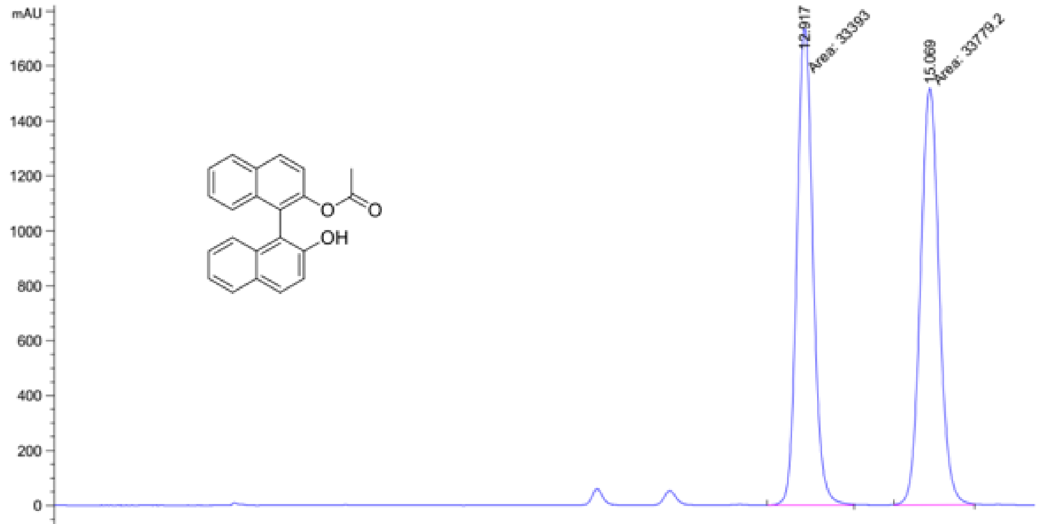

Peak #	RetTime [min]	Type	Width [min]	Area [mAU*s]	Height [mAU]	Area %
1	12.917	MF	0.3209	3.33930e4	1734.14417	49.7125
2	15.069	FM	0.3710	3.37792e4	1517.66113	50.2875

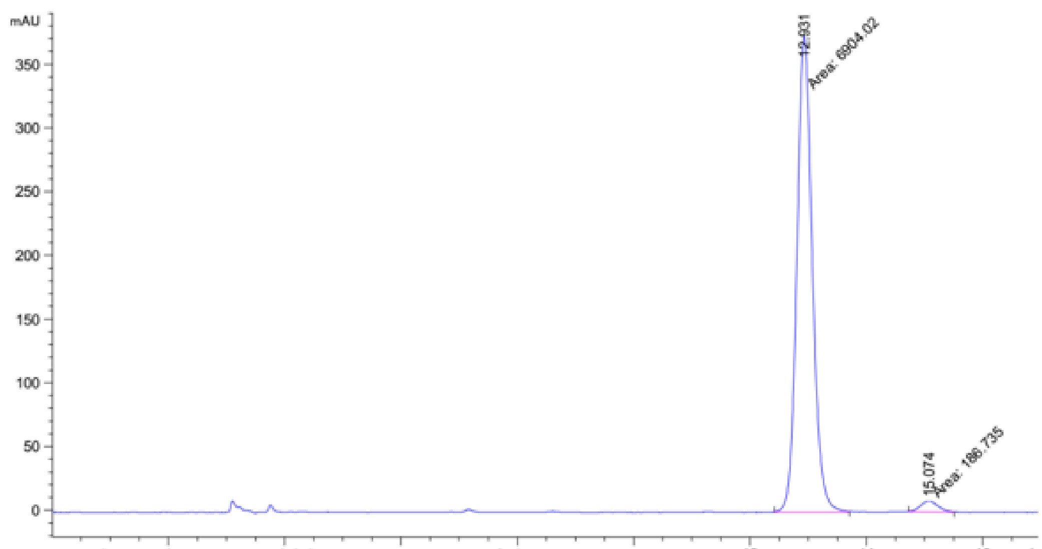

Peak #	RetTime [min]	Type	Width [min]	Area [mAU*s]	Height [mAU]	Area %
1	12.931	FM	0.3082	6904.01904	373.40613	97.3665
2	15.074	MF	0.3576	186.73489	8.70326	2.6335

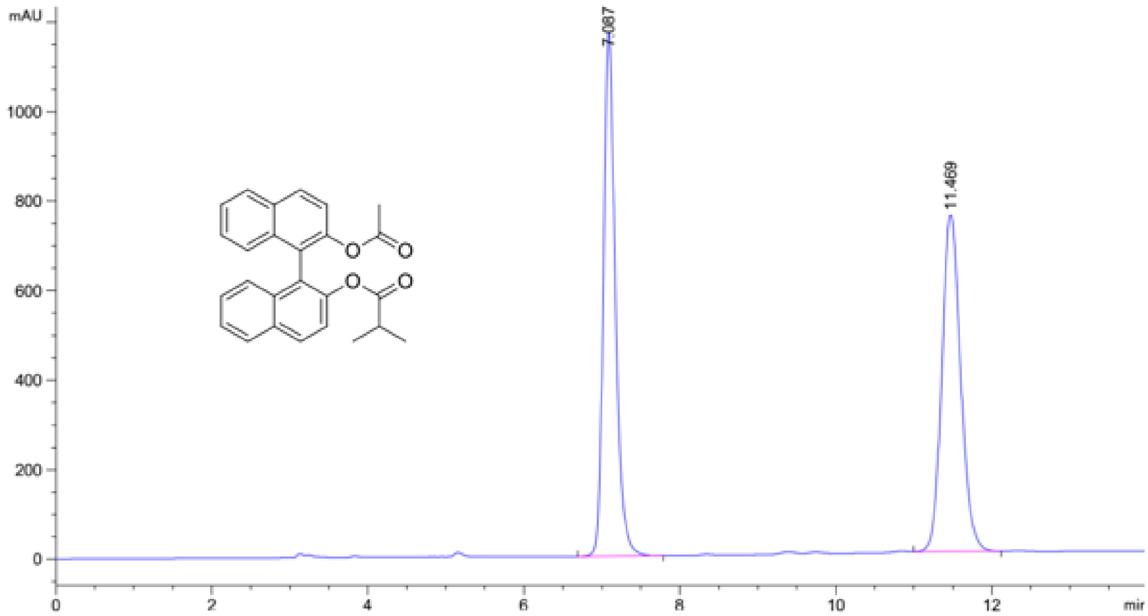

Peak #	RetTime [min]	Type	Width [min]	Area [mAU*s]	Height [mAU]	Area %
1	7.087	BB	0.1625	1.24945e4	1170.51831	49.8174
2	11.469	BB	0.2574	1.25861e4	751.38727	50.1826

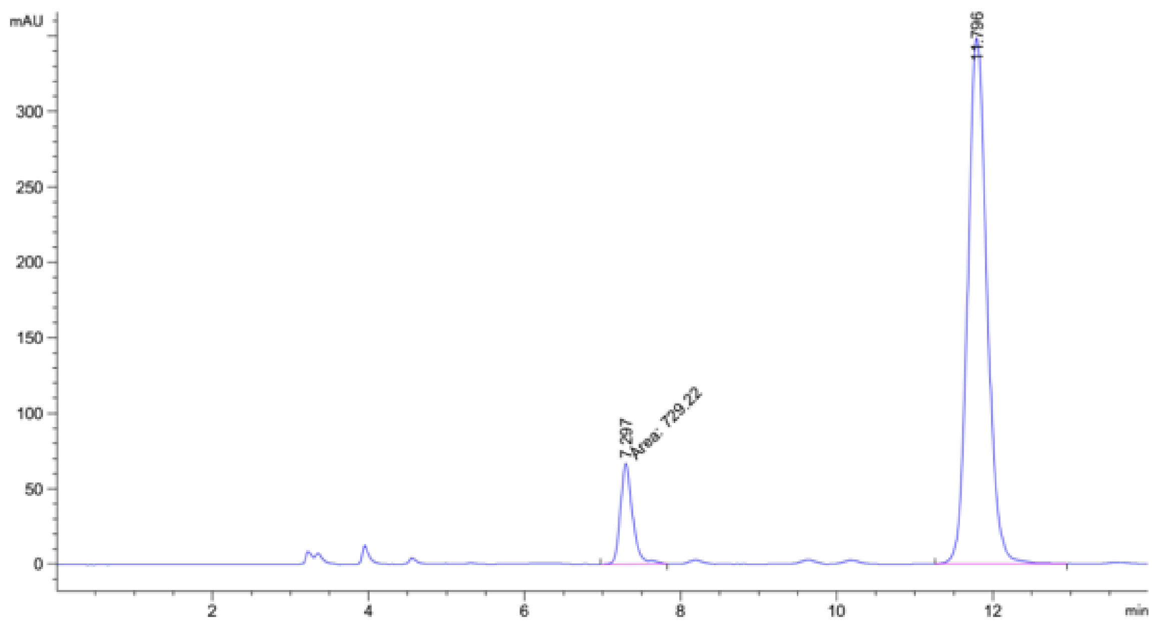

Peak #	RetTime [min]	Type	Width [min]	Area [mAU*s]	Height [mAU]	Area %
1	7.297	MM	0.1816	729.22009	66.91624	10.8805
2	11.796	BB	0.2639	5972.84082	348.52100	89.1195

The result of catalyst 5d´ in continue flow

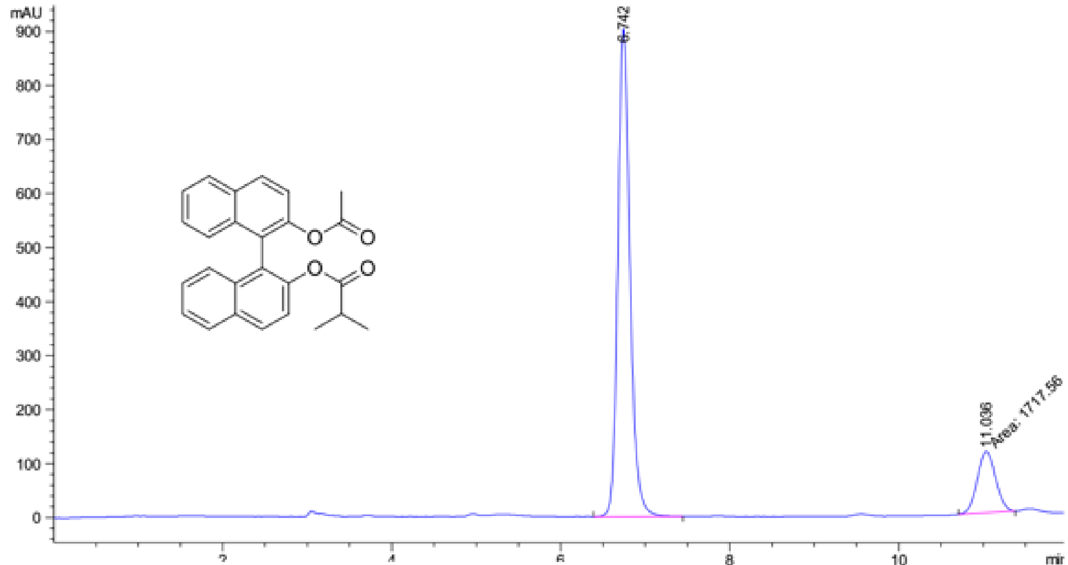

Peak #	Ret Time [min]	Type	Width [min]	Area [mAU*s]	Height [mAU]	Area %
1	6.742	BB	0.1507	9020.01660	901.81744	84.0042
2	11.036	FM	0.2516	1717.56104	113.76506	15.9958

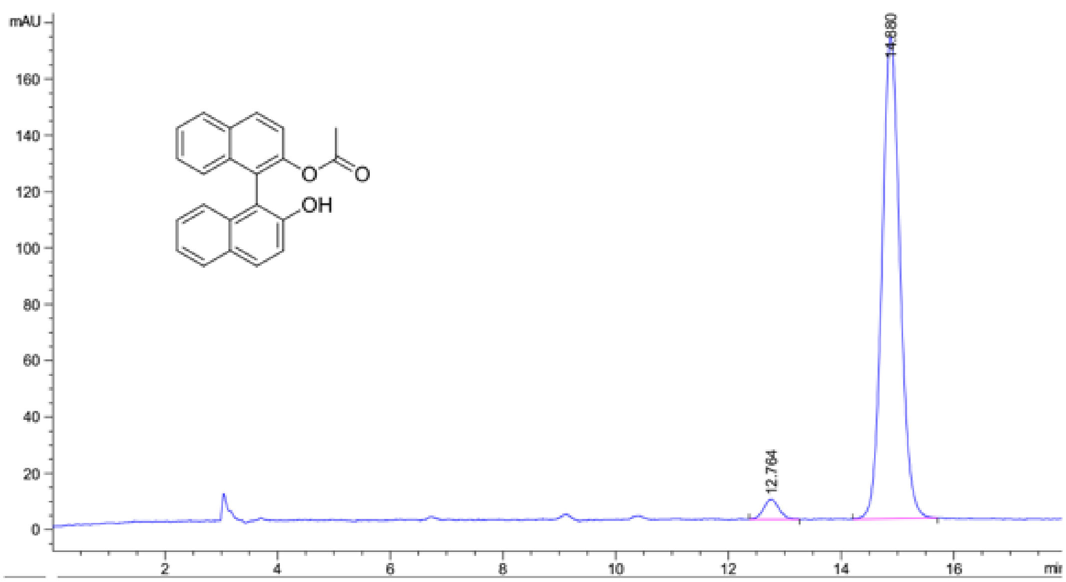

Peak #	Ret Time [min]	Type	Width [min]	Area [mAU*s]	Height [mAU]	Area %
1	12.764	BB	0.2744	133.75186	7.08153	3.3956
2	14.880	BB	0.3458	3805.20801	170.90968	96.6044

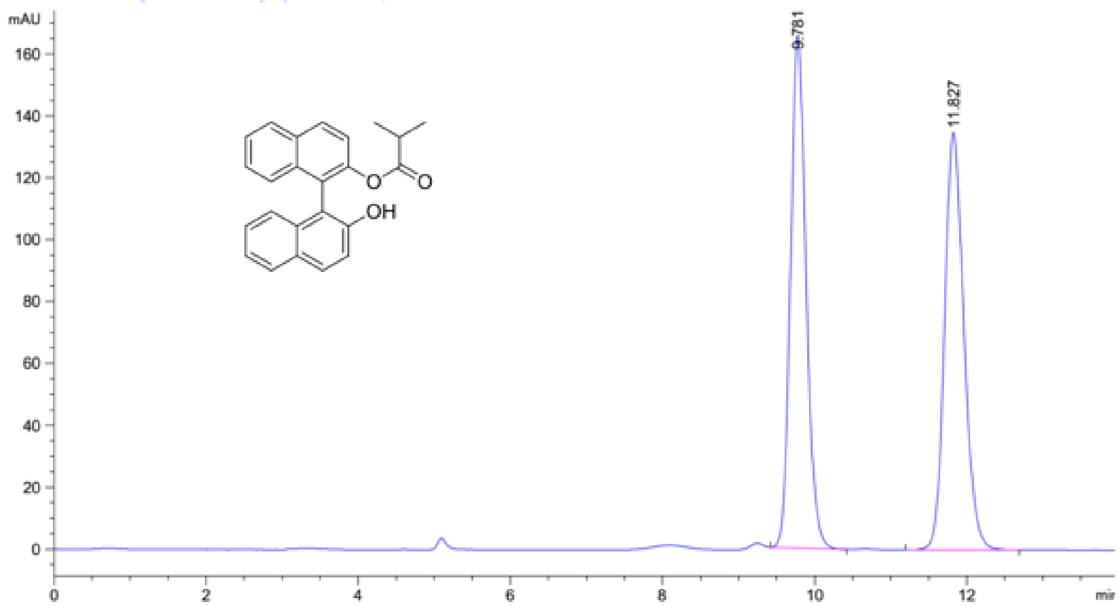

Peak #	RetTime [min]	Type	Width [min]	Area [mAU*s]	Height [mAU]	Area %
1	9.781	BB	0.2173	2345.27539	165.52708	49.7186
2	11.827	BB	0.2713	2371.82373	134.77007	50.2814

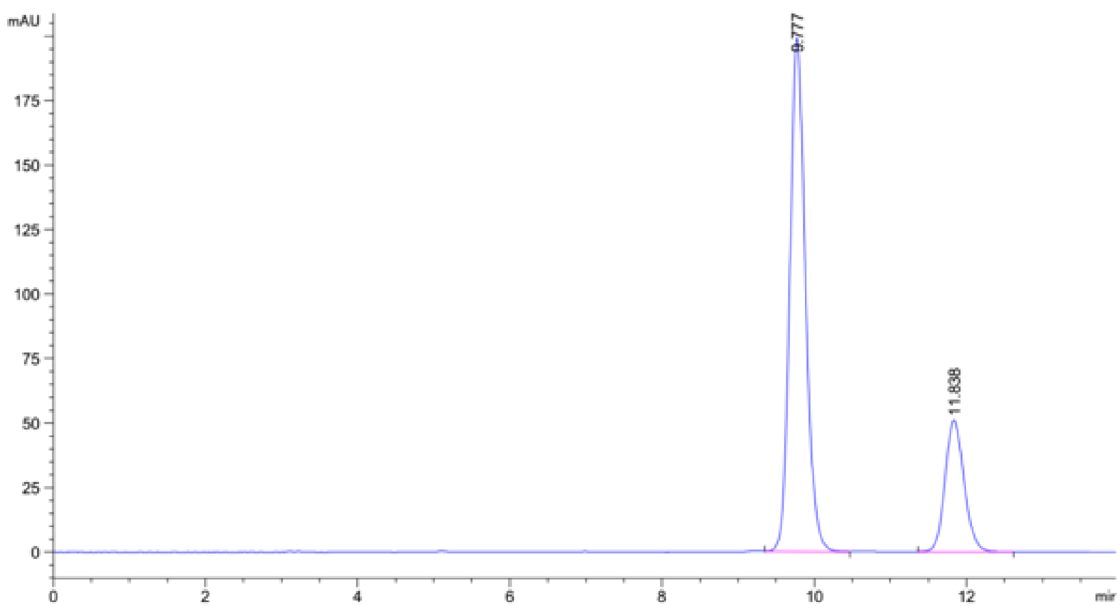

Peak #	RetTime [min]	Type	Width [min]	Area [mAU*s]	Height [mAU]	Area %
1	9.777	BB	0.2185	2837.57544	198.87733	76.1133
2	11.838	BB	0.2675	890.52051	51.06417	23.8867

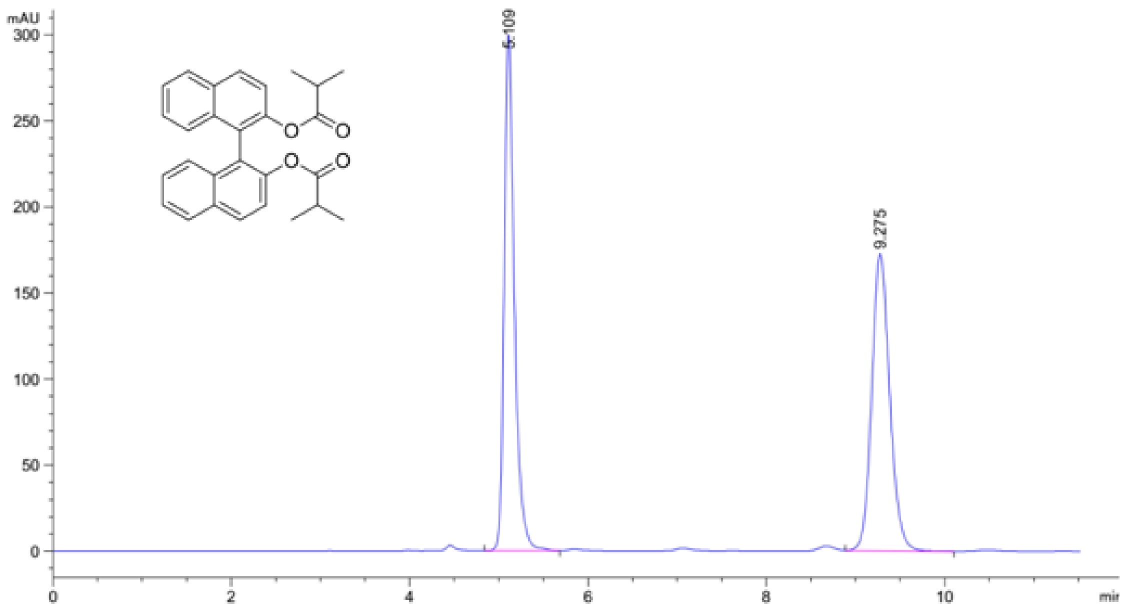

Peak #	RetTime [min]	Type	Width [min]	Area [mAU*s]	Height [mAU]	Area %
1	5.109	BB	0.1187	2387.17334	300.28049	49.7029
2	9.275	BB	0.2153	2415.71069	172.63086	50.2971

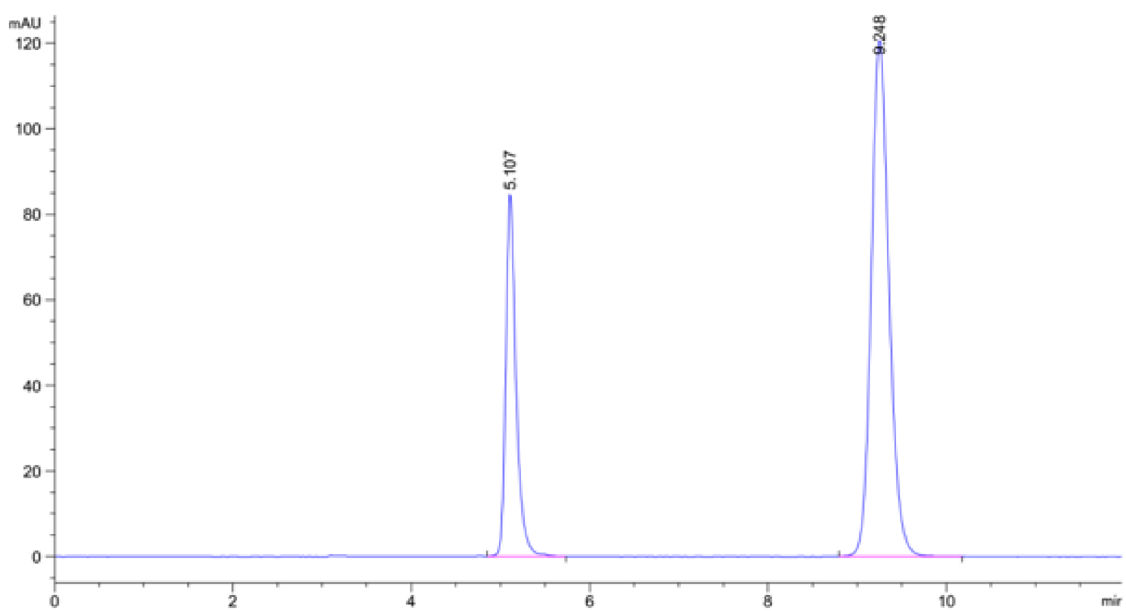

Peak #	RetTime [min]	Type	Width [min]	Area [mAU*s]	Height [mAU]	Area %
1	5.107	BB	0.1194	677.52356	84.61812	28.8301
2	9.248	BB	0.2137	1672.52942	120.67919	71.1699

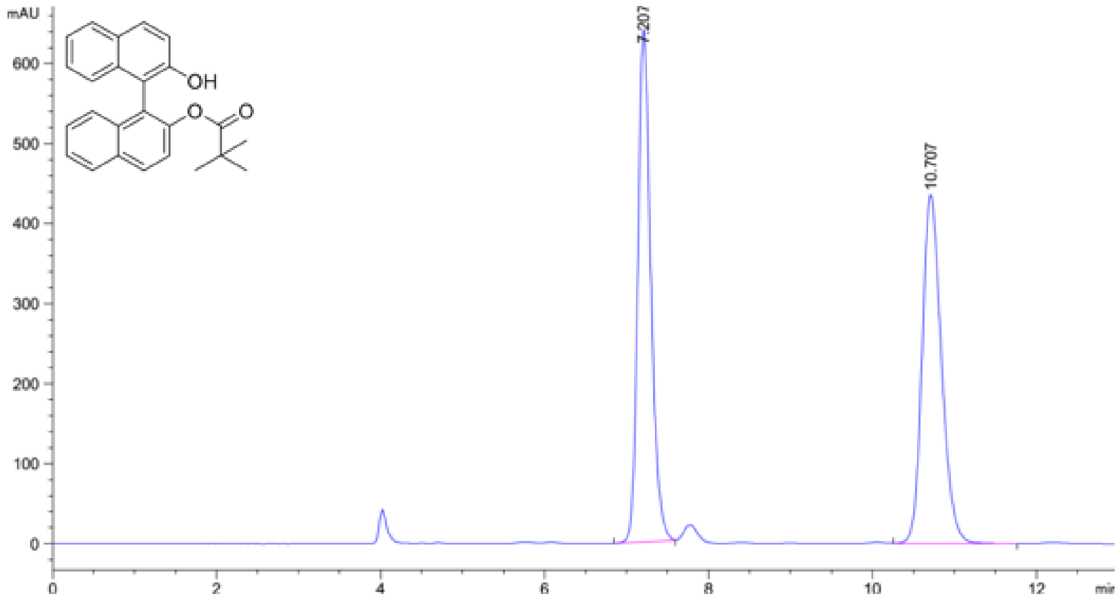

Peak #	RetTime [min]	Type	Width [min]	Area [mAU*s]	Height [mAU]	Area %
1	7.207	BB	0.1680	7027.37500	640.36743	49.5646
2	10.707	BB	0.2535	7150.85010	435.56982	50.4354

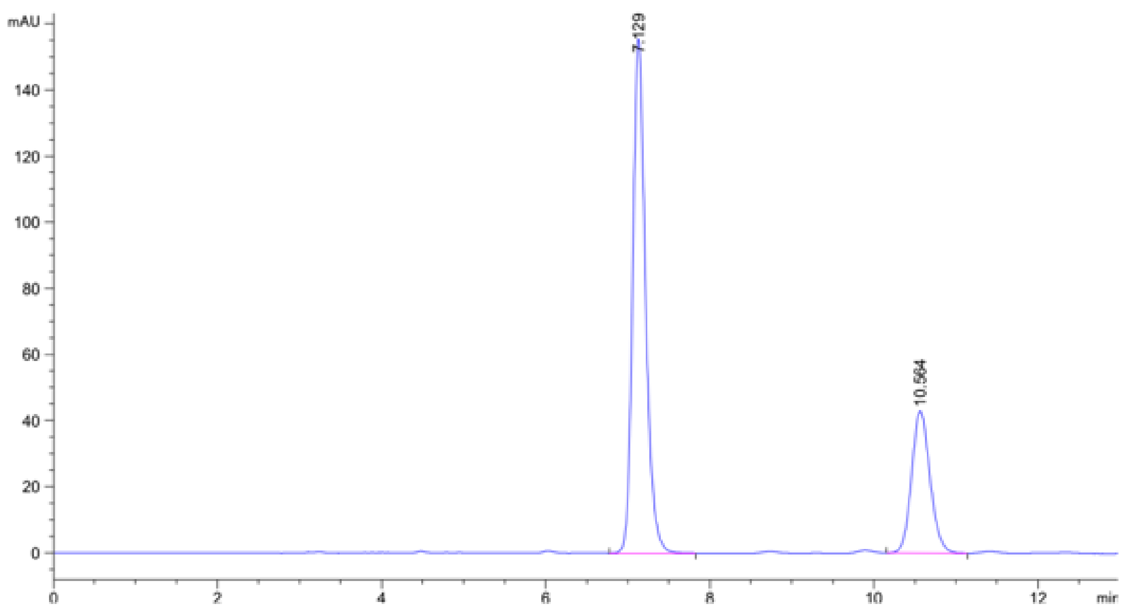

Peak #	RetTime [min]	Type	Width [min]	Area [mAU*s]	Height [mAU]	Area %
1	7.129	BB	0.1669	1693.52197	155.63924	71.6008
2	10.564	BB	0.2403	671.70697	42.98484	28.3992

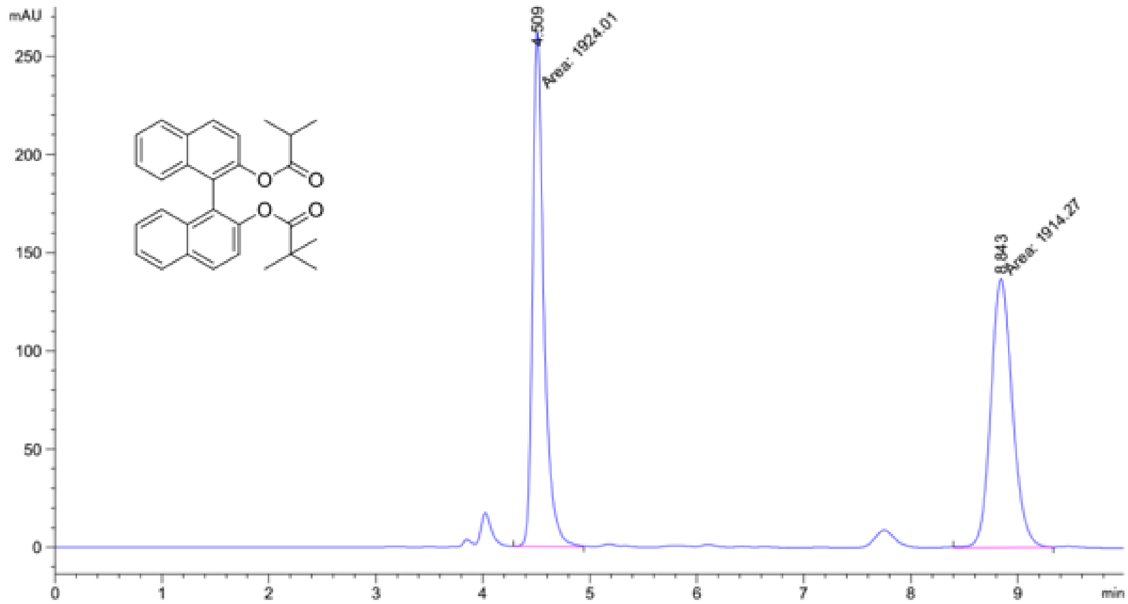

Peak #	RetTime [min]	Type	Width [min]	Area [mAU*s]	Height [mAU]	Area %
1	4.509	MF	0.1222	1924.00916	262.42426	50.1269
2	8.843	FM	0.2332	1914.26831	136.79175	49.8731

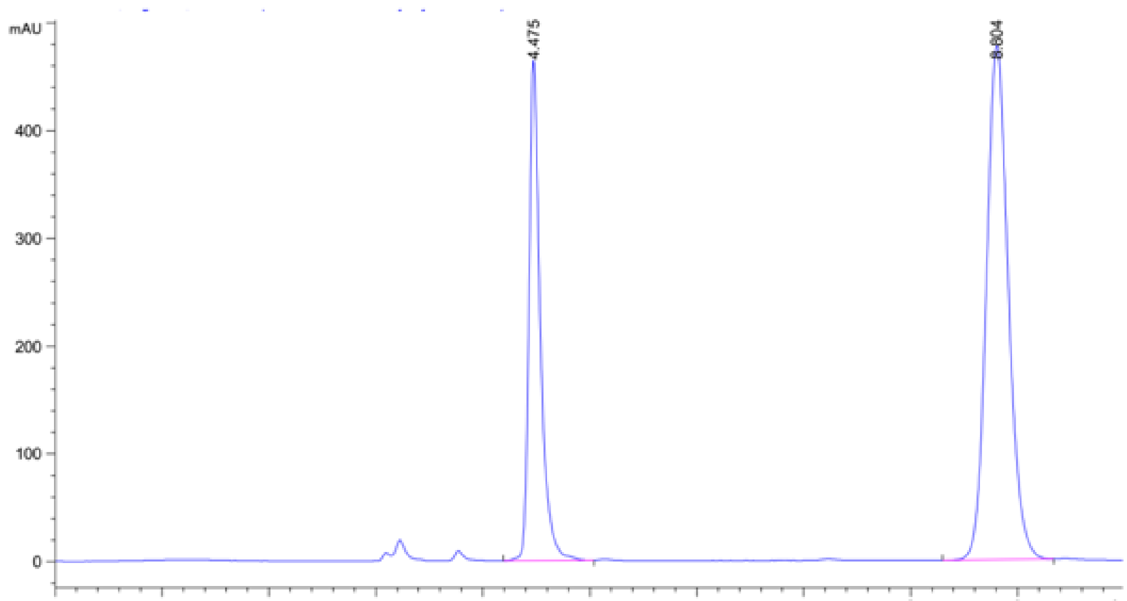

Peak #	RetTime [min]	Type	Width [min]	Area [mAU*s]	Height [mAU]	Area %
1	4.475	BB	0.1077	3410.00293	464.46292	33.4218
2	8.804	BB	0.2181	6792.93457	477.20874	66.5782

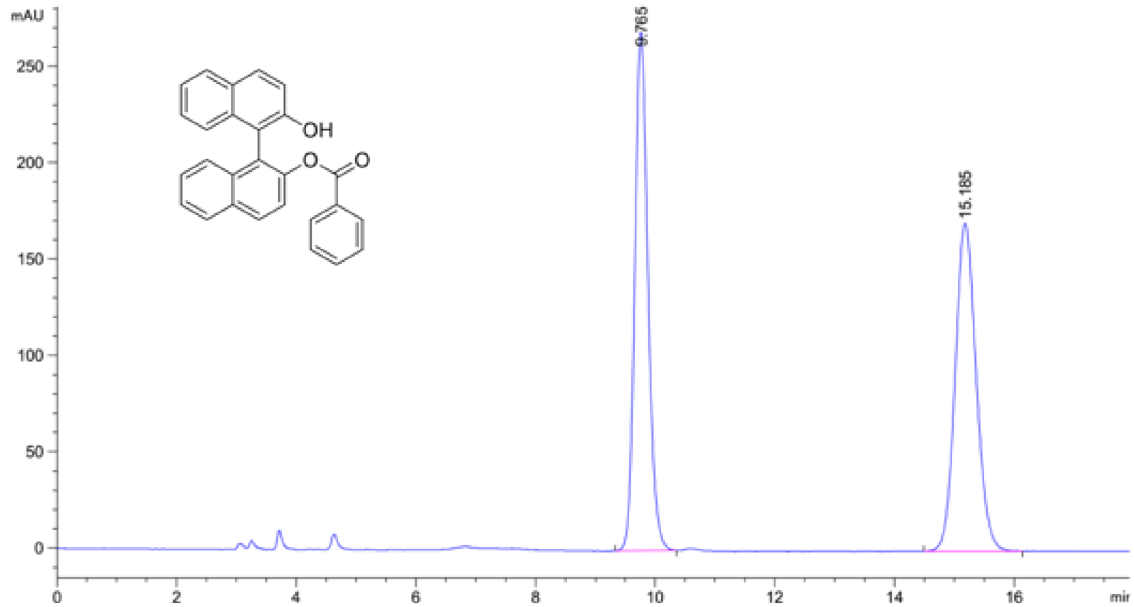

Peak #	RetTime [min]	Type	Width [min]	Area [mAU*s]	Height [mAU]	Area %
1	9.765	BB	0.2349	4125.72266	269.08008	49.8682
2	15.185	BB	0.3743	4147.53223	170.17354	50.1318

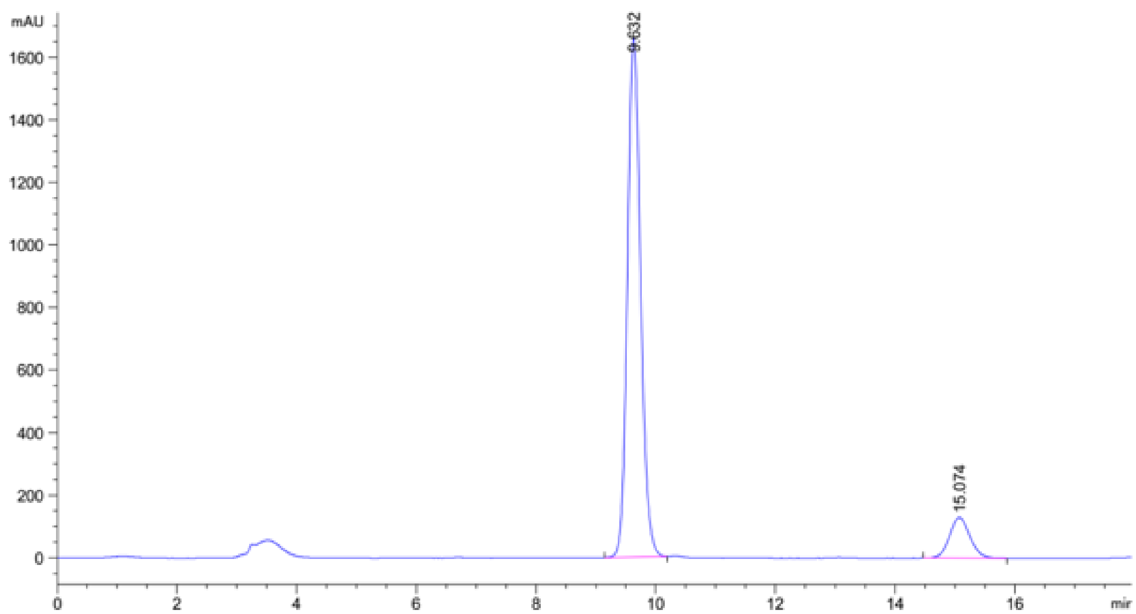

Peak #	RetTime [min]	Type	Width [min]	Area [mAU*s]	Height [mAU]	Area %
1	9.632	BB	0.2389	2.54527e4	1659.53333	89.2307
2	15.074	BB	0.3689	3071.90747	129.42276	10.7693

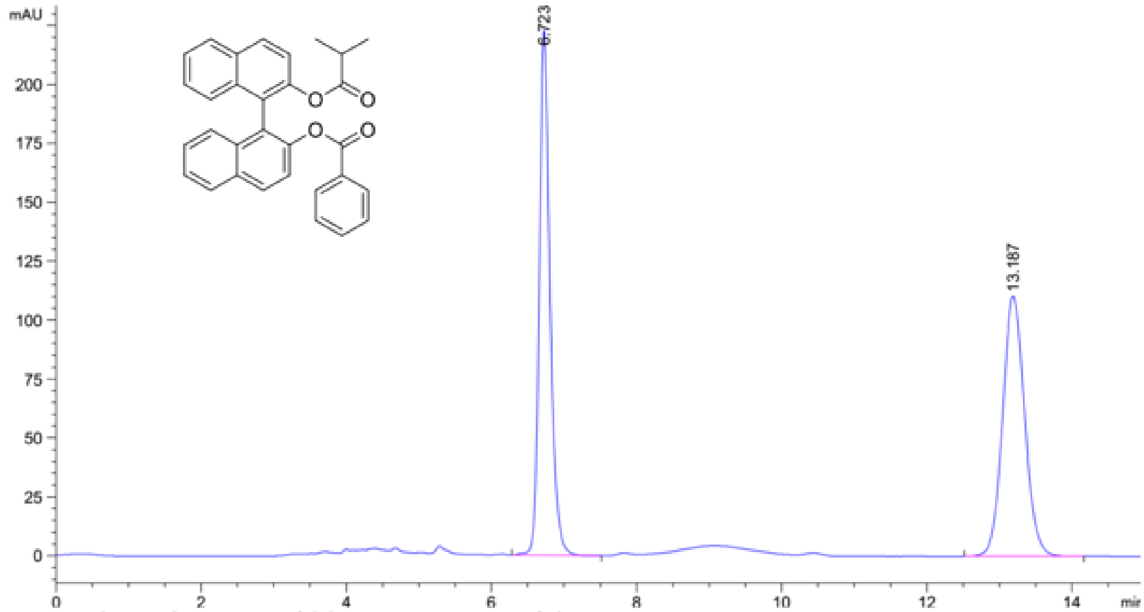

Peak #	RetTime [min]	Type	Width [min]	Area [mAU*s]	Height [mAU]	Area %
1	6.723	BB	0.1578	2320.31372	222.30287	49.9815
2	13.187	BB	0.3255	2322.02856	110.32584	50.0185

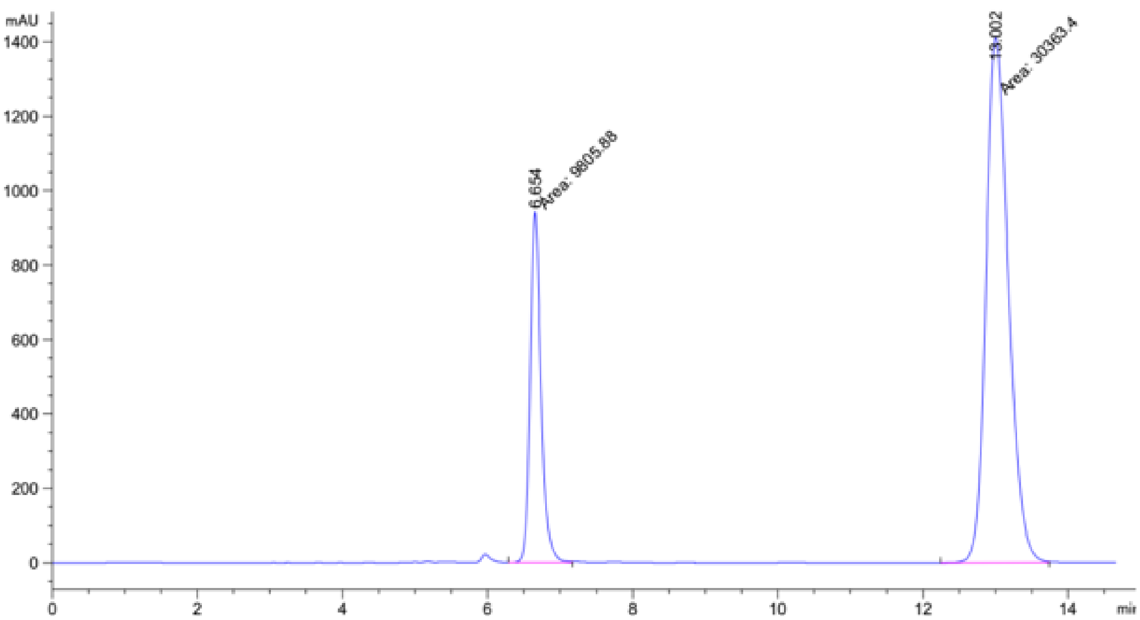

Peak #	RetTime [min]	Type	Width [min]	Area [mAU*s]	Height [mAU]	Area %
1	6.654	MF	0.1737	9805.88086	941.02795	24.4114
2	13.002	MF	0.3584	3.03634e4	1411.87000	75.5886

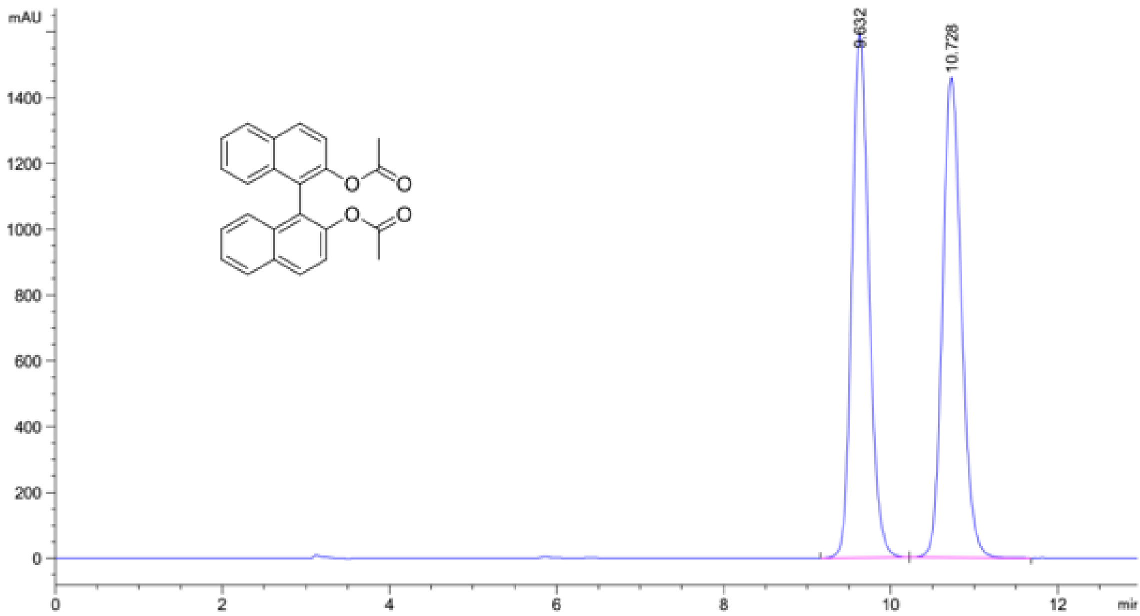

Peak #	RetTime [min]	Type	Width [min]	Area [mAU*s]	Height [mAU]	Area %
1	9.632	BB	0.2221	2.26580e4	1591.47412	49.6749
2	10.728	BB	0.2456	2.29546e4	1458.75085	50.3251

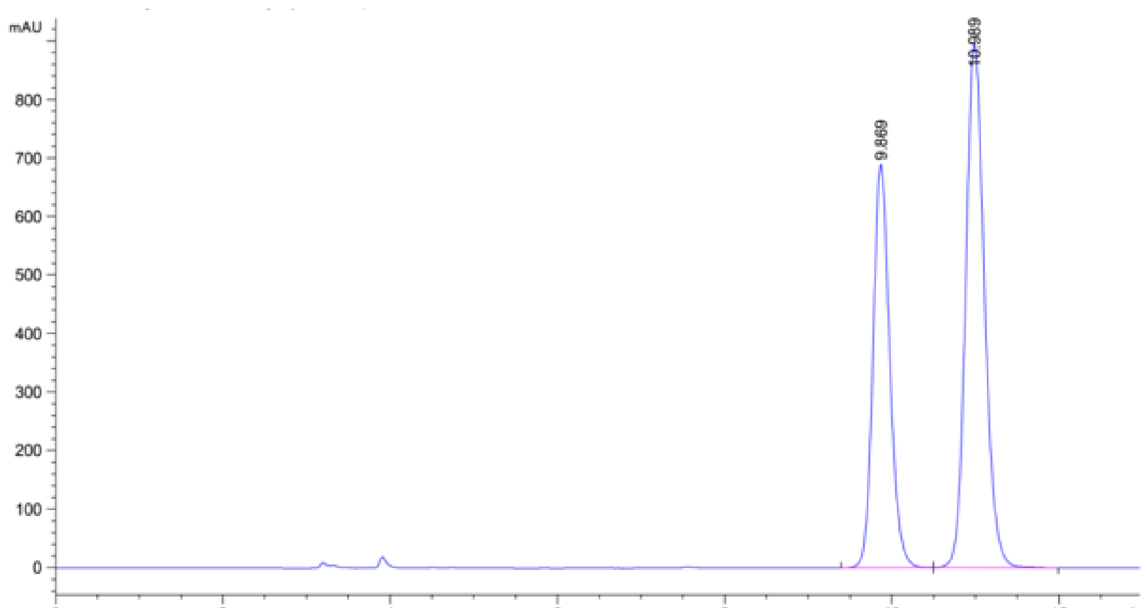

Peak #	RetTime [min]	Type	Width [min]	Area [mAU*s]	Height [mAU]	Area %
1	9.869	BB	0.2124	9593.43359	689.03296	40.7533
2	10.989	BB	0.2399	1.39468e4	894.38831	59.2467

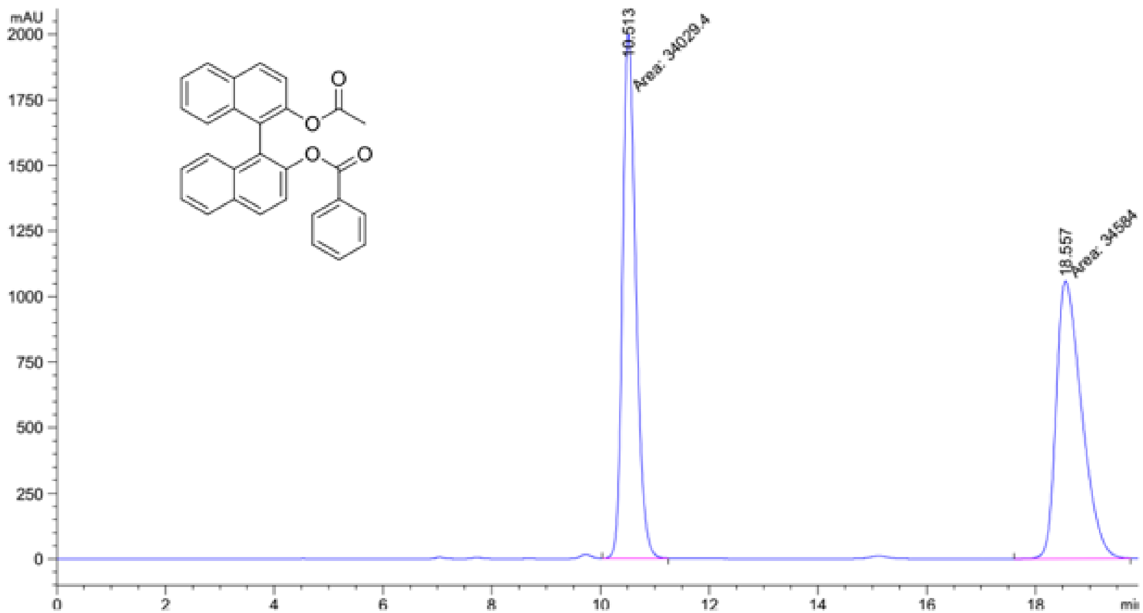

Peak #	RetTime [min]	Type	Width [min]	Area [mAU*s]	Height [mAU]	Area %
1	10.513	MF	0.2837	3.40294e4	1999.32153	49.5958
2	18.557	MF	0.5444	3.45840e4	1058.69482	50.4042

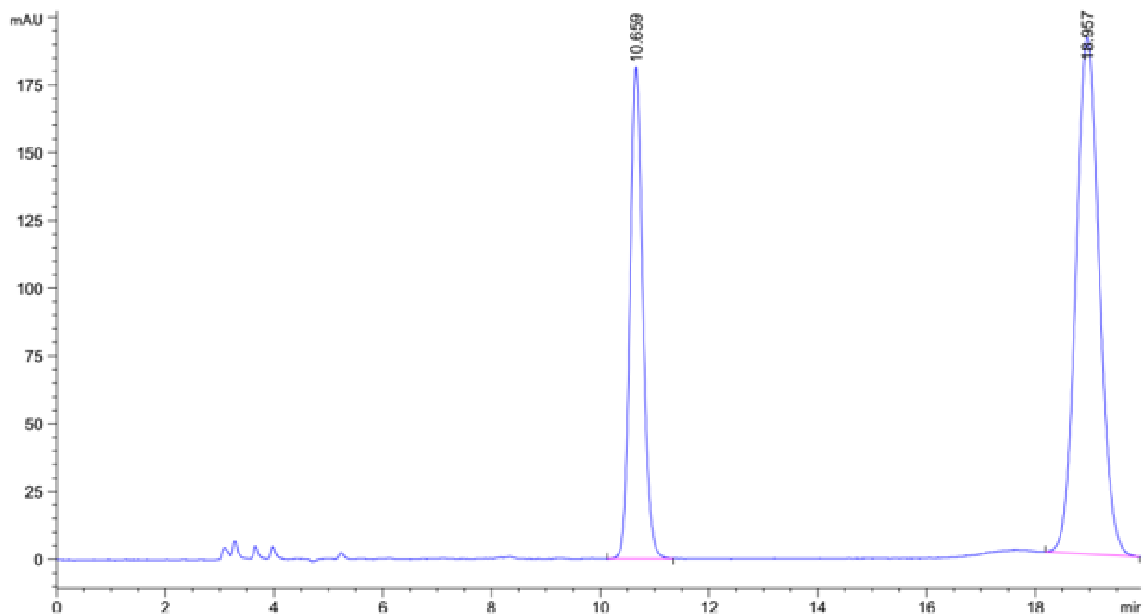

Peak #	RetTime [min]	Type	Width [min]	Area [mAU*s]	Height [mAU]	Area %
1	10.659	BB	0.2532	2970.30420	181.28345	34.2793
2	18.957	BB	0.4624	5694.69971	190.71109	65.7207

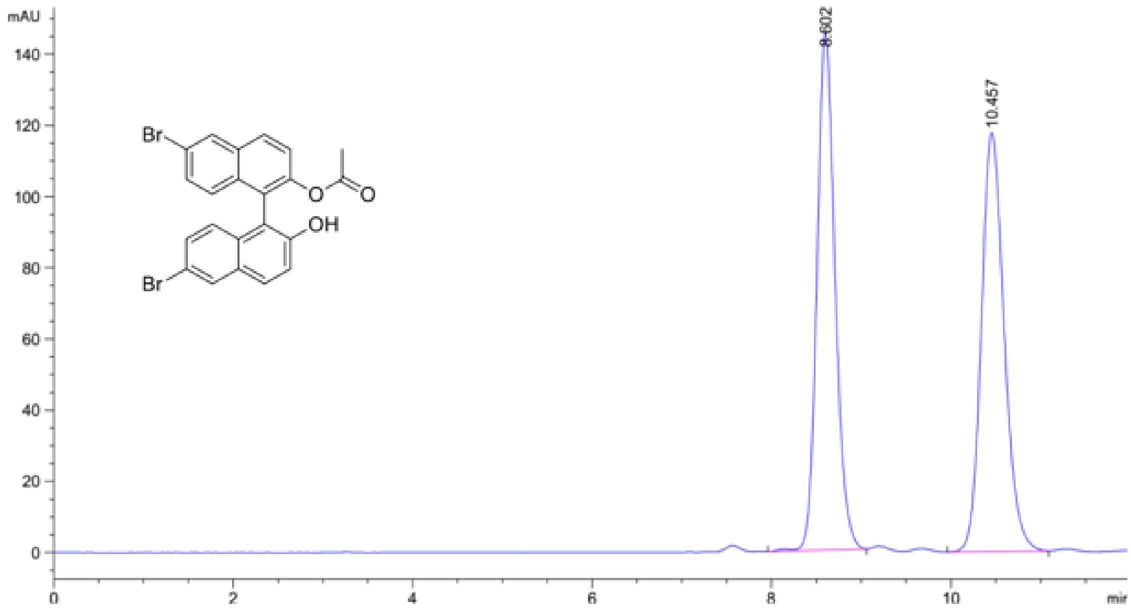

Peak #	RetTime [min]	Type	Width [min]	Area [mAU*s]	Height [mAU]	Area %
1	8.602	BB	0.2138	2038.79004	145.19525	49.4984
2	10.457	BB	0.2722	2080.11401	117.71638	50.5016

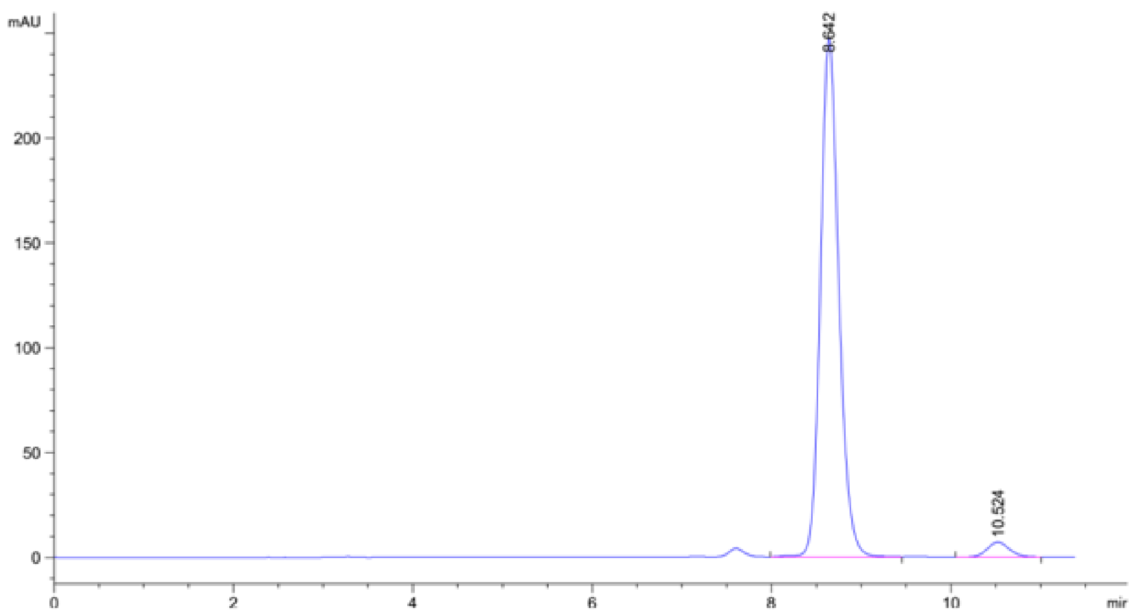

Peak #	RetTime [min]	Type	Width [min]	Area [mAU*s]	Height [mAU]	Area %
1	8.642	BB	0.2207	3531.91431	247.13925	96.6113
2	10.524	BB	0.2599	123.88401	7.15709	3.3887

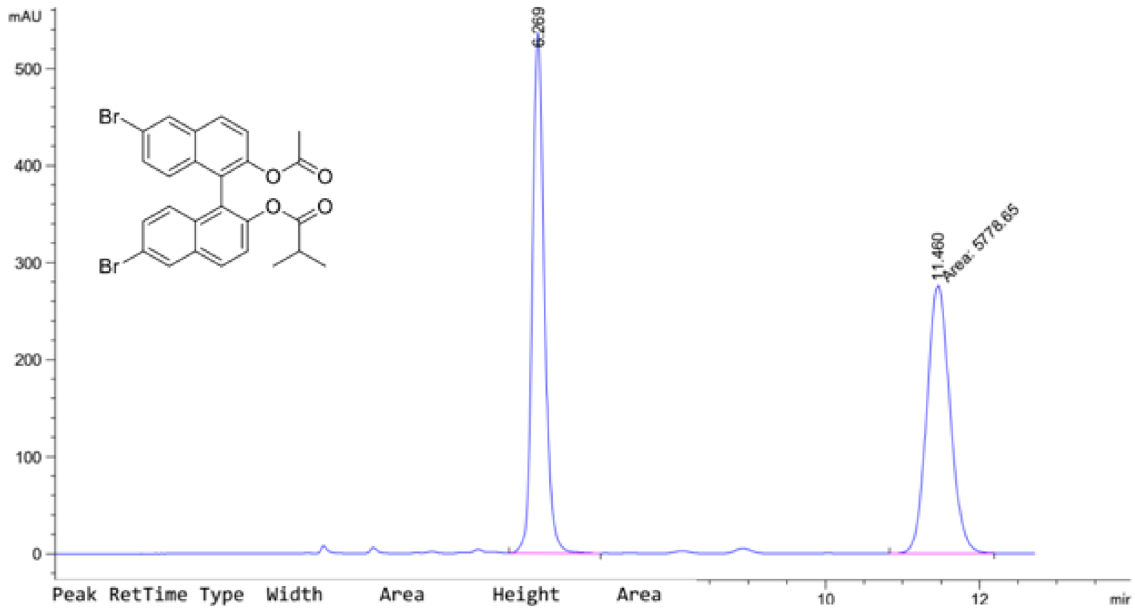

Peak #	RetTime [min]	Type	Width [min]	Area [mAU*s]	Height [mAU]	Area %
1	6.269	BB	0.1643	5798.60938	535.64050	50.0862
2	11.460	MF	0.3488	5778.65137	276.10025	49.9138

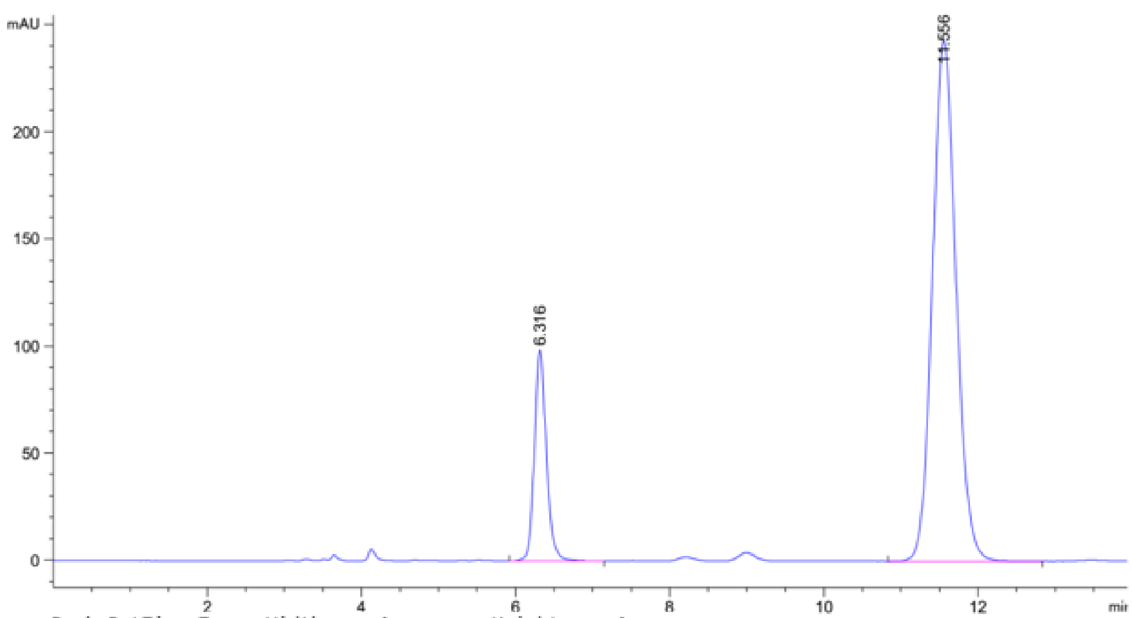

Peak #	RetTime [min]	Type	Width [min]	Area [mAU*s]	Height [mAU]	Area %
1	6.316	BB	0.1646	1069.10767	98.51842	17.1477
2	11.556	BB	0.3301	5165.59473	242.94791	82.8523

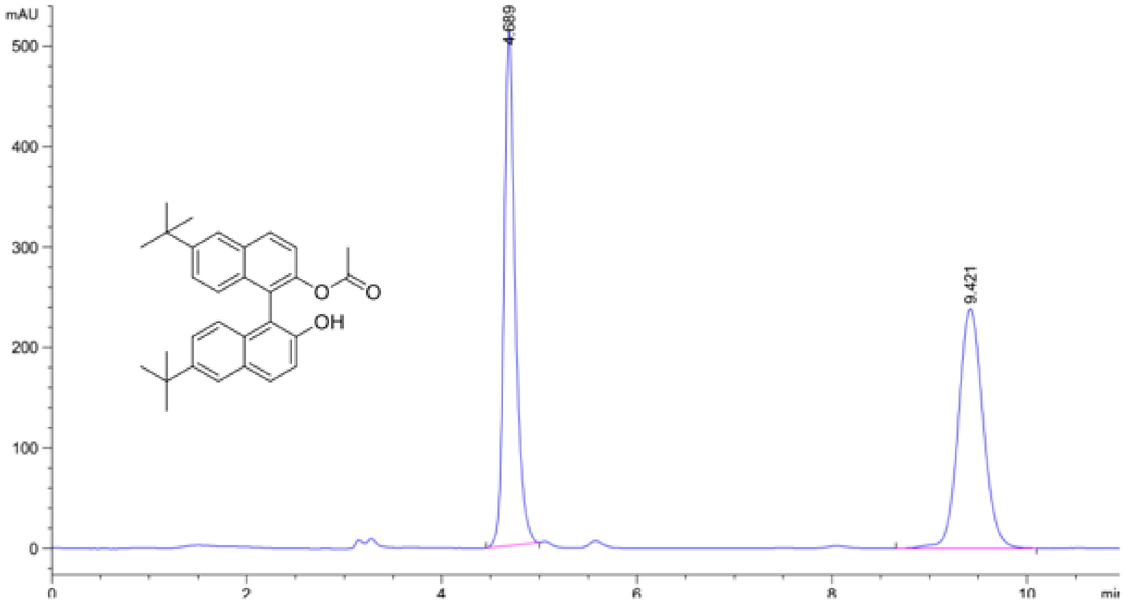

Peak #	RetTime [min]	Type	Width [min]	Area [mAU*s]	Height [mAU]	Area %
1	4.689	BB	0.1199	4122.69092	512.33838	49.5979
2	9.421	BB	0.2712	4189.54150	238.24367	50.4021

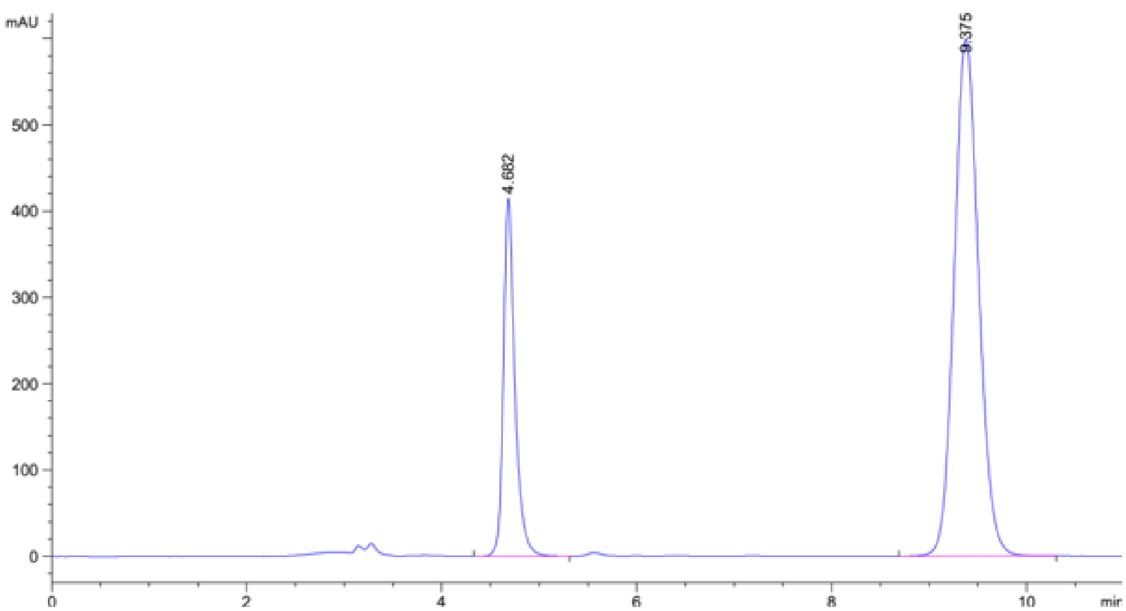

Peak #	RetTime [min]	Type	Width [min]	Area [mAU*s]	Height [mAU]	Area %
1	4.682	BB	0.1235	3397.33154	415.06268	24.5525
2	9.375	BB	0.2692	1.04397e4	599.40875	75.4475

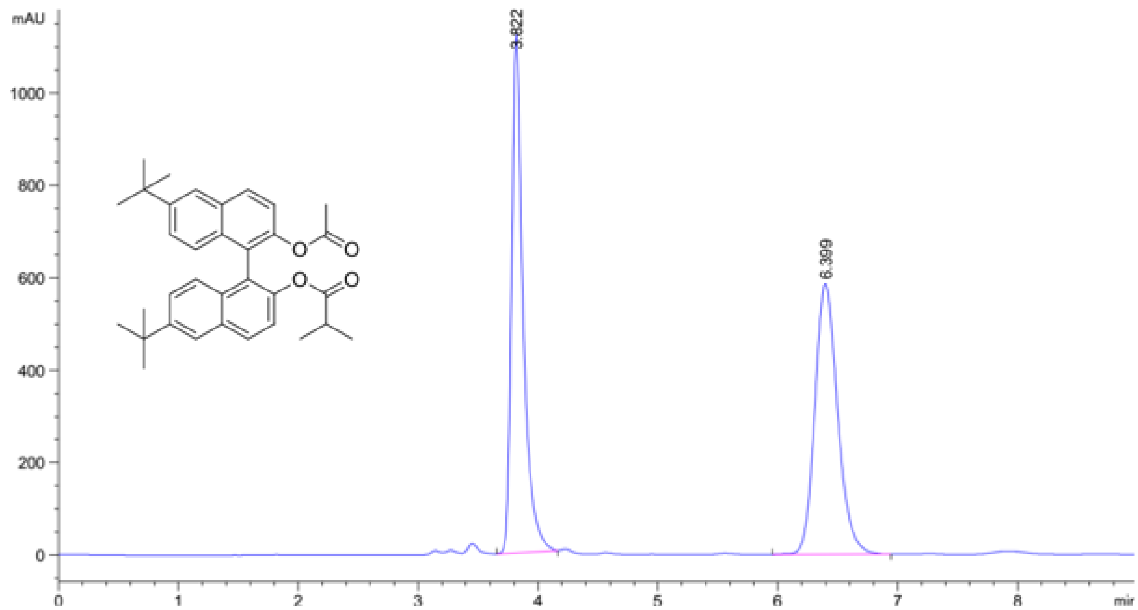

Peak #	RetTime [min]	Type	Width [min]	Area [mAU*s]	Height [mAU]	Area %
1	3.822	BB	0.0988	7566.61914	1120.22461	49.4880
2	6.399	BB	0.2019	7723.17627	585.47687	50.5120

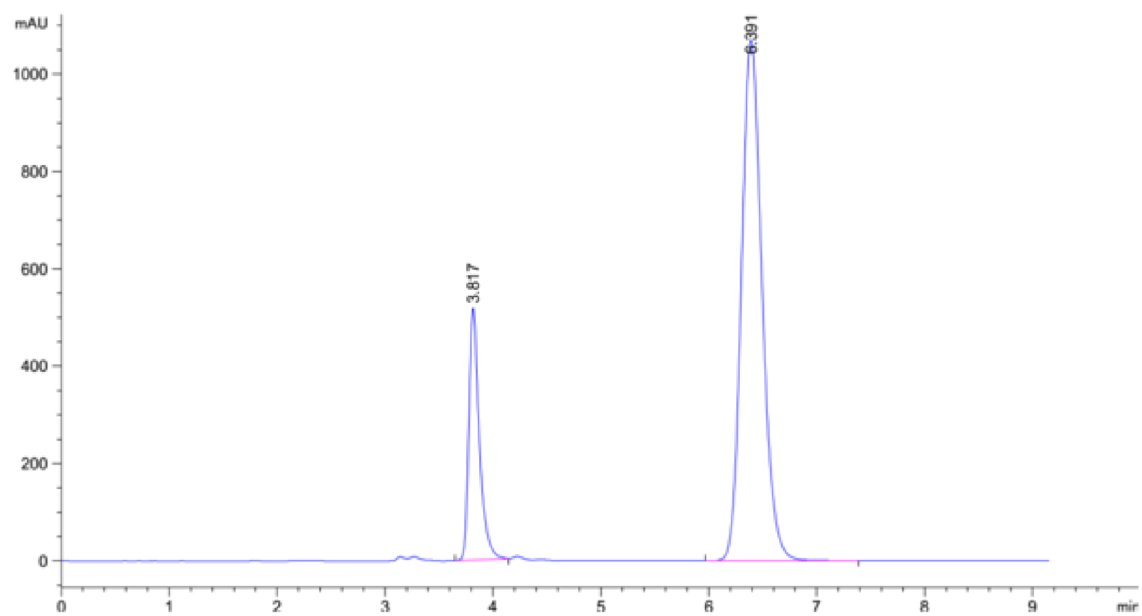

Peak #	RetTime [min]	Type	Width [min]	Area [mAU*s]	Height [mAU]	Area %
1	3.817	BB	0.0977	3454.08691	518.72284	19.5896
2	6.391	BB	0.2046	1.41782e4	1070.15125	80.4104

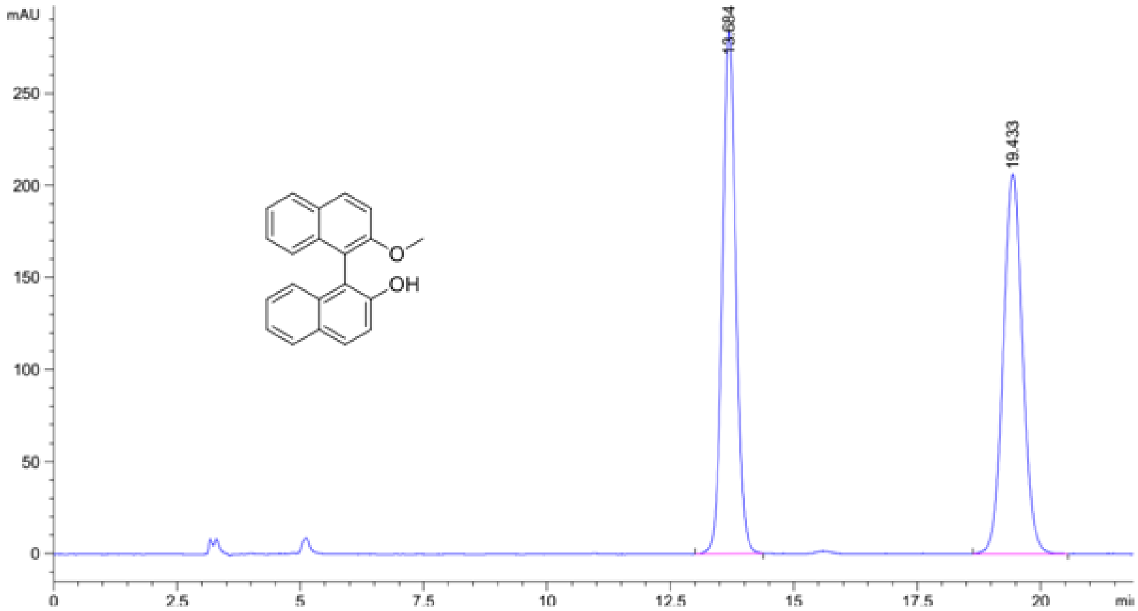

Peak #	RetTime [min]	Type	Width [min]	Area [mAU*s]	Height [mAU]	Area %
1	13.684	BB	0.2948	5413.35791	283.48343	49.0786
2	19.433	BB	0.4198	5616.60938	206.21181	50.9214

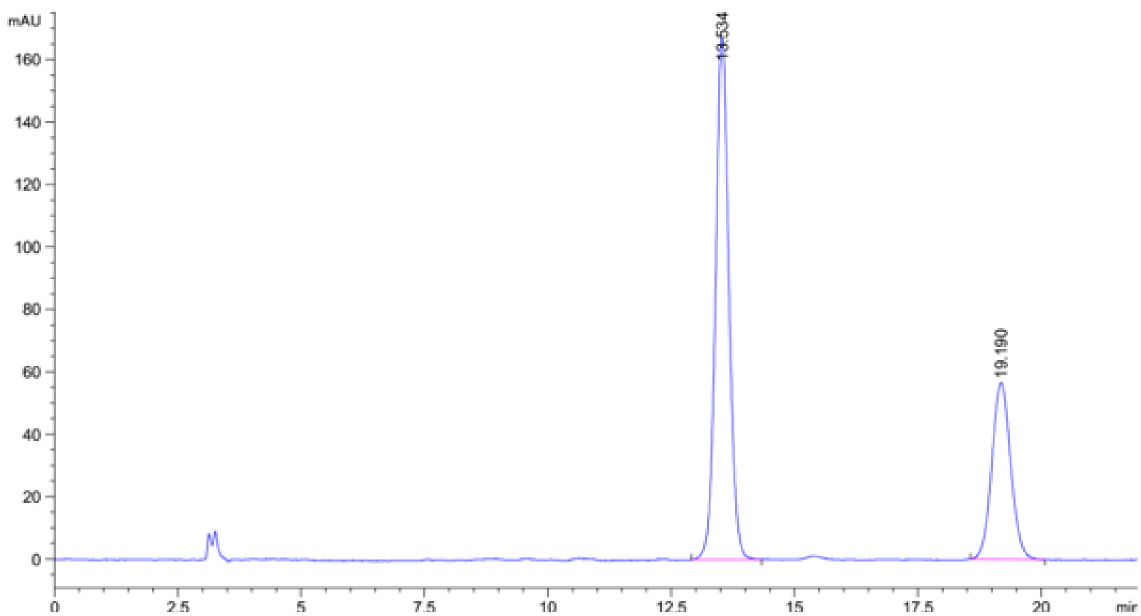

Peak #	RetTime [min]	Type	Width [min]	Area [mAU*s]	Height [mAU]	Area %
1	13.534	BB	0.2881	3153.56299	167.17210	67.7110
2	19.190	BB	0.4078	1503.82275	56.63585	32.2890

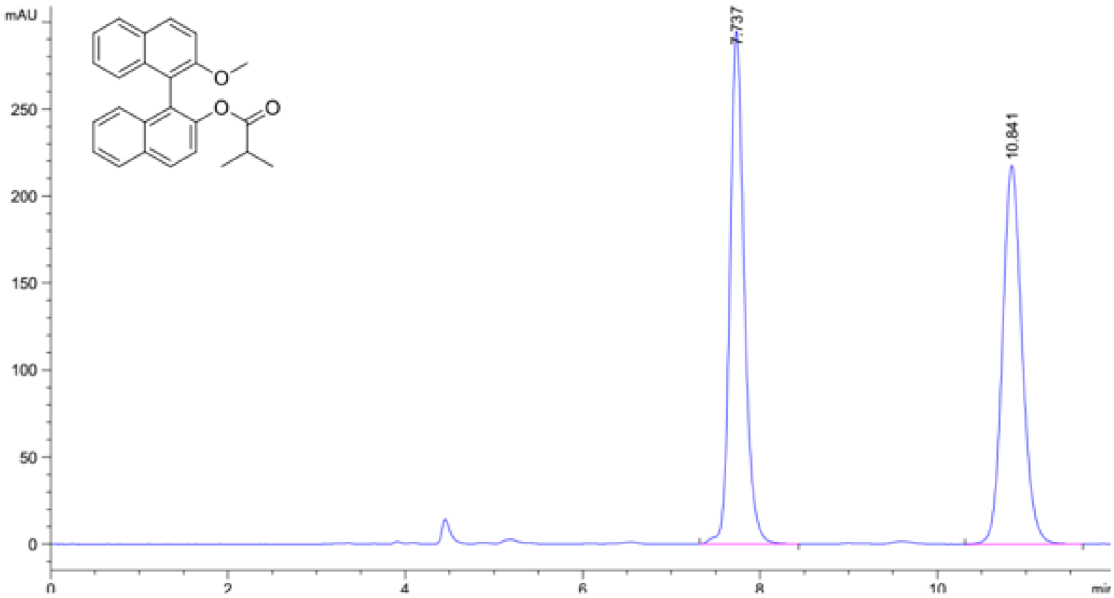

Peak #	RetTime [min]	Type	Width [min]	Area [mAU*s]	Height [mAU]	Area %
1	7.737	BB	0.1714	3315.38501	294.44278	49.7603
2	10.841	BB	0.2373	3347.32104	217.76512	50.2397

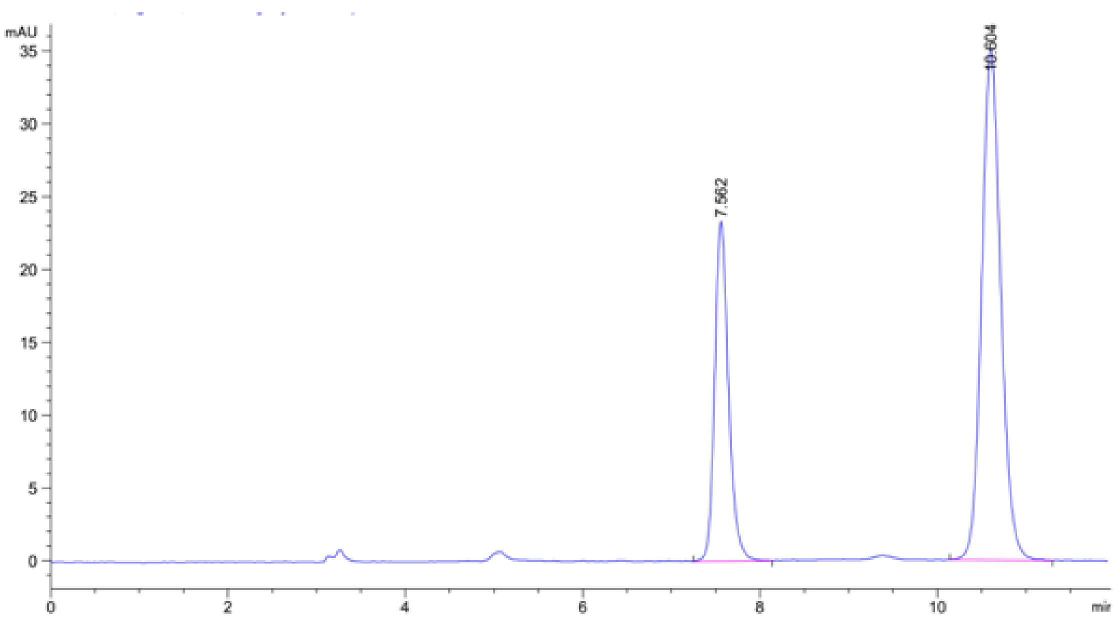

Peak #	RetTime [min]	Type	Width [min]	Area [mAU*s]	Height [mAU]	Area %
1	7.562	BB	0.1647	252.78839	23.28018	32.3860
2	10.604	BB	0.2316	527.76105	35.06016	67.6140

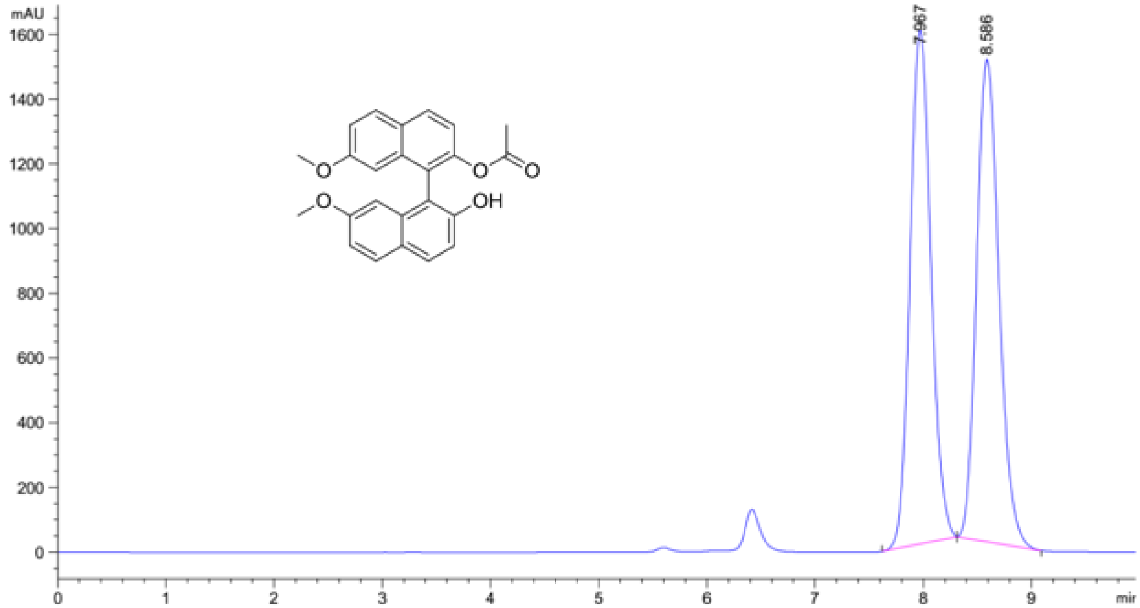

Peak #	RetTime [min]	Type	Width [min]	Area [mAU*s]	Height [mAU]	Area %
1	7.967	BB	0.2092	2.13849e4	1586.86646	49.9071
2	8.586	BBA	0.2241	2.14645e4	1489.40540	50.0929

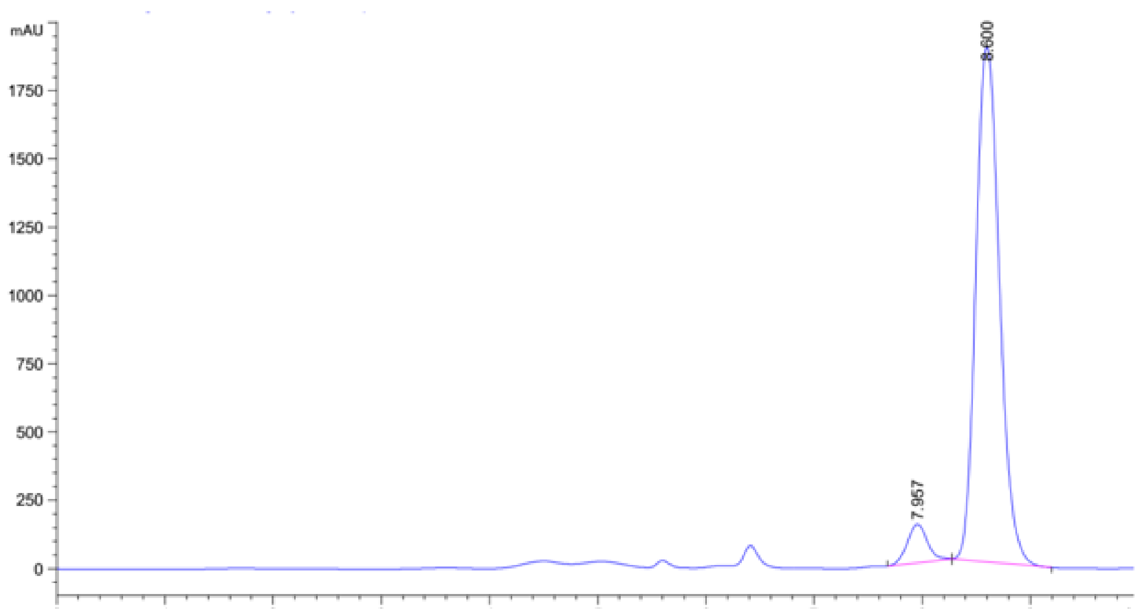

Peak #	RetTime [min]	Type	Width [min]	Area [mAU*s]	Height [mAU]	Area %
1	7.957	BB	0.1959	1811.55444	140.95947	5.9428
2	8.600	BB	0.2394	2.86718e4	1885.17419	94.0572

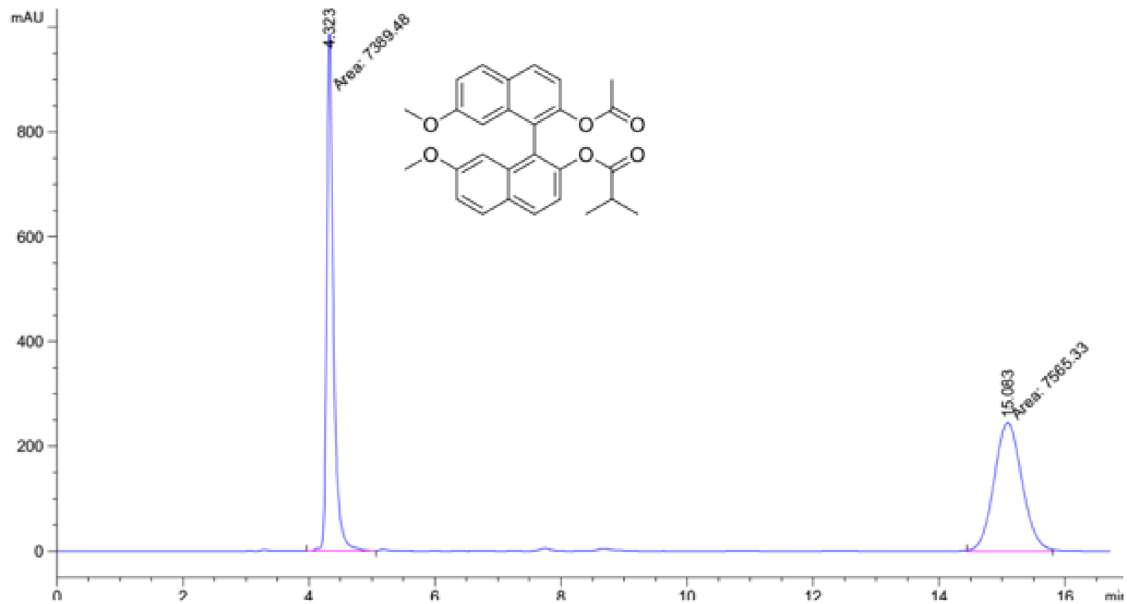

Peak #	RetTime [min]	Type	Width [min]	Area [mAU*s]	Height [mAU]	Area %
1	4.323	MM	0.1247	7389.48047	987.57294	49.4121
2	15.083	MF	0.5146	7565.33301	245.01817	50.5879

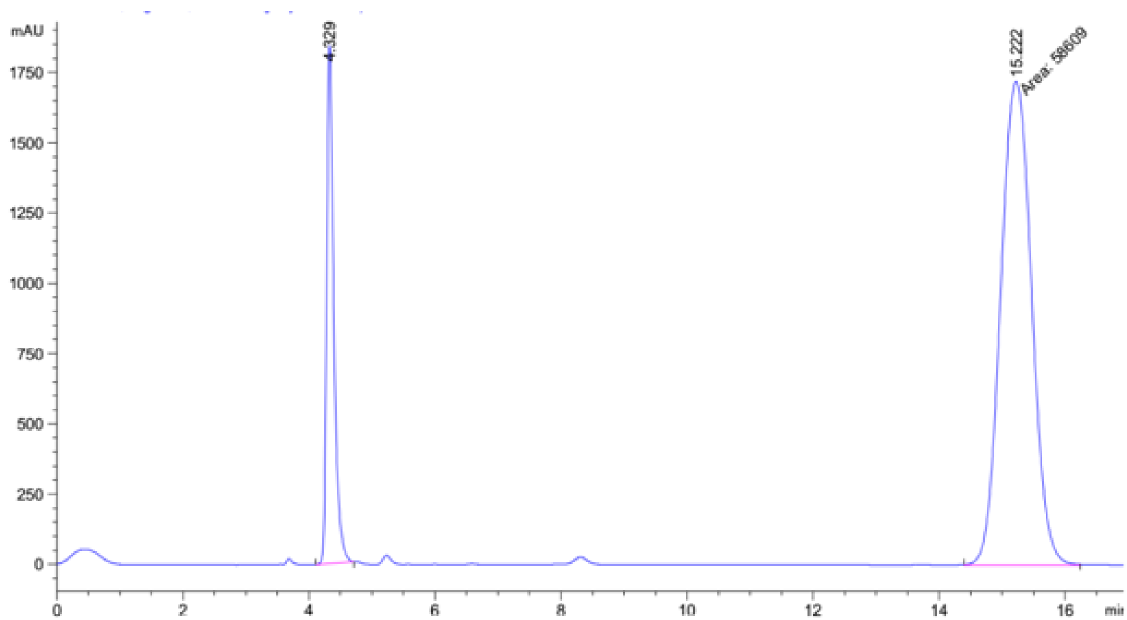

Peak #	RetTime [min]	Type	Width [min]	Area [mAU*s]	Height [mAU]	Area %
1	4.329	BB	0.1211	1.46575e4	1836.81372	20.0057
2	15.222	FM	0.5679	5.86090e4	1720.16174	79.9943

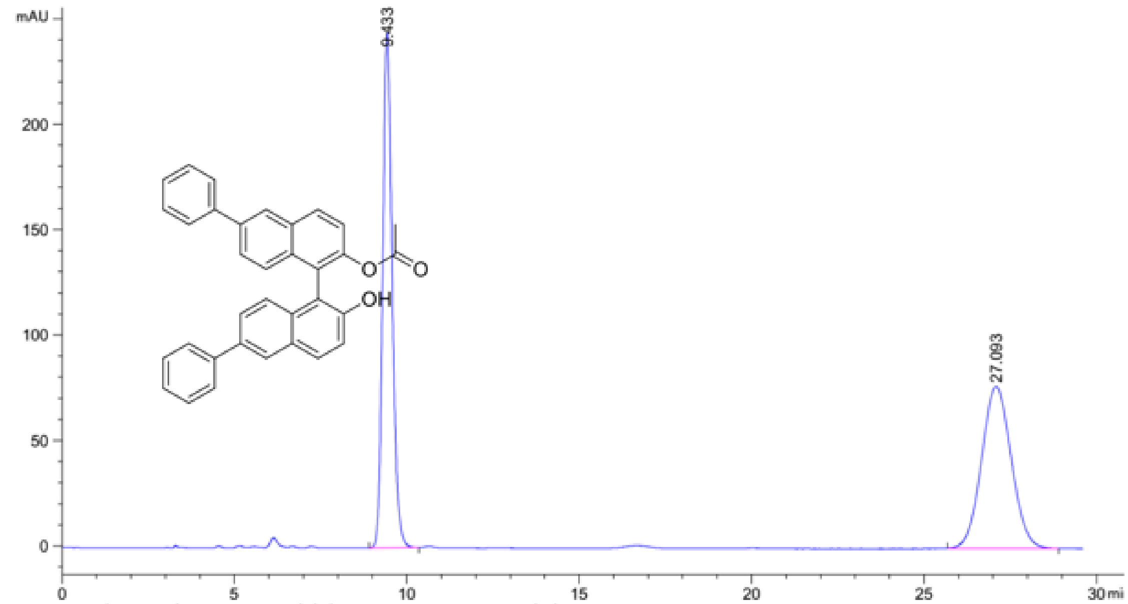

Peak #	RetTime [min]	Type	Width [min]	Area [mAU*s]	Height [mAU]	Area %
1	9.433	BB	0.2928	4661.43652	244.11710	50.3492
2	27.093	BB	0.9033	4596.77100	76.69217	49.6508

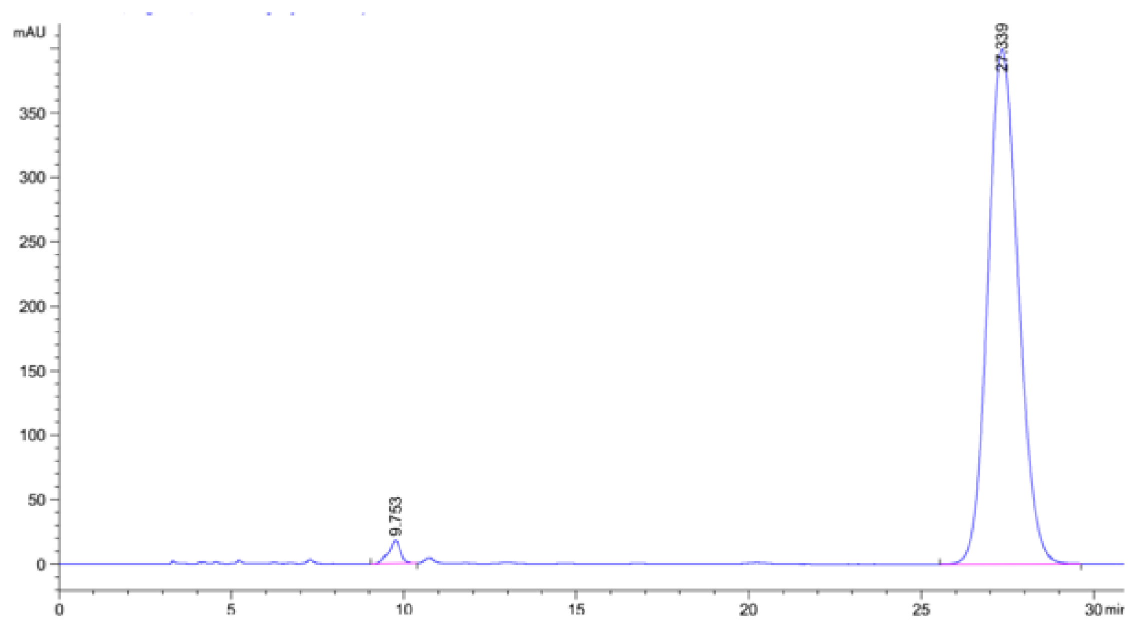

Peak #	RetTime [min]	Type	Width [min]	Area [mAU*s]	Height [mAU]	Area %
1	9.753	BB	0.3452	429.01816	17.92729	1.7195
2	27.339	BB	0.9440	2.45209e4	399.52658	98.2805

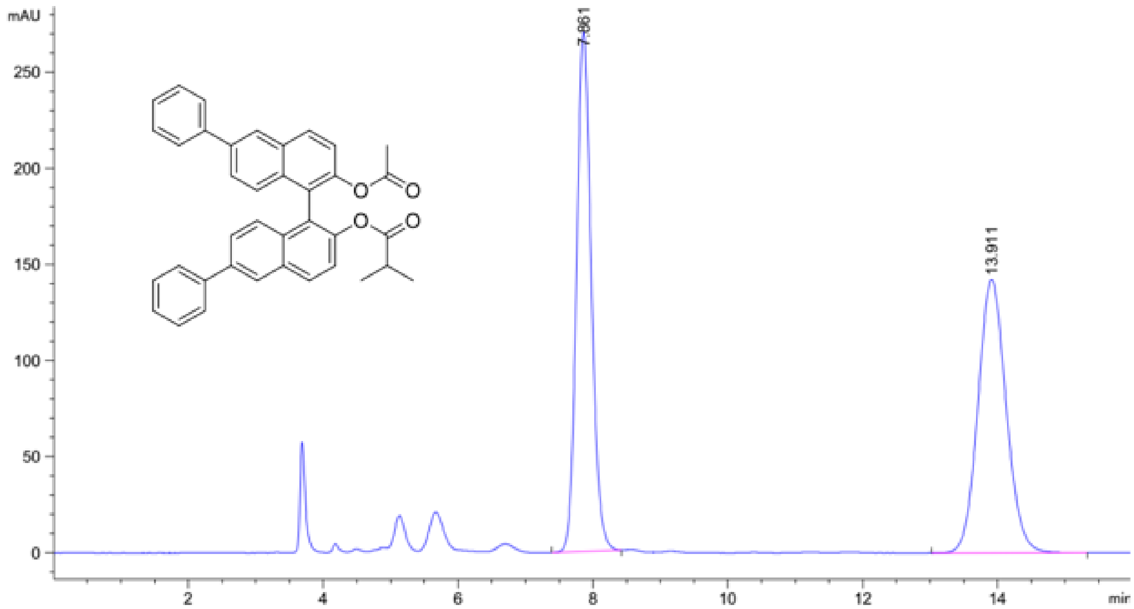

Peak #	RetTime [min]	Type	Width [min]	Area [mAU*s]	Height [mAU]	Area %
1	7.861	BB	0.2353	4102.46533	269.99124	49.8105
2	13.911	BB	0.4492	4133.67236	142.17194	50.1895

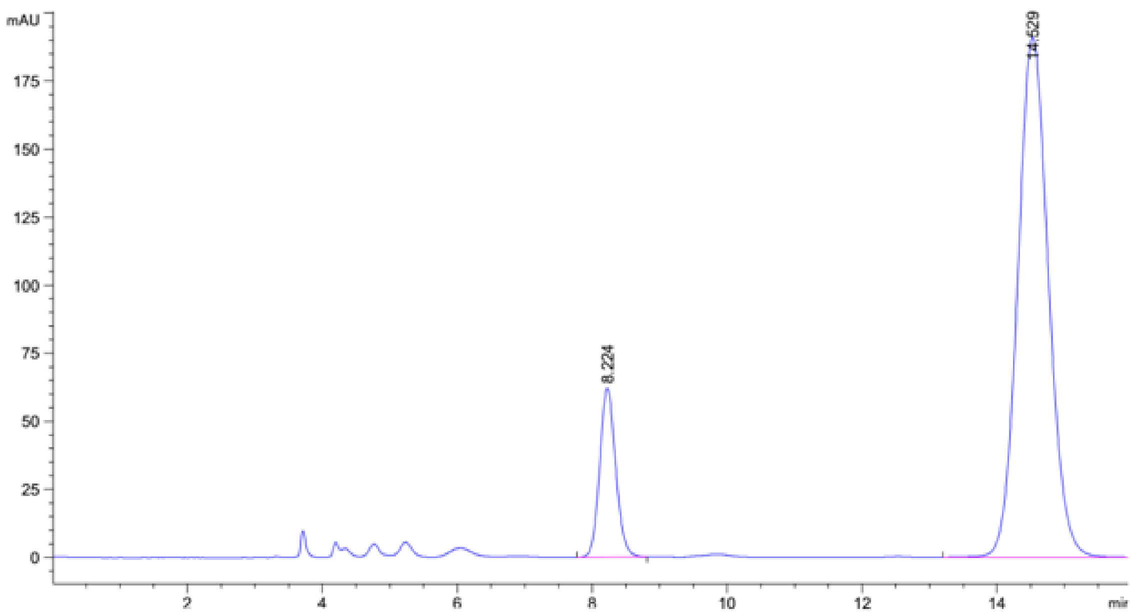

Peak #	RetTime [min]	Type	Width [min]	Area [mAU*s]	Height [mAU]	Area %
1	8.224	BB	0.2552	1026.80457	62.01259	14.5601
2	14.529	BBA	0.4879	6025.39746	191.07770	85.4399

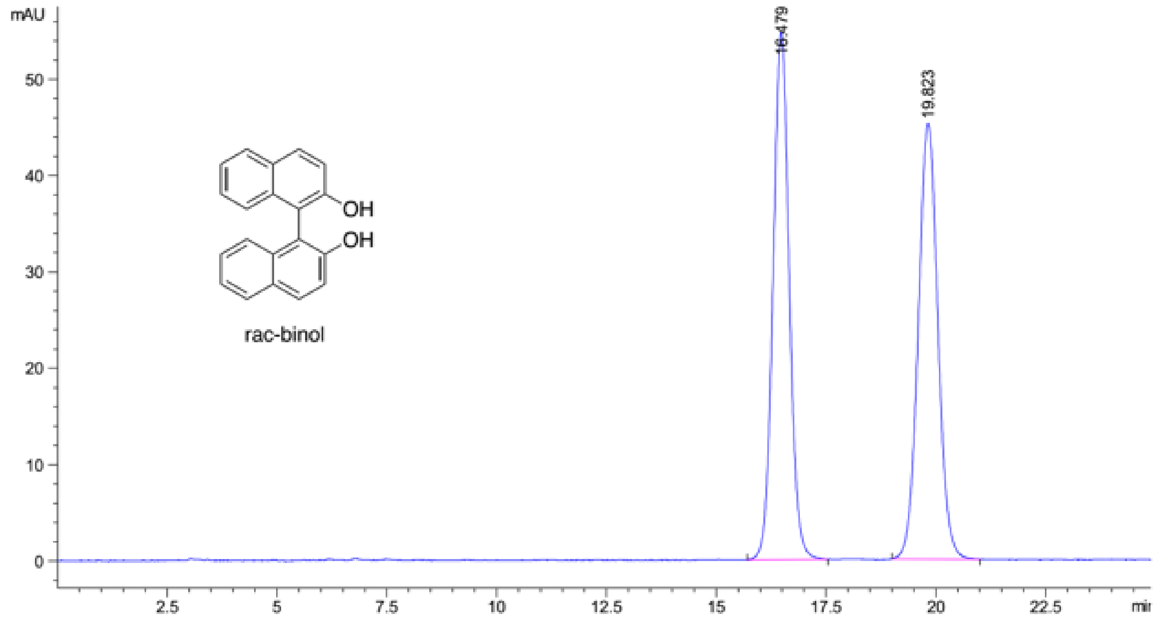

Peak #	Ret Time [min]	Type	Width [min]	Area [mAU*s]	Height [mAU]	Area %
1	16.479	BB	0.3955	1404.92468	54.73468	50.0003
2	19.823	BB	0.4784	1404.90649	45.23195	49.9997

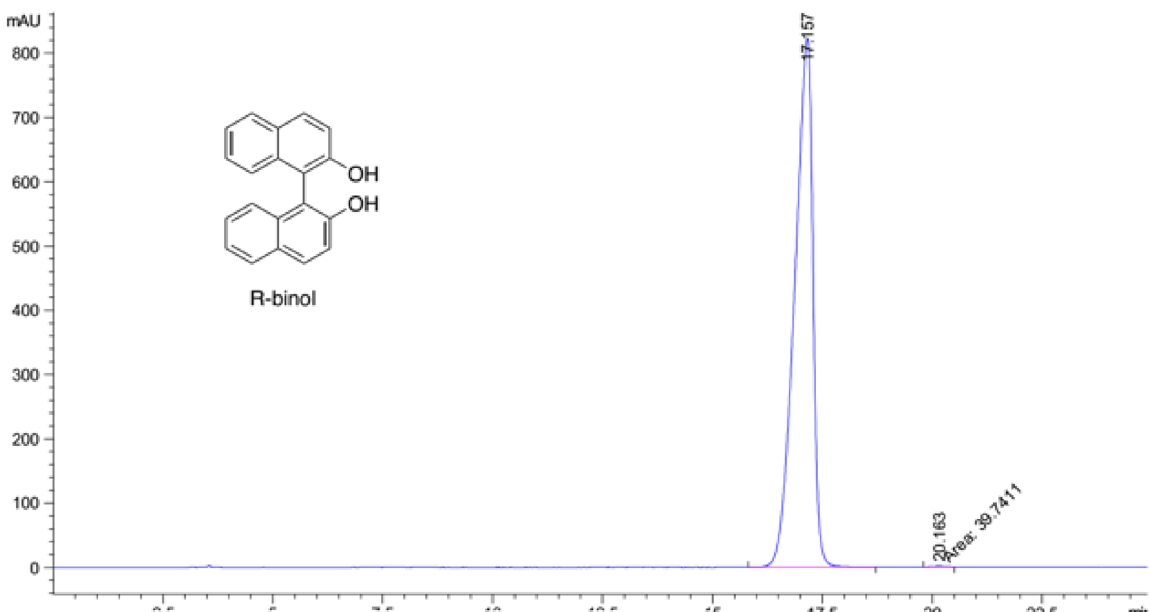

Peak #	Ret Time [min]	Type	Width [min]	Area [mAU*s]	Height [mAU]	Area %
1	17.157	BB	0.4324	2.37115e4	822.43158	99.8327
2	20.163	MM	0.4490	39.74109	1.47515	0.1673

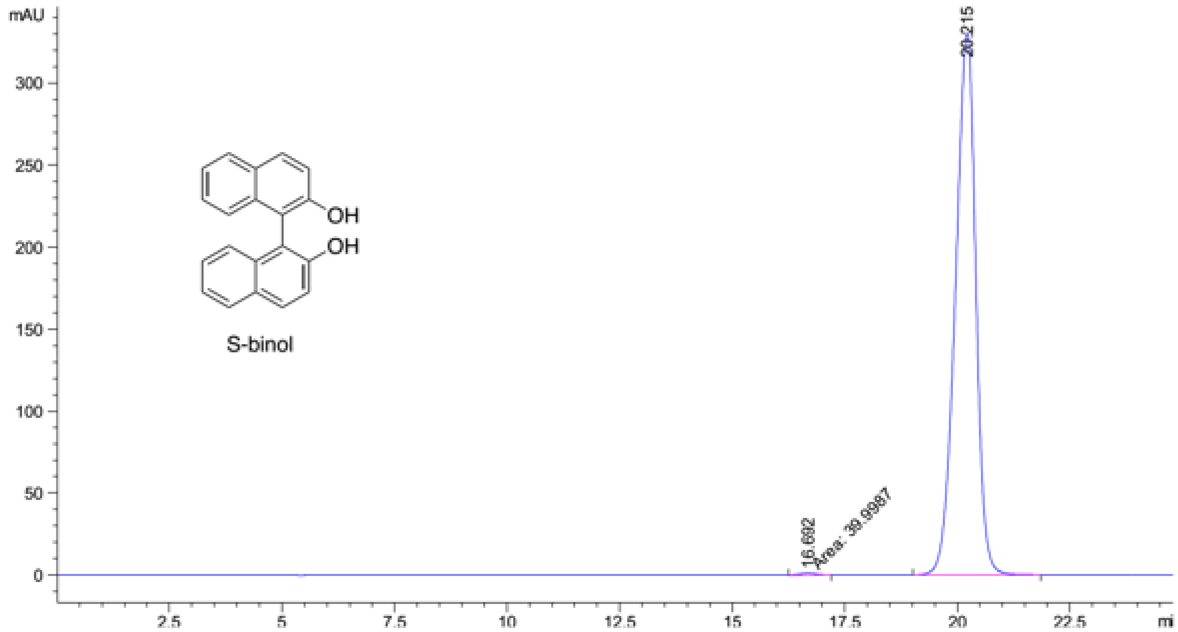

Peak #	Ret Time [min]	Type	Width [min]	Area [mAU*s]	Height [mAU]	Area %
1	16.692	MM	0.4797	39.99871	1.38965	0.3838
2	20.215	BB	0.4848	1.03817e4	330.16565	99.6162

Chapter IV

Development of Immobilized SPINOL-Derived Chiral Phosphoric Acids for Catalytic Continuous Flow Processes. Use in the Catalytic Desymmetrization of 3,3-Disubstituted Oxetanes

4.1. Polymer-immobilized chiral phosphoric acids

Chiral phosphoric acids (CPAs) are powerful and versatile Brønsted acid catalysts. Since the pioneer studies on these substances by the groups of Akiyama, [159] Terada and Uraguchi[160] in 2004, the use of CPAs in the development and application in asymmetric catalysis has experienced a rapid growth, and they have been applied in over 500 asymmetric transformations so far.[161]

---

[159] Akiyama, T.; Itoh, J.; Yokota, K.; Fuchibe, K. *Angew. Chem. Int. Ed.* **2004**, *43*, 1566-1568.

[160] Uraguchi, D.; Terada, M. *J. Am. Chem. Soc.* **2004**, *126*, 5356-5357.

[161] a) Akiyama, T.; Itoh, J.; Yokota, K.; Fuchibe, K. *Angew. Chem., Int. Ed.* **2004**, *43*, 1566-1568; b) Uraguchi, D.; Terada, M. *J. Am. Chem. Soc.* **2004**, *126*, 5356-5357; c) Akiyama, T.; Itoh, J.; Fuchibe, K. *Adv. Synth. Catal.* **2006**, *348*, 999-1010; d) Taylor, M. S.; Jacobsen, E. N. *Angew. Chem. Int. Ed.* **2006**, *45*, 1520-1543; e) Connon, S. J. *Angew. Chem. Int. Ed.* **2006**, *45*, 3909-3912; f) Akiyama, T. *Chem. Rev.* **2007**, *107*, 5744-5758; g) Doyle, A. G.; Jacobsen, E. N. *Chem. Rev.* **2007**, *107*, 5713-5743; h) Dondoni, A.; Massi, A. *Angew. Chem. Int. Ed.* **2008**, *47*, 4638-4660; i) Terada, M. *Chem. Commun.* **2008**, *44*, 4097-4112; j) You, S.-L.; Cai, Q.; Zeng, M. *Chem. Soc. Rev.* **2009**, *38*, 2190-2215; k) Adair, G.; Mukherjee, S.; List, B. *Aldrichimica Acta* **2009**, *41*, 31-39; l) Terada, M. *Synthesis* **2010**, 1929-1982; m) Rueping, M.; Kuenkel, A.; Atodiresei, I. *Chem. Soc. Rev.* **2011**, *40*, 4539-4549; n) Yu, J.; Shi, F.; Gong, L.-Z. *Acc. Chem. Res.* **2011**, *44*, 1156-1171; o) Parmar, D.; Sugiono, E.; Raja, S.; Rueping, M. *Chem. Rev.* **2014**, *114*, 9047-9153; p) Wu, H.; He, Y.-P.; Shi, F. *Synthesis* **2015**, *47*, 1990-2016; q) Merad, J.; Lalli, C.; Bernadat, G.; Maury, J.; Masson, G. *Chem. -Eur. J.* **2018**, *24*, 3925-2943; r) Maji, R.; Mallojjala, S. C.; Wheeler, S. E. *Chem. Soc. Rev.* **2018**, *47*, 1142-1158; s) Rahman, A.; Lin, X. *Org. Biomol. Chem.* **2018**, *16*, 4753–4777.

The reason for the excellent catalytic performance of CPAs can be ascribed to their unique structural features. For instance, a variety of bulky steric groups can be introduced by Suzuki coupling or Kumada coupling into the basic skeleton of CPAs (mostly BINOL) inducing excellent enantioselectivity and catalytic activity in many different processes. Moreover, they are stable and compatible with oxidation and hydrolysis conditions. In addition, both enantiomers of CPAs are available in most cases.

Attracted by the versatility displayed by these catalysts, our group, as well as several other groups have studied the immobilization of these species in an effort to minimize the problems associated to their tedious synthesis and purification and to lower their very high commercial cost by allowing recycling and reuse.

In 2011, Blechert, Thomas and coworkers reported a new concept for the immobilization of a thienyl-functionalized BINOL-derived CPA and to increase its enantioselectivity through a single step allowed introducing microporosity, chirality and catalytic active centers in a polymer network at the same time. This porous network (**IV-2**) was used as a recoverable heterogeneous organocatalyst in asymmetric transfer hydrogenation and showed increased enantioselectivty compared with the homogeneous reaction catalyzed by **IV-1** (Scheme 1).[162]

[162] Bleschke, C.; Schmidt, J.; Kundu, D. S.; Blechert, S.; Thomas, A. *Adv. Synth. Catal.* **2011**, *353*, 3101-3106.

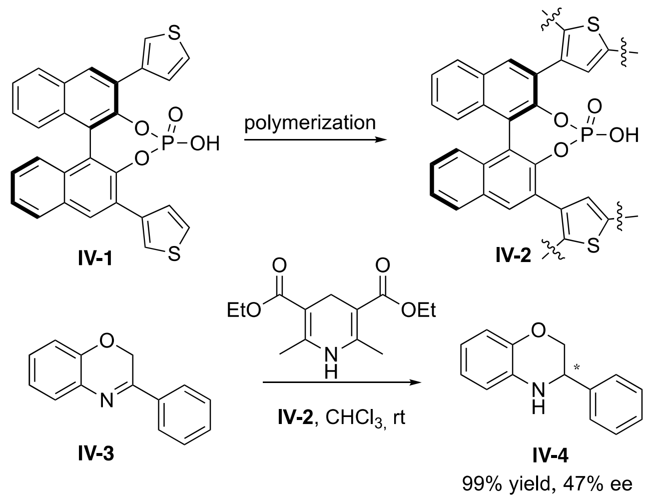

Scheme 1. Microporous polymer of thienyl-functionalized chiral phosphoric acid

In 2012, the same authors reported the synthesis of a new BINOL-derived CPA with 9-anthracenyl as bulky groups derived heterogeneous catalyst (**IV-6**) with high permanent surface area. The highly active and selective porous heterogeneous catalyst (**IV-6**) was evaluated in asymmetric organocatalytic processes, such as transfer hydrogenation, aza-ene-type reactions and the asymmetric Friedel-Crafts alkylation of pyrrole. The catalyst is stable, easily separable, and can be reused several times. The reaction rates are comparable with the corresponding homogeneous catalyst when using the same mass of both in different reactions (Scheme 2).[163]

[163] Kundu, D. S.; Schmidt, J.; Bleschke, C.; Thomas, A.; Blechert, S. *Angew. Chem., Int. Ed.* **2012**, *51*, 5456-5459.

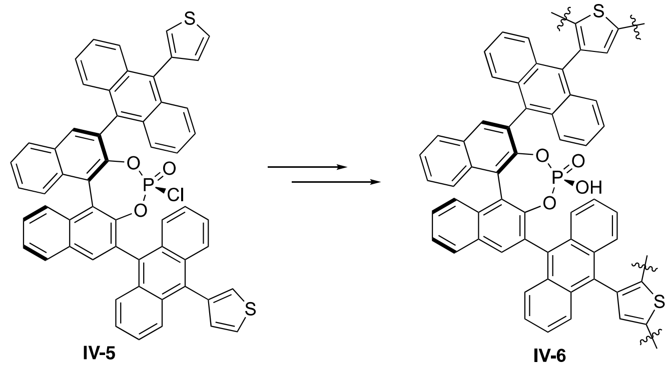

Scheme 2. Porous material of chiral phosphoric acid

In 2010, the Rueping group reported the synthesis of polymer-immobilized CPAs by radical copolymerization. The stick-type polymeric catalysts **IV-7** and **IV-8** were evaluated in the asymmetric transfer hydrogenation of quinolines and benzoxazines; **IV-8** in this reaction gave the products up to 97% yield with 96% ee. The monolithic materials were found to be stable and had the same catalytic activity and selectivity with their homogeneous counterparts. Moreover, the polymeric catalysts were easily recovered with a tea-bag approach and reused more than 12 cycles without any loss of reactivity and enantioselectivity (Scheme 3). [164]

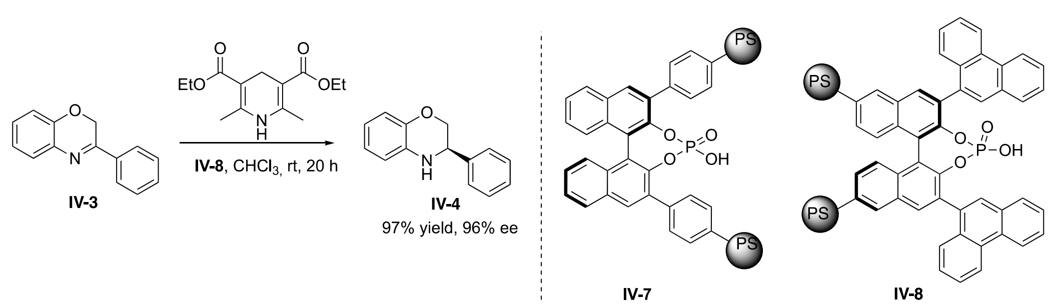

Scheme 3. Stick-type polymeric chiral phosphoric acid

In 2014, our group reported the synthesis of a very robust PS-supported BINOL derived CPA (**IV-9**). The highly active and selective polymeric catalyst **IV-9** was

[164] Rueping. M.; Sugiono. E.; Steck. A.; Theissmann. T. *Adv. Synth. Catal.* **2010**, *352*, 281-287.

applied in the enantioselective Friedel-Crafts reaction of indoles and sulfonylimines (Scheme 4),[165] producing a broad range of 3-indolylmethanamines **IV-12** in high yields and excellent enantioselectivities (up to 98 % ee). Moreover, the polymeric catalyst was recycled for 14 cycles without significant loss in catalytic performance. The versatility of the immobilization approach was also demonstrated in the rapid and convenient, sequential production of a library of enantiopure compounds in continuous-flow.

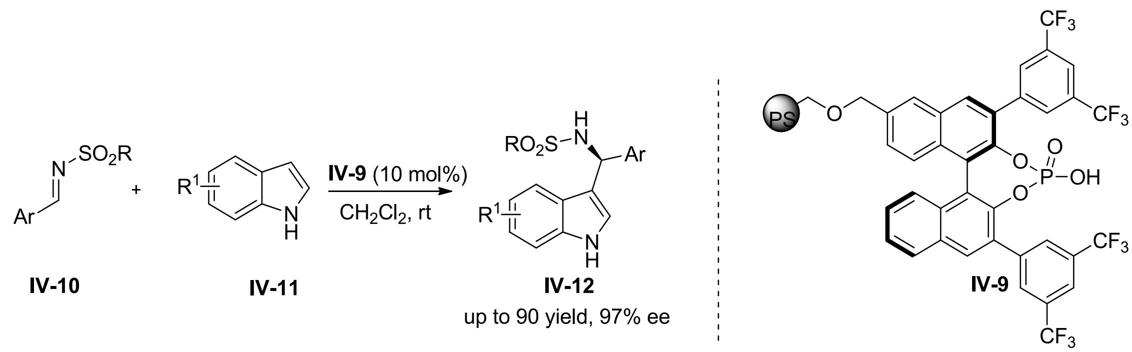

Scheme 4. PS-supported CPA in Friedel-Crafts reaction of indoles and sulfonylimines

In 2016, our laboratory reported the PS-immobilized TRIP phosphoric acid catalyst using a copolymerization-based strategy. The highly active and enantioselective polymeric resin (PS-TRIP, **IV-13**) was evaluated in the asymmetric allylboration of aldehydes leading to **IV-16** (Scheme 5, a).[166] Moreover, **IV-13** was reused for 18 times retaining its activity, showing great robust. Finally, the polymeric catalyst **IV-13** was able to be implemented into a continuous flow process operating for 28 h. In 2018, the supported TRIP was applied as efficient organocatalyst to the desymmetrisation of meso-1,3-diones to produce cyclohexenones **IV-18** in excellent yields and enantioselectivities(Scheme 5, b).[167]

---

[165] Osorio-Planes, L.; Rodríguez-Escrich, C.; Pericàs, M. A. *Chem. Eur. J.* **2014**, *20*, 2367-2372.

[166] Clot-Almenara, L.; Rodríguez-Escrich, C.; Osorio-Planes, L.; Pericàs, M. A. *ACS Catal.* **2016**, *6*, 7647-7651.

[167] Clot-Almenara, L.; Rodríguez-Escrich, C.; Pericàs, M. A. *RSC Adv.* **2018**, *8*, 6910-6914.

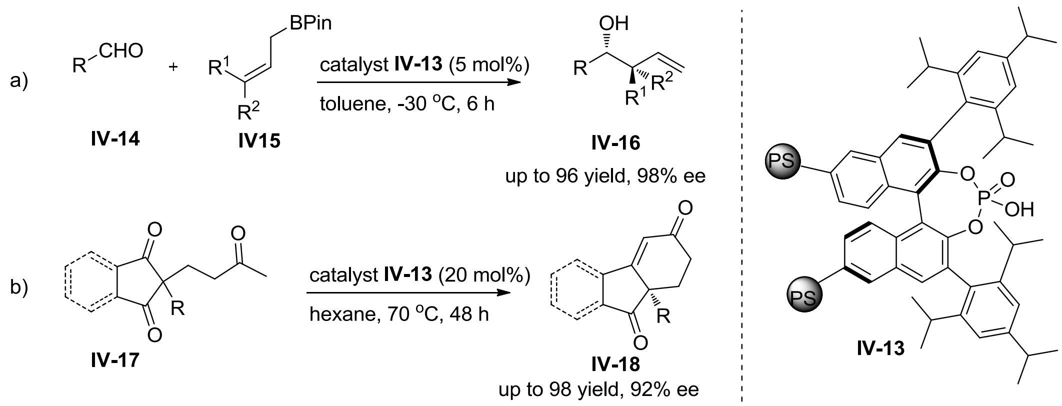

Scheme 5. PS-supported TRIP in the asymmetric allylboration of aldehydes and desymmetrisation of *meso*-diones

In 2017, the Zhang group reported the synthesis of a porous heterogeneous BINOL-derived chiral phosphoric acid BiCz-POF-1 (**IV-20**) using the mild, $FeCl_3$-promoted oxidative polymerization of carbazole units (Scheme 6).[168] Application of **IV-20** in the asymmetric transfer hydrogenation of quinolines and benzoxazines led to excellent yields and stereoselectivities, while reusability was proven for five consecutive runs.

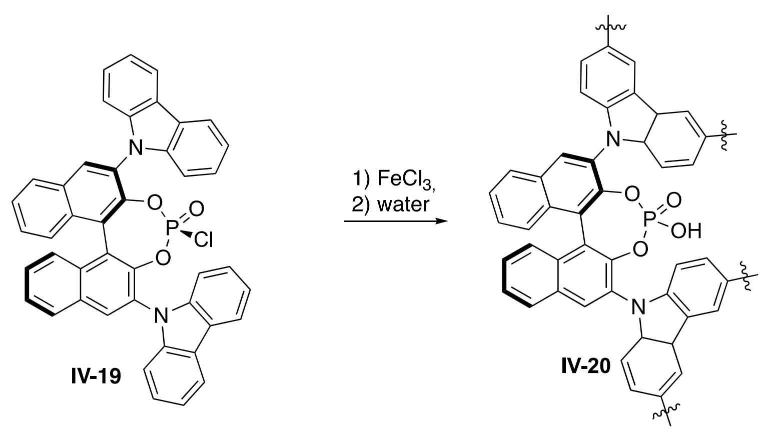

Scheme 6. $FeCl_3$-promoted oxidative polymerization to prepare BiCz-POF-1

[168] Zhang, X.; Kormos, A.; Zhang, J. *Org. Lett.* **2017**, *19*, 6072-6075.

At about the same time, the Kobayashi group reported the preparation of a novel chiral bifunctional heterogeneous materials (**IV-21**) with Au/Pd nanoparticles and CPAs as active orthogonal catalysts by using a facile pseudo-suspension co-polymerization method. With this bifunctional heterogeneous materials, they were able to carry out a sequential one-pot aerobic oxidation–cyclization process to provide **IV-24** in high yields and enantioselectivities (Scheme 7). The catalytic system was recycled several cycles without significant loss of activity or enantioselectivity. (Scheme 7) [169]

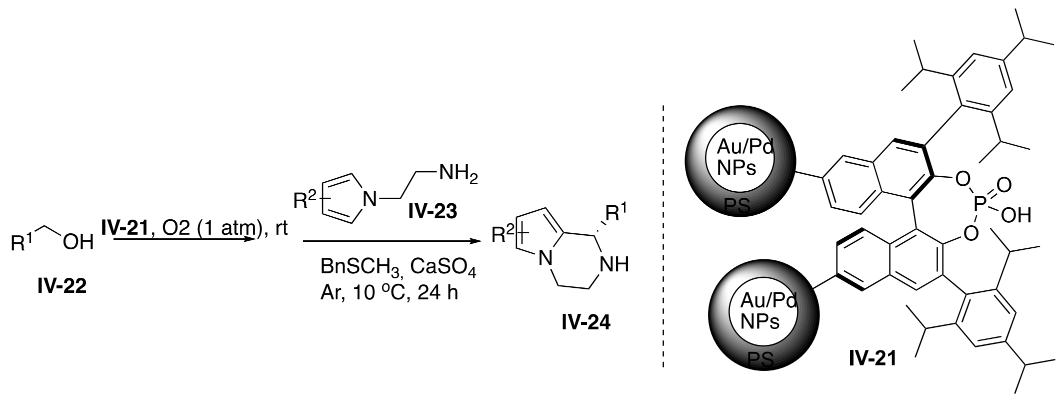

Scheme 7 CPAs on Au/Pd nanoparticles **IV-21** as active orthogonal catalysts for a one-pot, sequential oxidation–cyclization process

4.2. Synthesis of SPAs

SPAs are a class of chiral phosphoric acids derived from the C_2-symmetric chiral SPINOLs. The simple, highly rigid chiral C_2 symmetric spirocyclic backbone of SPINOL involving a quaternary center makes racemization virtually impossible; therefore, SPAs combine chemical robustness and conformational rigidity and this makes the catalyst characteristics (both electronic and steric) of SPAs very different from that of BINOL-derived phosphoric acids (BPAs).

[169] Cheng, H. G.; Miguélez, J.; Miyamura, H.; Yoo, W. J.; Kobayashi, S. *Chem. Sci.* **2017**, *8*, 1356-1359.

These characteristics convert SPINOL and its derivatives (like SPAs) into good candidates for immobilization in view of their use as reusable chiral catalysts. However, in spite of the different studies dealing with the immobilization of BINOL-derived phosphoric acid, the immobilization of SPINOL-derived phosphoric acid has not been explored up to date.

The synthesis of SPAs normally start with commercially available R- or S-configured SPINOL **IV-25** as shown in Scheme 8. Protection of the hydroxyl groups with MOMCl gives **IV-26**, which leads to the introduction of iodine atoms at the 6,6′-positions using a lithiation–halogenation strategy to yield **IV-27**. Intermediate **IV-28** can be then prepared by two different strategies: a) by performing a Suzuki coupling (for highly sterically hindered groups, Kumada coupling is used) to introduce the aryl groups before hydrolytic deprotection [In this method, Pd (0) in combination with suitable ligands is used, which increases the cost of the procedure],[170] and b) by performing hydrolytic deprotection before coupling. While this second approach presents the advantage of involving the use of comparatively cheaper Pd/C as catalyst in the Suzuki coupling when X = I, suffers from the limitation that highly hindered bulky groups cannot be introduced with this method.[171] Finally, the phosphorylation of **IV-28** affords the desired SPA catalysts **IV-29**.

A practical detail clearly advocating in favor of SPAs immobilization is the need for thorough removal of metal cations after the requisite purification of **IV-29** by flash chromatography on silica gel, since the metal phosphates originated during

[170] a) Čorić, I.; Müller, S.; List, B. *J. Am. Chem. Soc.* **2010**, *132*, 17370-17373; b) Xing, C. H.; Liao, Y. X.; J. Ng, J.; Hu, Q. S. *J. Org. Chem.* **2011**, *76*, 4125-4131; c) Xu, B.; Zhu, S.-F.; Xie, X. L.; Shen, J. J.; Zhou, Q.-L. *Angew. Chem. Int. Ed.* **2011**, *50*, 11483-11486.

[171] a) Xu, F.; Huang, D.; Han, C.; Shen, W.; Lin, X.; Wang, Y. *J. Org. Chem.* **2010**, *75*, 8677-8680; b) González, A. Z.; Benitez, D.; Tkatchouk, E.; Goddard III, W. A.; Toste, F. D. *J. Am. Chem. Soc.* **2011**, *133*, 5500-5507; c) Xing, C. H.; Liao, Y. X.; Ng, J.; Hu, Q. S. *J. Org. Chem.* **2011**, *76*, 4125-4131.

purification present catalytic characteristics very different from those of the free-acid forms of CPAs.

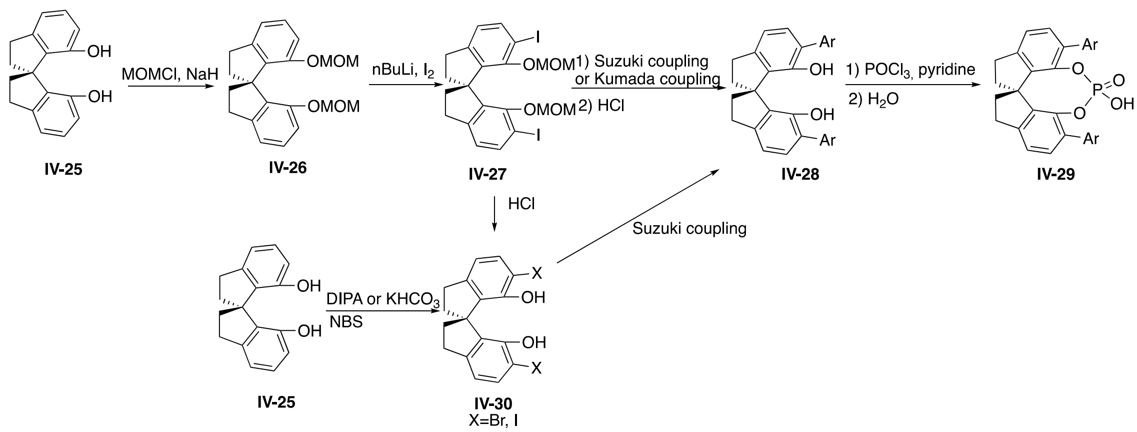

Scheme 8. Synthesis of SPAs

4.3 The synthesis of SPINOL derivatives

In 1999, the Birman group [172] reported the synthesis of SPINOL, and numerous important works by the Qilin Zhou group have later demonstrated the outstanding performance of 1,1'-spirobiindane-based chiral ligands in diverse asymmetric catalytic processes. [173] However, the seven steps synthetic procedure required to prepare SPINOL in enantiomerically pure form importantly increased the cost of this compound and hampered its application of catalysts. To solve this limitation and to enlarge the manifold of potential applications, in the following years, a number of synthesis of spirocyclic backbone structures was reported.

According to Birman´s procedure, [16] the synthesis of SPINOL started with the coupling of *m*-anisaldehyde **IV-31** with acetone in the present of NaOH. Then, both double bonds in **IV-32** were reduced by low-pressure hydrogenation with Raney Nickel. Before the

[172] Birman, B. V.; Rheingold, A. L.; Lam, K. C. *Tetrahedron: Asymmetry* **1999**, *10*, 125-131.

[173] Xie, J.-H.; Zhou, Q.-L. *Acc. Chem. Res.* **2008**, *41*, 581-593.

spirocyclization, the para positions of the aryl groups with respect to the MeO substituents were brominated to block these positions and to make sure only the *ortho* positions (with respect to methoxy) in **IV-34** react with the carbonyl carbon to produce the target spirobiindane **IV-35**. Then, the Br and O-methyl groups were sequentially cleaved with n-BuLi and BBr_3 producing SPINOL **IV-25** as a racemate. (±)-**IV-25** can be resolved by treating with L-menthyl chloroformate and NEt_3. Later on, in 2002, Zhou and coworkers reported a method to resolve SPINOL by inclusion crystallization with N-benzylcinchonidinium chloride.[174] This new method represents a highly efficient and practical way to resolve SPINOL in gram scale.

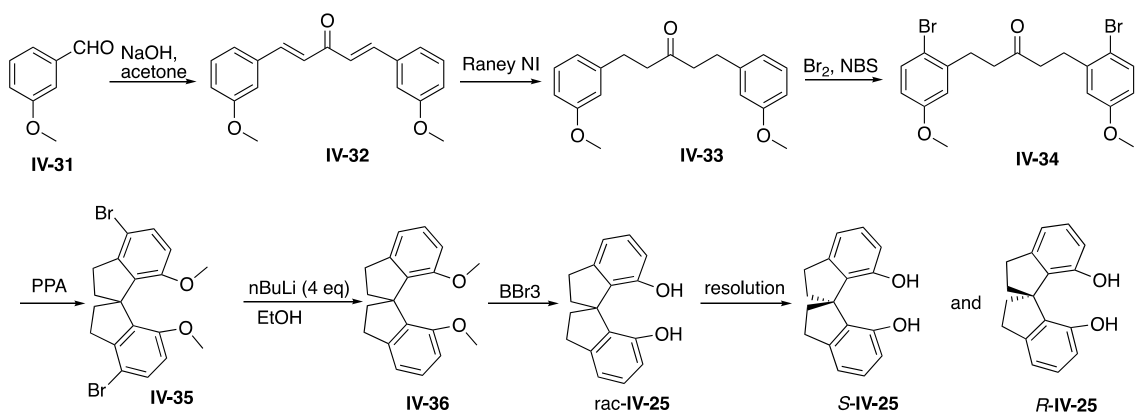

Scheme 9. Common procedure for the synthesis of SPINOL

In 2013, a US patent reported a five steps procedure to prepare (±)-**IV-25** (Scheme 10). In this patent, 3-hydroxybenzaldehyde **IV-37** was used as starting material instead of *m*-anisaldehyde. In this way, the deprotection of MeO- group is no longer required. In addition, the removal of the Br substituents by low-pressure hydrogenation with Pd/C is safer and cheaper than the use of *n*BuLi with the same purpose.[175]

[174] Zhang, J. H.; Liao, J.; Cui, X.; Yu, K. B.; Zhu, J.; Deng, J. G.; Zhu, S. F.; Wang, L. X.; Zhou, Q. L.; Chung, L. W.; Ye, T. *Tetrahedron: Asymmetry* **2002**, *13*, 1363-1366.
[175] Wang, Y. R.; Chin, C. L.; Cheng, K. L.; Liu, S. H. US20130135574.

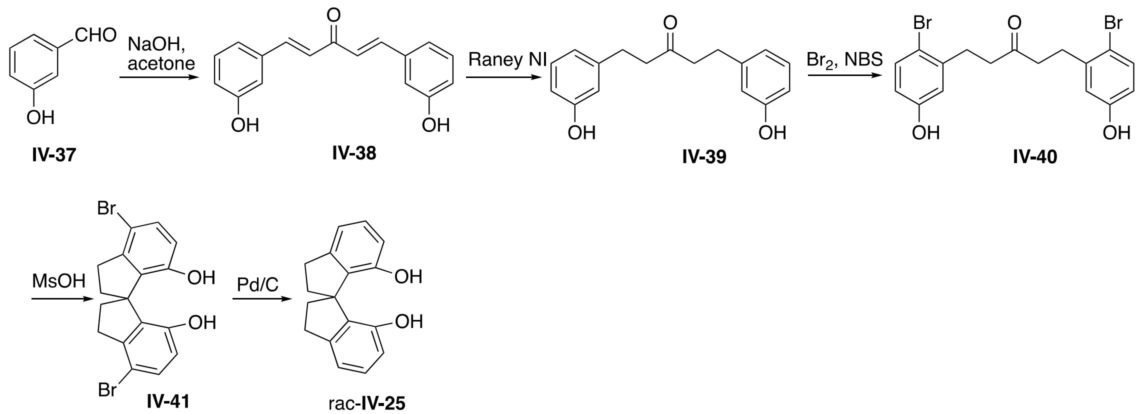

Scheme 10. Improved procedure for synthesis of SPINOL

In 2004, the Dai group reported the preparation of spiro-bisphenol by treatment of bisphenol A with concentrated sulfuric acid at room temperature.[176] Later in 2018, the Lin group reported the preparation of the corresponding spiro-bisphenol **IV-43** by treatment of bisphenol C with methanesulfonic acid (Scheme 11). This compound could be resolved by derivatization with L-menthyl chloroformate or by inclusion crystallization with N-benzylcinchonidinium chloride. A variety of ligands based on the structure of **IV-43** were later prepared ((**IV-44)** - (**IV-48)**) and showed good to excellent results in different catalytic asymmetric processes.[177]

The syntheses of **IV-43**, however, are poorly atom-economical; equivalent amounts of phenolic by-products are co-produced, and this increases the difficulty of isolation of the target derivatives while representing a heavy burden of environmental pollution.

---

[176] Chen, W. F.; Lin, H. Y.; Dai, S. A. *Org. Lett.* **2004**, 6, 2341-2343.

[177] a) Sun, W.; Gu, H.; Lin, X. *J. Org. Chem.* **2018**, *83*, 4034−4043; b) Shan, H.; Zhou, Q.; Yu, J.; Zhang, S.; Hong, X.; Lin, X. *J. Org. Chem.* **2018**, *83*, 11873−11885; c) Chang, S.; Wang, L.; Lin, X. *Org. Biomol. Chem.* **2018**, *16*, 2239-2247; d) Shan, H.; Pan, R.; Lin, X. *Org. Biomol. Chem.* **2018**, *16*, 6183-6186; e) Gu, H.; Han, Z.; Xie, H.; Lin, X. *Org. Lett.* **2018**, *20*, 6544-6549.

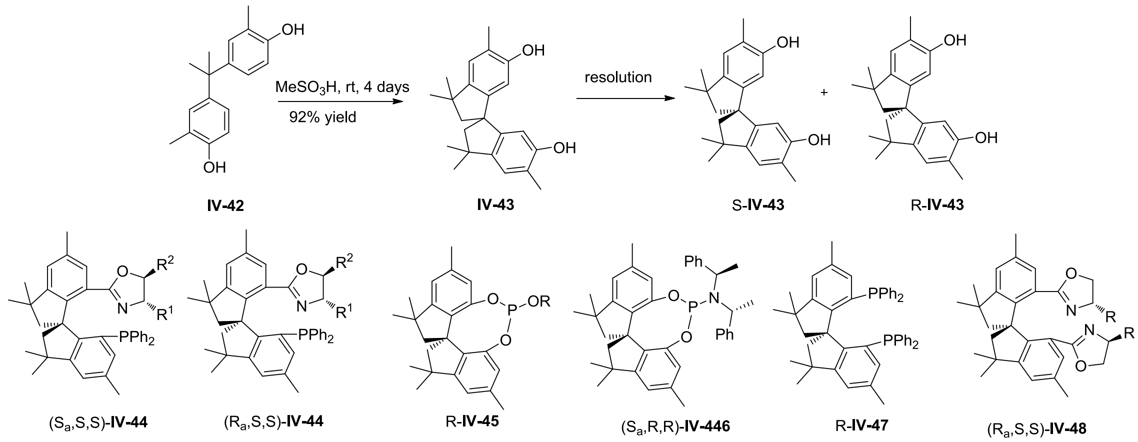

Scheme 11. Synthesis and application of spiro-bisphenol **IV-43**

In 2004, the Zhou group reported the synthesis and optical resolution of 9,9‘-spirobifluorene-1,1‘-diol (SBIFOL, **IV-51**). SBIFOL was synthesized from 1,2-dibromobenzene and 3-bromoanisole (Scheme 12). It can be resolved by inclusion resolution with 2,3-dimethoxy-N,N,N‘,N‘-tetracyclohexylsuccinamide. [178] In 2005, Zhou and coworkers used SBIFOL for preparing diphosphane ligands and applied them in the ruthenium‐catalyzed asymmetric hydrogenation of α,β‐unsaturated carboxylic acids.[179] However, during the next 16 years, no further studies about SBIFOL has been reported.

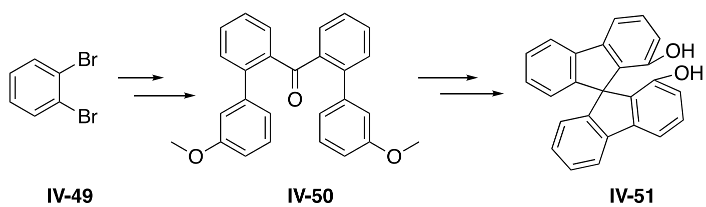

Scheme 12. Synthesis and SBIFOL

In 2007, the Zhou group reported the synthesis of a racemic 1,1′‐spirobitetralin‐8,8′‐diol (SBITOL, rac-**IV-57**) via a 9 steps synthetic procedure in 26% over yield,

[178] Cheng, X.; Hou, G. H.; Xie, J. H.; Zhou, Q. L. *Org. Lett.* **2004**, *6*, 2381-2383.
[179] Cheng, X.; Zhang, Q.; Xie, J. H.; Wang, L. X.; Zhou, Q. L. *Angew. Chem. Int. Ed.* **2005**, *44*, 1118-1121.

and it was resolved *via* bis‐(S)‐camphorsulfonates (Scheme 13).[180] The resolved enantiomerically pure SBITOL was applied to the synthesis of chiral spirobitetraline monophosphoramidite ligands and then applied in the Rh catalyzed enantioselective hydrogenation of dehydroamino esters.

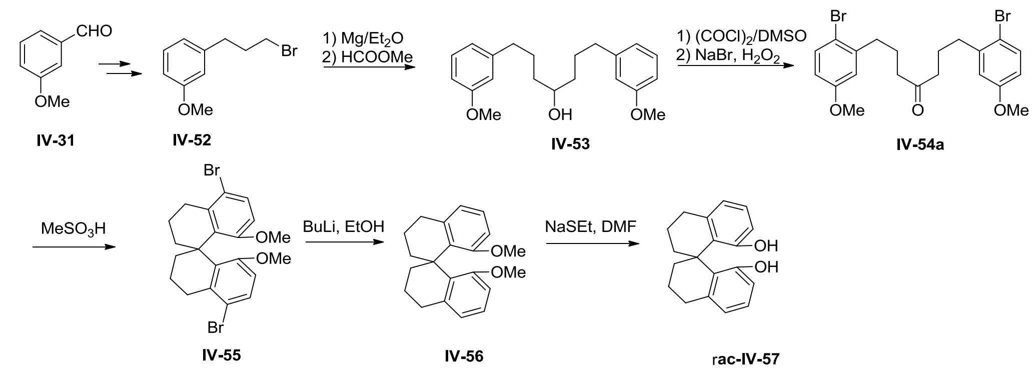

Scheme 13. Synthesis and SBITOL

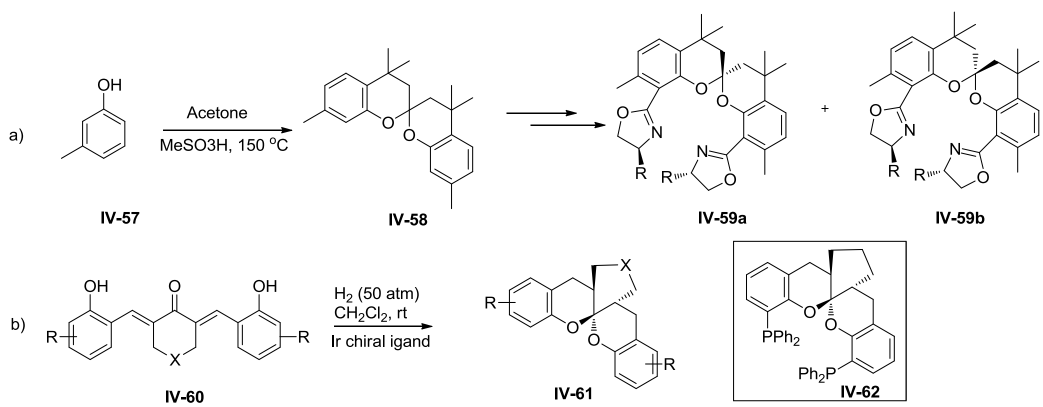

Scheme 14. Synthesis of SPINOL based on aromatic spiroketals backbones

In 1997, the Caruso group reported the preparation of **IV-58** in large scale by acid-catalyzed reaction of p-cresol with acetone.[181] Later in 2011, Ding and coworkers developed a new type of spiro bisoxazoline ligand (SPANbox) based on **IV-58** and two oxazoline chelating units **IV-59a** and **IV-59b** (Scheme 14, a). Their Zn(II)

---

[180] Huo, X. H.; Xie, J. H.; Wang, Q. S.; Zhou, Q. L. *Adv. Synth. Catal.* **2007**, *349*, 2477-2484.
[181] Caruso, A. J.; Lee, J. L. *J. Org. Chem.* **1997**, *62*, 1058-1063.

complexes showed excellent activity and enantioselectivity in the catalytic hydroxylation of various β-keto esters and 1,3-diesters.[182] In 2012, the same group reported a resolution-free preparation of aromatic spiroketals **IV-61** by catalytic asymmetric hydrogenation of α,α′ - bis(2 - hydroxyarylidene) ketones with an iridium(I) complex involving a spiranic P,N ligand (SpinPhox) in high yields with excellent diastereo - and enantioselectivities (Scheme 14, b).[183] **IV-61** was applied to the synthesis of diphosphine (SKP) ligands in one step with 78–95% yields on multigram scale.[184] After that, several asymmetric transformation have been reported with type ligands, showing its great application potential.

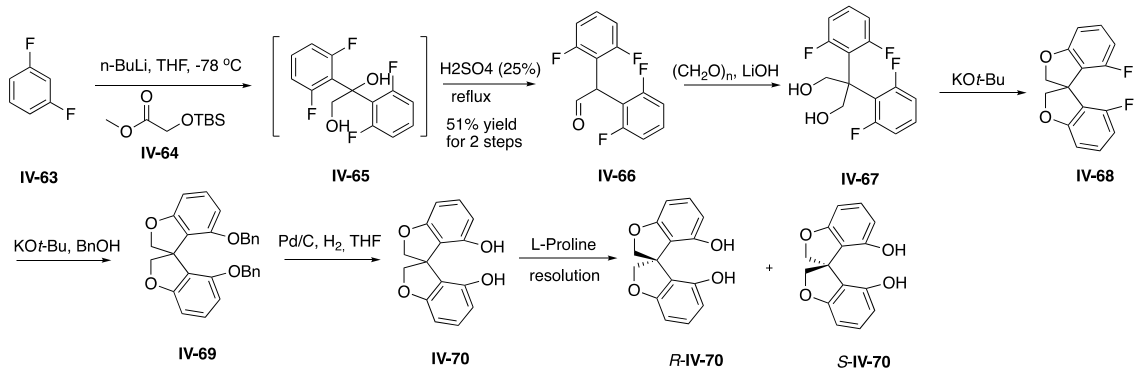

Scheme 15. Synthesis of *oxa*-SPINOL

In 2018, the Zhang group reported the synthesis of chiral *oxa*-spirocyclic ligands for Ir-catalyzed direct asymmetric reduction of bringmann's lactones with molecular hydrogen. The 6 steps synthetic procedure (Scheme 15) included the construction of the all-carbon quaternary center at an early stage, a key double intramolecular S_NAr reaction to create the spirocycles, and could be operated at >100 g scale. The *oxa*-SPINOL **IV-70** can be resolved with L-proline by control of the solvent.[185]

---

[182] Li, J.; Chen, G.; Wang, Z.; Zhang, R.; Zhang, X.; Ding, K. *Chem. Sci.* **2011**, *2*, 1141-1144.
[183] Wang, X.; Han, Z.; Wang, Z.; Ding, K. *Angew. Chem. Int. Ed.* **2012**, *51*, 936-940.
[184] Wang, X.; Guo, P.; Wang, X.; Wang, Z.; Ding, K. *Adv. Synth. Catal.* **2013**, *355*, 2900-2907.
[185] Chen, G. Q.; Lin, B. J.; Huang, J. M.; Zhao, L. Y.; Chen, Q. S.; Jia, S. P.; Yin, Q.; Zhang, X. *J. Am. Chem. Soc.* **2018**, *140*, 8064-8068.

Although the *oxa*-spirocyclic ligands prepared in this manner didn´t show any significant advantages in terms of catalytic activity and enantioselectivity, this work presented a new concept in the synthesis SPINOL analogs.

In 2018, Sun group reported the synthesis of a series of chiral spiroketal bisphosphine ligands containing 1,1′-spirobi(3*H*,3′*H*)isobenzofuran backbones. The synthesis (Scheme 16) was performed at gram scale, and no kinetic resolution of enantiomers is required. Enantiopure diphosphines **IV-73a** and **IV-73b** were applied in the enantioselective, Rh-catalyzed hydrogenation of α-dehydroamino acid esters.[186]

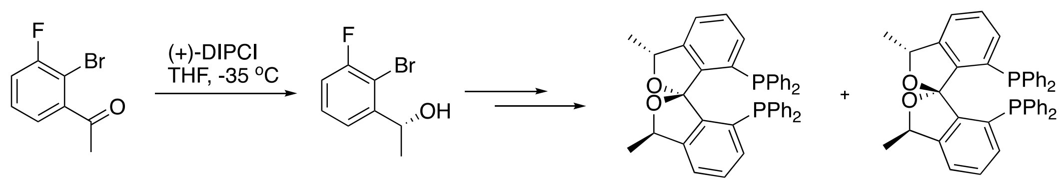

Scheme 16. Synthesis and SPINOL based on 1,1′-spirobi(3H,3′H)isobenzofuran backbones

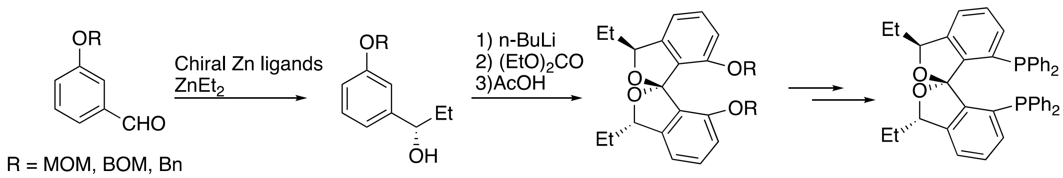

Scheme 17. Synthesis of spiroketal - based SPINOL

In 2018, the Nagorny group reported a new enantioselective route to the synthesis of spiroketal - based SPINOLs **IV-76** (Scheme 17). Based on it, several chiral ligands were generated and employed in an array of stereoselective

[186] Huang, J.; Hong, M.; Wang, C. C.; Kramer, S.; Lin, G. Q.; Sun, X. W. *J. Org. Chem.* **2018**, *83*, 12838-12846.

transformations.[187] Notably, this approach represents an expedient and economical method to prepare SPINOL analogs.

In 2016, Tan and coworkers reported a chiral phosphoric acid-catalyzed asymmetric synthesis of SPINOLs. Their approach is characterized by its highly convergent nature and functional group tolerance, and efficiently provides SPINOLs in good yield with excellent enantioselectivity.[188] For systems containing electron donating groups (EDG) in the *para* position with respect to OH, the corresponding spinols can be prepared from ketone directly by heating at 120 ºC for 2 days. However, the presence of electron withdrawing groups (EWG) such as F, Cl, Br and I in those *para* positions diverted the reaction towards the corresponding ketals **IV-79**, In general, the reaction conditions required for the formation of **IV-25** involve heating at 80 ºC for 4-7 days. The long reaction time and high reaction temperature required are the main limitations for the application of this method. (Scheme 18)

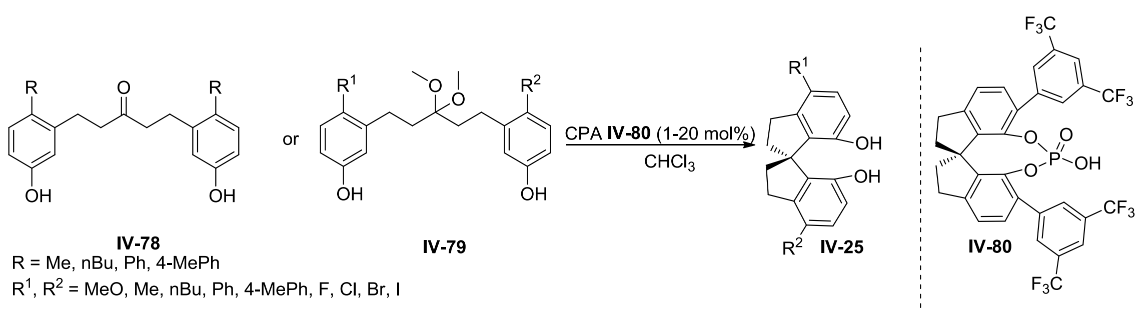

Scheme 18. Synthesis of SPINOL with CPA

In 2004, Venugopal reported the synthesis and resolution of new cyclohexyl fused spirobiindane 7,7′-diol CHEXDBSPINOL (**IV-84**).[189] The compound was prepared following birman's procedure, replacing acetone with cyclohexanone (Scheme 19). However, **IV-84** failed to be resolved by inclusion crystallization with N-benzyl

---

[187] Argüelles, A. J.; Sun, S.; Budaitis, B. G.; Nagorny, P. *Angew. Chem. Int. Ed.* **2018**, *57*, 5325 –5329.
[188] Li, S.; Zhang, J. W.; Li, X. L.; Cheng, D. J.; Tan, B. *J. Am. Chem. Soc.* **2016**, *138*, 16561-16566.
[189] Venugopal, M.; Elango, S.; Parthiban, A.; Eni. *Tetrahedron: Asymmetry* **2004**, *15*, 3427-3431.

cinchonidinium chloride in either toluene or a mixture of hexane and toluene. On the other hand, it could be resolved by treatment with L-menthyl chloroformate and NEt_3 followed by crystallization in hexane. In 2019, the Ding group presented a facile enantioselective synthesis of CHEXDBSPINOL in high yields and excellent stereoselectivities (up to >99% ee).[190] The protocol can be performed in one pot and is readily scalable. Notably a 25 g batch scale was performed without any chromatographic purification. SPINOL **IV-84** was evaluated as a chiral ligand in several transition metal (Rh, Au, or Ir) catalyzed enantioselective transformations (hydrogenation, hydroacylation, and [2 + 2] cycloaddition reaction).

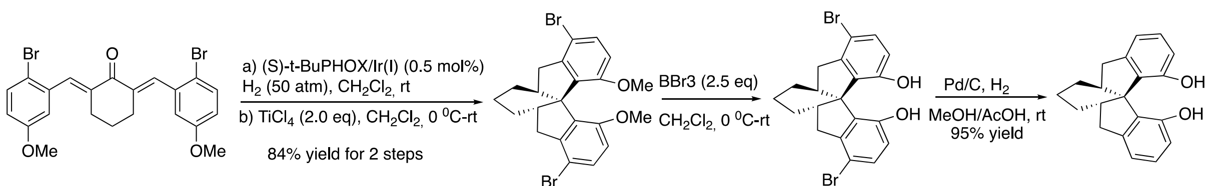

Scheme 19. Enantioselective synthesis of cyclohexyl-fused chiral SPINOL analog

Most recently, in 2019, the Dou group reported the synthesis of a series of 3,3′‐diaryl‐SPINOLs IV-86 by sequential Rh‐catalyzed asymmetric conjugate addition of arylboronic acids/BF3‐promoted diastereoselective spirocyclization with excellent yields and stereoselectivities (Scheme 20). Some phosphoramidite ligands prepared from 3,3′‐diphenyl‐SPINOL showed higher enantioselectivities than the privileged nonsubstituted ligand in several catalytic asymmetric reactions.[191]

---

[190] Zheng, Z.; Cao, Y.; Chong, Q.; Han, Z.; Ding, J.; Luo, C.; Wang, Z.;Zhu, D.; Zhou, Q. C.; Ding, K. *J. Am. Chem. Soc.* **2018**, *140*, 10374−10381.
[191] Yin, L.; Xing, J.; Wang, Y.; Shen, Y.; Lu, T.; Hayashi, T.; Dou, X. *Angew. Chem. Int. Ed.* **2019**, *58*, 2474-2478

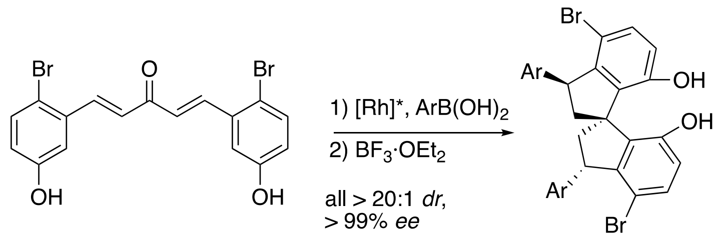

IV-85 **IV-86**

Scheme 20. Enantioselective synthesis of 3,3′ - diaryl - SPINOLs

4.4 Aim of this project

CPAs present many important advantages in asymmetric catalysis. For instance, a variety of bulky steric groups could be introduced into the structure of CPAs to optimize enantioselectivity up to very high levels. In addition, they are stable and compatible with oxidation and hydrolysis conditions. Not less important, in most cases, both enantiomers of CPAs are available.

The simple highly rigid chiral C_2 symmetric quaternary center of spirocyclic backbone of SPINOL makes racemization virtually impossible, and this converts SPINOL derivatives into potentially high profile, reusable chiral catalysts.

However, the seven steps procedure required to achieve enantiomerically pure SPINOLs can represent an unaffordable effort in cost and time required for their preparation. In particular, the introduction of optimal bulky substituents, highly beneficial for catalytic performance, is particularly painful.

Consequently, we thought that it would be highly desirable to immobilize these catalysts onto a solid support to allow their recovery, multiple reuse and, eventually, application in continuous flow.

According to Dou´s work, 3,3′ - diaryl - SPINOLs could be prepared in two steps (three steps if including the synthesis of the starting material) with excellent yield and stereoselectivities. As already mentioned, some phosphoramidite ligands prepared from 3,3′ - diphenyl - SPINOL exhibit superior catalytic performance than the privileged nonsubstituted ligand in several catalytic asymmetric reactions. For these reasons, this type of SPINOL derivative is an ideal candidate for immobilization and conversion (before or after immobilization) into chiral phosphoric acids.

With this aim in mind, we synthesized a family of immobilized 3,3'-diphenyl-SPINOLs derived chiral phosphoric acids with different bulky substituents at 6,6´-positions ((**IV-90)**- (**IV-94)**). The catalytic enantioselective desymmetrization of 3-substituted oxetanes (**IV-87**) with benzo[d]thiazole-2-thiol (**IV-88**) was chosen as a model reaction to evaluate this family of immobilized SPAs (Scheme 21).

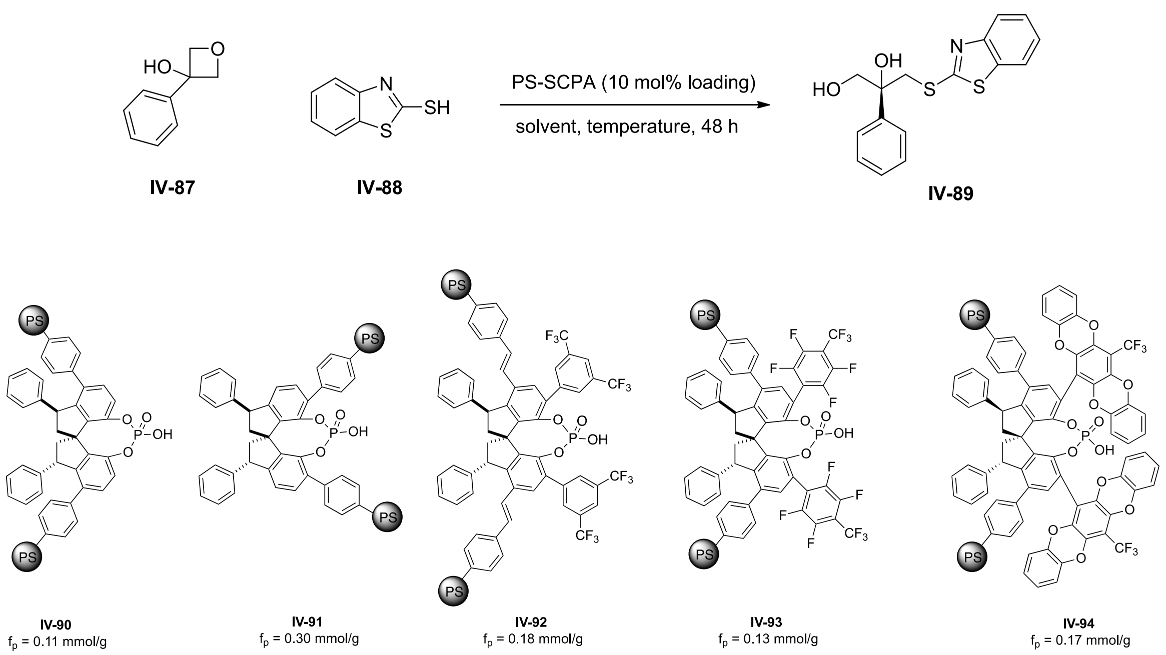

Scheme 21. Immobilized Chiral 3,3′ - diaryl - SPINOLs derived phosphoric acid and application

Development of Immobilized SPINOL-Derived Chiral Phosphoric Acids for Catalytic Continuous Flow Processes. Use in the Catalytic Desymmetrization of 3,3-Disubstituted Oxetanes

Junshan Lai, Mauro Fianchini, and Miquel A. Pericàs*

ABSTRACT: A family of C_2-symmetrical 1,1′-spirobiindane-7,7′-diol (SPINOL) derivatives containing polymerizable styryl units has been prepared through a highly convergent approach. Radical co-polymerization of these monomers with styrene has allowed the synthesis of a new family of immobilized SPINOL-derived chiral phosphoric acids (SPAs) where the combination of the restricted axial flexibility of the SPINOL units and the existence of extended and adaptable chiral walls adjacent to them leads to enhanced stereocontrol in catalytic processes. The optimal immobilized species (**Cat f**) brings about the catalytic desymmetrization of 3,3-disubstituted oxetanes in up to 90% yield with up to >99% enantioselectivity, exhibiting a very high recyclability (no decrease in conversion or enantioselectivity after sixteen, 16-hour runs). To exploit these characteristics, a continuous flow process has been implemented and operated for the sequential preparation of 17 diverse enantioenriched products. The suitability of the flow setup for gram scale preparations (20 mmol scale) and its deactivation/reactivation by treatment with pyridine/hydrochloric acid in dioxane have been demonstrated. Density Functional Theory has been employed to provide a rational justification of the deep effect on enantioselectivity arising from the presence of sterically bulky substituents at the 6,6´-positions of the SPINOL unit. The main structural features of **Cat f** have subsequently been incorporated to the design of a simplified homogeneous analog available in a straightforward manner (**Cat g**) that performs the benchmark desymmetrization reaction with similar yields and enantioselectivities as **Cat f**, providing a convenient alternative for cases when single use in solution is sought.

KEYWORDS: *Chiral Phosphoric Acids • Immobilization • SPINOL • Continuous Flow • Density Functional Theory*.

Among the different families of successful organocatalysts, chiral phosphoric acids stands out for the unique peculiarity of combining a Lewis basic site with a Brønsted acid site within the same catalytic unit.[1-5] Moreover, since the first pioneering works of Akiyama,[6] Terada and Uraguchi[7] in 2004, the high versatility of BINOL-derived chiral phosphoric acids (BPAs) as Brønsted acid-Lewis base catalysts translates in over 500 publications.[2-4, 6-20] Drawbacks in the use of BPAs in asymmetric catalysis can be ascribed to the conformational flexibility of the BINOL scaffold that may hamper enantioselection,[21] or to the unaffordable cost in derivatives like TRIP, where this problem has been solved through the introduction of very bulky substituents in the 2,2' positions.[12] A conceptual, synthetic evolution of BINOL, 1,1′-spirobiindane-7,7′-diol or SPINOL (**1**), first introduced by Birman in 1999,[22] and its derivatives found initial application as ligands in asymmetric metal catalysis.[23-24] From 2010 on, a new generation of SPINOL-derived phosphoric acids (SPAs) has been developed.[25-26] Over the last decade, both the number of synthetic procedures for the preparation of SPAs and their catalytic applications have sensibly grown, leading to the characterization of diverse chiral SPAs and their application in different catalytic processes resulting in over 100 publications.[27] The most significant advantage of SPAs over BPAs lays in the structural rigidity of the C_2-symmetric chiral spirocyclic backbone: the configuration of the quaternary carbon in SPINOLS is blocked. Thus, conformational mobility is completely restricted and racemization in solution becomes virtually impossible. Thus, the chemical robustness and conformational rigidity of **SPAs** enables different electronic and steric factors compared to those of **BPAs**. Following pioneering work by Birman,[22] a considerable amount of work involving the use in catalysis of structures with spirocyclic backbones has been reported.[24, 28-36] Thus, asymmetric syntheses of SPINOL and SPIROL derivatives (**2-5**) have been achieved by the Tan,[30] Ding,[29,35] Nagorny,[34] and Dou groups[36] (Figure 1).

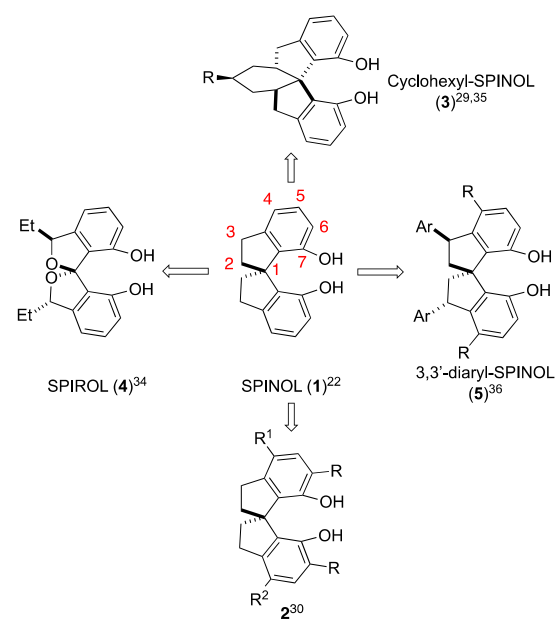

Figure 1. Development of SPINOL and SPIROL derivatives.

Most notably, Dou and coworkers reported in 2019 a highly diastereo- and enantioselective synthesis of 3,3'-diaryl-SPINOLS (**5**) and could show that the derived phosphoramidite ligands showcased higher enantioselectivities than those containing the non-substituted SPINOL skeleton in several different types of catalytic asymmetric processes.[36] In addition, it has been shown[27] that bulky substituents at the 6,6´-positions on the SPINOL skeleton in derived phosphoric acids are essential for the achievement of optimal enantiocontrol with SPINOL-derived ligands and organocatalysts. This is not a trivial detail, since the introduction of such substituents always requires additional synthetic steps leading to increased production costs that could hamper large scale application. This limitation, however, could be efficiently mitigated by immobilization of the catalyst onto solid supports. If correctly planned, this strategy could allow the easy recovery and recycling of the catalyst (thus extending its useful life span) and easy product isolation without paying a penalty in catalytic activity.[37,38] Moreover, catalytic processes based on immobilized catalysts often present the remarkable advantage of allowing implementation in continuous-flow.[39-56] As a consequence of these advantages, interest in the immobilization of homogeneous chiral catalysts onto diverse solid supports has spread in recent years,[57-61] chiral phosphoric acids clearly illustrating this tendency.

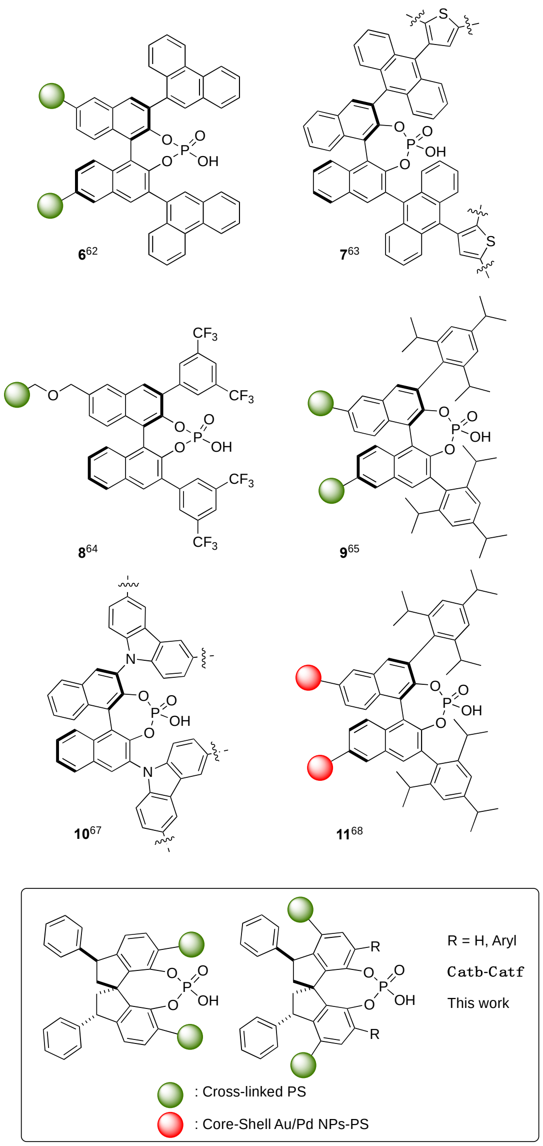

Figure 2. Immobilized chiral phosphoric acids.

Thus, Rueping[62] and Blechert[63] already envisioned the potential advantages of immobilization of chiral phosphoric acids onto stationary phases (Structures **6** and **7** in Figure 2). Later on, the Pericàs laboratory developed immobilized CPAs **8** and **9** and demonstrated their practicality for long-time operable, highly enantioselective processes in continuous flow.[64-66] Structures **10** and **11** correspond to more recent examples exemplifying the continued interest for the immobilization of CPAs.[67,68] We report in this manuscript the synthesis of a family of 3,3'-diphenyl-SPINOL bearing polymerizable substituents at either C4-C4' or C6-C6', their immobilization by copolymerization, the preparation of the corresponding CPAs (**Cat b-Cat f**) and the use of these catalytic species for the desymmetrization of 3-substituted oxetanes with benzothiazole thiols (up to 90% yield and >99% ee) has been tested both in batch and in flow. These experimental studied are complemented by a theoretical (DFT) analysis of the factors governing the enantioselectivity of the desymmetrization process that opens new perspectives for the design of even more efficient catalysts of this type.

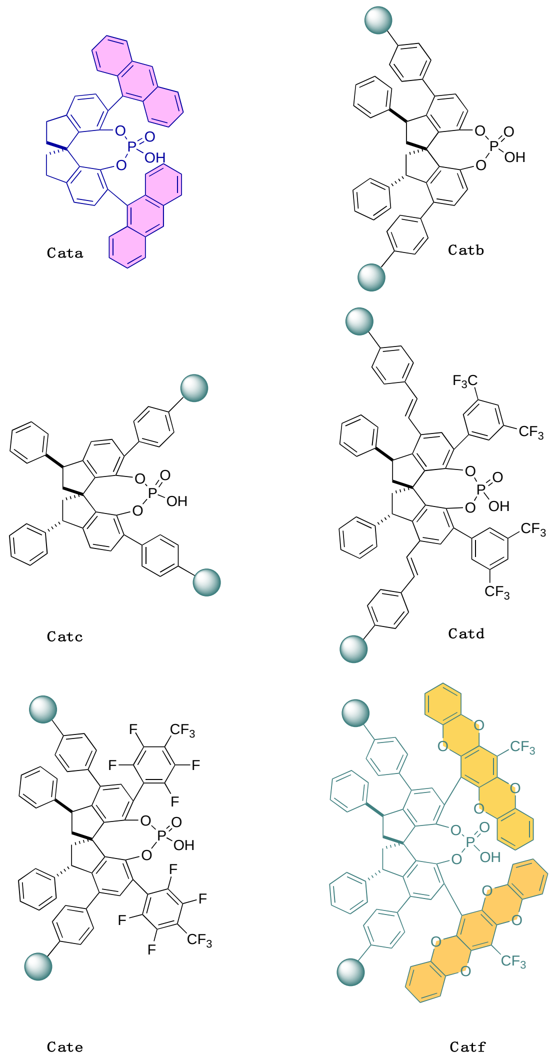

Figure 3. Immobilized SPINOL-derived chiral phosphoric acids prepared in this study.

For the preparation of polystyrene immobilized SPAs (**Cat b-Cat f**) in high enantiomeric purity, the Dou method was used as an efficient entry to the key SPINOL intermediates.[36] For comparison purposes, we designate the homogeneous 6,6'-bis(9-anthryl) SPA as **Cat a** (Figure 3). We will discuss here the preparation of **Cat f** as a most representative example of our modular approach to these catalytic species (Scheme 1). On the other hand, full details for the preparation of **Cat b-Cat e** can be found in the Supporting Information.

The starting material for the preparation of **Cat f**, 3,3'-diphenylSPINOL (**12**) was prepared in multigram amount with high enantiomeric purity (>99% ee) as a single diastereomer following the reported procedure.[36] To direct the introduction of 6,6' aryl substituents, the phenolic units were first protected as MOM ethers (**13**, 85% yield). Then, double *ortho* lithiation (*n*-BuLi, THF, 0 ºC to rt) followed by treatment with perfluorotoluene at -78 ºC, selectively led to the 6,6'-bis(arylated) product **14** in 89% yield. The standard deprotection of the MOM ethers in **14** (HCl in dioxane), followed by regioselective dibromination at 4,4' with NBS in dichloromethane afforded **16** in 64% yield (2 steps). At this stage, the phenolic units were re-protected as MOM ethers (**17**, 82% yield), and the protected intermediate was reacted with catechol in the presence of K_2CO_3 to increase the structural complexity of the aryl substituents at 6,6' (**18**, 90% yield).[69] Interestingly, monocrystals of **18** could be grown from a mixture of iodobenzene and hexane. X-ray diffraction (see Supporting Information) confirmed the structure and configuration of the compound, showing two molecules of **18** per unit cell that display p-p stacking between the heteroaromatic *wings* at the 6,6' positions, with interplane distances of 3.5-3.6 Å. As discussed below, the logic of the transformation leading to **18** was precisely that of creating a deep chiral groove around the active phosphoric acid site that will favor enantiocontrol in catalytic processes mediated by **Cat f**. It is also worth mentioning here that the apparently antieconomic protection/deprotection sequences of the phenolic units are necessary for: a) the selective introduction of the perfluoroaryl substituents at 6,6'; b) the subsequent bromination at 4,4'; c) the aromatic nucleophilic substitutions leading to the formation of the pentacyclic substituents at 6,6' and d) the ultimate Suzuki coupling with 4-vinylphenylboronic acid in the presence tetrakis(triphenylphino)palladium (0) leading to the introduction of the polymerizable units in **20** (19% yield, two steps). The polystyrene-supported SPINOL **21** was then prepared by copolymerization with styrene and DVB induced by AIBN, and **Cat f** was generated by reaction of **21** with $POCl_3$. The functionalization of the polymer was determined by phosphorus elemental analysis providing a value of f_P = 0.17 mmol/g, very appropriate for catalytic purposes.

Scheme 1. Synthesis of the polystyrene-supported SPA **Cat f**.

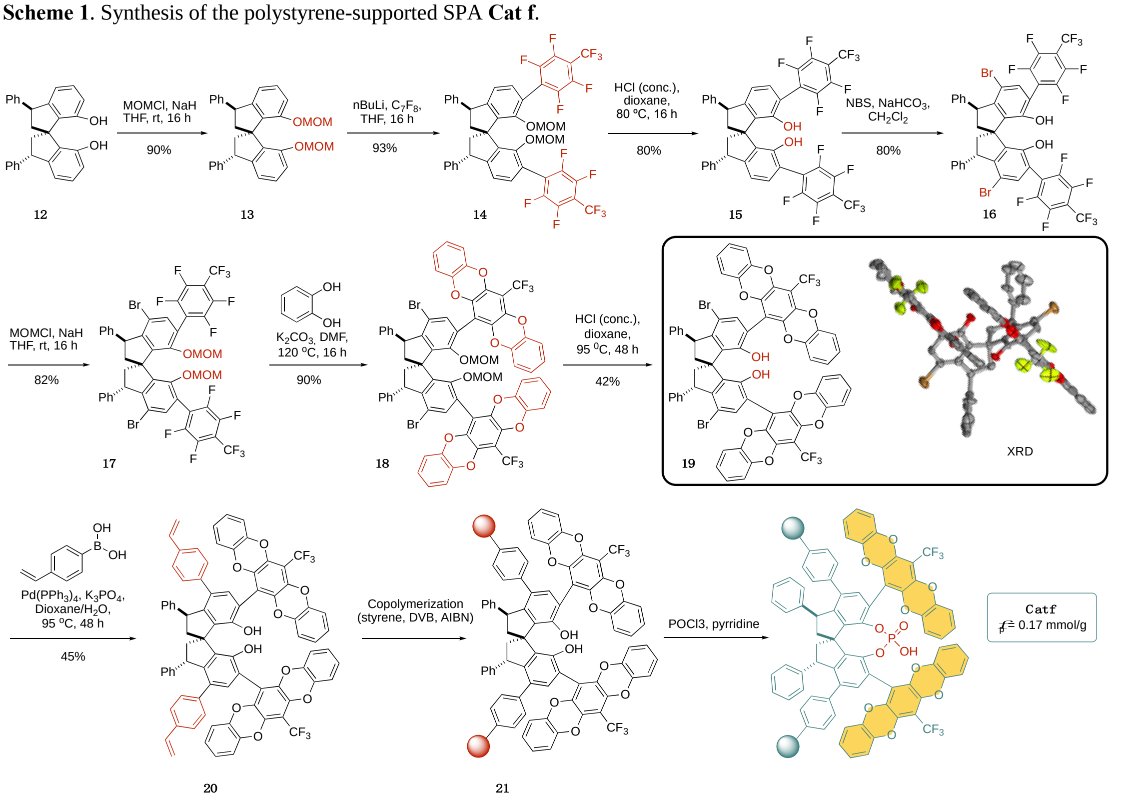

From a practical perspective, is it important to highlight that the preparation of **19** can be significantly shortened by obviating the isolation of some of its precursors. Thus, **16** can be advantageously prepared from **14** in 70% yield, while **19** can be reached from **16** in 59% yield (three steps). In this manner, the overall yield for the preparation of **19** from **12** increases from 16.6% in the step-by-step procedure to 34.5%, while three chromatographic purifications are avoided. Experimental details for these shortcuts can be found in the Supporting Information. As a benchmark of the catalytic performance of the PS-supported SPAs **Cat b-Cat f**, we selected the desymmetrization of 3,3-disubstituted oxetanes. This scaffold is increasingly used in drug design,[70] and the desymmetrizing ring-opening of these prochiral structures could be relevant to their use as prodrugs. The reaction of 3-phenyloxetan-3-ol (**22a**) with benzo[d]thiazole-2-thiol (**23a**) was used for the selection of the optimal immobilized catalytic species and for solvent optimization (Table 1). It is to be mentioned that this reaction had been previously studied by Sun and coworkers with homogeneous CPAs as catalysts,[71] 6,6'-bis(9-anthryl) SPA providing in that case the best results in terms of yield and enantioselectivity. As already mentioned, we have now used this compound (designated as **Cat a**) as a reference for the immobilized species.

Table 1. Catalyst and solvent optimization in the desymmetrization of **22a** with **23a** mediated by **Cat a-Cat f**.[a]

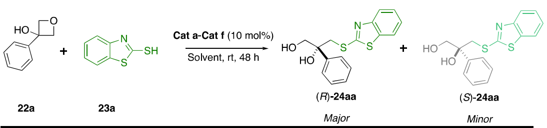

Entry	Solvent	Catalyst	Yield [%]	*ee* [%]
1[70]	CH_2Cl_2	**Cat a**	91	97
2	CH_2Cl_2	**Cat b**	85	20
3	CH_2Cl_2	**Cat c**	85	63
4	CH_2Cl_2	**Cat d**	87	72
5	CH_2Cl_2	**Cat e**	90	83
6	CH_2Cl_2	**Cat f**	81	90
7	toluene	**Cat e**	92	76
8	Et_2O	**Cat e**	90	81
9	1,2-DCE	**Cat e**	90	82
10	$CHCl_3$	**Cat e**	90	86
11	$CHCl_3$/toluene (1:9)	**Cat e**	86	86
12	$CHCl_3$	**Cat f**	92	95
13	$CHCl_3$/toluene (1:9)	**Cat f**	88	87
14[b]	$CHCl_3$	Cat f	92	98
15[b,c,d]	**$CHCl_3$**	**Cat f**	**95**	**97**
16[b,c,d,e]	**$CHCl_3$**	**Cat f**	**90**	**97**

[a]Standard conditions: **22a** (30 mg, 0.2 mmol), **23a** (42 mg, 0.25 mmol), **Cat a-f** (10 mol%; for the immobilized SPAs, calculated according to the determined functionalization) in the specified solvent (1 mL). shaking at room temperature for 48 h. Under these conditions, **23a** is only partially soluble. [b]Reaction under more dilute conditions (4 mL $CHCl_3$) to favor solubility of **23a**. [c]Reaction performed at 60 ºC. [d]Reaction time was 16 h (overnight). [e]5 mol% catalyst was used.

For the initial screening, the reaction of **22a** with **23a** was performed in dichloromethane in the presence of **Cat b-Cat f** and compared with the results reported for **Cat a** under identical conditions (entries 1-6). Although yields were satisfactory in all cases, it became clear from these results that a combination of bulky substituents at 6,6' and rotational mobility of these substituents was required for high enantioselectivity (entries 2 and 3). The more promising results were those achieved with **Cat e** and **Cat f** (entries 5 and 6), and for this reason special attention was paid to the optimization of reaction conditions with these two ligands.

It is important to point out that, from a chronological perspective, **Cat e** was designed and prepared first, with the aim of exploring the combination of steric and electronic effects by the perfluoroaryl substituents at 6,6' on enantioselectivity, already pointed out by **Cat d** (entry 4). At a later stage in the project, the susceptibility of those perfluoroaryl substituents towards nucleophilic aromatic substitution was used as a vehicle for the preparation of **Cat f** where, as discussed below, the pentacyclic heteroaryl substituents at 6,6' play a fundamental role on the catalytic performance.

The use of **Cat e** in combination with different solvents was studied in detail. The use of more benign solvents (THF, 2-methyltetrahydrofuran, ethyl acetate, acetone, 1,4-dioxane, methanol) was studied first, but none of these solvents led to measurable conversion in the studied process. When using toluene, diethyl ether or 1,2-dichoroethane (entries 7-9) the results were similar to those achieved with dichloromethane, and only with the use of chloroform (entry 10) some improvement in enantioselectivity (86%) was noticed. Interestingly, very similar results were recorded when a 9:1 mixture of toluene and chloroform was used as the solvent (entry 11).

When **Cat f** was used (entries 12, 14-16) in chloroform, yield and enantioselectivity even outperformed those recorded with the homogeneous reference **Cat a**. Thus, with 0.05M initial concentration of **22a**, enantioselectivity achieved 98% (entry 14). Interestingly, the reaction time in $CHCl_3$ could be significantly shortened by performing the reaction at 60 ºC, the reaction being completed overnight under these conditions (entry 15), and the catalyst loading could be decreased to 5 mol% without decrease in enantioselectivity (entry 16). On the other hand, with **Cat f** the use of 9:1 mixture of toluene and chloroform had a negative effect on the performance of the reaction (entry 13), so that advantages derived from the use of this more benign solvent are counterbalanced by a significant decrease in enantioselectivity.

Once we had established that **Cat f** exhibited optimal characteristics in the target desymmetrization of **22a** with thiol **23a**, we next studied the recyclability of this catalyst under the most productive conditions (those of entry 16 in Table 1). In this manner, sixteen consecutive cycles of sixteen hours could be run without substantial loss of yield and enantioselectivity. After each cycle the resin was simply separated by filtration and immediately reused in the next reaction cycle. Table S1 shows that there are negligible fluctuations in the results obtained for yields and enantioselectivity between the 1th and the 16th reaction cycles. The cumulative turnover number (TON) achieved in these sixteen runs was 280.

Previous experience in our laboratory with immobilized CPAs has shown that the only significant deactivation mode is deprotonation by basic components in reaction mixtures. Fortunately, this is a reversible process and previously studied immobilized CPAs have shown to be easily reactivated by treatment with acid.[64,65] Although **Cat f** did not show any sign of deactivation during the recycling experiment, we decided to force the base-induced deactivation of the catalyst to confirm the possibility of a subsequent reactivation. To this end (Scheme 2), a sample of **Cat f** was deactivated by treatment with excess pyridine for 6 h. Then, the use of this deactivated catalyst in the reaction of **22a** with **23a** under the standard conditions of Table

1 led to only 15% conversion, although enantioselectivity kept high (93%). Interestingly, the employed catalyst sample could be reactivated by treatment with 2M HCl in dioxane and reused in the reaction after washing with chloroform. In this manner, complete conversion of **22a** and 96% enantioselectivity in the formation of **24aa** were recorded.

Scheme 2. Deactivation/reactivation of the polystyrene-supported SPA **Cat f**.

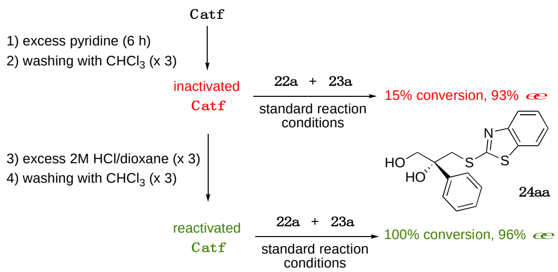

In view of the excellent recyclability depicted by **Cat f** and its compatibility with rather high temperatures, with the derived consequence of short reaction times, we decided to explore the desymmetrization as a genuine flow process, bypassing any intermediate scope development in batch. For the flow experiments, 2.0 g of **Cat f** (*f* = 0.17 mmol/g, 0.34 mmol) were loaded in a size adjustable, jacketed tubular reactor. The feed of the reactor could be selected through a three-way valve from the appropriate mixture of **22** and **23** (they are unreactive to one another in the absence of **Cat f**) to the reaction solvent (chloroform) for resin cleaning between distinct operations. At the reactor outlet, a back-pressure regulator was intercalated to secure uneventful operation near the boiling point of chloroform (Figure 4)

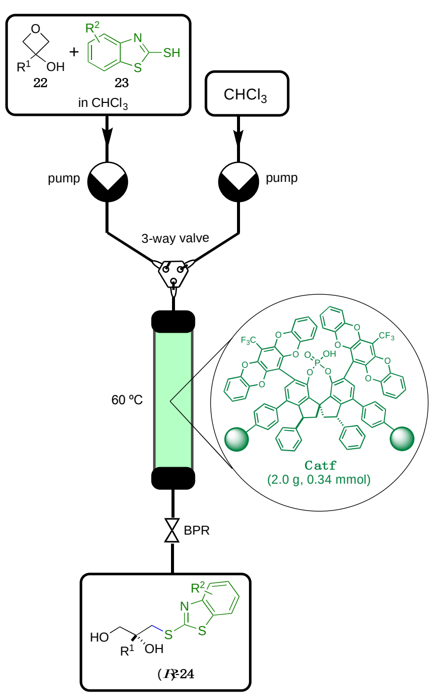

Figure 4. Schematic representation of the flow system for the desymmetrization of oxetanes mediated by the PS-supported SPA **Cat f**.

As an initial step, the parameters of reaction temperature, concentration of **22a**, and combined flow rate were optimized for the simultaneous achievement of high yield and enantioselectivity in the reaction with **23a** leading to **24aa**. Full data for the optimization process can be found in the Supporting Information (Table S3). In summary, work at 60 ºC is highly recommended for high yield with no penalty in enantioselectivity, and two sets of [**22a**]/flow rate conditions seem to be equally suitable: a) Work with 0.05 M **22a** in chloroform at 1 mL/min (residence time = 8 min) leads to a conversion of 92% and enantioselectivity of 97%, and b) Work with 0.1 M **22a** in chloroform at 0.5 mL/min (residence time = 15 min) leads to a conversion of 98% and enantioselectivity of 95%. In all these experiments, a 25 mol% excess of **23a** was used. As a general comment, the productivity of the experiments under any of the two optimal sets of experimental conditions is remarkable (*ca.* 8 $mmol_{24aa}.mmol_{Cat\,f}^{-1}.hour^{-1}$) and can be further increased till *ca.* 14 $mmol_{24aa}.mmol_{Cat\,f}^{-1}.hour^{-1}$ at the expense of a somewhat lower instant conversion.

The same flow system, with the same catalyst sample, was next used for the study of the scope of the desymmetrization process by reaction of **22a-n** with **23a-d**. For this study, we selected 3,3-disubstituted oxetanes as substrates. Besides having been comparatively less studied, they offer the additional interest of leading to products with a quaternary stereocenter. All the experiments were sequentially performed with 2 mmol of **22** and 2.5 mmol of **23** in 20 mL $CHCl_3$, operating the flow system at 0.5 mL/min. In this manner, every individual experiment lasted 40 minutes, and the packed bed reactor was rinsed for 20 min with $CHCl_3$ between individual experiments in order to remove traces of the previous product (Figure 5). In this manner, a family of fourteen different oxetanes **22a-n** was submitted to the desymmetrization process in flow in combination with the mercaptobenzothiazoles **23a-d** to produce the seventeen products depicted in Figure 5. The process tolerates well a variety of substituent types at C3 on the oxetane structure (aryl, heteroaryl, alkyl, alkenyl, alkynyl) defining in most cases tertiary alcohols at that position. In the same manner, substituents on the aromatic ring of **23** do not affect in a substantial manner the outcome of the reaction with the same oxetane (**22a**).

From the point of view of yield, it is important to remark that all the studied desymmetrization reactions are very clean, no significant byproducts being detected. Thus, although lower than optimal yields detected in some cases (>65%), it should be possible to increase them by simply adjusting flow rate in those particular examples. As for enantioselectivity, the results in Figure 5 tend to indicate that the differences between the steric requirements of the C3 substituents on the oxetane ring play a fundamental role on the outcome of the reaction. In tertiary alcohol-type substrates, the presence of an aromatic substituent at C3 generally leads to very high *ee*, whereas in the parallel cases involving linear alkyl substituents, a certain chain length is required for high enantioselectivity (40% *ee* in **24ha**, where R^1 = methyl, but 90% *ee* in **24ia**, where R^1 = butyl).

The success of the desymmetrization in the case of product **24ea**, containing a terminal propargyl alcohol moiety, offers an additional interest. Thus, this type of substrates easily undergo copper-catalyzed alkyne-azide (CuAAC) reactions in continuous flow,[72] and the integration of these two constructive reactions can lead to the telescoped, highly convergent preparation of modular enantioenriched triazoles.

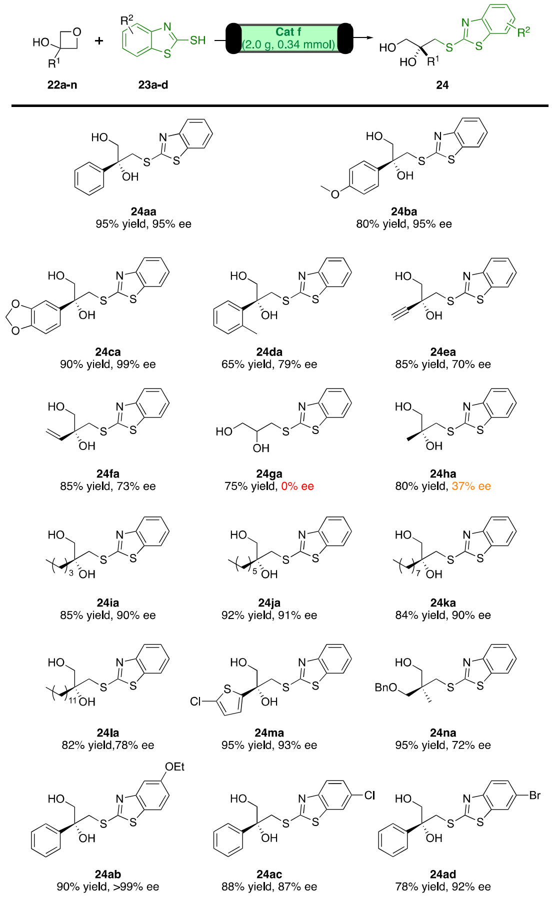

Figure 5. Oxetanes and benzothiazolethiols scope in the **Cat f** catalyzed desymmetrization reaction. All yields shown refer to isolated products. The reactions were performed with oxetane **22** (2 mmol) and benzothiazolethiol **23** (2.5 mmol) in 20 mL chloroform, flowing for 40 minutes (flow rate = 0.5 ml/min) through a packed bed reactor at 60 ºC containing 2.0 g (0.34 mmol) of **Cat f**. When the circulation of a given reactants mixture was complete, chloroform was circulated through the reactor for 20 minutes at 0.5 mL/min. Then the system is ready for the next reactant combination.

As a final test of the practical value of the desymmetrization in continuous flow catalyzed by **Cat f**, we planned to use the same packed bed reactor employed for the scope in Figure 5 for the gram scale preparation of **24aa** (two runs) and **24na**. In a first preparative experiment (Scheme 3, a), starting from 20 mmol of **22a** and 25 mmol of **23a** in chloroform (200 mL) the system was operated at 0.5 mL/min for *ca*. 400 minutes, till the reactants solution had completely circulated, and the packed bed reactor was then washed by circulating chloroform at 0.5 mL/min for 20 minutes. Product purification by the usual protocol afforded **24aa** (5.7g, 90% yield) with 95% ee. In the same manner, **22a** (0.24 g, 92% conversion) was recovered. After keeping the employed sample of **Cat. f** swollen with chloroform for 15 months, the flow preparation of **24aa** was performed again under identical conditions, starting from 18 mmol of **22a** and 22.5 mmol of **23a** in chloroform (180 mL) (Scheme 3, b). Gratifyingly, both yield and enantioselectivity of the previous run were duplicated. Subsequently, the preparation of **24na** was also performed at the 20 mmol scale using one more time the same packed bed reactor (Scheme 3, c), a slight improvement in yield and the same enantioselectivity with respect to the smaller scale preparation in Figure 5 being recorded. Data for instant conversion and enantioselectivity during experiments b) and c) are presented in the Supporting Information. Thus, all the data collected in our study, from recycling in batch to sequential scoping in flow and use at the multigram scale in flow point out to the important robustness of **Cat f** and its suitability for large scale production. In this respect it is worth mentioning that, setting apart the initial adjustment of flow rate, the 0.34 mmol sample of Cat. f used for the scope in Figure 5 and the preparative experiments in Scheme 3 accounts for a cumulative TON of *ca*. 243, without decreases in performance.

Scheme 3. Continuous flow preparation of **24aa** in gram scale using a multiply reused sample of **Cat f**.

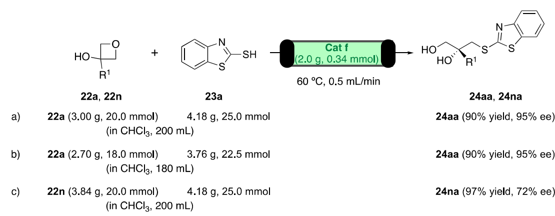

In order to rationalize the enantioselectivity performance of **Cat f** and the differences with the poorly behaving **Cat b**, we decided to undertake a theoretical study of the desymmetrization process. Early computational studies on organocatalytic reactions mediated by chiral phosphoric acids include Mannich reaction, 1,3-dipolar cycloadditions[73a] as well as desymmetrization processes.[73b-c] In particular, Seguin and Wheeler studied the desymmetrization of 3-substituted oxetanes catalyzed by 6,6'-bis(9-anthryl)SPINOL phosphoric acid, reaching the conclusion that competing noncovalent interactions are the main factor controlling enantioselectivity in that case.[74] The main focus of the present computational study has been directed to establishing the relevance of the pentacyclic substituents at the 6,6'-positions of **Cat f** in biasing the enantioselectivity of the oxetane desymmetrizations mediated by this species. **Cat b** and **Cat f** were selected for the computational study as they represent the two extremes in size of the substituents at the 6,6'-positions and of recorded enantioselectivity. Since our experimental studies have shown that the polymer backbone does not affect enantioselectivity (with respect to homogeneous models), the truncated versions of the real catalysts **25** and **26** were used in the calculations (Figure 6).

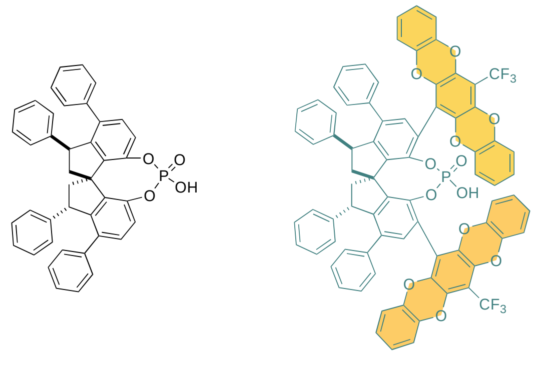

25 (model for Catb) 26 (model for Catf)

Figure 6. Structures **25** and **26**, models for **Cat b** and **Cat f** in the theoretical studies.

Focusing first our attention onto the reactants, we were surprised to find that the thiol tautomeric form of the reactant benzo[d]thiazole-2-thiol is not involved in the catalytic nucleophilic attack onto the 3-hydroxyoxetane structure. At the employed level of theory (M06-2X-D3/DGTZVP/SMD//M06-2X-D3/DGDZVP) the results of the theoretical studies suggest that the tautomeric form of **23a**, benzo[d]thiazole-2(3H)-thione, keto-**23a**, is thermodynamically preferred over the thiol form by DG = -8.4 kcal·mol^{-1} at 333 K (Figure 7). The interconversion between enethiol and thione tautomers can take place in either intermolecular or intramolecular fashions. In the former case, the calculated barrier is very low, DG‡ = +6.0 kcal·mol^{-1}, while the intramolecular process is not competitive at the considered temperature (DG‡ = +29.8 kcal·mol^{-1}). It is thus suggested that only the thione form of **23a** will be present in the reaction media and will likewise be the nucleophile acting in the desymmetrization reaction.

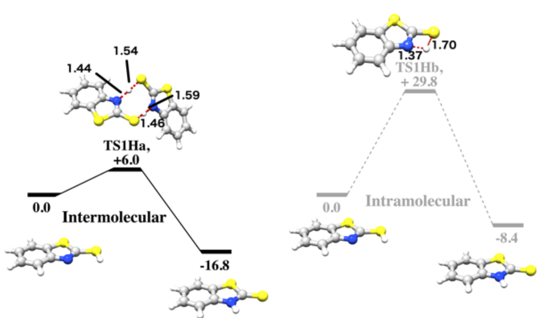

Figure 7. Free energy profiles for the intermolecular and the intramolecular tautomerization of benzo[d]thiazole-2-thiol (**23a**) into benzo[d]thiazole-2-thione (keto-**23a**) in $CHCl_3$ at 333K. Displacements associated to the imaginary frequencies in the relevant transition states are indicated by red dotted lines and related atomic distances in Å.

Xie and co-workers were able to isolate tautomeric 2-(methylthio)benzo[d]thiazole (**27a**) and 3-methylbenzo[d]thiazole-2(3H)-thione (**27b**) prepared through different synthetic routes and characterize them by NMR spectroscopy.[75] As expected, the thiol and thione tautomers present very different chemical shift in ^{13}C{^{1}H}NMR: d = 167.0 ppm for ***C***-SH, and d = 188.4 ppm for ***C***=S.[75] To determine the tautomeric form of **23** present in solution, we measured the ^{13}C{^{1}H}NMR spectrum on a freshly prepared sample of the reagent. A chemical shift of 190.9 ppm was found for the considered carbon, strongly suggesting that **27b** is the largely predominant tautomer present in $CHCl_3$ solution at 298 K (Figure 8). Moreover, a full geometrical optimization of a Van der Waals complex featuring the contact of a molecule of **23a** with **25** triggers a barrierless proton exchange to form keto-**23a**.

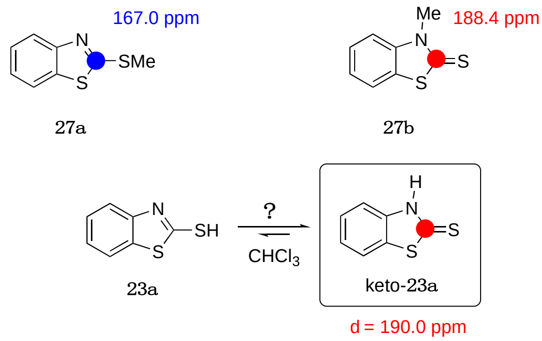

Figure 8. Tautomeric equilibrium of **23a** in chloroform

Interestingly, the benzo[d]thiazole-2(3H)-thione tautomer (keto-**23a**) exhibits nucleophilic character and easily undergoes nucleophilic attack to the oxetane partner in the presence of phosphoric acid catalysts. Figure 9 shows the calculated reaction profile for the reaction of **22a** with keto-**23a** catalyzed by the **Cat b** truncated model, **25**. Mechanistic information from the intrinsic reaction coordinates (IRC) following the hypersurface downhill from the transition states suggests that proton transfer from the catalyst to the ether oxygen of the oxetane ring happens first, followed by a nucleophilic attack of the thione sulphur atom onto one of the enantiotopic carbon atoms a to oxygen in the oxetane ring (C2 or C4). The transition states for these desymmetrizing processes exhibit marked S_N2 characteristics, with O•••C•••S angle of nearly 180º. As already pointed out by Seguin and Wheeler,[72] the shape of the oxetanol substrate provides a perfect interlocking match with the phosphoric acid catalyst via the formation of two complementary O-H•••O hydrogen interactions. The result is the formation of stable Van der Waals adducts between oxetanol **22a** and **25** (**I0_1** and **I0_2** in Figure 9). We also investigated the possible involvement of similar Van der Waals complexes of **25** with keto-**23a** in the early stages of the reaction; however, their higher endergonic nature (compared to **I0_1** and **I0_2**) discarded them as competent reaction intermediates.

To get a more comprehensive scenario of the possible transition states involved in the desymmetrization process, we considered four different geometric catalyst-to-reactants approaches, including two (*R*)- and two (*S*)-stereodifferentiating pathways. In this respect, Figures 9 and 10 show the lowest energetically demanding pathways leading to (*R*)- and two (*S*)-stereoisomers in processes mediated by **25** and **26**, respectively (data concerning redundant transition structures and minima thereof are included in the computational section of SI). Calculations at the M06-2X-D3/DGTZVP/SMD//M06-2X-D3/DGDZVP level estimate the reaction barrier for the process mediated by **25** as +25.5 kcal·mol^{-1} for the *(R)*-directing **TS1d_*R*** and +26.3 kcal·mol^{-1} for *(S)*-directing **TSb_*S***, Figure 9. This results in a calculated enantioselectivity at 333 K of 78:22 (65:35 without BSSE corrections) in favor of the *R* enantiomer (ee_R = 55% with BSSE corrections and ee_R = 29% without BSSE corrections). These data are in excellent agreement with the experimental results obtained with **Cat b** at the same temperature (ee_R = 20%).

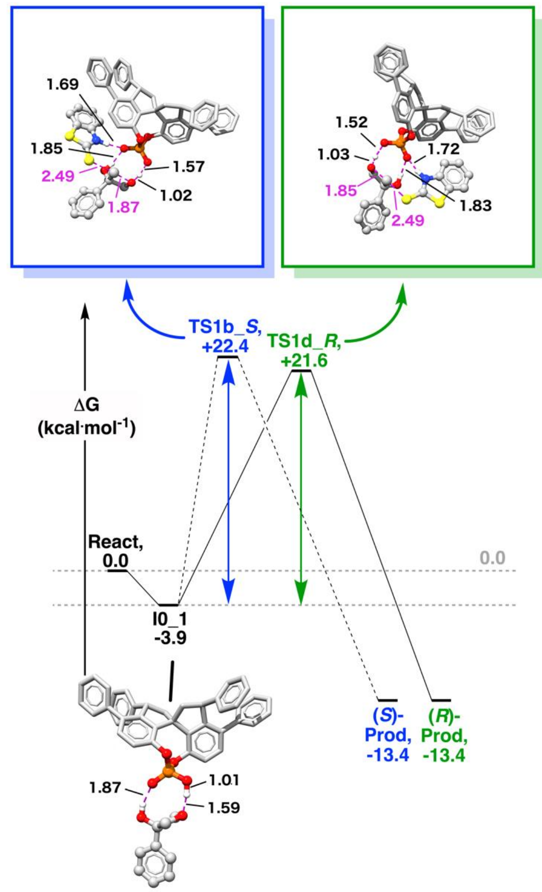

Figure 9. Free energy profiles for the desymmetrization of **22a** with keto-**23a** catalyzed by the **Cat b** model (**25**). The values are reported in kcal·mol^{-1}. **I0_1** represents the resting states of the catalyst. Relevant hydrogen bonds distances are reported in black (in Å). Relevant distances associated to displacements of the imaginary frequency for transition states are reported in magenta (in Å).

Figure 10 shows the calculated reaction profile for the reaction of **22a** with keto-**23a** catalyzed by the **Cat f** truncated model, **26**. The first substantial difference between catalysts **25** and **26** is that the latter binds the substrates somewhat stronger than the former, as it can be seen in the coordination of the oxetanol at **I0_1** and **I0_2** in Figure 10. Thus, **26** binds the oxetanol exergonically with a net gain of up to -13.2 kcal·mol^{-1}, while **25** binds oxetanol with a net gain up to -3.9 kcal·mol^{-1} (as comparison, an intermediate situation is seen for **Cat a**, with a net gain of up to -6.5 kcal·mol^{-1}, see Supporting Information). Consequently, while **25** expels easily the products at the end of the desymmetrization (the value of -13.4 kcal·mol^{-1} in Figure 9 and 10 refers to the separation of the product and catalyst at infinite distance), the product of the desymmetrization prefers to remain bound to catalyst **26** than to be separated from it. Catalyst-product adduct resides at -26.3 kcal·mol^{-1} in the free energy profile of Figure 10. In the case of **26** the system must pay an energetic penalty of +12.9 kcal·mol^{-1} to free the catalytic site and allows the release of the (*R*)-product (again, an intermediate situation is seen for **Cat a**, whose catalyst-product adduct resides at -18.6 kcal·mol^{-1} and the system has to pay a penalty of +5.2 kcal·mol^{-1} to free the catalytic site, see Supporting Information).

Secondly, **26** displays an enhanced reactivity towards the desymmetrization of **22a** with **23a**: the lowest free energy barrier stands out at +20.3 kcal·mol^{-1}, five kcal·mol^{-1} lower than that shown for catalysis carried out by **25**. Thus, the results of these calculations suggest that **Cat f** will kinetically outperfom even **Cat a**, whose activation barrier stands out at +21.5 kcal·mol^{-1} (see Supporting Information) and correctly reproduces the experimental enantioselectivity recorded for **Cat f** at 333 K, of up to ee ~ 98% (calculated ee is 100% with and without BSSE correction). The predominance of *R* product arises from **TS1d_*R***, represented in Figure 10 in side and bottom views. For comparison, calculations at the same level of theory also correctly predicts ee ~ 100% for **Cat a** (see Supporting Information).

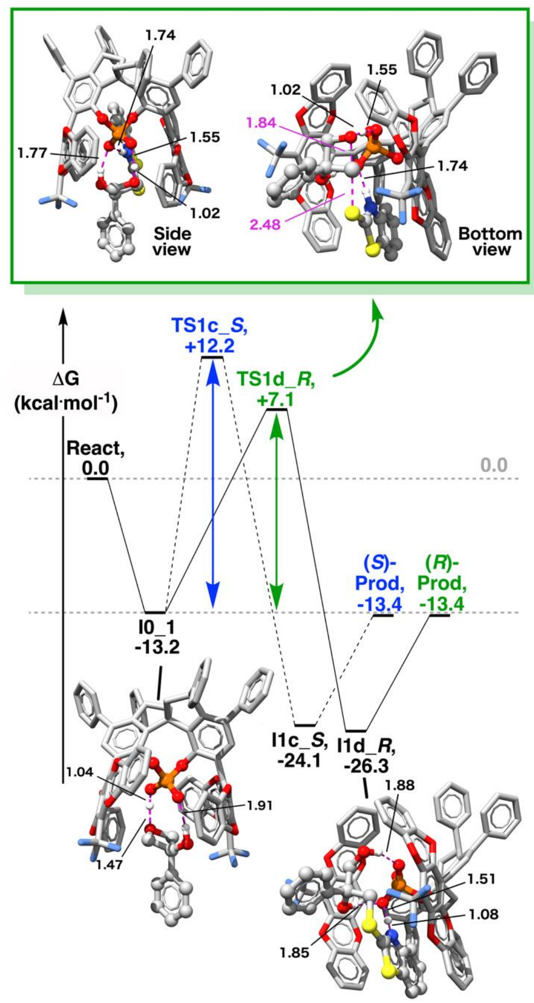

Figure 10. Free energy profiles for the desymmetrization of **22a** with keto-**23a** catalyzed by the **Cat f** model (**26**). The values are

reported in kcal·mol^{-1}. **I0_1** represents the resting states of the catalyst. Relevant hydrogen bond distances are represented in black (in Å). Relevant distances associated to displacements following the imaginary frequency for transition states are represented in magenta (in Å).

The stronger binding towards the substrates seen for **26**, compared to **25**, can be rationalized considering that the extended heteroaromatic wings do not only create a deep chiral groove of steric nature around the catalytic center but, even more importantly, they also offer extra differential stabilization via non-covalent interactions and p-p stacking. Figure 11a represents dg^{inter} isosurfaces mapping the non-covalent interactions between the anionic catalyst (Fragment 1, $[(RO)_2PO_2]^-$) and the protonated activated complex of the substrates (Fragment 2, Oxetanol + keto-**23a** + H$^+$) via Independent Gradient Model (IGM), developed by Henon and co-workers[76] and implemented by Lu and co-workers in MULTIWFN.[77] We found over 1300 weak interactions in **TS1d_*R*** of **26** including strong interfragment O-H•••O and N-H•••O hydrogen bonds, a plethora of F•••C, F•••O, F•••H, S•••O, S•••F and S•••C Van der Waals contacts and other interactions assimilable to p-p stacking. The cumulative effect of these weak interactions within **26** is so strong that the extended heteroaromatic conjugation of the wings is overcome, enabling the loss of planarity and the formation of a "templated" cradle around the catalytic center, reminiscent to the *induced fit* operating in enzymes.[78]

Figure 11b displays a quantitative measurement of these weak interactions at transition states between anionic catalyst (Fragment 1) and the protonated activated complex of the substrates (Fragment 2) for **Cat a**, **Cat b** (**25**) and **Cat f** (**26**): DPE$_{TS(R)}$ and DPE$_{TS(S)}$ represent the molar work (i.e., a difference of potential energies) that must be spent in order to separate Frag. 1 and 2 at infinite distance in chloroform, with a dielectric constant e = 4.7113, for (*R*)-directing TS and (*S*)-directing TS, respectively. Figure 11b conveys two fundamental concepts at glance: firstly, the **Cat f** model binds the (*R*)-activated complex 3.4 kcal·mol^{-1} stronger than **Cat a** and 19.6 kcal·mol^{-1} stronger than **Cat b** model **(25)** at transition state in chloroform and, secondly, the fragments within (*R*)-stereoinducing transition state are tighter bound than those in (*S*)-stereoinducing transition state for **Cat f** (and **Cat a**) compared to **Cat b (**the difference between DPE$_{TS(R)}$ and DPE$_{TS(S)}$ is essentially negligible for **25,** even more so considering that it is of the same order of magnitude as the differences between the (*R*)- and (*S*)-directing isolated fragments, DPE$_{Frag\#1}$ and DPE$_{Frag\#2,}$ Figure 11**)**. This is an unequivocal sign that cumulative weak interactions between Frag. 1 and 2 at (*R*)-stereoinducing **TS1d_*R*** of **Cat f** are competitively stronger than those within the fragments in (*S*)-stereoinducing **TS1c_*S***, causing an overall increased stabilization of the former structure over the latter.

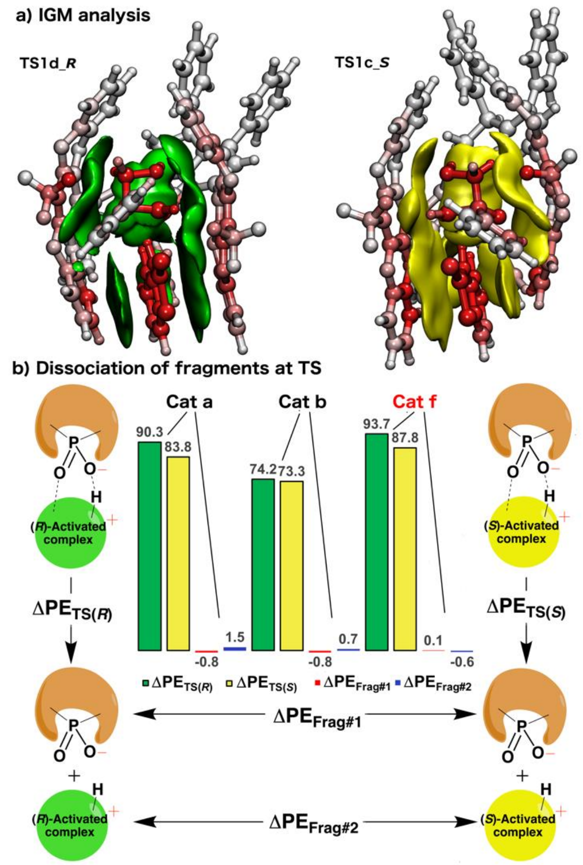

Figure 11. a) IGM on computational densities for **TS1d_*R*** and **TS1c_*S*** structures in reactions mediated by **Cat f** model (**26**). Green and yellow Dg^{inter} surfaces represent non-covalent interaction regions between anionic catalyst (Frag. 1) and protonated activated complex of substrates (Frag. 2) at 0.004 a.u. isovalue. The darker the red color of the atoms, the more they contribute to the Dg^{inter} isosurface (atoms in grey do not contribute). b) Energetics of the dissociation of Fragment 1 and Fragment 2 at transition states. Values are in kcal·mol^{-1}, being only valid for reactions in chloroform.

At the light of the results of the theoretical study, where the role of the pentacyclic substituents at 6,6' on the enantioselectivity recorded with **Cat. f** in the catalytic desymmetrization of 3,3-disubstituted oxetanes has been stressed, we considered the potential interest of developing a minimalistic, readily available analog of this species for work in homogeneous phase. Since substitution at 4,4' is required for immobilization, but does not seems to play an important role on enantioselectivity according to the calculated structures for the relevant transition states (see Figures 10 and 11), we conceived **Cat. g** as the candidate structure fulfilling the above conditions.

Scheme 4. Preparation of the monomeric phoshoric acid **Cat. g** from intermediate **14**.

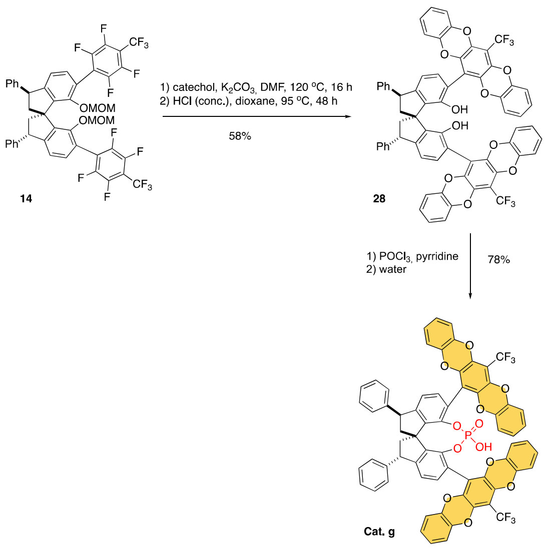

Interestingly, **Cat g** is available in only two steps, already optimized in the course of the present study, from intermediate **14** in 45% yield (four steps, 38% yield from **12**). With **Cat g** in hands, its use in the catalytic desymmetrization of a representative family of oxetanes **22** was studied. We have collected in Table 2 the results of this study. For comparison purposes, the results obtained with **Cat f** in continuous flow have also been included.

Table 2. Desymmetrization of **22** with **23** leading to **24** mediated by the homogeneous catalyst **Cat g**.[a]

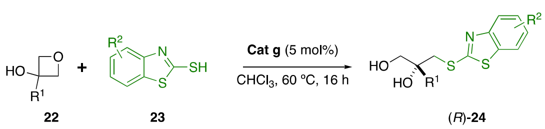

Entry	Product	with **Cat g** Yield [%]; ee [%]	with **Cat f**[b] Yield [%]; ee [%]
1	**24aa**	87; 95	95; 95
2	**24ba**	78; 98	80; 95
3	**24ca**	83; >99	90; 99
4	**24da**	86; 95	65; 79
5	**24ea**	90; 73	85; 70
6	**24ga**	84; 7[c]	75; 0
7	**24ha**	87; 13[d]	80; 37
8	**24ia**	90; 90	85; 90
9	**24ja**	85; 92	92; 91
10	**24ka**	88; 92	84; 90
11	**24ma**	87; 97	95; 93
12	**24na**	95; 78	95; 72
13	**24ab**	96; 95	90; >99
14	**24ac**	85; 85	88; 87
15	**24ad**	80; 74	78; 92

[a]Standard conditions: **22** (0.2 mmol), **23** (0.25 mmol) and **Cat g** (12 mg, 5 mol%) in chloroform (4 mL) stirred at 60 ºC (oil bath temp) in a sealed vial for 16 h. [b]Reaction conditions are those in Figure 5. [c]When the reaction was performed at rt for 16 h, yield was 82% and ee 4%. [d]When the reaction was performed at rt. for 16 h, yield was 86% and ee 10%.

To facilitate comparison with **Cat f**, the scope of the desymmetrization with **Cat g** was studied in chloroform solution at 60 ºC. Under these conditions, the parallelism with **Cat f** in terms of performance is remarkable. Thus, the preparations of **24ga** and **24ha** turned out to be poorly enantioselective, as it is the case with **Cat f**. For the rest of products **24**, although some differences can be noted in individual cases, the average yield and enantioselectivity recorded with the heterogeneous (**Caf f**) and the simplified homogeneous catalyst (**Cat g**) are essentially identical: 86.9% average yield with **Cat g** *vs*. 86.3% with **Cat f**, and 89.5% average ee with **Cat g** *vs*. 88.6% with **Cat f**. The desymmetrization of the two reluctant examples was also studied at room temperature in an attempt to improve the enantioselectivity of the transformations, but without success (entries 6 and 7). All together, these results tend to indicate that the pentacyclic substituents present at the 6,6' positions of **Cat f**, possess the power to impart optimal enantiocontrol characteristics to SPINOL-derived phosphoric acids without the need of other structural characteristics.

In summary, a new family of chiral phosphoric acids derived from 3,3'-diphenyl-SPINOL (SPAs) been successfully synthesized and immobilized onto cross-linked polystyrene using either the 4,4' or the 6,6' positions. The resulting catalytic polymers efficiently mediate the desymmetrization of 3-substituted oxetanes (**22**) with 3-mercaptobenzothiazoles (**23**). The optimal catalyst (**Cat f**) involves immobilization through positions 4,4', remote from the catalytic site, and presents two very extended heteroaromatic substituents at positions 6,6'. **Cat f** exhibits unlimited recyclability (to the extent of the attempted reuses) in batch and flow, providing the target desymmetrized products in high yield (up to 92%) and enantioselectivity and (up to >99% *ee*), high productivity being recorded under both types of experimental conditions. A DFT study on monomer models of **Cat b** and **Cat f**, the worst and the best-performing SPAs in this study, has demonstrated that the extended, geometrically adaptable heteroaromatic wings at the 6,6' positions of the SPINOL sketon in **Cat f** are key to improved kinetics and enantioselectivity in the desymmetrization process thanks to extended and cumulatively strong non-covalent interactions. The lessons learned from this theoretical study have guided the design of a readily available, minimalistic homogeneous analog (**Cat g**) with catalytic performance similar to **Cat f**, that could represent an interesting and economic alternative when single catalytic use in batch is considered.

Notes

The authors declare no competing financial interest.

ASSOCIATED CONTENT

Supporting Information. The Supporting Information is available free of charge on the ACS Publications website at http://pubs.acs.org.

Synthetic procedures and complete spectroscopic (NMR and HPLC) characterizations of the catalytic structures and their precursors. Synthetic procedures of immobilization of catalysts onto polystyrene stationary phase, full methodology of the flow chemistry implementation, complete characterization of all the products (NMR and HPLC). Cartesian coordinates and frequencies of all characterized stationary points, absolute values of thermodynamic state functions, absolute and relative values of RRHO-corrected thermodynamic state functions (PDF)

Accession Codes. CCDC 2018564 contains the supplementary crystallographic data for this paper. These data can be obtained free of charge via www.ccdc.cam.ac.uk/data_request/cif, or by emailing data_request@ccdc.cam.ac.uk, or by contacting The Cambridge Crystallographic Data Centre, 12 Union Road, Cambridge CB2 1EZ, UK; fax: +44 1223 336033.

.

AUTHOR INFORMATION

Corresponding Author

Miquel A. Pericàs − *Institute of Chemical Research of Catalonia (ICIQ), The Barcelona Institute of Science and Technology (BIST), E-43007 Tarragona, Spain*; *Departament de Química Inorgànica i Orgànica, Universitat de Barcelona, 08028 Barcelona, Spain*; orcid.org/0000-0003-0195-8846;
Email: mapericas@iciq.es

Authors

Junshan Lai − *Institute of Chemical Research of Catalonia (ICIQ), The Barcelona Institute of Science and Technology (BIST), E-43007 Tarragona, Spain; Universitat Rovira i Virgili, Departament de Química Analítica i Química Orgànica, c/Marcel·lí Domingo, 1, 43007 Tarragona, Spain*
Mauro Fianchini − *Institute of Chemical Research of Catalonia (ICIQ), The Barcelona Institute of Science and Technology (BIST), E-43007 Tarragona, Spain*; orcid.org/0000-0003-2619-7932. Inquiries on computational aspects of the manuscript should be addressed to this author at: mfianchini@iciq.es

ACKNOWLEDGMENT

This work was funded by MINECO/FEDER (grants CTQ2015-69136-R and PID2019-109236RB-I00) and the CERCA Program/Generalitat de Catalunya. J. L. thanks the MINECO for a FPI fellowship (BES-2016-078937). MF would like to thank Prof. E. Henon and Prof. T. Lu for the useful discussions on the nature and the implementation of Independent Gradient Model (IGM).

REFERENCES

1. Kampen, D.; Reisinger, C. M.; List, B. Chiral Brønsted Acids for Asymmetric Organocatalysis. In *Asymmetric Organocatalysis*, List, B., Ed. Springer Berlin Heidelberg: Berlin, Heidelberg, 2009; pp 1-37.

2. Akiyama, T.; Itoh, J.; Fuchibe, K. Recent Progress in Chiral Brønsted Acid Catalysis. *Adv. Synth. Catal.* **2006,** *348* (9), 999-1010.

3. Akiyama, T. Stronger Brønsted Acids. *Chem. Rev.* **2007,** *107* (12), 5744-5758.

4. Connon, S. J. Chiral Phosphoric Acids: Powerful Organocatalysts for Asymmetric Addition Reactions to Imines. *Angew. Chem. Int. Ed.* **2006,** *45*, 3909-3912.

5. Ouellet, S. G.; Walji, A. M.; Macmillan, D. W. C. Enantioselective Organocatalytic Transfer Hydrogenation Reactions using Hantzsch Esters. *Acc. Chem. Res.* **2007,** *40*, 1327-1339.

6. Akiyama, T.; Itoh, J.; Yokota, K.; Fuchibe, K., Enantioselective Mannich-Type Reaction Catalyzed by a Chiral Brønsted Acid. *Angew. Chem. Int. Ed.* **2004,** *43*, 1566-1568.

7. Uraguchi, D.; Terada, M. Chiral Brønsted Acid-Catalyzed Direct Mannich Reactions via Electrophilic Activation. *J. Am. Chem. Soc.* **2004,** *126*, 5356-5357.

8. Taylor, M. S.; Jacobsen, E. N., Asymmetric Catalysis by Chiral Hydrogen-Bond Donors. *Angew. Chem. Int. Ed.* **2006,** *45*, 1520-1543.

9. Doyle, A. G.; Jacobsen, E. N. Small-Molecule H-Bond Donors in Asymmetric Catalysis. *Chem. Rev.* **2007,** *107*, 5713-5743.

10.Dondoni, A.; Massi, A., Asymmetric Organocatalysis: From Infancy to Adolescence. *Angew. Chem. Int. Ed.* **2008,** *47*, 4638-4660.

11. Terada, M. Binaphthol-derived phosphoric acid as a versatile catalyst for enantioselective carbon–carbon bond forming reactions. *Chem. Commun.* **2008,** 4097-4112.

12. Adair, G.; Mukherjee, S.; List, B. TRIP-A Powerful Bronsted Acid Catalyst for Asymmetric Synthesis. *Aldrichimica Acta* **2008,** *41*, 31-39.

13. You, S.-L.; Cai, Q.; Zeng, M. Chiral Brønsted acid catalyzed Friedel–Crafts alkylation reactions. *Chem. Soc. Rev.* **2009,** *38*, 2190-2201.

14. Terada, M. Chiral Phosphoric Acids as Versatile Catalysts for Enantioselective Transformations. *Synthesis* **2010,** 1929-1982.

15. Yu, J.; Shi, F.; Gong, L.-Z. Brønsted-Acid-Catalyzed Asymmetric Multicomponent Reactions for the Facile Synthesis of Highly Enantioenriched Structurally Diverse Nitrogenous Heterocycles. *Acc. Chem. Res.* **2011,** *44*, 1156-1171.

16. Rueping, M.; Kuenkel, A.; Atodiresei, I. Chiral Brønsted acids in enantioselective carbonyl activations–activation modes and applications. *Chem. Soc. Rev.* **2011,** *40*, 4539-4549.

17. Parmar, D.; Sugiono, E.; Raja, S.; Rueping, M. Complete Field Guide to Asymmetric BINOL-Phosphate Derived Brønsted Acid and Metal Catalysis: History and Classification by Mode of Activation; Brønsted Acidity, Hydrogen Bonding, Ion Pairing, and Metal Phosphates. *Chem. Rev.* **2014,** *114*, 9047-9153.

18. Wu, H.; He, Y.-P.; Shi, F. Recent Advances in Chiral Phosphoric Acid Catalyzed Asymmetric Reactions for the Synthesis of Enantiopure Indole Derivatives. *Synthesis* **2015,** *47*, 1990-2016.

19. Merad, J.; Lalli, C.; Bernadat, G.; Maury, J.; Masson, G., Enantioselective Brønsted Acid Catalysis as a Tool for the Synthesis of Natural Products and Pharmaceuticals. *Chem. Eur. J.* **2018,** *24*, 3925-3943.

20. Maji, R.; Mallojjala, S. C.; Wheeler, S. E. Chiral phosphoric acid catalysis: from numbers to insights. *Chem. Soc. Rev.* **2018,** *47*, 1142-1158.

21. Xing, C.-H.; Liao, Y.-X.; Ng, J.; Hu, Q.-S. Optically Active 1,1′-Spirobiindane-7,7′-diol (SPINOL)-Based Phosphoric Acids as Highly Enantioselective Catalysts for Asymmetric Organocatalysis. *J. Org. Chem.* **2011,** *76*, 4125-4131.

22. Birman, V. B.; L. Rheingold, A.; Lam, K.-C., 1,1′-Spirobiindane-7,7′-diol: a novel, C2-symmetric chiral ligand. *Tetrahedron: Asymmetry* **1999,** *10*, 125-131.

23. Xie, J.-H.; Zhou, Q.-L. Chiral Diphosphine and Monodentate Phosphorus Ligands on a Spiro Scaffold for Transition-Metal-Catalyzed Asymmetric Reactions. *Acc. Chem. Res.* **2008,** *41*, 581-593.

24. Chung, Y. K.; Fu, G. C. Phosphine-Catalyzed Enantioselective Synthesis of Oxygen Heterocycles. *Angew. Chem. Int. Ed.* **2009,** *48*, 2225-2227.

25. Čorić, I.; Müller, S.; List, B. Kinetic Resolution of Homoaldols via Catalytic Asymmetric Transacetalization. *J. Amer. Chem. Soc.* **2010,** *132*, 17370-17373.

26. Xu, F.; Huang, D.; Han, C.; Shen, W.; Lin, X.; Wang, Y. SPINOL-Derived Phosphoric Acids: Synthesis and Application in Enantioselective Friedel−Crafts Reaction of Indoles with Imines. *J. Org. Chem.* **2010,** *75*, 8677-8680.

27. Rahman, A.; Lin, X. Development and application of chiral spirocyclic phosphoric acids in asymmetric catalysis. *Org. Biomol. Chem.* **2018,** *16*, 4753-4777.

28. Li, J.; Chen, G.; Wang, Z.; Zhang, R.; Zhang, X.; Ding, K. Spiro-2,2′-bichroman-based bisoxazoline (SPANbox) ligands for ZnII-catalyzed enantioselective hydroxylation of β-keto esters and 1,3-diester. *Chem. Sci.* **2011,** *2*, 1141-1144.

29. Wang, X.; Han, Z.; Wang, Z.; Ding, K. Catalytic Asymmetric Synthesis of Aromatic Spiroketals by SpinPhox/Iridium(I)-Catalyzed Hydrogenation and Spiroketalization of α,α′-Bis(2-hydroxyarylidene) Ketones. *Angew. Chem. Int. Ed.* **2012,** *51*, 936-940.

30. Li, S.; Zhang, J.-W.; Li, X.-L.; Cheng, D.-J.; Tan, B. Phosphoric Acid-Catalyzed Asymmetric Synthesis of SPINOL Derivatives. *J. Am. Chem. Soc.* **2016,** *138*, 16561-16566.

31. Sun, W.; Gu, H.; Lin, X. Synthesis and Application of Hexamethyl-1,1′-spirobiindane-Based Phosphine-Oxazoline Ligands in Ni-Catalyzed Asymmetric Arylation of Cyclic Aldimines. *J. Org. Chem.* **2018,** *83*, 4034-4043.

32. Huang, J.; Hong, M.; Wang, C.-C.; Kramer, S.; Lin, G.-Q.; Sun, X.-W. Asymmetric Synthesis of Chiral Spiroketal Bisphosphine Ligands and Their Application in Enantioselective Olefin Hydrogenation. *J. Org. Chem.* **2018,** *83*, 12838-12846.

33. Chen, G.-Q.; Lin, B.-J.; Huang, J.-M.; Zhao, L.-Y.; Chen, Q.-S.; Jia, S.-P.; Yin, Q.; Zhang, X. Design and Synthesis of Chiral oxa-Spirocyclic Ligands for Ir-Catalyzed Direct Asymmetric Reduction of Bringmann's Lactones with Molecular H_2. *J. Am. Chem. Soc.* **2018,** *140*, 8064-8068.

34. Argüelles, A. J.; Sun, S.; Budaitis, B. G.; Nagorny, P. Design, Synthesis, and Application of Chiral C2-Symmetric Spiroketal-Containing Ligands in Transition-Metal Catalysis. *Angew. Chem. Int. Ed.* **2018,** *57*, 5325-5329.

35. Zheng, Z.; Cao, Y.; Chong, Q.; Han, Z.; Ding, J.; Luo, C.; Wang, Z.; Zhu, D.; Zhou, Q.-L.; Ding, K. Chiral Cyclohexyl-Fused Spirobiindanes: Practical Synthesis, Ligand Development, and Asymmetric Catalysis. *J. Am. Chem. Soc.* **2018,** *140*, 10374-10381.

36. Yin, L.; Xing, J.; Wang, Y.; Shen, Y.; Lu, T.; Hayashi, T.; Dou, X. Enantioselective Synthesis of 3,3′-Diaryl-SPINOLs: Rhodium-Catalyzed Asymmetric Arylation/BF3-Promoted Spirocyclization Sequence. *Angew. Chem. Int. Ed.* **2019,** *58*, 2474-2478.

37. Rodríguez-Escrich, C.; Pericàs, M. A. Organocatalysis on Tap: Enantioselective Continuous Flow Processes Mediated by Solid-Supported Chiral Organocatalysts. *Eur. J. Org. Chem.* **2015**, 1173-1188.

38. Rodriguez-Escrich, C.; Pericàs, M. A. Catalytic Enantioselective Flow Processes with Solid-Supported Chiral Catalysts. *Chem. Rec.* **2019**, *19*, 1872-1890.

39. Jas, G.; Kirschning, A. Continuous Flow Techniques in Organic Synthesis. *Chem. Eur. J.* **2003,** *9*, 5708-5723.

40. Kirschning, A.; Jas, G. Applications of Immobilized Catalysts in Continuous Flow Processes. In *Immobilized Catalysts. Topics in Current Chemistry*, Kirschning, A., Ed. Springer: Berlin, Heidelberg, 2004; Vol. 242, pp 209-239.

41. Phan, N. T. S.; Brown, D. H.; Styring, P. A facile method for catalyst immobilisation on silica: nickel-catalysed Kumada reactions in mini-continuous flow and batch reactors. *Green Chem.* **2004,** *6*, 526-532.

42. Baxendale, I. R.; Deeley, J.; Griffiths-Jones, C. M.; Ley, S. V.; Saaby, S.; Tranmer, G. K. A flow process for the multi-step synthesis of the alkaloid natural product oxomaritidine: a new paradigm for molecular assembly. *Chem. Commun.* **2006,** 2566-2568.

43. Baxendale, I. R.; Griffiths-Jones, C. M.; Ley, S. V.; Tranmer, G. K. Microwave-Assisted Suzuki Coupling Reactions with an Encapsulated Palladium Catalyst for Batch and Continuous-Flow Transformations. *Chem. Eur. J.* **2006,** *12*, 4407-4416.

44. Kirschning, A.; Solodenko, W.; Mennecke, K. Combining Enabling Techniques in Organic Synthesis: Continuous Flow Processes with Heterogenized Catalysts. *Chem. Eur. J.* **2006,** *12*, 5972-5990.

45. Baxendale, I. R.; Ley, S. V.; Mansfield, A. C.; Smith, C. D. Multistep Synthesis Using Modular Flow Reactors: Bestmann–Ohira Reagent for the Formation of Alkynes and Triazoles. *Angewandte Chemie* **2009,** *121* (22), 4077-4081.(es la misma que 45)

46. Baxendale, I. R.; Ley, S. V.; Mansfield, A. C.; Smith, C. D. Multistep Synthesis Using Modular Flow Reactors: Bestmann–Ohira Reagent for the Formation of Alkynes and Triazoles. *Angew. Chem. Int. Ed.* **2009,** *48*, 4017-4021.

47. Ceylan, S.; Kirsching, A. Organic synthesis with mini flow reactors using immobilised catalysts. In *Recoverable and Recyclable Catalysts*, Benaglia, M., Ed. Wiley: Chichester, 2009; pp 379-410.

48. Alza, E.; Rodríguez-Escrich, C.; Sayalero, S.; Bastero, A.; Pericàs, M. A., A Solid-Supported Organocatalyst for Highly Stereoselective, Batch, and Continuous-Flow Mannich Reactions. *Chem. Eur. J.* **2009,** *15*, 10167-10172.

49. Bedore, M. W.; Zaborenko, N.; Jensen, K. F.; Jamison, T. F. Aminolysis of Epoxides in a Microreactor System: A Continuous Flow Approach to β-Amino Alcohols. *Organic Process Research & Development* **2010,** *14*, 432-440.

50. Alza, E.; Sayalero, S.; Cambeiro, X. C.; Martín-Rapún, R.; Miranda, P. O.; Pericàs, M. A. Catalytic Batch and Continuous Flow Production of Highly Enantioenriched Cyclohexane Derivatives with Polymer-Supported Diarylprolinol Silyl Ethers. *Synlett* **2011,** 464-468.

51. Wegner, J.; Ceylan, S.; Kirschning, A. Ten key issues in modern flow chemistry. *Chem. Commun.* **2011,** *47*, 4583-4592.

52. Ayats, C.; Henseler, A. H.; Pericàs, M. A. A Solid-Supported Organocatalyst for Continuous-Flow Enantioselective Aldol Reactions. *ChemSusChem* **2012,** *5*, 320-325.

53. Fan, X.; Sayalero, S.; Pericàs, M. A., Asymmetric α-Amination of Aldehydes Catalyzed by PS-Diphenylprolinol Silyl Ethers: Remediation of Catalyst Deactivation for Continuous Flow Operation. *Adv. Synth. Cat.* **2012,** *354* (16), 2971-2976.

54. Kasaplar, P.; Rodríguez-Escrich, C.; Pericàs, M. A. Continuous Flow, Highly Enantioselective Michael Additions Catalyzed by a PS-Supported Squaramide. *Org. Lett.* **2013,** *15*, 3498-3501.

55. Tsubogo, T.; Ishiwata, T.; Kobayashi, S. Asymmetric Carbon–Carbon Bond Formation under Continuous-Flow Conditions with Chiral Heterogeneous Catalysts. *Angew. Chem. Int. Ed.* **2013,** *52*, 6590-6604.

56. Puglisi, A.; Benaglia, M.; Chiroli, V. Stereoselective organic reactions promoted by immobilized chiral catalysts in continuous flow systems. *Green Chem.* **2013,** *15*, 1790-1813.

57. *Chiral Catalyst Immobilization and Recycling*; De Vos, D.; Vankelecom, I. F.; Jacobs, P. A., Eds.; Wiley-VCH: Weinheim, 2000.

58. Cozzi, F. Immobilization of Organic Catalysts: When, Why, and How. *Adv. Synth. Cat.* **2006,** *348*, 1367-1390.

59. *Handbook of Asymmetric Heterogeneous Catalysis*; Ding, K.; Uozumi, Y., Eds.; Wiley-VCH: Weinheim, 2008.

60. Gruttadauria, M.; Giacalone, F.; Noto, R. Supported proline and proline-derivatives as recyclable organocatalysts. *Chem. Soc. Rev.* **2008,** *37*, 1666-1688.

61. Jimeno, C.; Sayalero, S.; Pericàs, M. A. Covalent Heterogenization of Asymmetric Catalysts on Polymers and Nanoparticles. In *Heterogenized Homogeneous Catalysts for Fine Chemicals Production. Catalysis by Metal Complexes*, Barbato, P.; Liguori, F., Eds. Springer: Dordrecht, 2010; Vol. 33, pp 123-170.

62. Rueping, M.; Sugiono, E.; Steck, A.; Theissmann, T. Synthesis and Application of Polymer-Supported Chiral Brønsted Acid Organocatalysts. *Adv. Synth. Cat.* **2010,** *352*, 281-287.

63. Kundu, D. S.; Schmidt, J.; Bleschke, C.; Thomas, A.; Blechert, S. A Microporous Binol-Derived Phosphoric Acid. *Angew. Chem. Int. Ed.* **2012,** *51*, 5456-5459.

64. Osorio-Planes, L.; Rodríguez-Escrich, C.; Pericàs, M. A. Enantioselective Continuous-Flow Production of 3-Indolylmethanamines Mediated by an Immobilized Phosphoric Acid Catalyst. *Chem. Eur. J.* **2014,** *20*, 2367-2372.

65. Clot-Almenara, L.; Rodríguez-Escrich, C.; Osorio-Planes, L.; Pericàs, M. A. Polystyrene-Supported TRIP: A Highly Recyclable Catalyst for Batch and Flow Enantioselective Allylation of Aldehydes. *ACS Catal.* **2016,** *6*, 7647-7651.

66. Clot-Almenara, L.; Rodríguez-Escrich, C.; Pericàs, M. A., Desymmetrisation of meso-diones promoted by a highly recyclable polymer-supported chiral phosphoric acid catalyst. *RSC Adv.* **2018,** *8*, 6910-6914.

67. Zhang, X.; Kormos, A.; Zhang, J. Self-Supported BINOL-Derived Phosphoric Acid Based on a Chiral Carbazolic Porous Framework. *Org. Lett.* **2017,** *19*, 6072-6075.

68. Cheng, H.-G.; Miguélez, J.; Miyamura, H.; Yoo, W.-J.; Kobayashi, S. Integration of aerobic oxidation and intramolecular asymmetric aza-Friedel–Crafts reactions with a chiral bifunctional heterogeneous catalyst. *Chem. Sci.* **2017,** *8*, 1356-1359.

69. For a related, multiple nucleophilic aromatic substitution involving 2,3,5,6-tetrafluoroterephthalonitrile, see: Weng, X.; Baez, J. E.; Khiterer, M.; Hoe, M. Y.; Bao, Z.; Shea, K. J. Chiral Polymers of Intrinsic Microporosity: Selective Membrane Permeation of Enantiomers. *Angew. Chem. Int. Ed.* **2015,** *54*, 11214-11218.

70. (a) Wuitschik, G.; Rogers-Evans, M.; Mueller, K.; Fischer, H.; Wagner, B.; Schuler, F.; Polonnchuk, L.; Carreira, E. M. Oxetanes as promising modules in drug discovery. *Angew. Chem. Int. Ed.* **2006,** *45*, 7736-7739; (b) Wuitschik, G.; Carreira, E. M.; Wagner, B.; Fischer, H. Parrilla, I.; Schuler, F.; Rogers-Evans, M.; Muller, K. Oxetanes in Drug Discovery: Structural and Synthetic Insights. *J. Med. Chem.* **2010**, *53*, 3227-3246; (c) Burkhard, J. A.; Wuitschik, G.; Rogers-Evans, M.; Mueller, K.; Carreira, E. M. Oxetanes as Versatile Elements in Drug Discovery and Synthesis. *Angew. Chem. Int. Ed.* **2010,** *49*, 9052-9067;

(d) Burkhard, J. A.; Wuitschik, G.; Plancher, J.-M.; Rogers-Evans, M.; Carreira, E. M. Synthesis and Stability of Oxetane Analogs of Thalidomide and Lenalidomide. *Org. Lett.* **2013,** *15*, 4312-4315; (e) Moller, G. P.; Muller, S.; Wolfstadter, B. T.; Wolfrum, S.; Schepmann, D.; Wunsch, B.; Carreira, E. M. Oxetanyl amino acids for peptidomimetics. *Org. Lett.* **2017,** *19*, 2510-2513; (f) Geary, G. C.; Nortcliffe, A.; Pearce, C. A.; Hamza, D.; Jones, G.; Moody, C. J. Densely functionalised spirocyclic oxetane-piperidine scaffolds for drug discovery. *Bioorg. Med. Chem.* **2018**, *26*, 791-797.

71. Wang, Z.; Chen, Z.; Sun, J. Catalytic Enantioselective Intermolecular Desymmetrization of 3-Substituted Oxetanes. *Angew. Chem. Int. Ed.* **2013,** *52*, 6685-6688.

72 (a) Jumde, R. P.; Evangelisti, C.; Mandoli, A.; Scotti, N.; Psaro, R. Aminopropyl-silica-supported Cu nanoparticles: An efficient catalyst for continuous-flow Huisgen azide-alkyne cycloaddition (CuAAC). *J. Catal.* **2015**, *324*, 25-31; (b) Wen, J.; Wu, K.; Yang, D.; Tian, J.; Huang, Z.; Filatov, A. S.; Lei, A. Lin, X.-M. Low-Pressure Flow Chemistry of CuAAC Click Reaction Catalyzed by Nanoporous AuCu Membrane. *ACS Appl. Mater. Inter.* **2018**, *10*, 25930-25935; (c) Santos de Sa, D.; Bustamante, R. A.; Rocha, C. E. R.; Diniz da Silva, V.; Rodrigues, E. J. R. Muller, C. D. B.; Ghavami, K.; Massi, A.; Pandoli, O. G. Fabrication of Lignocellulose-Based Microreactors: Copper-Functionalized Bamboo for Continuous-Flow CuAAC Click Reactions. *ACS Sust. Chem. Eng.* **2019**, *7*, 3267-3273.

73. (a) Cheong, P. H.-Y.; Legault, C. Y.; Um, J. M.; Çelebi-Ölçüm, N.; Houk, K. N. Quantum Mechanical Investigations of Organocatalysis: Mechanisms, Reactivities, and Selectivities. *Chem. Rev.* **2011,** *111*, 5042-5137; (b) Champagne, A.; Houl, K. N. Origins of Selectivity and General Model for Chiral Phosphoric Acid-Catalyzed Oxetane Desymmetrizations. *J. Am. Chem. Soc.* **2016**, *138*, 12356-12359; (c) Duarte, F.; Patton, R. S. Molecular Recognition in Asymmetric Counteranion Catalysis: Understanding Chiral Phosphate-Mediated Desymmetrization. *J. Am. Chem. Soc.* **2017**, *139*, 8886-8896.

74. Seguin, T. J.; Wheeler, S. E. Competing Noncovalent Interactions Control the Stereoselectivity of Chiral Phosphoric Acid Catalyzed Ring Openings of 3-Substituted Oxetanes. *ACS Catal.* **2016,** *6*, 7222-7228.

75. Xie, J.-G.; Quan, J.; Li, S.-B.; Zheng, Y.; Zhu, L.-M. SH-Methylation of SH-Containing Heterocycles with Dimethyl Carbonate via Phase-Transfer Catalytic Reaction. *Synth. Commun.* **2011,** *41*, 871-878.

76. Lefebvre, C.; Rubez, G.; Khartabil, H.; Boisson, J.-C.; Contreras-García, J.; Hénon, E. Accurately extracting the signature of intermolecular interactions present in the NCI plot of the reduced density gradient versus electron density. *Chem. Phys. Phys. Chem.* **2017**, *17*, 17928-17936.

77. Lu, T.; Chen, F. Multiwfn: A multifunctional wavefunction analyzer. *J. Comput. Chem.* **2012**, *33*, 580-592.

78. It is worth mentioning that 9-antrhyl substituents in Cat a, one of the catalytic systems also studied by Seguin and Wheeler91 are unable and adapt to the substrates by bending while aromatic stabilization intact according to the reliable theoretical model used in the present calculations. Accordingly, the 9-anthryl wings in Cat a undergo very negligible deviations from planarity throughout the catalytic cycle.

Supporting Information

Development of Immobilized SPINOL-Derived Chiral Phosphoric Acids for Catalytic Continuous Flow Processes. Use in the Catalytic Desymmetrization of 3,3-Disubstituted Oxetanes

Junshan Lai,[†,§] Mauro Fianchini,[†] and Miquel A. Pericàs[†,‡,*]

[†] Institute of Chemical Research of Catalonia (ICIQ), The Barcelona Institute of Science and Technology, Av. Països Catalans, 16, 43007 Tarragona (Spain)

[§] Universitat Rovira i Virgili, Departament de Química Analítica i Química Orgànica, c/Marcel·lí Domingo, 1, 43007 Tarragona (Spain)

[‡] Departament de Química Inorgànica i Orgànica, Universitat de Barcelona (UB), 08028 Barcelona (Spain)

mapericas@iciq.es

Table of Contents

1. General information

Unless otherwise noted, all reactions were conducted under air. All commercial reagents were used as received; 3,3′-Diaryl-SPINOLs **S1** and **12** were synthesized according to the reported procedures.[1a] **22g** is commercially available, **22n** was prepared according to a reported procedure.[1b] All other oxetanes were prepared from the coupling of 3-oxetanone with the corresponding Grignard reagents. Flash chromatography was carried out using 60 mesh silicagel and dry-packed columns. For the continuous flow system, the packed bed reactor was an adjustable volume Omnifit glass column with 10 mm Ø, and a dual syringe pump was used for the circulation of reactants and solvent. Thin layer chromatography was carried out using Merck TLC Silicagel 60 F254 aluminum sheets. Components were visualized by UV light (λ = 254 nm) and stained with phosphomolybdic dip. NMR spectra were recorded at 298 K on a Bruker Avance 400 Ultrashield apparatus. ^{1}H NMR spectroscopy chemical shifts are quoted in ppm relative to tetramethylsilane (TMS). $CDCl_3$ was used as internal standard for ^{13}C NMR spectra. Chemical shifts are given in ppm and coupling constants in Hz. IR spectra were recorded on a Bruker Tensor 27 FT-IR spectrometer and are reported in wavenumbers (cm^{-1}). Elemental analyses were performed by MEDAC Ltd. (Surrey, UK) on a LECO CHNS 932 micro-analyzer. High performance liquid chromatography (HPLC) was performed on Agilent Technologies chromatographs (1100 and 1200 Series), using Chiralpak AD-H columns and guard columns. FAB mass spectra were obtained on a Fisons V6-Quattro instrument, ESI mass spectra were obtained on a Waters LCT Premier Instrument and CI and EI spectra were obtained on a Waters GCT spectrometer. Specific optical rotation measurements were carried out on a Jasco P-1030 polarimeter.

2. Preparation of the immobilized SPINOL-derived chiral phosphoric acids

2.1. Preparation of Cat b

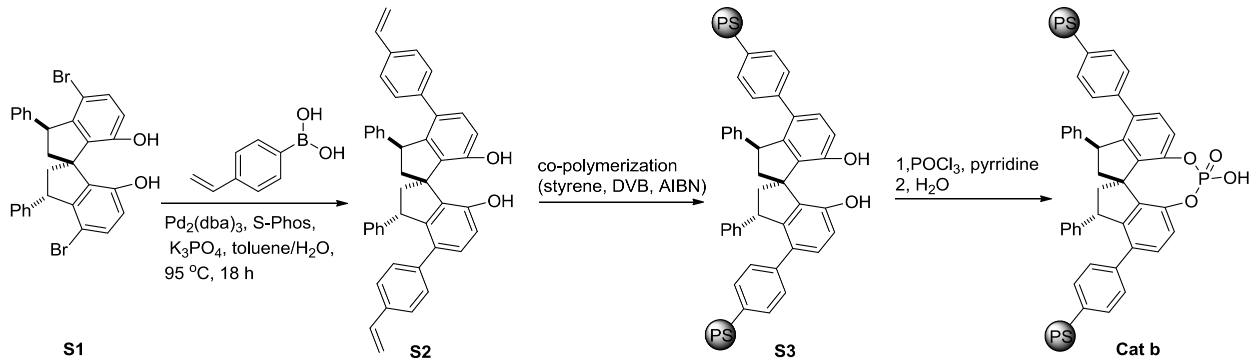

Scheme S1. The procedure of preparation of **Cat b**

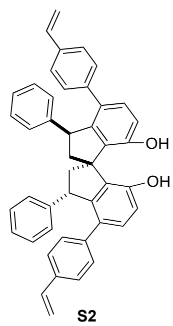

S2 was synthesized following a typical Suzuki coupling procedure. Under N_2, to a Schlenk tube containing **S1** (1.12 g, 2 mmol), 4-vinylphenylboronic acid (1.18 g, 8 mmol, 4.0 equiv), $Pd_2(dba)_3$ (36.8 mg, 2 mol %), S-Phos (66 mg, 8 mol %) and K_3PO_4 (1.7 g, 8 mmol, 4.0 equiv) was added degased toluene (15 mL) and water (5 mL). The reaction mixture was stirred and heated to 95 °C for 18 h. After being cooled to room temperature, HCl (2 N) was added to the reaction mixture. The mixture was then extracted with CH_2Cl_2 (40 mL × 3). The combined organic layers were dried over $MgSO_4$ and concentrated under reduced pressure. The crude product was purified by flash column chromatography on silicagel using cyclohexane/CH_2Cl_2 (5:1) as the eluent to give compound **S2** as a slightly yellow solid. (791 mg, 65% yield).

Yellow solid. Carbonization or polymerization starts from 280 °C; Melting point could not be detected.

^{1}H NMR (400 MHz, Chloroform-*d*) δ 7.12 (d, *J* = 8.2 Hz, 2H), 7.06 (d, *J* = 8.2 Hz, 4H), 6.99-6.79 (m, 16H), 6.58 (dd, *J* = 17.6, 10.9 Hz, 2H), 5.61 (dd, *J* = 17.6, 1.0 Hz, 2H), 5.15 (dd, *J* = 10.8, 1.0 Hz, 2H), 4.99 (s, 2H), 4.73 (dd, *J* = 10.1, 7.7 Hz, 2H), 2.94 (dd, *J* = 13.3, 7.7 Hz, 2H), 2.37 (dd, *J* = 13.2, 10.3 Hz, 2H).

^{13}C NMR (101 MHz, $CDCl_3$) δ 151.9 (x2), 145.3 (x2), 143.9 (x2), 139.7 (x2), 136.7 (x2), 135.3 (x2), 133.1 (x2), 131.8 (x2), 131.7 (x2), 128.8 (x4), 128.0 (x4), 127.7 (x4), 125.6 (x2), 125.3 (x4), 115.2 (x2), 113.0 (x2), 55.6 (x2), 50.0 (x3).

IR (neat): 3527, 3020, 2927, 2867, 1595, 1480, 1261, 1201, 988, 906, 822, 762, 698 cm^{-1}.

HRMS (ESI): m/z: $[M-H]^+$ ($C_{45}H_{35}O_2$), calcd.: 607.2643; found: 607.2627.

$[\alpha]_D^{25}$ = +288 (*c* = 0.1, CH_2Cl_2).

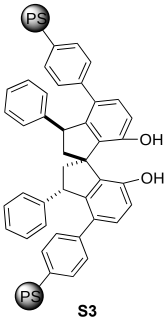

S3

S3 was synthesized Following a modification of a literature procedure.[2] A 100 mL reactor was charged with a suspension of polyvinyl alcohol (PV-OH) (100 mg, 0.96 µmol, 0.001 equiv.) in 72 mL of degassed MiliQ water. The solution was heated at 100 °C until PV-OH was dissolved. Then, it was cooled to RT and a solution of boric acid (449 mg, 7.26 mmol) in 18 mL of degassed MiliQ water was transferred to the reactor. Later, a degassed solution containing divinylbenzene (DVB), filtered on a short pad of silica immediately before use, (80%, 119 µL, 0.68 mmol, 0.65 equiv.), BINOL derivative **S2** (645 mg, 1.06 mmol), styrene (2.9 mL, 25.5 mmol, 23.66 equiv.) and AIBN (31 mg, 0.19 mmol, 0.18 equiv.) in toluene (2.4 mL) was transferred to the reactor. After that, the system was heated at 90 °C and magnetically stirred at 440 rpm overnight, the aqueous solution was decanted off and the resin was washed with water (50 °C) several times, followed by MeOH and CH_2Cl_2. Finally, it was dried overnight in a 40 °C vacuum oven to furnish 2.7 g of light-yellow beads.

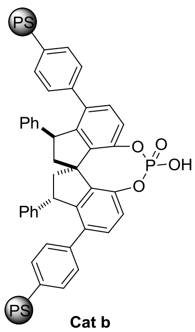

Cat b

Cat b was synthesized Following a modification of a literature procedure.[2] In a dry Schlenk tube, resin **S3** (2.7 g, ca. 1.06 mmol) was suspended in pyridine (20 mL) under Ar. Then, $POCl_3$ (495 µL, 5.3 mmol, 5 eq.) was added and the reaction mixture was heated in the closed Schlenk tube at 120 °C. After 2 days, it was cooled to RT and 5 mL of water were added. Then the system was closed again and heated at 100 °C overnight. The resin was filtered and washed with water, THF/water, THF, 2 M HCl/EtOAc, EtOAC/DCM, and DCM and dried overnight in a 40 °C vacuum oven to give 2.7 g of brown beads.

P elemental analysis (%): 0.34

$f_{(P)}$: 0.11 mmol/g resin

2.2. Preparation of Cat c

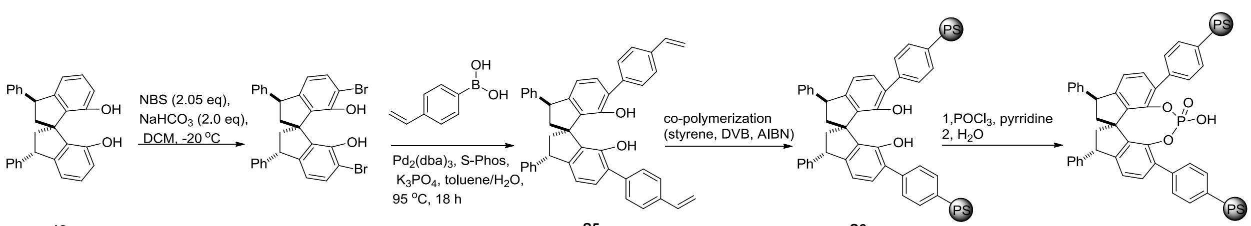

Scheme S2. The procedure of preparation of **Cat c**

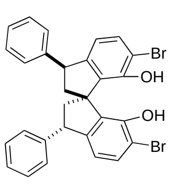

S4

S4 was synthesized according to the reported procedures.[3] In a Schlenk tube, SPINOL **12** (3.232 g, 8 mmol) and $NaHCO_3$ (1.344 g, 16 mmol, 2.0 equiv) were mixed with CH_2Cl_2 (80 mL), and the mixture was stirred and cooled to -20 °C. Then, NBS (2.92 g, 16.4 mmol, 2.05 equiv) was added slowly. After being stirred at -20 °C for 2 h, the reaction mixture was poured into HCl (2 N). The reaction mixture was then extracted with CH_2Cl_2 (40 mL × 3). After removal of solvent by rota-evaporation, the residue was subjected to column chromatography (silicagel, cyclohexane/ethyl acetate (v/v = 20/1) as eluent), affording the expected compound **S4** as a Light yellow solid (3.6 g, 80% yield).

m.p. 241 °C.

^{1}H NMR (500 MHz, Chloroform-*d*) δ 7.33-7.24 (m, 12H), 6.36 (dd, *J* = 8.1, 1.2 Hz, 2H), 5.43 (d, *J* = 1.4 Hz, 2H), 4.39 (dd, *J* = 10.6, 7.7 Hz, 2H), 2.76 (dd, *J* = 12.8, 7.6 Hz, 2H), 2.49 (dd, *J* = 12.9, 10.8 Hz, 2H).

^{13}C NMR (126 MHz, $CDCl_3$) δ 148.4 (x2), 144.0 (x2), 134.5 (x2), 131.2 (x2), 128.6 (x2), 128.4 (x2), 128.3 (x4), 126.7 (x2), 118.5 (x2), 108.5 (x2), 99.9 (x2), 57.4, 49.9 (x2), 48.0 (x2).

IR (neat): 3492, 3061, 3023, 2935, 2863, 1579, 1493, 1445, 1317, 1237, 1160, 907, 806, 759, 698 cm^{-1}.

HRMS (ESI): m/z: [M-H]$^+$ ($C_{29}H_{21}Br_2O_2$), calcd.: 558.9914; found: 558.9903.

$[\alpha]_D^{25}$ = +65 (*c* = 0.1, CH_2Cl_2).

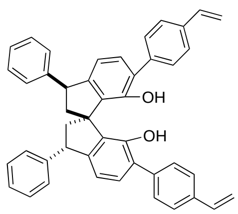

S5

S5 was synthesized Following a modification of a literature procedure.[3] Under N_2, to a Schlenk tube containing **S4** (1.12 g, 2 mmol), 4-vinylphenylboronic acid (1.18 g, 8 mmol, 4.0 equiv), $Pd_2(dba)_3$ (36.8 mg, 2 mol %), S-Phos (66 mg, 8 mol %) and K_3PO_4 (34 mmol) was added toluene (20 mL) and water (20 mL). The reaction mixture was stirred and heated to 95 °C for 18 h. After being cooled to room temperature, HCl (2 N) was added to the reaction mixture. The mixture was then extracted with CH_2Cl_2 (40 mL × 3). After removal of solvent by rota evaporation, the residue was subjected to column chromatography [silicagel, cyclohexane/ dichloromethane (v/v = 5/2) as eluent], affording the expected product as a white solid. (780 mg, 64% yield).

Light yellow solid. Carbonization or polymerization, Melting point cannot be detected.

^{1}H NMR (400 MHz, Chloroform-*d*) δ 7.46 (t, *J* = 2.1 Hz, 8H), 7.33 (dd, *J* = 4.1, 2.1 Hz, 8H), 7.29-7.20 (m, 2H), 7.20-7.12 (m, 2H), 6.72 (ddd, *J* = 17.7, 10.9, 1.8 Hz, 2H), 6.58 (dd, *J* = 7.6, 2.2 Hz, 2H), 5.76 (d, *J* = 17.6 Hz, 2H), 5.31-5.18 (m, 4H), 4.50 (dd, *J* = 10.8, 7.4 Hz, 2H), 2.87 (dd, *J* = 13.0, 7.5 Hz, 2H), 2.55 (t, *J* = 11.9 Hz, 2H).

^{13}C NMR (101 MHz, $CDCl_3$) δ 149.3 (x2), 148.3 (x2), 143.9 (x2), 136.7 (x2), 136.6 (x2), 136.4 (x2), 132.2 (x2), 130.6 (x2), 129.4 (x4), 128.6 (x4), 128.4 (x4), 126.9 (x2), 126.7 (x2), 126.5 (x4), 117.9(x2), 114.1 (x2), 56.3, 50.0 (x2), 48.0 (x2).

IR (neat): 3497, 3024, 2958, 2927, 2864, 1601, 1576, 1446, 1400, 1228, 1117, 990, 909, 848, 818, 759, 698 cm^{-1}.

HRMS (ESI): m/z: [M-H]$^+$ ($C_{45}H_{35}O_2$), calcd.: 607.2643; found: 607.2657.

$[\alpha]_D^{25}$ = +232 (*c* = 0.1, CH_2Cl_2).

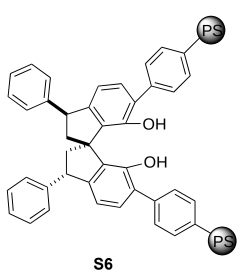

S6

S6 was synthesized Following a modification of a literature procedure.[2] A 100 mL reactor was charged with a suspension of polyvinyl alcohol (PV-OH) (100 mg, 0.96 µmol, 0.001 equiv.) in 72 mL of degassed MiliQ water. The solution was heated at 100 °C until PV-OH was dissolved. Then, it was cooled to RT and a solution of boric acid (449 mg, 7.26 mmol) in 18 mL of degassed MiliQ water was transferred to the reactor. Later, a degassed solution containing divinylbenzene (DVB), filtered on a short pad of silica immediately before use, (80%, 119 µL, 0.68 mmol, 0.65 equiv.), BINOL derivative **S5** (645 mg, 1.06 mmol), styrene (2.9 ml, 25.5 mmol, 23.66 equiv.) and AIBN (31 mg, 0.19 mmol, 0.18 equiv.) in toluene (2.4 mL) was transferred to the reactor. After that, the system was heated at 90 °C and magnetically stirred at 440 rpm overnight, the aqueous solution was decanted off and the resin was washed with water (50 °C) several times, followed by MeOH and CH_2Cl_2. Finally, it was dried overnight in a 40 °C vacuum oven to furnish 3.5 g of light-yellow beads.

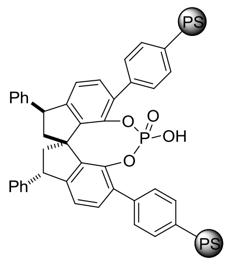

Cat c

Cat c was synthesized Following a modification of a literature procedure.[2] In a dry Schlenk tube, resin **S6** (3.5 g, ca. 1.06 mmol) was suspended in pyridine (20 mL) under Ar. Then, $POCl_3$ (495 µL, 5.3 mmol, 5 eq.) was added and the reaction mixture was heated in the closed Schlenk tube at 120 °C. After 2 days, it was cooled to RT and 5 mL of water were added. Then the system was closed again and heated at 100 °C overnight. The resin was filtered and washed with water, THF/water, THF, 2 M HCl/EtOAc, EtOAC/DCM, and DCM and dried overnight in a 40 °C vacuum oven to give 3.5 g of brown beads.

P elemental analysis (%): 0.93

$f_{(P)}$: 0.3 mmol/g resin

2.3. Preparation of Cat d

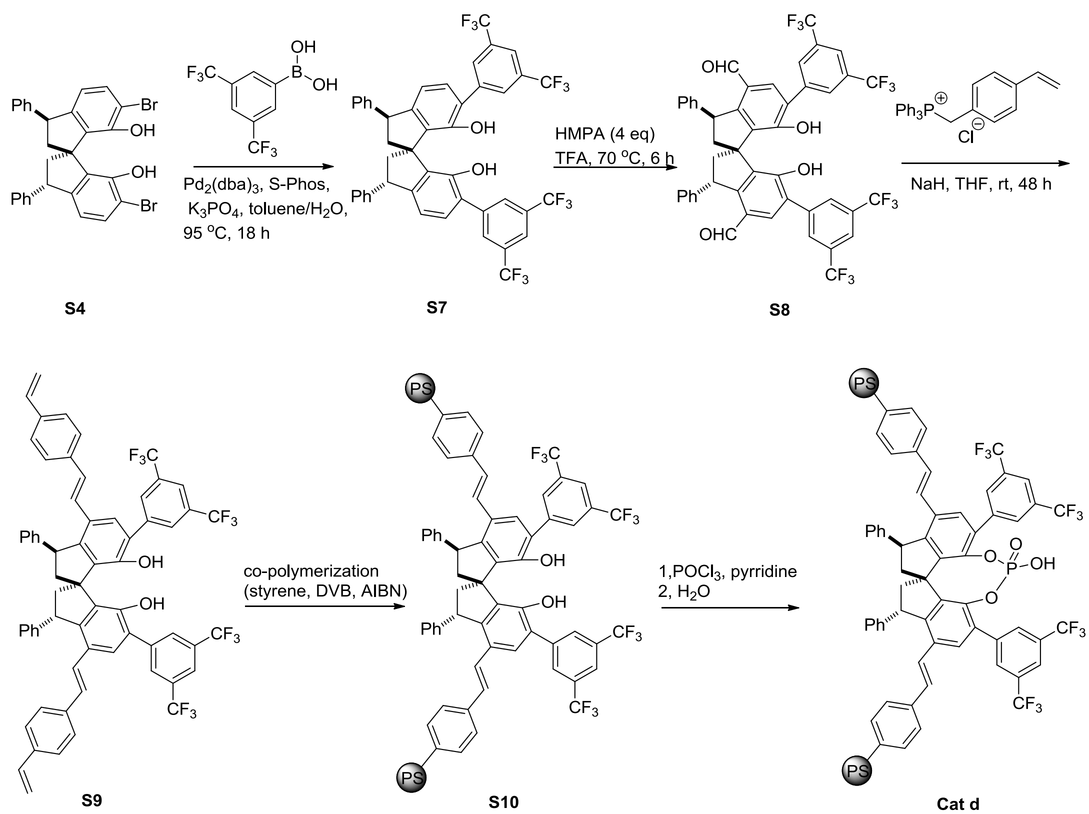

Scheme S3. The procedure of preparation of **Cat d**

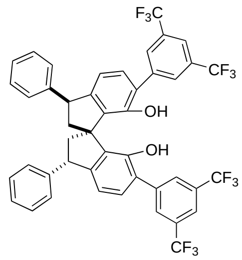

S7

S7 was synthesized Following a modification of a literature procedure.[3] Under N_2, to a Schlenk tube containing **S4** (1.124 g, 2 mmol), (3,5-bis(trifluoromethyl)phenyl)boronic acid (2.064 g, 8 mmol, 4.0 equiv), $Pd_2(dba)_3$ (36.8 mg, 2 mol %), S-Phos (66 mg, 8 mol %) and K_3PO_4 (34 mmol) was added toluene (20 mL) and water (20 mL). The reaction mixture was stirred and heated to 95 °C for 18 h. After being cooled to room temperature, HCl (2 N) was added to the reaction mixture. The mixture was then extracted with CH_2Cl_2 (30 mL × 3). After removal of solvent by rota evaporation, the residue was subjected to column chromatography [silicagel, cyclohexane/ dichloromethane (v/v = 5/2) as eluent], affording the expected product as a white solid. (1.34 g, 81% yield).

White solid. m.p. 140 °C.

^{1}H NMR (400 MHz, Chloroform-*d*) δ 8.01 (s, 4H), 7.84 (s, 2H), 7.44 – 7.23 (m, 12H), 6.73 (dq, *J* = 7.8, 1.3 Hz, 2H), 5.17 (t, *J* = 1.8 Hz, 2H), 4.57 (dd, *J* = 11.0, 7.5 Hz, 2H), 3.05 – 2.85 (m, 2H), 2.51 (t, *J* = 12.1 Hz, 2H).

^{13}C NMR (101 MHz, $CDCl_3$) δ 150.0 (x2), 149.6 (x2), 142.6 (x2), 139.5 (x2), 131.9 (x2), 131.7 (x4, q, $^2J_{(C-F)}$ = 33 Hz), 130.9 (x2), 129.5 (x4), 128.9 (x4), 128.3 (x4), 127.2 (x2), 125.1 (x2), 123.4 (x4, q, $^1J_{(C-F)}$ = 275 Hz), 121.0 (x2), 119.1 (x2), 55.8, 50.0 (x2), 48.0 (x2).

^{19}F NMR (376 MHz, $CDCl_3$) δ -62.90.

IR (neat): 3525, 3030, 2955, 2869, 1617, 1579, 1495, 1457, 1418, 1381, 1275, 1169, 1125, 1000, 897, 823, 762, 699, 682 cm^{-1}.

HRMS (ESI): m/z: $[M-H]^+$ ($C_{45}H_{27}F_{12}O_2$), calcd.: 827.1825; found: 829.1813.

$[\alpha]_D^{25}$ = +53 (*c* = 0.1, CH_2Cl_2).

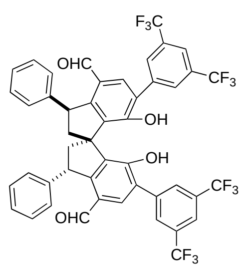

S8

For the preparation of **S8**, to a Schlenk tube containing **S7** (829 mg, 1 mmol) under Ar, hexamethylenetetramine (HMTA) (561 mg, 4 mmol, 4.0 equiv), and trifluoroacetic acid (4 mL) were added. The reaction mixture was stirred and heated to 70 °C for 6 h. After being cooled to room temperature, 4 mL HCl (6 N) was added to the reaction mixture and heated at 50 °C for two more hours. The mixture was then extracted with dichloromethane. After removal of solvent by rota evaporation, the residue was subjected to column chromatography [silicagel, cyclohexane/ ethyl acetate (v/v = 5/1) as eluent], affording the expected product as a light yellow solid. (575 mg, 65% yield).

Light yellow solid. m.p. 215 °C.

^{1}H NMR (400 MHz, Chloroform-*d*) δ 9.59 (s, 2H), 8.04 – 7.79 (m, 8H), 7.38 – 7.22 (m, 11H), 5.94 (d, *J* = 4.4 Hz, 2H), 4.98 (dd, *J* = 10.1, 7.8 Hz, 2H), 3.09 (dd, *J* = 13.4, 7.9 Hz, 2H), 2.51 (dd, *J* = 13.3, 10.2 Hz, 2H).

^{13}C NMR (101 MHz, $CDCl_3$) δ 188.7 (x2), 153.8 (x2), 151.6 (x2), 145.2 (x2), 137.9 (x2), 133.8 (x2), 132.4 (x4, q, $^2J_{(C-F)}$ = 33 Hz), 131.9 (x2), 129.5 (x2), 129.4 (x6), 127.3 (x6), 127.2 (x2), 126.2 (x2), 123.1 (x4, q, $^1J_{(C-F)}$ = 274 Hz), 122.0 (x2), , 56.4, 50.1 (x2), 49.2 (x2).

^{19}F NMR (376 MHz, $CDCl_3$) δ -62.99.

IR (neat): 3502, 3061, 2929, 2870, 1671, 1600, 1566, 1479, 1453, 1377, 1275, 1171, 1126, 1032, 896, 845, 767, 701, 682 cm^{-1}.

HRMS (ESI): m/z: $[M-H]^+$ ($C_{47}H_{27}F_{12}O_4$), calcd.: 883.1723; found: 883.1726.

$[\alpha]_D^{25}$ = +52 (*c* = 0.1, CH_2Cl_2).

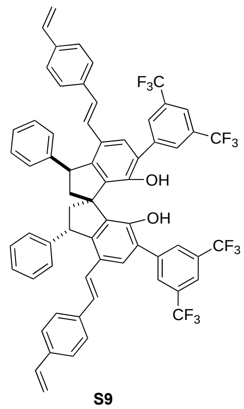

S9

S9: To a Schlenk tube, **S8** (500 mg, 0.56 mmol), (4-vinylbenzyl) triphenylphosphonium chloride (930 mg, 2.24 mmol, 4.0 equiv) and 15 mL THF were added under Ar. The mixture was cooled to 0 °C with an ice bath, then NaH (a mixture of 60% sodium hydride (w/w) in mineral oil, 134 mg, 3.36 mmol, 6 eq) suspended in 5 mL THF was added dropwise. The reaction mixture was stirred at rt for 48 h, then cooled to 0 °C with an ice bath, and 1 mL water was added dropwise to quench the reaction. The mixture was then extracted with dichloromethane. After removal of solvent by rota-evaporation, the residue was subjected to column chromatography [silicagel, cyclohexane/ dichloromethane (v/v = 5/2) as eluent], affording the expected product as a white solid. (377 mg, 62% yield).

White solid. Decomposed by carbonization or polymerization upon heating. A melting point could not be detected.

^1H NMR (400 MHz, Chloroform-*d*) δ 8.08 (d, *J* = 4.2 Hz, 4H), 7.90 (d, *J* = 3.7 Hz, 2H), 7.64 – 7.56 (m, 2H), 7.44 – 7.34 (m, 8H), 7.33 – 7.28 (m, 2H), 7.24 (dd, *J* = 8.3, 2.5 Hz, 4H), 6.92 (dd, *J* = 8.1, 3.2 Hz, 4H), 6.78 (dd, *J* = 16.2, 3.5 Hz, 2H), 6.63 (ddd, *J* = 16.2, 7.5, 3.1 Hz, 4H), 5.70 (dd, *J* = 17.7, 2.3 Hz, 2H), 5.37 (q, *J* = 3.2, 2.7 Hz, 2H), 5.19 (dd, *J* = 11.1, 2.0 Hz, 2H), 4.73 (td, *J* = 8.9, 7.5, 3.2 Hz, 2H), 3.13 – 2.92 (m, 2H), 2.50 (td, *J* = 10.5, 9.9, 5.4 Hz, 2H).

^{13}C NMR (101 MHz, $CDCl_3$) δ 149.0 (x2), 146.0 (x2), 144.3 (x2), 139.3 (x2), 136.8 (x2), 136.7 (x2), 136.4 (x4), 132.0 (x2), 131.8 (x4, q, $^2J_{(C-F)}$ = 33 Hz), 129.6 (x6), 129.2 (x6), 129.1 (x2), 128.3 (x2), 128.0 (x6), 127.9 (x2), 127.1 (x2), 126.5 (x4), 126.3 (x4), 124.7 (x2), 123.5 (x4, q, $^1J_{(C-F)}$ = 274 Hz), 121.3 (x2), 113.6 (x2), 55.7, 50.0 (x2), 49.6 (x2).

^{19}F NMR (376 MHz, $CDCl_3$) δ -62.73, -62.74.

IR (neat): 3501, 3028, 2937, 2865, 1600, 1510, 1479, 1463, 1407, 1380, 1333, 1275, 1171, 1127, 1031, 989, 961, 893, 845, 822, 767, 700, 681 cm^{-1}.

HRMS (ESI): m/z: $[M-H]^+$ ($C_{65}H_{43}F_{12}O_2$), calcd.: 1083.3064; found: 1083.3077.

$[\alpha]_D^{25}$ = -84 (*c* = 0.1, CH_2Cl_2).

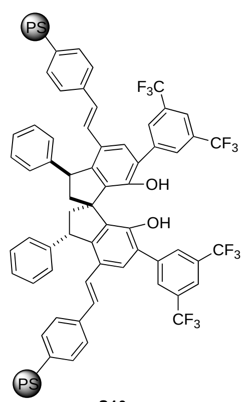

S10

S10 was synthesized Following a modification of a literature procedure.[2] A 100 mL reactor was charged with a suspension of polyvinyl alcohol (PV-OH) (50 mg, 0.58 μmol, 0.002 equiv.) in 36 mL of degassed MiliQ water. The solution was heated at 100 °C until PV-OH was dissolved. Then, it was cooled to RT and a solution of boric acid (225 mg, 3.63 mmol) in 9 mL of degassed MiliQ water was transferred to the reactor. Later, a degassed solution containing divinylbenzene (DVB), filtered on a short pad of silica immediately before use, (80%, 60 μL, 0.34 mmol, 1.3 equiv.), SPINOL derivative **S9** (293 mg, 0.27 mmol), styrene (1.45 ml, 12.75 mmol, 47.75 equiv.) and AIBN (15.5 mg, 0.1 mmol, 0.35 equiv.) in toluene (1.2 mL) were added to the reactor. After that, the system was heated at 80 °C and magnetically stirred at 440 rpm. After two days, the aqueous solution was decanted off and the resin was washed with water (50 °C) several times, followed by MeOH and CH_2Cl_2. Finally, it was dried overnight in a 40 °C vacuum oven to furnish 1.5 g of light-yellow beads.

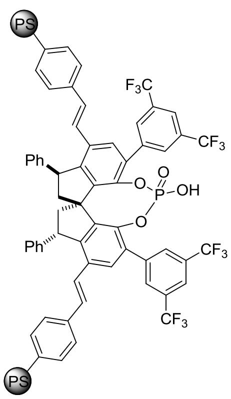

Cat d

Cat d was synthesized Following a modification of a literature procedure.[2] In a dry Schlenk tube, resin **S10** (1.5 g, ca. 0.27 mmol) was suspended in pyridine (5 mL) under Ar. Then, $POCl_3$ (126 μL, 1.35 mmol, 5 eq.) was added, and the reaction mixture was heated in the sealed Schlenk tube at 120 °C. After 2 days, it was cooled to room temperature and 1.25 mL of water were added. Then the system was sealed again and heated at 100 °C overnight. The resin was then filtered and sequentially washed with water, THF/water, THF, 2 M HCl/EtOAc, EtOAC/DCM, and DCM, and finally dried overnight in a vacuum oven at 40 °C to afford 1.5 g of brown beads.

P elemental analysis (%): 0.56

$f_{(P)}$: 0.18 mmol/g resin

2.4. Preparation of Cat e

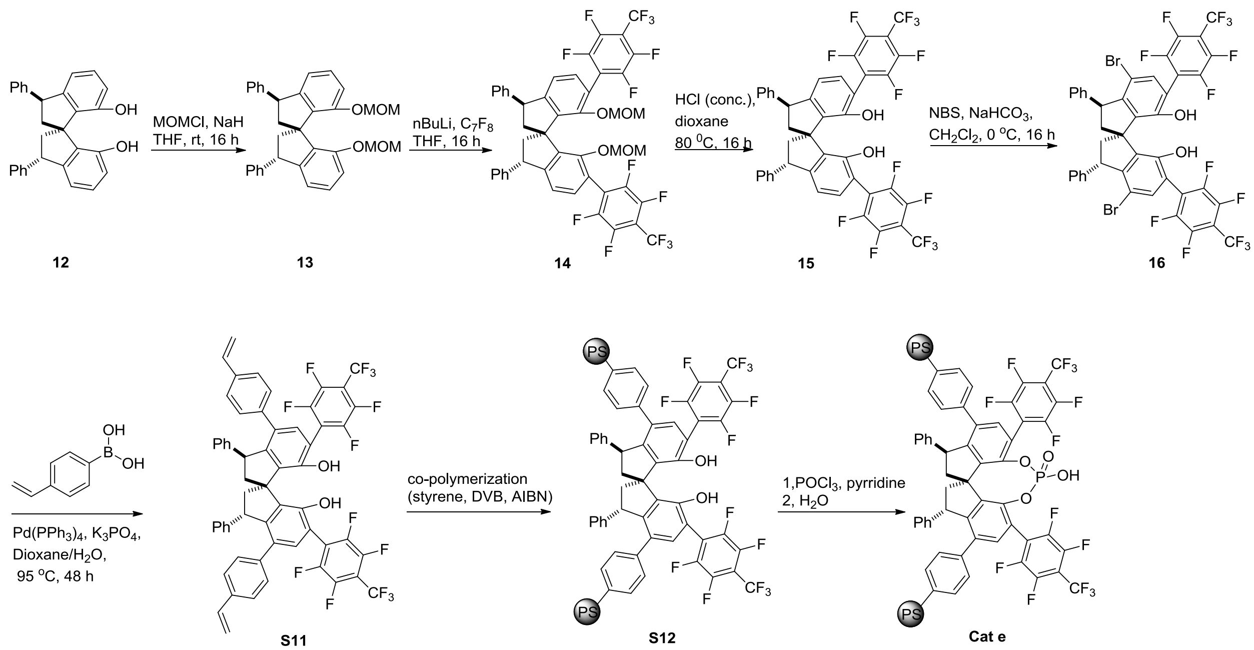

Scheme S4. The procedure of preparation of **Cat e**

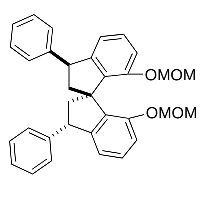

13

13: In a dry Schlenk tube under Argon, NaH (a mixture of 60% sodium hydride (w/w) in mineral oil, 2.4 g, 60 mmol, 3 eq) was suspended in 200 mL dry THF, and the mixture was stirred and cooled to 0 °C in an ice bath. SPINOL **12** (8.09 g, 20 mmol) was dissolved in 40 mL dry THF and added to the mixture dropwise with syringe. The mixture was stirred at this temperature for 1 hour, then removed the ice bath and stirred at rt for 15 min. The mixture was cooled to 0 °C again and Chloromethyl methyl ether (4.83 g, 4.56 mL, 60mmol, 3 eq) was added dropwise with syringe. After being stirred at rt for 16 h, the reaction mixture was quenched with 8 mL water. The reaction mixture was then extracted with CH_2Cl_2 (100 mL × 3). After removal of solvent by rota-evaporation, the residue was subjected to column chromatography (silicagel, cyclohexane/ethyl acetate (v/v = 20/1) as eluent), affording the expected compound **13** as a white solid (8.79 g, 90% yield).

White solid. m.p. 142.6 °C.

^{1}H NMR (400 MHz, Chloroform-*d*) δ 7.37 – 7.28 (m, 8H), 7.26 – 7.21 (m, 2H), 7.10 – 7.03 (m, 2H), 6.81 (d, *J* = 8.1 Hz, 2H), 6.53 (d, *J* = 7.5 Hz, 2H), 5.00 (d, *J* = 6.3 Hz, 2H), 4.95 (d, *J* = 6.3 Hz, 2H), 4.47 (t, *J* = 9.2 Hz, 2H), 3.17 (s, 6H), 2.77 (dd, *J* = 12.7, 7.9 Hz, 2H), 2.50 (t, *J* = 11.8 Hz, 2H).

^{13}C NMR (101 MHz, $CDCl_3$) δ 153.3 (x2), 148.1 (x2), 145.5 (x2), 137.4, 128.5 (x6), 128.4 (x2), 128.3, 128.0 (x2), 126.3 (x2), 118.2 (x2), 111.1 (x2), 93.7 (x2), 57.3 (x2), 55.8, 50.3 (x2), 48.5 (x2).

IR (neat): 3064, 3026, 2954, 2926, 2853, 2823, 1587, 1473, 1406, 1251, 1150, 1080, 1022, 918, 794, 764, 746, 698 cm^{-1}.

HRMS (ESI): m/z: $[M+Na]^+$ ($C_{33}H_{32}NaO_4$), calcd.: 515.2193; found: 515.2195.

$[\alpha]_D^{25}$ = +55 (*c* = 0.1, CH_2Cl_2).

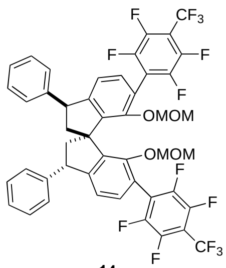

14

14 was synthesized Following a modification of a literature procedure.[4] In a Schlenk tube under Argon, **13** (7.88 g, 16 mmol) was dissolved in 160 mL dry THF, and the mixture was stirred and cooled to 0 °C with ice bath. *n*-BuLi (2.5 M in hexanes, 19.2 mL, 48 mmol) was added to the mixture dropwise with syringe. The mixture was stirred at rt for 3 hours, then cooled to -78 °C. Perfluorotoluene (26.43 g, 7.93 mL, 112 mmol, 7 eq) was added dropwise with syringe. The mixture was stirred at this temperature for one more hour and allowed to warm to rt slowly. After being stirred at rt for 16 h, the reaction mixture was quenched with 20 mL water by dropwise at 0 °C (ice bath). The reaction mixture was then extracted with CH_2Cl_2 (80 mL × 3). After removal of solvent by rota-evaporation, the residue was subjected to column chromatography (silica gel, cyclohexane/ dichloromethane (v/v = 5/2) as eluent), affording the expected compound **14** as a white solid (13.77 g, 93% yield).

White solid. m.p. 184.1 °C.

^{1}H NMR (400 MHz, Chloroform-*d*) δ 7.37 (dd, *J* = 4.3, 1.3 Hz, 8H), 7.32 – 7.26 (m, 2H), 7.06 (dd, *J* = 7.7, 1.4 Hz, 2H), 6.85 – 6.78 (m, 2H), 4.60 (dd, *J* = 6.0, 1.7 Hz, 2H), 4.53 (dd, *J* = 11.1, 7.4 Hz, 2H), 4.38 (dd, *J* = 6.0, 1.6 Hz, 2H), 2.94 (d, *J* = 1.6 Hz, 6H), 2.92 – 2.84 (m, 2H), 2.55 (t, *J* = 11.9 Hz, 2H).

^{13}C NMR (101 MHz, $CDCl_3$) δ 153.3 (x2), 150.8 (x2), 143.1 (x2), 141.6 (x2), 130.9 (x4), 128.8 (x8), 128.4 (x8), 126.9 (x4), 120.9 (x2), 117.6 (x4), 99.3 (x2), 57.6, 56.1 (x2), 50.0 (x2), 48.3 (x2).

^{19}F NMR (376 MHz, $CDCl_3$) δ -56.18 (t, J = 21.7 Hz, 6F), -137.85 (dd, J = 22.6, 12.5 Hz, 2F), -138.13 (dd, J = 21.7, 12.1 Hz, 2F), -141.13 – -141.52 (m, 2F), -141.56 – -141.89 (m, 2F).

IR (neat): 3064, 3030, 2954, 2934, 2838, 1657, 1601, 1478, 1430, 1392, 1338, 1258, 1187, 1136, 1086, 1013, 984, 944, 901, 827, 765, 714, 700 cm^{-1}.

HRMS (ESI): m/z: $[M+Na]^+$ ($C_{47}H_{30}F_{14}NaO_4$), calcd.: 947.1813; found: 947.1802.

$[\alpha]_D^{25}$ = +85 (*c* = 0.1, CH_2Cl_2).

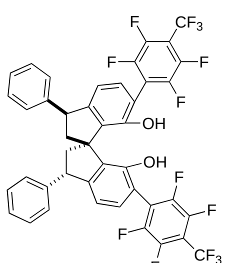

15

15: Compound **14** (6.50 g, 7 mmol) was dissolved in 35 mL 1,4-dioxane, 7 mL con. HCl was added and heated at 80 °C for 16 h. The reaction mixture was then extracted with dichloromethane. After removal of solvent by rota-evaporation, the residue was subjected to column chromatography (silicagel, cyclohexane/ dichloromethane (v/v = 5/2) as eluent), affording the expected compound **15** as a white solid (4.685 g, 80% yield).

Note: the polarity of ***14*** *and* ***15*** *are almost the same. The consumption of* ***14*** *couldn't be checked by TLC. It should be detected by 1H NMR.*

White solid. m.p. 169.7 °C.

^{1}H NMR (400 MHz, Chloroform-*d*) δ 7.37 (t, *J* = 7.4 Hz, 4H), 7.33 – 7.26 (m, 6H), 7.21 (d, *J* = 7.8 Hz, 2H), 6.74 (d, *J* = 7.8 Hz, 2H), 5.08 (s, 2H), 4.58 (dd, *J* = 11.0, 7.4 Hz, 2H), 2.98 (dd, *J* = 13.3, 7.4 Hz, 2H), 2.50 (dd, *J* = 13.1, 11.1 Hz, 2H).

^{13}C NMR (101 MHz, $CDCl_3$) δ 151.5 (x2), 150.4 (x2), 142.2 (x2), 132.6 (x4), 130.6 (x2), 128.9 (x8), 128.2 (x8), 127.3 (x4), 118.8 (x4), 113.0 (x2), 55.6, 50.3 (x2), 47.7 (x2).

^{19}F NMR (376 MHz, $CDCl_3$) δ -56.27 (t, J = 21.7 Hz, 6F), -136.93 (p, J = 16.3 Hz, 2F), -138.44 (dd, J = 22.2, 12.4 Hz, 2F), -140.61 – -141.52 (m, 4F).

IR (neat): 3530, 3029, 2954, 1659, 1602, 1479, 1454, 1428, 1338, 1257, 1186, 1145, 982, 901, 827, 763, 714, 699 cm^{-1}.

HRMS (ESI): m/z: $[M+Na]^+$ ($C_{43}H_{22}F_{14}NaO_2$), calcd.: 859.1294; found: 859,1290.

$[\alpha]_D^{25}$ = +85 (c = 0.1, CH_2Cl_2).

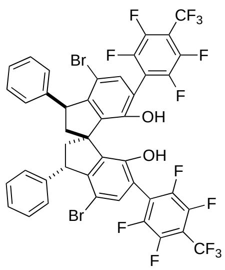

16

a) Preparation of **16** from **15**: In a Schlenk tube, **15** (4.6 g, 5.5 mmol) and $NaHCO_3$ (924 mg, 11 mmol, 2.0 equiv) were mixed with dichloromethane (55 mL), and the mixture was stirred and cooled to 0 °C. Then, NBS (2.007 g, 11.275 mmol, 2.05 equiv) was added slowly. After being stirred at 0 °C for 16 h, the reaction mixture was poured into HCl (2 N). The reaction mixture was then extracted with dichloromethane (50 mL x 3). After removal of solvent by rota-evaporation, the residue was subjected to column chromatography (silicagel, cyclohexane/ethyl acetate (v/v = 20/1) as eluent), affording the expected compound **16** as a white solid (4.375 g, 80% yield).

b) Preparation of **16** from **14**: Compound **14** (13.0 g, 14 mmol) was dissolved in 70 mL 1,4-dioxane, 14 mL con. HCl was added and heated at 80 °C for 16 h. The reaction mixture was then extracted with dichloromethane. After removal of solvent by rota-evaporation, we obtained 11.5 g yellow solid. The obtained yellow solid was used in the next step directly without purification.

In a 250 mL round bottle, the obtained yellow solid was dissolved in 100mL MeCN, and cooled with ice bath. One drop of Br_2 was added to the mixture. Then, NBS (5.11 g, 28.7 mmol, 2.05 equiv) was added slowly. After being stirred at 0 °C for 4 h and TLC showed SM consumed completely, 20 mL saturated $Na_2S_2O_4$ was added to the mixture to quench the reaction. The double phase mixture was separated and the aqueous phase was extracted with dichloromethane (20 mL x 3). After removal of solvent by rota-evaporation, the residue was subjected to column chromatography (silicagel, cyclohexane/ethyl acetate (v/v = 20/1) as eluent), affording the expected compound **16** as a white solid (9.71 g, 70% yield).

Light yellow solid. m.p. 175 °C.

^1H NMR (400 MHz, Chloroform-*d*) δ 7.37 – 7.18 (m, 12H), 5.11 (s, 2H), 4.59 (dd, *J* = 10.1, 7.9 Hz, 2H), 2.99 (dd, *J* = 13.6, 7.9 Hz, 2H), 2.37 (dd, *J* = 13.5, 10.3 Hz, 2H).

^{13}C NMR (126 MHz, CDCl3) δ 149.6 (x2), 148.2 (x2), 142.7 (x2), 136.0 (x4), 134.1 (x2), 128.8 (x8), 128.1 (x8), 126.9 (x4), 115.2 (x4), 112.5 (x2), 56.5, 51.6 (x2), 49.6 (x2).

^{19}F NMR (376 MHz, $CDCl_3$) δ -56.31 (t, J = 21.7 Hz, 6F), -136.21 – -137.16 (p, J = 16.0 Hz, 2F), -137.90 (dd, J = 21.8, 12.4 Hz, 2F), -139.56 – -140.78 (m, 4F).

IR (neat): 3538, 3067, 3028, 2956, 2937, 2871, 1660, 1602, 1480, 1454, 1337, 1261, 1232, 1143, 987, 843, 763, 715, 699, 676 cm^{-1}.

HRMS (ESI): m/z: $[M-H]^+$ ($C_{43}H_{19}Br_2F_{14}O_2$), calcd.: 990.9534; found: 990.9505.

$[\alpha]_D^{25}$ = +87 (*c* = 0.1, CH_2Cl_2).

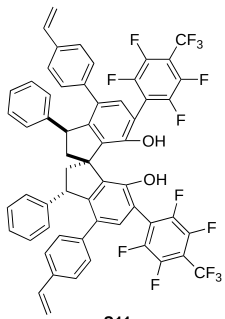

S11

S11: Under N_2, to a Schlenk tube containing **16** (2.0 g, 2 mmol), 4-vinylphenylboronic acid (0.9 g, 6 mmol, 3.0 equiv), Pd(PPh3)4 (116 mg, 0.1 mmol, 5 mol%) and K_3PO_4 (1.272 g, 6 mmol, 3.0 eq) was added degassed 1,4-dioxane (15 mL) and water (5 mL). The reaction mixture was stirred and heated to 95 °C for 48 h. and then it was cooled to room temperature and extracted with CH_2Cl_2 (20 mL×3). The combined organic layers were dried over $MgSO_4$ and concentrated under reduced pressure. The crude product was purified by flash column chromatography on silicagel using cyclohexane/CH_2Cl_2 (5:1) as the eluent to give compound **S11** as a slightly yellow solid. (1.33 g, 64% yield).

Light yellow solid. Decomposed upon heating by carbonization or polymerization; a melting point could not be detected.

^1H NMR (400 MHz, Chloroform-*d*) δ 7.91 (d, *J* = 1.3 Hz, 2H), 7.26 – 6.88 (m, 20H), 6.64 (dd, *J* = 17.6, 10.9 Hz, 2H), 5.69 (d, *J* = 17.6 Hz, 2H), 5.22 (d, *J* = 10.9 Hz, 2H), 5.00 (t, *J* = 8.6 Hz, 2H), 3.25 (ddd, *J* = 13.7, 8.6, 1.4 Hz, 2H), 2.77 (ddd, *J* = 13.7, 8.9, 1.5 Hz, 2H).

^{13}C NMR (101 MHz, $CDCl_3$) δ 152.4 (x2), 147.8 (x2), 144.5 (x2), 139.2 (x2), 137.4 (x2), 136.5 (x4), 136.1 (x2), 132.8 (x2), 128.9 (x6), 128.0 (x12), 125.9 (x4), 125.5 (x6), 124.3 (x2), 120.7 (x2), 113.7 (x4), 56.8, 52.0 (x2), 51.2 (x2).

^{19}F NMR (376 MHz, $CDCl_3$)δ -55.36 (t, J = 21.8 Hz, 6F), -138.61 – -139.77 (pd, J = 21.1, 5.8 Hz, 2F), -144.06 (pd, J = 21.1, 5.8 Hz, 2F), -145.79 (t, J = 19.6 Hz, 4F).

IR (neat): 3538, 3027, 2939, 2871, 1663, 1629, 1603, 1516, 1464, 1427, 1321, 1234, 1184, 1136, 986, 906, 841, 756, 714, 697 cm^{-1}.

HRMS (ESI): m/z: $[M-H]^+$ ($C_{59}H_{33}F_{14}O_2$), calcd.: 1039.2257; found: 1039.2268.

$[\alpha]_D^{25}$ = +24 (*c* = 0.1, CH_2Cl_2).

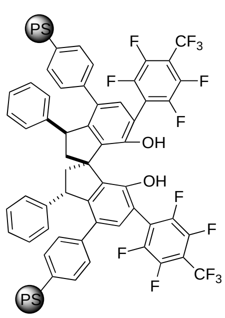

S12

S12 was synthesized Following a modification of a literature procedure.[2] A 100 mL reactor was charged with a suspension of polyvinyl alcohol (PV-OH) (100 mg, 0.96 µmol, 0.001 equiv.) in 72 mL of degassed MiliQ water. The solution was heated at 100 °C until PV-OH was dissolved. Then, it was cooled to RT and a solution of boric acid (449 mg, 7.26 mmol) in 18 mL of degassed MiliQ water was transferred to the reactor. Later, a degassed solution containing divinylbenzene (DVB), filtered on a short pad of silica immediately before use, (80%, 119 µL, 0.68 mmol, 0.65 equiv.), BINOL derivative **S11** (1.1 g, 1.06 mmol), styrene (2.9 ml, 25.5 mmol, 23.66 equiv.) and AIBN (31 mg, 0.19 mmol, 0.18 equiv.) in toluene (2.4 mL) was transferred to the reactor. After that, the system was heated at 90 °C and magnetically stirred at 440 rpm overnight, the aqueous solution was decanted off and the resin was washed with water (50 °C) several times, followed by MeOH and CH_2Cl_2. Finally, it was dried overnight in a vacuum oven at 40 °C to furnish 3.0 g of light-yellow beads.

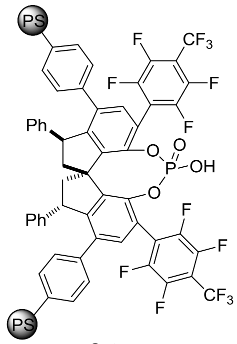

Cat e

Cat e was synthesized Following a modification of a literature procedure.[2] In a dry Schlenk tube, resin **S12** (3.0 g, ca. 1.06 mmol) was suspended in pyridine (20 mL) under Ar. Then, $POCl_3$ (495 µL, 5.3 mmol, 5 eq.) was added and the reaction mixture was heated in the closed Schlenk tube at 120 °C. After 2 days, it was cooled to RT and 5 mL of water were added. Then the system was closed again and heated at 100 °C overnight. The resin was filtered and washed with water, THF/water, THF, 2 M HCl/EtOAc, EtOAC/DCM, and DCM and dried overnight in a 40 °C vacuum oven to give 3.0 g of brown beads.

P elemental analysis (%): 0.40

$f_{(P)}$: 0.13 mmol/g resin

2.5. Preparation of Cat f

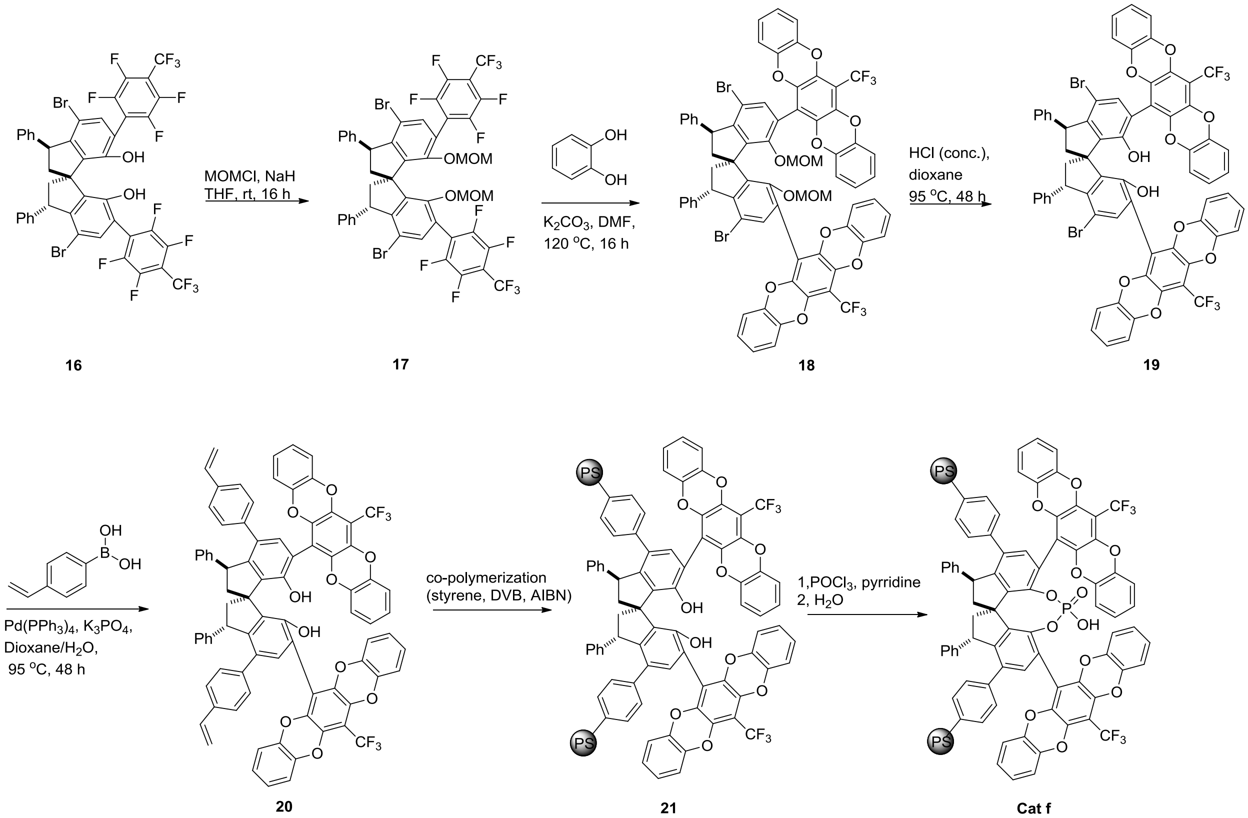

Scheme S5. The procedure of preparation of **Cat f**

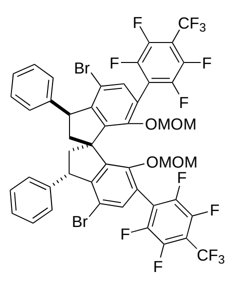

17

Preparation of **17**: In a Schlenk tube under Ar, NaH (a mixture of 60% sodium hydride (w/w) in mineral oil, 0.6 g, 15 mmol, 3 eq) was dissolved in 50 mL dry THF, and the mixture was stirred and cooled to 0 °C with ice bath. SPINOL **16** (5.0 g, 5 mmol) was dissolved in 10 mL dry THF and added to the mixture dropwise with syringe. The mixture was stirred at this temperature for 1 hour, then removed the ice bath and stirred at rt for 15 min. The mixture was cooled to 0 °C again and Chloromethyl methyl ether (1.21 g, 1.14 mL, 15mmol, 3 eq) was added dropwise with syringe. After being stirred at rt for 16 h, the reaction mixture was quenched with 2 mL water. The reaction mixture was then extracted with dichloromethane. After removal of solvent by rota-evaporation, the residue was subjected to column chromatography (silicagel, cyclohexane/CH_2Cl_2 (v/v = 5/2) as eluent), affording the expected compound **17** as a white solid (4.44 g, 82% yield).

White solid. m. p. 177.2 °C.

^{1}H NMR (400 MHz, Chloroform-*d*) δ 7.32 – 7.25 (m, 12H), 4.68 (dd, *J* = 6.1, 1.9 Hz, 2H), 4.55 (dd, *J* = 10.2, 7.9 Hz, 2H), 4.44 (dd, *J* = 6.2, 1.9 Hz, 2H), 3.06 (s, 6H), 2.95 – 2.89 (m, 2H), 2.34 (dd, *J* = 13.0, 10.3 Hz, 2H).

^{13}C NMR (101 MHz, $CDCl_3$) δ 152.5 (x2), 147.5 (x2), 144.5 (x2), 143.5 (x2), 135.0 (x4), 128.6 (x8), 128.2 (x8), 126.7 (x4), 121.9 (x2), 119.5 (x2), 115.3 (x2), 99.3 (x2), 58.4, 56.3 (x2), 51.4 (x2), 50.5 (x2).

^{19}F NMR (376 MHz, $CDCl_3$)δ -56.27 (t, *J* = 21.7 Hz, 6F), -137.37 (dd, *J* = 20.3, 12.3 Hz, 2F), -138.03 – -138.40 (m, 2F), -140.71 – -141.33 (m, 2F).

IR (neat): 3063, 3027, 2943, 1660, 1603, 1550, 1480, 1452, 1415, 1386, 1336, 1262, 1143, 1082, 1031, 986, 907, 845, 763, 733, 714, 699, 675 cm^{-1}.

HRMS (ESI): m/z: [M+Na]$^+$ ($C_{47}H_{28}Br_2F_{14}NaO_4$), calcd.: 1103.0023; found: 1103.0036.

$[\alpha]_D^{25}$ = +96 (*c* = 0.1, CH_2Cl_2).

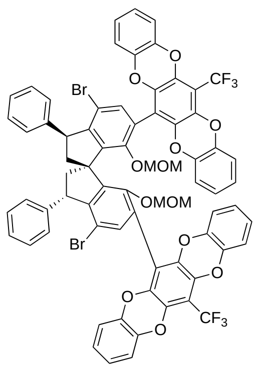

18

Preparation of **18**: In a Schlenk tube was added **17** (4.33 g, 4 mmol), pyrocatechol (1.98 g, 18 mmol, 4.5 equiv) and K_2CO_3 (11.04 g, 80 mmol, 20 equiv). The flask was reflashed with Ar three times. 50 mL degassed DMF was added and stirred at 120 ^{o}C overnight. The reaction mixture was cooled to rt and quenched with 100 mL water and 100 mL ethyl acetate. The biphasic solution was separated and the organic solution was washed with saturated $NaHCO_3$, water and brine, dried with $MgSO_4$. After removal of solvent by rota-evaporation, the residue was subjected to column chromatography (silicagel, cyclohexane/ethyl acetate (v/v = 20/1) as eluent), affording the expected compound **18** as a white solid (4.91 g, 90% yield).

White solid. m. p. 227.9 ^{o}C.

^{1}H NMR (400 MHz, Chloroform-*d*) δ 7.42 (dt, *J* = 5.8, 3.4 Hz, 4H), 7.30 – 7.25 (m, 8H), 6.89 (d, *J* = 4.3 Hz, 4H), 6.86 (d, *J* = 4.3 Hz, 4H), 6.81 – 6.77 (m, 2H), 6.69 – 6.65 (m, 2H), 6.59 (d, *J* = 7.9 Hz, 2H), 6.29 (d, *J* = 7.9 Hz, 2H), 4.77 – 4.71 (m, 2H), 4.64 – 4.56 (m, 4H), 3.02 (d, *J* = 3.0 Hz, 8H), 2.68 – 2.59 (m, 2H).

^{13}C NMR (101 MHz, $CDCl_3$) δ 152.7 (x2), 145.8 (x2), 144.5 (x2), 144.2 (x2), 141.3 (x2), 141.0 (x2), 140.8 (x2), 136.9 (x2), 136.6 (x2), 136.4 (x2), 135.8 (x2), 135.4 (x2), 128.7 (x6), 128.5 (x6), 126.3 (x2), 124.8 (x2), 124.6 (x2), 124.5 (x2), 124.2 (x2), 123.3 (x2, q, J = 277 Hz), 118.8 (x2), 116.6 (x2), 116.5 (x2), 116.3 (x2), 115.9 (x2), 114.2 (x2), 106.4 (x2, q, $^1J_{(C-F)}$ = 32 Hz), 98.9 (x2), 58.5, 56.5 (x2), 51.8 (x2), 50.6 (x2).

^{19}F NMR (376 MHz, $CDCl_3$) δ -55.00.

IR (neat): 3063, 3026, 2940, 1645, 1602, 1495, 1438, 1311, 1253, 1158, 1121, 1100, 1028, 986, 875, 744, 729, 697 cm^{-1}.

HRMS (ESI): m/z: [M+Na]$^+$ ($C_{71}H_{44}Br_2F_6NaO_{12}$), calcd.: 1383.0996; found: 1383.0974.

$[\alpha]_D^{25}$ = +185 (*c* = 0.1, CH_2Cl_2).

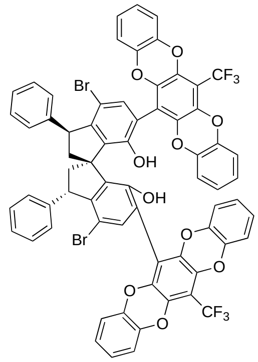

19

a) Preparation of **19** from **18**: In a round-bottom flask equipped with a condenser, compound **18** (4.85 g, 3.56 mmol) was dissolved in 30 mL 1,4-dioxane, 7 mL con. HCl was added, and the mixture was heated at 95 °C for 48 h. The reaction mixture was then extracted with dichloromethane. After removal of solvent by rota-evaporation, the residue was subjected to column chromatography (silicagel, cyclohexane/ dichloromethane (v/v = 5/2) as eluent), affording the expected compound **19** as a white solid (1.91 g, 42% yield). *Note: the polarity of **18** and **19** are almost the same. The consumption of **18** couldn't be checked by TLC; it should be detected by ^{1}H NMR or HPLC.*

b) Preparation of **19** from **16**: In a Schlenk tube under Argon, NaH (a mixture of 60% sodium hydride (w/w) in mineral oil, 1.08 g, 27 mmol, 3 eq) was suspended in 100 mL dry THF, and the mixture was stirred and cooled to 0 °C with an ice bath. SPINOL **16** (8.93 g, 9 mmol) was dissolved in 30 mL dry THF and added to the mixture dropwise *via* syringe. The mixture was stirred at this temperature for 1 hour, the ice bath was then removed and stirring was continued at rt for 15 min. The mixture was cooled again to 0 °C and chloromethyl methyl ether (2.17 g, 2.05 mL, 27 mmol, 3 eq) was added dropwise *via* syringe. After being stirred at rt for 16 h, the reaction mixture was quenched with 4 mL water and extracted with dichloromethane (3x 100 mL). After removal of solvent by rota-evaporation, the residue was passed through a short pad of silicagel eluting with cyclohexane/EA (v/v = 2/1) and the clear eluate was evaporated to dryness. The solid residue (9.23 g) was placed in a a Shlenck tube, catechol (4.46 g, 40.5 mmol, 4.5 equiv) and K_2CO_3 (24.84 g, 180 mmol, 20 equiv) were added, and an Ar atmosphere was established (3 X vacuum/refill). Degassed DMF (120 mL) was added, and the misture stirred at 120 °C for 48 h. The reaction mixture was cooled to rt and quenched with 400 mL water and 400 mL ethyl acetate. The biphasic solution was separated and the organic solution was washed with saturated $NaHCO_3$, water and brine, dried with $MgSO_4$. After removal of solvent by rota-evaporation, the residue was used in the next step without purification. The obtained yellow semi-solid was dissolved in 90 mL 1,4-dioxane, 9 mL con. HCl was added and the solution was heated at 95 °C for 48 h. The reaction mixture was then extracted with dichloromethane (3x 100 mL). After removal of solvent by rota-evaporation, the residue was subjected to column chromatography (silicagel, cyclohexane/ dichloromethane (v/v = 5/2) as eluent), affording the expected compound **19** as a white solid (6.75 g, 59% yield).

Light yellow solid. m. p. >300 °C.

^{1}H NMR (400 MHz, Chloroform-*d*) δ 7.34 – 7.22 (m, 12H), 6.93 – 6.88 (m, 4H), 6.85 – 6.76 (m, 4H), 6.72 (td, *J* = 7.7, 1.7 Hz, 2H), 6.66 – 6.57 (m, 6H), 5.16 (s, 2H), 4.62 (dd, *J* = 10.2, 7.5 Hz, 2H), 3.08 – 2.97 (m, 2H), 2.43 (dd, *J* = 13.2, 10.4 Hz, 2H).

^{13}C NMR (101 MHz, $CDCl_3$) δ 149.6 (x2), 146.4 (x2), 143.5 (x2), 141.1 (x2), 140.8 (x2), 140.3 (x2), 139.9 (x2), 136.7 (x2), 136.3 (x2), 135.8 (x2), 135.8 (x2), 135.4 (x2), 134.3 (x2), 128.7 (x4), 128.3 (x4), 126.6 (x2), 124.6 (x2), 124.5 (x2), 124.5 (x2), 124.3 (x2), 122.3 (x2, q, J = 274 Hz), 118.9 (x2), 116.5 (x4), 116.4 (x2), 116.1 (x2), 115.8 (x2), 111.9 (x2), 106.4 (x2, q, $^1J_{(C-F)}$ = 32 Hz), 56.6, 51.5 (x2), 49.9 (x2).

^{19}F NMR (376 MHz, $CDCl_3$) δ -55.11.

IR (neat): 3507, 3059, 3028, 2930, 2866, 1648, 1602, 1495, 1439, 1311, 1255, 1124, 1099, 1030, 988, 905, 876, 743, 728, 697 cm^{-1}.

HRMS (ESI): m/z: $[M+Na]^+$ ($C_{67}H_{36}Br_2F_6NaO_{10}$), calcd.: 1295.0472; found: 1295.0464.

$[\alpha]_D^{25}$ = -32 (*c* = 0.1, CH_2Cl_2).

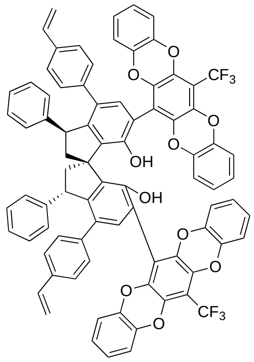

20

20: Under N_2, to a Schlenk tube containing **19** (1.8 g, 1.41 mmol), 4-vinylphenylboronic acid (626 mg, 4.23 mmol, 3.0 equiv), $Pd(PPh_3)_4$ (130 mg, 0.07 mmol, 5 mol%) and K_3PO_4 (0.9 g, 4.23 mmol, 3.0 eq) was added degassed 1,4-dioxane (9 mL) and water (3 mL). The reaction mixture was stirred and heated to 95 °C for 48 h. and then it was cooled to room temperature and extracted with CH_2Cl_2 (10 mL×3). The combined organic layers were dried over $MgSO_4$ and concentrated under reduced pressure. The crude product was purified by flash column chromatography on silicagel using cyclohexane/CH_2Cl_2 (5:2) as the eluent to give compound **20** (838 mg, 45% yield) as a slightly yellow solid. The reaction can also be performed with $Pd_2(dba)_3$ (2 mol %) and S-Phos (8 mol %) in 3:1 toluene/water (95 °C, 18 h), **20** being obtained in almost identical yield (44%).

Light yellow solid. m. p. >300 °C.

^{1}H NMR (500 MHz, Chloroform-*d*) δ 7.10 (s, 2H), 7.06 (d, *J* = 8.4 Hz, 4H), 7.02 (d, *J* = 8.3 Hz, 4H), 7.00 – 6.89 (m, 10H), 6.88 (d, *J* = 2.1 Hz, 1H), 6.86 (dd, *J* = 2.9, 1.7 Hz, 2H), 6.85 (d, *J* = 1.4 Hz, 1H), 6.84 – 6.80 (m, 2H), 6.76 – 6.72 (m, 6H), 6.66 – 6.62 (m, 2H), 6.57 (d, *J* = 10.9 Hz, 1H), 6.56 – 6.52 (m, 3H), 5.60 (dd, *J* = 17.5, 1.0 Hz, 2H), 5.37 (s, 2H), 5.14 (dd, *J* = 10.8, 1.0 Hz, 2H), 4.88 (dd, *J* = 10.3, 7.5 Hz, 2H), 3.14 (dd, *J* = 13.3, 7.5 Hz, 2H), 2.51 (dd, *J* = 13.1, 10.5 Hz, 2H).

^{13}C NMR (126 MHz, $CDCl_3$) δ 149.6 (x2), 146.0 (x2), 143.3 (x2), 141.3 (x2), 140.9 (x2), 140.5 (x2), 140.0 (x2), 139.0 (x2), 136.6 (x4), 136.2 (x2), 135.9 (x2), 135.6 (x2), 135.5 (x2), 133.5 (x2), 133.0 (x2), 131.9 (x2), 128.8 (x4), 128.0 (x4), 127.9 (x4), 125.8 (x2), 125.3 (x4), 124.4 (x2), 124.3 (x2), 124.2 (x2), 124.1 (x2), 122.4(x2, q, *J* = 222 Hz), 117.9 (x2), 117.2 (x2), 116.5 (x4), 116.4 (x2), 116.1 (x2), 113.2 (x2), 105.8 (x2, q, $^1J_{(C\text{-}F)}$ = 32 Hz), 55.9, 50.2 (x2), 50.1 (x2).

^{19}F NMR (376 MHz, $CDCl_3$) δ -55.00.

IR (neat): 3511, 3059, 3027, 2932, 2862, 1647, 1603, 1495, 1439, 1310, 1256, 1165, 1124, 1098, 1031, 988, 906, 885, 842, 743, 730, 698 cm^{-1}.

HRMS (ESI): m/z: $[M+Na]^+$ ($C_{83}H_{50}F_6NaO_{10}$), calcd.: 1343.3200; found: 1343.3176.

$[\alpha]_D^{25}$ = +50 (*c* = 0.1, CH_2Cl_2).

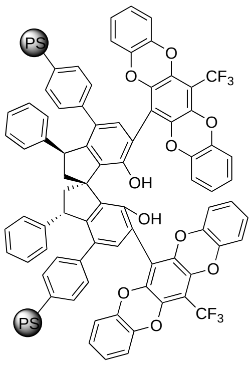

21

21 was synthesized Following a modification of a literature procedure.[2] A 100 mL reactor was charged with a suspension of polyvinyl alcohol (PV-OH) (100 mg, 0.96 µmol, 0.002 equiv.) in 72 mL of degassed MiliQ water. The solution was heated at 100 °C until PV-OH was dissolved. Then, it was cooled to rt and a solution of boric acid (449 mg, 7.26 mmol) in 18 mL of degassed MiliQ water was transferred to the reactor. Later, a degassed solution containing divinylbenzene (DVB), filtered on a short pad of silica immediately before use, (80%, 119 µL, 0.68 mmol, 1.3 equiv.), BINOL derivative **20** (700 mg, 0.53 mmol), styrene (2.9 ml, 25.5 mmol, 47.75 equiv.) and AIBN (31 mg, 0.19 mmol, 0.35 equiv.) in toluene (2.4 mL) was transferred to the reactor. After that, the system was heated at 90 °C and magnetically stirred at 440 rpm. After two days, the aqueous solution was decanted off and the resin was washed with water (50 °C) several times, followed by MeOH and CH_2Cl_2. Finally, it was dried overnight in a 40 °C vacuum oven to furnish 3.0 g of yellow beads.

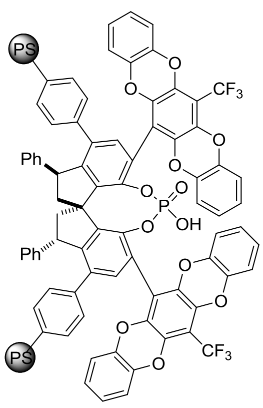

Cat f

Cat f was synthesized Following a modification of a literature procedure.[2] In a dry Schlenk tube, resin **21** (3.0 g, ca. 0.53 mmol) was suspended in pyridine (20 mL) under Ar. Then, $POCl_3$ (248 µL, 2.65 mmol, 5 eq.) was added and the reaction mixture was heated in the closed Schlenk tube at 120 °C. After 2 days, it was cooled to RT and 5 mL of water were added. Then the system was closed again and heated at 100 °C overnight. The resin was filtered and washed with water, THF/water, THF, 2 M HCl/EtOAc, EtOAC/DCM, and DCM and dried overnight in a 40 °C vacuum oven to give 3.0 g of brown beads.

P elemental analysis (%): 0.53

$f_{(P)}$: 0.17 mmol/g resin

2.6. Preparation of Cat g

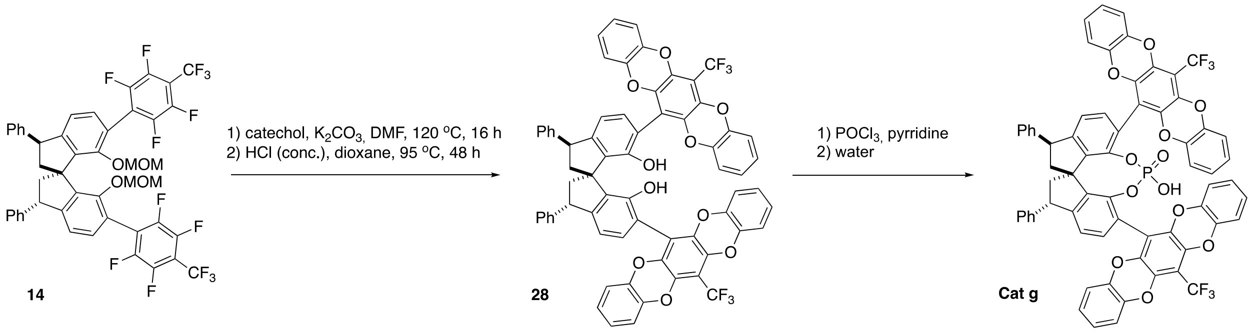

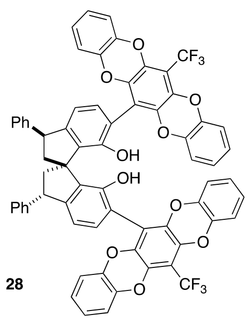

28: The protected diol **14** (924 mg, 1 mmol) was placed In a Schlenk tube, pyrocatechol (495 mg, 4.5 mmol, 4.5 equiv) and K_2CO_3 (2.75 g, 20 mmol, 20 equiv) were added, and an Ar atmosphere was established (3 X vacuum/refill). Degassed anhydrous DMF (12 mL) was added, and the mixture was stirred at 120 °C overnight. The reaction mixture was cooled to rt and quenched with 30 mL water and 30 mL ethyl acetate. Phases were separated, and the organic one was washed with saturated $NaHCO_3$, water and brine, and dried with $MgSO_4$. Removal of solvent by rota-evaporation afforded 1.2 g of a yellow semi-solid, which was dissolved in 1,4-dioxane (10 mL). Concentrated aqueous HCl (1.0 mL) was added, and the solution was heated at 95 °C for 48 h. The reaction mixture was then extracted with dichloromethane (3x15 mL). After solvent removal by rota-evaporation, the residue was puridied by column chromatography [silicagel, cyclohexane/ dichloromethane (v/v = 5/2) as eluent], affording the expected compound **28** as a white solid (647 mg, 58% yield).

Light yellow solid. m. p. >300 °C with decomposition.

^{1}H NMR (400 MHz, $CDCl_3$) δ 7.32-7.15 (m, 10H), 7.00 (d, *J* = 7.7 Hz, 2H), 6.79 (dd, *J* = 5.9, 1.8 Hz, 4H), 6.74-6.63 (m, 4H), 6.61-6.45 (m, 10H), 5.08 (s, 2H), 4.52 (dd, *J* = 11.0, 7.1 Hz, 2H), 2.92 (dd, *J* = 13.0, 7.1 Hz, 2H), 2.44 (t, *J* = 12.0 Hz, 2H).

^{13}C NMR (101 MHz, $CDCl_3$) δ 150.4 (x2), 149.7 (x2), 143.1 (x2), 141.4 (x2), 141.0 (x2), 140.4 (x2), 139.9 (x2), 136.5 (x2), 136.1 (x2), 135.8 (x2), 135.6 (x2), 132.3 (x2), 130.7 (x2), 128.8 (x4), 128.4 (x4), 126.9 (x2), 124.4 (x2), 124.2 (x2), 124.2 (x2), 124.1 (x2), 122.4 (x2, q, ^{1}J = 276 Hz), 118.3 (x2), 118.1 (x2), 116.6 (x2), 116.5 (x2), 116.3 (x2), 115.9 (x2), 106.1 (x2), 105.5 (x2, q, $^{1}J_{(C-F)}$ = 33 Hz), 55.8, 50.2 (x2), 48.0 (x2).

^{19}F NMR (376 MHz, $CDCl_3$) δ -54.96.

IR (neat): 3510, 3060, 3028, 2930, 2860, 1648, 1600, 1496, 1440, 1311, 1257, 1166, 1120, 1030, 985, 900, 887, 843 cm^{-1}.

HRMS (ESI): m/z: $[M+Na]^+$ ($C_{67}H_{38}F_6NaO_{10}$), calcd.: 1139.2261; found: 1139.2242.

$[\alpha]_D^{25}$ = -48 (*c* = 0.1, CH_2Cl_2).

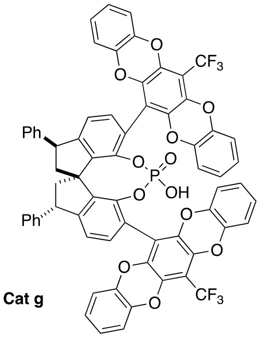

Cat g

Cat g: To a dry Schlenk tube, **28** (500 mg, 0.448 mmol) and pyridine (5 mL) were added under Ar. Then, $POCl_3$ (126 µL, 1.35 mmol, 3 eq.) was added, and the reaction mixture was heated at 100 °C in the sealed Schlenk tube. After 18 hours, the reaction mixture was cooled to room temperature and water (5 mL) was added. The system was sealed again and heated at 100 °C overnight. Afterwards, the solution was cooled to rt, diluted with DCM (20 mL), washed with 2N HCl (3x 10 mL). Volatiles were removed under vacuum and the residue was purified by column chromatography on silicagel (ethyl acetate/hexane=1:1). The collected product was redissolved in DCM (5 mL), 6N HCl (5 mL) was added, and the mixture stirred for 1 hour at room temperature. By evaporation of the organic phase, compound **Cat g** (413 mg, 78% yield) was obtained as a slightly yellow solid.

Light yellow solid. m. p. >300 °C or polymerized.

^{1}H NMR (500 MHz, $CDCl_3$) δ 7.40 (t, *J* = 7.4 Hz, 4H), 7.33 (dd, *J* = 12.4, 7.3 Hz, 6H), 7.23 (d, *J* = 7.7 Hz, 2H), 6.90 – 6.77 (m, 14H), 6.69 (d, *J* = 7.7 Hz, 2H), 6.45 (d, *J* = 8.0 Hz, 2H), 4.63 (dd, *J* = 10.8, 6.3 Hz, 2H), 2.98 (dd, *J* = 12.3, 6.3 Hz, 2H), 2.43 (t, *J* = 11.6 Hz, 2H).

^{13}C NMR (126 MHz, $CDCl_3$) δ 149.6 (x2), 143.6 (x2), 143.2 (x2), 141.6 (x2), 141.4 (x2), 141.3 (x2), 141.1 (x2), 139.7 (x2), 137.1 (x2), 136.5 (x2), 136.2 (x2), 135.7 (x2), 131.4 (x2), 128.8 (x4), 128.6(x4), 128.5 (x2), 127.1 (x2), 125.6 (x2), 124.3 (x2), 124.2 (x2), 124.1 (x4), 122.8 (x2), 122.4 (x2), 122.3 (x2, q, ^{1}J = 275 Hz), 117.9 (x2), 116.6 (x2), 116.5 (x2), 116.3 (x2), 116.0 (x2), 106.1 (x2, q, $^{1}J_{(C-F)}$ = 33 Hz), 57.7, 50.1 (x2), 49.2 (x2).

^{19}F NMR (471 MHz, $CDCl_3$) δ -54.91.

^{31}P NMR (162 MHz, $CDCl_3$) δ -7.09.

IR (neat): 3648, 3358, 3081, 3062, 3025, 2960, 2926, 2858, 1640, 1600, 1493, 1434, 1308, 1256, 1165, 1120, 1090, 1020, 985, 906, 834, 747, 730, 698 cm^{-1}.

HRMS (ESI): m/z: $[M-H]^+$ ($C_{67}H_{36}F_6O_{12}P$), calcd.: 1177.1854; found: 1177.1843.

$[\alpha]_D^{25}$ = 240 (c = 0.1, CH_2Cl_2).

3. Experimental procedures

3.1. Optimization of catalyst and solvent for the desymmetrization reaction

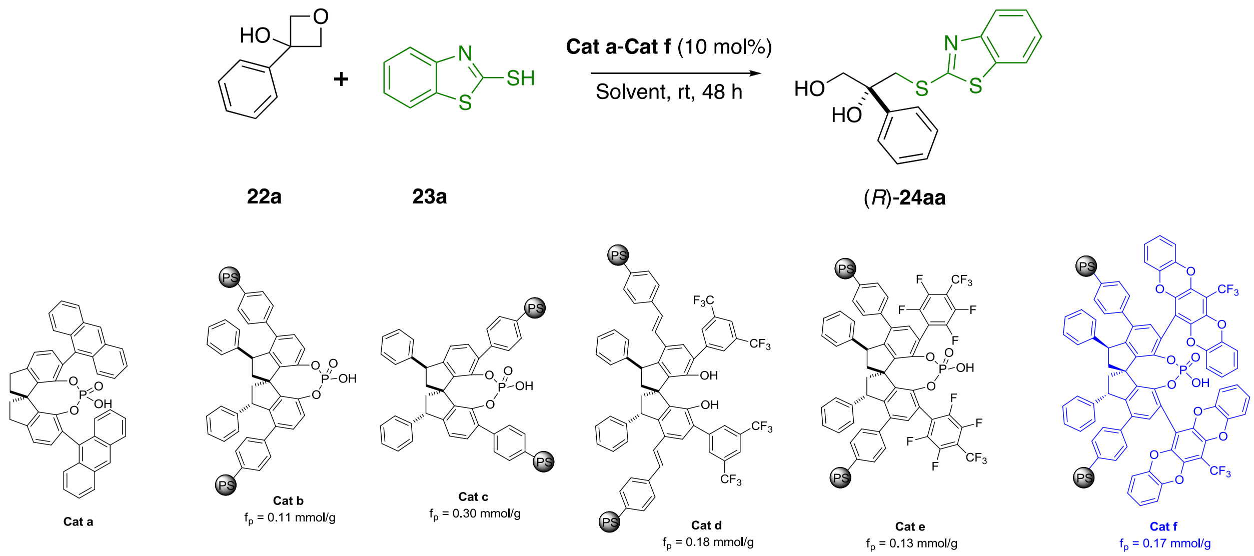

Scheme S6. Optimization of reaction conditions

These experiments refer to Table 1 in the main text. To a 10 mL glass vial were sequentially added **Cat b**-**Cat f** (10 mol % loading) and the indicated solvent (1 mL), followed by oxetane **22a** (30 mg, 0.2 mmol) and **23a** (42 mg, 0.25 mmol). The reaction mixture was shaken at room temperature for 48 h, or at 60 °C for 16 h in specified cases. Then, it was filtered and the resin beads were washed with DCM (3 x 0.25 mL). The solvent was concentrated under reduced pressure and the product was isolated after purification by column chromatography on silicagel with cyclohexane/ethyl acetate (EtOAc/*c*-Hex = 1:5) to yield **24aa.**

3.2. Recycling of Cat f in the desymmetrization of 22a with 23a in batch

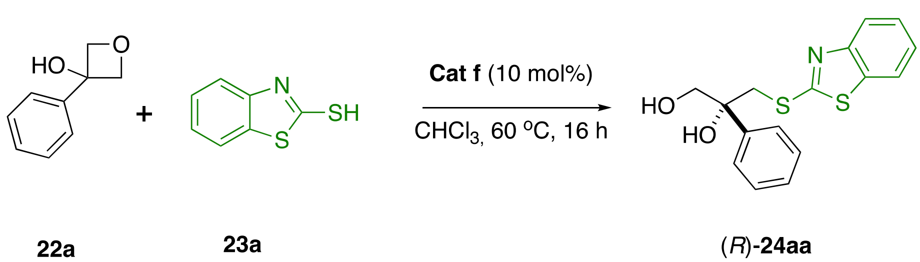

Scheme S7. Recycling experiments of Cat f in batch

To a 10 mL glass vial were sequentially **Cat f** (59 mg, f_p = 0.17 mmol/g, 5 mol % loading) and 4 mL $CHCl_3$, followed by oxetane **22a** (30 mg, 0.2 mmol) and **23a** (42 mg, 0.25 mmol). The reaction mixture was shaken at 60 °C for 16 h. Then, it was filtered and the resin beads were washed with $CHCl_3$ (3 x 0.25 mL). The solvent was removed under reduced pressure and the residue was purified by column chromatography on silicagel with cyclohexane/ethyl acetate (EtOAc/*c*-Hex = 1:5) to yield **24aa.**

Table S1. Recycling experiments in batch

Run	Conversion (%)	Yield (%)	ee (%)
1	92	90	95
2	89	90	96
3	92	85	97
4	90	89	97
5	93	90	97
6	90	90	97
7	90	85	97
8	90	87	95
9	93	90	96
10	92	90	95
11	91	90	95
12	89	85	95
13	92	89	95
14	91	82	94
15	91	85	95
16	90	84	94

Isolated yield.

3.3. Optimization of the desymmetrization of 22a with 23a mediated by Cat f in flow

Scheme S8. Parameter optimization for the flow experiment

Cat f (2.0 g, f_p = 0.17 mmol/g, 0.34 mmol) was placed in a size-adjustable, jacketed glass Omnifit column (10 mm Ø), and temperature was controlled at 60 °C by an external circulating pump. A stream of $CHCl_3$ was passed for 1 h at 0.1 mL min^{-1} to swell the polymer, and size of the packed bed was adjusted. The reagents were then introduced in the system using the two-pump system, represented in Figure 4 of the main text: One of the pumps was used to circulate a solution of **22a** (300 mg, 2 mmol, 1.0 eq) and **23a** (418 mg, 1.25 eq.) in $CHCl_3$ (40 mL for 0.05 M; 20 mL for 0.1 M), while the other was used to circulate $CHCl_3$ at 0.5 mL min^{-1} for 1 h between the eight individual experiments in Table S2. The collected outstream was concentrated under reduced pressure and purified by column chromatography on silicagel, eluting with cyclohexane/ethyl acetate (EtOAc/*c*-Hex = 1:5) to yield **24aa**.

Table S2. Parameter optimization for the flow experiment

Flow rate	concentration	Temperature	conversion	yield (%)	ee (%)
0.5 ml/min	0.05 M	rt	84	80	95
0.3 ml/min	0.05 M	rt	89	85	96
1 ml/min	**0.05 M**	**60 °C**	**92**	**90**	**97**
2 ml/min	0.05 M	60 °C	78	72	95
2 ml/min	0.1 M	60 °C	81	80	95
1.0 ml/min	0.1 M	60 °C	87	80	94
0.75 ml/min	0.1 M	60 °C	87	82	95
0.5 ml/min	**0.1 M**	**60 °C**	**98**	**90**	**95**

3.4. Continuous flow desymmetrization of oxetanes 22 with thiols 23 mediated by Cat f

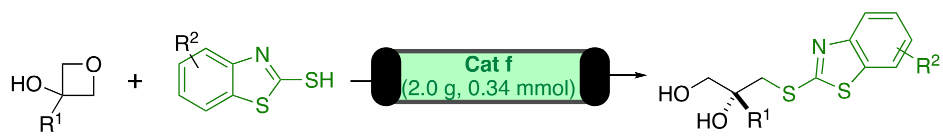

22a-n **23a-d** **24**

Scheme S9. Continuous flow process

a) Processes at 2 mmol scale: Using the same set-up depicted above, filled with the same sample of **Cat f** (2.0 g, f_p = 0.17 mmol/g, 0.34 mmol), previously swollen with $CHCl_3$ and operated at the same temperature (60 °C), the reactants were circulated through the reactor using the two-pump system. One of the syringes contained the oxetane (**22a-n**, 2.00 mmol, 1.00 eq) and the thiol (**23a-d**, 2.50 mmol, 1.25 eq) to be reacted, dissolved in $CHCl_3$ (20 mL), while the other syringe was filled with chloroform for rinsing the resin between individual experiments. A three-way valve was intercalated between the syringes and the reactor, to act as a flow selector, and a back pressure regulator was placed at the outlet of the reactor to prevent the formation of bubbles near the boiling point of chloroform. Flow rate in the preparative experiments was 0.5 mL/min. In each case, when the circulation of the solution containing the reactants was complete, the channel used for the addition of the reactants and the packed bed reactor was rinsed with $CHCl_3$ at 0.5 mL min^{-1} for 1 h. The collected outstream was concentrated under reduced pressure and purified by column chromatography on silicagel with cyclohexane/ethyl acetate (EtOAc/*c*-Hex = 1:5) to yield the corresponding products (**24aa-24ad**).

b) Processes at 20 mmol scale: With the same set-up and catalyst sample, operated under the same experimental conditions, the large-scale preparation of **24aa** (one run at 20 mmol scale and one run at 18 mmol scale) and **24na** (20 mmol scale) was performed with the results shown in Scheme 3 of the main text. Results for the two runs in the preparation of **24aa**, performed in a non-consecutive manner, indicate tha **Cat f** can be stored for 15 months without losses in its catalytic performance.

3.5. Desymmetrization of oxetanes 22 with thiols 23 mediated by Cat g in batch

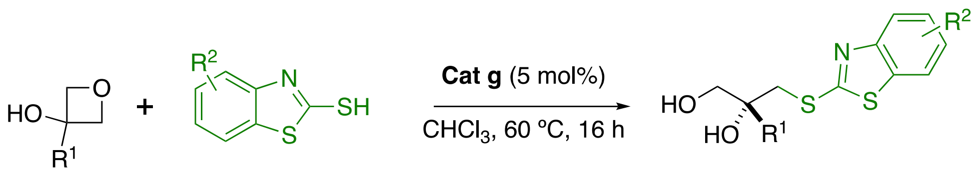

22 **23** (*R*)-**24**

In a tall reaction vial with screw-on cap, **22** (0.2 mmol), **23** (0.25 mmol), **Cat g** (12 mg, 5 mol%) and chloroform (4 mL) were placed. The system was stirred at 60 ºC (bath temperature) for 16 h. Then, the products were purified as in the flow experiments mediated by **Cat f**. The results (yield and enantiomeric excess) for the fifteen examples studied are summarized in Table S3. For comparison purposes, the results achieved with **Cat f** in the preparation of the same products in flow (Figure 5 in the main text) are also included in the table.

Table S3. Desymmetrization of 22 with 23 leading to 24 mediated by the homogeneous catalyst Cat g.

Entry	Product	with **Cat g** Yield [%]; ee [%]	with **Cat f**[b] Yield [%]; ee [%]
1	**24aa**	87; 95	95; 95
2	**24ba**	78; 98	80; 95
3	**24ca**	83; >99	90; 99
4	**24da**	86; 95	65; 79
5	**24ea**	90; 73	85; 70
6	**24ga**	84; 7[c]	75; 0
7	**24ha**	87; 13[d]	80; 37
8	**24ia**	90; 90	85; 90
9	**24ja**	85; 92	92; 91
10	**24ka**	88; 92	84; 90
11	**24ma**	87; 97	95; 93
12	**24na**	95; 78	95; 72
13	**24ab**	96; 95	90; >99
14	**24ac**	85; 85	88; 87
15	**24ad**	80; 74	78; 92

[a]Standard conditions: **22** (0.2 mmol), **23** (0.25 mmol) and **Cat g** (12 mg, 5 mol%) in chloroform (4 mL) stirred at 60 ºC (oil bath temp) in a sealed vial for 16 h. [b]Reaction conditions are those in Figure 5. [c]When the reaction was performed at rt for 16 h, yield was 82% and ee 4%. [d]When the reaction was performed at rt. for 16 h, yield was 86% and ee 10%.

4. Compound characterization data

(Data on prepared amounts and yields refer to the flow processes summarized in Figure 5 in the main text)

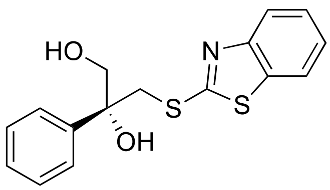

24aa

(R)-3-(benzo[d]thiazol-2-ylthio)-2-phenylpropane-1,2-diol

Colorless solid. 603 mg, 95% yield. Reported compound.[5]

^{1}H NMR (400 MHz, Chloroform-*d*) δ 7.86 (dt, *J* = 8.1, 0.9 Hz, 1H), 7.73 (dt, *J* = 7.9, 0.9 Hz, 1H), 7.56 – 7.49 (m, 2H), 7.47 – 7.26 (m, 5H), 5.37 (s, 1H), 4.00 (dd, *J* = 11.2, 7.3 Hz, 1H), 3.93 – 3.83 (m, 2H), 3.82 – 3.74 (m, 2H).

^{13}C NMR (101 MHz, $CDCl_3$) δ 169.2, 151.8, 142.5, 135.2, 128.4 (x2), 127.6, 126.4, 125.5 (x2), 124.8, 121.1, 121.0, 76.4, 68.3, 42.6.

$[\alpha]_D^{25}$ = +112.2 (*c* = 0.1, CH_2Cl_2).

HPLC (Daicel Chiralpak AD-H, hexane/*i*-PrOH = 80:20, flow rate 1.0 mL/min, λ = 210 nm): minor isomer: t_R = 12.6 min; major isomer: t_R = 15.4 min.

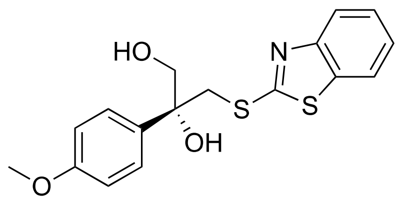

24ba

(*R*)-3-(benzo[*d*]thiazol-2-ylthio)-2-(4-methoxyphenyl)propane-1,2-diol

Colorless solid. M.p. 167.8 °C. 592 mg, 80% yield.

^{1}H NMR (400 MHz, Chloroform-*d*) δ 7.88 – 7.82 (m, 1H), 7.73 (dt, *J* = 8.0, 0.8 Hz, 1H), 7.48 – 7.40 (m, 3H), 7.33 (d, *J* = 1.0 Hz, 1H), 6.91 (d, *J* = 8.8 Hz, 2H), 5.18 (s, 1H), 4.02 – 3.94 (m, 1H), 3.90 (dd, *J* = 12.3, 5.3 Hz, 1H), 3.85 – 3.71 (m, 6H).

^{13}C NMR (101 MHz, $CDCl_3$) δ 169.2, 159.0, 151.8, 135.2, 134.5, 126.8 (x2), 126.4, 124.8, 121.1, 121.0, 113.7 (x2), 76.1, 68.2, 55.2, 42.7.

IR (neat): 3368, 2957, 1609, 1579, 1512, 1452, 1419, 1307, 1246, 1209, 1180, 1080, 1011, 968, 815, 751, 565 cm^{-1}.

HRMS (ESI): m/z: $[M+Na]^+$ ($C_{17}H_{17}NNaO_3S_2$), calcd.: 370.0542; found: 370.0538.

$[\alpha]_D^{25}$ = +132.0 (*c* = 0.1, CH_2Cl_2).

HPLC (Daicel Chiralpak AD-H, hexane/*i*-PrOH = 80:20, flow rate 1.0 mL/min, λ = 210 nm): minor isomer: t_R = 37.6 min; major isomer: t_R = 39.3 min.

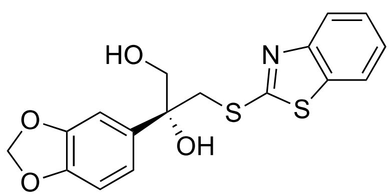

24ca

(*R*)-2-(benzo[*d*][1,3]dioxol-5-yl)-3-(benzo[*d*]thiazol-2-ylthio)propane-1,2-diol

Colorless solid. M.p. 120.4 °C. 650 mg, 90% yield.

^{1}H NMR (400 MHz, Chloroform-*d*) δ 7.82 (ddd, *J* = 8.2, 1.2, 0.6 Hz, 1H), 7.70 (ddd, *J* = 8.0, 1.3, 0.6 Hz, 1H), 7.41 (ddd, *J* = 8.3, 7.3, 1.3 Hz, 1H), 7.30 (ddd, *J* = 8.0, 7.3, 1.2 Hz, 1H), 7.05 (d, *J* = 1.8 Hz, 1H), 6.94 (dd, *J* = 8.1, 1.8 Hz, 1H), 6.78 (d, *J* = 8.1 Hz, 1H), 5.92 (s, 2H), 5.42 (s, 1H), 4.01 (d, *J* = 6.9 Hz, 1H), 3.94 – 3.81 (m, 2H), 3.77 – 3.66 (m, 2H).

^{13}C NMR (101 MHz, $CDCl_3$) δ 169.0, 151.7, 147.7, 146.8, 136.6, 135.1, 126.3, 124.7, 121.0, 120.9, 118.8, 107.9, 106.5, 101.0, 76.3, 68.4, 42.7.

IR (neat): 3366, 3200, 2888, 1501, 1419, 1396, 1244, 1079, 1039, 1011, 933, 858, 824, 749 cm^{-1}.

HRMS (ESI): m/z: $[M+Na]^+$ ($C_{17}H_{15}NNaO_4S_2$), calcd.: 384.0335; found: 384.0319.

$[\alpha]_D^{25}$ = +169.5 (*c* = 0.1, CH_2Cl_2).

HPLC (Daicel Chiralpak AD-H, hexane/*i*-PrOH = 80:20, flow rate 1.0 mL/min, λ = 210 nm): minor isomer: t_R = 22.5 min; major isomer: t_R = 24.3 min.

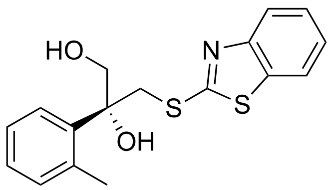

24da

(R)-3-(benzo[d]thiazol-2-ylthio)-2-(o-tolyl)propane-1,2-diol

Colorless solid. M.p. 106.7 °C. 457 mg, 65% yield.

^{1}H NMR (400 MHz, Chloroform-*d*) δ 7.89 (dd, *J* = 8.1, 1.1 Hz, 1H), 7.74 (d, *J* = 8.0 Hz, 1H), 7.53 – 7.43 (m, 2H), 7.39 – 7.31 (m, 1H), 7.25 – 7.13 (m, 3H), 5.38 (q, *J* = 2.4, 1.5 Hz, 1H), 4.21 (d, *J* = 8.0 Hz, 2H), 4.00 (s, 2H), 3.88 (d, *J* = 5.8 Hz, 1H), 2.62 (s, 3H).

^{13}C NMR (101 MHz, $CDCl_3$) δ 169.2, 151.7, 139.4, 136.0, 135.1, 132.7, 127.7, 126.9, 126.4, 125.6, 124.7, 121.1, 120.9, 77.7, 67.0, 41.0, 22.4.

IR (neat): 3398, 3054, 2928, 2856, 1492, 1451, 1417, 1390, 1344, 1309, 1235, 1208, 1075, 1053, 1022, 1005, 966, 882, 752, 722, 568 cm^{-1}.

HRMS (ESI): m/z: [M+Na]$^+$ ($C_{17}H_{17}NNaO_2S_2$), calcd.: 354.0593; found: 354.0583.

$[\alpha]_D^{25}$ = +81.9 (*c* = 0.1, CH_2Cl_2).

HPLC (Daicel Chiralpak AD-H, hexane/*i*-PrOH = 80:20, flow rate 1.0 mL/min, λ = 210 nm): minor isomer: t_R = 13.1 min; major isomer: t_R = 16.5 min.

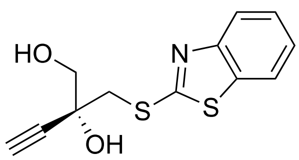

24ea

(R)-2-((benzo[d]thiazol-2-ylthio)methyl)but-3-yne-1,2-diol

Colorless solid. 411 mg, 85% yield. Reported compound. [5]

^{1}H NMR (400 MHz, Chloroform-*d*) δ 7.85 – 7.78 (m, 1H), 7.76 – 7.70 (m, 1H), 7.42 (ddd, *J* = 8.3, 7.2, 1.3 Hz, 1H), 7.32 (td, *J* = 7.6, 1.2 Hz, 1H), 5.15 (s, 1H), 4.51 (t, *J* = 8.1 Hz, 1H), 3.84 (dd, *J* = 11.8, 6.5 Hz, 1H), 3.80 – 3.71 (m, 2H), 3.65 (d, *J* = 14.6 Hz, 1H), 2.58 (s, 1H).

^{13}C NMR (101 MHz, $CDCl_3$) δ 168.9, 151.6, 135.0, 126.5, 124.9, 121.1, 120.9, 83.2, 74.6, 71.6, 66.8, 40.6.

$[\alpha]_D^{25}$ = -28.9 (*c* = 0.1, CH_2Cl_2).

HPLC (Daicel Chiralpak AD-H, hexane/*i*-PrOH = 80:20, flow rate 1.0 mL/min, λ = 210 nm): minor isomer: t_R = 12.9 min; major isomer: t_R = 15.3 min.

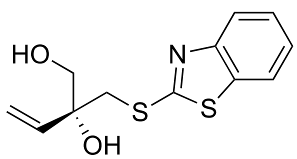

24fa

(*R*)-2-((benzo[*d*]thiazol-2-ylthio)methyl)but-3-ene-1,2-diol

Colorless solid. 455 mg, 85% yield.

^{1}H NMR (400 MHz, Chloroform-*d*) δ 7.83 (dd, *J* = 8.3, 1.1 Hz, 1H), 7.74 (d, *J* = 8.0 Hz, 1H), 7.50 – 7.38 (m, 1H), 7.36 – 7.25 (m, 1H), 6.04 (dd, *J* = 17.3, 10.9 Hz, 1H), 5.55 (dd, *J* = 17.3, 1.4 Hz, 1H), 5.32 (dd, *J* = 10.8, 1.4 Hz, 1H), 4.65 – 4.50 (m, 1H), 4.42 (d, *J* = 14.4 Hz, 1H), 3.79 – 3.51 (m, 4H).

^{13}C NMR (101 MHz, $CDCl_3$) δ 169.1, 151.7, 138.4, 134.9, 126.3, 124.7, 121.0, 120.9, 116.2, 75.3, 66.6, 40.2.

IR (neat): 3333, 2926, 2871, 2243, 1642, 1561, 1456, 1425, 1310, 1240, 1128, 1076, 1020, 993, 926, 754, 724, 670 cm^{-1}.

HRMS (ESI): m/z: [M+Na]$^+$ ($C_{12}H_{13}NNaO_2S_2$), calcd.: 290.0280; found: 290.0281.

$[\alpha]_D^{25}$ = +7.71 (*c* = 0.1, CH_2Cl_2).

HPLC (Daicel Chiralpak AD-H, hexane/*i*-PrOH = 80:20, flow rate 1.0 mL/min, λ = 210 nm): minor isomer: t_R = 22.6 min; major isomer: t_R = 24.1 min.

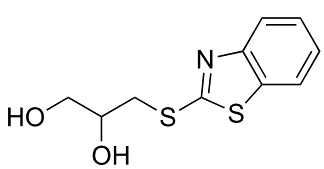

24ga

3-(benzo[*d*]thiazol-2-ylthio)propane-1,2-diol

Colorless oil. 394 mg, 75% yield.

^{1}H NMR (400 MHz, Chloroform-*d*) δ 7.80 (dd, *J* = 8.3, 1.3 Hz, 1H), 7.69 (dd, *J* = 8.1, 1.4 Hz, 1H), 7.42 – 7.33 (m, 1H), 7.33 – 7.18 (m, 1H), 4.67 (d, *J* = 5.4 Hz, 1H), 4.26 – 4.01 (m, 2H), 3.73 (d, *J* = 4.8 Hz, 2H), 3.60 – 3.39 (m, 2H).

^{13}C NMR (101 MHz, $CDCl_3$) δ 168.3, 152.0, 135.0, 126.3, 124.6, 121.0 (x2), 71.4, 64.1, 36.1.

IR (neat): 3320, 2926, 2872, 1644, 1455, 1424, 1310, 1238, 1074, 1020, 996, 905, 752, 724 cm^{-1}.

HRMS (ESI): m/z: [M+Na]$^+$ ($C_{10}H_{11}NNaO_2S_2$), calcd.: 264,0129; found: 264,0125.

HPLC (Daicel Chiralpak AD-H, hexane/*i*-PrOH = 80:20, flow rate 1.0 mL/min, λ = 210 nm): t_{R1} = 12.6 min; t_{R2} = 15.4 min.

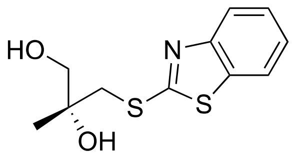

24ha

(*R*)-3-(benzo[*d*]thiazol-2-ylthio)-2-methylpropane-1,2-diol

Colorless oil. 445 mg, 80% yield.

^{1}H NMR (400 MHz, Chloroform-*d*) δ 7.82 (d, *J* = 8.1 Hz, 1H), 7.74 (dd, *J* = 8.1, 1.3 Hz, 1H), 7.46 – 7.39 (m, 1H), 7.36 – 7.30 (m, 1H), 4.90 (t, *J* = 7.6 Hz, 1H), 3.93 (t, *J* = 5.1 Hz, 1H), 3.69 – 3.56 (m, 2H), 3.49 – 3.34 (m, 2H), 1.33 (s, 3H).

^{13}C NMR (101 MHz, $CDCl_3$) δ 169.2, 151.7, 134.8, 126.4, 124.7, 121.0, 120.8, 73.18, 67.07, 40.7, 22.9.

IR (neat): 3347, 2971, 2930, 2871, 1456, 1426, 1375, 1310, 1238, 1167, 1127, 1077, 1046, 1003, 904, 754, 724 cm^{-1}.

HRMS (ESI): m/z: $[M+Na]^+$ ($C_{11}H_{13}NNaO_2S_2$), calcd.: 278.0280; found: 278.0275.

$[\alpha]_D^{25}$ = -10.9 (*c* = 0.1, CH_2Cl_2).

HPLC (Daicel Chiralpak AD-H, hexane/*i*-PrOH = 90:10, flow rate 1.0 mL/min, λ = 210 nm): minor isomer: t_R = 19.1 min; major isomer: t_R = 20.6 min.

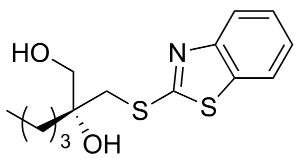

24ia

(R)-2-((benzo[d]thiazol-2-ylthio)methyl)hexane-1,2-diol

Colorless oil. 505 mg, 85% yield.

^{1}H NMR (400 MHz, Chloroform-*d*) δ 7.83 – 7.76 (m, 1H), 7.71 (dd, *J* = 8.0, 1.3 Hz, 1H), 7.40 (td, *J* = 8.2, 7.8, 1.4 Hz, 1H), 7.34 – 7.25 (m, 1H), 4.89 (ddt, *J* = 6.4, 4.3, 2.3 Hz, 1H), 3.72 (q, *J* = 4.6 Hz, 1H), 3.66 – 3.57 (m, 2H), 3.49 – 3.32 (m, 2H), 1.66 – 1.55 (m, 2H), 1.50 – 1.29 (m, 4H), 0.93 (t, *J* = 7.1 Hz, 3H).

^{13}C NMR (101 MHz, $CDCl_3$) δ 169.3, 151.7, 134.8, 126.3, 124.7, 121.0, 120.8, 74.7, 65.6, 38.8, 35.2, 25.0, 23.2, 14.0.

IR (neat): 3059, 3063, 2954, 2930, 2869, 1456, 1426, 1310, 1240, 1053, 1019, 1002, 906, 754, 724 cm^{-1}.

HRMS (ESI): m/z: $[M+Na]^+$ ($C_{14}H_{19}NNaO_2S_2$), calcd.: 320.0749; found: 320.0746.

$[\alpha]_D^{25}$ = -46.8 (*c* = 0.1, CH_2Cl_2).

HPLC (Daicel Chiralpak AD-H, hexane/*i*-PrOH = 80:20, flow rate 1.0 mL/min, λ = 210 nm): minor isomer: t_R = 10.4 min; major isomer: t_R = 12.8 min.

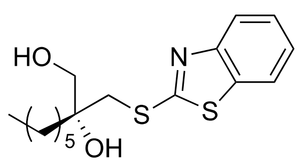

24ja

(R)-2-((benzo[d]thiazol-2-ylthio)methyl)octane-1,2-diol

Colorless oil. 585 mg, 92% yield.

^{1}H NMR (400 MHz, Chloroform-*d*) δ 7.80 (d, *J* = 8.1 Hz, 1H), 7.72 (d, *J* = 7.9 Hz, 1H), 7.41 (t, *J* = 7.7 Hz, 1H), 7.34 – 7.23 (m, 1H), 4.92 – 4.80 (m, 1H), 3.73 – 3.57 (m, 3H), 3.45 (dd, *J* = 11.9, 8.0 Hz, 1H), 3.36 (d, *J* = 14.7 Hz, 1H), 1.61 (dd, *J* = 10.1, 7.4 Hz, 2H), 1.51 – 1.19 (m, 8H), 0.93 – 0.83 (m, 3H).

^{13}C NMR (101 MHz, $CDCl_3$) δ 169.3, 151.8, 134.8, 126.3, 124.7, 121.0, 120.8, 74.8, 65.62, 38.8, 35.5, 31.7, 29.8, 22.9, 22.5, 14.0.

IR (neat): 3355, 2926, 2855, 1561, 1456, 1426, 1310,1277, 1240, 1060, 1003, 909, 753, 724 cm^{-1}.

HRMS (ESI): m/z: $[M+Na]^+$ ($C_{16}H_{23}NNaO_2S_2$), calcd.: 348,1068; found: 348,1058.

$[\alpha]_D^{25}$ = -46.1 (*c* = 0.1, CH_2Cl_2).

HPLC (Daicel Chiralpak AD-H, hexane/*i*-PrOH = 80:20, flow rate 1.0 mL/min, λ = 210 nm): major isomer: t_R = 14.2 min; minor isomer: t_R = 16.1 min.

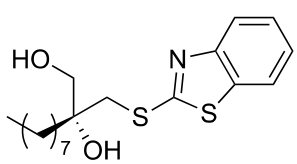

24ka

(R)-2-((benzo[d]thiazol-2-ylthio)methyl)decane-1,2-diol

Colorless oil. 593 mg, 84% yield.

^{1}H NMR (400 MHz, Chloroform-*d*) δ 7.80 (d, *J* = 8.1 Hz, 1H), 7.71 (d, *J* = 7.9 Hz, 1H), 7.40 (t, *J* = 7.8 Hz, 1H), 7.29 (dd, *J* = 14.9, 7.3 Hz, 1H), 4.94 – 4.81 (m, 1H), 3.74 – 3.55 (m, 3H), 3.48 – 3.31 (m, 2H), 1.60 (dd, *J* = 8.7, 6.1 Hz, 2H), 1.43 – 1.22 (m, 12H), 0.88 (t, *J* = 6.7 Hz, 3H).

^{13}C NMR (101 MHz, $CDCl_3$) δ 169.3, 151.7, 134.8, 126.3, 124.7, 121.0, 120.8, 74.8, 65.6, 38.8, 35.5, 31.8, 30.1, 29.5, 29.2, 22.9, 22.6, 14.1.

IR (neat): 3355, 2922, 2852, 1457, 1427, 1310, 1240, 1046, 1003, 753, 724 cm^{-1}.

HRMS (ESI): m/z: $[M+Na]^+$ ($C_{18}H_{27}NNaO_2S_2$), calcd.: 376.1375; found: 376.1371.

$[\alpha]_D^{25}$ = 41.2 (*c* = 0.1, CH_2Cl_2).

HPLC (Daicel Chiralpak AD-H, hexane/*i*-PrOH = 80:20, flow rate 1.0 mL/min, λ = 210 nm): minor isomer: t_R = 8.4 min; major isomer: t_R = 10.6 min.

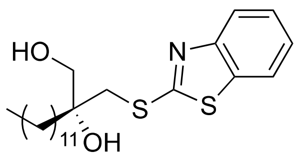

24la

(R)-2-((benzo[d]thiazol-2-ylthio)methyl)tetradecane-1,2-diol

Colorless oil. 708 mg, 82% yield.

^{1}H NMR (400 MHz, Chloroform-*d*) δ 7.82 (dd, *J* = 8.2, 1.1 Hz, 1H), 7.74 (dd, *J* = 8.1, 1.3 Hz, 1H), 7.46 – 7.40 (m, 1H), 7.35 – 7.29 (m, 1H), 4.91 (t, *J* = 7.2 Hz, 1H), 3.74 – 3.59 (m, 3H), 3.52 – 3.34 (m, 2H), 1.63 (dd, *J* = 8.8, 6.0 Hz, 2H), 1.30 (d, *J* = 17.4 Hz, 20H), 0.94 – 0.84 (m, 3H).

^{13}C NMR (101 MHz, $CDCl_3$) δ 169.3, 151.7, 134.8, 126.3, 124.7, 121.0, 120.8, 74.8, 65.6, 38.8, 35.5, 31.7, 30.1, 29.6, 29.6, 29.5, 29.5, 29.3, 22.9, 22.6, 14.1.

IR (neat): 3355, 2921, 2851, 1457, 1427, 1310, 1241, 1128, 1020, 1003, 908, 753, 724 cm^{-1}.

HRMS (ESI): m/z: $[M+Na]^+$ ($C_{22}H_{35}NNaO_2S_2$), calcd.: 432.2001; found: 432.1997.

$[\alpha]_D^{25}$ = -50.0 (*c* = 0.1, CH_2Cl_2).

HPLC (Daicel Chiralpak AD-H, hexane/*i*-PrOH = 80:20, flow rate 1.0 mL/min, λ = 210 nm): minor isomer: t_R = 6.7 min; major isomer: t_R = 7.6 min.

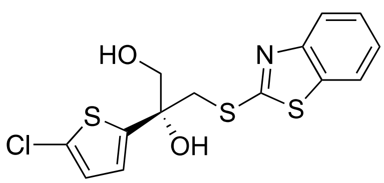

24ma

(*R*)-3-(benzo[*d*]thiazol-2-ylthio)-2-(5-chlorothiophen-2-yl)propane-1,2-diol

Colorless solid. M.p. 96.8 ºC. 675 mg, 95% yield.

^{1}H NMR (400 MHz, Chloroform-*d*) δ 7.82 (d, *J* = 8.2 Hz, 1H), 7.75 – 7.69 (m, 1H), 7.45 – 7.39 (m, 1H), 7.36 – 7.29 (m, 1H), 6.80 (d, *J* = 1.9 Hz, 2H), 5.69 (t, *J* = 4.7 Hz, 1H), 4.42 (s, 1H), 3.91 – 3.70 (m, 4H).

^{13}C NMR (101 MHz, $CDCl_3$) δ 169.0, 151.5, 146.0, 135.0, 129.5, 126.5, 126.0, 125.0, 122.6, 121.1, 121.0, 76.1, 67.8, 42.4.

IR (neat): 3212, 1453, 1423, 1399, 1238, 1215, 1081, 997, 924, 791, 755 cm^{-1}.

HRMS (ESI): m/z: $[M+Na]^+$ ($C_{14}H_{12}ClNNaO_2S_3$), calcd.: 379.9611; found: 379.9611.

$[\alpha]_D^{25}$ = +130.5 (*c* = 0.1, CH_2Cl_2).

HPLC (Daicel Chiralpak AD-H, hexane/*i*-PrOH = 80:20, flow rate 1.0 mL/min, λ = 210 nm): minor isomer: t_R = 12.7 min; major isomer: t_R = 15.6 min.

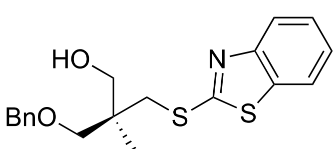

24na

(*R*)-3-(benzo[*d*]thiazol-2-ylthio)-2-((benzyloxy)methyl)-2-methylpropan-1-ol

Colorless oil. 682 mg, 95% yield.

^{1}H NMR (400 MHz, Chloroform-*d*) δ 7.84 (dd, *J* = 8.1, 1.1 Hz, 1H), 7.74 (dd, *J* = 8.0, 1.2 Hz, 1H), 7.44 – 7.27 (m, 7H), 5.00 (t, *J* = 7.2 Hz, 1H), 4.57 (d, *J* = 1.6 Hz, 2H), 3.63 (d, *J* = 14.3 Hz, 1H), 3.56 – 3.45 (m, 5H), 1.13 (s, 3H).

^{13}C NMR (101 MHz, $CDCl_3$) δ 169.6, 152.0, 138.2, 134.8, 128.3, 127.5, 127.4, 126.2, 124.5, 120.9, 120.8, 74.9, 73.4, 65.4, 41.7, 37.8, 19.5.

IR (neat): 3354, 3061, 3029, 2858, 1602, 1496, 1454, 1426, 1361, 1309, 1277, 1205, 1095, 1046, 994, 895, 842, 753, 725, 696, 608 cm^{-1}.

HRMS (ESI): m/z: $[M+Na]^+$ ($C_{19}H_{21}NNaO_2S_2$), calcd.: 382.0906; found: 382.0895.

$[\alpha]_D^{25}$ = -25.2 (*c* = 0.1, CH_2Cl_2).

HPLC (Daicel Chiralpak AD-H, hexane/*i*-PrOH = 80:20, flow rate 1.0 mL/min, λ = 210 nm): minor isomer: t_R = 9.0 min; major isomer: t_R = 13.9 min.

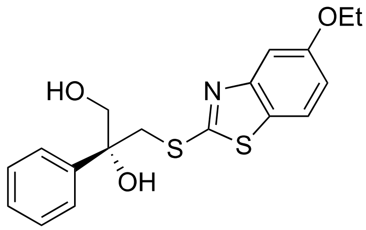

24ab

(*R*)-3-((5-ethoxybenzo[*d*]thiazol-2-yl)thio)-2-phenylpropane-1,2-diol

Colorless solid. 650 mg, 90% yield. Reported compound. [5]

^{1}H NMR (400 MHz, Chloroform-*d*) δ 7.75 (d, *J* = 8.8 Hz, 1H), 7.59 – 7.50 (m, 2H), 7.44 – 7.27 (m, 3H), 7.20 (d, *J* = 2.4 Hz, 1H), 7.04 (dd, *J* = 8.8, 2.4 Hz, 1H), 5.47 (d, *J* = 2.3 Hz, 1H), 4.16 – 3.94 (m, 4H), 3.92 – 3.69 (m, 3H), 1.47 (t, *J* = 7.0 Hz, 3H).

^{13}C NMR (101 MHz, $CDCl_3$) δ 165.7, 156.7, 146.2, 142.6, 136.5, 128.3, 127.5, 125.5, 121.5, 115.6, 104.8, 76.4, 68.3, 64.1, 42.8, 14.7.

$[\alpha]_D^{25}$ = +115.6 (*c* = 0.1, CH_2Cl_2).

HPLC (Daicel Chiralpak AD-H, hexane/*i*-PrOH = 80:20, flow rate 1.0 mL/min, λ = 210 nm): minor isomer: t_R = 19.7 min; major isomer: t_R = 28.5 min.

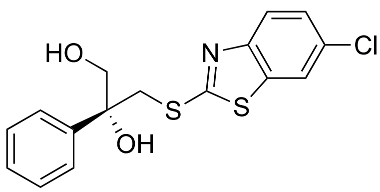

24ac

(*R*)-3-((6-chlorobenzo[*d*]thiazol-2-yl)thio)-2-phenylpropane-1,2-diol

Colorless solid. 620 mg, 88% yield. Reported compound. [5]

^{1}H NMR (400 MHz, Chloroform-*d*) δ 7.88 (d, *J* = 2.1 Hz, 1H), 7.64 (d, *J* = 8.5 Hz, 1H), 7.58 – 7.51 (m, 2H), 7.43 – 7.38 (m, 2H), 7.33 (td, *J* = 8.5, 1.7 Hz, 2H), 5.20 (d, *J* = 2.5 Hz, 1H), 4.03 – 3.88 (m, 2H), 3.86 – 3.77 (m, 2H), 3.69 (t, *J* = 6.7 Hz, 1H).

^{13}C NMR (101 MHz, $CDCl_3$) δ 171.3, 152.6, 142.3, 133.4, 132.6, 128.4, 128.3, 127.7, 125.5, 125.5, 125.2, 121.7, 121.0, 76.4, 68.5, 42.7.

$[\alpha]_D^{25}$ = +168.8 (*c* = 0.1, CH_2Cl_2).

HPLC (Daicel Chiralpak AD-H, hexane/*i*-PrOH = 80:20, flow rate 1.0 mL/min, λ = 210 nm): minor isomer: t_R = 7.5 min; major isomer: t_R = 8.3 min.

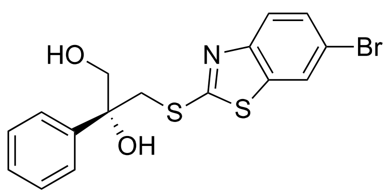

24ad

(*R*)-3-((6-bromobenzo[*d*]thiazol-2-yl)thio)-2-phenylpropane-1,2-diol

Light-yellow solid. M.p. 150.6 ºC. 616 mg, 78% yield.

^{1}H NMR (400 MHz, Chloroform-*d*) δ 8.05 (d, *J* = 1.9 Hz, 1H), 7.65 – 7.51 (m, 3H), 7.48 – 7.30 (m, 4H), 5.17 (d, *J* = 2.6 Hz, 1H), 3.98 (dd, *J* = 20.0, 13.8 Hz, 2H), 3.86 – 3.75 (m, 2H), 3.64 (d, *J* = 6.9 Hz, 1H).

^{13}C NMR (101 MHz, $CDCl_3$) δ 171.2, 152.9, 142.3, 134.0, 128.4, 127.8, 127.7, 125.5, 125.2, 124.0, 122.0, 121.7, 121.0, 120.1, 76.4, 68.5, 42.7.

IR (neat): 3529, 3089, 2911, 1497, 1446, 1409, 1246, 1202, 1071, 1050, 1024, 959, 858, 696, 569 cm^{-1}.

HRMS (ESI): m/z: $[M+Na]^+$ ($C_{16}H_{14}BrNNaO_2S_2$), calcd.: 417.9542; found: 417.9548.

$[\alpha]_D^{25}$ = +139.3 (*c* = 0.1, CH_2Cl_2).

HPLC (Daicel Chiralpak AD-H, hexane/*i*-PrOH = 80:20, flow rate 1.0 mL/min, λ = 210 nm): minor isomer: t_R = 7.8 min; major isomer: t_R = 8.8 min.

5. Computational section

The calculations were carried out using G09 D.01 program.[6] M06-2X was selected for this investigation given the excellent performances of this functional reported for kinetics and thermodynamics of the main group and the non-covalent interactions (particularly π-π stacking of arenes).[7] Our recent study pointed out that M06-2X-D3 is particularly suitable to produce kinetically relevant model for the chemistry of phosphine oxides vis-à-vis with experiments.[8] Furthermore, M06-2X-D3 delivers better performances than M06-2X in describing weak interactions.[9] Preliminary stationary points used as good guesses for higher level calculations have been located using multi-layer ONIOM[10-16] (DFT:PM6) calculations. Guesses structures were firstly optimized at M06-2X-D3/DGDZVP[17] level in gas phase and, secondly, the solvent correction was introduced during the single-point energy refinement at M06-2X-D3/DGTZVP/SMD[18] (chloroform, $\varepsilon = 4.7113$). Single-point energy corrections have been calculated using an "ultrafine" (99 radial shells by 590 angular points) grid to avoid potential problems deriving from quadrature issues of the Minnesota functionals.[19] Vibrational analysis was carried out to identify the nature of stationary points and to obtain ZPE, enthalpic (H) and free energy corrections (G) to the potential energy via statistical thermodynamics. ΔH, $-T\Delta S$ and ΔG have been calculated at 333K and 1M. GoodVibes v. 2.0.3[20] has been used to introduce the quasi-harmonic correction to the entropic term derived from low-frequency vibrations ($\nu < 100$ cm^{-1} cut off) via Grimme's RRHO corrections. Basis set superimposition error (BSSE) have been estimated at M06-2X-D3/DGTZVP level in gas phase for each stationary point using the counterpoise scheme implemented in G09 based on Boys and Bernardi method[21-22](the partition schemes for reactants, transition states and products are displayed in Fig. S1, S2 and S3) and added as a correction to the total single-point potential energy. For simplicity and clarity in the computational profiles, Van der Waals complexes found to be endergonic with respect to the reactants or the products separated at infinite distance have been removed from the profiles. CHIMERA v.1.13.1[23] and VMD v.1.9.3[24] have been used to visualize, render and generate all the graphical content included in the computational work via POV-Ray[25] and Tachyon[26] libraries, respectively.

Cartesian coordinates, vibrations and non-corrected values for energies

Benzo[d]thiazole-2-thiol

Center Number	Atomic Number	Atomic Type	Coordinates (Angstroms) X	Y	Z
1	6	0	-5.197433	-5.732430	-0.074661
2	6	0	-3.806657	-5.925135	0.032468
3	6	0	-2.949692	-4.818007	0.017625
4	6	0	-3.498127	-3.548786	-0.103458
5	6	0	-4.887310	-3.368910	-0.210385
6	6	0	-5.752396	-4.457232	-0.197110
7	6	0	-4.420597	-8.034746	0.132690
8	1	0	-1.879067	-4.973913	0.100985
9	1	0	-2.845872	-2.681660	-0.115837
10	1	0	-5.294044	-2.367387	-0.305097
11	1	0	-6.825224	-4.316067	-0.279644
12	16	0	-4.332215	-9.784615	0.257634
13	1	0	-2.991580	-9.788737	0.307133
14	16	0	-6.002580	-7.279050	-0.027200
15	7	0	-3.398468	-7.249414	0.148947

Frequencies --	104.1360	189.6270	191.9167
Frequencies --	257.6143	292.9460	374.3202
Frequencies --	387.7570	432.4147	511.7332
Frequencies --	531.1037	599.6660	601.4862
Frequencies --	659.7282	719.7802	741.3648
Frequencies --	777.7204	876.0156	876.4382
Frequencies --	917.5204	964.2259	1003.3537
Frequencies --	1051.3082	1060.8864	1114.9294
Frequencies --	1153.9121	1186.5066	1280.0095
Frequencies --	1314.7471	1360.6119	1486.8536
Frequencies --	1507.5366	1575.1762	1648.6841
Frequencies --	1685.1011	2764.3400	3227.9745
Frequencies --	3235.8498	3243.8381	3252.5495

SCF Done: E(RM062X/DGDZVP) = -1120.65058655
Sum of electronic and zero-point Energies= -1120.547701
Sum of electronic and thermal Energies= -1120.537731
Sum of electronic and thermal Free Energies= -1120.586309
SCF Done: E(RM062X/DGTZVP/SMD) = -1120.81574335

TS1Ha

Center Number	Atomic Number	Atomic Type	Coordinates (Angstroms) X	Y	Z
1	16	0	-1.473481	-3.787416	0.669706
2	6	0	-1.977063	-3.449680	-0.951264
3	16	0	-2.491276	-4.744429	-2.012884
4	7	0	-2.018660	-2.262290	-1.497572
5	6	0	-2.791159	-3.576982	-3.275803
6	6	0	-2.464242	-2.291791	-2.814314
7	6	0	-3.269671	-3.779701	-4.571262
8	6	0	-2.607366	-1.179170	-3.649944
9	6	0	-3.411917	-2.668770	-5.395015
10	1	0	-3.522388	-4.773110	-4.927289
11	6	0	-3.082940	-1.382141	-4.938229
12	1	0	-2.345041	-0.189776	-3.287181
13	1	0	-3.781682	-2.800622	-6.406438
14	1	0	-3.201416	-0.533714	-5.603998
15	1	0	-0.733582	-2.533570	0.795868
16	1	0	-1.956285	-1.022280	-0.773234
17	16	0	-1.895690	0.338794	-0.061592
18	6	0	-0.376256	-0.005234	0.689085
19	16	0	0.640687	1.305961	1.267513
20	7	0	0.120822	-1.198791	0.886286
21	6	0	1.809871	0.137629	1.825022
22	6	0	1.358788	-1.157850	1.516560
23	6	0	3.026980	0.345441	2.475586
24	6	0	2.136098	-2.271812	1.854706
25	6	0	3.789672	-0.768462	2.810632
26	1	0	3.371503	1.346882	2.712485
27	6	0	3.347195	-2.064609	2.501508
28	1	0	1.788526	-3.270414	1.606990
29	1	0	4.740681	-0.630899	3.314542
30	1	0	3.961783	-2.917171	2.771174

Frequencies --	-877.5730	12.5050	22.4898
Frequencies --	30.6378	49.6159	65.9400
Frequencies --	103.7174	106.6099	186.7690
Frequencies --	192.5403	196.3899	216.4836
Frequencies --	285.8666	297.6936	354.3899
Frequencies --	383.4696	389.6339	398.3790
Frequencies --	410.0559	429.8172	430.5120
Frequencies --	511.9237	512.9308	532.3886
Frequencies --	537.3675	599.1356	604.1531
Frequencies --	611.9578	615.9727	696.6839
Frequencies --	707.8178	725.1419	733.0035
Frequencies --	739.9246	742.1845	769.4200
Frequencies --	773.9651	842.5311	868.8566
Frequencies --	869.1053	881.7151	889.0184
Frequencies --	956.7807	957.9128	980.0724
Frequencies --	996.8577	1001.5645	1046.2482
Frequencies --	1049.1485	1059.2169	1060.3222
Frequencies --	1111.4573	1115.8374	1149.8279
Frequencies --	1157.7927	1167.4540	1184.9782
Frequencies --	1186.1485	1252.8510	1285.2786
Frequencies --	1290.2932	1297.5739	1341.8349
Frequencies --	1347.5923	1365.1360	1370.0329
Frequencies --	1489.9900	1493.6516	1510.1384
Frequencies --	1510.6733	1547.2346	1557.5746
Frequencies --	1654.1143	1658.0178	1684.4211
Frequencies --	1686.5783	3220.9730	3222.6524
Frequencies --	3226.9273	3227.7955	3235.7067
Frequencies --	3239.7196	3245.2103	3253.2800

SCF Done: E(RM062X/DGDZVP) = -2241.31134437
Sum of electronic and zero-point Energies= -2241.109213
Sum of electronic and thermal Energies= -2241.088358
Sum of electronic and thermal Free Energies= -2241.166226
SCF Done: E(RM062X/DGTZVP/SMD) = -2241.64215807

Benzo[d]thiazole-2(3H)-thione

Center Number	Atomic Number	Atomic Type	Coordinates (Angstroms) X	Y	Z
1	16	0	-0.000084	0.000000	-0.003844

2	6	0	0.002414	0.000000	1.639210
3	16	0	1.441255	0.000000	2.662505
4	7	0	-1.097081	0.000000	2.449341
5	6	0	0.481924	0.000000	4.131178
6	6	0	-0.884822	0.000000	3.822530
7	6	0	0.906254	0.000000	5.457015
8	6	0	-1.851089	0.000000	4.826276
9	6	0	-0.056759	0.000000	6.464996
10	1	0	1.963937	0.000000	5.699337
11	6	0	-1.420521	0.000000	6.150531
12	1	0	-2.908322	0.000000	4.579951
13	1	0	0.257290	0.000000	7.503078
14	1	0	-2.155788	0.000000	6.948005
15	1	0	-2.016575	0.000000	2.019252

Frequencies -- 90.2679 188.0419 209.0542
Frequencies -- 281.7423 384.9194 403.5443
Frequencies -- 430.1006 504.7645 523.1969
Frequencies -- 555.3698 576.3708 621.9335
Frequencies -- 668.5946 723.5974 734.7883
Frequencies -- 761.3246 870.6349 883.2073
Frequencies -- 951.5913 992.0682 1055.2400
Frequencies -- 1074.2844 1115.1751 1161.3382
Frequencies -- 1180.2769 1254.2635 1295.5396
Frequencies -- 1315.8380 1368.1783 1460.3870
Frequencies -- 1517.8067 1536.7507 1673.0820
Frequencies -- 1688.7806 3228.2050 3240.9820
Frequencies -- 3244.5452 3257.8298 3597.0997

SCF Done: E(RM062X/DGDZVP) = -1120.66395890
Sum of electronic and zero-point Energies= -1120.557749
Sum of electronic and thermal Energies= -1120.548147
Sum of electronic and thermal Free Energies= -1120.596096
SCF Done: E(RM062X/DGTZVP/SMD) = -1120.83289725

TS1Hb

Center Number	Atomic Number	Atomic Type	X	Y	Z
1	16	0	-1.972467	-2.043090	1.390312
2	6	0	-1.628666	-2.088370	-0.285707
3	16	0	-1.300976	-3.313174	-1.460024
4	7	0	-1.623344	-0.854746	-0.767183
5	6	0	-1.144772	-2.064266	-2.690865
6	6	0	-1.353520	-0.789697	-2.126458
7	6	0	-0.860768	-2.216943	-4.046712
8	6	0	-1.278171	0.354235	-2.925505
9	6	0	-0.787985	-1.071807	-4.834566
10	1	0	-0.701215	-3.200105	-4.477920
11	6	0	-0.995035	0.198847	-4.276682
12	1	0	-1.439805	1.332868	-2.486040
13	1	0	-0.568456	-1.166096	-5.892714
14	1	0	-0.934834	1.076291	-4.912100
15	1	0	-1.911863	-0.565860	0.541642

Coordinates (Angstroms)

Frequencies -- -1791.7319 96.6327 192.3924
Frequencies -- 231.5125 274.3485 392.1086
Frequencies -- 422.2681 427.5883 504.0108
Frequencies -- 513.4839 576.2388 643.0212
Frequencies -- 707.0575 719.4309 736.6681
Frequencies -- 768.8068 863.4105 877.2180
Frequencies -- 904.9025 960.5877 998.4210
Frequencies -- 1056.3680 1080.8570 1143.8096
Frequencies -- 1159.0840 1182.7738 1290.7266
Frequencies -- 1316.7638 1364.6377 1466.7644
Frequencies -- 1502.6788 1513.3681 1653.8101
Frequencies -- 1682.0835 1747.0970 3228.4493
Frequencies -- 3241.8355 3249.2991 3257.4515

SCF Done: E(RM062X/DGDZVP) = -1120.59695302
Sum of electronic and zero-point Energies= -1120.496832
Sum of electronic and thermal Energies= -1120.487519
Sum of electronic and thermal Free Energies= -1120.534950
SCF Done: E(RM062X/DGTZVP/SMD) = -1120.76598765

(*R*)-3-(benzo[d]thiazol-2-ylthio)-2-phenylpropane-1,2-diol ((*R*)-Product)

Center Number	Atomic Number	Atomic Type	X	Y	Z
1	8	0	-0.137702	0.169497	0.049577
2	6	0	-0.051436	0.047498	1.454043
3	6	0	2.448661	0.021304	1.235620
4	1	0	-0.048046	1.058219	1.867595
5	1	0	-0.910328	-0.498300	1.864997
6	6	0	1.222407	-0.714184	1.857707
7	8	0	1.061215	-1.974578	1.228583
8	1	0	-0.067433	-0.734033	-0.300271
9	6	0	1.283306	-0.826834	3.372721
10	6	0	1.179643	-2.067850	4.001951
11	6	0	1.426868	0.322316	4.159580
12	6	0	1.231518	-2.161106	5.393803
13	1	0	1.053756	-2.960535	3.397579
14	6	0	1.470627	0.232231	5.548139
15	1	0	1.521287	1.298347	3.687566
16	6	0	1.376833	-1.013816	6.170506
17	1	0	1.154747	-3.134168	5.869435
18	1	0	1.585081	1.132780	6.143676
19	1	0	1.416123	-1.087072	7.252951
20	1	0	2.235750	1.087695	1.115465
21	1	0	2.627584	-0.383504	0.237871
22	16	0	4.027536	0.046623	2.147091
23	6	0	4.408637	-1.648305	2.277567
24	16	0	5.849297	-2.094559	3.180661
25	7	0	3.725491	-2.630411	1.777491
26	6	0	5.491104	-3.769117	2.848139
27	6	0	4.311402	-3.853851	2.087382
28	6	0	6.191920	-4.912455	3.234661
29	6	0	3.813126	-5.104955	1.706976
30	6	0	5.686851	-6.149181	2.848309
31	1	0	7.102489	-4.842458	3.820733
32	6	0	4.506997	-6.243901	2.092353
33	1	0	2.901945	-5.164285	1.119420
34	1	0	6.214055	-7.052529	3.136986
35	1	0	4.134579	-7.221376	1.803956
36	1	0	1.936227	-2.418282	1.252864

Coordinates (Angstroms)

Frequencies -- 11.1939 29.0324 49.2269
Frequencies -- 68.6393 80.4601 112.4797
Frequencies -- 116.4288 141.3818 148.6469
Frequencies -- 190.5215 199.1509 255.5933
Frequencies -- 284.5231 301.4874 334.1762
Frequencies -- 342.1714 366.6704 383.0561
Frequencies -- 412.4321 414.6108 431.1679
Frequencies -- 456.2651 491.7236 512.7939

Frequencies -- 522.6731 531.3491 579.7863
Frequencies -- 599.5083 611.1904 628.1193
Frequencies -- 631.5738 698.4652 703.0788
Frequencies -- 714.6379 723.1534 726.9346
Frequencies -- 741.3095 773.9987 778.0558
Frequencies -- 818.3065 867.3160 872.4377
Frequencies -- 874.2167 883.8157 942.7161
Frequencies -- 955.7006 960.0461 996.6329
Frequencies -- 997.6510 1001.8410 1012.9175
Frequencies -- 1024.6269 1042.2414 1057.5915
Frequencies -- 1069.3870 1104.5157 1110.7913
Frequencies -- 1112.8711 1126.3255 1157.0529
Frequencies -- 1160.6458 1176.6521 1184.7379
Frequencies -- 1204.7347 1212.5312 1249.4947
Frequencies -- 1282.5411 1302.7544 1315.8339
Frequencies -- 1327.2899 1339.9790 1361.7935
Frequencies -- 1362.9560 1377.8497 1436.3385
Frequencies -- 1458.3976 1459.7340 1490.5292
Frequencies -- 1493.0060 1507.6419 1513.3575
Frequencies -- 1543.9612 1559.4381 1651.6138
Frequencies -- 1674.9336 1685.3041 1698.1197
Frequencies -- 3087.0660 3108.2393 3170.3140
Frequencies -- 3184.9543 3202.3310 3218.0584
Frequencies -- 3222.9988 3225.0828 3231.5270
Frequencies -- 3234.6647 3239.4312 3243.1136
Frequencies -- 3246.7554 3542.8085 3800.5642

SCF Done: E(RM062X/DGDZVP) = -1619.92929868
Sum of electronic and zero-point Energies= -1619.646631
Sum of electronic and thermal Energies= -1619.624138
Sum of electronic and thermal Free Energies= -1619.703320
SCF Done: E(RM062X/DGTZVP/SMD) = -1620.21479048

(*S*)-3-(benzo[d]thiazol-2-ylthio)-2-phenylpropane-1,2-diol ((*S*)-Product)

Center Number	Atomic Number	Atomic Type	Coordinates (Angstroms) X	Y	Z
1	8	0	0.007381	0.028286	0.004492
2	6	0	0.009477	-0.051927	2.894252
3	6	0	1.228962	0.003596	0.711640
4	1	0	-0.981012	-0.194152	2.456241
5	6	0	1.079042	-0.761597	2.040469
6	1	0	1.524925	1.040752	0.884901
7	1	0	2.018910	-0.492624	0.133100
8	8	0	0.647797	-2.054078	1.647136
9	1	0	-0.264932	-0.900905	-0.076841
10	6	0	2.425725	-0.808287	2.745840
11	6	0	3.088937	-2.021542	2.929969
12	6	0	3.026058	0.370510	3.205687
13	6	0	4.326882	-2.057755	3.573729
14	1	0	2.625835	-2.931477	2.564016
15	6	0	4.262083	0.335269	3.846826
16	1	0	2.530429	1.329907	3.071217
17	6	0	4.917009	-0.882741	4.034717
18	1	0	4.830592	-3.009402	3.714400
19	1	0	4.712156	1.257484	4.201442
20	1	0	5.879246	-0.913706	4.536426
21	1	0	0.208181	1.022677	2.917505
22	16	0	-0.058813	-0.492491	4.667163
23	6	0	-1.069012	-1.917622	4.639415
24	16	0	-1.829312	-2.426180	6.138192
25	7	0	-1.309442	-2.655923	3.601693
26	6	0	-2.528344	-3.774347	5.279427
27	6	0	-2.145414	-3.719390	3.926971
28	6	0	-3.350859	-4.792721	5.763560
29	6	0	-2.594976	-4.698023	3.033159
30	6	0	-3.791218	-5.757490	4.864476
31	1	0	-3.641797	-4.831206	6.808248
32	6	0	-3.416121	-5.709450	3.511522
33	1	0	-2.295100	-4.650930	1.991108
34	1	0	-4.434373	-6.557920	5.215140
35	1	0	-3.773960	-6.475257	2.831243
36	1	0	-0.031946	-2.389801	2.270611

Frequencies -- 7.3793 26.6969 44.4741
Frequencies -- 58.4343 79.5700 104.0162
Frequencies -- 127.1108 142.1247 184.0885
Frequencies -- 190.7003 207.1183 242.6401
Frequencies -- 289.3714 297.5904 332.8236
Frequencies -- 349.3119 364.9423 380.4041
Frequencies -- 410.7551 414.0055 434.0302
Frequencies -- 457.2284 490.3359 512.6722
Frequencies -- 515.5604 531.2132 580.9667
Frequencies -- 595.8564 612.2785 624.9165
Frequencies -- 629.1138 659.2603 700.3386
Frequencies -- 714.8316 719.7310 724.1803
Frequencies -- 741.8447 775.7372 778.9930
Frequencies -- 808.3213 871.0917 875.8713
Frequencies -- 877.5223 887.4267 940.6716
Frequencies -- 954.1881 964.5050 999.9646
Frequencies -- 1000.3282 1007.2379 1016.1054
Frequencies -- 1026.8347 1038.2963 1056.8233
Frequencies -- 1070.9474 1107.0287 1110.7151
Frequencies -- 1120.8695 1131.5375 1158.7500
Frequencies -- 1169.6011 1177.0084 1184.7394
Frequencies -- 1207.4729 1212.5091 1253.1698
Frequencies -- 1282.9883 1306.8909 1318.1476
Frequencies -- 1325.8941 1342.7872 1363.7224
Frequencies -- 1364.7489 1384.1251 1439.8099
Frequencies -- 1458.8594 1462.8623 1489.1134
Frequencies -- 1492.2632 1510.1182 1513.2463
Frequencies -- 1546.8266 1560.0568 1652.0152
Frequencies -- 1675.2617 1686.7621 1699.6260
Frequencies -- 3079.9400 3114.3386 3171.2100
Frequencies -- 3189.4115 3202.3302 3215.9925
Frequencies -- 3224.8059 3228.5957 3236.5053
Frequencies -- 3238.1836 3246.0368 3250.2697
Frequencies -- 3250.4507 3546.0167 3790.1303

SCF Done: E(RM062X/DGDZVP) = -1619.92907204
Sum of electronic and zero-point Energies= -1619.646255
Sum of electronic and thermal Energies= -1619.623754
Sum of electronic and thermal Free Energies= -1619.703735
SCF Done: E(RM062X/DGTZVP/SMD) = -1620.21547081

3-Phenyloxetan-3-ol

Center Number	Atomic Number	Atomic Type	Coordinates (Angstroms) X	Y	Z
1	8	0	0.137658	-1.198681	-0.829289
2	6	0	0.643784	-2.316164	-0.076728
3	6	0	0.627681	-1.756377	-2.062601
4	1	0	1.565488	-2.057008	0.460875
5	1	0	-0.098332	-2.716187	0.618987
6	6	0	0.908929	-3.116080	-1.375785
7	8	0	2.191843	-3.665920	-1.540846

8	1	0	2.850772	-2.983051	-1.346468
9	1	0	1.542429	-1.250796	-2.399142
10	1	0	-0.127271	-1.737493	-2.853028
11	6	0	-0.121405	-4.180875	-1.668324
12	6	0	-1.482843	-3.869581	-1.560073
13	6	0	0.258507	-5.469243	-2.045596
14	6	0	-2.449224	-4.835522	-1.825640
15	1	0	-1.787414	-2.865784	-1.267276
16	6	0	-0.713272	-6.436024	-2.311607
17	1	0	1.312669	-5.708626	-2.128060
18	6	0	-2.066496	-6.124414	-2.202785
19	1	0	-3.501660	-4.583345	-1.738465
20	1	0	-0.408402	-7.436311	-2.604027
21	1	0	-2.819737	-6.878855	-2.407977

Frequencies -- 53.1801 117.8919 140.2864
Frequencies -- 232.9607 309.8066 324.8309
Frequencies -- 342.7273 410.6848 413.7259
Frequencies -- 416.4638 522.9715 559.2501
Frequencies -- 628.6483 700.1318 718.0760
Frequencies -- 777.9285 803.7395 875.2143
Frequencies -- 921.3744 948.5266 965.0766
Frequencies -- 1005.3082 1015.2464 1019.6501
Frequencies -- 1043.8363 1064.9114 1087.4103
Frequencies -- 1090.0886 1098.6886 1117.9587
Frequencies -- 1154.2205 1178.9953 1182.4369
Frequencies -- 1210.6908 1217.0152 1263.9193
Frequencies -- 1298.0914 1342.7895 1368.1090
Frequencies -- 1389.4218 1422.9881 1499.0289
Frequencies -- 1526.5169 1548.2840 1555.3147
Frequencies -- 1678.5990 1700.9109 3062.7541
Frequencies -- 3072.4638 3158.3777 3164.8192
Frequencies -- 3194.7523 3216.8129 3224.3511
Frequencies -- 3240.2954 3250.9207 3833.2432

SCF Done: E(RM062X/DGDZVP) = -499.212120525
Sum of electronic and zero-point Energies= -499.037424
Sum of electronic and thermal Energies= -499.026165
Sum of electronic and thermal Free Energies= -499.077392
SCF Done: E(RM062X/DGTZVP/SMD) = -499.335004990

Cat a

Center Number	Atomic Number	Atomic Type	Coordinates (Angstroms) X	Y	Z
1	15	0	-0.266770	-0.212339	0.299723
2	8	0	-0.205384	-0.083627	1.908538
3	8	0	1.276424	-0.130695	-0.147704
4	8	0	-0.715947	1.211554	-0.243746
5	8	0	-1.046064	-1.383866	-0.099364
6	6	0	0.408371	1.036608	2.461450
7	6	0	2.048358	-1.224112	0.254419
8	6	0	1.781666	1.039539	2.652848
9	6	0	-0.379547	2.143945	2.803408
10	6	0	2.656003	-1.197117	1.500289
11	6	0	2.154724	-2.333480	-0.591821
12	6	0	2.803792	-0.070968	2.503877
13	6	0	2.404543	2.210316	3.098257
14	6	0	0.264016	3.277777	3.311032
15	6	0	3.297667	-2.347818	1.968791
16	6	0	2.861625	-3.446473	-0.122211
17	6	0	2.964324	-0.888247	3.817322
18	6	0	4.087826	0.766411	2.240402
19	6	0	3.906690	2.030816	3.101398
20	6	0	1.653280	3.329658	3.436390
21	6	0	3.756340	-2.141370	3.395960
22	6	0	3.409108	-3.473666	1.161402
23	1	0	2.949880	-4.311450	-0.774069
24	1	0	3.448304	-0.310452	4.609948
25	1	0	1.969287	-1.184265	4.166655
26	1	0	5.000053	0.207662	2.467485
27	1	0	4.110430	1.044262	1.181183
28	1	0	4.278058	1.878871	4.121166
29	1	0	4.837201	-1.965376	3.436349
30	1	0	3.908136	-4.368863	1.522232
31	1	0	2.135750	4.237257	3.788477
32	1	0	3.542489	-3.007171	4.027472
33	1	0	4.426954	2.899800	2.690985
34	6	0	1.568892	-2.325261	-1.962687
35	6	0	0.499732	-3.183239	-2.282229
36	6	0	2.127497	-1.480784	-2.943562
37	6	0	-0.140522	-4.012716	-1.302599
38	6	0	-0.000854	-3.216869	-3.627595
39	6	0	1.606485	-1.509560	-4.280870
40	6	0	3.221080	-0.594021	-2.668839
41	6	0	-1.167584	-4.841591	-1.648575
42	1	0	0.178099	-3.946227	-0.267940
43	6	0	-1.078276	-4.103775	-3.951602
44	6	0	0.562093	-2.381645	-4.593498
45	6	0	2.177284	-0.649670	-5.274255
46	1	0	3.644290	-0.568423	-1.669522
47	6	0	3.740441	0.210341	-3.642664
48	6	0	-1.640130	-4.898302	-2.996058
49	1	0	-1.649653	-5.448556	-0.888573
50	1	0	-1.440775	-4.124260	-4.976115
51	1	0	0.177341	-2.408731	-5.611303
52	6	0	3.209825	0.187968	-4.968431
53	1	0	1.768477	-0.682180	-6.280972
54	1	0	4.568313	0.873368	-3.410579
55	1	0	-2.459440	-5.564124	-3.249660
56	1	0	3.635042	0.836462	-5.728189
57	1	0	-0.342276	4.137442	3.583871
58	6	0	-1.862566	2.106130	2.653239
59	6	0	-2.503882	2.948136	1.721817
60	6	0	-2.619716	1.234506	3.463430
61	6	0	-1.777315	3.821226	0.841521
62	6	0	-3.936431	2.918499	1.607814
63	6	0	-4.048712	1.202615	3.329981
64	6	0	-2.017704	0.373603	4.439748
65	6	0	-2.429868	4.617034	-0.056846
66	1	0	-0.692879	3.821610	0.877030
67	6	0	-4.582296	3.775605	0.658133
68	6	0	-4.673698	2.045931	2.410303
69	6	0	-4.810794	0.307321	4.148474
70	1	0	-0.941028	0.396928	4.573424
71	6	0	-2.777042	-0.464367	5.204238
72	6	0	-3.856464	4.603944	-0.146714
73	1	0	-1.858683	5.260016	-0.719360
74	1	0	-5.666611	3.745558	0.590347
75	1	0	-5.757436	2.021093	2.314612
76	6	0	-4.197058	-0.505090	5.055500
77	1	0	-5.890882	0.291069	4.029031
78	1	0	-2.299915	-1.108794	5.936058
79	1	0	-4.354743	5.246844	-0.865578
80	1	0	-4.782529	-1.181491	5.670278
81	1	0	-1.672627	1.274015	-0.408686

Frequencies -- 17.2797 18.6374 26.9829

Frequencies --	31.1196	34.6001	45.8512
Frequencies --	55.4137	79.1476	84.6839
Frequencies --	91.1969	98.0679	105.4735
Frequencies --	122.2634	128.6238	138.8232
Frequencies --	140.0306	151.4566	176.2440
Frequencies --	176.8859	184.8938	197.3522
Frequencies --	206.0175	225.0428	230.3841
Frequencies --	234.4971	235.4947	249.8301
Frequencies --	271.5364	290.9841	292.4331
Frequencies --	295.8339	315.1145	329.0085
Frequencies --	340.8255	357.0824	363.7999
Frequencies --	368.0488	377.2281	390.4262
Frequencies --	401.5205	402.2687	414.9394
Frequencies --	419.4050	423.0265	425.7213
Frequencies --	433.4373	473.8577	482.8759
Frequencies --	487.8742	494.4587	497.5971
Frequencies --	497.7551	516.5549	524.8932
Frequencies --	539.8712	547.2890	554.7937
Frequencies --	559.3417	560.7609	569.2127
Frequencies --	571.1492	605.9515	608.4595
Frequencies --	615.6467	620.8618	623.2840
Frequencies --	639.8284	648.7340	649.4679
Frequencies --	650.3158	657.7776	662.8051
Frequencies --	675.2406	688.7008	705.6030
Frequencies --	707.3900	732.9997	748.4554
Frequencies --	753.9718	754.7425	756.4660
Frequencies --	757.5740	771.0109	778.6942
Frequencies --	795.2747	797.1568	808.8854
Frequencies --	809.5219	824.5988	833.2283
Frequencies --	842.6399	845.6957	847.0200
Frequencies --	866.1721	869.6048	870.7232
Frequencies --	870.8389	877.1128	880.1008
Frequencies --	881.0554	887.4461	902.8653
Frequencies --	921.5627	921.9452	939.3238
Frequencies --	939.8103	943.0637	947.6921
Frequencies --	955.4509	971.6029	972.7482
Frequencies --	982.8719	984.6692	989.8165
Frequencies --	991.0666	993.6883	994.4009
Frequencies --	1000.4959	1000.7867	1004.6221
Frequencies --	1005.7542	1014.4957	1020.8784
Frequencies --	1035.3713	1045.0489	1045.5161
Frequencies --	1047.3483	1047.5504	1049.1324
Frequencies --	1061.2444	1081.0801	1092.4476
Frequencies --	1103.2493	1139.1704	1140.3618
Frequencies --	1159.1298	1159.4924	1164.6924
Frequencies --	1168.6164	1178.3829	1186.4150
Frequencies --	1193.0399	1198.0830	1203.2723
Frequencies --	1206.5601	1207.1698	1207.5317
Frequencies --	1210.6692	1220.1341	1251.2436
Frequencies --	1252.9871	1253.4608	1257.2441
Frequencies --	1259.2153	1268.0727	1279.3609
Frequencies --	1295.3888	1296.3742	1304.4706
Frequencies --	1316.4070	1321.4690	1321.9581
Frequencies --	1324.9162	1344.1507	1347.9004
Frequencies --	1348.6212	1351.8509	1357.4634
Frequencies --	1362.3925	1371.2531	1409.6532
Frequencies --	1412.7543	1413.2735	1415.3051
Frequencies --	1442.7563	1443.1252	1482.6660
Frequencies --	1483.4934	1486.4844	1489.2073
Frequencies --	1489.9074	1493.0566	1498.2440
Frequencies --	1499.7011	1500.4743	1504.7434
Frequencies --	1512.5303	1518.0510	1529.4453
Frequencies --	1531.2780	1550.0117	1555.0333
Frequencies --	1602.1029	1604.2682	1648.9586
Frequencies --	1650.2780	1657.2535	1659.1745
Frequencies --	1661.9151	1665.4060	1706.2256
Frequencies --	1711.6739	1713.0722	1714.4358
Frequencies --	1718.0701	1719.6582	3076.1116
Frequencies --	3077.4972	3084.0342	3091.6913
Frequencies --	3140.5574	3145.1610	3155.9108
Frequencies --	3160.2232	3193.5982	3200.0272
Frequencies --	3204.2979	3205.6318	3206.8308
Frequencies --	3209.7512	3209.8432	3210.7514
Frequencies --	3214.7164	3218.3407	3219.5089
Frequencies --	3223.0951	3223.5955	3227.3226
Frequencies --	3230.5413	3232.3320	3233.0831
Frequencies --	3234.4238	3236.1983	3241.8853
Frequencies --	3243.0049	3247.4516	3803.0299

SCF Done: E(RM062X/DGDZVP) = -2375.13878930
Sum of electronic and zero-point Energies= -2374.494913
Sum of electronic and thermal Energies= -2374.448765
Sum of electronic and thermal Free Energies= -2374.576069
SCF Done: E(RM062X/DGTZVP/SMD) = -2375.67807820

Cat a I0_1

Center Number	Atomic Number	Atomic Type	Coordinates (Angstroms) X	Y	Z
1	15	0	-0.167938	-0.020550	0.097086
2	8	0	-0.080758	0.012287	1.698012
3	8	0	1.373657	-0.036155	-0.385163
4	6	0	0.586379	1.087547	2.284045
5	8	0	-0.964151	-1.178396	-0.351347
6	8	0	-0.610085	1.404779	-0.347686
7	6	0	2.100202	-1.172870	-0.038591
8	6	0	1.961823	1.025555	2.442435
9	6	0	-0.154142	2.210507	2.675248
10	6	0	2.731330	-1.208124	1.195791
11	6	0	2.144671	-2.258249	-0.921822
12	6	0	2.936568	-0.119527	2.233900
13	6	0	2.638180	2.155809	2.914081
14	6	0	0.544389	3.301028	3.203114
15	6	0	-1.640558	2.215366	2.551185
16	6	0	3.339412	-2.394970	1.614818
17	6	0	2.822862	-3.409312	-0.501455
18	6	0	1.517501	-2.198838	-2.273957
19	6	0	4.247528	0.677978	1.975483
20	6	0	3.089529	-0.987095	3.515864
21	6	0	4.131588	1.916490	2.884098
22	6	0	1.937671	3.292295	3.300819
23	1	0	-0.020961	4.175411	3.514226
24	6	0	-2.278250	3.066589	1.628310
25	6	0	-2.399010	1.343043	3.359034
26	6	0	3.829785	-2.251947	3.039141
27	6	0	3.396471	-3.496193	0.767894
28	1	0	2.868236	-4.257117	-1.179723
29	6	0	0.470987	-3.083117	-2.605168
30	6	0	2.012174	-1.289833	-3.235476
31	1	0	5.141991	0.077910	2.165470
32	1	0	4.261947	0.992678	0.926433
33	1	0	3.605832	-0.453002	4.318553
34	1	0	2.090435	-1.259948	3.872530
35	1	0	4.681272	2.778177	2.497253
36	1	0	4.511973	1.710929	3.891181
37	1	0	2.463416	4.168582	3.670044
38	6	0	-1.549557	3.945482	0.758041
39	6	0	-3.709279	3.036193	1.509464
40	6	0	-1.798647	0.472349	4.327906
41	6	0	-3.827974	1.316679	3.227610

42	1	0	3.597341	-3.130595	3.645755
43	1	0	4.916631	-2.114341	3.064684
44	1	0	3.872602	-4.418812	1.088230
45	6	0	-0.125860	-3.967030	-1.644058
46	6	0	-0.053063	-3.094547	-3.943364
47	6	0	3.075687	-0.369243	-2.955503
48	6	0	1.442115	-1.273209	-4.553906
49	6	0	-2.197115	4.741799	-0.141853
50	1	0	-0.465431	3.944163	0.798426
51	6	0	-4.449578	2.161977	2.307082
52	6	0	-4.352034	3.889640	0.554014
53	6	0	-2.559351	-0.366809	5.090229
54	1	0	-0.721335	0.490693	4.459595
55	6	0	-4.591643	0.420687	4.043813
56	6	0	-1.110989	-4.838448	-2.011135
57	1	0	0.193123	-3.912401	-0.608435
58	6	0	0.434214	-2.183594	-4.881701
59	6	0	-1.072439	-4.038357	-4.292195
60	6	0	3.508464	0.519255	-3.897975
61	1	0	3.544069	-0.382915	-1.976701
62	6	0	1.920534	-0.323900	-5.513906
63	6	0	-3.622955	4.719972	-0.245436
64	1	0	-1.624164	5.388151	-0.799556
65	1	0	-5.533082	2.136717	2.207168
66	1	0	-5.435896	3.855665	0.478584
67	6	0	-3.979899	-0.399579	4.945497
68	1	0	-2.083118	-1.016911	5.817723
69	1	0	-5.672215	0.410104	3.927196
70	6	0	-1.576060	-4.895837	-3.360772
71	1	0	-1.559297	-5.487848	-1.265491
72	1	0	0.016012	-2.179463	-5.886871
73	1	0	-1.441962	-4.043029	-5.314625
74	6	0	2.917936	0.551935	-5.197580
75	1	0	4.312448	1.208942	-3.660205
76	1	0	1.470078	-0.319640	-6.503385
77	1	0	-4.118150	5.360064	-0.969147
78	1	0	-4.567293	-1.075776	5.558749
79	1	0	-2.352570	-5.605672	-3.630021
80	1	0	3.273443	1.268655	-5.931341
81	8	0	-1.982811	1.159521	-2.472679
82	6	0	-3.195119	0.414358	-2.157598
83	6	0	-1.446066	0.048153	-3.253850
84	6	0	-2.756273	-0.765895	-3.064704
85	1	0	-3.228294	0.148086	-1.096271
86	1	0	-4.081950	0.977835	-2.454009
87	1	0	-1.200981	0.374039	-4.266963
88	1	0	-0.572789	-0.402086	-2.770315
89	6	0	-3.560131	-0.932780	-4.333190
90	8	0	-2.643124	-1.999307	-2.428487
91	6	0	-3.820404	0.174158	-5.149493
92	6	0	-4.036932	-2.188493	-4.711413
93	1	0	-2.058467	-1.898227	-1.648796
94	6	0	-4.543900	0.027442	-6.330163
95	1	0	-3.454061	1.159281	-4.862543
96	6	0	-4.760134	-2.334815	-5.896612
97	1	0	-3.831868	-3.038203	-4.068604
98	6	0	-5.014706	-1.231400	-6.709043
99	1	0	-4.741024	0.893372	-6.954936
100	1	0	-5.127892	-3.315455	-6.184461
101	1	0	-5.577457	-1.347909	-7.630257
102	1	0	-1.161411	1.430208	-1.215094

Frequencies --	9.5389	18.9454	21.2552
Frequencies --	29.6134	34.5037	35.5763
Frequencies --	39.7977	52.1634	58.2085
Frequencies --	61.4754	70.9651	76.5223
Frequencies --	81.4427	85.1005	93.8216
Frequencies --	100.1702	104.5680	110.2234
Frequencies --	120.2570	127.3986	135.8356
Frequencies --	141.8057	148.3270	153.7387
Frequencies --	172.6106	180.4064	181.2176
Frequencies --	190.5951	198.2905	221.6034
Frequencies --	229.3779	232.1071	236.6821
Frequencies --	241.8748	252.5578	274.8007
Frequencies --	289.2293	291.7385	294.4843
Frequencies --	296.1676	318.3300	331.4455
Frequencies --	336.7802	338.7773	359.8981
Frequencies --	363.7300	367.5401	376.2329
Frequencies --	381.9502	389.5873	402.2467
Frequencies --	402.6394	414.9935	417.1529
Frequencies --	421.5063	423.6669	424.2948
Frequencies --	431.2422	437.2453	441.9471
Frequencies --	474.5468	484.7386	485.1725
Frequencies --	495.9337	497.4306	502.0881
Frequencies --	517.2713	526.4251	529.2856
Frequencies --	539.7820	547.4317	554.5175
Frequencies --	559.1704	560.8963	563.9671
Frequencies --	568.2392	570.1834	593.6620
Frequencies --	605.4558	607.9697	615.2002
Frequencies --	620.9389	623.1878	627.8079
Frequencies --	639.3576	648.4667	648.8709
Frequencies --	650.1274	657.5237	662.7647
Frequencies --	675.2206	688.5203	703.8424
Frequencies --	706.8561	707.0925	719.4828
Frequencies --	733.3411	749.1575	751.9993
Frequencies --	753.4905	754.3007	756.5143
Frequencies --	772.4252	775.0033	775.4142
Frequencies --	795.3903	796.3364	807.7172
Frequencies --	808.4147	819.6267	824.8808
Frequencies --	834.6350	841.3451	844.4166
Frequencies --	853.4819	865.7377	868.1303
Frequencies --	869.8578	872.3462	874.1104
Frequencies --	875.7196	879.3476	880.8969
Frequencies --	888.9133	909.7676	915.3319
Frequencies --	916.5358	920.0635	938.9004
Frequencies --	939.5823	942.7430	944.0511
Frequencies --	951.7471	952.9773	971.9648
Frequencies --	975.7025	977.4554	985.2695
Frequencies --	987.5664	987.6971	988.7604
Frequencies --	991.2567	993.8155	1000.4172
Frequencies --	1000.7511	1003.4033	1003.9397
Frequencies --	1003.9614	1007.0316	1009.8133
Frequencies --	1014.3147	1019.6283	1020.1366
Frequencies --	1037.1540	1042.6964	1045.9372
Frequencies --	1047.0557	1047.5151	1048.3831
Frequencies --	1060.6314	1063.0866	1067.4524
Frequencies --	1080.6115	1083.1498	1088.5012
Frequencies --	1093.5377	1103.7436	1113.1222
Frequencies --	1139.0993	1139.7367	1158.7979
Frequencies --	1159.0603	1165.5220	1170.0105
Frequencies --	1173.0025	1177.7132	1181.6085
Frequencies --	1185.5017	1192.4194	1198.7963
Frequencies --	1204.1521	1204.3418	1206.3371
Frequencies --	1207.3051	1208.3575	1208.4363
Frequencies --	1211.0745	1220.2705	1240.4438
Frequencies --	1251.1225	1253.0014	1254.0293
Frequencies --	1257.9041	1260.0264	1268.6192
Frequencies --	1279.2232	1284.8242	1295.1203
Frequencies --	1296.1337	1299.3776	1305.1617
Frequencies --	1314.4940	1316.7907	1320.7975
Frequencies --	1321.1714	1325.6535	1335.7305

Frequencies -- 1344.6744 1344.8648 1347.9544
Frequencies -- 1348.4927 1351.0762 1362.4273
Frequencies -- 1365.9352 1370.4499 1391.2632
Frequencies -- 1408.8217 1412.4243 1412.5822
Frequencies -- 1413.9985 1440.1692 1443.9033
Frequencies -- 1471.9635 1482.7263 1483.6486
Frequencies -- 1485.6328 1488.8134 1489.9031
Frequencies -- 1492.6766 1498.3690 1498.7160
Frequencies -- 1500.3676 1500.6415 1504.4685
Frequencies -- 1510.8894 1511.6042 1517.6507
Frequencies -- 1529.7025 1531.1945 1532.4228
Frequencies -- 1549.6504 1551.2513 1554.0514
Frequencies -- 1601.5401 1603.2427 1646.2605
Frequencies -- 1649.8555 1654.7495 1658.1547
Frequencies -- 1660.9614 1664.9519 1676.3810
Frequencies -- 1700.7930 1705.7929 1711.7151
Frequencies -- 1712.8807 1714.6821 1718.1492
Frequencies -- 1718.2602 2687.7483 3077.7720
Frequencies -- 3079.6166 3085.4366 3091.4218
Frequencies -- 3109.7294 3116.8666 3141.8112
Frequencies -- 3148.0339 3158.0454 3161.2295
Frequencies -- 3183.1854 3189.7243 3192.6622
Frequencies -- 3194.8214 3197.7361 3201.5269
Frequencies -- 3202.8802 3207.5707 3208.3729
Frequencies -- 3208.5408 3209.6629 3209.8256
Frequencies -- 3216.4462 3217.7717 3217.9127
Frequencies -- 3221.8387 3222.0628 3224.1469
Frequencies -- 3228.4532 3230.7213 3231.3116
Frequencies -- 3232.1358 3233.7670 3234.5883
Frequencies -- 3240.9200 3241.9417 3242.8146
Frequencies -- 3245.3835 3250.3741 3649.4400

SCF Done: E(RM062X/DGDZVP) = -2874.40395778
Sum of electronic and zero-point Energies= -2873.583004
Sum of electronic and thermal Energies= -2873.524884
Sum of electronic and thermal Free Energies= -2873.678420
SCF Done: E(RM062X/DGTZVP/SMD) = -2875.05444715

Cat a I0_2

Center Number	Atomic Number	Atomic Type	Coordinates (Angstroms) X	Y	Z
1	15	0	-0.250624	-0.048558	0.273059
2	8	0	-0.046887	-0.002601	1.862649
3	8	0	1.245970	0.064787	-0.324646
4	8	0	-0.845221	1.331828	-0.131597
5	8	0	-0.976358	-1.272712	-0.114785
6	6	0	0.574862	1.120140	2.407590
7	6	0	2.091634	-1.006401	-0.046045
8	6	0	1.959058	1.158257	2.475925
9	6	0	-0.217854	2.188666	2.846442
10	6	0	2.812442	-0.996766	1.139914
11	6	0	2.163064	-2.078571	-0.943627
12	6	0	3.001368	0.094252	2.179945
13	6	0	2.580844	2.331000	2.918121
14	6	0	0.433544	3.319884	3.349341
15	6	0	3.551188	-2.129585	1.495355
16	6	0	2.973495	-3.166066	-0.593171
17	6	0	3.312364	-0.771907	3.433280
18	6	0	4.224824	0.993957	1.842474
19	6	0	4.082130	2.207696	2.779870
20	6	0	1.826742	3.408558	3.367406
21	1	0	-0.172112	4.152179	3.697913
22	6	0	4.124011	-1.962220	2.885965
23	6	0	3.646522	-3.212008	0.628008
24	1	0	3.038596	-4.002533	-1.283719
25	1	0	3.833819	-0.206172	4.210574
26	1	0	2.366028	-1.133970	3.849106
27	1	0	5.173829	0.462292	1.954392
28	1	0	4.136980	1.322898	0.801386
29	1	0	4.548571	2.020110	3.753518
30	1	0	5.194371	-1.731286	2.841799
31	1	0	-1.456287	1.315401	-0.959328
32	8	0	-2.334424	0.991548	-2.159568
33	6	0	-1.758644	-0.077588	-2.970855
34	6	0	-2.984208	-0.993919	-2.703047
35	1	0	-1.600962	0.261520	-3.996892
36	1	0	-0.824043	-0.450184	-2.540271
37	8	0	-2.733750	-2.207089	-2.066496
38	6	0	-3.468128	0.157221	-1.780537
39	6	0	-3.844458	-1.239672	-3.920803
40	1	0	-2.101911	-2.055991	-1.332385
41	1	0	-3.431571	-0.099748	-0.716961
42	1	0	-4.408870	0.647578	-2.038902
43	6	0	-4.273359	-2.528414	-4.240768
44	6	0	-4.212330	-0.170257	-4.746316
45	6	0	-5.053486	-2.744592	-5.378175
46	1	0	-3.990755	-3.350032	-3.591251
47	6	0	-4.991423	-0.386937	-5.879740
48	1	0	-3.888401	0.841076	-4.502836
49	6	0	-5.412573	-1.678788	-6.201460
50	1	0	-5.383566	-3.750757	-5.619832
51	1	0	-5.269731	0.450752	-6.512026
52	1	0	-6.018604	-1.850599	-7.085846
53	1	0	4.534884	3.114021	2.370432
54	1	0	2.310222	4.316632	3.717044
55	1	0	4.009732	-2.865668	3.490082
56	1	0	4.225696	-4.090626	0.898143
57	6	0	-1.705726	2.117742	2.768713
58	6	0	-2.402578	1.194006	3.573033
59	6	0	-2.405418	2.957735	1.879450
60	6	0	-1.737762	0.328684	4.503729
61	6	0	-3.832055	1.105106	3.476155
62	6	0	-3.835654	2.864801	1.795186
63	6	0	-1.740219	3.879699	1.003468
64	6	0	-2.439641	-0.562190	5.264009
65	1	0	-0.658823	0.392152	4.606126
66	6	0	-4.532699	0.156046	4.288362
67	6	0	-4.515020	1.941625	2.591841
68	6	0	-4.541288	3.705297	0.873143
69	1	0	-0.656480	3.924486	1.011530
70	6	0	-2.445650	4.660806	0.134071
71	6	0	-3.861048	-0.656283	5.154088
72	1	0	-1.915238	-1.207649	5.961905
73	1	0	-5.614325	0.098089	4.198064
74	1	0	-5.598602	1.869376	2.518658
75	6	0	-3.871337	4.579875	0.068963
76	1	0	-5.624278	3.624495	0.825841
77	1	0	-1.919177	5.339918	-0.529508
78	1	0	-4.400721	-1.374200	5.763806
79	1	0	-4.414036	5.208931	-0.629889
80	6	0	1.408933	-2.090469	-2.231276
81	6	0	0.417672	-3.070531	-2.445666
82	6	0	1.719815	-1.160752	-3.246665
83	6	0	-0.010950	-3.971368	-1.413697
84	6	0	-0.226382	-3.163668	-3.726684
85	6	0	1.025063	-1.225678	-4.502626
86	6	0	2.707265	-0.134162	-3.080267
87	6	0	-0.944407	-4.934691	-1.667860
88	1	0	0.391278	-3.854366	-0.412988

89	6	0	-1.182967	-4.204311	-3.960034
90	6	0	0.082597	-2.234768	-4.720353
91	6	0	1.307601	-0.250606	-5.512053
92	1	0	3.269331	-0.084191	-2.153198
93	6	0	2.950737	0.778497	-4.067033
94	6	0	-1.520780	-5.074937	-2.967832
95	1	0	-1.266690	-5.594675	-0.868341
96	1	0	-1.641031	-4.272901	-4.943635
97	1	0	-0.429006	-2.291920	-5.679688
98	6	0	2.234315	0.728897	-5.301478
99	1	0	0.762887	-0.308147	-6.451099
100	1	0	3.697724	1.551359	-3.914813
101	1	0	-2.251148	-5.857928	-3.148189
102	1	0	2.436638	1.467600	-6.070811

Frequencies --	15.2964	20.4916	25.5952
Frequencies --	31.2979	36.1362	40.5977
Frequencies --	43.4503	53.5314	59.8824
Frequencies --	63.0021	77.5221	81.6741
Frequencies --	87.2661	90.0945	97.4116
Frequencies --	100.6777	106.7585	109.1354
Frequencies --	123.6902	129.9232	140.2707
Frequencies --	143.0274	149.1809	155.3125
Frequencies --	171.7583	179.9138	184.1336
Frequencies --	191.6083	199.7200	225.7101
Frequencies --	230.7831	234.0027	239.5721
Frequencies --	244.2438	256.7259	275.1834
Frequencies --	287.0984	292.4542	294.4029
Frequencies --	297.4924	318.7974	331.8800
Frequencies --	336.3952	338.8227	361.1432
Frequencies --	366.1028	368.0646	376.7084
Frequencies --	384.4082	390.9592	402.7446
Frequencies --	403.0708	416.7906	419.5525
Frequencies --	422.8254	424.9041	425.8031
Frequencies --	432.9640	438.2402	442.6153
Frequencies --	476.2355	486.8542	488.5785
Frequencies --	497.4518	497.8164	503.7318
Frequencies --	517.5524	522.9141	529.2770
Frequencies --	539.6893	548.9251	556.3322
Frequencies --	560.2396	561.8442	564.7629
Frequencies --	568.9650	570.3269	605.7156
Frequencies --	608.1911	615.2870	621.1966
Frequencies --	624.1869	630.0048	639.7954
Frequencies --	649.3582	650.6696	650.9453
Frequencies --	658.7821	663.6966	675.6432
Frequencies --	688.8950	704.4134	706.6762
Frequencies --	707.4138	709.5794	723.3327
Frequencies --	733.3395	751.0587	753.4458
Frequencies --	754.6629	754.7702	757.1993
Frequencies --	773.9899	776.3050	777.8670
Frequencies --	794.6829	796.1422	807.6902
Frequencies --	809.5105	819.9379	825.7232
Frequencies --	836.6827	843.4688	846.6454
Frequencies --	854.6448	867.6034	867.7468
Frequencies --	872.7077	873.6517	875.6529
Frequencies --	881.0611	881.3192	885.4636
Frequencies --	889.4618	911.2060	915.1502
Frequencies --	917.4603	919.7669	940.4940
Frequencies --	941.0407	942.8776	947.4187
Frequencies --	952.9775	955.8399	972.4383
Frequencies --	974.8989	980.5476	985.2079
Frequencies --	986.5556	990.9603	992.8520
Frequencies --	994.4467	994.9010	1001.7251
Frequencies --	1002.6486	1004.5309	1007.5628
Frequencies --	1009.6847	1010.3933	1013.2028
Frequencies --	1019.2844	1019.7945	1022.7574
Frequencies --	1037.2922	1044.8872	1046.4610
Frequencies --	1047.7159	1050.5242	1050.9160
Frequencies --	1060.8764	1063.9229	1071.3167
Frequencies --	1080.6779	1084.6679	1089.7662
Frequencies --	1093.4623	1103.9351	1116.4516
Frequencies --	1138.0548	1143.2314	1160.8785
Frequencies --	1164.0108	1166.7115	1172.7782
Frequencies --	1174.9263	1175.8182	1178.7306
Frequencies --	1187.6091	1193.2668	1199.2483
Frequencies --	1202.3067	1202.6178	1206.6107
Frequencies --	1207.2083	1210.8134	1214.0622
Frequencies --	1214.6847	1220.9282	1239.8541
Frequencies --	1251.5560	1254.3277	1255.8884
Frequencies --	1259.3113	1260.5403	1269.7218
Frequencies --	1279.7527	1285.0497	1297.4802
Frequencies --	1299.4251	1301.0446	1305.4922
Frequencies --	1313.4548	1316.6794	1321.4120
Frequencies --	1324.9962	1326.9590	1338.7936
Frequencies --	1345.9114	1346.2126	1349.4834
Frequencies --	1351.8946	1354.3222	1361.6800
Frequencies --	1367.6821	1370.3094	1389.6139
Frequencies --	1408.5975	1410.9857	1413.7558
Frequencies --	1418.4360	1444.0625	1444.8785
Frequencies --	1463.5771	1484.5273	1485.4335
Frequencies --	1487.1152	1490.1317	1491.9576
Frequencies --	1494.3253	1497.7805	1498.1502
Frequencies --	1500.6006	1502.2865	1507.3061
Frequencies --	1511.0354	1511.4172	1519.0978
Frequencies --	1529.3446	1530.9573	1534.2249
Frequencies --	1549.8474	1554.0763	1555.1601
Frequencies --	1603.4648	1604.6358	1648.1402
Frequencies --	1650.8824	1657.2248	1659.8511
Frequencies --	1662.6430	1665.6474	1676.6225
Frequencies --	1701.9965	1706.5972	1711.8048
Frequencies --	1715.0207	1715.7857	1718.9536
Frequencies --	1720.6685	2678.4506	3079.3725
Frequencies --	3081.8296	3084.4409	3091.9911
Frequencies --	3102.2676	3117.4605	3141.1073
Frequencies --	3142.9388	3154.6252	3160.5531
Frequencies --	3186.6064	3187.5528	3193.6743
Frequencies --	3195.1369	3202.9146	3205.9538
Frequencies --	3207.6973	3208.1340	3208.2010
Frequencies --	3209.3406	3211.3992	3214.4655
Frequencies --	3218.2737	3218.4871	3218.9327
Frequencies --	3223.5851	3224.6399	3225.3565
Frequencies --	3230.8543	3231.1489	3232.5647
Frequencies --	3234.0879	3236.1989	3236.8766
Frequencies --	3239.5189	3242.0796	3247.0661
Frequencies --	3249.5843	3249.9395	3642.5239

SCF Done: E(RM062X/DGDZVP) = -2874.40451469
Sum of electronic and zero-point Energies= -2873.582442
Sum of electronic and thermal Energies= -2873.524644
Sum of electronic and thermal Free Energies= -2873.676204
SCF Done: E(RM062X/DGTZVP/SMD) = -2875.05432386

Cat a TS1a_*R*

Center Number	Atomic Number	Atomic Type	Coordinates (Angstroms) X	Y	Z
1	15	0	0.028777	-0.002382	0.012552
2	8	0	0.008829	0.000246	1.633286
3	8	0	1.634993	0.015650	-0.306234

4	8	0	-0.442304	1.313309	-0.544620
5	8	0	-0.613887	-1.275633	-0.432269
6	6	0	0.738349	0.992150	2.272316
7	6	0	2.284602	-1.182081	-0.045958
8	6	0	2.061677	0.729596	2.615320
9	6	0	0.150074	2.240113	2.532796
10	6	0	2.732075	-1.446389	1.235718
11	6	0	2.401440	-2.121049	-1.077989
12	6	0	2.900594	-0.525432	2.427464
13	6	0	2.822695	1.738024	3.215842
14	6	0	0.925541	3.206726	3.186708
15	6	0	3.177072	-2.733402	1.549030
16	6	0	2.929079	-3.375922	-0.759733
17	6	0	2.775921	-1.551171	3.586678
18	6	0	4.330092	0.095901	2.419670
19	6	0	4.249483	1.275954	3.401665
20	6	0	2.257752	2.971130	3.522668
21	1	0	0.472531	4.171987	3.396729
22	6	0	3.443707	-2.832436	3.037491
23	6	0	3.282170	-3.700954	0.554992
24	1	0	3.030598	-4.115482	-1.549577
25	1	0	3.228748	-1.188658	4.514222
26	1	0	1.713696	-1.739992	3.772929
27	1	0	5.101419	-0.636953	2.672935
28	1	0	4.539082	0.474360	1.411907
29	1	0	4.416374	0.948023	4.434310
30	1	0	4.520000	-2.843241	3.242893
31	1	0	-1.554593	-1.299235	-1.711715
32	8	0	-2.193882	-1.005093	-2.444793
33	6	0	-3.122243	-0.049346	-1.871251
34	6	0	-2.736943	1.160192	-2.740428
35	1	0	-4.144505	-0.409855	-1.989301
36	1	0	-2.892377	0.122315	-0.815917
37	8	0	-2.506777	2.328792	-2.022894
38	6	0	-1.477667	0.454079	-3.327662
39	6	0	-3.727607	1.447465	-3.852147
40	1	0	-1.899093	2.122561	-1.280655
41	1	0	-0.523624	0.440929	-2.811392
42	1	0	-1.504172	-0.001179	-4.310435
43	6	0	-4.144840	2.751739	-4.113356
44	6	0	-4.206555	0.395478	-4.640771
45	6	0	-5.036666	3.000459	-5.157792
46	1	0	-3.756264	3.558343	-3.500244
47	6	0	-5.094461	0.646669	-5.684051
48	1	0	-3.881951	-0.626345	-4.441667
49	6	0	-5.512454	1.952784	-5.944527
50	1	0	-5.355862	4.018395	-5.360354
51	1	0	-5.460083	-0.175138	-6.292159
52	1	0	-6.204334	2.150804	-6.757440
53	1	0	4.312294	3.662280	0.647327
54	6	0	3.831711	3.831927	-0.311625
55	6	0	2.717821	3.072330	-0.651539
56	6	0	4.341922	4.805819	-1.184218
57	6	0	2.117545	3.320774	-1.888018
58	1	0	2.327594	2.298177	0.006214
59	6	0	3.740253	5.046638	-2.417142
60	7	0	1.008525	2.665715	-2.411746
61	6	0	2.616680	4.294048	-2.759520
62	1	0	4.133603	5.799823	-3.092264
63	6	0	0.611894	3.053606	-3.633831
64	1	0	0.437149	2.051150	-1.793318
65	16	0	1.643165	4.350837	-4.214932
66	16	0	-0.651262	2.452952	-4.559847
67	1	0	5.215345	5.382171	-0.897412
68	1	0	4.978533	2.062027	3.187443
69	1	0	3.631046	-4.702748	0.790127

70	1	0	3.021699	-3.742964	3.469912
71	1	0	2.847643	3.750838	3.996915
72	6	0	1.971644	-1.729356	-2.450671
73	6	0	2.625602	-0.651223	-3.088694
74	6	0	0.890890	-2.375876	-3.083238
75	6	0	3.734158	0.040147	-2.494993
76	6	0	2.172098	-0.205811	-4.375007
77	6	0	0.484429	-1.959241	-4.397674
78	6	0	0.132764	-3.413200	-2.441921
79	6	0	4.313364	1.111897	-3.112362
80	1	0	4.119481	-0.296913	-1.538110
81	6	0	2.794707	0.929974	-4.986463
82	6	0	1.124127	-0.878865	-5.007699
83	6	0	-0.613192	-2.624673	-5.036775
84	1	0	0.376905	-3.685945	-1.421000
85	6	0	-0.915768	-4.012965	-3.078319
86	6	0	3.830306	1.574636	-4.374254
87	1	0	5.141819	1.628669	-2.635884
88	1	0	2.415559	1.272479	-5.946324
89	1	0	0.787382	-0.537359	-5.985088
90	6	0	-1.290358	-3.623743	-4.401769
91	1	0	-0.898889	-2.306831	-6.036855
92	1	0	-1.486028	-4.782259	-2.567104
93	1	0	4.294964	2.437090	-4.843587
94	1	0	-2.125085	-4.116975	-4.890154
95	6	0	-1.232654	2.571086	2.081836
96	6	0	-1.418275	3.580067	1.110582
97	6	0	-2.339012	1.868469	2.593959
98	6	0	-0.322670	4.251561	0.472070
99	6	0	-2.743297	3.899302	0.662364
100	6	0	-3.660024	2.183316	2.123758
101	6	0	-2.206349	0.834976	3.580870
102	6	0	-0.530440	5.170104	-0.517687
103	1	0	0.692632	4.002579	0.759681
104	6	0	-2.923916	4.892468	-0.354835
105	6	0	-3.832705	3.193765	1.177195
106	6	0	-4.779163	1.446993	2.633413
107	1	0	-1.219649	0.594685	3.963629
108	6	0	-3.296521	0.157197	4.044155
109	6	0	-1.854320	5.509642	-0.933090
110	1	0	0.323619	5.641083	-0.999907
111	1	0	-3.936490	5.112805	-0.682570
112	1	0	-4.833525	3.422977	0.816456
113	6	0	-4.606700	0.461701	3.560290
114	1	0	-5.770704	1.693741	2.262504
115	1	0	-3.170984	-0.622816	4.788653
116	1	0	-2.000323	6.240934	-1.721897
117	1	0	-5.460850	-0.091676	3.938360

Frequencies --	-545.3428	13.0686	19.3787
Frequencies --	22.3433	30.7183	31.5672
Frequencies --	37.1673	40.6320	43.2414
Frequencies --	49.4121	53.2587	57.3500
Frequencies --	62.4213	67.5637	77.4505
Frequencies --	85.3774	88.7007	92.1538
Frequencies --	93.5688	99.3714	105.2506
Frequencies --	108.2065	114.7835	124.3812
Frequencies --	132.0524	139.0702	143.0026
Frequencies --	149.4075	154.0602	163.0739
Frequencies --	173.0974	183.0577	184.6848
Frequencies --	190.4021	196.7584	202.3947
Frequencies --	205.8072	215.4573	225.3004
Frequencies --	232.1643	236.4757	242.4943
Frequencies --	248.0895	252.6617	274.8286
Frequencies --	279.9255	287.0010	294.4315

Frequencies -- 299.0326 303.1460 307.0105
Frequencies -- 321.6500 333.0835 345.1780
Frequencies -- 354.0148 364.6750 376.6255
Frequencies -- 377.6432 389.4284 393.0495
Frequencies -- 396.7759 400.8930 403.8120
Frequencies -- 404.4392 413.3813 417.7550
Frequencies -- 419.0297 423.8157 428.3316
Frequencies -- 435.6665 439.3429 441.0052
Frequencies -- 449.7799 455.3183 482.7301
Frequencies -- 485.2823 489.6858 497.9085
Frequencies -- 499.2553 508.3466 509.2716
Frequencies -- 523.5575 529.4015 530.5267
Frequencies -- 530.9840 540.4115 550.7007
Frequencies -- 556.9598 562.4034 566.7613
Frequencies -- 567.6344 573.5979 580.4616
Frequencies -- 583.2074 604.4310 608.3179
Frequencies -- 615.9578 617.8662 621.6110
Frequencies -- 624.9017 630.1379 644.5607
Frequencies -- 648.9939 651.2365 652.2610
Frequencies -- 658.4692 660.1275 662.5609
Frequencies -- 676.4937 677.3892 690.2776
Frequencies -- 702.4137 709.5928 710.3515
Frequencies -- 719.4178 726.1771 732.9877
Frequencies -- 734.8042 746.6765 748.1032
Frequencies -- 753.5368 755.0932 755.4532
Frequencies -- 756.1865 768.7037 776.8972
Frequencies -- 777.9541 779.0570 795.6426
Frequencies -- 799.8287 809.0886 812.0090
Frequencies -- 825.3245 837.6450 841.8442
Frequencies -- 844.9400 847.9493 855.5326
Frequencies -- 863.5191 867.1516 869.0197
Frequencies -- 872.1844 873.5473 877.7945
Frequencies -- 880.1503 880.7080 882.2957
Frequencies -- 884.2520 888.9004 889.8441
Frequencies -- 900.9755 916.1362 920.6941
Frequencies -- 935.6982 939.8078 940.2265
Frequencies -- 943.3663 950.8053 951.1129
Frequencies -- 964.6730 970.5873 978.7092
Frequencies -- 981.1565 981.7766 988.1825
Frequencies -- 988.7714 990.4595 995.5259
Frequencies -- 1000.5727 1001.0653 1002.1596
Frequencies -- 1003.1481 1004.8136 1012.3330
Frequencies -- 1013.0557 1015.9707 1019.3578
Frequencies -- 1019.9464 1029.9354 1033.7567
Frequencies -- 1045.7737 1047.8860 1049.1924
Frequencies -- 1051.1236 1053.5605 1054.3243
Frequencies -- 1055.6990 1064.1933 1067.0998
Frequencies -- 1074.6658 1077.5781 1090.8993
Frequencies -- 1100.7796 1103.6085 1111.2619
Frequencies -- 1114.7965 1115.6274 1135.4064
Frequencies -- 1140.3623 1144.2135 1159.2384
Frequencies -- 1160.7660 1167.1528 1168.9791
Frequencies -- 1170.2351 1179.3103 1180.4885
Frequencies -- 1184.8604 1187.9393 1194.4837
Frequencies -- 1196.1337 1200.4414 1201.2596
Frequencies -- 1203.6151 1206.8915 1208.6642
Frequencies -- 1208.8211 1212.8062 1218.9804
Frequencies -- 1222.6208 1236.7855 1250.2405
Frequencies -- 1253.9274 1257.2375 1259.5395
Frequencies -- 1261.5924 1271.9142 1277.5507
Frequencies -- 1281.5678 1287.4830 1297.6008
Frequencies -- 1298.7629 1303.5074 1304.1590
Frequencies -- 1313.3890 1315.7092 1321.4201
Frequencies -- 1323.4789 1326.4641 1341.4811
Frequencies -- 1344.1455 1347.6028 1350.7033
Frequencies -- 1351.6129 1355.5794 1362.1149
Frequencies -- 1366.0151 1369.1738 1370.5200
Frequencies -- 1388.2682 1408.6437 1412.9957
Frequencies -- 1414.8185 1418.8431 1421.2150
Frequencies -- 1437.0111 1440.9366 1447.1294
Frequencies -- 1466.0552 1480.9077 1482.1855
Frequencies -- 1482.8106 1484.8704 1490.7202
Frequencies -- 1491.9993 1494.5806 1497.0991
Frequencies -- 1499.4670 1500.5827 1501.2609
Frequencies -- 1505.4537 1511.0508 1520.1419
Frequencies -- 1520.9583 1525.0569 1528.1889
Frequencies -- 1532.2877 1547.9206 1551.1493
Frequencies -- 1552.3907 1557.8522 1601.9084
Frequencies -- 1604.0196 1646.6572 1648.8410
Frequencies -- 1655.5841 1658.0177 1661.3248
Frequencies -- 1665.4848 1672.2490 1679.5298
Frequencies -- 1684.5327 1697.0425 1700.9002
Frequencies -- 1711.8217 1713.6938 1714.2033
Frequencies -- 1717.4116 1717.5309 2928.7796
Frequencies -- 3074.6326 3076.9232 3080.2647
Frequencies -- 3086.9863 3096.6966 3121.5395
Frequencies -- 3137.5245 3141.9943 3150.3414
Frequencies -- 3155.6628 3181.6567 3195.6915
Frequencies -- 3196.0625 3200.2142 3200.9995
Frequencies -- 3203.2224 3205.5771 3208.1651
Frequencies -- 3208.5082 3209.2096 3211.0684
Frequencies -- 3212.9356 3213.0925 3219.1271
Frequencies -- 3222.2254 3222.3658 3222.8045
Frequencies -- 3225.1952 3226.4533 3227.4526
Frequencies -- 3228.9450 3230.3753 3230.6845
Frequencies -- 3233.8935 3236.5428 3239.6049
Frequencies -- 3240.7932 3241.5884 3244.6900
Frequencies -- 3245.6764 3254.4246 3256.4000
Frequencies -- 3260.3955 3351.6554 3632.3211

SCF Done: E(RM062X/DGDZVP) = -3995.08586802
Sum of electronic and zero-point Energies= -3994.157130
Sum of electronic and thermal Energies= -3994.088648
Sum of electronic and thermal Free Energies= -3994.262406
SCF Done: E(RM062X/DGTZVP/SMD) = -3995.88703288

Cat a I1a_*R*

Center Number	Atomic Number	Atomic Type	Coordinates (Angstroms) X	Y	Z
1	15	0	-0.017129	-0.010930	0.008492
2	8	0	-0.000580	-0.000692	1.631943
3	8	0	1.590770	-0.004269	-0.334890
4	8	0	-0.442739	1.351203	-0.506582
5	8	0	-0.693870	-1.245899	-0.447141
6	6	0	0.755487	0.965741	2.273478
7	6	0	2.221635	-1.215427	-0.095792
8	6	0	2.079039	0.674574	2.593766
9	6	0	0.192935	2.218037	2.574116
10	6	0	2.690683	-1.497166	1.174974
11	6	0	2.293362	-2.152843	-1.132963
12	6	0	2.894768	-0.590511	2.372253
13	6	0	2.864303	1.654532	3.210500
14	6	0	0.988815	3.150161	3.252502
15	6	0	3.117997	-2.794629	1.470376
16	6	0	2.802314	-3.420022	-0.833959
17	6	0	2.773586	-1.625316	3.524028
18	6	0	4.332618	0.009924	2.349813
19	6	0	4.287122	1.166988	3.361073
20	6	0	2.321626	2.884707	3.565026

21	1	0	0.552510	4.114158	3.500918
22	6	0	3.412711	-2.910631	2.952089
23	6	0	3.181383	-3.758637	0.469671
24	1	0	2.866322	-4.157833	-1.629388
25	1	0	3.246394	-1.278548	4.447635
26	1	0	1.711674	-1.799929	3.725028
27	1	0	5.098450	-0.739263	2.569504
28	1	0	4.526042	0.409684	1.347071
29	1	0	4.466776	0.811248	4.382250
30	1	0	4.492638	-2.937652	3.136225
31	1	0	-2.062566	-1.517614	-1.747999
32	8	0	-2.839552	-1.227074	-2.267961
33	6	0	-3.192327	0.054545	-1.787912
34	6	0	-2.759185	1.199356	-2.748643
35	1	0	-4.279054	0.102488	-1.667310
36	1	0	-2.737859	0.238341	-0.809369
37	8	0	-2.561214	2.392225	-2.019957
38	6	0	-1.467118	0.780664	-3.486579
39	6	0	-3.831071	1.462642	-3.795759
40	1	0	-2.008895	2.178307	-1.240512
41	1	0	-0.670653	0.431993	-2.821792
42	1	0	-1.670358	-0.029208	-4.189970
43	6	0	-4.286876	2.755451	-4.055588
44	6	0	-4.353635	0.387341	-4.525891
45	6	0	-5.254046	2.972566	-5.039794
46	1	0	-3.879566	3.580670	-3.480202
47	6	0	-5.318799	0.607393	-5.505946
48	1	0	-4.011400	-0.623836	-4.308636
49	6	0	-5.770518	1.902562	-5.768025
50	1	0	-5.604742	3.981578	-5.236342
51	1	0	-5.723853	-0.233230	-6.061602
52	1	0	-6.523624	2.073086	-6.531427
53	1	0	4.203627	3.709336	0.504258
54	6	0	3.680262	3.833867	-0.438852
55	6	0	2.583133	3.028657	-0.711467
56	6	0	4.122579	4.800167	-1.359205
57	6	0	1.931922	3.222175	-1.932159
58	1	0	2.240633	2.262738	-0.019066
59	6	0	3.472437	4.987143	-2.574855
60	7	0	0.822568	2.511282	-2.385624
61	6	0	2.364894	4.182399	-2.849328
62	1	0	3.816644	5.732498	-3.284323
63	6	0	0.406130	2.854759	-3.587945
64	1	0	0.265795	1.905752	-1.656549
65	16	0	1.338429	4.160152	-4.266609
66	16	0	-0.843630	2.149216	-4.530337
67	1	0	4.985911	5.412485	-1.120479
68	1	0	5.024038	1.947502	3.153462
69	1	0	3.514622	-4.768623	0.692116
70	1	0	2.986676	-3.818974	3.385092
71	1	0	2.928073	3.639060	4.059132
72	6	0	1.835305	-1.753716	-2.493830
73	6	0	2.491902	-0.689195	-3.151330
74	6	0	0.727724	-2.382258	-3.096129
75	6	0	3.612128	0.000411	-2.577753
76	6	0	2.028933	-0.255390	-4.438075
77	6	0	0.305908	-1.973929	-4.407782
78	6	0	-0.045866	-3.386654	-2.422380
79	6	0	4.191365	1.064219	-3.209166
80	1	0	4.006566	-0.331263	-1.622781
81	6	0	2.658526	0.865693	-5.069646
82	6	0	0.963021	-0.921906	-5.047615
83	6	0	-0.827346	-2.611513	-5.011263
84	1	0	0.210725	-3.649558	-1.402211
85	6	0	-1.130392	-3.957338	-3.023450
86	6	0	3.701085	1.514733	-4.472538
87	1	0	5.028913	1.578571	-2.746328
88	1	0	2.283715	1.190789	-6.037783
89	1	0	0.620237	-0.594087	-6.027783
90	6	0	-1.524887	-3.573029	-4.342418
91	1	0	-1.130037	-2.294922	-6.006622
92	1	0	-1.720563	-4.691235	-2.483988
93	1	0	4.170993	2.365194	-4.958889
94	1	0	-2.396238	-4.034400	-4.796256
95	6	0	-1.179600	2.579639	2.118430
96	6	0	-1.341005	3.615394	1.170870
97	6	0	-2.295613	1.849081	2.566270
98	6	0	-0.234502	4.332613	0.605413
99	6	0	-2.649728	3.913842	0.664074
100	6	0	-3.597566	2.140344	2.033347
101	6	0	-2.187772	0.799892	3.539188
102	6	0	-0.417571	5.275455	-0.367130
103	1	0	0.771651	4.109122	0.941226
104	6	0	-2.805875	4.924136	-0.339786
105	6	0	-3.745497	3.164322	1.098151
106	6	0	-4.721128	1.360072	2.461162
107	1	0	-1.216690	0.579681	3.971039
108	6	0	-3.281873	0.083965	3.928318
109	6	0	-1.726718	5.588035	-0.844697
110	1	0	0.445645	5.789563	-0.784493
111	1	0	-3.805503	5.119856	-0.718420
112	1	0	-4.728224	3.366912	0.677174
113	6	0	-4.571070	0.359684	3.375223
114	1	0	-5.696181	1.583158	2.035902
115	1	0	-3.175312	-0.707769	4.663338
116	1	0	-1.854570	6.336619	-1.620477
117	1	0	-5.427087	-0.229640	3.688835

Frequencies --	11.6326	15.5303	22.9722
Frequencies --	27.3323	32.4390	36.6823
Frequencies --	37.8316	45.9283	47.4365
Frequencies --	49.0452	54.5346	58.4733
Frequencies --	62.7541	71.5539	84.0371
Frequencies --	87.7365	94.4851	96.9311
Frequencies --	99.6006	106.9127	110.3230
Frequencies --	115.9825	121.4741	127.8502
Frequencies --	139.6278	142.5808	148.1334
Frequencies --	156.3592	172.3025	176.1057
Frequencies --	182.5215	187.2258	188.7017
Frequencies --	192.4408	201.5207	206.5749
Frequencies --	215.7504	220.2057	234.9888
Frequencies --	235.7463	240.7418	242.8057
Frequencies --	253.1689	256.7226	279.8168
Frequencies --	283.6892	294.3630	297.2574
Frequencies --	299.7804	306.4398	320.7110
Frequencies --	330.7708	339.6517	349.4056
Frequencies --	364.5699	369.7942	373.7247
Frequencies --	377.4044	385.9135	387.3915
Frequencies --	399.0295	403.3189	403.7019
Frequencies --	406.9531	409.4293	415.2423
Frequencies --	419.2106	424.2279	429.7880
Frequencies --	435.5265	435.8522	444.2038
Frequencies --	455.8077	485.1638	487.5737
Frequencies --	490.1609	497.0432	497.4898
Frequencies --	506.3313	510.1930	521.3213
Frequencies --	528.8636	529.9758	533.2380
Frequencies --	539.4733	550.8410	556.9829
Frequencies --	558.9217	566.6834	567.4018
Frequencies --	573.3226	580.4066	586.2013
Frequencies --	595.4291	603.7923	606.7574
Frequencies --	608.7547	615.4941	620.4353

Frequencies --	625.2857	629.7307	630.5485
Frequencies --	643.6940	648.7236	651.0569
Frequencies --	652.4461	655.2185	658.3237
Frequencies --	661.9406	672.1969	681.5430
Frequencies --	690.2958	710.0485	710.5736
Frequencies --	719.7548	724.3549	730.3102
Frequencies --	731.3244	733.7902	749.8353
Frequencies --	751.6088	754.5775	754.8011
Frequencies --	756.1501	762.7385	770.2861
Frequencies --	774.1965	779.8739	788.9567
Frequencies --	796.1951	800.2051	810.1642
Frequencies --	813.1307	824.7597	836.1865
Frequencies --	837.6040	843.4646	845.7457
Frequencies --	855.7479	865.1896	866.7859
Frequencies --	869.3491	871.1163	873.6192
Frequencies --	875.4788	878.9996	880.3230
Frequencies --	881.6232	884.7550	887.3205
Frequencies --	889.5525	917.8162	919.6475
Frequencies --	926.3545	939.4644	939.6296
Frequencies --	943.0554	950.7845	956.8818
Frequencies --	965.9515	970.6613	974.8009
Frequencies --	978.0095	985.9140	986.7148
Frequencies --	988.8908	990.5030	997.4308
Frequencies --	998.3041	1000.2750	1001.8055
Frequencies --	1005.1802	1005.4769	1005.9882
Frequencies --	1013.5579	1013.7124	1018.0684
Frequencies --	1019.2798	1020.2156	1034.4798
Frequencies --	1039.1052	1045.8675	1049.8724
Frequencies --	1051.8967	1053.4483	1055.1421
Frequencies --	1058.7087	1069.9434	1070.3099
Frequencies --	1077.7813	1090.9367	1103.4782
Frequencies --	1108.2952	1114.3399	1121.6167
Frequencies --	1126.1502	1137.7617	1140.9447
Frequencies --	1143.5382	1157.5710	1159.7283
Frequencies --	1162.8992	1164.3897	1165.8526
Frequencies --	1168.6547	1179.6724	1180.9442
Frequencies --	1186.8823	1188.3209	1195.8000
Frequencies --	1199.9423	1200.7537	1203.6421
Frequencies --	1206.5608	1208.2262	1210.3527
Frequencies --	1212.4787	1218.1453	1222.1254
Frequencies --	1245.8207	1250.4976	1252.8727
Frequencies --	1256.8286	1258.9281	1261.4087
Frequencies --	1266.4525	1272.6209	1282.1305
Frequencies --	1285.9804	1292.5834	1298.0571
Frequencies --	1303.1597	1303.3383	1308.1709
Frequencies --	1316.2309	1317.0135	1322.3961
Frequencies --	1322.9361	1326.6444	1341.5311
Frequencies --	1343.5479	1347.9448	1350.7866
Frequencies --	1355.1936	1361.6938	1365.2042
Frequencies --	1368.2552	1369.2902	1406.7381
Frequencies --	1408.9657	1413.7476	1415.9173
Frequencies --	1418.2550	1420.0170	1441.9771
Frequencies --	1442.2480	1446.8622	1454.2601
Frequencies --	1464.6665	1482.1099	1482.6799
Frequencies --	1485.3938	1490.8954	1492.5173
Frequencies --	1494.7654	1494.9577	1496.7964
Frequencies --	1498.0600	1499.0007	1500.9097
Frequencies --	1505.4731	1511.0343	1515.3059
Frequencies --	1515.6021	1520.5641	1527.9812
Frequencies --	1532.1497	1546.7023	1547.0475
Frequencies --	1552.6224	1581.9355	1601.0525
Frequencies --	1604.6209	1646.2124	1649.5092
Frequencies --	1656.7385	1658.7985	1662.2540
Frequencies --	1666.3665	1671.7851	1675.7991
Frequencies --	1684.4796	1694.3011	1694.7391
Frequencies --	1712.0689	1713.0809	1713.5741
Frequencies --	1717.9030	1719.5507	2159.9890
Frequencies --	3075.2232	3076.1558	3080.6910
Frequencies --	3086.9311	3101.1239	3128.7127
Frequencies --	3138.3662	3141.4823	3151.9548
Frequencies --	3155.7895	3163.4789	3190.6651
Frequencies --	3194.5646	3196.8792	3197.2018
Frequencies --	3199.3572	3201.2707	3203.2174
Frequencies --	3204.6136	3208.2699	3209.4735
Frequencies --	3212.3152	3213.2784	3217.0503
Frequencies --	3218.3291	3218.9282	3219.7406
Frequencies --	3220.1301	3223.4605	3224.8455
Frequencies --	3228.7705	3230.2050	3233.9839
Frequencies --	3235.6677	3236.9797	3237.2551
Frequencies --	3241.5700	3243.0320	3245.7878
Frequencies --	3246.1768	3248.9819	3252.9901
Frequencies --	3262.8209	3665.5673	3684.2073

SCF Done: E(RM062X/DGDZVP) = -3995.13807371
Sum of electronic and zero-point Energies= -3994.209234
Sum of electronic and thermal Energies= -3994.140233
Sum of electronic and thermal Free Energies= -3994.315529
SCF Done: E(RM062X/DGTZVP/SMD) = -3995.94025335

Cat a TS1b_*S*

Center Number	Atomic Number	Atomic Type	Coordinates (Angstroms) X	Y	Z
1	15	0	-0.038321	0.182197	0.423642
2	8	0	0.097787	-0.023876	2.028931
3	8	0	1.518892	0.281446	-0.035246
4	8	0	-0.649251	1.496504	0.074721
5	8	0	-0.685563	-1.082549	-0.078289
6	6	0	0.741979	0.974122	2.742312
7	6	0	2.276230	-0.867993	0.117814
8	6	0	2.110351	0.858613	2.955682
9	6	0	0.021834	2.093406	3.190054
10	6	0	2.910778	-1.111894	1.327616
11	6	0	2.341549	-1.778984	-0.947124
12	6	0	3.087013	-0.238511	2.559915
13	6	0	2.786090	1.888334	3.618441
14	6	0	0.714462	3.060741	3.929432
15	6	0	3.555461	-2.338796	1.518035
16	6	0	3.077361	-2.954050	-0.757200
17	6	0	3.236268	-1.333777	3.651999
18	6	0	4.402174	0.588730	2.469322
19	6	0	4.277497	1.639015	3.588614
20	6	0	2.090389	2.973143	4.140448
21	6	0	4.018338	-2.464889	2.953860
22	6	0	3.662403	-3.252773	0.475328
23	1	0	3.151626	-3.660320	-1.579971
24	1	0	3.726361	-0.956598	4.554188
25	1	0	2.238266	-1.690413	3.927129
26	1	0	5.294224	-0.038607	2.551841
27	1	0	4.428460	1.093047	1.497192
28	1	0	4.629870	1.245766	4.548887
29	1	0	5.100565	-2.310615	3.031954
30	1	0	-2.250979	-1.401823	0.453332
31	8	0	-3.220861	-1.529252	0.229708
32	6	0	-3.219358	-2.008385	-1.144149
33	6	0	-3.370304	-0.650978	-1.845632
34	1	0	-2.290329	-2.530907	-1.379055
35	1	0	-4.079441	-2.665546	-1.269278
36	8	0	-2.165064	-0.147155	-2.351475
37	6	0	-3.751111	0.073295	-0.528065

38	6	0	-4.417007	-0.638850	-2.937713
39	1	0	-1.434727	-0.466454	-1.780908
40	1	0	-4.756980	0.043625	-0.123277
41	1	0	-3.032975	0.715122	-0.022593
42	6	0	-4.075920	-0.247683	-4.232174
43	6	0	-5.729042	-1.033301	-2.661953
44	6	0	-5.042974	-0.242096	-5.237116
45	1	0	-3.056113	0.063618	-4.433684
46	6	0	-6.695518	-1.021918	-3.664556
47	1	0	-6.011710	-1.341831	-1.656740
48	6	0	-6.353746	-0.625113	-4.957802
49	1	0	-4.772323	0.070953	-6.241047
50	1	0	-7.713922	-1.321029	-3.436571
51	1	0	-7.105688	-0.613585	-5.740782
52	1	0	-1.664479	2.133521	-1.090106
53	7	0	-1.972215	2.861790	-1.765653
54	6	0	-3.242156	3.084062	-2.104432
55	6	0	-1.028045	3.736329	-2.282451
56	16	0	-4.601565	2.217809	-1.626538
57	16	0	-3.341996	4.477063	-3.169702
58	6	0	-1.608901	4.725121	-3.083913
59	6	0	0.347558	3.688155	-2.051387
60	6	0	-0.819474	5.713664	-3.671214
61	6	0	1.127026	4.676107	-2.640296
62	1	0	0.766244	2.904384	-1.423765
63	6	0	0.553595	5.679476	-3.437313
64	1	0	-1.260685	6.487533	-4.291141
65	1	0	2.200608	4.668569	-2.478306
66	1	0	1.186663	6.440731	-3.881830
67	1	0	4.177329	-4.198967	0.617706
68	1	0	2.612296	3.765677	4.669695
69	1	0	3.799416	-3.450842	3.371452
70	1	0	4.844538	2.549664	3.380100
71	6	0	1.597854	-1.502041	-2.209801
72	6	0	0.574668	-2.379535	-2.632689
73	6	0	1.881355	-0.338978	-2.956378
74	6	0	0.197852	-3.548260	-1.887728
75	6	0	-0.162348	-2.086539	-3.829697
76	6	0	1.106400	-0.033254	-4.126519
77	6	0	2.932756	0.569953	-2.597334
78	6	0	-0.780372	-4.390174	-2.338438
79	1	0	0.680993	-3.747004	-0.937712
80	6	0	-1.200322	-2.977853	-4.255044
81	6	0	0.110092	-0.916523	-4.540576
82	6	0	1.370608	1.175551	-4.850811
83	1	0	3.557881	0.342111	-1.740133
84	6	0	3.166001	1.703504	-3.320945
85	6	0	-1.490464	-4.107837	-3.546243
86	1	0	-1.044801	-5.267752	-1.755918
87	1	0	-1.754832	-2.732222	-5.157155
88	1	0	-0.474016	-0.684292	-5.428921
89	6	0	2.364126	2.023305	-4.460450
90	1	0	0.757049	1.402833	-5.718607
91	1	0	3.972848	2.370617	-3.031208
92	1	0	-2.273838	-4.780447	-3.882023
93	1	0	2.552612	2.939523	-5.011885
94	1	0	0.162611	3.924276	4.291368
95	6	0	-1.398046	2.317895	2.790531
96	6	0	-2.408477	1.404734	3.147388
97	6	0	-1.704033	3.427217	1.968814
98	6	0	-2.148777	0.245211	3.952116
99	6	0	-3.752451	1.609881	2.681959
100	6	0	-3.058024	3.646122	1.547290
101	6	0	-0.698826	4.307242	1.442940
102	6	0	-3.135373	-0.655316	4.234605
103	1	0	-1.145883	0.085601	4.334702
104	6	0	-4.762383	0.645137	3.004829
105	6	0	-4.050988	2.733489	1.909775
106	6	0	-3.368744	4.767762	0.709782
107	1	0	0.344501	4.109116	1.662133
108	6	0	-1.026499	5.354522	0.629304
109	6	0	-4.465005	-0.459960	3.747045
110	1	0	-2.910648	-1.530666	4.836035
111	1	0	-5.773299	0.816159	2.641753
112	1	0	-5.069904	2.891779	1.561791
113	6	0	-2.385967	5.605263	0.268841
114	1	0	-0.243033	5.987541	0.221935
115	1	0	-5.234239	-1.190701	3.977062
116	1	0	-4.403634	4.916344	0.410411
117	1	0	-2.626634	6.445401	-0.376536

Frequencies --	-531.2406	14.5734	18.9315
Frequencies --	22.1102	24.2096	33.7156
Frequencies --	34.3665	38.8776	42.9261
Frequencies --	51.0846	55.3673	59.6475
Frequencies --	60.9170	67.3060	74.4629
Frequencies --	77.8545	85.1113	91.8592
Frequencies --	94.5607	100.7795	102.6982
Frequencies --	108.4418	114.2368	119.0114
Frequencies --	130.0863	135.0727	139.2735
Frequencies --	145.2596	150.0827	161.0544
Frequencies --	167.4518	177.4402	183.4110
Frequencies --	191.9038	196.5879	198.1568
Frequencies --	200.9183	211.9438	232.5400
Frequencies --	236.7068	237.7189	241.0075
Frequencies --	245.0021	249.4786	272.2226
Frequencies --	277.9178	286.3218	293.4582
Frequencies --	294.7420	296.4382	302.2075
Frequencies --	322.3779	335.2823	341.8188
Frequencies --	346.8290	365.0653	374.0852
Frequencies --	376.7450	378.1090	385.8975
Frequencies --	393.1320	402.1469	403.2616
Frequencies --	403.7223	405.8479	417.8633
Frequencies --	419.0800	421.1941	427.2165
Frequencies --	432.4333	433.0683	436.5095
Frequencies --	448.1754	465.2322	484.4477
Frequencies --	486.5917	490.2685	491.8064
Frequencies --	498.3139	499.1894	504.6645
Frequencies --	506.7133	529.0340	529.9693
Frequencies --	530.4589	538.9596	551.6724
Frequencies --	557.8843	559.8996	565.3912
Frequencies --	567.0782	568.5815	570.3863
Frequencies --	578.6827	604.3133	607.6287
Frequencies --	615.7960	619.0857	620.8455
Frequencies --	625.2290	626.7540	644.3702
Frequencies --	648.9620	649.7279	654.7304
Frequencies --	657.7573	659.2153	666.5046
Frequencies --	675.3377	679.5000	682.2013
Frequencies --	690.3848	709.3698	712.6773
Frequencies --	715.0360	723.6000	730.5625
Frequencies --	736.1035	746.0297	751.8423
Frequencies --	753.4182	755.7765	756.9862
Frequencies --	765.1873	765.5738	772.5474
Frequencies --	773.3920	774.5352	795.7623
Frequencies --	798.6547	809.6576	814.9713
Frequencies --	821.9942	826.6432	838.3596
Frequencies --	845.4811	846.3518	850.4844
Frequencies --	861.1697	864.6307	870.0663
Frequencies --	871.4353	873.6697	875.1949
Frequencies --	879.2132	881.5549	881.7495
Frequencies --	888.8458	889.7789	891.3972

Frequencies -- 904.0686 915.8512 916.8031
Frequencies -- 932.2278 939.5908 941.0604
Frequencies -- 942.7470 946.1373 951.5148
Frequencies -- 963.8929 971.1811 980.9954
Frequencies -- 981.7461 983.5953 985.8061
Frequencies -- 990.4486 991.7024 992.5732
Frequencies -- 995.5739 1000.1454 1002.7458
Frequencies -- 1004.2675 1004.5745 1005.0214
Frequencies -- 1006.1581 1008.9797 1015.8350
Frequencies -- 1018.8292 1019.7718 1030.1213
Frequencies -- 1035.3821 1046.2880 1047.3928
Frequencies -- 1048.3388 1049.8752 1051.0282
Frequencies -- 1052.8895 1058.9932 1064.0885
Frequencies -- 1073.7059 1079.3908 1090.6934
Frequencies -- 1091.1209 1103.1836 1109.6575
Frequencies -- 1111.5665 1117.4121 1136.9626
Frequencies -- 1140.0204 1144.6351 1159.4081
Frequencies -- 1162.4531 1163.6942 1166.3776
Frequencies -- 1170.0281 1173.0824 1174.8999
Frequencies -- 1177.8068 1180.7040 1188.2920
Frequencies -- 1189.2042 1196.4592 1200.3344
Frequencies -- 1203.0352 1206.0068 1207.1828
Frequencies -- 1211.9715 1212.4567 1214.4515
Frequencies -- 1222.2553 1242.1075 1249.5416
Frequencies -- 1253.1329 1256.4405 1257.9286
Frequencies -- 1260.7425 1270.6378 1272.6211
Frequencies -- 1282.7745 1287.8697 1297.2292
Frequencies -- 1298.9039 1302.5321 1302.9714
Frequencies -- 1312.8098 1315.8253 1320.8691
Frequencies -- 1324.4011 1327.7716 1341.2892
Frequencies -- 1342.4437 1346.2282 1349.1842
Frequencies -- 1351.9101 1356.1534 1360.0928
Frequencies -- 1360.7092 1365.5092 1367.9781
Frequencies -- 1394.6754 1408.5138 1414.1448
Frequencies -- 1415.6258 1419.1491 1427.6876
Frequencies -- 1433.0782 1442.4568 1448.9410
Frequencies -- 1466.2316 1480.6000 1482.3875
Frequencies -- 1485.8216 1487.1624 1489.8902
Frequencies -- 1492.2772 1494.3736 1497.6071
Frequencies -- 1499.1308 1500.4223 1502.8719
Frequencies -- 1508.1311 1508.5868 1513.2541
Frequencies -- 1518.2025 1519.4706 1528.3990
Frequencies -- 1531.4898 1546.9259 1550.7992
Frequencies -- 1552.2881 1557.6777 1601.2693
Frequencies -- 1604.3437 1646.2019 1651.8510
Frequencies -- 1654.9199 1658.3813 1662.4099
Frequencies -- 1665.6589 1673.4850 1679.4412
Frequencies -- 1686.7829 1700.3020 1701.7821
Frequencies -- 1706.0048 1713.2359 1715.6255
Frequencies -- 1716.6599 1719.8868 3079.5832
Frequencies -- 3082.1627 3084.8301 3086.4848
Frequencies -- 3140.1082 3140.2448 3142.8699
Frequencies -- 3152.1100 3156.3222 3167.0094
Frequencies -- 3189.6546 3196.0316 3196.8312
Frequencies -- 3199.2840 3200.7708 3203.8062
Frequencies -- 3206.1352 3206.4547 3210.2509
Frequencies -- 3210.3970 3212.4265 3214.1187
Frequencies -- 3214.2007 3215.5911 3215.6824
Frequencies -- 3220.6996 3222.2758 3222.6286
Frequencies -- 3225.7491 3227.3397 3227.4921
Frequencies -- 3227.8171 3228.8399 3231.5623
Frequencies -- 3231.6462 3232.9165 3236.4592
Frequencies -- 3238.1972 3238.3202 3243.7518
Frequencies -- 3246.3445 3247.1751 3254.2640
Frequencies -- 3255.8545 3330.4644 3643.1582

SCF Done: E(RM062X/DGDZVP) = -3995.07424617
Sum of electronic and zero-point Energies= -3994.145600
Sum of electronic and thermal Energies= -3994.076824
Sum of electronic and thermal Free Energies= -3994.251549
SCF Done: E(RM062X/DGTZVP/SMD) = -3995.87663314

Cat a I1b_*S*

Center Number	Atomic Number	Atomic Type	Coordinates (Angstroms) X	Y	Z
1	15	0	-0.149419	0.073272	0.432866
2	8	0	0.115333	0.040713	2.033840
3	8	0	1.365984	0.251649	-0.154298
4	8	0	-0.850897	1.339792	0.047446
5	8	0	-0.729171	-1.255860	0.070054
6	6	0	0.772539	1.119791	2.598879
7	6	0	2.188020	-0.853271	0.008506
8	6	0	2.154993	1.054598	2.731428
9	6	0	0.055126	2.262232	2.991644
10	6	0	2.910263	-0.998792	1.186148
11	6	0	2.198716	-1.841598	-0.986409
12	6	0	3.132995	-0.047195	2.351896
13	6	0	2.842300	2.143729	3.275805
14	6	0	0.766588	3.300187	3.607694
15	6	0	3.597474	-2.195381	1.416294
16	6	0	2.980668	-2.981781	-0.768992
17	6	0	3.366244	-1.068605	3.498777
18	6	0	4.423656	0.797297	2.137976
19	6	0	4.334420	1.914594	3.192376
20	6	0	2.152850	3.253407	3.751440
21	6	0	4.140150	-2.222152	2.829106
22	6	0	3.660525	-3.177746	0.434595
23	1	0	3.001975	-3.749665	-1.537941
24	1	0	3.891631	-0.625176	4.349569
25	1	0	2.393230	-1.430821	3.846248
26	1	0	5.332482	0.193569	2.212155
27	1	0	4.387143	1.237680	1.135676
28	1	0	4.732261	1.583818	4.158671
29	1	0	5.220868	-2.041132	2.840490
30	1	0	-2.389927	-1.687748	0.712466
31	8	0	-3.365780	-1.756664	0.678623
32	6	0	-3.745472	-1.986943	-0.657567
33	6	0	-3.722715	-0.716939	-1.544648
34	1	0	-3.105513	-2.732834	-1.151043
35	1	0	-4.764229	-2.381881	-0.627975
36	8	0	-2.414138	-0.418633	-1.994948
37	6	0	-4.217980	0.466764	-0.682983
38	6	0	-4.597603	-0.942942	-2.769709
39	1	0	-1.762525	-0.836445	-1.390365
40	1	0	-5.106560	0.203602	-0.099719
41	1	0	-3.448307	0.768908	0.033618
42	6	0	-4.037343	-0.905039	-4.047573
43	6	0	-5.972829	-1.169785	-2.639392
44	6	0	-4.837568	-1.095088	-5.175382
45	1	0	-2.971474	-0.721986	-4.138821
46	6	0	-6.772013	-1.359937	-3.764337
47	1	0	-6.433204	-1.198077	-1.653425
48	6	0	-6.205450	-1.323876	-5.039617
49	1	0	-4.389674	-1.060753	-6.164805
50	1	0	-7.836933	-1.535956	-3.645977
51	1	0	-6.826967	-1.472141	-5.917501
52	1	0	-1.750202	1.781878	-1.061013
53	7	0	-2.102714	2.454769	-1.830492
54	6	0	-3.339994	2.667202	-2.205186

55	6	0	-1.155432	3.261490	-2.452903
56	16	0	-4.786345	1.923613	-1.632582
57	16	0	-3.465134	3.911666	-3.412677
58	6	0	-1.734465	4.162991	-3.351134
59	6	0	0.222255	3.226471	-2.226896
60	6	0	-0.949810	5.085391	-4.044771
61	6	0	0.996892	4.147398	-2.917417
62	1	0	0.643313	2.506464	-1.529021
63	6	0	0.421296	5.068142	-3.809858
64	1	0	-1.390282	5.791785	-4.740474
65	1	0	2.070760	4.155037	-2.762180
66	1	0	1.055924	5.777075	-4.331769
67	1	0	4.204133	-4.102380	0.608635
68	1	0	2.684537	4.091742	4.193254
69	1	0	3.966845	-3.185403	3.315434
70	1	0	4.879557	2.817037	2.904890
71	6	0	1.330946	-1.720771	-2.194855
72	6	0	0.297187	-2.662451	-2.397401
73	6	0	1.516253	-0.669352	-3.114632
74	6	0	-0.012278	-3.685602	-1.439033
75	6	0	-0.526052	-2.576278	-3.569970
76	6	0	0.654805	-0.565230	-4.259560
77	6	0	2.554661	0.310888	-2.966823
78	6	0	-1.016322	-4.583283	-1.663838
79	1	0	0.533579	-3.710886	-0.502891
80	6	0	-1.568388	-3.538644	-3.773722
81	6	0	-0.328956	-1.530803	-4.473108
82	6	0	0.826750	0.528393	-5.170014
83	1	0	3.237968	0.231632	-2.126789
84	6	0	2.699247	1.328101	-3.866394
85	6	0	-1.800071	-4.522425	-2.857412
86	1	0	-1.241861	-5.335867	-0.914415
87	1	0	-2.181175	-3.458929	-4.668436
88	1	0	-0.959633	-1.464824	-5.358402
89	6	0	1.811976	1.452068	-4.980572
90	1	0	0.151045	0.604088	-6.018199
91	1	0	3.499588	2.051615	-3.738934
92	1	0	-2.596846	-5.242749	-3.015983
93	1	0	1.932306	2.277941	-5.675498
94	1	0	0.215828	4.179916	3.930345
95	6	0	-1.390891	2.436242	2.665749
96	6	0	-2.365523	1.563479	3.185210
97	6	0	-1.762780	3.457275	1.761953
98	6	0	-2.037816	0.489715	4.078488
99	6	0	-3.741886	1.722221	2.802834
100	6	0	-3.143535	3.624826	1.408903
101	6	0	-0.803486	4.289471	1.092253
102	6	0	-2.996443	-0.371577	4.526801
103	1	0	-1.006948	0.361875	4.391760
104	6	0	-4.719943	0.802619	3.303440
105	6	0	-4.101882	2.756286	1.938098
106	6	0	-3.517064	4.655060	0.484136
107	1	0	0.253652	4.126088	1.272011
108	6	0	-1.191652	5.248418	0.199362
109	6	0	-4.360493	-0.219195	4.130479
110	1	0	-2.722556	-1.187468	5.188287
111	1	0	-5.755658	0.934244	2.999541
112	1	0	-5.146546	2.879410	1.655257
113	6	0	-2.573562	5.450531	-0.100632
114	1	0	-4.572122	4.779599	0.250299
115	1	0	-0.441260	5.846296	-0.310887
116	1	0	-5.104700	-0.922426	4.490621
117	1	0	-2.865116	6.227865	-0.801694

Frequencies -- 14.0147 15.8284 22.8076
Frequencies -- 25.2503 28.9004 34.4874
Frequencies -- 35.8041 40.9923 48.7082
Frequencies -- 53.8889 58.8675 59.7560
Frequencies -- 68.9002 74.7161 78.0438
Frequencies -- 89.1407 93.2714 99.9695
Frequencies -- 101.6435 105.6160 108.5441
Frequencies -- 121.5778 124.1187 130.3490
Frequencies -- 134.9677 142.4531 144.3060
Frequencies -- 149.2435 159.8402 168.4175
Frequencies -- 169.1983 176.8990 192.9388
Frequencies -- 196.8698 204.4776 211.6967
Frequencies -- 222.6019 231.4157 237.3680
Frequencies -- 240.5447 243.3308 245.9412
Frequencies -- 257.9571 265.5196 280.2033
Frequencies -- 290.7070 294.2723 296.8566
Frequencies -- 301.0897 306.4822 322.6892
Frequencies -- 328.7583 337.9434 345.3259
Frequencies -- 348.3670 366.0541 373.6064
Frequencies -- 377.0385 380.4397 385.4371
Frequencies -- 398.7614 403.3158 403.6231
Frequencies -- 404.3912 409.8420 417.8913
Frequencies -- 419.0266 424.8567 430.6590
Frequencies -- 433.5424 436.4469 444.5135
Frequencies -- 468.6841 480.7300 485.0965
Frequencies -- 487.4117 490.9482 497.0651
Frequencies -- 498.0854 504.6321 507.9635
Frequencies -- 523.3886 527.0955 531.8814
Frequencies -- 539.9023 550.6803 556.4770
Frequencies -- 558.5814 563.6848 566.7682
Frequencies -- 569.7773 581.4710 586.7067
Frequencies -- 605.1777 608.2487 610.0580
Frequencies -- 615.9927 619.3426 621.3285
Frequencies -- 626.5303 631.0217 635.9069
Frequencies -- 643.9080 648.7313 650.6627
Frequencies -- 654.7437 658.2900 661.1301
Frequencies -- 670.4533 682.2171 690.4767
Frequencies -- 705.5479 710.4319 712.7737
Frequencies -- 716.6684 722.1947 727.6976
Frequencies -- 733.5340 733.8253 744.4070
Frequencies -- 747.3399 750.5997 754.3810
Frequencies -- 758.7431 769.9173 771.3833
Frequencies -- 773.5407 776.5816 792.3163
Frequencies -- 796.8645 798.7539 809.9916
Frequencies -- 812.6276 827.9617 835.9681
Frequencies -- 842.1888 842.9113 851.5771
Frequencies -- 859.5112 860.5386 861.7245
Frequencies -- 865.9849 870.1400 871.0876
Frequencies -- 875.4881 879.6818 880.9817
Frequencies -- 888.1109 890.8290 891.9631
Frequencies -- 892.9491 906.9007 915.7306
Frequencies -- 934.0655 938.0771 940.1771
Frequencies -- 942.9924 949.1601 951.9711
Frequencies -- 957.6317 971.0269 974.1404
Frequencies -- 975.6019 976.5324 982.3544
Frequencies -- 983.7643 985.8483 990.4991
Frequencies -- 991.8439 995.7905 997.6673
Frequencies -- 999.8394 1000.3159 1002.0320
Frequencies -- 1002.4359 1004.9299 1019.1057
Frequencies -- 1019.6847 1021.9731 1023.5042
Frequencies -- 1035.1227 1046.2433 1046.5738
Frequencies -- 1047.8325 1050.1570 1052.8019
Frequencies -- 1059.6325 1067.1067 1071.8121
Frequencies -- 1077.8930 1092.2151 1104.0049
Frequencies -- 1108.5973 1113.2745 1118.5394
Frequencies -- 1124.2534 1136.8564 1140.9641
Frequencies -- 1145.5867 1155.6763 1160.6462

Frequencies --	1163.9552	1164.8836	1168.8641
Frequencies --	1171.1334	1173.9098	1177.7343
Frequencies --	1182.5962	1184.7773	1194.8119
Frequencies --	1199.1274	1203.1920	1203.6276
Frequencies --	1204.3963	1206.9333	1210.6147
Frequencies --	1211.4578	1213.0664	1222.4409
Frequencies --	1247.3130	1250.2195	1251.6968
Frequencies --	1255.1418	1256.7610	1258.7885
Frequencies --	1272.2177	1274.5292	1282.6298
Frequencies --	1293.7369	1297.0922	1298.8346
Frequencies --	1300.4849	1303.6081	1312.1135
Frequencies --	1313.2284	1315.7047	1318.1394
Frequencies --	1321.5145	1328.2065	1342.5431
Frequencies --	1342.6145	1344.4972	1347.7094
Frequencies --	1351.0458	1360.0406	1365.2547
Frequencies --	1366.4955	1368.2320	1400.7100
Frequencies --	1402.8783	1407.2686	1411.3608
Frequencies --	1414.4669	1415.2122	1431.8478
Frequencies --	1439.8745	1444.7341	1455.8023
Frequencies --	1481.5266	1481.9858	1484.0866
Frequencies --	1486.6500	1489.7186	1490.7638
Frequencies --	1492.9567	1494.8441	1496.8184
Frequencies --	1498.5560	1499.3682	1501.1443
Frequencies --	1507.2116	1507.9733	1511.2734
Frequencies --	1514.7943	1522.1430	1527.1889
Frequencies --	1529.3211	1546.1508	1546.5943
Frequencies --	1549.9399	1596.4914	1599.9271
Frequencies --	1601.6020	1646.2112	1648.6819
Frequencies --	1654.5556	1656.5258	1660.8943
Frequencies --	1664.1487	1674.2952	1676.2879
Frequencies --	1687.7474	1698.1256	1698.8025
Frequencies --	1704.5523	1709.9566	1713.2529
Frequencies --	1716.1078	1718.7304	2469.1413
Frequencies --	3077.4116	3077.4567	3081.4469
Frequencies --	3086.3918	3089.5409	3108.8860
Frequencies --	3141.4172	3144.0313	3154.3335
Frequencies --	3154.6229	3157.9989	3178.4374
Frequencies --	3180.7546	3190.0949	3191.8220
Frequencies --	3194.7439	3198.4453	3201.6228
Frequencies --	3204.3077	3204.6249	3205.5072
Frequencies --	3207.1690	3209.1707	3211.8454
Frequencies --	3217.5151	3219.3555	3219.8412
Frequencies --	3220.2725	3220.3865	3221.5893
Frequencies --	3223.1767	3226.9176	3232.3719
Frequencies --	3233.0739	3235.3671	3235.4058
Frequencies --	3235.4819	3242.5825	3243.5178
Frequencies --	3243.8505	3245.2268	3250.8034
Frequencies --	3253.4663	3574.0066	3644.6630

SCF Done: E(RM062X/DGDZVP) = -3995.13267500
Sum of electronic and zero-point Energies= -3994.204104
Sum of electronic and thermal Energies= -3994.135081
Sum of electronic and thermal Free Energies= -3994.310404
SCF Done: E(RM062X/DGTZVP/SMD) = -3995.93630212

Cat a TS1c_*S*

Center Number	Atomic Number	Atomic Type	Coordinates (Angstroms) X	Y	Z
1	15	0	0.079566	0.042670	-0.105938
2	8	0	-0.001430	-0.003626	1.518292
3	8	0	1.681414	0.006321	-0.363655
4	8	0	-0.379849	1.378290	-0.630508
5	8	0	-0.595709	-1.197448	-0.582863
6	6	0	0.500990	1.099926	2.188063
7	6	0	2.369263	-1.099660	0.110059
8	6	0	1.850631	1.143459	2.510894
9	6	0	-0.360632	2.169435	2.478254
10	6	0	2.917690	-1.041278	1.384959
11	6	0	2.461470	-2.260208	-0.675911
12	6	0	2.941144	0.088599	2.402188
13	6	0	2.379411	2.315306	3.062218
14	6	0	0.181240	3.285268	3.127549
15	6	0	3.563720	-2.168631	1.901504
16	6	0	3.192020	-3.338794	-0.161755
17	6	0	3.055963	-0.733328	3.719471
18	6	0	4.189076	1.001692	2.250939
19	6	0	3.886820	2.212600	3.156815
20	6	0	1.547622	3.377576	3.398786
21	1	0	-0.478849	4.111808	3.377206
22	6	0	3.938601	-1.939065	3.348385
23	6	0	3.736045	-3.307110	1.122444
24	1	0	3.282540	-4.235597	-0.769049
25	1	0	3.451239	-0.137728	4.547162
26	1	0	2.056341	-1.083748	3.998310
27	1	0	5.116582	0.482642	2.509005
28	1	0	4.256918	1.329542	1.208326
29	1	0	4.204526	2.029662	4.189601
30	1	0	5.004103	-1.701020	3.444718
31	1	0	-0.347338	1.707924	-2.250116
32	8	0	-0.831896	1.892629	-3.112854
33	6	0	-2.092350	2.491382	-2.704168
34	6	0	-2.929458	1.205374	-2.638931
35	1	0	-1.991094	3.007913	-1.748077
36	1	0	-2.406077	3.181333	-3.487068
37	8	0	-3.086859	0.711161	-1.336370
38	6	0	-1.860283	0.382345	-3.405577
39	6	0	-4.288152	1.312850	-3.295999
40	1	0	-2.299962	0.969215	-0.813513
41	1	0	-1.771423	0.419664	-4.485642
42	1	0	-1.227313	-0.327003	-2.876799
43	6	0	-5.439450	0.993146	-2.575864
44	6	0	-4.403432	1.735136	-4.623210
45	6	0	-6.691541	1.085123	-3.183004
46	1	0	-5.339930	0.655888	-1.549443
47	6	0	-5.653898	1.821811	-5.230394
48	1	0	-3.515249	1.988058	-5.200058
49	6	0	-6.803801	1.496124	-4.510170
50	1	0	-7.582165	0.825464	-2.618613
51	1	0	-5.730476	2.142389	-6.264759
52	1	0	-7.779120	1.562104	-4.982330
53	1	0	-2.056694	-1.679779	-1.237886
54	7	0	-2.881240	-2.304277	-1.350935
55	6	0	-3.571945	-2.436577	-2.482662
56	6	0	-3.264371	-3.112525	-0.291646
57	16	0	-3.340736	-1.618455	-3.934070
58	16	0	-4.829814	-3.643760	-2.281019
59	6	0	-4.335277	-3.948343	-0.627261
60	6	0	-2.677423	-3.139894	0.974130
61	6	0	-4.847536	-4.851907	0.303842
62	6	0	-3.192965	-4.043237	1.896245
63	1	0	-1.846947	-2.475136	1.201354
64	6	0	-4.262617	-4.891053	1.567426
65	1	0	-5.677093	-5.504751	0.052067
66	1	0	-2.757622	-4.092669	2.889622
67	1	0	-4.643531	-5.588338	2.306641
68	1	0	4.382424	3.126787	2.820497
69	1	0	3.741978	-2.815638	3.970848
70	1	0	1.953767	4.280865	3.845816
71	1	0	4.252816	-4.177657	1.517206

72	6	0	-1.788340	2.134760	2.047551
73	6	0	-2.277094	3.125681	1.164102
74	6	0	-2.644966	1.105415	2.490337
75	6	0	-1.441704	4.154673	0.611544
76	6	0	-3.652603	3.094983	0.751995
77	6	0	-4.001939	1.051559	2.020740
78	6	0	-2.218781	0.089630	3.411448
79	6	0	-1.953925	5.117070	-0.214414
80	1	0	-0.380486	4.147471	0.832648
81	6	0	-4.148832	4.108325	-0.130869
82	6	0	-4.479774	2.054858	1.180256
83	6	0	-4.843710	-0.037993	2.421645
84	1	0	-1.214615	0.135630	3.819640
85	6	0	-3.054684	-0.922606	3.784174
86	6	0	-3.333525	5.105238	-0.585374
87	1	0	-1.297802	5.881826	-0.619089
88	1	0	-5.191573	4.061735	-0.434795
89	1	0	-5.511264	2.018920	0.835141
90	6	0	-4.385134	-1.004014	3.266472
91	1	0	-5.856924	-0.078002	2.030345
92	1	0	-2.707055	-1.677360	4.483815
93	1	0	-3.720803	5.871411	-1.250023
94	1	0	-5.025111	-1.832467	3.554607
95	6	0	1.716120	-2.383818	-1.962070
96	6	0	0.685849	-3.345966	-2.067113
97	6	0	1.967042	-1.498935	-3.028334
98	6	0	0.292972	-4.189170	-0.973518
99	6	0	-0.075737	-3.439156	-3.279854
100	6	0	1.162192	-1.565591	-4.216578
101	6	0	2.995559	-0.499838	-2.971926
102	6	0	-0.716439	-5.100472	-1.106409
103	1	0	0.781602	-4.072693	-0.012475
104	6	0	-1.115138	-4.420283	-3.390547
105	6	0	0.169756	-2.541263	-4.321725
106	6	0	1.385105	-0.617862	-5.269216
107	1	0	3.634997	-0.452401	-2.096541
108	6	0	3.179108	0.385466	-3.994400
109	6	0	-1.421762	-5.237140	-2.341159
110	1	0	-1.008887	-5.709300	-0.255402
111	1	0	-1.670120	-4.480081	-4.323537
112	1	0	-0.438069	-2.594821	-5.223065
113	6	0	2.354271	0.335785	-5.160848
114	1	0	0.762019	-0.678149	-6.158525
115	1	0	3.959029	1.137286	-3.923669
116	1	0	-2.215558	-5.973320	-2.430637
117	1	0	2.509966	1.054538	-5.959351

Frequencies -- -535.3208 10.9249 16.5920
Frequencies -- 18.6192 26.2941 30.5180
Frequencies -- 34.1267 35.9212 39.6361
Frequencies -- 50.4122 51.1282 54.8654
Frequencies -- 60.5481 63.7729 66.4964
Frequencies -- 75.6647 83.5788 91.8862
Frequencies -- 94.8326 100.3533 104.1125
Frequencies -- 108.4730 115.2352 120.7578
Frequencies -- 129.0967 136.9571 144.4449
Frequencies -- 145.6585 150.0602 161.2617
Frequencies -- 169.6435 177.4161 184.8873
Frequencies -- 194.2494 196.8967 199.6933
Frequencies -- 202.5984 211.1434 232.1451
Frequencies -- 237.3704 238.5775 240.6267
Frequencies -- 245.5252 248.7801 274.7479
Frequencies -- 275.9927 283.8720 293.9267
Frequencies -- 294.6644 298.6829 302.1923
Frequencies -- 323.8088 335.1502 342.6756
Frequencies -- 348.0302 364.2459 373.1023
Frequencies -- 376.3722 378.1480 385.6251
Frequencies -- 390.4264 401.6233 402.9252
Frequencies -- 403.4456 404.4144 414.6054
Frequencies -- 418.2840 421.7637 427.0511
Frequencies -- 431.5860 435.0911 438.3692
Frequencies -- 443.6898 465.8340 483.0436
Frequencies -- 489.2393 489.6744 491.4057
Frequencies -- 499.9300 500.3220 502.2567
Frequencies -- 507.3494 527.2446 531.0383
Frequencies -- 531.4561 540.2328 547.9104
Frequencies -- 553.7024 558.0702 565.0884
Frequencies -- 567.8648 569.4662 571.5046
Frequencies -- 581.7082 598.9080 604.5727
Frequencies -- 607.2191 615.6744 618.5900
Frequencies -- 621.7822 627.5294 629.5915
Frequencies -- 646.8146 648.6060 649.4355
Frequencies -- 655.9609 657.7031 661.8259
Frequencies -- 675.2953 678.1739 686.4954
Frequencies -- 690.6130 708.7502 712.0162
Frequencies -- 717.5818 724.6583 731.5878
Frequencies -- 737.3670 753.3469 753.9480
Frequencies -- 755.5741 756.9753 758.2258
Frequencies -- 766.1829 769.5945 772.7788
Frequencies -- 777.8940 780.0878 796.9663
Frequencies -- 799.2568 811.7829 813.5778
Frequencies -- 826.0069 834.2957 836.8434
Frequencies -- 843.5602 845.6387 851.7299
Frequencies -- 863.4429 870.4640 872.7083
Frequencies -- 875.1516 876.8740 877.3987
Frequencies -- 880.3871 882.7335 883.6530
Frequencies -- 887.6031 889.1928 893.0453
Frequencies -- 904.4554 919.8430 928.6232
Frequencies -- 935.4737 939.6506 940.2788
Frequencies -- 942.2707 949.9769 951.0033
Frequencies -- 970.5262 970.7437 979.0682
Frequencies -- 980.1683 987.1069 987.5912
Frequencies -- 991.0763 991.5181 992.0898
Frequencies -- 1000.0455 1003.3715 1004.1092
Frequencies -- 1004.2143 1005.7877 1006.7803
Frequencies -- 1012.1540 1015.3630 1017.5280
Frequencies -- 1017.7724 1021.7243 1032.2921
Frequencies -- 1035.6325 1045.8136 1048.1576
Frequencies -- 1048.9068 1050.2112 1051.3898
Frequencies -- 1051.8947 1058.9168 1062.9968
Frequencies -- 1076.0615 1078.9306 1089.6712
Frequencies -- 1092.7190 1101.1077 1108.6022
Frequencies -- 1113.6231 1122.1658 1137.9498
Frequencies -- 1140.4876 1141.6130 1155.8897
Frequencies -- 1162.6507 1164.2103 1165.1614
Frequencies -- 1168.4236 1175.6100 1179.8685
Frequencies -- 1180.2334 1182.3552 1187.2681
Frequencies -- 1191.6763 1195.9131 1199.9572
Frequencies -- 1202.1511 1204.8382 1211.5697
Frequencies -- 1212.5203 1213.7271 1215.5173
Frequencies -- 1221.8054 1243.8686 1249.0284
Frequencies -- 1251.9850 1255.1677 1257.2835
Frequencies -- 1260.0260 1270.9080 1272.2353
Frequencies -- 1281.8947 1286.0454 1294.7059
Frequencies -- 1299.6526 1300.3937 1301.6764
Frequencies -- 1311.6935 1316.5070 1322.1293
Frequencies -- 1322.2652 1328.1579 1341.0673
Frequencies -- 1343.6299 1346.0561 1349.3671
Frequencies -- 1351.5245 1355.6557 1359.7230
Frequencies -- 1360.9678 1367.5345 1368.8165
Frequencies -- 1394.8377 1407.7174 1412.8703

Frequencies --	1415.7861	1417.8767	1436.0030
Frequencies --	1441.7336	1443.5532	1445.7203
Frequencies --	1460.7261	1481.2293	1483.1770
Frequencies --	1483.8697	1484.9589	1489.7749
Frequencies --	1492.5178	1493.7722	1497.9932
Frequencies --	1498.6049	1499.5742	1500.5380
Frequencies --	1503.7740	1508.2880	1513.8350
Frequencies --	1515.9158	1517.5794	1527.6354
Frequencies --	1530.4281	1546.2147	1549.2087
Frequencies --	1553.5968	1558.9588	1600.6840
Frequencies --	1602.7423	1647.3838	1648.2485
Frequencies --	1655.7441	1657.9689	1662.5323
Frequencies --	1665.2244	1670.0484	1679.8832
Frequencies --	1685.5860	1698.9403	1701.5258
Frequencies --	1704.8056	1712.2133	1713.2606
Frequencies --	1717.1468	1718.5471	3076.4086
Frequencies --	3078.3718	3083.7863	3086.8961
Frequencies --	3128.0533	3139.7793	3142.2891
Frequencies --	3150.5401	3151.9059	3155.7279
Frequencies --	3181.9445	3197.9959	3199.5882
Frequencies --	3203.9197	3204.0706	3204.5608
Frequencies --	3205.1085	3205.8216	3205.9754
Frequencies --	3206.3165	3211.0690	3216.1964
Frequencies --	3217.2868	3219.9388	3220.0349
Frequencies --	3221.5546	3221.5697	3222.1056
Frequencies --	3222.9758	3226.8328	3229.6248
Frequencies --	3231.4966	3231.6866	3232.9464
Frequencies --	3233.0624	3234.4867	3237.0426
Frequencies --	3238.9283	3241.5722	3246.9153
Frequencies --	3248.7281	3250.6719	3252.5307
Frequencies --	3254.8938	3338.3821	3661.2363

SCF Done: E(RM062X/DGDZVP) = -3995.07397851
Sum of electronic and zero-point Energies= -3994.145241
Sum of electronic and thermal Energies= -3994.076408
Sum of electronic and thermal Free Energies= -3994.252244
SCF Done: E(RM062X/DGTZVP/SMD) = -3995.87720105

Cat a I1c_*S*

Center Number	Atomic Number	Atomic Type	Coordinates (Angstroms) X	Y	Z
1	15	0	-0.099252	-0.038836	0.170419
2	8	0	0.003327	0.013208	1.799988
3	8	0	1.462845	0.030777	-0.266241
4	8	0	-0.748575	1.188764	-0.382423
5	8	0	-0.659940	-1.396600	-0.127868
6	6	0	0.418006	1.233524	2.311737
7	6	0	2.309689	-0.938509	0.243492
8	6	0	1.775298	1.490269	2.445968
9	6	0	-0.547331	2.208529	2.600964
10	6	0	2.990912	-0.663574	1.423585
11	6	0	2.440789	-2.177994	-0.403553
12	6	0	2.984257	0.579297	2.301601
13	6	0	2.190615	2.780321	2.792307
14	6	0	-0.102316	3.461119	3.037433
15	6	0	3.826599	-1.639530	1.974285
16	6	0	3.345381	-3.103025	0.134366
17	6	0	3.365194	-0.053751	3.672321
18	6	0	4.063089	1.619322	1.890665
19	6	0	3.697792	2.884778	2.693546
20	6	0	1.259677	3.762502	3.111093
21	1	0	-0.842354	4.222500	3.269944
22	6	0	4.348484	-1.182855	3.317887
23	6	0	4.036994	-2.847072	1.318124
24	1	0	3.464878	-4.058716	-0.369258
25	1	0	3.772978	0.683359	4.369581
26	1	0	2.461706	-0.483021	4.118722
27	1	0	5.079535	1.261180	2.078722
28	1	0	3.962382	1.821083	0.819174
29	1	0	4.159409	2.875942	3.687595
30	1	0	5.373944	-0.806009	3.230047
31	1	0	-0.765563	1.341977	-2.210454
32	8	0	-1.158810	1.252342	-3.101969
33	6	0	-2.548214	1.451959	-2.991198
34	6	0	-3.319173	0.225725	-2.440123
35	1	0	-2.797598	2.306112	-2.344982
36	1	0	-2.910954	1.672981	-3.998422
37	8	0	-3.259051	0.152719	-1.027609
38	6	0	-2.653458	-1.043827	-3.017758
39	6	0	-4.784342	0.334152	-2.839178
40	1	0	-2.469370	0.643915	-0.710957
41	1	0	-2.445541	-0.944817	-4.088338
42	1	0	-1.694773	-1.236286	-2.525801
43	6	0	-5.773868	0.427661	-1.859322
44	6	0	-5.164302	0.311204	-4.186505
45	6	0	-7.120333	0.501516	-2.220584
46	1	0	-5.468345	0.434407	-0.817778
47	6	0	-6.507549	0.383366	-4.547734
48	1	0	-4.410459	0.229936	-4.967438
49	6	0	-7.492569	0.479527	-3.563221
50	1	0	-7.881374	0.573888	-1.448523
51	1	0	-6.786286	0.363667	-5.597012
52	1	0	-8.540156	0.535049	-3.843126
53	1	0	-1.999544	-1.952090	-0.434560
54	7	0	-2.821857	-2.653963	-0.354942
55	6	0	-3.635437	-3.047460	-1.303526
56	6	0	-2.996607	-3.292279	0.869198
57	16	0	-3.696985	-2.545828	-2.950824
58	16	0	-4.744536	-4.272353	-0.763513
59	6	0	-4.012344	-4.251999	0.825898
60	6	0	-2.260212	-3.049582	2.031283
61	6	0	-4.317311	-5.022949	1.948594
62	6	0	-2.565982	-3.821466	3.143271
63	1	0	-1.483007	-2.288492	2.038542
64	6	0	-3.576460	-4.797426	3.103950
65	1	0	-5.102298	-5.771511	1.922139
66	1	0	-2.013996	-3.660545	4.063659
67	1	0	-3.790750	-5.383550	3.991763
68	1	0	4.012985	3.805469	2.196112
69	1	0	4.357724	-1.988161	4.056719
70	1	0	1.581035	4.762241	3.390267
71	1	0	4.700642	-3.598866	1.736426
72	6	0	-1.996399	1.922441	2.387362
73	6	0	-2.716189	2.644877	1.411490
74	6	0	-2.639521	0.916437	3.137328
75	6	0	-2.094002	3.615956	0.556503
76	6	0	-4.112003	2.374034	1.210967
77	6	0	-4.024592	0.623035	2.896400
78	6	0	-1.966030	0.170472	4.162122
79	6	0	-2.817974	4.300175	-0.377361
80	1	0	-1.023496	3.770382	0.629834
81	6	0	-4.839135	3.116488	0.224048
82	6	0	-4.731326	1.365560	1.949475
83	6	0	-4.663118	-0.417416	3.646638
84	1	0	-0.927023	0.396528	4.381537
85	6	0	-2.614510	-0.798592	4.873626
86	6	0	-4.217616	4.058581	-0.541287
87	1	0	-2.321184	5.017898	-1.023314
88	1	0	-5.897144	2.905052	0.089647

89	1	0	-5.785648	1.151575	1.781481
90	6	0	-3.983972	-1.109422	4.605951
91	1	0	-5.706213	-0.639449	3.436133
92	1	0	-2.087396	-1.336707	5.656570
93	1	0	-4.775169	4.608727	-1.293233
94	1	0	-4.479035	-1.894009	5.170734
95	6	0	1.582036	-2.555811	-1.564219
96	6	0	0.653555	-3.610312	-1.411157
97	6	0	1.649021	-1.844693	-2.776817
98	6	0	0.442747	-4.282297	-0.160271
99	6	0	-0.188612	-3.980009	-2.512551
100	6	0	0.781409	-2.204188	-3.864482
101	6	0	2.554574	-0.749941	-2.975212
102	6	0	-0.482217	-5.280561	-0.035437
103	1	0	1.005478	-3.964273	0.710946
104	6	0	-1.133863	-5.046211	-2.351645
105	6	0	-0.103335	-3.272750	-3.715066
106	6	0	0.832252	-1.449684	-5.081391
107	1	0	3.232909	-0.476140	-2.173967
108	6	0	2.568682	-0.050382	-4.146609
109	6	0	-1.274293	-5.685999	-1.153366
110	1	0	-0.635281	-5.757539	0.928883
111	1	0	-1.743704	-5.327538	-3.207086
112	1	0	-0.750476	-3.552586	-4.545293
113	6	0	1.689499	-0.398770	-5.217487
114	1	0	0.164409	-1.730842	-5.892083
115	1	0	3.253482	0.782823	-4.269515
116	1	0	-1.993164	-6.492742	-1.040312
117	1	0	1.709269	0.178282	-6.136557

Frequencies --	17.7067	20.3034	23.5363
Frequencies --	29.4337	32.4795	37.7710
Frequencies --	41.0607	45.9336	54.0417
Frequencies --	57.3580	60.0555	62.5943
Frequencies --	72.0528	77.2387	85.1183
Frequencies --	89.0162	92.4961	97.2450
Frequencies --	102.3017	109.4057	111.4690
Frequencies --	120.8958	123.9491	134.2329
Frequencies --	142.8368	143.4978	144.7883
Frequencies --	152.1104	160.1031	168.6409
Frequencies --	170.2345	176.5500	188.2395
Frequencies --	194.3112	205.8561	214.3964
Frequencies --	217.8155	230.9298	233.5958
Frequencies --	240.3169	244.1640	246.1656
Frequencies --	255.3940	267.4112	275.0492
Frequencies --	290.6072	294.9565	296.8315
Frequencies --	301.8843	307.7581	322.7314
Frequencies --	331.3119	333.9378	343.9169
Frequencies --	349.9681	362.1675	372.2262
Frequencies --	377.7075	379.4176	384.6112
Frequencies --	397.0550	402.7821	403.1799
Frequencies --	404.0633	408.5516	419.2939
Frequencies --	421.1999	425.6878	428.3397
Frequencies --	431.6659	437.7124	441.9903
Frequencies --	467.4185	483.1294	488.0064
Frequencies --	490.1071	492.5282	500.0736
Frequencies --	501.1755	502.8606	507.7678
Frequencies --	523.9279	527.7251	531.3632
Frequencies --	540.3479	550.1233	555.2115
Frequencies --	558.0520	564.3496	568.2656
Frequencies --	571.2824	579.4006	588.1415
Frequencies --	605.1959	607.2949	608.1151
Frequencies --	616.0223	616.4104	621.2442
Frequencies --	623.7576	627.7764	630.5833
Frequencies --	644.9710	649.5693	650.4373
Frequencies --	654.1157	657.5029	661.8400
Frequencies --	672.8317	683.0997	690.6838
Frequencies --	703.6430	709.2591	711.5789
Frequencies --	718.2129	724.9513	727.8205
Frequencies --	733.3267	736.8818	751.6204
Frequencies --	754.5557	755.4388	756.4150
Frequencies --	757.3406	776.2065	779.0810
Frequencies --	779.8534	785.6584	790.0162
Frequencies --	798.1157	800.2219	812.1534
Frequencies --	816.2122	826.0879	836.2815
Frequencies --	842.1079	845.2287	851.1409
Frequencies --	859.8108	866.2272	868.7592
Frequencies --	873.7095	874.5451	879.3053
Frequencies --	880.1509	881.5021	883.1622
Frequencies --	884.6191	887.3333	890.7536
Frequencies --	891.0197	914.4330	917.3020
Frequencies --	934.6615	939.2582	940.1202
Frequencies --	941.2169	951.5230	958.2114
Frequencies --	969.0912	969.6228	973.6672
Frequencies --	981.1025	986.2333	987.6148
Frequencies --	991.1270	992.9552	996.0670
Frequencies --	1002.1714	1002.8804	1004.2316
Frequencies --	1005.7021	1009.5022	1009.6217
Frequencies --	1018.5445	1019.5086	1021.3043
Frequencies --	1025.0433	1025.9906	1030.3883
Frequencies --	1036.7408	1046.9303	1047.2493
Frequencies --	1049.3565	1049.7033	1053.1506
Frequencies --	1059.1701	1061.0216	1070.7730
Frequencies --	1079.3639	1091.2707	1103.7624
Frequencies --	1104.6263	1112.4053	1115.0310
Frequencies --	1121.2229	1140.2438	1141.5319
Frequencies --	1148.2461	1160.7418	1163.8284
Frequencies --	1164.2855	1164.5267	1165.3065
Frequencies --	1171.1509	1174.2646	1177.6041
Frequencies --	1180.7355	1188.4656	1194.8736
Frequencies --	1200.2566	1203.5895	1206.9168
Frequencies --	1207.1550	1209.6311	1212.1879
Frequencies --	1212.8382	1213.7444	1223.6773
Frequencies --	1248.9804	1251.8591	1255.0077
Frequencies --	1256.3861	1258.2068	1260.6628
Frequencies --	1272.6885	1276.0782	1283.6305
Frequencies --	1290.1189	1297.5501	1298.8231
Frequencies --	1302.1820	1304.2379	1308.6938
Frequencies --	1312.1740	1316.8218	1322.0877
Frequencies --	1323.0861	1329.6168	1342.1242
Frequencies --	1343.5545	1347.7028	1349.0850
Frequencies --	1352.2601	1360.1582	1361.3052
Frequencies --	1362.3607	1368.8648	1398.8179
Frequencies --	1404.0720	1408.2206	1412.7859
Frequencies --	1415.0078	1417.8403	1433.0186
Frequencies --	1444.1477	1444.6316	1456.3063
Frequencies --	1484.3918	1485.0456	1485.5712
Frequencies --	1486.3361	1491.0494	1492.5772
Frequencies --	1493.8166	1494.0345	1495.0923
Frequencies --	1498.4668	1500.0726	1500.4292
Frequencies --	1502.9040	1507.3528	1510.0287
Frequencies --	1512.6528	1517.8811	1529.2841
Frequencies --	1531.9389	1546.2806	1547.9073
Frequencies --	1551.4047	1593.5452	1602.0226
Frequencies --	1602.6773	1648.6729	1649.1908
Frequencies --	1656.4039	1659.2419	1662.6274
Frequencies --	1665.6812	1671.3855	1672.8371
Frequencies --	1681.3211	1696.5692	1701.8355
Frequencies --	1707.4701	1711.4762	1715.4550
Frequencies --	1718.9801	1720.1492	2430.1352
Frequencies --	3072.7485	3074.8432	3076.7494

Frequencies -- 3085.6595 3086.8005 3103.9014
Frequencies -- 3138.4607 3140.3148 3154.2514
Frequencies -- 3156.1886 3158.9734 3172.0989
Frequencies -- 3185.8552 3190.4496 3198.2909
Frequencies -- 3200.7418 3202.3765 3205.7315
Frequencies -- 3207.2067 3209.8473 3212.4919
Frequencies -- 3214.8121 3215.8662 3216.2893
Frequencies -- 3221.1924 3221.4576 3221.6093
Frequencies -- 3224.3598 3225.5645 3229.9295
Frequencies -- 3230.8342 3231.0604 3231.9582
Frequencies -- 3234.5858 3235.1611 3237.4464
Frequencies -- 3240.5980 3243.5009 3243.8301
Frequencies -- 3246.9208 3251.8443 3253.8019
Frequencies -- 3254.8918 3566.0728 3657.3390

SCF Done: E(RM062X/DGDZVP) = -3995.13332598
Sum of electronic and zero-point Energies= -3994.203812
Sum of electronic and thermal Energies= -3994.134984
Sum of electronic and thermal Free Energies= -3994.308549
SCF Done: E(RM062X/DGTZVP/SMD) = -3995.93678555

Cat a TS1d_*R*

Center Number	Atomic Number	Atomic Type	Coordinates (Angstroms) X	Y	Z
1	15	0	0.040215	-0.015199	-0.102558
2	8	0	-0.035096	-0.043652	1.533309
3	8	0	1.640125	-0.042180	-0.365208
4	8	0	-0.480113	1.266343	-0.665617
5	8	0	-0.599425	-1.323303	-0.478485
6	6	0	0.375990	1.125025	2.154508
7	6	0	2.349454	-1.080472	0.220799
8	6	0	1.721690	1.321588	2.412362
9	6	0	-0.581022	2.102485	2.444880
10	6	0	2.892857	-0.882548	1.486275
11	6	0	2.474653	-2.311248	-0.443860
12	6	0	2.880361	0.345227	2.383646
13	6	0	2.156011	2.578103	2.841702
14	6	0	-0.130264	3.325713	2.952782
15	6	0	3.552053	-1.941668	2.120102
16	6	0	3.191282	-3.331071	0.196425
17	6	0	3.043398	-0.329422	3.778069
18	6	0	4.058781	1.323463	2.126282
19	6	0	3.669705	2.603883	2.899007
20	6	0	1.234398	3.582773	3.118994
21	1	0	-0.862077	4.095028	3.185139
22	6	0	3.954455	-1.541462	3.521552
23	6	0	3.721071	-3.162204	1.475575
24	1	0	3.298281	-4.283660	-0.315498
25	1	0	3.431441	0.363486	4.529898
26	1	0	2.058875	-0.678109	4.112224
27	1	0	5.021376	0.905550	2.435237
28	1	0	4.104752	1.539833	1.054042
29	1	0	4.021518	2.568387	3.936185
30	1	0	5.013310	-1.258909	3.551425
31	1	0	-1.959780	1.297876	-1.275443
32	8	0	-2.822945	1.013042	-1.727052
33	6	0	-2.490208	0.047436	-2.757659
34	6	0	-3.265718	-1.150824	-2.180059
35	1	0	-2.835586	0.408746	-3.726501
36	1	0	-1.412812	-0.136589	-2.774796
37	8	0	-2.522299	-2.322330	-2.086264
38	6	0	-3.570925	-0.423779	-0.835346
39	6	0	-4.558212	-1.444758	-2.917512
40	1	0	-1.654900	-2.106813	-1.681013
41	1	0	-2.877939	-0.415373	0.000718
42	1	0	-4.530206	0.051255	-0.671476
43	6	0	-4.890256	-2.752404	-3.269656
44	6	0	-5.430079	-0.398482	-3.238265
45	6	0	-6.085957	-3.010061	-3.940943
46	1	0	-4.207828	-3.553847	-3.006419
47	6	0	-6.624089	-0.658425	-3.907013
48	1	0	-5.176015	0.626542	-2.966620
49	6	0	-6.954405	-1.967620	-4.261257
50	1	0	-6.341351	-4.030465	-4.210463
51	1	0	-7.294367	0.159378	-4.153393
52	1	0	-7.884311	-2.172057	-4.782969
53	1	0	1.580568	-3.661470	3.815282
54	6	0	0.528380	-3.814249	3.591876
55	6	0	-0.054367	-3.072857	2.570450
56	6	0	-0.216225	-4.747879	4.328802
57	6	0	-1.406039	-3.294816	2.298229
58	1	0	0.509549	-2.333095	2.007813
59	6	0	-1.564172	-4.964705	4.052375
60	7	0	-2.168212	-2.650301	1.330172
61	6	0	-2.153125	-4.227860	3.024686
62	1	0	-2.140044	-5.687877	4.621002
63	6	0	-3.462092	-3.001451	1.258882
64	1	0	-1.692776	-2.052814	0.623111
65	16	0	-3.802987	-4.259585	2.437180
66	16	0	-4.651384	-2.390660	0.246660
67	1	0	0.261273	-5.311124	5.123881
68	1	0	4.083268	3.508640	2.446750
69	1	0	1.564676	4.560531	3.458683
70	1	0	3.811835	-2.345024	4.249365
71	1	0	4.238095	-3.982857	1.965554
72	6	0	-2.023562	1.803949	2.216315
73	6	0	-2.638728	0.758703	2.941516
74	6	0	-2.762560	2.539850	1.267842
75	6	0	-1.930207	-0.041569	3.899509
76	6	0	-4.027527	0.466925	2.723619
77	6	0	-4.160661	2.261369	1.083767
78	6	0	-2.158174	3.535028	0.427611
79	6	0	-2.545852	-1.066152	4.560483
80	1	0	-0.885186	0.170062	4.101230
81	6	0	-4.640784	-0.612467	3.437890
82	6	0	-4.760316	1.235434	1.815867
83	6	0	-4.905258	3.015522	0.118034
84	1	0	-1.089137	3.702787	0.500171
85	6	0	-2.898710	4.222729	-0.490615
86	6	0	-3.924524	-1.359988	4.327207
87	1	0	-1.982200	-1.667666	5.268716
88	1	0	-5.688076	-0.829959	3.245093
89	1	0	-5.814111	1.010456	1.659050
90	6	0	-4.297309	3.970788	-0.642001
91	1	0	-5.964797	2.801056	-0.000011
92	1	0	-2.417199	4.956831	-1.129110
93	1	0	-4.398809	-2.176704	4.862885
94	1	0	-4.866848	4.531882	-1.376462
95	6	0	1.833127	-2.557471	-1.767673
96	6	0	0.812644	-3.527474	-1.875539
97	6	0	2.221555	-1.808296	-2.895091
98	6	0	0.307100	-4.249954	-0.743146
99	6	0	0.181951	-3.756924	-3.144231
100	6	0	1.570064	-2.032405	-4.155703
101	6	0	3.257258	-0.816488	-2.842323
102	6	0	-0.722735	-5.138827	-0.869160
103	1	0	0.734469	-4.066836	0.236672
104	6	0	-0.872453	-4.722417	-3.243652
105	6	0	0.571712	-3.002676	-4.253038

106	6	0	1.957234	-1.251680	-5.293505
107	1	0	3.773348	-0.642059	-1.903743
108	6	0	3.601022	-0.094815	-3.948316
109	6	0	-1.315854	-5.394403	-2.143501
110	1	0	-1.099664	-5.651799	0.012528
111	1	0	-1.335629	-4.879205	-4.214309
112	1	0	0.078911	-3.167264	-5.209349
113	6	0	2.938397	-0.309497	-5.196315
114	1	0	1.450689	-1.430476	-6.238513
115	1	0	4.385760	0.652466	-3.882458
116	1	0	-2.132778	-6.104689	-2.223922
117	1	0	3.223542	0.277586	-6.063810

Frequencies --	-546.9229	14.5196	19.9889
Frequencies --	21.6014	33.6200	35.4574
Frequencies --	38.8182	43.3286	43.9461
Frequencies --	52.5249	56.1444	58.7776
Frequencies --	63.5817	67.5095	77.9058
Frequencies --	83.1890	87.1121	92.3002
Frequencies --	95.1214	100.4146	105.6313
Frequencies --	107.7791	118.5499	127.5688
Frequencies --	131.5560	139.3343	144.7295
Frequencies --	146.1605	155.8061	160.9130
Frequencies --	171.8629	181.6779	187.2917
Frequencies --	191.6912	197.2324	202.1441
Frequencies --	207.1293	215.6561	225.0466
Frequencies --	236.9797	239.4253	244.3256
Frequencies --	248.8517	255.0354	273.8406
Frequencies --	282.3679	291.1119	294.7927
Frequencies --	297.9338	299.2538	308.7122
Frequencies --	322.7981	336.2838	348.3247
Frequencies --	359.7975	366.9339	377.4699
Frequencies --	380.4817	386.6753	394.1331
Frequencies --	395.9938	400.8031	403.7217
Frequencies --	404.0273	411.9814	418.5308
Frequencies --	419.1563	424.8620	427.4271
Frequencies --	431.7535	434.8668	440.7849
Frequencies --	450.6535	455.0650	486.9556
Frequencies --	487.7457	488.1478	498.8205
Frequencies --	501.7243	506.9579	508.2196
Frequencies --	525.0763	531.1117	532.8191
Frequencies --	534.4854	540.9834	549.8774
Frequencies --	556.9225	565.0236	568.6685
Frequencies --	568.7078	574.8850	579.9001
Frequencies --	583.4612	604.8318	607.1723
Frequencies --	615.6400	616.7434	621.7609
Frequencies --	626.4422	628.5935	645.0383
Frequencies --	648.6918	649.5756	652.1529
Frequencies --	657.4070	660.7255	662.7607
Frequencies --	674.8181	676.9875	689.9115
Frequencies --	690.8013	708.7356	711.0703
Frequencies --	720.2814	724.3674	732.0070
Frequencies --	735.2365	748.8889	753.0827
Frequencies --	753.8190	757.1932	757.4821
Frequencies --	758.1267	764.7614	774.9465
Frequencies --	776.1747	780.6825	796.6152
Frequencies --	800.8283	813.0824	813.3449
Frequencies --	826.9421	839.1210	842.0058
Frequencies --	847.5680	850.3228	857.5618
Frequencies --	860.7560	869.8352	871.1598
Frequencies --	873.1820	874.3833	875.2627
Frequencies --	876.6378	881.4425	882.3449
Frequencies --	887.7009	890.1350	899.5462
Frequencies --	911.3640	921.0727	926.2399
Frequencies --	939.2143	939.6217	943.3880
Frequencies --	946.1901	951.6654	953.2255
Frequencies --	953.8575	972.1999	975.9932
Frequencies --	985.9604	987.9375	989.2715
Frequencies --	990.7057	993.2396	993.5957
Frequencies --	995.9844	1003.0952	1004.9705
Frequencies --	1005.4284	1008.0665	1010.9292
Frequencies --	1013.0204	1015.7820	1019.3691
Frequencies --	1020.7455	1027.0848	1034.7297
Frequencies --	1044.0822	1046.4607	1048.1567
Frequencies --	1050.0271	1050.8931	1053.2985
Frequencies --	1056.3430	1060.8714	1064.2871
Frequencies --	1078.1064	1080.2263	1092.3435
Frequencies --	1098.5760	1105.3131	1109.3828
Frequencies --	1114.6912	1119.4645	1133.3169
Frequencies --	1140.1223	1140.3856	1160.8780
Frequencies --	1161.8705	1163.8397	1165.1361
Frequencies --	1169.3548	1177.2246	1180.2008
Frequencies --	1180.3776	1187.4562	1188.0090
Frequencies --	1193.3419	1197.6683	1201.2396
Frequencies --	1201.6289	1205.9032	1207.1580
Frequencies --	1210.2721	1212.2382	1213.9897
Frequencies --	1221.8202	1234.1596	1251.0058
Frequencies --	1253.1537	1255.6527	1258.5542
Frequencies --	1260.1675	1271.2864	1277.8198
Frequencies --	1282.5077	1288.3598	1293.0393
Frequencies --	1293.9827	1298.2896	1304.4194
Frequencies --	1309.4834	1317.4977	1322.1083
Frequencies --	1322.6929	1328.2282	1343.1491
Frequencies --	1343.4629	1346.4320	1347.0432
Frequencies --	1348.9559	1352.0330	1361.4580
Frequencies --	1367.7728	1369.3603	1373.7664
Frequencies --	1385.0309	1407.4067	1412.1946
Frequencies --	1413.4474	1414.9464	1424.9054
Frequencies --	1436.8421	1443.3679	1443.6232
Frequencies --	1459.5104	1474.7218	1482.7498
Frequencies --	1483.1451	1487.3420	1490.0895
Frequencies --	1490.9439	1493.1777	1498.0098
Frequencies --	1498.4463	1500.6867	1501.0940
Frequencies --	1510.9920	1513.0573	1516.7820
Frequencies --	1523.2056	1529.8654	1530.7163
Frequencies --	1531.6304	1548.0203	1550.6114
Frequencies --	1551.8375	1552.6978	1601.4263
Frequencies --	1602.2635	1646.9706	1648.6168
Frequencies --	1655.1054	1657.7309	1661.0823
Frequencies --	1665.5339	1672.6008	1677.3630
Frequencies --	1684.4831	1699.9978	1701.7496
Frequencies --	1710.7812	1712.8065	1713.2086
Frequencies --	1717.7226	1717.8359	2961.2414
Frequencies --	3077.8180	3079.7952	3081.5772
Frequencies --	3088.8371	3125.6237	3137.9989
Frequencies --	3141.6677	3154.0847	3158.3254
Frequencies --	3169.0914	3188.8066	3191.2731
Frequencies --	3199.2470	3200.2636	3201.3377
Frequencies --	3207.8865	3208.3791	3208.9531
Frequencies --	3209.6673	3215.0886	3215.3963
Frequencies --	3215.4781	3217.7116	3218.2905
Frequencies --	3218.4139	3218.7636	3220.1341
Frequencies --	3223.7147	3226.3795	3227.3060
Frequencies --	3231.1537	3231.2254	3235.1310
Frequencies --	3235.9170	3236.0284	3238.1691
Frequencies --	3239.2738	3243.9853	3245.5540
Frequencies --	3246.2140	3247.2497	3248.4190
Frequencies --	3256.2916	3350.2118	3596.3437

SCF Done: E(RM062X/DGDZVP) = -3995.08584176

Sum of electronic and zero-point Energies= -3994.156783

Sum of electronic and thermal Energies= -3994.088416
Sum of electronic and thermal Free Energies= -3994.261394
SCF Done: E(RM062X/DGTZVP/SMD) = -3995.88726983

Cat a I1d_*R*

Center Number	Atomic Number	Atomic Type	Coordinates (Angstroms) X	Y	Z
1	15	0	0.034660	-0.036579	-0.092191
2	8	0	-0.038372	-0.070895	1.551206
3	8	0	1.639692	-0.061156	-0.347674
4	8	0	-0.514356	1.211113	-0.667099
5	8	0	-0.555157	-1.392033	-0.429948
6	6	0	0.364393	1.104047	2.164419
7	6	0	2.356501	-1.090720	0.237083
8	6	0	1.709225	1.308837	2.424313
9	6	0	-0.595529	2.082728	2.440032
10	6	0	2.896624	-0.889778	1.503642
11	6	0	2.498128	-2.319425	-0.430110
12	6	0	2.873845	0.338629	2.399734
13	6	0	2.137587	2.570375	2.844635
14	6	0	-0.150546	3.312901	2.936398
15	6	0	3.566434	-1.942391	2.137429
16	6	0	3.226557	-3.331478	0.208795
17	6	0	3.043009	-0.332818	3.794664
18	6	0	4.046967	1.322517	2.138613
19	6	0	3.650802	2.603577	2.905872
20	6	0	1.212122	3.575321	3.107650
21	1	0	-0.885820	4.083263	3.153712
22	6	0	3.963976	-1.537984	3.539358
23	6	0	3.751115	-3.159518	1.490309
24	1	0	3.349847	-4.280453	-0.306290
25	1	0	3.425949	0.364000	4.545492
26	1	0	2.061458	-0.688803	4.130001
27	1	0	5.012071	0.911125	2.448648
28	1	0	4.090977	1.534891	1.065503
29	1	0	4.000204	2.572884	3.944101
30	1	0	5.020409	-1.246774	3.570033
31	1	0	-2.137362	1.516772	-1.639919
32	8	0	-2.850395	1.228673	-2.246014
33	6	0	-2.490790	-0.055183	-2.717299
34	6	0	-3.313495	-1.196746	-2.050549
35	1	0	-2.661687	-0.097001	-3.797356
36	1	0	-1.429065	-0.248379	-2.536333
37	8	0	-2.567680	-2.394989	-2.044049
38	6	0	-3.696812	-0.767664	-0.614931
39	6	0	-4.599825	-1.458161	-2.820450
40	1	0	-1.666591	-2.184074	-1.725696
41	1	0	-2.851577	-0.424470	-0.009313
42	1	0	-4.418242	0.050946	-0.641237
43	6	0	-4.958946	-2.751474	-3.202393
44	6	0	-5.442825	-0.385697	-3.139426
45	6	0	-6.152587	-2.972147	-3.892428
46	1	0	-4.292322	-3.572717	-2.959472
47	6	0	-6.632014	-0.609312	-3.829743
48	1	0	-5.151103	0.626442	-2.861235
49	6	0	-6.992590	-1.905057	-4.206045
50	1	0	-6.425510	-3.981474	-4.186553
51	1	0	-7.275226	0.228986	-4.080394
52	1	0	-7.919746	-2.079019	-4.743854
53	1	0	1.602594	-3.823804	3.762172
54	6	0	0.545394	-3.910715	3.528538
55	6	0	0.013766	-3.111619	2.525231
56	6	0	-0.254879	-4.823606	4.236080
57	6	0	-1.347478	-3.252906	2.244035
58	1	0	0.621128	-2.394123	1.978625
59	6	0	-1.609425	-4.963082	3.951190
60	7	0	-2.063699	-2.541080	1.284015
61	6	0	-2.146461	-4.163149	2.941385
62	1	0	-2.226334	-5.668204	4.498444
63	6	0	-3.348814	-2.830900	1.231283
64	1	0	-1.502318	-1.954750	0.549319
65	16	0	-3.792324	-4.087355	2.351429
66	16	0	-4.570838	-2.113327	0.263429
67	1	0	0.187787	-5.432995	5.017101
68	1	0	4.061485	3.508609	2.451573
69	1	0	1.538205	4.557734	3.437811
70	1	0	3.827280	-2.341986	4.267894
71	1	0	4.280211	-3.974053	1.977896
72	6	0	-2.038875	1.787388	2.212144
73	6	0	-2.664429	0.763111	2.957236
74	6	0	-2.771269	2.512526	1.250860
75	6	0	-1.956697	-0.049035	3.906200
76	6	0	-4.064109	0.504480	2.769561
77	6	0	-4.175282	2.255837	1.083652
78	6	0	-2.152826	3.469223	0.377384
79	6	0	-2.582804	-1.053763	4.588422
80	1	0	-0.902299	0.136478	4.083060
81	6	0	-4.691434	-0.544195	3.516835
82	6	0	-4.791498	1.269498	1.854623
83	6	0	-4.909784	2.984921	0.091964
84	1	0	-1.080709	3.619343	0.439233
85	6	0	-2.883527	4.130349	-0.567313
86	6	0	-3.976284	-1.305720	4.395623
87	1	0	-2.019250	-1.662217	5.290634
88	1	0	-5.752202	-0.724813	3.360532
89	1	0	-5.853237	1.069725	1.717709
90	6	0	-4.285690	3.894084	-0.709151
91	1	0	-5.971652	2.779790	-0.020174
92	1	0	-2.390537	4.824458	-1.240548
93	1	0	-4.462702	-2.099196	4.955606
94	1	0	-4.842691	4.424615	-1.474834
95	6	0	1.857729	-2.561842	-1.755022
96	6	0	0.850256	-3.544298	-1.873203
97	6	0	2.223768	-1.784438	-2.870943
98	6	0	0.373845	-4.307456	-0.755083
99	6	0	0.201825	-3.747884	-3.137263
100	6	0	1.555853	-1.984603	-4.126641
101	6	0	3.251168	-0.784537	-2.810197
102	6	0	-0.642315	-5.210982	-0.890663
103	1	0	0.817486	-4.149986	0.221590
104	6	0	-0.842163	-4.723634	-3.246811
105	6	0	0.563907	-2.960002	-4.231984
106	6	0	1.917476	-1.173269	-5.251128
107	1	0	3.779637	-0.626302	-1.875694
108	6	0	3.571343	-0.034189	-3.903864
109	6	0	-1.255333	-5.436830	-2.161082
110	1	0	-0.989332	-5.762412	-0.020009
111	1	0	-1.321280	-4.856557	-4.213096
112	1	0	0.053928	-3.102233	-5.182683
113	6	0	2.891541	-0.224988	-5.146417
114	1	0	1.395798	-1.332451	-6.191236
115	1	0	4.349433	0.719443	-3.831741
116	1	0	-2.061406	-6.158282	-2.250768
117	1	0	3.156862	0.386546	-6.003158

Frequencies --	13.2831	18.5508	22.5658
Frequencies --	28.3357	32.1970	36.7233
Frequencies --	43.0725	45.0577	48.4185

Frequencies -- 51.8675 54.9403 61.1328
Frequencies -- 63.0492 67.8369 80.7959
Frequencies -- 82.4011 92.9023 95.9382
Frequencies -- 97.5343 102.4921 108.1257
Frequencies -- 117.9589 123.2193 125.4334
Frequencies -- 135.5158 142.9148 147.2731
Frequencies -- 154.1226 170.8782 174.1575
Frequencies -- 180.6490 184.5313 186.7979
Frequencies -- 192.7458 199.6531 203.2844
Frequencies -- 216.5547 223.7112 234.6891
Frequencies -- 238.2826 239.3226 243.7340
Frequencies -- 255.5812 257.0233 281.2737
Frequencies -- 284.1071 294.4234 295.5072
Frequencies -- 297.4189 304.7240 320.8453
Frequencies -- 331.9028 339.9356 349.8562
Frequencies -- 365.4690 366.4767 375.9728
Frequencies -- 378.4805 382.7744 388.1463
Frequencies -- 397.6608 402.6855 403.7197
Frequencies -- 406.4266 412.3291 414.5464
Frequencies -- 419.1666 425.4100 429.7189
Frequencies -- 434.0792 436.1273 445.5776
Frequencies -- 454.6289 487.0120 488.1764
Frequencies -- 489.6446 497.6685 497.7420
Frequencies -- 505.8649 510.0719 520.4784
Frequencies -- 525.8091 528.4337 532.2295
Frequencies -- 539.9951 549.1862 556.9346
Frequencies -- 561.9114 567.3606 567.7481
Frequencies -- 573.0362 576.4382 584.9287
Frequencies -- 595.1433 604.5397 606.4211
Frequencies -- 608.2221 615.5194 618.7585
Frequencies -- 623.0120 626.6565 628.2683
Frequencies -- 644.5863 648.7635 649.7929
Frequencies -- 652.5475 657.1812 660.7090
Frequencies -- 663.3770 675.5247 688.1377
Frequencies -- 690.9143 708.7889 711.5970
Frequencies -- 718.5679 723.6175 729.0661
Frequencies -- 732.5740 736.7345 750.2064
Frequencies -- 751.7995 755.0574 756.0057
Frequencies -- 756.9291 758.5970 764.4414
Frequencies -- 771.6510 774.9737 790.0946
Frequencies -- 797.1969 801.2731 812.4479
Frequencies -- 814.0193 825.9785 837.1424
Frequencies -- 839.4403 845.8214 849.0937
Frequencies -- 855.8531 866.1867 867.5204
Frequencies -- 868.3545 871.2634 873.4241
Frequencies -- 874.5640 879.1272 881.1035
Frequencies -- 881.2992 882.9863 886.8571
Frequencies -- 889.8525 919.3433 921.2350
Frequencies -- 923.0916 938.9765 940.0848
Frequencies -- 943.5741 951.7608 955.5814
Frequencies -- 961.8051 972.1674 976.9088
Frequencies -- 983.3597 987.7720 987.9456
Frequencies -- 990.6619 991.4248 992.3926
Frequencies -- 999.3527 1002.2632 1002.7591
Frequencies -- 1003.3577 1005.6468 1008.9306
Frequencies -- 1010.4913 1015.2498 1015.9650
Frequencies -- 1019.6943 1020.7488 1034.9040
Frequencies -- 1038.3593 1044.1885 1047.1036
Frequencies -- 1049.9730 1051.3412 1053.6472
Frequencies -- 1058.6518 1066.8814 1069.7624
Frequencies -- 1080.4790 1092.5116 1105.1570
Frequencies -- 1107.4187 1110.1285 1114.5105
Frequencies -- 1119.4631 1137.4068 1139.8457
Frequencies -- 1140.9755 1155.4280 1156.8022
Frequencies -- 1161.8215 1163.1387 1164.8119
Frequencies -- 1169.3277 1174.5520 1179.5351
Frequencies -- 1180.0363 1187.6568 1193.7329
Frequencies -- 1197.3850 1200.6281 1201.3582
Frequencies -- 1206.1990 1208.5782 1209.7694
Frequencies -- 1210.1152 1212.6376 1222.0301
Frequencies -- 1245.4401 1251.6721 1253.8078
Frequencies -- 1255.7929 1258.5717 1260.6965
Frequencies -- 1268.2444 1273.1130 1283.3365
Frequencies -- 1284.2156 1289.3937 1295.0327
Frequencies -- 1299.1992 1304.3674 1308.0150
Frequencies -- 1316.1894 1318.2860 1322.3265
Frequencies -- 1322.7251 1329.0613 1341.7294
Frequencies -- 1343.4835 1348.0023 1348.9586
Frequencies -- 1352.4782 1361.5964 1364.5246
Frequencies -- 1366.9214 1369.5852 1406.6958
Frequencies -- 1408.0652 1413.1065 1414.2812
Frequencies -- 1414.6459 1417.5915 1427.1202
Frequencies -- 1443.2646 1444.0432 1455.2035
Frequencies -- 1460.6192 1482.7501 1483.8415
Frequencies -- 1487.6221 1490.3352 1491.4208
Frequencies -- 1493.1537 1493.3085 1495.7874
Frequencies -- 1498.2977 1499.2485 1501.4135
Frequencies -- 1510.3877 1510.8785 1512.7523
Frequencies -- 1519.7037 1523.0833 1530.1430
Frequencies -- 1531.4225 1547.2670 1548.1465
Frequencies -- 1552.3984 1580.4755 1600.5622
Frequencies -- 1602.8816 1647.2631 1648.4522
Frequencies -- 1655.2275 1658.4248 1661.4000
Frequencies -- 1665.8027 1672.9261 1673.3200
Frequencies -- 1684.6622 1698.9887 1699.1498
Frequencies -- 1709.9421 1711.4972 1713.7710
Frequencies -- 1717.2505 1719.0193 2219.0128
Frequencies -- 3078.2756 3080.1674 3081.4184
Frequencies -- 3088.5041 3097.5407 3133.5768
Frequencies -- 3137.6344 3141.5772 3154.4149
Frequencies -- 3158.0983 3161.5657 3189.2214
Frequencies -- 3199.3264 3199.6558 3200.3361
Frequencies -- 3203.2748 3203.5591 3203.9999
Frequencies -- 3207.3991 3208.9804 3211.4100
Frequencies -- 3211.7949 3212.7602 3218.9261
Frequencies -- 3219.6625 3220.2598 3223.9206
Frequencies -- 3224.4506 3224.7319 3228.4011
Frequencies -- 3228.7069 3232.3650 3233.2481
Frequencies -- 3234.2766 3235.2461 3237.0489
Frequencies -- 3240.0311 3240.1319 3240.7049
Frequencies -- 3242.1439 3246.3191 3253.6744
Frequencies -- 3263.6757 3656.1665 3665.3294

SCF Done: E(RM062X/DGDZVP) = -3995.13801731
Sum of electronic and zero-point Energies= -3994.209289
Sum of electronic and thermal Energies= -3994.140240
Sum of electronic and thermal Free Energies= -3994.315334
SCF Done: E(RM062X/DGTZVP/SMD) = -3995.94092534

Cat b

Center Number	Atomic Number	Atomic Type	Coordinates (Angstroms) X	Y	Z
1	15	0	0.004905	0.010892	0.009161
2	8	0	0.011245	0.004531	1.604864
3	8	0	1.586463	0.010491	-0.281518
4	1	0	-0.450677	0.779296	1.964546
5	8	0	-0.461429	-1.468517	-0.397255
6	8	0	-0.787901	1.064101	-0.627253
7	6	0	1.928479	-0.110262	-1.635880

8	6	0	0.164262	-2.558635	0.219437
9	6	0	2.099161	-1.370684	-2.187871
10	6	0	2.022479	1.033804	-2.421480
11	6	0	1.355869	-3.062835	-0.282285
12	6	0	-0.409823	-3.096522	1.367242
13	6	0	2.128526	-2.739544	-1.544873
14	6	0	2.317236	-1.480287	-3.563419
15	6	0	2.320770	0.907737	-3.777040
16	6	0	2.005422	-4.080232	0.424872
17	6	0	0.211455	-4.163548	2.011649
18	6	0	3.564054	-3.130444	-1.107532
19	6	0	1.676292	-3.623330	-2.737330
20	6	0	2.258498	-2.939331	-3.998727
21	6	0	2.472225	-0.351091	-4.370540
22	1	0	2.419338	1.798344	-4.391451
23	6	0	3.386552	-4.342434	-0.162597
24	6	0	1.432682	-4.671420	1.552830
25	1	0	-0.247692	-4.602880	2.892883
26	1	0	4.215656	-3.348677	-1.959142
27	1	0	4.004690	-2.297286	-0.550278
28	1	0	1.999628	-4.663646	-2.634353
29	1	0	0.582966	-3.614290	-2.791486
30	6	0	1.422389	-3.153011	-5.243893
31	1	0	3.271122	-3.314846	-4.192832
32	6	0	2.793314	-0.491994	-5.817336
33	6	0	4.471880	-4.455294	0.887795
34	1	0	3.373385	-5.271380	-0.746449
35	6	0	2.105757	-5.805318	2.243554
36	6	0	0.095296	-2.708073	-5.283994
37	6	0	1.965428	-3.749840	-6.382396
38	6	0	1.862105	-0.144343	-6.800620
39	6	0	4.029428	-1.020699	-6.203737
40	6	0	4.661455	-3.429012	1.821519
41	6	0	5.269932	-5.596598	0.973027
42	6	0	2.649190	-5.643397	3.522143
43	6	0	2.239624	-7.038087	1.596727
44	6	0	-0.667648	-2.853642	-6.439595
45	1	0	-0.337204	-2.220981	-4.411591
46	6	0	1.206148	-3.894058	-7.544063
47	1	0	3.000900	-4.082568	-6.370140
48	6	0	2.157175	-0.338331	-8.149241
49	1	0	0.892873	0.246164	-6.501283
50	6	0	4.329584	-1.205193	-7.552553
51	1	0	4.757548	-1.283615	-5.439733
52	6	0	5.625840	-3.546990	2.819327
53	1	0	4.030722	-2.542277	1.783308
54	6	0	6.234073	-5.721576	1.973675
55	1	0	5.121415	-6.406738	0.262802
56	6	0	3.332717	-6.691948	4.135349
57	1	0	2.564124	-4.679798	4.017995
58	6	0	2.913652	-8.091401	2.213867
59	1	0	1.809538	-7.168834	0.606423
60	6	0	-0.112546	-3.444068	-7.576869
61	1	0	-1.693374	-2.497561	-6.456833
62	1	0	1.650427	-4.346252	-8.425721
63	6	0	3.390227	-0.870750	-8.528068
64	1	0	1.418180	-0.086394	-8.903820
65	1	0	5.294219	-1.611584	-7.841837
66	6	0	6.413797	-4.697100	2.901334
67	1	0	5.756985	-2.745951	3.540717
68	1	0	6.835527	-6.623728	2.032601
69	6	0	3.469002	-7.917265	3.481672
70	1	0	3.770386	-6.548171	5.118513
71	1	0	3.008520	-9.045587	1.704180
72	1	0	-0.703288	-3.548750	-8.481847
73	1	0	3.617019	-1.024167	-9.578688
74	1	0	7.159668	-4.794182	3.684291
75	1	0	4.004049	-8.732171	3.959524
76	1	0	1.845516	2.002932	-1.966470
77	1	0	-1.334603	-2.670333	1.742329

Frequencies --	20.2108	24.1348	32.6538
Frequencies --	34.1742	53.7400	57.6414
Frequencies --	61.6626	63.4364	70.4344
Frequencies --	77.7903	82.4323	94.8072
Frequencies --	100.8890	101.3679	108.3793
Frequencies --	120.9797	146.7988	159.3810
Frequencies --	174.5716	178.3907	186.1831
Frequencies --	209.9349	222.0607	232.4510
Frequencies --	233.9209	241.8311	249.5028
Frequencies --	273.9592	281.1523	287.1439
Frequencies --	301.2567	306.8007	326.4657
Frequencies --	350.0751	383.3047	392.7842
Frequencies --	399.2926	399.9569	408.3370
Frequencies --	408.5321	409.9830	413.8676
Frequencies --	427.1995	447.6436	463.6975
Frequencies --	486.1137	500.0977	504.3065
Frequencies --	529.5344	536.4151	541.6408
Frequencies --	549.6887	555.0252	576.1959
Frequencies --	592.4695	608.6947	613.6769
Frequencies --	621.8231	625.0454	629.4034
Frequencies --	629.5302	635.1476	638.8324
Frequencies --	654.3101	664.0253	669.1718
Frequencies --	677.5773	689.0892	708.4454
Frequencies --	708.9549	715.2742	716.3788
Frequencies --	720.6152	729.9644	736.5471
Frequencies --	772.5676	774.8792	778.8098
Frequencies --	789.6032	801.4722	817.1119
Frequencies --	825.3590	844.1629	849.5884
Frequencies --	857.0536	858.1233	865.8104
Frequencies --	867.8415	871.0639	871.3464
Frequencies --	895.5598	919.7475	929.1157
Frequencies --	931.1212	935.8550	936.0283
Frequencies --	941.3765	943.2493	953.4896
Frequencies --	970.2045	973.8824	989.4807
Frequencies --	990.2886	997.1993	997.7985
Frequencies --	999.2855	1001.4018	1005.9831
Frequencies --	1010.4227	1013.2684	1015.9801
Frequencies --	1019.0394	1019.5133	1019.7114
Frequencies --	1020.0258	1024.3514	1042.9734
Frequencies --	1049.7793	1062.5726	1065.9672
Frequencies --	1066.7658	1067.3869	1069.7582
Frequencies --	1085.9446	1099.4246	1104.2607
Frequencies --	1109.7194	1113.0434	1120.8771
Frequencies --	1122.1745	1138.6609	1174.8458
Frequencies --	1175.2610	1175.4087	1178.6650
Frequencies --	1188.0174	1198.6594	1203.2830
Frequencies --	1204.4053	1205.9489	1206.2132
Frequencies --	1213.1441	1224.1460	1232.2743
Frequencies --	1235.5923	1242.9416	1252.7690
Frequencies --	1272.4359	1282.0792	1292.9087
Frequencies --	1297.6846	1307.1994	1312.2353
Frequencies --	1325.1807	1327.4904	1334.3190
Frequencies --	1335.7495	1340.9499	1343.0208
Frequencies --	1357.1604	1358.6469	1358.8339
Frequencies --	1362.4827	1363.7536	1368.8618
Frequencies --	1377.4999	1383.9015	1390.2696
Frequencies --	1458.8017	1472.5565	1491.9148
Frequencies --	1492.6280	1496.6738	1498.3783
Frequencies --	1504.0219	1507.6912	1527.9676
Frequencies --	1530.9773	1545.0939	1547.0007

Frequencies -- 1564.8312 1568.9399 1668.3016
Frequencies -- 1668.6756 1675.2494 1675.6281
Frequencies -- 1682.6271 1684.5852 1686.1277
Frequencies -- 1689.8627 1696.6797 1698.2858
Frequencies -- 1699.8321 1702.4500 3072.2571
Frequencies -- 3072.3917 3088.1390 3092.3703
Frequencies -- 3152.9383 3157.5151 3190.8579
Frequencies -- 3198.6322 3200.0128 3201.2069
Frequencies -- 3204.9031 3209.1872 3212.5214
Frequencies -- 3215.2635 3215.2762 3217.1074
Frequencies -- 3217.7799 3218.6773 3221.5964
Frequencies -- 3225.6776 3225.8091 3227.2365
Frequencies -- 3230.0167 3235.6721 3236.6377
Frequencies -- 3237.0269 3243.9202 3249.0682
Frequencies -- 3249.8791 3252.5042 3823.0952

SCF Done: E(RM062X/DGDZVP) = -2222.74132429
Sum of electronic and zero-point Energies= -2222.122488
Sum of electronic and thermal Energies= -2222.078367
Sum of electronic and thermal Free Energies= -2222.202490
SCF Done: E(RM062X/DGTZVP/SMD) = -2223.24177564

Cat b I0_1

Center Number	Atomic Number	Atomic Type	Coordinates (Angstroms) X	Y	Z
1	15	0	0.000000	0.000000	0.000000
2	8	0	0.000000	0.000000	1.601596
3	8	0	1.559282	0.000000	-0.400122
4	8	0	-0.686096	1.135169	-0.649638
5	8	0	-0.559922	-1.429269	-0.301656
6	6	0	0.564892	1.137234	2.196230
7	6	0	2.340001	-1.065847	0.062448
8	6	0	1.925731	1.168612	2.461450
9	6	0	-0.240330	2.242748	2.448670
10	6	0	2.903628	-1.023803	1.329525
11	6	0	2.484969	-2.189264	-0.745156
12	6	0	2.984335	0.092577	2.349356
13	6	0	2.489755	2.352358	2.943172
14	6	0	0.327907	3.388536	3.002406
15	6	0	3.562794	-2.159443	1.809267
16	6	0	3.215272	-3.280643	-0.281038
17	6	0	3.105856	-0.724908	3.661997
18	6	0	4.252878	0.960747	2.137360
19	6	0	4.010238	2.258095	2.947627
20	6	0	1.701991	3.462765	3.258053
21	1	0	-0.298955	4.247402	3.225294
22	6	0	3.899827	-2.000206	3.286299
23	6	0	3.760668	-3.286223	1.007842
24	1	0	3.348673	-4.150997	-0.917528
25	1	0	3.579512	-0.154006	4.466569
26	1	0	2.103287	-1.009337	3.997082
27	1	0	5.167812	0.439893	2.435887
28	1	0	4.339265	1.209946	1.074883
29	1	0	4.380389	2.136695	3.973216
30	6	0	4.670987	3.478918	2.339693
31	6	0	2.317440	4.688316	3.836102
32	1	0	4.975743	-1.827495	3.413512
33	6	0	3.507210	-3.213458	4.105374
34	6	0	4.520076	-4.459086	1.520749
35	6	0	4.305175	3.906557	1.057393
36	6	0	5.609431	4.223796	3.054269
37	6	0	2.350733	5.884473	3.112221
38	6	0	2.912292	4.639433	5.101089
39	6	0	2.195211	-3.699702	4.047848
40	6	0	4.441597	-3.891918	4.888337
41	6	0	3.878145	-5.678482	1.759279
42	6	0	5.882270	-4.336505	1.813781
43	6	0	4.863555	5.056807	0.506394
44	1	0	3.556275	3.349444	0.496506
45	6	0	6.168306	5.380095	2.508145
46	1	0	5.888351	3.911981	4.058242
47	6	0	2.988310	7.007471	3.636970
48	1	0	1.905933	5.920493	2.121015
49	6	0	3.540424	5.765312	5.631547
50	1	0	2.877901	3.712813	5.669432
51	6	0	1.830563	-4.843891	4.752278
52	1	0	1.458986	-3.192834	3.425756
53	6	0	4.081804	-5.041950	5.592527
54	1	0	5.467692	-3.533522	4.928699
55	6	0	4.582914	-6.750997	2.302988
56	1	0	2.815920	-5.771743	1.548514
57	6	0	6.591176	-5.412561	2.346063
58	1	0	6.385197	-3.391804	1.620055
59	6	0	5.795487	5.801089	1.233005
60	1	0	4.563659	5.379655	-0.486080
61	1	0	6.884957	5.956606	3.085372
62	6	0	3.586884	6.949953	4.896136
63	1	0	3.028331	7.923926	3.056195
64	1	0	3.995511	5.716426	6.616355
65	6	0	2.775603	-5.522879	5.524626
66	1	0	0.810817	-5.212244	4.691552
67	1	0	4.826596	-5.566302	6.183698
68	6	0	5.940032	-6.619884	2.600344
69	1	0	4.069063	-7.685711	2.505702
70	1	0	7.649393	-5.307032	2.565851
71	1	0	6.223870	6.704054	0.808853
72	1	0	4.085184	7.824829	5.302430
73	1	0	2.494768	-6.420095	6.067666
74	1	0	6.486884	-7.455272	3.026917
75	1	0	-1.130304	-1.457247	-1.140690
76	8	0	-1.895843	-1.173237	-2.505772
77	6	0	-2.915220	-0.132323	-2.431474
78	6	0	-2.183357	0.717643	-3.503831
79	1	0	-3.893643	-0.533755	-2.701894
80	1	0	-2.931279	0.336675	-1.444372
81	8	0	-1.772438	1.986934	-3.098858
82	6	0	-1.100782	-0.393285	-3.443445
83	6	0	-2.902358	0.814304	-4.829219
84	1	0	-1.328583	1.900699	-2.230046
85	1	0	-0.160661	-0.054069	-2.994626
86	1	0	-0.917259	-0.958329	-4.359591
87	6	0	-3.057149	2.042057	-5.472734
88	6	0	-3.418555	-0.342639	-5.425411
89	6	0	-3.723204	2.110513	-6.697938
90	1	0	-2.654198	2.934253	-5.006771
91	6	0	-4.083324	-0.273052	-6.646470
92	1	0	-3.301766	-1.308285	-4.934419
93	6	0	-4.237882	0.957787	-7.287625
94	1	0	-3.839521	3.070533	-7.191785
95	1	0	-4.480380	-1.177316	-7.097492
96	1	0	-4.755946	1.014782	-8.239973
97	1	0	-1.294657	2.196619	2.196089
98	1	0	2.014705	-2.198784	-1.723656

Frequencies -- 1.5230 7.1214 18.5931
Frequencies -- 26.3407 28.6203 37.5423
Frequencies -- 39.6425 53.0236 56.2762
Frequencies -- 58.5006 62.1873 62.9376

Frequencies --	68.6424	74.8127	75.2746
Frequencies --	79.9946	92.6386	93.4719
Frequencies --	95.6179	101.9084	111.0114
Frequencies --	122.2369	126.0720	155.2031
Frequencies --	166.1652	168.5883	177.0836
Frequencies --	184.1034	198.6934	210.7253
Frequencies --	221.7196	234.0492	241.7045
Frequencies --	245.8420	254.8054	275.0152
Frequencies --	279.1382	281.1535	287.4597
Frequencies --	303.9633	307.7620	324.5156
Frequencies --	334.9213	351.3339	365.9124
Frequencies --	390.0711	391.9972	400.6796
Frequencies --	408.5489	411.1455	412.8910
Frequencies --	413.6037	416.6352	421.2921
Frequencies --	425.4401	426.2635	435.6215
Frequencies --	449.2960	466.5795	488.3988
Frequencies --	504.5541	505.0946	526.4303
Frequencies --	532.1096	537.5544	542.4073
Frequencies --	550.9636	559.4357	559.9755
Frequencies --	575.9817	591.5102	608.3690
Frequencies --	614.1339	622.7263	624.7085
Frequencies --	628.2575	629.3211	631.1226
Frequencies --	636.2820	638.4802	654.1950
Frequencies --	663.3660	670.2903	677.7151
Frequencies --	684.6799	688.4106	704.0136
Frequencies --	706.0936	713.8204	714.4043
Frequencies --	718.9790	720.1303	721.2527
Frequencies --	730.5591	737.1163	771.7592
Frequencies --	774.2599	776.5305	777.9053
Frequencies --	787.7798	800.4477	817.3449
Frequencies --	824.0522	825.4780	837.5774
Frequencies --	849.4240	850.8037	863.1577
Frequencies --	866.7549	868.3303	872.5005
Frequencies --	874.5156	878.7965	895.8669
Frequencies --	913.9678	917.9221	924.7160
Frequencies --	931.5492	934.2116	935.9925
Frequencies --	940.2927	943.8799	946.4736
Frequencies --	948.6311	958.4029	968.6741
Frequencies --	974.5109	986.4523	992.9708
Frequencies --	995.2554	996.0314	998.2979
Frequencies --	1001.0645	1005.2253	1006.5505
Frequencies --	1007.6854	1008.0296	1009.7296
Frequencies --	1013.4152	1017.8576	1019.1916
Frequencies --	1019.3041	1019.6955	1019.8484
Frequencies --	1019.9313	1024.1814	1034.9307
Frequencies --	1042.8611	1052.3890	1060.5724
Frequencies --	1062.3750	1064.0056	1067.7510
Frequencies --	1068.9215	1072.1709	1086.6725
Frequencies --	1089.8824	1090.1603	1100.3937
Frequencies --	1103.2177	1107.7794	1111.7507
Frequencies --	1116.2398	1121.8237	1126.4101
Frequencies --	1134.6386	1172.1159	1174.1896
Frequencies --	1175.9424	1178.2593	1179.0888
Frequencies --	1183.2665	1184.7302	1192.4636
Frequencies --	1200.1211	1201.1532	1202.0721
Frequencies --	1207.4232	1211.9900	1214.2846
Frequencies --	1214.4553	1223.2245	1230.9000
Frequencies --	1233.9011	1235.5292	1242.4274
Frequencies --	1252.0597	1254.0078	1270.6809
Frequencies --	1278.1864	1292.4882	1296.3972
Frequencies --	1297.7286	1306.1837	1310.9357
Frequencies --	1315.2133	1323.0692	1326.2838
Frequencies --	1329.4400	1336.0114	1336.1395
Frequencies --	1341.6947	1344.6739	1345.9381
Frequencies --	1356.6713	1359.1670	1365.7590
Frequencies --	1367.3296	1368.8841	1370.6753
Frequencies --	1376.0367	1382.2531	1387.7275
Frequencies --	1393.6966	1457.0870	1469.1381
Frequencies --	1470.6278	1489.0590	1492.3859
Frequencies --	1499.4004	1500.4612	1500.9175
Frequencies --	1506.5289	1510.0319	1513.5700
Frequencies --	1526.4895	1528.7279	1538.0248
Frequencies --	1546.9956	1551.4374	1555.5072
Frequencies --	1563.6022	1567.2844	1664.2900
Frequencies --	1669.2068	1677.0267	1678.0206
Frequencies --	1679.6804	1682.3887	1684.1353
Frequencies --	1685.3293	1691.7462	1697.7627
Frequencies --	1701.0679	1701.4340	1702.8930
Frequencies --	1703.1442	2908.0890	3072.2951
Frequencies --	3076.6858	3088.5436	3089.6066
Frequencies --	3104.5627	3122.9037	3153.1238
Frequencies --	3155.5995	3185.7581	3186.2935
Frequencies --	3190.0073	3190.3926	3200.2727
Frequencies --	3200.4754	3200.9593	3203.7095
Frequencies --	3204.1364	3208.9983	3210.2783
Frequencies --	3212.4118	3214.7877	3216.4124
Frequencies --	3216.6717	3217.4378	3217.4848
Frequencies --	3223.1245	3223.5641	3226.0116
Frequencies --	3226.4941	3228.8568	3228.9825
Frequencies --	3229.6540	3236.6202	3236.6623
Frequencies --	3238.6932	3239.0938	3239.1173
Frequencies --	3248.0873	3251.2192	3670.9629

SCF Done: E(RM062X/DGDZVP) = -2721.99270329
Sum of electronic and zero-point Energies= -2721.196670
Sum of electronic and thermal Energies= -2721.140300
Sum of electronic and thermal Free Energies= -2721.296791
SCF Done: E(RM062X/DGTZVP/SMD) = -2722.60970473

Cat b I0_2

Center Number	Atomic Number	Atomic Type	Coordinates (Angstroms) X	Y	Z
1	15	0	-0.032029	0.038638	0.121493
2	8	0	0.000433	0.040447	1.730151
3	8	0	1.511035	0.067296	-0.307985
4	8	0	-0.504719	1.457952	-0.336495
5	8	0	-0.815512	-1.113931	-0.366789
6	6	0	0.655035	1.105043	2.360411
7	6	0	2.244872	-1.070240	0.059388
8	6	0	2.026542	1.058081	2.568301
9	6	0	-0.081951	2.229114	2.719436
10	6	0	2.859484	-1.119391	1.301446
11	6	0	2.280738	-2.162145	-0.801000
12	6	0	3.030233	-0.058207	2.366738
13	6	0	2.664909	2.186652	3.088893
14	6	0	0.561422	3.314316	3.310931
15	6	0	3.472736	-2.308633	1.702210
16	6	0	2.966448	-3.312669	-0.415814
17	6	0	3.158708	-0.942818	3.634809
18	6	0	4.330606	0.759495	2.147691
19	6	0	4.178372	2.028433	3.022011
20	6	0	1.947522	3.311930	3.501801
21	1	0	-0.014781	4.183856	3.614521
22	6	0	3.873664	-2.236004	3.170363
23	6	0	3.571730	-3.405796	0.842813
24	1	0	3.017890	-4.160799	-1.092807
25	1	0	3.688666	-0.433396	4.445515
26	1	0	2.155996	-1.194199	3.995060
27	1	0	5.229130	0.183745	2.389812

28	1	0	4.392316	1.052308	1.094747
29	1	0	4.589264	1.852172	4.023803
30	6	0	4.857632	3.247006	2.429317
31	6	0	2.650599	4.464199	4.129196
32	1	0	4.960843	-2.120860	3.262579
33	6	0	3.451516	-3.466163	3.948592
34	6	0	4.292984	-4.635579	1.269182
35	6	0	4.434213	3.741821	1.189485
36	6	0	5.870233	3.920923	3.112688
37	6	0	2.744206	5.698620	3.479049
38	6	0	3.274033	4.297290	5.370617
39	6	0	2.114678	-3.882672	3.924338
40	6	0	4.379732	-4.227430	4.659531
41	6	0	3.607972	-5.837177	1.474636
42	6	0	5.668728	-4.583151	1.517343
43	6	0	5.007124	4.889768	0.649746
44	1	0	3.629878	3.238429	0.655088
45	6	0	6.445042	5.074672	2.576848
46	1	0	6.196482	3.556169	4.084006
47	6	0	3.468429	6.742628	4.052800
48	1	0	2.279036	5.824879	2.504810
49	6	0	3.989341	5.343996	5.950184
50	1	0	3.192393	3.340477	5.881213
51	6	0	1.718586	-5.038290	4.591972
52	1	0	1.382255	-3.310861	3.356417
53	6	0	3.988205	-5.389129	5.326561
54	1	0	5.424243	-3.924137	4.670894
55	6	0	4.285066	-6.962188	1.942808
56	1	0	2.536002	-5.876143	1.299180
57	6	0	6.349051	-5.710782	1.974211
58	1	0	6.204090	-3.651866	1.347089
59	6	0	6.013533	5.563919	1.345331
60	1	0	4.662353	5.264928	-0.309212
61	1	0	7.221594	5.595999	3.128444
62	6	0	4.095426	6.566786	5.287247
63	1	0	3.555336	7.689508	3.528650
64	1	0	4.465146	5.204390	6.916275
65	6	0	2.656743	-5.799291	5.292966
66	1	0	0.679343	-5.351535	4.558088
67	1	0	4.727108	-5.977801	5.861974
68	6	0	5.655966	-6.900739	2.196727
69	1	0	3.739468	-7.883541	2.122314
70	1	0	7.417782	-5.659762	2.159844
71	1	0	6.454907	6.464814	0.930148
72	1	0	4.661749	7.379888	5.731055
73	1	0	2.351172	-6.705458	5.807096
74	1	0	6.180946	-7.776978	2.564731
75	1	0	-1.457611	1.457389	-0.685048
76	8	0	-2.960062	1.126125	-1.102820
77	6	0	-3.109371	0.097253	-2.125488
78	6	0	-3.946673	-0.791605	-1.167682
79	1	0	-3.622560	0.498816	-3.001283
80	1	0	-2.144349	-0.342037	-2.391434
81	8	0	-3.409354	-2.045771	-0.879218
82	6	0	-3.665532	0.317236	-0.119151
83	6	0	-5.400152	-0.941280	-1.552887
84	1	0	-2.465908	-1.927133	-0.644935
85	1	0	-3.000933	-0.011026	0.687052
86	1	0	-4.528677	0.855763	0.277396
87	6	0	-6.003734	-2.198102	-1.584076
88	6	0	-6.154844	0.190856	-1.883691
89	6	0	-7.347479	-2.320639	-1.942390
90	1	0	-5.413862	-3.070206	-1.326049
91	6	0	-7.494977	0.067492	-2.240427
92	1	0	-5.695154	1.178580	-1.863989
93	6	0	-8.096120	-1.192174	-2.270483
94	1	0	-7.809390	-3.303120	-1.964955
95	1	0	-8.069903	0.952369	-2.495689
96	1	0	-9.140786	-1.290626	-2.549031
97	1	0	-1.149812	2.243349	2.525147
98	1	0	1.759594	-2.102874	-1.750970

Frequencies --	8.3217	14.3967	24.6890
Frequencies --	26.8680	30.1279	34.4649
Frequencies --	39.9360	57.7758	60.7013
Frequencies --	61.4472	64.0926	66.1560
Frequencies --	70.4235	75.3722	78.8713
Frequencies --	80.0374	88.5692	92.2220
Frequencies --	95.5411	98.2983	115.2854
Frequencies --	123.0360	126.7227	156.8571
Frequencies --	165.3816	168.1554	180.7965
Frequencies --	186.5963	200.6144	212.3613
Frequencies --	223.1028	234.0689	242.7512
Frequencies --	246.6981	256.3885	275.2250
Frequencies --	279.0048	281.9186	287.0393
Frequencies --	304.8369	308.4643	325.9598
Frequencies --	331.5200	351.4566	364.7929
Frequencies --	389.9736	393.7433	401.1693
Frequencies --	409.1075	411.5680	412.3089
Frequencies --	414.9880	416.1157	421.0541
Frequencies --	424.5452	427.0591	438.6201
Frequencies --	451.1544	467.9518	489.3522
Frequencies --	504.9295	506.2769	521.1513
Frequencies --	533.0518	538.8416	543.1955
Frequencies --	551.4166	559.5573	560.4969
Frequencies --	577.3237	591.9856	609.2372
Frequencies --	614.6432	623.0631	625.4629
Frequencies --	629.6324	630.5925	631.3927
Frequencies --	636.8949	640.1782	654.3233
Frequencies --	664.0756	670.3377	678.4581
Frequencies --	679.1963	689.9705	704.7786
Frequencies --	708.1434	714.2588	714.9698
Frequencies --	718.8945	720.9156	722.9795
Frequencies --	730.8200	738.4918	772.8017
Frequencies --	775.4325	777.4520	777.5829
Frequencies --	789.4340	801.9367	818.9639
Frequencies --	824.5817	827.3409	841.9501
Frequencies --	849.6216	859.4826	864.2728
Frequencies --	869.2436	869.9932	871.1681
Frequencies --	876.1026	878.8703	895.7946
Frequencies --	916.7173	919.4143	929.9260
Frequencies --	932.9921	936.5695	938.9904
Frequencies --	941.7927	945.4250	947.5346
Frequencies --	950.9145	965.1946	970.9047
Frequencies --	975.1350	991.7135	992.6255
Frequencies --	996.1919	997.9799	998.6567
Frequencies --	1003.5512	1005.0479	1006.7625
Frequencies --	1009.2059	1011.2904	1012.1971
Frequencies --	1014.3310	1017.2873	1019.0846
Frequencies --	1019.3642	1019.7109	1020.1248
Frequencies --	1020.2890	1026.4517	1034.1444
Frequencies --	1044.0648	1052.7256	1061.8591
Frequencies --	1063.9136	1065.0410	1065.8993
Frequencies --	1069.7142	1071.2623	1087.8288
Frequencies --	1090.7156	1091.6043	1102.4219
Frequencies --	1105.8677	1110.9809	1112.1342
Frequencies --	1121.0582	1121.5278	1127.5710
Frequencies --	1138.2531	1173.1197	1174.3469
Frequencies --	1176.4924	1177.5289	1177.6608
Frequencies --	1184.3473	1187.2523	1191.7921
Frequencies --	1201.9716	1203.5971	1203.9156

Frequencies -- 1206.0112 1215.1487 1216.6946
Frequencies -- 1220.0465 1225.0706 1230.8228
Frequencies -- 1233.9399 1237.9755 1244.7962
Frequencies -- 1256.6524 1260.4840 1273.4394
Frequencies -- 1280.8282 1292.6944 1298.3234
Frequencies -- 1300.4250 1309.9648 1314.4183
Frequencies -- 1315.9783 1327.1241 1327.4086
Frequencies -- 1330.4412 1336.6257 1338.0367
Frequencies -- 1342.9000 1346.0748 1348.2330
Frequencies -- 1358.8486 1359.3659 1362.5845
Frequencies -- 1367.5700 1370.1764 1372.1630
Frequencies -- 1376.1835 1381.2781 1387.3518
Frequencies -- 1393.8722 1460.0234 1471.2433
Frequencies -- 1473.3878 1491.7871 1492.8766
Frequencies -- 1497.3934 1502.5469 1502.9229
Frequencies -- 1505.6931 1510.7745 1510.8969
Frequencies -- 1528.3354 1530.3555 1531.1496
Frequencies -- 1543.7125 1550.5156 1556.9158
Frequencies -- 1564.5486 1568.3048 1666.6337
Frequencies -- 1670.1920 1674.3682 1676.2323
Frequencies -- 1678.8431 1682.6035 1684.8533
Frequencies -- 1687.5536 1691.6455 1697.4074
Frequencies -- 1700.3954 1701.0483 1702.8085
Frequencies -- 1703.7819 2936.7385 3080.2570
Frequencies -- 3082.1437 3090.6986 3094.2517
Frequencies -- 3098.9664 3119.8970 3156.0623
Frequencies -- 3159.3233 3181.3821 3184.7336
Frequencies -- 3189.4426 3198.5317 3199.8185
Frequencies -- 3202.5366 3204.9690 3206.3241
Frequencies -- 3206.8751 3207.7105 3212.5021
Frequencies -- 3215.8539 3216.0215 3218.5717
Frequencies -- 3218.6653 3219.0622 3224.9726
Frequencies -- 3225.0623 3226.6364 3227.3491
Frequencies -- 3228.5278 3234.6106 3235.9046
Frequencies -- 3235.9924 3238.9789 3239.0507
Frequencies -- 3241.4360 3242.3698 3243.2464
Frequencies -- 3243.2665 3270.7599 3659.9581

SCF Done: E(RM062X/DGDZVP) = -2721.99305799
Sum of electronic and zero-point Energies= -2721.196148
Sum of electronic and thermal Energies= -2721.139938
Sum of electronic and thermal Free Energies= -2721.293115
SCF Done: E(RM062X/DGTZVP/SMD) = -2722.60955718

Cat b TS1a_*R*

Center Number	Atomic Number	Atomic Type	X	Y	Z
1	15	0	0.000000	0.000000	0.000000
2	8	0	0.000000	0.000000	1.618772
3	8	0	1.592226	0.000000	-0.355332
4	8	0	-0.509173	1.314963	-0.534852
5	8	0	-0.652970	-1.270953	-0.449718
6	6	0	0.632436	1.075949	2.231535
7	6	0	2.294394	-1.135914	0.049513
8	6	0	1.980827	0.993145	2.551352
9	6	0	-0.082931	2.241570	2.487632
10	6	0	2.801607	-1.221533	1.339756
11	6	0	2.398951	-2.215965	-0.822333
12	6	0	2.921829	-0.186703	2.440575
13	6	0	2.631847	2.099956	3.112724
14	6	0	0.558190	3.313589	3.101150
15	6	0	3.340457	-2.435321	1.774667
16	6	0	3.024304	-3.387204	-0.401366
17	6	0	2.866483	-1.096563	3.694342
18	6	0	4.284335	0.544853	2.369417
19	6	0	4.124366	1.800551	3.257459
20	6	0	1.921754	3.266755	3.433256
21	1	0	-0.013482	4.204672	3.344981
22	6	0	3.579192	-2.408572	3.279682
23	6	0	3.496843	-3.520124	0.909313
24	1	0	3.125849	-4.222101	-1.089260
25	1	0	3.320182	-0.629299	4.573901
26	1	0	1.819460	-1.312356	3.928842
27	1	0	5.120210	-0.087731	2.683704
28	1	0	4.466503	0.853944	1.335092
29	1	0	4.342860	1.531457	4.298556
30	6	0	5.057827	2.919138	2.848034
31	6	0	2.528513	4.419227	4.150738
32	1	0	4.652135	-2.341940	3.498573
33	6	0	3.022557	-3.637700	3.969803
34	6	0	4.141238	-4.776585	1.378668
35	6	0	4.966018	3.471084	1.566540
36	6	0	6.034843	3.406705	3.718261
37	6	0	2.275476	5.736548	3.746482
38	6	0	3.314185	4.212112	5.290584
39	6	0	1.682030	-3.995471	3.779284
40	6	0	3.832476	-4.457386	4.756541
41	6	0	3.411965	-5.964975	1.485497
42	6	0	5.486205	-4.765296	1.764035
43	6	0	5.814720	4.501838	1.170738
44	1	0	4.218663	3.093764	0.871274
45	6	0	6.889609	4.437206	3.327502
46	1	0	6.118657	2.986606	4.718374
47	6	0	2.823145	6.813910	4.440263
48	1	0	1.645106	5.922312	2.880151
49	6	0	3.853625	5.286839	5.992560
50	1	0	3.482442	3.198452	5.644557
51	6	0	1.166210	-5.150513	4.360703
52	1	0	1.044391	-3.378525	3.147599
53	6	0	3.320743	-5.618821	5.337317
54	1	0	4.879823	-4.199995	4.897146
55	6	0	4.013593	-7.117963	1.987603
56	1	0	2.361653	-5.971530	1.205740
57	6	0	6.092044	-5.920371	2.256136
58	1	0	6.056913	-3.843898	1.672744
59	6	0	6.779132	4.991709	2.053069
60	1	0	5.721431	4.919151	0.171734
61	1	0	7.636346	4.811299	4.021302
62	6	0	3.619102	6.592999	5.563620
63	1	0	2.626248	7.826940	4.102785
64	1	0	4.455463	5.103577	6.877758
65	6	0	1.986755	-5.970048	5.139347
66	1	0	0.126442	-5.417706	4.196981
67	1	0	3.968624	-6.253542	5.934478
68	6	0	5.353670	-7.097841	2.376789
69	1	0	3.431972	-8.029475	2.086715
70	1	0	7.137844	-5.900631	2.548292
71	1	0	7.440393	5.797082	1.748451
72	1	0	4.046125	7.431578	6.104783
73	1	0	1.588505	-6.876952	5.584132
74	1	0	5.819150	-7.995959	2.771187
75	1	0	-1.480501	-1.365878	-1.718523
76	8	0	-2.042320	-1.168400	-2.557538
77	6	0	-3.047496	-0.191010	-2.199641
78	6	0	-2.537838	0.968578	-3.076805
79	1	0	-4.039093	-0.568300	-2.450337
80	1	0	-2.983468	0.044810	-1.133853
81	8	0	-2.346508	2.161232	-2.380567
82	6	0	-1.228969	0.216874	-3.462602

83	6	0	-3.395627	1.229348	-4.298460
84	1	0	-1.878744	1.954498	-1.543779
85	1	0	-0.346055	0.266089	-2.835207
86	1	0	-1.138680	-0.317836	-4.399789
87	6	0	-3.782583	2.526078	-4.632679
88	6	0	-3.793391	0.158492	-5.106151
89	6	0	-4.562195	2.748773	-5.767771
90	1	0	-3.463443	3.349454	-4.003728
91	6	0	-4.568233	0.383385	-6.241474
92	1	0	-3.500037	-0.859432	-4.849956
93	6	0	-4.955005	1.682171	-6.574810
94	1	0	-4.858305	3.761147	-6.024880
95	1	0	-4.870832	-0.453644	-6.862959
96	1	0	-5.558739	1.860614	-7.459264
97	1	0	2.720612	5.111015	1.137689
98	6	0	2.491881	5.035831	0.078791
99	6	0	1.713102	3.977346	-0.375335
100	6	0	3.011291	5.991215	-0.807802
101	6	0	1.467376	3.904786	-1.746568
102	1	0	1.306238	3.227341	0.301194
103	6	0	2.764380	5.909517	-2.175754
104	7	0	0.711359	2.933980	-2.395104
105	6	0	1.983006	4.851250	-2.637828
106	1	0	3.167456	6.647565	-2.861657
107	6	0	0.595465	3.056116	-3.724614
108	1	0	0.234805	2.205275	-1.832788
109	16	0	1.487442	4.463549	-4.273097
110	16	0	-0.243585	2.070003	-4.794176
111	1	0	-1.128952	2.291870	2.203336
112	1	0	1.970449	-2.130086	-1.815844
113	1	0	3.618148	6.804035	-0.421285

Frequencies --	-549.7239	11.2966	13.3012
Frequencies --	19.3456	23.8691	28.8128
Frequencies --	30.2262	30.7234	38.7619
Frequencies --	43.7776	44.8968	48.9787
Frequencies --	51.2076	57.9965	61.7455
Frequencies --	65.3092	73.0161	77.0646
Frequencies --	82.7495	85.6103	90.3757
Frequencies --	94.0883	97.4307	98.6858
Frequencies --	99.5185	113.6584	122.8922
Frequencies --	130.0576	131.8091	156.9583
Frequencies --	161.8679	171.2765	181.3600
Frequencies --	185.1235	193.2343	194.2303
Frequencies --	207.7187	210.3814	218.1021
Frequencies --	226.0023	231.3263	241.2168
Frequencies --	251.9956	261.8995	273.3999
Frequencies --	276.9322	284.1573	289.2470
Frequencies --	293.8888	304.7843	313.7676
Frequencies --	324.8935	330.0821	351.7046
Frequencies --	365.2607	385.4473	387.7907
Frequencies --	398.1744	406.0363	411.1028
Frequencies --	412.1627	412.9732	414.9469
Frequencies --	415.4702	418.2602	421.6718
Frequencies --	421.9875	433.6511	438.7661
Frequencies --	445.5222	452.8911	461.3236
Frequencies --	471.8565	493.7147	507.9045
Frequencies --	508.9477	511.9447	523.9004
Frequencies --	531.5615	536.4820	538.6139
Frequencies --	542.6686	555.2510	567.6414
Frequencies --	576.3773	576.7275	586.1916
Frequencies --	597.7045	609.2676	614.8005
Frequencies --	618.9233	623.3498	627.0654
Frequencies --	628.9191	629.5585	632.3067
Frequencies --	637.9256	639.9197	653.8270
Frequencies --	663.9226	664.8229	673.0238
Frequencies --	681.2067	683.8269	693.2976
Frequencies --	704.6898	712.2917	713.0174
Frequencies --	717.4250	719.3055	720.7706
Frequencies --	722.2896	725.7112	732.1741
Frequencies --	736.7359	739.8658	748.8462
Frequencies --	769.8775	771.9357	775.5007
Frequencies --	779.8519	780.4396	783.7047
Frequencies --	799.4480	817.6459	825.0657
Frequencies --	841.6531	849.8458	862.7805
Frequencies --	864.3374	866.1514	868.5120
Frequencies --	872.6014	873.3777	879.2431
Frequencies --	881.0133	885.4618	890.4430
Frequencies --	896.7844	901.2759	904.1417
Frequencies --	933.1828	934.7806	939.4745
Frequencies --	939.9291	942.1533	943.3234
Frequencies --	944.2371	954.0321	965.8221
Frequencies --	967.6953	974.7973	993.3685
Frequencies --	995.6968	997.4508	998.2229
Frequencies --	998.8910	1001.8149	1006.1902
Frequencies --	1010.2259	1010.4612	1011.1586
Frequencies --	1011.3027	1017.4616	1018.0736
Frequencies --	1019.1216	1019.2921	1019.9908
Frequencies --	1020.8501	1022.6789	1027.5733
Frequencies --	1042.5095	1045.5146	1051.5983
Frequencies --	1053.3305	1058.7613	1063.4426
Frequencies --	1064.7651	1068.2401	1069.8021
Frequencies --	1071.5099	1079.2893	1087.2321
Frequencies --	1089.2725	1102.0676	1103.2958
Frequencies --	1105.7129	1109.4813	1111.1481
Frequencies --	1114.3686	1117.6495	1119.8422
Frequencies --	1124.1738	1125.6342	1139.0890
Frequencies --	1153.7644	1158.9257	1175.2888
Frequencies --	1176.2361	1176.2917	1177.6660
Frequencies --	1178.9751	1180.3117	1189.0403
Frequencies --	1198.1238	1202.0466	1206.3841
Frequencies --	1207.5547	1209.4407	1209.8179
Frequencies --	1210.8214	1214.1901	1214.6140
Frequencies --	1224.7701	1230.9172	1232.8730
Frequencies --	1241.0772	1246.8046	1257.1405
Frequencies --	1264.9370	1277.4318	1289.9534
Frequencies --	1291.0639	1295.4487	1296.7475
Frequencies --	1300.3763	1306.0305	1308.3665
Frequencies --	1312.1854	1324.7021	1327.4939
Frequencies --	1333.6003	1337.2053	1343.3444
Frequencies --	1343.8922	1346.9664	1349.7928
Frequencies --	1357.2361	1358.6251	1366.1566
Frequencies --	1367.0073	1368.0774	1370.0194
Frequencies --	1371.5801	1376.9730	1382.6429
Frequencies --	1385.6343	1394.7940	1441.8145
Frequencies --	1451.7902	1465.0351	1468.4369
Frequencies --	1474.6896	1478.2164	1490.6592
Frequencies --	1494.2118	1499.5537	1500.6174
Frequencies --	1500.9803	1506.4187	1510.6853
Frequencies --	1514.9389	1523.7025	1527.6211
Frequencies --	1530.5881	1547.9568	1550.7214
Frequencies --	1552.9174	1555.5070	1563.8139
Frequencies --	1567.8984	1662.8643	1664.8815
Frequencies --	1673.5065	1675.6312	1676.4468
Frequencies --	1678.3727	1679.5446	1682.3186
Frequencies --	1684.7438	1686.4080	1690.1610
Frequencies --	1698.4869	1698.7700	1701.8319
Frequencies --	1702.0148	1702.9815	2690.9465
Frequencies --	3074.7061	3077.5782	3091.1751
Frequencies --	3092.8142	3121.3975	3155.1837
Frequencies --	3157.8132	3189.8592	3198.9895

Frequencies -- 3201.9876 3202.3093 3202.9041
Frequencies -- 3204.5087 3205.3540 3207.3949
Frequencies -- 3207.8445 3213.0652 3213.7088
Frequencies -- 3215.3823 3216.8504 3217.7117
Frequencies -- 3218.2762 3218.8263 3218.9176
Frequencies -- 3221.8018 3224.9566 3226.0826
Frequencies -- 3226.6571 3229.2161 3229.7456
Frequencies -- 3229.8253 3233.1269 3235.1881
Frequencies -- 3237.4690 3239.6311 3239.7516
Frequencies -- 3241.4530 3241.6534 3242.8627
Frequencies -- 3243.7242 3247.5105 3250.0473
Frequencies -- 3258.8232 3349.5619 3608.6537

SCF Done: E(RM062X/DGDZVP) = -3842.65727870
Sum of electronic and zero-point Energies= -3841.753818
Sum of electronic and thermal Energies= -3841.686876
Sum of electronic and thermal Free Energies= -3841.863287
SCF Done: E(RM062X/DGTZVP/SMD) = -3843.43434433

Cat b TS1b_*S*

Center Number	Atomic Number	Atomic Type	Coordinates (Angstroms) X	Y	Z
1	15	0	0.000000	0.000000	0.000000
2	8	0	0.000000	0.000000	1.635973
3	8	0	1.571144	0.000000	-0.374553
4	8	0	-0.546272	1.310179	-0.510647
5	8	0	-0.688819	-1.270068	-0.395588
6	6	0	0.535663	1.122420	2.256090
7	6	0	2.337882	-1.057994	0.108730
8	6	0	1.907113	1.234624	2.447734
9	6	0	-0.312789	2.158626	2.635878
10	6	0	2.940708	-0.955128	1.355287
11	6	0	2.448355	-2.224865	-0.640780
12	6	0	3.009281	0.203187	2.328028
13	6	0	2.431152	2.443657	2.913597
14	6	0	0.219109	3.335395	3.160188
15	6	0	3.623184	-2.060445	1.867900
16	6	0	3.199522	-3.289413	-0.146103
17	6	0	3.182914	-0.561612	3.668910
18	6	0	4.233921	1.118492	2.074371
19	6	0	3.954336	2.409325	2.884567
20	6	0	1.602630	3.503831	3.291269
21	1	0	-0.446075	4.140842	3.464668
22	6	0	3.995200	-1.834992	3.327383
23	6	0	3.800417	-3.224691	1.116139
24	1	0	3.308773	-4.194073	-0.738139
25	1	0	3.660315	0.049443	4.441299
26	1	0	2.194701	-0.854132	4.037677
27	1	0	5.177042	0.640045	2.356112
28	1	0	4.283607	1.359164	1.007601
29	1	0	4.337762	2.296409	3.906517
30	6	0	4.576134	3.653962	2.285649
31	6	0	2.170936	4.772649	3.821995
32	1	0	5.070066	-1.636595	3.423068
33	6	0	3.642037	-3.018852	4.205443
34	6	0	4.594167	-4.361959	1.656327
35	6	0	4.258155	4.048564	0.980818
36	6	0	5.451392	4.446588	3.030366
37	6	0	2.121208	5.939270	3.053065
38	6	0	2.785872	4.807063	5.077059
39	6	0	2.337228	-3.527493	4.195333
40	6	0	4.602724	-3.649550	4.996124
41	6	0	3.984708	-5.581745	1.967130
42	6	0	5.961957	-4.202404	1.902758
43	6	0	4.808813	5.206580	0.436277
44	1	0	3.567630	3.446977	0.391456
45	6	0	5.990389	5.616548	2.495428
46	1	0	5.697382	4.157818	4.049569
47	6	0	2.700542	7.117203	3.520665
48	1	0	1.654187	5.906819	2.071281
49	6	0	3.354543	5.988879	5.551885
50	1	0	2.814610	3.903459	5.681696
51	6	0	2.004206	-4.644363	4.956607
52	1	0	1.582861	-3.060790	3.563548
53	6	0	4.274724	-4.772808	5.757451
54	1	0	5.624338	-3.276335	4.997544
55	6	0	4.726735	-6.616250	2.534810
56	1	0	2.918550	-5.703734	1.794003
57	6	0	6.708088	-5.240482	2.459010
58	1	0	6.439976	-3.257957	1.652897
59	6	0	5.670839	6.000613	1.194471
60	1	0	4.573770	5.489946	-0.585578
61	1	0	6.654389	6.228821	3.098162
62	6	0	3.320370	7.144734	4.770820
63	1	0	2.676692	8.010644	2.903216
64	1	0	3.826373	6.007137	6.529925
65	6	0	2.974793	-5.274685	5.738566
66	1	0	0.989564	-5.030639	4.931685
67	1	0	5.039509	-5.260957	6.354163
68	6	0	6.089275	-6.447632	2.784787
69	1	0	4.237215	-7.550226	2.793728
70	1	0	7.770042	-5.105333	2.641755
71	1	0	6.091927	6.907987	0.772451
72	1	0	3.772469	8.062136	5.135475
73	1	0	2.718802	-6.151875	6.324940
74	1	0	6.664578	-7.253145	3.230979
75	1	0	-2.252159	-1.304869	-0.242882
76	8	0	-3.238918	-1.048958	-0.315514
77	6	0	-3.421630	-0.434324	-1.612538
78	6	0	-3.773061	0.991326	-1.144266
79	1	0	-2.483386	-0.456599	-2.173331
80	1	0	-4.210122	-0.951938	-2.159081
81	8	0	-2.947503	1.975254	-1.690961
82	6	0	-3.490383	0.679740	0.352937
83	6	0	-5.223490	1.367080	-1.367703
84	1	0	-2.016216	1.689086	-1.574824
85	1	0	-4.288134	0.395712	1.028744
86	1	0	-2.497824	0.787029	0.769815
87	6	0	-5.564139	2.576423	-1.970993
88	6	0	-6.232908	0.490706	-0.956813
89	6	0	-6.906529	2.907682	-2.156510
90	1	0	-4.774759	3.249491	-2.286503
91	6	0	-7.572709	0.825317	-1.137707
92	1	0	-5.976015	-0.461508	-0.492871
93	6	0	-7.912471	2.037708	-1.739333
94	1	0	-7.166142	3.851816	-2.625527
95	1	0	-8.349297	0.140228	-0.812107
96	1	0	-8.956029	2.300371	-1.882476
97	1	0	-1.229040	2.747167	0.069163
98	7	0	-1.524899	3.714627	0.307594
99	6	0	-2.705312	4.006900	0.860179
100	6	0	-0.653146	4.775364	0.110357
101	16	0	-3.964884	2.956672	1.241458
102	16	0	-2.800600	5.726941	1.192250
103	6	0	-1.194914	5.990508	0.541437
104	6	0	0.614843	4.698139	-0.465661
105	6	0	-0.476388	7.177131	0.395693
106	6	0	1.319451	5.886292	-0.621499
107	1	0	1.008400	3.736676	-0.784844

108	6	0	0.781862	7.111560	-0.197554
109	1	0	-0.886748	8.124412	0.729920
110	1	0	2.304540	5.865274	-1.073909
111	1	0	-1.388354	2.034194	2.524605
112	1	0	1.932432	-2.286363	-1.593439
113	1	0	1.356476	8.022799	-0.327555

Frequencies -- -551.3082 11.4255 16.8705
Frequencies -- 18.8554 24.8882 29.1649
Frequencies -- 33.1426 36.4211 36.8854
Frequencies -- 45.1772 50.8296 55.6331
Frequencies -- 56.5464 61.3090 63.0220
Frequencies -- 67.2065 69.9126 77.2147
Frequencies -- 77.4810 82.2687 83.0798
Frequencies -- 90.6767 93.4105 95.2208
Frequencies -- 107.6663 114.1708 121.1726
Frequencies -- 128.9696 133.3957 150.3469
Frequencies -- 163.0046 168.1643 178.8419
Frequencies -- 185.5186 192.2169 193.4189
Frequencies -- 205.7507 214.4970 226.9680
Frequencies -- 232.1842 240.3713 241.7539
Frequencies -- 249.7436 256.5519 270.5496
Frequencies -- 275.8069 280.1772 293.2751
Frequencies -- 297.5127 300.1951 307.6656
Frequencies -- 309.9414 335.1026 351.0721
Frequencies -- 354.0328 385.4807 390.9976
Frequencies -- 394.9181 405.8226 407.2998
Frequencies -- 408.6948 409.5498 411.4163
Frequencies -- 413.4232 418.2831 418.4471
Frequencies -- 428.6219 429.4348 433.3777
Frequencies -- 438.7741 454.0561 456.0592
Frequencies -- 472.9498 492.9442 507.4842
Frequencies -- 509.5132 516.1330 520.2876
Frequencies -- 531.0801 534.3359 538.4504
Frequencies -- 543.5424 558.2160 565.9310
Frequencies -- 574.0243 575.7059 584.1726
Frequencies -- 595.9591 608.3766 613.5775
Frequencies -- 617.3478 623.0307 625.2530
Frequencies -- 628.8878 628.9317 631.8394
Frequencies -- 637.1481 639.3562 654.7941
Frequencies -- 659.9733 664.5618 670.4184
Frequencies -- 680.5521 683.0100 693.3374
Frequencies -- 695.3628 707.9606 712.2936
Frequencies -- 713.4651 716.6396 718.3757
Frequencies -- 719.8810 725.2742 729.2203
Frequencies -- 733.6054 737.2771 747.8982
Frequencies -- 759.7774 772.6654 775.4707
Frequencies -- 777.1179 777.3845 787.9007
Frequencies -- 799.5768 817.7798 825.0761
Frequencies -- 845.9614 847.8729 852.3920
Frequencies -- 862.2181 864.3638 868.5190
Frequencies -- 869.9251 872.3074 874.0717
Frequencies -- 875.2745 885.8297 893.4606
Frequencies -- 896.7789 899.0820 926.5214
Frequencies -- 932.5394 934.3675 936.9247
Frequencies -- 939.8742 940.3512 944.1633
Frequencies -- 950.1128 953.4337 959.2908
Frequencies -- 967.7672 983.1536 986.5824
Frequencies -- 989.1193 992.2010 995.8840
Frequencies -- 997.5887 998.0719 999.5123
Frequencies -- 1005.7330 1007.7338 1008.7501
Frequencies -- 1008.8285 1010.0845 1014.7203
Frequencies -- 1018.9957 1019.9298 1019.9810
Frequencies -- 1019.9979 1020.0430 1023.4793
Frequencies -- 1041.2700 1042.9230 1049.0641
Frequencies -- 1051.9927 1057.3489 1061.5735
Frequencies -- 1061.7586 1067.9060 1068.5907
Frequencies -- 1069.6853 1072.1586 1077.6421
Frequencies -- 1085.0225 1098.4365 1100.4180
Frequencies -- 1104.0999 1108.5637 1109.4309
Frequencies -- 1109.9586 1115.6916 1118.0006
Frequencies -- 1122.4037 1123.0426 1133.8906
Frequencies -- 1137.7863 1155.7893 1173.2853
Frequencies -- 1175.6987 1176.2400 1178.6003
Frequencies -- 1181.3359 1182.7264 1183.8491
Frequencies -- 1187.1170 1199.4478 1199.8760
Frequencies -- 1201.4153 1208.2060 1208.5668
Frequencies -- 1210.3298 1210.7373 1212.8417
Frequencies -- 1224.6148 1230.6229 1232.9914
Frequencies -- 1236.8016 1243.3241 1252.8488
Frequencies -- 1263.0338 1278.3067 1286.9818
Frequencies -- 1292.4414 1292.9983 1295.4441
Frequencies -- 1297.9771 1309.4287 1310.6529
Frequencies -- 1312.0900 1324.9780 1325.6429
Frequencies -- 1335.4437 1336.7659 1340.5262
Frequencies -- 1344.1779 1344.9289 1356.7796
Frequencies -- 1357.6857 1357.7241 1366.0276
Frequencies -- 1366.5958 1367.9115 1368.1613
Frequencies -- 1374.1234 1375.5855 1382.8033
Frequencies -- 1392.1873 1392.8890 1437.9232
Frequencies -- 1454.9264 1456.4374 1468.3001
Frequencies -- 1470.1141 1481.5467 1490.6522
Frequencies -- 1491.1811 1499.3092 1500.6891
Frequencies -- 1502.2060 1505.7840 1509.3049
Frequencies -- 1518.3160 1525.9928 1527.3101
Frequencies -- 1529.5736 1547.7294 1548.0121
Frequencies -- 1553.4980 1561.3521 1563.9334
Frequencies -- 1568.3828 1667.0979 1668.0577
Frequencies -- 1672.5210 1676.0932 1678.6774
Frequencies -- 1679.7818 1681.5600 1681.6725
Frequencies -- 1682.9827 1689.5634 1689.9591
Frequencies -- 1696.8653 1698.7932 1699.4342
Frequencies -- 1702.5301 1703.2226 2812.0922
Frequencies -- 3069.7329 3072.8123 3088.5223
Frequencies -- 3089.6319 3120.3374 3152.5139
Frequencies -- 3155.1438 3168.4648 3178.3653
Frequencies -- 3188.9759 3191.8674 3196.8089
Frequencies -- 3198.1601 3199.1163 3205.5653
Frequencies -- 3207.8112 3209.1790 3209.8980
Frequencies -- 3213.3659 3214.4475 3215.1686
Frequencies -- 3217.4738 3217.6261 3219.1102
Frequencies -- 3219.1517 3222.3777 3222.7520
Frequencies -- 3223.3603 3224.9021 3225.5544
Frequencies -- 3226.3477 3228.2440 3228.9897
Frequencies -- 3231.6576 3235.9143 3237.5038
Frequencies -- 3240.7487 3242.0259 3243.1585
Frequencies -- 3244.6144 3245.2420 3249.1612
Frequencies -- 3249.7938 3362.3208 3602.2240

SCF Done: E(RM062X/DGDZVP) = -3842.65836648
Sum of electronic and zero-point Energies= -3841.755729
Sum of electronic and thermal Energies= -3841.688686
Sum of electronic and thermal Free Energies= -3841.864539
SCF Done: E(RM062X/DGTZVP/SMD) = -3843.43328230

Cat b TS1c_*S*

Center Number	Atomic Number	Atomic Type	Coordinates (Angstroms) X	Y	Z

1	15	0	0.000000	0.000000	0.000000
2	8	0	0.000000	0.000000	1.615391
3	8	0	1.589075	0.000000	-0.383170
4	8	0	-0.553265	1.261291	-0.587483
5	8	0	-0.616781	-1.317667	-0.401766
6	6	0	0.625577	1.071690	2.248234
7	6	0	2.339797	-1.100113	0.007261
8	6	0	1.982622	1.005632	2.535890
9	6	0	-0.107910	2.218486	2.535567
10	6	0	2.859351	-1.177319	1.293277
11	6	0	2.538071	-2.142434	-0.894076
12	6	0	2.979269	-0.124502	2.375741
13	6	0	2.611702	2.131486	3.072250
14	6	0	0.520469	3.301050	3.148161
15	6	0	3.483814	-2.358474	1.703415
16	6	0	3.217594	-3.290520	-0.489778
17	6	0	3.066306	-1.021484	3.637077
18	6	0	4.295776	0.683211	2.204556
19	6	0	4.125014	1.957577	3.067011
20	6	0	1.891371	3.275145	3.427181
21	1	0	-0.054798	4.187622	3.400378
22	6	0	3.842088	-2.282499	3.182620
23	6	0	3.689922	-3.422569	0.821262
24	1	0	3.383200	-4.098105	-1.199693
25	1	0	3.544745	-0.512656	4.479581
26	1	0	2.053489	-1.303476	3.942879
27	1	0	5.182152	0.102838	2.478335
28	1	0	4.396220	0.971772	1.153532
29	1	0	4.499694	1.783356	4.083332
30	6	0	4.835866	3.165360	2.488380
31	6	0	2.576699	4.425632	4.075890
32	1	0	4.920654	-2.107710	3.286144
33	6	0	3.496712	-3.533618	3.963135
34	6	0	4.416807	-4.647100	1.254650
35	6	0	4.462442	3.648811	1.228042
36	6	0	5.823147	3.844143	3.203218
37	6	0	2.694600	5.659232	3.427817
38	6	0	3.159286	4.260519	5.337542
39	6	0	2.178801	-4.002340	4.013622
40	6	0	4.490787	-4.260088	4.621910
41	6	0	3.732042	-5.851805	1.437193
42	6	0	5.789657	-4.594291	1.515589
43	6	0	5.059821	4.788933	0.698585
44	1	0	3.675715	3.143603	0.669723
45	6	0	6.421591	4.990965	2.678114
46	1	0	6.109305	3.490014	4.191054
47	6	0	3.402011	6.702877	4.022939
48	1	0	2.260716	5.784373	2.439141
49	6	0	3.857700	5.306568	5.938339
50	1	0	3.058996	3.304713	5.846729
51	6	0	1.866689	-5.166536	4.712915
52	1	0	1.394101	-3.456372	3.491979
53	6	0	4.185540	-5.435282	5.307726
54	1	0	5.521036	-3.914553	4.577414
55	6	0	4.405512	-6.981629	1.898556
56	1	0	2.662203	-5.888062	1.244131
57	6	0	6.466809	-5.727014	1.966488
58	1	0	6.325566	-3.660496	1.361452
59	6	0	6.040441	5.467991	1.425464
60	1	0	4.752379	5.155128	-0.276451
61	1	0	7.176303	5.517162	3.254954
62	6	0	3.988187	6.528195	5.277440
63	1	0	3.508015	7.648671	3.500270
64	1	0	4.302335	5.167516	6.919330
65	6	0	2.869846	-5.892124	5.357277
66	1	0	0.837451	-5.510034	4.764448
67	1	0	4.976768	-5.993616	5.798955
68	6	0	5.773925	-6.920991	2.167585
69	1	0	3.859029	-7.906641	2.058822
70	1	0	7.533617	-5.676927	2.163449
71	1	0	6.499567	6.363884	1.018682
72	1	0	4.541536	7.340868	5.738121
73	1	0	2.625991	-6.802739	5.895779
74	1	0	6.297703	-7.800580	2.529551
75	1	0	-0.811877	1.237116	-2.144171
76	8	0	-1.129899	0.950254	-3.071442
77	6	0	-2.420891	0.317848	-2.904052
78	6	0	-2.037250	-1.106092	-3.349990
79	1	0	-2.718380	0.346812	-1.852638
80	1	0	-3.162208	0.818192	-3.527507
81	8	0	-2.343624	-2.085186	-2.403812
82	6	0	-0.521604	-0.772664	-3.461811
83	6	0	-2.613749	-1.506197	-4.692788
84	1	0	-2.001580	-1.783475	-1.535341
85	1	0	-0.076871	-0.498527	-4.411152
86	1	0	0.137401	-0.858178	-2.608017
87	6	0	-3.227659	-2.746212	-4.862782
88	6	0	-2.515350	-0.628546	-5.777051
89	6	0	-3.736029	-3.105695	-6.110832
90	1	0	-3.295193	-3.421315	-4.017103
91	6	0	-3.020187	-0.990646	-7.023874
92	1	0	-2.042540	0.345449	-5.652481
93	6	0	-3.632928	-2.233063	-7.192875
94	1	0	-4.209355	-4.074357	-6.238614
95	1	0	-2.937820	-0.303562	-7.860259
96	1	0	-4.026759	-2.518115	-8.163533
97	1	0	-0.163316	-2.749108	-1.161905
98	7	0	0.015541	-3.724365	-1.475847
99	6	0	0.233928	-4.062691	-2.749498
100	6	0	0.083399	-4.746241	-0.541331
101	16	0	0.248483	-3.059994	-4.101157
102	16	0	0.549642	-5.785361	-2.862535
103	6	0	0.365548	-5.982692	-1.129977
104	6	0	-0.112227	-4.610700	0.833075
105	6	0	0.441110	-7.136332	-0.349164
106	6	0	-0.047585	-5.765968	1.603342
107	1	0	-0.315804	-3.630702	1.257955
108	6	0	0.222320	-7.014196	1.020905
109	1	0	0.657140	-8.101403	-0.795713
110	1	0	-0.205307	-5.701213	2.674014
111	1	0	2.169504	-2.042006	-1.913172
112	1	0	-1.157818	2.249246	2.263298
113	1	0	0.268908	-7.898590	1.647894

Frequencies --	-550.4680	15.0536	18.3299
Frequencies --	21.3497	25.8595	32.5099
Frequencies --	35.9578	37.5800	43.7581
Frequencies --	43.9935	51.6410	58.0689
Frequencies --	59.4875	65.3430	67.4357
Frequencies --	70.3083	72.8181	78.5221
Frequencies --	80.2129	84.1298	91.3177
Frequencies --	93.4051	97.4063	99.5105
Frequencies --	114.1915	117.1154	121.5759
Frequencies --	130.5529	137.5501	150.0111
Frequencies --	163.5884	169.6330	181.7332
Frequencies --	189.1263	193.2901	197.6020
Frequencies --	206.7836	215.3612	226.9782
Frequencies --	232.9651	240.2553	243.0599
Frequencies --	251.3020	257.7945	271.3404
Frequencies --	276.2701	280.9448	292.7332
Frequencies --	297.3359	302.3314	308.8142

Frequencies --	309.4999	333.9401	352.9562
Frequencies --	354.7359	386.6714	392.0680
Frequencies --	396.0379	406.8722	408.8800
Frequencies --	410.7192	412.1718	413.6843
Frequencies --	416.5310	420.1607	421.1822
Frequencies --	428.9706	431.5573	435.7274
Frequencies --	438.7534	454.1363	458.4675
Frequencies --	473.2010	493.2484	507.7284
Frequencies --	510.3631	516.7122	523.9324
Frequencies --	529.7062	536.2959	539.6585
Frequencies --	544.3247	558.2039	566.1188
Frequencies --	575.4236	576.5009	584.4632
Frequencies --	596.2445	609.3712	614.1290
Frequencies --	618.4841	623.4565	625.8917
Frequencies --	627.9074	629.5186	631.8093
Frequencies --	637.0754	640.9574	655.0182
Frequencies --	659.7231	665.9626	670.6371
Frequencies --	681.4934	684.4364	695.0432
Frequencies --	704.6601	712.7759	715.4162
Frequencies --	717.6469	721.3465	721.4669
Frequencies --	723.9074	725.3109	730.0078
Frequencies --	736.2047	738.0943	748.2267
Frequencies --	762.6645	773.8548	775.8796
Frequencies --	779.2043	780.2688	789.0648
Frequencies --	801.0697	818.5425	826.3998
Frequencies --	849.8636	852.5034	866.7285
Frequencies --	867.6684	870.8805	871.3971
Frequencies --	878.0748	880.2655	881.6525
Frequencies --	881.8348	887.7669	895.2239
Frequencies --	898.1323	900.9121	930.9715
Frequencies --	936.3198	938.3345	940.5586
Frequencies --	942.9611	947.6575	949.5457
Frequencies --	954.3918	955.6182	963.2474
Frequencies --	974.9825	991.6251	993.9779
Frequencies --	995.1508	997.0208	999.5323
Frequencies --	1000.6649	1005.3458	1005.5216
Frequencies --	1008.4775	1008.6954	1010.6864
Frequencies --	1013.4948	1014.6656	1019.4386
Frequencies --	1019.5704	1019.7573	1020.3496
Frequencies --	1020.6296	1021.2672	1026.2052
Frequencies --	1041.9652	1043.8727	1050.3781
Frequencies --	1052.5357	1057.4462	1061.7466
Frequencies --	1064.3276	1069.0294	1069.9192
Frequencies --	1071.8533	1074.8850	1080.0159
Frequencies --	1086.8045	1100.8203	1102.9558
Frequencies --	1105.6547	1108.9848	1110.1538
Frequencies --	1112.7034	1116.6512	1117.5322
Frequencies --	1122.3959	1125.6169	1136.5497
Frequencies --	1142.0949	1158.2197	1174.8166
Frequencies --	1176.1612	1178.0450	1178.2553
Frequencies --	1180.2613	1182.6249	1186.8881
Frequencies --	1190.5793	1200.6017	1203.2749
Frequencies --	1204.9759	1206.3914	1211.5738
Frequencies --	1211.6601	1214.6031	1214.7989
Frequencies --	1225.4941	1230.7506	1235.2275
Frequencies --	1235.3737	1243.3796	1253.8790
Frequencies --	1263.7100	1280.7892	1289.7946
Frequencies --	1293.3427	1294.0413	1295.6762
Frequencies --	1297.9398	1311.4818	1313.9081
Frequencies --	1315.3835	1325.7605	1327.5503
Frequencies --	1336.0423	1338.0007	1342.1936
Frequencies --	1344.5503	1344.8031	1358.3037
Frequencies --	1358.9311	1359.0630	1365.2258
Frequencies --	1366.4143	1367.2165	1368.1391
Frequencies --	1375.2452	1376.1382	1382.1371
Frequencies --	1389.8583	1394.3887	1438.3808
Frequencies --	1457.8875	1458.9870	1472.4070
Frequencies --	1474.9892	1482.7436	1490.3304
Frequencies --	1493.2546	1499.1861	1500.2616
Frequencies --	1501.5202	1505.6211	1509.7058
Frequencies --	1518.2821	1527.6411	1529.8650
Frequencies --	1531.4205	1545.6182	1548.0625
Frequencies --	1554.4498	1564.5365	1566.5045
Frequencies --	1569.3913	1666.3653	1669.5559
Frequencies --	1673.0069	1675.2055	1677.3423
Frequencies --	1678.4810	1681.2255	1683.3366
Frequencies --	1684.0246	1687.6015	1690.7479
Frequencies --	1697.9182	1699.5005	1700.2056
Frequencies --	1701.9976	1702.2818	2832.2765
Frequencies --	3072.3430	3075.6490	3090.5037
Frequencies --	3093.1120	3128.5516	3155.6189
Frequencies --	3157.3672	3158.0864	3192.7904
Frequencies --	3196.0775	3196.9260	3197.8182
Frequencies --	3198.8232	3199.0994	3205.7587
Frequencies --	3206.7544	3207.1018	3208.2968
Frequencies --	3210.9531	3213.5779	3215.6917
Frequencies --	3216.2714	3217.4602	3218.2383
Frequencies --	3223.2282	3224.2102	3224.7446
Frequencies --	3227.5016	3227.9670	3228.1609
Frequencies --	3228.6049	3231.7326	3232.1609
Frequencies --	3233.7300	3235.1146	3236.4430
Frequencies --	3241.2955	3241.3883	3243.8859
Frequencies --	3245.4994	3253.6201	3255.3749
Frequencies --	3256.1954	3362.0819	3626.9469

SCF Done: E(RM062X/DGDZVP) = -3842.65863965
Sum of electronic and zero-point Energies= -3841.754507
Sum of electronic and thermal Energies= -3841.687804
Sum of electronic and thermal Free Energies= -3841.861642
SCF Done: E(RM062X/DGTZVP/SMD) = -3843.43304769

Cat b TS1d_*R*

Center Number	Atomic Number	Atomic Type	Coordinates (Angstroms) X	Y	Z
1	15	0	0.000000	0.000000	0.000000
2	8	0	0.000000	0.000000	1.625213
3	8	0	1.583630	0.000000	-0.353781
4	8	0	-0.580426	1.272123	-0.538482
5	8	0	-0.624872	-1.311154	-0.406602
6	6	0	0.611963	1.092086	2.239017
7	6	0	2.286071	-1.124241	0.070825
8	6	0	1.977425	1.068599	2.491754
9	6	0	-0.141630	2.224439	2.533390
10	6	0	2.857518	-1.153403	1.335596
11	6	0	2.359780	-2.238936	-0.759540
12	6	0	2.997337	-0.043554	2.354324
13	6	0	2.592672	2.217941	2.991856
14	6	0	0.475049	3.333145	3.110734
15	6	0	3.464336	-2.329668	1.797967
16	6	0	3.029777	-3.375569	-0.320305
17	6	0	3.111124	-0.867922	3.658317
18	6	0	4.290757	0.782484	2.126066
19	6	0	4.108948	2.072831	2.963079
20	6	0	1.853906	3.349073	3.347845
21	1	0	-0.116579	4.207575	3.367385
22	6	0	3.865966	-2.160085	3.264024
23	6	0	3.593916	-3.449903	0.963561
24	1	0	3.122948	-4.226738	-0.988885
25	1	0	3.611816	-0.319846	4.462460

26	1	0	2.104920	-1.127229	4.003328
27	1	0	5.195617	0.228197	2.394055
28	1	0	4.359254	1.046387	1.065886
29	1	0	4.501106	1.924920	3.976979
30	6	0	4.791574	3.281858	2.355576
31	6	0	2.529401	4.523685	3.963499
32	1	0	4.945830	-1.980286	3.334782
33	6	0	3.513779	-3.324138	4.165129
34	6	0	4.325522	-4.682102	1.360262
35	6	0	4.394246	3.743488	1.094483
36	6	0	5.779473	3.982637	3.047991
37	6	0	2.620005	5.746450	3.291160
38	6	0	3.132496	4.390121	5.219193
39	6	0	2.198176	-3.795748	4.210173
40	6	0	4.470897	-3.932584	4.979211
41	6	0	3.806428	-5.950401	1.068281
42	6	0	5.577188	-4.602362	1.982189
43	6	0	4.969958	4.884347	0.542500
44	1	0	3.606884	3.220696	0.553547
45	6	0	6.356373	5.129570	2.500201
46	1	0	6.083318	3.644767	4.036216
47	6	0	3.320925	6.810692	3.856930
48	1	0	2.170400	5.847650	2.306772
49	6	0	3.824467	5.456657	5.790640
50	1	0	3.053593	3.442373	5.746898
51	6	0	1.848776	-4.861330	5.035939
52	1	0	1.438328	-3.326439	3.587110
53	6	0	4.127588	-4.999031	5.810051
54	1	0	5.499014	-3.577575	4.954116
55	6	0	4.502218	-7.105292	1.420263
56	1	0	2.846363	-6.035215	0.564905
57	6	0	6.279030	-5.754425	2.327628
58	1	0	6.014066	-3.626326	2.176030
59	6	0	5.951859	5.585047	1.246781
60	1	0	4.644963	5.234099	-0.432844
61	1	0	7.112438	5.672333	3.059631
62	6	0	3.927678	6.667509	5.105637
63	1	0	3.405415	7.748090	3.315534
64	1	0	4.284904	5.341528	6.767431
65	6	0	2.815636	-5.470125	5.837621
66	1	0	0.821384	-5.215331	5.050122
67	1	0	4.886911	-5.465968	6.430075
68	6	0	5.739893	-7.011915	2.056316
69	1	0	4.076382	-8.078890	1.197100
70	1	0	7.250709	-5.669589	2.805053
71	1	0	6.394212	6.481015	0.821991
72	1	0	4.475924	7.496357	5.543083
73	1	0	2.547657	-6.303702	6.479450
74	1	0	6.283227	-7.910644	2.330797
75	1	0	-1.886548	1.325503	-1.312147
76	8	0	-2.729697	1.111933	-1.861465
77	6	0	-2.351922	0.202117	-2.919760
78	6	0	-3.155402	-1.025440	-2.447956
79	1	0	-2.648824	0.611552	-3.885581
80	1	0	-1.274169	0.018482	-2.897578
81	8	0	-2.390173	-2.184986	-2.319145
82	6	0	-3.557319	-0.357688	-1.099871
83	6	0	-4.373067	-1.316622	-3.301536
84	1	0	-1.573758	-1.956606	-1.826156
85	1	0	-2.908414	-0.414137	-0.234093
86	1	0	-4.516321	0.128499	-0.973475
87	6	0	-4.642422	-2.611860	-3.740100
88	6	0	-5.241731	-0.275337	-3.644424
89	6	0	-5.773601	-2.862495	-4.516883
90	1	0	-3.966345	-3.412816	-3.462892
91	6	0	-6.373248	-0.528201	-4.416394
92	1	0	-5.036867	0.741682	-3.310377
93	6	0	-6.641338	-1.825370	-4.855194
94	1	0	-5.979561	-3.873765	-4.854024
95	1	0	-7.042350	0.286078	-4.676538
96	1	0	-7.522306	-2.025674	-5.457122
97	1	0	1.375398	-5.421738	2.176572
98	6	0	0.310240	-5.379609	1.969031
99	6	0	-0.227882	-4.230328	1.400273
100	6	0	-0.500630	-6.476096	2.299534
101	6	0	-1.604429	-4.211804	1.173537
102	1	0	0.386481	-3.371031	1.133538
103	6	0	-1.873672	-6.449895	2.068747
104	7	0	-2.330815	-3.163628	0.620034
105	6	0	-2.419617	-5.300951	1.497834
106	1	0	-2.499004	-7.298791	2.325489
107	6	0	-3.646733	-3.362102	0.468455
108	1	0	-1.828962	-2.320192	0.286078
109	16	0	-4.083325	-4.948984	1.071372
110	16	0	-4.786790	-2.314896	-0.182878
111	1	0	-1.199887	2.226507	2.293846
112	1	0	1.887725	-2.201501	-1.735903
113	1	0	-0.050494	-7.357418	2.745355

Frequencies --	-552.0767	5.2420	17.2492
Frequencies --	20.5026	22.0478	24.8205
Frequencies --	29.4406	31.3085	33.1234
Frequencies --	38.9704	43.5088	46.9708
Frequencies --	54.1368	57.7411	62.7327
Frequencies --	65.0232	69.1898	78.0490
Frequencies --	81.0418	89.4592	91.3351
Frequencies --	92.9733	98.9127	99.1619
Frequencies --	103.4471	113.9562	125.2369
Frequencies --	126.1241	131.6957	157.9127
Frequencies --	162.3587	170.1609	182.4592
Frequencies --	185.7412	191.3260	196.3646
Frequencies --	209.9996	215.0181	219.4835
Frequencies --	227.9607	232.3487	241.0595
Frequencies --	250.4036	260.3142	271.7328
Frequencies --	278.2090	283.4552	291.7094
Frequencies --	294.6652	305.5375	312.5884
Frequencies --	322.7372	334.3929	352.3720
Frequencies --	365.3297	385.6892	386.7269
Frequencies --	395.5273	405.0751	408.9836
Frequencies --	412.2042	413.0679	414.2908
Frequencies --	416.1511	418.5159	419.4532
Frequencies --	422.2806	435.0274	437.8154
Frequencies --	443.9155	452.9219	462.7903
Frequencies --	472.5053	495.8658	507.3898
Frequencies --	508.8360	513.4525	524.1191
Frequencies --	532.1587	537.6251	539.4909
Frequencies --	544.0565	555.0042	567.3071
Frequencies --	573.7267	576.8240	587.3243
Frequencies --	597.7316	609.9332	614.6525
Frequencies --	619.5166	624.3396	626.6218
Frequencies --	628.5213	629.6341	633.1819
Frequencies --	638.3831	640.8278	653.2095
Frequencies --	662.7901	664.2446	672.8698
Frequencies --	680.9273	685.2686	694.1679
Frequencies --	704.5586	714.8066	716.6594
Frequencies --	717.3349	720.3519	722.6744
Frequencies --	723.6399	725.4091	732.9486
Frequencies --	738.2858	740.2221	748.8472
Frequencies --	772.1379	775.2002	776.1659
Frequencies --	777.9921	784.4132	785.0616
Frequencies --	800.1086	818.7377	826.2736

Frequencies -- 844.1977 848.0302 866.6704
Frequencies -- 866.7909 869.4607 870.5377
Frequencies -- 871.8296 872.7397 878.7300
Frequencies -- 885.6925 890.2396 894.2034
Frequencies -- 896.2999 901.6227 912.5996
Frequencies -- 932.5332 935.7453 940.3284
Frequencies -- 943.2844 944.1883 948.7679
Frequencies -- 949.5946 950.0910 969.3717
Frequencies -- 971.3497 975.8408 994.0403
Frequencies -- 995.5971 997.6475 998.5582
Frequencies -- 1000.5369 1001.0064 1005.9970
Frequencies -- 1008.9735 1011.1846 1012.5121
Frequencies -- 1012.9272 1015.3172 1018.4893
Frequencies -- 1019.2298 1019.5737 1020.1698
Frequencies -- 1020.5231 1026.3977 1030.6214
Frequencies -- 1043.4067 1045.7303 1050.8543
Frequencies -- 1052.5386 1059.4411 1062.2270
Frequencies -- 1064.4672 1068.0749 1070.3401
Frequencies -- 1072.1129 1079.1700 1086.8482
Frequencies -- 1089.9906 1101.4962 1102.6195
Frequencies -- 1106.1342 1109.9996 1111.4735
Frequencies -- 1117.5803 1117.8191 1120.3948
Frequencies -- 1122.4462 1127.4279 1140.4012
Frequencies -- 1152.4574 1158.4741 1175.7218
Frequencies -- 1177.9434 1178.3823 1178.5829
Frequencies -- 1181.6376 1184.6526 1189.5452
Frequencies -- 1196.3664 1203.2017 1204.8305
Frequencies -- 1207.3941 1209.7159 1213.1332
Frequencies -- 1213.3276 1213.8663 1215.5551
Frequencies -- 1226.8625 1231.8132 1234.4464
Frequencies -- 1235.5785 1244.5622 1256.5957
Frequencies -- 1261.5993 1278.7585 1287.8941
Frequencies -- 1289.0637 1293.9297 1295.5501
Frequencies -- 1298.1862 1305.5631 1309.6652
Frequencies -- 1313.4025 1324.5014 1326.3205
Frequencies -- 1334.2558 1338.1032 1342.7207
Frequencies -- 1344.9393 1345.5050 1347.9965
Frequencies -- 1357.4379 1362.0709 1364.8432
Frequencies -- 1367.9251 1369.4705 1371.1113
Frequencies -- 1372.7405 1378.2756 1383.9419
Frequencies -- 1386.8263 1388.8221 1441.1532
Frequencies -- 1451.3884 1464.1632 1469.1224
Frequencies -- 1475.3377 1479.4434 1490.3460
Frequencies -- 1495.2060 1498.8656 1501.4713
Frequencies -- 1501.5537 1505.4269 1509.3208
Frequencies -- 1512.6071 1528.6286 1529.3758
Frequencies -- 1531.5548 1546.3705 1551.2592
Frequencies -- 1555.2368 1559.3871 1563.5578
Frequencies -- 1568.7252 1662.3953 1664.5643
Frequencies -- 1672.2432 1676.7472 1678.2448
Frequencies -- 1679.2131 1682.0114 1682.1528
Frequencies -- 1684.1337 1687.1233 1691.7958
Frequencies -- 1698.2335 1699.3204 1701.0107
Frequencies -- 1702.3032 1702.5795 2698.8358
Frequencies -- 3073.5321 3074.8948 3089.1919
Frequencies -- 3090.3582 3119.1289 3153.9746
Frequencies -- 3156.4886 3184.3325 3192.3029
Frequencies -- 3197.6784 3198.1548 3200.6265
Frequencies -- 3204.5064 3205.1120 3207.5609
Frequencies -- 3210.3682 3214.2512 3214.3311
Frequencies -- 3214.9813 3215.3476 3216.5764
Frequencies -- 3216.8092 3220.2040 3221.9524
Frequencies -- 3223.0664 3224.5383 3224.6312
Frequencies -- 3225.4291 3226.7463 3230.1254
Frequencies -- 3230.9078 3232.2186 3235.0888
Frequencies -- 3236.6774 3237.6071 3237.9849
Frequencies -- 3239.1073 3239.6288 3242.9018
Frequencies -- 3243.8772 3246.4005 3248.6883
Frequencies -- 3251.1052 3358.3602 3618.2220

SCF Done: E(RM062X/DGDZVP) = -3842.65693498
Sum of electronic and zero-point Energies= -3841.753274
Sum of electronic and thermal Energies= -3841.686352
Sum of electronic and thermal Free Energies= -3841.863671
SCF Done: E(RM062X/DGTZVP/SMD) = -3843.43435353

Cat f

Center Number	Atomic Number	Atomic Type	Coordinates (Angstroms) X	Y	Z
1	15	0	0.604621	0.259730	0.141339
2	8	0	0.409991	0.469504	1.698272
3	8	0	2.168469	-0.102282	0.187089
4	1	0	-0.473725	0.784098	1.978407
5	8	0	-0.087600	-1.160711	-0.242096
6	8	0	0.146839	1.327412	-0.748551
7	6	0	2.727037	-0.868472	-0.836261
8	6	0	-0.135067	-2.069568	0.812939
9	6	0	2.747688	-2.252972	-0.724016
10	6	0	3.219831	-0.234957	-1.977510
11	6	0	0.970421	-2.821418	1.153816
12	6	0	-1.290106	-2.079597	1.598339
13	6	0	2.216578	-3.160719	0.367917
14	6	0	3.287369	-3.002794	-1.769496
15	6	0	3.823955	-1.003929	-2.972969
16	6	0	3.002156	1.223259	-2.147958
17	6	0	0.982448	-3.474621	2.386890
18	6	0	-1.290899	-2.801871	2.789506
19	6	0	-2.470720	-1.365844	1.040400
20	6	0	3.220228	-3.421027	1.517774
21	6	0	1.949487	-4.461284	-0.443717
22	6	0	2.976200	-4.482434	-1.599253
23	6	0	3.887398	-2.394560	-2.876817
24	1	0	4.233592	-0.505189	-3.847736
25	6	0	3.800515	2.164446	-1.507250
26	6	0	1.915483	1.669942	-2.889034
27	6	0	2.376318	-4.020077	2.677834
28	6	0	-0.140885	-3.481233	3.217611
29	1	0	-2.188925	-2.828102	3.401523
30	6	0	-2.951097	-0.157466	1.528488
31	6	0	-3.052312	-1.878308	-0.120957
32	1	0	4.040458	-4.077665	1.211501
33	1	0	3.651858	-2.467159	1.837178
34	1	0	1.992538	-5.357427	0.182917
35	1	0	0.941650	-4.400329	-0.867557
36	6	0	2.411622	-5.084748	-2.872511
37	1	0	3.873531	-5.041635	-1.308841
38	6	0	4.530410	-3.215927	-3.935706
39	6	0	3.503674	3.517400	-1.591163
40	8	0	4.880477	1.715797	-0.783145
41	6	0	1.586959	3.024832	-2.959233
42	8	0	1.107745	0.731404	-3.487284
43	6	0	2.862968	-3.610941	4.053644
44	1	0	2.375069	-5.115264	2.618942
45	6	0	-0.110780	-4.197509	4.521836
46	6	0	-4.013973	0.514782	0.917998
47	8	0	-2.283046	0.422662	2.597135
48	6	0	-4.103791	-1.221748	-0.744294
49	8	0	-2.544405	-3.052792	-0.615695
50	6	0	1.339401	-4.455446	-3.518888

51	6	0	2.973856	-6.220356	-3.454796
52	6	0	4.043667	-3.210750	-5.246678
53	6	0	5.608594	-4.045780	-3.610197
54	6	0	2.383169	3.962759	-2.301379
55	8	0	4.306446	4.447795	-0.973283
56	6	0	5.327281	2.595193	0.182215
57	8	0	0.460203	3.397904	-3.647738
58	6	0	-0.224798	1.099219	-3.558526
59	6	0	2.879915	-2.256709	4.411009
60	6	0	3.245200	-4.563138	4.998666
61	6	0	-0.129891	-3.484631	5.724726
62	6	0	-0.010074	-5.592014	4.555505
63	6	0	-4.607808	-0.025316	-0.223209
64	8	0	-4.447674	1.713599	1.419267
65	6	0	-3.039073	1.327316	3.332610
66	8	0	-4.692706	-1.729672	-1.871990
67	6	0	-2.912244	-3.363805	-1.908045
68	6	0	0.852469	-4.943878	-4.728337
69	1	0	0.907401	-3.549295	-3.094060
70	6	0	2.484959	-6.717433	-4.664472
71	1	0	3.820374	-6.705752	-2.974726
72	6	0	4.612680	-4.041502	-6.210748
73	1	0	3.193593	-2.581144	-5.497442
74	6	0	6.185615	-4.867620	-4.576346
75	1	0	5.997069	-4.038719	-2.594437
76	6	0	2.109913	5.448514	-2.283622
77	6	0	5.040783	3.956078	0.088808
78	6	0	6.087149	2.108078	1.234817
79	6	0	-0.550577	2.447739	-3.631000
80	6	0	-1.216059	0.130683	-3.536071
81	6	0	3.270957	-1.866815	5.689318
82	1	0	2.559864	-1.503955	3.691147
83	6	0	3.632243	-4.176476	6.282588
84	1	0	3.217176	-5.618657	4.737982
85	6	0	-0.030925	-4.155107	6.942444
86	1	0	-0.188585	-2.399517	5.698882
87	6	0	0.077643	-6.264674	5.773673
88	1	0	-0.005365	-6.148800	3.621320
89	6	0	-5.787355	0.589568	-0.942882
90	6	0	-4.114955	1.971174	2.732205
91	6	0	-2.684547	1.601119	4.643788
92	6	0	-3.974079	-2.711569	-2.530149
93	6	0	-2.222952	-4.367995	-2.572129
94	6	0	1.425846	-6.078651	-5.306989
95	1	0	0.042054	-4.422245	-5.229773
96	1	0	2.945332	-7.592967	-5.112223
97	6	0	5.681243	-4.874519	-5.877158
98	1	0	4.212832	-4.047293	-7.220126
99	1	0	7.026397	-5.502759	-4.314002
100	9	0	1.036069	5.803233	-2.992640
101	9	0	1.913490	5.886258	-1.025790
102	9	0	3.153333	6.138335	-2.781060
103	6	0	5.514090	4.840759	1.046243
104	6	0	6.579464	2.996093	2.191975
105	1	0	6.287235	1.042441	1.280614
106	6	0	-1.873533	2.853708	-3.684304
107	6	0	-2.552583	0.531407	-3.602123
108	1	0	-0.931890	-0.915184	-3.456317
109	6	0	3.645168	-2.827285	6.631824
110	1	0	3.276112	-0.813405	5.953181
111	1	0	3.913271	-4.931246	7.011035
112	6	0	0.075903	-5.546319	6.969525
113	1	0	-0.024295	-3.590299	7.869587
114	1	0	0.150315	-7.347995	5.789032
115	9	0	-6.834603	-0.254404	-0.939001
116	9	0	-5.493983	0.845264	-2.230848
117	9	0	-6.205294	1.735076	-0.402231
118	6	0	-4.852449	2.907840	3.441397
119	6	0	-3.414735	2.552850	5.356446
120	1	0	-1.840051	1.077705	5.081000
121	6	0	-4.347539	-3.047329	-3.822703
122	6	0	-2.607041	-4.724431	-3.865191
123	1	0	-1.403809	-4.868010	-2.063802
124	1	0	1.057163	-6.453797	-6.256870
125	1	0	6.120593	-5.523384	-6.628599
126	6	0	6.294404	4.357630	2.097375
127	1	0	5.270601	5.893353	0.944954
128	1	0	7.183517	2.620103	3.010823
129	6	0	-2.879223	1.885850	-3.676471
130	1	0	-2.094724	3.915210	-3.726236
131	1	0	-3.342540	-0.214891	-3.593602
132	1	0	3.942395	-2.524985	7.631345
133	1	0	0.156019	-6.067417	7.918584
134	6	0	-4.492761	3.202912	4.756177
135	1	0	-5.684757	3.397847	2.947131
136	1	0	-3.139038	2.783707	6.379579
137	6	0	-3.662847	-4.063308	-4.491006
138	1	0	-5.175930	-2.514983	-4.279348
139	1	0	-2.077410	-5.523135	-4.373736
140	1	0	6.675571	5.048605	2.841582
141	1	0	-3.918568	2.192085	-3.719925
142	1	0	-5.059014	3.943147	5.310884
143	1	0	-3.960616	-4.336360	-5.497501

Frequencies --	6.5949	11.0183	12.8363
Frequencies --	21.3281	22.4683	24.6758
Frequencies --	26.8277	29.8956	32.9820
Frequencies --	35.5990	40.0641	41.5891
Frequencies --	44.1985	45.7741	49.1107
Frequencies --	54.5376	56.4049	59.8903
Frequencies --	61.8095	68.7883	70.1778
Frequencies --	73.1274	74.3869	76.7110
Frequencies --	79.5871	83.1208	87.4512
Frequencies --	93.9860	98.4450	98.9431
Frequencies --	101.8198	107.5072	118.4638
Frequencies --	121.7342	123.2292	127.2160
Frequencies --	129.7576	134.8964	139.2514
Frequencies --	154.7359	156.6357	163.2739
Frequencies --	170.1021	177.1527	181.8198
Frequencies --	190.2485	199.4558	203.8871
Frequencies --	211.9638	225.5579	230.3783
Frequencies --	232.6531	239.2671	244.2146
Frequencies --	247.1443	252.1636	268.0910
Frequencies --	269.2060	273.6640	275.2405
Frequencies --	277.9295	287.6285	290.4372
Frequencies --	291.2595	293.2154	295.0864
Frequencies --	299.4554	301.8184	302.3786
Frequencies --	307.2308	311.2750	316.8949
Frequencies --	321.7025	322.6261	327.2434
Frequencies --	330.0108	334.4525	347.3854
Frequencies --	367.0957	391.6637	403.8178
Frequencies --	406.6181	407.7330	409.6516
Frequencies --	414.3334	415.1751	417.1762
Frequencies --	418.1336	421.6280	441.9236
Frequencies --	443.0772	446.1157	447.7454
Frequencies --	449.8407	455.9824	456.6273
Frequencies --	466.5782	469.8898	484.3002
Frequencies --	490.7770	492.7089	501.0407
Frequencies --	505.5321	511.9629	516.5010
Frequencies --	521.2834	527.0236	530.1533
Frequencies --	536.4919	540.0263	543.4772

Frequencies -- 549.6209 555.5957 557.1799
Frequencies -- 558.3109 559.1892 564.4425
Frequencies -- 567.5656 569.4623 582.5970
Frequencies -- 588.5968 596.5473 598.2975
Frequencies -- 600.6716 602.4829 603.7161
Frequencies -- 605.5184 607.3441 608.9022
Frequencies -- 610.4493 617.5090 623.2335
Frequencies -- 624.8420 626.4982 631.2370
Frequencies -- 632.0580 633.9965 635.7907
Frequencies -- 646.2771 648.5785 653.5649
Frequencies -- 662.5912 665.6055 670.1387
Frequencies -- 680.1460 683.0841 702.8534
Frequencies -- 705.8721 712.8522 715.2799
Frequencies -- 715.4815 715.8693 716.4818
Frequencies -- 717.2009 720.7738 723.0324
Frequencies -- 727.4106 731.1988 734.9414
Frequencies -- 740.2823 743.6513 748.9917
Frequencies -- 755.1728 757.3442 768.9814
Frequencies -- 769.6638 770.4806 771.5483
Frequencies -- 774.2550 776.9325 779.4664
Frequencies -- 780.5170 784.9989 790.9371
Frequencies -- 797.0331 800.3661 805.5392
Frequencies -- 807.7348 820.0842 825.3152
Frequencies -- 828.3472 830.1484 857.8641
Frequencies -- 859.2484 862.9967 864.1081
Frequencies -- 866.3855 868.5618 870.4225
Frequencies -- 871.7789 873.0949 882.5993
Frequencies -- 887.6485 889.2213 890.0199
Frequencies -- 896.6662 909.9282 913.4304
Frequencies -- 915.5053 922.7787 931.6894
Frequencies -- 933.8809 934.3274 938.4076
Frequencies -- 942.5893 944.1054 945.6448
Frequencies -- 946.9729 948.4015 948.8867
Frequencies -- 955.8890 960.0686 966.2978
Frequencies -- 971.7662 986.7648 990.5078
Frequencies -- 991.1095 992.9956 993.7390
Frequencies -- 996.8167 998.3259 1002.1234
Frequencies -- 1003.3838 1011.7790 1013.5386
Frequencies -- 1013.6754 1017.5557 1018.5743
Frequencies -- 1019.2779 1019.6315 1020.4973
Frequencies -- 1026.5671 1031.5309 1036.9290
Frequencies -- 1037.9864 1042.6136 1054.5464
Frequencies -- 1057.4283 1063.0334 1063.6586
Frequencies -- 1066.1856 1067.0541 1069.9331
Frequencies -- 1071.5412 1074.3837 1091.8312
Frequencies -- 1101.9385 1107.0587 1110.3921
Frequencies -- 1113.5487 1114.9835 1123.0742
Frequencies -- 1127.2927 1129.5526 1130.4976
Frequencies -- 1135.3233 1136.6601 1166.5229
Frequencies -- 1167.7378 1169.6214 1172.8851
Frequencies -- 1173.6055 1175.7303 1177.6267
Frequencies -- 1179.0590 1179.3450 1180.6952
Frequencies -- 1186.7441 1195.6406 1202.8287
Frequencies -- 1204.9089 1207.1270 1209.7368
Frequencies -- 1212.3017 1215.8834 1216.4496
Frequencies -- 1218.6044 1223.7747 1228.2745
Frequencies -- 1231.5229 1232.6070 1233.4326
Frequencies -- 1234.8829 1241.3943 1246.0046
Frequencies -- 1249.0915 1257.2029 1258.3583
Frequencies -- 1267.0314 1275.9097 1276.4589
Frequencies -- 1291.8037 1293.2931 1296.1357
Frequencies -- 1302.1897 1303.1495 1303.1950
Frequencies -- 1306.8071 1307.4246 1311.6617
Frequencies -- 1313.0541 1314.1207 1316.3567
Frequencies -- 1320.3910 1325.2393 1327.1716
Frequencies -- 1330.4838 1335.0306 1337.4924
Frequencies -- 1340.5085 1350.7364 1357.2523
Frequencies -- 1357.8801 1358.7861 1359.0495
Frequencies -- 1362.0177 1362.5147 1364.2242
Frequencies -- 1364.3292 1370.8719 1372.1259
Frequencies -- 1375.1553 1376.4896 1385.0931
Frequencies -- 1395.3010 1411.4124 1452.6015
Frequencies -- 1463.6624 1472.9155 1475.0095
Frequencies -- 1490.9047 1494.0902 1498.2658
Frequencies -- 1499.7118 1506.1244 1507.1753
Frequencies -- 1508.8995 1509.3158 1510.9408
Frequencies -- 1515.7461 1519.7845 1523.3571
Frequencies -- 1529.9924 1534.8767 1544.8847
Frequencies -- 1550.7662 1555.9609 1557.6548
Frequencies -- 1560.5221 1563.2439 1564.1028
Frequencies -- 1565.6688 1569.4587 1578.2293
Frequencies -- 1666.7503 1667.5712 1671.0349
Frequencies -- 1671.5842 1673.5741 1674.2515
Frequencies -- 1676.2378 1679.2519 1691.3981
Frequencies -- 1693.1502 1695.8643 1696.9360
Frequencies -- 1698.4637 1699.1823 1701.7636
Frequencies -- 1703.0104 1703.7451 1704.0154
Frequencies -- 1704.9391 1707.1902 1722.7488
Frequencies -- 1722.8746 1740.1099 1743.2582
Frequencies -- 3076.5421 3084.2504 3088.5154
Frequencies -- 3089.0875 3151.9215 3155.8392
Frequencies -- 3178.7407 3187.5701 3200.8481
Frequencies -- 3201.5006 3205.2214 3206.6827
Frequencies -- 3211.0629 3211.3322 3211.7900
Frequencies -- 3214.4338 3218.6416 3219.7303
Frequencies -- 3221.7487 3222.3420 3225.2449
Frequencies -- 3225.5625 3227.4548 3228.6386
Frequencies -- 3229.5177 3230.2360 3231.3578
Frequencies -- 3231.8069 3234.4326 3235.0655
Frequencies -- 3237.0613 3237.4737 3239.4862
Frequencies -- 3239.8029 3239.9128 3241.3153
Frequencies -- 3243.1597 3247.3530 3248.0601
Frequencies -- 3253.0982 3253.7827 3254.5759
Frequencies -- 3258.7008 3259.0131 3679.6712

SCF Done: E(RM062X/DGDZVP) = -4879.40731991
Sum of electronic and zero-point Energies= -4878.341618
Sum of electronic and thermal Energies= -4878.250170
Sum of electronic and thermal Free Energies= -4878.478168
SCF Done: E(RM062X/DGTZVP/SMD) = -4880.43072127

Cat f I0_1

Center Number	Atomic Number	Atomic Type	Coordinates (Angstroms) X	Y	Z
1	15	0	0.225185	0.018377	0.027214
2	8	0	0.188651	0.254195	1.620224
3	8	0	1.802781	-0.000227	-0.308670
4	8	0	-0.464117	1.038332	-0.791645
5	8	0	-0.286949	-1.449833	-0.067253
6	6	0	0.833603	1.388863	2.113007
7	6	0	2.512193	-1.081054	0.221307
8	6	0	2.173521	1.310311	2.462953
9	6	0	0.146254	2.602969	2.175213
10	6	0	2.988511	-1.033013	1.519379
11	6	0	2.620189	-2.245556	-0.545464
12	6	0	3.112995	0.123051	2.488271
13	6	0	2.839619	2.469727	2.860595
14	6	0	0.817514	3.734192	2.644294
15	6	0	3.501251	-2.198769	2.091338

16	6	0	3.202845	-3.377645	0.022869
17	6	0	3.062480	-0.627411	3.843891
18	6	0	4.481102	0.832151	2.294738
19	6	0	4.339966	2.230073	2.945728
20	6	0	2.165307	3.686313	3.002507
21	1	0	0.281211	4.677492	2.706846
22	6	0	3.712482	-2.012919	3.588002
23	6	0	3.641161	-3.374975	1.351172
24	1	0	3.294381	-4.284045	-0.569818
25	1	0	3.555926	-0.069086	4.645401
26	1	0	2.014881	-0.768226	4.129335
27	1	0	5.310398	0.250948	2.710020
28	1	0	4.663547	0.953742	1.221747
29	1	0	4.668357	2.198636	3.991634
30	6	0	5.122364	3.307988	2.220717
31	6	0	2.874118	4.906083	3.472336
32	1	0	4.781970	-1.984625	3.828669
33	6	0	3.063475	-3.131083	4.380836
34	6	0	4.213770	-4.596795	1.977095
35	6	0	4.788240	3.641273	0.901266
36	6	0	6.131197	4.027014	2.860648
37	6	0	3.024317	6.008521	2.625024
38	6	0	3.433388	4.946943	4.753450
39	6	0	1.721321	-3.456553	4.144570
40	6	0	3.785629	-3.884084	5.306133
41	6	0	3.422829	-5.732772	2.175341
42	6	0	5.539067	-4.599763	2.424076
43	6	0	5.445795	4.677166	0.243541
44	1	0	3.976901	3.112710	0.400798
45	6	0	6.793811	5.065602	2.203774
46	1	0	6.384480	3.791924	3.891814
47	6	0	3.746275	7.124410	3.043971
48	1	0	2.598322	5.973387	1.625037
49	6	0	4.142646	6.069296	5.178803
50	1	0	3.304258	4.097067	5.419713
51	6	0	1.119206	-4.514755	4.818700
52	1	0	1.155834	-2.896894	3.399463
53	6	0	3.186173	-4.949363	5.980715
54	1	0	4.833585	-3.654016	5.484014
55	6	0	3.943385	-6.845888	2.832858
56	1	0	2.388354	-5.725907	1.840720
57	6	0	6.064454	-5.717449	3.070337
58	1	0	6.158964	-3.721855	2.256901
59	6	0	6.451169	5.395781	0.894474
60	1	0	5.156123	4.943998	-0.768739
61	1	0	7.566396	5.624913	2.722559
62	6	0	4.309496	7.156220	4.320202
63	1	0	3.875674	7.965637	2.369873
64	1	0	4.566667	6.094540	6.178180
65	6	0	1.851760	-5.268527	5.738706
66	1	0	0.081252	-4.763978	4.618027
67	1	0	3.767729	-5.535890	6.685493
68	6	0	5.263663	-6.839431	3.284925
69	1	0	3.314704	-7.714738	3.002351
70	1	0	7.096507	-5.711625	3.407964
71	1	0	6.955937	6.211930	0.386880
72	1	0	4.872262	8.026170	4.644520
73	1	0	1.385549	-6.100519	6.257347
74	1	0	5.667383	-7.706839	3.798080
75	1	0	-1.108209	-1.583600	-0.689538
76	8	0	-2.269000	-1.584412	-1.593776
77	6	0	-3.284462	-0.639696	-1.140977
78	6	0	-3.204864	0.144785	-2.475988
79	1	0	-4.218307	-1.156422	-0.911876
80	1	0	-2.929058	-0.065075	-0.278366
81	8	0	-2.809853	1.480866	-2.362551
82	6	0	-2.071884	-0.851433	-2.840370
83	6	0	-4.435441	0.041869	-3.341661
84	1	0	-1.954418	1.502141	-1.884890
85	1	0	-1.079894	-0.387283	-2.881628
86	1	0	-2.246383	-1.505150	-3.700678
87	6	0	-5.013708	1.177327	-3.905914
88	6	0	-5.010346	-1.212583	-3.574008
89	6	0	-6.157725	1.058189	-4.695920
90	1	0	-4.566580	2.146709	-3.714739
91	6	0	-6.150283	-1.330597	-4.363975
92	1	0	-4.565013	-2.104622	-3.131972
93	6	0	-6.728314	-0.191777	-4.928091
94	1	0	-6.606020	1.947592	-5.128233
95	1	0	-6.589768	-2.308157	-4.538383
96	1	0	-7.618892	-0.279772	-5.542727
97	6	0	-1.234177	2.689332	1.651641
98	6	0	-1.520305	3.512262	0.565908
99	6	0	-2.254224	1.871105	2.124830
100	6	0	-2.769171	3.508625	-0.057799
101	8	0	-0.503686	4.262524	0.020149
102	6	0	-3.500681	1.854545	1.512031
103	8	0	-2.006191	1.015575	3.175763
104	6	0	-3.773146	2.654466	0.400225
105	8	0	-2.944824	4.297382	-1.168399
106	6	0	-0.563995	4.315027	-1.363199
107	8	0	-4.458294	0.973199	1.965477
108	6	0	-2.657696	-0.194734	3.028319
109	6	0	-5.120095	2.483340	-0.258896
110	6	0	-1.813970	4.343772	-1.970034
111	6	0	0.596086	4.325588	-2.121841
112	6	0	-3.912234	-0.214419	2.422254
113	6	0	-2.072015	-1.368305	3.477472
114	9	0	-6.115499	2.765865	0.599983
115	9	0	-5.298426	1.201822	-0.649231
116	9	0	-5.297878	3.249804	-1.333432
117	6	0	-1.931942	4.398433	-3.349520
118	6	0	0.485432	4.400964	-3.510887
119	1	0	1.558281	4.260811	-1.622727
120	6	0	-4.608078	-1.403589	2.267682
121	6	0	-2.774031	-2.567118	3.340105
122	1	0	-1.085563	-1.321366	3.927962
123	6	0	-0.769587	4.440160	-4.120332
124	1	0	-2.921952	4.392804	-3.792984
125	1	0	1.386263	4.409987	-4.115333
126	6	0	-4.034177	-2.584690	2.741712
127	1	0	-5.582029	-1.383933	1.788672
128	1	0	-2.332451	-3.489677	3.702331
129	1	0	-0.847991	4.481207	-5.201512
130	1	0	-4.575772	-3.519450	2.640735
131	6	0	2.067117	-2.223552	-1.918874
132	6	0	1.050113	-3.085141	-2.318890
133	6	0	2.503182	-1.262129	-2.830388
134	6	0	0.436373	-2.962748	-3.567488
135	8	0	0.606364	-4.042167	-1.436950
136	6	0	1.889380	-1.114930	-4.068270
137	8	0	3.548559	-0.455649	-2.460311
138	6	0	0.830994	-1.948457	-4.443566
139	8	0	-0.582528	-3.828414	-3.890669
140	6	0	-0.749392	-4.293780	-1.548237
141	8	0	2.304006	-0.148664	-4.948279
142	6	0	3.637233	0.737814	-3.144924
143	6	0	0.154067	-1.647096	-5.760291
144	6	0	-1.349003	-4.205707	-2.799810
145	6	0	-1.497944	-4.603873	-0.424130
146	6	0	3.019735	0.891368	-4.384771
147	6	0	4.392915	1.766917	-2.603948

148	9	0	1.008970	-1.746482	-6.789657
149	9	0	-0.327055	-0.388465	-5.759923
150	9	0	-0.878404	-2.453472	-6.024205
151	6	0	-2.701564	-4.460597	-2.959167
152	6	0	-2.860795	-4.865002	-0.575681
153	1	0	-1.007704	-4.623518	0.544223
154	6	0	3.151337	2.074505	-5.094863
155	6	0	4.544006	2.953359	-3.322610
156	1	0	4.872318	1.614367	-1.641466
157	6	0	-3.457235	-4.801940	-1.835633
158	1	0	-3.137927	-4.384438	-3.950702
159	1	0	-3.456325	-5.115409	0.295755
160	6	0	3.925548	3.106991	-4.563166
161	1	0	2.657918	2.160669	-6.057660
162	1	0	5.160191	3.748588	-2.917046
163	1	0	-4.516275	-5.010825	-1.946949
164	1	0	4.049060	4.027553	-5.124378

Frequencies --	15.0586	17.3505	17.5656
Frequencies --	21.2992	22.2803	25.7151
Frequencies --	28.0341	29.4685	30.9976
Frequencies --	33.6934	36.1080	38.6201
Frequencies --	40.9607	41.9264	42.1176
Frequencies --	44.7181	52.8974	55.3088
Frequencies --	56.7875	61.6772	63.4852
Frequencies --	64.4061	66.8842	68.8113
Frequencies --	73.0031	73.3683	77.7801
Frequencies --	78.2200	81.4453	86.6609
Frequencies --	91.7249	92.3858	94.9593
Frequencies --	97.9237	100.3179	104.9519
Frequencies --	106.9101	113.1710	116.0094
Frequencies --	119.2255	123.3963	126.8867
Frequencies --	132.9618	135.1651	143.3184
Frequencies --	144.8866	155.0913	159.2866
Frequencies --	163.9471	171.0830	179.1515
Frequencies --	183.8827	195.8791	197.7571
Frequencies --	197.9333	204.8663	212.2355
Frequencies --	217.9689	227.6721	237.4993
Frequencies --	241.0942	244.9354	248.0462
Frequencies --	253.0668	262.1912	270.9953
Frequencies --	273.3648	275.0350	278.5445
Frequencies --	282.5253	291.2098	292.5240
Frequencies --	294.8600	297.0955	298.8239
Frequencies --	304.7809	310.6201	311.0855
Frequencies --	315.5745	316.1844	323.5768
Frequencies --	327.2962	330.2860	332.5741
Frequencies --	336.2482	337.3636	339.7138
Frequencies --	346.9937	358.1172	369.0445
Frequencies --	372.1082	403.6278	404.9467
Frequencies --	408.3130	409.0986	411.1875
Frequencies --	412.3846	415.4040	416.0888
Frequencies --	419.7126	424.2988	433.4024
Frequencies --	435.7794	437.4526	439.8937
Frequencies --	441.3944	444.0572	447.1312
Frequencies --	449.1953	451.4251	456.6806
Frequencies --	466.5410	474.2607	486.7288
Frequencies --	491.7529	501.0682	512.4864
Frequencies --	516.0950	516.5742	521.0950
Frequencies --	522.8553	529.0175	531.7190
Frequencies --	536.4528	539.6241	543.2070
Frequencies --	548.0926	555.4643	559.2820
Frequencies --	561.5231	563.5135	563.7656
Frequencies --	565.5937	566.8811	570.9788
Frequencies --	583.1423	588.4774	596.5233
Frequencies --	597.7494	600.9678	601.6026
Frequencies --	603.8427	607.7970	609.6840
Frequencies --	610.2600	617.3708	618.4805
Frequencies --	620.8805	624.4944	626.6328
Frequencies --	629.5229	630.3079	630.5365
Frequencies --	632.2177	633.3281	635.1315
Frequencies --	646.4380	649.8022	654.5384
Frequencies --	669.9417	673.2325	680.9496
Frequencies --	684.3933	691.2520	701.2297
Frequencies --	704.8629	705.8566	708.3002
Frequencies --	709.9230	714.5549	714.8257
Frequencies --	718.9381	721.7519	723.7115
Frequencies --	725.7556	728.7668	730.2308
Frequencies --	733.0960	737.6789	741.1310
Frequencies --	745.1639	747.3506	750.8984
Frequencies --	763.5565	768.1764	769.3057
Frequencies --	770.7712	772.9864	775.7955
Frequencies --	776.8005	778.7688	780.7033
Frequencies --	782.6429	787.7604	795.9955
Frequencies --	800.3295	801.3288	804.1713
Frequencies --	805.5643	820.3164	823.8014
Frequencies --	825.7864	827.9831	829.8032
Frequencies --	856.9067	857.6712	858.8975
Frequencies --	862.1523	863.4392	864.8139
Frequencies --	866.7608	867.4748	870.3444
Frequencies --	874.0959	883.9506	885.6014
Frequencies --	887.9306	890.1916	905.2601
Frequencies --	916.2019	918.4625	919.0076
Frequencies --	921.4004	923.8869	930.6513
Frequencies --	932.2823	933.4043	938.0923
Frequencies --	940.0770	942.1746	943.9883
Frequencies --	945.1060	945.9973	948.7185
Frequencies --	950.3730	954.5745	954.9240
Frequencies --	970.5364	974.2678	986.5446
Frequencies --	987.8880	988.5253	990.4508
Frequencies --	990.7747	991.0952	995.1526
Frequencies --	999.0324	1000.5665	1000.9352
Frequencies --	1006.8166	1008.3871	1009.8565
Frequencies --	1011.6415	1012.5492	1014.0509
Frequencies --	1018.8546	1019.0730	1019.5518
Frequencies --	1019.7808	1019.8600	1021.9618
Frequencies --	1023.0522	1029.3200	1033.6202
Frequencies --	1035.5542	1042.7093	1044.2502
Frequencies --	1053.8663	1055.0482	1056.6102
Frequencies --	1059.4738	1063.1208	1063.9225
Frequencies --	1066.8380	1069.2936	1072.0374
Frequencies --	1073.1969	1084.7665	1093.0950
Frequencies --	1093.7718	1100.6238	1107.9395
Frequencies --	1108.6584	1110.0215	1114.3961
Frequencies --	1116.4507	1122.7761	1125.9356
Frequencies --	1126.7919	1128.1093	1130.1983
Frequencies --	1132.1706	1162.6181	1167.4445
Frequencies --	1169.2957	1169.5771	1170.8104
Frequencies --	1171.1086	1171.8963	1172.3558
Frequencies --	1174.5660	1176.3075	1178.2108
Frequencies --	1181.3565	1183.8697	1192.7415
Frequencies --	1195.5758	1198.7185	1199.1905
Frequencies --	1202.9503	1210.1223	1212.8674
Frequencies --	1213.2845	1214.7639	1216.1698
Frequencies --	1221.4598	1223.3878	1224.6439
Frequencies --	1228.1749	1230.3011	1232.0992
Frequencies --	1233.9955	1236.5671	1241.3162
Frequencies --	1243.0894	1247.1884	1255.8997
Frequencies --	1259.4137	1266.2113	1273.7727
Frequencies --	1277.1246	1282.0329	1289.8495
Frequencies --	1290.5519	1291.7072	1296.0340
Frequencies --	1297.1621	1300.1367	1301.6125

Frequencies --	1304.5104	1307.1324	1308.0947
Frequencies --	1308.9848	1311.1095	1313.0418
Frequencies --	1314.6013	1318.3526	1324.5575
Frequencies --	1325.1005	1326.6540	1328.6839
Frequencies --	1336.4606	1339.7434	1341.1403
Frequencies --	1345.4665	1346.8459	1357.0047
Frequencies --	1357.1985	1359.9600	1362.8508
Frequencies --	1366.2705	1366.7279	1368.0001
Frequencies --	1368.3893	1370.3702	1371.7671
Frequencies --	1372.4276	1377.8782	1383.0772
Frequencies --	1383.8657	1394.4831	1410.3863
Frequencies --	1450.7909	1459.6268	1461.8143
Frequencies --	1468.9015	1471.6976	1490.4514
Frequencies --	1491.6375	1495.7035	1498.1596
Frequencies --	1499.6621	1499.9606	1505.1755
Frequencies --	1506.0904	1508.0555	1508.8069
Frequencies --	1512.5762	1512.7593	1516.1803
Frequencies --	1518.0218	1527.6113	1530.5183
Frequencies --	1530.7247	1548.8591	1549.4658
Frequencies --	1553.5087	1555.0029	1555.1627
Frequencies --	1555.8198	1560.6204	1562.2836
Frequencies --	1563.4762	1570.4679	1575.9468
Frequencies --	1664.9959	1665.6942	1668.5939
Frequencies --	1669.5727	1674.7456	1675.2259
Frequencies --	1676.9498	1677.2002	1677.6907
Frequencies --	1688.9312	1690.8408	1694.8390
Frequencies --	1696.7275	1696.9427	1698.8796
Frequencies --	1699.5025	1701.2443	1701.5184
Frequencies --	1702.7181	1702.8059	1705.4699
Frequencies --	1707.2217	1720.1828	1723.0785
Frequencies --	1733.7308	1734.2595	2476.8812
Frequencies --	3082.3016	3083.4024	3087.5789
Frequencies --	3089.3498	3096.3185	3110.0339
Frequencies --	3151.3111	3155.7250	3171.8656
Frequencies --	3180.3715	3183.2231	3192.0362
Frequencies --	3194.5391	3197.7578	3200.9900
Frequencies --	3204.0423	3205.3580	3210.3889
Frequencies --	3214.5410	3215.4609	3217.8993
Frequencies --	3218.4653	3218.9946	3219.3106
Frequencies --	3220.2219	3221.0137	3221.8544
Frequencies --	3223.3377	3223.5576	3224.9943
Frequencies --	3227.5234	3228.2147	3228.7927
Frequencies --	3230.0824	3231.9785	3232.5387
Frequencies --	3232.7792	3233.0250	3234.3384
Frequencies --	3237.5205	3238.2484	3240.2957
Frequencies --	3240.6899	3241.2959	3243.0468
Frequencies --	3243.1895	3243.3979	3247.2444
Frequencies --	3247.7246	3249.8742	3255.7207
Frequencies --	3256.6455	3258.4149	3647.2515

SCF Done: E(RM062X/DGDZVP) = -5378.68898726
Sum of electronic and zero-point Energies= -5377.446857
Sum of electronic and thermal Energies= -5377.343581
Sum of electronic and thermal Free Energies= -5377.594377
SCF Done: E(RM062X/DGTZVP/SMD) = -5379.82096920

Cat f I0_2

Center Number	Atomic Number	Atomic Type	Coordinates (Angstroms) X	Y	Z
1	15	0	-0.013767	-0.036707	0.365803
2	8	0	0.123276	0.075134	1.964628
3	8	0	1.507870	-0.105658	-0.136253
4	8	0	-0.437830	1.361693	-0.180642
5	8	0	-0.862674	-1.196666	0.023676
6	6	0	0.838989	1.142777	2.504785
7	6	0	2.239007	-1.236937	0.232542
8	6	0	2.213895	1.035253	2.664025
9	6	0	0.171357	2.333483	2.819820
10	6	0	2.923007	-1.235314	1.439445
11	6	0	2.202047	-2.382038	-0.573479
12	6	0	3.158963	-0.133250	2.454501
13	6	0	2.930506	2.143078	3.121507
14	6	0	0.904803	3.392109	3.362264
15	6	0	3.548294	-2.408466	1.864508
16	6	0	2.928942	-3.505738	-0.169853
17	6	0	3.306447	-0.968323	3.753777
18	6	0	4.480212	0.618824	2.144428
19	6	0	4.428832	1.919477	2.981318
20	6	0	2.287090	3.313860	3.529098
21	1	0	0.387031	4.307785	3.634375
22	6	0	3.963913	-2.304011	3.325112
23	6	0	3.611185	-3.539109	1.046158
24	1	0	2.927221	-4.389025	-0.802204
25	1	0	3.879926	-0.441486	4.522605
26	1	0	2.309788	-1.167704	4.161033
27	1	0	5.363832	0.010154	2.359431
28	1	0	4.500104	0.873689	1.079591
29	1	0	4.888000	1.758429	3.964217
30	6	0	5.115374	3.095204	2.314515
31	6	0	3.063725	4.450466	4.091151
32	1	0	5.054400	-2.241419	3.420793
33	6	0	3.470923	-3.497793	4.120844
34	6	0	4.333250	-4.758369	1.493698
35	6	0	4.632046	3.583545	1.093849
36	6	0	6.193889	3.741920	2.917366
37	6	0	3.129845	5.676565	3.422380
38	6	0	3.778425	4.281845	5.281580
39	6	0	2.117208	-3.854342	4.064573
40	6	0	4.344130	-4.289644	4.865995
41	6	0	3.647695	-5.960872	1.691613
42	6	0	5.703016	-4.698857	1.771036
43	6	0	5.214569	4.695539	0.492336
44	1	0	3.771949	3.103783	0.628136
45	6	0	6.776288	4.861941	2.322086
46	1	0	6.565534	3.384322	3.874762
47	6	0	3.920559	6.709110	3.923532
48	1	0	2.583312	5.805888	2.491346
49	6	0	4.557889	5.318605	5.791487
50	1	0	3.714765	3.333515	5.810313
51	6	0	1.649227	-4.977854	4.739565
52	1	0	1.432535	-3.261298	3.458795
53	6	0	3.880837	-5.422798	5.536883
54	1	0	5.401185	-4.036027	4.899457
55	6	0	4.317025	-7.079348	2.185059
56	1	0	2.581013	-6.005522	1.484999
57	6	0	6.376020	-5.820100	2.252651
58	1	0	6.240532	-3.768816	1.600416
59	6	0	6.287795	5.342893	1.108775
60	1	0	4.828202	5.064563	-0.453558
61	1	0	7.604633	5.363564	2.813028
62	6	0	4.638782	6.531455	5.106781
63	1	0	3.983067	7.649988	3.385377
64	1	0	5.102675	5.179266	6.720410
65	6	0	2.533017	-5.770653	5.475446
66	1	0	0.596869	-5.242963	4.687259
67	1	0	4.576575	-6.038326	6.099071
68	6	0	5.681279	-7.010147	2.470857
69	1	0	3.771762	-8.002424	2.356131
70	1	0	7.440679	-5.765102	2.459158

71	1	0	6.737444	6.216274	0.646645
72	1	0	5.255289	7.336397	5.494913
73	1	0	2.172870	-6.653992	5.993736
74	1	0	6.200862	-7.881576	2.857316
75	1	0	-1.417907	1.395299	-0.489643
76	8	0	-2.822805	1.183231	-1.075247
77	6	0	-2.637603	0.425271	-2.310226
78	6	0	-3.572512	-0.706291	-1.809373
79	1	0	-2.967497	1.004570	-3.173933
80	1	0	-1.593931	0.110418	-2.423285
81	8	0	-2.983797	-1.970041	-1.678348
82	6	0	-3.642329	0.119493	-0.501177
83	6	0	-4.876407	-0.824760	-2.558489
84	1	0	-2.223170	-1.881868	-1.067178
85	1	0	-3.133228	-0.365398	0.336480
86	1	0	-4.628371	0.490803	-0.212595
87	6	0	-5.304144	-2.050957	-3.065980
88	6	0	-5.664550	0.314727	-2.753198
89	6	0	-6.511076	-2.135509	-3.761941
90	1	0	-4.684845	-2.928619	-2.915370
91	6	0	-6.870047	0.228050	-3.444206
92	1	0	-5.339792	1.276937	-2.359138
93	6	0	-7.296893	-1.000537	-3.951589
94	1	0	-6.836404	-3.092480	-4.158905
95	1	0	-7.476101	1.117760	-3.585339
96	1	0	-8.235963	-1.070109	-4.492025
97	6	0	1.294788	-2.441901	-1.742121
98	6	0	0.332032	-3.450906	-1.822853
99	6	0	1.267602	-1.454952	-2.723591
100	6	0	-0.663029	-3.449477	-2.800831
101	8	0	0.328384	-4.434150	-0.856915
102	6	0	0.261025	-1.425909	-3.682959
103	8	0	2.212467	-0.452983	-2.723105
104	6	0	-0.725610	-2.410488	-3.730592
105	8	0	-1.611573	-4.442236	-2.792453
106	6	0	-0.927717	-4.918707	-0.550174
107	8	0	0.198701	-0.359690	-4.551319
108	6	0	1.654639	0.776431	-3.030914
109	6	0	-1.819992	-2.246823	-4.757697
110	6	0	-1.912477	-4.920503	-1.532054
111	6	0	-1.183550	-5.430073	0.712174
112	6	0	0.621429	0.823766	-3.961942
113	6	0	2.103408	1.932467	-2.412785
114	9	0	-1.309099	-2.201509	-6.000312
115	9	0	-2.484501	-1.086414	-4.569130
116	9	0	-2.727421	-3.222253	-4.740523
117	6	0	-3.174634	-5.426073	-1.263754
118	6	0	-2.443908	-5.966692	0.980950
119	1	0	-0.391383	-5.407709	1.455158
120	6	0	0.004941	2.024702	-4.280237
121	6	0	1.502536	3.146577	-2.742631
122	1	0	2.898461	1.856531	-1.678521
123	6	0	-3.434619	-5.961796	-0.001311
124	1	0	-3.925661	-5.403491	-2.046395
125	1	0	-2.649687	-6.388838	1.960012
126	6	0	0.454631	3.193566	-3.663029
127	1	0	-0.810822	2.024992	-4.996460
128	1	0	1.843240	4.059494	-2.265762
129	1	0	-4.415265	-6.374775	0.211192
130	1	0	-0.024690	4.140501	-3.890753
131	6	0	-1.255999	2.506637	2.465825
132	6	0	-2.236243	1.592227	2.839921
133	6	0	-1.646463	3.572343	1.648574
134	6	0	-3.542945	1.665346	2.347146
135	8	0	-1.906760	0.569279	3.698718
136	6	0	-2.950117	3.675484	1.182208
137	8	0	-0.703291	4.498976	1.265746
138	6	0	-3.912935	2.715817	1.505525
139	8	0	-4.424082	0.664436	2.678182
140	6	0	-2.519526	-0.620948	3.346380
141	8	0	-3.312394	4.710307	0.355422
142	6	0	-0.965773	5.122549	0.062759
143	6	0	-5.290266	2.903794	0.915233
144	6	0	-3.809481	-0.571803	2.832002
145	6	0	-1.855794	-1.829647	3.484649
146	6	0	-2.274729	5.220363	-0.401716
147	6	0	0.078980	5.684177	-0.653918
148	9	0	-5.241032	2.933349	-0.431625
149	9	0	-5.832864	4.065370	1.313133
150	9	0	-6.146248	1.932944	1.248563
151	6	0	-4.461516	-1.729246	2.433274
152	6	0	-2.508873	-2.999324	3.098447
153	1	0	-0.843326	-1.830040	3.874354
154	6	0	-2.552593	5.858302	-1.600741
155	6	0	-0.195555	6.350959	-1.849100
156	1	0	1.086202	5.595480	-0.258028
157	6	0	-3.799765	-2.950402	2.570170
158	1	0	-5.458193	-1.655933	2.009496
159	1	0	-1.998808	-3.952755	3.188766
160	6	0	-1.504874	6.432531	-2.323076
161	1	0	-3.582594	5.909331	-1.938192
162	1	0	0.616062	6.805528	-2.408488
163	1	0	-4.286264	-3.862804	2.241116
164	1	0	-1.716678	6.947726	-3.254027

Frequencies --	10.5971	16.7936	22.0905
Frequencies --	23.9448	25.3216	27.1427
Frequencies --	28.6361	32.5539	34.6652
Frequencies --	40.1437	41.6126	43.8277
Frequencies --	45.8657	49.0653	51.2733
Frequencies --	51.9092	56.8259	59.8138
Frequencies --	61.0369	63.3113	67.1341
Frequencies --	68.8889	69.3511	73.6333
Frequencies --	74.8818	78.2776	80.6437
Frequencies --	84.2855	85.1788	86.1571
Frequencies --	88.0580	94.1481	96.2555
Frequencies --	97.8718	100.4169	106.2258
Frequencies --	109.5045	122.1419	125.9967
Frequencies --	126.5676	128.0770	131.4409
Frequencies --	133.4991	140.5596	144.8193
Frequencies --	148.7991	157.1670	164.2800
Frequencies --	170.0752	173.3680	182.8238
Frequencies --	192.9021	193.5243	198.2582
Frequencies --	201.6174	206.1875	211.3806
Frequencies --	218.4412	225.1259	236.8547
Frequencies --	240.3816	241.9896	247.2060
Frequencies --	253.2009	261.9979	271.5909
Frequencies --	272.8420	276.4164	279.5568
Frequencies --	286.2421	288.5038	290.7619
Frequencies --	294.3827	299.0567	302.8022
Frequencies --	304.9047	309.2639	310.3690
Frequencies --	317.0490	318.6678	324.6691
Frequencies --	328.4785	329.7098	334.4486
Frequencies --	337.6510	342.2825	347.6485
Frequencies --	351.9375	358.9425	372.0355
Frequencies --	377.3686	403.3039	407.1352
Frequencies --	411.4537	412.7912	413.7780
Frequencies --	416.1798	416.7538	417.3103
Frequencies --	418.9438	424.8722	430.3126
Frequencies --	431.8085	435.3158	438.7144
Frequencies --	444.2120	446.5720	449.2418

Frequencies -- 450.2458 454.6076 456.9552
Frequencies -- 466.1186 471.7019 486.8416
Frequencies -- 492.6905 502.8709 514.2013
Frequencies -- 515.5056 518.0470 519.8489
Frequencies -- 521.3235 530.8620 535.1018
Frequencies -- 537.7663 541.4973 543.4343
Frequencies -- 545.0866 555.1233 557.6387
Frequencies -- 560.6556 561.8357 562.8939
Frequencies -- 564.4797 568.4868 572.3080
Frequencies -- 586.0052 589.5149 597.1876
Frequencies -- 598.7256 599.4675 601.1921
Frequencies -- 605.0070 606.4701 609.8179
Frequencies -- 614.6433 615.1721 617.6213
Frequencies -- 621.0488 624.1597 624.6751
Frequencies -- 626.6021 629.3821 630.1757
Frequencies -- 632.1224 633.3127 636.5338
Frequencies -- 644.8701 651.9887 655.4767
Frequencies -- 673.5766 675.4504 679.1735
Frequencies -- 682.7238 688.1760 700.1170
Frequencies -- 703.8674 704.7606 711.6160
Frequencies -- 713.1151 716.1776 717.2969
Frequencies -- 717.8261 718.9900 720.3542
Frequencies -- 727.5135 728.0424 730.1075
Frequencies -- 732.3668 737.6990 741.5686
Frequencies -- 745.5198 748.5813 749.9285
Frequencies -- 762.1948 766.3069 770.3125
Frequencies -- 771.3435 773.0453 773.4303
Frequencies -- 775.1162 775.8910 779.0943
Frequencies -- 785.8587 787.3474 795.4283
Frequencies -- 800.2692 801.8814 802.4889
Frequencies -- 804.8178 820.2650 824.9147
Frequencies -- 826.3371 829.5033 832.5146
Frequencies -- 852.8370 862.9506 863.3714
Frequencies -- 866.0128 866.4617 868.3913
Frequencies -- 869.5008 873.3342 873.9006
Frequencies -- 876.0492 876.5670 885.5745
Frequencies -- 887.8112 890.2702 907.5544
Frequencies -- 917.9117 919.4598 922.4636
Frequencies -- 923.6202 924.9351 935.4971
Frequencies -- 936.4972 937.2921 938.1243
Frequencies -- 940.4919 943.0292 945.1398
Frequencies -- 946.8300 947.5792 948.8828
Frequencies -- 949.9011 957.8936 962.1313
Frequencies -- 964.5652 973.7652 987.7140
Frequencies -- 988.0210 989.3623 992.4532
Frequencies -- 993.3283 995.2649 996.1513
Frequencies -- 996.3202 997.4876 997.6734
Frequencies -- 1002.7760 1005.9709 1007.8820
Frequencies -- 1008.7366 1009.0583 1011.6615
Frequencies -- 1014.9790 1019.5069 1019.5873
Frequencies -- 1019.8033 1020.3156 1020.9458
Frequencies -- 1025.5655 1027.4600 1031.7479
Frequencies -- 1033.5631 1037.4487 1044.4224
Frequencies -- 1051.1354 1055.0484 1056.3606
Frequencies -- 1057.0908 1058.3847 1060.7921
Frequencies -- 1064.0248 1067.0742 1068.3830
Frequencies -- 1072.6725 1074.0272 1091.3431
Frequencies -- 1095.0926 1095.4642 1099.0123
Frequencies -- 1106.9636 1111.9007 1113.0727
Frequencies -- 1117.8235 1123.1617 1123.5251
Frequencies -- 1125.8030 1129.2717 1130.1426
Frequencies -- 1131.3343 1160.8091 1164.5212
Frequencies -- 1165.7483 1166.4608 1170.8213
Frequencies -- 1171.5385 1172.6802 1173.4620
Frequencies -- 1174.0240 1176.5719 1177.4785
Frequencies -- 1186.5438 1192.8953 1195.5522
Frequencies -- 1198.0563 1202.5061 1204.4227
Frequencies -- 1207.3740 1211.3597 1211.5791
Frequencies -- 1215.3717 1216.1463 1217.3483
Frequencies -- 1219.0453 1222.4179 1224.5862
Frequencies -- 1229.2767 1230.3717 1232.7775
Frequencies -- 1235.5262 1237.0025 1242.0549
Frequencies -- 1243.4946 1248.0052 1254.8798
Frequencies -- 1258.5542 1266.1581 1272.7511
Frequencies -- 1280.7118 1283.3220 1285.5161
Frequencies -- 1289.0216 1294.8650 1295.5525
Frequencies -- 1296.9867 1297.6403 1301.8267
Frequencies -- 1305.9642 1307.6476 1308.0907
Frequencies -- 1309.8789 1310.8156 1312.9237
Frequencies -- 1315.7792 1318.2185 1321.8574
Frequencies -- 1324.3900 1327.9827 1329.1369
Frequencies -- 1335.5070 1337.5958 1341.0946
Frequencies -- 1344.2248 1345.2425 1356.9377
Frequencies -- 1360.6895 1362.1312 1362.9011
Frequencies -- 1363.9383 1365.3080 1366.1636
Frequencies -- 1367.8059 1369.5297 1370.1260
Frequencies -- 1371.9480 1378.4975 1384.0495
Frequencies -- 1389.6147 1392.3669 1405.6908
Frequencies -- 1448.1094 1456.7764 1457.7559
Frequencies -- 1467.1069 1470.2545 1490.3047
Frequencies -- 1494.6264 1497.2476 1499.9226
Frequencies -- 1502.2110 1502.4541 1505.1042
Frequencies -- 1506.5074 1510.5067 1510.6253
Frequencies -- 1511.8403 1512.5619 1515.0292
Frequencies -- 1519.1554 1526.2816 1527.4770
Frequencies -- 1539.1330 1543.9058 1551.8688
Frequencies -- 1553.3568 1553.9076 1554.3248
Frequencies -- 1557.5124 1559.1774 1561.2501
Frequencies -- 1562.9631 1567.3767 1570.1448
Frequencies -- 1661.6095 1662.4284 1667.6493
Frequencies -- 1669.4830 1673.0478 1673.6543
Frequencies -- 1675.2768 1677.6671 1678.4738
Frequencies -- 1690.2965 1691.0246 1694.4818
Frequencies -- 1695.7667 1698.6767 1700.4436
Frequencies -- 1701.6274 1701.7142 1702.2182
Frequencies -- 1702.9565 1703.3207 1703.8252
Frequencies -- 1706.1791 1718.9599 1719.7596
Frequencies -- 1728.1166 1731.9928 2673.2284
Frequencies -- 3083.0040 3088.7664 3089.6723
Frequencies -- 3094.3248 3112.9653 3126.8326
Frequencies -- 3152.0592 3159.2564 3183.7734
Frequencies -- 3184.2605 3195.7094 3198.8130
Frequencies -- 3201.4671 3201.4829 3205.0839
Frequencies -- 3205.7402 3208.1166 3208.1910
Frequencies -- 3213.4967 3214.1469 3214.9412
Frequencies -- 3215.3557 3216.5644 3216.8817
Frequencies -- 3219.3467 3219.8140 3221.1890
Frequencies -- 3223.3095 3224.6333 3225.6112
Frequencies -- 3225.6926 3226.2064 3226.6100
Frequencies -- 3227.7287 3230.6069 3232.9637
Frequencies -- 3235.1132 3235.4159 3235.5151
Frequencies -- 3235.5254 3235.6232 3235.7711
Frequencies -- 3236.4627 3237.3689 3238.5769
Frequencies -- 3241.8891 3243.0192 3244.6588
Frequencies -- 3246.2000 3248.2219 3248.5239
Frequencies -- 3248.6386 3248.9677 3646.0000

SCF Done: E(RM062X/DGDZVP) = -5378.68958244
Sum of electronic and zero-point Energies= -5377.446451
Sum of electronic and thermal Energies= -5377.343614
Sum of electronic and thermal Free Energies= -5377.591446
SCF Done: E(RM062X/DGTZVP/SMD) = -5379.82032726

Cat f I0a_*R*

Center Number	Atomic Number	Atomic Type	X	Y	Z
1	15	0	0.234062	-0.033140	-0.307778
2	8	0	0.121367	-0.090182	1.294472
3	8	0	1.802982	-0.225662	-0.602047
4	8	0	-0.168995	1.269992	-0.897968
5	8	0	-0.528920	-1.300523	-0.745181
6	6	0	0.821813	0.927603	1.944575
7	6	0	2.338951	-1.446816	-0.182740
8	6	0	2.140448	0.707406	2.298573
9	6	0	0.203545	2.164607	2.149671
10	6	0	2.745746	-1.600308	1.129545
11	6	0	2.328120	-2.517773	-1.079028
12	6	0	2.928494	-0.585253	2.241211
13	6	0	2.901927	1.756985	2.826370
14	6	0	0.967902	3.189288	2.702807
15	6	0	-1.226655	2.321895	1.790663
16	6	0	3.076728	-2.878367	1.579728
17	6	0	2.742587	-3.770049	-0.626810
18	6	0	1.871846	-2.256604	-2.465589
19	6	0	2.670569	-1.479231	3.482286
20	6	0	4.375556	-0.035215	2.232608
21	6	0	4.339950	1.284074	3.041333
22	6	0	2.318669	3.017080	3.043307
23	1	0	0.493116	4.148393	2.887784
24	6	0	-1.678043	3.325658	0.933193
25	6	0	-2.159212	1.414044	2.294527
26	6	0	3.174940	-2.897214	3.100351
27	6	0	3.115320	-3.970355	0.707502
28	1	0	2.757250	-4.607700	-1.319250
29	6	0	0.747784	-2.868887	-3.014370
30	6	0	2.533758	-1.306701	-3.240118
31	1	0	3.149276	-1.087434	4.385110
32	1	0	1.591466	-1.518902	3.664422
33	1	0	5.100388	-0.753099	2.628779
34	1	0	4.659662	0.191963	1.199449
35	1	0	4.492205	1.058491	4.104394
36	6	0	5.419859	2.241461	2.587521
37	6	0	3.050179	4.173655	3.623012
38	6	0	-3.012385	3.359941	0.529504
39	8	0	-0.768548	4.248404	0.484953
40	6	0	-3.491188	1.428090	1.885795
41	8	0	-1.726668	0.503923	3.230651
42	1	0	4.211758	-3.033884	3.429503
43	6	0	2.325431	-4.014768	3.677251
44	6	0	3.513320	-5.314014	1.203773
45	6	0	0.291612	-2.512768	-4.278689
46	8	0	0.046144	-3.795099	-2.278557
47	6	0	2.086153	-0.936335	-4.511245
48	8	0	3.662135	-0.733162	-2.707760
49	6	0	5.341262	2.817403	1.315875
50	6	0	6.516071	2.544540	3.395864
51	6	0	2.862980	5.460592	3.098975
52	6	0	3.903039	4.016802	4.720611
53	6	0	-3.921650	2.395414	0.974524
54	8	0	-3.483783	4.317504	-0.318430
55	6	0	-1.202616	5.079180	-0.536421
56	8	0	-4.367486	0.493496	2.377586
57	6	0	-2.460155	-0.661783	3.280544
58	6	0	0.998422	-4.163286	3.251386
59	6	0	2.858151	-4.954333	4.559738
60	6	0	2.618013	-6.387262	1.163902
61	6	0	4.780413	-5.501398	1.766876
62	6	0	0.940127	-1.535708	-5.039610
63	8	0	-0.848330	-3.106425	-4.772283
64	6	0	-1.318361	-3.727823	-2.508137
65	8	0	2.792760	-0.008079	-5.229340
66	6	0	3.938152	0.531540	-3.187291
67	6	0	6.317714	3.706002	0.874931
68	1	0	4.497590	2.576642	0.669985
69	6	0	7.506364	3.422159	2.953073
70	1	0	6.590715	2.102697	4.387534
71	6	0	3.535659	6.554291	3.638238
72	1	0	2.190980	5.605103	2.255619
73	6	0	4.571730	5.109874	5.265840
74	1	0	4.027949	3.033256	5.165311
75	6	0	-5.314649	2.454554	0.390426
76	6	0	-2.531911	5.089834	-0.949104
77	6	0	-0.280683	5.925760	-1.131506
78	6	0	-3.783133	-0.666923	2.847724
79	6	0	-1.890083	-1.808145	3.813010
80	6	0	0.232405	-5.242041	3.684189
81	1	0	0.576919	-3.457453	2.535262
82	6	0	2.088611	-6.030960	5.004435
83	1	0	3.893440	-4.862984	4.880090
84	6	0	2.976606	-7.621930	1.702475
85	1	0	1.628553	-6.240242	0.737974
86	6	0	5.144039	-6.738746	2.294458
87	1	0	5.483648	-4.671895	1.782440
88	6	0	0.357742	-1.226734	-6.400999
89	6	0	-1.773053	-3.387391	-3.779242
90	6	0	-2.213653	-3.968859	-1.477386
91	6	0	3.505975	0.893175	-4.460391
92	6	0	4.679188	1.410342	-2.412240
93	6	0	7.405651	4.012677	1.694422
94	1	0	6.223885	4.165574	-0.105614
95	1	0	8.350141	3.653465	3.595996
96	6	0	4.398281	6.381650	4.720566
97	1	0	3.386024	7.541277	3.211361
98	1	0	5.229491	4.968111	6.118041
99	9	0	-5.931290	3.605751	0.696985
100	9	0	-5.264935	2.370431	-0.953608
101	9	0	-6.106285	1.460093	0.806634
102	6	0	-2.940379	5.913277	-1.986430
103	1	0	0.741104	5.927849	-0.763258
104	6	0	-0.685698	6.757405	-2.175861
105	6	0	-4.548217	-1.820820	2.926897
106	1	0	-0.861362	-1.774278	4.159082
107	6	0	-2.662950	-2.964720	3.921970
108	6	0	0.775825	-6.182123	4.562888
109	1	0	-0.779026	-5.367078	3.308344
110	1	0	2.523792	-6.761824	5.679230
111	6	0	4.237775	-7.799196	2.272895
112	1	0	2.266888	-8.443393	1.685650
113	1	0	6.132111	-6.874694	2.723771
114	9	0	1.051849	-0.322554	-7.087117
115	9	0	-0.905008	-0.769556	-6.293849
116	9	0	0.304634	-2.341429	-7.153560
117	6	0	-3.129986	-3.305544	-4.049956
118	1	0	-1.827533	-4.193086	-0.487773
119	6	0	-3.581881	-3.894591	-1.743521
120	6	0	3.816244	2.139450	-4.980939
121	1	0	5.001864	1.095332	-1.424076
122	6	0	5.009577	2.660488	-2.936651
123	1	0	8.167881	4.706169	1.353253
124	1	0	4.924342	7.232739	5.141533
125	1	0	-3.984137	5.887428	-2.283697

126	6	0	-2.009966	6.744544	-2.609545
127	1	0	0.042057	7.410080	-2.648001
128	1	0	-5.576694	-1.788510	2.582060
129	6	0	-3.983987	-2.973813	3.474707
130	1	0	-2.228314	-3.851111	4.371452
131	1	0	0.183700	-7.031592	4.889277
132	1	0	4.514455	-8.761099	2.693497
133	1	0	-3.449820	-3.034666	-5.051569
134	6	0	-4.037103	-3.570953	-3.022630
135	1	0	-4.291879	-4.083452	-0.945036
136	1	0	3.454893	2.397334	-5.971821
137	6	0	4.582184	3.020741	-4.214245
138	1	0	5.593238	3.355393	-2.341494
139	1	0	-2.324652	7.383152	-3.427849
140	1	0	-4.583258	-3.874122	3.560038
141	1	0	-5.102319	-3.517750	-3.222780
142	1	0	4.831305	3.997850	-4.615928
143	1	0	-1.389110	-1.148327	-1.372903
144	8	0	-2.441657	-0.792226	-2.202880
145	6	0	-3.282113	0.254088	-1.627189
146	6	0	-2.887976	1.253431	-2.747757
147	1	0	-4.322466	-0.073510	-1.580036
148	1	0	-2.913099	0.543596	-0.637111
149	8	0	-2.239282	2.407599	-2.298973
150	6	0	-1.978153	0.102633	-3.270713
151	1	0	-1.489237	2.130024	-1.738158
152	1	0	-0.902706	0.287388	-3.195650
153	1	0	-2.228103	-0.311518	-4.249747
154	1	0	3.467341	4.595984	0.619402
155	6	0	3.100058	4.657353	-0.400533
156	6	0	2.304862	3.631945	-0.907653
157	6	0	3.436802	5.771082	-1.182720
158	6	0	1.852091	3.754427	-2.220819
159	1	0	2.029449	2.764599	-0.308779
160	6	0	2.971067	5.890006	-2.493759
161	1	0	4.061559	6.552536	-0.760924
162	7	0	1.068011	2.846086	-2.911800
163	6	0	2.168875	4.873169	-3.004940
164	1	0	3.224892	6.755407	-3.098608
165	6	0	0.737422	3.150872	-4.192741
166	1	0	0.696228	2.012056	-2.452202
167	16	0	1.426778	4.733004	-4.584785
168	16	0	-0.127994	2.217996	-5.242330
169	6	0	-3.997116	1.637530	-3.694071
170	6	0	-4.150251	2.960705	-4.104693
171	6	0	-4.866139	0.656705	-4.182251
172	6	0	-5.176963	3.300721	-4.985925
173	1	0	-3.455522	3.708064	-3.735144
174	6	0	-5.890307	0.997573	-5.061516
175	1	0	-4.740702	-0.382668	-3.877184
176	6	0	-6.050451	2.324842	-5.462841
177	1	0	-5.291511	4.332308	-5.305483
178	1	0	-6.562842	0.231058	-5.434338
179	1	0	-6.849225	2.593588	-6.147250

Frequencies --	11.4603	14.1677	20.7109
Frequencies --	22.2228	23.7521	26.4235
Frequencies --	29.6828	32.3005	33.3021
Frequencies --	33.9932	34.4809	38.7470
Frequencies --	40.4525	41.4294	43.9544
Frequencies --	45.6289	48.8468	53.6625
Frequencies --	55.3574	56.7206	58.0755
Frequencies --	61.0398	61.7049	65.0268
Frequencies --	66.8568	68.1225	73.6565
Frequencies --	75.5159	77.4056	78.5194
Frequencies --	82.7116	84.0719	88.1624
Frequencies --	91.1401	93.6033	98.2724
Frequencies --	103.5222	104.4990	106.2233
Frequencies --	109.0384	111.9642	116.7571
Frequencies --	118.9373	124.9710	126.1757
Frequencies --	127.0431	129.4082	131.1878
Frequencies --	137.7968	144.2597	144.7308
Frequencies --	147.3497	151.9952	154.8852
Frequencies --	166.0615	172.7669	177.2434
Frequencies --	181.8517	188.2311	192.7668
Frequencies --	195.9698	201.5120	207.6472
Frequencies --	213.5600	222.5552	224.5380
Frequencies --	230.9186	233.2361	237.6871
Frequencies --	244.5970	246.0123	248.5664
Frequencies --	251.3776	264.0551	269.0864
Frequencies --	271.6450	273.6263	278.0599
Frequencies --	281.1321	286.3964	289.9845
Frequencies --	295.7989	297.8423	298.8428
Frequencies --	301.1013	304.0234	305.7531
Frequencies --	309.1151	312.5313	316.5532
Frequencies --	319.4440	323.7337	324.8600
Frequencies --	331.9898	333.4998	335.8664
Frequencies --	338.1709	344.8225	359.4046
Frequencies --	368.5948	379.3210	386.0761
Frequencies --	402.6220	404.5269	408.3785
Frequencies --	409.6839	410.8549	414.5196
Frequencies --	415.0078	419.3148	420.5509
Frequencies --	420.9095	426.1002	428.1752
Frequencies --	432.9159	440.6678	441.2476
Frequencies --	444.5407	446.0611	449.6416
Frequencies --	451.4791	455.4276	459.5471
Frequencies --	467.8086	470.3936	474.7155
Frequencies --	485.8163	489.4662	502.2173
Frequencies --	506.2026	507.5398	511.9564
Frequencies --	516.6863	520.2577	521.1532
Frequencies --	524.0535	529.6250	531.5686
Frequencies --	535.6321	540.2032	540.6454
Frequencies --	547.0885	550.8613	555.0038
Frequencies --	556.3865	558.6393	559.2022
Frequencies --	561.0123	564.6384	569.2978
Frequencies --	571.0098	583.5942	584.3958
Frequencies --	588.4576	593.4685	597.2447
Frequencies --	599.7767	602.7477	603.2534
Frequencies --	604.5318	604.7982	611.3075
Frequencies --	612.7363	619.0510	621.1051
Frequencies --	622.3730	625.4138	626.8697
Frequencies --	629.7922	630.4840	631.0660
Frequencies --	633.3393	635.4349	645.6690
Frequencies --	649.3088	656.1811	657.7626
Frequencies --	665.7509	673.4503	675.2688
Frequencies --	681.3122	683.3972	701.3493
Frequencies --	704.5649	708.0145	711.5718
Frequencies --	717.5217	717.8107	719.6407
Frequencies --	719.7782	721.1895	721.2464
Frequencies --	722.1151	723.9332	727.1912
Frequencies --	727.9068	732.5318	733.4289
Frequencies --	737.6718	740.1279	741.7542
Frequencies --	744.0829	747.4161	752.6918
Frequencies --	760.8397	762.6652	771.0243
Frequencies --	771.1670	772.8805	773.1655
Frequencies --	775.1029	776.3607	779.9493
Frequencies --	783.4416	783.5460	784.9913
Frequencies --	791.1160	796.1403	802.0103
Frequencies --	804.9743	805.8985	819.6422
Frequencies --	820.5358	825.2619	827.8208
Frequencies --	829.8068	866.7256	867.2710

Frequencies -- 868.4121 868.8866 870.3532
Frequencies -- 872.5442 874.8434 875.6665
Frequencies -- 879.1985 880.8223 883.6605
Frequencies -- 886.6776 887.3568 889.4925
Frequencies -- 890.0080 891.0597 909.7850
Frequencies -- 913.4587 914.0498 920.5922
Frequencies -- 922.1122 925.8503 930.4163
Frequencies -- 936.6271 939.0516 939.8496
Frequencies -- 941.4966 942.1276 945.9833
Frequencies -- 947.2016 948.7446 951.7383
Frequencies -- 954.2371 954.5643 955.1893
Frequencies -- 960.5977 964.4194 970.1424
Frequencies -- 980.2166 988.3822 989.8655
Frequencies -- 992.5236 993.5626 994.8009
Frequencies -- 997.6630 1002.5432 1002.7409
Frequencies -- 1005.2151 1006.5050 1009.8475
Frequencies -- 1012.0562 1013.2890 1016.9793
Frequencies -- 1018.1020 1018.4889 1018.9815
Frequencies -- 1019.0997 1019.6186 1020.6795
Frequencies -- 1022.5698 1027.7103 1029.7070
Frequencies -- 1034.0384 1036.3204 1040.3212
Frequencies -- 1044.4818 1051.0312 1051.9384
Frequencies -- 1055.9414 1058.2317 1059.3494
Frequencies -- 1060.1606 1066.3177 1068.3403
Frequencies -- 1069.5418 1070.8512 1071.6771
Frequencies -- 1072.4549 1073.8876 1080.9508
Frequencies -- 1085.9293 1094.4352 1100.3799
Frequencies -- 1109.1974 1112.7222 1114.1949
Frequencies -- 1114.8558 1117.5417 1120.4188
Frequencies -- 1124.2452 1125.4542 1127.2888
Frequencies -- 1129.7048 1132.6477 1157.3180
Frequencies -- 1162.1010 1163.7626 1167.3439
Frequencies -- 1168.3135 1169.9112 1171.4693
Frequencies -- 1171.8230 1173.2772 1174.4150
Frequencies -- 1175.6271 1175.7757 1177.3329
Frequencies -- 1178.4105 1182.3058 1189.8388
Frequencies -- 1198.0656 1201.5684 1204.8002
Frequencies -- 1207.0280 1207.3469 1208.5467
Frequencies -- 1208.8254 1209.8404 1210.6681
Frequencies -- 1213.0768 1221.6218 1223.4953
Frequencies -- 1225.5658 1227.5171 1229.8426
Frequencies -- 1230.9504 1233.3285 1236.3619
Frequencies -- 1240.9963 1245.2848 1251.3323
Frequencies -- 1257.1050 1257.5487 1262.8796
Frequencies -- 1268.3852 1278.2172 1279.1906
Frequencies -- 1282.5382 1285.1628 1287.9242
Frequencies -- 1294.1624 1294.5768 1297.6934
Frequencies -- 1298.1432 1300.5568 1302.6414
Frequencies -- 1302.7764 1304.6607 1306.3054
Frequencies -- 1309.3473 1309.7561 1311.0599
Frequencies -- 1314.9231 1323.4390 1324.7010
Frequencies -- 1326.8099 1329.4769 1331.1501
Frequencies -- 1332.4589 1334.2332 1339.1964
Frequencies -- 1340.4705 1344.3054 1344.8310
Frequencies -- 1356.5643 1358.7676 1360.5133
Frequencies -- 1361.0699 1362.5333 1363.4408
Frequencies -- 1365.5921 1366.2886 1366.7406
Frequencies -- 1371.1873 1371.9410 1374.9923
Frequencies -- 1378.0677 1381.0631 1381.3719
Frequencies -- 1393.7755 1408.2744 1446.1556
Frequencies -- 1457.9505 1461.6298 1464.6102
Frequencies -- 1470.3236 1471.2682 1491.9135
Frequencies -- 1495.3799 1496.2912 1496.7535
Frequencies -- 1498.8024 1499.8752 1503.4661
Frequencies -- 1504.3698 1504.7190 1506.6935
Frequencies -- 1509.9027 1510.9447 1517.1492
Frequencies -- 1517.9036 1520.3499 1522.2939
Frequencies -- 1526.4357 1532.7563 1536.9366
Frequencies -- 1543.3113 1545.7890 1552.1682
Frequencies -- 1554.6662 1555.9413 1558.1653
Frequencies -- 1559.0862 1559.7328 1566.3863
Frequencies -- 1571.6980 1576.2811 1652.8574
Frequencies -- 1665.3326 1667.5184 1667.6066
Frequencies -- 1668.0533 1671.8385 1674.1204
Frequencies -- 1674.8919 1677.1553 1679.5854
Frequencies -- 1682.4064 1688.8080 1690.5533
Frequencies -- 1696.2440 1696.5661 1698.9018
Frequencies -- 1699.2985 1699.9540 1700.6972
Frequencies -- 1702.5687 1702.6609 1703.1622
Frequencies -- 1705.4110 1708.8866 1721.6180
Frequencies -- 1722.5862 1732.1861 1734.9530
Frequencies -- 2026.7079 3068.3208 3082.2497
Frequencies -- 3085.2355 3090.4511 3104.3729
Frequencies -- 3130.0328 3146.5841 3156.5508
Frequencies -- 3166.7806 3189.4020 3191.9924
Frequencies -- 3195.8879 3198.7252 3199.5415
Frequencies -- 3200.3250 3200.8348 3209.0071
Frequencies -- 3210.6866 3211.6614 3212.1418
Frequencies -- 3213.7189 3213.8306 3216.2597
Frequencies -- 3217.5682 3217.9775 3219.0441
Frequencies -- 3221.0845 3221.8871 3222.0312
Frequencies -- 3222.9721 3223.8740 3225.8298
Frequencies -- 3227.1110 3228.9319 3230.0541
Frequencies -- 3231.7538 3232.6443 3232.7910
Frequencies -- 3233.0613 3234.1365 3234.5693
Frequencies -- 3236.7832 3236.8359 3237.5133
Frequencies -- 3238.4133 3241.0637 3241.5955
Frequencies -- 3241.5996 3241.6125 3243.4495
Frequencies -- 3243.4967 3243.8529 3244.6170
Frequencies -- 3245.7849 3248.7428 3250.2793
Frequencies -- 3250.3553 3479.2680 3686.7433

SCF Done: E(RM062X/DGDZVP) = -6499.39950806
Sum of electronic and zero-point Energies= -6498.049855
Sum of electronic and thermal Energies= -6497.935546
Sum of electronic and thermal Free Energies= -6498.208075
SCF Done: E(RM062X/DGTZVP/SMD) = -6500.68639466

Cat f TS1a_*R*

Center Number	Atomic Number	Atomic Type	Coordinates (Angstroms) X	Y	Z
1	15	0	-0.026717	0.008552	0.003297
2	8	0	-0.013331	0.020778	1.626204
3	8	0	1.568125	0.011530	-0.349501
4	8	0	-0.498933	1.330399	-0.539897
5	8	0	-0.702605	-1.257077	-0.421269
6	6	0	0.721910	1.043110	2.212010
7	6	0	2.215095	-1.177756	-0.043589
8	6	0	2.050483	0.803841	2.530196
9	6	0	0.146163	2.305682	2.408317
10	6	0	2.654482	-1.421238	1.246049
11	6	0	2.258494	-2.175438	-1.017977
12	6	0	2.825874	-0.491472	2.429026
13	6	0	2.836706	1.840391	3.034825
14	6	0	0.945981	3.324290	2.933319
15	6	0	-1.274869	2.505047	2.037166
16	6	0	3.029309	-2.716092	1.599331
17	6	0	2.733995	-3.440706	-0.669838
18	6	0	1.742432	-1.861258	-2.370397

19	6	0	2.555084	-1.472193	3.596165
20	6	0	4.290108	0.026599	2.465947
21	6	0	4.276033	1.374737	3.226788
22	6	0	2.289124	3.110013	3.262101
23	1	0	0.507355	4.303952	3.102939
24	6	0	-1.685917	3.511179	1.160306
25	6	0	-2.238167	1.605012	2.489767
26	6	0	3.104290	-2.845566	3.117706
27	6	0	3.109989	-3.735036	0.645395
28	1	0	2.779378	-4.221201	-1.425174
29	6	0	0.697696	-2.592926	-2.927248
30	6	0	2.264916	-0.797486	-3.109870
31	1	0	3.008000	-1.138024	4.534996
32	1	0	1.473580	-1.549663	3.748095
33	1	0	4.973903	-0.700027	2.915184
34	1	0	4.626190	0.196345	1.439167
35	1	0	4.462272	1.205820	4.294734
36	6	0	5.321308	2.339566	2.702507
37	6	0	3.093970	4.204088	3.868927
38	6	0	-2.996755	3.550620	0.693405
39	8	0	-0.757416	4.427186	0.724995
40	6	0	-3.539473	1.600934	1.986848
41	8	0	-1.877686	0.688713	3.450913
42	1	0	4.137923	-2.980054	3.457361
43	6	0	2.278882	-4.026712	3.592465
44	6	0	3.543039	-5.101333	1.038691
45	6	0	0.214033	-2.291097	-4.193767
46	8	0	0.114282	-3.606760	-2.206811
47	6	0	1.792139	-0.486014	-4.390283
48	8	0	3.272715	-0.080455	-2.515435
49	6	0	5.326214	2.688394	1.348022
50	6	0	6.287787	2.899973	3.539118
51	6	0	3.311139	5.404577	3.185682
52	6	0	3.643395	4.041018	5.145502
53	6	0	-3.924956	2.570324	1.059353
54	8	0	-3.411912	4.531085	-0.166747
55	6	0	-1.087143	5.087958	-0.447875
56	8	0	-4.418404	0.632843	2.405706
57	6	0	-2.533369	-0.519621	3.341610
58	6	0	0.958216	-4.175273	3.146026
59	6	0	2.833714	-5.020964	4.397796
60	6	0	2.677602	-6.191759	0.906036
61	6	0	4.809174	-5.299129	1.600624
62	6	0	0.752999	-1.242970	-4.944649
63	8	0	-0.832454	-3.023747	-4.705035
64	6	0	-1.244795	-3.708977	-2.447474
65	8	0	2.332532	0.545145	-5.114614
66	6	0	3.852389	0.913010	-3.266917
67	6	0	6.264106	3.585383	0.842495
68	1	0	4.576038	2.263715	0.681945
69	6	0	7.230025	3.799765	3.039720
70	1	0	6.294954	2.643312	4.595823
71	6	0	4.096562	6.408153	3.751679
72	1	0	2.865653	5.547735	2.203898
73	6	0	4.416494	5.048233	5.718686
74	1	0	3.452879	3.120788	5.693057
75	6	0	-5.281232	2.621372	0.394421
76	6	0	-2.405264	5.132723	-0.893473
77	6	0	-0.088388	5.736613	-1.159970
78	6	0	-3.817548	-0.547503	2.807371
79	6	0	-1.933354	-1.683947	3.794745
80	6	0	0.221587	-5.306995	3.485825
81	1	0	0.519038	-3.423813	2.488532
82	6	0	2.094245	-6.152679	4.746412
83	1	0	3.864637	-4.926675	4.731183
84	6	0	3.064092	-7.454891	1.351696
85	1	0	1.687708	-6.036559	0.483611
86	6	0	5.200876	-6.563720	2.035689
87	1	0	5.488854	-4.454782	1.690425
88	6	0	0.187363	-1.047982	-6.334322
89	6	0	-1.725344	-3.430866	-3.724098
90	6	0	-2.112668	-4.064492	-1.426734
91	6	0	3.406418	1.204411	-4.551067
92	6	0	4.904997	1.627895	-2.709435
93	6	0	7.220585	4.147436	1.689523
94	1	0	6.239758	3.850466	-0.212234
95	1	0	7.966397	4.233945	3.709146
96	6	0	4.656193	6.230147	5.017093
97	1	0	4.272222	7.329184	3.204353
98	1	0	4.832901	4.911177	6.712214
99	9	0	-5.909787	3.780971	0.639737
100	9	0	-5.161832	2.507184	-0.943990
101	9	0	-6.099788	1.639496	0.788455
102	6	0	-2.735262	5.804159	-2.060393
103	1	0	0.929244	5.711379	-0.781432
104	6	0	-0.413806	6.411459	-2.337235
105	6	0	-4.517882	-1.739672	2.705085
106	1	0	-0.931733	-1.634074	4.210407
107	6	0	-2.643005	-2.883238	3.723487
108	6	0	0.787560	-6.301804	4.286556
109	1	0	-0.786709	-5.427639	3.099568
110	1	0	2.548258	-6.925038	5.359892
111	6	0	4.324153	-7.643003	1.921246
112	1	0	2.375791	-8.290071	1.264720
113	1	0	6.187617	-6.706163	2.466145
114	9	0	0.729982	-0.033599	-7.003656
115	9	0	-1.145158	-0.833805	-6.295636
116	9	0	0.375245	-2.156589	-7.073646
117	6	0	-3.076453	-3.533591	-4.013421
118	1	0	-1.710704	-4.219871	-0.430369
119	6	0	-3.474312	-4.180489	-1.712795
120	6	0	4.035105	2.187351	-5.304427
121	1	0	5.223380	1.377815	-1.701586
122	6	0	5.523416	2.631119	-3.452855
123	1	0	7.951209	4.849968	1.300648
124	1	0	5.266956	7.011968	5.457795
125	1	0	-3.775334	5.819367	-2.370753
126	6	0	-1.732320	6.442394	-2.789367
127	1	0	0.371378	6.913000	-2.894606
128	1	0	-5.517384	-1.725340	2.282490
129	6	0	-3.926240	-2.912623	3.176958
130	1	0	-2.187738	-3.790508	4.106455
131	1	0	0.217127	-7.190095	4.540084
132	1	0	4.622638	-8.626783	2.270194
133	1	0	-3.417566	-3.308360	-5.019245
134	6	0	-3.952059	-3.923700	-2.998460
135	1	0	-4.162691	-4.461812	-0.922833
136	1	0	3.668173	2.379604	-6.307685
137	6	0	5.093664	2.906131	-4.752023
138	1	0	6.344550	3.190962	-3.017296
139	1	0	-1.984812	6.965399	-3.705556
140	1	0	-4.474453	-3.847371	3.123065
141	1	0	-5.011758	-4.014965	-3.212575
142	1	0	5.581200	3.678192	-5.337983
143	1	0	-1.949055	-1.232294	-1.409053
144	8	0	-2.649407	-0.951295	-2.086062
145	6	0	-3.382280	0.190177	-1.572328
146	6	0	-2.921536	1.214986	-2.627636
147	1	0	-4.449817	-0.031171	-1.559574
148	1	0	-3.029008	0.452072	-0.569900
149	8	0	-2.412076	2.396933	-2.090939
150	6	0	-1.851117	0.250806	-3.227665

151	1	0	-1.807573	2.148033	-1.360271
152	1	0	-0.855708	0.160829	-2.801043
153	1	0	-2.045422	-0.310856	-4.136008
154	1	0	3.581823	4.334712	0.395963
155	6	0	3.186971	4.280119	-0.613396
156	6	0	2.244748	3.303830	-0.923331
157	6	0	3.626276	5.203292	-1.573777
158	6	0	1.735615	3.297790	-2.222386
159	1	0	1.885564	2.590519	-0.183774
160	6	0	3.118543	5.182575	-2.871616
161	1	0	4.365951	5.949632	-1.300094
162	7	0	0.741688	2.456689	-2.712092
163	6	0	2.156590	4.223840	-3.183506
164	1	0	3.452618	5.900214	-3.614660
165	6	0	0.314489	2.699743	-3.966007
166	1	0	0.231224	1.854836	-2.044353
167	16	0	1.246878	4.011040	-4.663564
168	16	0	-0.905594	1.928025	-4.809847
169	6	0	-3.979764	1.537684	-3.660951
170	6	0	-4.232145	2.857529	-4.027987
171	6	0	-4.697578	0.499334	-4.262252
172	6	0	-5.204063	3.137644	-4.987868
173	1	0	-3.656794	3.648655	-3.558466
174	6	0	-5.664739	0.780949	-5.224182
175	1	0	-4.502544	-0.535773	-3.978917
176	6	0	-5.921536	2.103565	-5.587574
177	1	0	-5.399082	4.167527	-5.271644
178	1	0	-6.217532	-0.029526	-5.689143
179	1	0	-6.676369	2.324386	-6.335978

Frequencies -- -543.8153 10.0599 15.9684
Frequencies -- 18.2324 20.3338 24.5509
Frequencies -- 26.2233 28.4622 31.3556
Frequencies -- 34.3215 35.9874 37.7787
Frequencies -- 39.9412 40.5073 41.4971
Frequencies -- 43.7443 45.5274 47.2644
Frequencies -- 50.2729 52.3670 58.5803
Frequencies -- 59.8156 63.2984 64.5206
Frequencies -- 66.4591 68.6765 74.7620
Frequencies -- 75.0899 78.9614 81.1879
Frequencies -- 83.9804 85.6960 91.3872
Frequencies -- 92.4877 93.4292 96.4668
Frequencies -- 98.2597 101.7933 106.5896
Frequencies -- 109.3033 112.1100 113.8695
Frequencies -- 119.0002 119.6186 122.2850
Frequencies -- 127.0014 131.5961 134.4501
Frequencies -- 136.7112 139.8112 146.7820
Frequencies -- 150.8336 155.5844 163.1330
Frequencies -- 167.4185 170.9407 174.9303
Frequencies -- 187.5222 188.9673 192.9908
Frequencies -- 195.7078 203.9153 209.8729
Frequencies -- 216.5480 218.8343 226.1028
Frequencies -- 227.9613 229.6503 232.1187
Frequencies -- 232.7892 244.4593 249.3967
Frequencies -- 252.6916 261.2427 269.7950
Frequencies -- 271.6604 274.1688 275.2418
Frequencies -- 278.2295 284.6152 289.4405
Frequencies -- 291.9502 292.4395 296.8329
Frequencies -- 299.6578 302.0215 302.6551
Frequencies -- 306.9544 308.6280 309.6916
Frequencies -- 315.6957 317.5247 320.6299
Frequencies -- 321.4841 331.6523 334.0125
Frequencies -- 338.7599 342.6018 351.6656
Frequencies -- 362.2807 377.8670 385.1959
Frequencies -- 399.5360 407.1587 409.5930
Frequencies -- 410.9346 412.1076 413.1918
Frequencies -- 415.8853 417.2507 419.9970
Frequencies -- 421.8847 424.1463 424.5886
Frequencies -- 435.1620 435.9464 442.7173
Frequencies -- 445.0173 449.0529 452.4711
Frequencies -- 454.9931 460.4990 463.3727
Frequencies -- 464.4240 466.8878 469.9622
Frequencies -- 475.8676 485.6376 490.0740
Frequencies -- 500.7194 505.8125 509.2466
Frequencies -- 512.1159 520.1731 522.1187
Frequencies -- 526.6107 530.7741 534.1029
Frequencies -- 537.6442 539.7053 545.8639
Frequencies -- 548.1001 552.2494 552.5609
Frequencies -- 557.4303 558.6468 561.7319
Frequencies -- 563.2629 569.2045 570.5132
Frequencies -- 577.8996 582.3944 584.2641
Frequencies -- 586.2311 590.9848 596.6580
Frequencies -- 596.8505 599.1571 601.3404
Frequencies -- 603.3286 609.3339 609.7914
Frequencies -- 610.7205 613.9654 618.4903
Frequencies -- 620.8624 624.7716 626.6676
Frequencies -- 630.2509 630.9638 632.0704
Frequencies -- 634.9337 635.2035 646.1418
Frequencies -- 648.0722 656.2915 658.8931
Frequencies -- 663.6839 664.5644 674.6204
Frequencies -- 677.3013 677.7158 682.2374
Frequencies -- 684.5655 698.7308 706.9220
Frequencies -- 714.0327 714.8256 715.1876
Frequencies -- 716.2271 718.9011 721.8649
Frequencies -- 722.8857 724.6964 726.4352
Frequencies -- 726.6500 729.4250 731.6919
Frequencies -- 733.4872 736.5559 740.2195
Frequencies -- 745.5292 745.9743 751.1390
Frequencies -- 752.5164 762.5788 765.2598
Frequencies -- 768.1780 768.3550 771.4910
Frequencies -- 775.5227 776.2979 779.7318
Frequencies -- 780.1890 781.7088 782.7049
Frequencies -- 789.1739 794.4900 798.9287
Frequencies -- 801.5408 804.3111 804.7308
Frequencies -- 822.5611 825.3063 826.9545
Frequencies -- 831.9396 858.4870 866.9145
Frequencies -- 868.3082 868.6584 869.5116
Frequencies -- 871.4536 871.8443 873.8475
Frequencies -- 874.8061 876.5094 878.7008
Frequencies -- 884.0624 886.7652 887.6554
Frequencies -- 888.1683 889.4424 897.2506
Frequencies -- 900.0715 901.8452 912.7162
Frequencies -- 918.2185 919.5318 923.8272
Frequencies -- 928.6366 935.6488 936.9902
Frequencies -- 940.4739 941.8618 946.6357
Frequencies -- 946.8174 948.0873 951.2701
Frequencies -- 952.8153 953.8867 956.1125
Frequencies -- 958.0579 961.7330 968.3835
Frequencies -- 974.9717 984.9991 986.2857
Frequencies -- 990.7737 992.3633 996.9463
Frequencies -- 997.0614 1001.5242 1002.9144
Frequencies -- 1004.3197 1006.3163 1006.8618
Frequencies -- 1009.4057 1012.9364 1013.7538
Frequencies -- 1015.0759 1015.9510 1018.1634
Frequencies -- 1018.5437 1019.9916 1020.7949
Frequencies -- 1021.1202 1023.3198 1024.4769
Frequencies -- 1028.0176 1036.1027 1036.2522
Frequencies -- 1043.0803 1048.9286 1051.7157
Frequencies -- 1054.7520 1056.4733 1057.6442
Frequencies -- 1058.7856 1062.8574 1065.1424
Frequencies -- 1065.3972 1067.6662 1068.2405

Frequencies -- 1071.2681 1073.9437 1078.7389
Frequencies -- 1092.2564 1094.4459 1099.3242
Frequencies -- 1108.9911 1109.3094 1111.3366
Frequencies -- 1112.4304 1113.9862 1115.8409
Frequencies -- 1121.9863 1124.7658 1126.4721
Frequencies -- 1128.2152 1129.2607 1130.4555
Frequencies -- 1132.4655 1160.5353 1164.3031
Frequencies -- 1165.3845 1167.1245 1170.4661
Frequencies -- 1171.2072 1171.8633 1172.8981
Frequencies -- 1174.6931 1175.3196 1177.2628
Frequencies -- 1177.6115 1180.8072 1180.8623
Frequencies -- 1186.8321 1194.6528 1196.7266
Frequencies -- 1201.6441 1203.6604 1204.4951
Frequencies -- 1207.1623 1209.3338 1209.8891
Frequencies -- 1210.0793 1210.9503 1218.6449
Frequencies -- 1222.3684 1226.1312 1227.5466
Frequencies -- 1230.4024 1231.8493 1233.5582
Frequencies -- 1237.8112 1242.0991 1248.4289
Frequencies -- 1251.6018 1255.4723 1257.2483
Frequencies -- 1268.3027 1272.3266 1279.4785
Frequencies -- 1281.1369 1284.2255 1286.8201
Frequencies -- 1289.4205 1292.7264 1296.9907
Frequencies -- 1297.7847 1298.7260 1300.7534
Frequencies -- 1302.4373 1305.2449 1306.7200
Frequencies -- 1307.9203 1309.9967 1310.9932
Frequencies -- 1313.5116 1321.5498 1324.7771
Frequencies -- 1327.0590 1328.5434 1333.6781
Frequencies -- 1337.1650 1340.2375 1340.6824
Frequencies -- 1341.9326 1346.5961 1357.0386
Frequencies -- 1358.2425 1360.5440 1361.4950
Frequencies -- 1362.8705 1363.9039 1364.2943
Frequencies -- 1365.9020 1366.7486 1368.5533
Frequencies -- 1369.7395 1370.1428 1375.3453
Frequencies -- 1382.0852 1383.4832 1392.7903
Frequencies -- 1407.7710 1438.5960 1447.8536
Frequencies -- 1452.7362 1459.9143 1466.0527
Frequencies -- 1468.8645 1470.4815 1481.4026
Frequencies -- 1490.4666 1494.7287 1496.8107
Frequencies -- 1498.5727 1502.7408 1503.0991
Frequencies -- 1503.7506 1505.5835 1506.3209
Frequencies -- 1510.5002 1511.4018 1512.8702
Frequencies -- 1516.5652 1517.6792 1524.8469
Frequencies -- 1526.1039 1528.7913 1540.6590
Frequencies -- 1544.2945 1547.1640 1552.1723
Frequencies -- 1555.2430 1557.2026 1557.3927
Frequencies -- 1559.1727 1560.9513 1561.6739
Frequencies -- 1568.8871 1572.8729 1657.0064
Frequencies -- 1662.7883 1665.6089 1666.9161
Frequencies -- 1668.3969 1672.7198 1674.3773
Frequencies -- 1675.2555 1677.7653 1678.8615
Frequencies -- 1682.0462 1688.1044 1689.5761
Frequencies -- 1694.1778 1695.3793 1697.3103
Frequencies -- 1698.8802 1700.0645 1700.2263
Frequencies -- 1700.8066 1701.3908 1702.2237
Frequencies -- 1704.2268 1705.6893 1718.1462
Frequencies -- 1719.8847 1730.5691 1731.1433
Frequencies -- 2957.2369 3072.4779 3082.7544
Frequencies -- 3088.5799 3093.4304 3118.1340
Frequencies -- 3152.9324 3155.5223 3177.4440
Frequencies -- 3177.5739 3189.8996 3199.5083
Frequencies -- 3201.7773 3202.4241 3203.1910
Frequencies -- 3203.8165 3211.5375 3212.9189
Frequencies -- 3213.0326 3213.9782 3215.9208
Frequencies -- 3216.1715 3216.4372 3217.7495
Frequencies -- 3219.5642 3220.4931 3221.7935
Frequencies -- 3222.1381 3223.1203 3223.3711
Frequencies -- 3223.5569 3225.2824 3229.2385
Frequencies -- 3229.5726 3230.7391 3231.3946
Frequencies -- 3231.5937 3232.6342 3232.9204
Frequencies -- 3233.0211 3233.3467 3234.8630
Frequencies -- 3238.1756 3238.2304 3240.2514
Frequencies -- 3240.7121 3240.9133 3241.5480
Frequencies -- 3243.1767 3243.3329 3243.5354
Frequencies -- 3246.4141 3246.9661 3247.4004
Frequencies -- 3248.0780 3250.5248 3252.9636
Frequencies -- 3266.6789 3331.0438 3596.5203

SCF Done: E(RM062X/DGDZVP) = -6499.37479158
Sum of electronic and zero-point Energies= -6498.024768
Sum of electronic and thermal Energies= -6497.911090
Sum of electronic and thermal Free Energies= -6498.181743
SCF Done: E(RM062X/DGTZVP/SMD) = -6500.65713238

Cat f I1a_*R*

Center Number	Atomic Number	Atomic Type	Coordinates (Angstroms) X	Y	Z
1	15	0	0.044349	0.060565	-0.042029
2	8	0	0.002249	0.033213	1.580893
3	8	0	1.655957	0.079396	-0.343740
4	8	0	-0.368704	1.437691	-0.523767
5	8	0	-0.625911	-1.159164	-0.555962
6	6	0	0.707196	1.044370	2.217809
7	6	0	2.300360	-1.112263	-0.050734
8	6	0	2.030071	0.809332	2.565635
9	6	0	0.114669	2.295983	2.434029
10	6	0	2.708611	-1.378942	1.246899
11	6	0	2.366219	-2.096884	-1.037205
12	6	0	2.826878	-0.473258	2.455963
13	6	0	2.788383	1.838929	3.122785
14	6	0	0.889515	3.306502	3.012190
15	6	0	-1.292352	2.518436	2.024058
16	6	0	3.083309	-2.677009	1.587234
17	6	0	2.849325	-3.362962	-0.698765
18	6	0	1.809815	-1.812255	-2.379975
19	6	0	2.527421	-1.482443	3.591668
20	6	0	4.283049	0.061671	2.555919
21	6	0	4.225061	1.387049	3.351800
22	6	0	2.223913	3.095453	3.370106
23	1	0	0.439105	4.279013	3.191824
24	6	0	-1.664091	3.573080	1.184923
25	6	0	-2.285690	1.620919	2.408330
26	6	0	3.105975	-2.839748	3.103627
27	6	0	3.201145	-3.677482	0.616827
28	1	0	2.905377	-4.133793	-1.463297
29	6	0	0.766476	-2.592618	-2.872959
30	6	0	2.251876	-0.743122	-3.161013
31	1	0	2.944352	-1.164329	4.552526
32	1	0	1.442177	-1.573473	3.705359
33	1	0	4.959913	-0.669473	3.008358
34	1	0	4.651016	0.262086	1.545872
35	1	0	4.373978	1.191864	4.421380
36	6	0	5.268372	2.389502	2.898632
37	6	0	3.019885	4.179623	4.008752
38	6	0	-2.968680	3.680123	0.716981
39	8	0	-0.704978	4.480246	0.785734
40	6	0	-3.582772	1.684409	1.892659
41	8	0	-1.969063	0.639014	3.319258
42	1	0	4.127815	-2.974682	3.477039
43	6	0	2.274298	-4.037054	3.524327

44	6	0	3.621825	-5.051811	0.994160
45	6	0	0.210931	-2.342566	-4.121936
46	8	0	0.253042	-3.602101	-2.101018
47	6	0	1.712256	-0.490939	-4.426618
48	8	0	3.234546	0.058423	-2.624853
49	6	0	5.337402	2.768128	1.553228
50	6	0	6.161064	2.969589	3.801261
51	6	0	3.414179	5.303547	3.276151
52	6	0	3.408344	4.068074	5.347406
53	6	0	-3.936200	2.721606	1.030750
54	8	0	-3.335901	4.713284	-0.106462
55	6	0	-0.991208	5.143627	-0.395412
56	8	0	-4.484181	0.708750	2.234728
57	6	0	-2.636299	-0.549519	3.099809
58	6	0	0.972153	-4.190480	3.027148
59	6	0	2.808558	-5.039397	4.333302
60	6	0	2.759834	-6.136435	0.802047
61	6	0	4.864661	-5.266407	1.599684
62	6	0	0.684828	-1.301305	-4.923144
63	8	0	-0.833328	-3.115325	-4.564191
64	6	0	-1.111867	-3.761467	-2.273786
65	8	0	2.162175	0.563918	-5.185662
66	6	0	3.837444	0.942003	-3.485558
67	6	0	6.269460	3.709343	1.122315
68	1	0	4.647484	2.325794	0.835160
69	6	0	7.089423	3.920946	3.377750
70	1	0	6.115002	2.692048	4.851583
71	6	0	4.208524	6.286525	3.864107
72	1	0	3.107093	5.393288	2.236622
73	6	0	4.191718	5.057020	5.941198
74	1	0	3.090489	3.202177	5.923485
75	6	0	-5.305010	2.894521	0.411846
76	6	0	-2.304837	5.246771	-0.847581
77	6	0	0.038934	5.739821	-1.109109
78	6	0	-3.908542	-0.513105	2.539053
79	6	0	-2.059179	-1.755533	3.464063
80	6	0	0.234691	-5.333857	3.322784
81	1	0	0.551489	-3.433115	2.364251
82	6	0	2.068082	-6.183197	4.637056
83	1	0	3.825330	-4.940631	4.706399
84	6	0	3.126323	-7.411019	1.231242
85	1	0	1.786422	-5.968181	0.346852
86	6	0	5.236806	-6.542533	2.018348
87	1	0	5.541473	-4.426299	1.737924
88	6	0	0.051598	-1.153471	-6.288410
89	6	0	-1.663947	-3.535680	-3.530794
90	6	0	-1.912393	-4.138971	-1.207127
91	6	0	3.323624	1.173691	-4.757410
92	6	0	4.967587	1.625399	-3.053120
93	6	0	7.147140	4.295253	2.036264
94	1	0	6.310585	3.986120	0.071134
95	1	0	7.764268	4.372030	4.098955
96	6	0	4.602177	6.163398	5.197276
97	1	0	4.523074	7.146640	3.280928
98	1	0	4.483182	4.963144	6.983089
99	9	0	-5.863122	4.055639	0.800702
100	9	0	-5.238259	2.917248	-0.929240
101	9	0	-6.158848	1.920196	0.741893
102	6	0	-2.598150	5.909650	-2.029203
103	1	0	1.051592	5.678893	-0.722555
104	6	0	-0.250701	6.416618	-2.295540
105	6	0	-4.618115	-1.681886	2.311975
106	1	0	-1.065927	-1.755377	3.902346
107	6	0	-2.782026	-2.933718	3.273043
108	6	0	0.780396	-6.336219	4.128010
109	1	0	-0.757893	-5.459534	2.899491
110	1	0	2.506673	-6.960941	5.254922
111	6	0	4.363263	-7.616357	1.843760
112	1	0	2.439581	-8.241373	1.098139
113	1	0	6.206014	-6.698148	2.482765
114	9	0	0.541512	-0.138302	-7.004629
115	9	0	-1.280741	-0.957061	-6.192860
116	9	0	0.226565	-2.269085	-7.015184
117	6	0	-3.019164	-3.713420	-3.755607
118	1	0	-1.460037	-4.250668	-0.226731
119	6	0	-3.276809	-4.331393	-1.428401
120	6	0	3.951590	2.061675	-5.620439
121	1	0	5.339658	1.428729	-2.052026
122	6	0	5.586566	2.537752	-3.905899
123	1	0	7.870576	5.033515	1.704183
124	1	0	5.220200	6.929540	5.655295
125	1	0	-3.634178	5.962605	-2.348370
126	6	0	-1.563541	6.494406	-2.759147
127	1	0	0.556588	6.888103	-2.848040
128	1	0	-5.601356	-1.618093	1.857540
129	6	0	-4.050306	-2.898440	2.692945
130	1	0	-2.348712	-3.877281	3.587643
131	1	0	0.208990	-7.232858	4.347644
132	1	0	4.646019	-8.609123	2.180184
133	1	0	-3.419318	-3.521248	-4.746103
134	6	0	-3.824958	-4.127743	-2.694556
135	1	0	-3.915167	-4.615693	-0.598961
136	1	0	3.527767	2.204871	-6.609615
137	6	0	5.084771	2.751179	-5.191078
138	1	0	6.465579	3.075708	-3.566181
139	1	0	-1.787960	7.018118	-3.682373
140	1	0	-4.605052	-3.818306	2.539599
141	1	0	-4.889198	-4.262858	-2.853905
142	1	0	5.574163	3.449490	-5.861817
143	1	0	-2.332189	-1.408535	-1.388179
144	8	0	-3.165544	-1.094297	-1.794088
145	6	0	-3.298957	0.267143	-1.448326
146	6	0	-2.842300	1.239626	-2.576963
147	1	0	-4.352344	0.470556	-1.228838
148	1	0	-2.714532	0.493293	-0.548740
149	8	0	-2.428240	2.468355	-2.008089
150	6	0	-1.676215	0.594400	-3.363928
151	1	0	-1.832070	2.240391	-1.266921
152	1	0	-0.852097	0.256578	-2.726927
153	1	0	-2.026700	-0.275271	-3.926681
154	1	0	3.845977	4.368515	0.083855
155	6	0	3.364767	4.262107	-0.883084
156	6	0	2.371352	3.302713	-1.045786
157	6	0	3.741361	5.113455	-1.934931
158	6	0	1.752803	3.240534	-2.295856
159	1	0	2.054181	2.644694	-0.238139
160	6	0	3.126445	5.036661	-3.181178
161	1	0	4.521968	5.850144	-1.773079
162	7	0	0.697363	2.399750	-2.643829
163	6	0	2.114746	4.090832	-3.344233
164	1	0	3.416418	5.695537	-3.993205
165	6	0	0.224603	2.574479	-3.865356
166	1	0	0.217023	1.854917	-1.846799
167	16	0	1.087508	3.807550	-4.732201
168	16	0	-1.040674	1.725481	-4.652645
169	6	0	-3.976768	1.520719	-3.547068
170	6	0	-4.314566	2.827278	-3.899495
171	6	0	-4.677366	0.448822	-4.112229
172	6	0	-5.346521	3.061573	-4.808837
173	1	0	-3.769486	3.649145	-3.446022
174	6	0	-5.706658	0.686256	-5.020720
175	1	0	-4.425027	-0.570580	-3.823215

176	6	0	-6.043214	1.994302	-5.373281
177	1	0	-5.608273	4.081450	-5.075334
178	1	0	-6.248931	-0.149918	-5.451914
179	1	0	-6.845962	2.178685	-6.080741

Frequencies --	12.3355	17.7047	21.9561
Frequencies --	23.2482	23.7798	28.7654
Frequencies --	29.6561	31.3176	35.7652
Frequencies --	36.2451	36.9302	39.0885
Frequencies --	40.6167	43.0241	46.0745
Frequencies --	46.8128	49.7203	55.3701
Frequencies --	57.9242	58.6943	60.7509
Frequencies --	62.3020	65.9268	66.9975
Frequencies --	68.1853	70.5986	73.6158
Frequencies --	78.7961	80.8268	81.8787
Frequencies --	86.8627	90.7283	92.4656
Frequencies --	94.1844	96.2791	98.5037
Frequencies --	104.2701	104.7427	109.4344
Frequencies --	111.2814	113.1262	118.2921
Frequencies --	119.6304	126.4481	129.7021
Frequencies --	132.0800	135.3187	136.8440
Frequencies --	140.2413	146.0130	152.5852
Frequencies --	156.2171	164.1442	167.2591
Frequencies --	171.4842	184.5054	186.7448
Frequencies --	188.4637	194.3274	195.8607
Frequencies --	201.1304	211.4605	215.2485
Frequencies --	217.4483	220.6530	226.2928
Frequencies --	228.6235	231.7870	233.8279
Frequencies --	245.0071	249.2438	255.3837
Frequencies --	260.4188	268.2033	271.7208
Frequencies --	273.9516	275.2980	277.5362
Frequencies --	285.4822	288.3743	289.8965
Frequencies --	292.1632	293.9414	298.5480
Frequencies --	299.9622	304.0270	307.2278
Frequencies --	308.8657	311.0336	313.7029
Frequencies --	316.8870	320.0723	322.4935
Frequencies --	330.0312	333.3019	338.6369
Frequencies --	341.7748	346.0636	354.2065
Frequencies --	370.0581	380.9735	388.8152
Frequencies --	406.3332	408.4914	409.4854
Frequencies --	410.6917	411.4127	413.0075
Frequencies --	415.1334	417.4171	420.4070
Frequencies --	422.1971	423.2802	428.4926
Frequencies --	432.1442	439.8899	442.8048
Frequencies --	445.1901	446.7370	452.5895
Frequencies --	457.5082	460.3912	463.6997
Frequencies --	465.5574	466.3201	474.5753
Frequencies --	487.2805	491.3845	500.8799
Frequencies --	507.6977	509.1552	513.4269
Frequencies --	520.4826	521.9446	525.3800
Frequencies --	528.9614	530.7297	533.6114
Frequencies --	537.5301	539.0071	546.2548
Frequencies --	551.0619	553.8656	555.6006
Frequencies --	559.1197	560.1226	561.9207
Frequencies --	566.7676	570.9509	574.6180
Frequencies --	576.0736	584.8036	586.3641
Frequencies --	589.0087	592.8838	595.7270
Frequencies --	596.9983	597.5234	599.1145
Frequencies --	601.9157	604.9787	609.0366
Frequencies --	610.1745	611.0273	613.0488
Frequencies --	617.7860	620.8224	624.0874
Frequencies --	625.8680	630.1009	630.8535
Frequencies --	632.2545	634.2005	634.7839
Frequencies --	645.7985	648.0759	656.5591
Frequencies --	663.8458	672.5687	676.9330
Frequencies --	678.7100	681.9739	685.4854
Frequencies --	698.0584	703.9048	711.2516
Frequencies --	712.8388	714.0924	715.2816
Frequencies --	715.6644	718.7810	718.8667
Frequencies --	721.8183	722.5254	724.5886
Frequencies --	726.3907	728.5836	730.8308
Frequencies --	732.5617	733.7408	736.9013
Frequencies --	740.9920	746.0538	749.3397
Frequencies --	751.9343	762.2173	764.0165
Frequencies --	764.1449	767.2309	770.3158
Frequencies --	771.3361	773.9447	779.4878
Frequencies --	780.1450	783.2198	784.1992
Frequencies --	786.7072	787.4043	797.2940
Frequencies --	799.5947	800.6261	804.6163
Frequencies --	805.4312	823.4382	824.7434
Frequencies --	827.0117	832.2505	855.3410
Frequencies --	863.6386	866.0950	867.6183
Frequencies --	868.6590	869.4892	871.7347
Frequencies --	872.5595	874.5806	876.0175
Frequencies --	876.3818	883.1545	885.4555
Frequencies --	887.4247	887.8591	888.6984
Frequencies --	889.8755	892.5942	909.3995
Frequencies --	912.3191	918.5958	923.5091
Frequencies --	929.4998	930.3462	934.0608
Frequencies --	936.1610	938.9208	941.9670
Frequencies --	942.6870	944.6723	945.1029
Frequencies --	950.9236	953.2948	953.4041
Frequencies --	958.5512	968.0548	968.5065
Frequencies --	970.2813	986.6061	988.5305
Frequencies --	990.3697	991.9491	994.7884
Frequencies --	997.1011	998.0927	998.4843
Frequencies --	1001.5278	1006.0132	1007.9073
Frequencies --	1008.7854	1012.6065	1013.1396
Frequencies --	1013.4229	1015.0877	1017.2343
Frequencies --	1018.5499	1019.2553	1019.4308
Frequencies --	1021.1094	1023.2070	1024.4169
Frequencies --	1028.4487	1035.0885	1036.2278
Frequencies --	1040.7475	1044.4518	1051.5337
Frequencies --	1052.5917	1057.0575	1059.5910
Frequencies --	1062.5822	1062.8343	1065.9129
Frequencies --	1068.5374	1069.1141	1070.3448
Frequencies --	1071.0408	1073.2561	1094.8138
Frequencies --	1099.1036	1105.2459	1108.9210
Frequencies --	1109.5357	1109.5913	1112.6460
Frequencies --	1113.3809	1117.9249	1124.3398
Frequencies --	1125.6502	1127.1553	1129.7735
Frequencies --	1130.3114	1132.2306	1134.8767
Frequencies --	1158.0867	1162.8079	1163.9211
Frequencies --	1164.5408	1166.2681	1167.8827
Frequencies --	1171.4200	1171.9798	1173.3552
Frequencies --	1174.6526	1175.1844	1177.5048
Frequencies --	1177.7471	1181.4651	1187.2263
Frequencies --	1195.7057	1197.7310	1199.6169
Frequencies --	1202.7675	1204.5236	1206.3148
Frequencies --	1211.9626	1212.3040	1212.8643
Frequencies --	1215.5560	1220.6682	1222.1883
Frequencies --	1226.7022	1228.8415	1230.6325
Frequencies --	1232.0788	1238.1603	1244.2270
Frequencies --	1246.8902	1250.3638	1253.3696
Frequencies --	1255.3678	1258.4753	1270.5184
Frequencies --	1275.5001	1278.1272	1279.8031
Frequencies --	1280.0520	1285.9269	1290.4216
Frequencies --	1293.2978	1297.1647	1299.5532
Frequencies --	1300.4926	1301.1735	1301.7677
Frequencies --	1307.8740	1309.1600	1310.0694
Frequencies --	1311.4623	1312.2436	1314.8443

Frequencies --	1314.8538	1321.2948	1324.5792
Frequencies --	1325.7919	1327.5504	1333.9641
Frequencies --	1335.4258	1342.7026	1342.9425
Frequencies --	1345.4352	1356.2334	1357.3404
Frequencies --	1358.2943	1360.6299	1361.6342
Frequencies --	1363.3090	1364.3983	1366.6091
Frequencies --	1367.2172	1368.8185	1370.1125
Frequencies --	1370.4773	1377.0491	1383.9653
Frequencies --	1390.5642	1405.4779	1408.1608
Frequencies --	1409.6333	1427.5394	1448.7831
Frequencies --	1458.9740	1463.6159	1468.9019
Frequencies --	1470.3631	1478.8837	1489.8311
Frequencies --	1491.5848	1492.5167	1495.7805
Frequencies --	1496.0553	1498.6757	1503.5434
Frequencies --	1504.6071	1506.0024	1506.8284
Frequencies --	1510.4595	1512.9191	1513.9255
Frequencies --	1516.4664	1518.4955	1519.8830
Frequencies --	1527.6875	1528.0852	1545.2620
Frequencies --	1548.1745	1549.3430	1554.2157
Frequencies --	1555.7476	1558.0155	1560.1740
Frequencies --	1561.1702	1562.0815	1569.3346
Frequencies --	1573.1807	1575.2568	1659.0827
Frequencies --	1664.1336	1666.7056	1668.1408
Frequencies --	1671.7783	1672.0179	1673.4016
Frequencies --	1674.4733	1674.9614	1678.4708
Frequencies --	1680.8067	1686.8525	1689.4725
Frequencies --	1693.2663	1695.9860	1696.9794
Frequencies --	1698.1889	1698.3713	1698.7466
Frequencies --	1701.2828	1702.0158	1702.2539
Frequencies --	1704.2093	1704.6172	1719.4872
Frequencies --	1721.6325	1728.7645	1731.9945
Frequencies --	2474.8630	3069.7673	3083.3826
Frequencies --	3090.2035	3093.0962	3093.3578
Frequencies --	3120.4555	3153.6682	3154.9500
Frequencies --	3155.9384	3178.7085	3186.4777
Frequencies --	3190.6885	3198.4543	3200.8447
Frequencies --	3201.4204	3203.3525	3208.5265
Frequencies --	3208.8397	3210.4908	3213.1708
Frequencies --	3213.5763	3215.9521	3217.9985
Frequencies --	3218.3355	3220.0055	3221.4061
Frequencies --	3221.6401	3222.5006	3224.6137
Frequencies --	3225.9349	3226.1010	3226.5779
Frequencies --	3226.7596	3228.1420	3229.9152
Frequencies --	3230.7643	3230.7992	3230.8224
Frequencies --	3233.0805	3234.4907	3235.8543
Frequencies --	3239.9359	3240.5587	3240.6748
Frequencies --	3240.7737	3241.7861	3242.4114
Frequencies --	3242.5345	3243.1380	3243.8802
Frequencies --	3245.4045	3247.8421	3248.0912
Frequencies --	3249.4349	3250.4502	3251.2078
Frequencies --	3257.1589	3663.8535	3672.7923

SCF Done: E(RM062X/DGDZVP) = -6499.42943890
Sum of electronic and zero-point Energies= -6498.078550
Sum of electronic and thermal Energies= -6497.964524
Sum of electronic and thermal Free Energies= -6498.234677
SCF Done: E(RM062X/DGTZVP/SMD) = -6500.71237674

Cat f I0b_*S*

Center Number	Atomic Number	Atomic Type	Coordinates (Angstroms) X	Y	Z
1	15	0	0.104248	0.082937	-0.034561
2	8	0	0.022003	0.002543	1.573980
3	8	0	1.675752	0.086588	-0.342175
4	8	0	-0.517608	1.311107	-0.572550
5	8	0	-0.447447	-1.300796	-0.453068
6	6	0	0.525352	1.094646	2.268783
7	6	0	2.435686	-1.006997	0.073064
8	6	0	1.869337	1.077041	2.617974
9	6	0	-0.287402	2.201990	2.549848
10	6	0	2.909009	-1.057876	1.376901
11	6	0	2.625304	-2.078856	-0.808662
12	6	0	2.890272	-0.039653	2.504486
13	6	0	2.433052	2.191854	3.238858
14	6	0	0.290390	3.273282	3.245261
15	6	0	-1.699763	2.266191	2.086998
16	6	0	3.537593	-2.223879	1.818083
17	6	0	3.367018	-3.179290	-0.370361
18	6	0	1.906050	-2.102305	-2.103774
19	6	0	2.834219	-0.984337	3.733291
20	6	0	4.209665	0.774013	2.519437
21	6	0	3.936108	2.009121	3.409764
22	6	0	1.640568	3.286401	3.601395
23	1	0	-0.329676	4.124377	3.511007
24	6	0	-2.172948	3.389110	1.398237
25	6	0	-2.594487	1.211339	2.273574
26	6	0	3.667918	-2.229001	3.335592
27	6	0	3.832145	-3.271433	0.942000
28	1	0	3.545566	-4.002322	-1.056795
29	6	0	1.053541	-3.169063	-2.398776
30	6	0	1.938780	-1.038455	-3.000418
31	1	0	3.201671	-0.503271	4.644989
32	1	0	1.794096	-1.280602	3.906145
33	1	0	5.060238	0.182005	2.870622
34	1	0	4.432923	1.099809	1.498926
35	1	0	4.152642	1.765386	4.457533
36	6	0	4.768797	3.216230	3.026462
37	6	0	2.218382	4.427879	4.359721
38	6	0	-3.468455	3.447910	0.872567
39	8	0	-1.291521	4.429556	1.211099
40	6	0	-3.888988	1.265443	1.769099
41	8	0	-2.216386	0.097615	2.986041
42	1	0	4.712538	-2.102792	3.644115
43	6	0	3.140360	-3.522507	3.926387
44	6	0	4.569637	-4.469593	1.420545
45	6	0	0.229944	-3.139486	-3.514450
46	8	0	0.991941	-4.233541	-1.524931
47	6	0	1.071209	-0.972855	-4.094693
48	8	0	2.844200	-0.028179	-2.778521
49	6	0	4.743695	3.711172	1.717962
50	6	0	5.579190	3.857100	3.966206
51	6	0	2.275904	5.706949	3.799102
52	6	0	2.735806	4.222099	5.642813
53	6	0	-4.350414	2.382149	1.071766
54	8	0	-3.882119	4.520885	0.131898
55	6	0	-1.834749	5.617766	0.767526
56	8	0	-4.728253	0.192466	1.950474
57	6	0	-2.757647	-1.062738	2.454635
58	6	0	1.861114	-3.972135	3.575556
59	6	0	3.922841	-4.313030	4.767719
60	6	0	3.975689	-5.735042	1.395911
61	6	0	5.856230	-4.329404	1.951980
62	6	0	0.204539	-2.030366	-4.363402
63	8	0	-0.638365	-4.181277	-3.764928
64	6	0	-0.221772	-4.885911	-1.506784
65	8	0	1.070371	0.141908	-4.888020
66	6	0	2.425566	1.211491	-3.217936
67	6	0	5.518247	4.812414	1.356703
68	1	0	4.110741	3.234651	0.969965

69	6	0	6.340018	4.971846	3.615668
70	1	0	5.605463	3.488253	4.988725
71	6	0	2.881729	6.754429	4.491651
72	1	0	1.860253	5.869711	2.807220
73	6	0	3.324083	5.272543	6.344733
74	1	0	2.669112	3.233608	6.091670
75	6	0	-5.796199	2.368855	0.628125
76	6	0	-3.107720	5.655348	0.207564
77	6	0	-1.074535	6.774020	0.860378
78	6	0	-4.054328	-1.020054	1.950221
79	6	0	-2.026983	-2.239548	2.424967
80	6	0	1.376971	-5.185638	4.055141
81	1	0	1.253735	-3.377733	2.894086
82	6	0	3.445454	-5.535839	5.243361
83	1	0	4.925838	-3.985614	5.031601
84	6	0	4.647141	-6.837754	1.921201
85	1	0	2.973030	-5.844596	0.989588
86	6	0	6.534292	-5.433541	2.464712
87	1	0	6.325895	-3.348326	1.956174
88	6	0	-0.777795	-2.055912	-5.511960
89	6	0	-1.041133	-4.864854	-2.633347
90	6	0	-0.599340	-5.592115	-0.374853
91	6	0	1.519812	1.294572	-4.271709
92	6	0	2.953192	2.360944	-2.649436
93	6	0	6.314831	5.451916	2.307017
94	1	0	5.495577	5.173849	0.332016
95	1	0	6.951939	5.463440	4.365899
96	6	0	3.412265	6.537981	5.763711
97	1	0	2.941779	7.738775	4.037281
98	1	0	3.718176	5.103373	7.342403
99	9	0	-6.607529	2.178781	1.683966
100	9	0	-6.189439	3.492006	0.030012
101	9	0	-6.040822	1.358790	-0.233570
102	6	0	-3.621495	6.842114	-0.294255
103	1	0	-0.081464	6.712005	1.296886
104	6	0	-1.582267	7.970017	0.353145
105	6	0	-4.659784	-2.156603	1.440285
106	1	0	-1.008261	-2.232733	2.797855
107	6	0	-2.629923	-3.390036	1.913487
108	6	0	2.172374	-5.976400	4.887864
109	1	0	0.382035	-5.520518	3.775078
110	1	0	4.074548	-6.147683	5.882694
111	6	0	5.925784	-6.688883	2.460467
112	1	0	4.168321	-7.812206	1.917262
113	1	0	7.534417	-5.314006	2.870376
114	9	0	-2.045657	-2.206795	-5.075914
115	9	0	-0.526145	-3.096982	-6.326935
116	9	0	-0.754445	-0.954980	-6.262899
117	6	0	-2.252151	-5.541187	-2.636972
118	1	0	0.062286	-5.585191	0.486528
119	6	0	-1.806290	-6.292887	-0.379334
120	6	0	1.107952	2.527363	-4.754669
121	1	0	3.660227	2.261257	-1.831405
122	6	0	2.582856	3.604724	-3.164779
123	1	0	6.911969	6.314635	2.028502
124	1	0	3.884257	7.353750	6.302464
125	1	0	-4.613031	6.831015	-0.734842
126	6	0	-2.848477	8.001796	-0.230106
127	1	0	-0.980014	8.870881	0.408148
128	1	0	-5.669930	-2.086106	1.049809
129	6	0	-3.938244	-3.351331	1.430954
130	1	0	-2.070654	-4.319251	1.886466
131	1	0	1.801550	-6.928546	5.254465
132	1	0	6.446280	-7.548664	2.871032
133	1	0	-2.869048	-5.502595	-3.529235
134	6	0	-2.630313	-6.265322	-1.504419
135	1	0	-2.099838	-6.861461	0.497413
136	1	0	0.388229	2.559852	-5.566619
137	6	0	1.657296	3.687659	-4.204830
138	1	0	3.009452	4.509763	-2.741044
139	1	0	-3.242225	8.929054	-0.632337
140	1	0	-4.392607	-4.250455	1.027352
141	1	0	-3.568252	-6.810339	-1.507238
142	1	0	1.362491	4.655498	-4.597221
143	1	0	-1.484790	-1.329940	-0.635736
144	8	0	-2.876953	-1.302591	-1.009796
145	6	0	-2.924099	-1.744270	-2.400882
146	6	0	-2.964529	-0.288022	-2.898324
147	1	0	-2.028437	-2.304425	-2.667067
148	1	0	-3.834454	-2.320688	-2.581395
149	8	0	-1.640272	0.082368	-3.217419
150	6	0	-3.293678	0.043367	-1.424736
151	1	0	-1.582725	1.057785	-3.129685
152	1	0	-4.353089	0.172234	-1.201352
153	1	0	-2.683239	0.825115	-0.967150
154	1	0	-0.466429	2.898916	-1.172164
155	7	0	-0.439910	3.858382	-1.557070
156	6	0	-1.317340	4.233278	-2.510239
157	6	0	0.505007	4.791767	-1.173184
158	16	0	-2.538880	3.307300	-3.158213
159	16	0	-0.972476	5.895585	-2.989857
160	6	0	0.385725	5.989052	-1.890002
161	6	0	1.472322	4.631638	-0.180349
162	6	0	1.261437	7.047518	-1.655898
163	6	0	2.338650	5.695086	0.055637
164	1	0	1.527653	3.703897	0.388330
165	6	0	2.242750	6.887515	-0.678845
166	1	0	1.171460	7.976694	-2.209930
167	1	0	3.099592	5.600731	0.823906
168	1	0	2.936269	7.698118	-0.478400
169	6	0	-3.971615	0.080803	-3.961201
170	6	0	-5.341227	-0.107457	-3.741802
171	6	0	-3.546044	0.601190	-5.184942
172	6	0	-6.268814	0.224112	-4.726282
173	1	0	-5.697915	-0.512273	-2.797102
174	6	0	-4.474413	0.934027	-6.170218
175	1	0	-2.484512	0.740112	-5.363682
176	6	0	-5.837136	0.748023	-5.945230
177	1	0	-7.328232	0.078673	-4.538975
178	1	0	-4.128665	1.339668	-7.115984
179	1	0	-6.559348	1.010415	-6.712267

Frequencies --	8.8639	12.4468	19.0733
Frequencies --	20.7079	23.6541	24.3654
Frequencies --	27.8710	28.7406	31.4018
Frequencies --	32.9612	35.9684	37.1273
Frequencies --	40.2870	41.0594	42.6379
Frequencies --	44.9607	46.5297	48.2715
Frequencies --	53.3008	54.1272	58.4884
Frequencies --	61.1485	62.2120	64.7427
Frequencies --	66.0417	67.5098	70.1412
Frequencies --	72.5810	77.3656	78.6369
Frequencies --	79.5837	81.4691	82.1158
Frequencies --	84.0282	90.5929	95.4302
Frequencies --	98.5766	99.3080	101.7792
Frequencies --	104.7669	110.8497	113.1186
Frequencies --	117.5956	120.0250	126.0408
Frequencies --	130.1342	131.9988	136.0778
Frequencies --	138.7324	140.4523	143.9839
Frequencies --	146.8277	154.9668	158.7079
Frequencies --	165.7554	171.9356	175.0380

Frequencies --	179.6764	186.2973	189.3457
Frequencies --	195.3081	198.8426	206.9547
Frequencies --	215.4331	224.4213	226.1610
Frequencies --	230.3882	235.1114	236.8572
Frequencies --	241.1885	244.6586	250.1392
Frequencies --	251.1847	258.6324	272.3469
Frequencies --	274.1437	276.7194	277.5691
Frequencies --	282.3177	285.7947	291.7571
Frequencies --	294.2071	295.0353	300.6213
Frequencies --	302.2189	303.9389	306.5432
Frequencies --	308.5324	312.4475	316.3440
Frequencies --	318.1150	321.7699	323.0277
Frequencies --	323.3363	330.7383	335.8306
Frequencies --	339.4067	348.4409	355.1380
Frequencies --	371.2257	377.3021	389.2043
Frequencies --	400.9643	403.4869	410.1970
Frequencies --	411.1996	412.7589	413.4878
Frequencies --	415.1941	417.2754	417.8015
Frequencies --	419.8508	422.3105	425.6836
Frequencies --	430.8036	434.2108	438.3118
Frequencies --	440.6582	443.2063	449.9082
Frequencies --	450.8966	453.4987	455.9291
Frequencies --	457.0789	466.2324	472.4140
Frequencies --	486.9576	490.6359	497.8756
Frequencies --	501.6636	507.8430	511.8355
Frequencies --	512.3619	517.4182	521.7659
Frequencies --	524.3686	533.0716	534.2641
Frequencies --	536.1613	537.0254	543.8043
Frequencies --	545.7201	550.7249	552.0930
Frequencies --	555.7321	560.7003	561.7806
Frequencies --	563.0137	566.9911	570.8743
Frequencies --	572.7012	583.3968	586.0388
Frequencies --	589.6277	592.8451	597.4831
Frequencies --	599.0667	601.0102	603.0891
Frequencies --	605.3285	610.0044	610.5799
Frequencies --	612.3506	617.4690	619.8061
Frequencies --	621.7242	625.2757	627.4335
Frequencies --	629.5436	631.0210	632.9013
Frequencies --	633.5787	636.9334	644.2098
Frequencies --	651.2874	656.9185	670.0924
Frequencies --	671.4520	673.2529	677.5024
Frequencies --	680.2808	682.9621	695.8880
Frequencies --	699.6193	703.0498	709.9706
Frequencies --	715.5252	716.0877	716.3840
Frequencies --	717.7242	717.8713	720.4657
Frequencies --	723.3167	724.0469	724.8955
Frequencies --	725.6640	730.9962	731.7921
Frequencies --	735.3484	740.3404	745.0385
Frequencies --	746.9130	753.2294	764.6785
Frequencies --	768.6633	768.7816	770.6090
Frequencies --	771.3943	774.8672	776.0820
Frequencies --	776.6636	781.0513	781.6448
Frequencies --	784.6882	785.3807	795.3186
Frequencies --	798.5620	801.3412	805.3892
Frequencies --	805.7323	819.7635	826.0275
Frequencies --	827.3045	829.5847	847.2916
Frequencies --	849.1823	858.8392	861.2395
Frequencies --	863.4733	865.4695	867.8377
Frequencies --	868.3038	870.8085	873.1477
Frequencies --	873.3373	875.1123	876.6011
Frequencies --	876.8197	888.0856	888.3019
Frequencies --	890.0613	892.9309	907.9975
Frequencies --	916.4550	917.8934	922.9548
Frequencies --	925.5912	931.8167	933.9990
Frequencies --	935.3082	939.8801	940.0517
Frequencies --	941.9417	943.0684	945.2556
Frequencies --	947.2982	950.9344	951.7257
Frequencies --	952.1098	952.7903	957.8553
Frequencies --	958.4751	963.2502	971.1121
Frequencies --	975.8853	987.9274	993.7823
Frequencies --	995.4756	995.5670	996.3419
Frequencies --	996.6565	997.2444	999.3588
Frequencies --	1001.8168	1008.2028	1010.6563
Frequencies --	1011.5606	1012.1324	1014.6677
Frequencies --	1015.1061	1018.8285	1019.2145
Frequencies --	1019.5525	1019.8003	1020.2287
Frequencies --	1023.6624	1024.2857	1028.1704
Frequencies --	1032.9296	1035.7098	1037.2595
Frequencies --	1044.7901	1046.1336	1049.8245
Frequencies --	1053.2684	1057.0975	1058.5136
Frequencies --	1060.7701	1061.0276	1062.9311
Frequencies --	1065.0298	1068.0141	1069.3028
Frequencies --	1069.8736	1071.2688	1072.3422
Frequencies --	1074.7722	1092.8761	1096.2382
Frequencies --	1096.9848	1110.7247	1110.8138
Frequencies --	1111.9038	1113.2460	1119.3202
Frequencies --	1123.8284	1124.9168	1127.6323
Frequencies --	1129.6848	1130.8499	1132.5087
Frequencies --	1160.5256	1166.7667	1167.0442
Frequencies --	1167.3132	1169.3626	1170.4566
Frequencies --	1172.5352	1173.2174	1175.3861
Frequencies --	1176.4716	1178.0699	1178.3936
Frequencies --	1182.1129	1183.9059	1185.0389
Frequencies --	1194.8463	1199.7958	1202.5429
Frequencies --	1202.7846	1204.9973	1207.4620
Frequencies --	1209.6132	1211.6196	1211.9408
Frequencies --	1214.7722	1215.6969	1221.8507
Frequencies --	1224.7784	1228.8719	1232.9537
Frequencies --	1235.3969	1238.3590	1243.3933
Frequencies --	1245.1344	1247.5741	1253.3930
Frequencies --	1255.5453	1257.4884	1267.4136
Frequencies --	1280.0883	1282.1759	1289.1011
Frequencies --	1293.3430	1293.9958	1297.9532
Frequencies --	1298.2902	1299.3847	1301.4000
Frequencies --	1303.7995	1305.5104	1307.0279
Frequencies --	1308.0717	1309.4024	1311.0813
Frequencies --	1311.5952	1314.5320	1317.0460
Frequencies --	1320.3689	1324.2121	1327.3556
Frequencies --	1328.7750	1332.2027	1333.6326
Frequencies --	1336.7199	1341.1374	1343.6939
Frequencies --	1347.7585	1348.5545	1358.6647
Frequencies --	1359.6325	1360.6031	1363.6676
Frequencies --	1364.0758	1365.0300	1366.7501
Frequencies --	1366.9989	1368.6214	1370.8484
Frequencies --	1372.7142	1373.6412	1376.6747
Frequencies --	1384.5218	1386.7297	1389.0296
Frequencies --	1403.5941	1424.1407	1435.6512
Frequencies --	1448.6862	1458.1858	1464.9056
Frequencies --	1470.2378	1479.7415	1493.1092
Frequencies --	1493.7204	1494.1011	1497.1513
Frequencies --	1497.4374	1500.5494	1502.7562
Frequencies --	1504.9924	1506.6894	1508.0464
Frequencies --	1510.5666	1511.2182	1516.2168
Frequencies --	1518.6936	1520.4817	1526.8059
Frequencies --	1529.0648	1532.0254	1548.3391
Frequencies --	1549.7185	1550.9857	1552.7700
Frequencies --	1553.6994	1554.8674	1559.4326
Frequencies --	1560.2950	1562.4744	1564.1866
Frequencies --	1566.0879	1572.5263	1657.1603
Frequencies --	1662.8068	1668.3782	1668.5542
Frequencies --	1669.8393	1672.1207	1674.1038
Frequencies --	1674.1752	1678.7281	1679.4580

Frequencies -- 1683.6334 1687.7375 1690.6082
Frequencies -- 1691.0565 1694.9062 1696.7421
Frequencies -- 1697.9183 1698.9899 1699.2656
Frequencies -- 1700.5866 1701.5046 1702.7881
Frequencies -- 1703.7733 1704.3639 1719.2121
Frequencies -- 1722.5182 1730.0656 1737.0533
Frequencies -- 2281.6037 3079.7842 3079.9190
Frequencies -- 3086.8408 3092.4186 3132.1048
Frequencies -- 3145.3900 3151.0634 3154.5246
Frequencies -- 3183.0963 3186.9339 3195.5326
Frequencies -- 3197.9503 3202.1843 3204.3047
Frequencies -- 3206.3708 3206.4822 3208.2920
Frequencies -- 3213.8072 3214.3723 3214.6986
Frequencies -- 3216.4166 3217.5214 3218.0879
Frequencies -- 3218.5845 3219.9541 3223.2718
Frequencies -- 3224.0448 3224.4385 3225.6282
Frequencies -- 3225.8925 3228.5209 3229.6452
Frequencies -- 3230.7426 3231.6861 3232.4811
Frequencies -- 3232.4913 3232.8526 3232.8912
Frequencies -- 3233.4465 3233.5426 3235.3700
Frequencies -- 3236.3856 3236.8651 3237.1021
Frequencies -- 3238.7110 3241.2543 3241.6132
Frequencies -- 3244.2895 3245.8851 3246.4224
Frequencies -- 3247.5767 3248.4736 3249.0617
Frequencies -- 3251.6502 3251.9492 3252.8465
Frequencies -- 3257.6975 3278.2045 3635.0847

SCF Done: E(RM062X/DGDZVP) = -6499.39696055
Sum of electronic and zero-point Energies= -6498.046728
Sum of electronic and thermal Energies= -6497.932205
Sum of electronic and thermal Free Energies= -6498.206737
SCF Done: E(RM062X/DGTZVP/SMD) = -6500.68236596

Cat f TS1b_*S*

Center Number	Atomic Number	Atomic Type	Coordinates (Angstroms) X	Y	Z
1	15	0	0.052661	0.008195	-0.056709
2	8	0	0.020621	0.009593	1.567332
3	8	0	1.646649	-0.005739	-0.361149
4	8	0	-0.414758	1.325591	-0.610821
5	8	0	-0.674495	-1.228451	-0.476816
6	6	0	0.561473	1.085653	2.238522
7	6	0	2.382594	-1.096974	0.066472
8	6	0	1.913912	1.067670	2.551731
9	6	0	-0.246456	2.184675	2.573297
10	6	0	2.902791	-1.114933	1.353150
11	6	0	2.516325	-2.205996	-0.778022
12	6	0	2.928968	-0.055924	2.440563
13	6	0	2.493259	2.186430	3.152242
14	6	0	0.347293	3.261563	3.243225
15	6	0	-1.680772	2.183981	2.185095
16	6	0	3.519883	-2.278360	1.814145
17	6	0	3.236697	-3.314662	-0.326764
18	6	0	1.762339	-2.223708	-2.053189
19	6	0	2.902519	-0.957757	3.703668
20	6	0	4.247862	0.756778	2.395011
21	6	0	4.001656	2.004778	3.276920
22	6	0	1.712475	3.280988	3.541020
23	1	0	-0.267634	4.105150	3.541920
24	6	0	-2.266404	3.279329	1.537023
25	6	0	-2.487194	1.064143	2.399042
26	6	0	3.704373	-2.229973	3.324927
27	6	0	3.751138	-3.368175	0.969932
28	1	0	3.364057	-4.168335	-0.987113
29	6	0	0.816802	-3.225472	-2.280586
30	6	0	1.851093	-1.192933	-2.984858
31	1	0	3.303553	-0.452643	4.587941
32	1	0	1.864345	-1.233944	3.917735
33	1	0	5.110955	0.171091	2.725799
34	1	0	4.433711	1.067018	1.361943
35	1	0	4.253699	1.774771	4.319779
36	6	0	4.810348	3.213884	2.852377
37	6	0	2.313067	4.419698	4.286381
38	6	0	-3.575835	3.234850	1.044880
39	8	0	-1.479932	4.397151	1.369704
40	6	0	-3.766886	0.985386	1.859429
41	8	0	-2.035327	0.014353	3.161030
42	1	0	4.760992	-2.109059	3.592509
43	6	0	3.176213	-3.488314	3.986691
44	6	0	4.475270	-4.565313	1.472241
45	6	0	-0.043904	-3.161210	-3.368287
46	8	0	0.725402	-4.249439	-1.366506
47	6	0	0.981694	-1.109367	-4.073722
48	8	0	2.808664	-0.219484	-2.810907
49	6	0	4.725455	3.700463	1.543303
50	6	0	5.643771	3.875350	3.756893
51	6	0	2.346090	5.705340	3.738804
52	6	0	2.875082	4.203511	5.549314
53	6	0	-4.331795	2.064546	1.179802
54	8	0	-4.133472	4.303942	0.397382
55	6	0	-2.103903	5.522610	0.876065
56	8	0	-4.482072	-0.174429	1.996490
57	6	0	-2.426583	-1.209056	2.640089
58	6	0	1.888179	-3.944000	3.676674
59	6	0	3.961570	-4.240320	4.859596
60	6	0	3.844863	-5.811645	1.538806
61	6	0	5.785882	-4.438907	1.945321
62	6	0	0.021686	-2.100330	-4.276313
63	8	0	-1.023260	-4.109289	-3.556863
64	6	0	-0.463684	-4.939870	-1.363632
65	8	0	1.078011	-0.030849	-4.915484
66	6	0	2.385849	1.031816	-3.216541
67	6	0	5.461947	4.815902	1.147243
68	1	0	4.070756	3.207255	0.825442
69	6	0	6.366975	5.003669	3.372253
70	1	0	5.714587	3.513688	4.779853
71	6	0	2.972563	6.747630	4.421225
72	1	0	1.893534	5.879119	2.765183
73	6	0	3.484079	5.248335	6.241737
74	1	0	2.826475	3.210308	5.990125
75	6	0	-5.746848	1.887480	0.677126
76	6	0	-3.404530	5.470715	0.381978
77	6	0	-1.396041	6.715818	0.863218
78	6	0	-3.669865	-1.300775	2.025837
79	6	0	-1.586895	-2.308793	2.707107
80	6	0	1.394832	-5.119482	4.234644
81	1	0	1.284717	-3.388934	2.959088
82	6	0	3.475554	-5.427036	5.412565
83	1	0	4.972369	-3.911598	5.090178
84	6	0	4.504753	-6.906644	2.093821
85	1	0	2.821704	-5.908741	1.183809
86	6	0	6.452290	-5.536053	2.487943
87	1	0	6.283246	-3.473860	1.879710
88	6	0	-0.970307	-2.094865	-5.414344
89	6	0	-1.338878	-4.863336	-2.444550
90	6	0	-0.757079	-5.758060	-0.282646
91	6	0	1.495534	1.125751	-4.281256
92	6	0	2.867543	2.175074	-2.595368
93	6	0	6.280962	5.476714	2.063523

94	1	0	5.392196	5.172346	0.122709
95	1	0	6.996936	5.511918	4.096012
96	6	0	3.548495	6.520017	5.671397
97	1	0	3.013532	7.737010	3.975725
98	1	0	3.912391	5.070199	7.223663
99	9	0	-6.596138	1.676861	1.694343
100	9	0	-6.207366	2.929765	-0.017879
101	9	0	-5.841028	0.813913	-0.139249
102	6	0	-4.001206	6.606581	-0.146078
103	1	0	-0.378688	6.721369	1.246518
104	6	0	-1.991503	7.861780	0.336355
105	6	0	-4.086143	-2.481839	1.431094
106	1	0	-0.620417	-2.196988	3.186863
107	6	0	-2.007140	-3.507048	2.133279
108	6	0	2.191335	-5.869605	5.103127
109	1	0	0.392790	-5.458764	3.987033
110	1	0	4.106738	-6.010135	6.076337
111	6	0	5.808307	-6.770719	2.573328
112	1	0	3.997297	-7.864095	2.162234
113	1	0	7.470941	-5.426825	2.847936
114	9	0	-2.239278	-2.017025	-4.956523
115	9	0	-0.887420	-3.229165	-6.131408
116	9	0	-0.802101	-1.083302	-6.265847
117	6	0	-2.526412	-5.580467	-2.439110
118	1	0	-0.043872	-5.807856	0.534864
119	6	0	-1.938330	-6.500343	-0.280974
120	6	0	1.045147	2.361077	-4.722778
121	1	0	3.561368	2.066891	-1.767610
122	6	0	2.457227	3.423081	-3.066812
123	1	0	6.848818	6.350452	1.759166
124	1	0	4.036348	7.331847	6.201932
125	1	0	-5.010824	6.524777	-0.535085
126	6	0	-3.289236	7.805848	-0.171447
127	1	0	-1.433700	8.792306	0.318997
128	1	0	-5.045636	-2.506631	0.925144
129	6	0	-3.243129	-3.592021	1.488894
130	1	0	-1.355382	-4.373951	2.165229
131	1	0	1.813582	-6.793551	5.530018
132	1	0	6.319562	-7.623746	3.008826
133	1	0	-3.186777	-5.497208	-3.296346
134	6	0	-2.824518	-6.406318	-1.353925
135	1	0	-2.163395	-7.149791	0.559000
136	1	0	0.330091	2.400612	-5.537707
137	6	0	1.539858	3.515585	-4.115148
138	1	0	2.845779	4.326963	-2.606329
139	1	0	-3.751811	8.693289	-0.589762
140	1	0	-3.544346	-4.520374	1.013823
141	1	0	-3.744738	-6.980703	-1.355292
142	1	0	1.209694	4.488650	-4.466038
143	1	0	-2.375112	-0.810941	-0.567067
144	8	0	-3.214074	-0.579198	-1.060650
145	6	0	-2.957419	-0.987791	-2.437088
146	6	0	-2.707956	0.406231	-3.044958
147	1	0	-2.078847	-1.631119	-2.476619
148	1	0	-3.843836	-1.494390	-2.817428
149	8	0	-1.356334	0.652589	-3.338758
150	6	0	-3.167067	1.147876	-1.773713
151	1	0	-0.865233	0.816739	-2.508010
152	1	0	-4.218841	1.356008	-1.618098
153	1	0	-2.456377	1.537129	-1.057325
154	1	0	-0.736517	2.858134	-1.099155
155	7	0	-0.782106	3.831218	-1.455812
156	6	0	-1.723015	4.266522	-2.308426
157	6	0	0.226003	4.727347	-1.135989
158	16	0	-3.095979	3.463596	-2.839859
159	16	0	-1.334000	5.898563	-2.834260
160	6	0	0.101551	5.933049	-1.832020
161	6	0	1.240559	4.518497	-0.201605
162	6	0	1.019712	6.964410	-1.635610
163	6	0	2.142244	5.557165	0.005284
164	1	0	1.304410	3.572699	0.335648
165	6	0	2.040870	6.762249	-0.709491
166	1	0	0.929281	7.902857	-2.173375
167	1	0	2.940037	5.433588	0.730819
168	1	0	2.765545	7.550933	-0.532951
169	6	0	-3.554616	0.697166	-4.266448
170	6	0	-4.945126	0.572884	-4.195347
171	6	0	-2.958213	1.075487	-5.467757
172	6	0	-5.733994	0.838278	-5.312563
173	1	0	-5.427559	0.273497	-3.265497
174	6	0	-3.747221	1.325547	-6.589328
175	1	0	-1.878987	1.169704	-5.513404
176	6	0	-5.134754	1.213051	-6.515195
177	1	0	-6.813709	0.749679	-5.243569
178	1	0	-3.274541	1.612024	-7.523827
179	1	0	-5.746777	1.416211	-7.388541

Frequencies --	-536.1650	14.5663	18.3956
Frequencies --	20.2953	21.5980	26.5025
Frequencies --	29.6366	32.2953	35.0943
Frequencies --	35.4727	37.6086	38.2773
Frequencies --	40.0524	41.4346	43.5995
Frequencies --	47.3657	49.4088	50.8097
Frequencies --	52.1250	55.0032	55.9538
Frequencies --	58.2618	62.1292	65.2789
Frequencies --	67.9417	70.1692	72.6024
Frequencies --	74.8677	76.8797	78.1724
Frequencies --	78.5734	84.7349	86.7235
Frequencies --	88.2508	92.1646	95.4583
Frequencies --	97.3509	99.1617	102.2562
Frequencies --	103.5594	106.5100	113.0879
Frequencies --	116.1108	119.2134	125.6296
Frequencies --	127.9022	130.4621	136.1459
Frequencies --	138.8387	141.5651	147.1759
Frequencies --	153.2783	157.6317	163.1577
Frequencies --	165.3926	168.8911	172.8180
Frequencies --	176.6739	188.3196	190.8608
Frequencies --	197.0608	197.2792	200.4621
Frequencies --	208.6689	217.3079	224.1307
Frequencies --	227.5815	230.5316	232.8871
Frequencies --	237.2120	243.2696	249.1655
Frequencies --	254.3597	256.4596	267.5147
Frequencies --	271.9452	274.6500	276.8527
Frequencies --	277.9311	279.9278	281.0791
Frequencies --	287.7637	290.1021	293.2671
Frequencies --	295.6019	297.5423	300.3679
Frequencies --	306.2166	312.8670	315.0235
Frequencies --	317.1396	321.4446	324.2815
Frequencies --	328.4353	331.2804	335.8448
Frequencies --	339.0081	344.2211	348.6694
Frequencies --	353.2126	375.5528	387.4340
Frequencies --	398.5064	404.8472	408.9945
Frequencies --	410.6089	411.3197	412.6543
Frequencies --	414.2209	414.5066	415.1763
Frequencies --	419.0847	421.1546	421.8479
Frequencies --	428.1765	434.7383	437.8572
Frequencies --	441.5531	444.1168	448.5571
Frequencies --	450.8172	452.8415	460.2049
Frequencies --	464.9060	466.6527	468.3511
Frequencies --	473.6206	486.9808	490.4285
Frequencies --	500.7041	508.2077	510.3366

Frequencies --	512.2657	512.5238	521.7266
Frequencies --	522.0852	525.5376	530.9887
Frequencies --	534.3832	535.3461	537.3300
Frequencies --	542.9759	546.6640	555.2956
Frequencies --	555.6806	558.9038	559.2437
Frequencies --	563.5008	566.2852	571.3300
Frequencies --	575.0004	582.4079	585.4734
Frequencies --	586.7445	590.5781	591.1894
Frequencies --	596.0324	599.0071	601.2084
Frequencies --	602.6629	603.8494	610.3480
Frequencies --	612.3219	614.0361	618.4424
Frequencies --	620.1097	621.2906	625.7901
Frequencies --	626.7412	629.4949	631.2784
Frequencies --	632.8760	633.9636	636.5594
Frequencies --	644.6278	651.0498	657.3347
Frequencies --	669.6467	670.4935	673.8908
Frequencies --	675.9614	678.8791	679.9787
Frequencies --	683.2676	696.3602	703.8505
Frequencies --	711.0482	712.7453	717.0182
Frequencies --	717.7098	718.0203	718.6818
Frequencies --	718.9088	722.7821	724.9531
Frequencies --	726.1556	727.0176	732.4594
Frequencies --	732.9491	734.2540	739.3993
Frequencies --	744.6271	747.7057	752.8511
Frequencies --	762.5377	764.7629	766.5996
Frequencies --	769.0336	771.1785	773.2922
Frequencies --	775.0343	776.4056	776.9352
Frequencies --	778.9181	781.2540	783.6068
Frequencies --	785.9099	796.5742	799.4763
Frequencies --	801.0158	804.2504	806.4029
Frequencies --	822.4986	826.7017	828.2329
Frequencies --	831.1637	856.1050	860.6752
Frequencies --	862.4115	862.5341	864.8382
Frequencies --	865.7099	866.4350	867.1833
Frequencies --	867.3025	871.1229	874.1207
Frequencies --	881.4671	881.9122	888.1594
Frequencies --	888.9439	890.3600	893.7820
Frequencies --	895.9887	912.9780	914.3888
Frequencies --	920.5094	923.1620	926.1842
Frequencies --	930.1303	931.9446	935.0365
Frequencies --	938.9681	941.2503	942.3794
Frequencies --	942.9031	944.6212	946.2772
Frequencies --	947.4926	951.7570	953.9414
Frequencies --	954.9456	958.0443	966.5399
Frequencies --	971.4149	974.0476	987.2651
Frequencies --	989.0287	991.7373	994.0492
Frequencies --	995.4310	996.3894	998.2829
Frequencies --	998.7082	999.8191	1001.8424
Frequencies --	1009.1432	1009.7689	1011.8772
Frequencies --	1013.2090	1014.8989	1018.7522
Frequencies --	1019.3967	1019.4812	1019.8970
Frequencies --	1020.1000	1022.4813	1028.0877
Frequencies --	1030.4572	1036.5496	1037.7553
Frequencies --	1038.9266	1045.4142	1045.9538
Frequencies --	1052.1023	1054.4625	1054.7543
Frequencies --	1061.3293	1064.1069	1066.1965
Frequencies --	1066.7682	1067.0667	1069.1667
Frequencies --	1070.3487	1073.9119	1075.8142
Frequencies --	1078.9194	1092.6923	1096.8049
Frequencies --	1105.7928	1110.0485	1111.9047
Frequencies --	1112.9305	1113.9792	1115.1787
Frequencies --	1120.7471	1123.3467	1126.5583
Frequencies --	1129.1158	1131.9910	1134.7970
Frequencies --	1135.5618	1164.1507	1164.4102
Frequencies --	1166.7608	1168.0770	1168.3218
Frequencies --	1170.3180	1173.5896	1175.4492
Frequencies --	1175.9663	1176.8717	1178.1974
Frequencies --	1178.7757	1179.0138	1179.2105
Frequencies --	1187.1648	1193.7343	1193.9592
Frequencies --	1200.1071	1201.4618	1204.5631
Frequencies --	1204.6639	1205.2304	1206.4375
Frequencies --	1209.0120	1212.0440	1215.6090
Frequencies --	1220.1271	1225.5277	1228.0452
Frequencies --	1234.2522	1237.5865	1239.4283
Frequencies --	1239.6489	1244.3983	1246.0619
Frequencies --	1252.1664	1255.9814	1262.2438
Frequencies --	1275.2338	1276.8542	1280.5306
Frequencies --	1283.1138	1286.8228	1287.6140
Frequencies --	1293.1946	1294.1335	1294.6765
Frequencies --	1298.2585	1299.3743	1305.8154
Frequencies --	1306.9205	1308.0141	1310.5626
Frequencies --	1311.7056	1313.0375	1317.6051
Frequencies --	1318.6729	1321.9598	1325.7976
Frequencies --	1326.9743	1329.0145	1334.8341
Frequencies --	1338.4204	1340.7894	1340.8941
Frequencies --	1343.5930	1354.2158	1358.6084
Frequencies --	1359.7943	1361.1378	1361.9541
Frequencies --	1362.3859	1363.3955	1365.1177
Frequencies --	1365.2851	1365.5047	1366.8805
Frequencies --	1370.2616	1373.5315	1374.1444
Frequencies --	1386.3717	1388.5903	1391.9082
Frequencies --	1404.7398	1420.5694	1447.3758
Frequencies --	1449.9054	1458.3766	1461.8742
Frequencies --	1467.7011	1472.6708	1482.0069
Frequencies --	1492.2415	1493.6845	1494.5614
Frequencies --	1496.9707	1498.8240	1499.6461
Frequencies --	1501.4092	1504.0374	1507.2619
Frequencies --	1507.7585	1510.5413	1511.8056
Frequencies --	1514.1971	1520.2868	1520.9507
Frequencies --	1530.1467	1533.2350	1544.6532
Frequencies --	1546.7101	1550.7644	1553.5890
Frequencies --	1554.4362	1556.9591	1557.6192
Frequencies --	1560.0152	1561.9115	1566.1805
Frequencies --	1568.3205	1573.0786	1655.5437
Frequencies --	1662.8322	1667.4393	1669.8764
Frequencies --	1671.8334	1672.6809	1674.5166
Frequencies --	1677.9492	1677.9655	1679.1566
Frequencies --	1685.5518	1687.1663	1690.3320
Frequencies --	1692.9071	1694.6223	1696.0159
Frequencies --	1697.2391	1699.2037	1700.0464
Frequencies --	1700.9668	1701.3607	1703.6079
Frequencies --	1704.1748	1704.4057	1718.7163
Frequencies --	1722.9416	1725.0694	1738.9729
Frequencies --	3077.8636	3080.4097	3086.7217
Frequencies --	3092.9530	3149.6094	3150.4892
Frequencies --	3155.7979	3181.0384	3181.8454
Frequencies --	3181.9449	3184.8552	3196.9825
Frequencies --	3202.7441	3203.2148	3203.7146
Frequencies --	3203.8200	3206.0299	3210.2123
Frequencies --	3211.3595	3213.4097	3214.7142
Frequencies --	3214.7946	3216.4583	3217.1448
Frequencies --	3217.5966	3220.4437	3221.7891
Frequencies --	3222.7164	3226.2978	3227.4004
Frequencies --	3227.4336	3228.4018	3228.6988
Frequencies --	3229.8993	3230.1696	3231.0759
Frequencies --	3232.0386	3235.0939	3236.7504
Frequencies --	3237.2563	3238.0607	3238.0667
Frequencies --	3238.6696	3239.2289	3239.6033
Frequencies --	3241.3194	3242.9975	3243.7977
Frequencies --	3243.9505	3244.2388	3246.1314
Frequencies --	3247.8091	3248.8624	3249.2033
Frequencies --	3250.1148	3256.8112	3260.6075

Frequencies -- 3279.1630 3377.3051 3662.0271

SCF Done: E(RM062X/DGDZVP) = -6499.36618258
Sum of electronic and zero-point Energies= -6498.015868
Sum of electronic and thermal Energies= -6497.901949
Sum of electronic and thermal Free Energies= -6498.171987
SCF Done: E(RM062X/DGTZVP/SMD) = -6500.64666827

Cat f I1b_*S*

Center Number	Atomic Number	Atomic Type	Coordinates (Angstroms) X	Y	Z
1	15	0	0.013282	0.020951	0.056719
2	8	0	0.028359	-0.009813	1.686511
3	8	0	1.612016	0.097306	-0.268632
4	8	0	-0.528634	1.340211	-0.429276
5	8	0	-0.614070	-1.248949	-0.395705
6	6	0	0.566446	1.071851	2.347402
7	6	0	2.369465	-1.001760	0.100872
8	6	0	1.925855	1.074880	2.637234
9	6	0	-0.246044	2.165805	2.684071
10	6	0	2.920494	-1.057997	1.374929
11	6	0	2.478709	-2.096194	-0.767829
12	6	0	2.947879	-0.037511	2.498226
13	6	0	2.502702	2.201485	3.225597
14	6	0	0.346888	3.258355	3.328714
15	6	0	-1.677541	2.153894	2.286426
16	6	0	3.555830	-2.227736	1.792027
17	6	0	3.228390	-3.205159	-0.366510
18	6	0	1.663055	-2.128768	-2.004023
19	6	0	2.934720	-0.980353	3.730151
20	6	0	4.264710	0.778063	2.471442
21	6	0	4.012460	2.021014	3.357049
22	6	0	1.715504	3.294032	3.610100
23	1	0	-0.272755	4.101117	3.621703
24	6	0	-2.228888	3.212562	1.557180
25	6	0	-2.490309	1.041976	2.501732
26	6	0	3.749894	-2.228736	3.302875
27	6	0	3.781936	-3.288921	0.911659
28	1	0	3.340149	-4.042287	-1.050477
29	6	0	0.732220	-3.153732	-2.182084
30	6	0	1.676813	-1.094625	-2.934680
31	1	0	3.335482	-0.500423	4.628669
32	1	0	1.900723	-1.275060	3.938961
33	1	0	5.125048	0.191259	2.807203
34	1	0	4.461310	1.090606	1.441750
35	1	0	4.253024	1.785263	4.401634
36	6	0	4.832188	3.228117	2.947519
37	6	0	2.311313	4.444070	4.344066
38	6	0	-3.506095	3.142640	1.002829
39	8	0	-1.416220	4.305841	1.322410
40	6	0	-3.751728	0.946123	1.917894
41	8	0	-2.054765	0.001644	3.285190
42	1	0	4.806057	-2.104513	3.571011
43	6	0	3.239903	-3.516312	3.921440
44	6	0	4.525676	-4.494638	1.360043
45	6	0	-0.163458	-3.123493	-3.241826
46	8	0	0.692808	-4.165216	-1.250700
47	6	0	0.767907	-1.041877	-3.991874
48	8	0	2.620501	-0.100389	-2.792874
49	6	0	4.809336	3.684798	1.625786
50	6	0	5.616159	3.918322	3.875117
51	6	0	2.382869	5.716186	3.768566
52	6	0	2.829774	4.250585	5.629089
53	6	0	-4.286467	1.995557	1.176305
54	8	0	-3.968715	4.145262	0.175919
55	6	0	-2.036073	5.427293	0.825648
56	8	0	-4.464932	-0.211223	2.053038
57	6	0	-2.423108	-1.229772	2.759218
58	6	0	1.952474	-3.972025	3.608069
59	6	0	4.043715	-4.294773	4.753667
60	6	0	3.910626	-5.750240	1.381857
61	6	0	5.840161	-4.372158	1.823521
62	6	0	-0.145777	-2.080634	-4.171589
63	8	0	-1.115806	-4.102513	-3.396999
64	6	0	-0.465043	-4.906357	-1.219724
65	8	0	0.784754	0.036913	-4.844491
66	6	0	2.198574	1.129962	-3.242510
67	6	0	5.539470	4.808951	1.242576
68	1	0	4.210376	3.157157	0.884960
69	6	0	6.338592	5.051036	3.502057
70	1	0	5.647672	3.576318	4.906579
71	6	0	3.002515	6.765476	4.446590
72	1	0	1.966131	5.874271	2.776552
73	6	0	3.431722	5.302825	6.316888
74	1	0	2.753576	3.268303	6.089714
75	6	0	-5.674343	1.800479	0.611093
76	6	0	-3.300859	5.346435	0.247105
77	6	0	-1.361683	6.639723	0.869898
78	6	0	-3.648070	-1.332905	2.112358
79	6	0	-1.578236	-2.323241	2.855326
80	6	0	1.479873	-5.175718	4.122480
81	1	0	1.332233	-3.394007	2.923222
82	6	0	3.577912	-5.509174	5.262126
83	1	0	5.053605	-3.964124	4.985624
84	6	0	4.589188	-6.858948	1.884402
85	1	0	2.884839	-5.844414	1.033592
86	6	0	6.525155	-5.482505	2.313557
87	1	0	6.325648	-3.399333	1.791998
88	6	0	-1.098446	-2.179236	-5.339423
89	6	0	-1.368830	-4.867711	-2.278453
90	6	0	-0.697833	-5.736539	-0.133003
91	6	0	1.270350	1.198483	-4.278902
92	6	0	2.740701	2.287676	-2.703007
93	6	0	6.302211	5.502190	2.182994
94	1	0	5.512940	5.142302	0.208160
95	1	0	6.928335	5.581145	4.243836
96	6	0	3.533149	6.560016	5.720362
97	1	0	3.074225	7.743108	3.979471
98	1	0	3.826230	5.141131	7.315659
99	9	0	-6.556658	1.539477	1.587528
100	9	0	-6.133976	2.872456	-0.053077
101	9	0	-5.726115	0.770052	-0.253026
102	6	0	-3.899375	6.473362	-0.298962
103	1	0	-0.372336	6.668921	1.319580
104	6	0	-1.953237	7.773947	0.312814
105	6	0	-4.043006	-2.520038	1.517429
106	1	0	-0.624184	-2.204615	3.358322
107	6	0	-1.978551	-3.528583	2.281629
108	6	0	2.295145	-5.952969	4.948888
109	1	0	0.478554	-5.516033	3.873480
110	1	0	4.223293	-6.111921	5.893942
111	6	0	5.896543	-6.727266	2.354931
112	1	0	4.093299	-7.824283	1.918779
113	1	0	7.546586	-5.375974	2.666573
114	9	0	-2.379841	-2.044597	-4.952536
115	9	0	-0.996289	-3.378721	-5.940957
116	9	0	-0.866256	-1.264486	-6.287393
117	6	0	-2.524756	-5.633540	-2.244982
118	1	0	0.034107	-5.753846	0.669348

119	6	0	-1.846881	-6.528169	-0.103599
120	6	0	0.867913	2.426072	-4.783942
121	1	0	3.454680	2.196015	-1.890205
122	6	0	2.370777	3.523724	-3.234246
123	1	0	6.868355	6.380687	1.889226
124	1	0	4.015312	7.377242	6.247823
125	1	0	-4.884488	6.371557	-0.742989
126	6	0	-3.217312	7.690577	-0.271956
127	1	0	-1.423370	8.720451	0.340135
128	1	0	-4.985644	-2.550546	0.981432
129	6	0	-3.197883	-3.625691	1.608125
130	1	0	-1.323966	-4.392296	2.337971
131	1	0	1.932440	-6.898125	5.340987
132	1	0	6.422833	-7.591525	2.748489
133	1	0	-3.209568	-5.574318	-3.084689
134	6	0	-2.762054	-6.471250	-1.154325
135	1	0	-2.024837	-7.185298	0.741741
136	1	0	0.140998	2.451373	-5.589681
137	6	0	1.434843	3.592706	-4.266907
138	1	0	2.807262	4.433879	-2.830845
139	1	0	-3.678834	8.571930	-0.704251
140	1	0	-3.481639	-4.559538	1.132935
141	1	0	-3.658628	-7.081583	-1.133318
142	1	0	1.149960	4.554584	-4.682611
143	1	0	-2.359849	-0.889846	-0.633659
144	8	0	-3.190929	-0.394864	-0.800336
145	6	0	-3.501885	-0.459125	-2.176291
146	6	0	-3.001902	0.785091	-2.943681
147	1	0	-3.051776	-1.336550	-2.656406
148	1	0	-4.589009	-0.534258	-2.268030
149	8	0	-1.589827	0.774253	-3.063739
150	6	0	-3.411189	2.038734	-2.152235
151	1	0	-1.215120	0.688875	-2.164624
152	1	0	-4.487153	2.070604	-1.960699
153	1	0	-2.892964	2.063865	-1.190145
154	1	0	-0.832796	2.684276	-1.170321
155	7	0	-0.813658	3.673228	-1.551348
156	6	0	-1.650685	4.205835	-2.424417
157	6	0	0.233294	4.510375	-1.164744
158	16	0	-3.095498	3.573366	-3.093782
159	16	0	-1.183404	5.811419	-2.891075
160	6	0	0.203211	5.735539	-1.833307
161	6	0	1.202364	4.224352	-0.202078
162	6	0	1.161975	6.718581	-1.587892
163	6	0	2.140094	5.214498	0.059828
164	1	0	1.198945	3.265132	0.313909
165	6	0	2.129785	6.440656	-0.629361
166	1	0	1.138876	7.669647	-2.109777
167	1	0	2.898683	5.041194	0.815061
168	1	0	2.886239	7.185711	-0.402270
169	6	0	-3.599739	0.827505	-4.338281
170	6	0	-4.988742	0.855907	-4.510536
171	6	0	-2.774414	0.885526	-5.461409
172	6	0	-5.541772	0.927093	-5.788002
173	1	0	-5.653102	0.822486	-3.649375
174	6	0	-3.327438	0.947532	-6.739556
175	1	0	-1.698488	0.865468	-5.323734
176	6	0	-4.711039	0.969830	-6.908125
177	1	0	-6.620735	0.944254	-5.907450
178	1	0	-2.672194	0.969585	-7.605332
179	1	0	-5.140747	1.017744	-7.904031

Frequencies --	16.2088	23.2722	24.5065
Frequencies --	26.9300	28.5304	29.2366
Frequencies --	34.3766	35.5432	36.4923
Frequencies --	38.6415	39.6321	40.4153
Frequencies --	43.4979	46.8181	48.2219
Frequencies --	50.8122	53.9439	58.0681
Frequencies --	59.4981	60.1991	63.4720
Frequencies --	64.9387	68.0709	70.7553
Frequencies --	73.7054	74.8834	76.5074
Frequencies --	79.6947	84.9297	87.1915
Frequencies --	88.0531	90.3564	92.9829
Frequencies --	96.5624	97.7781	98.8785
Frequencies --	100.4841	103.1982	108.6668
Frequencies --	108.9198	114.0983	120.0681
Frequencies --	120.3279	123.6299	128.0893
Frequencies --	132.1800	133.6040	140.9894
Frequencies --	141.7193	147.9132	158.0491
Frequencies --	161.5647	164.8319	166.5209
Frequencies --	169.2495	172.7394	177.6006
Frequencies --	188.8377	191.3830	194.9312
Frequencies --	195.5624	209.3342	213.4123
Frequencies --	217.5388	225.6541	229.9606
Frequencies --	234.4791	236.3078	237.0311
Frequencies --	242.4258	245.0843	247.6240
Frequencies --	255.5757	256.3163	271.9500
Frequencies --	273.6686	276.6969	279.7626
Frequencies --	282.1588	287.1881	289.6167
Frequencies --	294.0780	295.9420	298.3067
Frequencies --	301.3734	304.5664	306.2240
Frequencies --	311.7989	314.9186	318.1905
Frequencies --	321.1972	322.9353	328.2217
Frequencies --	330.9664	331.8824	336.6460
Frequencies --	339.0924	346.9233	349.6159
Frequencies --	355.1467	376.2411	388.6437
Frequencies --	393.2240	404.8733	410.5962
Frequencies --	411.3833	412.6588	414.2150
Frequencies --	415.6566	418.4418	419.6647
Frequencies --	421.8780	423.5720	425.8254
Frequencies --	434.6682	436.3303	441.7602
Frequencies --	442.6140	447.4771	449.6066
Frequencies --	450.6712	455.1990	460.8721
Frequencies --	467.3937	471.1592	472.7671
Frequencies --	486.2631	491.7368	500.9330
Frequencies --	502.3137	510.2633	511.2095
Frequencies --	512.7163	521.1904	523.9518
Frequencies --	524.6830	524.9553	530.8869
Frequencies --	534.5001	536.1975	543.4526
Frequencies --	548.3756	554.2845	556.9417
Frequencies --	557.3917	559.5996	563.2096
Frequencies --	567.6753	569.9178	572.5663
Frequencies --	584.1965	585.3552	588.3777
Frequencies --	588.8622	592.6730	596.6535
Frequencies --	599.0294	600.4266	602.1688
Frequencies --	605.0500	610.0283	610.5452
Frequencies --	611.6392	614.8908	618.0024
Frequencies --	622.2604	625.5449	626.7187
Frequencies --	630.1758	630.9285	632.7879
Frequencies --	633.9385	636.5274	640.4598
Frequencies --	644.6026	650.5051	656.8814
Frequencies --	669.6288	672.5930	675.6031
Frequencies --	678.2510	683.0259	694.9611
Frequencies --	697.3248	703.8961	707.9908
Frequencies --	714.0214	715.6883	717.1569
Frequencies --	718.9808	719.8533	721.4315
Frequencies --	723.1178	723.6041	725.7590
Frequencies --	729.1826	731.6154	734.0067
Frequencies --	735.1417	735.1855	738.8411
Frequencies --	744.2477	748.1645	751.0164
Frequencies --	755.9045	758.6539	767.0168

Frequencies --	767.8565	770.0828	771.2018
Frequencies --	775.1926	779.1973	780.2482
Frequencies --	780.5821	781.4739	784.3685
Frequencies --	795.3084	797.2300	799.9864
Frequencies --	800.7290	801.9533	804.1706
Frequencies --	806.1317	823.2887	826.4492
Frequencies --	829.1135	832.0040	858.4411
Frequencies --	860.0591	860.9567	862.2527
Frequencies --	864.2275	866.0392	869.6686
Frequencies --	870.6736	871.8183	874.4196
Frequencies --	880.1573	882.6198	883.4875
Frequencies --	887.7107	889.6480	891.4633
Frequencies --	894.4607	905.8897	911.9776
Frequencies --	916.4577	921.0959	924.9136
Frequencies --	930.8056	934.5160	938.6713
Frequencies --	939.7632	939.9839	942.1109
Frequencies --	943.7102	944.2605	946.3744
Frequencies --	948.8215	952.1844	954.3087
Frequencies --	955.1821	960.5582	966.9406
Frequencies --	969.9318	978.7929	984.5928
Frequencies --	986.9440	987.1187	991.5457
Frequencies --	992.7422	994.1297	997.5831
Frequencies --	998.7522	1000.5154	1005.6777
Frequencies --	1007.3262	1011.1212	1012.4816
Frequencies --	1014.9912	1018.4367	1018.8541
Frequencies --	1019.6099	1019.9327	1021.6533
Frequencies --	1023.5167	1027.8729	1028.4617
Frequencies --	1030.9341	1034.7274	1036.0502
Frequencies --	1036.6093	1044.3788	1051.7547
Frequencies --	1053.3703	1059.7483	1059.8062
Frequencies --	1062.1569	1064.8190	1066.0868
Frequencies --	1067.4574	1069.3509	1070.8261
Frequencies --	1071.0916	1072.5088	1091.8119
Frequencies --	1096.8882	1109.6453	1110.8215
Frequencies --	1112.2999	1115.0045	1118.3941
Frequencies --	1120.4714	1124.1450	1125.0938
Frequencies --	1126.3693	1127.2719	1129.6621
Frequencies --	1131.3062	1132.9075	1142.7731
Frequencies --	1153.9375	1160.9814	1163.3937
Frequencies --	1163.7585	1164.3487	1165.9965
Frequencies --	1170.6663	1173.2528	1174.4462
Frequencies --	1175.3344	1177.8735	1178.3301
Frequencies --	1179.1563	1180.7728	1183.0931
Frequencies --	1195.6183	1197.2861	1199.5895
Frequencies --	1201.4766	1206.6135	1207.5311
Frequencies --	1211.2903	1212.8579	1214.1917
Frequencies --	1215.2917	1217.0496	1221.0692
Frequencies --	1225.0102	1228.5205	1235.9709
Frequencies --	1237.0706	1238.2496	1243.8026
Frequencies --	1246.9018	1249.7064	1252.9677
Frequencies --	1253.6028	1259.1581	1271.1374
Frequencies --	1276.0275	1277.7282	1280.1628
Frequencies --	1286.7607	1290.0530	1293.9421
Frequencies --	1295.4176	1297.0493	1298.6082
Frequencies --	1300.8130	1301.9491	1306.0689
Frequencies --	1307.0590	1308.0970	1309.5370
Frequencies --	1310.5872	1311.9365	1313.2002
Frequencies --	1317.7623	1321.3327	1326.1684
Frequencies --	1326.8585	1327.5414	1334.2373
Frequencies --	1337.5621	1340.8624	1342.0867
Frequencies --	1347.6790	1357.5337	1359.0267
Frequencies --	1360.7915	1361.6856	1361.8683
Frequencies --	1364.0285	1365.4802	1365.9907
Frequencies --	1366.3202	1366.5680	1367.3158
Frequencies --	1369.9451	1374.1154	1384.3034
Frequencies --	1387.4757	1397.2706	1400.2007
Frequencies --	1404.1688	1442.3693	1448.5951
Frequencies --	1458.5897	1462.0239	1467.0073
Frequencies --	1471.7690	1488.5297	1492.2958
Frequencies --	1493.8167	1495.9901	1496.2122
Frequencies --	1498.6019	1498.7399	1500.4748
Frequencies --	1502.8337	1503.7649	1506.1956
Frequencies --	1506.4369	1510.4142	1510.6758
Frequencies --	1514.4171	1515.1783	1519.7168
Frequencies --	1529.3768	1533.2788	1544.9879
Frequencies --	1546.7793	1549.1377	1553.9641
Frequencies --	1555.2485	1559.8018	1561.0436
Frequencies --	1562.6485	1564.9986	1567.9965
Frequencies --	1569.2680	1570.6954	1655.1933
Frequencies --	1663.0008	1669.1037	1669.6979
Frequencies --	1672.5339	1673.6173	1674.2758
Frequencies --	1677.0672	1677.2795	1677.3236
Frequencies --	1682.1246	1686.4708	1689.4384
Frequencies --	1691.3284	1692.8003	1695.4890
Frequencies --	1696.2275	1698.9226	1699.0150
Frequencies --	1700.2340	1700.4837	1702.5701
Frequencies --	1702.9925	1703.9928	1720.9273
Frequencies --	1723.3716	1728.4501	1739.2016
Frequencies --	2818.9736	3077.4628	3077.8769
Frequencies --	3085.2208	3087.9589	3095.3432
Frequencies --	3124.3819	3148.5995	3156.7781
Frequencies --	3164.5082	3183.8506	3183.8820
Frequencies --	3199.1284	3199.2195	3202.2201
Frequencies --	3202.2738	3204.9367	3206.7981
Frequencies --	3209.0348	3209.3903	3211.7599
Frequencies --	3211.8673	3212.4268	3213.8694
Frequencies --	3214.4184	3215.5946	3215.6903
Frequencies --	3216.0099	3216.3645	3222.1318
Frequencies --	3223.4214	3224.2935	3224.5778
Frequencies --	3225.1552	3226.4632	3227.7556
Frequencies --	3228.4936	3229.7159	3231.0712
Frequencies --	3231.9951	3233.5162	3234.0969
Frequencies --	3234.1890	3234.6413	3236.4960
Frequencies --	3236.6196	3237.7401	3238.2193
Frequencies --	3239.8165	3242.8895	3244.3707
Frequencies --	3246.8880	3248.0338	3249.7087
Frequencies --	3250.8610	3253.2864	3254.6722
Frequencies --	3265.8913	3559.3416	3704.0212

SCF Done: E(RM062X/DGDZVP) = -6499.42805541
Sum of electronic and zero-point Energies= -6498.076245
Sum of electronic and thermal Energies= -6497.962393
Sum of electronic and thermal Free Energies= -6498.230158
SCF Done: E(RM062X/DGTZVP/SMD) = -6500.70849985

Cat f I0c_*S*

Center Number	Atomic Number	Atomic Type	Coordinates (Angstroms) X	Y	Z
1	15	0	-0.039786	-0.092427	0.115302
2	8	0	-0.027364	-0.094574	1.718269
3	8	0	1.517618	-0.032500	-0.292154
4	8	0	-0.543571	1.297606	-0.338799
5	8	0	-0.714684	-1.310472	-0.382069
6	6	0	0.503239	1.017258	2.372338
7	6	0	2.328913	-1.093065	0.091575
8	6	0	1.875345	1.113142	2.563631
9	6	0	-0.350029	2.068342	2.731352
10	6	0	2.950626	-1.014175	1.332146
11	6	0	2.481161	-2.224633	-0.724673

12	6	0	3.006700	0.127392	2.329451
13	6	0	2.402571	2.306268	3.062933
14	6	0	0.200693	3.191860	3.354584
15	6	0	-1.765941	2.073232	2.296658
16	6	0	3.723984	-2.083240	1.784068
17	6	0	3.346522	-3.235735	-0.280304
18	6	0	1.664189	-2.425381	-1.952201
19	6	0	3.319403	-0.646908	3.637309
20	6	0	4.168178	1.099331	1.995221
21	6	0	3.906626	2.374119	2.837324
22	6	0	1.577618	3.334937	3.522383
23	1	0	-0.457016	3.999942	3.662396
24	6	0	-2.244009	3.157245	1.552848
25	6	0	-2.635269	1.006874	2.508360
26	6	0	4.189818	-1.851651	3.213093
27	6	0	3.970504	-3.187778	0.965347
28	1	0	3.514176	-4.100058	-0.915109
29	6	0	0.955331	-3.621010	-2.121524
30	6	0	1.489246	-1.441474	-2.926172
31	1	0	3.805996	-0.015050	4.386631
32	1	0	2.379046	-1.007619	4.066147
33	1	0	5.148724	0.655342	2.192543
34	1	0	4.124262	1.350054	0.930492
35	1	0	4.458734	2.334411	3.783285
36	6	0	4.276059	3.652598	2.106974
37	6	0	2.162275	4.580581	4.082362
38	6	0	-3.524838	3.152946	1.023681
39	8	0	-1.402953	4.219617	1.286489
40	6	0	-3.905936	0.968335	1.923521
41	8	0	-2.220400	-0.025858	3.316558
42	1	0	5.248652	-1.562943	3.205082
43	6	0	4.036649	-3.059438	4.114546
44	6	0	4.855255	-4.295611	1.421290
45	6	0	0.035155	-3.801939	-3.157824
46	8	0	1.146817	-4.607656	-1.181569
47	6	0	0.603483	-1.623826	-3.983182
48	8	0	2.218989	-0.278980	-2.857985
49	6	0	3.597549	3.990942	0.928622
50	6	0	5.237020	4.531182	2.605717
51	6	0	1.933027	5.811797	3.459429
52	6	0	2.997512	4.526821	5.203118
53	6	0	-4.367146	2.049234	1.177145
54	8	0	-3.954707	4.212135	0.251367
55	6	0	-1.646579	4.834310	0.076203
56	8	0	-4.685309	-0.144323	2.074799
57	6	0	-2.762033	-1.253540	2.991147
58	6	0	2.777530	-3.634447	4.324846
59	6	0	5.146818	-3.633622	4.736101
60	6	0	4.309018	-5.525079	1.802352
61	6	0	6.236468	-4.103584	1.514832
62	6	0	-0.144398	-2.796123	-4.110430
63	8	0	-0.720734	-4.941515	-3.233931
64	6	0	0.673658	-5.860892	-1.502366
65	8	0	0.448920	-0.631307	-4.921947
66	6	0	1.526271	0.816403	-3.344906
67	6	0	3.878431	5.180907	0.264170
68	1	0	2.822123	3.327008	0.546504
69	6	0	5.514615	5.730989	1.947263
70	1	0	5.755147	4.290314	3.531113
71	6	0	2.552380	6.966604	3.933610
72	1	0	1.291018	5.851321	2.582490
73	6	0	3.607449	5.683216	5.685773
74	1	0	3.161901	3.572703	5.698618
75	6	0	-5.702121	2.093246	0.471428
76	6	0	-2.937905	4.838808	-0.444812
77	6	0	-0.612585	5.468501	-0.596324
78	6	0	-3.993835	-1.309230	2.344429
79	6	0	-2.110352	-2.419712	3.362553
80	6	0	2.634238	-4.752601	5.143809
81	1	0	1.900299	-3.206659	3.840439
82	6	0	5.011170	-4.764486	5.541100
83	1	0	6.132142	-3.203154	4.573594
84	6	0	5.128629	-6.541915	2.288036
85	1	0	3.231682	-5.665555	1.742876
86	6	0	7.059808	-5.124014	1.990943
87	1	0	6.664519	-3.151735	1.209135
88	6	0	-1.065254	-2.908543	-5.305590
89	6	0	-0.274668	-6.021388	-2.505581
90	6	0	1.123761	-6.952560	-0.774752
91	6	0	0.659233	0.642990	-4.420607
92	6	0	1.709918	2.070566	-2.783028
93	6	0	4.837012	6.059542	0.775161
94	1	0	3.346584	5.429331	-0.650345
95	1	0	6.253488	6.412372	2.357946
96	6	0	3.394534	6.904139	5.044539
97	1	0	2.385240	7.913946	3.430331
98	1	0	4.249197	5.632667	6.560270
99	9	0	-6.451083	1.007824	0.664940
100	9	0	-6.424403	3.150866	0.882390
101	9	0	-5.543955	2.227609	-0.862643
102	6	0	-3.212651	5.468694	-1.649570
103	1	0	0.383935	5.441938	-0.164937
104	6	0	-0.886865	6.125840	-1.797124
105	6	0	-4.570920	-2.527795	2.022290
106	1	0	-1.155055	-2.344313	3.873330
107	6	0	-2.714734	-3.650492	3.095787
108	6	0	3.753257	-5.327639	5.748664
109	1	0	1.647754	-5.175600	5.313769
110	1	0	5.889405	-5.205887	6.002456
111	6	0	6.506680	-6.342233	2.385208
112	1	0	4.691578	-7.485433	2.601106
113	1	0	8.132384	-4.967145	2.054976
114	9	0	-2.010614	-1.947787	-5.289897
115	9	0	-1.697776	-4.076975	-5.391700
116	9	0	-0.371144	-2.750540	-6.448240
117	6	0	-0.811876	-7.272030	-2.771948
118	1	0	1.873748	-6.795007	-0.006103
119	6	0	0.580035	-8.210770	-1.029312
120	6	0	0.006159	1.724990	-4.988854
121	1	0	2.368066	2.166819	-1.925638
122	6	0	1.047315	3.163896	-3.343864
123	1	0	5.049738	6.993498	0.264274
124	1	0	3.877585	7.804303	5.412030
125	1	0	-4.228242	5.445974	-2.032103
126	6	0	-2.178937	6.122911	-2.322843
127	1	0	-0.087651	6.640470	-2.321082
128	1	0	-5.521451	-2.536253	1.498258
129	6	0	-3.930021	-3.705107	2.414360
130	1	0	-2.224465	-4.568230	3.408630
131	1	0	3.643581	-6.203678	6.380481
132	1	0	7.146275	-7.133299	2.764345
133	1	0	-1.563808	-7.359084	-3.549558
134	6	0	-0.391863	-8.368276	-2.018174
135	1	0	0.912395	-9.064490	-0.448117
136	1	0	-0.655818	1.555069	-5.832411
137	6	0	0.211595	2.994553	-4.447486
138	1	0	1.180659	4.150092	-2.911314
139	1	0	-2.388068	6.631336	-3.258037
140	1	0	-4.389528	-4.663336	2.194083
141	1	0	-0.820155	-9.345905	-2.212400
142	1	0	-0.299027	3.849537	-4.878351
143	1	0	-1.017128	1.335205	-1.284415

144	8	0	-1.750488	1.344664	-2.506987
145	6	0	-3.118268	1.765696	-2.225776
146	6	0	-3.596634	0.303529	-2.189340
147	1	0	-3.178459	2.295689	-1.277099
148	1	0	-3.504116	2.365019	-3.053988
149	8	0	-3.595480	-0.094501	-0.834091
150	6	0	-2.234376	0.003318	-2.855359
151	1	0	-3.457187	-1.065214	-0.816091
152	1	0	-2.253712	-0.096358	-3.941524
153	1	0	-1.644036	-0.786536	-2.384810
154	1	0	-1.267338	-2.904850	-0.205800
155	7	0	-1.639754	-3.868288	-0.137027
156	6	0	-2.750672	-4.211947	-0.825843
157	6	0	-1.119917	-4.816917	0.726659
158	16	0	-3.606040	-3.255059	-1.883795
159	16	0	-3.186783	-5.871529	-0.425288
160	6	0	-1.857423	-6.007522	0.707491
161	6	0	0.003755	-4.670228	1.541141
162	6	0	-1.504061	-7.074191	1.532820
163	6	0	0.353802	-5.739472	2.359200
164	1	0	0.581025	-3.747219	1.517771
165	6	0	-0.395727	-6.927092	2.363630
166	1	0	-2.075130	-7.997152	1.522159
167	1	0	1.224050	-5.652899	3.003833
168	1	0	-0.103099	-7.745613	3.013457
169	6	0	-4.860560	-0.065157	-2.926725
170	6	0	-4.975218	0.162290	-4.302811
171	6	0	-5.939556	-0.622772	-2.238640
172	6	0	-6.146643	-0.167294	-4.980273
173	1	0	-4.147145	0.596908	-4.858955
174	6	0	-7.111669	-0.954416	-2.916542
175	1	0	-5.858090	-0.789767	-1.169070
176	6	0	-7.219375	-0.729383	-4.287659
177	1	0	-6.219207	0.008769	-6.049096
178	1	0	-7.941772	-1.391501	-2.370161
179	1	0	-8.131117	-0.991417	-4.815545

Frequencies -- 15.9512 17.4436 20.6167
Frequencies -- 22.8275 24.8579 26.3977
Frequencies -- 30.4297 32.3133 33.3978
Frequencies -- 35.3831 39.5374 40.9859
Frequencies -- 41.9673 44.0721 47.1162
Frequencies -- 48.9774 50.3321 55.8603
Frequencies -- 56.5115 57.6028 60.2180
Frequencies -- 63.0108 63.9489 64.9193
Frequencies -- 69.0734 71.1584 73.2443
Frequencies -- 74.4793 80.5813 83.9368
Frequencies -- 85.9914 87.5423 89.3580
Frequencies -- 90.3299 94.3423 95.1056
Frequencies -- 98.4728 101.4901 103.1762
Frequencies -- 106.6276 110.3212 116.7364
Frequencies -- 119.8200 123.7016 129.1505
Frequencies -- 131.8128 134.4373 135.1882
Frequencies -- 141.4101 142.9436 147.5843
Frequencies -- 150.6608 157.7756 165.2203
Frequencies -- 169.3445 171.7398 174.6537
Frequencies -- 178.1950 182.3863 192.9331
Frequencies -- 196.4814 201.3169 208.0064
Frequencies -- 216.8754 224.5820 226.9652
Frequencies -- 231.7278 234.6412 239.8060
Frequencies -- 240.7640 242.0369 250.2215
Frequencies -- 252.1180 258.4218 272.8573
Frequencies -- 275.2753 275.7366 278.6959
Frequencies -- 283.3010 286.7465 290.1472
Frequencies -- 297.2308 297.6970 301.9883
Frequencies -- 303.6910 307.2088 308.2666
Frequencies -- 311.7391 314.5774 317.8478
Frequencies -- 319.6611 322.0723 323.1387
Frequencies -- 324.8559 330.9046 337.4664
Frequencies -- 342.6706 345.3734 356.9737
Frequencies -- 369.5723 375.1487 388.7025
Frequencies -- 401.3916 402.5688 408.5374
Frequencies -- 410.4431 412.4675 414.3433
Frequencies -- 416.0523 416.6659 419.4416
Frequencies -- 421.7851 423.4710 427.0509
Frequencies -- 435.1226 439.9388 442.4465
Frequencies -- 443.3853 447.0069 449.7600
Frequencies -- 452.3821 454.9739 455.1840
Frequencies -- 457.1328 467.3231 472.9172
Frequencies -- 488.2670 489.2932 491.0137
Frequencies -- 502.4158 506.9264 511.0663
Frequencies -- 513.0652 519.1821 521.9548
Frequencies -- 522.5609 533.3139 536.5722
Frequencies -- 537.0806 538.7258 545.2753
Frequencies -- 546.9862 552.2799 553.2090
Frequencies -- 555.2590 560.3660 564.2287
Frequencies -- 565.3291 569.9976 572.2081
Frequencies -- 574.3307 582.5968 586.1099
Frequencies -- 590.0320 592.6507 597.7496
Frequencies -- 598.8664 601.1826 602.3366
Frequencies -- 606.3982 609.0627 610.3850
Frequencies -- 611.6802 616.3717 621.2553
Frequencies -- 622.4813 624.6443 626.1294
Frequencies -- 628.6873 630.3657 632.1349
Frequencies -- 633.1919 635.9412 643.7134
Frequencies -- 651.7652 656.3959 668.8665
Frequencies -- 672.6748 675.6273 678.1943
Frequencies -- 680.7522 683.2188 694.7988
Frequencies -- 699.9667 702.7082 709.3461
Frequencies -- 711.6709 714.7235 716.7001
Frequencies -- 719.0429 720.4143 720.9140
Frequencies -- 724.2608 724.4201 725.1398
Frequencies -- 728.0251 732.9841 735.0002
Frequencies -- 737.3942 740.9347 745.7396
Frequencies -- 747.2311 751.6373 760.1732
Frequencies -- 762.3193 769.1259 770.0070
Frequencies -- 771.1827 773.8744 775.1341
Frequencies -- 777.1240 780.1681 782.2903
Frequencies -- 783.4508 793.7524 795.3925
Frequencies -- 798.9686 800.9704 804.4460
Frequencies -- 804.6228 820.3409 826.3231
Frequencies -- 827.3589 829.7471 847.2914
Frequencies -- 857.9332 858.7610 861.7044
Frequencies -- 863.5985 864.3396 865.6737
Frequencies -- 866.6864 870.0932 870.6785
Frequencies -- 874.2856 878.7836 879.2448
Frequencies -- 885.1985 887.4987 887.9861
Frequencies -- 889.4345 891.8265 907.5995
Frequencies -- 913.2968 919.2588 921.5782
Frequencies -- 923.7039 929.5504 930.1090
Frequencies -- 933.6673 935.3305 938.6138
Frequencies -- 940.3956 942.3083 943.1606
Frequencies -- 944.9477 945.8220 948.0989
Frequencies -- 951.3647 952.6296 952.9662
Frequencies -- 956.8413 958.4982 971.1087
Frequencies -- 976.3055 987.9087 988.7461
Frequencies -- 991.6825 992.1177 993.2555
Frequencies -- 996.0095 999.7238 1002.9188
Frequencies -- 1005.8109 1007.3777 1009.4159
Frequencies -- 1011.6766 1013.8912 1014.7703
Frequencies -- 1017.0795 1018.8651 1019.2574

Frequencies -- 1019.4528 1019.7939 1020.1387
Frequencies -- 1020.4102 1020.6120 1025.5417
Frequencies -- 1028.5232 1034.5134 1036.1937
Frequencies -- 1040.4755 1047.1621 1048.0410
Frequencies -- 1053.7112 1056.4688 1057.3962
Frequencies -- 1061.0784 1061.9825 1063.4257
Frequencies -- 1064.4387 1067.8134 1068.2117
Frequencies -- 1068.5147 1070.3340 1071.4028
Frequencies -- 1074.9953 1093.2350 1094.2838
Frequencies -- 1097.9565 1107.4037 1110.2097
Frequencies -- 1111.4013 1113.3691 1122.0264
Frequencies -- 1122.7169 1123.8408 1126.3500
Frequencies -- 1128.4530 1131.0812 1134.1306
Frequencies -- 1159.5948 1161.7934 1164.3439
Frequencies -- 1167.2773 1167.7083 1169.8972
Frequencies -- 1172.4087 1173.0248 1174.2671
Frequencies -- 1175.1433 1175.4741 1177.3064
Frequencies -- 1177.6496 1181.0201 1181.1680
Frequencies -- 1195.2315 1199.4490 1201.1209
Frequencies -- 1203.6017 1204.2500 1205.5786
Frequencies -- 1211.2569 1212.4495 1214.1174
Frequencies -- 1214.9759 1217.7378 1224.5863
Frequencies -- 1227.4146 1229.2466 1230.6082
Frequencies -- 1235.6009 1238.4045 1243.6085
Frequencies -- 1244.7138 1247.4293 1249.3956
Frequencies -- 1257.6880 1260.3476 1266.4593
Frequencies -- 1280.7695 1281.9543 1286.7033
Frequencies -- 1292.8350 1295.8688 1297.1645
Frequencies -- 1297.6274 1298.8676 1300.3744
Frequencies -- 1302.8451 1303.0004 1305.3385
Frequencies -- 1306.6528 1308.7852 1310.0415
Frequencies -- 1311.1953 1314.2259 1316.2236
Frequencies -- 1321.2315 1323.6295 1325.4509
Frequencies -- 1329.9608 1332.2575 1332.5454
Frequencies -- 1337.3695 1342.2242 1343.3219
Frequencies -- 1345.0363 1345.7689 1355.7506
Frequencies -- 1360.1288 1361.1953 1362.2927
Frequencies -- 1362.5563 1363.1707 1364.9337
Frequencies -- 1365.5699 1368.1310 1368.8973
Frequencies -- 1370.2562 1373.6902 1378.0535
Frequencies -- 1381.3201 1384.7471 1387.5463
Frequencies -- 1403.1128 1416.2293 1418.5767
Frequencies -- 1447.4465 1457.7734 1464.2699
Frequencies -- 1468.9227 1474.8708 1489.2360
Frequencies -- 1489.4612 1494.5624 1495.9603
Frequencies -- 1496.6706 1500.7565 1502.3076
Frequencies -- 1505.5257 1505.8386 1509.1454
Frequencies -- 1510.4854 1511.5210 1515.5298
Frequencies -- 1516.1925 1517.4340 1518.7892
Frequencies -- 1528.1669 1529.4134 1545.3966
Frequencies -- 1549.0171 1549.1430 1550.6814
Frequencies -- 1552.5853 1554.0798 1559.4806
Frequencies -- 1560.2488 1561.6748 1562.6418
Frequencies -- 1567.2926 1569.0696 1656.8502
Frequencies -- 1663.2799 1666.7647 1666.9665
Frequencies -- 1668.5897 1669.0855 1673.8788
Frequencies -- 1674.3011 1677.3818 1679.2595
Frequencies -- 1683.6049 1688.0246 1690.6458
Frequencies -- 1691.5750 1694.5940 1696.8687
Frequencies -- 1699.8229 1699.8857 1700.1921
Frequencies -- 1700.9744 1701.2057 1702.4543
Frequencies -- 1702.7833 1703.4342 1717.8749
Frequencies -- 1720.9435 1730.4507 1735.0926
Frequencies -- 2228.5931 3077.2263 3088.2874
Frequencies -- 3091.0396 3093.1378 3132.2840
Frequencies -- 3142.5084 3154.3062 3157.8723
Frequencies -- 3179.4874 3181.5587 3196.5133
Frequencies -- 3197.0597 3198.8917 3201.9373
Frequencies -- 3205.3450 3207.3249 3209.9081
Frequencies -- 3210.6746 3213.0373 3215.0523
Frequencies -- 3215.6456 3216.2683 3217.9402
Frequencies -- 3218.2179 3218.5397 3219.0846
Frequencies -- 3220.9967 3222.8649 3225.2299
Frequencies -- 3225.8714 3227.2912 3227.3082
Frequencies -- 3227.9223 3228.3672 3228.5270
Frequencies -- 3229.8143 3230.1501 3231.9810
Frequencies -- 3233.1943 3233.8498 3234.9913
Frequencies -- 3235.9129 3236.2924 3236.8996
Frequencies -- 3238.2884 3239.0720 3239.6340
Frequencies -- 3240.4984 3241.5211 3241.6009
Frequencies -- 3243.3031 3243.3332 3247.8976
Frequencies -- 3251.0468 3252.0071 3255.1308
Frequencies -- 3256.1861 3262.2097 3634.8402

SCF Done: E(RM062X/DGDZVP) = -6499.39694452
Sum of electronic and zero-point Energies= -6498.046953
Sum of electronic and thermal Energies= -6497.932831
Sum of electronic and thermal Free Energies= -6498.203599
SCF Done: E(RM062X/DGTZVP/SMD) = -6500.6820721

Cat f TS1c_*S*

Center Number	Atomic Number	Atomic Type	Coordinates (Angstroms) X	Y	Z
1	15	0	-0.014269	-0.009930	0.010924
2	8	0	-0.020468	-0.004823	1.635637
3	8	0	1.573248	0.000148	-0.326187
4	8	0	-0.580947	1.228542	-0.602597
5	8	0	-0.624025	-1.336574	-0.352506
6	6	0	0.506645	1.107948	2.268745
7	6	0	2.344124	-1.063171	0.097777
8	6	0	1.872019	1.181984	2.510651
9	6	0	-0.333291	2.187064	2.566607
10	6	0	2.917407	-0.997542	1.360971
11	6	0	2.516914	-2.194033	-0.717677
12	6	0	2.978562	0.156723	2.342673
13	6	0	2.409191	2.377955	2.988308
14	6	0	0.218305	3.330145	3.151504
15	6	0	-1.749593	2.149209	2.134798
16	6	0	3.635669	-2.088821	1.847954
17	6	0	3.311298	-3.241284	-0.231634
18	6	0	1.817839	-2.280195	-2.026406
19	6	0	3.220779	-0.606529	3.671311
20	6	0	4.180205	1.087476	2.030379
21	6	0	3.923630	2.393130	2.828377
22	6	0	1.592365	3.447557	3.365911
23	1	0	-0.431965	4.163339	3.404023
24	6	0	-2.244239	3.153765	1.299760
25	6	0	-2.605231	1.099207	2.457250
26	6	0	4.043801	-1.863411	3.297291
27	6	0	3.876171	-3.208167	1.044769
28	1	0	3.488830	-4.107968	-0.861042
29	6	0	1.087680	-3.420514	-2.390339
30	6	0	1.807994	-1.205900	-2.918812
31	1	0	3.718368	0.015614	4.421703
32	1	0	2.253279	-0.911093	4.082778
33	1	0	5.139900	0.621894	2.276099
34	1	0	4.182379	1.311615	0.958457
35	1	0	4.432747	2.357476	3.798467
36	6	0	4.369927	3.638276	2.083708

37	6	0	2.190053	4.697947	3.901951
38	6	0	-3.526744	3.081650	0.776414
39	8	0	-1.416771	4.201546	0.963082
40	6	0	-3.895847	1.010194	1.927031
41	8	0	-2.159075	0.121707	3.317363
42	1	0	5.116426	-1.636580	3.343882
43	6	0	3.770123	-3.050643	4.199141
44	6	0	4.712696	-4.334516	1.540543
45	6	0	0.298587	-3.455634	-3.545720
46	8	0	1.147621	-4.502836	-1.539507
47	6	0	0.981932	-1.209292	-4.038001
48	8	0	2.631396	-0.124854	-2.714749
49	6	0	3.734480	3.982249	0.883015
50	6	0	5.357830	4.483692	2.586998
51	6	0	2.028536	5.910765	3.224273
52	6	0	2.977523	4.662972	5.057819
53	6	0	-4.369194	2.005665	1.074496
54	8	0	-3.976103	4.039748	-0.104259
55	6	0	-1.693997	4.780734	-0.255077
56	8	0	-4.674718	-0.072154	2.242568
57	6	0	-2.679159	-1.128543	3.043487
58	6	0	2.466210	-3.536477	4.349869
59	6	0	4.804409	-3.691092	4.884223
60	6	0	4.147247	-5.591066	1.777952
61	6	0	6.070369	-4.136581	1.810966
62	6	0	0.212633	-2.326005	-4.366493
63	8	0	-0.414278	-4.569465	-3.893895
64	6	0	0.542602	-5.664909	-1.967838
65	8	0	0.928102	-0.099722	-4.838339
66	6	0	2.027253	1.071092	-3.066015
67	6	0	4.087274	5.141426	0.199035
68	1	0	2.927706	3.353183	0.506185
69	6	0	5.705958	5.654530	1.909481
70	1	0	5.842050	4.241545	3.530355
71	6	0	2.666595	7.063083	3.679543
72	1	0	1.424537	5.937088	2.320443
73	6	0	3.606285	5.817095	5.521308
74	1	0	3.091052	3.723841	5.594536
75	6	0	-5.720664	1.980079	0.403029
76	6	0	-2.974846	4.695703	-0.795524
77	6	0	-0.698696	5.486126	-0.913208
78	6	0	-3.958695	-1.224714	2.504529
79	6	0	-1.955593	-2.272716	3.346324
80	6	0	2.202423	-4.626308	5.177270
81	1	0	1.648369	-3.057832	3.811910
82	6	0	4.549636	-4.798042	5.693772
83	1	0	5.823731	-3.329992	4.771188
84	6	0	4.916151	-6.621301	2.316599
85	1	0	3.093248	-5.746884	1.558926
86	6	0	6.845700	-5.171396	2.332107
87	1	0	6.517292	-3.165691	1.609414
88	6	0	-0.608672	-2.245584	-5.633095
89	6	0	-0.245535	-5.689203	-3.114717
90	6	0	0.718958	-6.817219	-1.215580
91	6	0	1.141591	1.079450	-4.137973
92	6	0	2.291675	2.233787	-2.360069
93	6	0	5.074104	5.985947	0.713198
94	1	0	3.587691	5.396510	-0.731378
95	1	0	6.464719	6.311357	2.324037
96	6	0	3.460989	7.017957	4.825911
97	1	0	2.552638	7.994513	3.133424
98	1	0	4.211520	5.779681	6.422132
99	9	0	-6.488737	0.957050	0.777372
100	9	0	-6.413424	3.103382	0.655480
101	9	0	-5.583527	1.901446	-0.939872
102	6	0	-3.268235	5.295692	-2.010839
103	1	0	0.286456	5.535626	-0.458971
104	6	0	-0.994535	6.117330	-2.121887
105	6	0	-4.532844	-2.461421	2.255117
106	1	0	-0.958336	-2.164688	3.761610
107	6	0	-2.541785	-3.521956	3.131212
108	6	0	3.245991	-5.266968	5.847543
109	1	0	1.180925	-4.977535	5.298702
110	1	0	5.370794	-5.292079	6.204251
111	6	0	6.266388	-6.412110	2.599819
112	1	0	4.460766	-7.586281	2.518016
113	1	0	7.900054	-5.007686	2.534083
114	9	0	-1.433839	-1.174455	-5.607605
115	9	0	-1.381020	-3.311643	-5.845065
116	9	0	0.178983	-2.099019	-6.710411
117	6	0	-0.883650	-6.857504	-3.505619
118	1	0	1.335268	-6.765880	-0.322130
119	6	0	0.079014	-7.994722	-1.602065
120	6	0	0.472967	2.236404	-4.504797
121	1	0	2.986539	2.193880	-1.527591
122	6	0	1.644056	3.408689	-2.739985
123	1	0	5.342335	6.896663	0.186713
124	1	0	3.960104	7.915745	5.177479
125	1	0	-4.274444	5.205652	-2.407458
126	6	0	-2.272194	6.016871	-2.672291
127	1	0	-0.223523	6.686167	-2.632379
128	1	0	-5.530342	-2.503664	1.830246
129	6	0	-3.819938	-3.616082	2.580363
130	1	0	-1.994342	-4.424224	3.388446
131	1	0	3.042212	-6.121590	6.485251
132	1	0	6.865354	-7.214402	3.019625
133	1	0	-1.500306	-6.834430	-4.398165
134	6	0	-0.725937	-8.012983	-2.741065
135	1	0	0.208240	-8.892212	-1.006174
136	1	0	-0.239387	2.195405	-5.322035
137	6	0	0.731948	3.409670	-3.796570
138	1	0	1.837657	4.326089	-2.193625
139	1	0	-2.500615	6.503811	-3.614422
140	1	0	-4.267619	-4.589662	2.406636
141	1	0	-1.230589	-8.925239	-3.040622
142	1	0	0.210052	4.322155	-4.065157
143	1	0	-1.194286	0.914164	-2.206518
144	8	0	-1.923862	0.691382	-2.853592
145	6	0	-3.165644	0.990191	-2.151885
146	6	0	-3.597531	-0.451429	-1.816331
147	1	0	-2.959765	1.583795	-1.260705
148	1	0	-3.830847	1.515666	-2.836209
149	8	0	-3.452640	-0.774165	-0.456357
150	6	0	-2.492704	-1.085208	-2.684772
151	1	0	-2.507816	-0.936982	-0.257455
152	1	0	-2.655771	-1.232693	-3.745128
153	1	0	-1.570713	-1.451276	-2.252268
154	1	0	-1.147269	-2.885209	-0.506397
155	7	0	-1.554380	-3.837052	-0.436214
156	6	0	-2.597974	-4.245702	-1.177006
157	6	0	-1.095065	-4.722288	0.528017
158	16	0	-3.347081	-3.461835	-2.455228
159	16	0	-3.120088	-5.833262	-0.638244
160	6	0	-1.859626	-5.892335	0.574274
161	6	0	0.020449	-4.543319	1.346877
162	6	0	-1.547307	-6.911561	1.472543
163	6	0	0.337885	-5.569784	2.230550
164	1	0	0.611993	-3.631068	1.278911
165	6	0	-0.440523	-6.737365	2.300265
166	1	0	-2.137427	-7.821693	1.510661
167	1	0	1.202786	-5.465077	2.878599
168	1	0	-0.172140	-7.519047	3.003977

169	6	0	-5.005812	-0.782828	-2.264824
170	6	0	-5.384097	-0.578029	-3.594528
171	6	0	-5.939551	-1.267563	-1.351259
172	6	0	-6.681905	-0.867513	-4.010012
173	1	0	-4.668997	-0.192595	-4.320269
174	6	0	-7.241817	-1.543320	-1.764081
175	1	0	-5.636083	-1.419904	-0.321151
176	6	0	-7.616343	-1.348776	-3.092611
177	1	0	-6.963325	-0.712684	-5.046965
178	1	0	-7.966182	-1.911903	-1.044144
179	1	0	-8.630125	-1.568598	-3.412668

Frequencies --	-538.5894	2.3415	12.7084
Frequencies --	19.8835	20.8353	22.9470
Frequencies --	23.8380	28.0338	31.6982
Frequencies --	35.5325	37.1717	38.3091
Frequencies --	40.1047	43.3487	44.0209
Frequencies --	48.0409	51.5601	52.8818
Frequencies --	53.3189	55.1646	58.1321
Frequencies --	60.4880	62.0651	63.6796
Frequencies --	69.1110	69.5195	71.6234
Frequencies --	74.4294	76.1841	79.6532
Frequencies --	80.3261	83.4500	83.9574
Frequencies --	90.4817	91.5305	93.9990
Frequencies --	97.6831	100.0964	100.9613
Frequencies --	102.1170	107.0551	109.3873
Frequencies --	113.8080	118.2896	125.4361
Frequencies --	127.1271	131.9349	136.2682
Frequencies --	138.1700	140.5873	149.2239
Frequencies --	156.3463	158.1003	164.3626
Frequencies --	165.3535	168.1780	172.4872
Frequencies --	182.7637	187.1283	189.5298
Frequencies --	197.2498	200.0484	201.2862
Frequencies --	210.9235	216.6744	220.8454
Frequencies --	224.4681	229.9748	233.5997
Frequencies --	236.6019	241.6229	250.3218
Frequencies --	252.9247	256.9342	267.8432
Frequencies --	272.8635	274.4898	276.0129
Frequencies --	280.2519	281.1279	288.7780
Frequencies --	290.4636	292.5424	294.3376
Frequencies --	296.7070	300.0644	302.7050
Frequencies --	305.7927	310.4171	313.9984
Frequencies --	318.0819	319.0940	323.1438
Frequencies --	325.3823	331.1503	337.0493
Frequencies --	339.4562	343.2849	347.4156
Frequencies --	354.1434	374.9705	385.8687
Frequencies --	396.6766	403.9318	408.5137
Frequencies --	408.5893	411.5381	412.0105
Frequencies --	413.4957	414.3270	415.7202
Frequencies --	418.3352	418.7997	419.6207
Frequencies --	428.5358	438.6625	439.4746
Frequencies --	441.7710	444.5083	447.9530
Frequencies --	450.7667	452.4806	459.8010
Frequencies --	466.4183	467.4431	469.3198
Frequencies --	473.6892	487.7993	491.0435
Frequencies --	500.8144	505.9987	507.0283
Frequencies --	512.0012	513.9506	521.4397
Frequencies --	522.4579	522.6447	530.5404
Frequencies --	534.1118	535.7238	538.0652
Frequencies --	543.7397	546.9458	554.4879
Frequencies --	556.5234	559.9780	561.2111
Frequencies --	564.4113	567.1731	571.6457
Frequencies --	574.8333	583.3612	585.9061
Frequencies --	587.7816	589.6631	593.7220
Frequencies --	595.5787	599.4273	601.6283
Frequencies --	602.7093	605.8311	609.6877
Frequencies --	610.8563	613.7036	617.4957
Frequencies --	620.0853	621.4898	624.2433
Frequencies --	626.1375	630.0817	630.7719
Frequencies --	632.0928	634.4780	635.8472
Frequencies --	644.0808	651.2025	656.7087
Frequencies --	666.6633	669.9041	673.6694
Frequencies --	676.9657	680.8743	682.1449
Frequencies --	684.1847	695.7241	703.6652
Frequencies --	709.8803	714.4797	714.7008
Frequencies --	717.3454	717.9969	718.2265
Frequencies --	720.2990	722.8794	723.6101
Frequencies --	724.3093	726.1523	732.0525
Frequencies --	732.8563	734.6723	739.1237
Frequencies --	744.0436	748.1123	751.7374
Frequencies --	763.5368	764.1364	765.4389
Frequencies --	766.5218	770.3966	771.4491
Frequencies --	772.1297	774.5392	776.4258
Frequencies --	779.7161	782.2200	783.5029
Frequencies --	794.9151	796.1059	798.9730
Frequencies --	800.7702	804.3502	804.9721
Frequencies --	822.9091	826.4330	827.7029
Frequencies --	830.9976	857.6053	862.9928
Frequencies --	865.8142	866.3028	867.6771
Frequencies --	869.7850	871.1645	871.9702
Frequencies --	873.7254	877.1632	878.0584
Frequencies --	881.2119	886.4070	888.0122
Frequencies --	888.9871	889.1533	894.5442
Frequencies --	900.7593	913.7157	917.1325
Frequencies --	923.4478	924.0078	927.0769
Frequencies --	931.5753	934.2407	935.3453
Frequencies --	935.5422	936.1232	941.7562
Frequencies --	943.9116	946.7657	947.1380
Frequencies --	950.4414	952.1711	956.7392
Frequencies --	959.9152	961.0902	963.0817
Frequencies --	970.4349	970.6935	987.5023
Frequencies --	988.5548	989.5813	991.0769
Frequencies --	993.8750	995.6139	996.4003
Frequencies --	999.7710	1003.3543	1005.4719
Frequencies --	1005.9598	1008.7938	1013.4239
Frequencies --	1014.2322	1016.3015	1018.4035
Frequencies --	1019.3654	1019.8092	1020.1905
Frequencies --	1020.9803	1021.3551	1024.4764
Frequencies --	1026.0100	1033.6646	1036.2112
Frequencies --	1038.0397	1044.0675	1045.7069
Frequencies --	1049.0367	1054.6551	1057.8247
Frequencies --	1058.7335	1059.2424	1064.3142
Frequencies --	1066.3762	1067.3975	1068.7661
Frequencies --	1070.6002	1073.2365	1077.0699
Frequencies --	1088.3680	1091.6923	1096.7488
Frequencies --	1106.7492	1108.0839	1110.6008
Frequencies --	1111.7184	1113.3951	1117.8935
Frequencies --	1119.8018	1122.7532	1126.0653
Frequencies --	1129.2270	1130.7189	1132.2486
Frequencies --	1133.6761	1154.3296	1160.6653
Frequencies --	1165.8681	1168.0423	1170.0331
Frequencies --	1171.2372	1171.8555	1174.0102
Frequencies --	1174.1463	1175.7639	1176.4997
Frequencies --	1177.1456	1178.8228	1179.2311
Frequencies --	1189.1441	1193.6826	1200.4499
Frequencies --	1201.9134	1203.4375	1203.8322
Frequencies --	1204.3996	1204.7569	1205.9587
Frequencies --	1212.6853	1214.3820	1216.0868
Frequencies --	1223.4582	1225.6002	1227.1120
Frequencies --	1232.3340	1234.1475	1240.5112
Frequencies --	1242.2424	1242.6302	1247.0578

Frequencies --	1252.0971	1256.0105	1262.6010
Frequencies --	1274.3505	1275.9520	1279.2554
Frequencies --	1279.9726	1284.6065	1286.2994
Frequencies --	1287.9506	1293.5092	1296.2866
Frequencies --	1298.7996	1299.0808	1304.7167
Frequencies --	1308.2313	1308.8102	1309.4251
Frequencies --	1311.0395	1314.4430	1315.0406
Frequencies --	1318.3867	1321.3349	1324.0571
Frequencies --	1326.7367	1330.1039	1333.9677
Frequencies --	1338.7431	1341.5286	1343.6361
Frequencies --	1343.9407	1352.7054	1357.2167
Frequencies --	1359.9232	1360.6988	1360.8413
Frequencies --	1362.5688	1363.5244	1364.6975
Frequencies --	1365.1481	1366.8591	1369.3263
Frequencies --	1371.4628	1373.1744	1376.6353
Frequencies --	1381.1380	1386.9038	1390.0020
Frequencies --	1403.3334	1416.2171	1445.7391
Frequencies --	1448.8493	1456.1603	1459.9066
Frequencies --	1467.5717	1472.0596	1477.2061
Frequencies --	1490.3333	1492.0715	1495.7910
Frequencies --	1496.7339	1499.1124	1499.9821
Frequencies --	1502.1399	1504.6001	1507.5024
Frequencies --	1507.5961	1509.7771	1510.9720
Frequencies --	1514.0978	1515.7373	1518.1585
Frequencies --	1528.8883	1530.0845	1544.1729
Frequencies --	1544.7675	1553.1505	1554.0055
Frequencies --	1555.1455	1555.7515	1558.8415
Frequencies --	1559.8473	1561.5105	1564.6060
Frequencies --	1567.3062	1571.6896	1654.6789
Frequencies --	1662.4102	1665.5668	1669.2158
Frequencies --	1669.2806	1669.8715	1674.1524
Frequencies --	1674.9877	1679.1163	1680.1925
Frequencies --	1682.8327	1687.4121	1689.9963
Frequencies --	1691.5293	1695.2355	1696.1210
Frequencies --	1698.2881	1698.7366	1701.3030
Frequencies --	1701.6763	1702.3572	1703.2961
Frequencies --	1704.0902	1705.3766	1719.2132
Frequencies --	1721.2429	1725.6563	1734.8157
Frequencies --	3071.6309	3085.0795	3087.7032
Frequencies --	3090.4746	3148.9033	3153.5447
Frequencies --	3154.0177	3173.4036	3184.5596
Frequencies --	3188.8777	3195.3281	3198.7255
Frequencies --	3200.8070	3203.9077	3204.9151
Frequencies --	3205.6265	3207.5338	3208.3962
Frequencies --	3208.8296	3211.0998	3217.2300
Frequencies --	3217.9271	3218.2244	3220.5857
Frequencies --	3221.0173	3221.7789	3222.0532
Frequencies --	3222.5085	3223.5701	3225.1960
Frequencies --	3227.9029	3228.6926	3229.7075
Frequencies --	3229.7468	3230.4458	3231.5470
Frequencies --	3233.9608	3234.4636	3234.6550
Frequencies --	3234.7330	3236.8390	3238.5237
Frequencies --	3239.1760	3239.2088	3240.3231
Frequencies --	3241.2180	3241.2973	3241.3669
Frequencies --	3241.8912	3243.7206	3246.0711
Frequencies --	3246.1923	3246.4637	3247.4418
Frequencies --	3248.5482	3249.7101	3255.6843
Frequencies --	3287.7949	3382.7171	3650.7059

SCF Done: E(RM062X/DGDZVP) = -6499.36575894
Sum of electronic and zero-point Energies= -6498.015603
Sum of electronic and thermal Energies= -6497.901639
Sum of electronic and thermal Free Energies= -6498.174468
SCF Done: E(RM062X/DGTZVP/SMD) = -6500.64748533

Cat f I1c_*S*

Center Number	Atomic Number	Atomic Type	Coordinates (Angstroms) X	Y	Z
1	15	0	-0.073518	-0.078696	0.088959
2	8	0	-0.024747	-0.113580	1.721330
3	8	0	1.514372	-0.013913	-0.274063
4	8	0	-0.694386	1.158395	-0.454552
5	8	0	-0.636212	-1.423708	-0.289108
6	6	0	0.481850	1.007830	2.357042
7	6	0	2.308409	-1.067028	0.125593
8	6	0	1.848444	1.112245	2.590311
9	6	0	-0.369697	2.080415	2.654109
10	6	0	2.911411	-1.016164	1.376679
11	6	0	2.469905	-2.185258	-0.706060
12	6	0	2.984698	0.130580	2.365200
13	6	0	2.365682	2.312622	3.079598
14	6	0	0.160383	3.213539	3.276228
15	6	0	-1.748789	2.090029	2.112517
16	6	0	3.655188	-2.107068	1.830079
17	6	0	3.261306	-3.244920	-0.247735
18	6	0	1.752944	-2.239476	-2.005431
19	6	0	3.320052	-0.630045	3.673615
20	6	0	4.133959	1.110404	2.012864
21	6	0	3.872074	2.381519	2.862834
22	6	0	1.530415	3.351120	3.499415
23	1	0	-0.503958	4.034781	3.531677
24	6	0	-2.105509	3.101040	1.219117
25	6	0	-2.656045	1.056522	2.318646
26	6	0	4.157402	-1.858191	3.248630
27	6	0	3.863583	-3.223998	1.012756
28	1	0	3.414849	-4.106919	-0.891119
29	6	0	0.932007	-3.324902	-2.325960
30	6	0	1.771805	-1.171015	-2.899513
31	1	0	3.840439	0.002007	4.399632
32	1	0	2.384660	-0.960352	4.134604
33	1	0	5.122425	0.675657	2.192472
34	1	0	4.067073	1.364481	0.949760
35	1	0	4.422437	2.332850	3.809658
36	6	0	4.251284	3.663138	2.143138
37	6	0	2.103602	4.601270	4.060191
38	6	0	-3.317490	3.063354	0.545466
39	8	0	-1.197838	4.106156	0.978551
40	6	0	-3.870359	0.994760	1.632940
41	8	0	-2.329631	0.077819	3.231614
42	1	0	5.219385	-1.583705	3.203217
43	6	0	4.017868	-3.040304	4.186170
44	6	0	4.742720	-4.345124	1.448558
45	6	0	0.107560	-3.321082	-3.449347
46	8	0	0.894524	-4.374753	-1.428221
47	6	0	0.926136	-1.142236	-4.005962
48	8	0	2.618672	-0.110454	-2.691960
49	6	0	3.564329	4.028753	0.977042
50	6	0	5.230656	4.520436	2.643115
51	6	0	1.879652	5.830724	3.431510
52	6	0	2.929532	4.553838	5.188476
53	6	0	-4.224584	2.021581	0.756415
54	8	0	-3.648720	4.033064	-0.372268
55	6	0	-1.369942	4.793046	-0.200354
56	8	0	-4.703963	-0.081847	1.829800
57	6	0	-2.865465	-1.155454	2.941650
58	6	0	2.752000	-3.520783	4.537116
59	6	0	5.141769	-3.688745	4.703372
60	6	0	4.212440	-5.596761	1.775205

61	6	0	6.123335	-4.144898	1.550332
62	6	0	0.093792	-2.216809	-4.306801
63	8	0	-0.790474	-4.346825	-3.660558
64	6	0	0.310395	-5.533869	-1.879599
65	8	0	0.890731	-0.027322	-4.794199
66	6	0	2.025864	1.101166	-3.018394
67	6	0	3.861584	5.221817	0.325041
68	1	0	2.764292	3.389507	0.601355
69	6	0	5.521548	5.724595	1.998300
70	1	0	5.753959	4.259079	3.560066
71	6	0	2.495632	6.987452	3.905338
72	1	0	1.244477	5.866974	2.549475
73	6	0	3.535514	5.712038	5.671660
74	1	0	3.090892	3.601343	5.688106
75	6	0	-5.555404	2.112425	0.048399
76	6	0	-2.586301	4.754024	-0.877013
77	6	0	-0.326215	5.570488	-0.678798
78	6	0	-4.059448	-1.235749	2.227987
79	6	0	-2.244487	-2.303405	3.412203
80	6	0	2.611667	-4.629316	5.370514
81	1	0	1.862728	-3.024143	4.152280
82	6	0	5.008900	-4.803743	5.529751
83	1	0	6.133714	-3.330011	4.439894
84	6	0	5.043152	-6.620603	2.228544
85	1	0	3.140740	-5.758705	1.687207
86	6	0	6.957745	-5.171761	1.989899
87	1	0	6.541634	-3.178404	1.278598
88	6	0	-0.773432	-2.089737	-5.536606
89	6	0	-0.535749	-5.519409	-2.986048
90	6	0	0.542230	-6.715122	-1.188528
91	6	0	1.130651	1.139311	-4.080483
92	6	0	2.313628	2.245674	-2.292636
93	6	0	4.839864	6.077956	0.836240
94	1	0	3.325390	5.495177	-0.579673
95	1	0	6.274104	6.389352	2.411541
96	6	0	3.328806	6.930218	5.023350
97	1	0	2.333279	7.932353	3.395794
98	1	0	4.170602	5.664848	6.551265
99	9	0	-6.443934	1.207189	0.473958
100	9	0	-6.121031	3.317070	0.247601
101	9	0	-5.426145	1.956319	-1.281158
102	6	0	-2.761251	5.472667	-2.050147
103	1	0	0.606598	5.580968	-0.121462
104	6	0	-0.503399	6.315738	-1.845233
105	6	0	-4.638446	-2.468502	1.964188
106	1	0	-1.311254	-2.203161	3.957977
107	6	0	-2.845157	-3.542713	3.188399
108	6	0	3.742140	-5.280080	5.865743
109	1	0	1.618509	-4.982190	5.636650
110	1	0	5.896745	-5.301223	5.908391
111	6	0	6.417725	-6.409214	2.341089
112	1	0	4.617109	-7.582326	2.498402
113	1	0	8.028612	-5.005346	2.059660
114	9	0	-1.626266	-1.052041	-5.442867
115	9	0	-1.526769	-3.175392	-5.771076
116	9	0	-0.027301	-1.888192	-6.633197
117	6	0	-1.162545	-6.682961	-3.409303
118	1	0	1.201730	-6.690570	-0.324739
119	6	0	-0.095040	-7.885801	-1.601103
120	6	0	0.478043	2.312867	-4.420933
121	1	0	3.015438	2.181275	-1.467204
122	6	0	1.679726	3.436092	-2.644714
123	1	0	5.062369	7.014519	0.334307
124	1	0	3.809826	7.831861	5.390000
125	1	0	-3.719810	5.414825	-2.555653
126	6	0	-1.716196	6.263026	-2.531748
127	1	0	0.308058	6.934722	-2.215532
128	1	0	-5.563086	-2.504646	1.396649
129	6	0	-4.033815	-3.625044	2.461858
130	1	0	-2.375036	-4.443958	3.573469
131	1	0	3.636845	-6.145372	6.512947
132	1	0	7.064985	-7.206658	2.692951
133	1	0	-1.815224	-6.635587	-4.275123
134	6	0	-0.946426	-7.869149	-2.706562
135	1	0	0.079363	-8.808945	-1.058233
136	1	0	-0.243392	2.296240	-5.231036
137	6	0	0.760534	3.469523	-3.694556
138	1	0	1.889941	4.340989	-2.084417
139	1	0	-1.855677	6.837583	-3.441500
140	1	0	-4.503998	-4.588821	2.291756
141	1	0	-1.440509	-8.779324	-3.029398
142	1	0	0.248325	4.395238	-3.936792
143	1	0	-1.252216	0.739679	-2.128477
144	8	0	-1.561824	0.201757	-2.888315
145	6	0	-2.972483	0.243570	-2.945502
146	6	0	-3.621880	-0.955705	-2.218590
147	1	0	-3.372414	1.154457	-2.483675
148	1	0	-3.260066	0.234567	-3.999891
149	8	0	-3.463119	-0.838253	-0.815586
150	6	0	-2.924632	-2.246300	-2.678637
151	1	0	-2.510786	-0.713993	-0.637017
152	1	0	-2.948221	-2.361768	-3.765732
153	1	0	-1.881233	-2.245491	-2.354230
154	1	0	-1.414058	-2.751635	-0.335378
155	7	0	-1.762192	-3.747657	-0.197961
156	6	0	-2.784994	-4.326851	-0.799378
157	6	0	-1.130327	-4.535280	0.763190
158	16	0	-3.785106	-3.741274	-2.063573
159	16	0	-3.082522	-5.928501	-0.195869
160	6	0	-1.751960	-5.775164	0.923397
161	6	0	0.010146	-4.186366	1.488279
162	6	0	-1.274539	-6.709126	1.844074
163	6	0	0.495539	-5.125617	2.388394
164	1	0	0.485163	-3.218349	1.335595
165	6	0	-0.141488	-6.366155	2.573331
166	1	0	-1.757424	-7.672478	1.970959
167	1	0	1.390076	-4.900759	2.959095
168	1	0	0.264951	-7.071776	3.291342
169	6	0	-5.105766	-1.020950	-2.529622
170	6	0	-5.544965	-1.143693	-3.853513
171	6	0	-6.046126	-1.004755	-1.499794
172	6	0	-6.905991	-1.230804	-4.140951
173	1	0	-4.829185	-1.172790	-4.672869
174	6	0	-7.407891	-1.082962	-1.788050
175	1	0	-5.700750	-0.916659	-0.475188
176	6	0	-7.842766	-1.196226	-3.107626
177	1	0	-7.233866	-1.320672	-5.172061
178	1	0	-8.128924	-1.046320	-0.976723
179	1	0	-8.903531	-1.254904	-3.331437

Frequencies --	12.3769	18.4719	21.9104
Frequencies --	23.6748	25.4271	28.1406
Frequencies --	30.8569	32.0678	35.1082
Frequencies --	37.6298	38.6131	40.2655
Frequencies --	44.9349	47.5925	50.3056
Frequencies --	52.2965	56.1535	59.7080
Frequencies --	60.8176	62.0028	64.6564
Frequencies --	68.4931	69.5594	70.8703
Frequencies --	73.4892	74.0299	78.2005
Frequencies --	80.2222	88.0661	88.8451
Frequencies --	91.0201	92.1741	94.1629

Frequencies -- 95.1515 96.5310 98.7892
Frequencies -- 100.1584 101.8867 104.0110
Frequencies -- 106.3322 113.7882 116.4690
Frequencies -- 120.5235 122.1062 126.3862
Frequencies -- 128.8856 134.3722 139.6385
Frequencies -- 141.4355 146.6303 152.5743
Frequencies -- 158.2629 161.7887 166.0794
Frequencies -- 167.4012 173.2606 179.1358
Frequencies -- 188.4989 191.1984 194.6911
Frequencies -- 198.8595 207.6144 212.3056
Frequencies -- 212.9642 223.1345 227.0583
Frequencies -- 231.7590 236.4527 240.2386
Frequencies -- 240.9065 242.9507 250.4250
Frequencies -- 254.1146 254.7924 269.6198
Frequencies -- 274.4692 277.8436 279.9289
Frequencies -- 282.4031 287.0493 289.8679
Frequencies -- 293.1213 294.4474 298.2748
Frequencies -- 300.0246 303.2468 304.8276
Frequencies -- 308.6638 312.5260 315.5659
Frequencies -- 318.6578 321.9472 328.7685
Frequencies -- 329.0340 332.6802 334.9775
Frequencies -- 337.7357 348.5656 351.2970
Frequencies -- 355.4958 375.7316 382.6894
Frequencies -- 395.0627 404.5587 405.6195
Frequencies -- 413.1681 415.5067 415.7917
Frequencies -- 416.5611 417.8542 420.1459
Frequencies -- 422.2567 423.2662 424.0295
Frequencies -- 433.1470 434.5242 443.2117
Frequencies -- 445.2981 448.6551 448.9718
Frequencies -- 453.0507 454.2881 459.2526
Frequencies -- 462.9679 467.5188 472.1596
Frequencies -- 481.8604 486.1132 491.8438
Frequencies -- 499.8776 501.7238 511.2122
Frequencies -- 511.7108 512.8823 522.0066
Frequencies -- 522.5470 522.9455 525.9692
Frequencies -- 531.8073 533.7357 538.3084
Frequencies -- 544.3293 549.3356 556.3100
Frequencies -- 557.6498 558.4888 562.5129
Frequencies -- 564.1718 568.4138 569.9211
Frequencies -- 583.2778 584.6692 586.6755
Frequencies -- 589.4298 593.2002 597.8280
Frequencies -- 598.4761 600.0248 601.9776
Frequencies -- 604.5258 609.6236 610.1977
Frequencies -- 611.2135 614.0222 617.0902
Frequencies -- 621.9693 624.8202 626.1217
Frequencies -- 628.7775 630.4064 632.0346
Frequencies -- 633.8926 636.2211 640.9251
Frequencies -- 643.9516 650.0556 655.9731
Frequencies -- 667.9062 670.4866 675.3577
Frequencies -- 678.4626 682.5340 693.9841
Frequencies -- 695.8223 701.0041 710.7691
Frequencies -- 712.9933 716.3166 716.4882
Frequencies -- 717.6540 719.2854 720.4154
Frequencies -- 722.9968 725.3125 725.6694
Frequencies -- 727.3059 730.8386 732.2805
Frequencies -- 732.7879 734.9490 739.1115
Frequencies -- 744.5000 748.4578 751.5302
Frequencies -- 755.5151 762.0617 765.1931
Frequencies -- 767.5931 770.3412 771.6685
Frequencies -- 772.0792 773.1230 777.0546
Frequencies -- 779.1194 781.8639 784.5836
Frequencies -- 789.2072 796.5207 798.6071
Frequencies -- 799.4558 800.6029 804.1659
Frequencies -- 805.0761 822.7960 826.3857
Frequencies -- 828.6760 830.2172 858.8719
Frequencies -- 859.4325 861.8011 863.1029
Frequencies -- 865.8835 867.2866 868.8848
Frequencies -- 869.1702 873.2013 874.0270
Frequencies -- 876.4146 880.8276 881.7115
Frequencies -- 888.7291 889.2331 890.6695
Frequencies -- 893.1932 907.1399 911.8109
Frequencies -- 915.6344 919.5790 922.5162
Frequencies -- 930.4141 933.5214 935.7587
Frequencies -- 936.6615 939.3072 941.1405
Frequencies -- 941.3228 944.2978 944.5407
Frequencies -- 950.7730 952.1504 953.3477
Frequencies -- 955.9626 958.5573 969.8351
Frequencies -- 975.6378 982.7743 986.7313
Frequencies -- 986.9567 989.1320 991.8527
Frequencies -- 992.1712 994.3216 995.7812
Frequencies -- 996.7749 1004.0719 1004.5407
Frequencies -- 1004.7634 1006.3748 1007.6882
Frequencies -- 1008.4787 1012.6035 1018.3575
Frequencies -- 1019.1020 1019.2159 1019.7338
Frequencies -- 1020.5093 1024.3504 1025.9532
Frequencies -- 1027.2318 1034.2691 1036.1536
Frequencies -- 1036.9296 1043.8068 1052.3269
Frequencies -- 1053.1623 1057.0554 1059.2331
Frequencies -- 1062.6892 1062.9803 1066.7670
Frequencies -- 1068.3599 1069.8482 1070.2608
Frequencies -- 1071.8136 1072.3355 1091.5792
Frequencies -- 1096.9110 1108.7507 1111.7091
Frequencies -- 1113.2289 1114.7485 1116.5282
Frequencies -- 1120.1227 1123.4397 1126.0404
Frequencies -- 1126.2433 1128.1523 1129.0016
Frequencies -- 1129.7584 1131.7980 1145.4862
Frequencies -- 1157.2710 1158.6046 1161.4399
Frequencies -- 1166.0389 1166.1257 1166.5310
Frequencies -- 1168.9592 1170.1291 1173.7034
Frequencies -- 1175.3740 1175.8574 1176.9718
Frequencies -- 1177.1567 1178.5003 1188.7894
Frequencies -- 1195.9801 1200.0548 1201.9617
Frequencies -- 1203.2140 1207.7894 1207.9415
Frequencies -- 1211.0181 1211.6886 1213.1570
Frequencies -- 1214.9478 1216.2124 1222.7106
Frequencies -- 1225.4258 1229.9120 1235.4265
Frequencies -- 1236.9198 1238.2333 1243.1974
Frequencies -- 1244.6826 1247.9211 1251.1265
Frequencies -- 1253.2940 1259.3809 1271.7237
Frequencies -- 1272.9342 1275.4259 1280.6367
Frequencies -- 1284.4827 1292.6824 1294.6323
Frequencies -- 1297.1451 1297.4596 1298.1973
Frequencies -- 1299.1801 1303.2326 1305.0558
Frequencies -- 1307.1856 1308.4016 1309.6856
Frequencies -- 1311.1559 1314.5471 1316.0651
Frequencies -- 1316.5801 1322.2743 1324.2517
Frequencies -- 1327.6846 1329.4082 1333.0793
Frequencies -- 1336.5052 1341.2938 1342.7602
Frequencies -- 1346.5980 1356.2687 1359.6490
Frequencies -- 1360.7753 1361.1909 1362.8273
Frequencies -- 1365.0114 1365.2297 1366.2422
Frequencies -- 1366.6500 1367.5991 1368.3855
Frequencies -- 1369.9431 1375.0514 1383.8912
Frequencies -- 1387.8990 1392.9610 1402.6748
Frequencies -- 1404.5871 1433.8025 1447.2844
Frequencies -- 1458.2810 1459.2091 1466.3337
Frequencies -- 1470.6932 1488.6944 1490.5037
Frequencies -- 1493.1932 1495.3218 1496.1878
Frequencies -- 1498.8622 1499.2449 1502.2061
Frequencies -- 1502.6986 1505.1878 1506.4695
Frequencies -- 1506.7439 1507.6267 1509.5016
Frequencies -- 1515.7002 1517.6458 1518.4873

Frequencies --	1528.9346	1532.3265	1546.2673
Frequencies --	1547.7616	1548.3481	1553.3845
Frequencies --	1555.0480	1559.5209	1561.1979
Frequencies --	1564.1234	1565.0989	1568.3422
Frequencies --	1570.5119	1575.0257	1654.7961
Frequencies --	1661.8383	1667.7931	1668.6154
Frequencies --	1672.1087	1672.5535	1673.8815
Frequencies --	1677.1508	1677.2552	1678.1222
Frequencies --	1683.4447	1687.7644	1689.3553
Frequencies --	1691.6362	1694.7917	1697.6152
Frequencies --	1698.3998	1698.6553	1699.1441
Frequencies --	1699.7919	1701.1245	1702.1540
Frequencies --	1703.2142	1704.2203	1721.2905
Frequencies --	1723.0625	1733.1362	1737.3862
Frequencies --	2728.4014	3070.9951	3085.0614
Frequencies --	3086.5625	3094.1462	3101.4561
Frequencies --	3126.4783	3150.8468	3158.3692
Frequencies --	3170.8090	3174.6135	3185.5325
Frequencies --	3193.7343	3198.7598	3200.1867
Frequencies --	3203.1756	3203.5139	3205.1253
Frequencies --	3206.2391	3207.7171	3209.3001
Frequencies --	3209.6252	3211.8860	3212.5723
Frequencies --	3212.8800	3215.4470	3215.9389
Frequencies --	3216.2783	3217.3163	3219.7170
Frequencies --	3220.3213	3220.4506	3222.2005
Frequencies --	3222.7440	3223.8615	3224.2408
Frequencies --	3224.4595	3228.4246	3230.1258
Frequencies --	3232.1194	3232.2911	3232.9517
Frequencies --	3233.0401	3234.0328	3235.2374
Frequencies --	3235.3511	3236.6170	3236.8278
Frequencies --	3239.5907	3239.9401	3240.7039
Frequencies --	3241.9591	3243.8294	3245.9272
Frequencies --	3247.4657	3248.8134	3250.4116
Frequencies --	3260.8317	3588.0535	3714.1814

SCF Done: E(RM062X/DGDZVP) = -6499.42768961
Sum of electronic and zero-point Energies= -6498.076763
Sum of electronic and thermal Energies= -6497.962686
Sum of electronic and thermal Free Energies= -6498.231810
SCF Done: E(RM062X/DGTZVP/SMD) = -6500.70823578

Cat f I0d_*R*

Center Number	Atomic Number	Atomic Type	X	Y	Z
1	15	0	0.380511	0.396154	-0.477466
2	8	0	0.392812	0.470910	1.129326
3	8	0	1.938575	0.428943	-0.863687
4	8	0	-0.139714	1.737361	-1.039921
5	8	0	-0.334343	-0.848339	-0.871388
6	6	0	0.783993	1.708037	1.649598
7	6	0	2.742353	-0.519435	-0.223267
8	6	0	2.124666	2.039175	1.734846
9	6	0	-0.215024	2.650486	1.895689
10	6	0	3.362434	-0.155682	0.961253
11	6	0	2.854552	-1.813432	-0.745229
12	6	0	3.377673	1.191785	1.647920
13	6	0	2.471561	3.374545	1.936417
14	6	0	0.159532	3.957491	2.211466
15	6	0	-1.628885	2.243620	1.726773
16	6	0	4.110127	-1.103565	1.660553
17	6	0	3.619866	-2.742414	-0.032709
18	6	0	2.148625	-2.131853	-2.009744
19	6	0	3.829842	0.798377	3.082004
20	6	0	4.360385	2.210185	1.021041
21	6	0	3.942882	3.592117	1.598618
22	6	0	1.504000	4.344083	2.213699
23	1	0	-0.609643	4.698670	2.411514
24	6	0	-2.459567	2.915266	0.831187
25	6	0	-2.154996	1.147227	2.412952
26	6	0	4.650000	-0.507257	2.957119
27	6	0	4.263753	-2.403367	1.161933
28	1	0	3.727972	-3.748641	-0.427946
29	6	0	1.227991	-3.175967	-2.111059
30	6	0	2.304133	-1.295278	-3.115644
31	1	0	4.392401	1.600368	3.569206
32	1	0	2.940747	0.610973	3.689526
33	1	0	5.405933	1.962673	1.229158
34	1	0	4.219751	2.216736	-0.064620
35	1	0	4.528053	3.826436	2.495366
36	6	0	4.095153	4.731602	0.608395
37	6	0	1.901363	5.755624	2.454595
38	6	0	-3.771572	2.505423	0.633970
39	8	0	-1.963099	3.986470	0.122863
40	6	0	-3.487830	0.750249	2.252532
41	8	0	-1.304482	0.469258	3.251718
42	1	0	5.713344	-0.271637	2.821504
43	6	0	4.510083	-1.406979	4.169826
44	6	0	5.128445	-3.392917	1.861663
45	6	0	0.400979	-3.305614	-3.232295
46	8	0	1.106618	-4.042900	-1.050267
47	6	0	1.483573	-1.414890	-4.228453
48	8	0	3.265594	-0.309265	-3.086842
49	6	0	3.313027	4.750438	-0.555142
50	6	0	4.940465	5.809474	0.870212
51	6	0	1.471361	6.775104	1.599386
52	6	0	2.759066	6.068726	3.514436
53	6	0	-4.306853	1.427078	1.343498
54	8	0	-4.559209	3.167128	-0.278792
55	6	0	-2.528378	4.115148	-1.133552
56	8	0	-3.994979	-0.296997	2.974143
57	6	0	-1.898650	-0.367890	4.169149
58	6	0	3.240026	-1.774137	4.625391
59	6	0	5.628926	-1.906271	4.839470
60	6	0	4.584939	-4.527254	2.471706
61	6	0	6.508992	-3.177971	1.927080
62	6	0	0.498775	-2.399828	-4.289373
63	8	0	-0.541053	-4.294000	-3.278071
64	6	0	-0.120598	-4.678589	-0.944318
65	8	0	1.603101	-0.519483	-5.265815
66	6	0	2.889607	0.834931	-3.762479
67	6	0	3.366601	5.838218	-1.422846
68	1	0	2.624475	3.929795	-0.762251
69	6	0	5.002117	6.896912	-0.002886
70	1	0	5.536198	5.813819	1.780025
71	6	0	1.911923	8.083874	1.788863
72	1	0	0.817101	6.530183	0.766031
73	6	0	3.189637	7.379111	3.712302
74	1	0	3.081351	5.279136	4.189431
75	6	0	-5.765555	1.109381	1.091460
76	6	0	-3.841234	3.700327	-1.336028
77	6	0	-1.779422	4.630482	-2.179767
78	6	0	-3.235287	-0.726564	4.043854
79	6	0	-1.128020	-0.867603	5.210278
80	6	0	3.088692	-2.635399	5.709856
81	1	0	2.353512	-1.397860	4.117743
82	6	0	5.484929	-2.771976	5.923413
83	1	0	6.624147	-1.636054	4.494702
84	6	0	5.405664	-5.412447	3.169410
85	1	0	3.514594	-4.708136	2.408406

86	6	0	7.332553	-4.071513	2.609318
87	1	0	6.936166	-2.306195	1.436636
88	6	0	-0.409863	-2.393264	-5.498070
89	6	0	-0.965063	-4.753161	-2.046882
90	6	0	-0.483297	-5.271555	0.256103
91	6	0	2.044785	0.728898	-4.864902
92	6	0	3.375461	2.071309	-3.366076
93	6	0	4.210162	6.917348	-1.149003
94	1	0	2.727906	5.857681	-2.301524
95	1	0	5.653638	7.734923	0.225293
96	6	0	2.774349	8.388259	2.842925
97	1	0	1.588890	8.864750	1.107175
98	1	0	3.849424	7.612584	4.542528
99	9	0	-6.528966	2.180813	1.384880
100	9	0	-5.982534	0.821622	-0.203794
101	9	0	-6.228728	0.091967	1.813543
102	6	0	-4.429515	3.796470	-2.587292
103	1	0	-0.748542	4.917213	-1.994671
104	6	0	-2.368155	4.740408	-3.440466
105	6	0	-3.828601	-1.560924	4.981320
106	1	0	-0.084326	-0.574376	5.271280
107	6	0	-1.710999	-1.729641	6.137393
108	6	0	4.213692	-3.142272	6.361412
109	1	0	2.089959	-2.914326	6.037687
110	1	0	6.367890	-3.163059	6.419964
111	6	0	6.780065	-5.184488	3.243577
112	1	0	4.970459	-6.279839	3.656059
113	1	0	8.403728	-3.897634	2.648688
114	9	0	-1.032514	-1.200380	-5.622728
115	9	0	-1.356677	-3.326485	-5.476909
116	9	0	0.301671	-2.573227	-6.626523
117	6	0	-2.219802	-5.333348	-1.942623
118	1	0	0.205121	-5.236548	1.095567
119	6	0	-1.727173	-5.896935	0.354203
120	6	0	1.659218	1.855879	-5.575148
121	1	0	4.038743	2.127330	-2.508495
122	6	0	3.016701	3.206583	-4.094117
123	1	0	4.241326	7.770601	-1.819553
124	1	0	3.117797	9.407878	2.988043
125	1	0	-5.452542	3.454762	-2.713140
126	6	0	-3.685523	4.327680	-3.642630
127	1	0	-1.791141	5.141989	-4.266844
128	1	0	-4.875704	-1.816943	4.855313
129	6	0	-3.060430	-2.069651	6.027591
130	1	0	-1.109559	-2.131220	6.946330
131	1	0	4.101200	-3.819286	7.202640
132	1	0	7.417763	-5.875160	3.786657
133	1	0	-2.864970	-5.336963	-2.814571
134	6	0	-2.603232	-5.905372	-0.730341
135	1	0	-2.013653	-6.363084	1.291599
136	1	0	0.993796	1.736802	-6.424438
137	6	0	2.157458	3.101078	-5.188109
138	1	0	3.420114	4.170255	-3.801405
139	1	0	-4.138291	4.416331	-4.624913
140	1	0	-3.517633	-2.732698	6.754398
141	1	0	-3.584336	-6.358165	-0.636234
142	1	0	1.878796	3.986101	-5.750362
143	1	0	-0.987883	1.691019	-1.689476
144	8	0	-2.063002	1.467833	-2.554598
145	6	0	-1.654082	0.596428	-3.653835
146	6	0	-2.671488	-0.493481	-3.225717
147	1	0	-1.810746	1.089494	-4.614481
148	1	0	-0.607977	0.288528	-3.536429
149	8	0	-2.102330	-1.727059	-2.900384
150	6	0	-2.994031	0.457535	-2.037273
151	1	0	-1.442597	-1.575433	-2.196032
152	1	0	-2.678360	0.090498	-1.057007
153	1	0	-4.010355	0.857736	-1.990572
154	1	0	1.839706	-3.435832	3.297932
155	6	0	0.762549	-3.477916	3.175940
156	6	0	0.157111	-2.675910	2.211434
157	6	0	0.012707	-4.350690	3.974703
158	6	0	-1.221917	-2.796147	2.043026
159	1	0	0.741440	-2.008509	1.582141
160	6	0	-1.369442	-4.451642	3.812624
161	1	0	0.512580	-4.961813	4.720188
162	7	0	-1.997176	-2.161787	1.082343
163	6	0	-1.979613	-3.674248	2.831883
164	1	0	-1.955522	-5.131320	4.423803
165	6	0	-3.304868	-2.535981	0.997487
166	1	0	-1.563731	-1.607916	0.335568
167	16	0	-3.648127	-3.680791	2.298695
168	16	0	-4.412653	-2.027546	-0.111176
169	6	0	-3.820007	-0.701680	-4.180920
170	6	0	-4.228829	-1.985838	-4.536193
171	6	0	-4.489842	0.407584	-4.708196
172	6	0	-5.295517	-2.157061	-5.419478
173	1	0	-3.708285	-2.839367	-4.115541
174	6	0	-5.555245	0.235033	-5.587120
175	1	0	-4.179679	1.414515	-4.426440
176	6	0	-5.959660	-1.051852	-5.947499
177	1	0	-5.607856	-3.159669	-5.695271
178	1	0	-6.070091	1.101329	-5.991782
179	1	0	-6.788601	-1.189469	-6.634940

Frequencies --	11.9102	15.4349	20.7485
Frequencies --	23.3587	25.0632	27.7685
Frequencies --	30.2232	32.7748	34.8830
Frequencies --	36.6369	39.8931	41.4741
Frequencies --	42.3241	43.8269	45.6852
Frequencies --	48.9314	51.7691	55.4877
Frequencies --	58.1617	58.7210	62.2207
Frequencies --	64.6192	65.5908	68.1146
Frequencies --	69.0971	71.6339	73.1325
Frequencies --	74.6223	78.8863	81.3304
Frequencies --	85.9017	88.4777	90.3893
Frequencies --	92.7519	95.0912	95.7542
Frequencies --	100.5960	102.5834	105.5284
Frequencies --	107.5343	114.3219	117.1162
Frequencies --	121.0254	122.9199	124.0839
Frequencies --	125.1230	130.1275	134.4293
Frequencies --	137.5497	142.6331	146.2461
Frequencies --	146.7441	153.8088	160.6709
Frequencies --	167.5208	172.8149	174.3989
Frequencies --	184.0242	187.1821	192.4385
Frequencies --	199.6204	201.9574	211.8364
Frequencies --	218.9613	223.0543	226.4657
Frequencies --	227.7326	231.7741	233.3865
Frequencies --	236.0998	243.0469	245.1429
Frequencies --	251.0681	259.3659	269.6757
Frequencies --	271.7375	276.9692	281.3348
Frequencies --	284.9972	289.1857	291.9073
Frequencies --	293.9602	296.9888	299.4220
Frequencies --	302.6654	303.2964	308.5334
Frequencies --	311.5171	314.6690	316.5796
Frequencies --	317.8122	321.2924	325.2965
Frequencies --	329.3276	334.2452	337.0938
Frequencies --	344.4043	346.0000	357.1704
Frequencies --	371.5842	373.9925	385.3285
Frequencies --	404.2285	405.5978	406.2147
Frequencies --	409.4068	410.8591	412.6406

Frequencies --	413.0773	418.0007	418.7711
Frequencies --	425.5998	429.1438	436.2433
Frequencies --	436.9286	437.2065	439.8282
Frequencies --	445.0715	447.0234	449.4265
Frequencies --	452.9746	458.1605	461.6106
Frequencies --	463.1417	467.2943	474.9066
Frequencies --	486.6456	489.7384	499.3647
Frequencies --	505.2268	506.2083	513.2143
Frequencies --	519.4668	519.9857	521.6472
Frequencies --	530.2682	533.5494	537.9329
Frequencies --	539.7911	541.4924	544.2286
Frequencies --	551.9526	554.1445	556.4888
Frequencies --	557.4314	560.6748	562.2883
Frequencies --	563.6560	567.9521	568.9067
Frequencies --	581.8018	583.2615	589.4521
Frequencies --	593.5800	595.7378	596.8629
Frequencies --	598.0105	601.4783	604.9697
Frequencies --	607.1328	609.6235	610.0681
Frequencies --	611.1173	618.6572	620.9965
Frequencies --	624.7720	626.5897	627.8033
Frequencies --	630.4439	631.0220	632.4048
Frequencies --	633.4991	634.7575	646.4650
Frequencies --	648.3919	655.7512	659.6941
Frequencies --	666.1217	673.2781	675.8146
Frequencies --	682.1149	682.9870	697.2982
Frequencies --	705.5144	705.8590	711.7072
Frequencies --	711.9678	714.1571	716.5603
Frequencies --	717.6500	719.7652	720.3548
Frequencies --	722.8472	725.4626	725.9741
Frequencies --	729.0686	730.0903	732.5509
Frequencies --	735.3851	740.9153	744.0096
Frequencies --	746.1733	749.9233	753.6841
Frequencies --	760.9584	764.9087	767.8699
Frequencies --	769.8586	771.0754	773.0242
Frequencies --	773.2260	776.1889	779.9017
Frequencies --	780.3818	782.2357	785.0398
Frequencies --	793.8312	796.9966	801.5814
Frequencies --	803.0439	805.5881	820.3861
Frequencies --	824.7338	825.2949	827.5378
Frequencies --	830.0429	864.9012	865.1933
Frequencies --	867.1290	867.8757	868.3209
Frequencies --	869.1975	871.1403	872.1560
Frequencies --	872.9772	875.8565	877.0038
Frequencies --	885.8015	887.6236	888.5309
Frequencies --	889.9425	891.1129	909.4508
Frequencies --	918.7935	920.0371	921.6850
Frequencies --	923.3969	925.9621	932.6144
Frequencies --	934.0911	937.0986	940.0074
Frequencies --	941.9675	943.1069	943.5096
Frequencies --	944.1407	947.2963	951.6412
Frequencies --	952.8937	953.6766	954.2536
Frequencies --	964.1531	968.1142	973.5817
Frequencies --	982.5423	986.8071	987.8303
Frequencies --	989.9380	993.5849	994.6571
Frequencies --	997.2153	997.9157	998.9681
Frequencies --	999.4541	1008.3874	1010.2094
Frequencies --	1010.6312	1010.7882	1011.4864
Frequencies --	1011.6466	1014.4451	1018.0455
Frequencies --	1018.6483	1019.1621	1019.7537
Frequencies --	1020.6805	1020.8610	1025.2056
Frequencies --	1030.0968	1035.5916	1036.0728
Frequencies --	1044.0577	1051.8603	1054.6170
Frequencies --	1055.8809	1059.5835	1061.0872
Frequencies --	1062.1281	1062.9876	1068.4841
Frequencies --	1068.8169	1071.0305	1071.6328
Frequencies --	1073.1579	1077.5874	1080.9561
Frequencies --	1090.5877	1094.3447	1100.4299
Frequencies --	1110.7956	1111.7949	1113.1461
Frequencies --	1114.2186	1117.1703	1124.1990
Frequencies --	1126.2912	1127.7592	1129.5968
Frequencies --	1130.6259	1132.7908	1160.7806
Frequencies --	1164.8330	1165.5527	1167.2225
Frequencies --	1168.2800	1170.0783	1171.2107
Frequencies --	1171.4696	1174.0566	1175.0046
Frequencies --	1176.6341	1178.0528	1178.2059
Frequencies --	1179.1822	1182.8044	1196.1177
Frequencies --	1198.9181	1202.0367	1202.9458
Frequencies --	1203.8910	1206.2654	1208.1387
Frequencies --	1210.8662	1212.1016	1213.3669
Frequencies --	1214.0962	1223.4581	1226.1021
Frequencies --	1227.1581	1227.9990	1229.1657
Frequencies --	1232.1791	1234.9978	1238.1151
Frequencies --	1241.9834	1242.7984	1247.7050
Frequencies --	1256.4659	1259.2549	1265.4988
Frequencies --	1268.3549	1277.0426	1283.0144
Frequencies --	1284.1799	1287.1587	1293.5597
Frequencies --	1294.9657	1295.0704	1296.7741
Frequencies --	1298.3637	1300.3017	1301.5481
Frequencies --	1303.0078	1306.4193	1306.9700
Frequencies --	1308.0879	1311.1981	1311.6634
Frequencies --	1318.8755	1323.1946	1324.3888
Frequencies --	1326.0254	1326.6402	1327.7821
Frequencies --	1335.2568	1337.8477	1340.0472
Frequencies --	1340.6971	1345.4585	1350.5466
Frequencies --	1358.8294	1359.0471	1360.2490
Frequencies --	1362.4214	1363.0080	1366.3002
Frequencies --	1367.0510	1368.8673	1370.3276
Frequencies --	1371.2406	1372.8339	1375.8233
Frequencies --	1378.0851	1383.9299	1388.0391
Frequencies --	1392.6010	1407.6261	1449.1464
Frequencies --	1457.3820	1461.4914	1468.4924
Frequencies --	1471.6849	1474.5128	1491.9173
Frequencies --	1493.2199	1497.1047	1498.5710
Frequencies --	1499.9098	1503.1057	1504.2161
Frequencies --	1504.8302	1506.8798	1507.3663
Frequencies --	1510.0167	1511.9961	1515.3635
Frequencies --	1515.6472	1517.6645	1525.0122
Frequencies --	1526.8032	1529.3416	1532.8840
Frequencies --	1546.8639	1549.3573	1554.9874
Frequencies --	1555.2984	1555.9673	1558.1905
Frequencies --	1560.3231	1561.2774	1563.2095
Frequencies --	1565.5286	1571.8813	1660.6540
Frequencies --	1663.5765	1668.2337	1668.6744
Frequencies --	1669.3801	1672.4946	1674.7353
Frequencies --	1677.3604	1677.7010	1679.5012
Frequencies --	1680.1919	1689.2929	1691.1252
Frequencies --	1696.1458	1697.7970	1699.8068
Frequencies --	1700.2802	1701.2298	1701.6104
Frequencies --	1702.6594	1703.1482	1703.6035
Frequencies --	1704.2991	1706.0935	1719.1781
Frequencies --	1719.7074	1731.2491	1733.2763
Frequencies --	2074.7398	3068.4911	3086.1156
Frequencies --	3090.8013	3097.6422	3101.6318
Frequencies --	3124.7764	3156.9002	3163.2700
Frequencies --	3169.1761	3170.1690	3187.5337
Frequencies --	3194.9113	3199.3374	3201.5426
Frequencies --	3201.9421	3205.3628	3205.4191
Frequencies --	3206.6626	3207.3590	3209.5158
Frequencies --	3210.0565	3212.8146	3216.0687
Frequencies --	3216.8626	3218.5095	3218.5169
Frequencies --	3220.7502	3221.2918	3222.4731
Frequencies --	3222.7066	3225.7128	3226.1017

Frequencies -- 3226.7027 3227.2731 3227.4188
Frequencies -- 3228.0106 3228.7419 3229.0763
Frequencies -- 3231.2172 3231.8935 3232.5486
Frequencies -- 3232.5863 3233.1725 3235.5165
Frequencies -- 3236.6065 3236.9852 3237.0255
Frequencies -- 3238.1063 3239.6689 3241.2972
Frequencies -- 3246.8391 3247.3661 3247.6744
Frequencies -- 3248.2595 3248.4988 3252.4109
Frequencies -- 3260.2839 3428.6563 3710.8780

SCF Done: E(RM062X/DGDZVP) = -6499.40019055
Sum of electronic and zero-point Energies= -6498.050144
Sum of electronic and thermal Energies= -6497.936044
Sum of electronic and thermal Free Energies= -6498.206875
SCF Done: E(RM062X/DGTZVP/SMD) = -6500.6845574

Cat f TS1d_*R*

Center Number	Atomic Number	Atomic Type	Coordinates (Angstroms) X	Y	Z
1	15	0	-0.011846	-0.020306	0.006666
2	8	0	0.000717	-0.003940	1.639022
3	8	0	1.570245	0.001360	-0.346108
4	8	0	-0.588988	1.241529	-0.555824
5	8	0	-0.626391	-1.351673	-0.336588
6	6	0	0.371845	1.217558	2.184252
7	6	0	2.374164	-0.949131	0.267455
8	6	0	1.711756	1.552530	2.302844
9	6	0	-0.626091	2.161951	2.431320
10	6	0	2.980775	-0.614508	1.470735
11	6	0	2.526019	-2.228358	-0.286520
12	6	0	2.967496	0.709326	2.204348
13	6	0	2.056397	2.880250	2.550370
14	6	0	-0.256725	3.458449	2.796088
15	6	0	-2.042170	1.800359	2.192538
16	6	0	3.745151	-1.565652	2.145184
17	6	0	3.319120	-3.156519	0.397634
18	6	0	1.792203	-2.571035	-1.527859
19	6	0	3.397463	0.271987	3.632452
20	6	0	3.958829	1.747742	1.625082
21	6	0	3.529757	3.112750	2.232718
22	6	0	1.085965	3.842915	2.842185
23	1	0	-1.029101	4.196779	2.995510
24	6	0	-2.806213	2.540607	1.290681
25	6	0	-2.649192	0.708315	2.815939
26	6	0	4.240842	-1.015345	3.477027
27	6	0	3.943017	-2.842337	1.606988
28	1	0	3.453577	-4.147611	-0.026165
29	6	0	0.937569	-3.675044	-1.589511
30	6	0	1.824586	-1.722065	-2.633486
31	1	0	3.935747	1.065411	4.159654
32	1	0	2.499194	0.047532	4.213742
33	1	0	5.001096	1.495577	1.844542
34	1	0	3.838221	1.782677	0.537476
35	1	0	4.106858	3.330080	3.139049
36	6	0	3.682229	4.275125	1.268965
37	6	0	1.477936	5.248149	3.123673
38	6	0	-4.137009	2.225666	1.048588
39	8	0	-2.230446	3.590183	0.615893
40	6	0	-3.994549	0.391120	2.591150
41	8	0	-1.875401	-0.048510	3.663611
42	1	0	5.305167	-0.763064	3.388619
43	6	0	4.070590	-1.972456	4.640137
44	6	0	4.808182	-3.837574	2.298087
45	6	0	0.052739	-3.854147	-2.655685
46	8	0	0.939610	-4.560571	-0.534218
47	6	0	0.944876	-1.890165	-3.695652
48	8	0	2.723427	-0.680543	-2.663897
49	6	0	2.902175	4.316221	0.104277
50	6	0	4.525273	5.348822	1.553809
51	6	0	1.051464	6.286820	2.289583
52	6	0	2.328013	5.538835	4.195974
53	6	0	-4.754786	1.155006	1.700559
54	8	0	-4.855496	2.970001	0.142781
55	6	0	-2.735758	3.741279	-0.663690
56	8	0	-4.572196	-0.675316	3.229952
57	6	0	-2.562394	-0.846463	4.550658
58	6	0	2.791703	-2.408922	5.003666
59	6	0	5.168778	-2.454223	5.353525
60	6	0	4.257440	-4.970501	2.904914
61	6	0	6.188881	-3.627990	2.371319
62	6	0	0.027539	-2.940062	-3.710339
63	8	0	-0.833351	-4.898430	-2.646925
64	6	0	-0.236310	-5.263672	-0.351273
65	8	0	0.941433	-0.980236	-4.727021
66	6	0	2.220446	0.446000	-3.285040
67	6	0	2.958457	5.419618	-0.742753
68	1	0	2.212956	3.499781	-0.117193
69	6	0	4.587555	6.453417	0.701964
70	1	0	5.118263	5.336713	2.465433
71	6	0	1.488383	7.591586	2.511642
72	1	0	0.403752	6.058896	1.446166
73	6	0	2.755135	6.845122	4.426507
74	1	0	2.647841	4.734388	4.854366
75	6	0	-6.224575	0.939944	1.414517
76	6	0	-4.074998	3.446042	-0.900622
77	6	0	-1.909151	4.156275	-1.695710
78	6	0	-3.905560	-1.142621	4.345576
79	6	0	-1.885123	-1.377642	5.639686
80	6	0	2.615376	-3.313042	6.048415
81	1	0	1.923636	-2.041973	4.457129
82	6	0	4.999216	-3.365660	6.396368
83	1	0	6.169703	-2.130076	5.078977
84	6	0	5.071444	-5.866211	3.596397
85	1	0	3.183989	-5.135814	2.848480
86	6	0	7.006039	-4.529028	3.052512
87	1	0	6.621067	-2.754703	1.888247
88	6	0	-0.938495	-2.999791	-4.871156
89	6	0	-1.146834	-5.386488	-1.395902
90	6	0	-0.483090	-5.876151	0.868188
91	6	0	1.315874	0.294093	-4.333060
92	6	0	2.631305	1.708625	-2.887113
93	6	0	3.799983	6.494444	-0.446261
94	1	0	2.323759	5.456590	-1.623579
95	1	0	5.236467	7.288301	0.948503
96	6	0	2.343930	7.873243	3.577631
97	1	0	1.169235	8.387266	1.845368
98	1	0	3.410033	7.060687	5.265478
99	9	0	-6.930036	2.034460	1.752050
100	9	0	-6.440803	0.732245	0.098529
101	9	0	-6.759060	-0.088897	2.069316
102	6	0	-4.622630	3.592537	-2.164474
103	1	0	-0.857473	4.326907	-1.487075
104	6	0	-2.454683	4.311890	-2.971520
105	6	0	-4.594611	-1.952123	5.236915
106	1	0	-0.834088	-1.136323	5.766345
107	6	0	-2.565963	-2.209938	6.527475
108	6	0	3.721912	-3.799956	6.746818
109	1	0	1.612907	-3.637796	6.317661
110	1	0	5.867764	-3.740659	6.929430

111	6	0	6.447145	-5.645358	3.674989
112	1	0	4.630529	-6.732849	4.079421
113	1	0	8.077548	-4.358911	3.098839
114	9	0	-1.661765	-1.862050	-4.956482
115	9	0	-1.807392	-4.006686	-4.808416
116	9	0	-0.275254	-3.121162	-6.035477
117	6	0	-2.352301	-6.046319	-1.209778
118	1	0	0.257932	-5.794790	1.656025
119	6	0	-1.678640	-6.572054	1.052639
120	6	0	0.800698	1.398940	-4.993807
121	1	0	3.335051	1.800250	-2.065803
122	6	0	2.139510	2.823878	-3.565629
123	1	0	3.832299	7.359985	-1.100824
124	1	0	2.685399	8.889754	3.747560
125	1	0	-5.670573	3.352416	-2.315004
126	6	0	-3.803739	4.040298	-3.202828
127	1	0	-1.818426	4.637663	-3.787588
128	1	0	-5.642984	-2.157479	5.044659
129	6	0	-3.918187	-2.493441	6.330005
130	1	0	-2.036563	-2.635053	7.373832
131	1	0	3.588686	-4.510055	7.557123
132	1	0	7.080345	-6.342610	4.214997
133	1	0	-3.049907	-6.100387	-2.038962
134	6	0	-2.619184	-6.639860	0.024640
135	1	0	-1.871724	-7.050867	2.007267
136	1	0	0.092524	1.244549	-5.801741
137	6	0	1.226161	2.671655	-4.609257
138	1	0	2.480379	3.812041	-3.275841
139	1	0	-4.220885	4.164073	-4.196670
140	1	0	-4.450467	-3.133660	7.025558
141	1	0	-3.558444	-7.161120	0.175770
142	1	0	0.845955	3.542801	-5.132664
143	1	0	-1.837642	1.264549	-1.481347
144	8	0	-2.653864	1.015134	-2.035702
145	6	0	-2.272338	-0.022550	-2.971100
146	6	0	-3.145565	-1.154121	-2.389598
147	1	0	-2.513403	0.291325	-3.986309
148	1	0	-1.202860	-0.240237	-2.881769
149	8	0	-2.444567	-2.326904	-2.105399
150	6	0	-3.550199	-0.318419	-1.138051
151	1	0	-1.642636	-2.076149	-1.598211
152	1	0	-2.925803	-0.293212	-0.249730
153	1	0	-4.495483	0.210822	-1.091312
154	1	0	0.980932	-4.004014	3.934807
155	6	0	-0.075769	-3.984235	3.686718
156	6	0	-0.516831	-3.158554	2.656016
157	6	0	-0.962673	-4.812044	4.389510
158	6	0	-1.872933	-3.208274	2.334329
159	1	0	0.161231	-2.516427	2.097326
160	6	0	-2.319239	-4.842080	4.071266
161	1	0	-0.589826	-5.441139	5.192065
162	7	0	-2.501846	-2.509894	1.307140
163	6	0	-2.763793	-4.038571	3.023423
164	1	0	-3.007520	-5.481332	4.615295
165	6	0	-3.811591	-2.761915	1.126139
166	1	0	-1.922222	-1.977741	0.633118
167	16	0	-4.365530	-3.915306	2.326087
168	16	0	-4.840390	-2.121911	-0.029448
169	6	0	-4.354373	-1.478852	-3.239553
170	6	0	-4.650575	-2.796305	-3.582888
171	6	0	-5.182100	-0.442061	-3.682519
172	6	0	-5.770801	-3.073728	-4.366677
173	1	0	-4.001832	-3.590755	-3.229797
174	6	0	-6.303537	-0.722199	-4.458909
175	1	0	-4.949896	0.591579	-3.422998
176	6	0	-6.599666	-2.041938	-4.803650
177	1	0	-5.997192	-4.101335	-4.634188
178	1	0	-6.944501	0.086853	-4.795386
179	1	0	-7.472530	-2.263531	-5.409953

Frequencies --	-552.7541	12.4527	20.8232
Frequencies --	23.7898	27.1042	27.7565
Frequencies --	29.0629	31.3692	32.6736
Frequencies --	35.3367	38.0973	39.2407
Frequencies --	40.4993	41.3025	46.3748
Frequencies --	49.1444	53.3944	54.0185
Frequencies --	56.3718	57.3914	59.8365
Frequencies --	61.1203	63.5454	66.8795
Frequencies --	68.6020	73.2119	73.4533
Frequencies --	76.1126	77.7387	80.1871
Frequencies --	84.8460	86.8601	89.5372
Frequencies --	90.7442	95.2133	97.4311
Frequencies --	99.5382	101.3712	105.7059
Frequencies --	112.2881	114.3535	115.5224
Frequencies --	117.9096	120.0963	125.7284
Frequencies --	127.8410	129.4743	134.9356
Frequencies --	135.6885	143.9663	148.7049
Frequencies --	153.7822	156.4510	163.4244
Frequencies --	167.1755	172.3393	174.9815
Frequencies --	187.4484	190.4327	194.1920
Frequencies --	198.6641	202.9501	209.5304
Frequencies --	218.0597	219.1890	221.5578
Frequencies --	224.0243	230.7450	233.8772
Frequencies --	237.0964	244.2379	247.7907
Frequencies --	252.4343	262.6099	269.4463
Frequencies --	272.5573	277.2497	278.5555
Frequencies --	283.3400	284.9554	288.7623
Frequencies --	292.2701	295.5984	298.5916
Frequencies --	300.5277	302.8837	304.2531
Frequencies --	306.7618	312.9422	315.8557
Frequencies --	316.4561	319.5838	321.5177
Frequencies --	324.4290	329.9961	336.7100
Frequencies --	339.2488	345.4777	353.2025
Frequencies --	364.5557	377.9343	386.8573
Frequencies --	398.3449	406.0942	406.7691
Frequencies --	411.5799	412.6880	414.6242
Frequencies --	416.6148	419.0657	421.0897
Frequencies --	422.3198	423.8044	429.1359
Frequencies --	430.4711	436.3501	442.1372
Frequencies --	445.4013	446.6342	452.0536
Frequencies --	454.3121	460.8834	461.2751
Frequencies --	462.9862	463.8507	466.6894
Frequencies --	474.9541	486.5073	491.4859
Frequencies --	501.3735	506.4999	508.7153
Frequencies --	513.9643	519.6707	521.3587
Frequencies --	526.0155	530.4357	536.1259
Frequencies --	538.5323	540.3806	541.3060
Frequencies --	545.2367	553.0228	556.1832
Frequencies --	559.4719	561.2971	562.3204
Frequencies --	563.2819	569.0796	571.2145
Frequencies --	578.4027	584.8029	587.6264
Frequencies --	590.3505	594.0802	596.0194
Frequencies --	597.2736	598.1640	601.0530
Frequencies --	604.4628	608.6163	610.3434
Frequencies --	610.8736	616.8075	618.9920
Frequencies --	621.1796	624.8033	626.7164
Frequencies --	630.3997	630.9860	632.6814
Frequencies --	635.1647	635.6787	645.7446
Frequencies --	648.8150	655.7594	665.9646
Frequencies --	666.5232	671.8712	677.3237
Frequencies --	681.7032	683.4081	684.9672

Frequencies -- 696.5411 703.9562 709.3956
Frequencies -- 713.4996 716.1188 719.1995
Frequencies -- 719.8033 720.1593 722.2923
Frequencies -- 723.8206 724.6613 726.5706
Frequencies -- 727.6856 729.4609 731.2745
Frequencies -- 732.5676 738.0177 740.1883
Frequencies -- 745.4872 747.2176 750.9953
Frequencies -- 752.1131 762.0874 764.0903
Frequencies -- 764.1726 769.4941 771.9782
Frequencies -- 772.5770 773.8477 778.5429
Frequencies -- 781.2766 781.5697 782.4285
Frequencies -- 788.2319 795.8983 798.3878
Frequencies -- 801.6277 803.5922 806.3243
Frequencies -- 822.9616 824.9833 826.3525
Frequencies -- 831.5468 859.7779 862.0607
Frequencies -- 863.4151 866.8594 867.4694
Frequencies -- 868.6484 868.9061 869.0300
Frequencies -- 874.0814 875.1169 876.0660
Frequencies -- 880.0921 883.3348 886.8821
Frequencies -- 887.5360 888.8568 890.5430
Frequencies -- 897.8386 912.5686 915.7165
Frequencies -- 916.6477 920.4459 923.1043
Frequencies -- 930.7767 932.7322 937.6827
Frequencies -- 941.4938 943.4598 944.0037
Frequencies -- 944.6593 947.5728 949.5946
Frequencies -- 951.2613 951.5449 952.9327
Frequencies -- 957.5075 959.3462 966.7271
Frequencies -- 968.9655 984.3275 988.0680
Frequencies -- 988.6723 992.1135 995.0516
Frequencies -- 996.5005 997.6095 1001.2278
Frequencies -- 1004.5897 1005.4413 1005.9168
Frequencies -- 1007.4534 1008.4151 1009.8545
Frequencies -- 1011.0832 1011.3082 1018.5256
Frequencies -- 1018.8390 1019.5244 1019.8215
Frequencies -- 1020.1602 1020.8582 1021.3161
Frequencies -- 1028.9416 1034.7917 1035.9004
Frequencies -- 1043.5748 1047.0831 1053.0941
Frequencies -- 1056.9672 1057.8317 1058.8886
Frequencies -- 1059.5782 1060.7658 1062.0718
Frequencies -- 1063.5260 1068.3524 1068.8152
Frequencies -- 1071.9820 1073.3797 1079.3797
Frequencies -- 1094.5260 1098.2800 1100.1207
Frequencies -- 1109.6713 1110.4173 1111.6474
Frequencies -- 1113.0374 1115.2708 1118.5375
Frequencies -- 1123.6462 1125.2770 1126.9466
Frequencies -- 1127.9236 1128.8267 1130.1631
Frequencies -- 1132.1420 1158.5447 1162.3926
Frequencies -- 1165.0185 1165.6808 1166.5682
Frequencies -- 1166.7477 1172.3126 1173.2423
Frequencies -- 1175.3248 1176.9618 1178.0515
Frequencies -- 1178.7496 1178.9547 1183.2123
Frequencies -- 1192.2803 1196.5870 1200.8777
Frequencies -- 1201.4139 1201.9709 1202.9171
Frequencies -- 1205.2870 1207.7316 1210.6585
Frequencies -- 1213.6822 1213.8502 1214.7732
Frequencies -- 1222.6709 1225.5818 1226.6505
Frequencies -- 1227.0370 1231.7282 1233.9813
Frequencies -- 1237.2860 1241.5345 1246.8189
Frequencies -- 1249.2234 1255.3013 1261.7293
Frequencies -- 1268.1664 1271.4173 1281.1063
Frequencies -- 1283.0376 1286.4106 1286.7627
Frequencies -- 1293.2139 1294.0641 1296.3362
Frequencies -- 1299.4137 1299.7570 1301.5822
Frequencies -- 1305.4886 1307.5194 1308.9858
Frequencies -- 1309.9115 1310.9100 1311.9149
Frequencies -- 1313.0612 1320.7134 1324.7988
Frequencies -- 1326.3296 1327.8959 1335.5341
Frequencies -- 1338.2322 1341.6296 1342.5034
Frequencies -- 1342.6976 1345.0558 1358.2718
Frequencies -- 1359.5705 1359.8809 1360.2786
Frequencies -- 1361.8829 1364.8928 1365.1605
Frequencies -- 1366.1860 1367.5265 1370.0747
Frequencies -- 1371.0898 1371.5142 1375.4569
Frequencies -- 1382.7391 1384.1253 1390.8220
Frequencies -- 1406.1717 1435.4121 1445.6524
Frequencies -- 1450.2888 1459.6189 1468.0515
Frequencies -- 1471.4778 1472.7426 1478.8963
Frequencies -- 1491.6462 1493.5987 1497.8548
Frequencies -- 1498.4375 1502.4421 1503.8265
Frequencies -- 1504.8263 1506.2272 1508.2530
Frequencies -- 1509.8275 1510.0509 1512.5325
Frequencies -- 1515.3756 1518.0802 1525.7150
Frequencies -- 1526.8238 1531.0718 1545.5210
Frequencies -- 1548.1902 1549.8750 1554.3660
Frequencies -- 1555.0021 1556.0934 1558.1177
Frequencies -- 1559.3139 1562.0185 1563.1685
Frequencies -- 1566.2275 1571.5850 1660.3157
Frequencies -- 1663.2093 1668.6320 1669.1558
Frequencies -- 1670.9387 1672.6173 1674.5098
Frequencies -- 1677.2089 1677.3622 1678.6621
Frequencies -- 1681.9180 1687.7121 1689.9528
Frequencies -- 1694.1741 1696.0850 1698.1248
Frequencies -- 1698.8829 1699.7415 1700.3217
Frequencies -- 1700.4230 1701.9674 1702.4637
Frequencies -- 1703.5276 1705.9765 1718.5086
Frequencies -- 1720.8440 1728.9086 1731.7200
Frequencies -- 2866.8281 3071.5135 3083.6356
Frequencies -- 3091.4855 3099.5697 3122.7769
Frequencies -- 3157.1785 3160.9293 3168.5127
Frequencies -- 3184.6081 3185.3383 3200.1067
Frequencies -- 3200.9211 3201.8194 3201.9330
Frequencies -- 3205.2445 3207.5006 3207.8739
Frequencies -- 3208.4693 3211.0078 3213.6974
Frequencies -- 3215.0725 3217.0667 3218.4089
Frequencies -- 3219.6169 3220.0945 3220.5201
Frequencies -- 3220.5565 3221.2469 3222.4078
Frequencies -- 3225.2317 3226.7175 3226.9187
Frequencies -- 3227.2562 3228.4782 3229.9372
Frequencies -- 3230.4343 3231.1909 3231.8789
Frequencies -- 3232.2885 3233.1166 3234.6785
Frequencies -- 3235.7151 3236.6814 3238.5364
Frequencies -- 3238.6095 3239.1678 3239.5018
Frequencies -- 3241.4230 3241.6127 3242.4421
Frequencies -- 3244.9142 3245.9961 3246.7960
Frequencies -- 3246.9771 3249.6374 3253.5768
Frequencies -- 3256.1366 3338.6295 3601.0779

SCF Done: E(RM062X/DGDZVP) = -6499.37689259
Sum of electronic and zero-point Energies= -6498.026708
Sum of electronic and thermal Energies= -6497.913330
Sum of electronic and thermal Free Energies= -6498.181075
SCF Done: E(RM062X/DGTZVP/SMD) = -6500.65858215

Cat f I1d_*R*

Center Number	Atomic Number	Atomic Type	Coordinates (Angstroms) X	Y	Z
1	15	0	0.398421	0.435629	-0.462442
2	8	0	0.455291	0.463923	1.176477
3	8	0	1.971977	0.487221	-0.855668

4	8	0	-0.262634	1.640059	-1.023232
5	8	0	-0.141105	-0.954415	-0.743349
6	6	0	0.824087	1.693072	1.702121
7	6	0	2.809199	-0.452230	-0.273332
8	6	0	2.165660	2.030608	1.805135
9	6	0	-0.170041	2.640956	1.952453
10	6	0	3.433876	-0.124414	0.924232
11	6	0	2.978965	-1.720606	-0.847841
12	6	0	3.418782	1.187111	1.682137
13	6	0	2.514387	3.355766	2.059786
14	6	0	0.204643	3.935188	2.321716
15	6	0	-1.588172	2.302372	1.690018
16	6	0	4.229522	-1.070607	1.569683
17	6	0	3.812042	-2.638068	-0.196876
18	6	0	2.224015	-2.089391	-2.069185
19	6	0	3.860806	0.725627	3.097983
20	6	0	4.409340	2.232179	1.112525
21	6	0	3.986601	3.589710	1.739932
22	6	0	1.547359	4.317248	2.366523
23	1	0	-0.565616	4.675444	2.522484
24	6	0	-2.309743	3.052343	0.761891
25	6	0	-2.233000	1.225016	2.298805
26	6	0	4.732462	-0.536373	2.904845
27	6	0	4.450216	-2.331500	1.005947
28	1	0	3.961604	-3.618589	-0.639660
29	6	0	1.422947	-3.235218	-2.104629
30	6	0	2.189660	-1.253501	-3.183797
31	1	0	4.381656	1.517579	3.644593
32	1	0	2.968104	0.465212	3.673382
33	1	0	5.452218	1.975346	1.323723
34	1	0	4.285290	2.281359	0.025831
35	1	0	4.566685	3.792322	2.647896
36	6	0	4.143390	4.762775	0.790299
37	6	0	1.942227	5.720438	2.654702
38	6	0	-3.639568	2.763070	0.480087
39	8	0	-1.689065	4.083971	0.108231
40	6	0	-3.575362	0.934455	2.035238
41	8	0	-1.496477	0.448593	3.166409
42	1	0	5.788690	-0.255532	2.805829
43	6	0	4.606039	-1.522222	4.049356
44	6	0	5.344646	-3.321082	1.667610
45	6	0	0.542861	-3.481816	-3.158251
46	8	0	1.474168	-4.104968	-1.033446
47	6	0	1.315115	-1.493515	-4.239670
48	8	0	3.020038	-0.158535	-3.241158
49	6	0	3.367832	4.815166	-0.376439
50	6	0	4.991571	5.829901	1.084120
51	6	0	1.518284	6.762936	1.823989
52	6	0	2.793192	6.005363	3.727723
53	6	0	-4.297147	1.711700	1.124264
54	8	0	-4.322088	3.511414	-0.444855
55	6	0	-2.171745	4.288300	-1.172591
56	8	0	-4.187457	-0.134224	2.647524
57	6	0	-2.223247	-0.336129	4.030517
58	6	0	3.345869	-2.002152	4.425296
59	6	0	5.729103	-1.987469	4.734282
60	6	0	4.819185	-4.460700	2.284326
61	6	0	6.724925	-3.100488	1.706170
62	6	0	0.469061	-2.600898	-4.238587
63	8	0	-0.297716	-4.565771	-3.107369
64	6	0	0.314911	-4.816569	-0.805241
65	8	0	1.249148	-0.597331	-5.278030
66	6	0	2.422569	0.929610	-3.852675
67	6	0	3.438379	5.918584	-1.221798
68	1	0	2.673305	4.004452	-0.601118
69	6	0	5.064104	6.937695	0.237066

70	1	0	5.581447	5.809709	1.997656
71	6	0	1.958906	8.065743	2.049923
72	1	0	0.869677	6.539343	0.980064
73	6	0	3.223705	7.309880	3.962438
74	1	0	3.111848	5.197809	4.382895
75	6	0	-5.763544	1.529040	0.804652
76	6	0	-3.508820	4.020804	-1.449494
77	6	0	-1.327309	4.766154	-2.161917
78	6	0	-3.565098	-0.611114	3.784249
79	6	0	-1.590663	-0.880046	5.140355
80	6	0	3.213676	-2.928440	5.457047
81	1	0	2.460368	-1.646304	3.899660
82	6	0	5.603736	-2.923651	5.761454
83	1	0	6.715662	-1.631396	4.447549
84	6	0	5.657867	-5.354833	2.947429
85	1	0	3.745282	-4.630573	2.259359
86	6	0	7.566825	-3.999152	2.360577
87	1	0	7.137290	-2.220844	1.217394
88	6	0	-0.455944	-2.781338	-5.421319
89	6	0	-0.601373	-4.999975	-1.836637
90	6	0	0.092032	-5.384019	0.440334
91	6	0	1.518736	0.705827	-4.887838
92	6	0	2.731645	2.219496	-3.451502
93	6	0	4.285324	6.986667	-0.916802
94	1	0	2.815826	5.959673	-2.110792
95	1	0	5.716738	7.767776	0.489991
96	6	0	2.815331	8.341711	3.116753
97	1	0	1.642214	8.864238	1.385866
98	1	0	3.879720	7.521003	4.801690
99	9	0	-6.457209	2.634403	1.122052
100	9	0	-5.956562	1.313752	-0.513473
101	9	0	-6.333686	0.509407	1.452104
102	6	0	-4.032881	4.252746	-2.709910
103	1	0	-0.279599	4.921989	-1.923879
104	6	0	-1.851769	5.015896	-3.430704
105	6	0	-4.294619	-1.411022	4.651770
106	1	0	-0.540771	-0.654592	5.301559
107	6	0	-2.312639	-1.701947	6.005562
108	6	0	4.345438	-3.398474	6.126293
109	1	0	2.226958	-3.282269	5.746411
110	1	0	6.491757	-3.285278	6.271064
111	6	0	7.033690	-5.124177	2.989713
112	1	0	5.236675	-6.227577	3.437132
113	1	0	8.637790	-3.820666	2.379694
114	9	0	-1.238003	-1.705699	-5.608103
115	9	0	-1.265350	-3.837272	-5.317155
116	9	0	0.259822	-2.943793	-6.551296
117	6	0	-1.795409	-5.668508	-1.610025
118	1	0	0.844990	-5.264223	1.211611
119	6	0	-1.088173	-6.094373	0.664912
120	6	0	0.892814	1.763947	-5.527677
121	1	0	3.438283	2.364829	-2.640520
122	6	0	2.129005	3.290986	-4.112007
123	1	0	4.329616	7.852475	-1.570274
124	1	0	3.160004	9.356677	3.289472
125	1	0	-5.077968	4.026043	-2.895155
126	6	0	-3.196317	4.765988	-3.701675
127	1	0	-1.200892	5.394313	-4.211522
128	1	0	-5.341654	-1.594067	4.430868
129	6	0	-3.661991	-1.964519	5.765438
130	1	0	-1.817828	-2.133315	6.869422
131	1	0	4.245109	-4.125339	6.926395
132	1	0	7.686793	-5.820350	3.506989
133	1	0	-2.499195	-5.769848	-2.429587
134	6	0	-2.039146	-6.215839	-0.349000
135	1	0	-1.259189	-6.548345	1.635625

136	1	0	0.175163	1.555145	-6.314422
137	6	0	1.211235	3.065445	-5.138055
138	1	0	2.379930	4.305182	-3.819553
139	1	0	-3.595069	4.948702	-4.693624
140	1	0	-4.227122	-2.594100	6.444578
141	1	0	-2.964443	-6.753196	-0.169216
142	1	0	0.736112	3.901446	-5.640101
143	1	0	-1.492457	1.954140	-2.404761
144	8	0	-2.098658	1.668159	-3.116933
145	6	0	-1.734287	0.343267	-3.437461
146	6	0	-2.676593	-0.726918	-2.802149
147	1	0	-1.760781	0.226985	-4.522453
148	1	0	-0.710651	0.136352	-3.099117
149	8	0	-1.964278	-1.932610	-2.588410
150	6	0	-3.218289	-0.177705	-1.464571
151	1	0	-1.139362	-1.692375	-2.119064
152	1	0	-2.425192	0.145770	-0.782920
153	1	0	-3.866028	0.684645	-1.637968
154	1	0	1.260170	-3.536104	3.580176
155	6	0	0.224617	-3.492641	3.257158
156	6	0	-0.122588	-2.656306	2.202420
157	6	0	-0.729439	-4.301263	3.895264
158	6	0	-1.456629	-2.674175	1.794105
159	1	0	0.600911	-2.022164	1.694130
160	6	0	-2.061065	-4.302045	3.490733
161	1	0	-0.426698	-4.935946	4.722282
162	7	0	-1.998442	-1.941414	0.737985
163	6	0	-2.410486	-3.481896	2.418761
164	1	0	-2.799121	-4.922921	3.987986
165	6	0	-3.286271	-2.142934	0.523217
166	1	0	-1.316545	-1.419849	0.085737
167	16	0	-3.964663	-3.294092	1.637041
168	16	0	-4.308272	-1.386484	-0.627658
169	6	0	-3.848263	-1.025329	-3.720838
170	6	0	-4.122787	-2.326338	-4.142057
171	6	0	-4.664457	0.027968	-4.151727
172	6	0	-5.209782	-2.573577	-4.981917
173	1	0	-3.475401	-3.134540	-3.817396
174	6	0	-5.750571	-0.223338	-4.986677
175	1	0	-4.432785	1.048530	-3.849233
176	6	0	-6.028527	-1.526869	-5.401936
177	1	0	-5.413735	-3.588103	-5.311296
178	1	0	-6.377805	0.599119	-5.317258
179	1	0	-6.873980	-1.722930	-6.054429

Frequencies --	8.3351	17.6539	19.6299
Frequencies --	22.4037	23.7277	26.4324
Frequencies --	26.8980	30.5191	32.0641
Frequencies --	34.6127	36.9726	40.2626
Frequencies --	40.9799	43.2646	48.1517
Frequencies --	52.1221	52.8996	54.5355
Frequencies --	55.3199	58.8957	59.5577
Frequencies --	60.3124	64.5774	66.4507
Frequencies --	70.0698	71.7166	73.5414
Frequencies --	74.7413	77.0846	82.7797
Frequencies --	85.5396	87.4616	89.3765
Frequencies --	92.5220	94.9208	98.7999
Frequencies --	100.0367	103.2383	109.2509
Frequencies --	112.1496	113.9955	117.4310
Frequencies --	121.4827	126.1624	128.9620
Frequencies --	132.7400	134.3416	138.6043
Frequencies --	142.7708	146.1173	152.7247
Frequencies --	157.3947	163.3538	167.4488
Frequencies --	171.7562	181.5937	185.9193
Frequencies --	187.9648	190.9503	197.3918
Frequencies --	199.1105	207.2593	211.7314
Frequencies --	216.8492	219.0558	224.1393
Frequencies --	230.0577	233.6162	236.2804
Frequencies --	244.1374	247.4928	254.2494
Frequencies --	256.6996	265.1935	270.2410
Frequencies --	275.0777	276.4343	282.0002
Frequencies --	285.8577	287.3790	288.3815
Frequencies --	292.5772	296.8251	297.8201
Frequencies --	299.1056	302.8000	306.0328
Frequencies --	309.1162	311.6533	314.5982
Frequencies --	319.6611	320.1852	322.7764
Frequencies --	329.8448	335.8785	337.0097
Frequencies --	338.0826	347.0648	355.4660
Frequencies --	376.9086	381.4271	391.5916
Frequencies --	405.1261	407.7200	409.7618
Frequencies --	412.0914	412.8704	414.8056
Frequencies --	417.6436	418.7948	419.7210
Frequencies --	421.1206	422.9367	425.1886
Frequencies --	428.7947	436.9811	440.8121
Frequencies --	443.4430	446.8036	452.8169
Frequencies --	458.7217	460.5763	462.2532
Frequencies --	464.7623	468.3356	473.5090
Frequencies --	487.6831	492.6575	501.5958
Frequencies --	507.0986	509.7123	515.7371
Frequencies --	521.9541	523.1536	528.0600
Frequencies --	530.4683	531.7419	534.4927
Frequencies --	538.0529	540.4745	545.9161
Frequencies --	552.3168	556.1822	558.4369
Frequencies --	560.8616	561.7301	563.7376
Frequencies --	567.4533	572.0760	580.0431
Frequencies --	585.3755	588.5318	591.2692
Frequencies --	595.3593	596.9659	597.4746
Frequencies --	598.5540	598.9516	601.6282
Frequencies --	607.2558	607.4744	609.9628
Frequencies --	611.8064	612.5080	614.3660
Frequencies --	618.5998	621.3454	624.7966
Frequencies --	626.3855	629.8864	631.0960
Frequencies --	632.5184	634.7814	635.6451
Frequencies --	645.1969	648.8903	656.2816
Frequencies --	664.9115	672.2804	677.2736
Frequencies --	681.4923	685.4169	685.7365
Frequencies --	696.9750	703.0297	710.0910
Frequencies --	713.3949	715.7985	717.4299
Frequencies --	718.1943	719.9215	720.5333
Frequencies --	720.8074	724.4780	725.8010
Frequencies --	727.9511	729.0168	731.3066
Frequencies --	731.8030	733.1713	737.3529
Frequencies --	740.8951	746.1605	749.1913
Frequencies --	751.8032	760.7034	763.1175
Frequencies --	764.7376	768.4338	769.0539
Frequencies --	771.4480	772.4400	773.2522
Frequencies --	778.1928	779.9354	784.1638
Frequencies --	788.5844	797.2645	798.0201
Frequencies --	799.1788	801.2515	805.5598
Frequencies --	806.2566	823.2106	825.4236
Frequencies --	826.8569	831.6818	853.9857
Frequencies --	857.3723	863.0403	864.4806
Frequencies --	864.8697	866.3216	868.1702
Frequencies --	870.2845	871.8924	873.9528
Frequencies --	875.8386	880.8249	883.8649
Frequencies --	887.4147	888.7837	889.5302
Frequencies --	891.0452	892.2175	911.9719
Frequencies --	912.8292	919.7630	924.7406
Frequencies --	930.7244	931.6276	934.1243
Frequencies --	936.7165	941.7587	942.4656
Frequencies --	943.2984	944.8755	945.6611

Frequencies --	947.2339	954.0790	955.6189
Frequencies --	957.7743	958.4169	968.6560
Frequencies --	969.7355	984.7736	989.2410
Frequencies --	989.6235	992.4402	992.7215
Frequencies --	994.1857	997.3516	1000.6231
Frequencies --	1006.1278	1007.7749	1008.2504
Frequencies --	1008.5953	1011.1672	1011.8462
Frequencies --	1014.3794	1017.5828	1017.9971
Frequencies --	1018.4891	1019.2292	1019.4562
Frequencies --	1019.6371	1020.3208	1022.6413
Frequencies --	1029.4505	1033.9633	1036.8377
Frequencies --	1042.3246	1043.2749	1053.1678
Frequencies --	1053.5809	1058.7458	1059.1609
Frequencies --	1060.9068	1064.4612	1065.6798
Frequencies --	1068.1097	1069.7780	1070.5532
Frequencies --	1071.7212	1072.9499	1093.4922
Frequencies --	1094.9049	1098.8837	1108.8941
Frequencies --	1109.3504	1111.4070	1113.0136
Frequencies --	1114.4909	1118.9038	1123.3704
Frequencies --	1124.6647	1127.0821	1127.8416
Frequencies --	1129.9666	1132.6107	1137.1829
Frequencies --	1157.5832	1161.5399	1164.7838
Frequencies --	1165.2952	1165.8148	1167.1259
Frequencies --	1170.1646	1170.5050	1174.4276
Frequencies --	1175.8907	1177.0129	1177.2829
Frequencies --	1177.9793	1182.9895	1185.7393
Frequencies --	1196.3476	1200.0814	1200.8372
Frequencies --	1201.6795	1204.8877	1207.0338
Frequencies --	1207.3277	1211.6184	1212.3671
Frequencies --	1215.0899	1219.1557	1221.7896
Frequencies --	1223.1749	1225.6017	1226.8703
Frequencies --	1234.6199	1239.4366	1242.9391
Frequencies --	1247.5324	1250.3136	1253.2557
Frequencies --	1254.4173	1261.0055	1270.1543
Frequencies --	1274.2974	1277.1730	1282.9908
Frequencies --	1285.0627	1286.7503	1290.7369
Frequencies --	1291.0590	1298.3583	1298.6649
Frequencies --	1300.3342	1303.0733	1303.5816
Frequencies --	1304.3098	1308.2134	1309.3726
Frequencies --	1311.2078	1313.5073	1313.6965
Frequencies --	1314.8896	1321.5546	1325.9551
Frequencies --	1326.3881	1328.2750	1335.3349
Frequencies --	1338.2065	1341.3402	1342.0569
Frequencies --	1344.3504	1358.2344	1358.3370
Frequencies --	1359.4744	1360.0870	1362.8194
Frequencies --	1363.8236	1364.4491	1364.6097
Frequencies --	1365.6523	1368.6226	1369.0801
Frequencies --	1371.0095	1374.6801	1382.1273
Frequencies --	1389.4250	1404.9680	1406.9488
Frequencies --	1413.3347	1439.2692	1449.1266
Frequencies --	1458.9795	1467.3375	1470.4771
Frequencies --	1471.3335	1476.7087	1491.3444
Frequencies --	1493.7155	1495.1812	1497.4943
Frequencies --	1497.9815	1498.7083	1504.2075
Frequencies --	1504.9543	1506.6806	1508.4559
Frequencies --	1508.7199	1510.6784	1513.1543
Frequencies --	1515.8812	1519.3503	1520.7268
Frequencies --	1528.2543	1531.9673	1545.6807
Frequencies --	1547.4812	1550.0407	1554.9435
Frequencies --	1555.7399	1559.2294	1559.6713
Frequencies --	1562.6535	1564.1562	1568.4251
Frequencies --	1572.1152	1576.4927	1660.0961
Frequencies --	1664.1617	1668.7527	1669.6374
Frequencies --	1672.2223	1674.5947	1674.7890
Frequencies --	1676.1187	1677.0422	1677.5652
Frequencies --	1681.5639	1688.2583	1689.6352
Frequencies --	1693.4878	1695.4368	1697.5569
Frequencies --	1698.2926	1698.6092	1699.5027
Frequencies --	1700.2631	1701.8767	1702.1780
Frequencies --	1703.6454	1705.6127	1719.7108
Frequencies --	1720.0878	1729.4579	1732.7466
Frequencies --	2432.4827	3070.9289	3082.0548
Frequencies --	3091.0329	3091.1541	3098.3028
Frequencies --	3124.9366	3156.3999	3159.5663
Frequencies --	3172.9519	3179.3179	3181.8973
Frequencies --	3192.0812	3197.3789	3199.5689
Frequencies --	3200.7266	3201.1288	3201.8151
Frequencies --	3204.3229	3207.1216	3207.7832
Frequencies --	3212.3704	3214.4196	3217.0565
Frequencies --	3218.3856	3220.4757	3221.2281
Frequencies --	3221.9008	3222.5271	3222.8662
Frequencies --	3223.0289	3224.0801	3225.6909
Frequencies --	3225.7136	3226.7835	3228.3065
Frequencies --	3229.5151	3233.0509	3234.5906
Frequencies --	3234.9438	3235.6263	3236.3056
Frequencies --	3236.4445	3236.6922	3237.8564
Frequencies --	3239.2786	3239.9249	3241.6503
Frequencies --	3242.3829	3242.3981	3243.4835
Frequencies --	3244.1749	3245.5774	3247.9230
Frequencies --	3248.3856	3252.2627	3253.8564
Frequencies --	3262.2893	3648.2542	3659.4336

SCF Done: E(RM062X/DGDZVP) = -6499.42926344
Sum of electronic and zero-point Energies= -6498.078417
Sum of electronic and thermal Energies= -6497.964364
Sum of electronic and thermal Free Energies= -6498.235515
SCF Done: E(RM062X/DGTZVP/SMD) = -6500.71185914873

RRHO- and BSSE-corrected absolute and relative energies

Table S3. RRHO- and BSSE-corrected thermodynamics for tautomerization N•••H•••S at M06-2X-D3/DGTZVP/SMD//M06-2X-D3/DGDZVP: absolute H, TS and G are presented in Hartrees and relative ΔH, -TΔS and ΔG are presented in kcal·mol^{-1}.

Structures	H	T·qh-S	qh-G(T)	ΔH	-TΔS	ΔG
2*Benzo[d]thiazole–2–thiol	-2241.40287	0.09196	-2241.49483	**0.0**	**0.0**	**0.0**
I0Ha	-2241.41350	0.07346	-2241.48695	**-6.7**	**11.6**	**4.9**
TS1Ha	-2241.41494	0.07033	-2241.48527	**-7.6**	**13.6**	**6.0**
I1Ha	-2241.44392	0.07169	-2241.51561	**-25.8**	**12.7**	**-13.0**
2*Benzo[d]thiazole–2(3H)–thione	-2241.43109	0.09052	-2241.52161	**-17.7**	**0.9**	**-16.8**
Benzo[d]thiazole–2–thiol	-1120.70144	0.04598	-1120.74742	**0.0**	**0.0**	**0.0**
TS1Hb	-1120.65510	0.04479	-1120.69989	**29.1**	**0.7**	**29.8**
Benzo[d]thiazole–2(3H)–thione	-1120.71555	0.04526	-1120.76080	**-8.9**	**0.5**	**-8.4**

Table S4. RRHO- and BSSE-corrected thermodynamics for reaction of **22a** and **23a** catalyzed by **Cat b** at M06-2X-D3/DGTZVP/SMD//M06-2X-D3/DGDZVP: absolute H, TS and G are presented in Hartrees and relative ΔH, -TΔS and ΔG are presented in kcal·mol^{-1}.

Structures	H	T·qh-S	qh-G(T)	ΔH	-TΔS	ΔG
Benzo[*d*]thiazole-2(3*H*)-thione	-1120.71555	0.04526	-1120.76080	**Reactants**		
3-Phenyloxetan-3-ol	-499.14799	0.04801	-499.19600			
Catalyst b	-2222.57703	0.11320	-2222.69023	**0.0**	**0.0**	**0.0**
I0_1	-2721.75349	0.13899	-2721.89248	**-17.9**	**13.9**	**-3.9**
TS1a_*R*	-3842.45492	0.15747	-3842.61239	**-9.0**	**30.7**	**21.7**
(*R*)-Product	-1619.90535	0.07278	-1619.97813	**-26.2**	**12.9**	**-13.4**
TS1b_*S*	-3842.45407	0.15729	-3842.61136	**-8.5**	**30.9**	**22.4**
(*S*)-Product	-1619.90535	0.07278	-1619.97813	**-26.2**	**12.9**	**-13.4**
I0_2	-2721.75265	0.13732	-2721.88997	**-17.3**	**15.0**	**-2.3**
TS1c_*S*	-3842.45271	0.15626	-3842.60897	**-7.6**	**31.5**	**23.9**
(*S*)-Product	-1619.90535	0.07278	-1619.97813	**-26.2**	**12.9**	**-13.4**
TS1d_*R*	-3842.45479	0.15787	-3842.61266	**-8.9**	**30.5**	**21.6**
(*R*)-Product	-1619.90535	0.07278	-1619.97813	**-26.2**	**12.9**	**-13.4**

Table S5. RRHO- and BSSE-corrected thermodynamics for reaction of **22a** and **23a** catalyzed by **Cat a** at M06-2X-D3/DGTZVP/SMD//M06-2X-D3/DGDZVP: absolute H, TS and G are presented in Hartrees and relative ΔH, -TΔS and ΔG are presented in kcal·mol^{-1}.

Structures	H	T.qh-S	qh-G(T)	ΔH	-TΔS	ΔG
Benzo[*d*]thiazole-2(3*H*)-thione	-1120.71555	0.04526	-1120.76080	**Reactants**		
3-Phenyloxetan-3-ol	-499.14799	0.04801	-499.19600			
Catalyst f	-2374.98632	0.11650	-2375.10282	**0.0**	**0.0**	**0.0**
I0_1	-2874.16993	0.13918	-2874.30911	**-22.4**	**15.9**	**-6.5**
TS1a_*R*	-3994.87786	0.15784	-3995.03570	**-17.6**	**32.6**	**15.0**
I1a_*R*	-3994.92965	0.15891	-3995.08856	**-50.1**	**31.9**	**-18.2**
(R)-Product	-1619.90535	0.07278	-1619.97813	**-26.2**	**12.9**	**-13.4**
TS1b_S	-3994.86796	0.15855	-3995.02651	**-11.4**	**32.1**	**20.8**
I1b_*S*	-3994.92658	0.15901	-3995.08559	**-48.1**	**31.9**	**-16.3**
(S)-Product	-1619.90535	0.07278	-1619.97813	**-26.2**	**12.9**	**-13.4**
I0_2	-2874.16898	0.13812	-2874.30709	**-21.8**	**16.6**	**-5.2**
TS1c_*S*	-3994.86830	0.15898	-3995.02728	**-11.6**	**31.9**	**20.3**
I1c_*S*	-3994.92641	0.15820	-3995.08461	**-48.0**	**32.4**	**-15.7**
(S)-Product	-1619.90535	0.07278	-1619.97813	**-26.2**	**12.9**	**-13.4**
TS1d_*R*	-3994.87796	0.15742	-3995.03538	**-17.6**	**32.8**	**15.2**
I1d_*R*	-3994.93045	0.15884	-3995.08929	**-50.6**	**32.0**	**-18.6**
(R)-Product	-1619.90535	0.07278	-1619.97813	**-26.2**	**12.9**	**-13.4**

Table S6. RRHO- and BSSE-corrected thermodynamics for reaction of **22a** and **23a** catalyzed by **Cat f** at M06-2X-D3/DGTZVP/SMD//M06-2X-D3/DGDZVP: absolute H, TS and G are presented in Hartrees and relative ΔH, -TΔS and ΔG are presented in kcal·mol^{-1}.

Structures	H	T.qh-S	qh-G(T)	ΔH	-TΔS	ΔG
Benzo[*d*]thiazole-2(3*H*)-thione	-1120.71555	0.04526	-1120.76080	**Reactants**		
3-Phenyloxetan-3-ol	-499.14799	0.04801	-499.19600			
Catalyst f	-4879.27182	0.20274	-4879.47456	**0.0**	**0.0**	**0.0**
I0_1	-5378.46810	0.22350	-5378.69160	**-30.3**	**17.1**	**-13.2**
I0a_*R*	-6499.20831	0.24364	-6499.45195	**-45.8**	**32.9**	**-12.9**
TS1a_*R*	-6499.17765	0.24227	-6499.41992	**-26.5**	**33.7**	**7.2**
I1a_*R*	-6499.23096	0.24238	-6499.47333	**-60.0**	**33.7**	**-26.3**
(R)-Product	-1619.90535	0.07278	-1619.97813	**-26.2**	**12.9**	**-13.4**
I0b_*S*	-6499.20325	0.24455	-6499.44779	**-42.6**	**32.3**	**-10.3**
TS1b_S	-6499.16758	0.24222	-6499.40980	**-20.2**	**33.8**	**13.5**
I1b_*S*	-6499.22711	0.24145	-6499.46856	**-57.6**	**34.2**	**-23.3**
(S)-Product	-1619.90535	0.07278	-1619.97813	**-26.2**	**12.9**	**-13.4**
I0_2	-5378.46681	0.22209	-5378.68890	**-29.5**	**18.0**	**-11.5**
I0c_*S*	-6499.20303	0.24279	-6499.44582	**-42.5**	**33.4**	**-9.1**
TS1c_*S*	-6499.16842	0.24358	-6499.41200	**-20.8**	**32.9**	**12.2**
I1c_*S*	-6499.22745	0.24238	-6499.46983	**-57.8**	**33.7**	**-24.1**
(S)-Product	-1619.90535	0.07278	-1619.97813	**-26.2**	**12.9**	**-13.4**
I0d_*R*	-6499.20551	0.24287	-6499.44838	**-44.0**	**33.3**	**-10.7**
TS1d_*R*	-6499.17923	0.24085	-6499.42008	**-27.5**	**34.6**	**7.1**
I1d_*R*	-6499.23044	0.24281	-6499.47325	**-59.7**	**33.4**	**-26.3**
(R)-Product	-1619.90535	0.07278	-1619.97813	**-26.2**	**12.9**	**-13.4**

Table S7. Accounting for weak interactions in the principal (*R*)- and (*S*)-enantiodirecting transition states for **Cat a**, **Cat b** and **Cat f**: BSSE-corrected ΔPE is calculated as difference of single point energies between the aggregated complex (TS) and Fragment 1 (Catalyst$^-$) and Fragment 2 (H^+-Activated complex of reactants) separated at infinite distance at M06-2X-D3/DGTZVP/SMD level. ΔPEs are BSSE-corrected and calculated in kcal·mol^{-1}.

Structures	E+BSSE (DGTZVP)	BSSE	E (DGTZVP)
Cat b TS1d_*R*	-3843.42643	0.00792	-3843.43435
Fragment 1	-2222.77256	0.00000	-2222.77256
Fragment 2	-1620.53565	0.00353	-1620.53919
ΔPE (R-directing)	**74.2**	**-2.8**	**76.9**
Cat b TS1b_*S*	-3843.42480	0.00848	-3843.43328
Fragment 1	-2222.77134	0.00000	-2222.77134
Fragment 2	-1620.53672	0.00353	-1620.54025
ΔPE (S-directing)	**73.3**	**-3.1**	**76.4**
Cat a TS1a_*R*	-3995.87614	0.01089	-3995.88703
Fragment 1	-2375.19727	0.00000	-2375.19727
Fragment 2	-1620.53498	0.00340	-1620.53838
ΔPE (R-directing)	**90.3**	**-4.7**	**95.0**
Cat a TS1c_*R*	-3995.86693	0.01027	-3995.87720
Fragment 1	-2375.19594	0.00000	-2375.19594
Fragment 2	-1620.53738	0.00359	-1620.54097
ΔPE (S-directing)	**83.8**	**-4.2**	**88.0**
Cat f TS1d_*R*	-6500.64385	0.01473	-6500.65858
Fragment 1	-4879.95945	0.00000	-4879.95945
Fragment 2	-1620.53502	0.00345	-1620.53847
ΔPE (R-directing)	**93.7**	**-7.1**	**100.8**
Cat f TS1c_*S*	-6500.63360	0.01389	-6500.64749
Fragment 1	-4879.95954	0.00000	-4879.95954
Fragment 2	-1620.53409	0.00340	-1620.53749
ΔPE (S-directing)	**87.8**	**-6.6**	**94.4**

Fragmentation schemes for counterpoise corrections

In order to counterpoise the energies of the structures and ensure the best and most reliable partition of the system in different fragments, thus properly accounting for BSSE corrections, we fragmented the stationary points as follows: three examples are given for reactant, transition state and product.

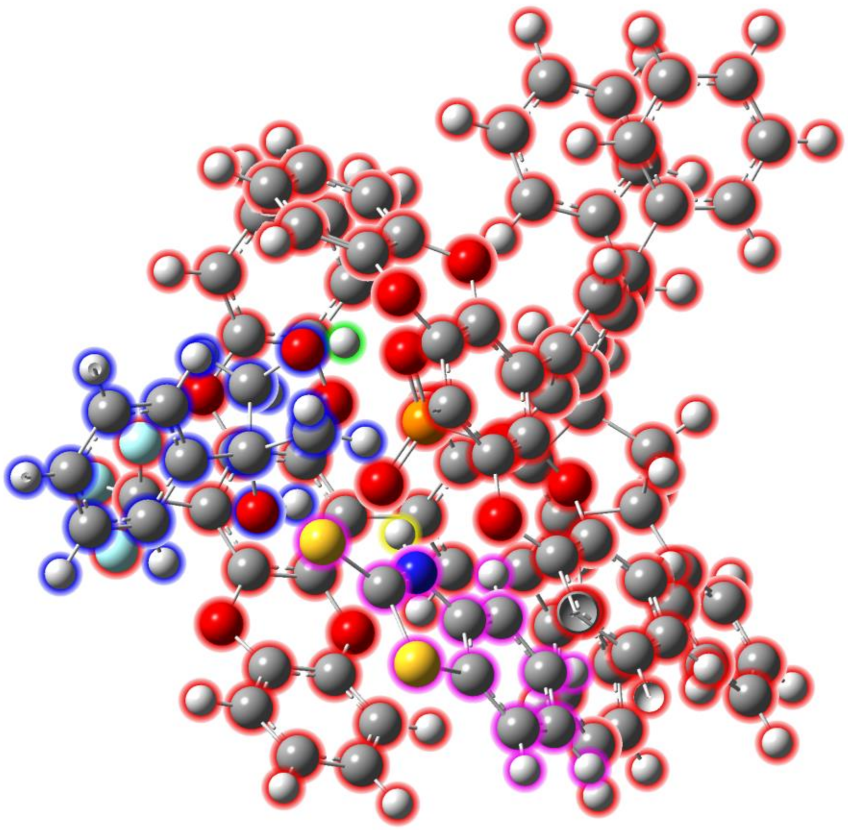

Figure S1. Clipped structure of **Cat f** TS1d_*R* transition state. Five fragments for counterpoise corrections are defined with their relative assigned charges: Catalyst^{-1}, H^+, Oxetane^0, H^+ and R_2N^-.

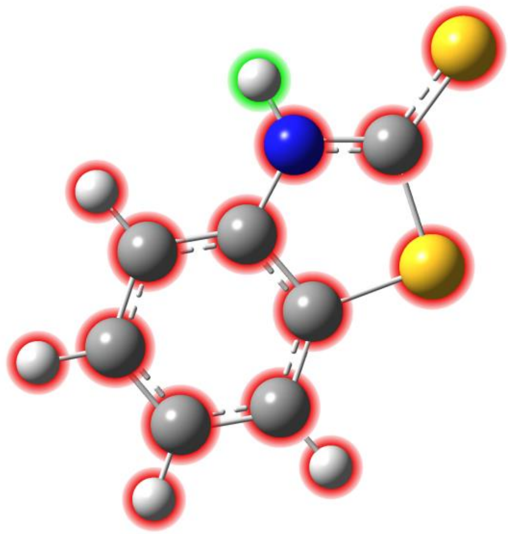

Figure S2. Two fragments are defined for the reactant with their relative assigned charges: R_2N^- and H^+.

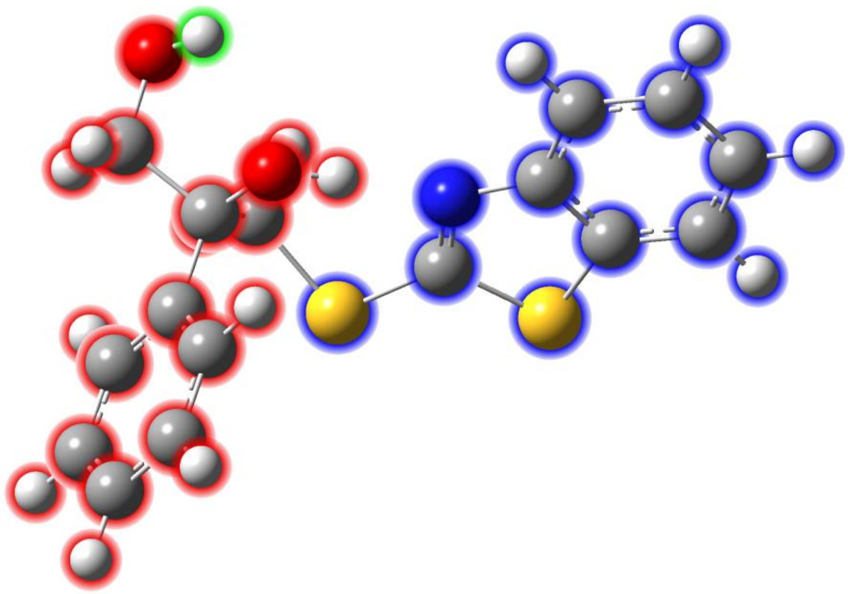

Figure S3. Three fragments are defined for the product with their relative assigned charges: $Oxetane^0$, R_2N^- and H^+.

6. X-ray diffraction data

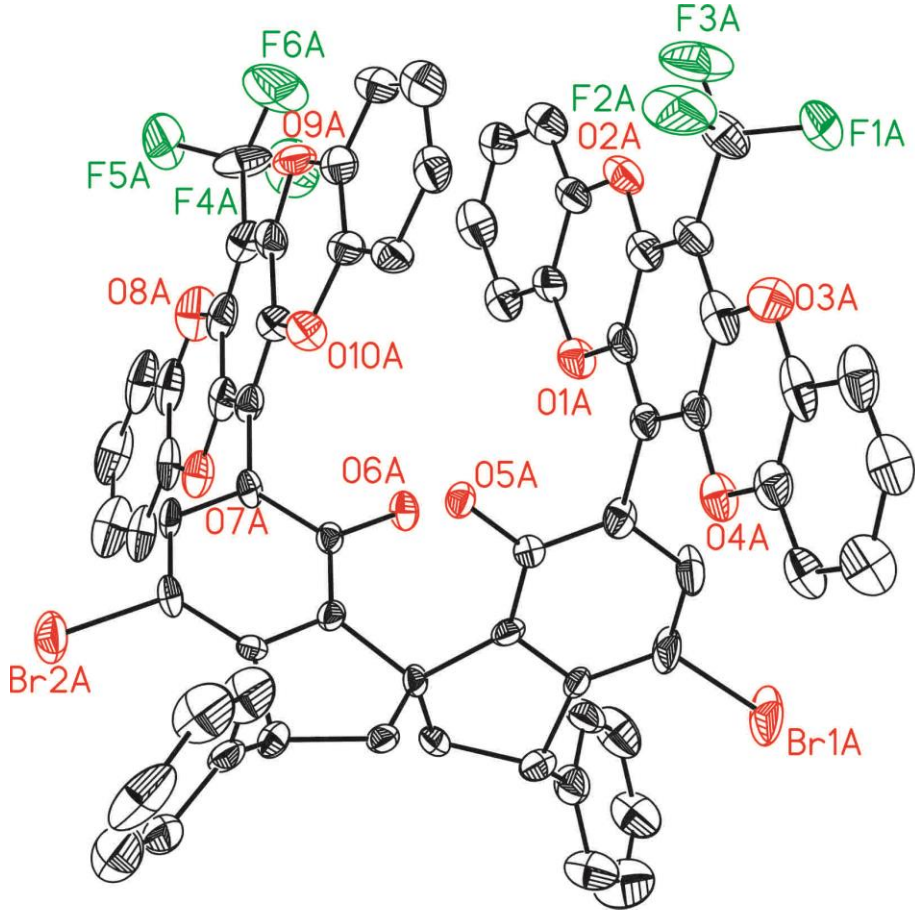

Figure S4. ORTEP X-ray structure of Compound **19**

Table S8. Crystal data and structure refinement for Compound **19**.

Empirical formula	C79 H45.50 Br2 F6 I2 O10	
Formula weight	1682.27	
Temperature	293(2) K	
Wavelength	0.71073 Å	
Crystal system	monoclinic	
Space group	P 21	
Unit cell dimensions	a = 18.5988(4) Å	α = 90°
	b = 13.7054(3) Å	β = 104.1331(16)°
	c = 26.5064(4) Å	γ = 90°
Volume	6552.1(2) Å^3	
Z	4	
Density (calculated)	1.705 Mg/m^3	
Absorption coefficient	2.261 mm^{-1}	
F(000)	3318	
Crystal size	0.250 x 0.120 x 0.050 mm^3	
Theta range for data collection	2.258 to 29.786°.	
Index ranges	-25<=h<=25,-19<=k<=19,-36<=l<=36	
Reflections collected	52522	
Independent reflections	52522[R(int) = ?]	
Completeness to theta =29.786°	95.1%	
Absorption correction	Multi-scan	
Max. and min. transmission	1.00 and 0.91	
Refinement method	Full-matrix least-squares on F^2	
Data / restraints / parameters	52522/ 755/ 2003	
Goodness-of-fit on F^2	1.151	
Final R indices [I>2sigma(I)]	R1 = 0.0676, wR2 = 0.1666	
R indices (all data)	R1 = 0.0993, wR2 = 0.1756	
Flack parameter	x =0.002(4)	
Largest diff. peak and hole	1.388 and -0.979 e.Å^{-3}	

7. References

1. a) Yin, L.; Xing, J.; Wang, Y.; Shen, Y.; Lu, T.; Hayashi, T.; Dou, X. Enantioselective Synthesis of 3,3′-Diaryl-SPINOLs: Rhodium-Catalyzed Asymmetric Arylation/BF_3-Promoted Spirocyclization Sequence. *Angew. Chem. Int. Ed.* **2019**, *58*, 2474-2478; b) St John-Campbell, S.; White, A. J.; Bull, J. A. Single operation palladium catalysed C (sp3)–H functionalisation of tertiary aldehydes: investigations into transient imine directing groups. *Chem. Sci.* **2017**, *8*, 4840-4847.

2. Clot-Almenara, L.; Rodríguez-Escrich, C.; Osorio-Planes, L.; Pericàs, M.A. Polystyrene-Supported TRIP: A Highly Recyclable Catalyst for Batch and Flow Enantioselective Allylation of Aldehydes. *ACS Catalysis* **2016**, *6*, 7647–7651.

3. Xing, C.H.; Liao, Y.X.; Ng, J.; Hu, Q.S. Optically Active 1,1′-Spirobiindane-7,7′-diol (SPINOL)-Based Phosphoric Acids as Highly Enantioselective Catalysts for Asymmetric Organocatalysis. *J. Org. Chem.* **2011**, *76*, 4125–4131.

4. a) Shih, J.L.; Nguyen, T.S.; May, J.A. Organocatalyzed Asymmetric Conjugate Addition of Heteroaryl and Aryl Trifluoroborates: a Synthetic Strategy for Discoipyrrole D. *Angew. Chem. Int. Ed.* **2015**, *54*, 9931-9935; b) Le, P.Q.; Nguyen, T.S.; May, J.A. A General Method for the Enantioselective Synthesis of α-Chiral Heterocycles. *Org. Lett.* **2012**, *14*, 6104-6107.

5. Wang, Z.; Chen, Z.; Sun, J. Catalytic Enantioselective Intermolecular Desymmetrization of 3-Substituted Oxetanes. *Angew. Chem. Int. Ed.* **2013**, *52*, 6685 –6688.

6. M. J. Frisch, G. W. T., H. B. Schlegel, G. E. Scuseria, M. A. Robb, J. R. Cheeseman, G. Scalmani, V. Barone, G. A. Petersson, H. Nakatsuji, X. Li, M. Caricato, A. Marenich, J. Bloino, B. G. Janesko, R. Gomperts, B. Mennucci, H. P. Hratchian, J. V. Ortiz, A. F. Izmaylov, J. L. Sonnenberg, D. Williams-Young, F. Ding, F. Lipparini, F. Egidi, J. Goings, B. Peng, A. Petrone, T. Henderson, D. Ranasinghe, V. G. Zakrzewski, J. Gao, N. Rega, G. Zheng, W. Liang, M. Hada, M. Ehara, K. Toyota, R. Fukuda, J. Hasegawa, M. Ishida, T. Nakajima, Y. Honda, O. Kitao, H. Nakai, T. Vreven, K. Throssell, J. A. Montgomery, Jr., J. E. Peralta, F. Ogliaro, M. Bearpark, J. J. Heyd, E. Brothers, K. N. Kudin, V. N. Staroverov, T. Keith, R. Kobayashi, J. Normand, K. Raghavachari, A. Rendell, J. C. Burant, S. S. Iyengar, J. Tomasi, M. Cossi, J. M. Millam, M. Klene, C. Adamo, R. Cammi, J. W. Ochterski, R. L. Martin, K. Morokuma, O. Farkas, J. B. Foresman, and D. J. Fox Gaussian 09, Revision D.01, Gaussian, Inc., Wallingford CT, 2016.

7. Zhao, Y.; Truhlar, D. G., The M06 suite of density functionals for main group thermochemistry, thermochemical kinetics, noncovalent interactions, excited states, and transition elements: two new functionals and systematic testing of four M06-class functionals and 12 other functionals. *Theor. Chem. Acc.* **2008**, *120*, 215-241.

8. Fianchini, M.; O'Brien, C. J.; Chass, G. A., Reduction Rate of 1-Phenyl Phospholane 1-Oxide Enhanced by Silanol Byproducts: Comprehensive DFT Study and Kinetic Modeling Linked to Reagent Design. *J. Org. Chem.* **2019**, *84*, 10579-10592.

9. Sedlak, R.; Janowski, T.; Pitoňák, M.; Řezáč, J.; Pulay, P.; Hobza, P., Accuracy of Quantum Chemical Methods for Large Noncovalent Complexes. *J. Chem. Theory Comput.* **2013**, *9*, 3364-3374.

10. Dapprich, S.; Komáromi, I.; Byun, K. S.; Morokuma, K.; Frisch, M. J., A new ONIOM implementation in Gaussian98. Part I. The calculation of energies, gradients, vibrational frequencies and electric field derivatives. *J. Mol. Struct. (THEOCHEM)* **1999**, *461-462*, 1-21.

11. Maseras, F.; Morokuma, K., IMOMM: A new integrated ab initio + molecular mechanics geometry optimization scheme of equilibrium structures and transition states. *J. Comp. Chem.* **1995**, *16*, 1170-1179.

12. Vreven, T.; Byun, K. S.; Komáromi, I.; Dapprich, S.; Montgomery, J. A.; Morokuma, K.; Frisch, M. J., Combining Quantum Mechanics Methods with Molecular Mechanics Methods in ONIOM. *J. Chem. Theory Comput.* **2006**, *2*, 815-826.

13. Vreven, T.; Frisch, M. J.; Kudin, K. N.; Schlegel, H. B.; Morokuma, K., Geometry optimization with QM/MM methods II: Explicit quadratic coupling. *Mol. Phys.* **2006**, *104*, 701-714.

14. Vreven, T.; Morokuma, K.; Farkas, Ö.; Schlegel, H. B.; Frisch, M. J., Geometry optimization with QM/MM, ONIOM, and other combined methods. I. Microiterations and constraints. J. *Comp. Chem.* **2003**, *24*, 760-769.

15. Vreven, T.; Morokuma, K., On the application of the IMOMO (integrated molecular orbital + molecular orbital) method. *J. Comput. Chem.* **2000**, *21*, 1419-1432.

16. Vreven, T.; Mennucci, B.; da Silva, C. O.; Morokuma, K.; Tomasi, J., The ONIOM-PCM method: Combining the hybrid molecular orbital method and the polarizable continuum model for solvation. Application to the geometry and properties of a merocyanine in solution. *J. Chem. Phys.* **2001**, *115*, 62-72.

17. Godbout, N.; Salahub, D. R.; Andzelm, J.; Wimmer, E., Optimization of Gaussian-type basis sets for local spin density functional calculations. Part I. Boron through neon, optimization technique and validation. *Can. J. Chem.* **1992**, *70*, 560-571.

18. Marenich, A. V.; Cramer, C. J.; Truhlar, D. G., Universal Solvation Model Based on Solute Electron Density and on a Continuum Model of the Solvent Defined by the Bulk Dielectric Constant and Atomic Surface Tensions. *J. Phys. Chem. B* **2009**, *113*, 6378-6396.

19. Wheeler, S. E.; Houk, K. N., Integration Grid Errors for Meta-GGA-Predicted Reaction Energies: Origin of Grid Errors for the M06 Suite of Functionals. *J. Chem. Theory Comput.* **2010**, *6*, 395-404.

20. Funes-Ardoiz, I.; Paton, R., GoodVibes, v.2.0.3. DOI: 10.5281/zenodo.1435820.

21. Boys, S. F.; and Bernardi, F., Calculation of Small Molecular Interactions by Differences of Separate Total Energies - Some Procedures with Reduced Errors. *Mol. Phys.* **1970**, *19*, 553-566.

22. Simon, S.; Duran, M.; Dannenberg, J.J. How does basis set superposition error change the potential surfaces for hydrogen bonded dimers? *J. Chem. Phys.* **1996**, *105*, 11024-11031.

23. Pettersen, E. F.; Goddard, T. D.; Huang, C. C.; Couch, G. S.; Greenblatt, D. M.; Meng, E. C.; Ferrin, T. E., UCSF Chimera—A visualization system for exploratory research and analysis. *J. Comput. Chem.* **2004**, *25*, 1605-1612.

24. Humphrey, W.; Dalke, A.; Schulten, K., VMD: Visual molecular dynamics. *J. Mol. Graphics*. **1996**, *14*, 33-38.
25. Persistence of Vision(TM) Raytracer, 3.6; Williamstown, Victoria, Australia, 2004.
26. Stone, J. An Efficient Library for Parallel Ray Tracing and Animation. University of Missouri-Rolla, 1998.

8. NMR spectra

^{1}H NMR of **S1**

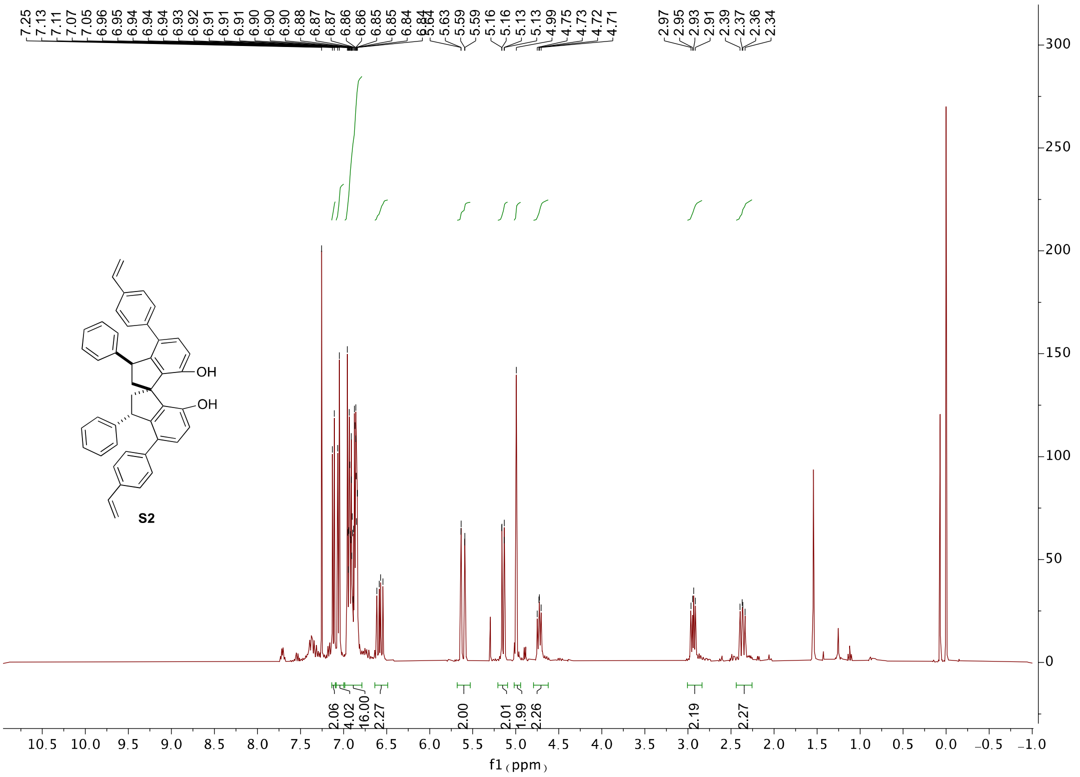

^{13}C NMR of **S1**

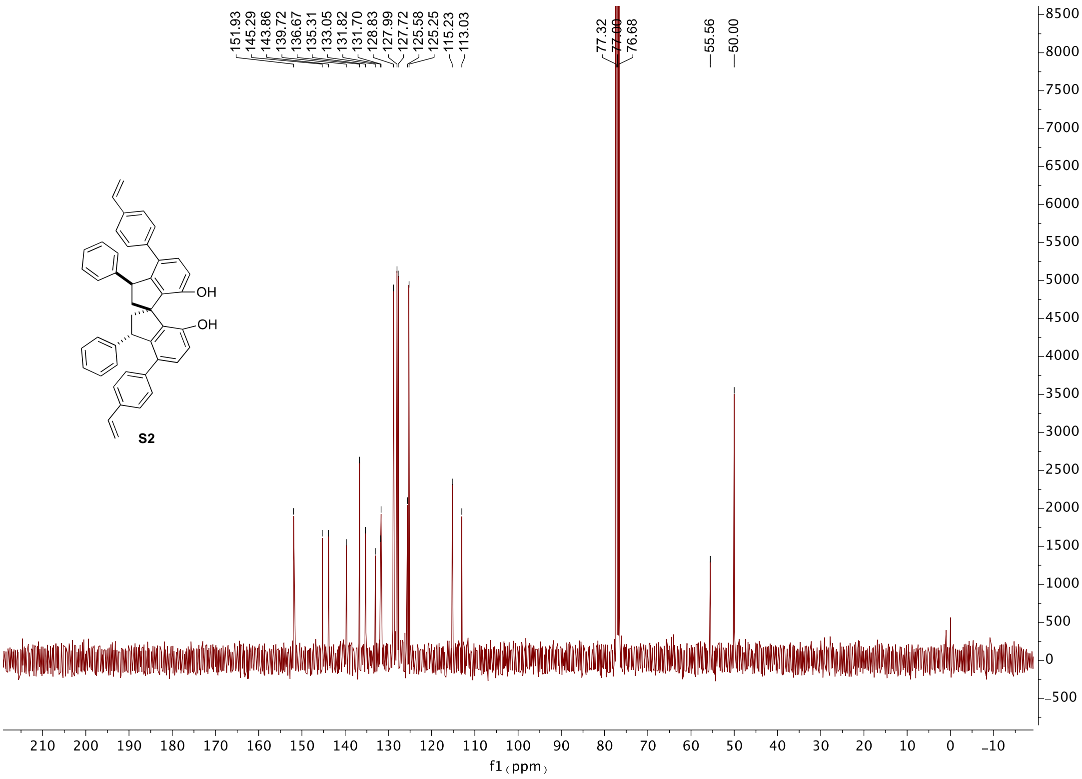

^{1}H NMR of **S4**

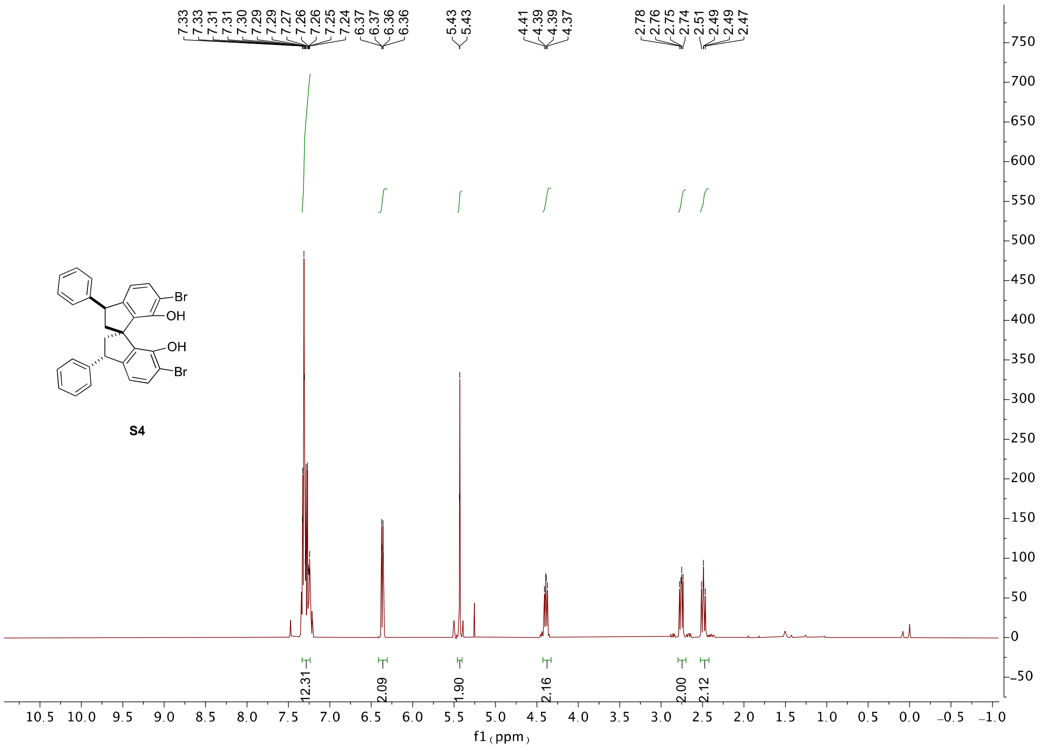

^{13}C NMR of **S4**

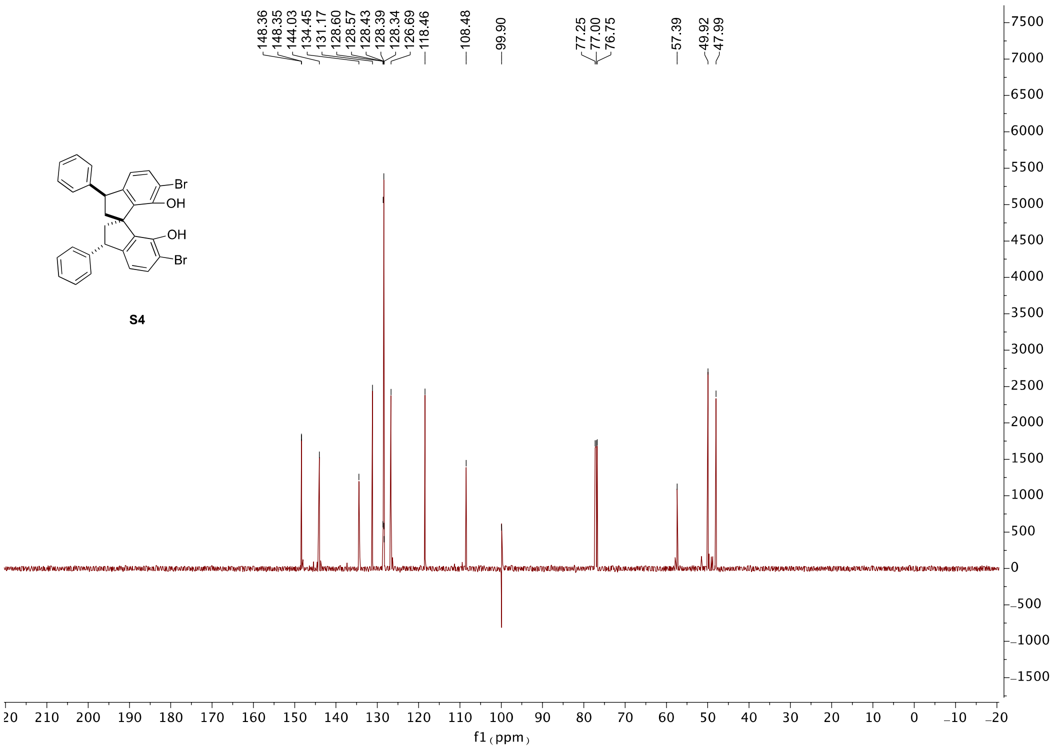

^{1}H NMR of **S5**

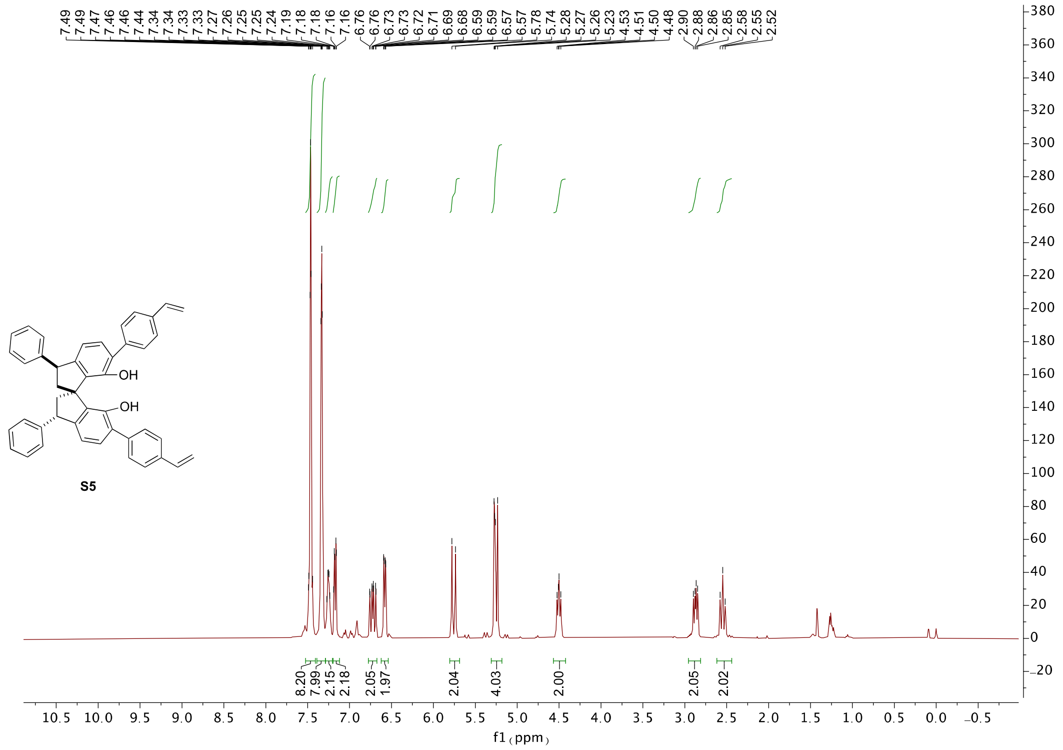

^{13}C NMR of **S5**

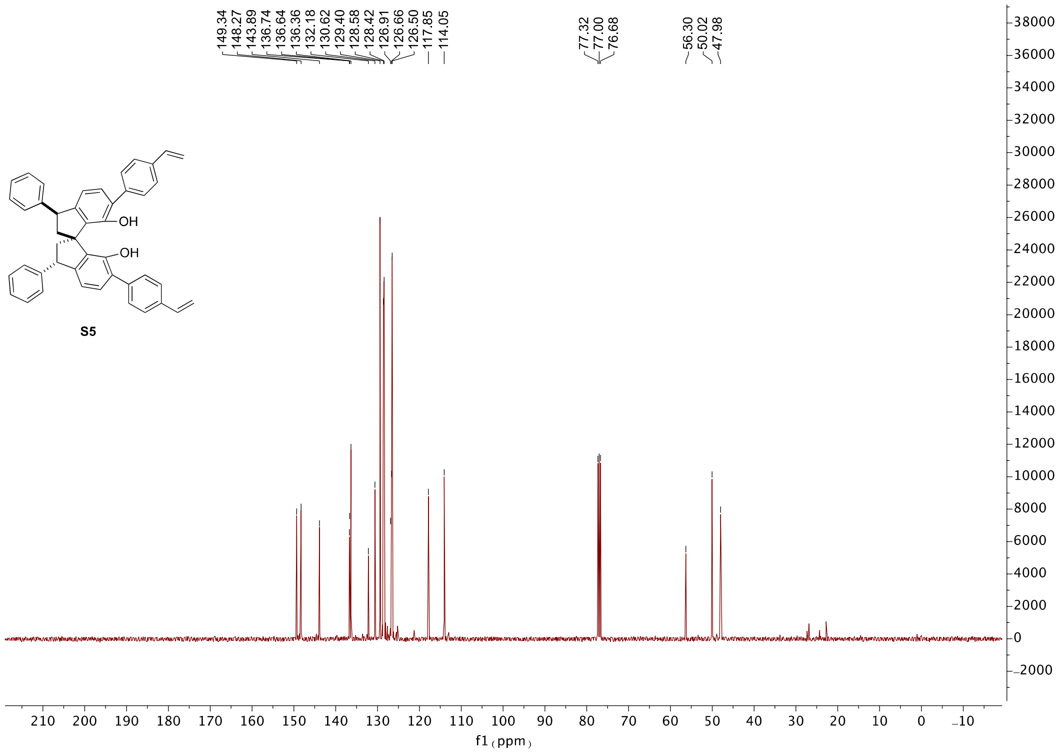

^{1}H NMR of **S7**

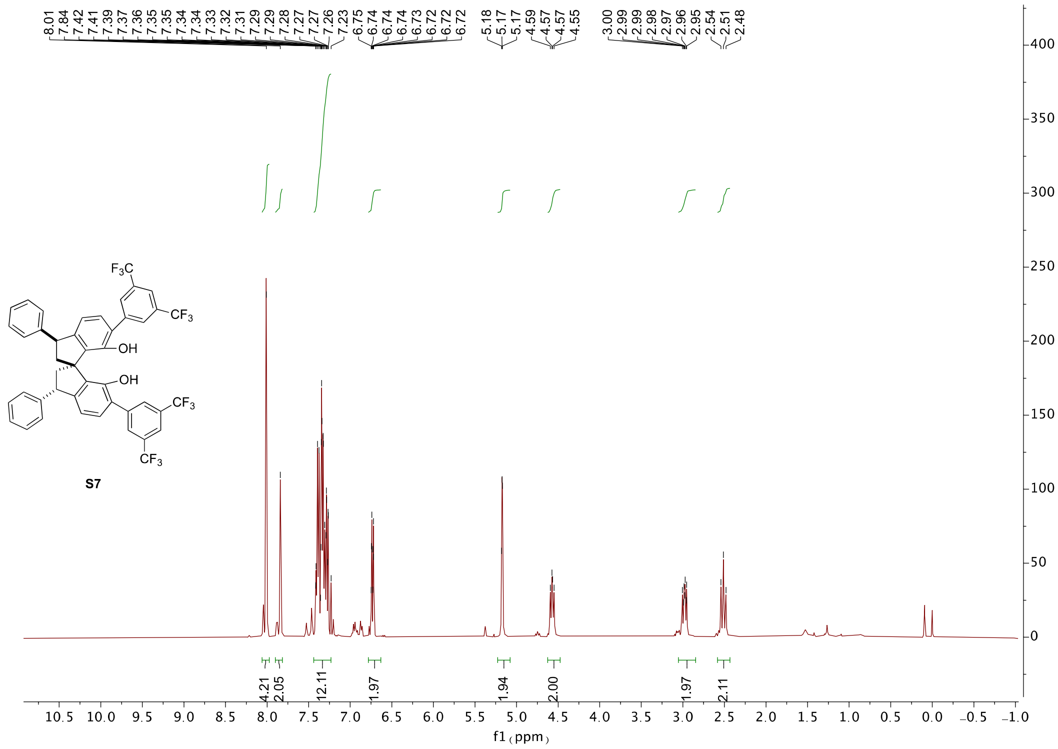

^{13}C NMR of **S7**

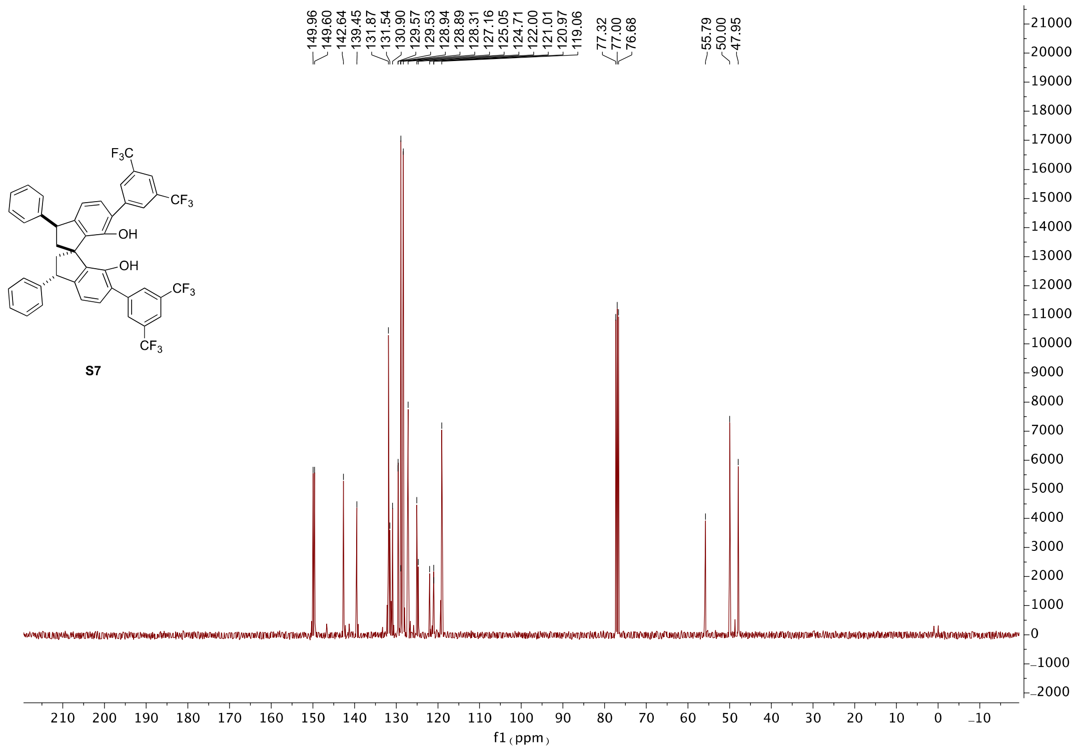

^{19}F NMR of **S7**

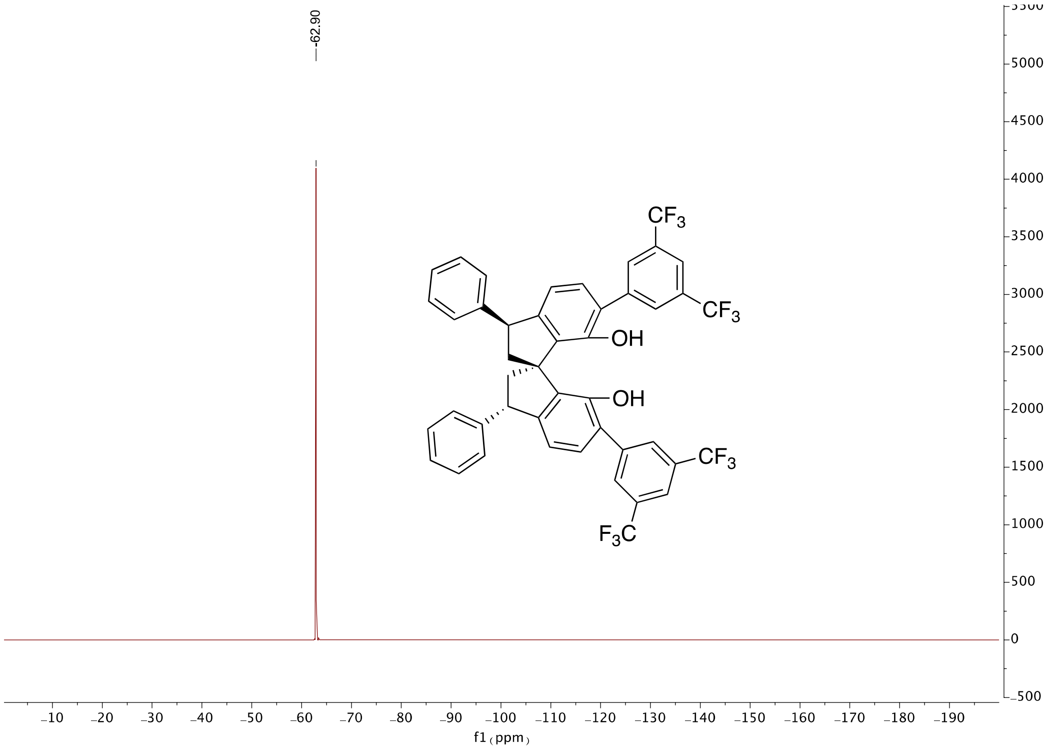
-62.90
CF3
CF3
OH
OH
CF3
F3C
5000
4500
4000
3500
3000
2500
2000
1500
1000
500
0
-500
-10 -20 -30 -40 -50 -60 -70 -80 -90 -100 -110 -120 -130 -140 -150 -160 -170 -180 -190
f1 (ppm)

^{1}H NMR of **S8**

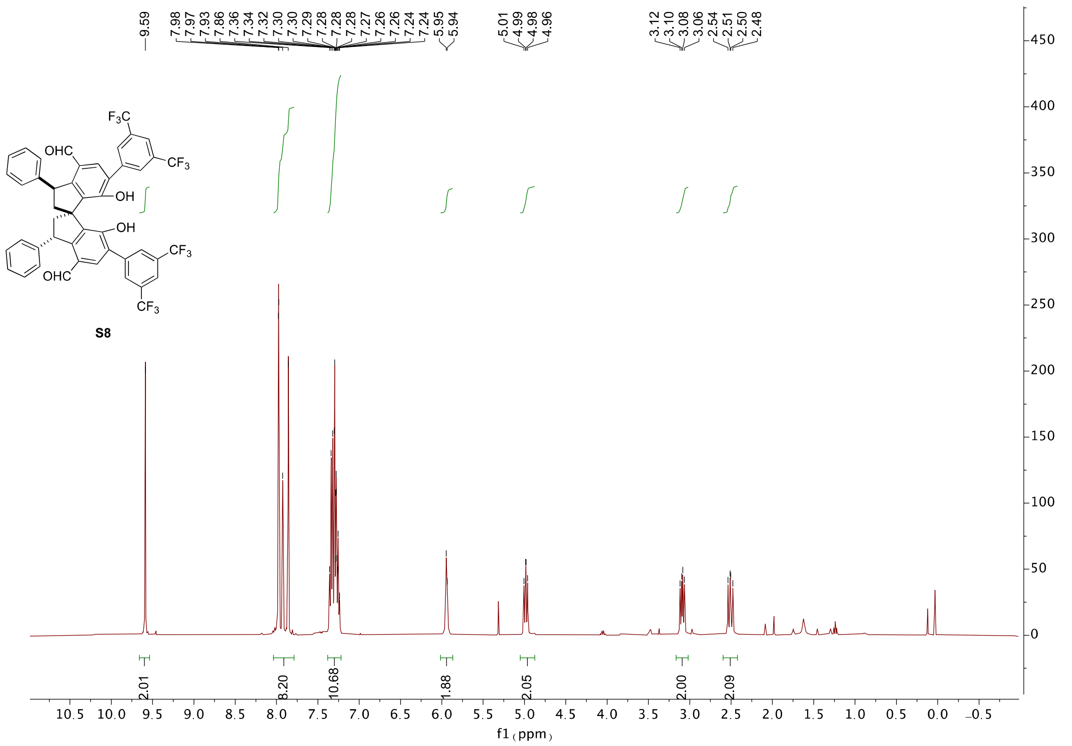

^{13}C NMR of **S8**

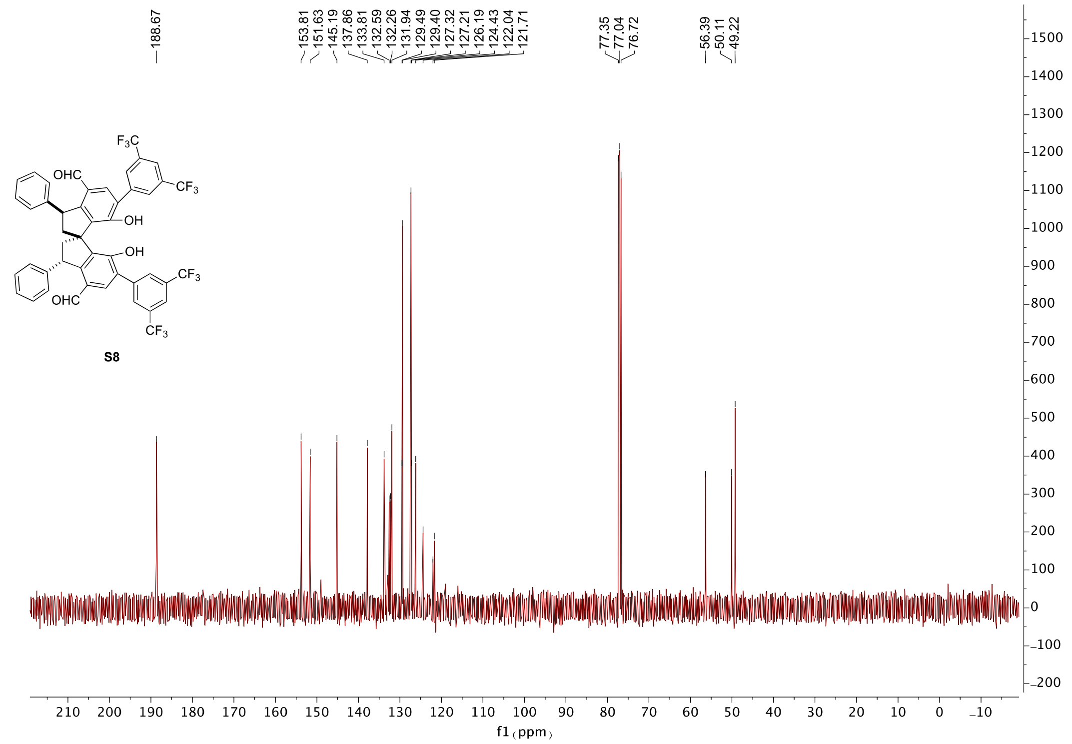

^{19}F NMR of **S8**

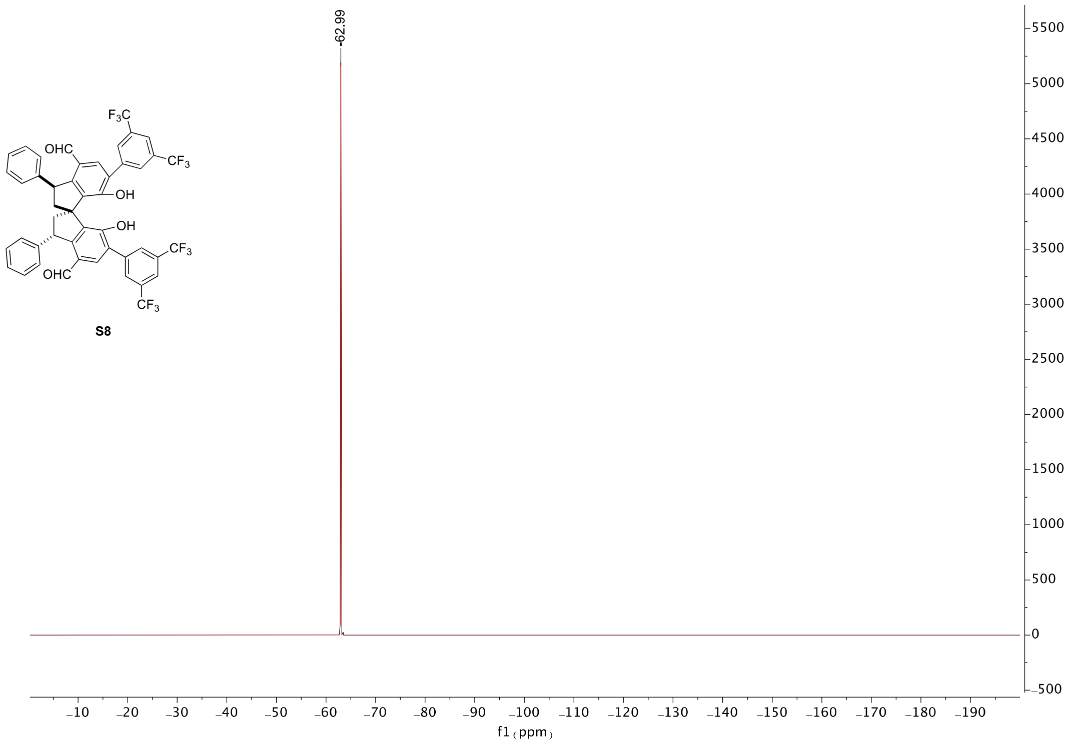

^{19}F NMR of **S9**

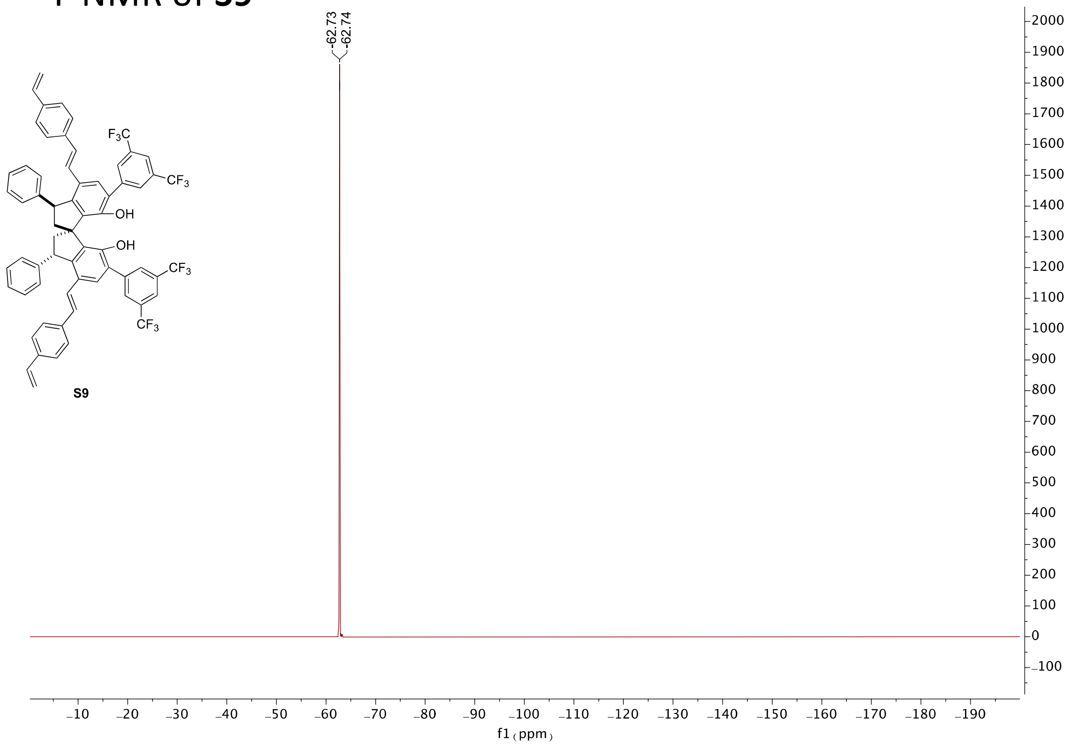

^{1}H NMR of **S9**

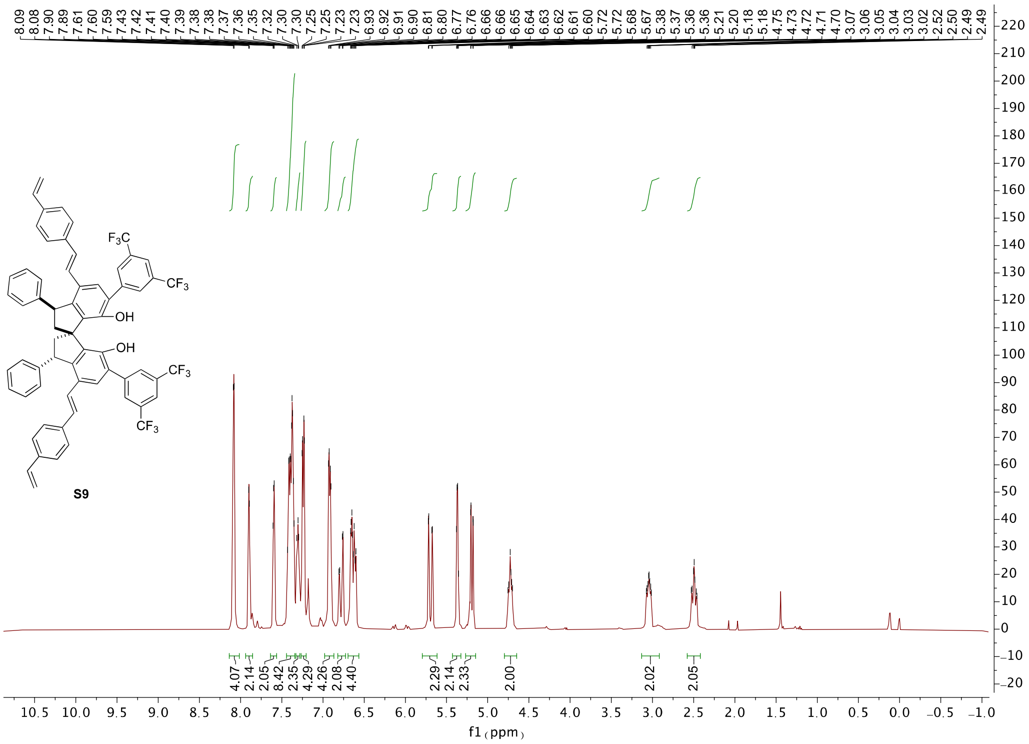

^{13}C NMR of **S9**

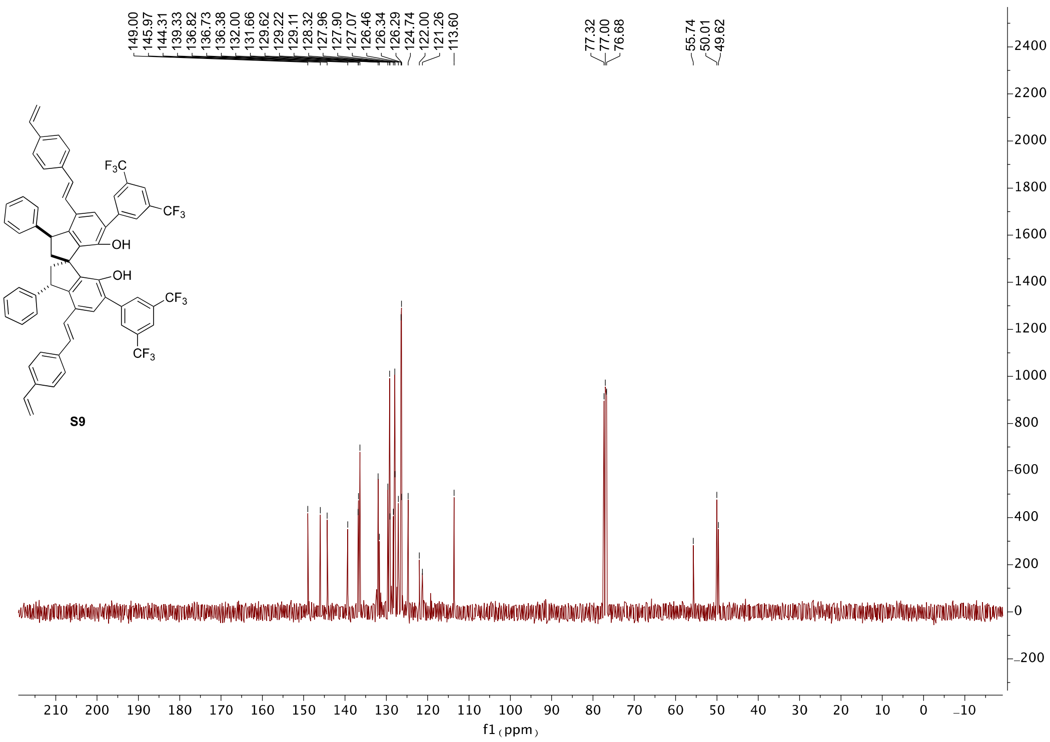

^{1}H NMR of **13**

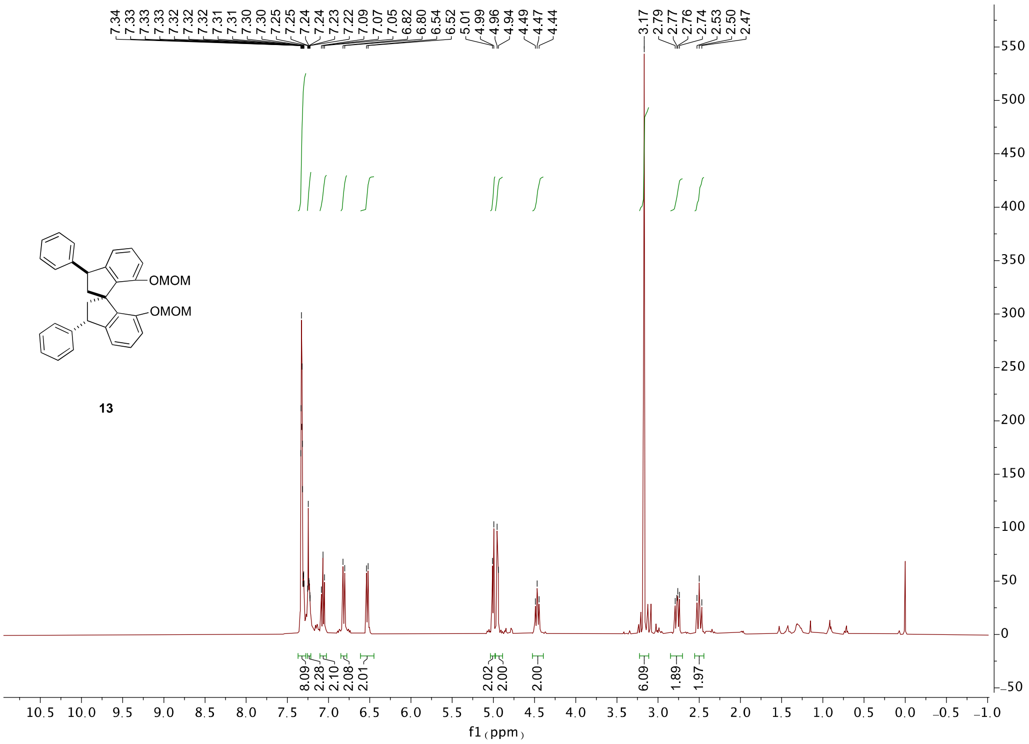

^{13}C NMR of **13**

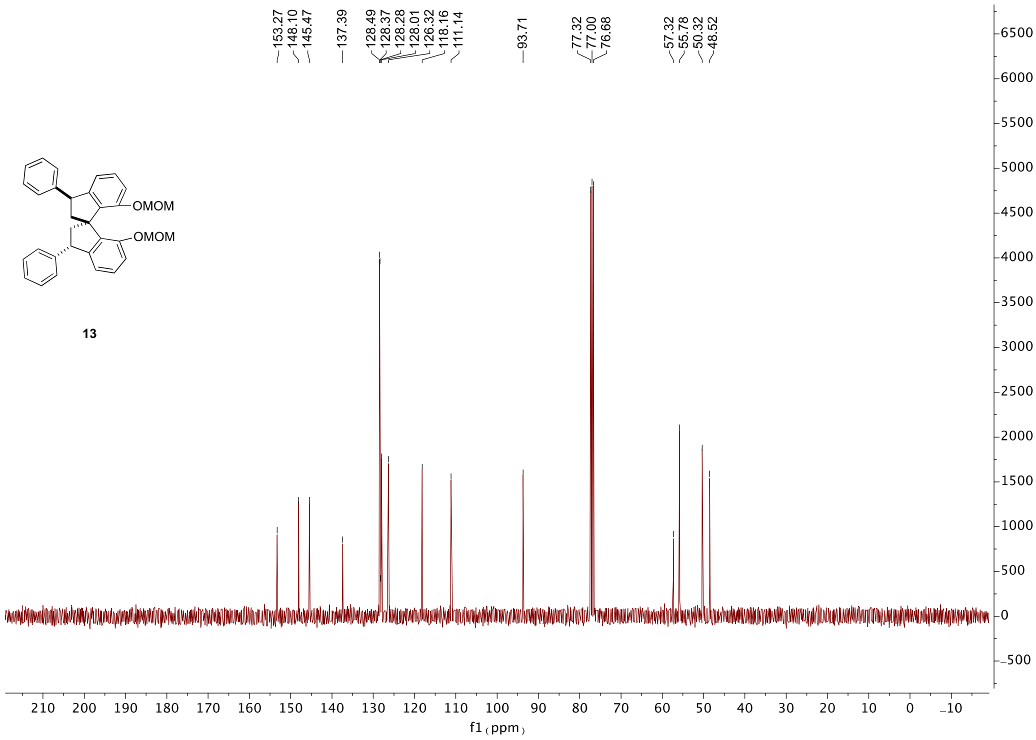

^{1}H NMR of **14**

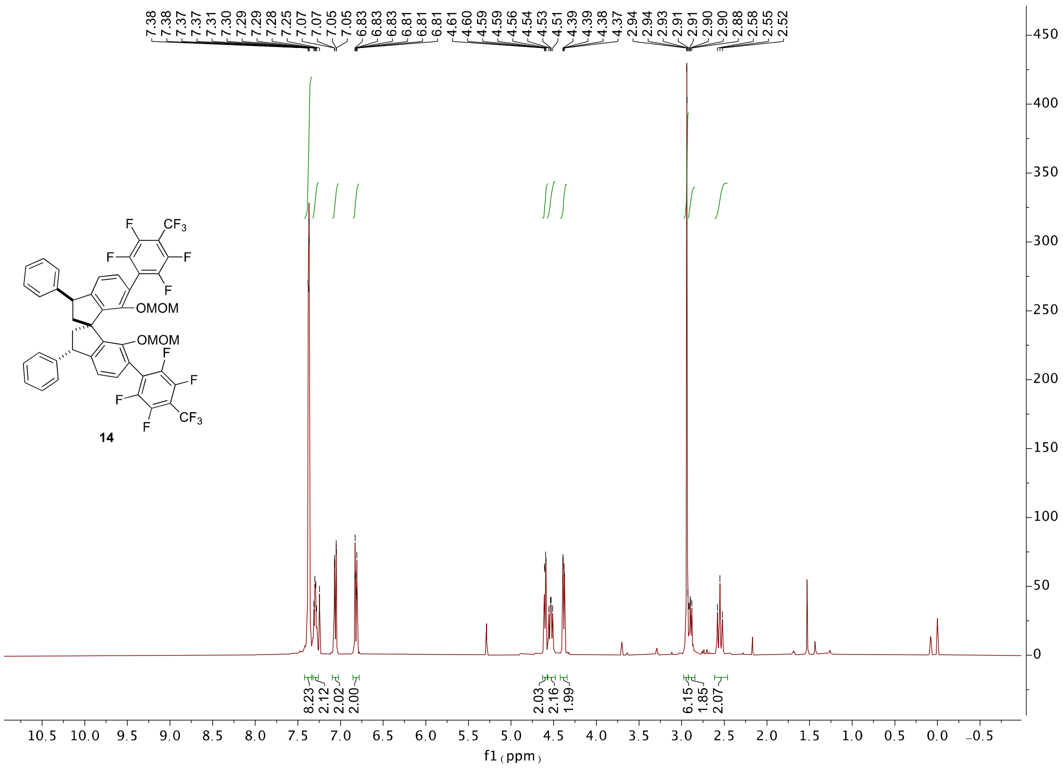

^{13}C NMR of **14**

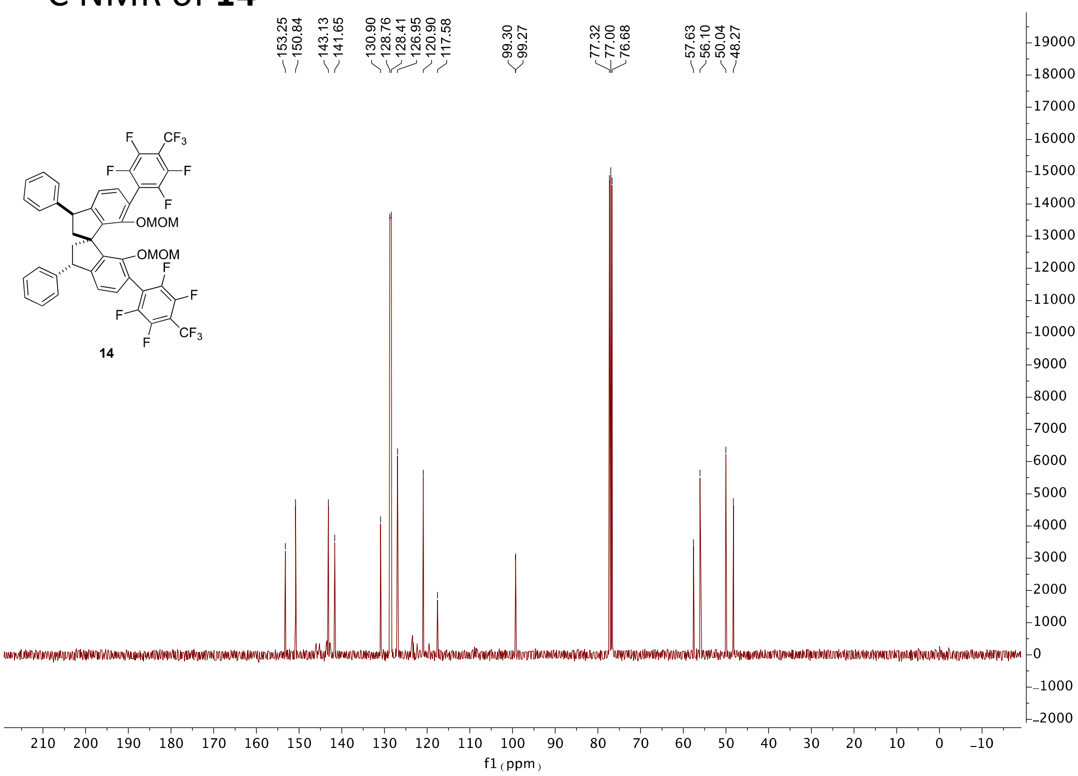

^{19}F NMR of **14**

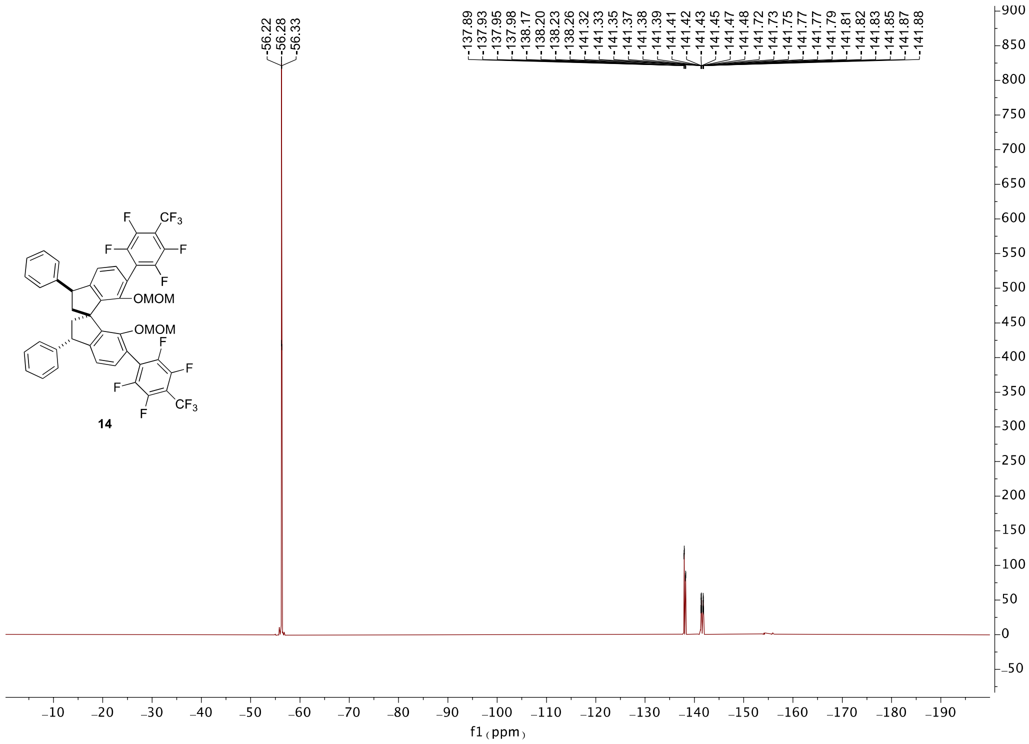

^{19}F NMR of **15**

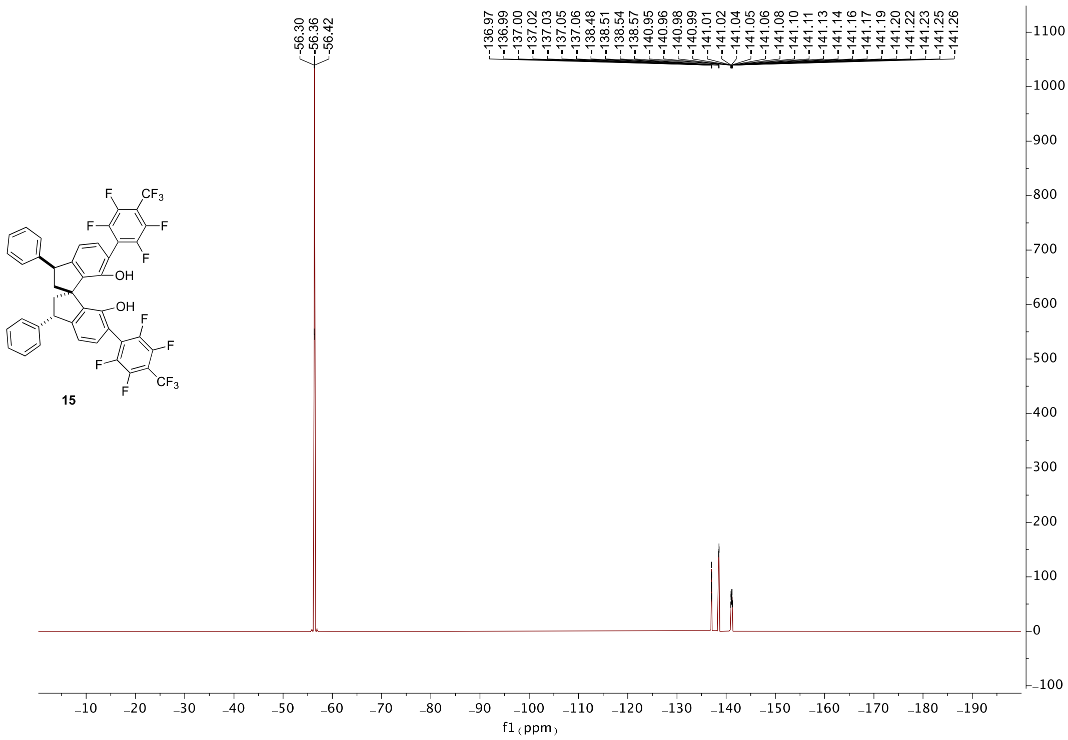

^{1}H NMR of **15**

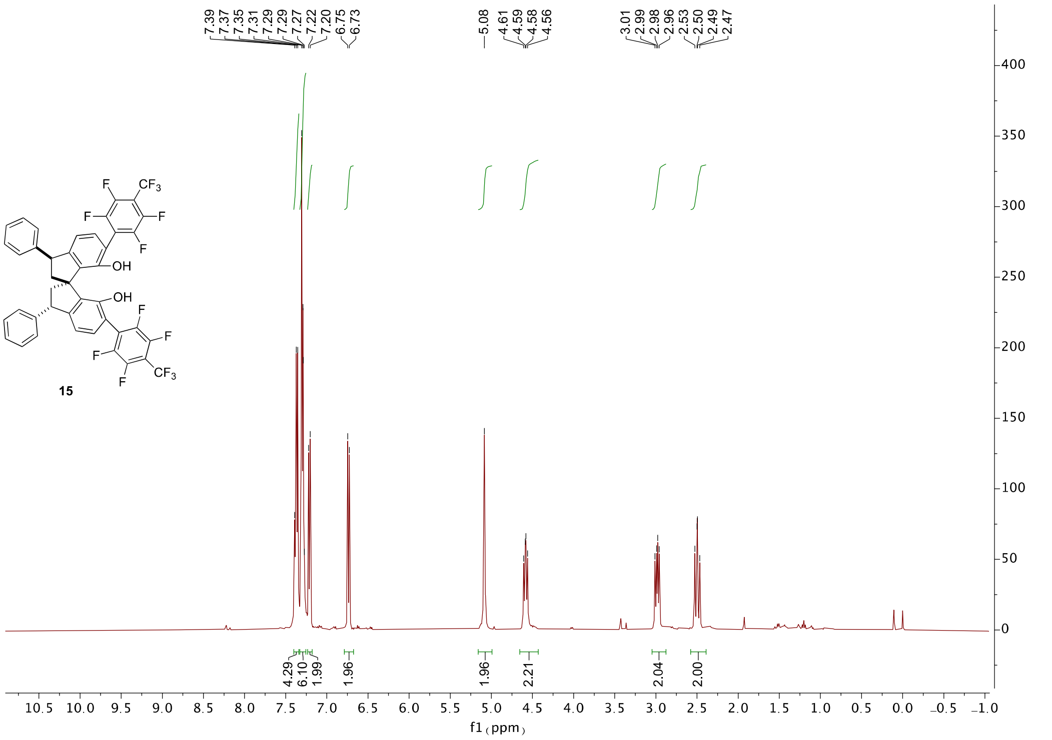

^{13}C NMR of **15**

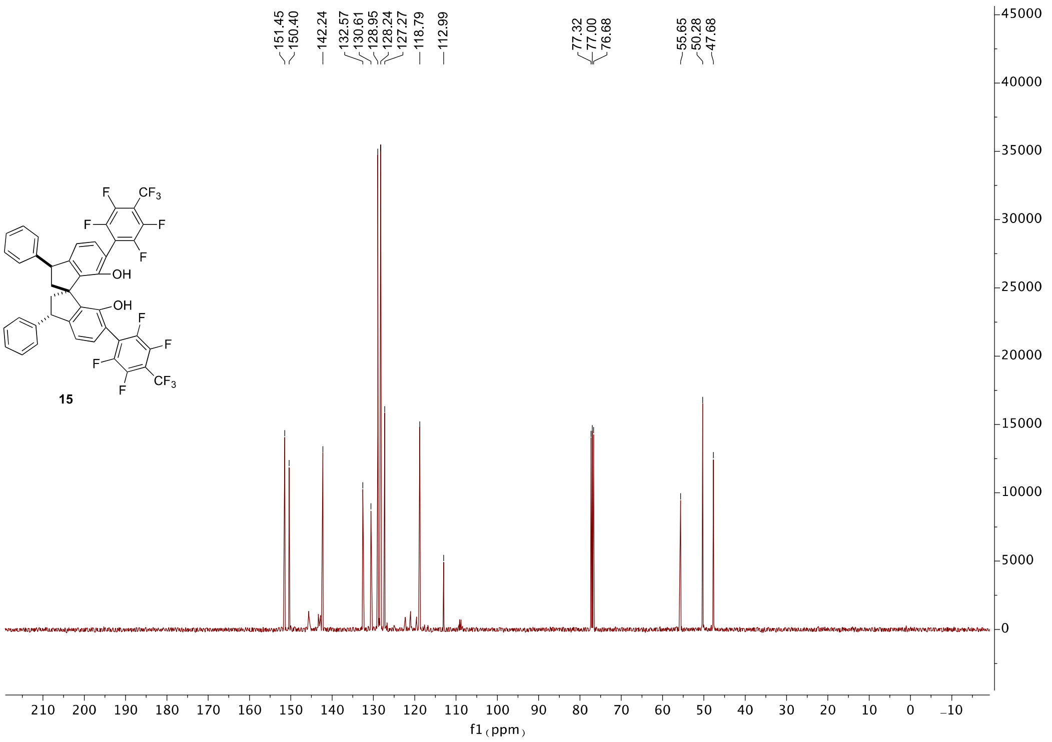

^{1}H NMR of **16**

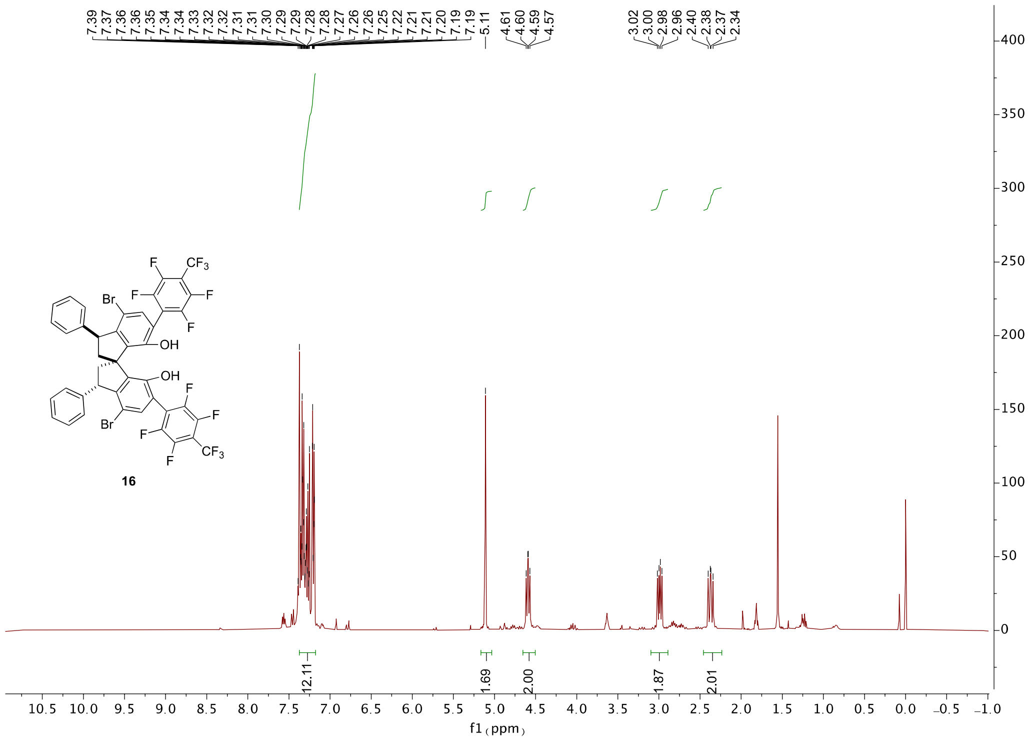

^{13}C NMR of **16**

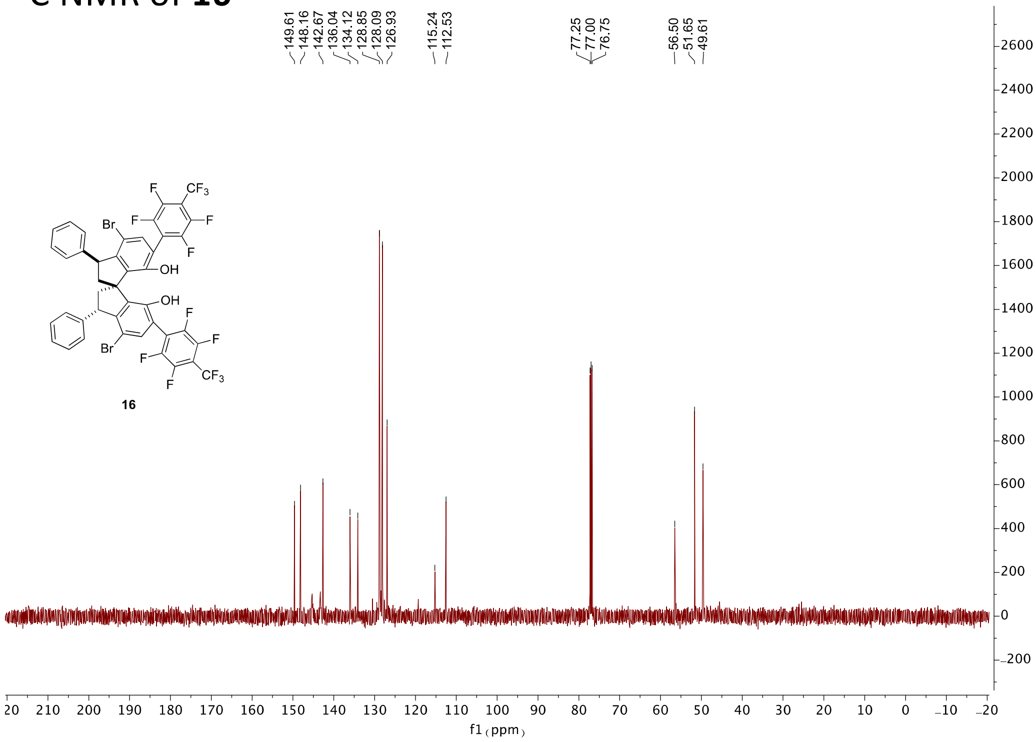

^{19}F NMR of **16**

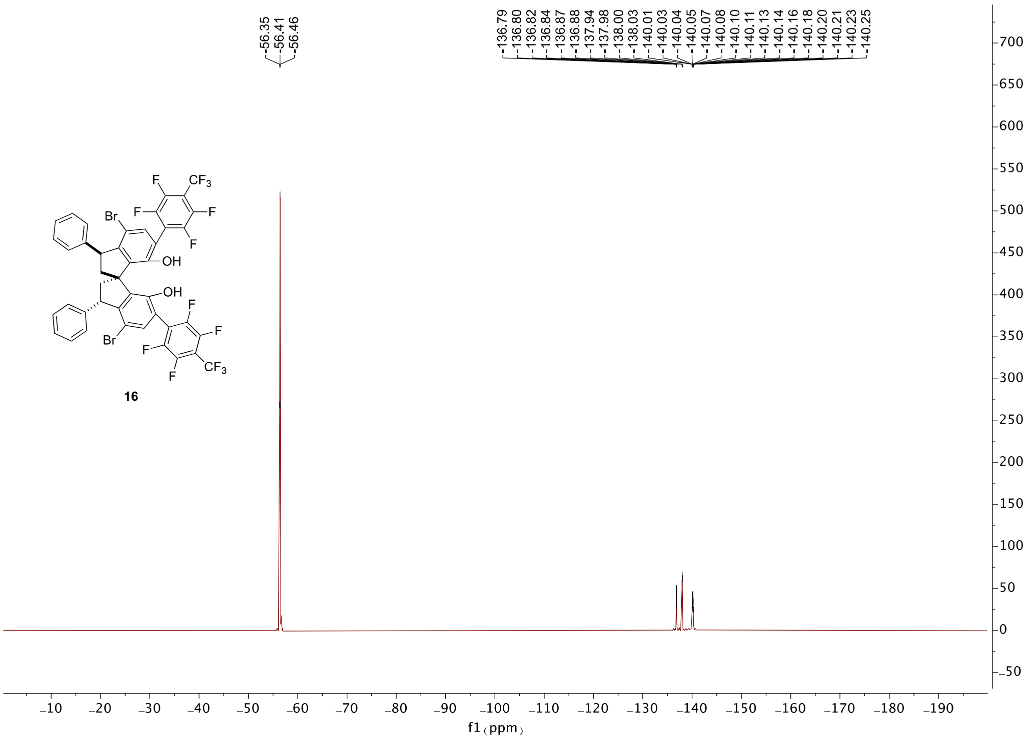

^{19}F NMR of **S11**

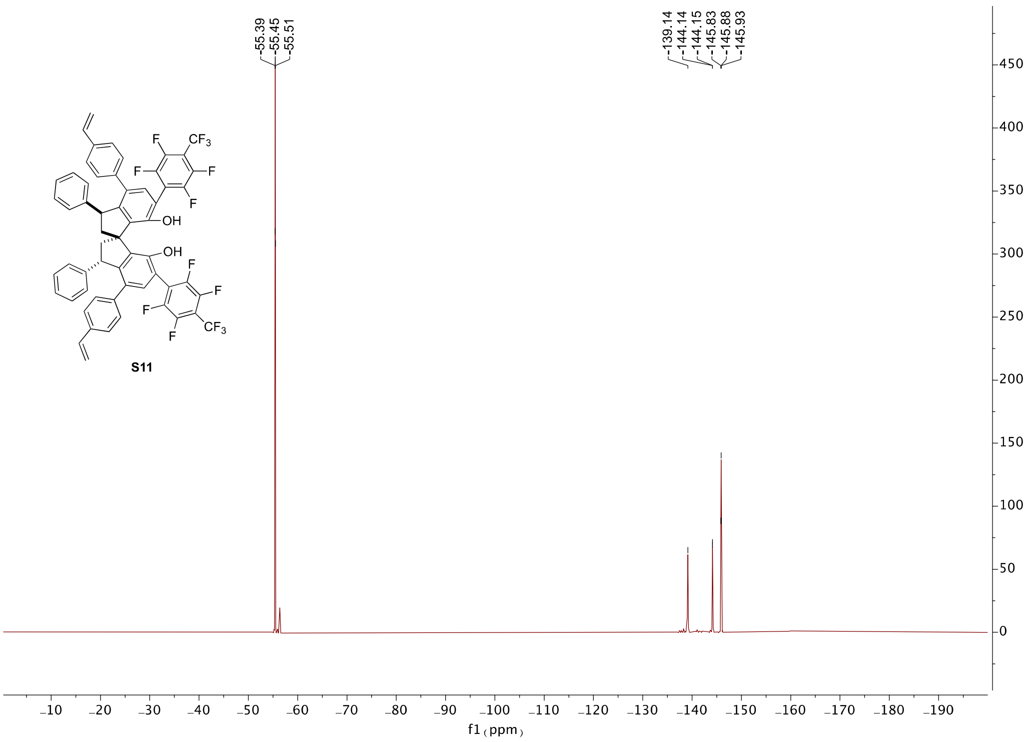

^{1}H NMR of **S11**

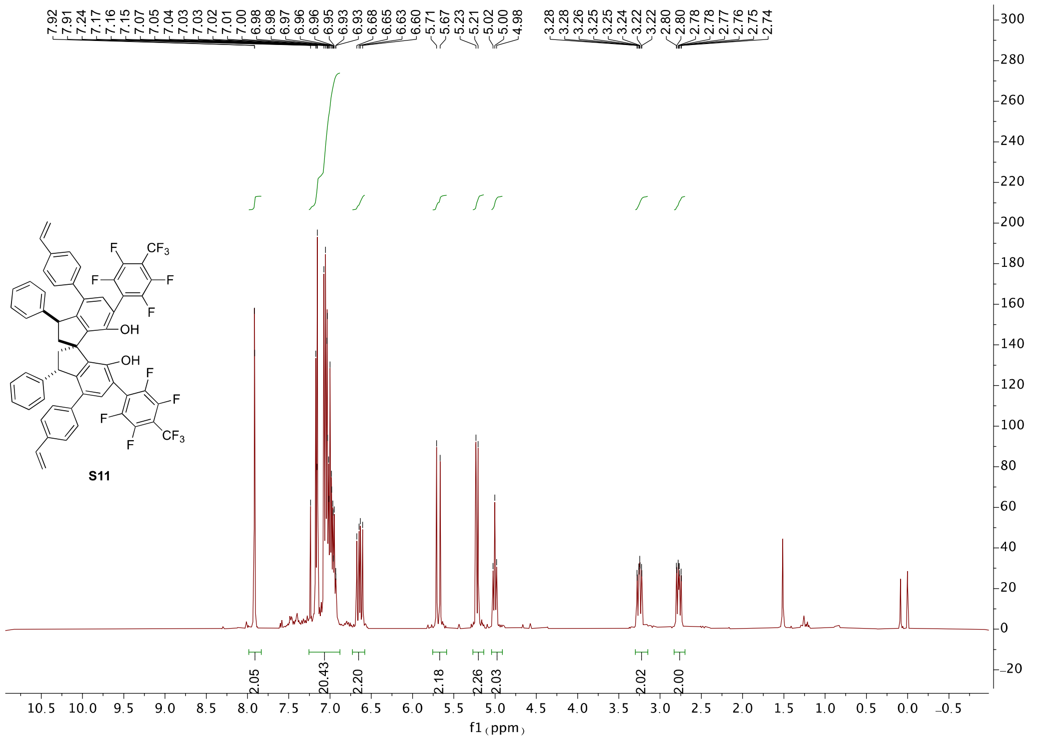

^{13}C NMR of **S11**

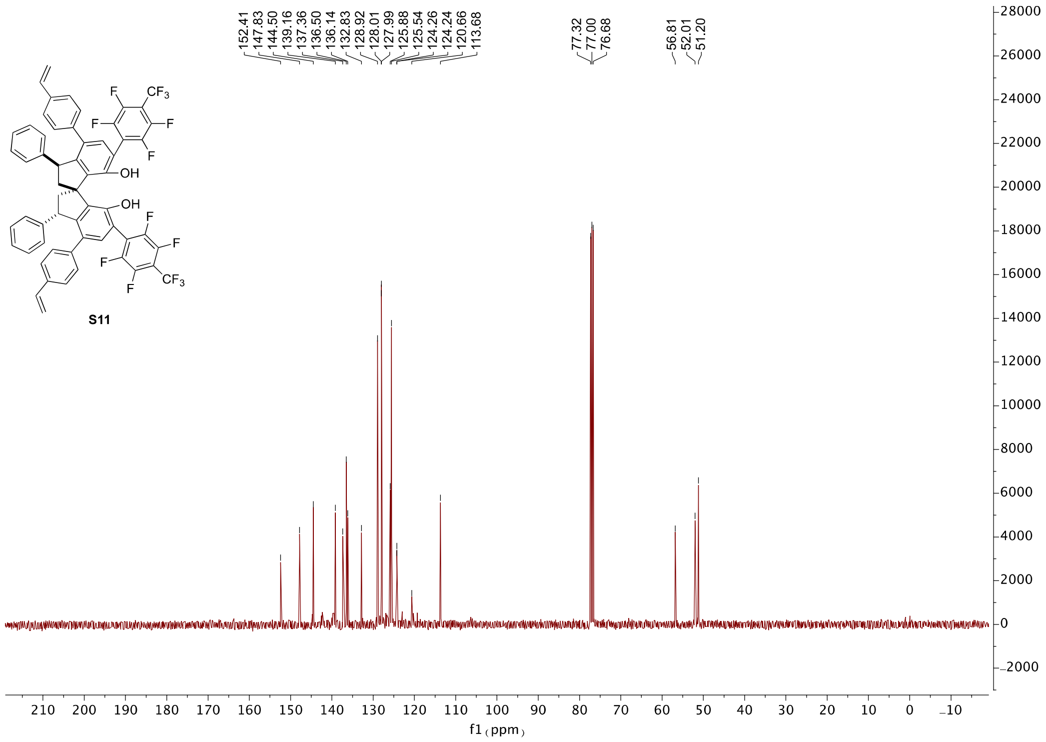

^{1}H NMR of **17**

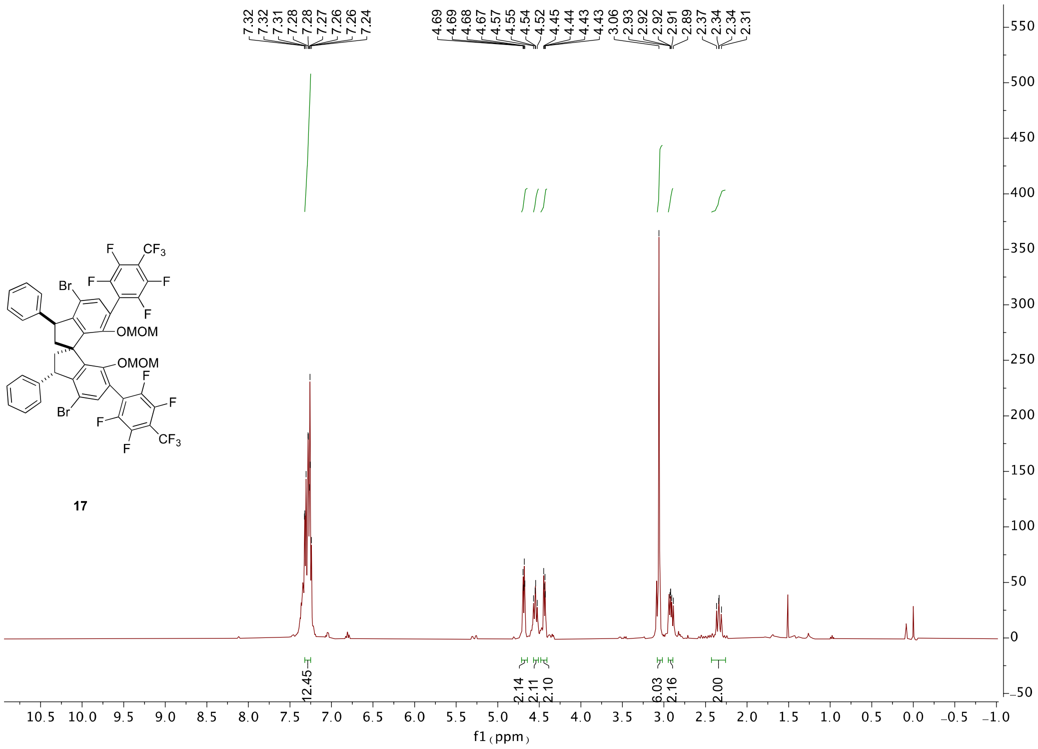

^{13}C NMR of **17**

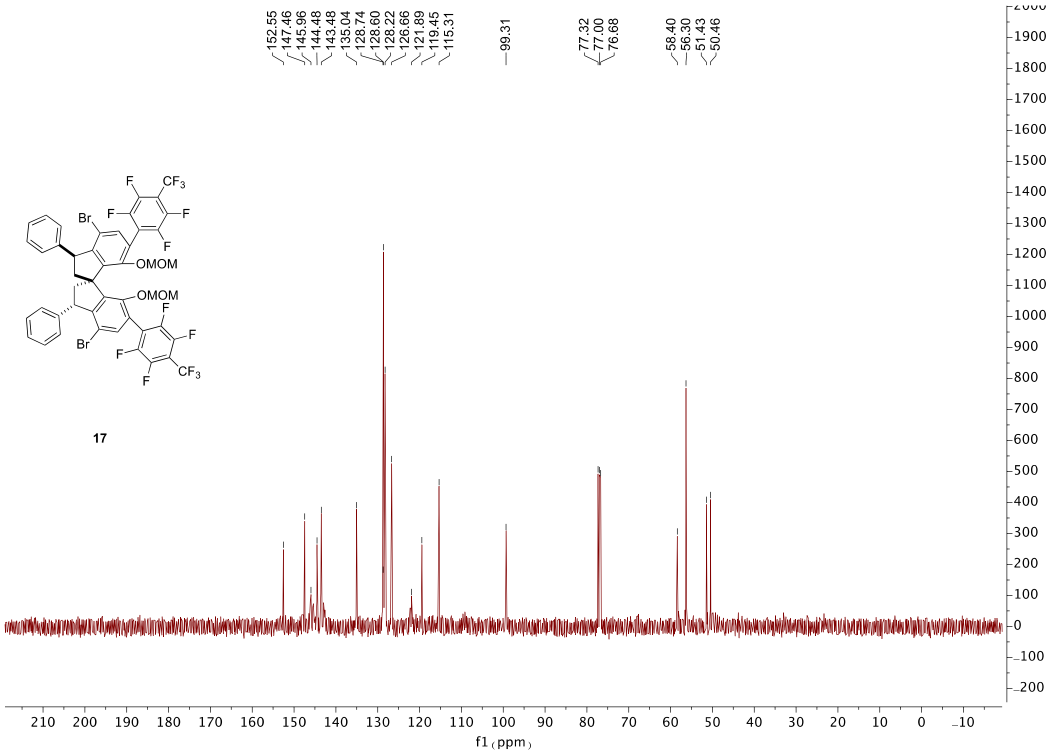

^{19}F NMR of **17**

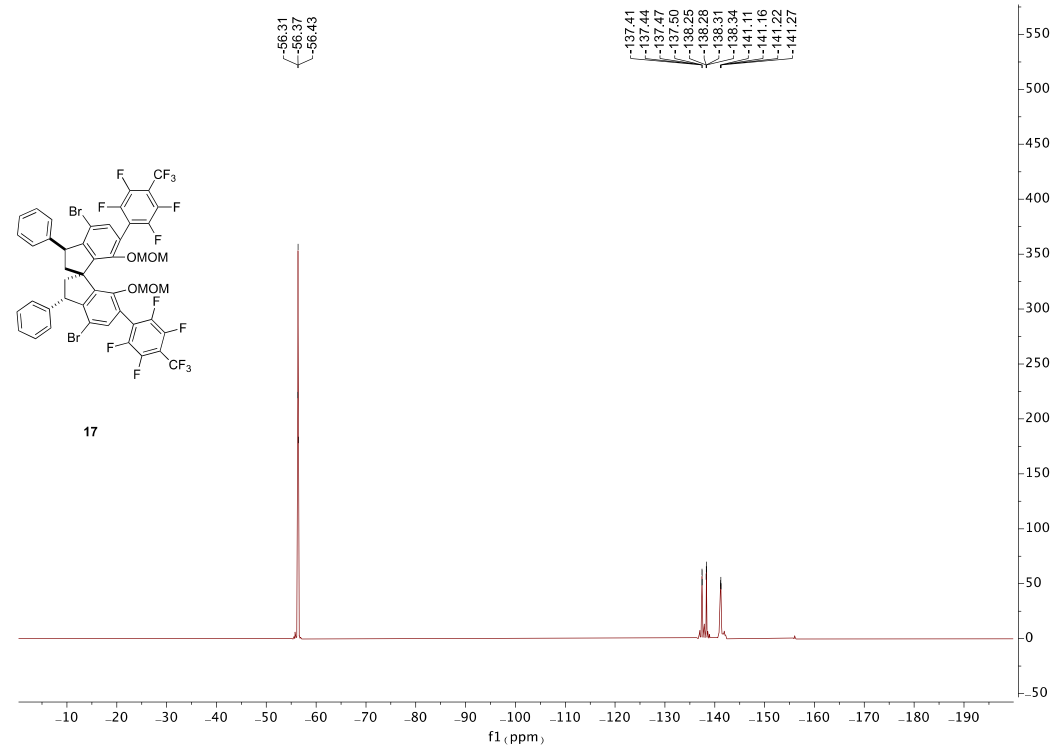

^{19}F NMR of **18**

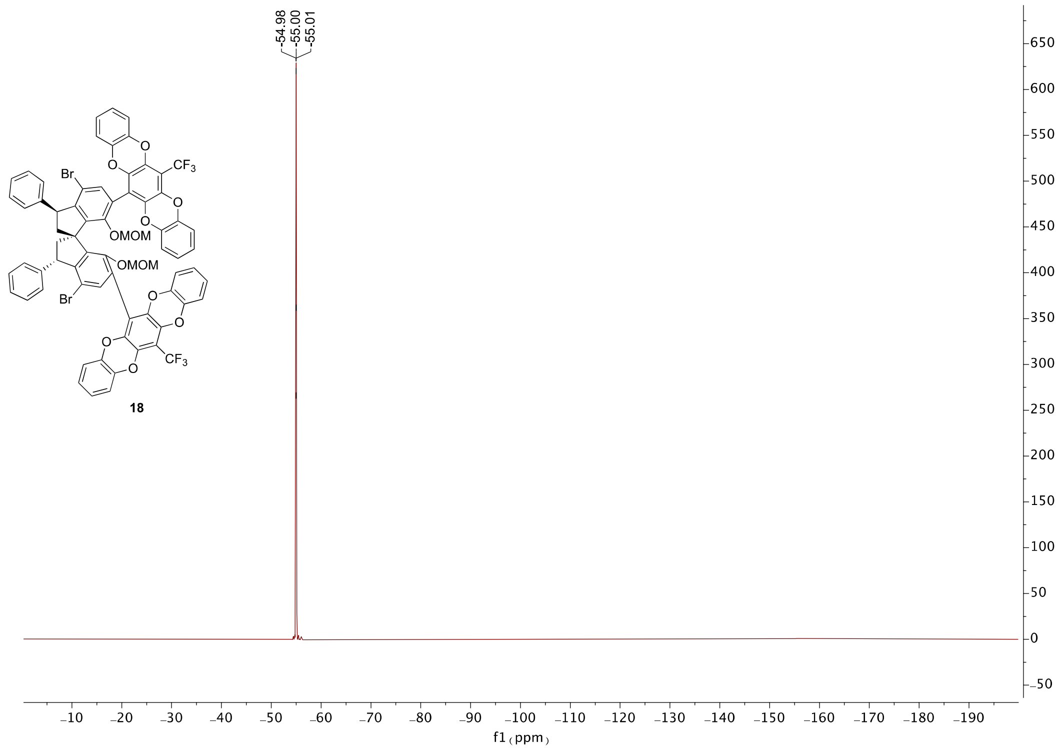

^{1}H NMR of **18**

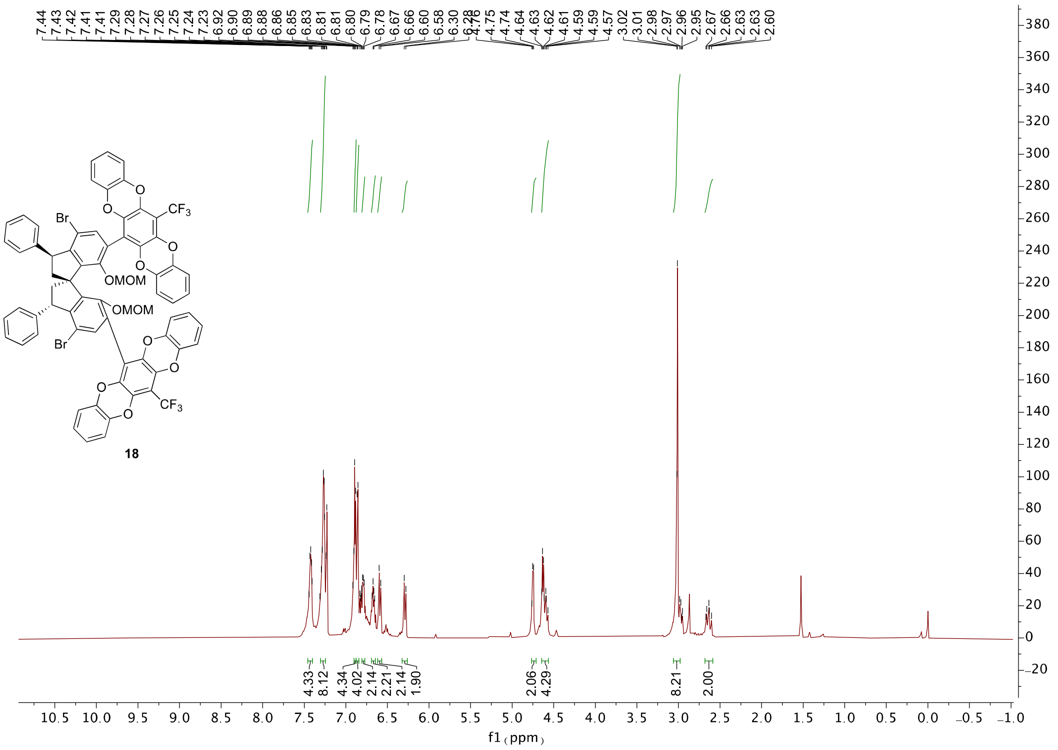

^{13}C NMR of **18**

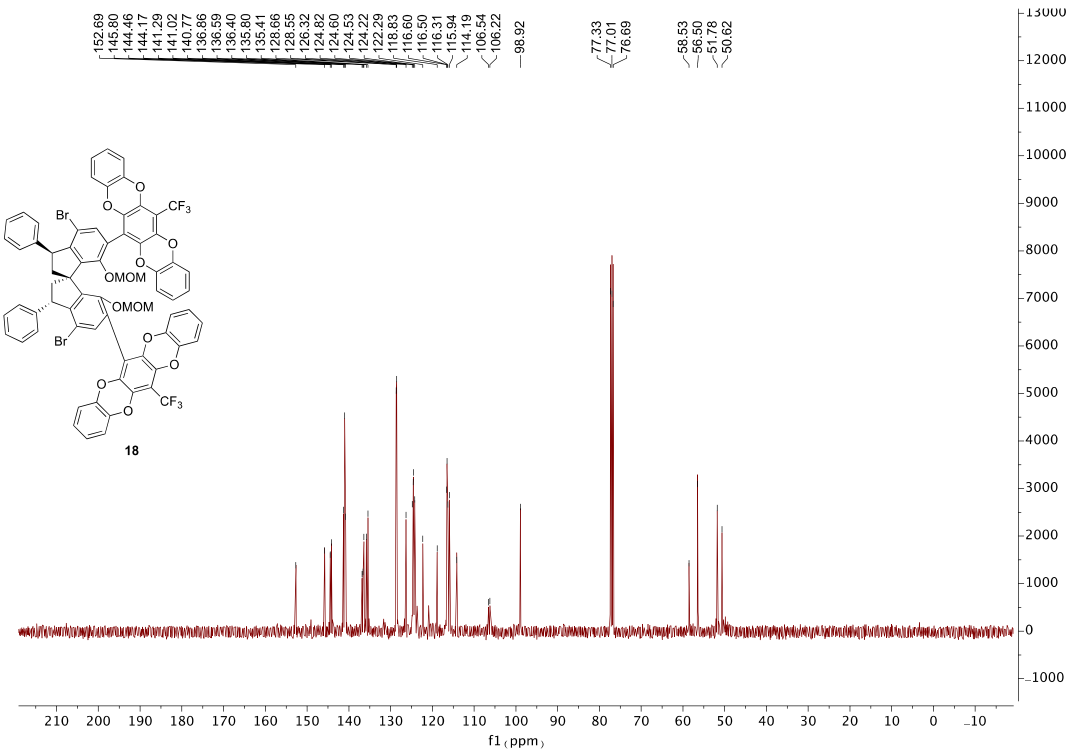

^{1}H NMR of **19**

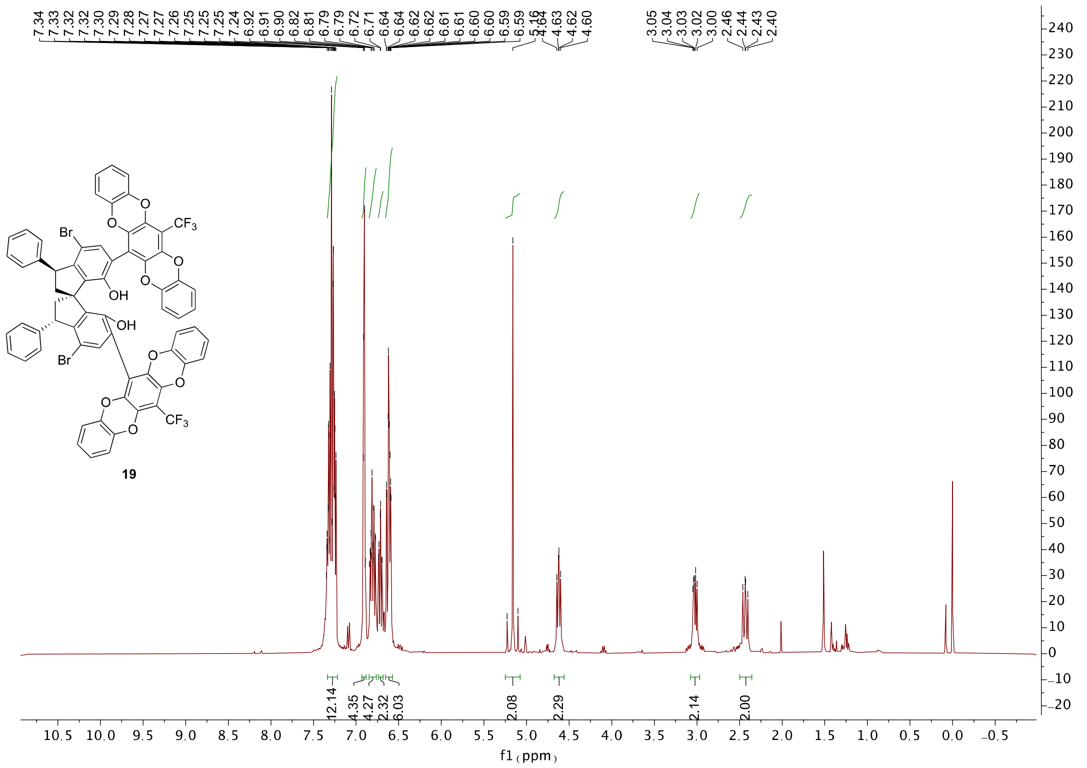

^{13}C NMR of **19**

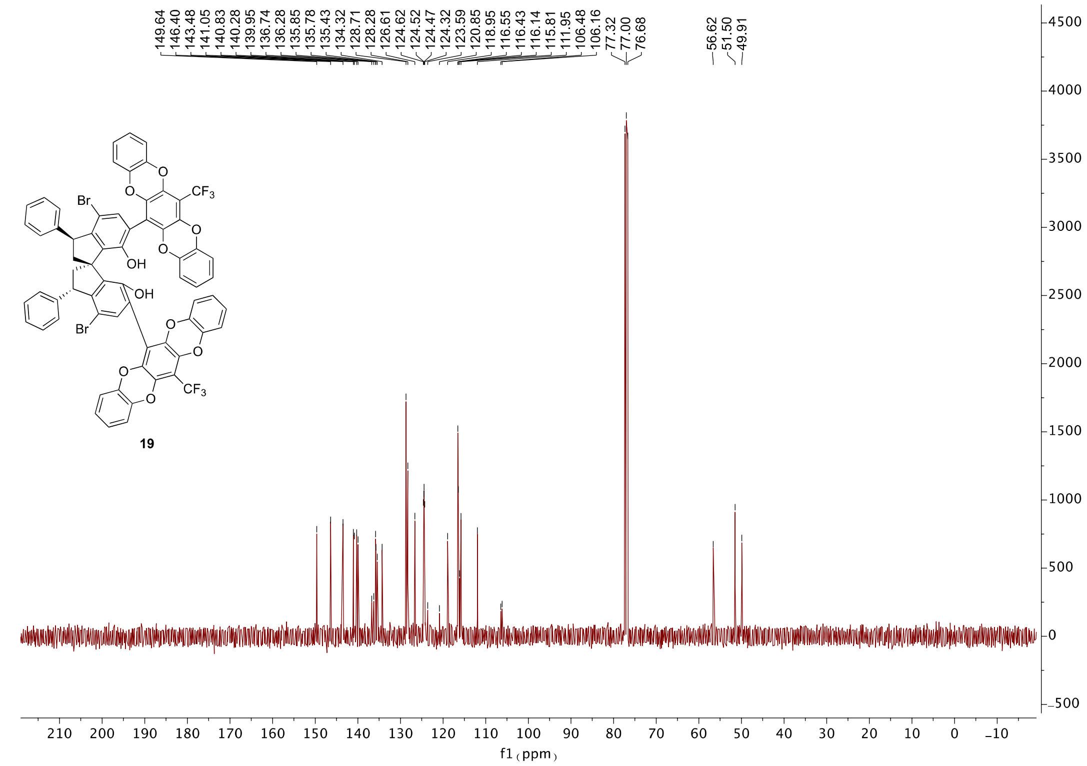

^{19}F NMR of **19**

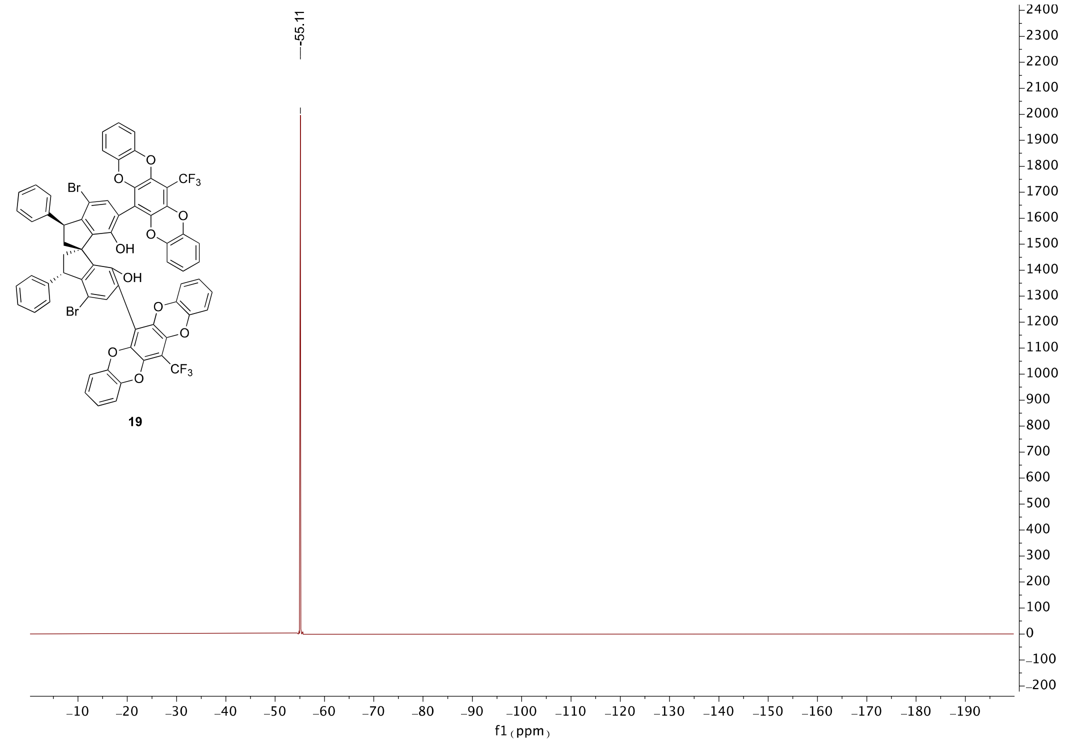

^{19}F NMR of **20**

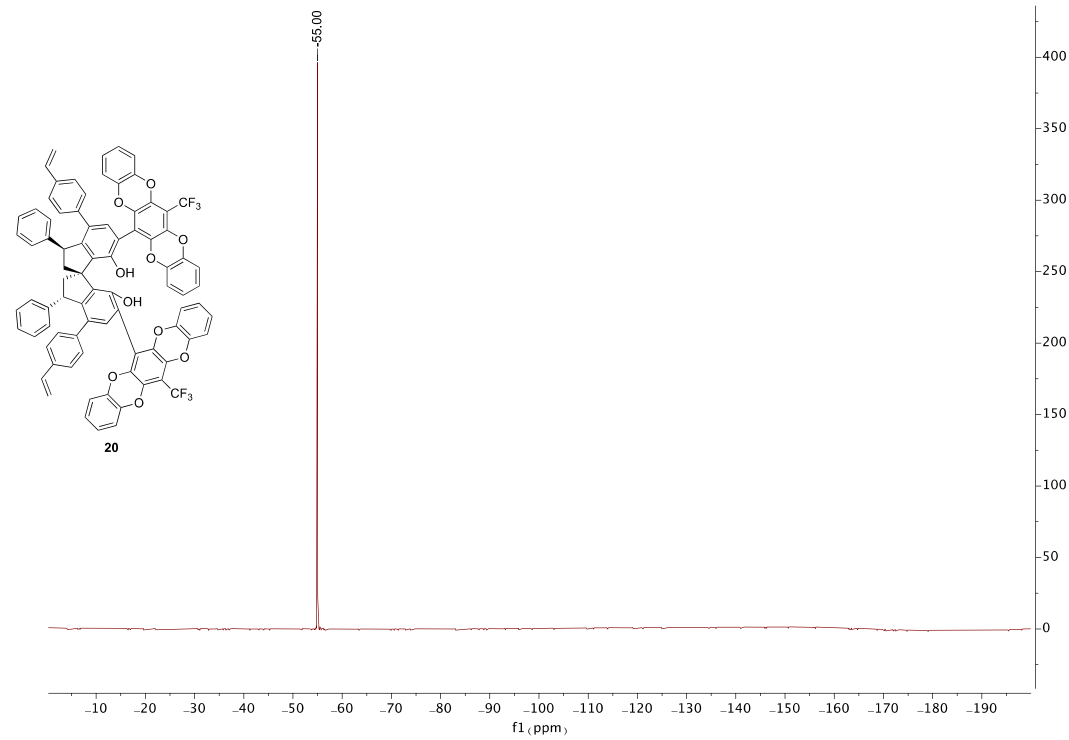

^{1}H NMR of **20**

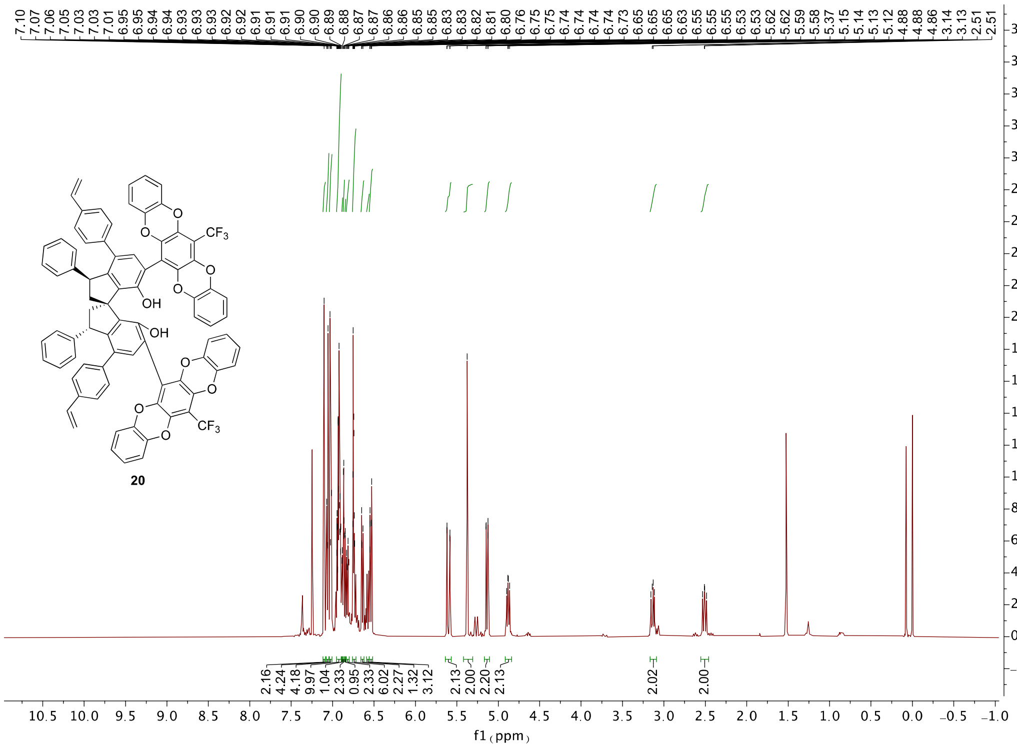

^{13}C NMR of **20**

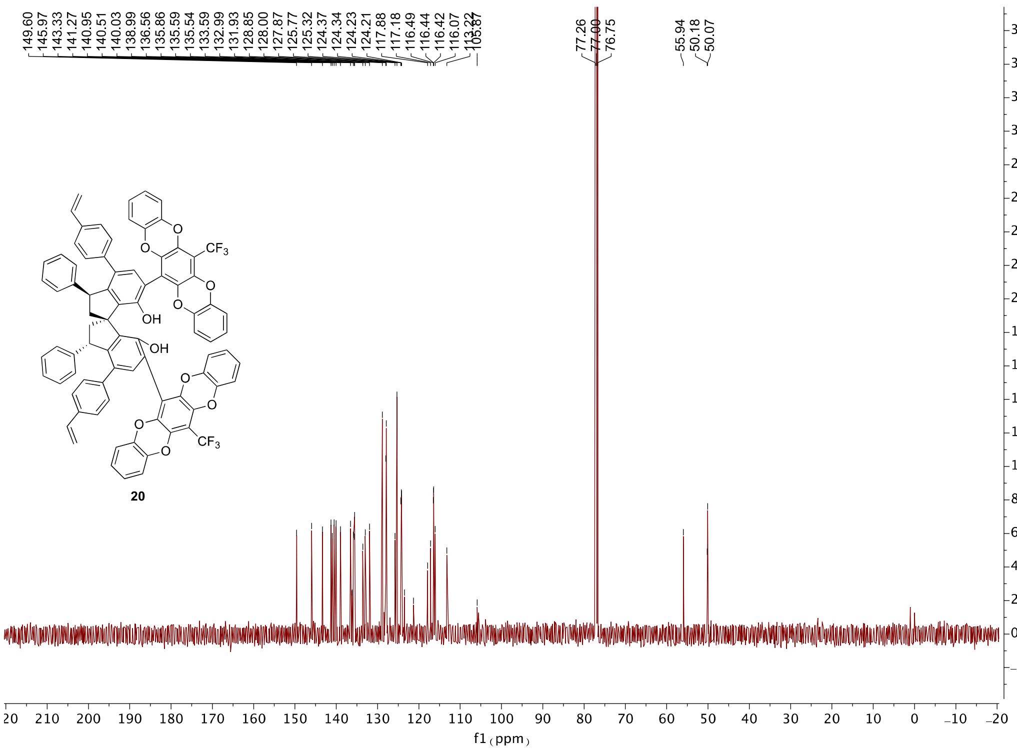

[1]H NMR of **28**

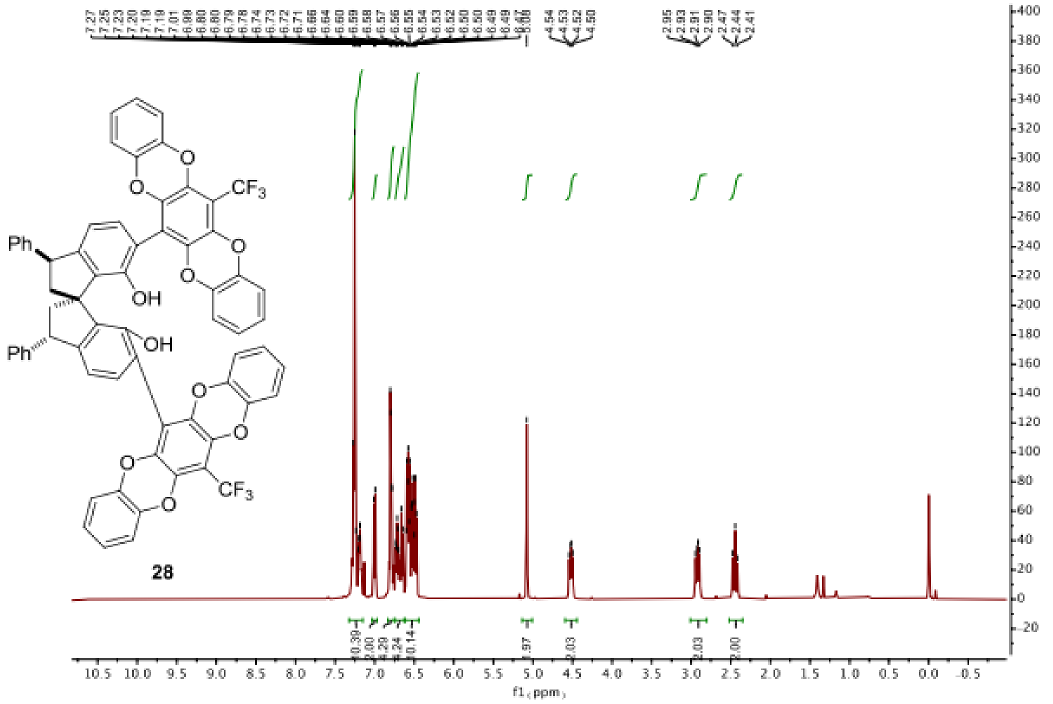

[13]C NMR of **28**

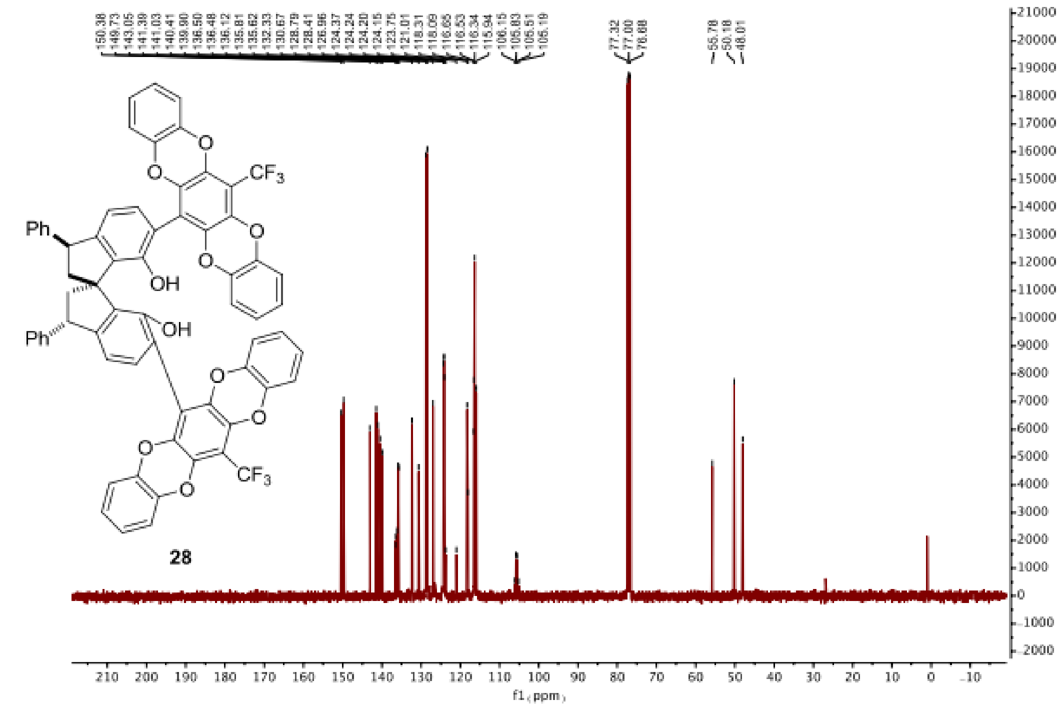

^{19}F NMR of **28**

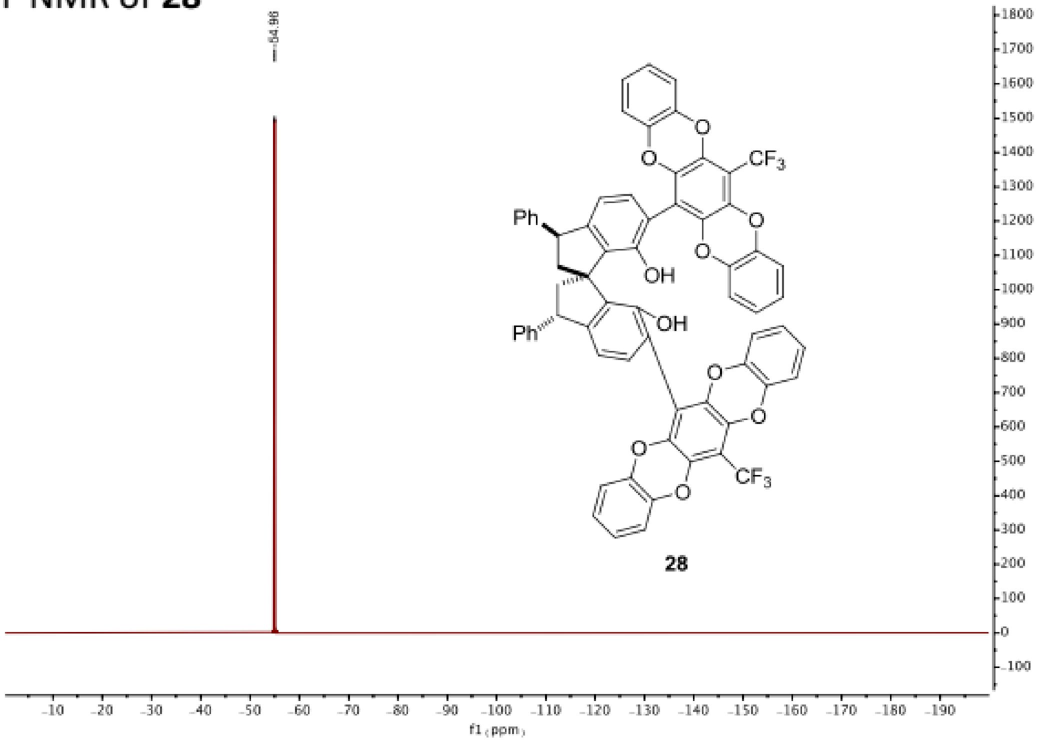
-54.96
CF3
O
OH
Ph
28
f1 (ppm)
-10
-20
-30
-40
-50
-60
-70
-80
-90
-100
-110
-120
-130
-140
-150
-160
-170
-180
-190
1800
1700
1600
1500
1400
1300
1200
1100
1000
900
800
700
600
500
400
300
200
100
0
-100

^{1}H NMR of **Cat g**

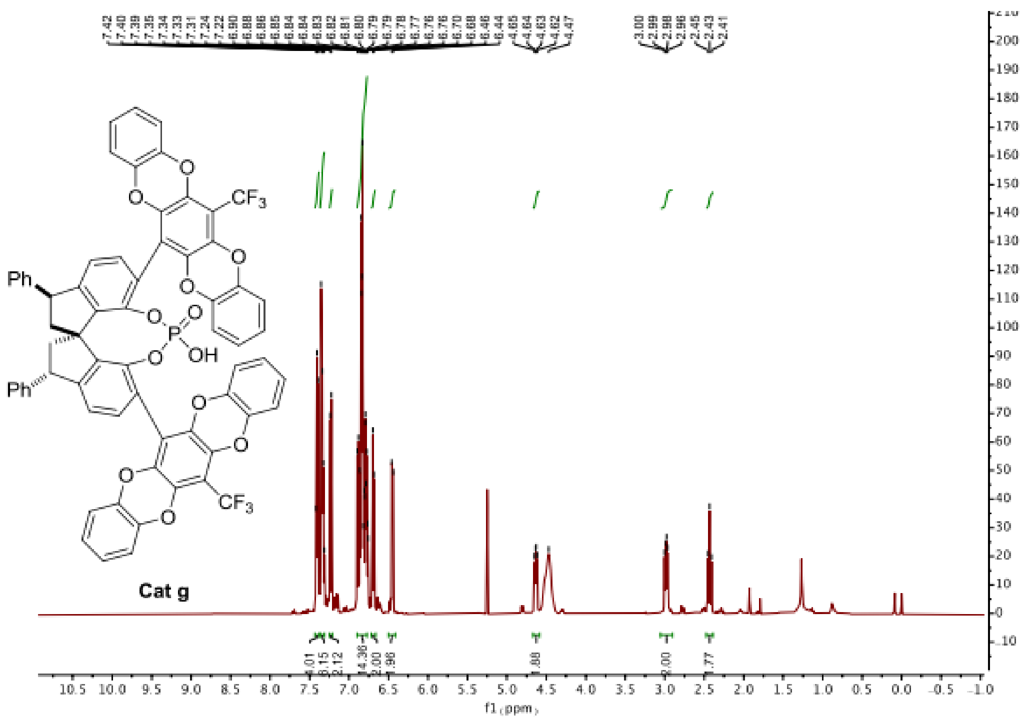

^{13}C NMR of **Cat g**

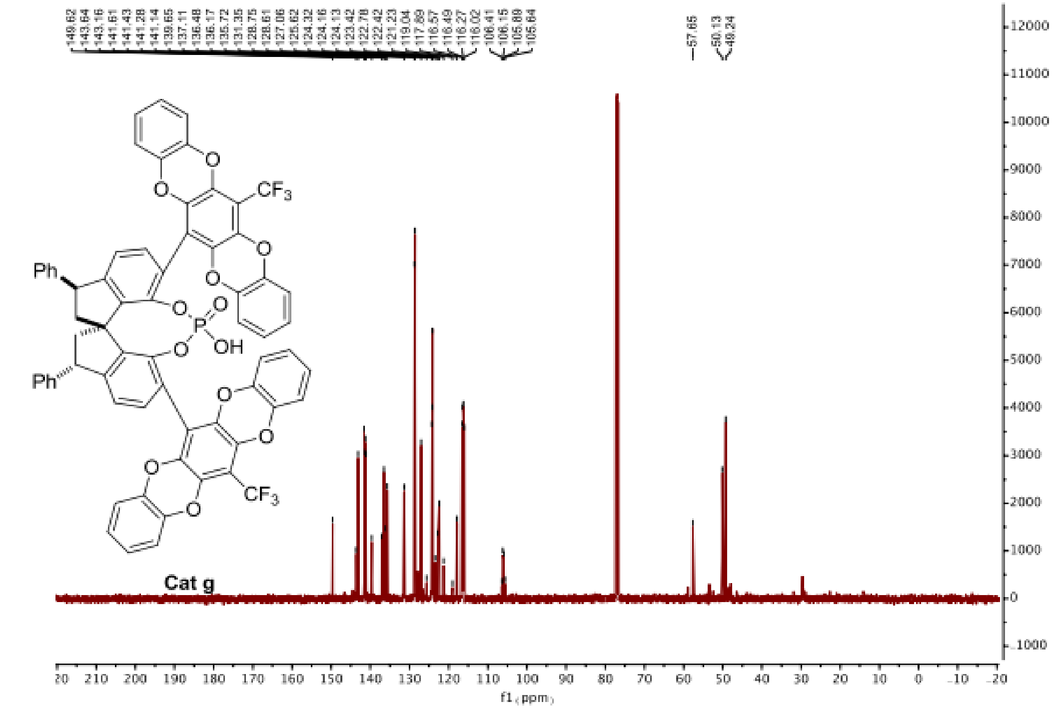

^{19}F NMR of **Cat g**

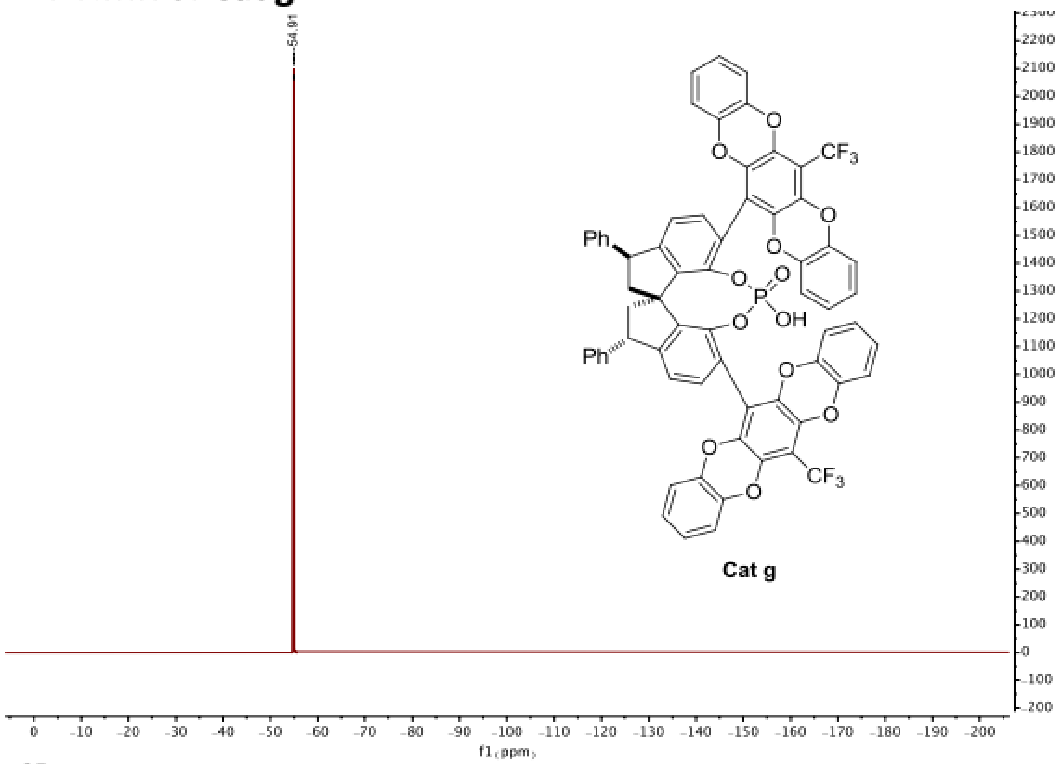

^{35}P NMR of **Cat g**

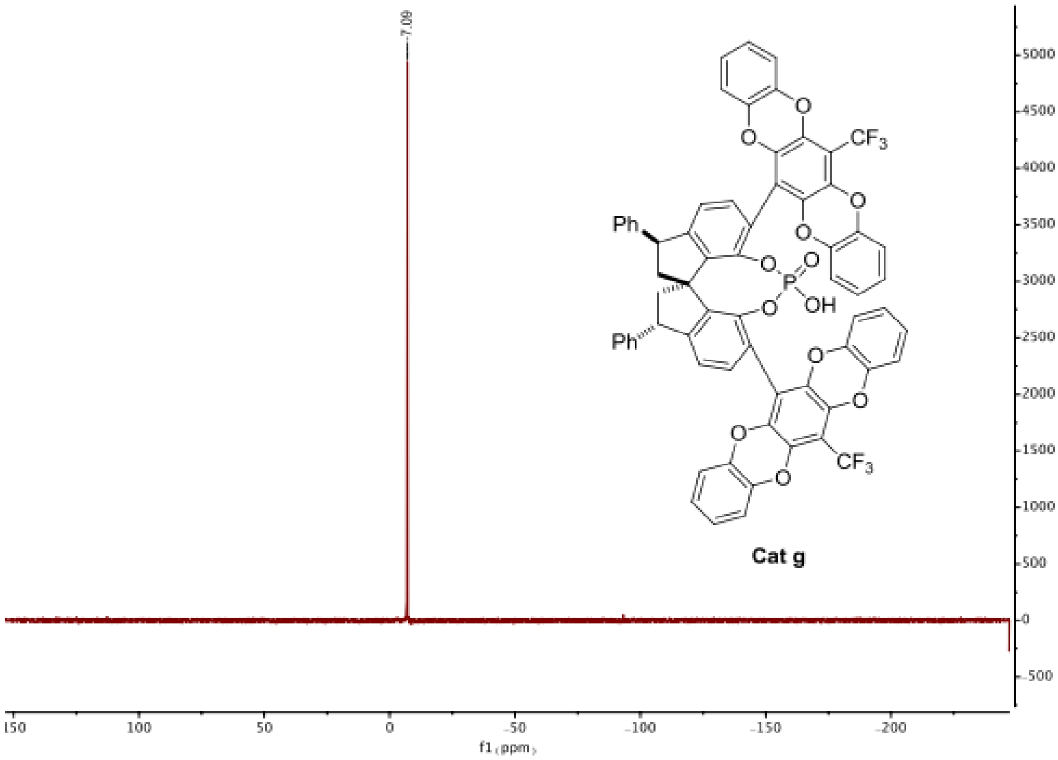

^{1}H NMR of **24aa**

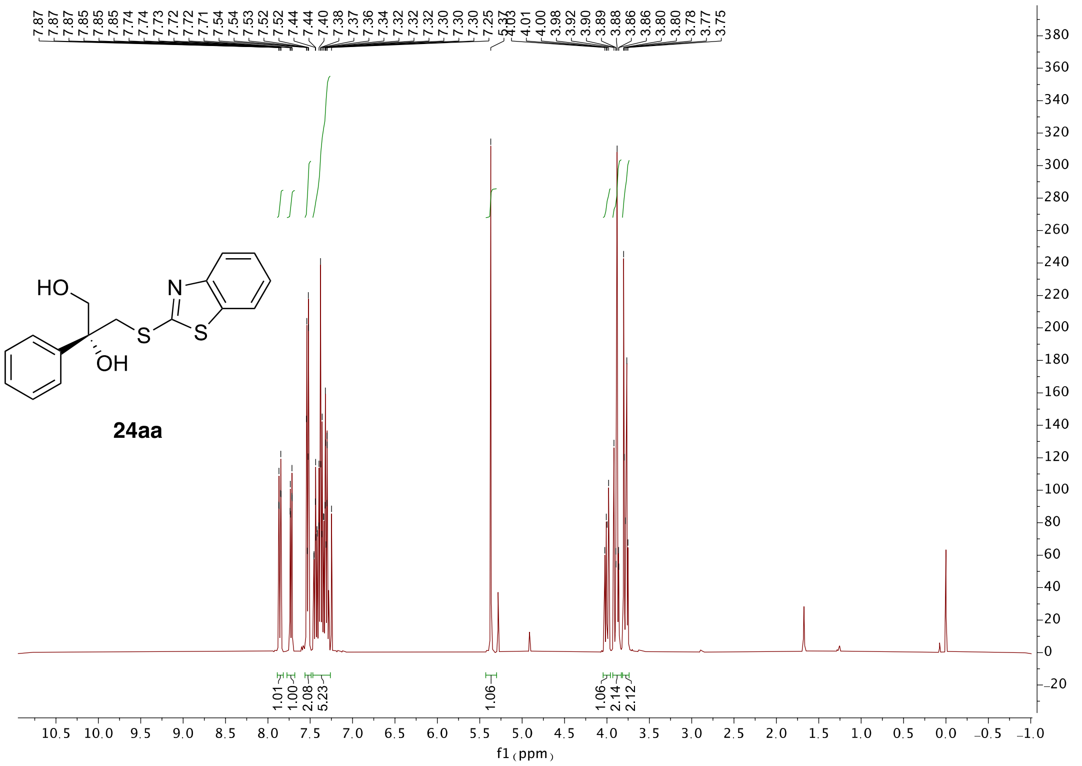

^{13}C NMR of **24aa**

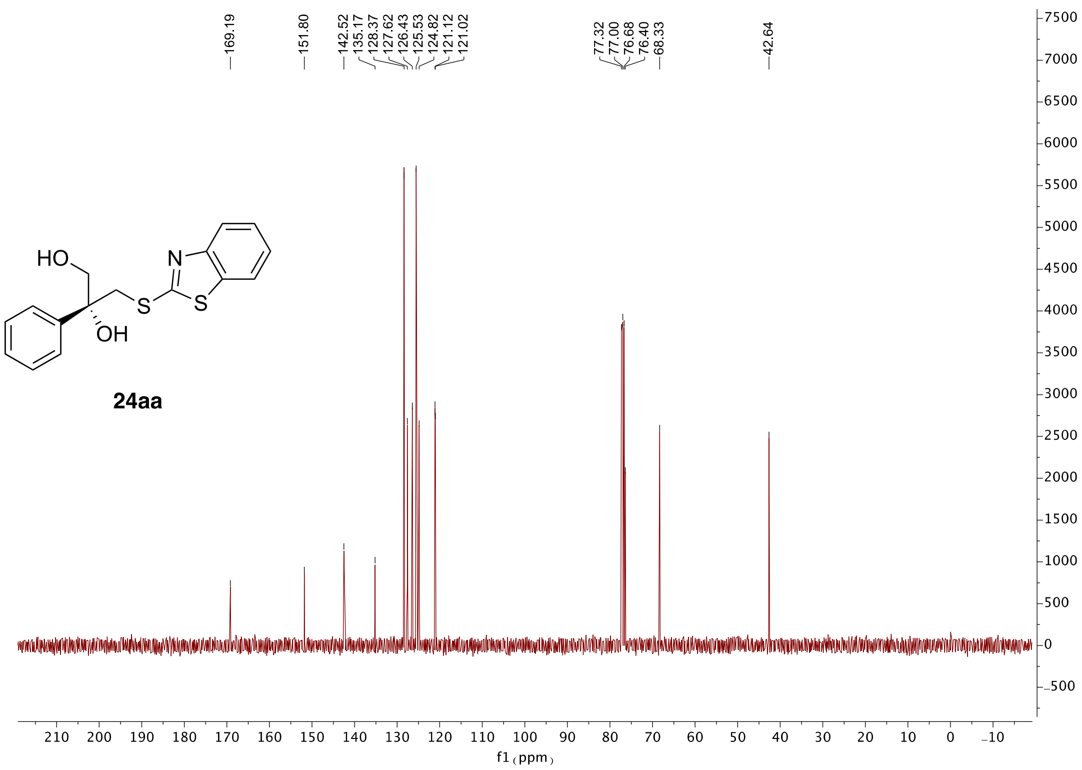

^{1}H NMR of **24ba**

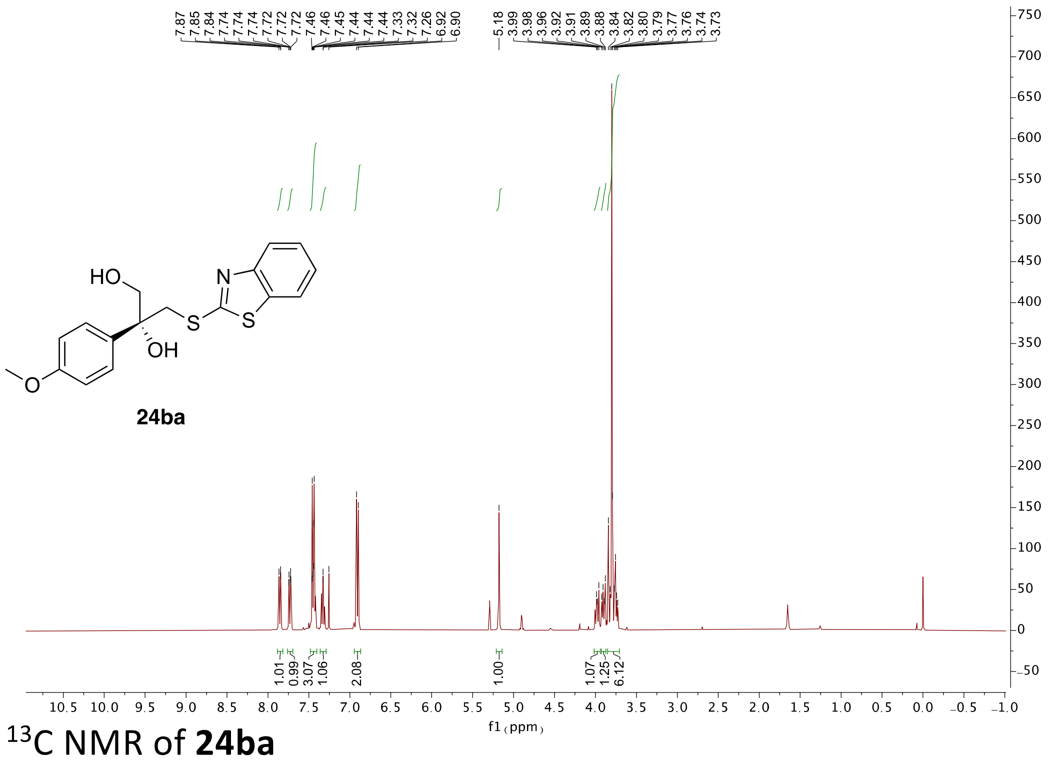

^{13}C NMR of **24ba**

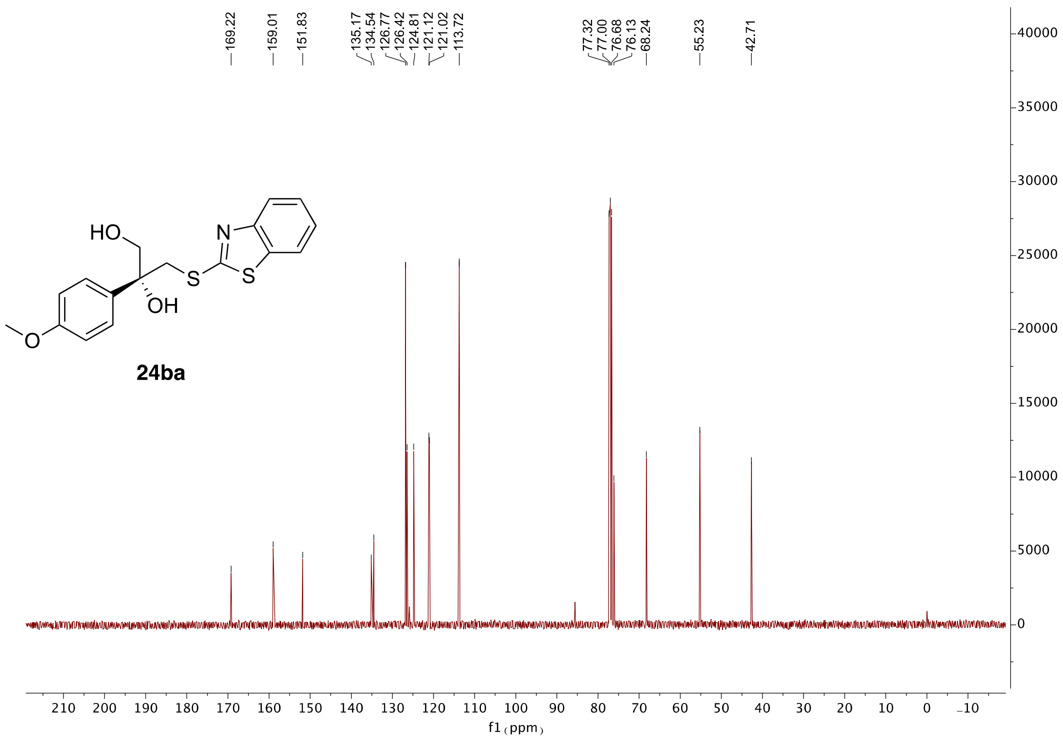

[1]H NMR of **24ca**

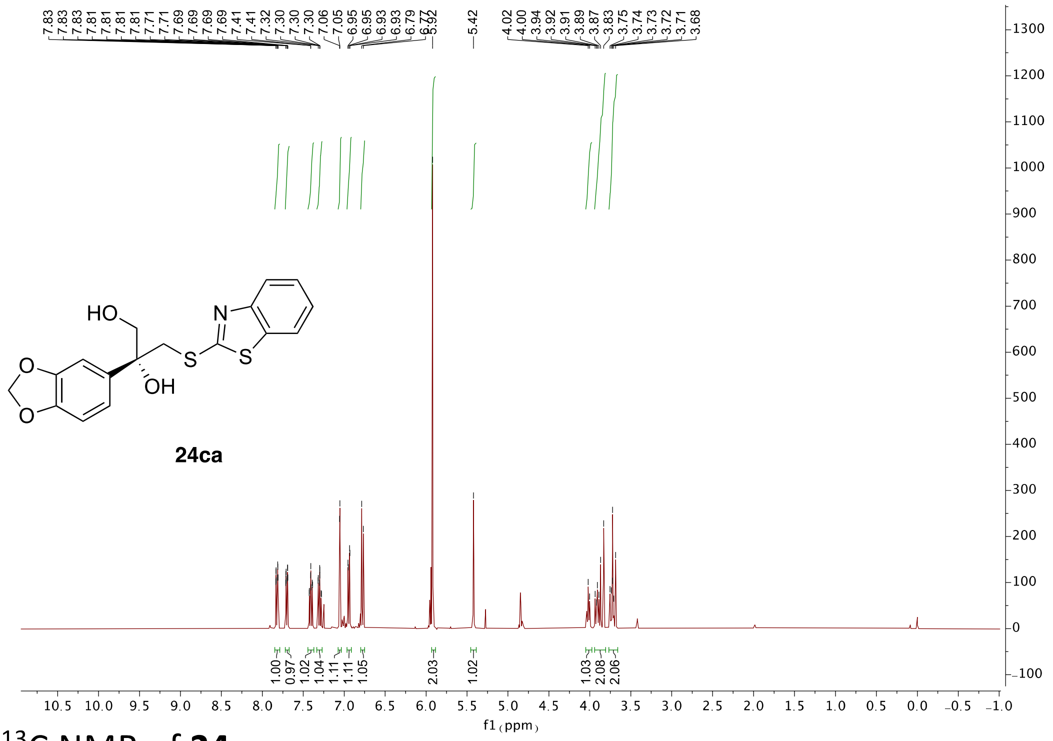

[13]C NMR of **24ca**

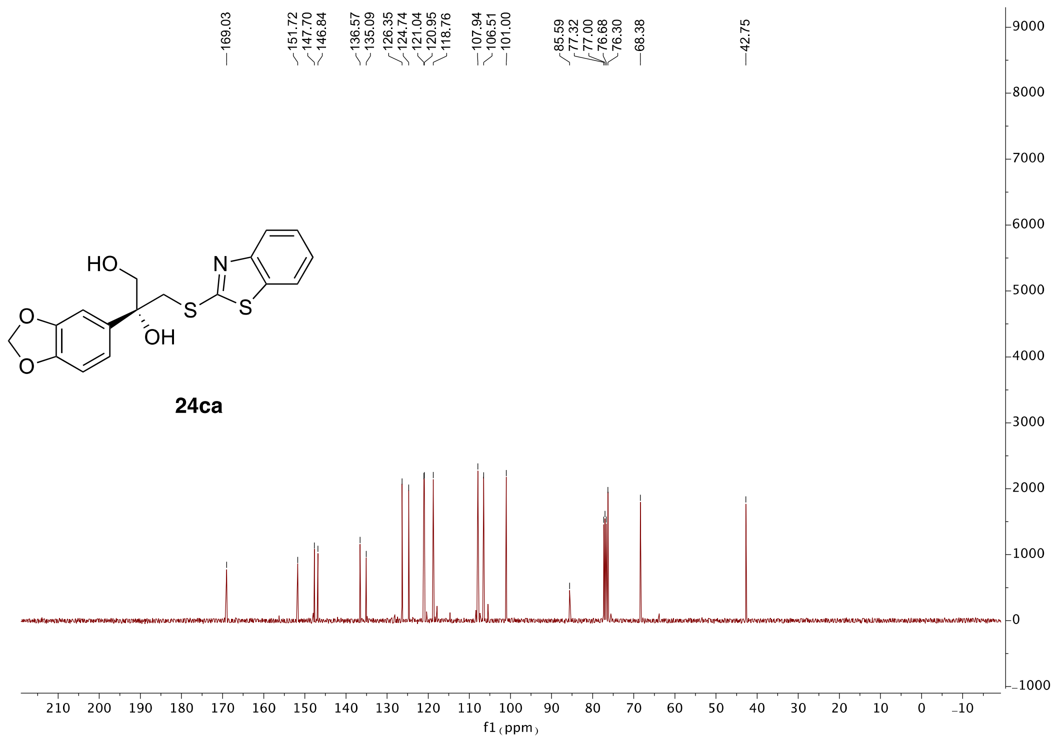

^{1}H NMR of **24da**

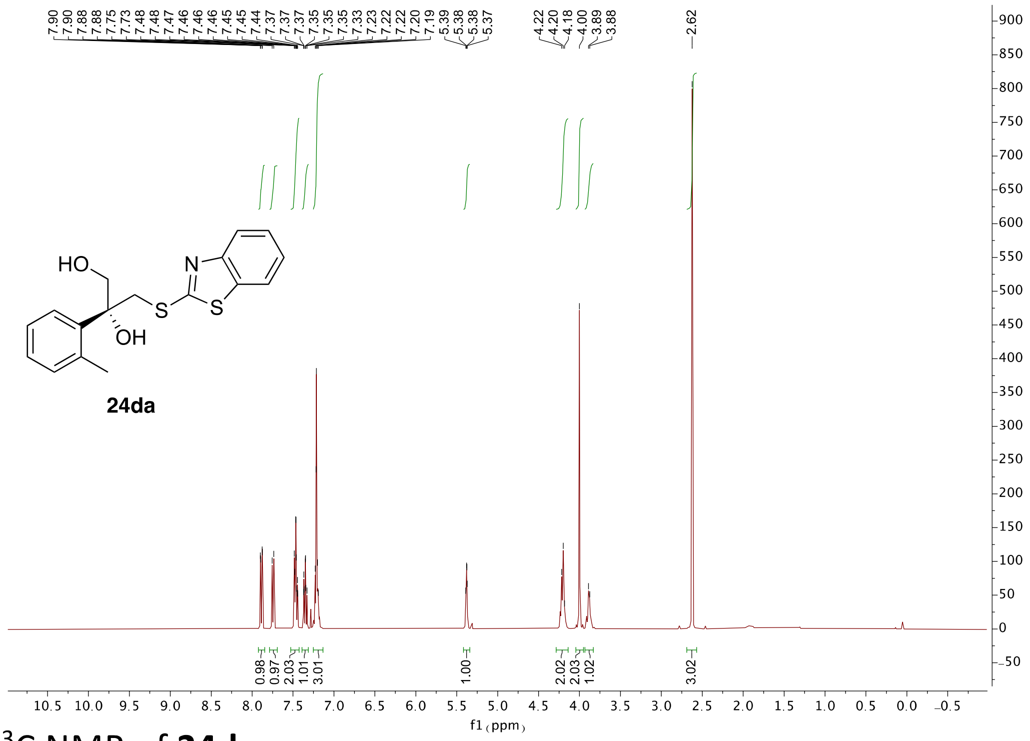

^{13}C NMR of **24da**

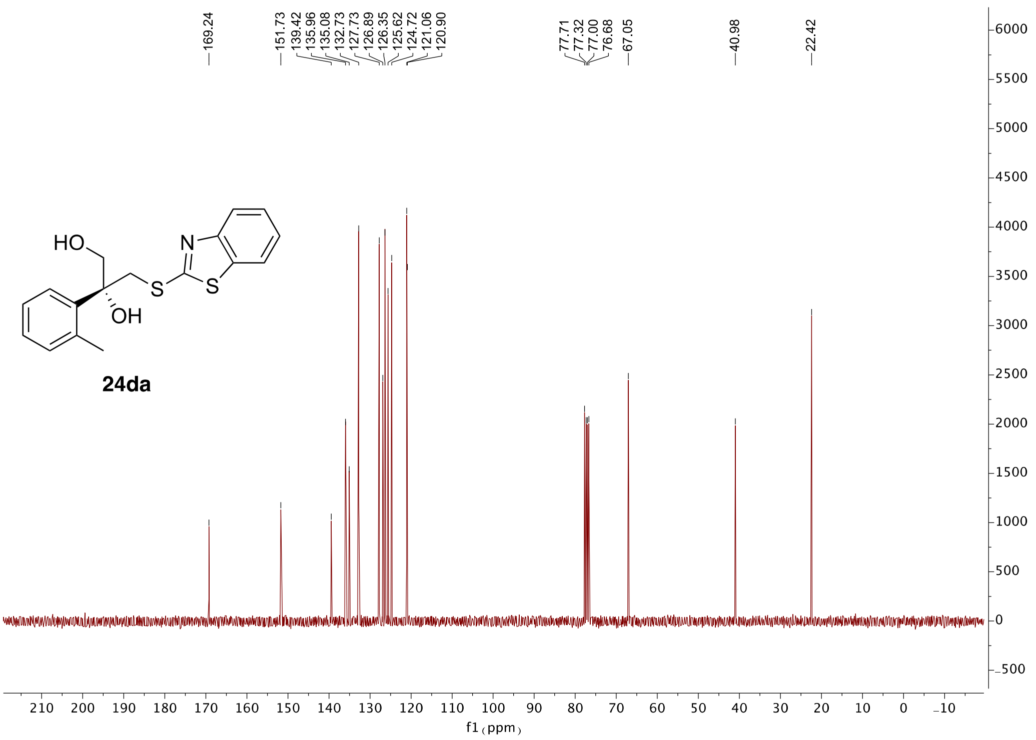

^{1}H NMR of **24ea**

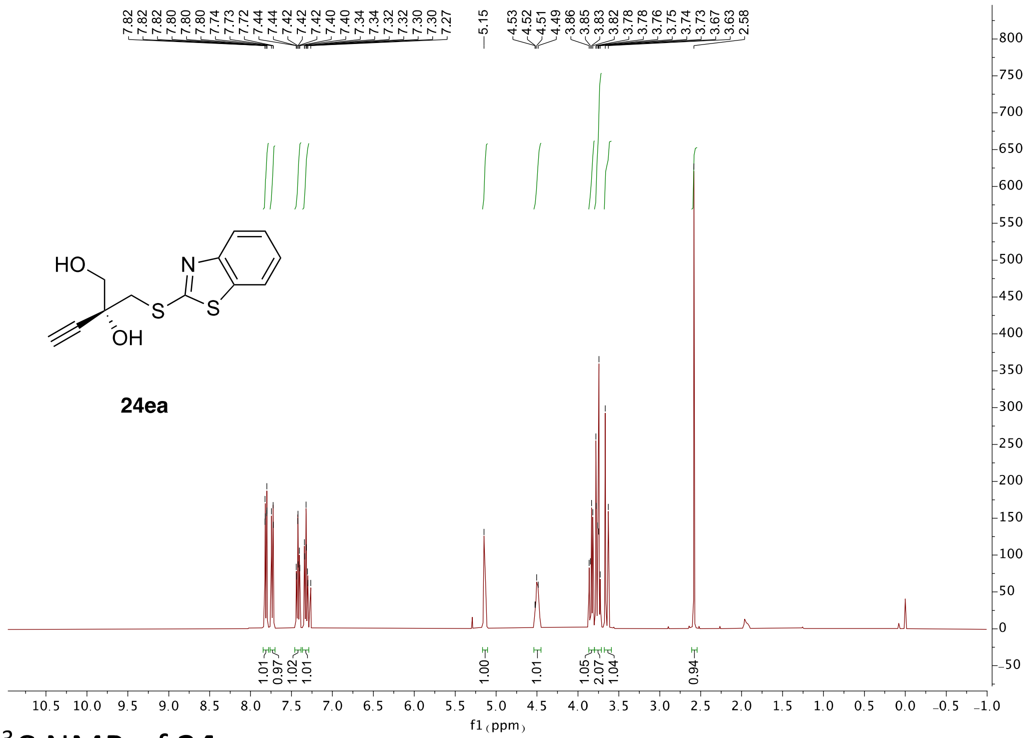

^{13}C NMR of **24ea**

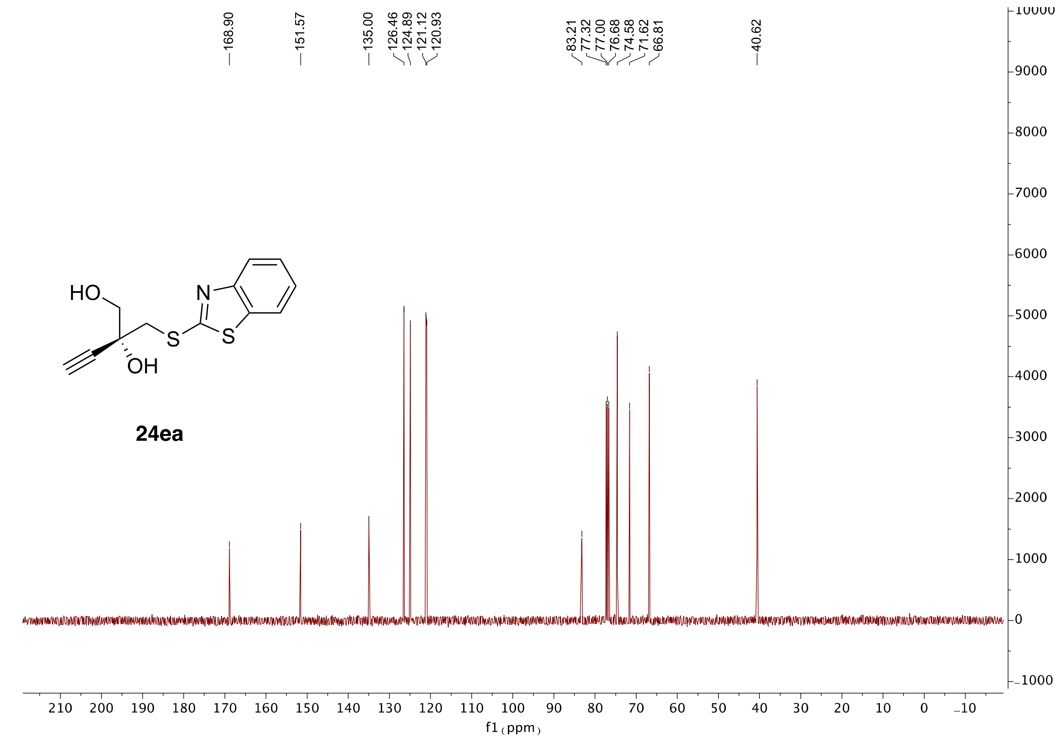

^{1}H NMR of **24fa**

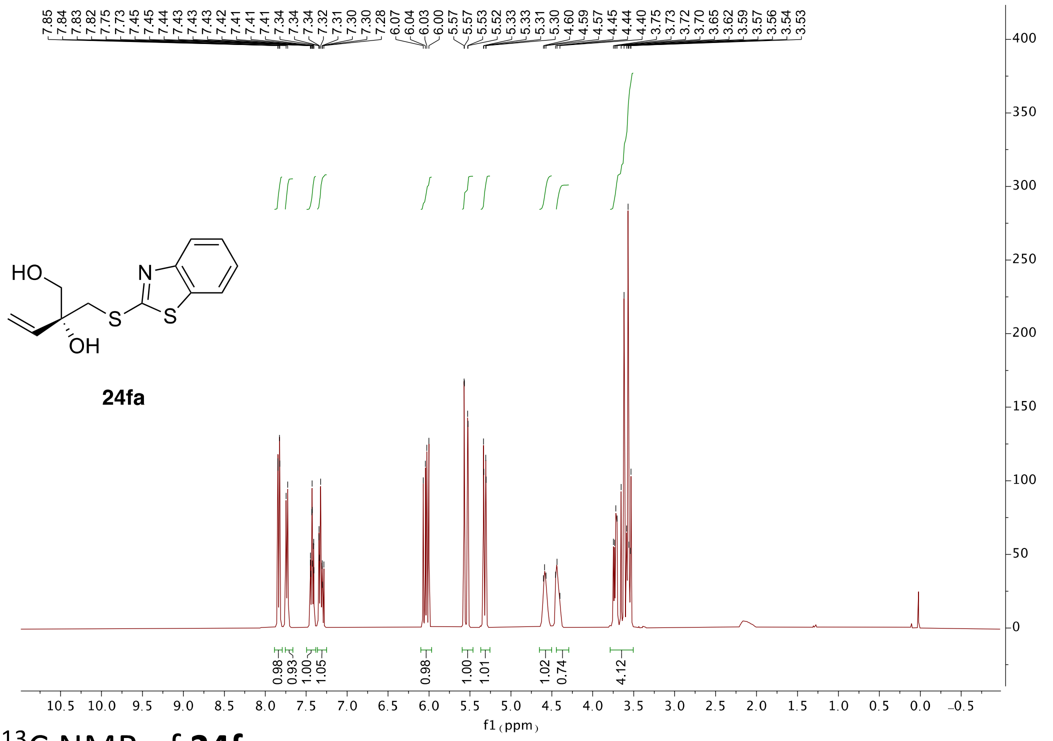

^{13}C NMR of **24fa**

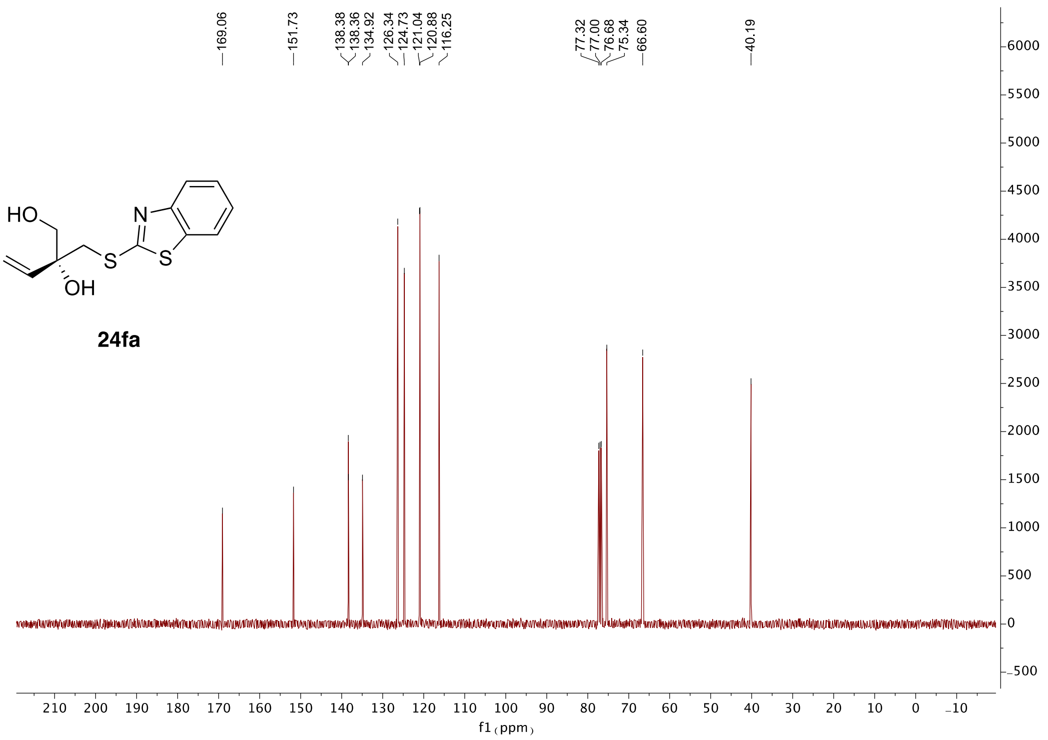

^{1}H NMR of **24ga**

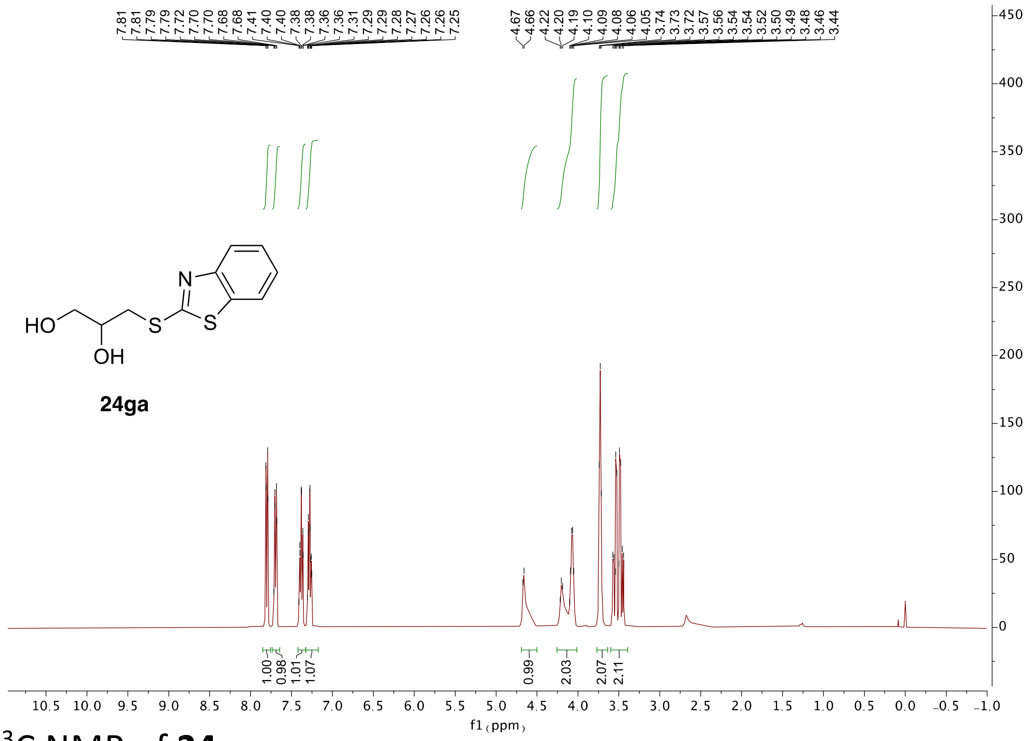

^{13}C NMR of **24ga**

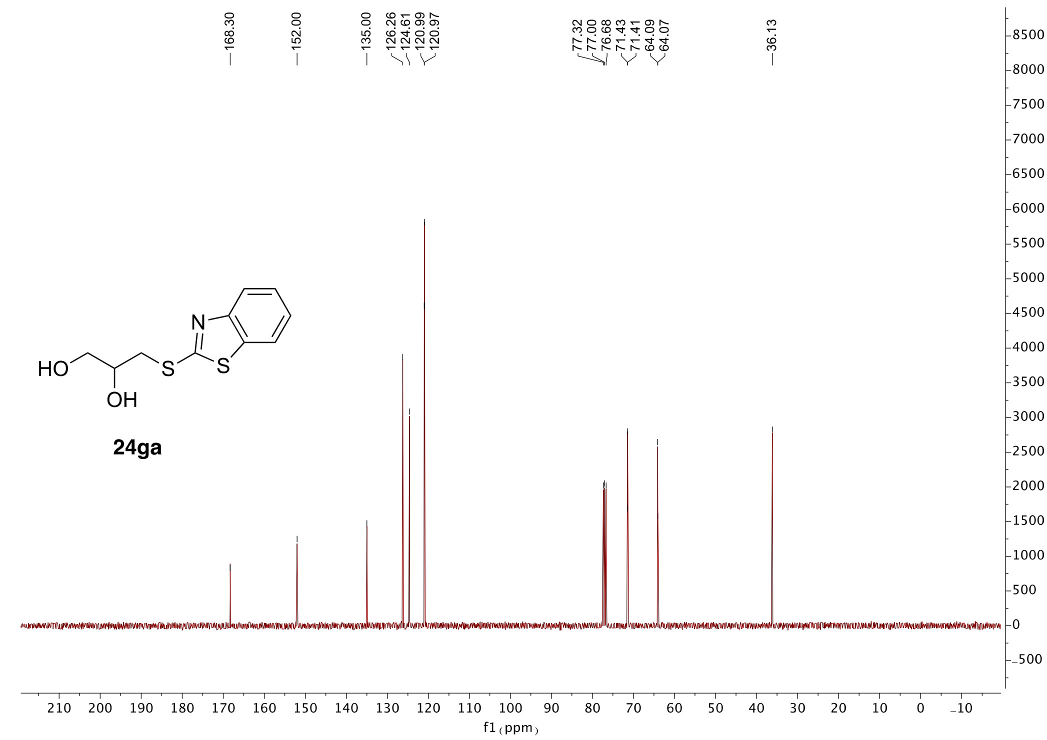

^{1}H NMR of **24ha**

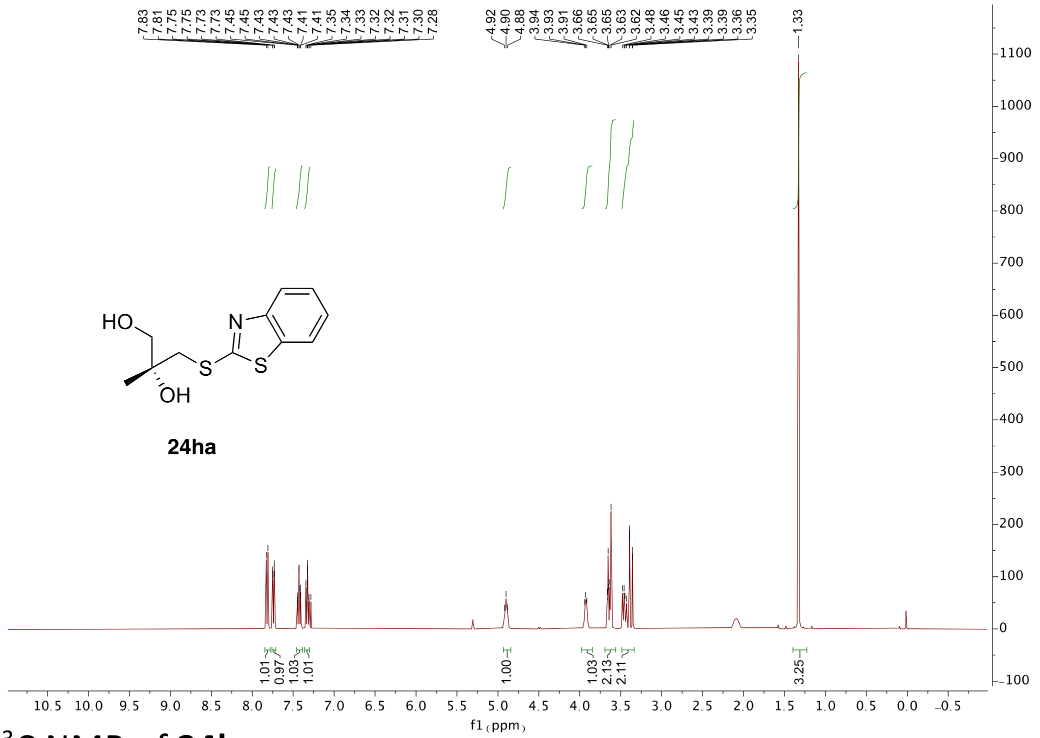

^{13}C NMR of **24ha**

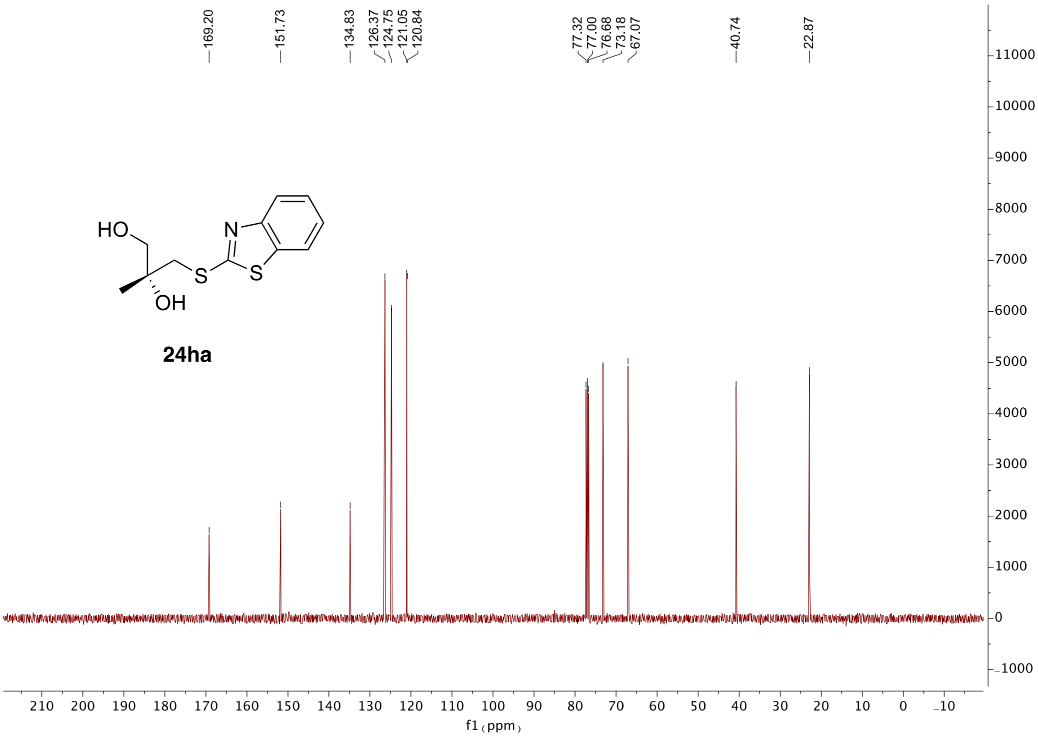

^{1}H NMR of **24ia**

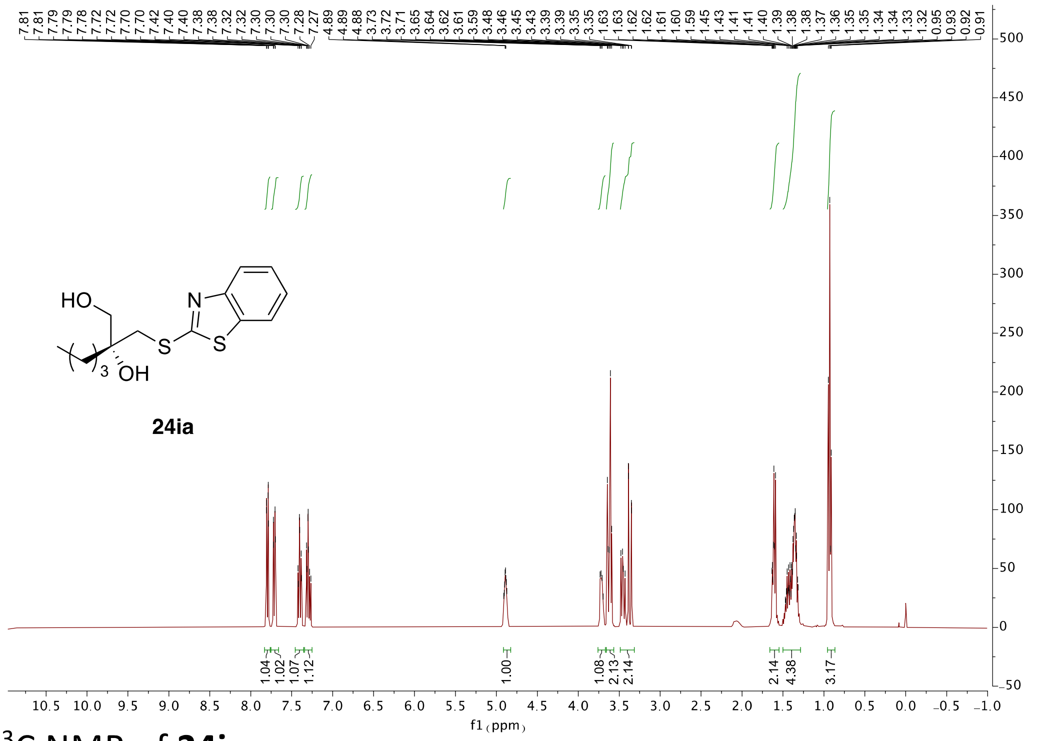

^{13}C NMR of **24ia**

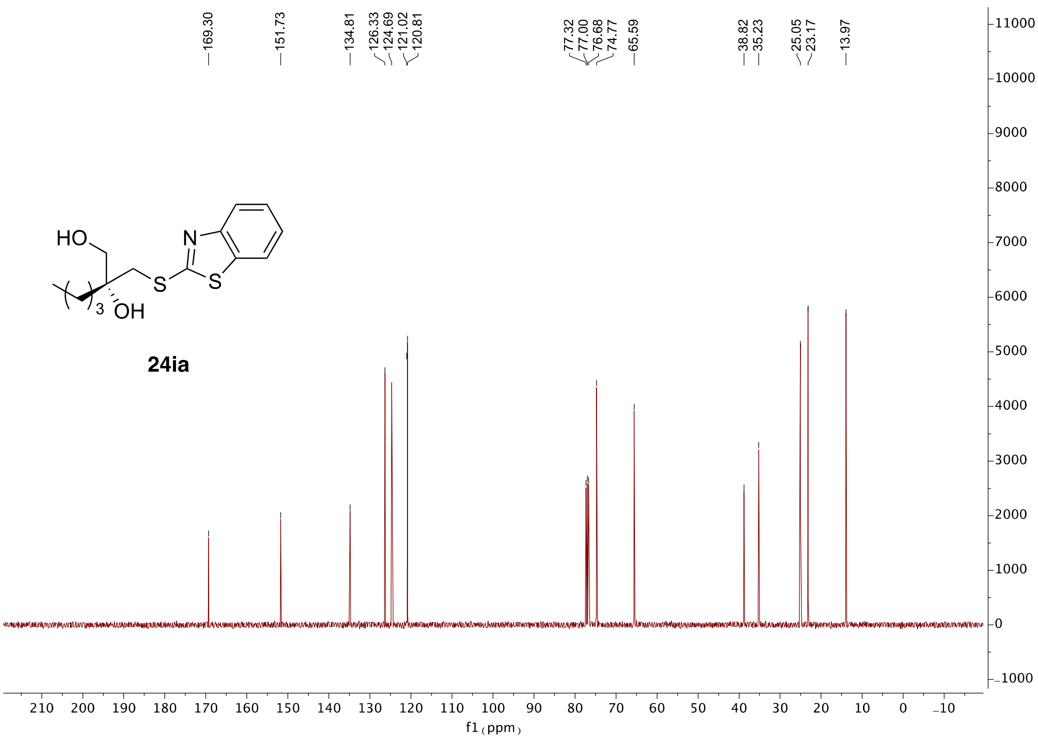

^{1}H NMR of **24ja**

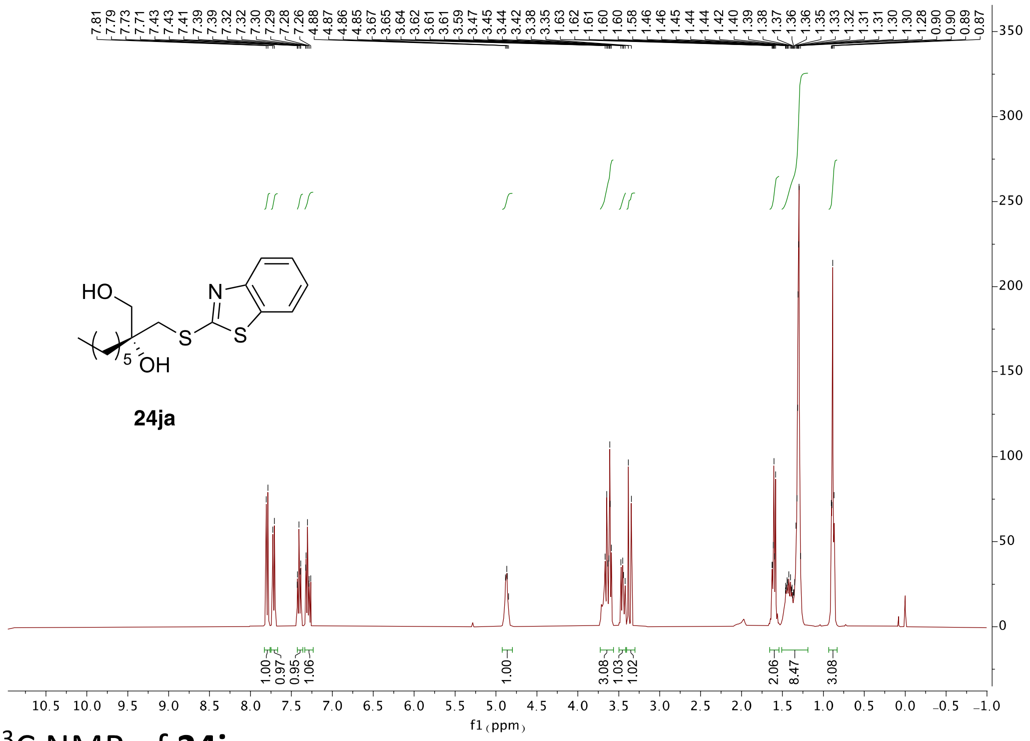

^{13}C NMR of **24ja**

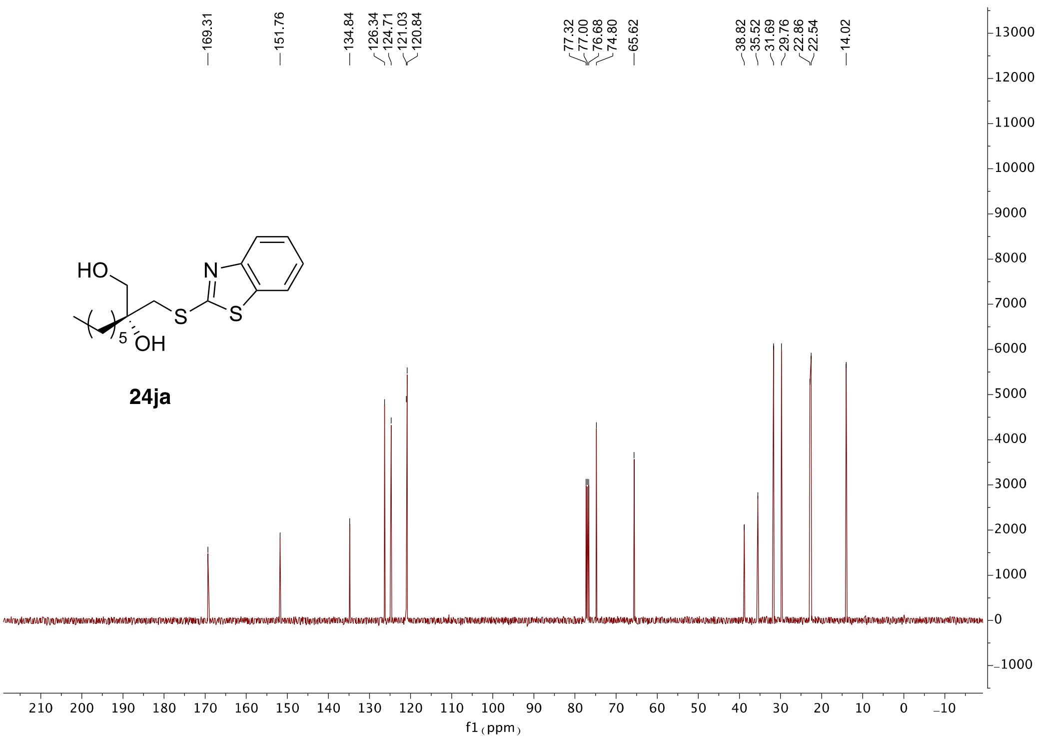

^{1}H NMR of **24ka**

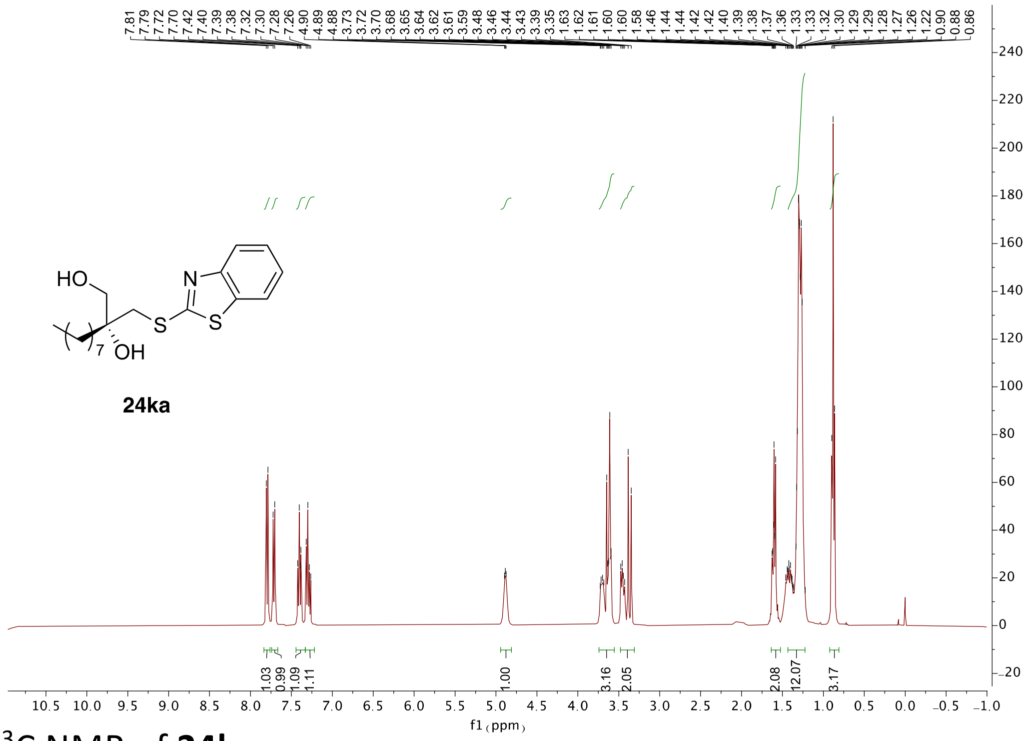

^{13}C NMR of **24ka**

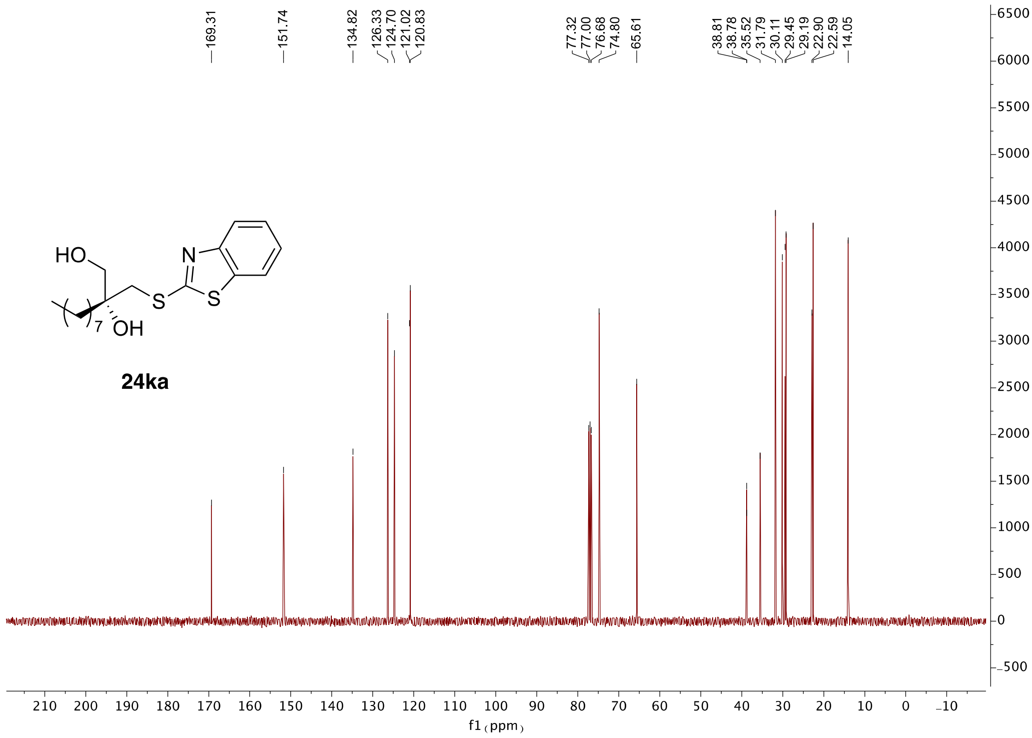

^{1}H NMR of **24la**

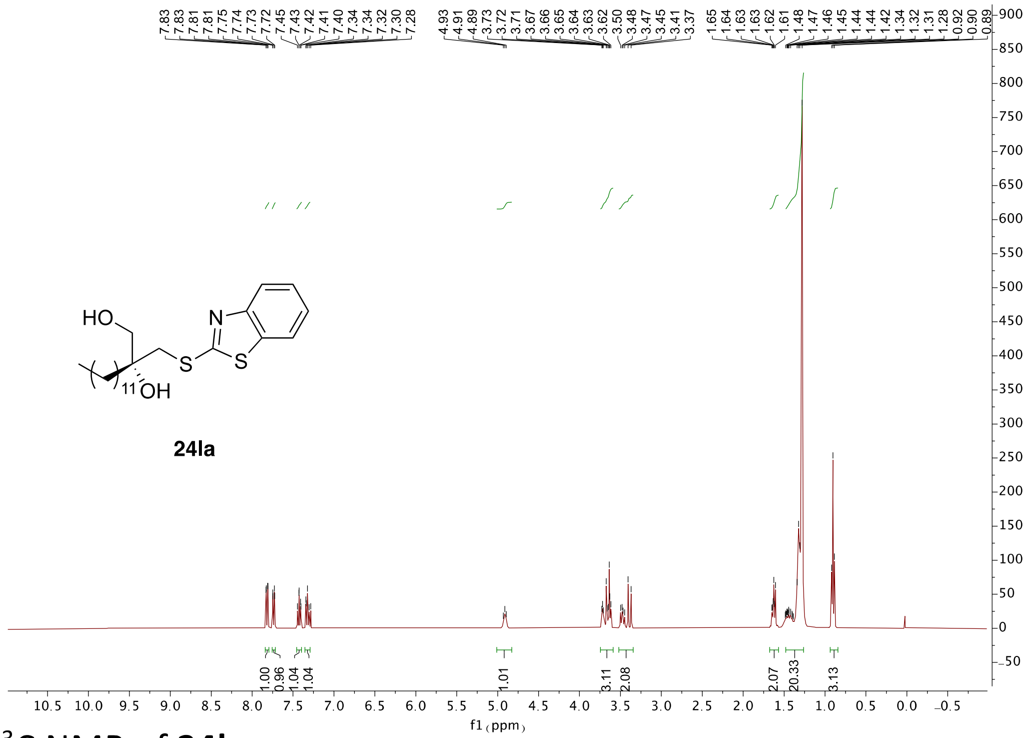

^{13}C NMR of **24la**

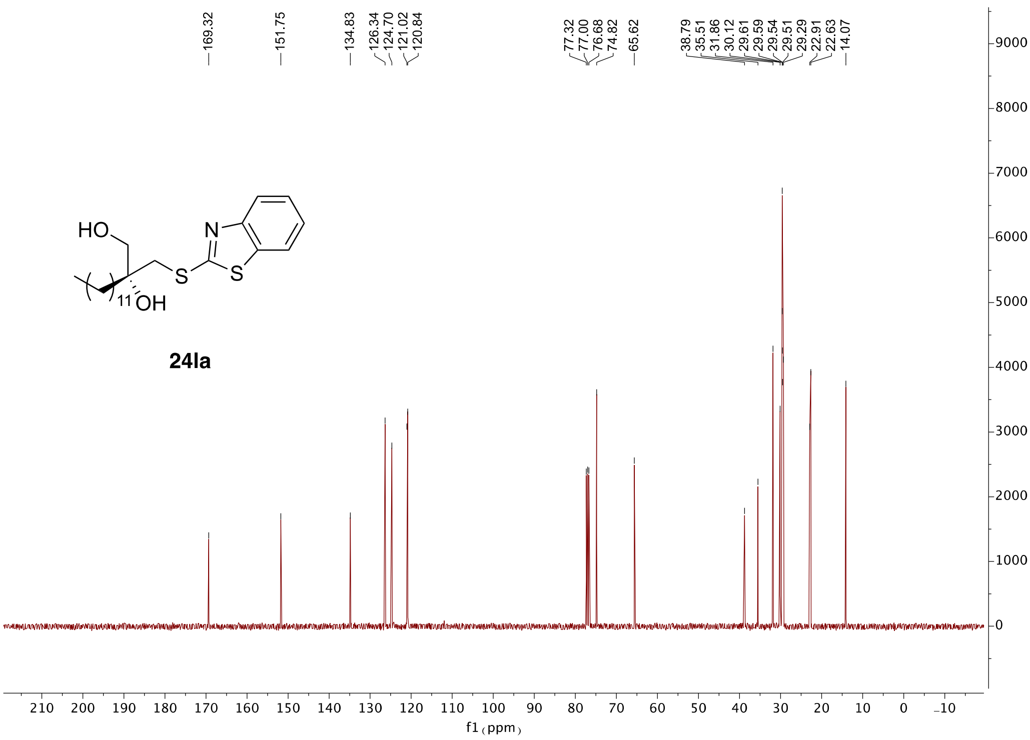

^{1}H NMR of **24ma**

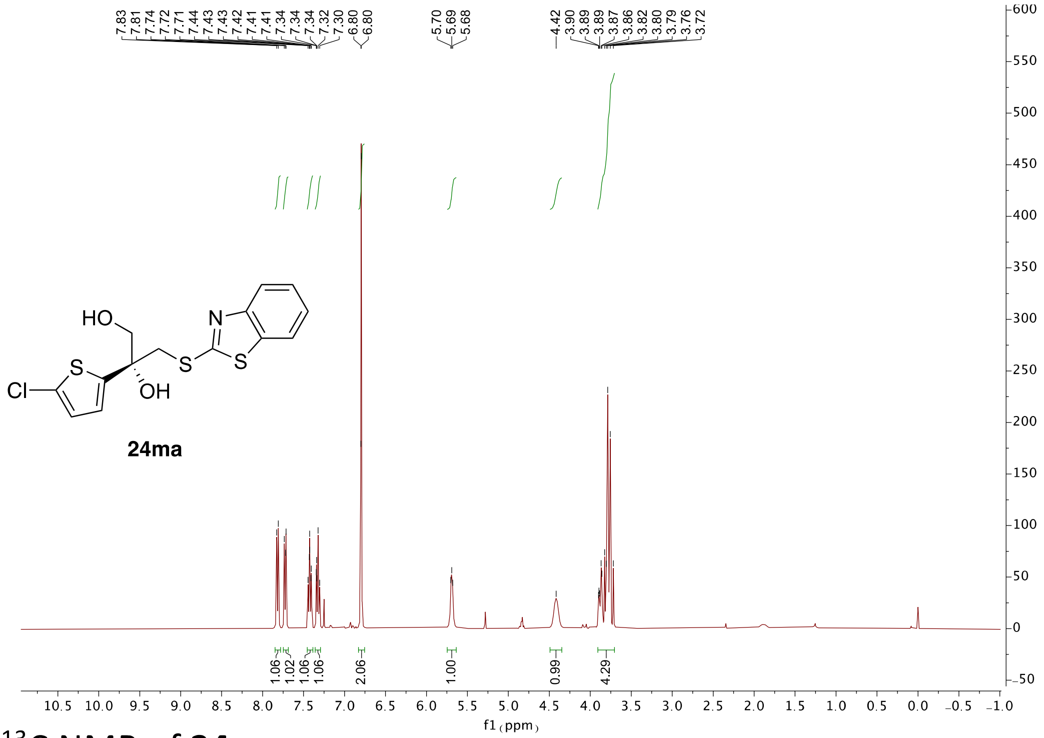

^{13}C NMR of **24ma**

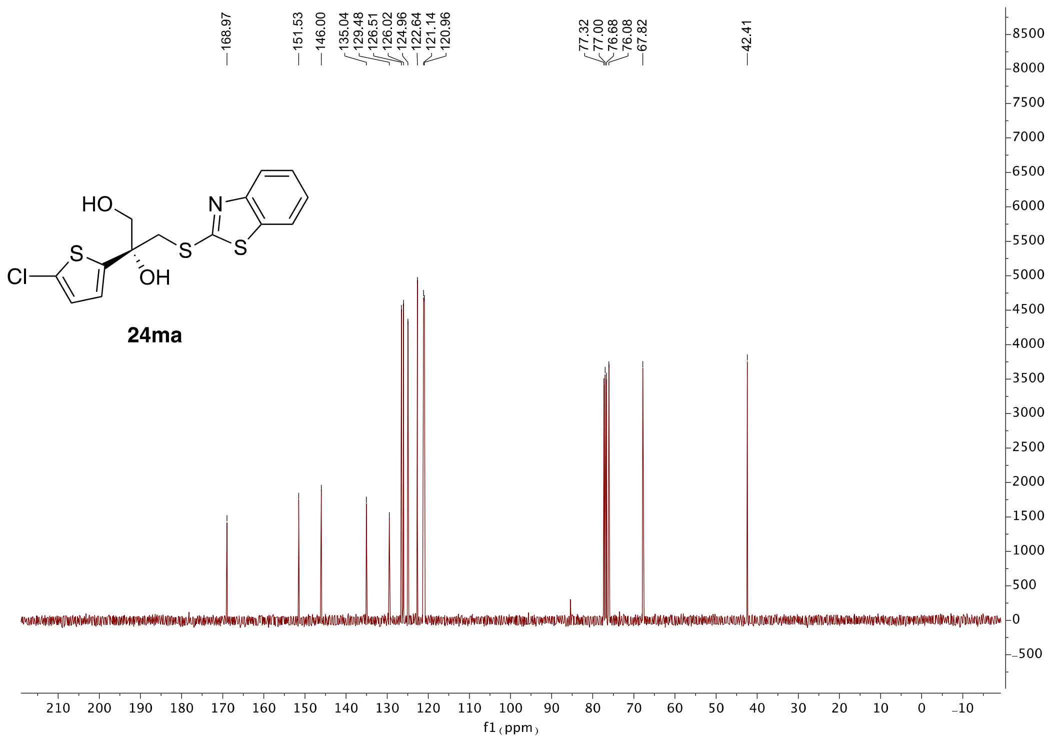

^{1}H NMR of **24na**

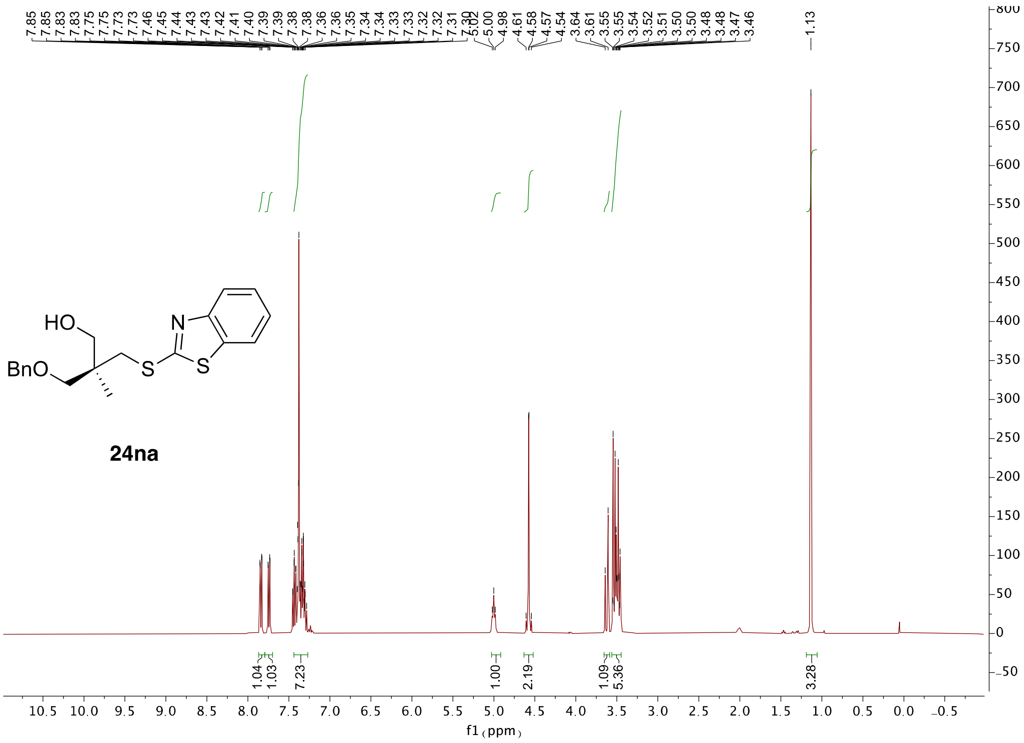

^{13}C NMR of **24na**

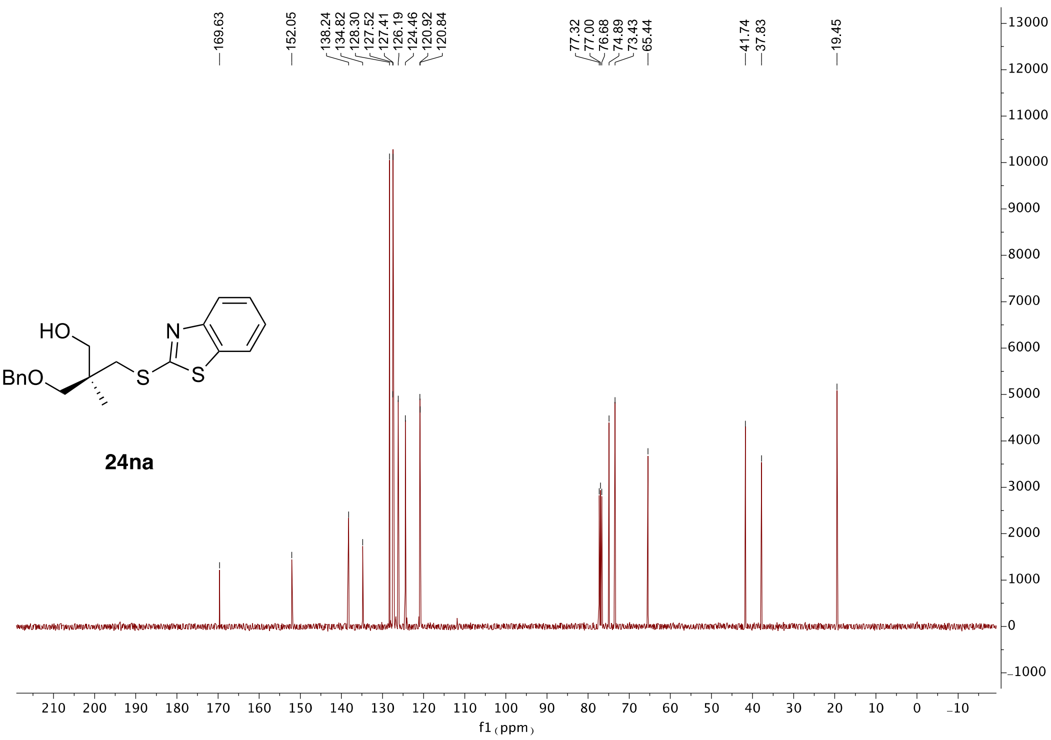

^{1}H NMR of **24ab**

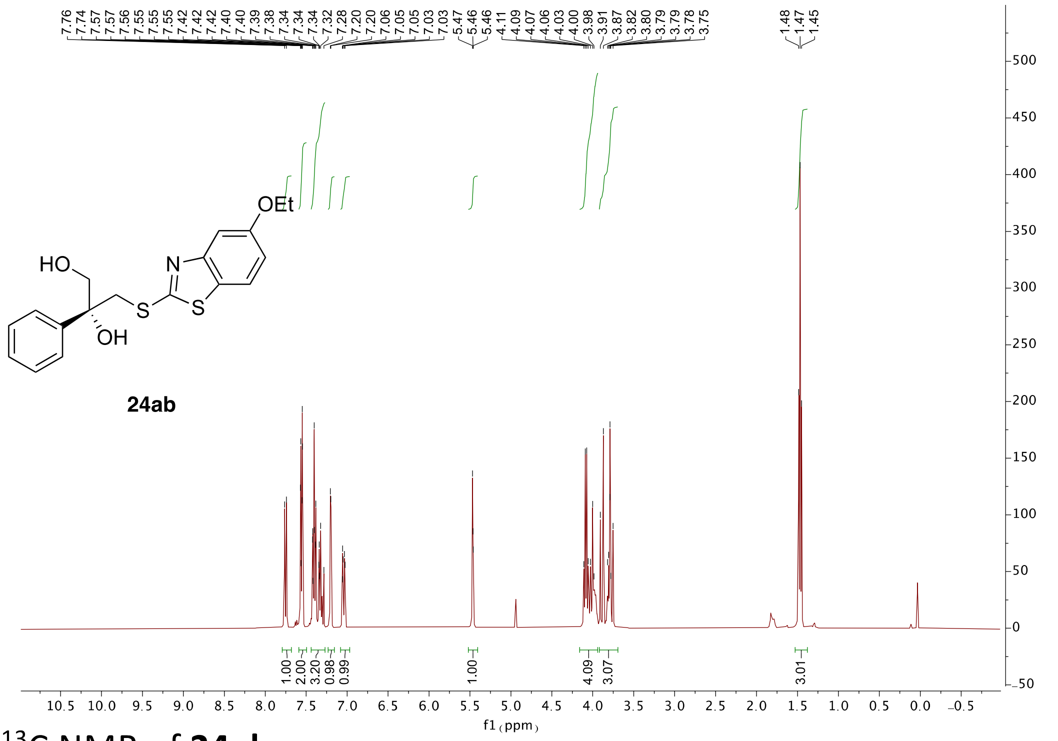

^{13}C NMR of **24ab**

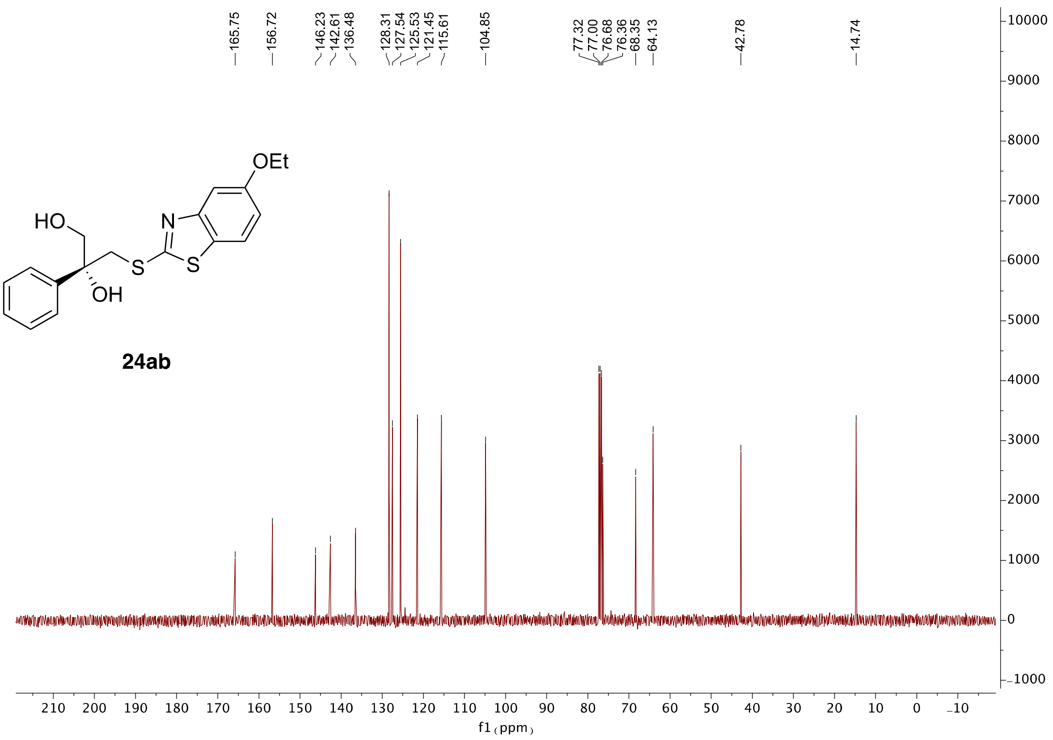

^{1}H NMR of **24ac**

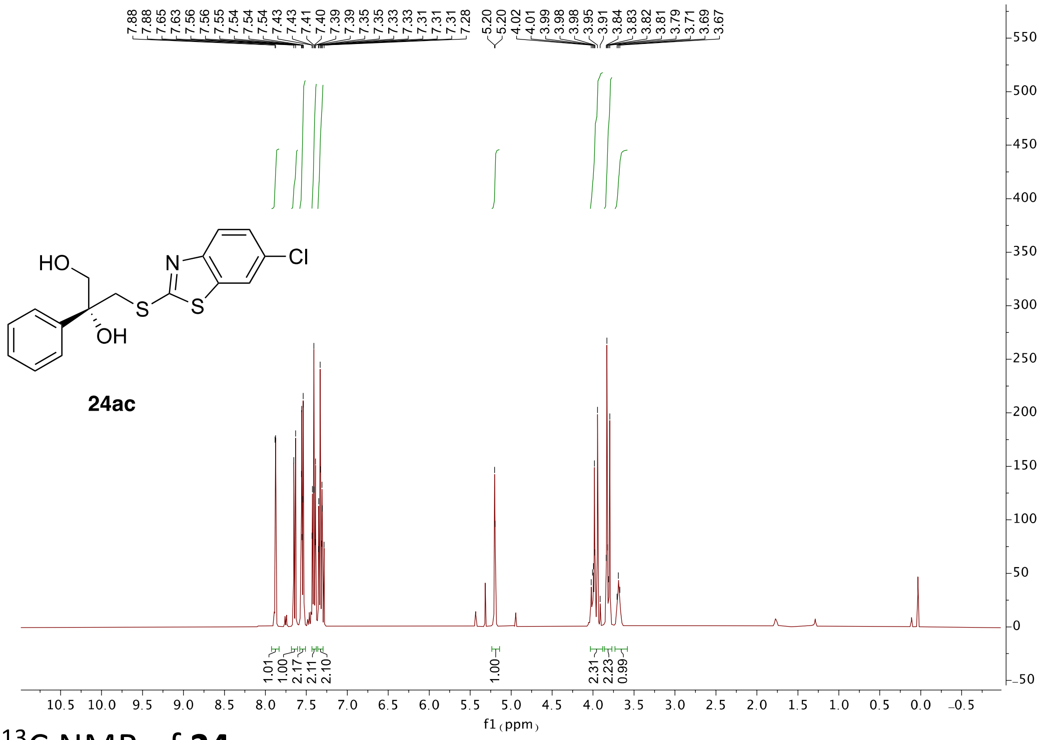

^{13}C NMR of **24ac**

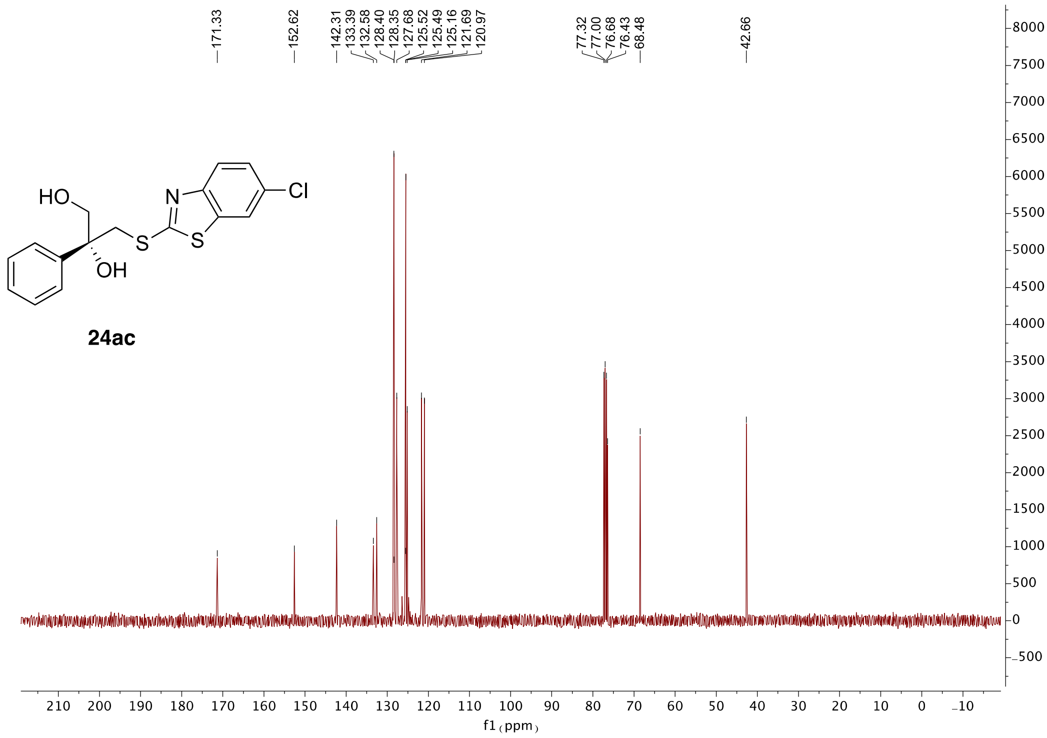

^{1}H NMR of **24ad**

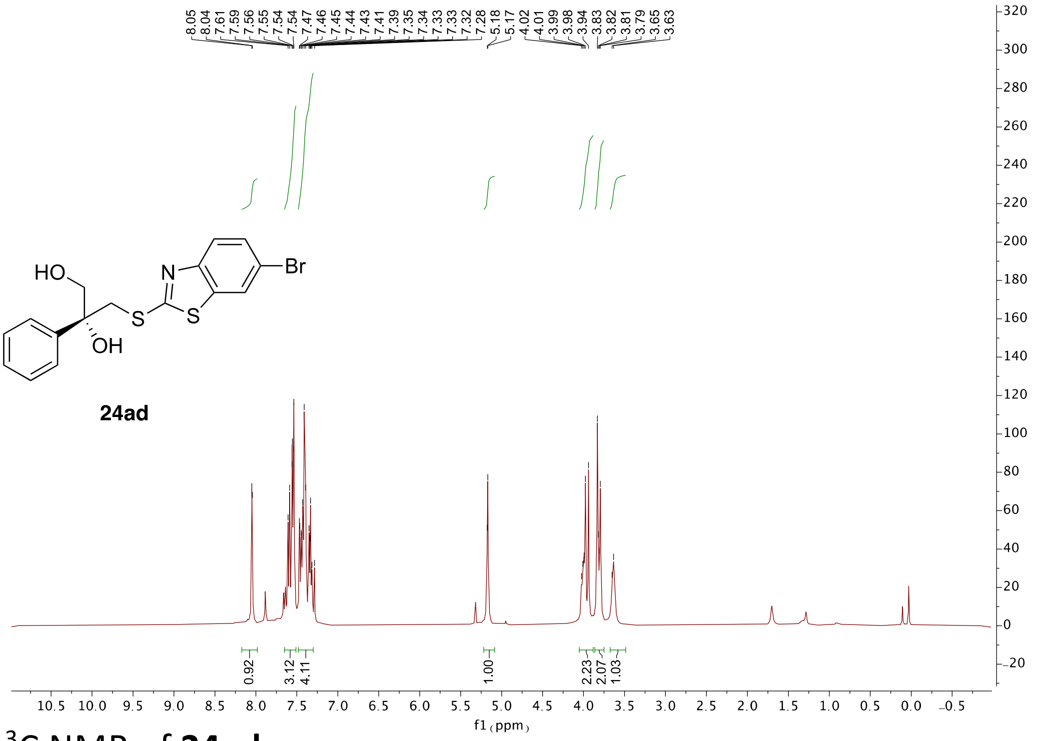

^{13}C NMR of **24ad**

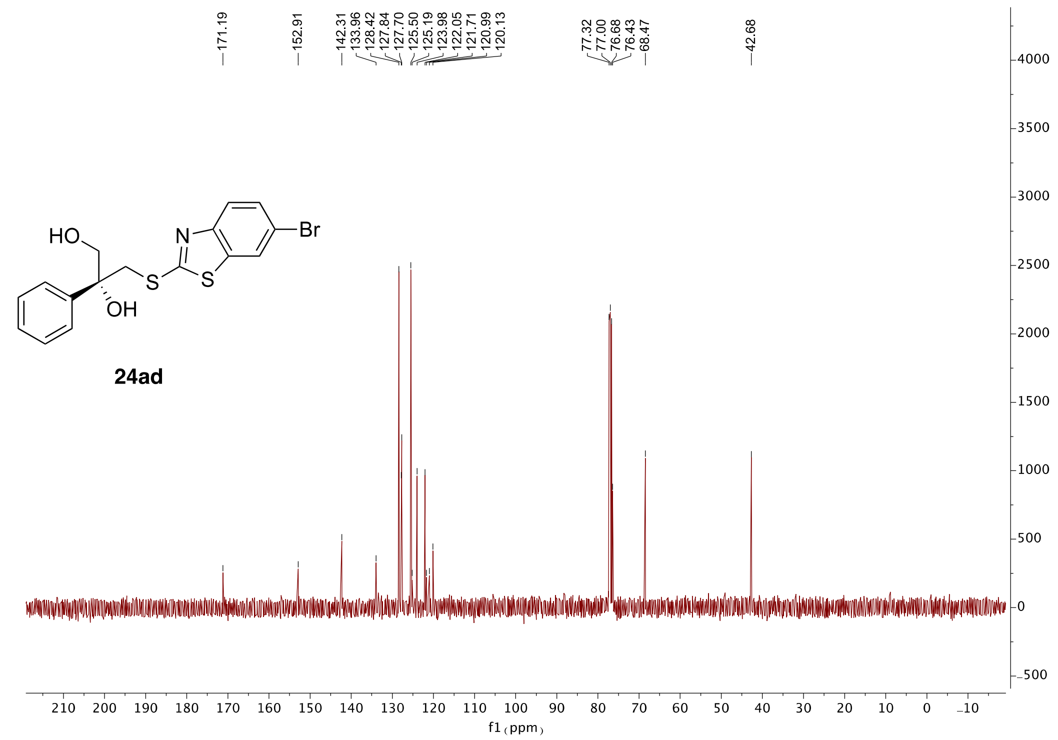

9. HPLC chromatograms

HPLC of *rac* **24aa**

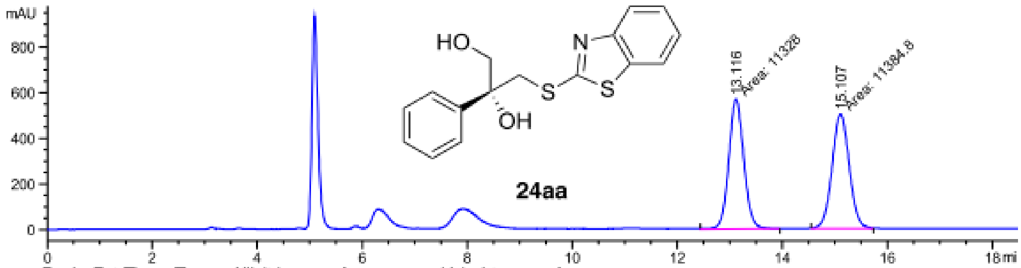

Peak #	Ret Time [min]	Type	Width [min]	Area [mAU*s]	Height [mAU]	Area %
1	13.116	MM	0.3321	1.13280e4	568.48718	49.8751
2	15.107	FM	0.3789	1.13848e4	500.76028	50.1249

HPLC of **24aa** (result for **Cat f**)

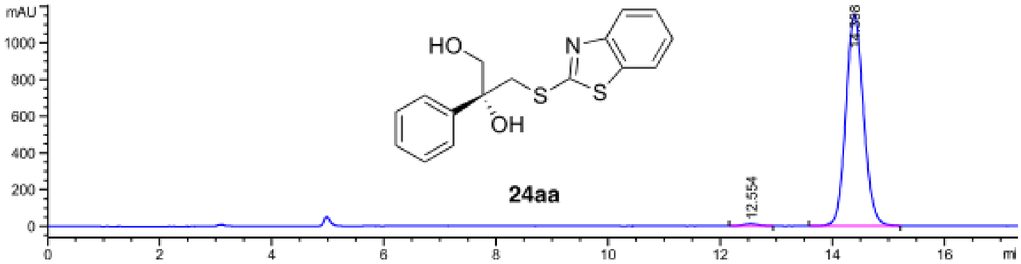

Peak #	Ret Time [min]	Type	Width [min]	Area [mAU*s]	Height [mAU]	Area %
1	12.554	BB	0.2396	231.46095	12.29906	0.9070
2	14.398	BB	0.3443	2.52892e4	1150.95044	99.0930

HPLC of **24aa** (result for **Cat g**)

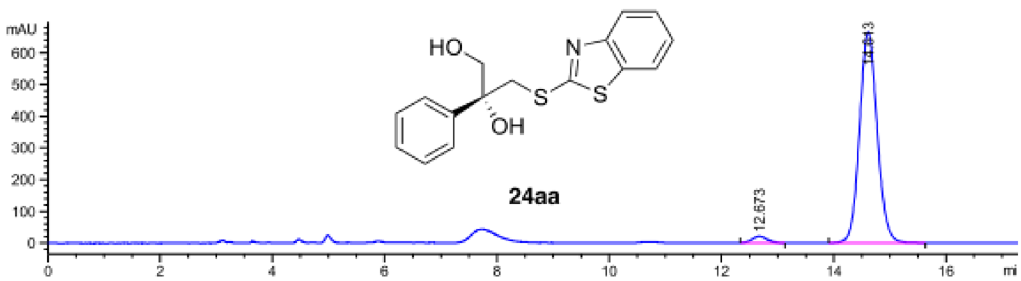

Peak #	Ret Time [min]	Type	Width [min]	Area [mAU*s]	Height [mAU]	Area %
1	12.673	BB	0.2397	386.56558	20.90881	2.5953
2	14.613	BB	0.3405	1.45080e4	665.02570	97.4047

HPLC of *rac* **24ba**

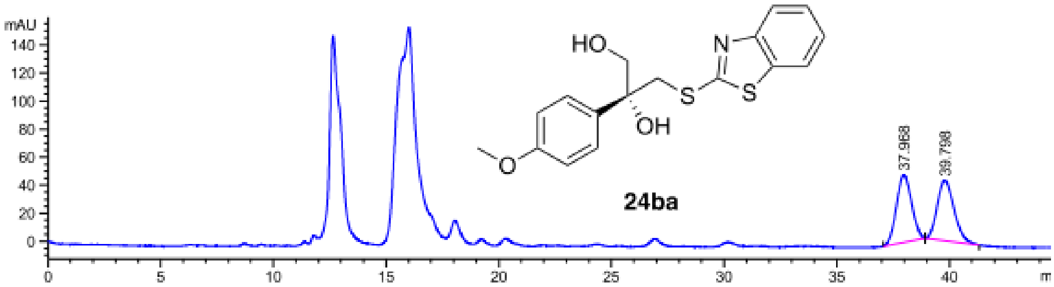

Peak #	RetTime [min]	Type	Width [min]	Area [mAU*s]	Height [mAU]	Area %
1	37.968	BB	0.5747	2241.27563	48.00397	49.9815
2	39.798	BB	0.6482	2242.93921	43.02361	50.0185

HPLC of **24ba** (result for **Cat f**)

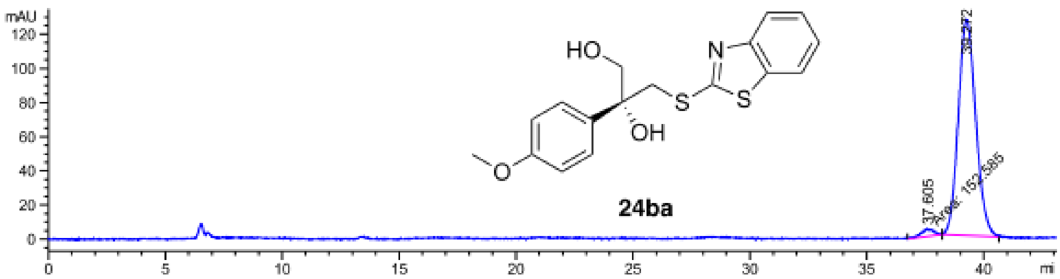

Peak #	RetTime [min]	Type	Width [min]	Area [mAU*s]	Height [mAU]	Area %
1	37.605	MM	0.6046	152.58478	4.20593	2.2842
2	39.272	BB	0.6714	6527.34131	126.19650	97.7158

HPLC of **24ba** (result for **Cat g**)

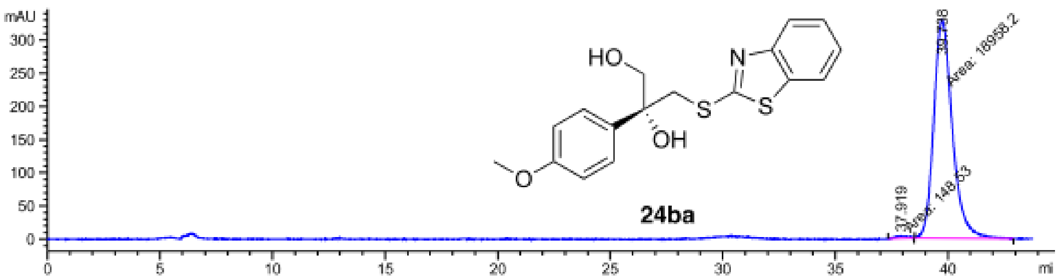

Peak #	RetTime [min]	Type	Width [min]	Area [mAU*s]	Height [mAU]	Area %
1	37.919	MM	0.6300	148.52953	3.92940	0.7774
2	39.738	MM	0.9591	1.89582e4	329.43411	99.2226

HPLC of *rac* **24ca**

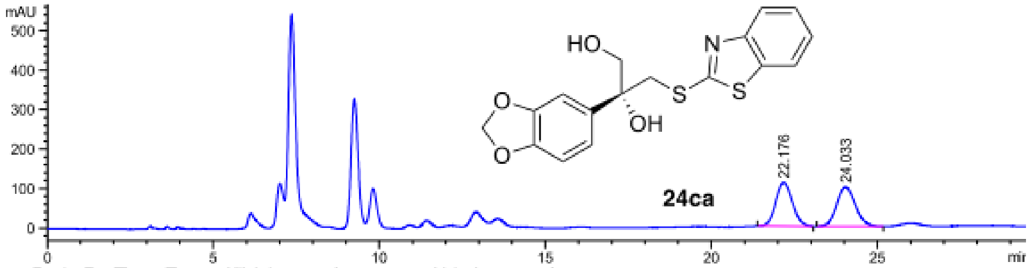

Peak #	RetTime [min]	Type	Width [min]	Area [mAU*s]	Height [mAU]	Area %
1	22.176	BB	0.4955	3866.35718	110.69800	49.5929
2	24.033	BB	0.5626	3929.83594	100.40834	50.4071

HPLC of **24ca** (result for **Cat f**)

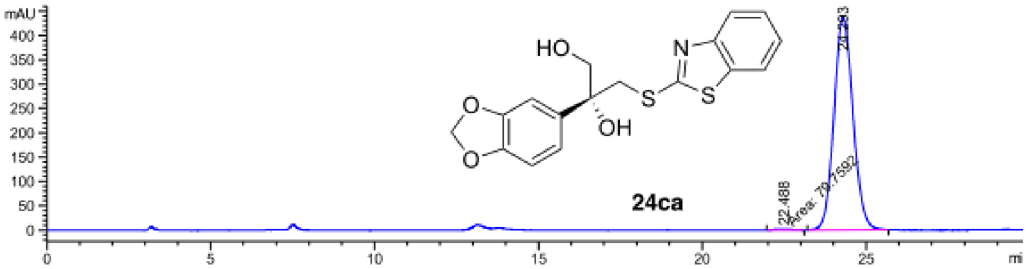

Peak #	RetTime [min]	Type	Width [min]	Area [mAU*s]	Height [mAU]	Area %
1	22.488	MM	0.5815	79.75922	2.28610	0.4499
2	24.293	BB	0.6038	1.76476e4	438.26343	99.5501

HPLC of *rac* **24ca**

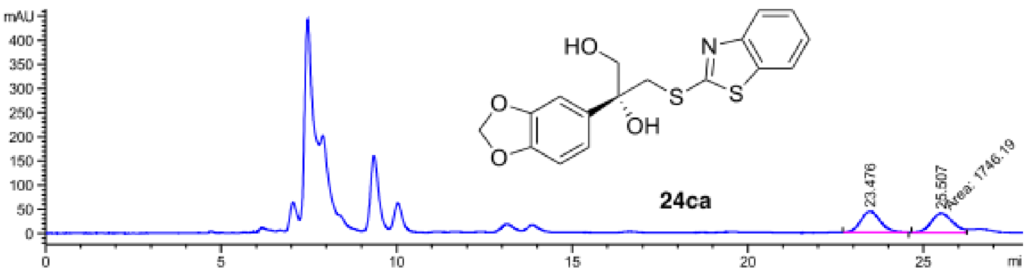

Peak #	RetTime [min]	Type	Width [min]	Area [mAU*s]	Height [mAU]	Area %
1	23.476	BB	0.5327	1683.54736	43.38780	49.0867
2	25.507	MM	0.7270	1746.19299	40.02989	50.9133

HPLC of **24ca** (result for **Cat g**)

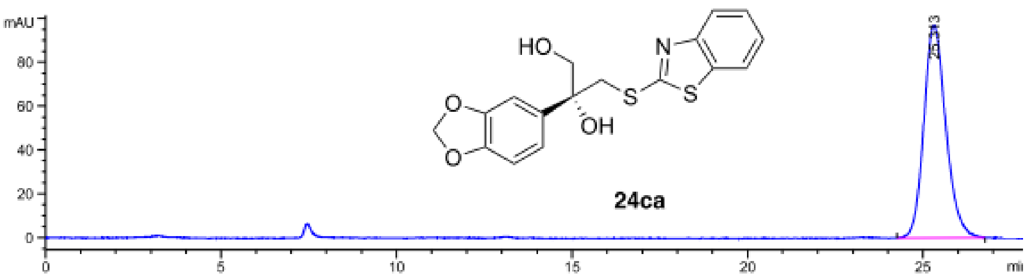

Peak #	RetTime [min]	Type	Width [min]	Area [mAU*s]	Height [mAU]	Area %
1	25.313	BB	0.6340	4236.57324	96.90931	100.0000

HPLC of *rac* **24da**

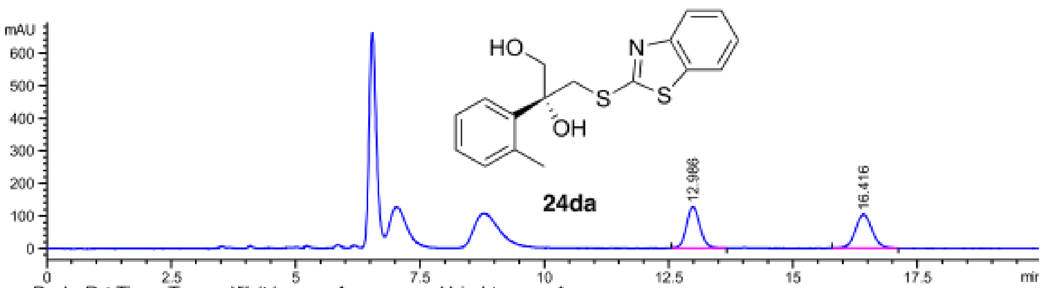

Peak #	Ret Time [min]	Type	Width [min]	Area [mAU*s]	Height [mAU]	Area %
1	12.986	BB	0.2838	2354.28369	127.28961	49.4780
2	16.416	BB	0.3565	2403.95801	103.68298	50.5220

HPLC of **24da** (result for **Cat f**)

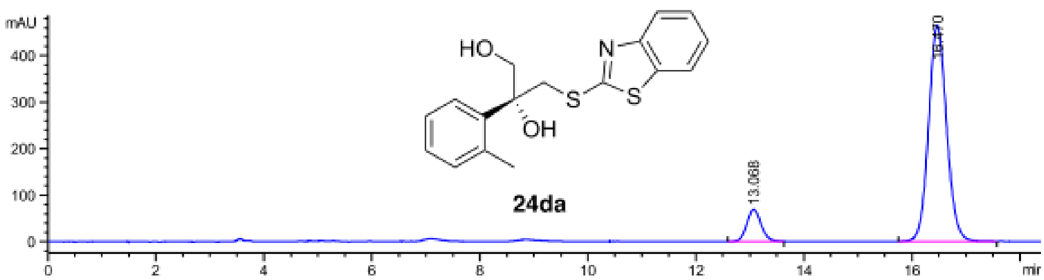

Peak #	Ret Time [min]	Type	Width [min]	Area [mAU*s]	Height [mAU]	Area %
1	13.068	BB	0.2841	1277.28369	68.94384	10.5983
2	16.470	BB	0.3589	1.07745e4	464.06689	89.4017

HPLC of *rac* **24da**

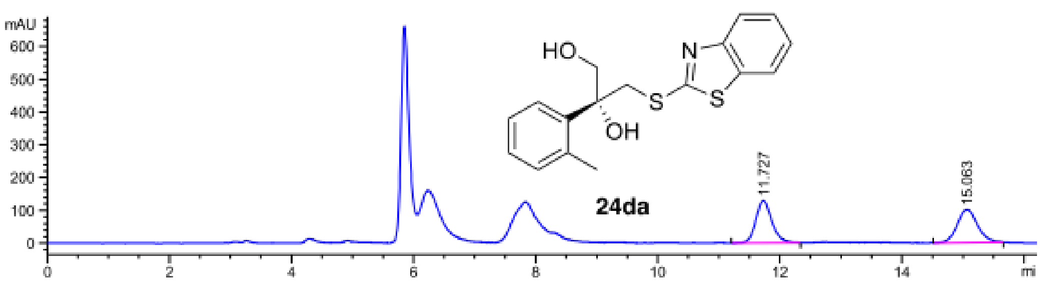

Peak #	Ret Time [min]	Type	Width [min]	Area [mAU*s]	Height [mAU]	Area %
1	11.727	BB	0.2740	2349.50903	129.31506	50.3147
2	15.063	BB	0.3484	2320.11670	100.11675	49.6853

HPLC of **24da** (result for **Cat g**)

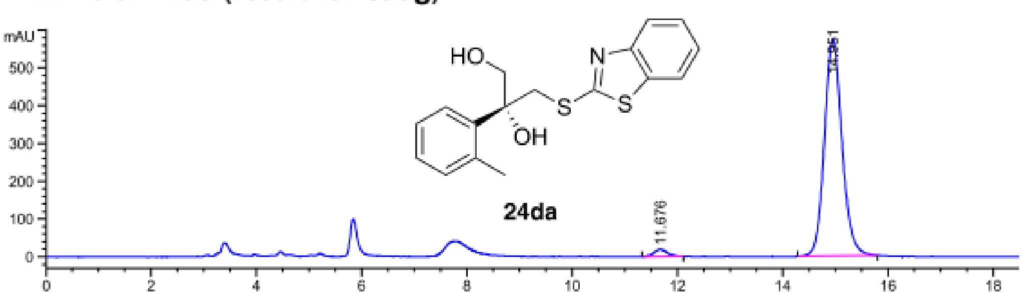

Peak #	Ret Time [min]	Type	Width [min]	Area [mAU*s]	Height [mAU]	Area %
1	11.676	BB	0.2208	334.17621	19.22446	2.4437
2	14.951	BB	0.3594	1.33411e4	573.49298	97.5563

HPLC of *rac* **24ea**

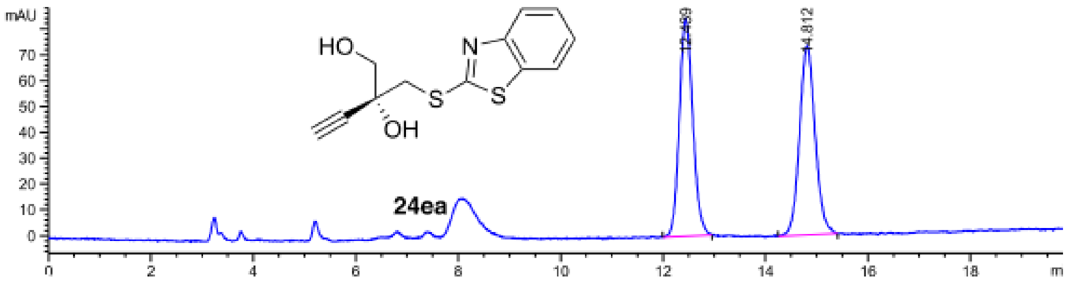

Peak #	Ret Time [min]	Type	Width [min]	Area [mAU*s]	Height [mAU]	Area %
1	12.439	BB	0.2794	1525.86462	84.19196	49.5195
2	14.812	BB	0.3213	1555.47351	73.37554	50.4805

HPLC of **24ea** (result for **Cat f**)

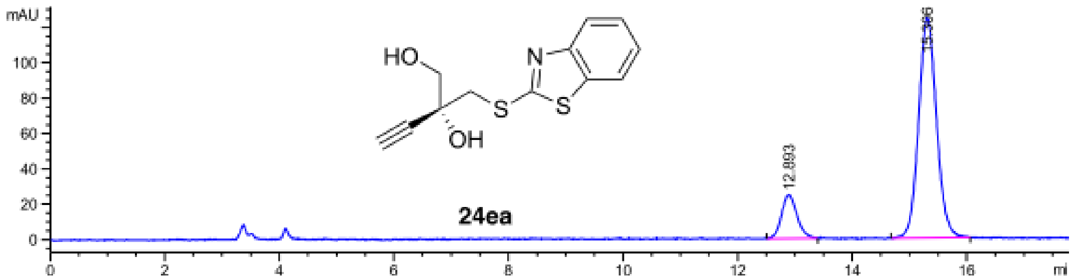

Peak #	Ret Time [min]	Type	Width [min]	Area [mAU*s]	Height [mAU]	Area %
1	12.893	BB	0.2789	463.04398	24.67975	14.6259
2	15.306	BB	0.3372	2702.87109	124.53317	85.3741

HPLC of **24ea** (result for **Cat g**)

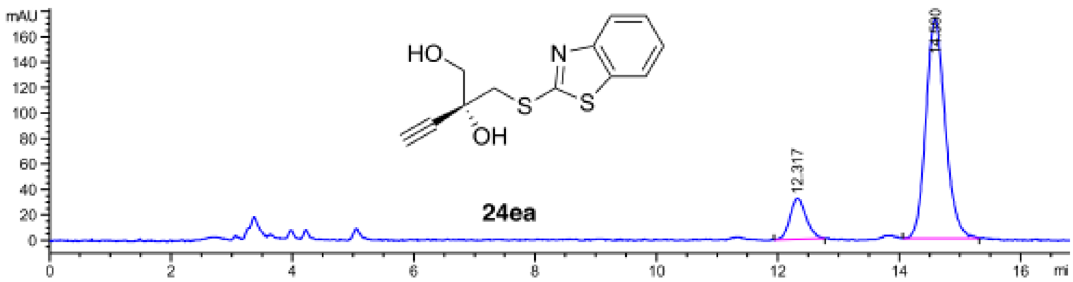

Peak #	Ret Time [min]	Type	Width [min]	Area [mAU*s]	Height [mAU]	Area %
1	12.317	BB	0.2486	595.66949	32.08870	13.4608
2	14.590	BB	0.3334	3829.55225	172.25470	86.5392

HPLC of *rac* **24fa**

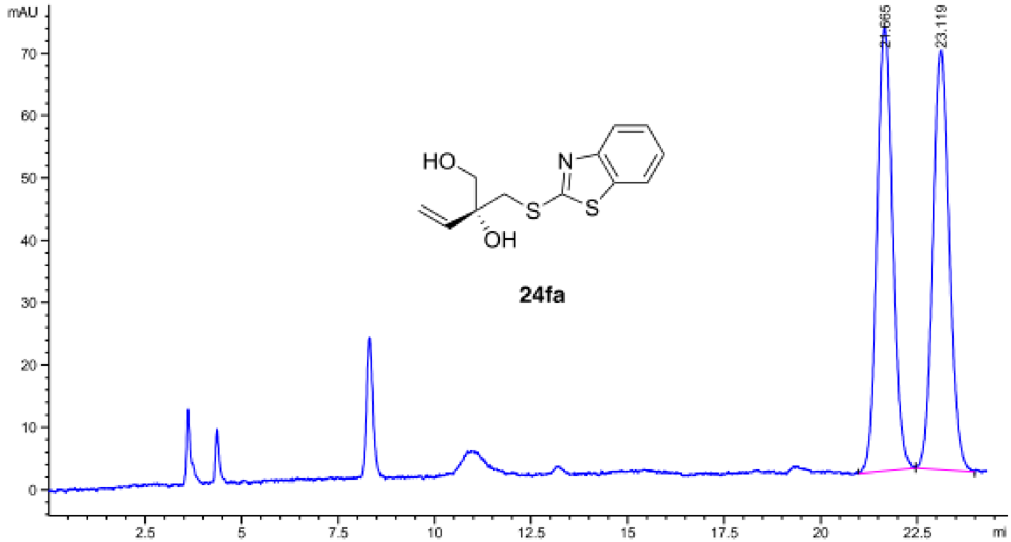

Peak #	Ret Time [min]	Type	Width [min]	Area [mAU*s]	Height [mAU]	Area %
1	21.665	BB	0.4253	2009.13757	71.17097	50.2055
2	23.119	BB	0.4417	1992.68945	67.24532	49.7945

HPLC of **24fa** (result for **Cat f**)

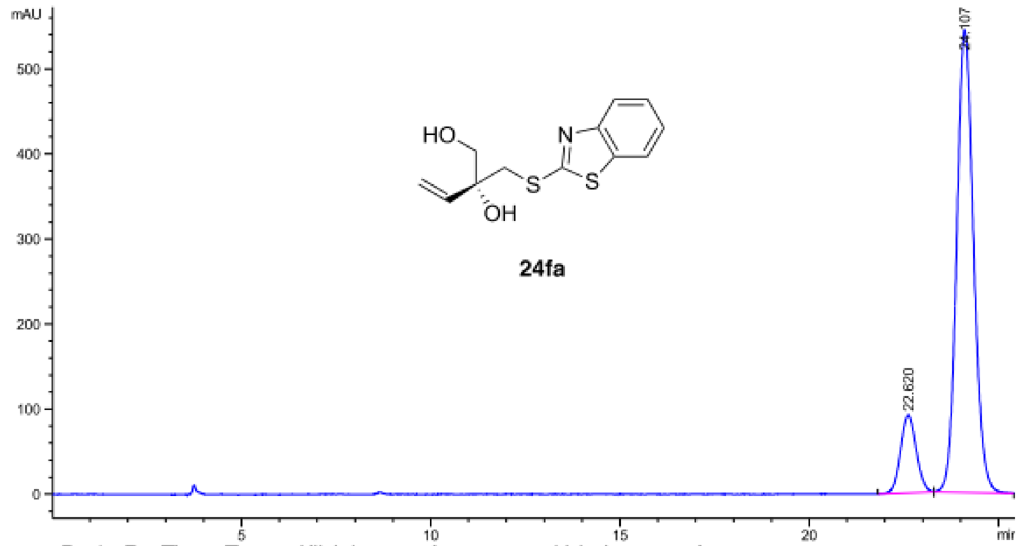

Peak #	Ret Time [min]	Type	Width [min]	Area [mAU*s]	Height [mAU]	Area %
1	22.620	BB	0.4301	2603.20435	90.89788	13.3701
2	24.107	BB	0.4781	1.68671e4	543.47510	86.6299

HPLC of *rac* 24ga

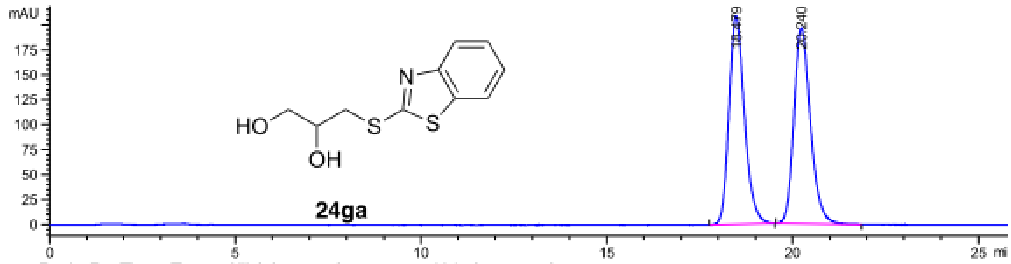

Peak #	Ret Time [min]	Type	Width [min]	Area [mAU*s]	Height [mAU]	Area %
1	18.479	BB	0.4394	7582.94922	263.74222	49.9291
2	20.241	BB	0.4648	7604.48877	247.26479	50.0709

HPLC of 24ga (result for Cat f)

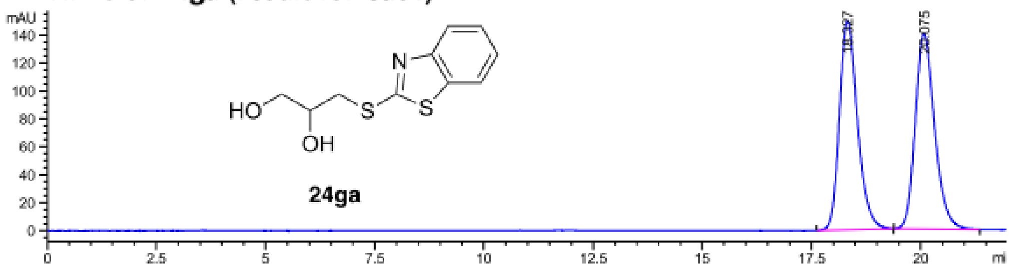

Peak #	Ret Time [min]	Type	Width [min]	Area [mAU*s]	Height [mAU]	Area %
1	18.326	BB	0.4382	5469.94971	189.83385	50.1288
2	20.075	BB	0.4601	5441.83057	177.30464	49.8712

HPLC of *rac* 24ga

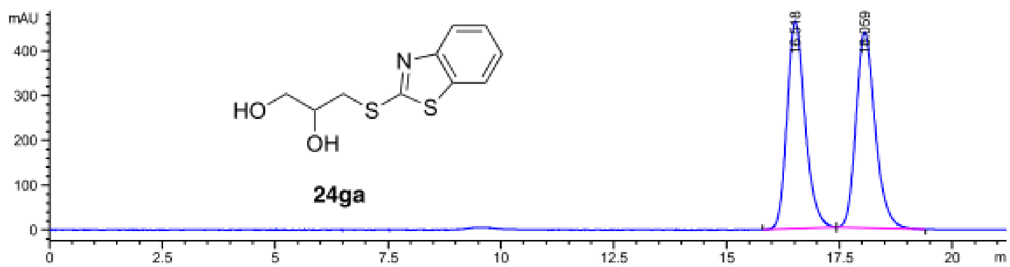

Peak #	Ret Time [min]	Type	Width [min]	Area [mAU*s]	Height [mAU]	Area %
1	16.518	BB	0.4260	1.28723e4	463.55728	49.8237
2	18.059	BB	0.4519	1.29634e4	437.27228	50.1763

HPLC of 24ga (result for Cat g)

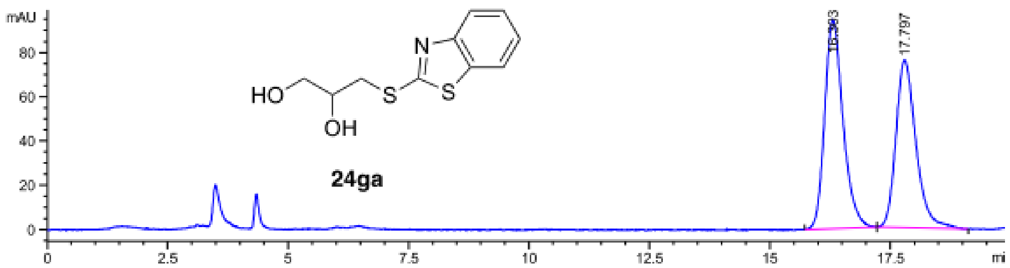

Peak #	Ret Time [min]	Type	Width [min]	Area [mAU*s]	Height [mAU]	Area %
1	16.303	BB	0.4069	2512.88354	94.28459	53.5876
2	17.797	BB	0.4252	2176.41821	75.75809	46.4124

HPLC of *rac* **24ha**

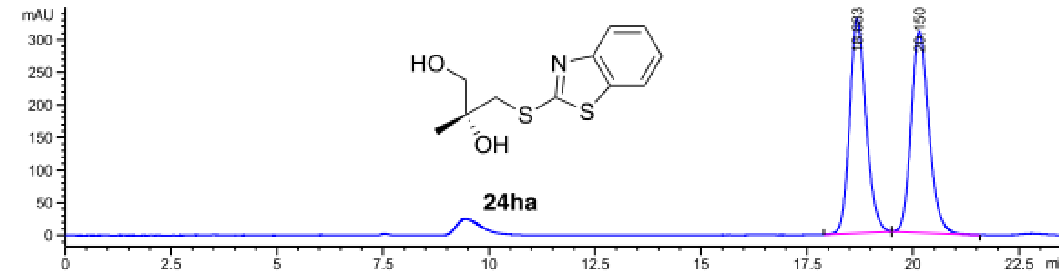

Peak #	Ret Time [min]	Type	Width [min]	Area [mAU*s]	Height [mAU]	Area %
1	18.683	BB	0.4119	8874.68359	329.82800	49.8972
2	20.150	BB	0.4387	8911.23633	308.80643	50.1028

HPLC of **24ha** (result for **Cat f**)

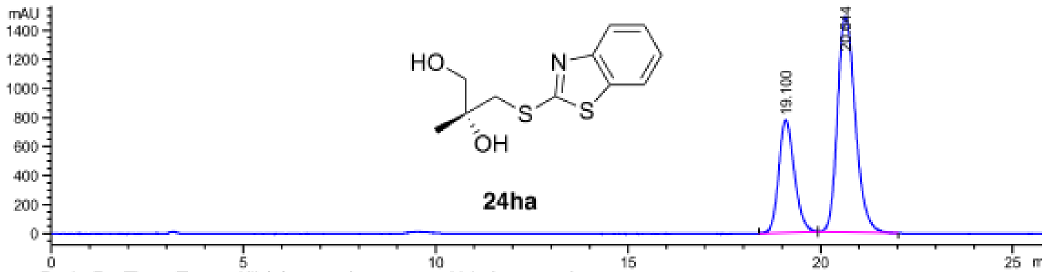

Peak #	Ret Time [min]	Type	Width [min]	Area [mAU*s]	Height [mAU]	Area %
1	19.100	BB	0.4290	2.19083e4	776.98950	31.3815
2	20.644	BB	0.4026	4.79045e4	1484.09680	68.6185

HPLC of **24ha** (result for **Cat g**)

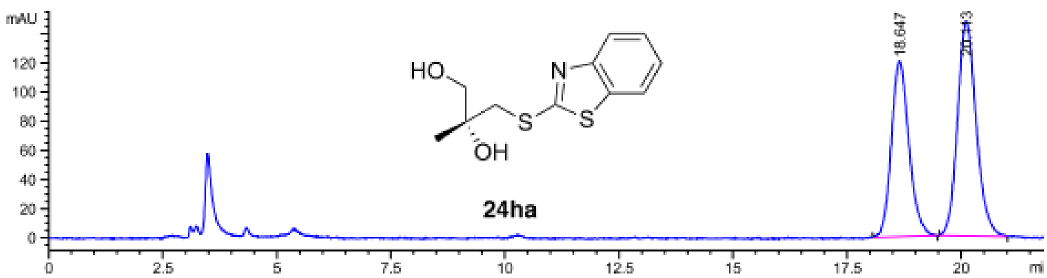

Peak #	Ret Time [min]	Type	Width [min]	Area [mAU*s]	Height [mAU]	Area %
1	18.647	BB	0.3948	3227.81641	120.39771	43.3719
2	20.113	BB	0.4225	4214.37549	146.99960	56.6281

HPLC of *rac* **24ia**

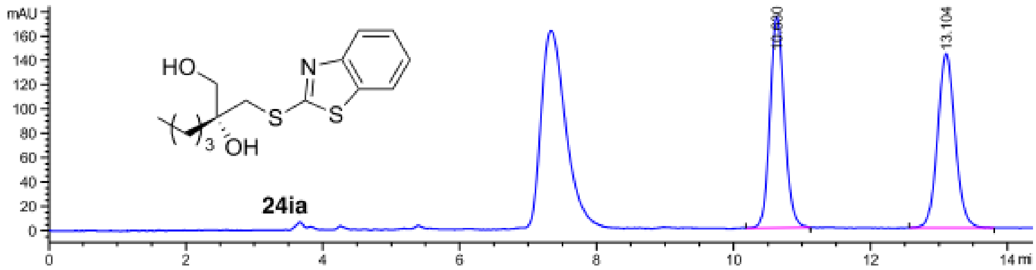

Peak #	Ret Time [min]	Type	Width [min]	Area [mAU*s]	Height [mAU]	Area %
1	10.630	BB	0.2283	2566.76025	173.84071	49.8406
2	13.104	BB	0.2801	2583.17920	143.42546	50.1594

HPLC of **24ia** (result for **Cat f**)

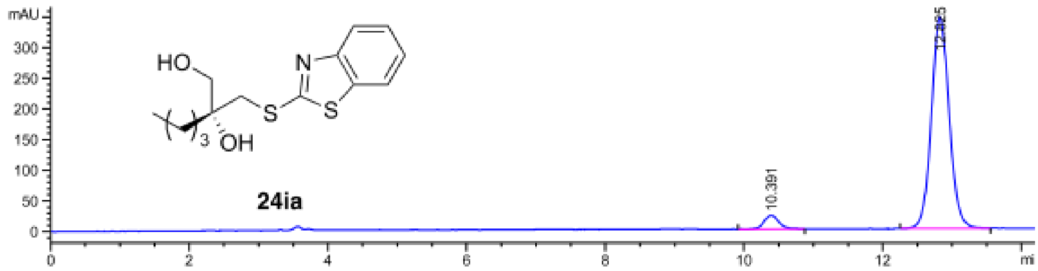

Peak #	Ret Time [min]	Type	Width [min]	Area [mAU*s]	Height [mAU]	Area %
1	10.391	BB	0.2260	340.11365	22.80517	5.2254
2	12.825	BB	0.2767	6168.76904	344.84219	94.7746

HPLC of *rac* **24ia**

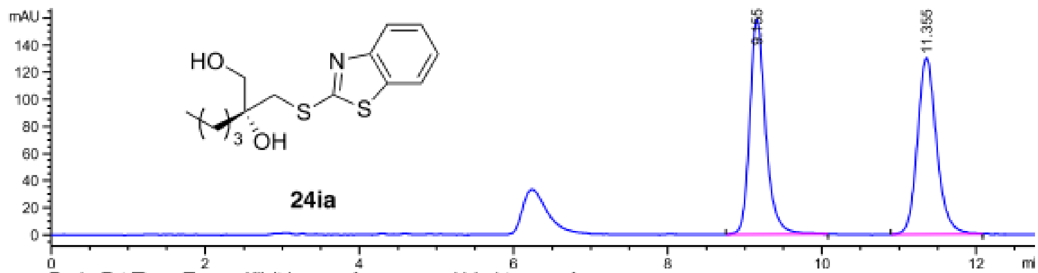

Peak #	Ret Time [min]	Type	Width [min]	Area [mAU*s]	Height [mAU]	Area %
1	9.155	BB	0.2176	2282.28174	158.83603	50.3522
2	11.355	BB	0.2637	2250.35400	130.14139	49.6478

HPLC of **24ia** (result for **Cat g**)

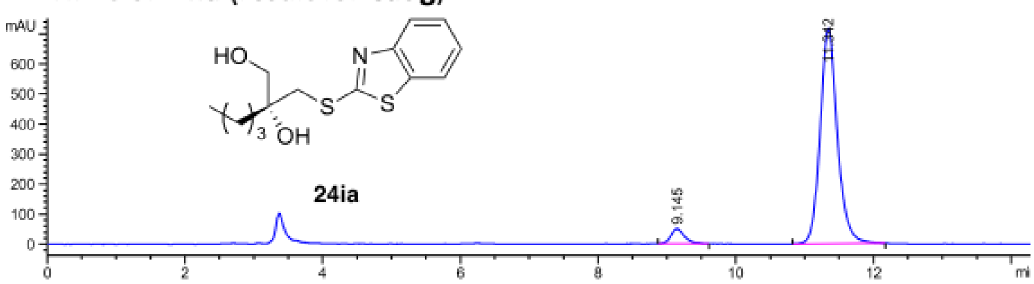

Peak #	Ret Time [min]	Type	Width [min]	Area [mAU*s]	Height [mAU]	Area %
1	9.145	BB	0.2096	694.80420	49.53904	5.2651
2	11.342	BB	0.2658	1.25016e4	715.77429	94.7349

HPLC of *rac* **24ja**

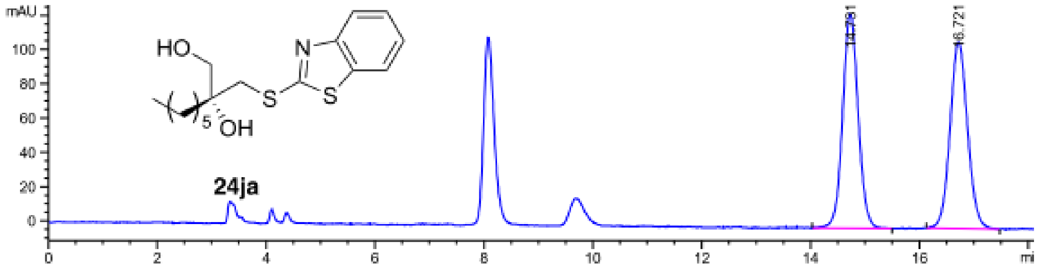

Peak #	Ret Time [min]	Type	Width [min]	Area [mAU*s]	Height [mAU]	Area %
1	14.731	BB	0.3085	2467.66895	124.90371	50.3041
2	16.721	BB	0.3494	2437.83081	108.79567	49.6959

HPLC of **24ja** (result for **Cat f**)

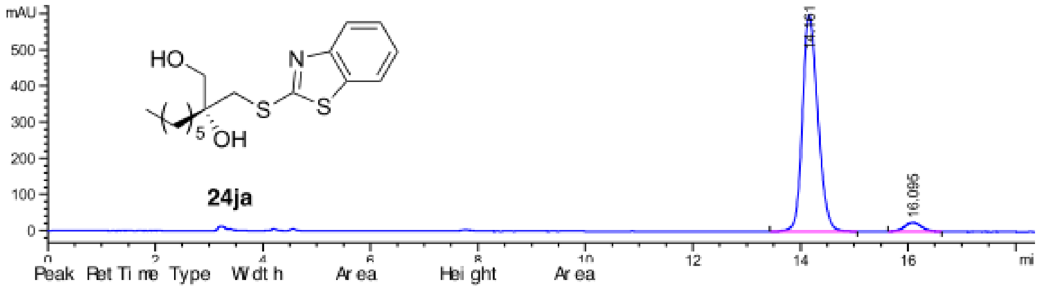

Peak #	Ret Time [min]	Type	Width [min]	Area [mAU*s]	Height [mAU]	Area %
1	14.161	BB	0.3086	1.18986e4	596.74194	95.6829
2	16.095	BB	0.3236	536.85510	24.69729	4.3171

HPLC of *rac* **24ja**

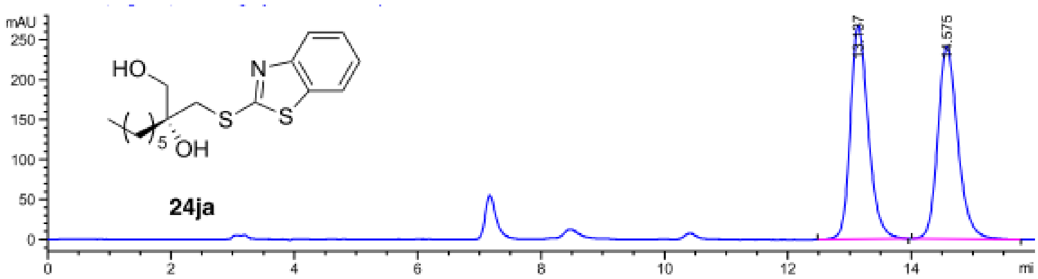

Peak #	Ret Time [min]	Type	Width [min]	Area [mAU*s]	Height [mAU]	Area %
1	13.137	BB	0.3075	5402.95410	267.64554	49.9405
2	14.575	BB	0.3421	5415.82373	241.07443	50.0595

HPLC of **24ja** (result for **Cat g**)

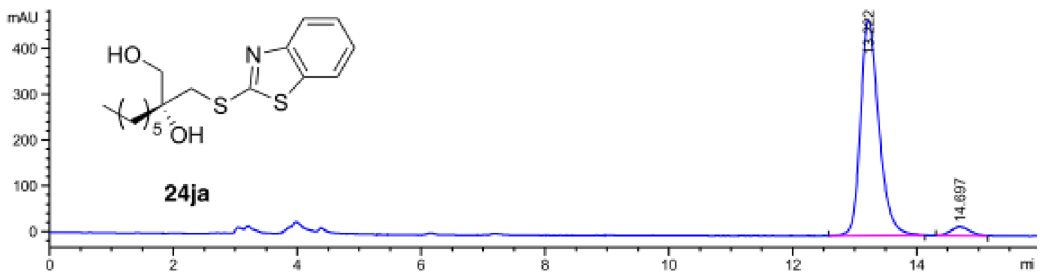

Peak #	Ret Time [min]	Type	Width [min]	Area [mAU*s]	Height [mAU]	Area %
1	13.222	BB	0.3152	9719.80859	470.07578	95.9814
2	14.697	BB	0.2759	406.95444	19.79124	4.0186

HPLC of *rac* **24ka**

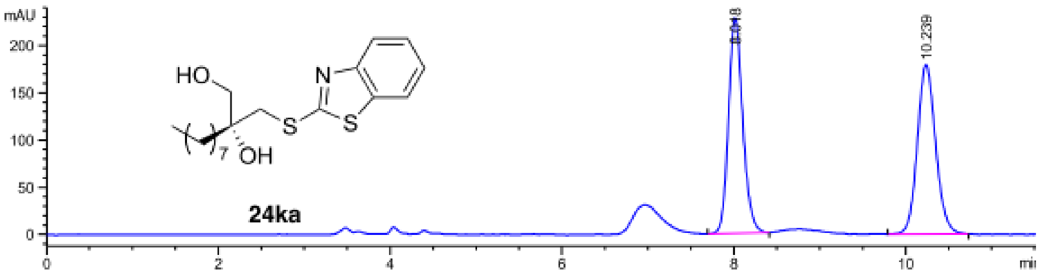

Peak #	RetTime [min]	Type	Width [min]	Area [mAU*s]	Height [mAU]	Area %
1	8.018	BB	0.1768	2630.15674	227.56409	49.6619
2	10.239	BB	0.2292	2665.96558	179.60493	50.3381

HPLC of **24ka** (result for **Cat f**)

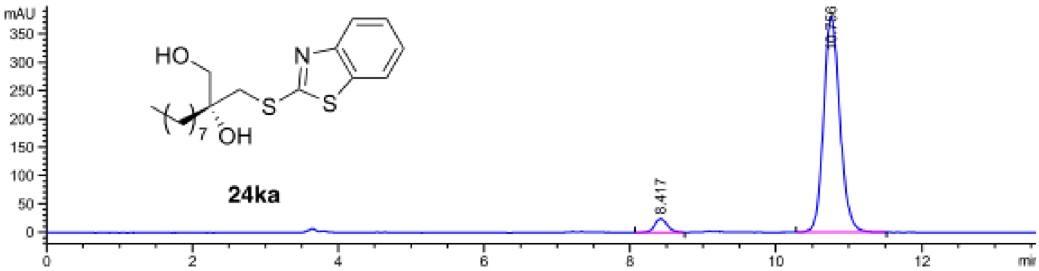

Peak #	RetTime [min]	Type	Width [min]	Area [mAU*s]	Height [mAU]	Area %
1	8.417	BB	0.1869	295.76129	24.15221	4.7778
2	10.756	BB	0.2388	5894.60596	380.37833	95.2222

HPLC of *rac* **24ka**

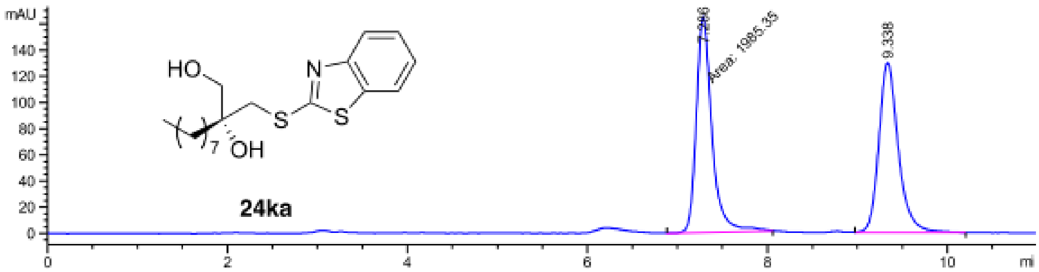

Peak #	RetTime [min]	Type	Width [min]	Area [mAU*s]	Height [mAU]	Area %
1	7.286	MM	0.2012	1985.35327	164.47823	50.4404
2	9.338	BB	0.2278	1950.68457	129.48407	49.5596

HPLC of **24ka** (result for **Cat g**)

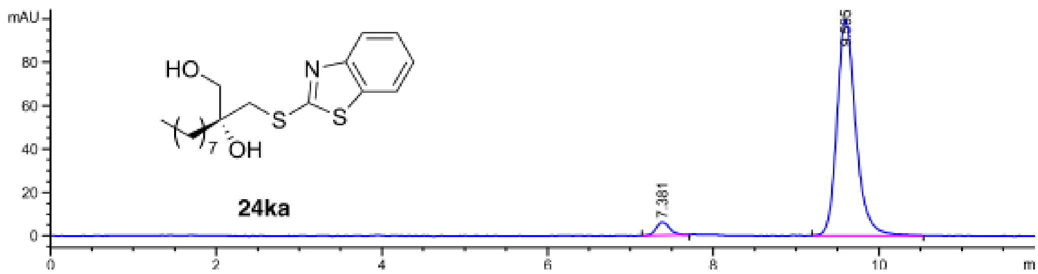

Peak #	RetTime [min]	Type	Width [min]	Area [mAU*s]	Height [mAU]	Area %
1	7.381	BB	0.1749	68.45732	6.01104	4.1749
2	9.595	BB	0.2402	1571.27258	99.51608	95.8251

HPLC of *rac* **24la**

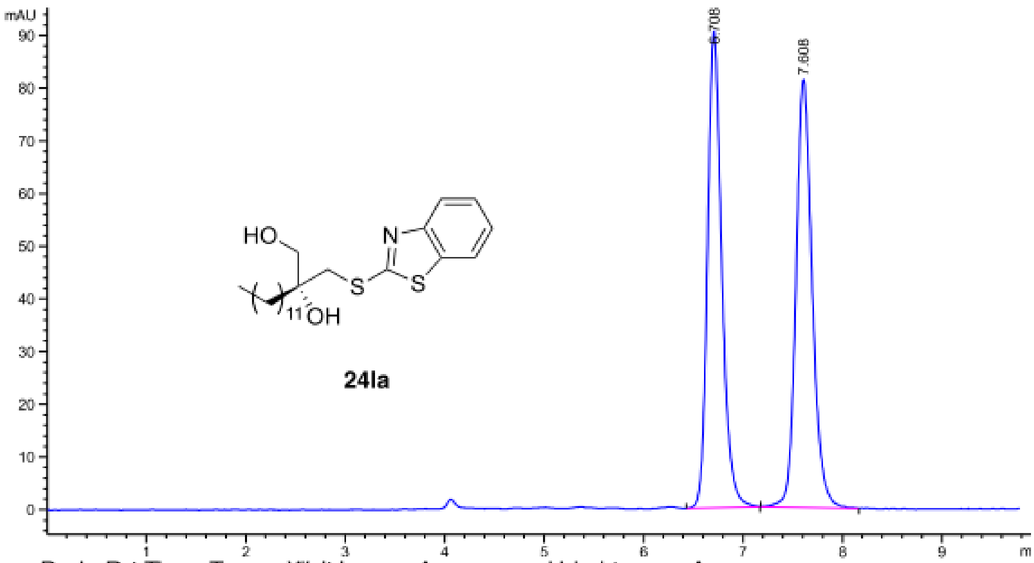

Peak #	Ret Time [min]	Type	Width [min]	Area [mAU*s]	Height [mAU]	Area %
1	6.708	BB	0.1526	904.13763	90.48456	49.5284
2	7.608	BB	0.1724	921.35657	81.19044	50.4716

HPLC of **24la** (result for **Cat f**)

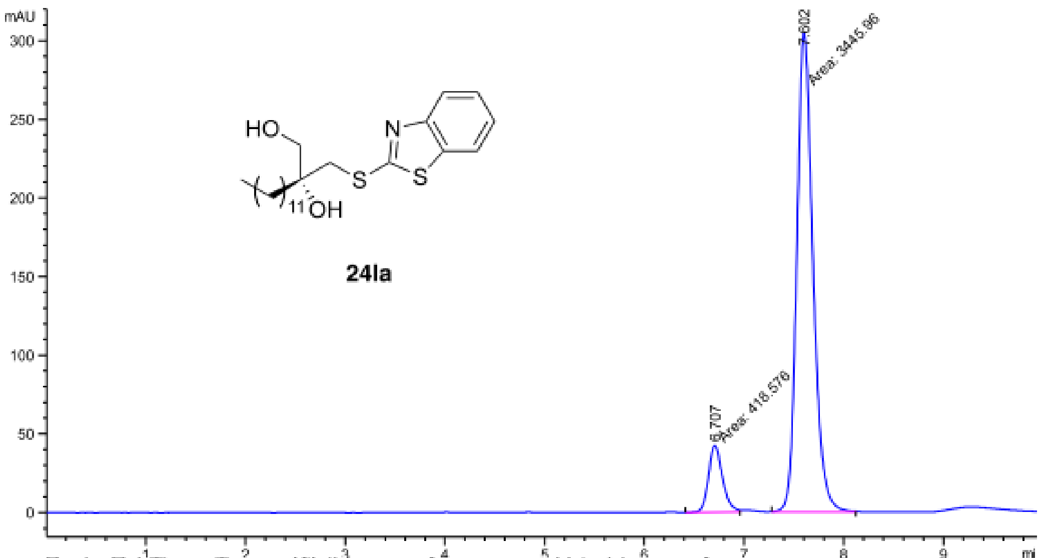

Peak #	Ret Time [min]	Type	Width [min]	Area [mAU*s]	Height [mAU]	Area %
1	6.707	MF	0.1644	418.57611	42.43792	10.8312
2	7.602	FM	0.1883	3445.95874	304.97391	89.1688

HPLC of *rac* **24ma**

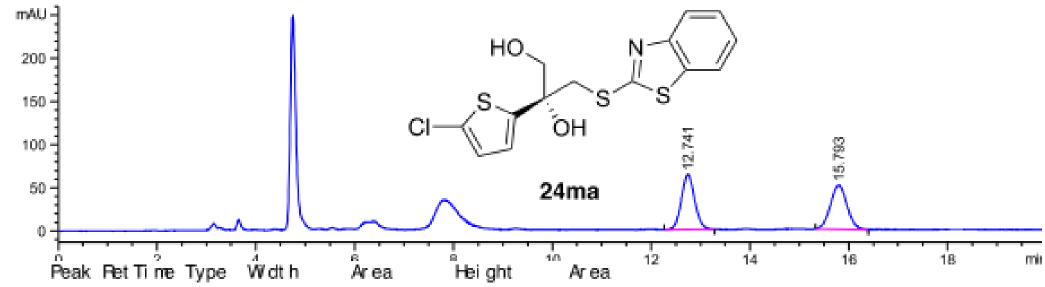

Peak #	Ret Time [min]	Type	Width [min]	Area [mAU*s]	Height [mAU]	Area %
1	12.741	BB	0.2919	1207.89124	64.07797	50.3296
2	15.793	BB	0.3282	1192.07239	51.09183	49.6704

HPLC of **24ma** (result for **Cat f**)

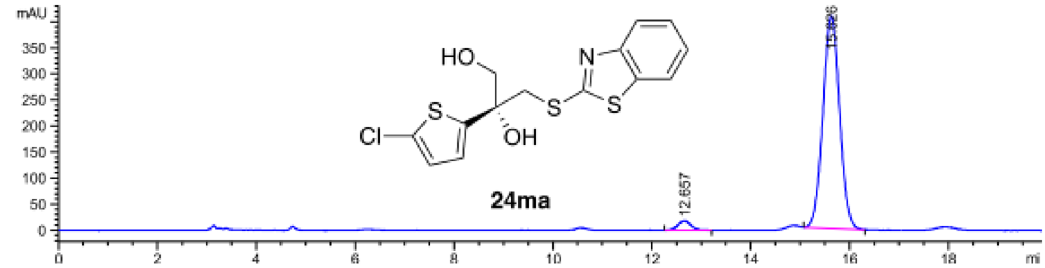

Peak #	Ret Time [min]	Type	Width [min]	Area [mAU*s]	Height [mAU]	Area %
1	12.657	BB	0.2765	340.74243	18.02709	3.4558
2	15.626	BB	0.3649	9519.21484	406.99600	96.5442

HPLC of *rac* **24ma**

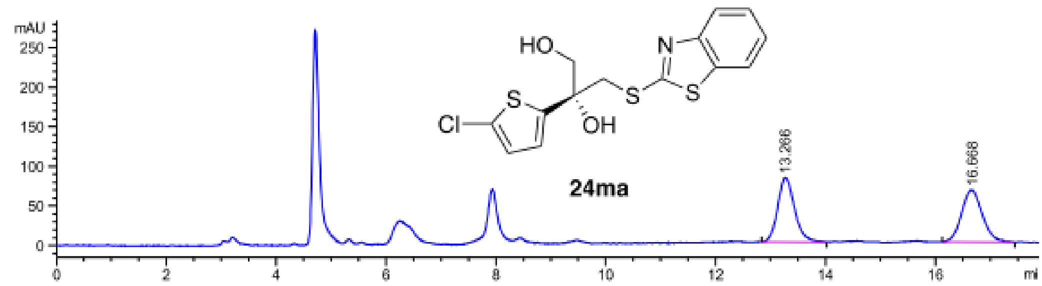

Peak #	Ret Time [min]	Type	Width [min]	Area [mAU*s]	Height [mAU]	Area %
1	13.266	BB	0.2998	1754.47656	81.28252	50.2306
2	16.668	BB	0.3429	1738.36853	66.07320	49.7694

HPLC of **24ma** (result for **Cat g**)

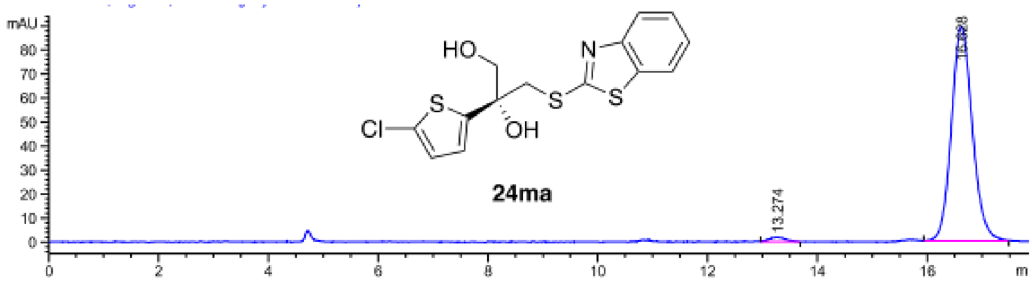

Peak #	Ret Time [min]	Type	Width [min]	Area [mAU*s]	Height [mAU]	Area %
1	13.274	BB	0.2380	37.32738	1.87726	1.5578
2	16.628	BB	0.4040	2358.82813	89.34995	98.4422

HPLC of *rac* **24na**

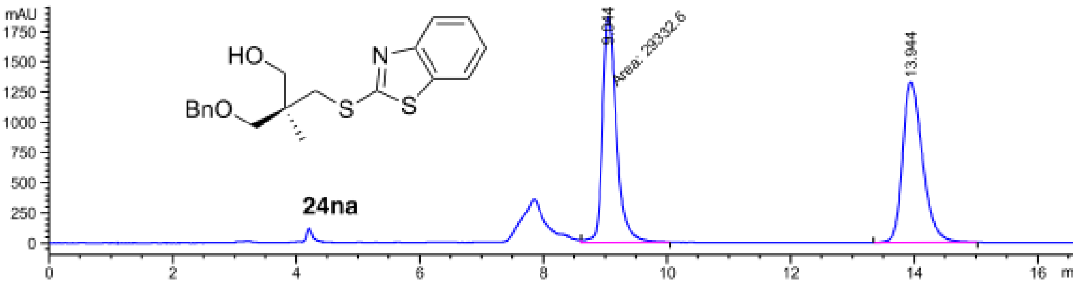

Peak #	Ret Time [min]	Type	Width [min]	Area [mAU*s]	Height [mAU]	Area %
1	9.044	MM	0.2618	2.93326e4	1867.45239	49.4191
2	13.944	BB	0.3416	3.00222e4	1328.84326	50.5809

HPLC of **24na** (result for **Cat f**)

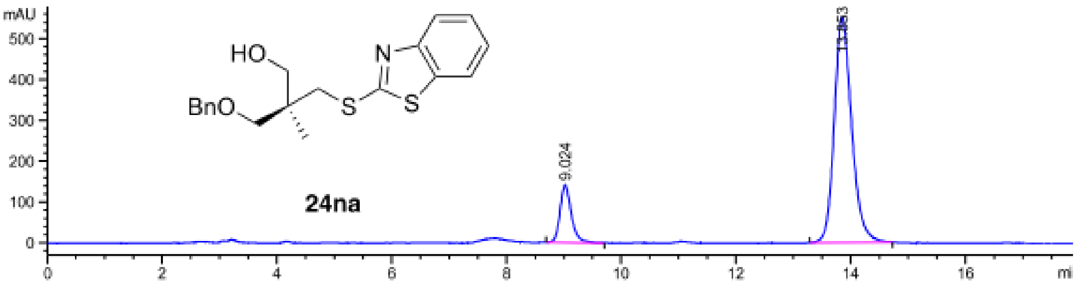

Peak #	Ret Time [min]	Type	Width [min]	Area [mAU*s]	Height [mAU]	Area %
1	9.024	BB	0.2097	1929.77136	141.00459	14.1735
2	13.853	BB	0.3192	1.16856e4	551.44299	85.8265

HPLC of **24na** (result for **Cat g**)

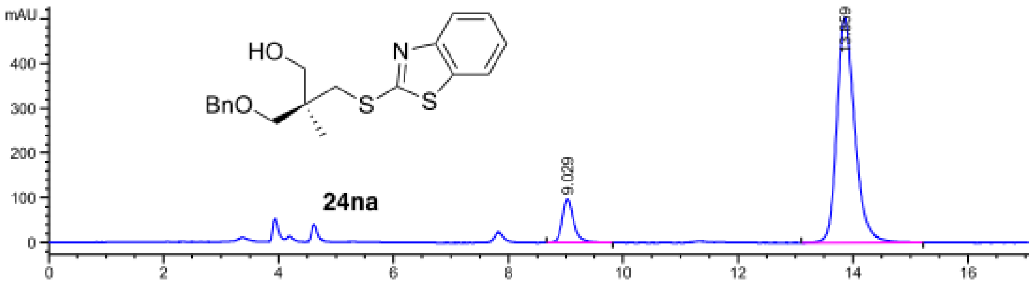

Peak #	Ret Time [min]	Type	Width [min]	Area [mAU*s]	Height [mAU]	Area %
1	9.029	BB	0.2142	1361.98108	96.79556	11.0911
2	13.859	BB	0.3278	1.09179e4	501.79672	88.9089

HPLC of *rac* **24ab**

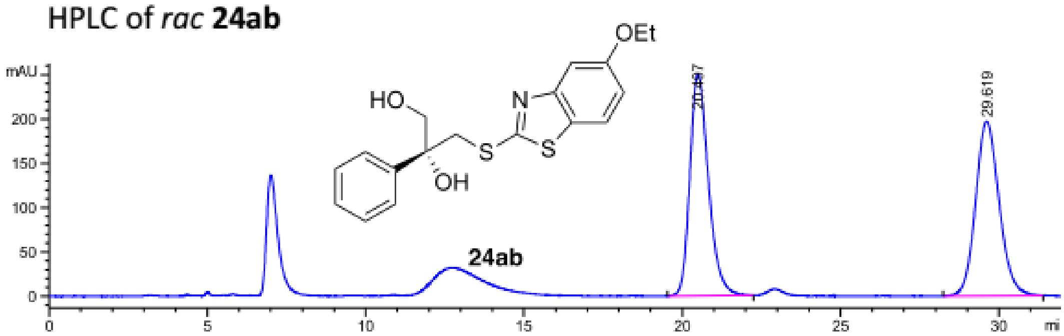

Peak #	Ret Time [min]	Type	Width [min]	Area [mAU*s]	Height [mAU]	Area %
1	20.497	BB	0.6070	1.01637e4	249.65979	49.8290
2	29.619	BB	0.7706	1.02334e4	196.81686	50.1710

HPLC of **24ab** (result for **Cat f**)

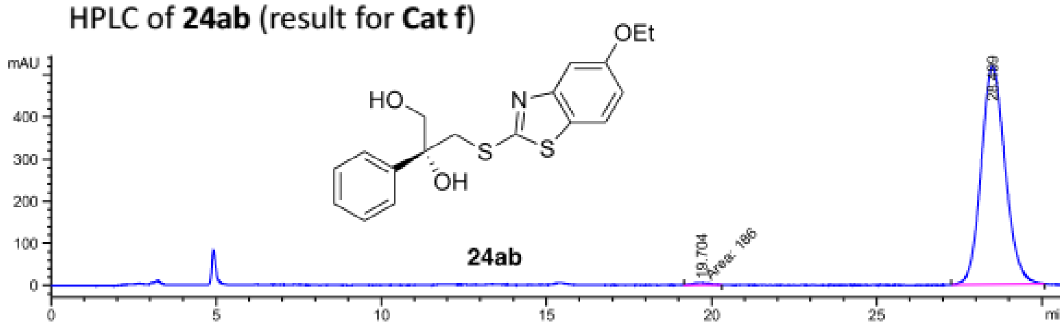

Peak #	Ret Time [min]	Type	Width [min]	Area [mAU*s]	Height [mAU]	Area %
1	19.704	MM	0.5795	185.99971	5.34953	0.7044
2	28.499	BB	0.6043	2.62180e4	518.14020	99.2956

HPLC of **24ab** (result for **Cat g**)

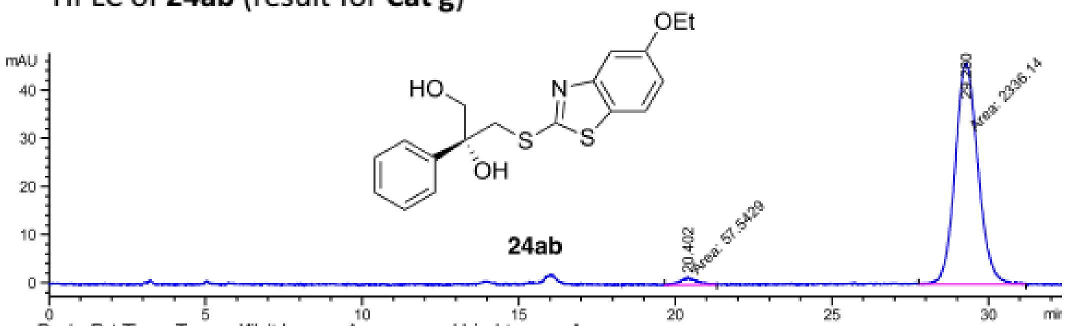

Peak #	Ret Time [min]	Type	Width [min]	Area [mAU*s]	Height [mAU]	Area %
1	20.402	MM	0.6097	57.54285	1.57298	2.4039
2	29.280	MM	0.8502	2336.13672	45.79684	97.5961

HPLC of *rac* **24ac**

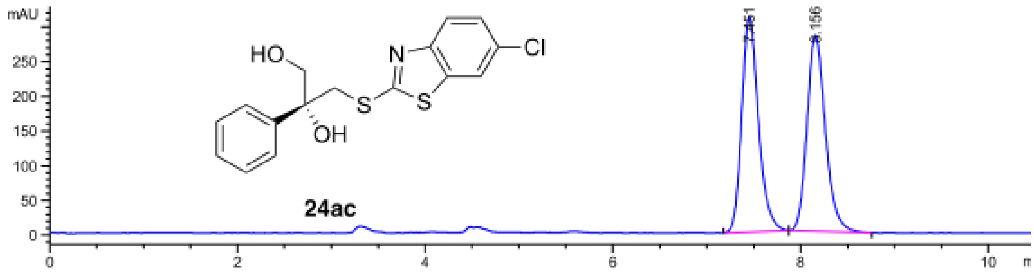

Peak #	RetTime [min]	Type	Width [min]	Area [mAU*s]	Height [mAU]	Area %
1	7.451	BB	0.1886	3836.87817	309.46826	50.0024
2	8.156	BB	0.2087	3836.50757	282.03986	49.9976

HPLC of **24ac** (result for **Cat f**)

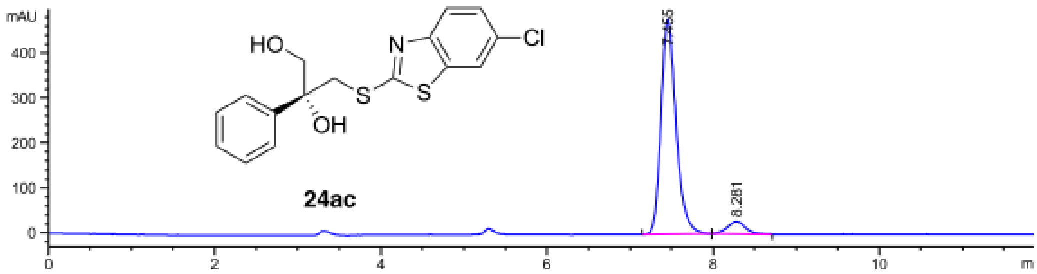

Peak #	RetTime [min]	Type	Width [min]	Area [mAU*s]	Height [mAU]	Area %
1	7.455	BB	0.1899	5979.53027	478.10236	93.5845
2	8.281	BB	0.2250	409.91687	27.32908	6.4155

HPLC of **24ac** (result for **Cat g**)

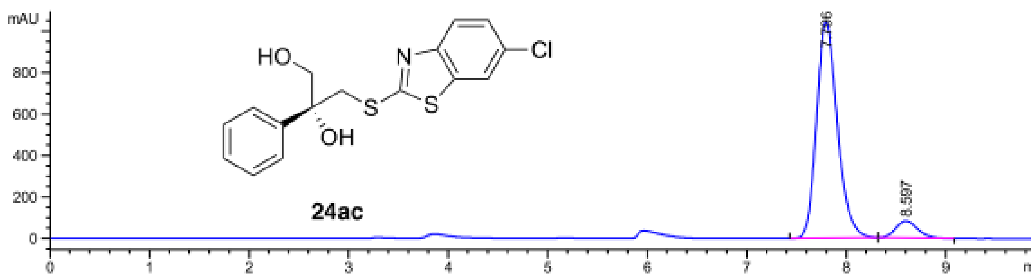

Peak #	RetTime [min]	Type	Width [min]	Area [mAU*s]	Height [mAU]	Area %
1	7.796	BB	0.2230	1.51223e4	1044.15747	92.4169
2	8.597	BB	0.2345	1240.83838	82.02414	7.5831

HPLC of *rac* **24ad**

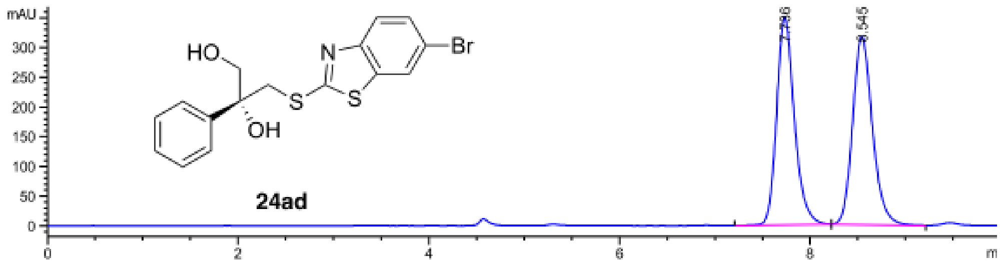

Peak #	RetTime [min]	Type	Width [min]	Area [mAU*s]	Height [mAU]	Area %
1	7.736	BB	0.1977	4546.08301	349.69937	49.9879
2	8.545	BB	0.2219	4548.28320	316.08212	50.0121

HPLC of **24ad** (result for **Cat f**)

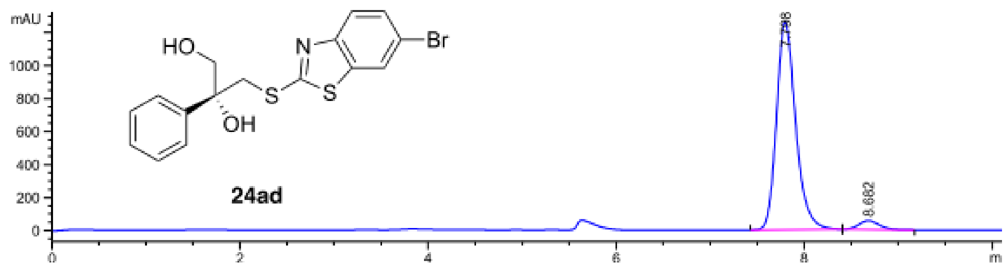

Peak #	RetTime [min]	Type	Width [min]	Area [mAU*s]	Height [mAU]	Area %
1	7.798	BB	0.2181	1.79290e4	1259.12231	95.8007
2	8.682	BB	0.2313	785.89990	52.91985	4.1993

HPLC of **24ad** (result for **Cat g**)

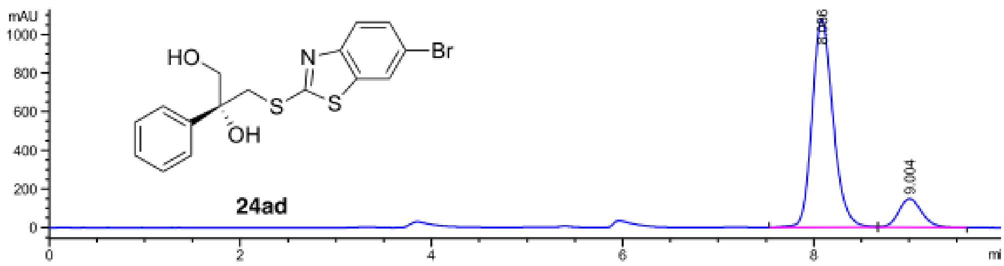

Peak #	RetTime [min]	Type	Width [min]	Area [mAU*s]	Height [mAU]	Area %
1	8.086	BB	0.2328	1.62947e4	1075.38013	87.1605
2	9.004	BB	0.2529	2400.34058	146.71199	12.8395

Chapter V

Manganese/Copper Co-Catalyzed Electrochemical Wacker-Tsuji-Type Oxidation of Aryl-Substituted Alkenes

5.1. Introduction

The oxidation of olefins represents a powerful tool for converting mineral oil into high value-added chemicals. The Wacker process, which was originally developed by *Wacker Chemie* in the 1950s and 1960s, was one of the first homogeneous catalytic processes applied on an industrial scale for the oxidation of ethylene to acetaldehyde. It involves the use of palladium (II) chloride and copper (II) as catalysts, the reaction taking place in aqueous media under oxygen.[192] The lab scale modified version, namely the Wacker-Tsuji Oxidation, is one of the most useful methods for the conversion of terminal olefins into methyl ketones.[193] In the Wacker-Tsuji Oxidation, water serves as the oxygen source, and the reduced palladium is re-oxidized by copper (II) and, ultimately, by atmospheric oxygen.[194] A variety of methods based on this reaction, resulting by modifying the re-oxidation process for palladium, have been reported during the past decades. In this part, some examples of recent developments of Wacker-type process will be described below.

5.2. Palladium catalyzed Wacker-Tsuji oxidation

In 2004, Sigman group reported the use of low catalyst loading of Pd[(−)-sparteine]Cl_2 as catalyst to prevent olefin isomerization and led to selective formation of corresponding methyl ketones from terminal olefins (Scheme 1).

[192] *Organometallics;* Elschenbroich, C., Ed.; Wiley-VCH: Weinheim, **2006**.

[193] (a) *Organic Synthesis with Palladium Compounds;* Tsuji, J., Ed.; Springer Verlag, Berlin, **1980**. (b) *Palladium Reagents in Organic Synthesis*; Heck, R. F., Ed.; Academic Press, London, **1985**.

[194] *Palladium Reagents and Catalysts*, First Edition; Tsuji, J., Ed.; Wiley, **2004**, 29-35.

Oxidation of enantiomerically enriched substrates in this process didn't led to racemization.[195]

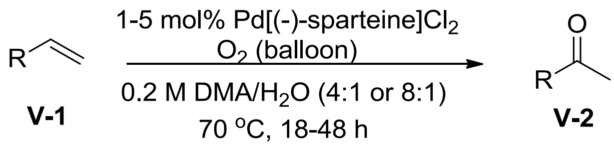

Scheme 1. Pd[(−)-sparteine]Cl_2 as catalyst for Wacker oxidation

In 2006, the Kaneda group reported that the combination of $PdCl_2$ and N,N - dimethylacetamide (DMA) constituted a highly efficient and reusable catalytic system for converting terminal olefins into methyl ketones. In this system, if water is replaced with HOAc in the present of 20 mol% NaOAc the reaction produced the corresponding linear allylic acetates (Scheme 2).[196]

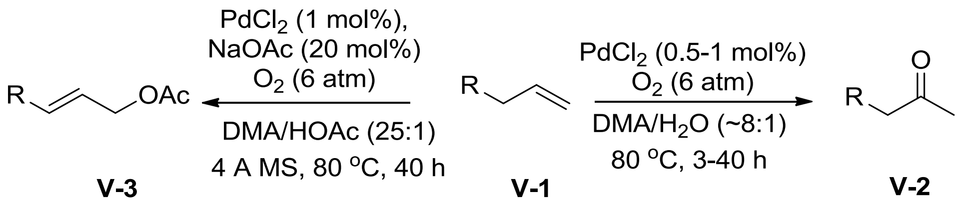

Scheme 2. $PdCl_2$ and N,N - dimethylacetamide (DMA) for Wacker oxidation

In 2009, the Sigman group reported the use of 2-(4,5-dihydro-2-oxazolyl)quinoline (Quinox) ligand and aqueous TBHP for the efficient conversion of protected allylic alcohols to the corresponding acylation products and the conversion of terminal olefins into methyl ketones in short reaction times (Scheme 3). The catalytic system used by Sigman is scalable and can be performed with a low loading (1 mol%) of catalyst.[197]

---

[195] Cornell, C. N.; Sigman, M. S. *Org. Lett.* **2006**, *8*, 4117-4120.

[196] Mitsudome, T.; Umetani, T.; Nosaka, N.; Mori, K.; Mizugaki, T.; Ebitani, K.; Kaneda, K. *Angew. Chem., Int. Ed.* **2006**, *45*, 481-485.

[197] Michel, B. W.; Camelio, A. M.; Cornell, C. N.; Sigman, M. S. *J. Am. Chem. Soc*. **2009**, *131*, 6076-6077.

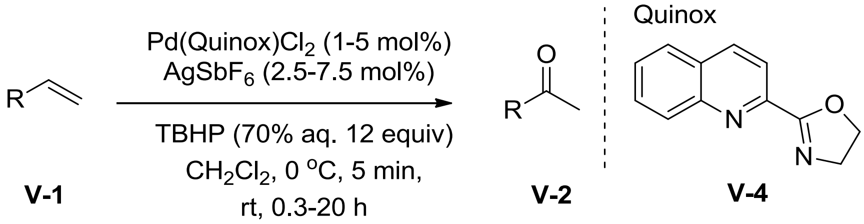

Scheme 3. Pd(Quinox)Cl_2 and aqueous TBHP for Wacker oxidation of protected allylic alcohols

In a 2013 update, Sigman and coworkers applied this methodology to the oxidation of internal alkenes and in the total synthesis of the antimalarial drug artemisinin (Scheme 4).[198]

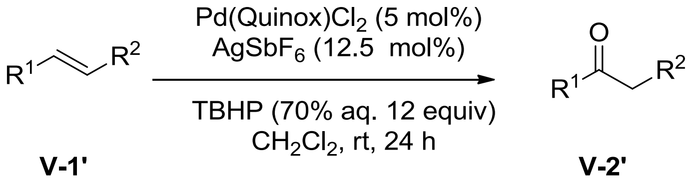

Scheme 4. Pd(Quinox)Cl_2 and aqueous TBHP for Wacker oxidation of internal alkenes

In 2017, the Ishida group reported the Wacker oxidation of terminal alkenes into methyl ketones by using reusable ZrO_2 supported Pd^0 nanoparticles (NPs) under acid- and cocatalyst-free conditions (Scheme 5). For this application, the Pd NPs with a diameter of 4–12 nm exhibited the highest activity.[199]

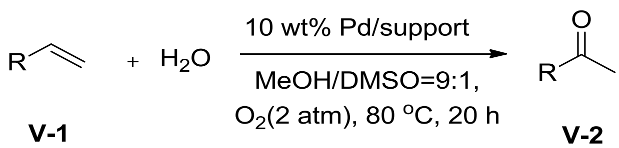

Scheme 5. ZrO_2 supported Pd0 NPs for Wacker oxidation

In 2014, the Wang group reported a palladium-catalyzed oxidation system using molecular oxygen as the sole oxidant and involving any palladium ligand. Terminal olefins, and especially styrene, can be oxidized to methyl ketones by

[198] DeLuca, R. J.; Edwards, J. L.; Steffens, L. D.; Michel, B. W.; Qiao, X.; Zhu, C.; Cook, S. P.; Sigman, M. S. *J. Org. Chem.* **2013**, *78*, 1682-1686.

[199] Zhang, Z.; Kumamoto, Y.; Hashiguchi, T.; Mamba, T.; Murayama, H.; Yamamoto, E.; Ishida, T.; Honma, T.; Tokunaga, M. *ChemSusChem* **2017**, *10*, 3482-3489.

this system. In addition, for some substrates, oxidation–dehydrogenation of terminal olefins to α,β-unsaturated ketones was observed.[200]

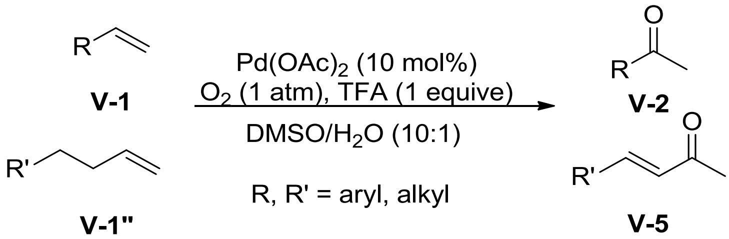

Scheme 6. Non ligand palladium-catalyzed Wacker oxidation

In 2016, the Fernandes group reported a combination of Pd(II) and Dess–Martin periodinane to produce methyl ketones from terminal olefins in high yields (Scheme 7). This operationally simple and scalable method has good functional group compatibility.[201]

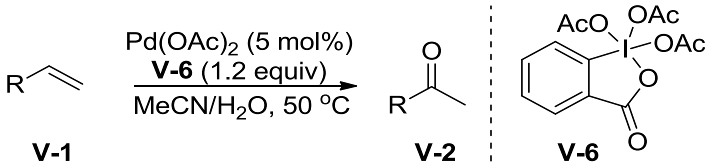

Scheme 7. Pd(II) and Dess–Martin periodinane for Wacker oxidation

In the same year, the Fernandes group reported a traceless one-pot synthesis of α,β-unsaturated and non-conjugated ketones from homo-allyl alcohols by a sequential $PdCl_2/CrO_3$-promoted Wacker process followed by an acid-mediated dehydration reaction (Scheme 8).[202] Remarkably, internal homo-allyl alcohols delivered regioselectively non-conjugated unsaturated carbonyl compounds by using the same protocol.

---

[200] Wang, Y. F.; Gao, Y. R.: Mao, S.; Zhang, Y. L.; Guo, D. D.; Yan, Z. L.; Guo, S. H.; Wang, Y. Q. *Org. Lett.* **2014**, *16*, 1610-1613.

[201] Chaudhari, D. A.; Fernandes, R. A. *J. Org. Chem.* **2016**, *81*, 2113-2121.

[202] Bethi, V.; Fernandes, R. A. *J. Org. Chem.*, **2016**, *81*, 8577-8584.

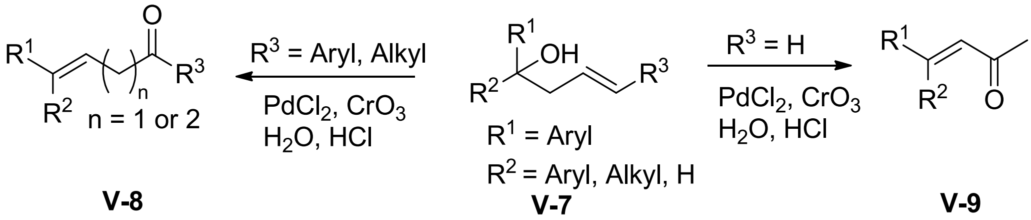

Scheme 8. One-pot synthesis of α,β-unsaturated and non-conjugated ketones

In 2017, the Peng group showed that a 5% palladium on charcoal catalyst displayed excellent catalytic activity in the oxidation of styrenes to the corresponding ketones with H_2O_2 as oxidant (Scheme 9). The method offers an option for avoiding the use of a copper salt as a co-catalyst.[203]

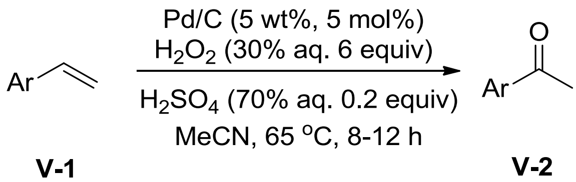

Scheme 9. Pd(0)/C catalyst for Wacker oxidation

In 2018, the Kang group reported a regioselectivity switchable aerobic Wacker–Tsuji oxidation using catalytic *tert*-butyl nitrite as a redox co-catalyst (Scheme 10). Either substituted aldehydes or ketones could be prepared with this procedure by simply switching the reaction solvent from *tert*-butyl alcohol to wet ethanol.[204]

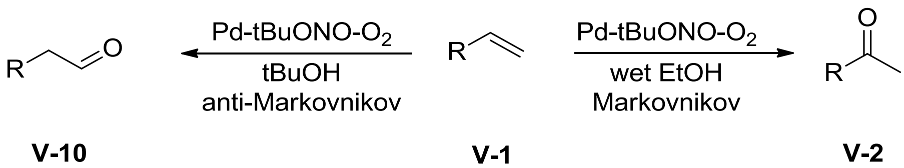

Scheme 10. *tert*-Butyl nitrite as a redox cocatalyst for Wacker oxidation

In 2019, Brunzel and coworkers reported a selective procedure for the conversion of an isomeric mixture of 1,9-cyclohexadecadiene to the corresponding monounsaturated cyclohexadec-8-en-1-one *via* Wacker type oxidation at room

---

[203] Xia, X.; Gao, X.; Xu,J.; Hu, C.; Peng, X. *Synlett* **2017**, *28*, 607-610.

[204] Hu, K. F., Ning, X. S., Qu, J. P., & Kang, Y. B. *J. Org. Chem.* **2018**, *83*, 11327-11332.

temperature (Scheme 11). Iron (III) salts were used as co-catalysts in this process.[205]

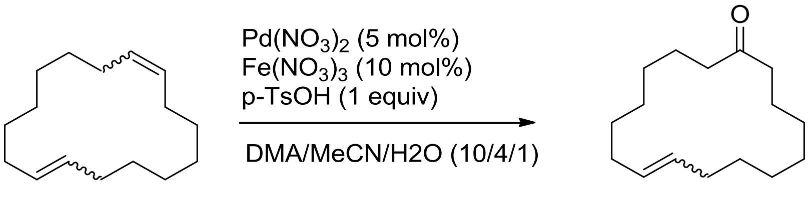

V-11 **V-12**

Scheme 11. Iron (III) salts as co-catalysts for Wacker oxidation

In the same year, the Gotor - Fernández group reported a sequential and selective chemoenzymatic approach involving the Wacker-Tsuji oxidation of allylbenzenes to the corresponding ketones followed by an enzyme catalyzed *biotransamination* with good to excellent yields and excellent selectivities in aqueous medium (Scheme 12).[206]

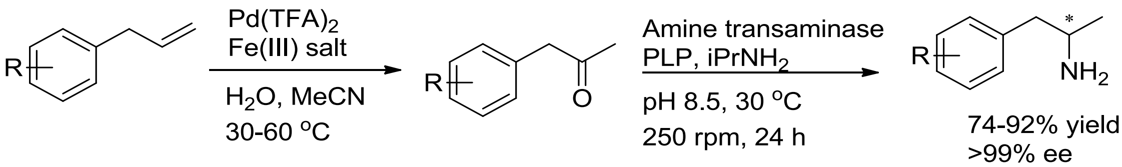

V-1 **V-2** **V-13**

Scheme 12. Iron (III) salts as co-catalysts for Wacker oxidation in aqueous medium

Visible light has been used as a green oxidant in the Wacker-type oxidations. In 2019, the Fabry group reported a catalytic Wacker-type oxidation using a combined palladium/photoredox catalytic system (Scheme 13). A broad range of substrates was examined affording the desired products in good yields.[207]

---

[205] Brunzel, T.; Heppekausen, J.; Panten, J.; Köckritz, A. *RSC Adv.* **2019**, *9*, 27865-27873.

[206] González‒Martínez, D.; Gotor, V.; Gotor‒Fernández, V. *Adv. Synth. Catal.* **2019**, *361*, 2582-2593.

[207] Ho, Y. A.; Paffenholz, E.; Kim, H. J.; Orgis, B., Rueping, M.; Fabry, D. C. *ChemCatChem* **2019**, *11*, 1889-1892.

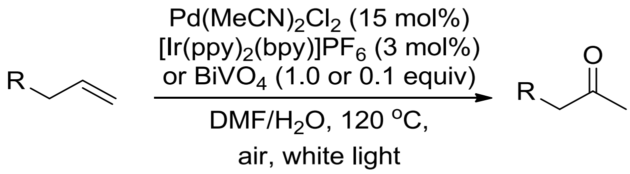

V-1 V-2

Scheme 13. Visible light was used as green oxidant for Wacker oxidation

Most recently, in 2020, the Kang group reported a regioselective Wacker-Tsuji oxidation of internal olefins to the corresponding ketones in ^{t}BuOH, using oxygen as the terminal oxidant and *tert*-butyl nitrite as a co-catalyst. The reaction takes place in generally good yields and with high regioselectivities.[208]

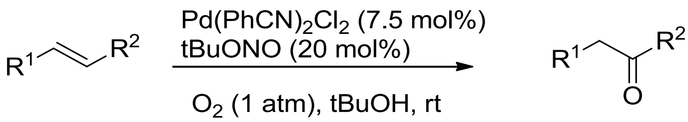

V-1' V-2'

Scheme 14. *tert*-Butyl nitrite as co-catalyst for Wacker oxidation of internal olefins

5.3. Non-palladium catalysed Wacker-Tsuji-type oxidation

In 2016, the Lei group presented a direct anti-Markovnikov oxidation of β-alkyl styrenes with H_2O under external-oxidant-free conditions by utilizing a photo redox-metal dual catalytic system to access the corresponding carbonyl compounds (Scheme 15).[209]

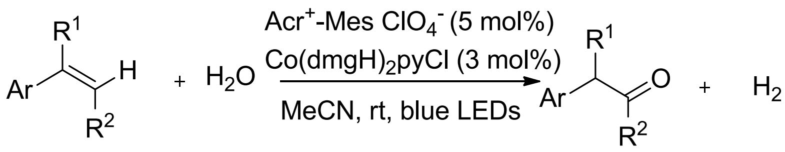

V-1' V-2'

Scheme 15. Anti-Markovnikov oxidation of β-alkyl styrenes with H_2O

---

[208] Huang, Q.; Li, Y. W.; Ning, X. S.; Jiang, G. Q.; Zhang, X. W.; Qu, J. P.; Kang, Y. B. *Org. Lett.* **2020**, *22*, 965-969.

[209] Zhang, G.; Hu, X.; Chiang, C. W.; Yi, H.; Pei, P.; Singh, A. K.; Lei, A. *J. Am. Chem. Soc.* **2016**, *138*, 12037-12040.

In 2017, Han and coworkers reported a $FeCl_2$ catalyzed Wacker - type oxidation of olefins to ketones using polymethylhydrosiloxane (PMHS) as an additive and air as the sole oxidant (Scheme 16). The process demonstrated excellent functional - group tolerance and could be applied to oxidize derivatives of complex natural product and polyfunctionalized molecules.[210]

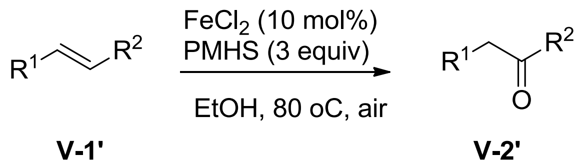

Scheme 16. $FeCl_2$ catalyzed Wacker - type oxidation

In 2018, the Knölker group described the oxidation of olefins into ketones catalyzed by the iron–complex $FePcF_{16}$ with stoichiometric amounts of triethylsilane as an additive under oxygen atmosphere with functional group tolerance (Scheme 17). The process was not completely selective, and the corresponding alcohols were observed as by-products.[211]

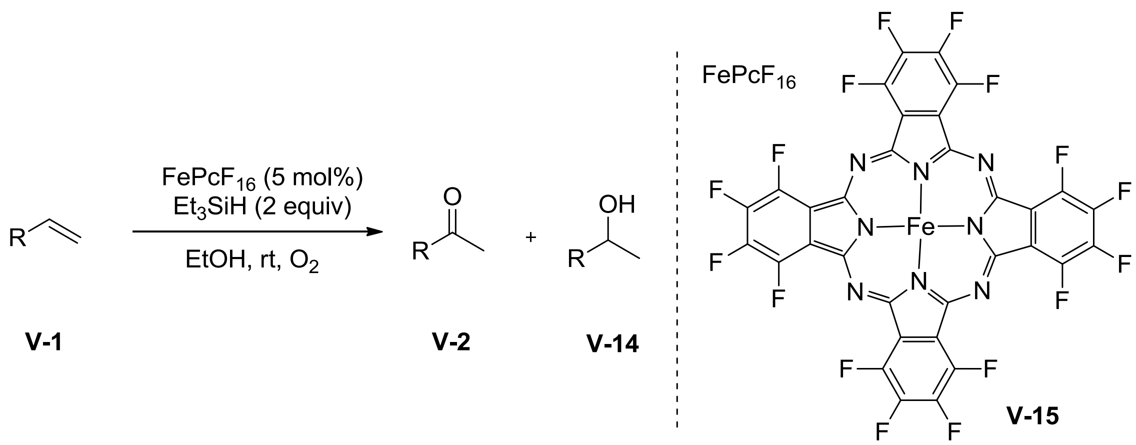

Scheme 17. $FePcF_{16}$ catalyzed Wacker-type oxidation

5.4. Aim of this project

[210] Liu, B.; Jin, F.; Wang, T.; Yuan, X.; Han, W. *Angew. Chem. Int. Ed.* **2017**, *56*, 12712-12717.

[211] Puls, F.; Knölker, H. J. *Angew. Chem. Int. Ed.* **2018**, *57*, 1222-1226.

Organic electrochemistry offers a mild and efficient alternative to conventional chemical approaches, with electricity representing a green oxidant or reducing agent in these processes. Electro oxidation methods have been employed for the direct oxidation of Pd(0) to Pd(II)[212,213,214,215] or for the generation of recyclable oxidants such as p-benzoquinone, ferric chloride or triarylamine, and as a co-oxidant for regeneration of Pd(II) catalysts. In these studies, divided cell systems have been usually utilized to avoid the deposition of palladium metal onto the cathode, which often led to unsatisfactory reaction conversion.[216]

Hitherto, the most significant progress on the knowledge and mastering of the Wacker-type oxidation is focused on palladium catalysis. However, challenges in the Wacker-Tsuji Oxidation remains, such as the poor activity for internal alkenes, degradation of the palladium catalyst, isomerization of the olefin, the formation of chlorinated byproducts, the generation of copper waste, high cost derived from the use of palladium, the generation of chemical waste, and/or safety concerns. Therefore, less hazardous, cost-effective, and noble-metal-free oxidation of alkenes is still in challenging and deserves further effort.

The electrochemical functionalization of olefins has received considerable attention in recent times and the use of manganese catalysis for this purpose, pioneered by Lin, has played a central role in these developments. In 2017, the Song Lin group reported the electrochemical diazidation of alkenes catalyzed by Manganese salts.[217] They later reported a Mn-catalyzed electrochemical dichlorination of alkenes using $MgCl_2$ as the chlorine source[218] and a

[212] (a) Blake, A. R.; Sunderland, J. G. *J. Chem. Soc. A*, **1969**, 3015-3018; (b) Goodridge, F.; King, C. J. H. *Trans. Faraday Soc.* **1970**, *66*, 2889-2896.

[213] Tsuji, J.; Minato, M. *Tetrahedron Lett.***1987**, *28*, 3683-3686.

[214] Horrowitz, H. H. *J. Appl. Electrochem.* **1984**, *14*, 779-790.

[215] a) Inokuchi, T.; Ping, L.; Hamaue, F.; Izawa, M.; Torii, S. *Chem. Lett*. **1994**, 121; b) Tesfu, E.; Maurer, K.; Ragsdale, S. R.; Moeller, K. D. *J. Am. Chem. Soc.* **2004**, *126*, 6212-6213.

[216] Wayner, D. D. M.; Hartstock, F. W. *J. Mol. Catal.* **1988**, *48*, 15-19.

[217] Fu, N.; Sauer, G. S.; Saha, A.; Loo, A; Lin, S. *Science* **2017**, *357*, 575-579.

[218] Fu, N.; Sauer, G. S.; Lin, S. *J. Am. Chem. Soc.* **2017**, *139*, 15548-15553.

chlorotrifluoromethylation of alkenes.[219] Encouraged by those works, most recently the Chen group reported a Mn-catalyzed electrochemical oxychlorination of styrenes via the oxygen reduction reaction, with $MgCl_2$ as the chlorine source.[220] At the light of these findings, we decided to explore the possibility of developing an electrochemical alternative to the Wacker-Tsuji-type process where toxic and expensive palladium could be replaced by abundant and less harmful metals used as catalysts.

Herein we wish to report the successful development of an electrochemical Wacker-Tsuji-type oxidation of aryl-substituted alkenes through a manifold of parallel oxidative events taking place at a carbon felt anode in an undivided cell using cheap, environmentally friendly $MnBr_2$ and $CuCl_2$ as co-catalysts in acetonitrile/water under *forbidden* conditions (2.8 V) as shown in Scheme 18.

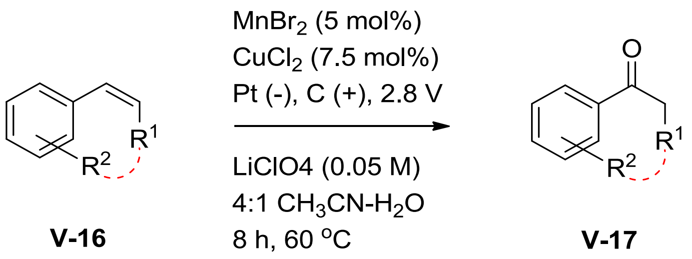

Scheme 18. Aim of this project

[219] Ye, K.; Pombar, G.; Fu, N.; Sauer, G. S.; Keresztes, I.; Lin, S. *J. Am. Chem. Soc.* **2018**, *140*, 2438-2441.

[220] Tian, S.; Jia, X.; Wang, L.; Li, B.; Liu, S.; Ma, L.; Gao, W.; Wei, Y.; Chen, J. *Chem. Commun.* **2019**, *55*, 12104-12107.

This manuscript was later published in Organic letters. (*Org. Lett.* **2020**, *22*, 7338-7342)

Manganese/Copper Co-Catalyzed Electrochemical Wacker-Tsuji-Type Oxidation of Aryl-Substituted Alkenes

Junshan Lai, and Miquel A. Pericàs*

Supporting Information Placeholder

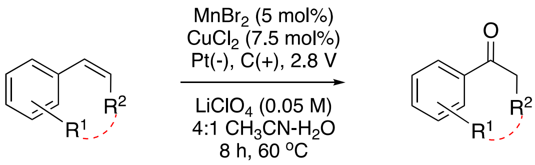

ABSTRACT: A manganese/copper co-catalyzed electrochemical Wacker-Tsuji-type oxidation of aryl-substituted alkenes has been developed. The process involves the use of 5 mol% $MnBr_2$ and 7.5 mol% $CuCl_2$, in 4:1 acetonitrile/water in an undivided cell at 60 ºC, with 2.8 V constant applied potential. α-Aryl ketones are formed in moderate to excellent yields, with the advantages of avoidance of palladium as a catalyst and any external chemical oxidant, in an easily operated, cost effective procedure.

The oxidation of olefins is a powerful tool for the industrial conversion of petrochemical feedstocks into high value-added chemicals.[1] Among the processes used with this purpose, the Wacker oxidation for the preparation of acetaldehyde from ethylene in aqueous media, with palladium (II) chloride and copper (II) as catalysts under oxygen, was one of the first homogeneous catalytic processes applied on an industrial scale.[2] The laboratory scale modification, namely the Wacker-Tsuji oxidation, is one of the most useful methods for convert terminal olefins into methyl ketones.[3] In this protocol water serves as the oxygen source, and the reduced palladium generated in the process is re-oxidized by copper (II) and ultimately by atmospheric oxygen.[4] A variety of synthetic methods based on this reaction by modification of the palladium re-oxidation process[5] or the nature of the involved nucleophile[6] have been reported during the past decades, and the process has found application in broadly different fields.[7]

Organic electrochemistry offers a mild and efficient alternative to conventional chemical approaches to redox chemistry, electricity representing (depending on its origin) a potentially *green* oxidizing or reducing agent[8] with no limitations for large scale application.[9] Electrooxidation methods have already been used for the partial oxidation of ethylene on palladium electrodes[10] and for the regeneration of recyclable oxidants such as quinone,[11] iron trichloride[12] or triarylamines,[13] used for the regeneration of the Pd(II) catalyst in Wacker-Tsuji reactions. In these studies, divided cell systems have been normally used to avoid the deposition of palladium metal onto the cathode that could result in unsatisfactory conversion.[14]

Hitherto, progress in the Wacker-type oxidation has rarely escaped from the palladium catalysis paradigm. There are, however, important limitations in the Wacker-Tsuji Oxidation still remaining, such as cost and toxicity to humans of palladium compounds, low activity for internal alkene substrates, moderate TON due to degradation of the palladium catalyst, and the formation of chlorinated by-products,[15] among others. Therefore, the development of cost-effective, noble-metal-free procedures for the oxidation of alkenes offers considerable interest. In this respect, Lei and coworkers reported a direct anti-Markovnikov oxidation of β-alkylstyrenes to carbonyl compounds involving a dual photoredox-metal catalytic system,[16] while the Han group reported the iron-catalyzed Wacker-type oxidation of olefins to ketones using ambient air as the sole oxidant under mild reaction conditions.[17]

The electrochemical functionalization of olefins has received considerable attention in recent times[18-23] and the use of manganese catalysis, pioneered by Li, has played a central role in these developments.[19-23] At the light of these findings, we decided to explore the possibility of developing an electrochemical alternative to the Wacker-Tsuji process where toxic and expensive palladium could be replaced by abundant and less harmful metals used as catalysts. Herein we wish to report the successful development of an electrochemical Wacker-Tsuji-type oxidation of aryl-substituted alkenes through a manifold of parallel oxidative events taking place at a carbon felt anode in an undivided cell using cheap, environmentally friendly $MnBr_2$ and $CuCl_2$ as co-catalysts in acetonitrile/water under *forbidden* conditions (2.8 V) as shown in Scheme 1.

Scheme 1. Standard and Electrochemical Wacker-Tsuji Oxidation

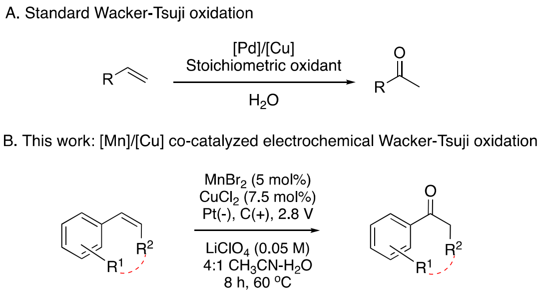

Our initial study targeted the oxidation of styrene (**1a**) to acetophenone (**2a**), as shown in Table S1. An undivided cell with Pt as cathode and carbon felt as anode was used in the experiments, operated at an applied voltage of 3.0 V. Since it has been previously reported that Mn(II) salts catalyze the coupling of styrenes and aliphatic alcohols under oxidative conditions (TBHP),[24] we wanted to discard first the operation of this mechanism under electrooxidative conditions. As shown in entries S1-S2, no coupling took place between primary alcohols used as co-solvents and styrene **1a**, while acetophenone **2a** was detected in low yield when 1:1 isopropanol/water was used as a solvent in the presence of 5 mol% $MnBr_2$ as catalyst at 60 ºC (entry S3). Binary mixtures of polar aprotic solvents and water also afforded poor results (entries S4-S5) but the use of 4:1 vol/vol acetonitrile/water was somewhat promising, especially when performing the reaction at 60 ºC (entries S7-S8). The use of $NiCl_2$ (entry S9), $FeCl_3$ (entry S10), or even $PdCl_2$ (entry S11) instead of $MnBr_2$ was deleterious. On the other hand, the combined use of $MnBr_2$ and $CuCl_2$ (5 mol% each) led to a very significant yield increase (67%, entry S12). Alternatively, the exclusive use of $CuCl_2$ didn't produce any detectable amount of **2a** (entry S13).

Once we had established the determining roles in the reaction of $MnBr_2$ and $CuCl_2$, we proceeded to optimize the relative amounts of these two species (Figures S1 and S2). The initial concentration of **1a** (Figure S4) and of the support electrolyte $LiClO_4$ (Figure S5) were also optimized.

Interestingly, the reaction gave a similar yield in the presence or in the absence of oxygen in the reaction cell. Besides the operative advantage in reaction practicality, this observation provides a clear indication that oxygen reduction is not involved in the observed reaction and that the oxygen atom in the final product arises from water. We accordingly studied the effect of the proportion of water in the solvent system on the efficiency of the process (Figure S3). As anticipated, the presence of water in the solvent is a requisite for the reaction to take place, and the optimal yield (77%) is achieved with a volumetric composition of 80% MeCN and 20% water. Further increases in the amount of water lead to a rather sharp decrease in yield, probably because of the insolubility of styrene in those solvent mixtures.

As a final parameter, we studied the effect of the applied potential on the reaction yield while working in constant voltage mode (Figure S6). The onset voltage for the reaction to proceed was shown to be 1.7 V. Yield slightly increased with the applied potential and, at *ca*. 2.5 V, a sudden increase in the slope of the yield *vs*. voltage graph occurs, a maximum 85% yield being achieved at 2.8 V.[25] These experiments were later repeated in a single compartment, three electrode cell including a AgCl reference electrode (see Figure S7). Interestingly, the results between 2.4 and 3.0 V are exactly duplicated, the highest (85%) yield being achieved again at 2.8 V. The observed yield *vs*. applied voltage behavior is strongly indicative of some additional redox process, on top of Cu^{I}/Cu^{II} and Mn^{II}/Mn^{III}, taking also place above 2.5 V. According to the known electrochemical oxidation behavior of acetonitrile at platinum electrodes in the presence of water, solvent oxidation appears as a logical, and in this case synergistic, candidate.[26]

Once the optimization process was completed, different combinations of manganese and copper compounds were tested as potential catalytic systems (Table S2). It is interesting to note that combinations of chlorides and bromides of Mn(II) and Cu(II) are almost equally suitable catalysts for the process (entries S1, S5, and S15), the combined use of both dibromides (entry S1) leading to the highest (86%) yield. By the contrary, the combination of both chlorides (entry S12) results in a mediocre catalyst. Thus, the presence of bromide ions is of primordial importance for catalytic activity. The reaction didn't produce any **2a** when $Cu(acac)_2$, involving a highly chelated Cu(II) species, was used as a cocatalyst (entry S6). It is also worth mentioning that polymerization of styrene was observed when $Cu(OTf)_2$ replaced $CuCl_2$ as the Cu(II) source (entry S4).[27] As already mentioned, no acetophenone was detected in the absence of a Mn(II) source (entries S16-S20).

Once the optimal reaction conditions had been fully established, the applicability of the Mn/Cu co-catalyzed electrochemical oxidation was studied on a representative series of substrates **1a-z** containing in their structures an aryl group conjugated with a carbon-carbon double bond (Scheme 2). In general, the reaction tolerates well alkyl groups and medium polarity substituents, such as halogen or trifluoromethyl groups and even groups with strong withdrawing character (**2n**). With respect to regiochemistry, *para*-substituted substrates are those leading to higher yields.

Scheme 2. Substrate Scope in the Mn/Cu Co-Catalyzed Wacker-Tsuji Electrochemical Oxidation[a]

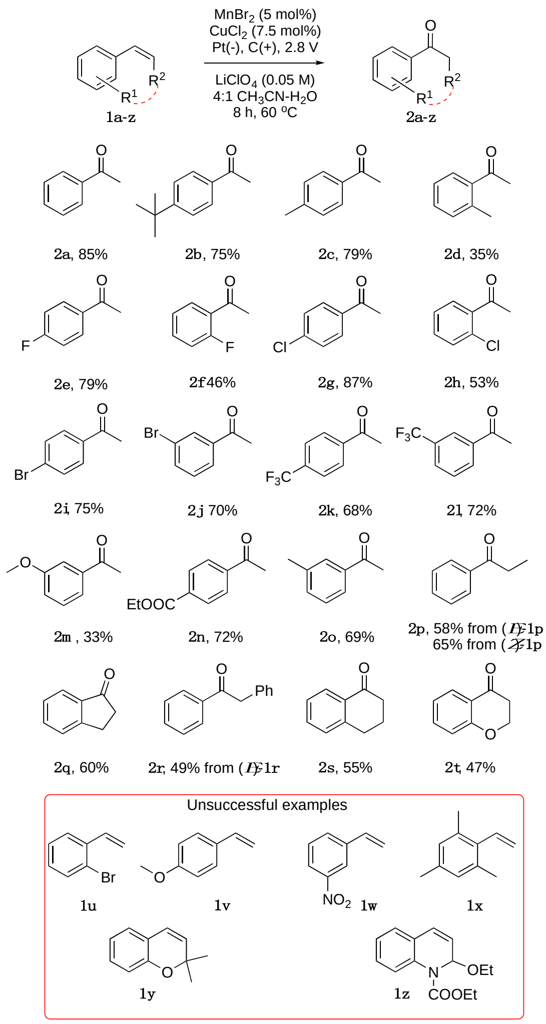

[a]Reaction conditions: Substrate (**1a-z**) (1mmol), $CuCl_2$ (7.5 mol%), $MnBr_2$ (5 mol%), 4:1 acetonitrile:water (3 mL), Constant applied potential: 2.8 V (Pt cathode, Carbon felt anode, 0.05 M $LiClO_4$), 60 °C, 8 h. Isolated yield.

Also in this respect, the reaction appears to be sensitive to steric effects, since *ortho*-substituted substrates, like **1d**, **1f**, and **1h** afford the corresponding oxidation products in lower yield than the corresponding *para*-isomers, and heavily *ortho*-substituted substrates, like **1u** and **1x**, fail to react. Interestingly, substrates containing 1,2-disubstituted double bonds are efficiently oxidized, irrespectively of their cyclic (**1q**, **1s**) or acyclic nature (**1p**, **1r**). In the case of **1p**, no appreciable bias exists with respect to the stereochemistry of the double bond in the substrate. 2*H*-Chromene (**1t**), a substrate belonging to an important class of natural substances, was successfully oxidized to chromanone **2t** (47% yield). However, the analogue 2,2,-dimethyl-2*H*-chromene **1y** failed to react, thus indicating that heavy substitution on the double bond is deleterious to the reaction. On the other hand, when extension of the electrochemical oxidation to commercially available dihydroquinoline **1z** was attempted, fast deprotection of the carbamate moiety took place, but oxidation did not proceed. It is also worth mentioning that allylbenzene, a regioisomer of **1o** of non-styrene nature, completely failed to provide the corresponding oxidation product.[28] Finally, *p*-methoxystyrene (**1t**) and m-nitrobenzaldehyde (**1u**) failed to provide the corresponding acetophenone products **2t** and **2u** for completely different reasons. While **1t** underwent a very fast reaction, but led to ill-defined products of oligomeric nature, **1u** was reluctant to electrochemical Wacker-Tsuji oxidation. This behavior can be rationalized through the tentative mechanistic proposal shown in Figure 1.

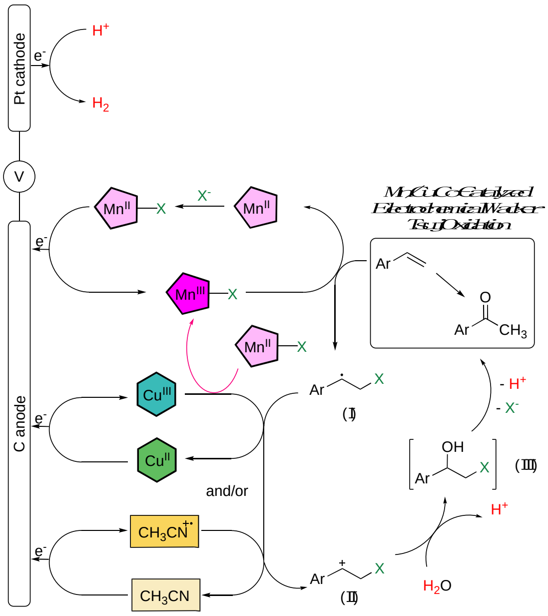

Figure 1. Tentative mechanistic proposal for the Mn/Cu co-catalyzed electrochemical oxidation of styrenes.

As it can be seen, we propose that three parallel oxidative events could take place at the carbon felt anode: the standard oxidation of Mn(II) to Mn(III) [E° = 1.56 V,[29] and peak at *ca*. 1.50 V in the cyclic voltammogram (CV, Figure 2)], the oxidation of Cu(II) to Cu(III) [E° = 2.4 V,[29] and peaks at *ca*. 1.85 and 2.45 V in the CV (Figure 2)], and the oxidation of acetonitrile to its radical cation which, as discussed above (Figure S6), becomes possible at the high applied potential [E° = 1.78 V,[23] and peak at *ca*. 2.32 V in the cyclic voltammogram (Figure 2)]. Interestingly, the peak at ca. 2.5 V in the CV which, according to our optimization studies appears to be very relevant to the overall oxidation process, cannot be observed when water is not present in the solvent system (see SI). We discard the possibility that oxidation of Mn(III) to Mn(IV) can also occur, since MnO_2 does not appear to be a competent chemical oxidant in the overall process (see Table S2, entry S11) and no assignable peak is observed in the CV.

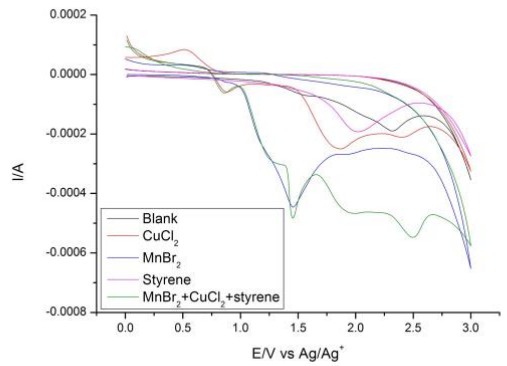

Figure 2. Cyclic voltammetry studies

A chemically or electrochemically generated Mn(III) halide, preferably containing bromide anions (X = Br) according to our optimization studies (Table S2), would transfer a halogen atom onto the starting styrene, generating the intermediate radical (**I**). Evolution of this species towards the final ketone product requires hydration, but this is hardly conceivable at this oxidation level. We accordingly propose that **I** could be further oxidized to carbocation **II** by electrogenerated Cu(III) or, more probably, by electrogenerated acetonitrile radical cation.

Hydration of **II** would lead to bromohydrin **III**, already possessing the overall oxidation state of the product acetophenone **2**. Then, either chemically or electrochemically promoted dehydrobromination would lead to the acetophenone product via. keto-enol tautomerism. It is worth mentioning that **III** has been detected as a minor byproduct in most oxidation crudes (see SI). On the other hand, independently prepared **III**[30] has been converted to acetophenone under the electrochemical conditions employed in our study with high selectivity (91%, corresponding to 50% yield at 55% conversion, see SI). Interestingly this transformation also occurs, albeit in a less selective manner (70%) in the absence of any metal halide. The intermediacy of carbocation **II** is consistent with the behavior in the reaction of highly electron-deficient substrates like **1w**, where the highly electron poor carbocation intermediate would be hardly available, and highly electron-rich ones like **1v**, where the exceeding electron density of the corresponding intermediate could trigger a highly promiscuous behavior leading to oligomeric product mixtures.

In conclusion, we have developed an electrochemical Wacker-Tsuji-type oxidation of aryl-substituted alkenes, applicable to monosubstituted and 1,2-disubstituted substrates. The process relies on a dual Mn/Cu catalytic system with solvent (acetonitrile) participation, and likely operates by means to three parallel electrochemical oxidative events where Mn(III), Cu(III) and acetonitrile radical cation are likely generated. By this process, a-aryl ketones are formed in moderate to excellent yields, with the advantages of avoidance of palladium as a catalyst and of any external chemical oxidant, in an easily operated, cost effective procedure.

ASSOCIATED CONTENT

Supporting Information

The Supporting Information is available free of charge at https://pubs.acs.org/doi/10.1021/acs.orglett.xxxxxxx.

Experimental procedures and spectral data (PDF)

AUTHOR INFORMATION

Corresponding Author

Miquel A. Pericàs − *Institute of Chemical Research of Catalonia (ICIQ), The Barcelona Institute of Science and Technology (BIST), E-43007 Tarragona, Spain*; *Departament de Química Inorgànica i Orgànica, Universitat de Barcelona, 08028 Barcelona, Spain*; orcid.org/0000-0003-0195-8846;
Email: mapericas@iciq.es

Authors

Junshan Lai − *Institute of Chemical Research of Catalonia (ICIQ), The Barcelona Institute of Science and Technology (BIST), E-43007 Tarragona, Spain; Universitat Rovira i Virgili, Departament de Química Analítica i Química Orgànica, c/Marcel·lí Domingo, 1, 43007 Tarragona, Spain*

Notes

The authors declare no competing financial interest.

ACKNOWLEDGMENT

Financial support from CERCA Programme/Generalitat de Catalunya, MINECO/FEDER (grants CTQ2015-69136-R and PID2019-1092336RB-I00) and AGAUR/ Generalitat de Catalunya (2017 SGR 1139) is gratefully acknowledged. J.L. thanks MINECO for a FPI fellowship (BES-2016-078937). We also thank Prof. Antoni Llobet (ICIQ) for helpful discussions and Dr. Marcos Gil-Sepulcre (ICIQ) for technical assistance.

REFERENCES

(1) *Industrial Organic Chemistry*, Fifth, completely revised Edition; Arpe, H.-J.; Wiley-VCH: Weinheim, 2010.

(2) Jira, R. Acetaldehyde from Ethylene-A Retrospective on the Discovery of the Wacker Process. *Angew. Chem. Int. Ed.* **2009**, *48*, 9034-9037.

(3) (a)Tsuji, J. Synthetic applications of the palladium-catalyzed oxidation of olefins to ketones. *Synthesis*, **1984**, 369-384; (b) Li, J. J. Wacker-Tsuji oxidation, in *Name Reactions for Functional Group Transformations*, Li, J. J.; Corey, E. J., Eds. Wiley-Interscience: Hoboken, NJ, 2007, pp. 309-326; (c) Baiju, T. V.; Gravel, E.; Doris, E.; Namboothiri, I. N. N. Recent developments in Tsuji-Wacker oxidation. *Tetrahedron Lett.* **2016**, *57*, 3993-4000.

(4) (a) Keith, J. A.; Henry, P. M. The Mechanism of the Wacker Reaction: A Tale of Two Hydroxypalladations. *Angew. Chem. Int. Ed.* **2009**, *48*, 9038-9049; (b) Vidossich, P.; Lledós, A.; Ujaque, G. First-Principles Molecular Dynamics Studies of Organometallic Complexes and Homogeneous Catalytic Processes. *Acc. Chem. Res.* **2016**, *49*, 1271-1278.

(5) (a) Tsuji, J.; Nokami, J.; Mandai, T. Oxidation of Olefins to Ketones Catalyzed by Pd^{2+} Salts and Its Applications to Organic Synthesis. *J. Syn. Org. Chem. Jpn*, **1989**, *47*, 649-659; (b) Cornell, C. N.; Sigman, M. S. Discovery of a Practical Direct O_2-Coupled Wacker Oxidation with Pd[(-)sparteine]Cl_2. *Org. Lett.* **2006**, *8*, 4117-4120; (c) Mitsudome, T.; Umetani, T.; Nosaka, N.; Mori, K.; Mizugaki, T.; Ebitani, K.; Kaneda, K. Convenient and Efficient Pd-Catalyzed Regioselective Oxyfunctionalization of Terminal Olefins by Using Molecular Oxygen as Sole Reoxidant. *Angew. Chem., Int. Ed.* **2006**, *45*, 481-485. (d) Michel, B. W.; Camelio, A. M.; Cornell, C. N.; Sigman, M. S. A general and efficient catalyst system for a Wacker-type oxidation using TBHP as the terminal oxidant: application to classically challenging substrates. *J. Am. Chem. Soc*. **2009**, *131*, 6076-6077. (e) DeLuca, R. J.; Edwards, J. L.; Steffens, L. D.; Michel, B. W.; Qiao, X.; Zhu, C.; Cook, S. P.; Sigman, M. S. Wacker-type oxidation of internal alkenes using Pd(Quinox) and TBHP. *J. Org. Chem.* **2013**, *78*, 1682-1686. (f) Wang, Y.-F.; Gao, Y.-R.: Mao, S.; Zhang, Y.-L.;

Guo, D.-D.; Yan, Z.-L.; Guo, S.-H.; Wang, Y.-Q. Wacker-type oxidation and dehydrogenation of terminal olefins using molecular oxygen as the sole oxidant without adding ligand. *Org. Lett.* **2014**, *16*, 1610-1613; (g) Chaudhari, D. A.; Fernandes, R. A. Hypervalent Iodine as a Terminal Oxidant in Wacker-Type Oxidation of Terminal Olefins to Methyl Ketones. *J. Org. Chem.* **2016**, *81*, 2113-2121. (h) Xia, X.; Gao, X.; Xu,J.; Hu, C.; Peng, X. Selective Oxidation of Styrene Derivatives to Ketones over Palladium(0)/Carbon with Hydrogen Peroxide as the Sole Oxidant. *Synlett* **2017**, *28*, 607-610.

(6) McDonald, R. I.; Liu, G.; Stahl, S. S. Palladium(II)-Catalyzed Alkene Functionalization via Nucleopalladation: Stereochemical Pathways and Enantioselective Applications. *Chem. Rev.* **2011**, *111*, 2981-3019.

(7) Fong, D.; Luo, S.-X.; Andre, R. S.; Swager, T. M. Trace Ethylene Sensing via Wacker Oxidation. *ACS Cent. Sci.* **2020**, *6*, 507-512.

(8) Frontana-Uribe, B. A.; Little, R. D.; Ibanez, J. G.; Palma A.; Vasquez-Medrano, R. Organic electrosynthesis: a promising green methodology in organic chemistry. *Green Chem.* **2010**, *12*, 2099–2119.

(9) (a) Cardoso, D. S. P.; Šljukic, B.; Santos, D. M. F.; Sequeira C. A.C. Organic Electrosynthesis: From Laboratorial Practice to Industrial Applications. *Org. Process Res. Dev.* **2017**, *21,* 1213−1226; (b) Leow, W. R.; Lum, Y.; Ozden, A.; Wang, Y.; Nam, D.-H.; Chen, B.; Wicks, J.; Zhuang, T.-T.; Li, F.; Sinton, D.; Sargent, E. H. Chloride-mediated selective electrosynthesis of ethylene and propylene oxides at high current density. *Science* **2020**, *368*, 1228-1233.

(10) (a) Blake, A. R.; Sunderland, J. G.; Kuhn, A. T. The partial anodic oxidation of ethylene on palladium. *J. Chem. Soc. A*, **1969**, 3015-3018; (b) Goodridge, F.; King, C. J. H. Oxidation of ethylene at a palladium electrode. *Trans. Faraday Soc.* **1970**, *66*, 2889-2896; (c) Otsuka, K.; Kobayashi, A. Design of the Catalyst for Partial Oxidation of Ethylene by Applying an Electrochemical Device. *Chem. Lett.***1991**, *20*, 1197-1200.

(11) (a) Tsuji, J.; Minato, M. Oxidation of olefins to ketones in combination with electrooxidation. *Tetrahedron Lett.***1987**, *28*, 3683-3686; (b) Bäckvall, J.-E.; Gogoll, A. Palladium-hydroquinone catalysed electrochemical 1,4-oxidation of conjugated dienes. *J. Chem. Soc., Chem. Commun.***1987**, 1236-1238.

(12) Horowitz, H. H. Preliminary examination of an electrochemical process for converting olefins to ketones. *J. Appl. Electrochem.* **1984**, *14*, 779-790.

(13) Inokuchi, T.; Ping, L.; Hamaue, F.; Izawa, M.; Torii, S. Electrochemical Wacker Type Reaction with a Double Mediatory System Consisting of Palladium Complex and Tri(4-bromophenyl)amine *Chem. Lett*. **1994**, *23*, 121-124.

(14) Wayner, D. D. M.; Hartstock, F. W. Electrode-mediated catalytic carbonylation of olefins. *J. Molecular Catalysis* **1988**, *48*, 15-19.

(15) Stangl, H.; Jira, R. Die durch palladium(II) chlorid und kupfer(II) chlorid katalysierte oxychlorierung von äthylen zu äthylenchlorhydrin. *Tetrahedron Lett.* **1970,** *11*, 3589-3592.

(16) Zhang, G.; Hu, X.; Chiang, C. W.; Yi, H.; Pei, P.; Singh, A. K.; Lei, A. Anti-Markovnikov Oxidation of β-Alkyl Styrenes with H_2O as the Terminal Oxidant. *J. Am. Chem. Soc.* **2016**, *138*, 12037-12040.

(17) Liu, B.; Jin, F.; Wang, T.; Yuan, X.; Han, W. Wacker-Type Oxidation Using an Iron Catalyst and Ambient Air: Application to Late-Stage Oxidation of Complex Molecules. *Angew. Chem. Int. Ed.* **2017**, *56*, 12712-12717.

(18) Imada, Y.; Okada, Y.; Noguchi, K.; Chiba, K. Selective Functionalization of Styrenes with Oxygen Using Different Electrode Materials: Olefin Cleavage and Synthesis of Tetrahydrofuran Derivatives. *Angew. Chem. Int. Ed.* **2019**, *58*, 125-129.

(19) Fu, N.; Sauer, G. S.; Saha, A.; Loo, A; Lin, S. Metal-catalyzed electrochemical diazidation of alkenes. *Science* **2017**, *357*, 575-579.

(20) Fu, N.; Sauer, G. S.; Lin, S. Electrocatalytic Radical Dichlorination of Alkenes with Nucleophilic Chlorine Sources. *J. Am. Chem. Soc.* **2017**, *139*, 15548-15553.

(21) Ye, K.; Pombar, G.; Fu, N.; Sauer, G. S.; Keresztes, I.; Lin, S. Anodically Coupled Electrolysis for the Heterodifunctionalization of Alkenes. *J. Am. Chem. Soc.* **2018**, *140*, 2438-2441.

(22) Zhang, Z.; Zhang, L.; Cao, Y.; Li, F.; Bai, G.; Liu, G.; Yang, Y.; Mo, F. Mn-Mediated Electrochemical Trifluoromethylation/C(sp^2)-H Functionalization Cascade for the Synthesis of Azaheterocycles. *Org. Lett.* **2019**, *21*, 762-766

(23) Tian, S.; Jia, X.; Wang, L.; Li, B.; Liu, S.; Ma, L.; Gao, W.; Wei, Y.; Chen, J. The Mn-catalyzed paired electrochemical facile oxychlorination of styrenes *via* the oxygen reduction reaction. *Chem. Commun.* **2019**, *55*, 12104.

(24) Zhang, W.; Wang, N. X.; Bai, C. B.; Wang, Y. J.; Lan, X. W.; Xing, Y.; Li, Y. H.; Wen, J. L. Manganese-Mediated Coupling Reaction of Vinylarenes and Aliphatic Alcohols. *Sci. Rep*. **2015**, *5*, 15250.

(25) Current intensity was also optimized for reactions ran in constant current mode. A highest 80 % yield was recorded in 8 hours for a reaction ran at 25 mA.

(26) Foley, J. K.; Korzeniewski, C.; Pons, S. Anodic and cathodic reactions in acetonitrile/tetra-n-butylammonium tetrafluoroborate: an electrochemical and infrared spectroelectrochemical study. *Can. J. Chem.* **1988**, *66*, 201–206.

(27) (a) Iroh, J. O.; Bell, J. P.; Scola, D. A. Mechanism of the electrocopolymerization of styrene and *N*-(3 carboxyphenyl)maleimide onto graphite fibers in aqueous solution. *Applied Pol. Sci*. **1993**, *47*, 93-104; (b) Lorandi, F.; Fantin, M.; Shanmugam, S.; Wang, Y.; Isse, A. A.; Gennaro, A.; Matyjaszewski, K. Toward Electrochemically Mediated Reversible Addition-Fragmentation Chain-Transfer (eRAFT) Polymerization: Can Propagating Radicals Be Efficiently Electrogenerated from RAFT Agents? *Macromolecules* **2019**, *52*, 1479−1488.

(28) However, when ethylbenzene was used as starting material, acetophenone could be isolated in 20% yield. This is probably related with the behavior in the reaction of the allyl ether of *p*-vinylbenzyl alcohol, where polymerization, and not selective oxidation of the aryl-substituted vinyl group, was the major reaction pathway.

(29) Bratsch, S. G. Standard Electrode Potentials and Temperature Coefficients in Water at 298.15 K. *J. Phys. Chem. Ref. Data* **1989**, *18*, 1–21.

(30) Das, B.; Venkateswarlu, K.; Damodar, K.; Suneel, K. Ammonium acetate catalyzed improved method for the regioselective conversion of olefins into halohydrins and haloethers at room temperature. *J. Mol. Catal. A-Chem.* **2007**, *269*, 17-21.

Supporting Information

Manganese/Copper Co-Catalyzed Electrochemical Wacker-Tsuji-Type Oxidation of Aryl-Substituted Alkenes

Junshan Lai,[a,b] and Miquel A. Pericàs[a,c,*]

[a] Institute of Chemical Research of Catalonia (ICIQ), The Barcelona Institute of Science and Technology, Av. Països Catalans, 16, 43007 Tarragona,Spain

[b] Departament de Química Analítica i Química Orgànica, Universitat Rovira i Virgili, 43007 Tarragona, Spain

[c] Departament de Química Inorgànica i Orgànica, Universitat de Barcelona, Martí i Franquès 1-11,08028 Barcelona, Spain

*mapericas@iciq.es

Table of Contents

1. General information

Unless otherwise noted, all reactions were conducted under air. All commercial reagents and solvents were used as received. Starting compounds **1a-z** are all known. **1a-x,** and **1z** were commercially available and were used as received, while **1y** was prepared by a reported procedure[1]. Flash chromatography was carried out using 60 mesh silica gel and dry-packed columns. Thin layer chromatography was carried out using Merck TLC Silicagel 60 F254 aluminum sheets. Components were visualized by UV light (λ = 254 nm) and stained with phosphomolybdic dip. NMR spectra were recorded at 298 K on a Bruker Avance 400 Ultrashield apparatus. ^{1}H NMR spectroscopy chemical shifts are quoted in ppm relative to tetramethylsilane (TMS). $CDCl_3$ was used as internal standard for ^{13}C NMR spectra. Chemical shifts are given in ppm and coupling constants in Hz.

2. General procedure for the electrochemical Wacker-Tsuji-type oxidation

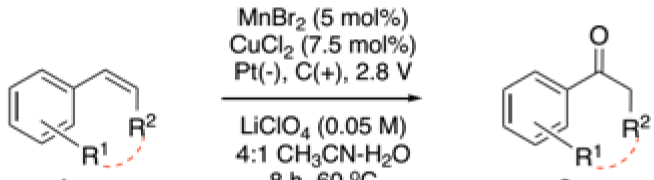

Experiments were performed using a DC power supply. The reaction vessel was a simple glass tube equipped with a rubber septum and carbon felt (G200, 10 mm x 10 mm x 5 mm) as the anode and platinum plate (10 mm x 10 mm x 0.25 mm) as the cathode. Experiments were normally performed under air atmosphere. For experiments under exclusion of oxygen, the cell was sealed and flushed with argon for 15 minutes. To the undivided glass tube (10 mL) used as electrochemical cell, $MnBr_2$ (10.7 mg, 0.05 mmol, 5 mol %), $CuCl_2$ (10.1 mg, 0.075 mmol, 7.5 mol %) and $LiClO_4$ solution (3 mL, 0.05 M in a 4:1 vol/vol MeCN/water) were added, followed by the addition of the reacting olefins (1 mmol) via syringe. The cell was placed in an oil bath heated at 60 ºC, and current pass was then started at a constant potential of 2.8 V and kept under these conditions for 8 h, when TLC analysis indicated that the reaction was complete. The solution was then transferred to a round-bottom flask, and the reaction flask and the electrodes were washed with DCM which was combined with the reaction mixture. The solvents were directly evaporated under reduced pressure, and the residue was submitted to purification by flash column chromatography on silicagel, eluting with solvent mixtures specified in Section 7 for each particular case.

3. Initial screening of solvents and catalysts

3.1 Table S1. Screening of reaction conditions: solvent and catalyst[a]

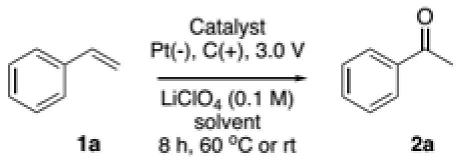

entry	Solvent/H_2O (v:v)[b]	Catalyst[c]	yield [%][d]
S1	MeOH (1:1)	$MnBr_2$	trace
S2	EtOH (1:1)	$MnBr_2$	trace
S3	^{i}PrOH (1:1)	$MnBr_2$	10
S4	DMF (1:1)	$MnBr_2$	trace
S5	Acetone (1:1)	$MnBr_2$	12
S6	MeCN (1:1)	$MnBr_2$	23
S7	MeCN (4:1)	$MnBr_2$	28
S8[e]	MeCN (4:1)	$MnBr_2$	15
S9	MeCN (4:1)	$NiCl_2$	nd[e]
S10	MeCN (4:1)	$FeCl_3$	nd[e]
S11	MeCN (4:1)	$PdCl_2$	trace
S12	MeCN (4:1)	$MnBr_2$, $CuCl_2$	67
S13	MeCN (4:1)	$CuCl_2$	nd[f]

[a]Reaction conditions: styrene (1mmol), catalyst (5 mol%), solvent (3 mL), 3.0 V (Pt cathode, Carbon felt anode, 0.1 M $LiClO_4$), 60 °C, Argon, 8 h. [b]Solvent:water ratio. [c]5 mol [d]Isolated yield.%. [e]Reaction at room temperature. [f]Not detected.

3.2 Table S2. Optimization of reaction conditions: copper and manganese sources[a]

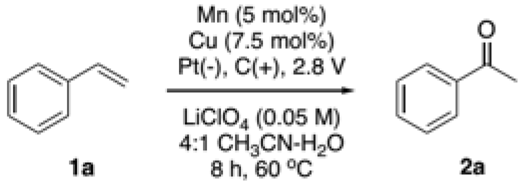

entry	Cu source	Mn or Br source	yield [%][b]
S1	$CuBr_2$	$MnBr_2$	86
S2	$Cu(OAc)_2$	$MnBr_2$	35
S3	CuI	$MnBr_2$	10
S4	$Cu(OTf)_2$	$MnBr_2$	44
S5	$CuCl_2$	$MnBr_2$	85
S6	$Cu(acac)_2$	$MnBr_2$	trace
S7	CuCN	$MnBr_2$	10
S8	$CuSO_4$	$MnBr_2$	27
S9	$Cu(TFA)_2$	$MnBr_2$	49
S10	Cu beads	$MnBr_2$	53
S11	Cu beads	MnO_2	trace
S12	$CuCl_2$	$MnCl_2$	40
S13	$Cu(OAc)_2$	$Mn(OAc)_2$	trace
S14	$CuSO_4$	$MnSO_4$	trace
S15	$CuBr_2$	$MnCl_2$	80
S16	$CuBr_2$	-	trace
S17	$CuCl_2$	NaBr	trace
S18	$CuCl_2$	HBr	trace
S19	$CuCl_2$	$^{n}Bu_4N^+Br^-$	trace
S20	$CuCl_2$	-	trace

[a]Reaction conditions: styrene (1mmol), copper source (7.5 mol%), Mn or Br source (5 mol%), MeCN/water (5:1) (3 mL), 2.8 V (Pt cathode, Carbon felt anode, 0.05 M $LiClO_4$), 60 °C, 8 h. [b]Isolated yield.

4. Optimization of the different reaction parameters

4.1. Amount of $MnBr_2$

Different experiments were performed according to the general procedure varying the amount of $MnBr_2$ between 0 and 10 mol%. Results are summarized in Figure S1.

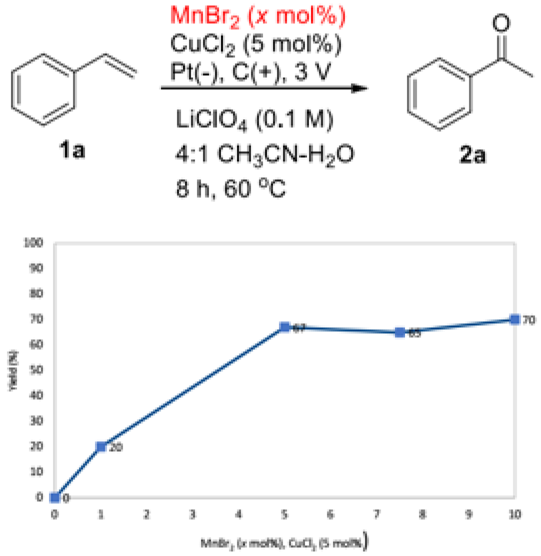

Figure S1. Reaction conditions: $MnBr_2$ (x mol%), $CuCl_2$ (6.8 mg, 0.05 mmol, 5 mol %), styrene (104 mg, 1 mmol), $LiClO_4$ solution [0.1 M in 4:1 MeCN/water (3 mL)], Pt(-), C(+), 3.0 V, 8 h, 60 ℃.

4.2. Amount of $CuCl_2$

Different experiments were performed according to the general procedure varying the amount of $CuCl_2$ between 0 and 15 mol%. Results are summarized in Figure S2.

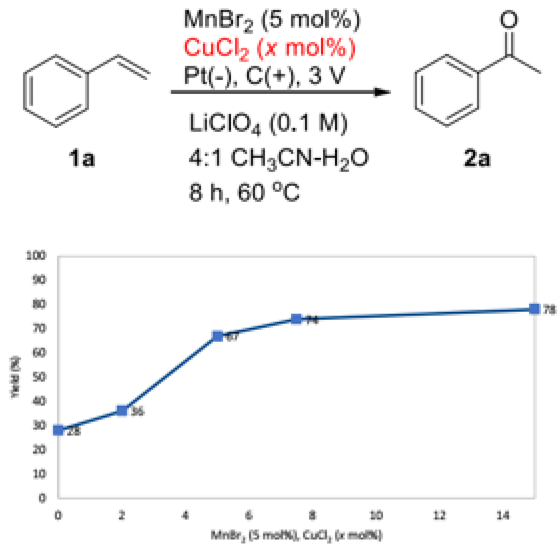

Figure S2. Reaction conditions: $MnBr_2$ (10.7 mg, 0.05 mmol, 5 mol%), $CuCl_2$ (x mol%), styrene (104 mg, 1 mmol), $LiClO_4$ solution [0.1 M in 4:1 MeCN/water (3 mL)], Pt(-), C(+), 3.0 V, 8 h, 60 ℃.

4.3. Amount of water in acetonitrile/water solvent mixtures

Different experiments were performed according to the general procedure in acetonitrile/water solvent mixtures with compositions ranging from 100% acetonitrile to 100% water. Results are summarized in Figure S3.

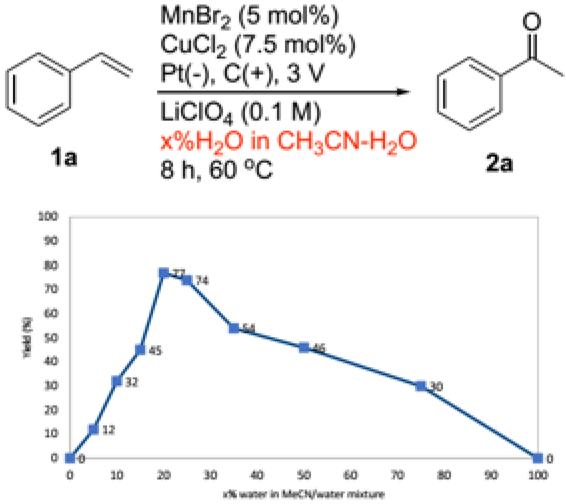

Figure S3. Reaction conditions: $MnBr_2$ (10.7 mg, 0.05 mmol, 5 mol%), $CuCl_2$ (10.1 mg, 0.075 mmol, 7.5 mol%), styrene (104 mg, 1 mmol), $LiClO_4$ solution (0.1 M in 3 mL of MeCN/water with the indicated vol/vol compositions), Pt(-), C(+), 3.0 V, 8 h, 60 °C.

4.4. Amount of Styrene

Different experiments were performed according to the general procedure varying the amount of styrene between 0.25 mmol and 3.00 mmol. Results are summarized in Figure S4.

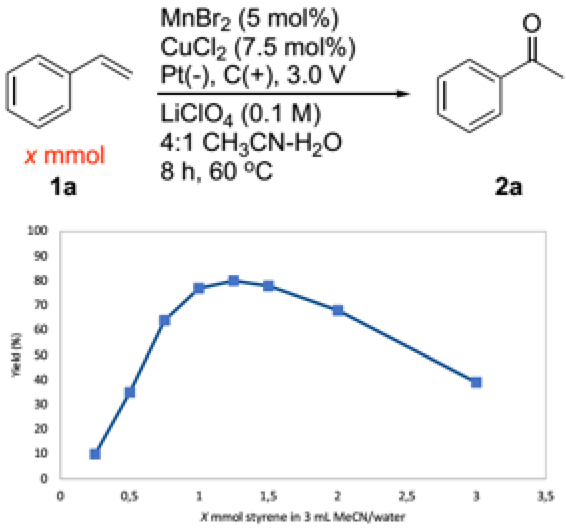

Figure S4. Reaction conditions: $MnBr_2$ (10.7 mg, 0.05 mmol, 5 mol%), $CuCl_2$ (10.1 mg, 0.075 mmol, 7.5 mol%), styrene (x mmol), $LiClO_4$ solution [0.1 M in 4:1 MeCN/water (3 mL)], Pt(-), C(+), 3.0 V, 8 h, 60 °C.

4.5. Concentration of $LiClO_4$ solution

Different experiments were performed according to the general procedure varying the concentration of $LiClO_4$ in 4:1 MeCN/water between 0.025 and 0.30 M. Results are summarized in Figure S5.

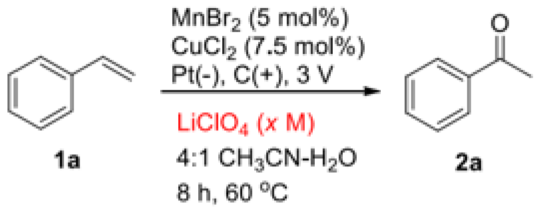

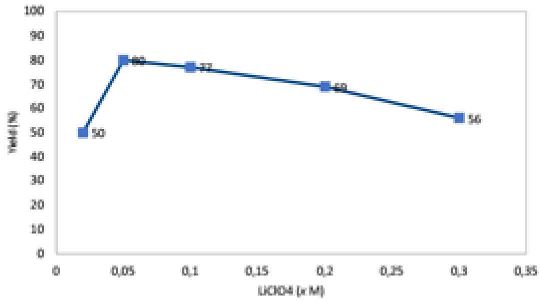

Figure S5. Reaction conditions: $MnBr_2$ (10.7 mg, 0.05 mmol, 5 mol%), $CuCl_2$ (10.1 mg, 0.075 mmol, 7.5 mol%), styrene (104 mg, 1 mmol), $LiClO_4$ solution [*x* M in 4:1 MeCN/water(3 mL)], Pt(-), C(+), 3.0 V, 8 h, 60 °C.

4.6. Applied potential

Different experiments were performed according to the general procedure varying the applied potential between 1.7 and 3.4 V. Results are summarized in Figure S6.

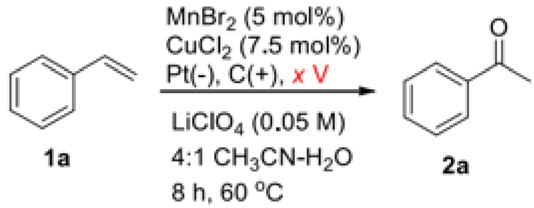

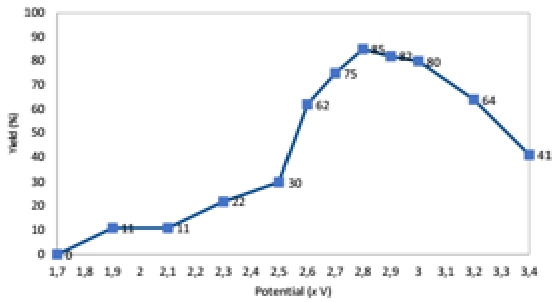

Figure S6. Reaction conditions: $MnBr_2$ (10.7 mg, 0.05 mmol, 5 mol%), $CuCl_2$ (10.1 mg, 0.075 mmol, 7.5 mol%), styrene (104 mg, 1 mmol), $LiClO_4$ solution [0.05 M in 4:1 MeCN/water(3 mL)], Pt(-), C(+), x V, 8 h, 60 °C.

The study was repeated in a single compartment, three electrode cell including an Ag/AgCl reference electrode. The results are summarized in Figure S7 for potentials ranging from 2.4 to 3.0 V. Each point corresponds to the mean value of two independent determinations.

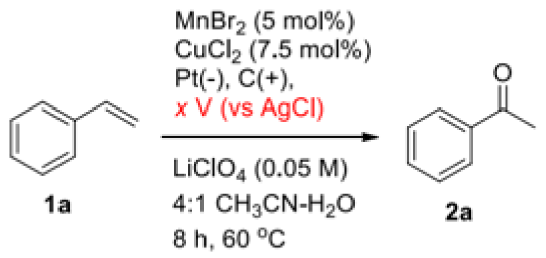

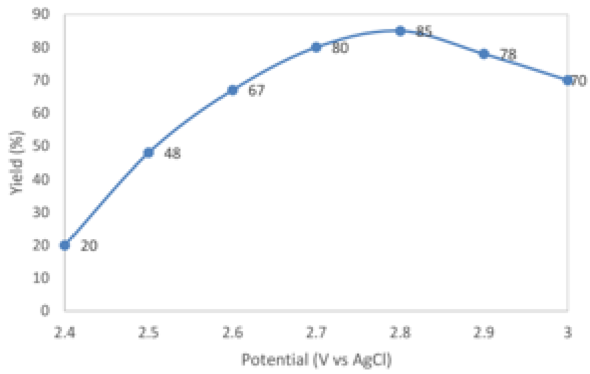

Figure S7. Reaction conditions: $MnBr_2$ (10.7 mg, 0.05 mmol, 5 mol%), $CuCl_2$ (10.1 mg, 0.075 mmol, 7.5 mol%), styrene (104 mg, 1 mmol), $LiClO_4$ solution [0.05 M in 4:1 MeCN/water(3 mL)], Pt(-), C(+), (x V vs AgCl), 8 h, 60 °C.

5. Cyclic voltammetry studies

Cyclic voltammetry (CV) experiments were conducted in a 5 mL glass vial equipped with a glassy carbon working electrode, an Ag/AgCl reference electrode, and a platinum wire counter electrode. Ag/AgCl reference electrodes were stored in 0.1 M $LiClO_4$ in acetonitrile. Concentrations of the individual individual components were 8 mM. The blank experiment refers to 0.1 M $LiClO_4$ in 4:1(v/v) CH_3CN/ H_2O. Scan rate was 50 mV/s. In the case of 5 eq. styrene, the concentration of styrene is 40 mM.

a)

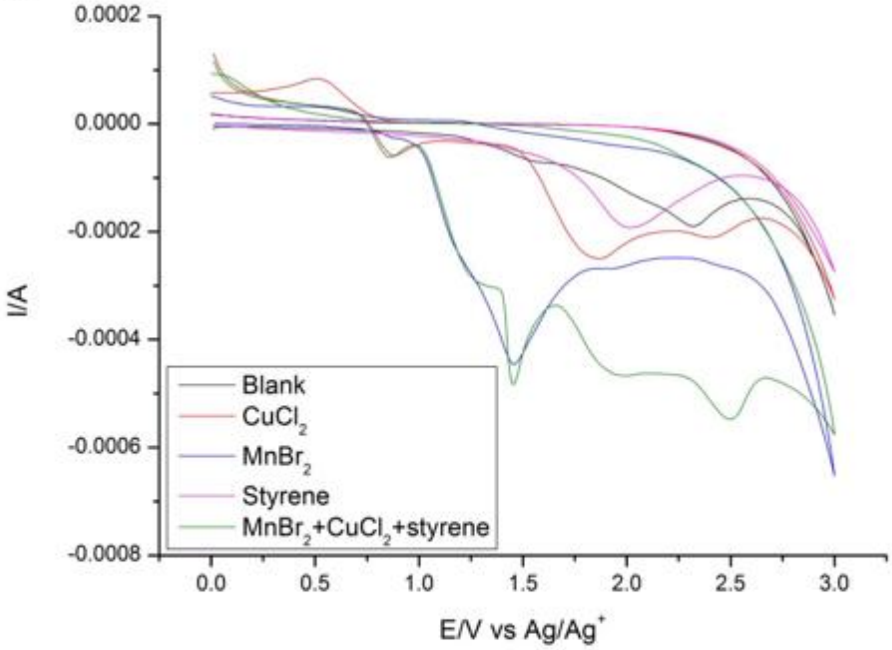

b)

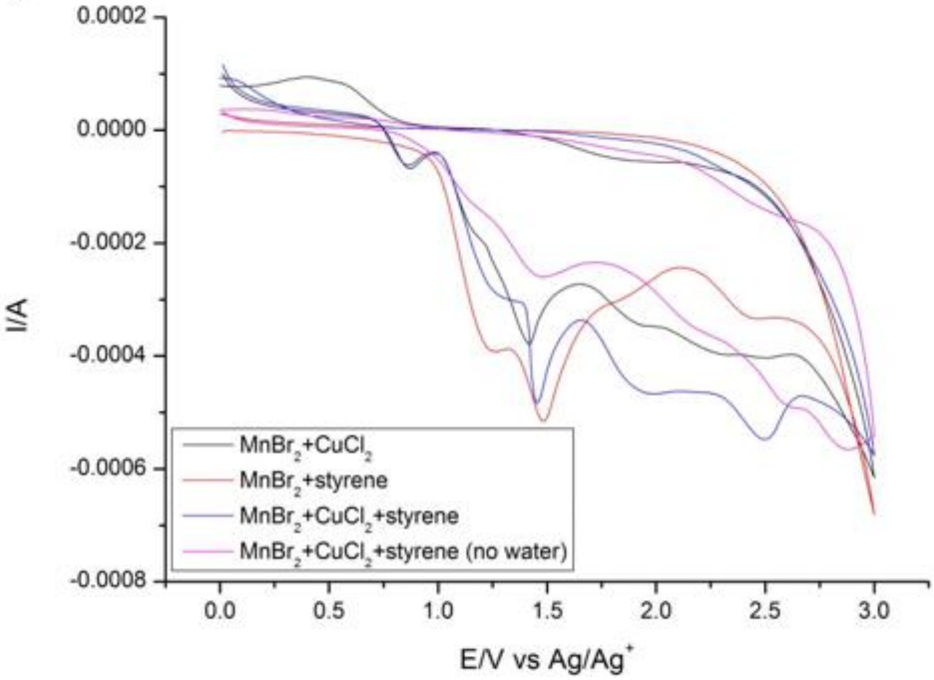

6. Mechanistic studies: detection of bromohydrin III and conversion into acetophenone 2a under electrochemical conditions.

a) ^{1}H NMR spectra of a reaction crude of the electrochemical oxidation of styrene leading to **2a**, showing the presence of bromohydrin **III**.

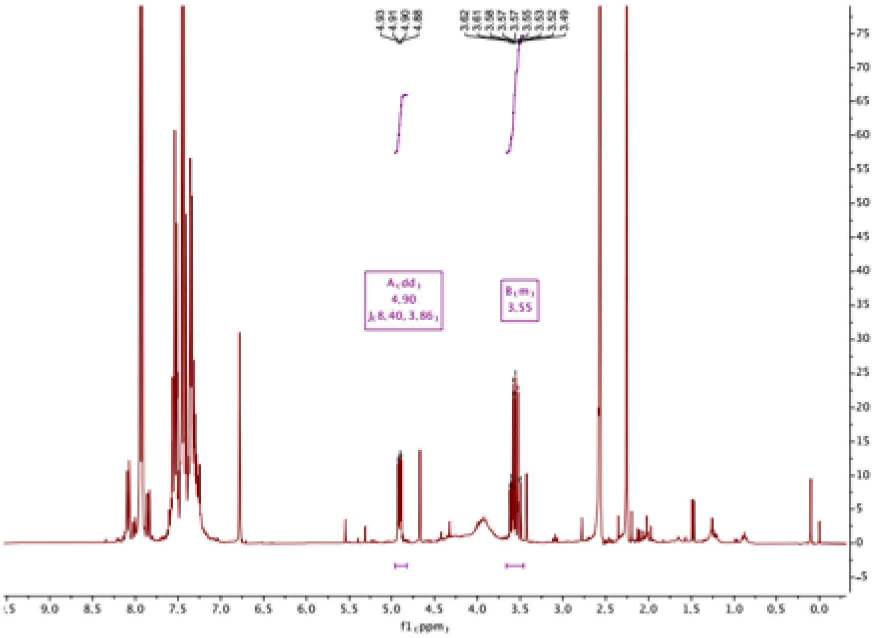

b) ^{1}H NMR spectra of an authentic sample of bromohydrin **III**

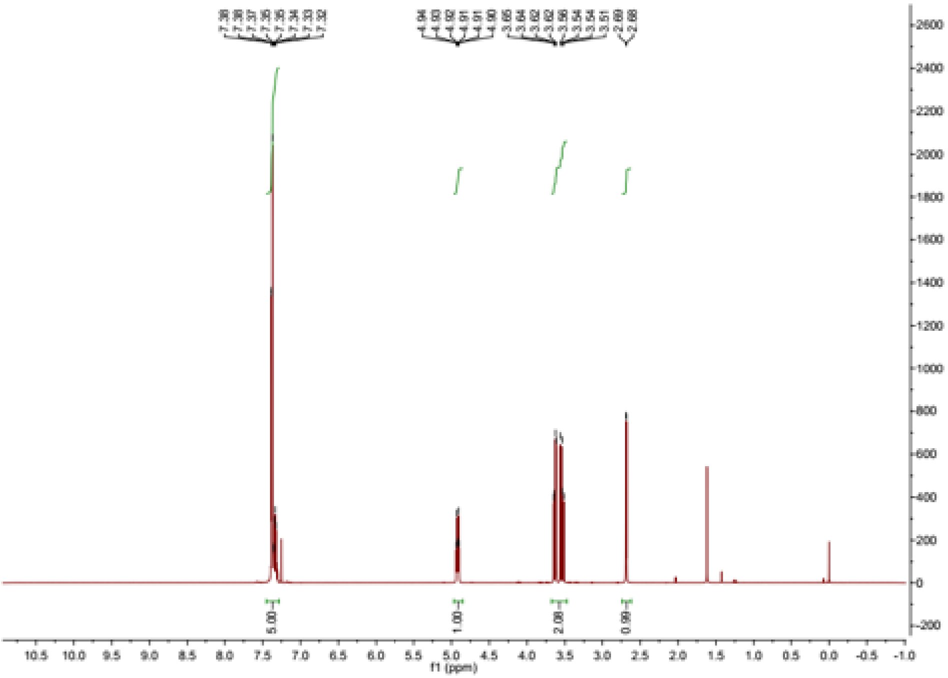

c) Conversion of bromohydrin **III** into acetophenone **2a** under electrochemical conditions

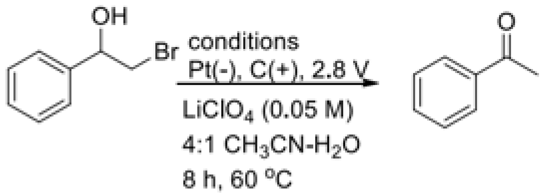

Conditions	Conversion [%]	Yield [%]	Selectivity [%] (100.yield.conv^{-1})
$CuCl_2$ (7.5 mol%)	40	35	87.5
$MnBr_2$ (5 mol%)	58	50	86.2
$CuCl_2$ (7.5 mol%), $MnBr_2$ (5 mol%)	55	50	90.9
no metal catalyst	50	35	70.0

7. Compound characterization data

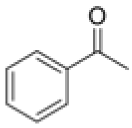

2a

Acetophenone (**2a**). The general procedure was followed from **1a** (0.104 g, 1 mmol) to afford **2a** (0.103 g, 0.85 mmol, 85% yield) as colorless oil. **2a** was purified by column chromatography on silica gel, eluting with ethyl acetate cyclohexane mixtures ($EtOAc/C_6H_{12}$ = 1:20). The structure of **2a** was confirmed by comparing its ^1H- and ^{13}C-NMR spectra with previously reported data described in the literature.[2] **^1H NMR** (400 MHz, $CDCl_3$) δ 8.00 – 7.91 (m, 2H), 7.61 – 7.52 (m, 1H), 7.52 – 7.39 (m, 2H), 2.61 (s, 3H) ppm. **^{13}C NMR** (101 MHz, $CDCl_3$) δ 198.0, 137.0, 132.9, 128.4 (x2), 128.1 (x2), 26.4 ppm.

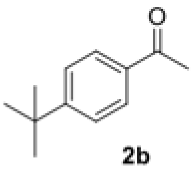

2b

***p-tert*-Butylacetophenone** (**2b**). The general procedure was followed from **1b** (0.160 g, 1 mmol) to afford **2b** (0.132 g, 0.75 mmol, 75% yield) as colorless oil. **2b** was purified by column chromatography on silica gel, eluting with ethyl acetate cyclohexane mixtures ($EtOAc/C_6H_{12}$ = 1:20). The structure of **2b** was confirmed by comparing its ^1H- and ^{13}C-NMR spectra with previously reported data described in the literature.[3] **^1H NMR** (400 MHz, $CDCl_3$) δ 7.91 (d, J = 8.5 Hz, 2H), 7.49 (d, J = 8.4 Hz, 2H), 2.59 (s, 3H), 1.35 (s, 9H). **^{13}C NMR** (101 MHz, $CDCl_3$) δ 197.7, 156.7, 134.6, 128.2 (x2), 125.4 (x2), 35.0, 31.0 (x3), 26.4 ppm.

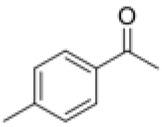

2c

***p*-Methylacetophenone** (**2c**). The general procedure was followed from **1c** (0.118 g, 1 mmol) to afford **2c** (0.106 g, 0.79 mmol, 79% yield) as colorless oil. **2c** was purified by column chromatography on silica gel, eluting with ethyl acetate cyclohexane mixtures ($EtOAc/C_6H_{12}$ = 1:20). The structure of **2c** was confirmed by comparing its ^1H- and ^{13}C-NMR spectra with previously reported data described in the literature.[4] **^{1}H NMR** (400 MHz, $CDCl_3$) δ 7.85 (d, *J* = 8.2 Hz, 2H), 7.25 (d, *J* = 8.0 Hz, 2H), 2.57 (s, 3H), 2.40 (s, 3H) ppm. **^{13}C NMR** (101 MHz, $CDCl_3$) δ 197.7, 143.8, 134.6, 129.1 (x2), 128.3 (x2), 26.4, 21.5 ppm.

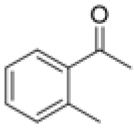

2d

***o*-Methylacetophenone** (**2d**). The general procedure was followed from **1d** (0.118 g, 1 mmol) to afford **2d** (0.047 g, 0.35 mmol, 35% yield) as colorless oil. **2d** was purified by column chromatography on silica gel, eluting with ethyl acetate cyclohexane mixtures (EtOAc/C_6H_{12} = 1:20). The structure of **2d** was confirmed by comparing its ^{1}H- and ^{13}C-NMR spectra with previously reported data described in the literature.[5] **^{1}H NMR** (400 MHz, $CDCl_3$) δ 7.68 (dd, *J* = 7.7, 1.4 Hz, 1H), 7.37 (td, *J* = 7.5, 1.4 Hz, 1H), 7.30 – 7.20 (m, 2H), 2.57 (s, 3H), 2.53 (s, 3H) ppm. **^{13}C NMR** (101 MHz, $CDCl_3$) δ 201.6, 138.3, 137.6, 131.9, 131.4, 129.3, 125.6, 29.4, 21.5 ppm.

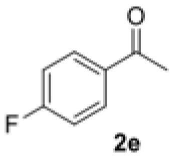

2e

***p*-Fluoroacetophenone** (**2e**). The general procedure was followed from **1e** (0.122 g, 1 mmol) to afford **2e** (0.109 g, 0.79 mmol, 79% yield) as colorless oil. **2e** was purified by column chromatography on silica gel, eluting with ethyl acetate cyclohexane mixtures (EtOAc/C_6H_{12} = 1:20). The structure of **2e** was confirmed by comparing its ^{1}H- and ^{13}C-NMR spectra with previously reported data described in the literature.[6] **^{1}H NMR** (400 MHz, $CDCl_3$) δ 7.96 (dd, *J* = 5.3, 3.0 Hz, 2H), 7.10 (dd, *J* = 8.7, 3.4 Hz, 2H), 2.58 (s, 3H) ppm. **^{13}C NMR** (101 MHz, $CDCl_3$) δ 196.3, 165.7 (d, *J* = 256 Hz), 133.5 (d, *J* = 3 Hz), 130.9 (d, *J* = 9 Hz) (x2), 115.6 (d, *J* = 21 Hz) (x2), 26.4 ppm.

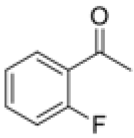

2f

***o*-Fluoroacetophenone** (**2f**). The general procedure was followed from **1f** (0.122 g, 1 mmol) to afford **2f** (0.063 g, 0.46 mmol, 46% yield) as colorless oil. **2f** was purified by column chromatography on silica gel, eluting with ethyl acetate cyclohexane mixtures (EtOAc/C_6H_{12} = 1:20). The structure of **2f** was confirmed by comparing its ^{1}H- and ^{13}C-NMR spectra with previously reported data described in the literature.[7] **^{1}H NMR** (400 MHz, $CDCl_3$) δ 7.95 – 7.79 (m, 1H), 7.52 (dq, *J* = 7.6, 2.5 Hz, 1H), 7.27 – 7.02 (m, 2H), 2.65 (dd, *J* = 5.3, 3.3 Hz, 3H) ppm. **^{13}C NMR** (101 MHz, $CDCl_3$) δ 195.8, 162.2 (d, *J* = 256 Hz), 134.6 (d, *J* = 9 Hz), 130.5(d, *J* = 4 Hz), 125.7(d, *J* = 13 Hz), 124.3(d, *J* = 4 Hz), 116.7(d, *J* = 23 Hz), 31.4(d, *J* = 8 Hz) ppm.

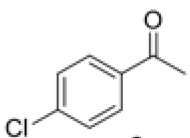

2g

***p*-Chloroacetophenone** (**2g**). The general procedure was followed from **1g** (0.138 g, 1 mmol) to afford **2g** (0.134 g, 0.87 mmol, 87% yield) as colorless oil. **2g** was purified by column chromatography on silica gel, eluting with ethyl acetate cyclohexane mixtures (EtOAc/C_6H_{12} = 1:20). The structure of **2g** was confirmed by comparing its ^{1}H- and ^{13}C-NMR spectra with previously reported data described in the literature.[4] **^{1}H NMR** (400 MHz, $CDCl_3$) δ 7.88 (d, *J* = 8.6 Hz, 2H), 7.42 (d, *J* = 8.6 Hz, 2H), 2.58 (s, 3H) ppm. **^{13}C NMR** (101 MHz, $CDCl_3$) δ 196.6, 139.4, 135.3, 129.6 (x2), 128.7 (x2), 26.4 ppm.

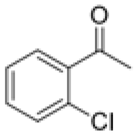

2h

***o*-Chloroacetophenone** (**2h**). The general procedure was followed from **1h** (0.138 g, 1 mmol) to afford **2h** (0.082 g, 0.53 mmol, 53% yield) as colorless oil. **2h** was purified by column chromatography on silica gel, eluting with ethyl acetate cyclohexane mixtures (EtOAc/C_6H_{12} = 1:20). The structure of **2h** was confirmed by comparing its ^{1}H- and ^{13}C-NMR spectra with previously reported data described in the literature.[5] **^{1}H NMR** (400 MHz, $CDCl_3$) δ 7.55 (ddd, *J* = 7.6, 1.7, 0.6 Hz, 1H), 7.45 – 7.26 (m, 3H), 2.64 (s, 3H) ppm. **^{13}C NMR** (101 MHz, $CDCl_3$) δ 200.3, 139.1, 131.9, 131.2, 130.6, 129.3, 126.8, 30.6 ppm.

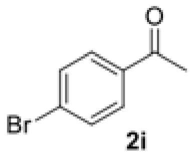

2i

***p*-Bromoacetophenone** (**2i**). The general procedure was followed from **1i** (0.183 g, 1 mmol) to afford **2i** (0.149 g, 0.75 mmol, 75% yield) as colorless oil. **2i** was purified by column chromatography on silica gel, eluting with ethyl acetate cyclohexane mixtures (EtOAc/C_6H_{12} = 1:20). The structure of **2i** was confirmed by comparing its ^{1}H- and ^{13}C-NMR spectra with previously reported data described in the literature.[8] **^{1}H NMR** (400 MHz, $CDCl_3$) δ 7.81 (d, *J* = 8.6 Hz, 2H), 7.60 (d, *J* = 8.6 Hz, 2H), 2.58 (s, 3H) ppm. **^{13}C NMR** (101 MHz, $CDCl_3$) δ 196.9, 135.8, 131.8 (x2), 129.8 (x2), 128.2, 26.5 ppm.
Known compound.[7]

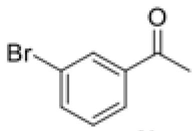

2j

***m*-Bromoacetophenone** (**2j**). The general procedure was followed from **1j** (0.183 g, 1 mmol) to afford **2i** (0.140 g, 0.70 mmol, 70% yield) as colorless oil. **2j** was purified by column chromatography on silica gel, eluting with ethyl acetate cyclohexane mixtures (EtOAc/C_6H_{12} = 1:20). The structure of **2i** was confirmed by comparing its ^{1}H- and ^{13}C-NMR spectra with previously reported data described in the literature.[7] **^{1}H NMR** (400 MHz, $CDCl_3$) δ 8.08 (t, *J* = 1.9 Hz, 1H), 7.94 – 7.85 (m, 1H), 7.69 (ddd, *J* = 8.0, 2.0, 1.0 Hz, 1H), 7.35 (t, *J* = 7.9 Hz, 1H), 2.60 (s, 3H) ppm. **^{13}C NMR** (101 MHz, $CDCl_3$) δ 196.5, 138.7, 135.8, 131.2, 130.1, 126.7, 122.8, 26.5 ppm.

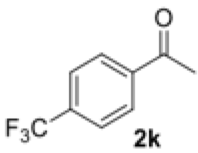

2k

***p*-Trifluoromethylacetophenone** (**2k**). The general procedure was followed from **1k** (0.172 g, 1 mmol) to afford **2k** (0.128 g, 0.68 mmol, 68% yield) as colorless oil. **2k** was purified by column chromatography on silica gel with pentane/DCM (4:1), and further purified by Kugelrohr distillation. The structure of **2k** was confirmed by comparing its ^{1}H- and ^{13}C-NMR spectra with previously reported data described in the literature.[9] **^{1}H NMR** (400 MHz, $CDCl_3$) δ 8.09 – 7.98 (m, 2H), 7.79 – 7.62 (m, 2H), 2.65 (s, 3H) ppm. **^{13}C NMR** (101 MHz, $CDCl_3$) δ 196.9, 139.7, 134.4 (q, *J* = 33 Hz), 128.6 (x2), 125.6 (q, *J* = 4 Hz) (x2), 123.6 (q, *J* = 271 Hz), 26.7 ppm.

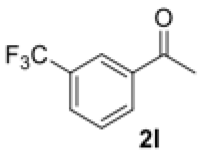

2l

***m*-Trifluoromethylacetophenone** (**2l**). The general procedure was followed from **1l** (0.172 g, 1 mmol) to afford **2l** (0.135 g, 0.72 mmol, 72% yield) as colorless oil. **2l** was purified by column chromatography on silica gel, eluting with ethyl acetate cyclohexane mixtures (EtOAc/C_6H_{12} = 1:20). The structure of **2l** was confirmed by comparing its ^{1}H- and ^{13}C-NMR spectra with previously reported data described in the literature.[10] **^{1}H NMR** (400 MHz, $CDCl_3$) δ 8.27 – 8.08 (m, 2H), 7.87 – 7.74 (m, 1H), 7.68 – 7.51 (m, 1H), 2.64 (d, *J* = 0.8 Hz, 3H) ppm. **^{13}C NMR** (101 MHz, $CDCl_3$) δ 196.5, 137.5, 131.4, 131.3 (q, *J* = 33 Hz), 129.5 (q, *J* = 4 Hz), 129.3, 125.1(q, *J* = 5 Hz), 123.7 (q, *J* = 271 Hz), 26.5 ppm.

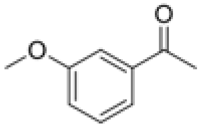

2m

***m*-Methoxyacetophenone** (**2m**). The general procedure was followed from **1m** (0.134 g, 1 mmol) to afford **2m** (0.049 g, 0.33 mmol, 33% yield) as colorless oil. **2m** was purified by column chromatography on silica gel, eluting with ethyl acetate cyclohexane mixtures (EtOAc/C_6H_{12} = 1:5). The structure of **2m** was confirmed by comparing its ^{1}H- and ^{13}C-NMR spectra with previously reported data described in the literature.[11] **^{1}H NMR** (400 MHz, $CDCl_3$) δ 7.57 – 7.44 (m, 2H), 7.36 (ddd, *J* = 8.2, 7.6, 0.4 Hz, 1H), 7.10 (ddd, *J* = 8.2, 2.7, 1.0 Hz, 1H), 3.85 (s, 3H), 2.59 (s, 3H) ppm. **^{13}C NMR** (101 MHz, $CDCl_3$) δ 197.8, 159.7, 138.4, 129.5, 121.0, 119.5, 112.3, 55.3, 26.6 ppm.

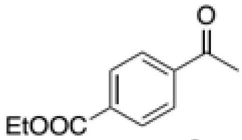

2n

***p*-Methoxycarbonylacetophenone** (**2n**). The general procedure was followed from **1n** (0.176 g, 1 mmol) to afford **2n** (0.138 g, 0.72 mmol, 72% yield) as white solid. **2n** was purified by column chromatography on silica gel, eluting with ethyl acetate cyclohexane mixtures (EtOAc/C_6H_{12} = 1:10). The structure of **2n** was confirmed by comparing its ^{1}H- and ^{13}C-NMR spectra with previously reported data described in the literature.[12] **^{1}H NMR** (400 MHz, $CDCl_3$) δ 8.13 (d, *J* = 8.7 Hz, 2H), 8.01 (d, *J* = 8.7 Hz, 2H), 3.95 (s, 3H), 2.65 (s, 3H) ppm. **^{13}C NMR** (101 MHz, $CDCl_3$) δ 197.5, 166.2, 140.2, 133.9, 129.8, 128.17, 52.4, 26.8 ppm.

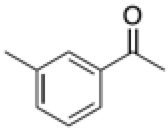

2o

***m*-Methylacetophenone** (**2o**). The general procedure was followed from **1n** (0.118 g, 1 mmol) to afford **2n** (0.093 g, 0.69 mmol, 69% yield) as colorless oil. **2o** was purified by column chromatography on silica gel, eluting with ethyl acetate cyclohexane mixtures (EtOAc/C_6H_{12} = 1:20). The structure of **2n** was confirmed by comparing its ^{1}H- and ^{13}C-NMR spectra with previously reported data described in the literature.[6] **^{1}H NMR** (400 MHz, $CDCl_3$) δ 7.81 – 7.68 (m, 2H), 7.39 – 7.30 (m, 2H), 2.58 (s, 3H), 2.40 (s, 3H) ppm. **^{13}C NMR** (101 MHz, $CDCl_3$) δ 198.2, 138.2, 137.1, 133.7, 128.7, 128.3, 125.5, 26.5, 21.2 ppm.

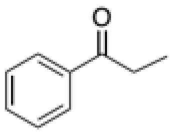

2p

Propiophenone (**2p**). The general procedure was followed from (*E*)-**1o** or (*Z*)-**1o** (0.118 g, 1 mmol in each case) to afford **2o** [0.078 g, 0.58 mmol, 58% yield from (*E*)-**1o** or 0.087 g, 0.65 mmol, 65% yield from (*Z*)-**1o**] as colorless oil. **2p** was purified by column chromatography on silica gel, eluting with ethyl acetate cyclohexane mixtures (EtOAc/C_6H_{12} = 1:20). The structure of **2n** was confirmed by comparing its ^{1}H- and ^{13}C-NMR spectra with previously reported data described in the literature.[13] **^{1}H NMR** (400 MHz, $CDCl_3$) δ 8.02 – 7.89 (m, 2H), 7.58 – 7.48 (m, 1H), 7.50 – 7.37 (m, 2H), 3.00 (qd, *J* = 7.2, 0.9 Hz, 2H), 1.22 (td, *J* = 7.2, 0.6 Hz, 3H) ppm. **^{13}C NMR** (101 MHz, $CDCl_3$) δ 200.7, 136.9, 132.8, 128.5 (x2), 127.9 (x2), 31.7, 8.2 ppm.

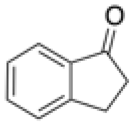

2q

1-Indanone (**2p**). The general procedure was followed from indene (**1p**) (0.116 g, 1 mmol) to afford **2p** (0.079 g, 0.60 mmol, 60% yield) as colorless oil. **2q** was purified by column chromatography on silica gel, eluting with ethyl acetate cyclohexane mixtures (EtOAc/C_6H_{12} = 1:20). The structure of **2p** was confirmed by comparing its ^{1}H- and ^{13}C-NMR spectra with previously reported data described in the literature.[14] **^{1}H NMR** (400 MHz, $CDCl_3$) δ 7.76 (d, *J* = 7.7 Hz, 1H), 7.59 (td, *J* = 7.4, 1.3 Hz, 1H), 7.48 (dt, *J* = 7.7, 1.0 Hz, 1H), 7.41 – 7.34 (m, 1H), 3.20 – 3.09 (m, 2H), 2.72 – 2.63 (m, 2H) ppm. **^{13}C NMR** (101 MHz, $CDCl_3$) δ 206.9, 155.1, 137.0, 134.5, 127.2, 126.6, 123.6, 36.1, 25.7 ppm.

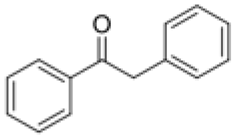

2r

1,2-Diphenylethan-1-one (**2r**). The general procedure was followed from (*E*)-**1r** (0.180 g, 1 mmol) to afford **2r** (0.096 g, 0.49 mmol, 49% yield) as white solid. **2r** was purified by column chromatography on silica gel, eluting with ethyl acetate cyclohexane mixtures (EtOAc/C_6H_{12} = 1:20). The structure of **2r** was confirmed by comparing its ^{1}H- and ^{13}C-NMR spectra with previously reported data described in the literature.[15] **^{1}H NMR** (400 MHz, $CDCl_3$) δ 8.00 (dd, *J* = 8.3, 1.4 Hz, 2H), 7.56 – 7.37 (m, 3H), 7.36 – 7.17 (m, 5H), 4.27 (s, 2H) ppm. **^{13}C NMR** (101 MHz, $CDCl_3$) δ 197.6, 136.5, 134.5, 133.1, 130.1, 129.4, 128.6, 128.6, 128.5, 128.4, 126.8, 45.4 ppm.

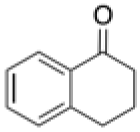

2s

1-Tetralone (**2s**). The general procedure was followed from **1s** (0.130 g, 1 mmol) to afford **2s** (0.080 g, 0.55 mmol, 55% yield) as colorless oil. **2s** was purified by column chromatography on silica gel, eluting with ethyl acetate cyclohexane mixtures (EtOAc/C_6H_{12} = 1:20). The structure of **2s** was confirmed by comparing its ^{1}H- and ^{13}C-NMR spectra with previously reported data described in the literature.[4] **^{1}H NMR** (400 MHz, $CDCl_3$) δ 8.02 (dd, *J* = 7.9, 1.5 Hz, 1H), 7.46 (td, *J* = 7.5, 1.5 Hz, 1H), 7.33 – 7.18 (m, 2H), 2.95 (t, *J* = 6.1 Hz, 2H), 2.64 (dd, *J* = 7.3, 5.9 Hz, 2H), 2.13 (tt, *J* = 7.4, 5.7 Hz, 2H) ppm. **^{13}C NMR** (101 MHz, $CDCl_3$) δ 198.3, 144.4, 133.3, 132.5, 128.7, 127.0, 126.5, 39.0, 29.6, 23.2 ppm.

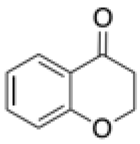

2t

4-Chromanone (**2t**). The general procedure was followed from **1t** (0.132 g, 1 mmol) to afford **2t** (0.070 g, 0.47 mmol, 47% yield) as white solid. **2t** was purified by column chromatography on silica gel, eluting with ethyl acetate cyclohexane mixtures (EtOAc/C_6H_{12} = 1:20). The structure of **2t** was confirmed by comparing its ^{1}H- and ^{13}C-NMR spectra with previously reported data described in the literature.[16] **^{1}H NMR** (400 MHz, $CDCl_3$) δ 7.89 (ddd, *J* = 7.9, 1.8, 0.5 Hz, 1H), 7.47 (ddd, *J* = 8.3, 7.2, 1.8 Hz, 1H), 7.06 – 6.94 (m, 2H), 4.56 – 4.50 (m, 2H), 2.85 – 2.78 (m, 2H) ppm. **^{13}C NMR** (101 MHz, $CDCl_3$) δ 191.7, 161.8, 135.9, 127.1, 121.3, 117.8, 66.9, 37.7 ppm.

8. References

1. de Boer, J. W.; Browne, W. R.; Harutyunyan, S. R.; Bini, L.; Tiemersma-Wegman, T. D.; Alsters, P. L.; Hage, R.; Feringa, B. L. *Chem. Commun.* **2008**, 3747-3749.
2. Yuan, Y.; Shi, X.; Liu, W. *Synlett*, **2011**, 559-564.
3. Nobuta, T.; Hirashima, S. I.; Tada, N.; Miura, T.; Itoh, A. *Org. Lett.* **2011**, *13*, 2576-2579.
4. Cunningham, A.; Mokal-Parekh, V.; Wilson, C.; Woodward, S. *Org. Biomol. Chem.* **2004**, *2*, 741-748.
5. Ruan, J.; Li, X.; Saidi, O.; Xiao, J. *J. Am. Chem. Soc.* **2008**, *130*, 2424-2425.
6. Murphy, J. A.; Commeureuc, A. G. J.; Snaddon, T. N.; McGuire, T. M.; Khan, T. A.; Hisler, K.; Dewis, M. L.; Carling, R. *Org. Lett.* **2005**, *7*, 1427-1429.
7. Genna, D. T.; Posner, G. H. *Org. Lett.* **2011**, *13*, 5358-5361.
8. Scheiper, B.; Bonnekessel, M.; Krause, H.; Fuerstner, A. *J. Org. Chem.* **2004**, *69*, 3943-3949.
9. Chu, L.; Qing, F. -L. *Org. Lett.* **2010**, *12*, 5060-5063.
10. Schultz, M. J.; Hamilton, St. S.; Jensen, D. R.; Sigman, M. S. *J. Org. Chem.* **2005**, *70*, 3343-3352.
11. Liu, M.; Hyder, Z.; Sun, Y.; Tang, W.; Xu, L.; Xiao, J. *Org. Biomol. Chem.* **2010**, *8*, 2012-2015.
12. Liu, S.; Berry, N.; Thomson, N.; Pettman, A.; Hyder, Z.; Mo, J.; Xiao, J. *J. Org. Chem.* **2006**, *71*, 7467-7470.
13. (a) Zhao, B.; Lu, X. *Tetrahedron Lett*. **2006**, *47*, 6765-6768; (b) Iinuma, M.; Moriyama, K.; Togo, H. *Tetrahedron* **2013**, *69*, 2961-2970.
14. Dohi, T.; Takenaga, N.; Goto, A.; Fujioka, H.; Kita, Y. *J. Org. Chem.* **2008**, *73*, 7365-7368.
15. Zhao, B.; Lu, X. *Org. Lett.* **2006**, *8*, 5987-5990.
16. Kotani, S.; Osakama, K.; Sugiura, M.; Nakajima, M. *Org. Lett.* **2011**, *13*, 3968–3971.

7. NMR Spectra

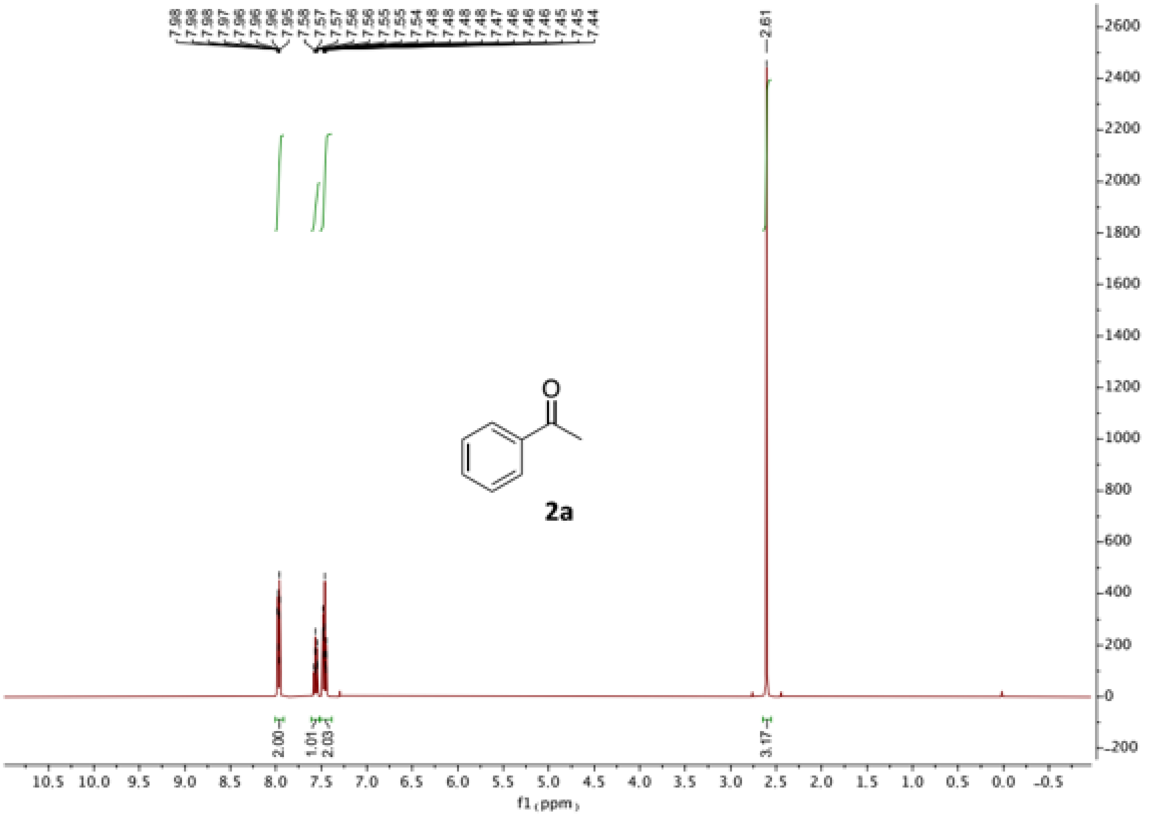

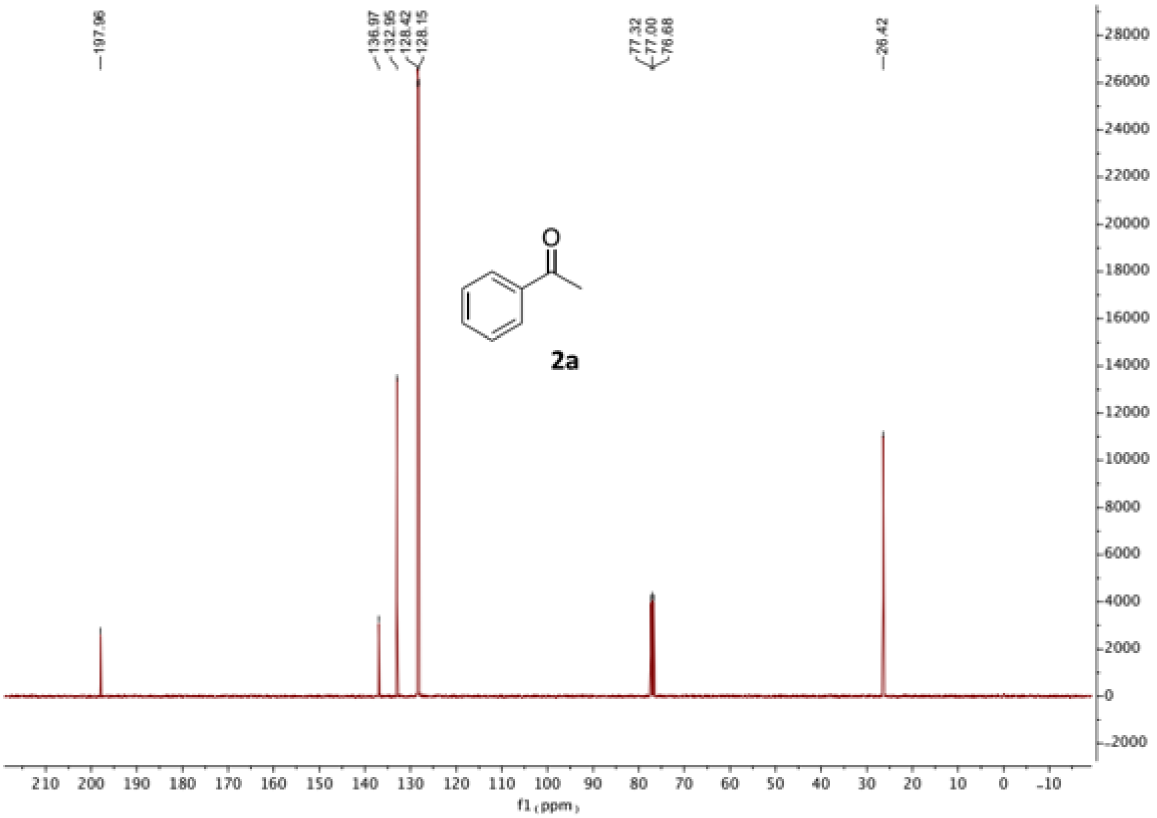

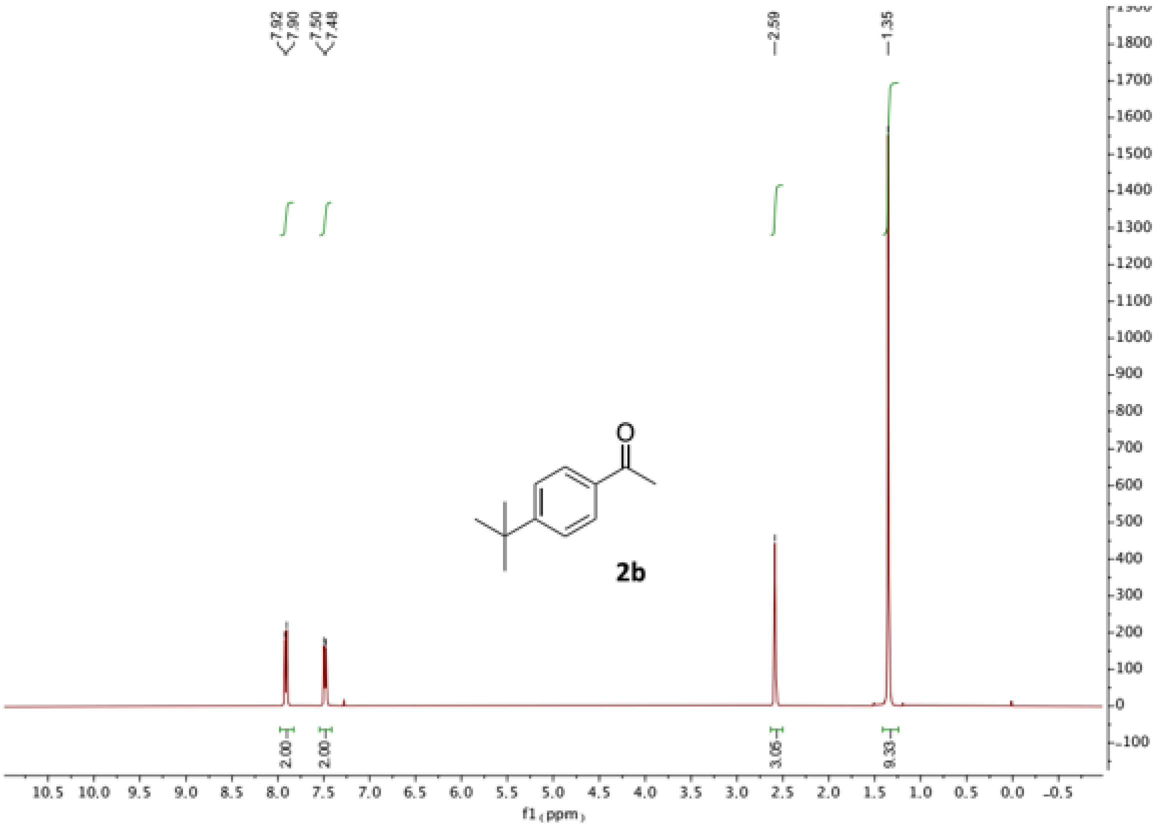
7.92
7.90
7.50
7.48
2.59
1.35
2b
2.00
2.00
3.05
9.33
f1 (ppm)

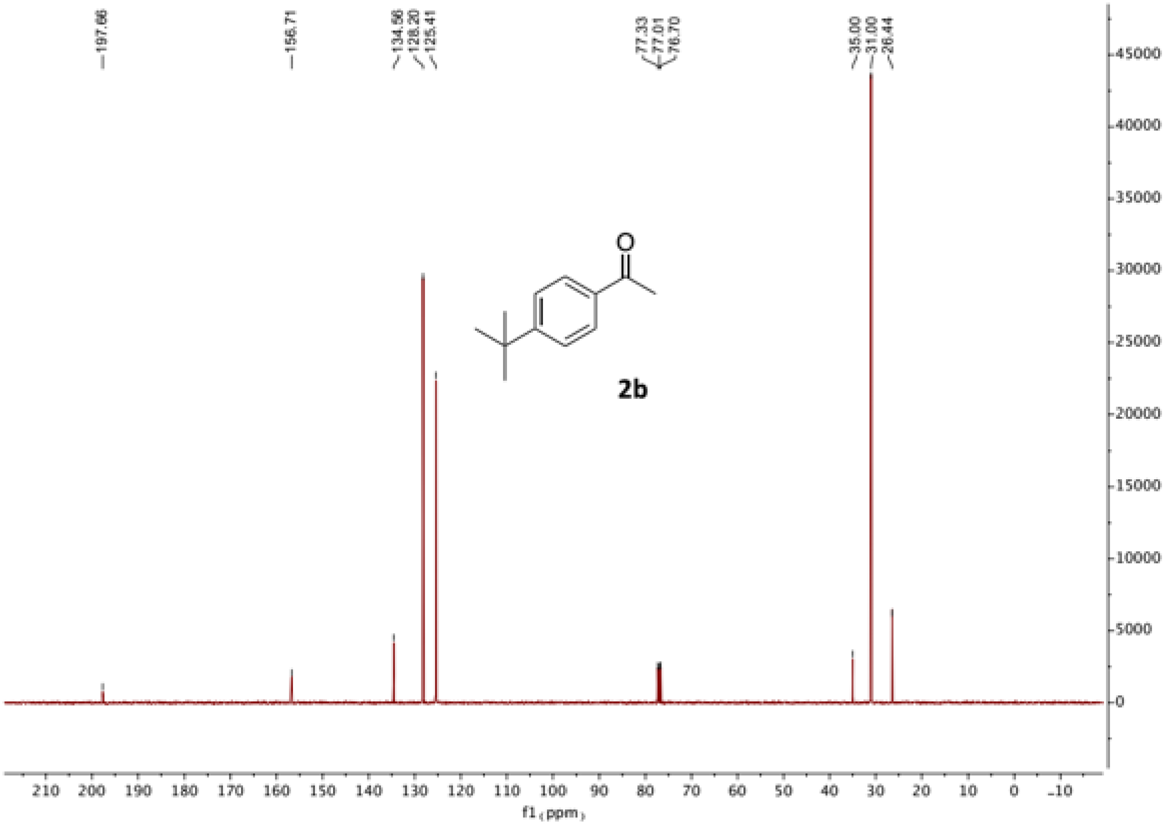
197.66
156.71
134.56
128.20
125.41
77.33
77.01
76.70
35.00
31.00
26.44
2b
f1 (ppm)

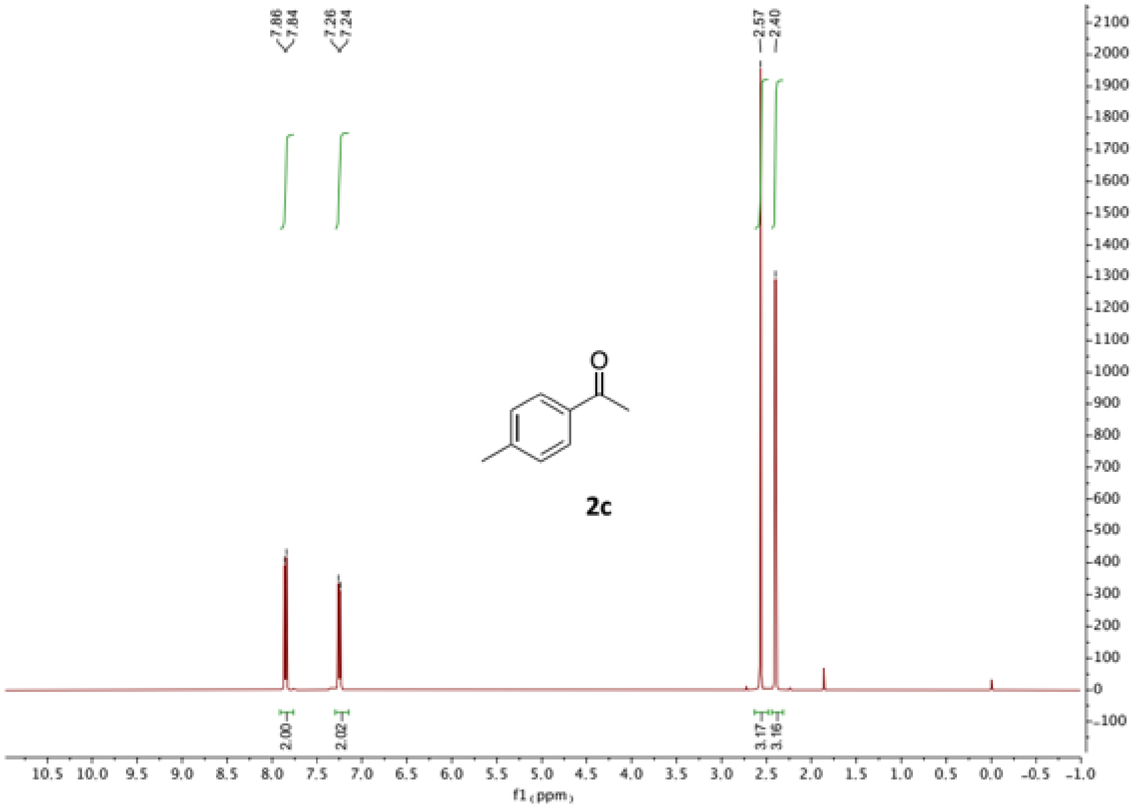
7.86
7.84
7.26
7.24
2.57
2.40
2c
2.00
2.02
3.17
3.16
f1 (ppm)

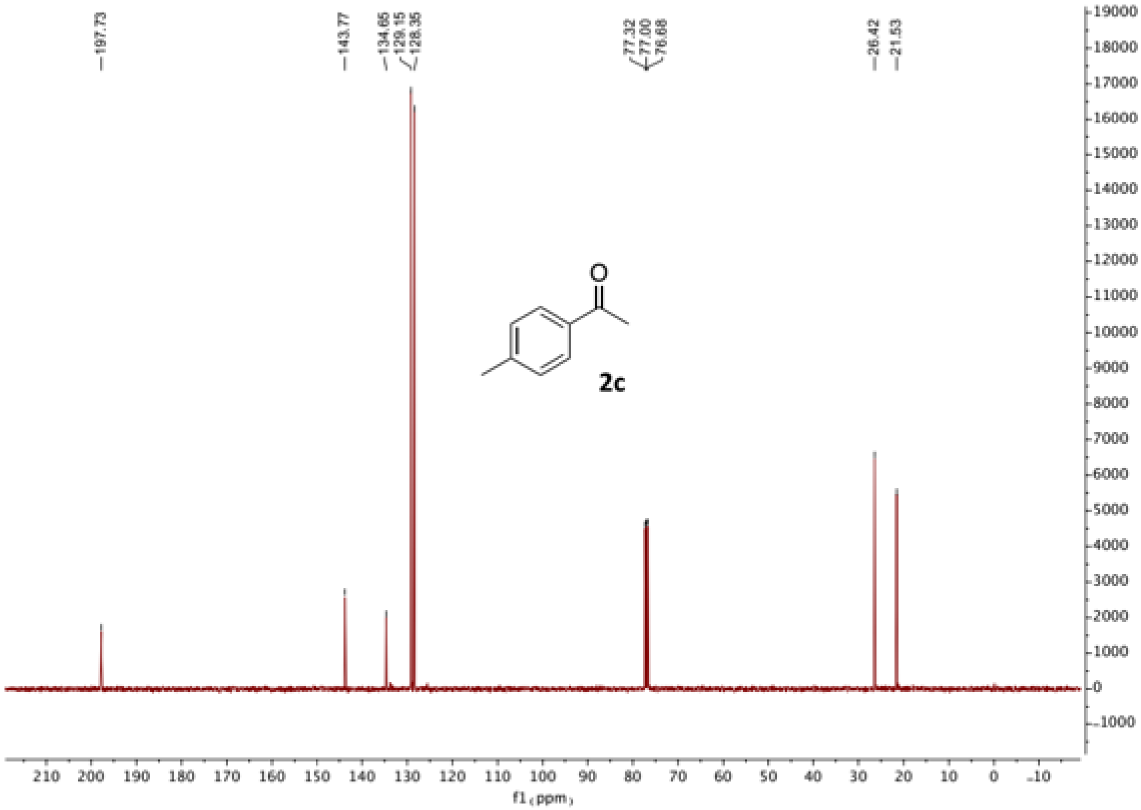
197.73
143.77
134.65
129.15
128.35
77.32
77.00
76.68
26.42
21.53
2c
f1 (ppm)

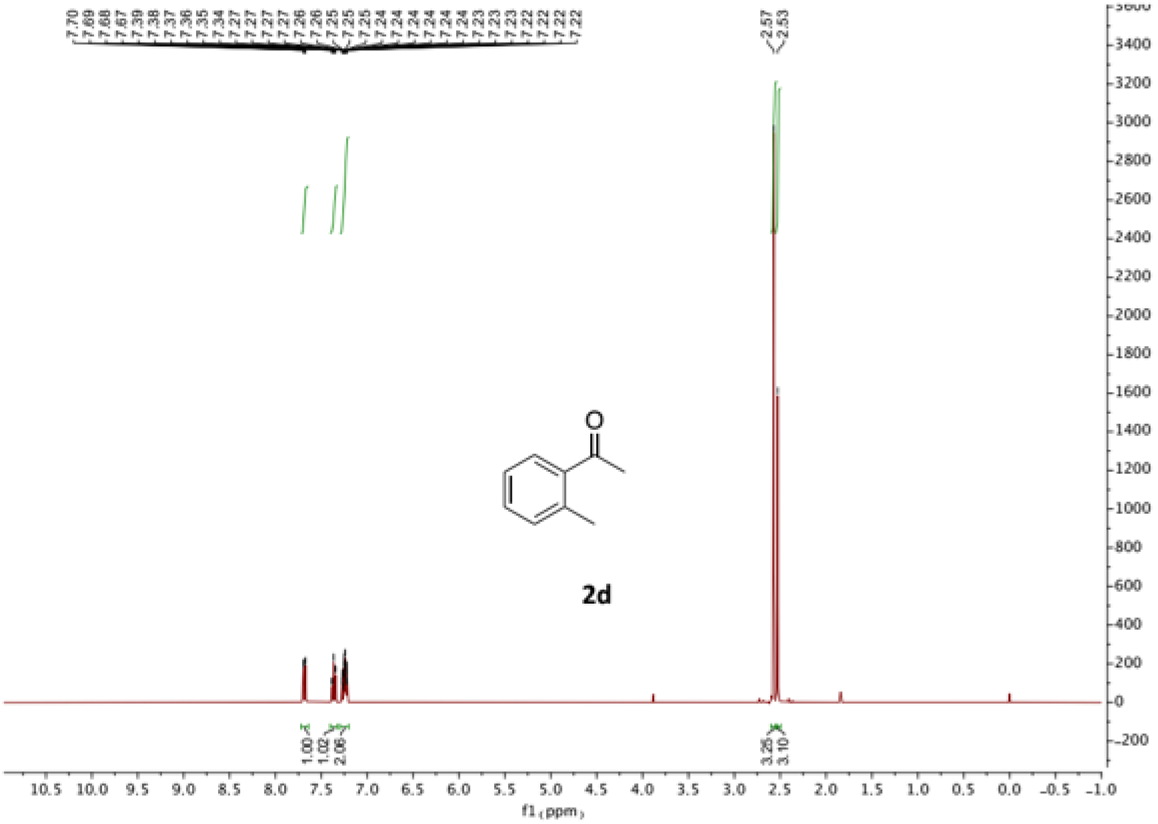
2d
f1 (ppm)

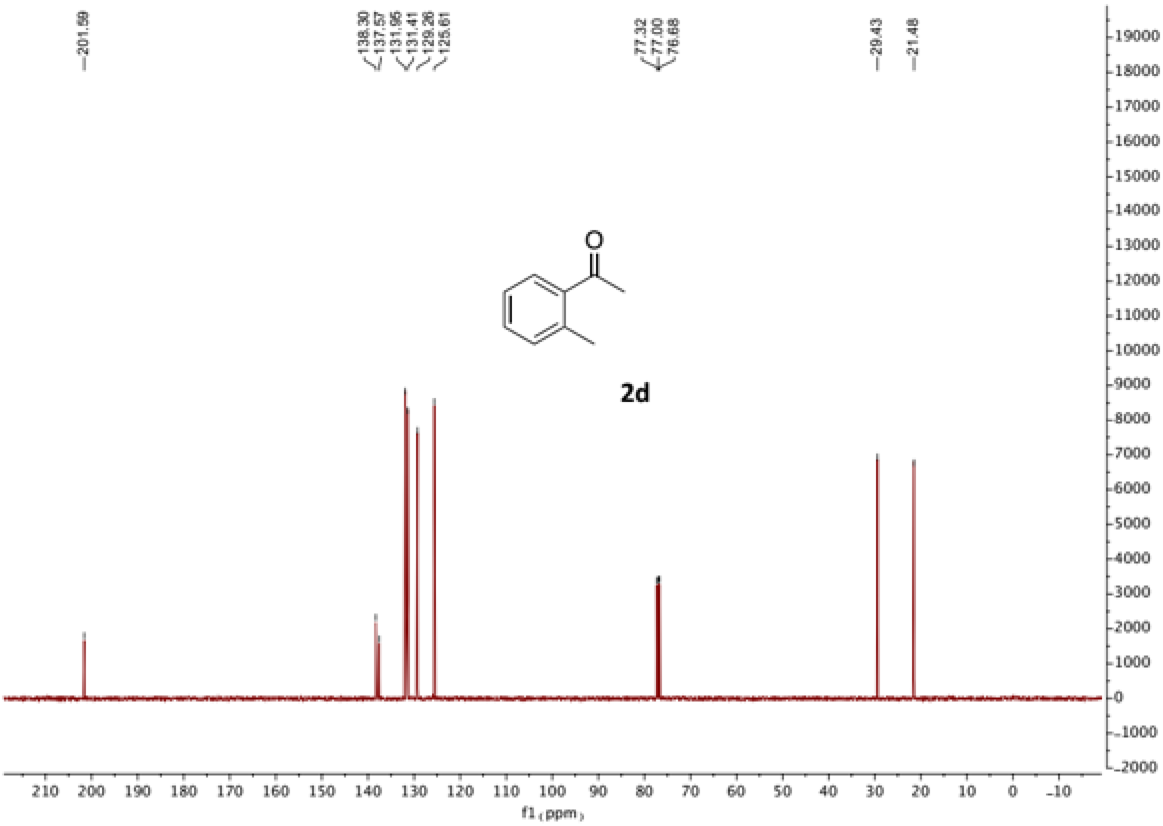
2d
f1 (ppm)

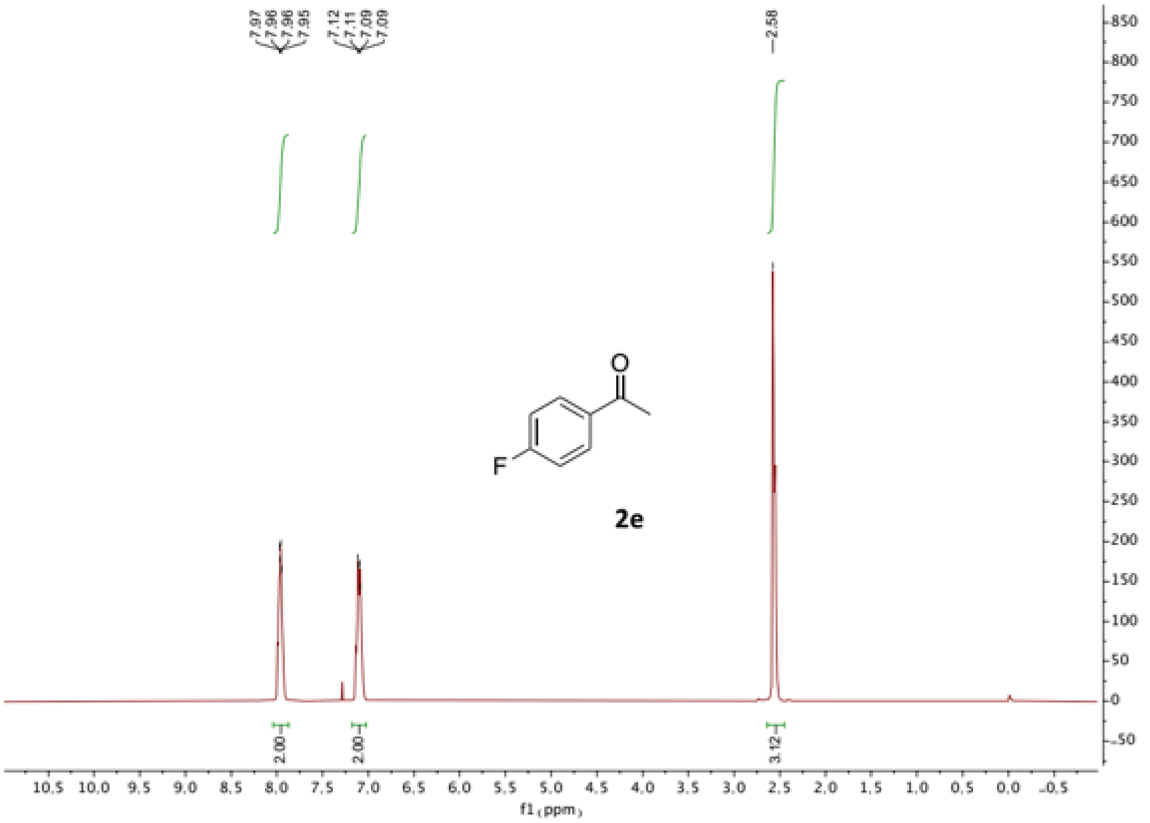
7.97
7.96
7.96
7.95
7.12
7.11
7.09
7.09
2.58
F
O
2e
2.00
2.00
3.12
f1 (ppm)

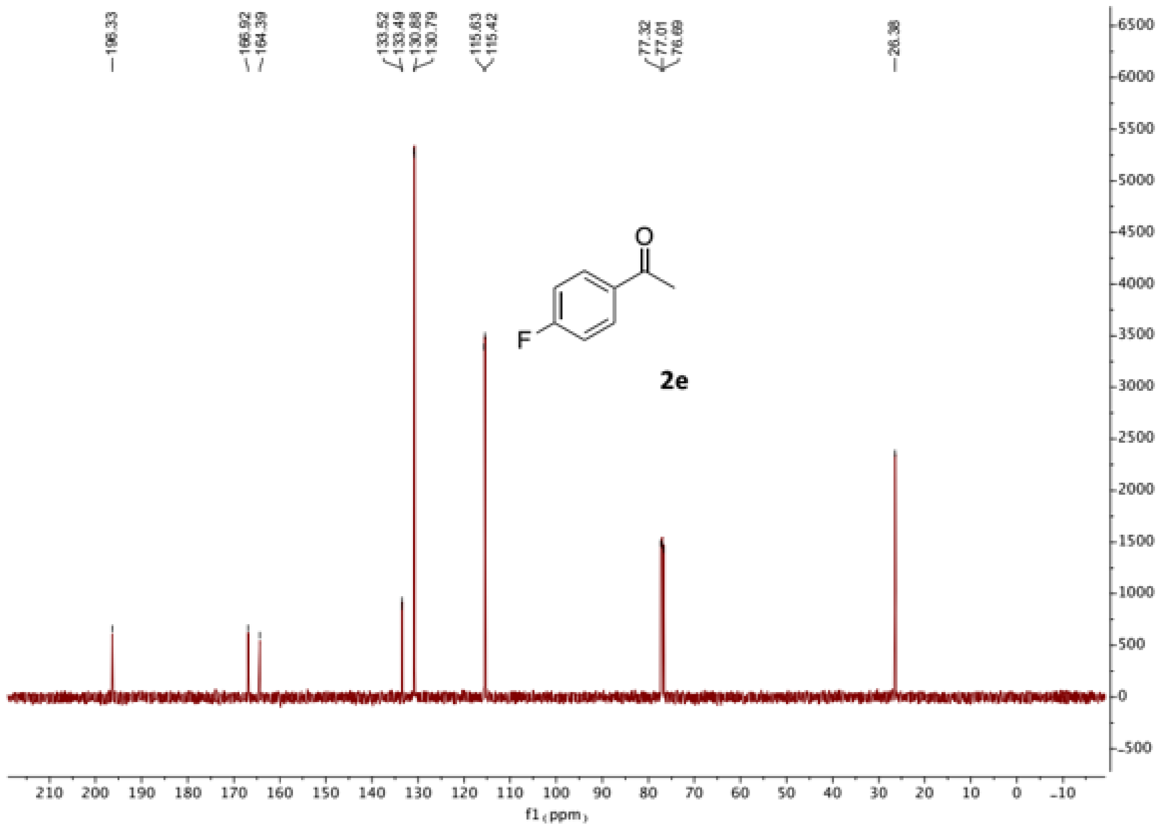
196.33
166.92
164.39
133.52
133.49
130.88
130.79
115.63
115.42
77.32
77.01
76.69
26.38
F
O
2e
f1 (ppm)

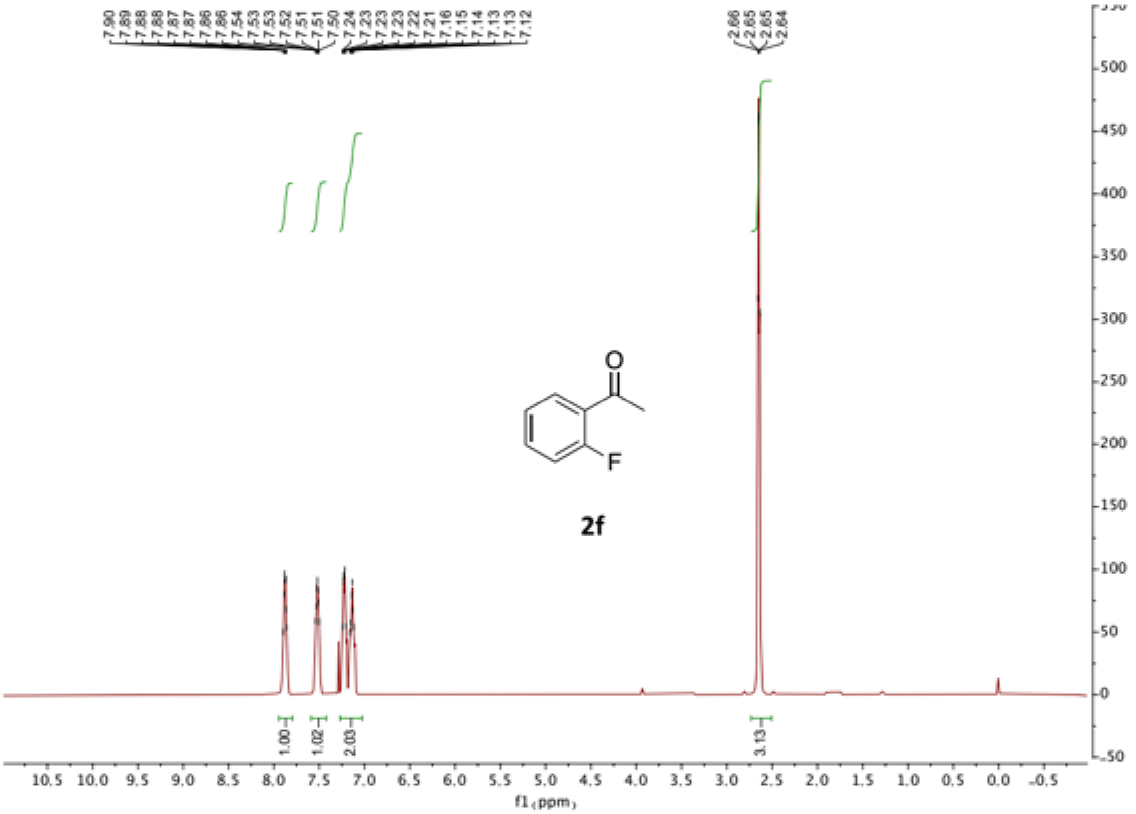
7.90
7.89
7.88
7.88
7.87
7.87
7.86
7.86
7.54
7.53
7.53
7.52
7.51
7.51
7.50
7.24
7.23
7.23
7.23
7.22
7.21
7.16
7.15
7.14
7.13
7.13
7.12
2.66
2.65
2.65
2.64
2f
1.00
1.02
2.03
3.13
f1 (ppm)

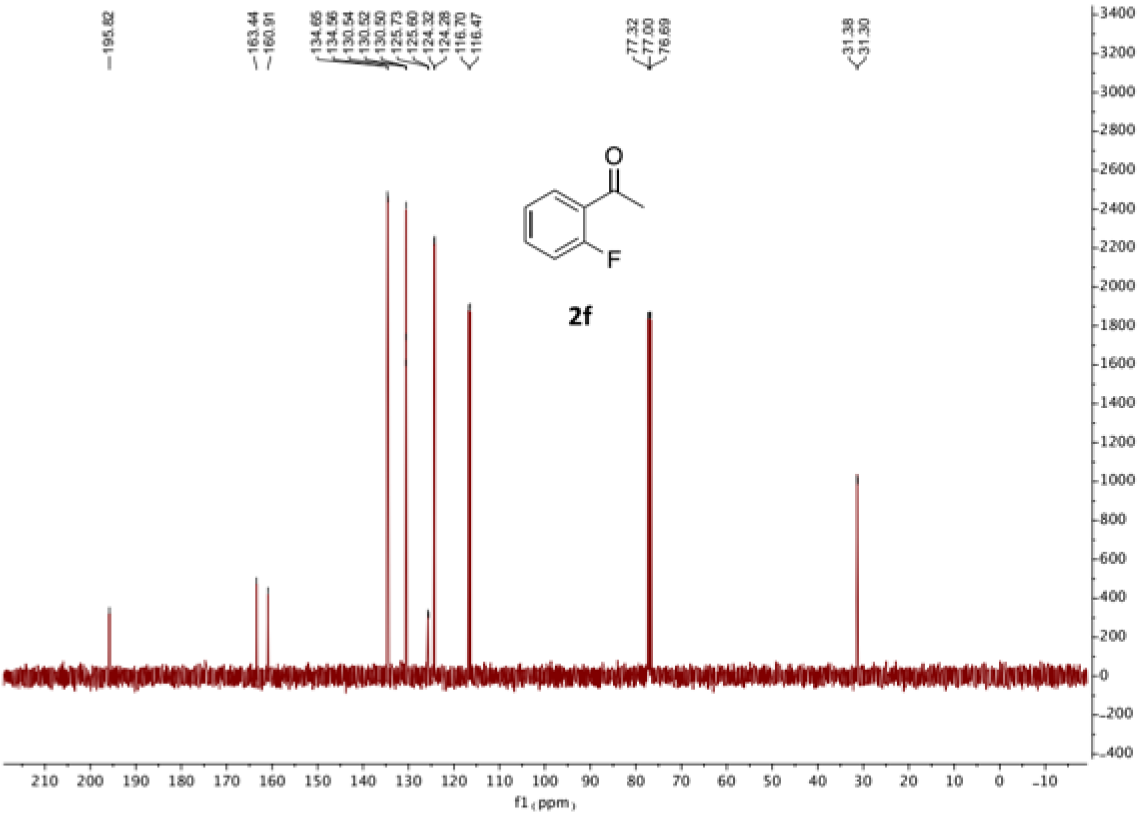
195.82
163.44
160.91
134.65
134.56
130.54
130.52
130.50
125.73
125.60
124.32
124.28
116.70
116.47
77.32
77.00
76.69
31.38
31.30
2f
f1 (ppm)

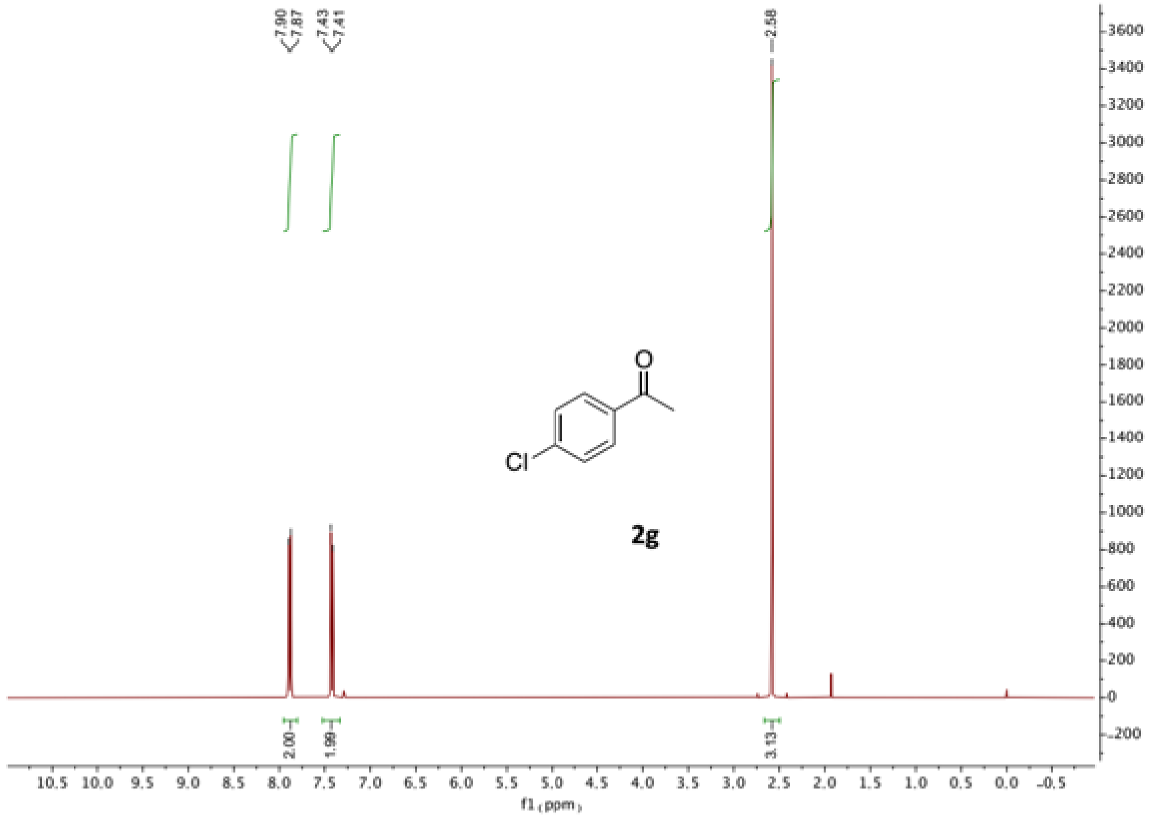
7.90
7.87
7.43
7.41
2.58
2.00
1.99
3.13
2g
f1 (ppm)

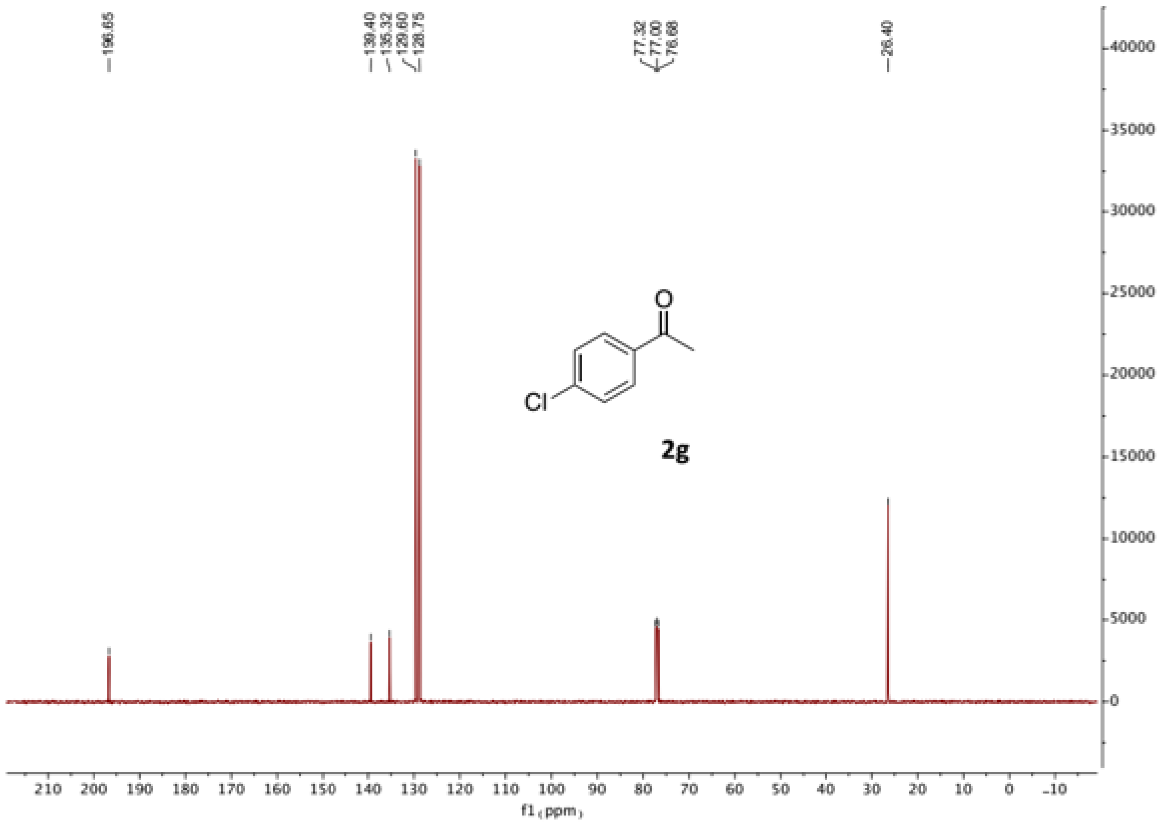
196.65
139.40
135.32
129.60
128.75
77.32
77.00
76.68
26.40
2g
f1 (ppm)

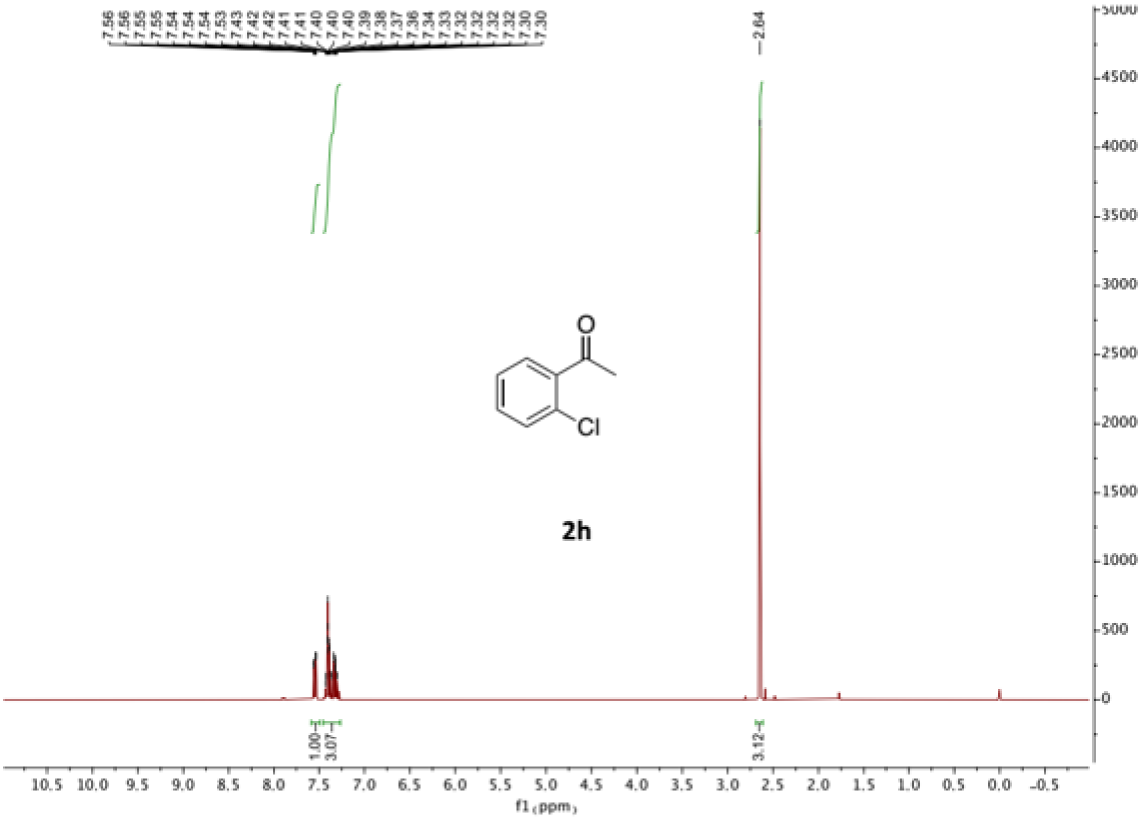
2h
Cl
O
f1 (ppm)
2.64
1.00
3.07
3.12

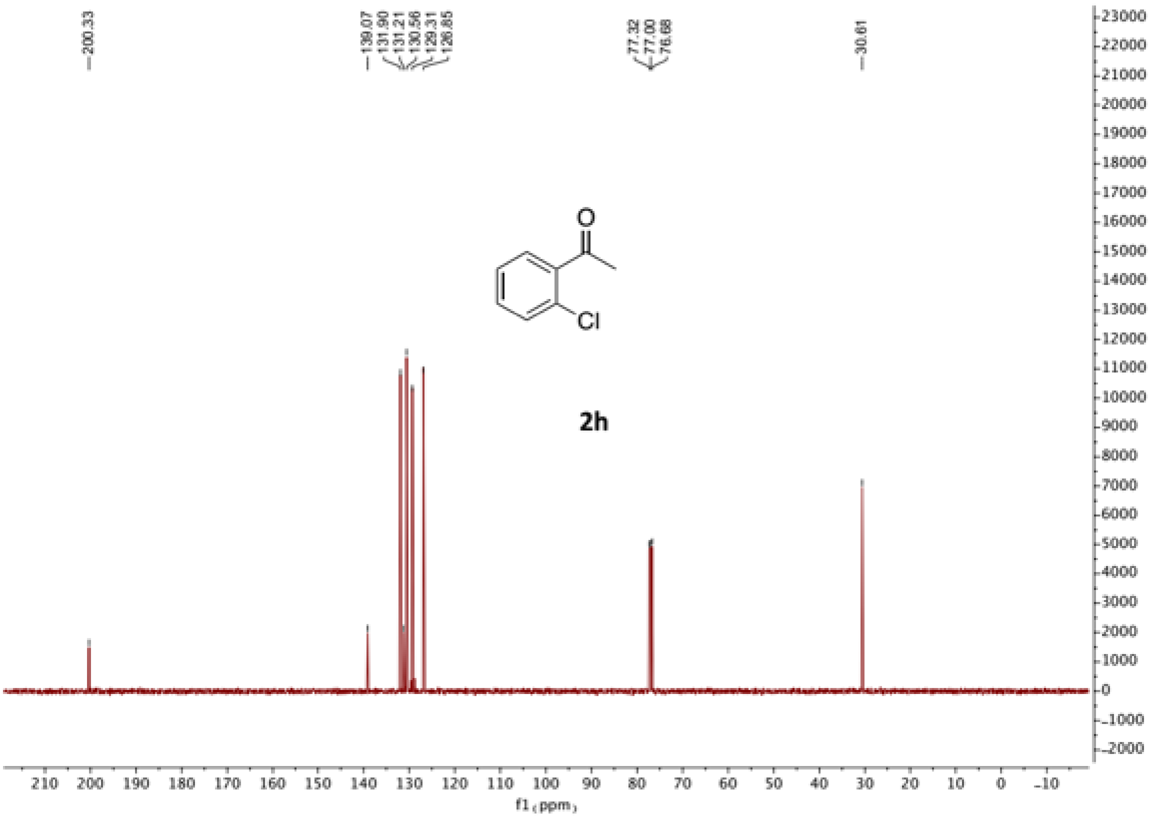
2h
Cl
O
f1 (ppm)
200.33
139.07
131.90
131.21
130.56
129.31
126.85
77.32
77.00
76.68
30.61

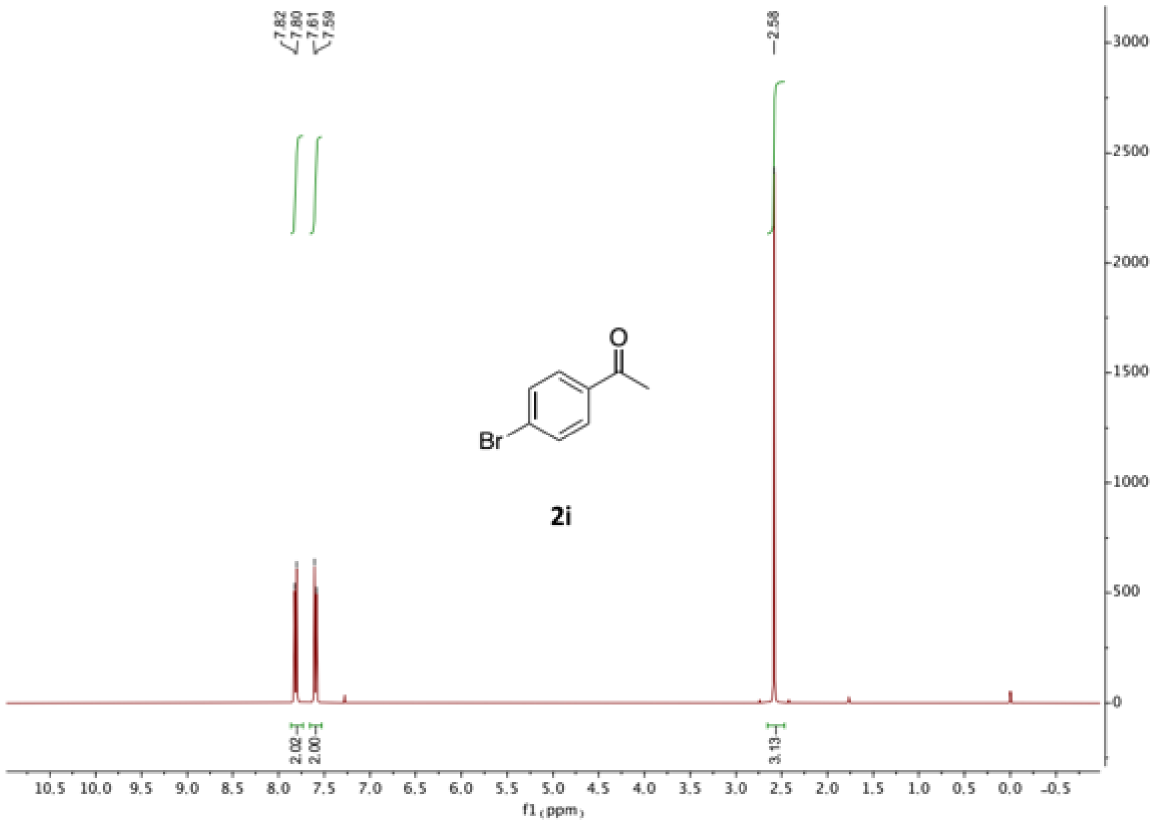
7.82
7.80
7.61
7.59
2.58
Br
O
2i
2.02
2.00
3.13
f1 (ppm)

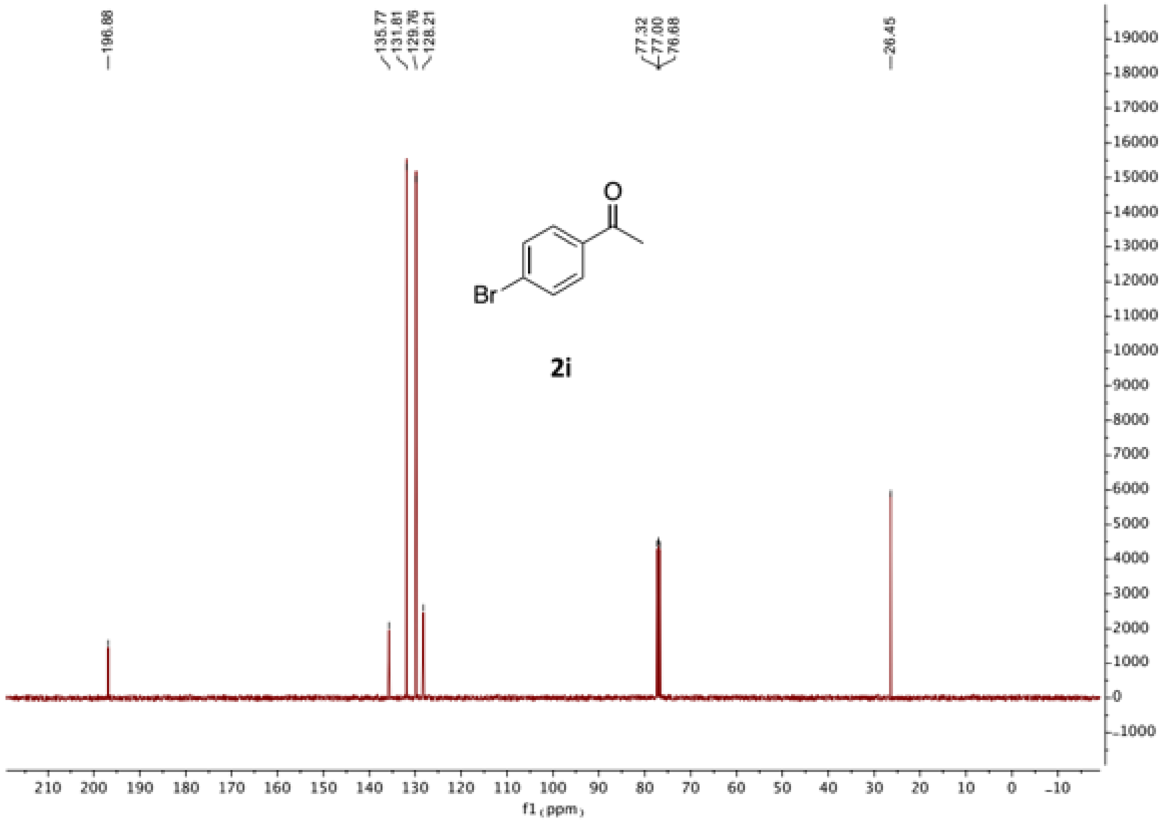
196.88
135.77
131.81
129.76
128.21
77.32
77.00
76.68
26.45
Br
O
2i
f1 (ppm)

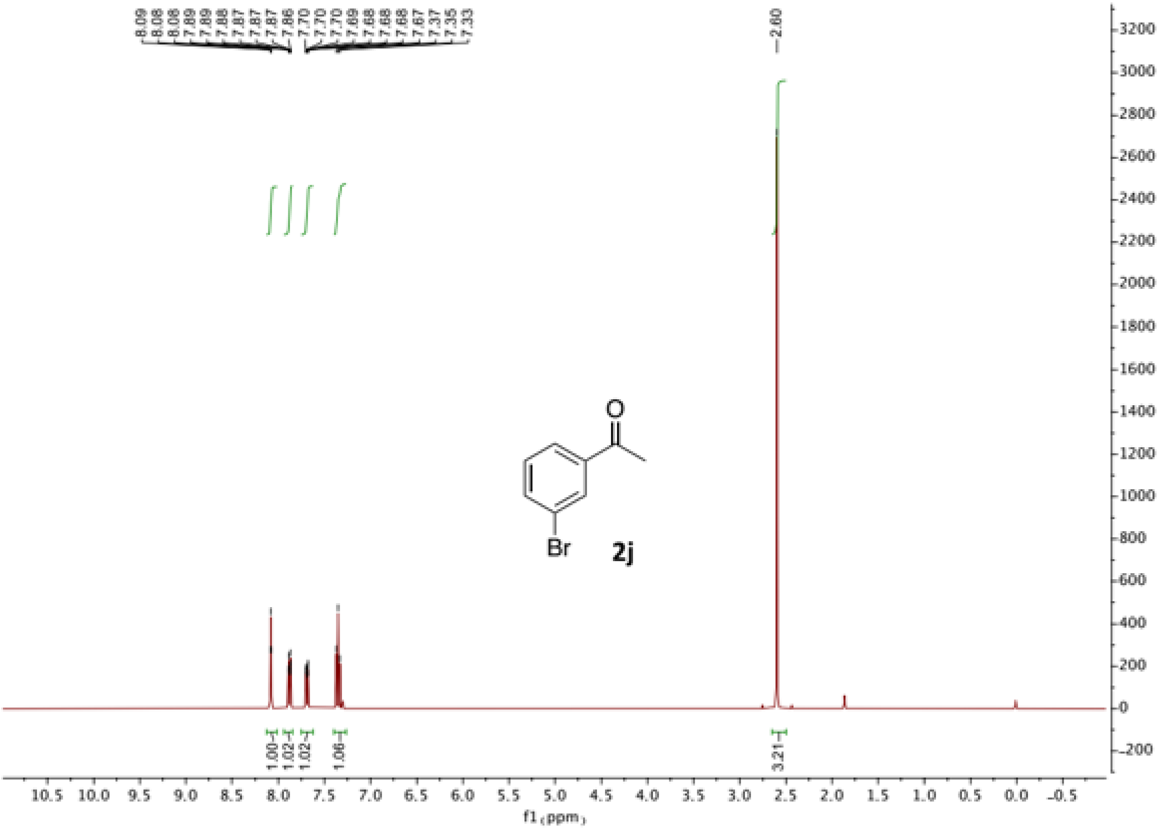
8.09
8.08
8.08
7.89
7.89
7.88
7.87
7.87
7.86
7.70
7.70
7.70
7.69
7.68
7.68
7.68
7.67
7.37
7.35
7.33
2.60
Br
2j
1.00
1.02
1.02
1.06
3.21
f1 (ppm)

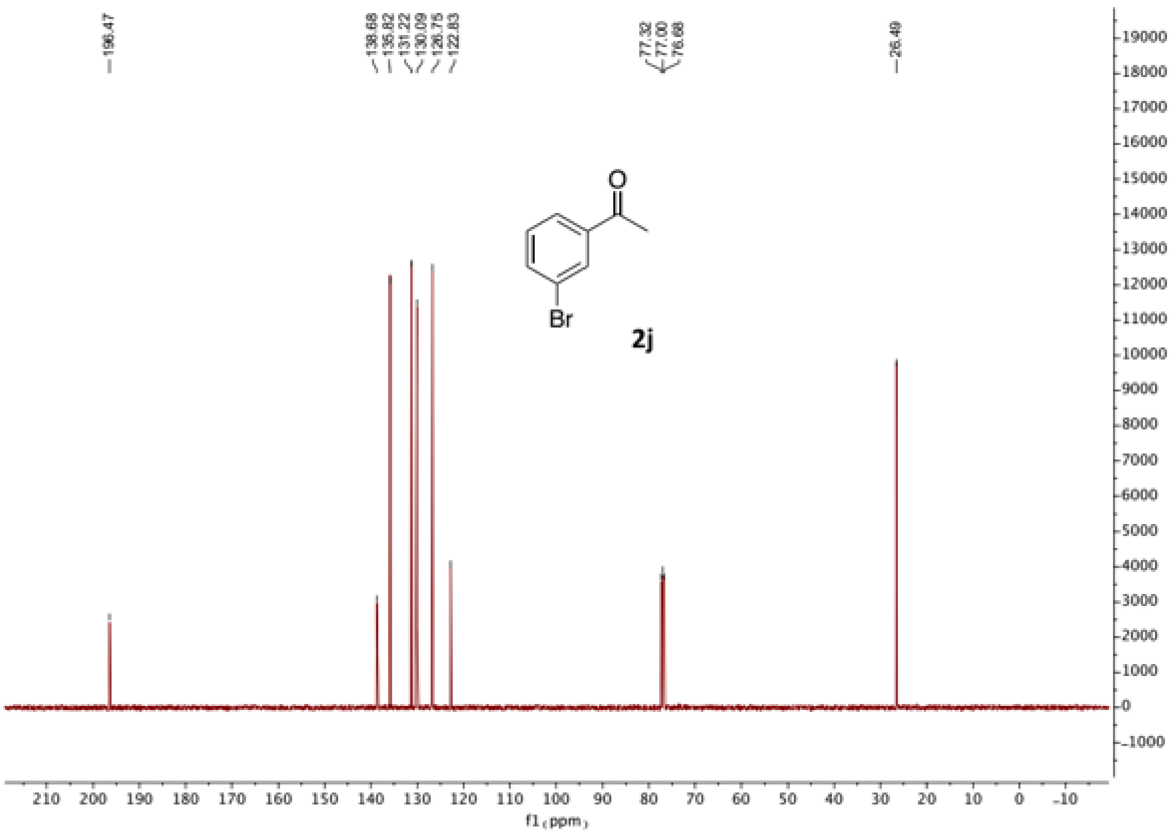
196.47
138.68
135.82
131.22
130.09
126.75
122.83
77.32
77.00
76.68
26.49
Br
2j
f1 (ppm)

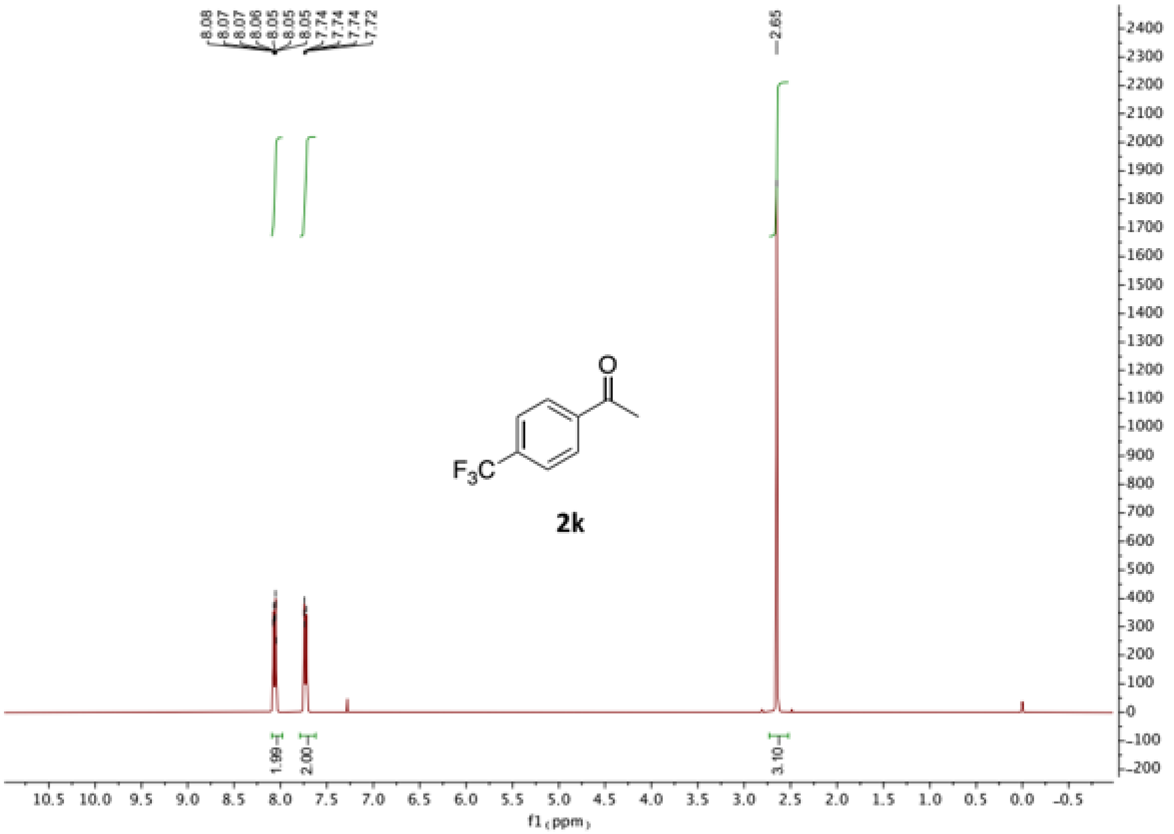
8.08
8.07
8.07
8.06
8.05
8.05
8.05
7.74
7.74
7.74
7.72
2.65
F3C
2k
1.99
2.00
3.10
f1 (ppm)

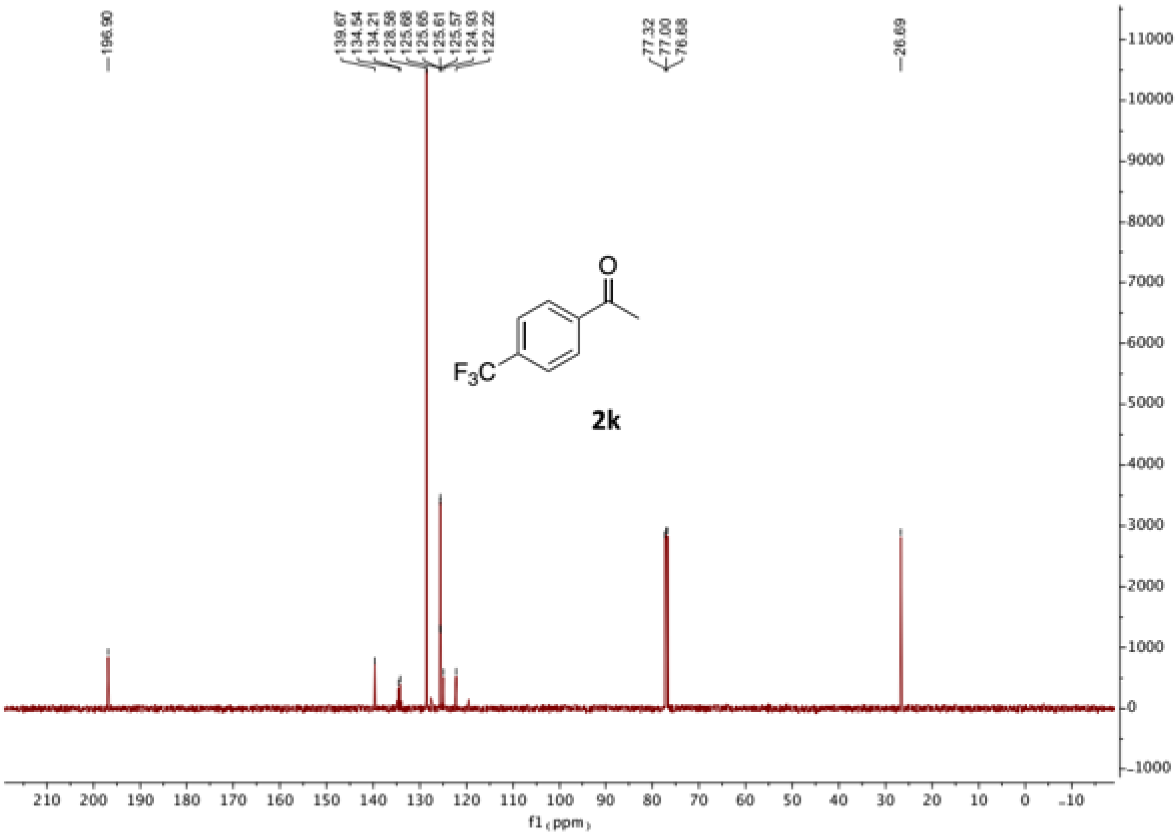
196.90
139.67
134.54
134.21
128.58
125.68
125.65
125.61
125.57
124.93
122.22
77.32
77.00
76.68
26.69
F3C
2k
f1 (ppm)

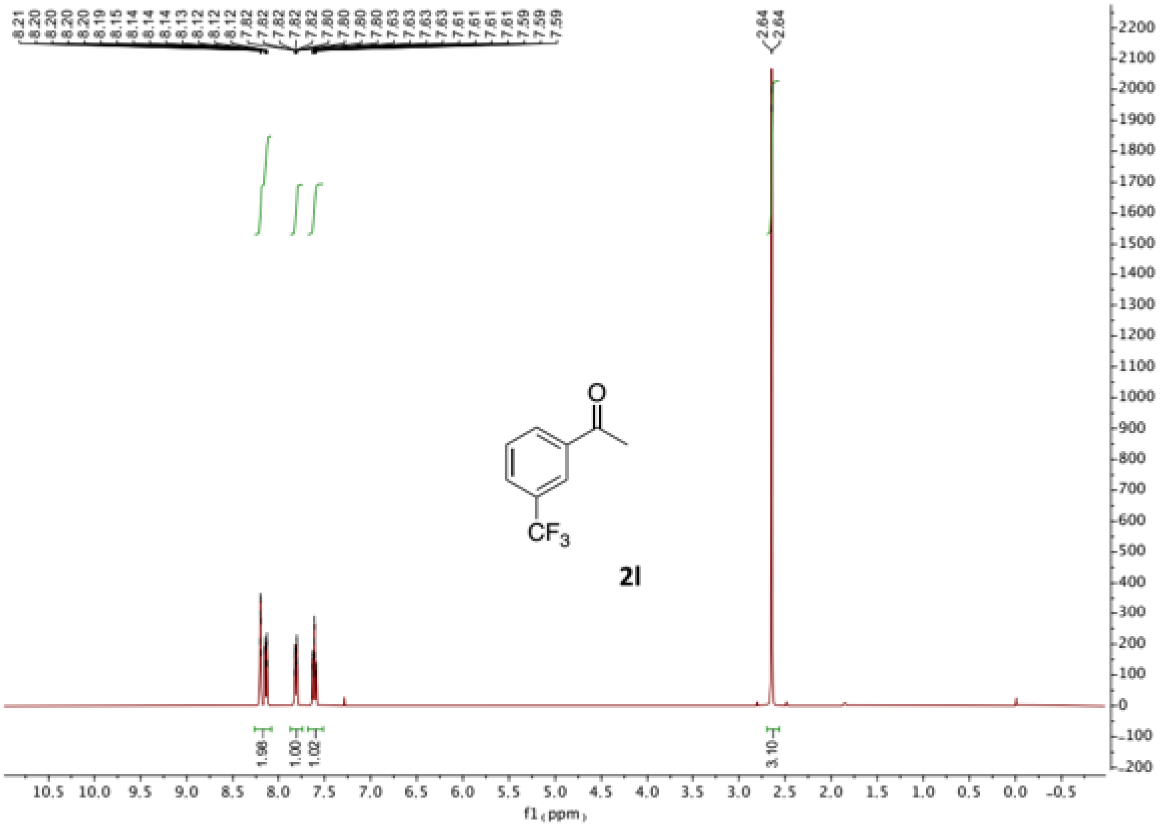
2l
f1 (ppm)

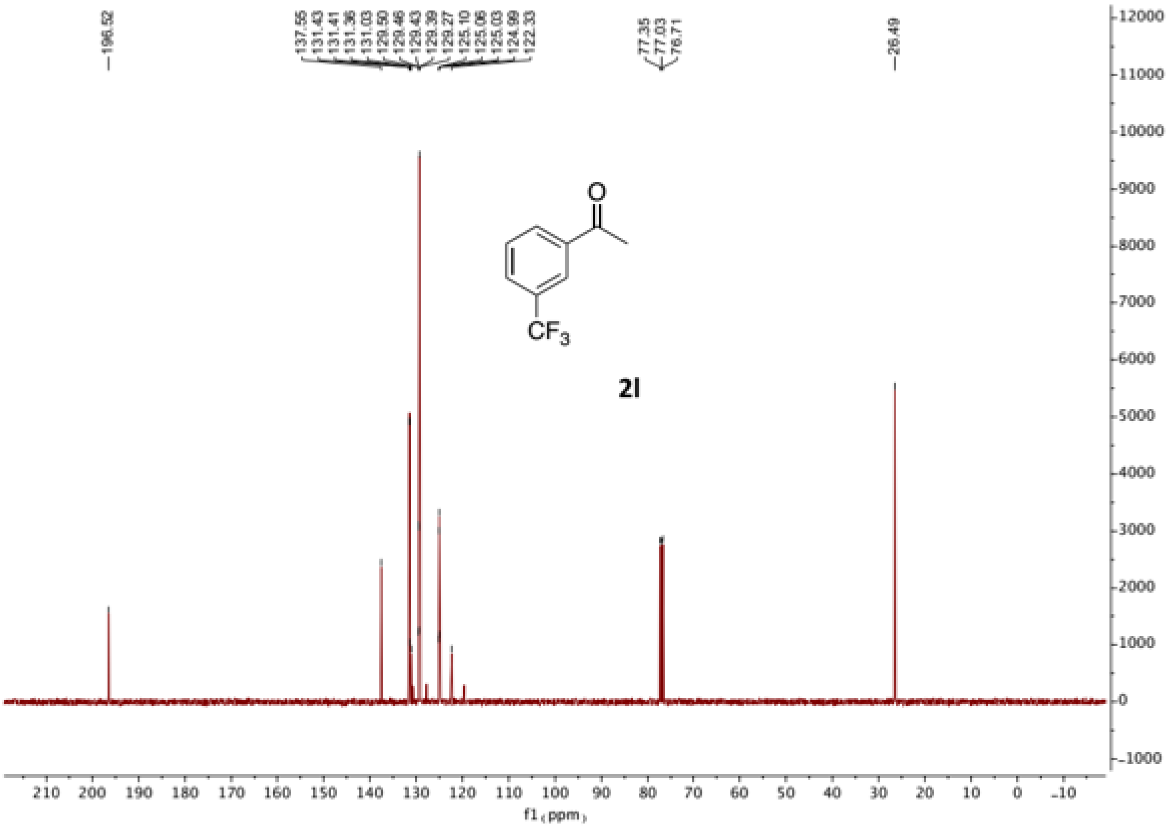
2l
f1 (ppm)

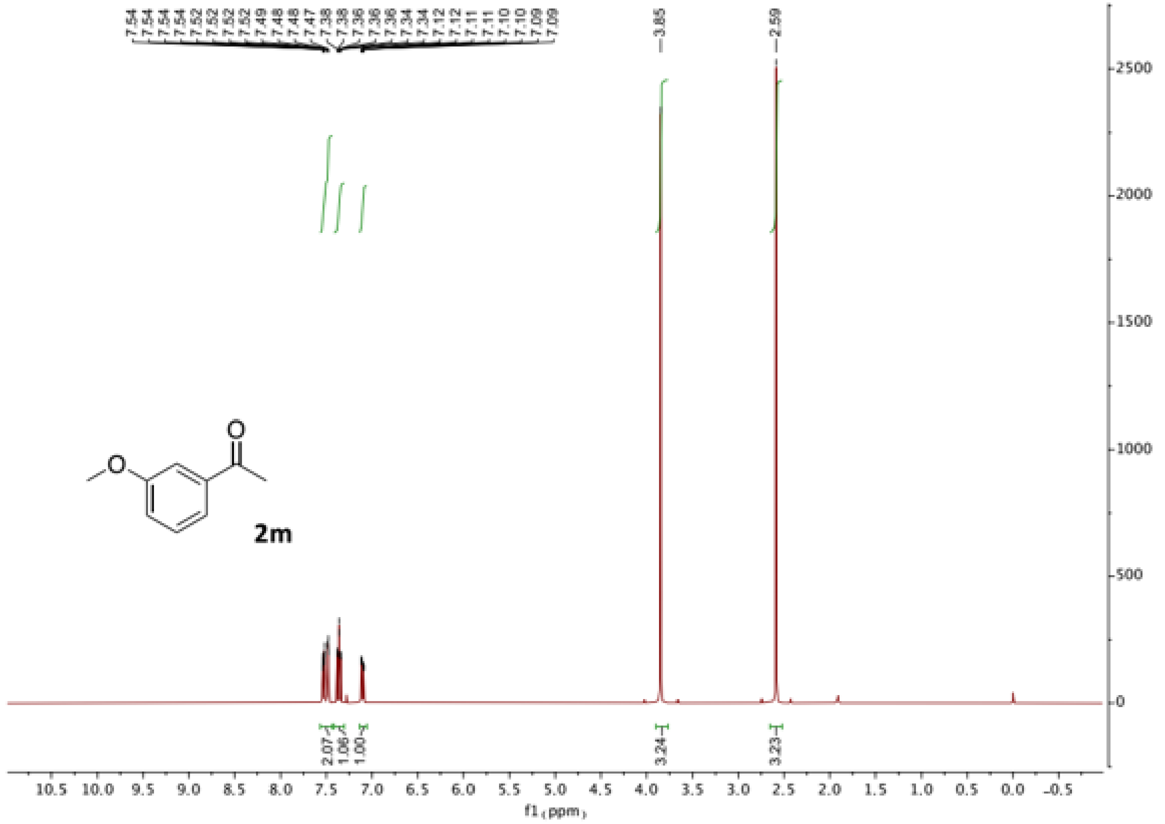
2m
3.85
2.59
2.07
1.06
1.00
3.24
3.23
f1 (ppm)

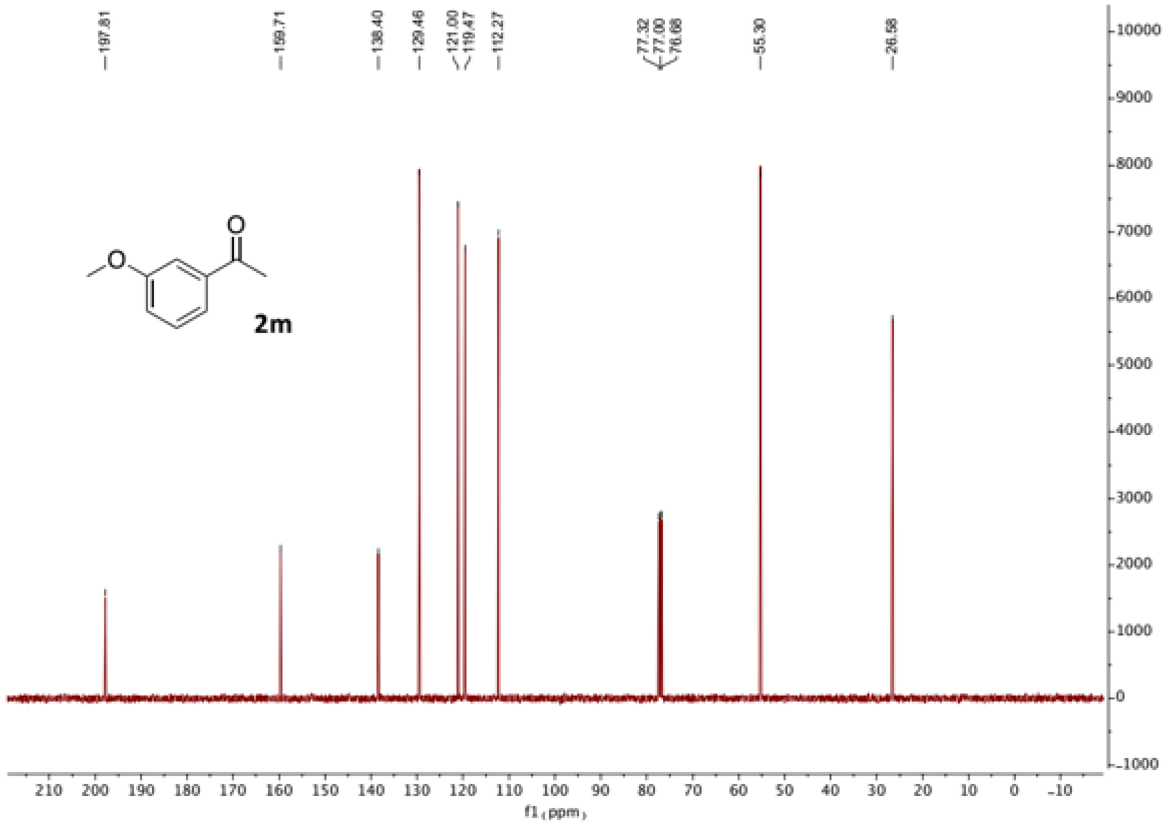
2m
197.81
159.71
138.40
129.46
121.00
119.47
112.27
77.32
77.00
76.68
55.30
26.58
f1 (ppm)

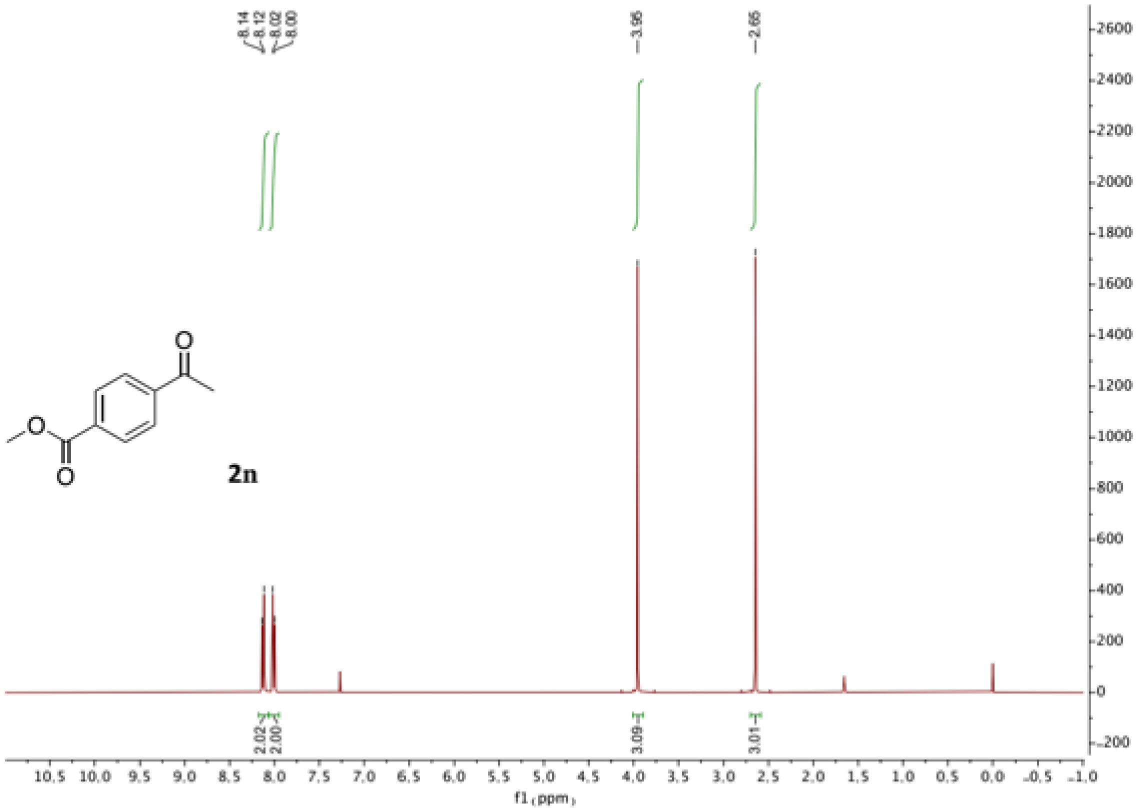
2n
8.14
8.12
8.02
8.00
3.95
2.65
2.02
2.00
3.09
3.01
f1 (ppm)

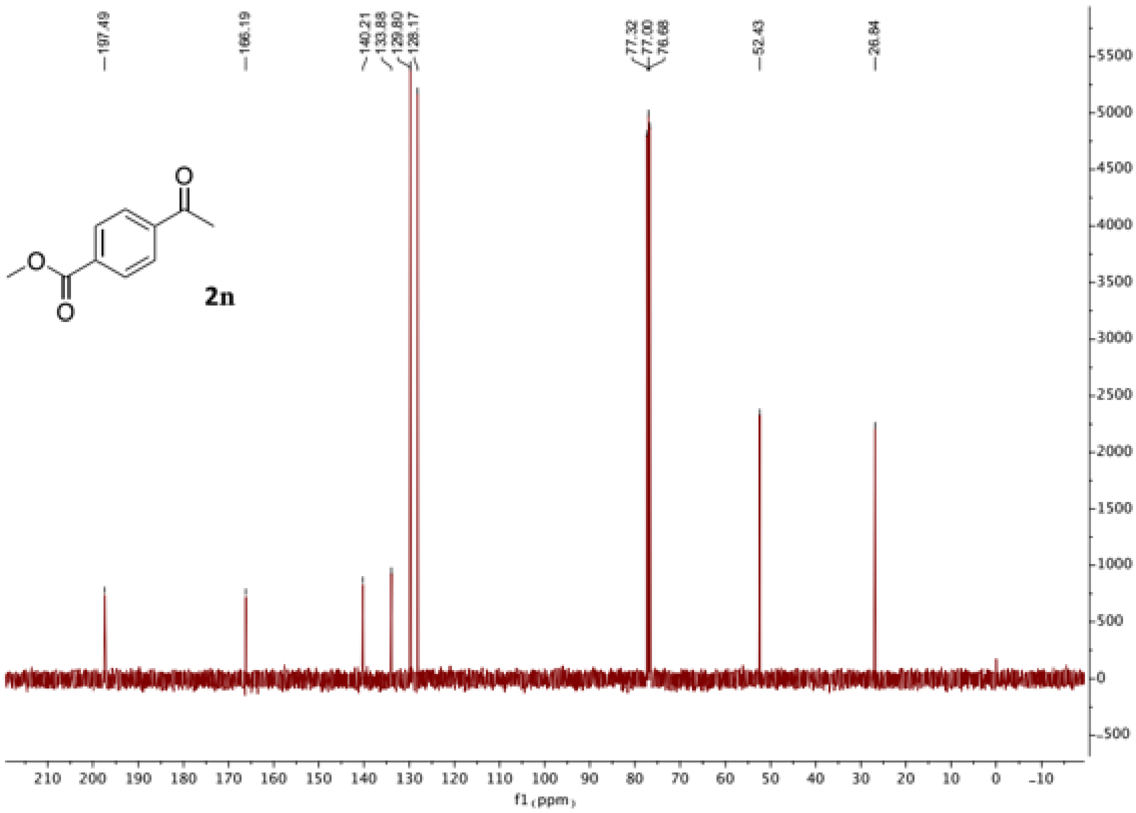
2n
197.49
166.19
140.21
133.88
129.80
128.17
77.32
77.00
76.68
52.43
26.84
f1 (ppm)

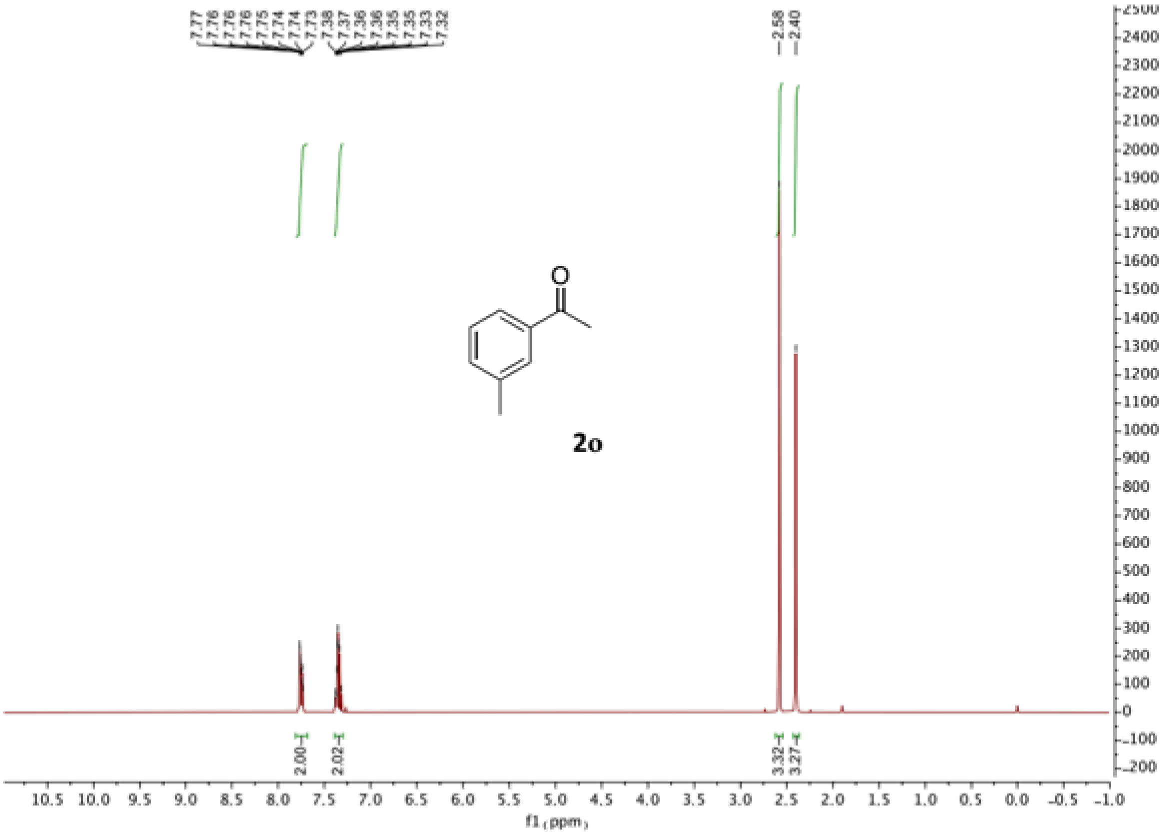
2o
f1 (ppm)

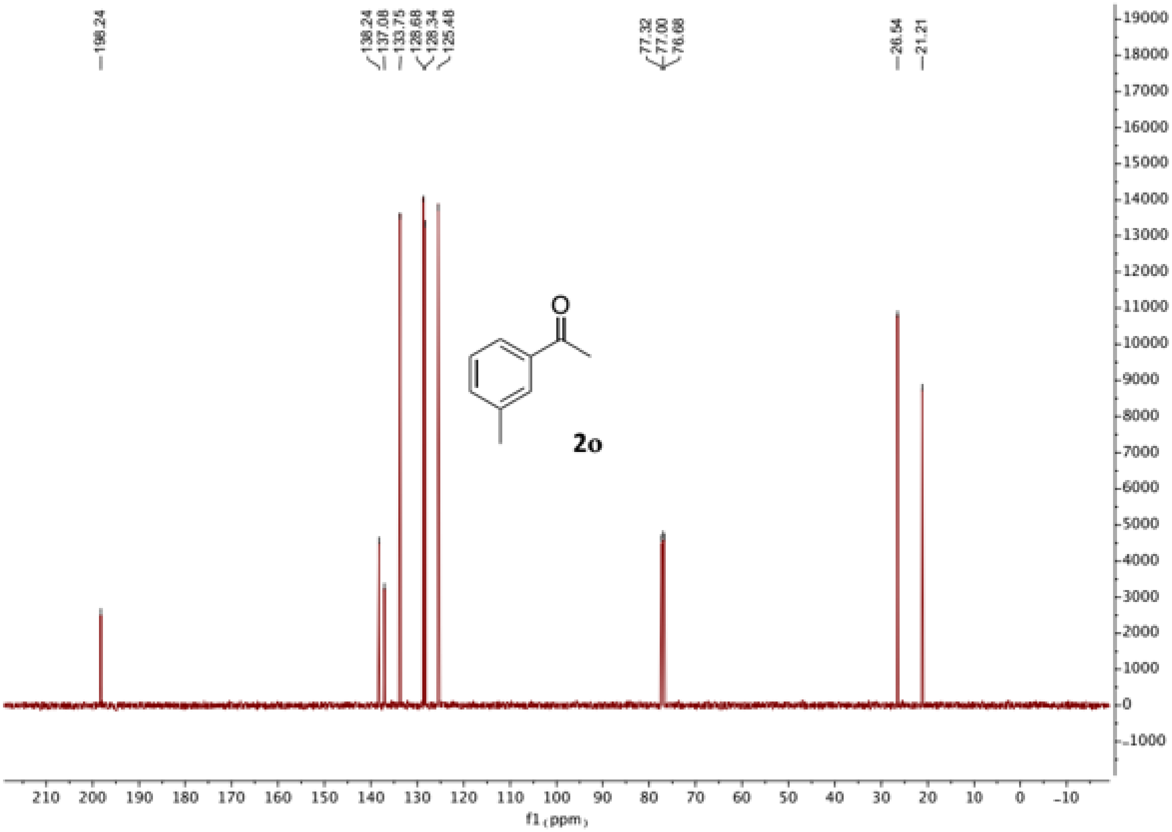
2o
f1 (ppm)

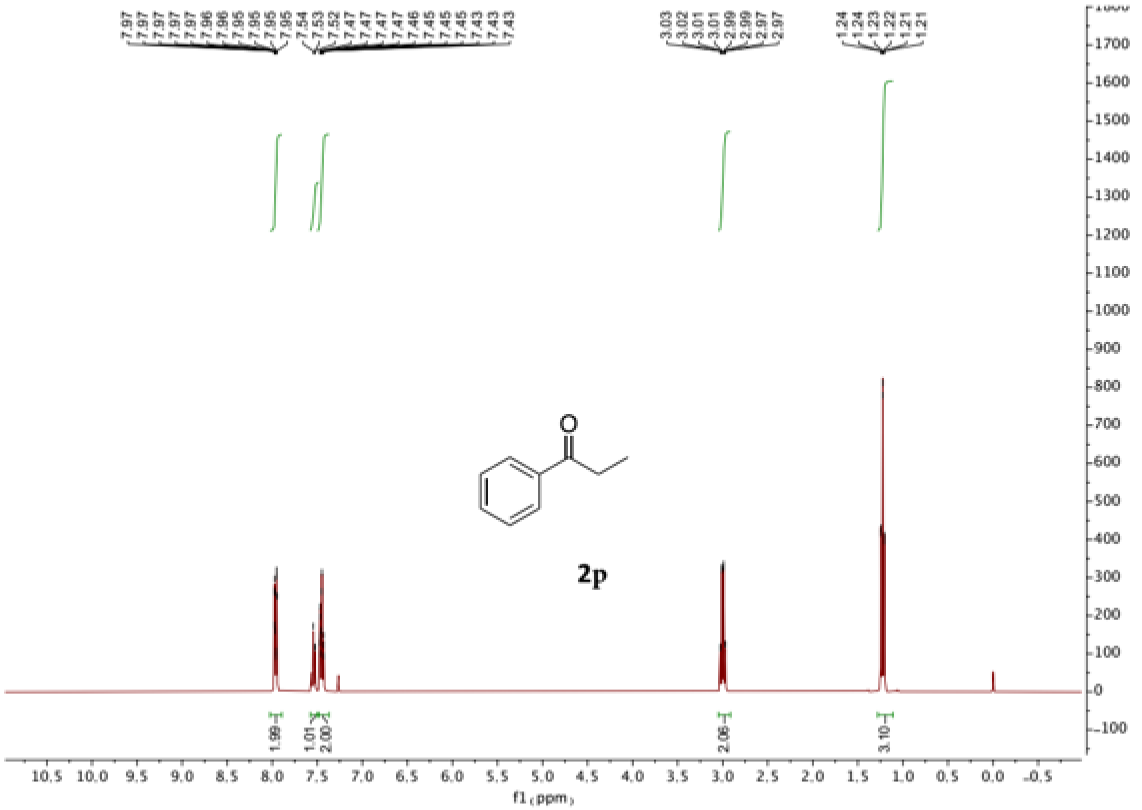
2p
1.99
1.01
2.00
2.06
3.10
f1 (ppm)

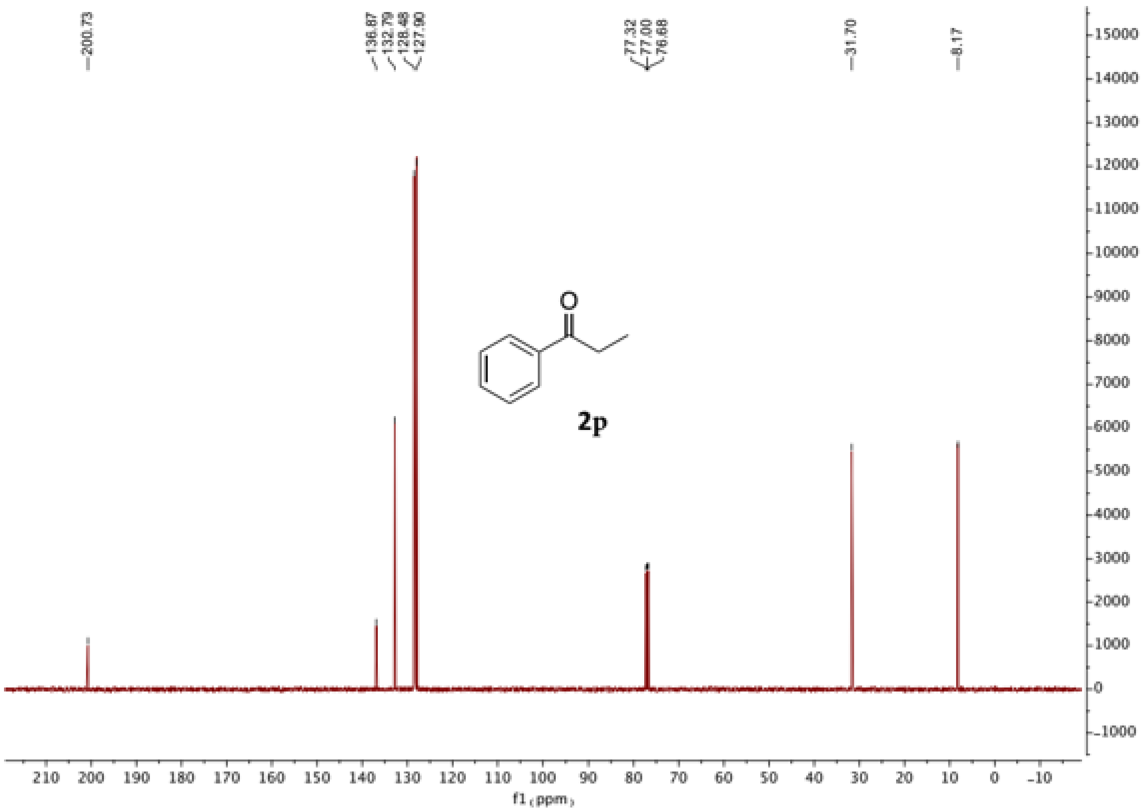
200.73
136.87
132.79
128.48
127.90
77.32
77.00
76.68
31.70
8.17
2p
f1 (ppm)

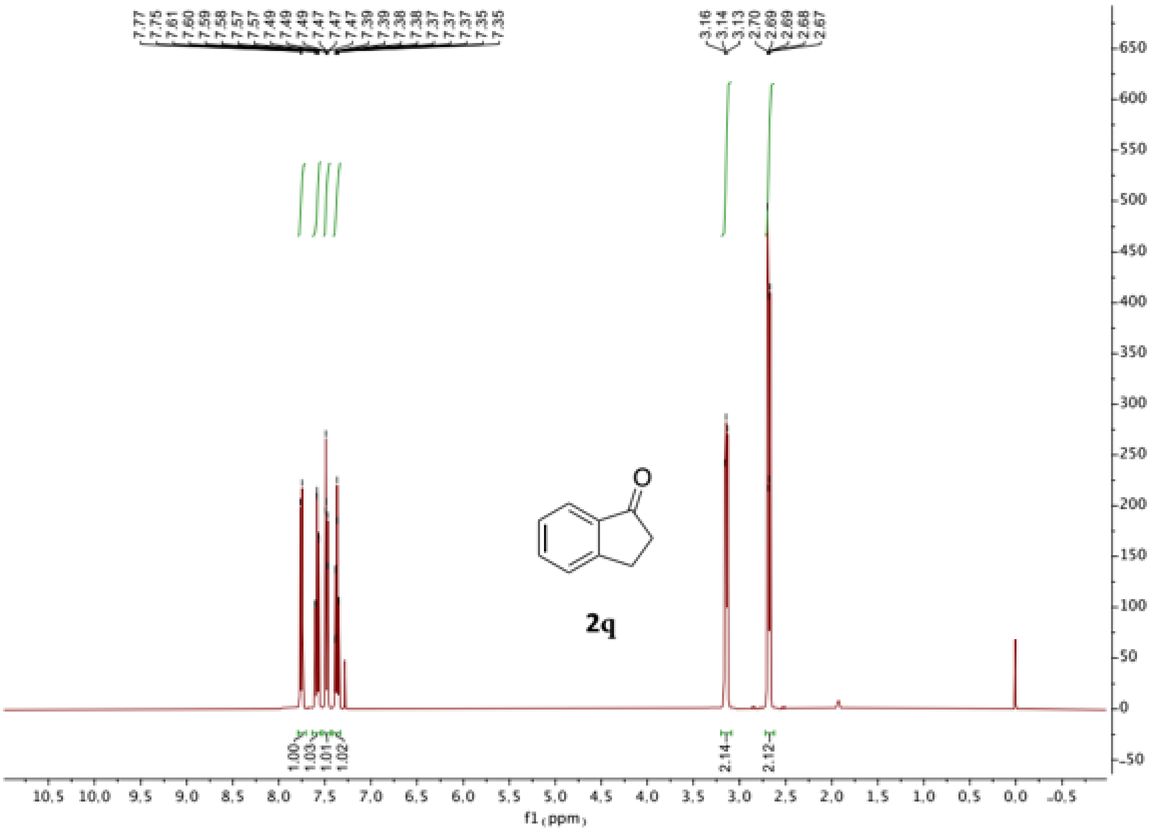
2q
f1 (ppm)

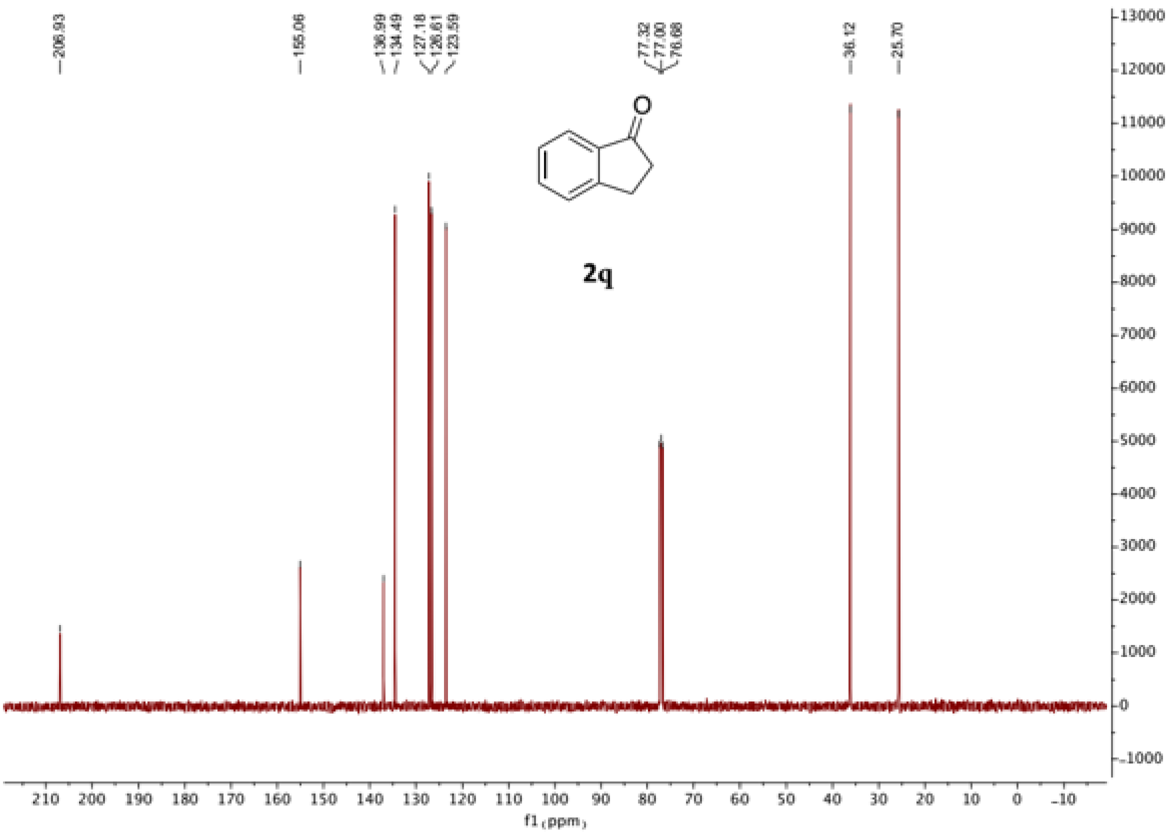
2q
f1 (ppm)

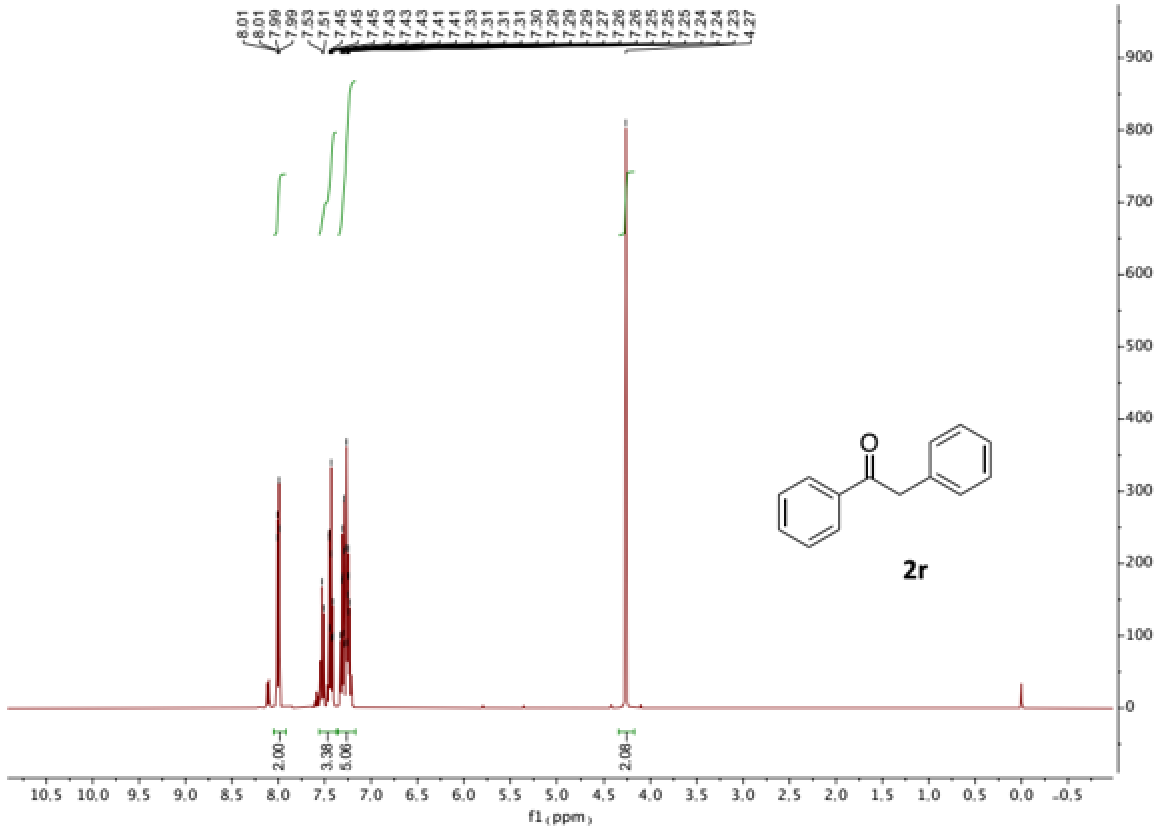
2r
f1 (ppm)

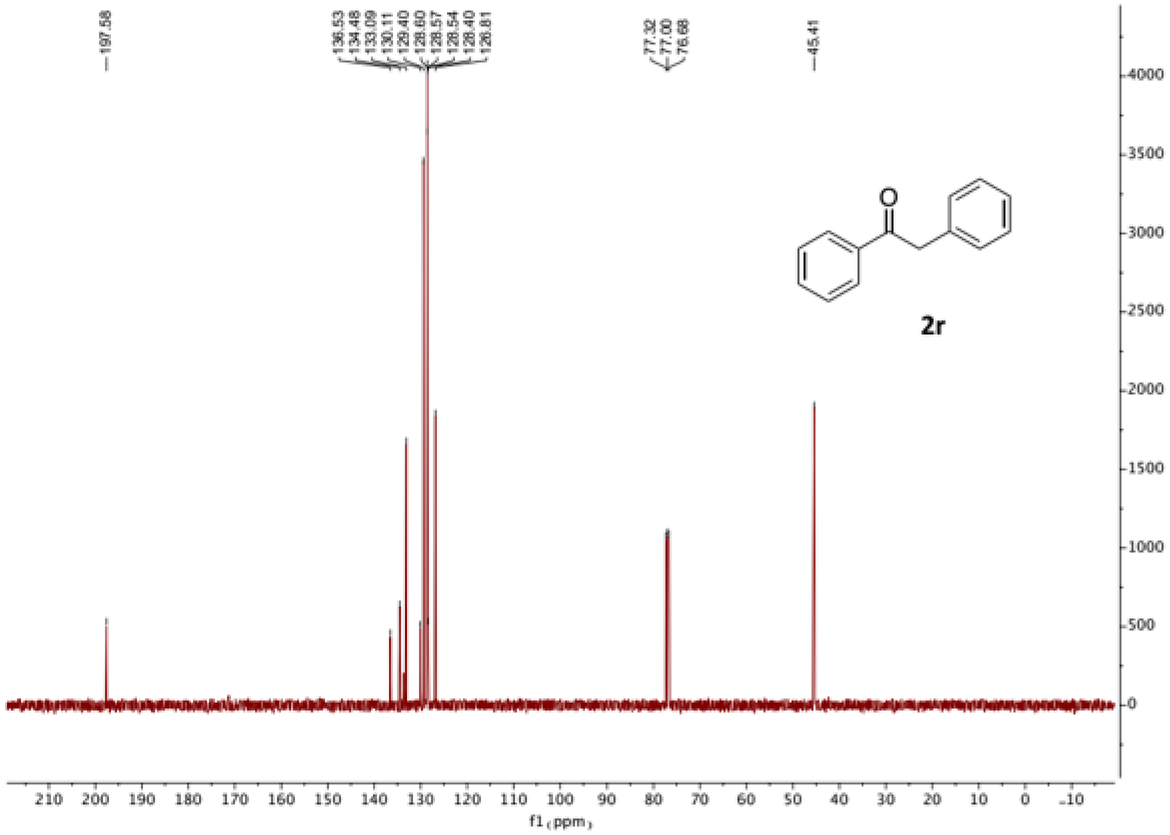
2r
f1 (ppm)

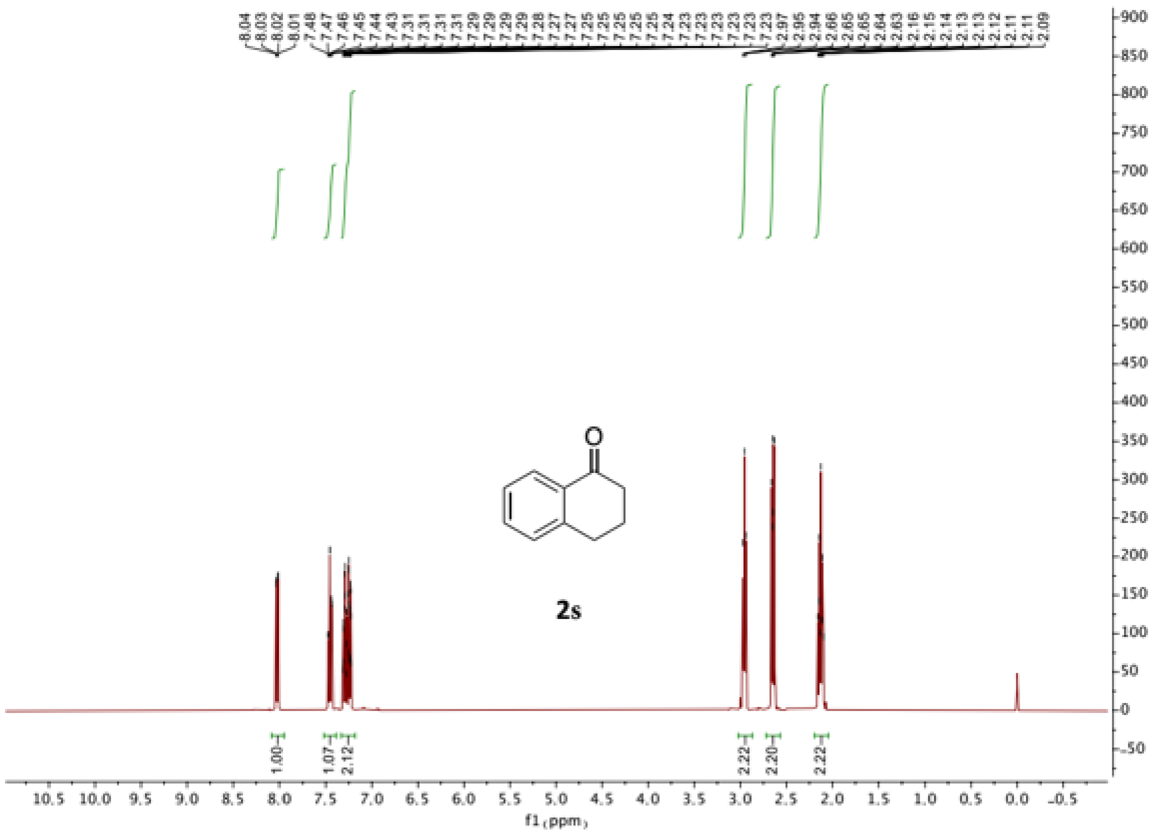
2s
f1 (ppm)

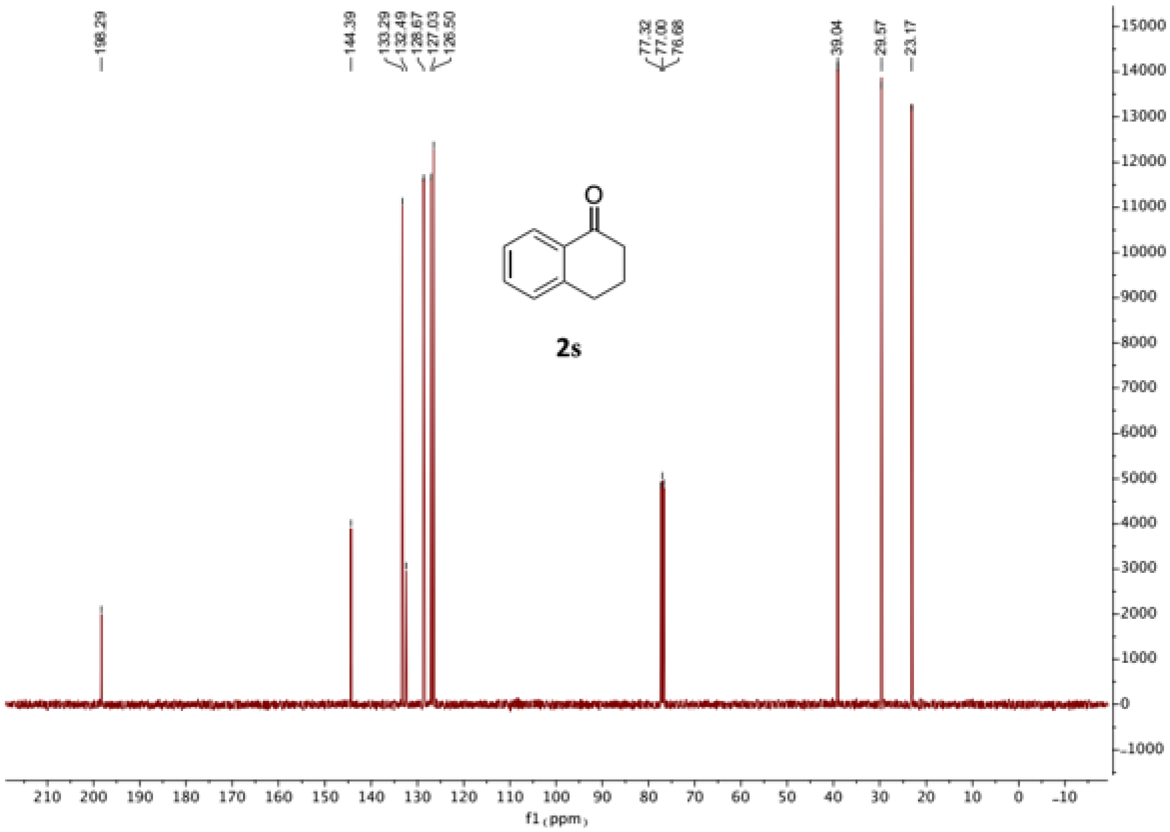
198.29
144.39
133.29
132.49
128.67
127.03
126.50
77.32
77.00
76.68
39.04
29.57
23.17
2s
f1 (ppm)

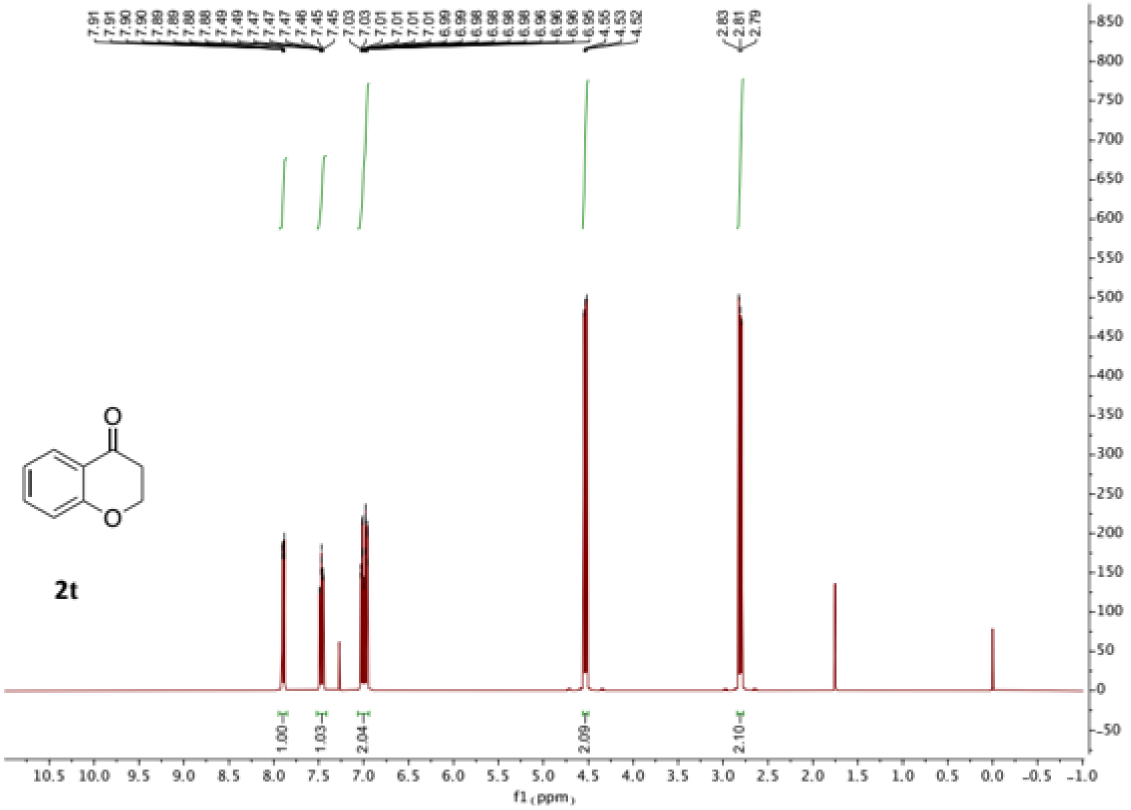
7.91
7.91
7.90
7.90
7.89
7.89
7.88
7.88
7.49
7.49
7.47
7.47
7.46
7.45
7.45
7.03
7.03
7.01
7.01
7.01
6.99
6.99
6.98
6.98
6.98
6.98
6.96
6.96
6.96
6.95
4.55
4.53
4.52
2.83
2.81
2.79
2t
1.00
1.03
2.04
2.09
2.10
f1 (ppm)

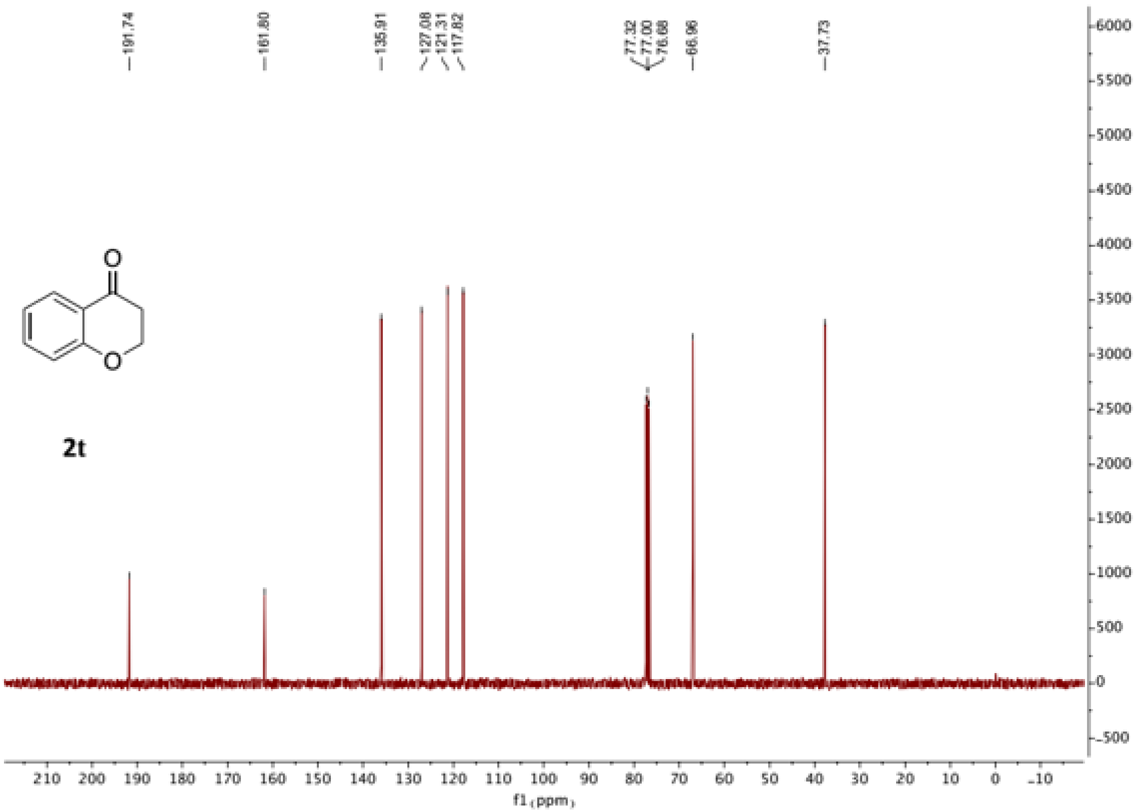
191.74
161.80
135.91
127.08
121.31
117.82
77.32
77.00
76.68
66.96
37.73
2t
f1 (ppm)

Conclusions

The present thesis focuses on developing processes and products, ultimately suitable for industrial use, that exploit resources more efficiently and minimize waste, with the goal of contributing to a more sustainable practice of chemistry. The main goal in this research has been to develop novel immobilization strategies leading to heterogenized catalysts with improved catalytic properties. The work also includes the design of new immobilized organocatalytic systems acting through non-covalent activation (SPINOL-derived CPAs) and the development of new flow processes for the sustainable production of high added-value chemicals. In addition, the use of electricity as a green oxidant in combination with salts of abundant metals as catalysts has also been explored.

In the first project, a new family of polystyrene-supported *cis*-4-hydroxydiphenylprolinol derivatives has been prepared, and the resulting functional polymers have been evaluated as organocatalysts to promote the tandem reaction between *N*-protected hydroxylamines and α,β-unsaturated aldehydes in batch and flow. The new PS-supported catalysts compare favorably with well-established immobilized Jørgensen-Hayashi catalysts belonging to the *trans*-4-hydroxydiphenylprolinol series, affording 5-hydroxyisoxazolidines as single diastereoisomers with high enantioselectivities and good yields (up to 83% yield, up to 99% ee).

In the second project, a polystyrene-immobilized isothiourea has been applied to the enantioselective acylative kinetic resolution (KR) of monoacylated BINOL(s) with inexpensive isobutyric anhydride in batch and flow. High selectivity values (s = 35 at 0 ^{o}C) and a remarkable stability of the catalytic system in the operation conditions have been recorded for unsubstituted BINOL. No significant loss of activity/selectivity is recorded after 10 consecutive KR cycles in batch. A continuous flow process has been implemented and operated with a 100 mmol (32.8 g) sample of racemic monoacetylated BINOL in an 84 hours experiment with a packed bed reactor containing 1g (f = 0.37 mmol.g^{-1}) of the functional resin. Residence time can be decreased to 10 min with the same reactor to achieve a conversion of 58% with a selectivity factor s = 17 in dichloromethane solution when a more highly functionalized catalyst (f = 0.88 mmol.g^{-1}) is used. This translates into a remarkable combined productivity of 5.5 mmol$_{prod}$·mmol$_{cat}$$^{-1}$·h^{-1}.

In the third project, a family of C2-symmetrical 1,1′-spirobiindane-7,7′-diol (SPINOL) derivatives containing polymerizable styryl units has been prepared through a highly convergent approach. Radical co-polymerization of these monomers with styrene has allowed the synthesis of a new family of immobilized SPINOL-derived chiral phosphoric acids (SPAs) where the combination of the restricted axial flexibility of the SPINOL units and the existence of extended and adaptable chiral walls adjacent to them leads to enhanced stereocontrol in catalytic processes. The optimal immobilized species (**Cat f**) brings about the catalytic desymmetrization of 3,3-disubstituted oxetanes in up to 90% yield with up to >99% enantioselectivity, exhibiting a very high recyclability (no decrease in conversion or enantioselectivity after sixteen, 16-hour runs). To exploit these characteris-tics, a continuous flow process has been implemented and operated for the sequential preparation of 17 diverse enantioen-riched products. The suitability of the flow setup for gram scale preparations (20 mmol scale) and its deactiva-tion/reactivation by treatment with pyridine/hydrochloric acid in dioxane have been demonstrated. Density Functional Theo-ry has been employed to provide a rational justification of the deep effect on enantioselectivity arising from the presence of sterically bulky substituents at the 6,6´-positions of the SPINOL unit. The main structural features of **Cat f** have subse-quently been incorporated to the design of a simplified homogeneous analog available in a straightforward manner (**Cat g**) that performs the benchmark desymmetrization reaction with similar yields and enantioselectivities as **Cat f**, providing a convenient alternative for cases when single use in solution is sought.

In the fourth project, a manganese/copper co-catalyzed electrochemical Wacker-Tsuji-type oxidation of aryl-substituted alkenes has been developed. The process involves the use of 5 mol% $MnBr_2$ and 7.5 mol% $CuCl_2$, in 4:1 acetonitrile/water in an undivided cell at 60 ºC, with 2.8 V constant applied potential. *α*-Aryl ketones are formed in moderate to excellent yields, with the advantages of avoidance of palladium as a catalyst and any external chemical oxidant, in an easily operated, cost effective procedure.

List of Publications

Publications in prof. Miquel A. Pericàs group in ICIQ (included in the thesis book).

(1) **Junshan Lai,** Sonia Sayalero, Alessandro Ferrali, Laura Osorio-Planes, Fernando Bravo, Carles Rodríguez-Escrich, Miquel A. Pericàs. Immobilization of cis-4-hydroxydiphenylprolinol silyl ethers onto polystyrene. Application in the catalytic enantioselective synthesis of 5-hydroxyisoxazolidines in batch and flow. *Adv. Synth. Catal.* **2018,** *360*, 2914-2924;

(2) **Junshan Lai,** Rifahath M. Neyyappadath, Andrew D. Smith, Miquel A. Pericàs. Continuous flow preparation of enantiomerically pure binol(s) by acylative kinetic resolution. *Adv. Synth. Catal.* **2020,** 362, 1370-1377;

(3) **Junshan Lai,** Mauro Fianchini, Miquel A. Pericàs. Development of Immobilized SPINOL-Derived Chiral Phosphoric Acids for Catalytic Continuous Flow Processes. Use in the Catalytic Desymmetrization of 3,3-Disubstituted Oxetanes. **Submitted**;

(4) **Junshan Lai,** Miquel A. Pericàs. Manganese/Copper Co-catalyzed Electrochemical Wacker–Tsuji-Type Oxidation of Aryl-Substituted Alkenes. *Org. Lett.* **2020**, *22*, 7338-7342.

Publications before join prof. Miquel A. Pericàs group in ICIQ (not included in the thesis book).

(1) **Junshan Lai**, Wenbin Du, Lixia Tian, Changgui Zhao, Xuegong She, Shouchu Tang. Fe-catalyzed direct dithioacetalization of aldehydes with 2-chloro-1, 3-dithiane. *Org. Lett*. **2014**, *16*, 4396–4399.

(2) **Junshan Lai**, Lixia Tian, Xing Huo, Yuan Zhang, Xingang Xie, Shouchu Tang. Metal-free difunctionalization of alkynes with 2-chlorodithiane for synthesis of β-ketodithianes. *J. Org. Chem.* **2015**, *80*, 5894–5899.

(3) **Junshan Lai**, Lixia Tian, Yongping Liang, Yuan Zhang, Xingang Xie, Bowen Fang, Shouchu Tang. Di-tertbutyl peroxide mediated atom transfer radical addition of 2-chlorodithiane to aryl alkynes under mild conditions. *Chem. Eur. J.* **2015**, *21*, 14328–14331.

(4) **Junshan Lai**, Yongping Liang, Teng Liu, Shouchu Tang. Dithiane induced cycloaddition/ aromatization tactic for the synthesis of multisubstituted furans. *Org. Lett*. **2016**, *18*, 2066-2069.

(5) Wenbin Du, **Junshan Lai**, Lixia Tian, Xingang Xie, Xuegong She, Shouchu Tang. Metal-free Mizoroki-Heck type reaction: a radical oxidative coupling reaction of 2-chloro-dithiane with substituted olefins. *Chem. Commun.* **2014**, *50*, 14017-14020.

(6) Yongping Liang, **Junshan Lai**, Teng Liu, Shouchu Tang. Direct regioselective [3+2] -cyclization reactions of ambivalent electrophilic/nucleophilic β-chlorovinyl dithianes: access to cyclopentene derivatives. *Org. Lett*. **2016**, 18, 5086-5089.

(7) Wenbin Du, Lixia Tian, **Junshan Lai**, Xing Huo, Xingang Xie, Xuegong She, Shouchu Tang. Iron-catalyzed radical oxidative coupling reaction of aryl olefins with 1, 3-dithiane. *Org. Lett.* **2014**, *16*, 2470-2473.

(8) Teng Liu, Lixia Tian, **Junshan Lai**, Deng Min, Mengnan Qu, Shouchu Tang. Alcohol-mediated direct dithioacetalization of alkynes with 2-chloro-1,3-dithiane for the synthesis of Markovnikov dithianes. *Org. Biomol. Chem.* **2017**, *15*, 4068-4071.